Indian J. Chem. Vol. 27A No. 1 pp. 1-88
January 1988
CODEN: IJOCAP ISSN: 0019-5103
27(A)(1) 1-88 (1988)

Indian Journal of
CHEMISTRY

SECTION A
(Inorganic, Physical, Theoretical & Analytical)

Published by
PUBLICATIONS & INFORMATION DIRECTORATE, CSIR, NEW DELHI
in association with
THE INDIAN NATIONAL SCIENCE ACADEMY, NEW DELHI

—THE WEALTH OF INDIA

An Encyclopaedia of Indian Raw Materials and Industrial Products, published in two series :
(i) Raw Materials, and (ii) Industrial Products.

RAW MATERIALS

The articles deal with Animal Products, Dyes & Tans, Essential Oils, Fats & Oils, Fibres & Pulps, Foods & Fodders, Drugs, Minerals, Spices & Flavourings, and Timbers and other Forest products. Names in Indian languages, and trade names are provided.

For important crops, their origin, distribution, evolution of cultivated types and methods of cultivation, harvesting and storage are mentioned in detail. Data regarding area and yield and import and export are provided. Regarding minerals, their occurrence and distribution in the country and modes of exploitation and utilization are given. The articles are well illustrated. Adequate literature references are provided.

Eleven volumes of the series covering letters A–Z have been published.

Vol. I A (Revised) Rs. 300.00, Vol. I (A-B) Rs. 120.00; Vol. II (C) Rs. 143.00; Vol. III (D-E) with index to Vols. I-III Rs. 158.00; Vol. IV (F-G) Rs. 98.00; Vol. IV Suppl. Fish & Fisheries Rs. 84.00; Vol. V (H-K) Rs. 171.00; Vol. VI (L-M) Rs. 135.00, Vol. VI. Suppl. on Livestock including poultry Rs. 153.00, Vol. VII (N-Pe) Rs. 150.00; Vol. VIII (Ph-Re) Rs. 129.00; Vol. IX (Rh-Se) Rs. 156.00; Vol. X (Sp-W) Rs. 338.00, Vol. XI (X-Z) with Cumulative Index to Vols. I-XI Rs. 223.00.

INDUSTRIAL PRODUCTS

Includes articles giving a comprehensive account of various large, medium and small scale industries. Some of the major industries included are: Acids, Carriages, Diesel Engines, Fertilizers, Insecticides & Pesticides, Iron & Steel, Paints & Varnishes, Petroleum Refining, Pharmaceuticals, Plastics, Ship & Boatbuilding, Rubber, Silk, etc.

The articles include an account of the raw materials and their availability, manufacturing processes, and uses of products, and industrial potentialities. Specifications of raw materials as well as finished products and statistical data regarding production, demand, exports, imports, prices, etc. are provided. The articles are suitably illustrated. References to the sources of information are provided.

Nine volumes of the series covering letters A–Z have been published.

Part I (A-B) Rs. 87.00; Part II (C) Rs. 111.00; Part III (D-E) with Index to Parts I-III Rs. 150.00; Part IV (F-H) Rs. 189.00; Part V (I-L) Rs. 135.00; Part VI (M-Pi) Rs. 42.00; Part VII (Pl-Sh) Rs. 90.00; Part VIII (Sl-Tl) Rs. 99.00; Part IX (To-Z) with Index to Parts I-IX Rs. 120.00.

SV02 121632
२५।५।८९

HINDI EDITION : BHARAT KI SAMPADA—PRAKRITIK PADARTH

Vols. I to VII and two supplements of Wealth of India—Raw
Materials series in Hindi already published.

Published Volumes

Vol. I (अ-औ) Rs. 57.00; Vol. II (क) Rs. 54.00; Vol. III (ख-न) Rs. 54.00; Vol. IV (प) Rs. 125.00; Vol. V (फ-मेरे) Rs. 90.00; Vol. VI (मेल-रु) Rs. 120.00, Vol. VII (रे-वाटा) Rs. 203.00; Vol. VIII (वाय-सीम) Rs. 300.00.

Supplements :

Fish & Fisheries (Matsya & Matsyaki) Rs. 74.00;

Livestock (Pashudhan aur Kukkut Palan) Rs. 51.00

Vols. IX to XI under publication.

Please contact :

SALES AND DISTRIBUTION OFFICER
PUBLICATIONS & INFORMATION DIRECTORATE, CSIR
Hillside Road, New Delhi 110 012

Indian Journal of Chemistry

Sec. A: Inorganic, Physical, Theoretical & Analytical

VOL. 27A NUMBER 1 JANUARY 1988

CONTENTS

Fluorescence Emission of *trans*-4,4'-Diphenylstilbene . . . 1
Joy T Kunjappu & K N Rao*

Adenosine-sensitised Photolysis of Alanine . . . 4
T Mukherjee, A M Wani & J P Mittal*

Apparent Molal Volumes & Apparent Molal Compressibilities of Some Carbohydrates in Dilute Aqueous Solutions at Different Temperatures . . . 6
M V Kaulgud* & S S Dhondge

Apparent Molal Compressibility Behaviour of Sodium Salts of Some Fatty Acids at Different Temperatures . . . 12
M V Kaulgud* & K Surya Mohan Rao

Permeation Studies on Binary Liquid Mixtures of Acetone with Benzene & Chloroform . . . 18
Kehar Singh* & M M Pandey

Kinetics & Mechanism of Oxidation of D-Glucopyranose 1-Phosphate by Chromium(VI) . . . 23
Kalyan Kali Sen Gupta*, Shipra Sen Gupta, Subrata Kumar Mandal & Samarendra Nath Basu

Kinetics of Oxidation of Mono-, Di- & Tri-chloroacetic Acids by Chloramine-T in Acid Medium: Catalysis by Iridium(III) . . . 27
S Ramakrishna & Sushma Kandlikar*

Kinetics of Reaction of Aromatic Anils with Acid Bromate: Interactive Free Energy Relationship . . . 31
P Narasimha Char, S Sondu, B Sethuram & T Navaneeth Rao*

Effect of Formaldehyde on Kinetics & Mechanism of Oxidation of Amino Acids by Bromamine-T in Perchloric Acid Medium . . . 34
B Thimme Gowda* & (Mrs) R Vijayalakshmi Rao

Role of Chloride Ion in Kinetics & Mechanism of Oxidation of Amino Acids by Chloramine-T in Perchloric Acid Medium . . . 39
B Thimme Gowda* & (Mrs) R Vijayalakshmi Rao

Synthesis & X-Ray Study of 4,4'-Bis(isoamylamino)biphenyl . . . 44
N K Sharma*, Asha Tiku, K N Goswami & Tarsaim Raj

Mixed Ligand Complexes of Copper(II) with L-Asparagine as Primary Ligand & Imidazole, Histamine & L-Histidine as Secondary Ligands . . . 48
M Sivasankaran Nair*, B Sivasankar & K Rengaraj

Pd(II) & Pt(IV) Complexes with Some Bi-, Tri- & Tetra-dentate Ligands . . . 52
N Rama Rao & M C Ganorkar*

Continued overleaf

CONTENTS

Notes

Solvent Effect on the Dipole Moments of Some-N-Substituted Maleimides ... 56
Magdi M Naoum*, Mohamed M Abdel-Moteleb & Samia M Wahba

Polarographic Reduction of Furfural Semicarbazone ... 58
R Venugopal Setty, V Suryanarayana Rao & S Brahmaji Rao*

Reaction of Dianion from Benzil-4,4′-dimethyldianil with Molybdenum Hexacarbonyl Leading to a Dianilinostilbene Complex ... 60
(Mrs) Geeta Singh & K N Mehrotra*

NMR Study of Brominated Yttrium Acetylacetonate ... 61
G Shankar & S K Ramalingam*

Pyridinium Hydrobromide Perbromide as a Brominating Agent for Metal β-Diketonates ... 63
S Abdul Samath, M Raman & S K Ramalingam*

Trivalent Nickel Complexes Containing Uninegative Bidentate Ligands & Bromine ... 66
(Miss) Minati Baral, B K Kanungo & B Pradhan*

Nickel(II) & Cobalt(II) Complexes of N,N-Diethylpyridine-2-carboxamide ... 68
Pamela Lyall & Gurdev Singh*

Anionic Complexes of Organotin(IV) with Onium Hydrochlorides ... 71
T N Srivastava*, M A Siddiqui & S K Srivastava

Synthesis & Structural Studies of Oxovanadium(IV), Manganese(II), Iron(II), Cobalt(II), Nickel(II) & Copper(II) Complexes of N-(4-Methyl-8-acetoumbelliferonylidene)-N′-(isonicotinoyl)hydrazine ... 73
P Venkateswar Rao, N Rama Rao & M C Ganorkar*

Nicotine Complexes of Zinc(II), Cadmium(II) & Mercury(II) ... 76
S Muralidharan, M R Udupa* & K S Nagaraja

Mixed Ligand Chelates of Chromium(III) ... 78
Sarbeshwar Mishra & K M Purohit*

Anionic Complexes of Nickel(II) ... 80
C M Dani & A K Das*

Complexometric Titration of Thallium(III) using Hydrazine Sulphate As Demasking Agent ... 82
A Nityananda Shetty, R V Gadag & M R Gajendragad*

Rapid Determination of Manganese by Differential Pulse and Alternating Current (Ist harmonic) Polarography ... 85
Rashmi Lakhani, S S Deshpande & A P Joshi*

Book Reviews

Homogeneous and Heterogeneous Photocatalysis (Editors: E. Pelizzetti & N Serpone) ... 87
V Vishwanathan

Organometallic Compounds of Iron (Editor: G R Knox) ... 88
B Majee

Authors for correspondence are indicated by (*)

12/12-99

Indian Journal of Chemistry

Sect. A : Inorganic, Physical, Theoretical & Analytical

VOL. 27A NUMBER 2 FEBRUARY 1988

CONTENTS

Solvent & *p*H Effects on Photochemistry & Photostability of Two Possible Laser Dyes, 7-Amino-3-(2′-benzoxazolyl)quinoline and 6-Amino-2-(2′-benzimidazolyl)indole 89
T Mukherjee*, K N Rao & J P Mittal

Spectroscopic Studies on 4-(*p*-Dimethylamino)benzylidene/phenylimino-3-methyl-1-phenyl-2-pyrazolin-5-ones 94
Anwar S El-Shahawy*, Maher M Girgis & Zarief H Khalil

Mode of Lithium Addition to Alumina on Reducibility of Nickel-Alumina 98
S Narayanan* & K Uma

Oxygen Chemisorption & X-Ray Diffraction Studies on Molybdena-Titania Catalysts . 101
B Mahipal Reddy

Adsorption of Sodium Oleate as Surfactant at the Interfacial Surface in Benzene-Water Emulsions 104
S Sharan Singh*, N Nath Pandey & R Pratap Singh

Accurate Kinetic Parameters from Thermogravimetric Data 110
K N Somasekharan

Effects of Surfactants on Kinetics of Alkaline Fading of Crystal Violet & Acid-catalysed Inversion of Sucrose 115
Jayati Datta, Abhijit Bhattacharya & Kiron K Kundu*

Kinetics of Oxidation of Some α-Hydroxy Acids by Sodium N-Bromobenzenesulphonamide 123
Abha Mathur, Vinita Sharma & Kalyan K Banerji*

Flexibly Bridged Binuclear Ruthenium(II) Complexes of Dithiobis (β-diketones) . . 126
(Mrs) Sarada Gopinathan, (Mrs) S S Deshpande & C Gopinathan*

Synthesis & Reactions of Some Cyclobutadiene Complexes of Cobalt 129
Jasim U Ahmad, Shariff E Kabir & Sayed S Ulah*

New Schiff Bases Derived from 2-Benzoylpyridine & Their Complexes with Transition Metals 133
R L Dutta* & Kuntala De

Chelating Ion-Exchanger Containing Benzoylacetanilide Group: Part I—Separation of Titanium(IV) 137
Swapan Majee, Chandrima Ray & Jyotirmoy Das*

Notes

Deduction Rules for Spectroscopic Properties of One-electron Diatomic Systems 141
B Joulakian

Continued overleaf

CONTENTS

Improved Calculation of Binding Energies of Molecules in Singlet Ground States 145
S C Rakshit* & B Hazra

Simple & Two Dimensional Hückel Molecular Orbital Treatments of Conjugated Polyolefins & Polyacetylenes 148
Lalji Dixit, Santanu Bhattacharjee & R P Semwal*

Coablt-60 Gamma Radiolysis of Tris(oxalato)cobalt(III) Ion in Oxygenated Aqueous Solution 151
B K Sharma* & Purshottam Saran

Synthesis & Characterisation of Organotin(IV) Complexes of Acetoin & Benzoin Semicarbazones & Thiosemicarbazones 153
(Miss) Purnima Dixit & J P Tandon*

Fe(III) Complexes of 2-Mercaptocarboxylic Acids 156
L D Dave* & V Pandit Rao

Synthesis & Characterisation of Oxovanadium(IV), Manganese(II), Iron(II), Cobalt(II), Nickel(II) & Copper(II) Complexes of N-(4-Methyl-8-acetoumbelliferonylidene)-N′-(salicyloyl)hydrazine 160
P Venkateswar Rao, N Rama Rao & M C Ganorkar*

Complexes of Cu(II), Ni(II), Co(II), Fe(II), Mn(II), Zn(II) & Oxovanadium(IV) with Schiff Base Derived from 2-Hydrazinopyridine & 6-Chloro-4-hydroxy-3-acetylcoumarin 163
(Miss) L Nalanda Sharada & M C Ganorkar*

Some Three-coordinate Complexes of Cadmium(II) 166
I S Ahuja*, Shailendra Tripathi & C L Yadava

Synthesis & Characterization of a Neutral, Monomeric, Dinuclear Tetrahedral Manganese(II) Species 169
I S Ahuja* & C L Yadava

Synthesis & Characterization of Pyrazinamide Complexes with Some Uranyl Salts . 171
I S Ahuja*, C L Yadava & Shailendra Tripathi

Lanthanide(III) Nitrate Complexes of the Schiff Base Vanillideneanthranilic Acid . . 174
Jessy Chacko & Geetha Parameswaran*

Analysis of Chromium(III) by a Kinetic Method 176
S A Chimatadar, G S Gokavi, S T Nandibewoor & J R Raju*

Trace Level Determination of Zinc by Differential Pulse Anodic Stripping Voltammetry 179
S S Deshpande & A P Joshi*

Book Reviews

Symmetry Through the Eyes of a Chemist (Authors: Istvan Hargittai & Magdolna Hargittai) 181
S Bhaduri

The Art of Scientific Writing (Authors: Hans F Ebel, Claus Bliefert & William E Russey) 181
B C Sharma

Authors for correspondence are indicated by (*)

Indian Journal of Chemistry

Sect. A: Inorganic, Physical, Theoretical & Analytical

VOL. 27A NUMBER 3 MARCH 1988

CONTENTS

Molecular Branching Topology & Quantum Mechanical Quantities 183
S C Rakshit*, M Banerjee & Biren Hazra

A Study of Quantitative Structure-Property Correlations (QSPC) Applying an Unusual Additivity Scheme 188
S Singh, B K Mishra & R K Mishra*

Hot Atom Chemistry in Oxyanion Targets: Part 3—Some Theoretical Aspects of Reincorporation of Parent Form in Permanganates 192
Shuddhodan P Mishra* & (Miss) Jyoti Singh

Current Efficiency, Dielectric Measurements & Ion Mobility Studies of Anodic Oxide Films Formed on Tantalum in Aqueous Electrolytes 198
R K Nigam*, K C Kalra & Parveen Katyal

Permeability of Nitrogen, Oxygen, Argon & Helium through Porous Medium (Fuel Cell Grade Asbestos + 5% Polyvinyl Alcohol) 204
R L Blokhra

Kinetics & Mechanism of Oxidation of Sulphanilamide by Peroxomonophosphoric Acid 207
G P Panigrahi* & R C Paichha

Kinetics of Co-oxidation of Ethylene Glycol & Propan-2-ol by Acid Bromate . 211
P Narasimha Char, S Sondu, B Sethuram & T Navaneeth Rao*

2,2,2-Trifluoroethoxy Derivatives of Chromium(III): Synthesis & Coordination Chemistry 214
S L Chadha* & Kamini Uppal

Synthesis & Spectral Studies of Complexes of Co(II), Ni(II), Cu(II), Zn(II), Ru(II), Pd(II) & Pt(II) with 2,3-Disubstituted Quinazolin-(3H)-4-ones 217
B Prabhakar, K Laxma Reddy & P Lingaiah*

Synthetic & Structural Studies on the Polymeric Complexes of Terephthaloyl-bis-(N-phenylhydroxamic Acid) (TPHA) & Sebacyl-bis-(N-phenylhydroxamic Acid) (SPHA) with Co(II), Ni(II), Cu(II) & Zn(II) 222
K N Munshi*, V W Kharche & H D Juneja

Synthesis & Characterization of Nitrato & Acetato Complexes of Dioxouranium(VI) with Disalicylaldehyde Acyl Hydrazones 225
S Das & R A Lal*

Mixed Ligand Complexes of Fe(II) & Cu(II) with Alizarin Maroon as a Primary Ligand & 5-Sulphosalicylic Acid as a Secondary Ligand 231
M M Seleim, K A Idriss*, M S Abu-Bakr & M K Hassan

Continued overleaf

CONTENTS

Notes

Internal Pressure & Free Volume of Potassium Chloride Solutions in Water-Dimethylformamide Mixtures 235
S O Pillai* & S Natarajan

Absorption & Fluorescence Spectra of Phenosafranin in Aqueous Solutions in Presence of Alkylamines 237
Benoy B Bhowmik* & Sharmila Roy

Electronic Spectra & Ionisation Equilibria of Thymol 240
Mannam Krishnamurthy & Sneh K Dogra*

Hydrolysis of 1-*p*-Anisyl-2,2-dimethylbutyl Chloride: Special Salt Effects . . . 242
M R Nair* & V R Shaji

Effects of Anionic & Non-ionic Surfactants in Differential Pulse Polarography . . 244
Vinay Kumar*, Gary L Baker, Patrick T Farrell, Linda M Milewski & Sandra L Zimmerman

Kinetics of Interaction of Nickel(II) & Cobalt(II) with α-Amino-β-methylbutyric Acid . 246
H C Malhotra* & Amitabh K Jain

Ru(III)-catalysed Decomposition of Ni(III) in Aqueous Sulphuric Acid Medium: A Kinetic & Ionic Strength Effect Study 250
G Krishna Reddy, T Rayapa Reddy & V Jagannadham*

Kinetics & Mechanism of Oxidation of Dimethyl Sulphoxide by Chromic Acid in Aqueous Acid Medium 252
S Venkateswara Rao & V Jagannadham*

Dipole Moments & Structure of Some Hydrazonomalononitriles 254
Magdi M Naoum*, Mohamed M Abdel-Moteleb & Zaghlol E Kandeel

^{13}C & ^{19}F NMR Studies of *para*-Substituted Monothio-β-diketones & Their Zn(II) Complexes 256
B R Dubey, R K Bansal & A K Rai*

Structural Studies of Cu(II) & Ni(II) Complexes with A Chiral Schiff Base . . . 258
L D Dave, Cherian Mathew*, Varughese Oommen & P K Krishnan Namboori

Synthesis & Characterisation of Ternary Complexes of Copper(II) with 2-Hydroxy-1-naphthaldehyde & α-Amino Acids 261
B V Mrudula Rao, G Venkatnarayana & P Lingaiah*

Stabilities & Thermodynamic Functions of the Complexes of Dimethyltin(IV) Ion with Some Amino Acids 264
K H Ajit Singh, (Miss) G Singh & V D Gupta*

Formation Constants of Binary Complexes of Lanthanides with 2-Hydroxymethylbenzimidazole 267
A Nagendram, K L Omprakash, A V Chandra Pal* & M L N Reddy

Atomic Absorption Spectrophotometric Determination of Palladium After Separation by Co-precipitation of Its 2-Mercaptobenzimidazole Complex with Microcrystalline Naphthalene 268
M Satake, G Kano, S Usami & B K Puri*

Indian Journal of Chemistry

Sect. A : Inorganic, Physical, Theoretical & Analytical

VOL. 27A NUMBER 4 APRIL 1988

CONTENTS

Communication

Structure of Conducting Polyaniline 279
Akheel A Syed*, Maravattickal K Dinesan & K N Somasekharan*

Papers

Porphyrin-sensitised Photodecomposition of Thymine in Aqueous Triton X-100 Solution 281
V V Lobko, L V Shastri, T Mukherjee & J P Mittal*

Molybdena Dispersion in Nickel Promoted Molybdena Hydrodesulfurisation Catalysts . 286
M O Alias & V Srinivasan*

Water Sorption & Ion Exchange Properties of Hydrous Oxides 290
B Venkataramani & A R Gupta*

Solubilities of Amino Acids in Methanol + Water Mixtures at Different Temperatures . 297
B P Dey & S C Lahiri*

Thermodynamic & Optical Studies on Binary Liquid Mixtures 303
T M Aminabhavi*, L S Manjeshwar, R H Balundgi & S B Halligudi

Kinetics & Mechanism of Thallium(III) Oxidation of Benzilic, Phenyllactic & 2-Hydroxyisobutyric Acids in Acid Perchlorate Solution & Comparison with Other Substituted Glycollic Acids 308
Dinesh Kumar, Pushpa Gupta & Yugul K Gupta*

Kinetics & Mechanism of Bromination of Phenols by N-Bromoacetamide: Effect of Substituents on Decomposition of Intermediate Adduct 314
S Venkateshwarlu & V Jagannadahm*

Studies on Metal-Vitamin B_6 Systems: Part II – Reaction of Iron(III) – Pyridoxol Complexes with Vitamins & Amino Acids 318
Sumitra Sen, S Gangopadhyay, B K Sen & P Bandyopadhyay*

Chemistry of Bis(fluorosulphuryl)amine: Part V – Reactions of Bis(fluorosulphuryl)amine with Antimony(V) Chloride & Protonic Acids 323
P L Dhingra, Pamela Lyall & R D Verma*

Polymeric Dioxouranium(VI) Complexes with Malonoyldihydrazine 327
R A Lal*, M N Singh & R K Thapa

Stabilities of Proton, Binary & Ternary Lanthanide Complexes of 2-Methyl-8-hydroxyquinoline-5-sulphonic Acid in Various Aquo-Organic Solvents 332
Anup Kumar Bandopadhyay & A K Chaudhury*

Continued overleaf

CONTENTS

Notes

Application of Refractive Index Mixing Rules in the Analysis of Binary Liquid Mixtures 336
J D Pandey, A K Shukla, R K Shukla & R D Rai*

Volumetric & Solvation Behaviour of Amino Acids in Some Aqueous Binaries: Part II – Behaviour of DL-Alanine in Aqueous Solutions of Strong Electrolytes in the Temperature Range 25-45°C 338
Rajani K Mohanty, Indra N Basumallick* & Utsabananda Chakraborty

Kinetic Study of Oxidation of Iodide Ion by N-Bromoacetamide by Stopped-flow Technique 341
Seema Kothari, Vinita Sharma & Kalyan K Banerji*

Separation of Polar & Steric Effects: Reactions of *ortho*-Substituted Benzoate & 3-Substituted 2-Naphthoate Ions with Picryl Bromide 343
P Ananthakrishnanadar

Kinetics & Mechanism of Aquation & of Silver Ion Catalysed Peroxydisulphate Oxidation of Pentaammineformatocobalt(III) Ion 347
Nirod Kumar Mohanty*, Bishnu Prasad Panda & Sangita Pani

Electro-reduction & Coulometric Determination of Titanium(III) in Calcium Nitrate Tetrahydrate Melt 350
C K Bhaskare* & K N Ganage

Preparation & Characterization of Some New Titanium(IV) Alkyl Acetopyruvates . . 353
(Mrs) P Pardasani, A Singh, A K Rai & R C Mehrotra*

Addition Compounds of Dithiophosphinates of Cobalt & Nickel with Acetylpyridines. 355
R N Mukherjee* & B B S Shastri

Lanthanide(III) Complexes of ONO Donor Schiff Bases Derived from Salicylaldehyde & *o*-Hydroxybenzylamine or *o*-Aminobenzylalcohol 357
A Syamal* & M R Maurya

Some Novel Cationic Mixed Ligand Complexes of Cobalt(III) 360
N Thankarajan* & K Mohanan

Synthesis & Characterisation of Some Lanthanide Perchlorate Complexes of 4-Nitrosoantipyrine 362
H Jayasankar & P Indrasenan*

Mixed Ligand Complexes of Sulphadiazine & Sulphadimidine as Secondary Ligands & Ethylenediaminetetraacetic Acid & Nitrilotriacetic Acid as Primary Ligands: Complexes of Lanthanides(III) & Transition Metal Ions 364
Mohamed M Shoukry* & Eman M Shoukry

Spectrophotometric Determination of Traces of Osmium with 4-Sulpho-2-aminobenzenethiol 366
Anil K Chakrabarty

Spectrophotometric Titration of Oxazine Dyes with Iron(II) in Triethanolamine Medium 368
K Vijaya Raju

Indian Journal of Chemistry

Sect. A: Inorganic, Physical, Theoretical & Analytical

VOL. 27A NUMBER 5 MAY 1988

CONTENTS

On the Utility of Akima's Bivariate Interpolation Method: Rotational Energy Transfer in HF-M (M = Ar, He) and HCl-Ar Collisions 373
I P Dubey, S K Upadhyay* & K Raghavan

Calculation of Quantum Chemical Parameters of S-N Ring Systems by Graph Theoretical Techniques 377
R K Mishra*, B K Mishra & S Singh

Studies on Some Novel Silica Clathrates 380
R P Gunawardane

Composition of Chromate & Chromate-Phosphate Conversion Coatings on Aluminium using Rutherford Backscattering Spectroscopy 387
M Oki

Ionic Conduction through Anodic Oxide Films Formed on Niobium in Oxalic Acid . . . 390
R K Nigam*, K C Singh & Sanjeev Maken

Solvent Effects on Solvolysis of Transition Metal Complexes: Part III—Kinetics of Aquation of Chloropentaamminecobalt(III) in Aquo-Organic Solvent Media 394
Anadi C Dash*, Nimai C Naik & Rabindra K Nanda*

Solvent Effects on Reactions of Coordination Complexes: Part IV—Acid Catalysed Aquation of Oxygen Bonded ($\alpha\beta$S)-(Sulphito)(tetraethylenepentamine)cobalt(III) in Aqueous Binary Mixtures of Protic & Dipolar Aprotic Cosolvents—A Flash Photolysis Study on Sulphur Bonded ($\alpha\beta$S)(Sulphito)(tetraethylenepentamine)cobalt(III) Ion 398
Anadi C Dash*, Neelamadhab Dash, Sukumar Aditya & Ansuman Roy

'Antispectrochemical' Behaviour of Cobalt(II) & Nickel(II) Chelates of Substituted Trialkylphosphates 404
Suraj P Narula*, Suniti Kumar, S K Bharadwaj & Rajeev Sharma

Metal Complexes of Some Nitrogen-Sulfur Donor Ligands 407
M T H Tarafder* & S Roy

Preparation & Structural Investigations of Copper(II), Cobalt(II), Nickel(II) & Zinc(II) Derivatives of 2,9,16,23-Phthalocyanine Tetracarboxylic Acid 411
B N Achar*, G M Fohlen, J A Parker & J Keshavayya

Pd(II), Pt(II), Rh(III), Ir(III) & Ru(III) Complexes of Some Nitrogen-Oxygen Donor Ligands 417
Sulekh Chandra* & Rajendra Singh

Characterisation of Some Copper(II), Nickel(II) & Cobalt(II) Complexes with Schiff Bases Derived from 3-Hydroxyiminobutane-2-one & Aromatic Amines 421
H C Rai*, (Mrs) Jaya Tiwary, (Mrs) Ranjana Prakash & (Mrs) Susan

Continued overleaf

CONTENTS

Synthesis & IR & NMR Spectral Studies on Some Triorganotin(IV) Compounds Containing 2-Pyridylcarbinols 427
R Visalakshi, V K Jain* & G S Rao

Open Shell Hexamethyleneiminecarbodithioates of VO(IV), Cr(III), Mn(II & III), Fe(III), Co(II) & Cu(II)—Magnetic, Spectral & Antimicrobial Investigations. 430
A K Singh*, B K Puri & R K Rawlley

Notes

Solvent Effects on Rates of Reduction of *trans*-Diazidobis(dimethylglyoximato)cobaltate(III) by Iron(II). 434
N Mani & V R Vijayaraghavan*

Kinetics & Mechanism of Oxidation of Diphenyl Sulphoxide by N-Chloro-3-methyl-2,6-diphenylpiperidin-4-one in Perchloric Acid Medium. 436
K Ganapathy* & K Iyanar

Kinetics & Mechanism of Oxidation of *m*-Cresol by Osmium Tetroxide in Alkaline Medium 438
A K Singh*, Sangeeta Saxena, Madhu Saxena, Rajana Gupta & R K Mishra

Effect of Ion-pairing on Solvolytic Aquation of Bromopentaamminecobalt(III) Ion in Presence of Oxalate Anion. 439
A Panda & N C Naik*

Kinetics of Chlorination of Some Substituted Piperidin-4-ones by 1-Chlorobenzotriazole. 442
R Gurumurthy* & E Arunanthi

^{13}C NMR Studies of Thiocyanato Complexes. 444
M T H Tarafder* & Kaniz Fatema

Complexes of La(III), Pr(III), Nd(III), Sm(III) & Tb(III) with 2-Thioorotic Acid 447
Madhulika Shrivastava & G S Pandey*

Studies on Lanthanide(III) Hexamethylenedithiocarbamate Complexes 449
K K Dahiya & N K Kaushik*

Magnetic, Spectral & Thermal Studies on Some New Polymeric Complexes of Mn(II), Co(II), Ni(II), Cu(II) & Zn(II) with Bis-phenylhydrazides of Suberic & Sebacic Acids. . . . 451
H D Juneja & K N Munshi*

Stability Constants of N-(2-Hydroxy-3-methoxybenzylidene)phenylhydrazine, N-(2-Hydroxy-3-methoxybenzylidene)semicarbazide & N-(2-hydroxy-3-methoxybenzylidene)thiosemicarbazide Complexes with La^{3+}, Y^{3+}, Nd^{3+}, Dy^{3+}, Pr^{3+} & Sm^{3+} . . . 454
M S Mayadeo* & Sujata S Kale

Stability Constants of Some Bivalent Metal Ion Chelates of Schiff Bases Derived from 2-Hydroxy-5-bromobenzaldehyde 456
M S Mayadeo* & Jyoti V Nalgirkar

Extraction Chromatographic Separation of Cobalt(II) Thiocyanate Complex with Dibenzo-18-Crown-6 458
Yi Yu Vin & S M Khopkar*

Use of Nickel Phosphate Membrane as an Ion Sensor with Special Reference to Phosphate Ion 460
M N Beg* & M Arshad

Indian Journal of Chemistry

Sect. A: Inorganic, Physical, Theoretical & Analytical

VOL 27A NUMBER 6 JUNE 1988

CONTENTS

Topological Investigations of the Viscous Behaviour of Binary Mixtures of Non-electrolytes . . . 469
Prem Paul Singh

Charge-Transfer Complexes of Hydroxystyrylcyanine Dyes & Their Analogues with Nicotine: Structure-Activity Relationship Studies . . . 474
Maher M Girgis* & Zarif H Khalil

Solution Densities of Aqueous Potassium Chloride-Barium Chloride Mixtures at 298.15K & Different Ionic Strengths . . . 479
Anil Kumar

Electrochemical Behaviour of Bisazo Dye, Acid Red-150 . . . 482
R N Goyal* & Anoop Kumar

Redox Chemistry of Hyponitrous Acid: Part I—Stoichiometry, Kinetics & Mechanism of Its Oxidation by Ethylenediaminetetraacetatothallium (III) in Aqueous Perchloric Acid Medium . . . 487
Muni R Goyal, Rama K Mittal & Y K Gupta*

Chromium(VI) Oxidation of Thallium (I) in Aqueous Acetic Acid & Effect of Added Vanadium (V) on the Reaction . . . 494
G S Gokavi & J R Raju*

Kinetics & Mechanism of Oxidation of Glutamine & Serine by Peroxomonosulphate in the Absence & Presence of Acetaldehyde & Propionaldehyde . . . 498
M S Ramachandran*, T S Vivekanandam & C Newman Paul Devasingh

Synthesis & Characterisation of Potassium, Cesium & Ammonium Oxotetrafluorotitanates (IV) . . . 504
Mihir K Chaudhuri* & Bimalendu Das

Synthesis & Infrared, ^{1}H, ^{13}C, ^{119}Sn NMR & ^{119}Sn Mössbauer Studies of Some New Diorganotin Dichloride Adducts . . . 507
A S Kothiwal, A Singh, A K Rai & R C Mehrotra*

Synthesis & Characterization of Complexes of Ru(II), Pt(II) & Pd(II) with Substituted Chalcones . . . 510
T Seetharama Rao, K Laxma Reddy & P Lingaiah*

Metal Complexes of Some Peptide Derivatives: Part V—Complex Formation of Copper(II) with N-Salicyloyl Derivatives of Some Amino Acids. . . . 514
G N Mukherjee* & (Miss) S Sarkar

Continued overleaf

CONTENTS

Coordination Compounds of Organometallic Bases of Group(IV) Elements: Part XI—Reactions of N,N′-(Phenyl/*o*-chlorophenyl/*p*-methylphenyl/benzyl/diethyl)-1,1-di-*n*-propoxy/*n*-butoxy-silanediamines with Tin(IV) & Titanium (IV) Chlorides at −10°C 519
Suraj P Narula*, Neeta Kapur, Ravi Shankar, Arun Chodha & Rajesh Malhotra

Solvent Extraction Studies of Mixed Chelates of Europium. 523
P R Sangurdekar & M Sudersanan*

Notes

Application of Mean Spherical Approximation in Estimating Activity Coefficients of Aqueous Mixed Electrolyte Solutions 527
Anil Kumar

Excess Properties of Binary Liquid Mixtures at 293.15K 529
T M Aminabhavi*, L S Manjeshwar, S B Halligudi & R H Balundgi

Studies of New Zeolite Derivatives of Stilbite. 532
Neelu Singhai & Sati Prasad Banerjee*

Studies of New Mesogens: Part II—*p*-(*p*′-*n*-Alkoxycinnamoyloxy)benzylidene-*p*″-*n*-butoxyanilines 536
J M Lohar & D N Dhabhai*

Charge Density-Activation Energy Correlations in Bromination of Thiophenes by N-Bromosuccinimide in Solution 538
Lalitha Rajaraman, M J Nanjan & V Kannappan*

Mechanism of Ligand Substitution Reaction of Monobipyridyl Complex of Manganese(II) 540
H M Abu El-Nader* & M N H Moussa

Complexes of Oxovanadium(IV), Chromium(III), Manganese(II), Iron(II), Cobalt(II), Nickel(II) & Copper(II) with 6-Chloro-4-hydroxy-3-acetylcoumarin (Cl-HAC). 542
(Miss) L Nalanda Sharada & M C Ganorkar*

Lanthanide Nitrate Complexes of Schiff Base Derived from 1-Isonicotinyl-Hydrazide & 2-Hydroxy-1-naphthaldehyde 545
H Jayasankar & P Indrasenan*

Mixed Valence Paramagnetic Trinuclear Complexes of Rhodium with N-Alkylphenothiazines 547
B Keshavan* & R Janardhan

Molecular Adducts of Tellurocyclopentane Diperchlorate with Neutral Donors . . 550
T N Srivastava*, M A Siddiqui & S K Srivastava

Mixed Ligand Complexes of Uranium 552
S G Deshpande & S C Jain*

Studies on the Formation Equilibria of Binary & Ternary Complexes of Copper(II) with Acetylacetone & Some Amino Acids 555
Y Anjaneyulu*, N Kameswara Rao & R Prabhakara Rao

Atomic Absorption Spectrophotometric Determination of Copper after Adsorption of Its Rubeanate onto Microcrystalline Naphthalene 558
B K Puri, M Katyal, M Satake* & L F Chang

Authors for correspondence are indicated by (*)

Indian Journal of Chemistry
Vol. 27A, January, 1988, pp. 1-3

Fluorescence Emission of *trans*-4,4′-Diphenylstilbene

JOY T KUNJAPPU & K N RAO*
Chemistry Division, Bhabha Atomic Research Centre, Trombay, Bombay 400 085

Received 12 *December* 1986; *revised and accepted* 23 *March* 1987

The fluorescence quantum yields of *trans*-4,4′-diphenylstilbene have been measured in solvents of different polarities using anthracene as the fluorescence standard, and compared with quantum yields of isomerisation in these solvents. The fluorescence emission is quenched by compounds containing heavy atoms. From the Stern-Volmer plots for quenching by propyl bromide, methylene dibromide and tetrabromoethylene, the bimolecular quenching rate constants (k_q) are calculated as 2.03×10^7, 1.05×10^8 and 7.45×10^8 dm³ mol⁻¹ S⁻¹, respectively. k_q is found to be proportional to $n^{5/2}$, where n is the number of bromine atoms in the quencher molecule. k_q values for methylene dibromide and methylene diiodide are in the ratio 1.100. This is approximately related to the sixth power of spin-orbital coupling factors of bromine and iodine atoms.

The *trans*-4,4′-diphenylstilbene (t-DPS) is an efficient laser dye[1] which lases in the range of 396-416 nm (λ_{max} 406 nm) in *p*-dioxane when excited within its first absorption band using pump sources like nitrogen laser or flash lamp. The photochemical processes occurring parallel to its fluorescence emission is its isomerisation to the *cis*-form (c-DPS). The *cis*-form is non-fluorescent[2] and hence the efficiency of this laser dye is limited to the extent of isomerization process.

While investigating the photoisomerisation process of t-DPS in detail, it became necessary to study its complementary process, viz. fluorescence emission. We report herein the results of studies on the determination of the quantum yields of fluorescence in different solvents and the process of quenching of fluorescence of this dye by some heavy atom containing quenchers.

Materials and Methods

The compound t-DPS was synthesised from *p*-phenylbenzaldehyde[3], purified by repeated crystallisation and its purity checked by HPLC on an ODS column using methanol-water (80:20) as the eluent. Its fluorescence spectrum in benzene with an emission maximum of 406 nm, and its fluorescence quantum yield (0.85) were in good agreement with those reported in literature[4,5].

The solvents were of either GR or spectro grade. They were found to be non-fluorescent in the region of fluorescence emission of the dye.

Solutions of the dye and anthracene standard were prepared in the respective solvents so as to have an absorbance of ~0.01. For deoxygenation, nitrogen was bubbled through the solutions taken in a tightly stoppered quartz cell.

The fluorescence emission spectrum was recorded from 380 to 580 nm on an Aminco Bowman spectrophotofluorometer, model No. 4-8202B, after exciting the solution at 370 nm.

The absolute fluorescence quantum yield of the compound was calculated relative to anthracene solution as standard; fluorescence emission is in the same range as that of the dye. Appropriate corrections were made to compensate for the different absorption of the sample and the standard. Each time, the total intensity of fluorescence emission was measured for the standard and the sample from the area of fluorescence spectrum recorded over the whole range of emission, under identical conditions.

Results and Discussion

The fluorescence quantum yields of t-DPS as determined in benzene solutions saturated with (i) nitrogen, (ii) air and (iii) oxygen are represented in Table 1. Oxygen quenches the fluorescence of this compound. The ϕ_f values decrease in the order: nitrogen saturated > air saturated > O_2 saturated (Table 1). The emission intensity reduces by 23.5% and 39% in air and oxygen saturated solutions respectively. The quantum yield of isomerisation of *trans*-to *cis*-forms is the highest for O_2-saturated solution. It is obvious that oxygen quenches the fluorescence of t-DPS, and this effect is usually explained on the basis of hypothesis suggested by Tsubomura *et al.*[6] (see Eq. 1).

$$S^* + O_2(T) \rightarrow (S^*.O_2)CT \rightarrow S + O_2(T), \quad \ldots (1)$$

where S, T and CT stand for singlet, triplet and charge-transfer states. Our study[2] on the complementary process of fluorescence, viz. isomerisation of t-DPS in deaerated and aerated cyclohexane solutions has shown that the triplet state of t-DPS is not

Table 1 — Fluorescence Quantum Yields* of t-DPS in Benzene Solutions

No	Sample solution	ϕ_f (t-DPS)	$\phi(t \rightarrow c) \times 10^3$
1	Nitrogen Saturated	0.85	0.60
2	Air saturated	0.65	3.22
3	Oxygen Saturated	0.52	5.79

*ϕ_f (Anthracene) in benzene = 0.29

Table 2 — Fluorescence Quantum Yields of t-DPS in Different Solvents

Solvent	Dielectric constant	λ_{max} (nm)	ϕ_f (Anthracene)	ϕ_f (t-DPS)
n-Hexane	1.89	326	0.31	0.84
Cyclohexane	2.02	337	0.27	0.81
Chloroform	4.81	341	0.15	0.66
Ethyl acetate	6.02	342	0.19	0.40
Methylene dichloride	8.90	342	0.37	0.44
Isopropanol	18.30	337	0.23	0.62
Ethanol	24.30	337	0.32	0.82
Acetonitrile	36.20	339	0.16	0.62
Dimethyl sulphoxide	49.0	350	0.16	0.62

Table 3 — Fluorescence Quantum Yields of t-DPS in Different Benzene-Methanol Mixtures

Solvent composition		ϕ_F (Anthracene)	ϕ_F(t-DPS)	$\phi_F(t \rightarrow c) \times 10^3$
Benzene (%)	Methanol (%)			
100	0	0.29	0.85	0.60
90	10	0.28	0.80	1.09
45	55	0.20	0.66	1.52
25	75	0.18	0.57	1.90
0	100	0.17	0.46	—

formed by this quenching process. Using a value of 1.91×10^{-3} mol dm^{-3} for the solubility of oxygen in aerated benzene, the rate constant for the quenching of fluorescence of t-DPS in benzene by oxygen was calculated to be ~ 10^{10} dm^3 mol^{-1} s^{-1}. This value is characteristic of a diffusion-controlled process.

The ϕ_f values of t-DPS as measured in a variety of solvents with a wide range of polarities along with the ϕ_f values of anthracene standard are listed in Table 2. The ϕ_f values did not show any regular behaviour with respect to dielectric constant of the solvent. This only shows that the dielectric constant of a solvent does not represent the true polarity of the solvent.

The ϕ_f values in methanol-benzene mixtures of different compositions are given in Table 3. Quantum yields of isomerisation are also included in Table. A comparison of the quantum yields of fluorescence and isomerisation reveals that these two are complementary processes. Similar observation was also made in the quenching studies with oxygen (Table 1).

The fluorescence emission was also followed in the presence of different heavy atom containing solvents. The effect of bromine atom was observed by choosing propyl bromide, methylene dibromide and tetrabromoethane as fluorescence quenchers. Stern-

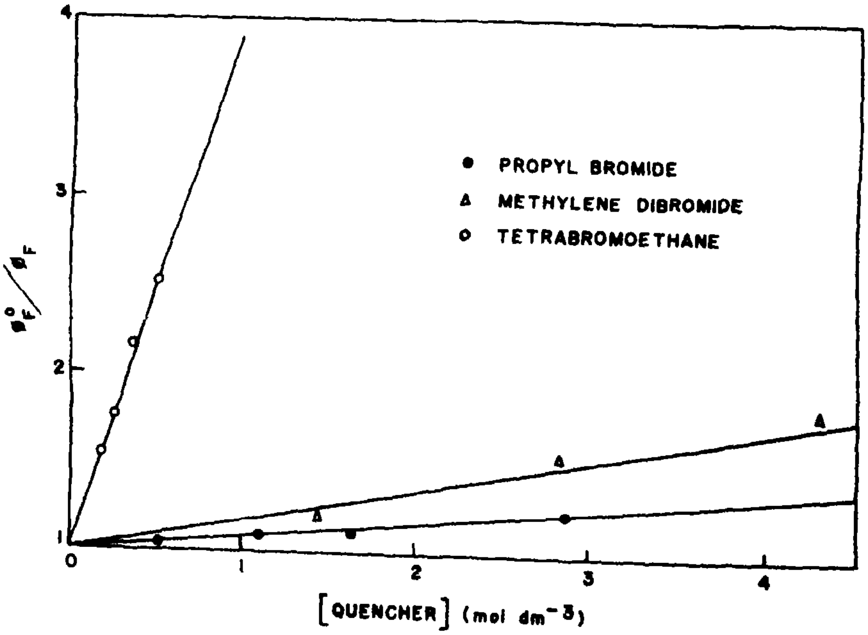

Fig. 1 — Stern Volmer plots for quenching of fluorescence of t-DPS by brominated hydrocarbons

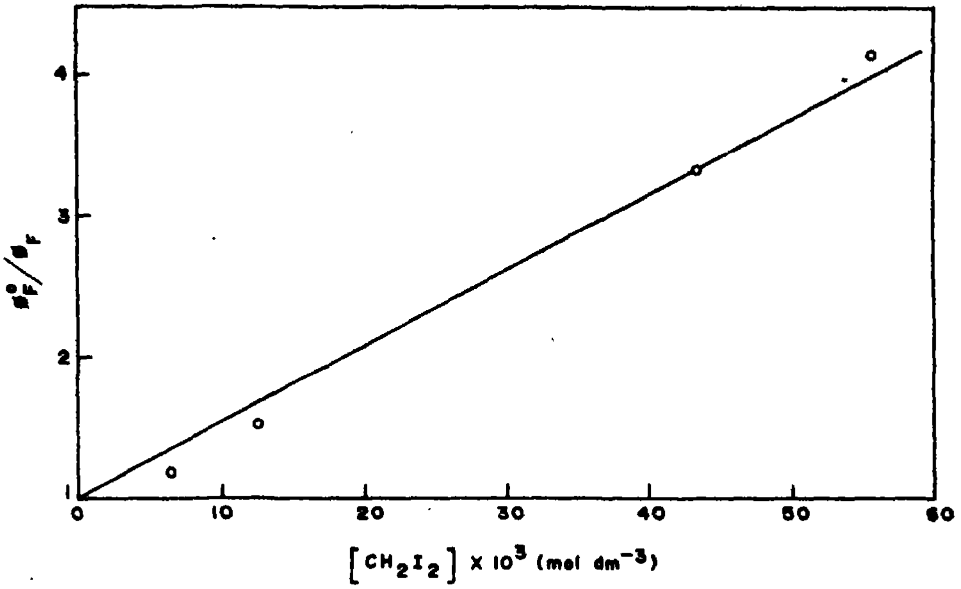

Fig. 2 — Stern-Volmer plot for quenching of fluorescence of t-DPS by methylene diiodide

Volmer plots drawn from the above data (Fig. 1) gave the quenching rate constants of 2.03×10^7, 1.05×10^8 and 7.45×10^8 dm^3 mol^{-1} s^{-1} for mono-, di-, and tetrabromoalkanes. Here, the fluorescent singlet state is quenched by the heavy atom due to spin-orbital coupling[7] which enhances the transition of singlets to triplets. This interaction can serve to relax the forbiddenness of singlet-triplet transitions of non-radiative ($T \leftarrow S^*$ and $S \leftarrow T$) and radiative ($S \leftarrow T$) types aside from enhancing the probability of $T \leftarrow S$ absorption. However, the net effect would be a reduction in the ϕ_f values[8]. As the number of bromine atoms is increased, the quenching rate constants also increase. Quenching rate constants are nearly related to the number of bromine atoms of the quencher molecule (n) and $k_q \propto n^{5/2}$, where k_q is the second order rate constant for quenching. The ratio of quenching rate constants is obtained as 1:5.3:36 where as the calculated value based on the above empirical relation is 1:5.6:32.

The quenching of fluorescence of t-DPS was studied with methylene diiodide also. k_q was obtained as 1.3×10^{10} dm^3 mol^{-1} s^{-1} from Fig. 2. Methylene dichloride showed only negligible quenching under normal concentrations. The k_q values for methylene dibromide and methylene diiodide were found to be in the ratio 1:100. This is approximately related to the ratio of the sixth powers of spin-orbital coupling factor values for bromine and iodine atoms[9] (2460 and 5060 cm^{-1} respectively). The quenching rate constants are smaller by about two orders of magnitude than the rate constants under diffusion-controlled conditions in benzene (k_{diff} in benzene is 1.6×10^{10} dm^3 mol^{-1} s^{-1} at 25°C[10] in the case of bromo compounds whereas methylene diiodide gave a value of 1.3×10^{10} dm^3 mol^{-1} s^{-1} which is very close to the k_{diff} value in benzene.

The reduction in the fluorescence emission of t-DPS in bromo- and iodo- compounds reinforces the earlier observations on laser dyes that heavy atom containing solvents should not be used in dye lasers[11]. Since it is the fluorescence emission property of the laser dye which is responsible for lasing action, both internal and external heavy atom effects are detrimental to its performance.

References

1 Meyer J A, Itzkan I & Kierstead E, *Nature*, **225** (1970) 544.
2 Kunjappu J T, *Ph D Thesis*, University of Bombay, 1985, pp 186.
3 Suzuki H, *Bull chem Soc Jpn*, **33** (1960) 415.
4 Bearlman I, *Handbook of Fluorescence Spectra of Aromatic molecules* (A P, New York) 1965
5 Fischer G & Fischer E, *Mol Photochem*, **6** (1974) 463.
6 Tsubomura H & Mulliken R S, *J Am chem Soc*, **82** (1960) 5966.
7 Kasha M, *J chem Phys*, **40** (1964) 507.
8 Cowan D O & Drisko R L E, *J Am chem Soc*, **92** (1970) 6281.
9 McClure, *J chem Phys*, **17** (1949) 905.
10 Murov S L, *Handbook of photochemistry* (Marcel Dekker, New York) 1973, pp. 63.
11 Drexhage K H, *Dye lasers*, edited by F P Schafer (Springer-Verlag, New York) 1973, pp. 58.

Indian Journal of Chemistry
Vol. 27A, January, 1988, pp. 4-5

Adenosine-sensitised Photolysis of Alanine

T MUKHERJEE, A M WANI† & J P MITTAL*
Chemistry Division, Bhabha Atomic Research Centre, Trombay, Bombay 400 085

Received 9 *April* 1987; *revised and accepted* 8 *May* 1987

Photoexcitation of an aqueous solution of adenosine containing alanine with 253.7 nm light, leads to sensitised photodecomposition of the latter to afford NH_3. The presence of O_2 reduces the quantum yield of NH_3 formation, while the presence of N_2O, CO_2 and other quenchers reduces the yield to zero, indicating that the sensitisation occurs via photoionisation of adenosine mediated via the triplet excited state.

The effect of UV radiation on nucleic acids has been extensively investigated[1-3]. As DNA intercalates to the proteins in the cells, the effect of UV radiation on the amino acids can be studied by selectively exciting nucleic acids and following subsequent reactions of the excited states of the latter. Electronically excited purines have been shown to react with alcohols[4], amines[5,6] and aliphatic amino acids[7], to give substituted purines. In several cases the functional groups of the substrates do not appear in the final product, suggesting that the substrates are cleaved by interaction with the excited purines. With amino acids as substrates, loss of amino groups has also been observed[8]. The effect of UV irradiation on aliphatic amino acids (e.g. alanine) in the presence of adenosine should serve as a useful model for photosensitisation in biological systems[8,9], since light is almost exclusively absorbed by adenosine, producing excited adenosine, which then interacts with the amino acid. In this paper, estimation of ammonia formed and luminescence studies have been used to elucidate the mechanism of photosensitisation.

Materials and Methods

Alanine (SISCO Research Laboratories, India) was recrystallised seven times from water. Adenosine (Sigma) was used as received. Triply distilled water was de-ionised by passing it in succession through cation and anion exchanger columns. High purity oxygen and purified N_2O (Indian Oxygen Ltd) were bubbled through the solution when necessary. Carbon dioxide used was generated by reacting $CaCO_3$ with $HClO_4$ *in situ*.

Ammonia was estimated with an Orion 95-10 gas-sensing electrode fitted with improved multilayer gas diffusion membranes, coupled with an Orion 407A specific ion meter (sensitivity better than 0.1 mV). Degassing was done by freeze-pump-thaw method at 77K, using a vacuum line. Photolysis was done in quartz tubes (int. diam. 15 mm), using a Rayonet RPR-100 photochemical reactor (Southern New England Ultraviolet Co., USA), fitted with 16 low pressure mercury resonance lamps (253.7 nm) in a cylindrical symmetry and a merry-go-round rotating at 4 rpm for uniform irradiation.

Absorption spectra were recorded on a Hitachi model 200-10 spectrophotometer. Fluorescence at room temperature and phosphorescence at 77K were studied using an Aminco Bowman spectrophotofluorometer (model 4-8202 B) fitted with an Aminco Keirs phosphoroscope). The photon flux was determined using a uranyl oxalate actinometer[10]. Typical photon flux used was 1.65×10^{19} $dm^{-3}s^{-1}$ for a 90-min irradiation.

The quantum yield (ϕ) for the sensitised photodecomposition was defined as:—

ϕ = (Number of NH_3 molecules produced due to sensitisation)/(Number of photons absorbed by sensitiser molecules)

Results and Discussion

In solutions containing 5×10^{-5} mol dm^{-3} adenosine and 1 mol dm^{-3} alanine, 253.7 nm UV light was absorbed exclusively by adenosine ($\varepsilon^{253.7} = 1.7 \times 10^4$ $dm^3mol^{-1}cm^{-1}$ for adenosine and ~0.014 $dm^3mol^{-1}cm^{-1}$ for alanine). Hence $(C\varepsilon)_{adenosine}/(C\varepsilon)_{alanine} \approx 61$. Ammonia was found to be a product formed by the photosensitisation of alanine by excited adenosine. Typical quantum yield in degassed solution was 5.6×10^{-4}. Increase in O_2 concentration in solution decreased the quantum yield of ammonia to 2.6×10^{-4} and 2.4×10^{-5} in air and oxygen saturated solutions respectively, indicating that triplets of adenosine were probably involved.

At room temperature, an aqueous solution of adenosine (*p*H 7) was devoid of any fluorescence. At *p*H 1, a very weak fluorescence was observed with λ_{max} at ~ 395 nm (λ_{exc} ~ 285 nm). Addition of alanine had no effect on this fluorescence, indicating that adenosine singlet states do not possibly interact with alanine. Steele and Szent-Gyorgyi[11] also did not observe any fluorescence from adenosine at any *p*H at room temperature. However, they reported phosphorescence from a 10^{-3}mol dm^{-3} adenosine solution frozen at 77K with $\lambda_{max} \sim 420$ nm and life-time (τ) of ~ 2.5 s. Due to such a long life-time of T_1 state, further photon absorption to T_n state becomes very probable. Hélène *et al.*[12] and Rosenthal *et al.*[8] have actually established that even in steady state photolysis, biphotonic excitation from T_1 to higher triplet states occurs in adenosine, followed by auto-ionisation. The π-electron ionisation energy of adenosine has been calculated quantummechanically as ~ 8 eV[13], but 253.7 nm corresponds only to ~ 5 eV, while $E(T_1) \sim 3.4$ eV. Evidently, direct photoionisation from T_1 state is not possible, while biphotonic absorption via T_1 state to $T_n > 8$ eV followed by ionisation becomes feasible. Hélène and coworkers[12,14] also suggested that any subsequent chemical transformation in the adenosine-sensitised reactions is due to interaction between the photoejected electrons and the substrate.

---

† Present address: Nuclear Research Laboratory, Srinagar 190 006 (J&K)

Presently it has been observed that an increase in O_2 concentration decreases the quantum yield of NH_3 production via sensitisation, indicating that triplets of adenosine are probably involved. However, the autoionisation process must be competing with the reaction with O_2, since, otherwise O_2 should have reacted completely with such a long-lived triplet, giving no NH_3 as the product. In the presence of metal ions (Cu^{2+}), no NH_3 could be detected, indicating complete inhibition due to triplet quenching[15].

At lower *p*H (< 4) no sensitisation was observed. This is possibly due to the lowering of triplet yield of adenosine, since it is found that the phosphorescence from adenosine is quenched by protonation ($pK_a \approx 4$). Acid inhibition could also be due to scavenging of photoejected electrons by acid protons (see Eq. 1)

$$e_{aq}^- + H^+ \rightarrow H \qquad \ldots(1)$$

When N_2O, an efficient electron scavenger[16], was bubbled through the mixture before photolysis, the quantum yield for sensitised photodecomposition decreased to zero, indicating the intermediacy of hydrated electrons in the sensitised photodecomposition in the absence of N_2O. Since the NH_3 yield actually decreased, involvement of OH produced by the reaction between e_{aq}^- and N_2O was also ruled out. Similar results were observed when N_2O was replaced by CO_2, another efficient electron scavenger.

The mechanism involving the generation of triplet adenosine, followed by ionisation from higher T_n state, explains our observations (see Scheme 1)

$$A(S_0) \xrightarrow{h\nu_1} {}^1A(S_1) \qquad (2)$$

$$^1A(S_1) \xrightarrow{ISC} {}^3A(T_1) \qquad (3)$$

$$^3A(T_1) \xrightarrow{h\nu_2} {}^3A(T_n)\ (n \geqslant 2) \qquad (4)$$

$$^3A(T_n) \longrightarrow A^+ + e_{aq}^- \qquad (5)$$

$$e_{aq}^- + CH_3CH(NH_3^+)COO^- \longrightarrow NH_3 + CH_3\dot{C}HCOO^- \qquad (6)$$

$$CH_3\dot{C}HCOO^- \longrightarrow PRODUCTS \qquad (7)$$

(ISC = INTER – SYSTEM CROSSING)

SCHEME 1

Reaction (6) is also supported by some earlier observations[17-19] that reactions between e_{aq}^- and amino acids lead to deamination. However, in Scheme 1, the fate of the adenosine cation is still not fully known. It probably reacts with water (see Eq. 8)

$$A^+ + H_2O \rightarrow AOH + H^+ \qquad \ldots (8)$$

In conclusion, triplet state of adenosine and its subsequent photoionisation are involved in the sensitised photodecomposition of alanine.

Acknowledgement

The authors thank Ms Indira Rau, a National Science Talent Search Scholar from IIT, Delhi, for help in some of the preliminary experiments.

References

1 Wang S Y, *Photochemistry and photobiology of nucleic acids*, Vol I & II (Academic Press, New York) 1976.
2 Steiner R F & Weinryb I, *Excited states of proteins and nucleic acids* (Plenum Press, New York) 1971.
3 Bensasson R V, Land E J & Truscot T G, *Flash photolysis and pulse radiolysis* (Pergamon Press, London) 1983.
4 Steinmaus H, Rosenthal I & Elad D, *J org Chem*, **36** (1971) 3594.
5 Stankunas A, Rosenthal I & Pitts (Jr) J N, *Tetrahedron Lett*, (1971) 4779.
6 Solomon J & Elad D, *Photochem Photobiol*, **19** (1974) 21.
7 Elad D & Rosenthal I, *Chem Commun*, (1969) 905.
8 Rosenthal I, Pupko R, Muszkat K A & Sharefi-Ozeri S, *J phys Chem*, **80** (1976) 454.
9 Mittal L J, Mittal J P & Hayon E, *J phys Chem*, **77** (1973) 1482.
10 Murov S L, *Handbook of photochemistry* (Marcel Dekker, New York) 1973.
11 Steele R H & Szent-Gyorgyi A, *Proc natl Aca Sci U S*, **43** (1957) 477.
12 Hélène C, Santus R & Douzon P, *Photochem Photobiol*, **5** (1966) 127.
13 Pullman A & Rossi M, *Biochim Biophys Acta*, **88** (1964) 211.
14 Santus R, Hélène C & Ptak M, *C R Acad Sci Paris, Series D*, **262** (1966) 2077.
15 Hélène C, Ptak M & Santos R, *J chim Phys*, **65** (1968) 160.
16 Gordon S, Hart E J, Matheson M S, Rabani J & Thomas J K, *Disc Faraday Soc*, **36** (1963) 193.
17 Braams R, *Radiat Res*, **27** (1966) 319.
18 Neta P, Simic M & Hayon D, *J phys Chem*, **74** (1970) 1214.
19 Sevilla M D, *J phys Chem*, **74** (1970) 2096.

Indian Journal of Chemistry
Vol. 27A, January, 1988, pp. 6-11

Apparent Molal Volumes & Apparent Molal Compressibilities of Some Carbohydrates in Dilute Aqueous Solutions at Different Temperatures

M V KAULGUD* & S S DHONDGE
Department of Chemistry, Nagpur University Campus, Nagpur 440 010

Received 9 December 1986; revised and accepted 23 April 1987

Apparent molal volumes (ϕ_v) and apparent molal compressibilities (ϕ_k) of some monosaccharides, disaccharides and methyl pyranosides in dilute aqueous solutions are reported at 5°, 15° and 25°C. The results are discussed in the light of solute-solvent interactions. The results suggest that the OH groups in D-glucose, D-fructose, sucrose, α-methyl and β-methyl glucosides interact with water in the manner similar to that of normal alcohols whereas galactose and lactose behave differently. Also the strength of stabilization of water structure in the case of galactose and lactose is more than that of other compounds. On the basis of results of ϕ_k^0, $d\phi_k^0/dT$ and viscosity *B*-coefficients, a cooperative hydration model is proposed for the hydration of lactose and galactose.

Carbohydrates play an important role in animal and plant life. Understanding the behaviour of these in dilute aqueous solutions is of utmost importance in biology and medicine. This behaviour can be understood, among others, by measuring thermodynamic properties in dilute solutions, like limiting aparent molal volumes, adiabatic compressibilities, specific heats etc. It is known[1,2] that the hydration of carbohydrates depends upon the percentage of axial and equatorial hydroxyl groups and it is more favourable when the hydroxyl group is at equatorial position. Lot of work has been done on such properties, albeit in the higher concentration range[3-7]. The extrapolated limiting parameters obtained from such measurements are not always reliable. Franks and coworkers[8] were the first to study the thermodynamic properties of several carbohydrates like ribose, galactose, glucose, methyl pyranosides etc. and cyclic ethers at 5° and 25°C in low concentration region. Their density data (obtained by magnetic float method) were very accurate but sound velocity data measured by conventional interferometer (± 0.3 m/s) were not reliable so as to enable extrapolations to give true limiting apparent molal compressibilities. The aim of the present study is to measure the densities and sound velocities of glucose, fructose, galactose, sucrose, lactose, α-methyl glucoside and β methyl glucoside in dilute aqueous solutions to obtain limiting apparent molal volumes (ϕ_v^0) and limiting apparent molal compressibilities (ϕ_k^0).

Materials and Methods

The compounds used in this work were of A R grade. D-Glucose, sucrose (S M Chemicals); D-fructose, D-galactose, lactose (Loba Chemic Indoaustrnal Co); and α-methyl glucoside and β-methyl glucoside (Sigma Chemical Co). All compounds were dried *in vacuo* at 50°C and kept in vacuum dessicator for at least 24 hr before use. The measurements were made in doubly distilled water.

Density measurements

The single float method[9] using a Sartorius model 2474 single pan semi-microbalance having facility to weigh below the pan was adopted.

A weighed quantity (~ 1850 g) of water was taken in the stainless steel cylinder. To this was added a weighed quantity of solid, which gave a difference of ~ 100 mg in the weight of plunger in water and solution at lowest concentration. The solution was stirred by a glass stirrer. In this way by adding solute successively to the water in stainless steel cylinder, 6-7 observations were taken in the concentration range 0-0.05 *m*. Density measurement of each compound in aqueous solution was made in 2-3 different runs. Considering the accuracy of temperature (± 0.002°C), weight (± 0.01 mg) and the volume of the float (~ 166 cc) the accuracy in density determination was of the order of 3 ppm.

The volume of the plunger was determined accurately first by weighing it in air and then in distilled water held at 5°, 15°, and 25°C. It was calibrated by measuring the densities of dilute aqueous solutions of sodium chloride at 5°, 15° and 25°C. It was observed that our density values were in good agreement with literature.

The density data were fitted into Eq (1)

$$d = d_0 + Am + Bm^2 + Cm^3 \qquad \dots(1)$$

with the help of microprocessor HCl-1800 model S_2 of Hindustan Computers Ltd. at the National Environmental Engineering Research Institute, Nagpur.

Table 1—Coefficients of Density Interpolation Equation (see Eq. 1)

	d_0 = 0.999965 g/cc			d_0 = 0.999098 g/cc			d_0 = 0.997048 g/cc		
	A	*B*	*C*	*A*	*B*	*C*	*A*	*B*	*C*
		Temp. = 5°C			Temp. = 15°C			Temp. = 25°C	
D-Glucose	0.070290	0.007873	−0.116074	0.070431	−0.007112	−0.299865	0.069069	−0.016452	0.042237
D-Fructose	0.073260	−0.029318	0.149379	0.069545	0.048604	−0.630238	0.070687	−0.029093	0.146833
D-Galactose	0.070100	0.102667	−1.431279	0.070218	0.036196	−0.537876	0.069988	0.007659	−0.210868
Sucrose	0.133204	0.053994	−1.106920	0.131331	0.048304	−1.016690	0.128570	0.085986	−1.353346
Lactose	0.135540	0.037798	−0.752183	0.135120	−0.006860	−0.325900	0.134858	−0.071095	0.533130

Apparent molal volumes

The apparent molal volumes were calculated using Eq. (2)

$$\phi_v = \frac{1000}{m d d_0}(d_0 - d) + \frac{M_2}{d} \qquad \ldots (2)$$

where d and d_0 are the densities of solution and solvent respectively; m is the molality; and M_2 is the molecular weight of the solute. The limiting apparent molal volumes (ϕ_v^0) were obtained by the method of least squares. For the extrapolation of ϕ_v versus m to zero concentration, the points at low concentration, which deviated considerably from linearlity were not considered. The same procedure was adopted by Franks *et al.*[8] because of the possibility of systematic error at low concentration due to dissolved air in solution.

Sound velocity measurements

The sound velocities were measured differentially in the carbohydrate concentration range of 0.0 to 0.05m using a phase-comparison interferometer. The details of the apparatus and method of measurements adopted were the same as those described in the earlier works[10,11].

Solutions of carbohydrates of different concentrations were prepared *in situ* by successively adding known weight of sugar solution into the interferometer vessel containing a known amount of water.

Accuracies in sound velocity measurements were 1, 2 and 3 cm s^{-1} for a velocity change of 1, 3 and 8 m s^{-1} respectively.

The sound velocity data were fitted into Eq. (3)

$$U = U_0 + am + bm^2 \qquad \ldots (3)$$

From the sound velocity and density values the apparent molal compressibility (ϕ_k) was calculated using Eq. (4)

$$\phi_k = \frac{1000}{m d d_0}(d_0 \beta - d\beta^0) + \beta \frac{M_2}{d} \qquad \ldots (4)$$

where d_0, d and β^0, β are the densities and compressibilities of solvent and solution, respectively; m is the molality; and M_2 is the molecular weight of the solute. The limiting apparent molal compressibility (ϕ_k^0) was obtained by extrapolating (using a least squares fit making use of a programmable calculator) ϕ_k versus m curves to zero concentrations, neglecting the points at low concentration, which deviated considerably from linearity as in the case of apparent molal volumes.

Results and Discussion

Values of the parameters A, B and C of Eq. (1) are listed in Table 1. The coefficients a and b of sound velocity interpolation equation (Eq. 3) are given in Table 2. Figure 1 shows the variation of apparent molal volume (ϕ_v) as a function of concentration at 25°C. Similar plots are obtained at 5° and 15°C. It is observed that the slopes are generally weakly positive and sometimes zero or even negative. The magnitudes of slopes are not significant from the point of view of solute-solvent interactions. Figure 2 shows the variation of ϕ_k as a function of concentration at 25°C. Similar curves are obtained at 5° and 15°C. It is observed that ϕ_k varies linearly with concentration. *Our* ϕ_k *values obtained at 25°C at 0.025* m concentration are accurate to ± 0.7 units, whereas the ϕ_k values obtianed by Franks *et al.*[8] at same concentration are accurate to ± 4.5 units. Hence our extrapolations yield more reliable ϕ_k^0 values than those of Franks *et al.*

As observed in the case of ϕ_v, ϕ_k weakly depends upon concentration. The slopes of these curves are not very important for the interpretation of solute-solute interactions.

The limiting apparent molal volumes (ϕ_v^0) for carbohydrates at 5°, 15° and 25°C, listed in Table 3, show that ϕ_v^0 values of glucose at all temperatures are higher than those of galactose and fructose, though the difference is not very large. The higher ϕ_v^0 values in the case of glucose suggest that it is comparatively

Table 2—Coefficients of Sound Velocity Interpolation Equation (see Eq. 3)

Compound	$U_0 = 1426.71$ m/s		$U_0 = 1466.4$ m/s		$U_0 = 1497$ m/s	
	a	*b*	*a*	*b*	*a*	*b*
	Temp. = 5°C		Temp. = 15°C		Temp. = 25°C	
D-Glucose	95.72	−20.0	90.00	34.0	58.66	94.0
D-Fructose	87.49	−56.0	82.58	−90.0	59.38	86.0
D-Galactose	162.06	−6.0	115.55	78.0	46.75	263.0
Sucrose	118.30	85.0	119.37	23.0	110.19	−26.0
Lactose	252.03	−87.0	161.16	−21.0	168.92	−120.0
α-Methyl glucoside	119.40	−79.0	—	—	60.92	306.0
β-Methyl glucoside	108.49	27.0	—	—	78.48	−109.75

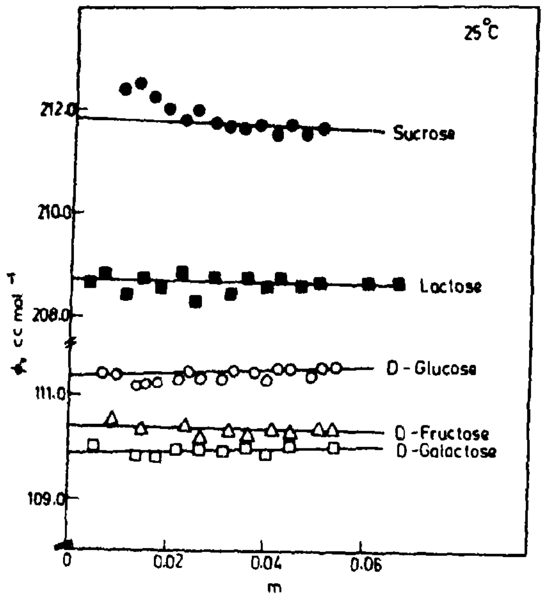

Fig. 1—Plots of ϕ_v (cc/mol) versus *m* for different carbohydrates at 25°C

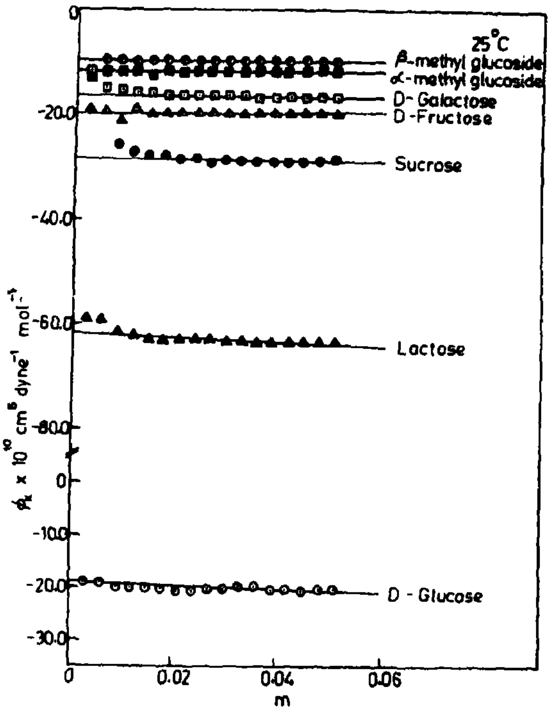

Fig. 2—Plots of $\phi_k \times 10^{10}$ (cm^5 dyne^{-1} mol^{-1}) versus *m* for different carbohydrates at 25°C

more hydrated than fructose and galactose. Glucose and galactose are present in the form of pyranose forms, with the difference that in galactose the OH group at C-4 is configurationally different from that in glucose. Galactose has higher percentage of axial OH groups than that in glucose and hence will exhibit lower values of ϕ_v^0 as compared to glucose[8]. Slightly higher hydration in glucose over fructose can be ascribed to six-membered pyranose ring being more favourable for interaction with water than the five-membered furanose ring in fructose.

The stereospecific hydration observed in aqueous monosaccharide solutions is also observed in solutions of disaccharides. The ϕ_v^0 values of sucrose and lactose bear this out (Table 3). On the basis of the discussion made earlier, one should have expected higher ϕ_v^0 values for lactose than those for sucrose, since sucrose is made up to glucose and fructose and lactose that of glucose and galactose. But a reverse trend is observed i.e. ϕ_v^0 (sucrose) > ϕ_v^0 (lactose). We believe that this is due to specific configuration of furanose and pyranose ring playing an important role in hydration.

It is seen from the data in Table 3 that limiting apparent molal expansibility (ϕ_E^0) increases sharply with increase in temperature for glucose, only slightly in the case of sucrose and lactose and decreases slightly for galactose and sharply for fructose. These results suggest that water around glucose is loosely bound and in other compounds it is relatively firmly bound, as has been concluded by Neal and Goring from expansibility studies[25].

In Table 4 are collected the limiting apparent molal compressibilities (ϕ_k^0) of carbohydrates at 5°, 15° and 25° and of NaCl and MeOH, EtOH etc at 25°C

Table 3—Limiting Apparent Molal Volumes (ϕ_v^0) and Mean Limiting Expansibilities ($\phi_E^0 = d\phi_v^0/dT$) of Carbohydrates

Compound	ϕ_v^0 (cc/mol)			ϕ_E^0 (cm^3 mol^{-1} deg^{-1})	
	5°C	15°C	25°C	10°C	20°C
D-Glucose	109.5(109.5^8)	110.0	111.4 (111.9^8, 112.04^4, 111.7^3, 112.2^5)	0.05	0.14
D-Fructose	107.2	109.2	110.4 (110.4^5)	0.20	0.12
D-Galactose	107.8 (107.7^8)	109.0	109.9 (110.7^8, 110.2^3, 111.9^5)	0.12	0.09
Sucrose	207.8 (207.62^{15})	209.6 (209.97^{15})	211.8 (211.32^4, 211.6^3, 211.82^{14}, 210.2^5)	0.18 (0.23^{15})	0.22 (0.16^{15})
Lactose	205.4	206.8	208.7 (209.1^3, 207.6^5)	0.14	0.19
α-Methyl-glucoside	(130.9^8)	—	(133.2^8)	—	—
β-Methyl-glucoside	(134.6^8)	—	(135.5^8)	—	—

Literature values are given in parentheses.

Table 4—Limiting Apparent Molal Compressibilities (ϕ_k^0) and $(d\phi_k^0/dT)_4$. of Carbohydrates (This Work) and Some Other Solutes

Compound	$\phi_k^0 \times 10^{10}$ (cm^5 dyne^{-1} mol^{-1})			$(d\phi_k^0/dT)_4$. (cm^5 dyne^{-1} mol^{-1} deg^{-1})
	5°C	15°C	25°C	
D-Glucose	−45.19 (−38.8^8)	−40.17	−20.13 (−16.0^8, −16.0^6)	0.502
D-Fructose	−42.02	−32.22	−19.79	0.98
D-Galactose	−91.25	−59.68	−16.06	3.157
Sucrose	−46.39	−39.81	−28.53 (−16.0^6)	0.65
Lactose	−133.55	−68.18	−62.88	6.06
α-Methyl-glucoside	−48.32 (−35.3^8)	—	−11.95 (−13.0^8, −11.0^6)	—
β-Methyl-glucoside	−39.51 (−29.2^8)	—	−9.81 (−5.9^8)	—
NaCl			−50.5^{16}	
MeOH			12.6^{11}	0.50^{13}, 0.29^{12}
EtOH			9.9^{11}	
THFA			4.4^{16}	
$EtNH_2$			13.32^{18}	
$N\text{-}Bu_4Br$			−15.2^{18}	

for comparison. It is observed that ϕ_k^0 values for all the carbohydrates at all temperatures are negative. The values at 25°C are less negative than those of NaCl, more negative than those of alcohols, ethylamine and THFA and are of comparable magnitude with those of tetraalkylammonium bromide.

The negative ϕ_k^0 values obtained in the case of carbohydrates can be explained by postulating that polar OH groups interact with the surrounding solvent water through dipole-dipole interaction in such a way that the surrounding water loses its own compressibility to a certain extent but not as completely as in the case of electrolytes. Water in the hydration shell of these molecules must be less compressible than that of bulk water but certainly not having zero compressibility as in the case of highly electrostricted water.

As a first approximation, one can expect a one to one relationship between the number of dipoles interacting with solvent water and the magnitude of ϕ_k^0. To examine this point further we have plotted ϕ_k^0 against the number of OH groups in a carbohydrate (Fig. 3) at 25°C. It is observed that as the number of OH groups increases, the ϕ_k^0 becomes more and more negative. The relationship is almost linear. This indicates that OH groups of carbohydrates interact with water in a manner similar to the OH groups in alcohols. This fact is also supported by the viscosity *B*-coefficients of alcohols and carbohydrates. It is observed that the *B*-coefficient increases linearly with number of OH groups (Fig. 3). *B*-coefficient gives direct idea about the amount of water attached firmly to the solute molecule when the molecule is in motion.

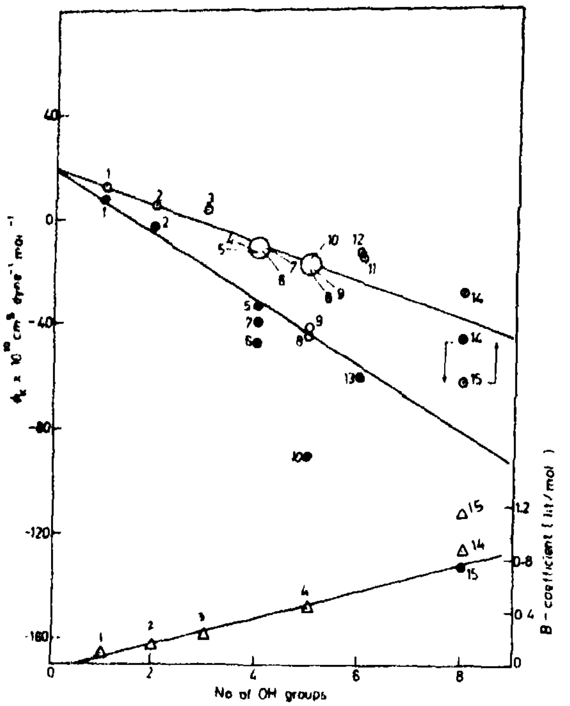

Fig. 3—Plots of ϕ_k^0 versus number of OH groups (○—○) at 25°C and (●—●) 5°C (left hand scale [1, Methanol (ref. 11); 2, ethylene glycol (ref. 19); 3, glycerol (ref. 20); 4, xylose (ref. 3); 5, ribose (ref. 8); 6, α-methyl glucoside (this work); 7, β-methyl glucoside (this work); 8, D-glucose (this work); 9, D-fructose (this work); 10, D-galactose (this work); 11, manitol (ref. 3); 12, glucitol (ref. 3); 13, myoinositol (ref. 8); 14, sucrose (this work); 15, lactose (this work)]; and plot of *B*-coefficient versus number of OH groups (Δ—Δ) (right hand scale) [1, methanol (ref. 21); 2, ethylene glycol (ref. 21); 3, glycerol (ref. 21); 8-D-glucose (ref. 22); 14, sucrose (ref. 23); 15, lactose (ref. 24)]

The only notable exception, lactose, shows more negative value of ϕ_k^0 and higher value of *B*-coefficient as compared to those of sucrose. This suggests that lactose is more extensively hydrated than sucrose. Since the number of interacting OH groups in sucrose and lactose is same, the authors strongly feel that hydration of lactose must be of different type than that of sucrose and other sugar molecules. In the case of other carbohydrates the OH groups can be visualized to interact with water as if they are separate alcohols. But in the case of lactose the water molecule which is attached to one OH group must be involved in H-bond formation with another water molecules attached to adjacent OH group. This type of hydration may be called as cooperative hydration which yields more negative value of ϕ_k^0 and also higher *B*-coefficient.

It is observed from the data in Table 4 that at 25°C, negative ϕ_k^0 values increase in the order galactose < fructose < glucose. The ϕ_k^0 values are in the order: galactose < fructose < glucose. It is shown by Franks *et al*[1] that the hydration is more favoured when the OH group are in equatorial position and compound fits well with tetrahydral arrangement of water molecules. However, they could not distinguish the hydration of glucose and galactose. Our ϕ_k^0 values of glucose and galactose clearly indicate that glucose is more hydrated than galactose for the same reason that glucose has more number of equatorial OH groups than galactose. This differentiation in the hydration of glucose and galactose on the basis of ϕ_k^0 values has been possible on account of more reliable estimate of ϕ_k^0.

The ϕ_k^0 values of α-methyl and β-methyl glucosides at 25°C are aproximately equal. This indicates that the hydration of the remaining three OH groups, which are all equatorial is similar.

Further Fig. 3 shows that ϕ_k^0 varies linearly as a function of OH groups at 5°C also. It means that even at 5°C, like at 25°C, carbohydrates behave like alcohols in water. The slope of the plot of ϕ_k^0 versus number of OH groups (Fig. 3) is higher than that at 25°C. However, galactose and lactose show deviations from linearity. These carbohydrates show high negative values. Also sucrose, α-methyl glucoside and β-methyl glucoside show deviation from linearity. This might be due to the fact that at 5°C, the ordered structure of solvent water must be forcing these carbohydrates into such stereochemical configuration which is more favourable for interaction with water dipoles. At 5° and 15°C galactose shows much larger negative values for ϕ_k^0 than those of glucose and fructose. Here the changed order of negative value of ϕ_k^0 is fructose < glucose < galactose. This indicates that at low temperature galactose seems to acquiring such a stereochemical reorientation/transformation that still more extensive hydration is made possible. The results of ϕ_k^0 for sucrose and lactose also strongly support the above contention, as lactose molecules are built-up of glucose and galactose of necessity show very large negative value (− 133.5) than sucrose which is made up of fructose and glucose.

The ϕ_k^0 values of α-methyl and β-methyl glucosides at 5°C and like the one at 25°C were expected to be identical. However, the values are more negative for α-methyl glucoside than those for β-methyl glucoside. This points to some stereochemical orientation/transformation in the case of α-methyl glucoside favouring extensive hydration. However, further experimentation on methyl derivatives of other pyranosides is necessary before drawing final conclusion.

Temperature coefficient of ϕ_k^0 at 4°C has been shown to give an idea of relative structure strengthening abilities of solutes on structure of water[13]. As an approximation $(d\phi_k^0/dT)_4$. values have been computed from values of ϕ_k^0 at 15° and 5°C (Table 4). The values of temperature coefficient of ϕ_k^0 for glucose, fructose and sucrose are of the order of methyl alcohol, whereas the values are very high for galactose and lactose. This suggests that glucose, fructose and sucrose behave like alcohols and strength of stabilization of water structure is of the same order even though there are more number of hydroxyl groups. In the case of galactose and lactose the strength appears to be more than that of other carbohydrates. This might be due to the cooperative hydration in the case of galactose and lactose.

Acknowledgement

S S D thanks the UGC, New Delhi for the award of a junior research fellowship.

References

1 Franks F, Tait M J, Suggett A, Ablett S & Quickenden P A, *J soln Chem*, **1** (1972) 131.
2 Franks F, Reid D S & Suggett A, *J soln Chem*, **2** (1973) 99.
3 Høiland H & Holvik H, *J soln Chem*, **7** (1978) 587.
4 Millero F J, Surdo A Lo & Shin C, *J chem & Engng Data*, **23** (1978) 197.
5 Edward J T, Shahidi F & Farrell P G, *J soln Chem*, **5** (1976) 807.
6 Shiio H, *J Am chem Soc*, **80** (1958) 70.
7 Gerecze N G, *Acoustica*, **32** (1975) 201.
8 Franks F, Ravenhill J R & Reid D S, *J soln Chem*, **1** (1972) 3.
9 Kaulgud M V, Bhagde V S & Shrivastava A, *J chem Soc Faraday Trans-I*, (1982) 313.
10 Kaulgud M V, Pandya G H & Rao K S M, *Indian J pure & appl Phys*, **16** (1978) 459.
11 Kaulgud M V & Rao K S M, *J chem soc Faraday Trans-I*, (1979) 2237.
12 Moharil A G, Ph D Thesis, Nagpur University (1985).
13 Kaulgud M V, *J chem Soc Faraday Trans-I*, (1979) 2246.
14 Dipaola G & Belleau B, *Can J Chem*, **55** (1977) 3825.
15 Garrod J E & Herrington T M, *J phys Chem*, **74** (1970) 363.
16 Owen B B & Kronik K L, *J phys Chem*, **65** (1961) 84.
17 Kaulgud M V, Shrivastava A & Awode M R, *Indian J pure & appl Phys*, **18** (1980) 864.
18 Desnoyers J E & Philip P R, *Can J Chem*, **50** (1972) 1094.
19 Nakajima T, Komatsu T & Nakagawa T, *Bull chem Soc Japan*, **48** (1975) 788.
20 Kuhnkies & Schaaffs W, *Akust Beih*, **12** (1962) 254; *Chem Abstr*, **58** (1963) 3918a.
21 Heroskovitz T T & Kelly T M, *J phys Chem*, **77** (1973) 381.
22 Ihnat M, Szabo A & Goring D A I, *J chem Soc (A)*, (1968) 1500.
23 Jones G & Talley S K, *J Am chem Soc*, **55** (1933) 624.
24 Palvermacher, *Z anorg allgm chem*, **113** (1920) 141.
25 Neal J L & Goring D A I, *J phys Chem*, **74** (1970) 658.

Indian Journal of Chemistry
Vol. 27A, January, 1988, pp. 12-17

Apparent Molal Compressibility Behaviour of Sodium Salts of Some Fatty Acids at Different Temperatures

M V KAULGUD* & K SURYA MOHAN RAO†

Department of Chemistry, Nagpur University, Nagpur 440 010

Received 9 *December* 1986; *revised and accepted* 23 *April* 1987

Sound velocity measurements in dilute solutions (0-0.06 *m*) of sodium salts of fatty acids from formic to caproic acids with the help of a differential phase-comparison interferometer at 5°, 15°, 20°, 25°, 30° and 45°C coupled with density measurements using buoyancy method have enabled the evaluation of precise limiting apparent molal compressibilities (ϕ_k^0) for all the salts. By subtracting the $\phi_k^0(Na^+)$ it is possible to evaluate ϕ_k^0 for all the anions. The $\phi_k^0(T)$ trends for the anions are interpreted in terms of electrostrictive and hydrophobic interaction of the anion moiety with solvent water The ϕ_k^0 values in addition enable one to estimate the thickness of the Frank and Wen disordered B-region in water as 3 Å. The deviation constants b_k and b_v for apparent compressibility and apparent volume have been interpreted in terms of ion pair formation and cosphere overlap using Gurney's model. It has been shown that the hydration numbers cannot be easily evaluated.

Sodium salts of higher fatty acids behave as surface active agents in aqueous solutions. Measurements of densities[1,2], entropies of transfer[3], enthalpies of dilution[4], heats of solutions[5] and activity and osmotic coefficients[6] in aqueous solutions of salts have been used to throw light on solute-solvent interactions.

The apparent molal compressibility (ϕ_k) is also a useful parameter in elucidating the solute-solvent interactions. Except for the work in the authors laboratory[8], not much work seems to have been done on compressibility behaviour of dilute solutions of sodium carboxylates. The reported measurements were carried out at high concentrations (> 0.2 *m*). These limiting apparent compressibility (ϕ_k^0) values are not considered reliable, for the following reasons: (a) extrapolations were done employing limiting law equation not applicable at higher concentrations; and (b) due to limited accuracy of measurements points at lower concentrations show considerable scatter. Hence extrapolation to infinite dilution are not unique.

Recently, Bhowmik and Mohanty[9] have measured the apparent compressibilities in aqueous solutions of sodium salts of fatty acids (formate to valerate) at different temperatures (25-55°C). However, on account of the limited accuracy of the interferometric method of measuring sound velocities, they could not carry out measurements in really dilute solutions. Consequently, extrapolations to obtain ϕ_k^0 using the limiting law are unsatisfactory for reason (a) mentioned above. They have also calculated hydration numbers from the ϕ_k^0 values.

The present work reports accurate ϕ_k^0 values and describes ϕ_k-concentration dependence of sodium salts of formic, acetic, propionic, *n*-butyric, valeric and caproic acids in low concentration region (0-0.06 *m*) at six different temperatures, 5°, 15°, 20°, 25°, 30° and 45°C obtained from sound velocity measurements using the differential phase-comparison-interferometer. This is the first systematic work on compressibility of sodium salts of fatty acids at low concentrations and different temperatures. The aim was to have a clear picture of anion-water interactions.

Materials and Methods

Sodium formate and acetate (both AR, BDH) were further recrystallised with ethanol and dried *in vacuo* for two to three days. Sodium propionate, butyrate, valerate and caproate were prepared from the respective carboxylic acid (AR) as follows: To a sample of carboxylic acid was added sodium hydroxide solution which was just a little less than required for complete neutralisation of the acid. The solution was evaporated to dryness and washed with ethanol or acetone to remove excess acid. The samples were recrystallised from ethanol or ethanol-water mixtures and dried *in vacuo* for two to three days before use.

The purity of the samples was checked by conductometric titration and it was found to be better

---

†*Present address*. Basic Research and Training Division, National Environmental Engineering Research Institute, Nagpur 440 020

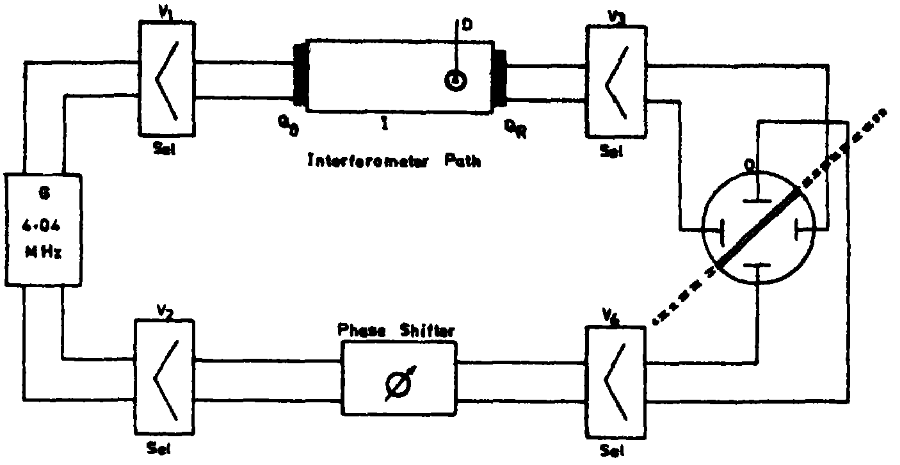

Fig. 1—Block diagram of the phase-comparison interferometer

than 99.9%, except in the case of sodium caproate where it was found to be 99.5%.

Sound velocity measurements

The sound velocities were measured differentially using a phase-comparison interferometer[9-11]. In this method a r.f. voltage from a generator (G) (see Fig. 1) was applied to the two plates of a detector oscilloscope (O) through two different channels. One of the channels consisted of an interferometer path (I) having an oscillating crystal, (Q_0) and a receiving crystal (Q_R). In the second channel a calibrated phase shifting network was incorporated. Small changes in sound velocity caused on the addition of solute in (I) resulted in a small splitting of the Lissajous figure of the oscilloscope screen which was compensated by the fine phase shifting network.

Provided there was a travelling wave between Q_0 and Q_R the relation between phase shift and the change in velocity was given by Eq. (1)

$$\Delta U = \frac{U_0^2}{2\pi \nu l} \cdot \frac{\Delta\alpha}{57.3} \qquad \ldots (1)$$

where U_0 is the initial velocity of sound in solvent, l is the interferometer path length, ν is the frequency and $\Delta\alpha$ is the phase shift in degrees.

The change in velocity at any desired concentration was found by summing the sound velocity changes measured after successive additions of small quantities of solute (see Eq. 2)

$$(\Delta U)_c = \sum_{c=0}^{c=c} \Delta U_i \qquad \ldots (2)$$

Solutions of salts of different concentrations were prepared *in situ* in a separate stainless vessel having sound transparent windows placed in (I). Salt solutions were added using a weighing pipette. Concentrations were calculated by knowing the initial mass of water taken and the mass of the added salt solution of known molality.

The temperature in the interferometer path was maintained at the desired temperature for 2 hr with an accuracy of ± 0.001°C by circulating thermostated liquid from a MK-70 cryostat (− 30 to + 30° ± 0.02°C) through copper coils placed in the path(I). A set of 20 to 25 measurements were carried out.

Accuracy in sound velocity measurements was 1, 2 and 3 cm/s for a velocity change of 1, 3 and 8 m s^{-1} respectively. The details of measurements and accuracy obtained have been described earlier[10,12].

The densities were measured using a differential float density balance. With an accuracy of 5 ppm. Details have been described elsewhere[13].

From the sound velocity and density values the apparent molal compressibility (ϕ_k) was calculated using Eq. (3)

$$\phi_k = \frac{1000}{mdd_0}(d_0\beta - d\beta^\circ) + \beta \cdot \frac{M_2}{d} \qquad \ldots (3)$$

where d_0, d and β°, β are the densities and compressibilities of solvent and solution respectively, m is the molality, and M_2 is the molecular weight of the solute. The limiting apparent molal compressibility (ϕ_k^0) was obtained by extrapolating (using a least squares fit making use of a DCM 1120 microcomputer) ($\phi_k - S_k\sqrt{m}$) versus m plot to zero concentration using the well

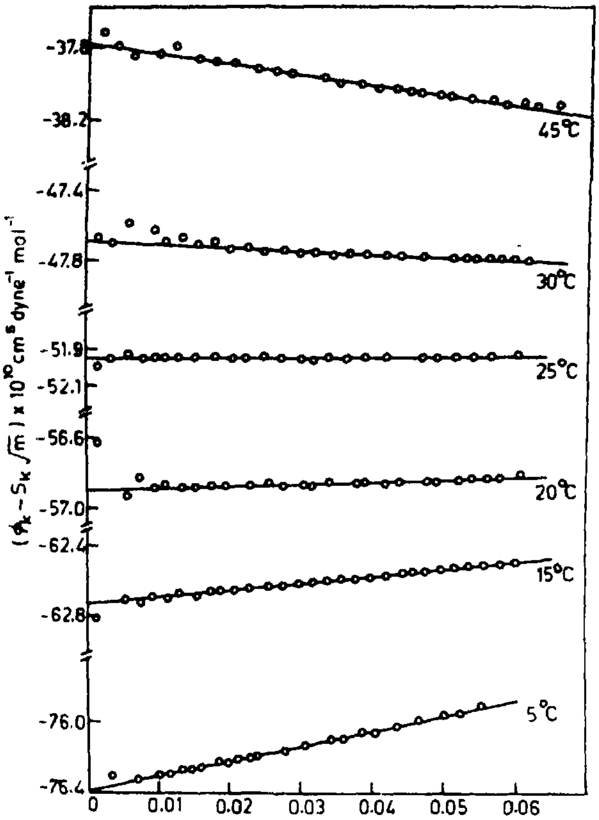

Fig. 2—Plot of $(\phi_k^0 - S_k\sqrt{m}) \times 10^{10}$ (cm^5 dyne^{-1} mole^{-1}) versus molality (m) for sodium acetate at 5°, 15°, 20°, 25°, 30° and 45°C

known equation (Eq. 4), which takes into account the deviations from the Debye-Hückel theory.

$$\phi_k = \phi_k^0 + S_k\sqrt{m} + b_k m \qquad \ldots (4)$$

In Eq (4) S_k is the isothermal constant since adiabatic constant S_{ks} has not been calculated but it is expected to be close to the isothermal constant.

From the extrapolated ϕ_k^0 values (obtained by least squares fit) of salts, those of the anions were obtained by subtracting the ϕ_k^0 of Na^+ ion. The ϕ_k^0 values of Na^+ ion at 15°, 30° and 45°C were taken from the work of Millero *et al.*[15] Values at intermediate temperatures were obtained by interpolations.

Results and Discussion

Errors in the measurement of correct limiting parameters

Figure 2 shows plots of $(\phi_k - S_k\sqrt{m})$ versus m at different temperatures for sodium acetate. Similar plots were obtained for other salts. Slope (b_k) of the plots at different temperatures are given in Table 1 for all the salts studied presently. In Table 2 are given the corresponding deviation constants (b_v) for apparent volumes obtained[13] from the plots of $(\phi_v - S_v\sqrt{m})$ versus m for all the salts at the same temperatures. These plots and the values of b_k and b_v clearly show that merely plotting ϕ_k (or ϕ_v) against $\sqrt{c}$ (or $\sqrt{m}$) and extrapolating to zero concentration do not give correct limiting parameters at different temperatures even from measurements at low concentrations, and much less from those at higher concentrations. This is a point which was generally overlooked by many workers in this field.

The ϕ_k^0 of the anions are given in Table 3 and are plotted graphically in Fig. 3.

Table 1—Deviation Constants (b_k) for Apparent Molal Compressibility of Sodium Salts of Fatty Acids

Sodium salt	$b_k \times 10^{10}$ (kg cm^5 dyne^{-1} mol^{-2})					
	5°	15°	20°	25°	35°	45°C
Formate	5.0	2.0	0	−1.2	−3.0	−6.3
Acetate	8.6	2.0	1.3	0.1	−1.9	−5.8
Propionate	14.8	7.6	3.3	1.0	−1.3	−4.8
Butyrate	11.7	7.2	3.2	1.1	−0.16	−6.7
Valerate	18.7	5.8	2.0	0.0	−2.2	−1.7(?)
Caproate	17.2	7.4	3.7	0.8	−1.7	−6.0

Table 2—Deviation Constants (b_v) for Apparent Molal Volumes of Sodium Salts of Fatty Acids

Sodium salt	b_v (kg cm^3 mol^{-2})					
	5°	15°	20°	25°	30°	45°C
Formate	0.7	0.2	0	0	−0.3	−1.2
Acetate	0.7	0.3	0.1	0	−0.2	−0.7
Propionate	1.2	0.5	0.1	0	−0.4	−1.2
Butyrate	0.6	0.1	0	−0.2	−0.4	−0.9
Valerate	−0.1	−0.34	−0.6	−0.5	−0.7	−0.9
Caproate	−0.4	−0.4	−0.5	−0.6	−0.75	−0.91

Table 3—Limiting Apparent Molal Compressibilities (ϕ_k^0) of Sodium and Fatty Acid Anions

Ion	$-\phi_{k(\text{ion})}^0 \times 10^{10}$ (cm^5 dyne^{-1} mol^{-1})					
	5°	15°	20°	25°	30°	45°C
Sodium*	45.4	36.5	32.8	30.0	27.7	25.6
Formate	14.3	15.3	15.0	14.7	14.8	11.4
Acetate	33.0	26.2	24.1	22.0	20.0	12.2
Propionate	53.9	35.1	31.3	28.6	26.4	18.8
Butyrate	56.3	37.5	33.0	29.0	25.5	12.8
Valerate	60.2	35.5	32.5	28.3	24.9	11.9
Caproate	62.7	34.6	30.3	26.3	23.5	11.6

*Taken from Millero *et al.*[15]

Limiting apparent molal compressibilities (ϕ_k^0) and their temperature dependence

The ϕ_k^0 for fatty acid anions are all negative and become more negative with increase in chain length of

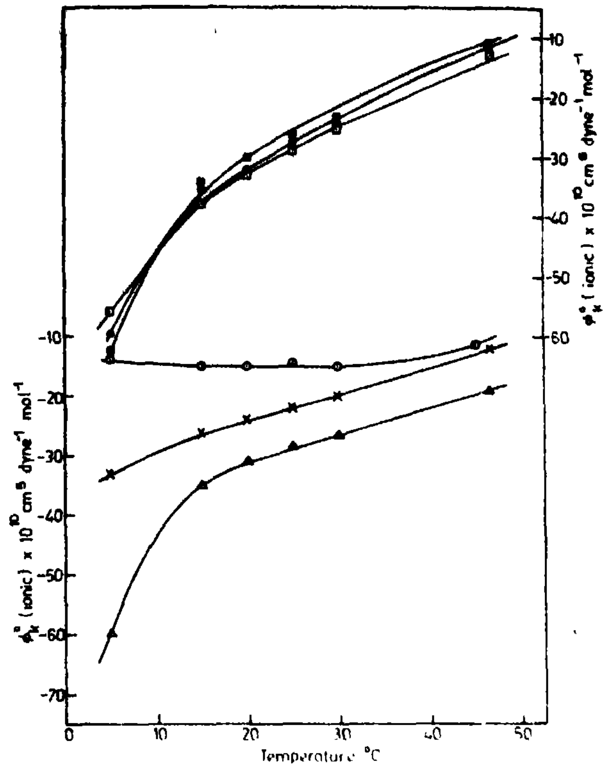

Fig. 3—Plots of limiting apparent ionic compressibility ($\phi_k^0 \times 10^{10}$, cm^5 $dyne^{-1}$ mol^{-1}) against temperature for different fatty acid anions

○ – ○ Formate, × – × Acetate and Δ – Δ Propionate (left hand scale); □ – □ Butyrate, ● – ● Valerate and ■ – ■ Caproate (right hand scale)

the salt. Negative ϕ_k^0 of ions in aqueous solutions are interpreted[16] in terms of loss of compressibility of water due to strong electrostrictive forces in the vicinity of ions, causing electrostrictive hydration of ions. The fatty acid anions carry a negative charge centre and also possess a hydrophobic tail. As has been rightly observed by Bhowmik and Mohanty[9], negative ϕ_k^0 for these ions manifests both electrostrictive and hydrophobic hydration effects. However, due to intrinsic limitations of their data (see above), it was not possible to visualize the nature and extent of these two hydration effects separately.

The results of ϕ_k^0 in this work obtained by adopting the extrapolation procedure making due allowance for the deviations from the Debey-Hückel theory are decidely more reliable, and also more informative on account of the measurements at lower temperatures. The flattening off of ϕ_k^0 values after butyrate ion appears to indicate some sort of saturation effect similar to that observed by Krishnan and Friedmann[18] in structure-making tendency of alcohols and alkylammonium cations.

A comparison of ϕ_k^0 value of formate ion with that of a negative monovalent ion of similar size namely Cl^- ion is revealing (the fact that negative charge in the formate anion is slightly more diffuse does not vitiate the comparison). ϕ_k^0 values for Cl^- ion in water at 15°, 30° and 45° are -19.1, -14.5 and -13.4×10^{-10} cm^5 $dyne^{-1}$ mol^{-1} respectively[15], which are similar to those of formate ion both in magnitude and temperature dependence. This fact suggests a similarity in their mode of interaction with water, which is predominantly electrostrictive. The near constancy of $\phi_k^0(T)$ values further shows that this electrostriction is relatively insensitive to rise in temperature. It is thus reasonable to assume that formate ion also interacts with water in electrostrictive way. We assume next the validity of the Frank and Wen model[19] for the interaction of ions with water resulting in three regions of water, namely A (highly electrostricted), B (partially disordered) and C (normal bulk water). The near constancy of ϕ_k^0 for formate ion means that the A-region is firmly held even at elevated temperatures and structural changes in B- and C-regions undergo such changes with rising temperature which nearly compensate each other, leaving ϕ_k^0 relatively unaffected.

The temperature variation of ϕ_k^0 for all the other fatty acid anions studied in this work (Fig. 3, Table 3) and more importantly the difference in the behaviour of consecutive members is quite interesting. At 5°C the change in ϕ_k^0 ($\Delta\phi_k^0$) in going from formate to acetate is large (18.7 units) and negative. It becomes larger and more negative in going from acetate to propionate ($\Delta\phi_k^0 = -21$ units). This decreasing trend in ϕ_k^0 does not continue after propionate ion, and the next member, i.e. the butyrate ion, has ϕ_k^0 more negative by only 3 units than propionate ion. Subsequent members, i.e. the valerate and caproate ions have ϕ_k^0 values only marginally more negative than the previous members (Table 3). The above features can be explained on the basis that the additional CH_2 group in acetate as compared to formate ion protrudes beyond the electrostricted A-zone into the disordered B-zone (Frank and Wen model) and imparts protection to the disordered water molecules due to hydrophobic hydration. This leads to more negative ϕ_k^0. This view is consistent with the large negative value of entropy of ionization ($\Delta S = -22.1$ eu mol^{-1})[20] for acetate ion, which together with viscosity and conductance[21] properties shows its structure-strengthening ability. Similar arguments can be put forth in the case of propionate ion, where the additional CH_2 group in comparison to acetate continues to be in the disordered B-zone bringing about further structural ordering in the solvent water. The $\Delta\phi_k^0$ values become much smaller after propionate (~ 2-4 units) at all temperatures. This shows that the additional $-CH_2-$ groups beyond propionate now protrude into the C-zone (Frank and

Wen) model of normal bulk water, which is more structured than the disordered B-zone. Hence, the CH_2 groups have diminished chance of hydrophobic interaction with disordered solvent molecules resulting in smaller variation in ϕ_k^0. This is consistent with lower solubilities of higher fatty acids in water. The ϕ_k^0 value at low temperature thus appears to be governed by the structural or disordered effects. The above analysis further leads to the estimation of thickness of the Frank and Wen B-region for fatty acid anions as roughly equivalent to two C – C bond lengths or about 3Å. This is a very important outcome of the present study of ϕ_k^0 of fatty acid anions.

The large variation in ϕ_k^0 with temperature for all ions ($d\phi_k^0/dT$ + ve) other than the formate ion ($d\phi_k^0/dT \approx 0$) bears further scrutiny of the mode of interaction proposed above. It can be seen that the ϕ_k^0 values for other members become less negative with increase in temperature—gradually for acetate ion and more rapidly for higher members—showing that the structural stabilisation imparted to water by the hydrophobic chain is temperature labile. It can further be observed that at sufficiently high temperature (45°C) the ϕ_k^0 values for all the anions tend towards a common limit, (-12×10^{-10} cm^5 dyne^{-1} mol^{-1}) which is not very different from that for formate ion (-11.4×10^{-10}). This important observation strongly suggests that at sufficiently high temperatures all acid anions interact with water predominantly through $-COO^-$ group, i.e. electrostrictively; and that the hydrophobic chain ceases to interact with water. This might be taken to mean that solutes tend to cluster together at higher tempeatures offering only the $-COO^-$ end for interaction with water. The $\phi_k^0(T)$ results for the fatty acid anions presented here thus clearly demonstrate the operation of structural hydration effects at low temperature and electrostrictive hydration at higher temperatures.

Hydration numbers

No attempt is made in this work to calculate the hydration numbers of the acid anions using Eq. (5):

$$n_H = -\frac{\phi_k^0}{\beta^0 V^0} \quad \ldots (5)$$

as is generally done by many authors, and also by Bhoumik and Mohanty[9]. Equation (5) yields physically meaningful hydration numbers only in those cases where the electrostrictive pressure exerted by the ions on the surrounding water molecules is sufficiently high ($\approx 10^7$ e.s.u.) to render the solvent molecules incompressible. In fact this has been the underlying assumption in arriving at Eq (5)[17]. However, as shown by Desnoyers *et al.*[22], this condition is obtained strictly only for ions like Li^+, Mg^{++} etc. having small diameters and hence high charge densities. The method is inapplicable in the case of ions like Cl^-, $HCOO^-$ where the electrostatic pressure would be of the order of $\sim 5 \times 10^5$ e.s.u. so that the compressibility of the hydrated water cannot be assumed to be zero.

Viewed in the light of the above, the hydration behaviour of fatty acid anions—partly electrostrictive and partly hydrophobic—is far from fulfilling the presumption of Eq(5). Even formate ion with a radius of about 1.35 Å fails to satisfy this equation. The hydrocarbon chain of fatty acid anion interacts with water molecules through Van der Waals forces giving rise to 'soft hydration' (hydrophobic hydration), which is qualitatively different from the hard electrostrictive hydration. It is thus not very correct to extend Eq. (5) to ions studied in this work. Values of n_H derived by earlier workers[9] are thus not correct and hence do not reflect the correct physical picture of ion-solvent interaction. The proper procedure to arrive at n_H would be to first substract the electrostrictive part of ϕ_k^0 (-12 units, see above) from the measured values to obtain ϕ_k^0 due to hydrophobic interaction followed by use of two different and well-founded equations to calculate (n_H)-electrostriction and (n_H)-hydrophobic, separately from the above division of ϕ_k^0. Such equations do not exist. Further theoretical work in this direction is very much called for.

Also no attempt has been made in this work to calculate incremental $\Delta\phi_k^0$ per CH_2 group, for the simple reason that the present results show that this is not constant but varies according to whether it is close to the COO^- group or farther away from it.

Deviation constants b_v and b_k

The b_v-values decrease with increase in the size of anions. Also db_v/dT is negative. These features are exhibited by other electrolytes (e.g. NaCl) and the size effect is similar to that shown by tetraalkylammonium ions[21]. However, the db_v/dT for tetra-salts (Bu_4NBr) shows positive values.

Positive deviations of b_v at lower temperatures can be interpreted in terms of ion-pair formation[23], reflecting the structural compatibility of hydration cospheres of cation and anions. The negative b_v-values for valerate and caproate at 5°C can be understood as the combined effect of ion-pair formation (+ve b_v) and overlap of hydration cospheres of the chain leading to $-$ve b_v-values. As discussed by Desnoyers *et al.*[24] such overlap of cospheres in the case of species with long hydrocarbon chain takes place to offset the thermodynamically unfavourable hydrophobic hydration of such species. The observed small b_v-values are a net result of these two opposing effects. At higher temperatures thermal agitation renders the weak ion-pair formation less probable and gives way to anion-anion interaction leading to increased overlap of cospheres, and consequent release of bulky ice-like hydration water into bulk as normal water having smaller volume. This explains the uniformly negative b_v-values for all members at 45°C and their near constancy points to the tendency of anions to cluster together in such a way that they interact with water only through COO^- groups.

The b_k-values (Table 1) can also be interpreted in a similar way as above. Positive b_k-values are to be understood as release of water from the incompressible electrostricted sheaths around the ions into the more compressible bulk water due to ion-pair formation. Rapid increase of b_k in the series at 5°C from a value of 5 units for formate to 18.7 units for valerate should then mean additional release of the less compressible hydrophobically hydrated water into the bulk on account of increased overlap of cosphere due to anion-anion interaction. Since the hydrophobic hydration melts off with increase in temperature this leads to a gradual decrease in b_k with increase in temperature for all the members. At 45°C all members tend to have the same (− ve) value of b_k indicating cluster formation due to anion-anion interactions, thereby achieving an economy of the number of structured water molecules per molecule of the dissolved solute. Since individual ionic contributions to b_k are not yet available, it is not possible to evaluate and interprete ionic b_k individually.

It can be concluded that the precise measurements of ϕ_k^0 of fatty acid anions over an extended temperature range including low temperatures enable a clear distinction between electrostrictive and hydrophobic interaction of water and the charge centre and hydrocarbon tail respectively. The trends in ϕ_k^0 have ben used to arrive at the thickness of the Frank and Wen B-region, which is about 3 Å wide. Convergence of ϕ_k^0 values for all members to approximately the same negative value at high temperature suggests exclusive interaction between charge centre and water only implying that the hydrocarbon chains tend to form clusters. The deviation constants b_v and b_k show trends which indicate ion-pair formation, at low temperature going over into anion-anion interaction at elevated temperature corroborating results of ϕ_k^0.

Acknowledgement

One of us (K S M R) is thankful to the UGC, New Delhi for the award of a junior research fellowship.

References

1 Watson G M & Felsing W A, *J Am Chem Soc*, **63** (1941) 410.
2 Sakurai M, *Bull Chem Soc* (*Japan*), **46** (1973) 1596.
3 Snell H & Greyson H, *J Phys Chem*, **74** (1970) 2148.
4 Lindenbaum S, *J Phys Chem*, **74** (1970) 3027.
5 Ahluwalia J C & Chawla B, *J Soln Chem*, **6** (1975) 383.
6 Diamond R M, *J Phys Chem*, **45** (1966) 2513.
7 Worley J D & Klotz I M, *J Phys Chem*, **45** (1966) 2868.
8 Kaulgud M V & Rao K S M, *Indian J Chem*, **13** (1975) 616.
9 Bhowmik S & Mohanty R K, *Indian J Chem*, **25A** (1986) 416.
10 Kaulgud M V, *Acustica*, **15** (1965) 377.
11 Kaulgud M V, *Z Phys Chem* (Neue Folge), **47** (1963) 24.
12 Kaulgud M V, Rao K S M & Pandya G H, *Indian J Pure Appl Phys*, **15** (1978) 459.
13 Kaulgud M V, Rao K S M & Dole H G, *Indian J Chem*, **16A** (1978) 955.
14 Rao K S M, Ph D Thesis, Nagpur University 1978.
15 Millero F J, Ward G K, Lipple L K & Hoff E V, *J Phys Chem*, **78** (1974) 1636.
16 Corey V B, *Phys Rev*, **64** (1943) 350
17 Passynski A, *Acta Physicochim*, **8** (1938) 385.
18 Krishnan C V & Friedman H L, *J Phys Chem*, **73** (1979) 1572.
19 Frank H S & Wen W Y, *Discu Faraday Soc*, **24** (1957) 133.
20 Coetzee J F, *Solute-solvent interactions* (Marcel-Dekker, New York) 1969.
21 Gurney R W, *Ionic process in solutions* (McGraw Hill, New York) 1953.
22 Desnoyers J E, Verrall R E & Conway B E, *J Chem Phys*, **43** (1965) 243.
23 Millero F J, *Chem Rev*, **71** (1971) 147.
24 Desnoyers J E, Perron M, Arel G & Jolicoeur C, *J Phys Chem*, **73** (1969) 3346

Indian Journal of Chemistry
Vol. 27A, January, 1988, pp. 18-22

Permeation Studies on Binary Liquid Mixtures of Acetone with Benzene & Chloroform

KEHAR SINGH* & M M PANDEY†
Department of Chemistry, Gorakhpur University, Gorakhpur 273 009

Received 25 *November* 1986; *revised and accepted* 23 *April* 1987

An experimental investigation on the electrokinetic transport of the binary mixtures of benzene-acetone and acetone-chloroform through a pyrex membrane is described. The linear phenomenological equations between the thermodynamic fluxes and forces hold good in both the cases. Dependence of the phenomenological coefficients on composition of the mixtures has been investigated. Onsager reciprocity relationship has also been tested. The experimental results indicate that permation is non-ideal in character. Characterization of membrane-permeant interface in terms of zeta-potential has also been carried out.

Membrane permeation under the action of gradients of pressure and/or electric potnetial difference is studied with the twin object of dimensional and electrochemical characterization of membranes[1-4], and examination of applicability of the transport equations deduced on the basis of non-equilibrium thermodynamic principles[5-10]. To obviate complications arising on account of membrane and electrode polarization, non-aqueous permeants are preferably used in such studies. In very few investigations mixtures have been used[11-13]. In this paper we report studies on hydrodynamic and electro-osmotic permeation of the binary mixtures of benzene and acetone, and acetone and chloroform through a pyrex membrane to investigate the dependence of transport coefficients on composition and nature of the permeating mixtures. Streaming potential and membrane conductance measurements have also been carried out. The results have been analysed to investigate alteration in the electrical character of the membrane-permeant interface with change in permeant composition. An attempt has also been made to express non-ideality in permeation in terms of excess phenomenological coefficients.

Materials and Methods

Benzene, acetone, and chloroform were BDH, (India) reagents and were used without further purification. Pyrex sinter of porosity grade G-4 obtained from M/s Corning, India, was used as the membrane.

An experimental cell similar to that described earlier[14] was used for the measurement of electro-osmotic and hydrodynamic permeabilities. The membrane was cleaned by boiling it with 50% conc. nitric acid (AR). It was washed with distilled water and dried at 120° for ~ 3 hr. The membrane was then equilibrated with the experimental liquid. The cell was filled with fresh permeant to ensure that concentration of the experimental solution remained the same as that compounded before equilibration. An electronically operated power supply (Toshniwal, India) was used to apply potential gradients. The platinum electrodes were cleaned with nitric acid and washed before use and kept in direct contact with the membrane. The volumetric flux was measured by following the rate of movement of the permeant in a horizontal fixed capillary tube having cross-sectional area equal to 1.0×10^{-2} cm^2. The electroosmotic flow in all instances was found to be from positive to negative electrode.

Hydrodynamic permeability was measured with the same cell. A known hydrodynamic pressure was applied across the membrane and volumetric flux was measured as already described. The electrodes were kept short-circuited throughout the hydrodynamic permeability measurements.

Streaming potnetials at different pressures were recorded using a digital multimeter, HIL 2142.

Results and Discussion

According to the theory of non-equilibrium thermodynamics, the volumetric flux, J_v, and the flow of electric current, I, under the simultaneous action of pressure difference, ΔP, and electrical potential difference, $\Delta \phi$, across the membrane may be expressed as[15,16],

$$J_v = \frac{L_{11}}{T} \Delta P + \frac{L_{12}}{T} \Delta \phi \qquad \ldots (1)$$

---

†Present address: Department of Chemistry, M.D.P.G. College, Pratapgarh.

Table 1—Phenomenological Coefficients L_{11}/T and L_{12}/T for Benzene-Acetone and Acetone-Chloroform/Pyrex Systems (T = 30 ± 0.5°C)

Benzene-acetone			Acetone-chloroform		
$x_{benzene}$	$(L_{11}/T)\times 10^{12}$ $(m^5s^{-1}N^{-1})$	$(L_{12}/T)\times 10^{11}$ $(m^3s^{-1}V^{-1})$	$x_{chloroform}$	$(L_{11}/T)\times 10^{12}$ $(m^5s^{-1}N^{-1})$	$(L_{12}/T)\times 10^{11}$ $(m^3s^{-1}V^{-1})$
0.00	9.44	20.08	0.00	9.00	20.57
0.20	6.87	8.48	0.17	8.43	10.60
0.40	5.27	3.59	0.40	7.19	5.38
0.60	3.91	1.00	0.60	6.16	1.94
0.73	3.49	0.37	0.80	5.83	0.53
1.00	4.14	—	1.00	5.00	0.25

Table 2—Examination of Validity of Onsager's Reciprocity Relationship for Acetone-chloroform/Pyrex System (T = 30 ± 0.5 °C)

Mol fr. of chloroform	$(\Delta\phi/\Delta P)\times 10^4$ $I=0$ $(N^{-1}m^2V)$	$(L_{22}/T)\times 10^6$ (Ohm^{-1})	$(L_{21}/T)\times 10^{11}$ $(m^3s^{-1}V^{-1})$	$(L_{12}/T)\times 10^{11}$ $(m^3s^{-1}V^{-1})$
0.00	1.02	2.00	20.4	20.57
0.17	1.33	0.74	9.8	10.6
0.40	1.74	0.31	5.4	5.38
0.60	1.40	0.15	2.10	1.94
0.80	0.71	0.07	0.50	0.58
1.00	0.08	—	—	—

$$I = \frac{L_{21}}{T}\Delta P + \frac{L_{22}}{T}\Delta\phi \qquad \ldots (2)$$

L_{ij} (i, j = 1, 2) are the phenomenological coefficients. From Eq. (1) it easily follows that,

$$(J_v)_{\Delta\phi=0} = \frac{L_{11}}{T}\Delta P \qquad \ldots (3)$$

and

$$(J_v)_{\Delta P=0} = \frac{L_{12}}{T}\Delta\phi \qquad \ldots (4)$$

According to Eqs (3) and (4), $(J_v)_{\Delta\phi=0}$ and $(J_v)_{\Delta P=0}$ are linearly related to ΔP and $\Delta\phi$ respectively. The experimental results show that Eqs (3) and (4) are valid for the benzene-acetone and the acetone-chloroform systems within the domain of investigation. The values of L_{11}/T and L_{12}/T obtained from the plots of $(J_v)_{\Delta\phi=0}$ versus ΔP and $(J_v)_{\Delta P=0}$ versus $\Delta\phi$ are recorded in Table 1.

The streaming potential, $(\Delta\phi)_{I=0}$, according to eq. (2), is given by,

$$(\Delta\phi)_{I=0} = -\frac{L_{21}}{L_{22}}\Delta P \qquad \ldots (5)$$

and

$$\left(\frac{I}{\Delta\phi}\right)_{\Delta P=0} = \frac{L_{22}}{T} \qquad \ldots (6)$$

So that the membrane conductance, K_m may be expressed as

$$(I/\Delta\phi)_{\Delta P=0} = \frac{L_{22}}{T} = K_m \qquad \ldots (7)$$

According to Onsager's reciprocity relationship[15,16],

$$\frac{L_{12}}{T} = \frac{L_{21}}{T} \qquad \ldots (8)$$

The validity of Eq. (5) has been tested and it is found that $(\Delta\phi)_{I=0}$ varies linearly with the applied pressure difference on the two sides of the membrane. The values of (L_{22}/T) and $(\Delta\phi/\Delta P)_{I=0}$ have been recorded in Table 2. Using Eqs (5) and (7), we have calculated values of L_{21}/T for chloroform-acetone system to test the validity of Eq. (8). The values of L_{12}/T and L_{21}/T recorded in Table 2 are in reasonable agreement. It may be noted that uncertainty in the values of the cross phenomenological coefficients does not exceed ± 5%.

Following the treatment of Overbeek[17], it can be shown that in the case of flow through membrane

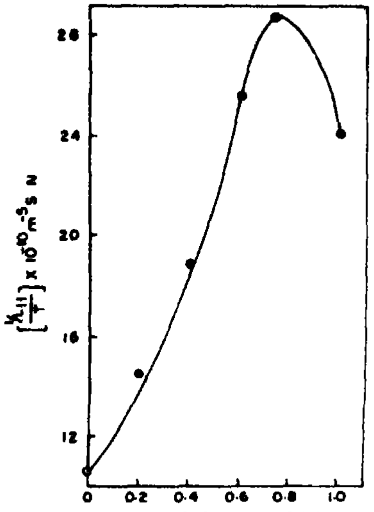

Fig. 1—Test of the validity of Eq. (13) for acetone-benzene/pyrex system.

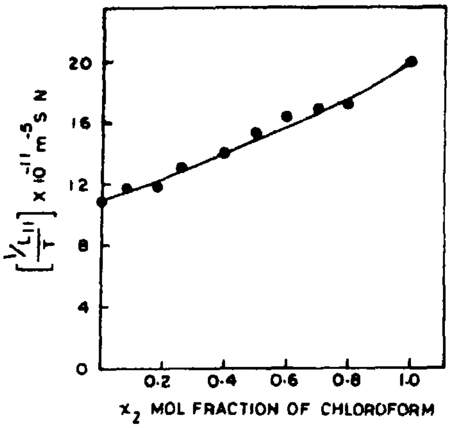

Fig. 2—Test of the validity of Eq. (13) for acetone-chloroform/pyrex system

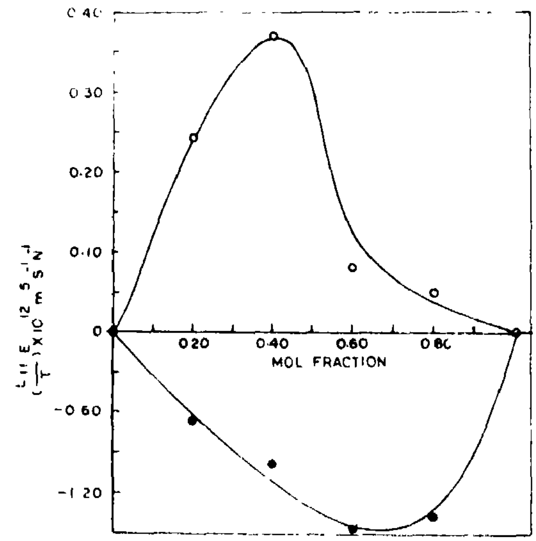

Fig. 3—Dependence of $(L_{11}/T)^E$ on composition [–○–, mole fraction of benzene in acetone-benzene mixture; –●–, mole fraction of chloroform in acetone-chloroform mixture]

consisting of n capillaries of equivalent pore radius, r, we have,

$$\frac{L_{11}}{T} = \frac{n\pi r^4}{8\eta l} \qquad \dots (9)$$

and

$$\frac{L_{12}}{T} = \frac{n\varepsilon r^2 \zeta}{4\eta l} \qquad \dots (10)$$

wherein η is viscosity coefficient, ε, is the dielectric constant of the permeant and l is the thickness of the membrane. ζ denotes electrokinetic potential at the membrane-permeant interfacial region.

$$\frac{L_{11}}{T} = \frac{n\pi r^4}{8\eta_i^m l} \qquad \dots (11)$$

η_i^m, the coefficient of viscosity for the ideal mixture may be expressed as[18],

$$\eta_i^m = x_1\eta_1 + x_2\eta_2 \qquad \dots (12)$$

where x_1 and x_2 are mole fractions of components 1 and 2 respectively. Using Eqs (11) and (12), it is possible to write,

$$\left(\frac{L_{11}}{T}\right)_i^m = \frac{(L_{11}/T)_1\,(L_{11}/T)_2}{(L_{11}/T)_2 + x_2[(L_{11}/T)_1 - (L_{11}/T)_2]} \qquad \dots (13)$$

The difference between the observed and ideal phenomenological coefficients, called excess phenomenological coefficients, may be expressed as[14,19],

$$\left(\frac{L_{11}}{T}\right)^E = \left(\frac{L_{11}}{T}\right) - \left(\frac{L_{11}}{T}\right)_i^m \qquad \dots (14)$$

For ideal permeation $(L_{11}/T)^E = 0$ and the total permeation is such that permeation of one component is not influenced by that of the other. Non-ideality in permeation arises on account of interaction amongst the components of the mixture and their interactions with the membrane matrix. If hydrodynamic permeation were ideal, Eq. (13) should hold good. Validity of this equation for acetone-benzene and acetone-chloroform mixtures were examined by plotting $1/(L_{11}/T)$ against x_2. The experimental results (Figs 1 and 2) are not consistent with Eq. (13). The permeation is thus non-ideal in both the cases.

For quantitative description of non-ideality in hydrodynamic permeation, excess phenomenological coefficients defined by Eq. (14) were estimated.

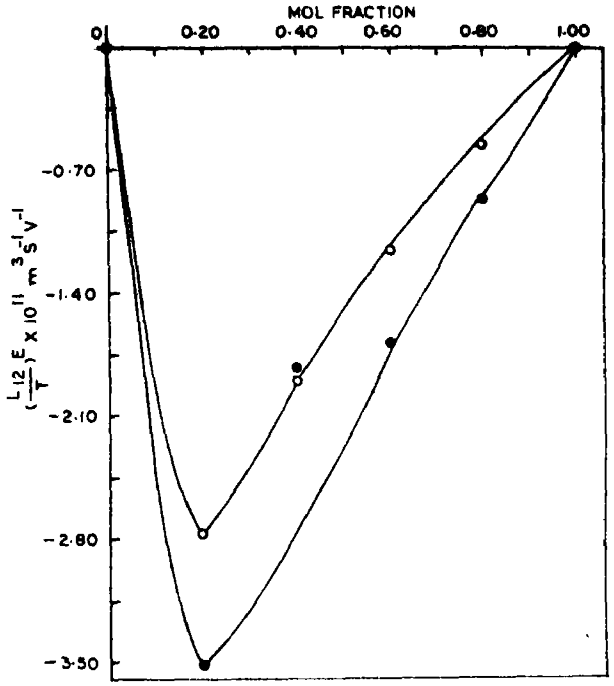

Fig. 4—Dependence of $(L_{12}/T)^E$ on composition [–○–, mole fraction of benzene in acetone-benzene mixture; –●–, mole fraction of chloroform in acetone-chloroform mixture]

Their dependence on composition is depicted in Fig. 3. In the case of acetone-benzene mixture, benzene acts as a Π-electron donor and may form a complex[20]. In case of acetone-chloroform system the non-ideal permeation may also be attributed to the formation of a complex[21,22] between acetone and chloroform.

The permeation behaviour of mixtures through a membrane under the action of electrical potential gradient can also be analysed by studying electro-osmotically driven flux which is attributed to the existence of an electrical double layer. Using Eq. (10), we may write

$$\left(\frac{L_{12}}{T}\Big/\zeta\right) = \frac{(A/l)\varepsilon}{4\pi\eta} \qquad \ldots (15)$$

where $(A/l) = \frac{n\pi r^2}{l}$

For ideal mixtrue, ε_i^m, the dielectric constant may be expressed as[23],

$$\varepsilon_i^m = x_1\varepsilon_1 + x_2\varepsilon_2 \qquad \ldots (16)$$

From Eqs (15) and (16), for ideal permeation, one may write,

$$\left(\frac{L_{12}}{T}\right)_i^m = [x_1(L_{12}/\zeta T)_1\eta_1 + x_2(L_{12}/T\zeta)_2]\frac{\zeta_i^m}{\eta_i^m} \qquad \ldots (17)$$

Table 3—Zeta-Potential for Different Compositions of Acetone-Benzene, and Acetone-Chloroform/Pyrex Systems (T = 30 ± 0.5°C)

Acetone-benzene system		Acetone-chloroform system	
Mol. fr. of benzene	ζ (mV)	Mol fr. of chloroform	ζ (mV)
0.00	50.5	0.00	55.5
0.20	24.2	0.20	34.8
0.40	14.1	0.40	25.3
0.60	4.7	0.60	12.3
0.73	5.3	0.80	5.5
1.00	—	1.00	4.8

Eq. (17) can be used to compute $(L_{12}/T)_i^m$ values and the excess electroosmotic phenomenological coefficient, $(L_{12}/T)^E$, defined as[14,19],

$$\left(\frac{L_{12}}{T}\right)^E = \left(\frac{L_{12}}{T}\right) - \left(\frac{L_{12}}{T}\right)_i^m \qquad \ldots (18)$$

If one of the permeants is such that it shows no electroosmotic permeability, e.g., benzene, Eq. (17) reduces to,

$$(L_{12}/T)_i^m = x_1(L_{12}/T\zeta)_1\frac{\eta_1\zeta_i^m}{\eta_i^m} \qquad \ldots (19)$$

since $(L_{12}/T)_2 = 0$.

Values of $(L_{12}/T)_i^m$ for acetone-chloroform and acetone-benzene mixtures computed using Eqs (17) and (19) respectively have been used to estimate $(L_{12}/T)^E$ values given in Fig. 4. It is seen that is both the cases electro-osmotic permeation is non-ideal.

Using Eq. (9) and definition of (A/l), the cell constant, average pore radius of the membrane may be expressed as,

$$r = \left[\frac{8\eta(L_{11}/T)}{(A/l)}\right]^{1/2} \qquad \ldots (20)$$

where (A/l) is given by[26],

$$\left(\frac{A}{l}\right) = \frac{K_m}{k} \qquad \ldots (21)$$

K_m is conductance of the membrane equilibrated with permeant of specific conductance k. The average pore radius of the membrane has been found to be of the order of 10^{-4} cm.

For the characterization of membrane-permeant interface in terms of zeta-potential, Eqs (10) and (21) may be used to obtain[18],

$$\zeta = \frac{4\pi\eta k}{K_m}\left(\frac{J_v}{\Delta\phi}\right)_{\Delta P=0} \times 9 \times 10^4 \text{ Volt}$$

Table 4—Coefficient of Viscostity, Dielectric Constant, Specific Conductance and Membrane Conductance ($T = 30 \pm 0.5$°C; x_2 = Mole fraction of the second component in the mixture)

x_2	Viscosity coefficient × 10^4 N m^{-2} S		Dielectric constant		Specific conductance K × 10^3 ohm^{-1} m^{-1} (experimental)	Membrane conductance K_m × 10^5 ohm^{-1} (experimental)
	η	η_s^m (eq 12)	ε	ε_s^m (eq. 16)		
			Acetone-benzene system			
0.00	2.95	2.95	19.3	19.3	0.320	0.220
0.20	3.02	3.67	14.1	15.9	0.112	0.095
0.40	3.22	4.43	10.4	12.5	0.056	0.050
0.60	3.34	5.16	6.4	9.1	0.004	0.005
0.73	3.42	5.64	4.3	6.8	0.0008	0.0005
1.00	6.64	6.64	2.2	2.2	—	—
			Acetone-chloroform system			
0.00	3.32	3.32	20.9	20.9	0.30	0.20
0.20	3.92	3.74	17.3	17.7	0.088	0.047
0.40	4.40	4.16	15.4	14.5	0.045	0.031
0.60	4.83	4.57	12.6	11.2	0.022	0.015
0.80	5.29	4.99	9.1	7.1	—	—
1.00	5.41	5.41	4.8	4.8	0.001	—

Values for the acetone-benzene system are from ref. 24, while those for the acetone-chloroform system are from ref. 25; η values for acetone-benzene system are experimental, and those for the acetone-chloroform system are from ref. 25.

The zeta-potentials for different compositions of acetone-benzene and acetone-chloroform mixtures have been recorded in Table 3. The values of coefficient of viscosity, η, dielectric constant, ε, specific conductance of the permeant, k, and the membrane conductance, K_m, used for the purpose of calculation are given in Table 4. It is noticed that zeta-potential always decreases by the addition of the other solvent and passes through a minimum in all cases at some concentration. η_s^m and ε_s^m values estimated using Eqs (12) and (16) respectively are also included in Table 4. Their comparison with η and ε values clearly shows that both the systems exhibit non-ideality. This supports the conclusion earlier derived on the basis of permeability measurements.

Acknowledgement

The authors are extremely grateful to the Head of the Chemistry Department, Gorakhpur University for providing research facilities. One of them (M.M.P.) is also grateuful to the UGC, New Delhi, for financial assistance.

References

1 Renkin E M, *J gen Physiol*, **38** (1954) 225.
2 Robinson E & Mamo A, *J gen Physiol*, **43** (1960) 523.
3 Lakshminarayanaiah N, *Biophys J*, **7** (1967) 511
4 Singh K & Raj Kumar, *Indian J Chem*, **17** (1979) 607.
5 Rastogi R P & Jha K M, *J phys Chem*, **70** (1966) 1017.
6 Tombalakian A S, *J phys Chem*, **72** (1968) 1566.
7 Blokhra R L & Kaul C L, *Electrochem Acta*, **11** (1966) 1391.
8 Singh K & Srivastava V N, *J non-equilib Thermodyn*, **6** (1981) 195.
9 Handermann A F, Waters P F & Woo J W, *J phys Chem*, **78** (1974) 65.
10 Srivastava R C & Awasthi P K, *J Hydrology*, **20** (1973) 37.
11 Rastogi R P, Singh K & Singh J, *J phys Chem*, **79** (1975) 2574.
12 Srivastava R C & Abraham M C, *J Colloid Interface Sci*, **57** (1976) 58.
13 Singh K & Srivastava V N, *J non-equilib Thermodyn*, **6** (1981) 181.
14 Singh K, Srivastava V N & Chandra N, *J non-equilib Thermodyn*, **6** (1981) 181.
15 de Groot S R, *Thermodynamics of irreversible processes* (North Holland Publishing Company, Amsterdam) 1952.
16 Katchalsky A & Curran P F, *Non-equilibrium thermodynamics in biophysics* (Harvard University Press, Cambridge Massechuset) 1974.
17 Overbeek J Th G, *Colloid science*, Vol 1, edited by H R Kruyt (Elsevier, Amsterdam, New York) 1952.
18 Fort R L & Moore W R, *Trans Faraday Soc*, **62** (1966) 1112.
19 Singh K, Shahd R, Kumar R & Pandey M M, *Indian J Chem*, **19A** (1980) 1062.
20 Yadava R R & Yadav S S, *Indian J Chem*, **16A** (1978) 826.
21 Hammes G G & Knoche W, *J chem Phys*, **45**, (1966) 4041.
22 Franks F & Ives D J G, *Quart Rev chem Soc*, **20** (1966) 1.
23 Singh R P & Sinha C P, *J Indian chem Soc*, **LV** (1983) 356
24 Washburn E W, *International critical tables*, Vol. VI (McGraw Hill, New York) 1929.
25 Timmermans J, *Physico-chemical constants of binary systems in concentrated solutions*, Vol. I (Interscience Publication, NY) 1959.
26 Singh K & Pandey M M, *J Membrane*, **11(6)** (1986) 363.

Indian Journal of Chemistry
Vol. 27A, January, 1988, pp. 23-26

Kinetics & Mechanism of Oxidation of D-Glucopyranose 1-Phosphate by Chromium(VI) & Vanadium(V) in Perchloric Acid Medium

KALYAN KALI SEN GUPTA*, SHIPRA SEN GUPTA & SUBRATA KUMAR MANDAL
Department of Chemistry, Jadavpur University, Calcutta 700 032
and
SAMARENDRA NATH BASU
Department of Chemistry, Asutosh College, Calcutta 700 026

Received 8 *January* 1987; *revised* 5 *May* 1987; *accepted* 25 *May* 1987

The kinetics of oxidation D-glucopyranose 1-phosphate by Cr(VI) and V(V) have been studied in perchloric acid medium spectrophotometrically in the UV and visible regions respectively. Comparison of the present results with those observed in the oxidation of glucose and glucose 6-phosphate by these metal ion oxidants reveals that the present substrate undergoes oxidation by Cr(VI) or V(V) by mechanisms which are different from those suggested for the oxidation of glucose or glucose 6-phosphate.

The mechanism of oxidation of aldose phosphates[1,2] by Cr(VI) and V(V), studied in our laboratory, is reported to be different from that of the parent aldoses[3,4] in perchloric acid medium. The mechanism of oxidation of glucose 1-phosphate by these oxidants is yet to be understood. The present investigation has been undertaken to correlate the results obtained with those for the oxidation of glucose[3,4] and glucose 6-phosphate[1,2] by these metal ions.

Materials and Methods

Glucose 1-phosphate and glucose 1,6-diphosphate were commercial products. Inorganic reagents were of the highest purity available. Aqueous solutions of the sugar phosphates were always prepared afresh in doubly distilled water. Chromium (VI), vanadium(V) and other reagents were the same as previously described[1,2].

Kinetic measurements

The measurements were carried out spectrophotometrically using a cell of 1 cm path length. Chromium(VI) oxidation was carried out in the presence of excess [substrate] at 355 nm. The pseudo-first order rate constants (k_{obs}) were determined from the plots of log [Cr(VI)] versus time (t). The rates of oxidation of the substrates by V(V) were determined as follows. Equivalent amounts of the substrate and oxidant were used in the runs except in the case of determining the effect of varying [substrate], where [substrate]$\gg$[V(V)]. In the former case the rate of formation of V(IV) was measured at 760 nm[5] and the second order rate constants (k_2) were determined from the plots of $1/A_\infty - A_t$ against t whereas in the latter case the reduction of V(V) was followed at 350 nm and the values of k_{obs} were determined from log [V(V)] versus t plots[6]. In all these experiments, no other reagents except Cr(VI), V(IV) and V(V) absorb in the respective wavelengths.

Product analysis

The aldose phosphate was oxidized under the kinetic conditions and the product was tested by the preparation of 2,4-DNP derivative. The oxidation of glucopyranose 1,6-diphosphate by these metal ion oxidants was too slow to be studied indicating that groups at C-2, C-3 and C-4 were not susceptible to oxidation under the condition of the experiment. Consequently the formation of 2,4-DNP derivative in the oxidation of glucose 1-phosphate indicated that $-CH_2OH$ group was oxidized to $-CHO$. This is in keeping with the fact[7] that when C-1 is blocked, then the oxidation occurs at C-6.

Test for free radicals

These oxidation reactions were studied in the presence of 8% acrylamide (w/v). The oxidation of the substrate by Cr(VI) was carried out at $[Cr(VI)]_0 = 1.66 \times 10^{-4}$ mol dm^{-3}; $[substrate]_0 = 1.0 \times 10^{-3}$ mol dm^{-3} and $[HClO_4]_0 = 2.4$ mol dm^{-3} whereas for that by V(V) reaction the respective reactant concentrations were 2×10^{-2}, 1.0×10^{-2} and 2.4 mol dm^{-3} respectively. Our attempts to identify free radicals were unsuccessful in the Cr(VI) oxidation of the substrate. However, appearance of gel in the initially clear solution in the oxidation of substrate by V(V) indicated that reaction proceeded by a free radical mechanism.

Results and Discussion

Effect of varying reactant concentration

The pseudo-first order rate constants were earlier found to be nearly independent of initial gross [Cr(VI)] in the oxidation of some aldoses[1] unlike the present reaction where k_{obs} slightly decreased with increase in gross [Cr(VI)]. This is to be expected[8] since the present reaction was studied at much wider range of initial gross [Cr(VI)]. Acid chromate ion exists[9,10] in aqueous medium either as CrO_4^{2-} (Eq. 1) or as $Cr_2O_7^{2-}$ (Eq. 2)

$$HCrO_4^- \overset{K_d}{\rightleftharpoons} H^+ + CrO_4^{2-} \qquad \ldots (1)$$

$$2\,HCrO_4^- \overset{K_{d'}}{\rightleftharpoons} Cr_2O_7^{2-} + H_2O \qquad \ldots (2)$$

Since the reaction was carried out at $[HClO_4]_0 = 1.0$ mol dm^{-3} and K_d is of the order of 10^{-7} at 35°, the equilibrium (1) was neglected. The $[HCrO_4^-]$ was then calculated, using equilibrium (2) and the value[11] of $K_{d'} = 78$ at 35°C. The results are recorded in Table 1. The pseudo-first order rate constants were also determined at different [substrate] but at fixed [oxidant], $[HClO_4]$ and temperature. The plot of k_{obs} versus [substrate] indicates that the rate is directly proportional to initial $[\text{substrate}]_0$ for both the reactions and the order in [substrate] is unity. In the case of V(V) oxidation the plot of $1/A_0 - A_t$ versus t is linear indicating the reaction to be of second order. Since the order in [substrate] is unity, so the order in V(V) is also unity.

Effect of varying acid concentration

The rate constant increased with increase in $[H^+]$ varied by the addition of perchloric acid. The plots of log k_{obs} against log $[H^+]_0$ in the oxidation by Cr(VI) and of log k_2 against log $[H^+]_0$ in V(V) oxidation were linear with slopes of 1.9 each.

Effect of varying salt concentration

The rate constants increased with the increase in sodium perchlorate concentration (Table 2) and nearly two-fold and 15-fold increase in rate constant in 1.0 mol dm^{-3} $NaClO_4$ was observed in oxidations by Cr(VI) and V(V), respectively.

Influence of temperature

The reactions were investigated at different temperatures. The plots of log (k_2/T) against $1/T$ are linear. The enthalpies of activation ($\Delta H^\ddagger$) and entropies of activation ($\Delta S^\ddagger$) were calculated[12] (Table 3) and then compared with those found for the oxidations of D-glucose and D-glucose 6-phosphate by these metal ion oxidants. The enthalpies of activation follow the order: glucose 1-phosphate > glucose > glucose 6-phosphate.

Disodium D-glucopyranose 1-phosphate exists as a dinegative ion in aqueous solution; but under acidic conditions (> 1.0 mol dm^{-3}), it undergoes fast diprotonation to yield D-glucopyranose 1-phosphate. This is believed to exist mainly in the β-conformation for accomodating the bulkier phosphate group. Unusually strong ionisation[13] of the first acid hydrogen of D-glucopyranose 1-phosphate ($pK_{a1} = 1.10$; $pK_{a2} = 6.13$) indicates the formation of hydrogen bond between the ring oxygen of the sugar moiety in β-conformation and

Table 1—Effect of Varying [Oxidant] on Cr(VI) Oxidation of Glucose 1-Phosphate

([D-glucose 1-phosphate]$_0$ = 1×10^{-2} mol dm^{-3}, $[HClO_4]_0$ = 1.0 mol dm^{-3}, temp. = 35°C)

$[Cr(VI)]_0 \times 10^4$ (mol dm^{-3})	$[HCrO_4^-]_0 \times 10^4$ (mol dm^{-3})	$k_{obs} \times 10^5$ (s^{-1})	$k_{cor} \times 10^5$ (s^{-1})
0.833	1.625	5.13	2.63
1.666	3.175	4.79	2.52
3.333	6.09	4.51	2.47
5.000	8.79	4.26	2.42
6.667	11.33	4.14	2.43
8.330	13.77	4.10	2.48
9.163	14.93	4.00	2.45

Table 2—Effect of Varying [Salt] on Second Order Rate Constants

(a) $[Cr(VI)]_0 = 1.66 \times 10^{-4}$ mol dm^{-3}; [D-glucose 1-phosphate]$_0$ = 1×10^{-1} mol dm^{-3}; $[HClO_4]_0$ = 2.4 mol dm^{-3}; temp. = 40°C.
(b) $[V(V)]_0 = 4.0 \times 10^{-2}$ mol dm^{-3}; [D-glucose 1-phosphate]$_0$ = 2×10^{-2} mol dm^{-3}; $[HClO_4]_0$ = 2.4 mol dm^{-3}; temp. = 40°C.)

$[NaClO_4]_0^a$ (mol dm^{-3})	$k_2 \times 10^4$ (dm^3 mol^{-1} s^{-1})	$[NaClO_4]_0^b$ mol dm^{-3}	$k_2 \times 10^3$ (dm^3 mol^{-1} s^{-1})
0.0	0.9596	0.0	0.764
0.4	1.37	0.24	4.30
0.8	1.78	0.48	7.52
1.0	2.05	0.8	11.8
1.2	2.24		–
2.4	3.53	1.0	13.95

Table 3—Activation Parameters for Oxidation of Glucose and Its Phosphate Derivatives by Cr(VI) and V(V) in Perchloric Acid Medium

Substrates	$\Delta H^\ddagger$ (kJ mol^{-1})		$\Delta S^\ddagger$ (J deg^{-1} mol^{-1})	
	Cr(VI)	V(V)	Cr(VI)	V(V)
D-Glucose	56 ± 4	97 ± 5	−89.7 ± 14	+3.6 ± 5
D-Glucose 6-phosphate	50 ± 5	89.5 ± 4	−105 ± 16	−3.4 ± 12
D-Glucose 1-phosphate	63 ± 4	111 ± 8	−60.9 ± 13.5	+59 ± 26.7

the second acid hydrogen atom of the phosphate group. Consequently, unlike glucose, reversible protonation of ethereal oxygen in strongly acidic medium is not feasible for the corresponding 1-phosphate derivative (like 6-phosphate). The order in acid which is found to be less for sugar phosphates as compared to that for the parent sugar corroborates the above contention. Again, the autoprotolysis of alcoholic hydroxyl group is very small[14], specially in the presence of strong acid. Moreover, the hydroxyl groups, acting as Lewis bases, can accept protons yielding alkoxonium ion. But the protonation of the sugar phosphate is not so favoured unlike the parent sugar, as the stability of protonated sugar phosphate due to hydration will be less favoured because of its relatively bigger size. So the concentration of alkoxonium ion is not expected to be appreciable. Thus, the molecular species of the sugar phosphate is regarded to be the reactive reductant. Since the C-1 position is being blocked by phosphate group, the reactive site is believed to be C-6. Thus it is the $-CH_2OH$ group which is oxidized.

The order in acid (= 1.9) and also the increase of pseudo-first order rate constant with increase in [salt] (sodium perchlorate) indicate that the path involving substrate and $HCrO_3^+$ predominates[15]. The kinetic results do not indicate the formationof 1:1 complex between substrate and Cr(VI). The UV spectra of the oxidant with and without substrate were recorded. Increase in absorbance for solutions at the absorption maximum of Cr(VI) indicates that an intermediate species between the protonated chromic acid molecule and the substrate is formed[3] where the formation constant is small and insignificant. The intermediate then decomposes to give the product of oxidation and Cr(IV) as shown in Scheme 1. The mechanism involving reactions of alcohols and Cr(VI) is known to be quite complex[16]. It is to be mentioned that initial oxidation product, i.e. aldehyde will be more reactive towards intermediate valence states of chromium. However, since [aldehyde] is much smaller as compared to that of the parent substrate, viz. glucose 1-phosphate, the intermediate state of chromium will preferably react with the partent substrate rather than with aldehyde. It is pertinent to mention that the reaction of Cr(VI) with substrate does not proceed by a free radical mechanism and the reaction fails to polymerize added acrylamide. There are convincing evidences in the literature[17,18] that Cr(V) is formed during the oxidation of some organic compounds by Cr(VI). Since Cr(IV) and Cr(V) are strong oxidants[19] (the redox potentials of the couples Cr(V)/Cr(III), Cr(VI)/Cr(IV) and Cr(IV)/Cr(III) are 1.65, 0.95 and > 1.75 V at 25° respectively), their reactions with the substrate will be fast as compared to the decomposition of the ester.

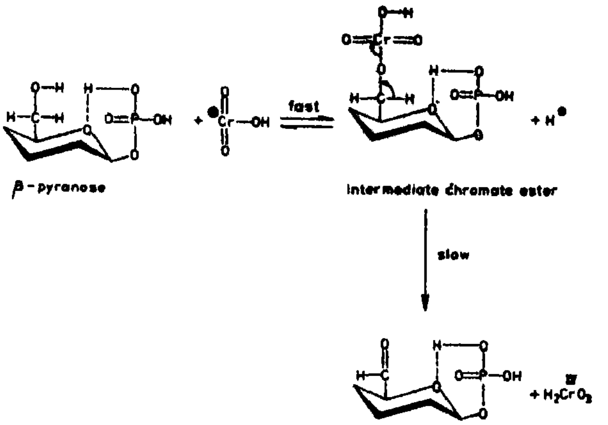

Scheme 1—Oxidation of β-pyranose by chromium (VI)

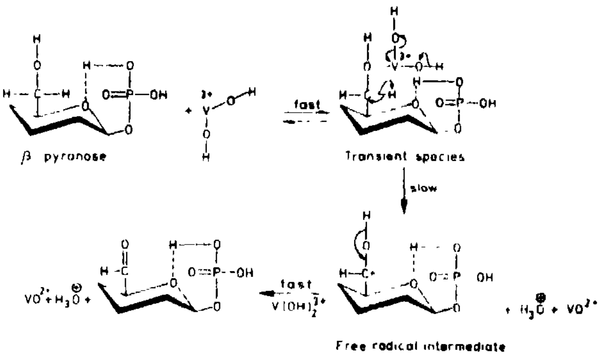

Scheme 2 Oxidation of β-pyranose by vanadium (V)

In V(V) oxidation, vanadate yields pervanadyl ion (VO_2^+) in acid medium which gets protonated in stronger acid medium to yield $V(OH)_2^{3+}$ (ref. 2). The order in acid (= 1.9) and the higher positive salt effect indicate ion-dipole interaction involving substrate and $V(OH)_2^{3+}$. The reaction takes place through the intermediate formation of free radicals[4] followed by reaction with another V(V) to give reaction products (Scheme 2).

Oxidation of D-glucopyranose 1-phosphate by Cr(VI) and V(V) in perchloric acid medium proceeds at a rate where the order in [substrate] and [oxidant] is unity each, but the order in acid is slightly less than two (1.9). However, the order in acid for the oxidation of D-glucopyranose 6-phosphate and the parent D-glucose are different. So, the parent reactions are kinetically different from those reported earlier[1,2,4], irrespective of which metal ion is used as oxidant. Again, D-glucopyranose 1,6-diphosphate practically does not undergo substantial oxidation under the comparable experimental conditions, indicating that C-1 and C-6 of glucose are the reactive sites. This is also the observation of Taha *et al.*[20] However, from the enthalpy of activation data, C-1 appears to be more reactive than C-6. The faster oxidation of the C_6-phosphate as compared to the C_1-phosphate may be due to the fact that C-1 has a potential –CHO group whereas C-6 possesses a –CH_2OH group. This may also be due to the fact that oxygen atom of the ring exerts –I effect[21] which is more pronounced on the nearer C-1 position than that at C-6. This investigation, therefore, shows that the mechanism of the oxidation of D-glucopyranose 1-phosphate by Cr(VI) and V(V) in perchloric acid medium is different from those of the parent sugar and its 6-phosphate derivative by the same oxidants. This further justifies our proposed mechanisms of the oxidation of D-glucose as well as D-glucose 6-phosphate by these metal ion oxidants.

Acknowledgement

Thanks are due to the CSIR and UGC, New Delhi for the award of a fellowship (to SKM) and an associateship (to SSG), respectively.

References

1 Sen Gupta K K, Sen Gupta S & Basu S N, *Carbohydr Res*, **71** (1979) 75.

2 Sen Gupta K K & Basu S N, *Carbohydr Res*, **80** (1980) 223

3 Sen Gupta K K, Sen Gupta S, Mandal S K & Basu S N, *Carbohydr Res* **139** (1985) 185.

4 Sen Gupta K K, Sen Gupta S, Mandal S K & Basu S N, *Carbohydr Res*, **145** (1986) 193.

5 Sen Gupta K K & Chatterjee H R, *Inorg Chem*, **17** (1978) 2429.

6 Rocek J & Aylward D E, *J Am chem Soc*, **97** (1975) 5452.

7 Finar I L, *Organic chemistry*, Vol. I (Longman, ELBS, UK), 1973, pp. 505.

8 Sen Gupta K K, Samanta T & Basu S N, *Tetrahedron*, **42** (1986) 5681.

9 Sen Gupta K K, Chakladar J K, *J chem Soc, Perkin II*, (1973) 929.

10 Wiberg K B, *Oxidation in organic chemistry*, Part-A (Academic Press, New York) 1965, pp. 71.

11 Pladziewcz J R & Espenson J H, *Inorg Chem*, **10** (1971) 634.

12 Laidler K J, *Chemical kinetics*, (Tata McGraw Hill, New Delhi) 1976, pp. 88.

13 Vanwazer J R, *Phosphorus and its compounds*, Vol. 1, (Interscience, New York) 1964, pp. 577.

14 Covington A V & Dickinson T, *Physical chemistry of organic solvent systems*, (Plenum Pres, London) 1973, pp. 390.

15 Frost A A & Pearson R G, *Kinetics and mechanism* (Wiley, New York) 1953, pp. 139.

16 March J, *Advanced organic chemistry* (2nd edition) (McGraw-Hill, Tokyo) pp. 1077.

17 Hasan F & Rocek J, *J Am chem Soc*, **94** (1972) 9073.

18 Haight G P, Jursich G M, Terrykelso M & Perrill P J, *Inorg Chem*, **24** (1985) 2740.

19 Dellien I, Hall F M & Hepler L G, *Chem Rev*, **76** (1976) 283.

20 Taha M I, Basudev W C & Wasif S, *Carbohydr Res*, **2** (1966) 175.

21 Capon B & Overend W G, *Advances in carbohydrate chemistry*, Vol. 15 (Academic Press, New York) 1960, pp. 10.

Indian Journal of Chemistry
Vol. 27A, January, 1988, pp. 27-30

Kinetics of Oxidation of Mono-, Di- & Tri-chloroacetic Acids by Chloramine-T in Acid Medium: Catalysis by Iridium(III)

S RAMAKRISHNA & SUSHMA KANDLIKAR*
Department of Chemistry, Nizam College (Osmania University), Hyderabad 500 001

Received 29 *July* 1986; *re-revised* 31 *March* 1987; *accepted* 18 *May* 1987

Kinetics of Ir(III) catalysed and uncatalysed oxidations of mono-, di- and tri-chloroacetic acids by chloramine-T (CAT) in acid medium have been studied. The order in [CAT] and [H$^+$] is unity each in both the catalysed and uncatalysed reactions. The order in [substrate] is zero in the uncatalysed reaction while it is fractional in the catalysed reaction. Reaction kinetics indicate first order dependence in [Ir(III)]. Salt and solvent effects on the reactions are negligible. Plausible mechanisms and the rate laws consistent with the experimental results have been proposed for the catalysed and uncatalysed reactions.

Chloramine-T (CAT), a two-electron oxidant in both acidic and basic media, has been widely used for the study of kinetics of oxidation of a variety of organic compounds[1-9]. In recent years Ir(III) has been employed as an efficient homogeneous catalyst in several redox systems[10-12]; however, such studies are not reported in CAT oxidations. Hence it is thought worthwhile to study the kinetics of Ir(III) catalysed and uncatalysed oxidations of mono-, di- and tri-chloroacetic acids by CAT in acid medium.

Materials and Methods

All the chemicals used were of AR grade. CAT (Veblabor Chemie Apolda), chloroacetic (E. Merck) and di- and tri-chloroacetic acids (Riedel, Seelze) were used as such. Iridium (III) solution, prepared from Ir(III) (Johnson-Mathew) was standardised by the Literature method[13]. CAT solution was prepared and stored in black coated bottles and was standardised iodometrically. Acetic acid was purified by the usual methods before use. Initial rate method[3] was followed to calculate the reaction rates. The reaction was followed by estimating the unreacted CAT by standard iodometric method. Since the overall rate (gross rate V_g) is the algebraic sum of catalysed and uncatalysed paths, uncatalysed rates (V_u) have been always substracted from gross rates (V_g) in the determination of order of the reaction.

Results and Discussion

Stoichiometric investigations under the conditions [CAT] ≫ [substrate] revealed that one mol of CAT was consumed by one mol of substrate yielding formaldehyde and CO_2 as the products in accord with Eq. (1).

$$ClCH_2COOH + RNCl^- + H^+ + H_2O \rightarrow RNH_2 + CH_2O + CO_2 + 2HCl \qquad \ldots(1)$$

Under the conditions [CAT] ≪ [substrate] the linear plot of log $a/(a-x)$ versus time passed through the origin indicating the order in [CAT] to be unity in both catalysed and uncatalysed systems. First order dependence in [CAT] was followed at all concentrations of the reactants and it was observed that the decrease in rate with increase in [CAT] may be attributed[14] to the corresponding increase in [RNH_2], since some RNH_2 (*p*-toluene sulphonamide or PTS) is always known to exist in equilibrium with CAT[15]. For varying [PTS] an indirect method has been followed by varying [CAT] under the conditions: [substrate] = 0.10 mol dm^{-3}, [H$^+$] = 6.6 × 10^{-3} mol dm^{-3} and temp. = 314 K. Increase in [CAT] (1.0-7.0 × 10^{-3} mol dm^{-3}) retarded the reaction rate, initial rates are: 7.30 to 1.04 × 10^{-7} mol dm^{-3} s^{-1} for Ir(III)-catalysed reaction ([Ir(III)] = 8.00 × 10^{-5} mol dm^{-3}); and 5.10 to 0.70 × 10^{-7} mol dm^{-3} s^{-1} for uncatalysd reaction. This observation shows inverse first order dependence in [PTS].

The rate of oxidation increased with increase in [substrate] (Table 1) showing zero order dependence on [substrate] for uncatalysed reaction and fractional order for catalysed reaction. Limiting rates have been observed at higher [substrate] (Table 2). Iridium (III) (10^{-5} mol dm^{-3}) was found to be effective in catalysing the reactions. The plot of (V_g-V_u) versus [Ir(III)] showed first order dependence in [Ir(III)] (Table 2).

The results in Table 1 show that the increase in percentage of acetic acid in the reaction mixture increases the rate of oxidation. It was reported

Table 1—Order of CAT-Chloroacetic Acid Reaction*

(10^3[CAT] = 1.25 mol dm^{-3}; temp = 304K)

[substrate]	10^2[H$^+$]	10^5[Ir(III)]	HOAc (% v/v)	10^7 × Rate (mol dm^{-3}s^{-1})					
(mol dm^{-3})				CA		DCA		TCA	
0.010	0.660	8.00	10.0	(0.780)	1.00	(0.900)	1.35	(1.14)	1.73
0.020	0.660	8.00	10.0	(0.770)	1.32	(0.910)	1.89	(1.15)	2.20
0.050	0.660	8.00	10.0	(0.780)	1.92	(0.890)	2.50	(1.15)	3.00
0.100	0.660	8.00	10.0	(0.780)	2.78	(0.900)	3.32	(1.15)	4.05
0.200	0.660	8.00	10.0	(0.780)	3.453	(0.900)	3.65	(1.15)	4.68
0.300	0.660	8.00	10.0	(0.800)	3.81	(0.900)	4.10	(1.15)	4.72
0.100	0.660	8.00	10.0	—	0.90	—	1.03	—	1.36
0.100	0.660	1.00	10.0	—	1.00	—	1.20	—	1.50
0.100	0.660	2.50	10.0	—	1.40	—	1.60	—	2.25
0.100	0.660	5.00	10.0	—	1.98	—	2.26	—	3.25
0.100	0.660	7.50	10.0	—	2.39	—	2.76	—	3.89
0.100	0.660	10.00	10.0	—	3.25	—	3.80	—	4.64
0.100	0.660	8.00	10.0	—	—	—	—	—	—
0.100	0.660	8.00	10.0	—	—	—	—	—	—
0.100	0.660	8.00	10.0	—	—	—	—	—	—
0.100	0.200	8.00	10.0	(0.190)	0.370	(0.230)	0.490	(0.250)	(0.61
0.100	0.500	8.00	10.0	(0.500)	1.01	(0.580)	1.23	(0.600)	1.76
0.100	1.00	8.00	10.0	(1.00)	2.15	(1.15)	2.54	(1.25)	3.52
0.100	1.50	8.00	10.0	(1.50)	3.05	(1.75)	3.58	(1.88)	4.74
0.100	2.00	8.00	10.0	(1.90)	3.68	(2.30)	4.77	(2.53)	6.05
0.100	0.660	8.00	5.0	(0.610)	1.93	(0.700)	2.50)	(0.810)	3.10
0.100	0.660	8.00	20.0	(0.960)	2.20	(1.05)	2.90	(1.20)	3.47
0.100	0.660	8.00	30.0	(1.04)	2.30	(1.21)	3.10)	(1.34)	3.63
0.100	0.660	8.00	40.0	(1.30)	2.40	(1.56)	3.45	(1.80)	3.93

*Values in parentheses include uncatalysed rate and CA, DCA and TCA represent mono-, di- and tri-chloroacetic acids respectively.
Temp = 298K for [H$^+$] and solvent effects.

Table 2—Effect of Varying [substrate] and [Ir(III)] in Ir(III) Catalysed Oxidation of Chloroacetic Acid

[Substrate] (mol dm^{-3})	10^7V (mol dm^{-3}s^{-1}) (V_s)			10^7V (mol dm^{-3}s^{-1}) (V_c) ($V_s - V_u = V_c$)		
	TCA	DCA	CA	TCA	DCA	CA
0.01	1.73 (1.15)	1.35 (0.90)	1.00 (0.75)	0.58	0.45	0.25
0.02	2.20	1.89	1.32	1.05	0.99	0.57
0.05	3.00	2.50	1.92	1.85	1.60	1.17
0.10	4.05	3.32	2.78	2.90	2.42	2.03
0.20	4.68	3.65	3.45	3.53	2.75	2.70
0.30	4.72	4.10	3.81	3.57	3.20	3.06
10^5[Ir(III)] mol dm^{-3}						
1.00	1.50	1.20	1.00	0.35	0.30	0.25
2.50	2.25	1.60	1.40	1.10	0.70	0.65
5.00	3.25	2.26	1.98	2.10	1.36	1.23
7.50	3.89	2.76	2.39	2.74	1.86	1.64
10.00	4.64	3.80	3.25	3.49	2.90	2.50

Values in parentheses are uncatalysed rates (V_u); for [substrate] variation, [Ir(III)] is kept constant at 1.00 × 10^{-5} and for [catalyst] variation [substrate] is kept constant at 1 × 10^{-2} (mol dm^{-3})

earlier that the lowering of dielectric constant of the medium favours the reactions involving protonation[16] of any reactant, in general, and anion of the oxidant in the present work. The plot of ln k' versus 1/D is linear with a positive slope indicating the involvement of a positive ion in the reaction.

Effect of varying [H$^+$] on the rate was studied by varying [HCl] and keeping [Cl^-] constant by additing KCl so as to keep ionic strength constant. The results in Table 1 show that the rates are proportional to [H^+] for both catalysed and uncatalysed reactions giving first order in [H^+]. It has been found that variation in [KCl] (from 0.10 to 1.00 mol dm^{-3}) and negligible effect in both catalysed and uncatalysed reactions.

In terms of the substrates the rates increased in the order: $Cl_3HOAc > Cl_2HOAc > ClHOAc$ (Table 1).

Mechanism and rate law in the absence of [*Ir*(*III*)]

From the experimental observations and from the earlier work of Dikshitulu[14], Mahadevappa[16,17], Higuichi[18] and Mushran[19], it is believed that HOCl which arises from CAT in acid medium is the active oxidant species and reacts with the substrate in a fast step. A general mechanism for the oxidation of chloroacetic acids by CAT in acidic medium may thus be proposed as shown in Scheme 1.

$$\underset{(CAT^-)}{RNNaCl \rightleftharpoons RNCl^-} + Na^+ \qquad \ldots (2)$$

$$RNCl^- + H^+ \underset{k_{-2}}{\overset{k_2}{\rightleftharpoons}} \underset{(CAT')}{RNHCl} \qquad \ldots (3)$$

$$RNCl + H_2O \underset{k_{-3}}{\overset{k_3}{\rightleftharpoons}} RNH_2 + HOCl \text{ (slow)} \qquad \ldots (4)$$

$$HOCL + ClCH_2COOH \xrightarrow[\text{fast}]{k_4} HCHO + CO_2 + 2HCl \qquad \ldots (5)$$

(where R = p-$MeC_6H_4SO_2$)

Scheme 1

After applying steady state treatment with respect to CAT' and HOCl and making reasonable approximation, viz. $k_4\{k_{-2} + k_3[H_2O]\}$ [substrate] $\gg k_{-2}k_{-3}$[PTS], rate law (6) is obtained.

$$-\frac{d}{dt}[CAT^-] = \frac{k_2k_3[H_2O]}{k_{-2} + k_3[H_2O]}[CAT^-][H^+] \qquad \ldots (6)$$

In acidic solution CAT^- may be taken as CAT and thus Eq. (6) becomes

$$\frac{-d[CAT]}{dt} = k[CAT][H^+] \qquad \ldots (7)$$

where

$$k = \frac{k_2k_3[H_2O]}{k_{-2} + k_3[H_2O]}$$

The derived rate equation (7) is in complete agreement with the experimental results.

Mechanism in the presence of [*Ir*(*III*)]

First order dependence each in [CAT] and [H^+] and fractional order dependence each in [substrate] and [Ir(III)] when the gross rate law includes uncatalysed rate and enhanced rates in presence of Ir(III) indicate that the substrate may probably form complex with Ir(III), which may further react with HOCl in a slow step. The proposed mechanism for catalysed reaction is shown in Scheme. 2.

$$RNNaCl \rightleftharpoons RNCl^- + Na^+ \qquad \ldots (8)$$

$$RNCl^- + H^+ \overset{K_1}{\rightleftharpoons} \underset{(CAT')}{RNHCl} \qquad \ldots (9)$$

$$\underset{(CAT')}{RNHCl} + H_2O \overset{K_2}{\rightleftharpoons} RNH_2 + \underset{(PTS)}{HOCl} \qquad \ldots (10)$$

$$ClCH_2COOH + Ir(III) \overset{K_3}{\rightleftharpoons} [Complex]^{III} \qquad \ldots (11)$$

$$[Complex]^{III} + HOCl \xrightarrow[\text{slow}]{k} [Complex]^{V} \rightarrow Products \qquad \ldots (12)$$

Scheme 2

Scheme 2 leads to rate law (13)

$$Rate = k[HOCl][Complex]^{III} \qquad \ldots (13)$$

From reaction (10)

$$[HOCl] = \frac{K_2[CAT'][H_2O]}{[PTS]} \qquad \ldots (14)$$

Substituting [CAT'] = $K_1[CAT^-][H^+]$ ... (15)

$$[HOCl] = \frac{K_1K_2[CAT^-][H_2O][H^+]}{[PTS]} \qquad \ldots (16)$$

and

$$[Complex]^{III} = \frac{K_3\,[substrate][Ir(III)]}{1 + K_3[substrate]} \qquad \ldots (17)$$

Substituting Eqs (16) and (17) in Eq. (13) we get,

$$Rate = \frac{\{kK_1K_2K_3[CAT^-][H^+][H_2O]\,[substrate][Ir(III)]\}}{[PTS]\{1 + K_3[substrate]\}} \qquad \ldots (18)$$

After considering the contribution due to the rates of uncatalysed reaction the gross rate law could be written as

$$\frac{-d[\mathrm{CAT}]}{dt}=\left\{\frac{kK_1K_2K_3[\mathrm{CAT}^-][\mathrm{H}^+][\mathrm{H_2O}][\text{substrate}][\mathrm{Ir(III)}]}{[\mathrm{PTS}]\{1+K_3[\text{substrate}]\}}\right\}+k[\mathrm{CAT}][\mathrm{H}^+] \quad \ldots(19)$$

Since in acidic media $[\mathrm{CAT}^-]=[\mathrm{CAT}]$

$$\frac{-d[\mathrm{CAT}]}{dt}=[\mathrm{CAT}][\mathrm{H}^+]\times\left\{\frac{kK_1K_2K_3[\mathrm{H_2O}][\text{substrate}][\mathrm{Ir(III)}]}{[\mathrm{PTS}]\{1+K_3[\text{substrate}]\}}+k_{\mathrm{uncat}}\right\} \quad \ldots(20)$$

Rate equation (20) is in agreement with the experiment observations, viz first order each in [CAT] and $[\mathrm{H}^+]$ in both catalysed and uncatalysed reactions, zero order in [substrate] in the case of uncatalysed reaction and fractional order in [substrate] and first order in [Ir(III)] in the case of catalysed reaction. However, when gross rate is considered reaction kinetics show fractional order in [Ir(III)] because of the contribution of uncatalysed path.

From Eq. (18) at constant $[\mathrm{H}^+]$, [PTS] and ionic strength the rate law for the catalysed system could be given by Eq. (21).

$$\text{Rate}=\frac{kK_1K_2K_3[\mathrm{CAT}\ \ ][\text{substrate}][\mathrm{Ir(III)}]}{1+K_3[\text{substrate}]} \quad \ldots(21)$$

$$\frac{\text{Rate}}{[\mathrm{CAT}]}=k'=\frac{kK_1K_2K_3[\text{substrate}][\mathrm{Ir(III)}]}{1+K_3[\text{substrate}]} \quad \ldots(22)$$

Thus Eq. (22) satisfies the experimental observations obtained under catalytic conditions.

Taking reciprocals, we get

$$\frac{1}{k'}=\frac{1}{kK_1K_2K_3[\text{substrate}][\mathrm{Ir(III)}]}+\frac{1}{kK_1K_2[\mathrm{Ir(III)}]} \quad \ldots(23)$$

It is clear from (23) that $1/k'$ versus 1/[substrate] at constant [Ir(III)] should be linear. Such Michaelis-Menten reciprocal plots were obtained for all the three chloroacetic acids studied with an intercept on $1/k'$ axis confirming the derived rate law, under catalytic conditions.

Acknowledgement

The authors are thankful to Prof. T Navaneeth Rao and Prof. B Sethuram, for their constant encouragement and to Principal, Nizam College, Hyderabad for facilities.

References

1 Ganapathy K & Jayagandhi P, *Indian J Chem*, **16A** (1978) 421.
2 Shailendra Jha, Sharma P D & Gupta Y K, *Inorg Chem*, **22** (1983) 1393 and references therein.
3 Latika Bhatt, Sharma P D & Gupta Y K, *Indian J Chem*, **21A** (1982) 926.
4 Kalyan K Banerji, *Indian J Chem*, **15A** (1977) 615.
5 Katgeri S N, Mahadevappa D S & Naidu H M K, *Bull chem Soc Japan*, (1979) 9.
6 Mushran S P, Sharma, Janardhan & Panday, *Proc Natl Acad Sci* (*A*, **50**(3) (1980).
7 Joesjacob T & Ramachandran Nair C G, *Curr Sci*, **535**(13) (1966) 334.
8 Mushran S P, Agarwal M C & Prasad B, *J chem Soc*, **75** (1971).
9 Srinivasan C & Pitchumani K, *Bull chem Soc Japan*, **55** (1982) 289.
10 Uma V, Sethuram B & Navaneeth Rao T, *React Kinet Catal Lett*, **18** (1981) 283.
11 Rajeswar Rao Y & Saiprakash P K, *Curr Sci*, **47** (1978) 763.
12 Ramananda Sarma Y, Rajenna K C & Saiprakash P K, *Indian J Chem*, **19A** (1980) 825.
13 Singh A K, Mohan Katyal & Singh R P, *J Indian chem Soc*, **53** (1976) 671.
14 Dikshitulu L S A, Vani P & Hanumantha Rao V, *Indian J Chem*, **20A** (1981) 36.
15 Bishop E & Jennings V J, *Talanta*, **1** (1958) 201, 197.
16 Mahadevappa D S & Naidu H M K, *Mh Chem*, **109** (1978) 269.
17 Yathirajan H S, Rangaswamy & Mahadevappa D S, *Chemical Coll Czech Chem Commun*, **47**(7) (1982) 1825.
18 Higuchi T & Hussain A, *J chem Soc*, (1967) 549(**B**).
19 Mushran S P, Mehrotra R M & Sanehi R, *J Indina chem Soc*, **LI**(1974) 594.

Indian Journal of Chemistry
Vol. 27A, January, 1988, pp. 31-33

Kinetics of Reaction of Aromatic Anils with Acid Bromate: Interactive Free Energy Relationship

P NARASIMHA CHAR, S SONDU, B SETHURAM & T NAVANEETH RAO*
Department of Chemistry, Osmania University, Hyderabad 500 007

Received 8 *September* 1986; *revised* 23 *April* 1987; *accepted* 14 *May* 1987

Oxidation of aromatic anils by acid bromate in H_2SO_4-HOAc mixture is enhanced by electron withdrawing substituents both in benzaldehyde as well as in aniline moieties. The magnitude of ρ-value obtained for various substituents in benzaldehyde moiety decreases with the introduction of electron releasing groups in aniline moiety and vice-versa. A linear plot is obtained between $\rho_{X(Y)}$ (obtained from Hammett's plot for various substituents in benzaldehyde moiety) and σ_Y (substituent constants for substituents in aniline moiety) with a slope of 0.70 ± 0.01. This relationship has been analysed quantitatively in terms of interactive free energy relationships for multiple substituent effects.

Acid bromate acts as a good oxidising agent for organic compounds[1-4]. Aromatic anils are known to get cleaved oxidatively by lead tetraacetate (LTA)[5,6], phenyl iodoacetate[7] and bromate[8], and the main products reported were benzaldehyde and azobenzene. The effect of substituents has also been studied with the help of Hammett equation[9]. However owing to the lack of a general method for treating cumulative effects of multiple substituents the additive model of Jaffe[10] is usually applied and the most outstanding deviations are assigned to some specific interactions[11]. Aromatic anils, $X-CH=N-Y$ have two phenyl rings X and Y, the ring X-originates from the aromatic aldehyde moiety and Y from aniline moiety. It is possible to evaluate the reaction constant (ρ) from the Hammett's plot by varying substituents is one of the rings X or Y, keeping the same substituent in the other ring. It is therefore possible to get several reaction constants for different substituents in one of the two rings. The purpose of the present investigation is to show that the multiple substituent effects (MSE) in the acid bromate oxidation of aromatic anils can be quantitatively analysed in terms of interactive free energy relationship by extending the classical Hammett relationship established for one substituent.

Materials and Methods

All the chemicals used were of either A R grade (BDH) or were purified by standard procedures. Purified acetic acid was used. Aromatic anils were prepared and purified by the literature procedure. The rate of reaction was followed iodometrically. All the experiments were carried out under pseudo-first order conditions, viz. [substrate] ≫ [oxidant]. The products of oxidation were identified as the corresponding benzaldehyde and azobenzene. The rate constants were calculated by the method of least squares.

The stoichiometry of the reaction was determined by studying the reaction under the conditions of [bromate] ≫ [anil] and it was found to be 3:1 (see. Eq. 1).

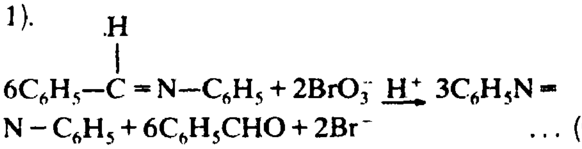

$$6C_6H_5-\overset{H}{C}=N-C_6H_5+2BrO_3^- \xrightarrow{H^+} 3C_6H_5N=N-C_6H_5+6C_6H_5CHO+2Br^- \quad \ldots (1)$$

Results and Discussion

The kinetics of oxidation of aromatic anils by potassium bromate in H_2SO_4-HOAc medium showed the following features.

(i) Under the condition [anil] ≫ $[BrO_3^-]$ the order in $[BrO_3^-]$ was unity as revealed by the linear plot of log $(a/a\text{-}x)$ versus time.

(ii) The order in [anil] was also one as revealed by the unit slope of the plot of log k_{obs} against log [substrate]. The plot of $1/k_{obs}$ against 1/[anil] was also linear but no intercept on Y-axis was obtained, suggesting the absence of complex formation between the reactant molecules.

(iii) The rate of the reaction increased with increase in $[H_2SO_4]$ indicating the involvement of protons in the rate-determining step. The plot of log k_{obs} versus log $[H^+]$ was linear with a slope of two.

(iv) The rate constants increased with increase in the percentage of acetic acid in the solvent medium and the plot of log k_{obs} against 1/D was linear with a positive slope confirming that the reaction is between a positive ion and a dipole.

(v) No polymerization was observed when acrylonitrile was added to the reaction system indicating that the reaction does not proceed by a free radical mechanism.

(vi) From the effect of [acid] it is clear that two protons are involved in the rate-determining step; protonation of the base anil and negative ion BrO_3^- is a distinct possibility.

Based on the above experimental observations a probable mechanism, shown in Scheme 1, is suggested. Considering Scheme 1 the rate of disappearance of bromate is given by Eq. (2)

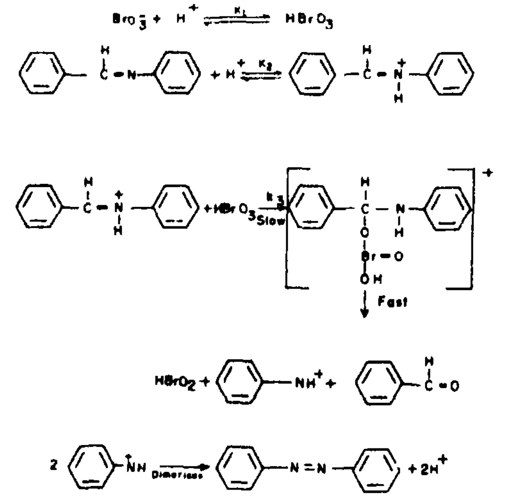

$BrO_3^- + H^+ \underset{}{\overset{K_1}{\rightleftharpoons}} HBrO_3$
K_2
k_3
Slow
Fast
Dimerises

Scheme 1

$$-\frac{d[BrO_3^-]}{dt} = k_3[HBrO_3][\text{protonated anil}] \quad \ldots (2)$$

Substituting the concentrations of $HBrO_3$ and protonated anil in the rate expression (2) the rate law (3) is obtained

$$-\frac{d}{dt}[BrO_3^-] = K_1K_2k_3[\text{anil}][BrO_3^-][H^+]^2 \quad \ldots (3)$$

This rate law satisfactorily explains all the experimental results.

The effect of substituents on rate was studied by varying the substituents in both the rings, i.e. X and Y. The order of reactivities with substituents in the ring-X is: $p\text{-}NO_2 > m\text{-}NO_2 > m\text{-}Cl > p\text{-}Cl > H > p\text{-}CH_3 > p\text{-}OCH_3$ (Table 1). The Hammet plot is linear with a slope of 0.76. It is clear from the order of reactivities that electron withdrawing groups increase the rate and vice versa; *para* and *meta* substituents also fall on the same Hammett's plot indicating that inductive effects are more important than the mesomeric effects. With substituents in the Y-ring the order of reactivities of substituents is: $p\text{-}NO_2 > m\text{-}NO_2 > m\text{-}Cl > p\text{-}Cl > H > p\text{-}CH_3 > p\text{-}OCH_3$. The Hammett's plot for this also is linear with $\rho = 0.50$.

Reaction constants determined for various substituents in ring-X for a particular substituent in ring-Y are given in Table 2. The ρ-value for H in ring-Y is 0.76 at 303 K. This value increased to 0.90 and 1.30 when the substituent in ring-Y was *p*-Cl and $p\text{-}NO_2$ respectively and decreased to 0.57 for $p\text{-}OCH_3$. This trend was observed at other temperatures as well. Introduction of $p\text{-}NO_2$ in Y decreases the electron density at the reaction site (i.e. C = N) due to $-I$ effect and this appears to increase the sensitivity of the reaction to the presence of substituents in ring-X. When $-OCH_3$ group is introduced in ring-Y at *para*-position, the electron density at C = N is considerably high in comparison to H or NO_2 group and this appears to decrease the sensitivity of reaction to the presence of substituents in X. Therefore it is obvious that the magnitude of ρ for various substitu-

Table 2 — Hammett ρ-values for Substituents in Ring-X and Cross-interaction Constant Values (*q*) for Various Substituents in Ring-Y

(Conditions are the same as in Table 1)

Substituents in ring-Y	ρ-Values for substituents in ring-X	*q*
$p\text{-}OCH_3$	0.57	0.704
H	0.76	0.00
$m\text{-}CH_3$	0.71	0.714
p-Cl	0.90	0.609
m-Cl	1.04	0.757
$p\text{-}NO_2$	1.30	0.692

Table 1 — Rate Constants for Various Substituents in both the Rings of Aromatic Anils in Their Oxidation by Acid Bromate

($[BrO_3^-] = 0.002$ mol dm^{-3}, [Anil] = 0.02 mol dm^{-3}; $[H_2SO_4] = 0.2$ mol dm^{-3}; $[Hg(OAc)_2] = 0.01$ mol dm^{-3}; [HOAc] = 80% (v/v); temp. = 303 K)

Substituents in aniline ring (Y)	$k' \times 10^2$ (dm^3 mol^{-1} sec^{-1}) for substituent in ring-X							
	$p\text{-}OCH_3$	$p\text{-}CH_3$	$m\text{-}CH_3$	H	*p*-Cl	*m*-Cl	$m\text{-}NO_2$	$p\text{-}NO_2$
H	0.933	1.10	1.32	1.51	2.29	2.88	5.01	5.62
$p\text{-}OCH_3$	0.70	0.81	0.93	1.00	1.41	1.61	2.51	2.88
$m\text{-}CH_3$	0.86	1.00	1.09	1.78	2.14	3.45	3.88	—
p-Cl	1.02	1.32	1.70	1.90	3.39	4.37	8.91	10.9
m-Cl	1.35	1.68	1.89	4.06	5.62	9.96	11.4	—
$p\text{-}NO_2$	1.77	2.51	3.24	3.98	7.76	12.0	39.8	—

ents in ring-X depends to a large extent on the nature of substituent in ring-Y. Electron releasing groups decrease the magnitude of ρ-value and vice versa. A linear plot is obtained when $\rho_{X(Y)}$ (obtained from the Hammett's plot for various substituents in ring-X) is plotted against σ_Y (substituent constants for substituents in ring-Y) with a slope of 0.70 (correlation coefficient = 0.986). This type of relationship is different from the simple Hammett equation and therefore an attempt is made to explain this relationship in terms of interactive free energy relationship (IFER) for multiple substituent effect (MSE) discussed earlier by Ruasse *et al.*[12,13] during their study on the bromination of α-methylstilbenes. We have derived the expression (4) for the variation of reaction constant with various substituents in both the rings.

$$\frac{[\rho_{Y(X)} - \rho_{Y(X_0)}]}{\sigma_X} = \frac{[\rho_{X(Y)} - \rho_{X(Y_0)}]}{\sigma_Y} = q \qquad \ldots (4)$$

where $\rho_{X(Y_0)}$ and $\rho_{Y(X_0)}$ are reaction constants for substituents in the rings X and Y respectively for H in the other ring. Similarly $\rho_{X(Y)}$ and $\rho_{Y(X)}$ are reaction constants for various substituents in X and Y respectively for a particular substituent in the other ring. σ_X and σ_Y are the substituent constants in rings X and Y respectively. This equation must be true whatever substituent in X and Y are. Therefore the ratios are equal to a constant (q) which is known as the cross-interaction constant[12]. From Eq. (4) it is clear that the reaction constants are not random variables and are directly dependent on substituent constants.

$$\rho_{X(Y)} = \rho_{X(Y_0)} + q\sigma_Y \qquad \ldots (5)$$

$$\text{or } \rho_{Y(X)} = \rho_{Y(X_0)} + q\sigma_X \qquad \ldots (6)$$

From Eq. (5) it is clear that a plot of $\rho_{X(Y)}$ versus σ_Y should be linear if q is a constant. In the present work a good linear plot is obtained experimentally with a slope of 0.70 (Fig. 1). Calculation of q values from Eq. (5) shows that it is a constant for all the substituents studied (Table 2) indicating that IFERs for MSEs are applicable for the oxidation of aromatic anils by acid bromate also. It also emphasises the fact that polysubstituted reaction system like substituted aromatic anil-BrO_3^- is accurately defined only if one knows the reaction constant and the cross-interaction (q). The value of q cannot be determined *a priori* but only from experimental results.

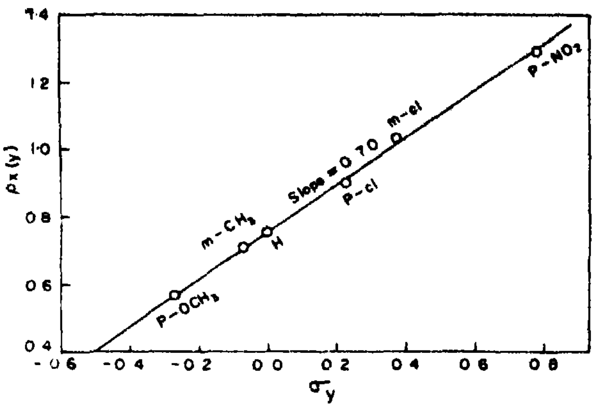

Fig. 1 — Plot of $\rho_{X(Y)}$ versus σ_Y

References

1 Vijayalakshmi & Sundaram E V, *Indian J Chem*, **15A** (1977) 612.
2 Sanjeeva Reddy Ch, Vijayalakshmi & Sundaram E V, *Indian J Chem*, **19A** (1980) 544.
3 Radhakrishna Murthy P S & Mahapatro D K, *Indian J Chem*, **18A** (1979) 53.
4 Natarajan R & Venkatasubramanian N, *Tetrahedron Lett*, (1969) 5021 and (1970) 785.
5 Rindone B, Santaniello E & Scolastico C, *Tetrahedron Lett*, (1972) 19.
6 Catto A, Corbani F, Rindone B & Scolastico C, *Tetrahedron Lett*, **29** (1973) 2723.
7 Narasimha Bharati S, Sundaram S & Venkatasubramanian N, *Indian J Chem*, **15B** (1977) 376.
8 Krishnamurthy N, "*A kinetic and mechanistic study of bromate oxidations*, Ph D thesis, Kakatiya University, 1986.
9 Wells Peter R, *Chem Rev*, **63** (1962) 171.
10 Jaffe H H, *Chem Rev*, **53** (1953) 191.
11 Nishida S, *J org Chim*, **32** (1967) 2692.
12 Alain Argile & Marie-Francoise Ruasse, *J org Chem*, **48** (1983) 209.
13 Marie-Francoise Ruasse & Alain Argile, *J org Chem*, **48** (1983) 202

Indian Journal of Chemistry
Vol. 27A, January, 1988, pp. 34-38

Effect of Formaldehyde on Kinetics & Mechanism of Oxidation of Amino Acids by Bromamine-T in Perchloric Acid Medium

B THIMME GOWDA* & (Mrs) R VIJAYALAKSHMI RAO
Department of Post-Graduate Studies and Research in Chemistry, Mangalore University,
Mangalagangothri, Mangalore 574 199

Received 21 *July* 1986; *re-revised* 21 *April* 1987; *accepted* 25 *May* 1987

The kinetics of oxidation of amino acids by bromamine-T (BAT) have been investigated both in the presence and absence of formaldehyde in perchloric acid medium. The reaction is first order in [BAT], zero order in both [amino acid] and [H^+] and fractional order in [HCHO] in the presence of formaldehyde, and first order each in [oxidant], and [amino acid] and inverse first order in [H^+] in the absence of formaldehyde. Addition of *p*-toluenesulphonamide or variation in ionic strength of the medium does not have any significant effect on the rate, but the decrease in dielectric constant of the reaction medium decreases the rate. Activation parameters have been computed from the Arrhenius plots and mechanisms in conformity with the observed kinetics have been suggested and related rate laws deduced. The oxidation process in the presence of formaldehyde proceeds via two pathways.

It is well known that amino acids react with aldehydes to give schiff bases[1]. The importance of amino acid-aldehyde condensations in biosystems is well established[2-4]. The title investigation has been undertaken to find out the role of schiff bases in the oxidative decarboxylation of α-amino acids.

Materials and Methods

A pure sample of bromamine-T (BAT) was prepared in the laboratory and its aqueous stock solution (~0.1 mol dm^{-3}) was prepared in doubly distilled water, standardised and stored in dark coloured bottles. Chromatographically pure amino acids, viz. L-glycine (Gly), L-alanine (Ala), L-valine (Val), L-leucine (Leu), L-serine (Ser) and L-threonine (Thr) (Sisco Research Laboratories, India) were used and their aqueous stock solutions (~0.1 mol dm^{-3}) were standardised. An aqueous solution of formaldehyde (Glaxo, BDH) was prepared and standardised by hypoiodite method. All other reagents employed were of accepted grades of purity. Preliminary investigations showed that the ionic strength of the medium has no significant effect on the rate of reaction.

The kinetic studies were made under pseudo-first order conditions ([amino acid] ≫ [BAT]; at least by 5-10 times). The reactions were initiated by the quick addition of requisite amounts of BAT solution, thermally equilibrated at a desired temperature, to a reaction mixture containing known amounts of amino acid solution, formaldehyde, perchloric acid and water, pe-equilibrated at the same temperature. The progress of the reaction was monitored for at least two half-lives by iodometric estimation of unreacted BAT at regular intervals of time. The pseudo-first order rate constants computed by the method of least squares were reproducible within ± 3%.

The stoichiometries of BAT-amino acid reactions were determined both in the presence and absence of HCHO in aqueous perchloric acid medium (0.005-0.20 mol dm^{-3}). The observed stoichiometries may be represented by Eq. (1) in the absence of HCHO and Eqs (2) and (3) in the presence of HCHO.

$$\mathrm{R'CH(NH_2)COOH + RNHBr + H_2O \rightarrow RNH_2 + R'CHO + CO_2 + NH_4^+ + Br^-} \quad \ldots (1)$$

$$\mathrm{H_2C(OH)_2 + RNHBr \rightarrow HCOOH + RNH_2 + H^+ + Br^-} \quad \ldots (2)$$

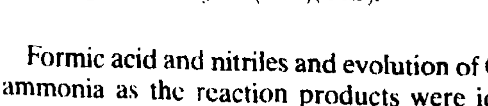

$$\mathrm{R'CH(NH_2)COOH + H_2C(OH)_2 + 3RNHBr \rightarrow 3RNH_2 + R'CN + HCOOH + CO_2 + 3H^+ + 3Br^-} \quad \ldots (3)$$

where $R = CH_3C_6H_4SO_2$ and $R' = H$(Gly), CH_3(Ala), $(CH_3)_2CH$(Val), $(CH_3)_2CHCH_2$(Leu), $HOCH_2$(Ser), $CH_3CH(OH)$(Thr).

Formic acid and nitriles and evolution of CO_2 and ammonia as the reaction products were identified by conventional tests, and formation of *p*-toluenesulphonamide (RNH_2 in Eqs 1-3) was detected by paper chromatography using benzyl alcohol saturated with water as the solvent and 0.5% vanillin in 1% HCl solution in ether as the spray reagent. The aldehyde formed in the absence of formaldehyde was quantitatively estimated.

Results and Discussion

Kinetics of oxidations of Gly, Ala, Val, Leu, Ser and Thr, both in the presence and absence of formaldehyde, by BAT was investigated in perchloric acid medium (0.005-0.2 mol dm^{-3}). The results are presented in Tables 1-5. The effect of varying [HCHO] on the kinetics of oxidation of α-amino acids was negligible upto [HCHO] = 0.02 mol dm^{-3} as the oxidation of formaldehyde to formic acid was very slow below this concentration. At [HCHO] > 0.02 mol dm^{-3} not only the rates increased but also order in [amino acid] changed form one to zero (Table 5).

At constant [HCHO] and [$HClO_4$] with amino acid in excess (at least by 5-10 times) plots of log $[BAT]_0/[BAT]$ versus time were linear upto 75% completion of reaction for all the substrates and the pseudo-first order rate constants were unaffected by the changes in $[BAT]_0$, establishing first order dependence in [BAT] (Table 1). The rates were unaffected by changes in [amino acid] and [$HClO_4$] except for glycine where the rate increased with increase in [Gly] with fractional order dependence and decreased with increase in [$HClO_4$] showing inverse fractional order in [H^+]. The rates increased with increase in [HCHO] and the double log plots of k_{obs} versus [HCHO] were linear with varying fractional slopes indicating fractional order dependence in [HCHO]. Plots of k_{obs} versus [HCHO] were also linear with almost the same intercept for all the substrates. Further the double reciprocal plots were non-linear indicating that the oxidation of HCHO occurs as a separate and independent reaction, in addition to formaldehyde-catalysed oxidation of amino acids. To substantiate this we have separately studied the kinetics of oxidation of HCHO by BAT in perchloric acid medium. As can be seen from the data in Table 3 the rate is first order each in [oxidant] and [HCHO] and is independent of [H^+]. The rate constants are also of the same order of magnitude.

Addition of *p*-toluenesulphonamide or the variation in ionic strength of the medium had no significant effect on the rates of oxidations of all the amino acids. But the rates decreased with decrease in dielectric constant of medium by changing the solvent composition by the addition of methanol (Table 4). The rates were measured at different temperatures and the activation parameters were computed from the Arrhenius plots (Table 5).

Mechanism

In acid solutions of BAT, the probable oxidising species are RNHBr, RNH_2Br^+, HOBr, H_2OBr^+ and $RNBr_2$ (see refs 5-8). If $RNBr_2$ were to be the reactive species, a second order dependence of rate on [BAT] was expected which is contrary to the present experimental observation. Further the kinetics of oxidation of glycine by HOBr was investigated, independently, under identical conditions (Table 6). As can be seen from the data in Table 6, orders in [Gly] and [H^+] in HOBr oxidations are different from those in BAT oxidations. It is therefore evident that RNH_2Br^+ gets hydrolysed to H_2O^+Br, in a slow step, which in turn interacts with the schiff bases (formed from the condensation of amino acid and formaldehyde) in fast steps to give formic acid and the corresponding nitrile as the final products (see Scheme 1). As already indicated oxidation of formaldehyde occurs parallel to formaldehyde-catalysed oxidation of amino acids. This can be accounted for by the mechanism shown in Scheme 2. Schemes 1 and 2 are compatible with first order dependence in [BAT], zero order each in [amino acid] and [H^+] and fractional order in [HCHO] (Formaldehyde is known to exist almost completely in the hydrated from, [$H_2C(OH)_2$] in aqueous solutions).

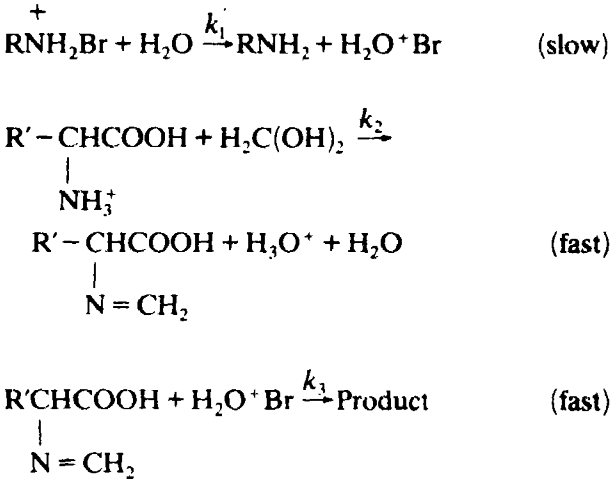

$$\overset{+}{RNH_2Br} + H_2O \xrightarrow{k_1} RNH_2 + H_2O^+Br \qquad \text{(slow)}$$

$$R'-\underset{\underset{NH_3^+}{|}}{C}HCOOH + H_2C(OH)_2 \xrightarrow{k_2} R'-\underset{\underset{N=CH_2}{|}}{C}HCOOH + H_3O^+ + H_2O \qquad \text{(fast)}$$

$$R'\underset{\underset{N=CH_2}{|}}{C}HCOOH + H_2O^+Br \xrightarrow{k_3} \text{Product} \qquad \text{(fast)}$$

Scheme 1

$$H_2C(OH)_2 + RNHBr \xrightarrow{k_4} H_2C(OH)OBr + RNH_2 \qquad \text{(slow)}$$

$$H_2C(OH)OBr \xrightarrow{k_5} HCOOH + H^+ + Br^- \qquad \text{(fast)}$$

Scheme 2

Schemes 1 and 2 lead to combined rate law (4).

$$-\frac{d[BAT]}{dt} = k_1[BAT] + k_4[BAT][HCHO]$$

Table 1—Pseudo-first Order Rate Constants (k) for Oxidation of Amino Acids (AA) by Bromamine-T (BAT) at 303 K in the Presence of HCHO at Different [Reactant] and [$HClO_4$]

[X] (mol dm^{-3})				$10^4 k$ (s^{-1})					
10^2[AA]$_0$	10^3[BAT]$_0$	10^2[$HClO_4$]	10^2[HCHO]$_0$	Gly	Ala	Val	Leu[a]	Ser	Thr
5.0	5.0	5.0	3.8	—	—	—	—	—	8.79
5.0	5.0	5.0	5.0	5.6	7.1	7.0	6.3	4.9	—
5.0	5.0	5.0	10.0	7.0	10.0	9.5	7.7	6.7	14.4
5.0	5.0	5.0	20.0	8.6	14.7	15.0	11.8	—	—
5.0	5.0	5.0	25.0	—	—	—	—	10.1	22.3
5.0	5.0	5.0	40.0	10.5	20.0	22.9	15.1	11.8	28.0
5.0	5.0	0.5	10.0	29.4	—	—	—	—	—
5.0	5.0	1.0	10.0	18.4	—	—	—	—	—
5.0	5.0	2.0	10.0	12.3	9.9	9.5	7.7	6.4	14.2
5.0	5.0	4.0	10.0	—	9.8	9.6	7.6	6.5	14.3
5.0	5.0	5.0	10.0	7.0	10.0	9.5	7.7	6.7	14.4
5.0	5.0	7.5	10.0	5.3	9.9	9.5	7.6	6.8	14.1
5.0	5.0	10.0	10.0	4.6	10.0	9.5	7.6	6.6	14.6
5.0	5.0	20.0	10.0	—	9.9	9.5	7.7	6.3	14.3
5.0	0.5	5.0	10.0	—	—	—	7.6	—	—
5.0	1.0	5.0	10.0	7.0	9.6	9.5	7.7	6.4	14.1
5.0	2.0	5.0	10.0	6.8	9.9	9.6	7.6	6.5	14.3
5.0	4.0	5.0	10.0	—	—	—	7.7	—	—
5.0	5.0	5.0	10.0	7.0	10.0	9.5	—	6.7	14.4
5.0	7.5	5.0	10.0	6.9	10.0	9.7	—	6.4	14.3
5.0	10.0	5.0	10.0	6.9	9.9	9.6	—	6.7	14.3
1.0	5.0	5.0	10.0	—	—	—	7.5	—	—
2.0	5.0	5.0	10.0	4.4	9.9	9.6	7.6	6.6	14.2
4.0	5.0	5.0	10.0	—	9.9	9.6	7.7	6.5	14.3
5.0	5.0	5.0	10.0	7.0	10.0	9.5	7.7	6.7	14.4
7.5	5.0	5.0	10.0	8.9	10.0	9.6	7.6	6.5	14.5
10.0	5.0	5.0	10.0	11.0	10.0	9.6	—	6.7	14.2

(a)With Leu standard run [X] were: 10^3[BAT]$_0$ = 10^2[Leu]$_0$ = 2.0 mol dm^{-3}.

Table 2—Pseudo-first Order Rate Constants (k) for Oxidation of Amino Acids (AA) by Bromamine-T (BAT) at 303 K in the Absence of HCHO at Different [BAT], [AA] and [$HClO_4$]

[X] (mol dm^{-3})			$10^4 k$ (s^{-1})					
10^2[AA]$_0$	10^3[BAT]$_0$	10^2[$HClO_4$]	Gly	Ala	Val	Leu[a]	Ser	Thr
5.0	5.0	2.0	13.3	—	—	—	6.1	6.0
5.0	5.0	3.0	7.7	9.7	11.1	4.9	—	—
5.0	5.0	4.0	—	6.5	8.2	4.3	—	—
5.0	5.0	5.0	5.3	5.5	6.5	3.2	3.0	3.0
5.0	5.0	7.5	3.2	4.0	4.9	2.2	—	—
5.0	5.0	10.0	2.0	2.4	4.0	1.6	1.5	1.8
5.0	5.0	20.0	—	1.7	2.1	0.8	0.9	1.2
5.0	0.5	5.0	—	—	—	3.2	—	—
5.0	1.0	5.0	5.2	5.4	6.9	3.2	2.9	3.1
5.0	2.0	5.0	5.5	5.5	7.0	3.3	2.7	3.2
5.0	4.0	5.0	5.3	5.5	6.9	3.2	2.8	3.1
5.0	5.0	5.0	5.3	5.5	6.5	—	2.8	3.0
5.0	10.0	5.0	5.4	5.4	7.0	—	2.9	3.1
1.0	5.0	5.0	—	—	—	1.4	—	—
2.0	5.0	5.0	2.1	2.0	2.6	3.2	1.3	1.5
4.0	5.0	5.0	—	4.2	—	5.4	2.2	2.5
5.0	5.0	5.0	5.3	5.5	6.5	6.5	2.8	3.0
7.5	5.0	5.0	8.7	9.6	9.1	9.6	4.5	4.0
10.0	5.0	5.0	10.9	12.5	11.4	—	—	4.8

(a)With Leu standard run [X] were 10^3[BAT]$_0$ = 10^2[Leu]$_0$ = 2.0 mol dm^{-3}.

Table 3—Pseudo-first Order Rate Constants (k) for Oxidation of Formaldehyde by Bromamine-T at 303 K

[X] (mol dm^{-3})			$10^4 k$ (s^{-1})
10^2 [HCHO]$_0$	10^3 [BAT]$_0$	10^2 [HClO$_4$]	
4.0	1.0	5.0	2.5
5.0	1.0	5.0	3.0
7.5	1.0	5.0	4.9
10.0	1.0	5.0	6.5
20.0	1.0	5.0	15.0
5.0	1.0	1.0	2.9
5.0	1.0	2.0	2.9
5.0	1.0	4.0	3.1
5.0	1.0	5.0	3.0
5.0	1.0	7.5	3.0
5.0	1.0	10.0	2.9
5.0	1.0	20.0	2.9
5.0	0.5	5.0	2.9
5.0	1.0	5.0	3.0
5.0	2.0	5.0	2.9
5.0	4.0	5.0	3.0

Table 4—Effect of Dielectric Constant (D) and Reaction Product (PTS) on Rates of Oxidation of Amino Acids by BAT at 303 K in Presence of HCHO (0.1 mol dm^{-3})[a]

D	$10^4 k$ (s^{-1})					
	Gly	Ala	Val	Leu[b]	Ser	Thr
74.3	7.0	10.0	9.5	7.7	6.7	14.4
72.1	5.4	7.4	8.4	5.4	4.9	13.8
67.6	5.4	7.4	7.9	5.3	4.8	13.6
63.1	5.3	7.4	7.2	5.3	4.4	13.6
10^3 [PTS] (mol dm^{-3})						
1.0	7.0	10.0	9.6	7.7	6.6	14.5
2.0	6.9	9.9	9.6	7.6	6.7	14.4
5.0	7.0	10.0	9.5	7.7	6.7	14 4
7.5	6.9	10.0	9.6	7.7	6.7	14.6

[a] 10^3 [BAT]$_0$ = 10^2 [AA]$_0$ = 10^2 [HClO$_4$] = 5.0 mol dm^{-3}.
[b] 10^3 [BAT]$_0$ = 10^2 [AA]$_0$ = 2.0 mol dm^{-3} and 10^2 [HClO$_4$] = 5.0 mol dm^{-3}.

or

$$k_{obs} = k_1 + k_4\,[\text{HCHO}] \qquad \ldots (4)$$

(where $k_1 = k_1'[\text{H}_2\text{O}]$)

Rate law (4) predicts a linear plot between k_{obs} and [HCHO] which is found to be so for all the substrates. The constants k_1 and k_4 were calculated from the slopes and intercepts of such plots (Table 7).

First order in [BAT], first order in [amino acid] and inverse first order in [H$^+$], generally observed in

Table 6—Pseudo-first Order Rate Constants for Oxidation of Glycine by Hypobromite in Perchloric Acid Medium at 303 K

[X] (mol dm^{-3})			$10^4 k$[a] (s^{-1})
10^2 [Gly]$_0$	10^3 [HOBr]$_0$	10^2 [HClO$_4$]	
5.0	2.0	5.0	3.8 (7.5)
5.0	5.0	5.0	4.0 (7.4)
5.0	7.5	5.0	3.8 (7.4)
5.0	10.0	5.0	3.9 (7.4)
2.5	5.0	5.0	1.2 (5.8)
5.0	5.0	5.0	4.0 (7.4)
10.0	5.0	5.0	9.3 (13.1)
20.0	5.0	5.0	23.0 (24.6)
5.0	5.0	2.0	12.8 (18.2)
5.0	5.0	5.0	4.0 (7.4)
5.0	5.0	10.0	1.4 (4.3)
5.0	5.0	20.0	0.65 (3.5)

[a] Values in parentheses are the rate constants in the presence of 0.1 mol dm^{-3} HCHO.

Table 7—The Rate Constants for Oxidation of Amino Acids by BAT in Presence of HCHO

Amino Acid	$10^4 k_1$ (s^{-1})	$10^3 k_4$ (dm^{3}mol^{-1}s^{-1})	Amino Acid	$10^4 k_1$ (s^{-1})	$10^3 k_4$ (dm^{3}mol^{-1}s^{-1})
Gly	--	2.0	Leu	4.8	2.5
Ala	4.7	5.0	Ser	4.7	1.7
Val	4.6	5.0	Thr	4.7	10.2

Table 5—Kinetic and Activation Parameters for Oxidation of Amino Acids by BAT in the Absence and Presence of HCHO

Order in	In the absence of HCHO						In the presence of HCHO (0.1 mol dm^{-3})					
	Gly	Ala	Val	Leu	Ser	Thr	Gly	Ala	Val	Leu	Ser	Thr
[BAT]	1.0	1.0	1.0	1.0	1.0	1.0	1.0	1.0	1.0	1.0	1.0	1.0
[H$^+$]	−1.0	−1.0	−1.0	−1.0	−0.9	−0.7	−0.6	0	0	0	0	0
[AA]	1.0	1.0	1.0	1.0	0.9	0.7	0.6	0	0	0	0	0
[HCHO]	—	—	—	—	—	—	0.3	0.5	0.56	0.44	0.46	0.5
Activation parameters												
E_a (kJ mol^{-1})	92.3	65.8	57.4	56.8	53.1	101.3	75.3	60.5	46.5	57.8	29.8	56.5
log A	13.0	6.52	6.69	6.29	9.63	17.7	13.8	11.4	9.0	10.4	5.93	10.8
$\Delta H^{\ddagger}$ (kJ mol^{-1})	89.8	54.3	54.9	54.2	50.6	98.7	72.8	58.0	44.0	55.5	27.2	54.0
$\Delta S^{\ddagger}$ (JK^{-1} mol^{-1})	4.3	−120.4	−117.1	−124.7	−60.2	−93.3	19.7	−26.1	−72.7	−37.7	−131.5	39.3
$\Delta G^{\ddagger}$ (kJ mol^{-1})	88.5	91.3	91.0	92.6	68.6	127.0	66.8	65.9	66.0	66.7	67.1	65.9

the absence of HCHO, can be explained by mechanisms reported in our earlier papers[8,9].

The anomaly in the case of glycine in the presence of HCHO, is due to the instability of schiff base[1], as equilibrium of step (ii) of Scheme 1 lies towards left and hence unconverted amino acid also reacts with the oxidant in addition to reaction pathways shown in Schemes 1 and 2. This was verified by studying the effect of formaldehyde on the kinetics of oxidation of amino acids under the condition [amino acid] $\gg$ [HCHO] where rates showed dependence on [amino acid], as under these conditions free amino acid present reacts independently with its characteristic rate.

The kinetics and stoichiometrics of oxidation of amino acids by BAT in the presence and absence of HCHO reveals that the kinetics are different (Table 5). The kinetic order in [amino acid] generally changes from one to zero and in $[H^+]$ from inverse first order to zero order and the product changes from the corresponding aldehyde to nitrile thus establishing the role of schiff base (aldimine) formation in the oxidative decarboxylation of amino acids.

The suggested mechanisms are also supported by the moderate values of activation parameters. The constancy of $\Delta G^{\ddagger}$ for the oxidation of amino acids in the presence of HCHO shows the operation of a similar mechanism for all the amino acids. The negative $\Delta S^{\ddagger}$ indicates the formation of more ordered activated complexes. Further the plot of $\Delta H^{\ddagger}$ versus $\Delta S^{\ddagger}$ is linear with an isokinetic temperature of 312 K. The latter is very much closer to the temperature range employed in the present investigations (293-313 K).

The observed effects of dielectric constant of the reaction medium on the rates of oxidation are in conformity with Amis' and other concepts[10-12].

References

1 Barton D & Ollis W D, *Comprehensive organic chemistry* (Pergamon, Oxford) 1979, Vol. 2, p. 824.
2 Braunstein A E, *Enzymes*, (Academic, New York) 1973, Vol. 9, p. 379.
3 Metzler D E, *Adr Enzymol*, **50** (1979) 1.
4 Walsh C, *Enzymatic reaction mechanisms* (Freeman, Sanfrancisco) 1979, p. 777
5 Bishop E & Jennings V J, *Talanta*, **1** (1958) 197.
6 Campbell M M & Johnson G, *J chem Soc, Perkin Trans* 2, **78** (1978) 65.
7 Hardy F E & Johnston J P, *J chem Soc, Perkin Trans* 2, (1973) 742.
8 Gowda B T & Mahadevappa D S, *J chem Soc, Perkin Trans* 2, (1983) 323 and references therein.
9 Gowda B T & (Mrs) Rao R V, *Indian J Chem*, **24A** (1985) 1021; **25A** (1986) 578.
10 Amis E S, *Solvent effects on reaction rate and mechanisms*, (Academic Press, New York) 1966.
11 Entelis S G & Tiger R P, *Reaction kinetics in the liquid phase*. (Wiley, New York) 1976.
12 Frost A A & Pearson R G, *Kinetics and Mechanism*, (Wiley, New York) 1961

Indian Journal of Chemistry
Vol. 27A, January, 1988, pp. 39-43

Role of Chloride Ion in Kinetics & Mechanism of Oxidation of Amino Acids by Chloramine-T in Perchloric Acid Medium

B THIMME GOWDA* & (Mrs) R VIJAYALAKSHMI RAO
Department of Post-Graduate Studies and Research in Chemistry, Mangalore University, Mangalagangothri 574 199

Received 4 *September* 1986; *revised* 6 *April* 1987; *accepted* 6 *May* 1987

The kinetics of oxidation of L-alanine, L-valine and L-phenylalanine by chloramine-T (CAT) have been studied under varying conditions of acidity and [chloride]. Chloride ion catalyses the oxidation and catalytic effect is $[H^+]$-dependent, being more pronounced at high $[H^+]$ (> 0.05 mol dm^{-3}). In the presence of Cl^- the reaction is first order in $[CAT]_0$, and zero order each in $[substrate]_0$ and $[H^+]$ with all the amino acids as against second order in $[CAT]_0$, first order in $[substrate]_0$ and inverse first order in $[H^+]$ in the absence of Cl^-. At low $[H^+]$, effect of added Cl^- is not kinetically significant and hence the kinetics are similar to those in the absence of Cl^-. Plausible mechanisms have been proposed and rate laws consistent with mechanisms deduced.

In continuation of our efforts on chloramine-T (CAT) oxidations[1-4]. We report herein the kinetics of oxidative decarboxylation of L-alanine (Ala), L-valine (Val) and L-phenylalanine (Phe) by CAT in aqueous perchloric acid medium both in the presence and absence of chloride ion.

Materials and Methods

Aqueous stock solutions (0.1 mol dm^{-3}) of chloramine-T (Fluka AG) and amino acids (0.2 mol dm^{-3}) (SRL, India) were prepared and standardised as reported elsewhere. All other reagents employed were of AR grade.

Preliminary investigations showed that the variation in ionic strength of the medium had no significant effect on the rate of oxidation.

The kinetics were followed as described earlier, under pseudo-first or second order conditions (employing 5-10 fold excess of amino acid over CAT). The rate constants computed by the method of least squares were reproducible within 3%.

The stoichiometric studies revealed that nitrile was the major product in the absence of Cl^- and presence of Cl^- at low $[H^+]$, and aldehyde was the major product in the presence of Cl^- at high $[H^+]$ (> 0.05 mol dm^{-3}). It was also noticed that aldehydes did not get oxidised under the present experimental conditions. The nitriles, aldehydes and the reduced product of the oxidant were identified by conventional tests[5,6] and by recording the spectra of the reaction mixtures. The observed stoichiometries in the absence and presence of Cl^- may be represented by Eqs (1) and (2), respectively.

$$R'CH(NH_2)COOH + 2RNCl^-Na^+ \rightarrow R'CN + 2RNH_2 + CO_2 + 2Na^+ + 2Cl^- \quad \ldots (1)$$

$$R'CH(NH_2)COOH + RNCl^-Na^+ + H_2O \rightarrow R'CHO + RNH_2 + CO_2 + NH_3 + Na^+ + Cl^- \quad \ldots (2)$$

where $R = CH_3C_6H_4SO_2$, $R' = CH_3$ (Ala), $(CH_3)_2CH$ (Val) and $C_6H_5CH_2$ (Phe).

Results and Discussion

(*a*) *Kinetics in absence of Cl*$^-$

At fixed [acid] and with amino acids (herein after referred to as substrates, S) in excess, plots of 1/[CAT] versus time were linear at least upto 75% completion of reaction and the pseudo-second order rate constants were insensitive towards the variation in $[CAT]_0$ (Table 1) establishing second order kinetics in $[CAT]_0$. But at fixed $[CAT]_0$ and [substrate], the rates decreased with increase in $[HClO_4]$ (Table 1) with inverse first order dependence on $[H^+]$ in all cases. At fixed $[CAT]_0$ and $[HClO_4]$ rates increased with increase in [substrate] showing first order dependence in $[substrate]_0$. Addition of *p*-toluenesulphonamide (PTS) and variation in ionic strength of the medium had no significant effect on the rate of oxidation (Table 2).

(*b*) *Kinetics in presence of Cl*$^-$

The catalytic effect of Cl^- was not kinetically significant at low [acid] (< 0.05 mol dm^{-3}) but affected the kinetics at high $[H^+]$ (> 0.05 mol dm^{-3}). At fixed $[CAT]_0$, [substrate] and $[Cl^-]$, the rates decreased with increase in $[HClO_4]$ upto 0.05 mol dm^{-3} and remained constant thereafter (Tables 3 and 4) with the order in [CAT] being changed from second to first. The plots of log k_{obs} versus log $[HClO_4]$ were linear with negative unit slopes at low [acid] showing inverse first order dependence in $[H^+]$.

Table 1 — Effect of Varying $[\text{Substrate}]_0$, $[HClO_4]$ and $[CAT]_0$ on the Rate of Uncatalysed Oxidation of Amino Acids at 303 K

[X] (mol dm^{-3})				$10^2 k_{obs}$ (dm^3 mol^{-1} s^{-1})		
10^2 [substrate]	10^3 $[CAT]_0$	10^2 $[HClO_4]$	10^2 $[H^+]^a$	Ala	Val	Phe
1.0	2.0	5.0	4.57	3.0	3.4	4.9
2.0	2.0	5.0	4.57	5.6	6.7	9.8
5.0	2.0	5.0	4.57	15.7	17.5	20.3
10.0	2.0	5.0	4.57	30.8	36.8	38.0
2.0	2.0	1.0	0.96	28.3	29.3	46.3
2.0	2.0	2.0	1.89	13.8	15.0	21.8
2.0	2.0	5.0	4.57	5.6	6.7	9.8
2.0	2.0	10.0	8.77	2.7	3.0	5.1
2.0	0.5	5.0	4.57	5.5	6.7	9.5
2.0	1.0	5.0	4.57	5.6	6.6	9.6
2.0	2.0	5.0	4.57	5.6	6.7	9.8
2.0	4.0	5.0	4.57	5.6	6.3	9.8

$^a[H^+]$ at different $[HClO_4]$ computed from the equivalent conductance measurements.

Table 2 — Effect of Varying Dielectric Constant D, Ionic Strength μ and Addition of Product on the Rate of Oxidation at 303 K ($10^3[CAT]_0 = 10^2$ [substrate] $= 2.0$ mol dm^{-3})

CH_3OH (% v/v)	In the absence of Cl^- $10^2 k_{obs}$ (dm^3 mol^{-1} s^{-1})			In the presence of Cl^- $10^2 k_{obs}$ (dm^3 mol^{-1} s^{-1})			In the presence of Cl^- at high H^+ $10^4 k_{obs}$ (s^{-1})		
	Ala^a	Val^a	Phe^a	Ala^b	Val^b	Phe^b	Ala^c	Val^c	Phe^c
0	5.6	6.7	9.8	3.8	7.6	4.8	10.0	10.4	12.2
10	3.5	3.9	6.0	3.1	5.1	4.0	10.6	11.6	13.5
20	2.0	2.5	3.8	2.3	3.2	3.1	10.8	11.9	15.0
30	1.3	1.5	2.2	1.8	1.8	2.3	10.9	12.2	16.8
40	0.69	0.85	1.13	1.2	1.1	1.2	11.2	13.4	19.9
				μ (mol dm^{-3})					
0.2	5.6	6.7	9.8	3.8	7.6	4.8	10.0	10.4	12.2
0.4	5.6	6.5	9.8	3.9	7.6	4.9	9.9	10.3	12.2
0.5	5.6	6.5	9.8	3.8	7.5	4.8	10.0	10.4	12.2
0.75	5.5	6.6	9.8	3.9	7.6	4.8	10.0	10.5	12.3
				10^3 [PTS] (mol dm^{-3})					
1.0	5.6	6.6	9.8	3.9	7.6	4.8	10.1	10.4	12.3
2.0	5.6	6.5	9.8	3.8	7.5	4.9	10.0	10.3	12.2
5.0	5.6	6.6	9.9	3.8	7.6	4.8	10.0	10.4	12.2

$^a10^2[H^+] = 4.57$ mol dm^{-3}

$^b10^2[H^+] = 2.85$ mol dm^{-3}; $10[Cl^-] = 1.0$ mol dm^{-3}

$^c10^2[H^+] = 8.77$ mol dm^{-3}; $10[Cl^-] = 1.0$ mol dm^{-3}.

At constant $[\text{substrate}]_0$, and $[Cl^-]$ and $[H^+] = 0.03$ mol dm^{-3} pseudo-second order rate constants remained unaffected by the changes in $[CAT]_0$ (Table 3) showing second order dependence in $[CAT]_0$. However, at $[H^+] = 0.1$ mol dm^{-3}, plots of log $[CAT]_0/[CAT]$ versus time were linear for two half-lives and pseudo-first order rate constants were unaffected by changes in $[CAT]_0$. The rates at $[H^+] = 0.03$ mol dm^{-3} increased with increase in [substrate] showing nearly first order dependence in [substrate] (Tables 3 and 5). However, at $[H^+] = 0.1$ mol dm^{-3} the rates remained unaffected by the changes in either [substrate] or $[HClO_4]$ indicating zero order dependence in [substrate] and $[H^+]$ (Table 5). The rates increased with increase in $[Cl^-]$ at both $[H^+] = 0.03$ and 0.1 mol dm^{-3} and the plots of log k_{obs} versus log $[Cl^-]$ were linear with fractional slopes (Table 5) for Ala, Val and Phe indicating fractional order dependence in $[Cl^-]$.

Addition of PTS and variation in ionic strength of the medium had no significant effect on the rates at both $[H^+]$. But the rates decreased with decrease in

Table 3—Effect of Varying [Substrate]$_0$, [HClO$_4$], [CAT]$_0$ and [Cl$^-$] on the Rate of Chloride Catalysed Oxidation of Amino Acids at Low [Acid] at 303 K

[X] (mol dm^{-3})					10 k_{obs} (dm^3 mol^{-1} s^{-1})		
10^2 [substrate]$_0$	10^3 [CAT]$_0$	10^2 [HClO$_4$]	10^2 [H$^+$]*	10 [Cl$^-$]	Ala	Val	Phe
1.0	2.0	3.0	2.85	1.0	2.05	4.0	2.5
2.0	2.0	3.0	2.85	1.0	3.8	7.7	4.8
5.0	2.0	3.0	2.85	1.0	12.6	17.8	9.6
10.0	2.0	3.0	2.85	1.0	24.8	35.2	21.1
2.0	2.0	1.0	0.96	1.0	—	26.6	[illegible]
2.0	2.0	1.5	1.45	1.0	8.3	17.6	7.5
2.0	2.0	2.0	1.89	1.0	6.3	13.0	—
2.0	2.0	3.0	2.85	1.0	3.8	7.7	4.8
2.0	2.0	4.0	3.69	1.0	3.2	5.7	3.8
2.0	2.0	5.0	4.57	1.0	2.8	—	—
2.0	0.5	3.0	2.85	1.0	3.9	7.8	4.9
2.0	1.0	3.0	2.85	1.0	3.8	7.6	4.7
2.0	2.0	3.0	2.85	1.0	3.8	7.7	4.8
2.0	4.0	3.0	2.85	1.0	3.9	7.7	4.8
2.0	2.0	3.0	2.85	0.2	2.2	2.2	3.4
2.0	2.0	3.0	2.85	0.5	2.9	4.3	4.2
2.0	2.0	3.0	2.85	1.0	3.8	6.1	4.8
2.0	2.0	3.0	2.85	2.0	5.1	7.2	5.9

*[H$^+$] at different [HClO$_4$], computed from the equivalent conductance measurements.

Dr. Zakir Husain Library
JAMIA
☆ JAMIA NAGAR
New Delhi

Table 4—Effect of Varying [Substrate]$_0$, [HClO$_4$], [CAT]$_0$ and [Cl$^-$] on the Rate of Cl$^-$ Catalysed Oxidation of Amino Acids at High [Acid] at 303 K

[X] (mol dm^{-3})					10^4 k_{obs} (s^{-1})		
10^2 [substrate]$_0$	10^3 [CAT]$_0$	10^2 [HClO$_4$]	10^2 [H$^+$]*	10 [Cl$^-$]	Ala	Val	Phe
1.0	2.0	10.0	8.77	1.0	9.9	10.4	12.3
2.0	2.0	10.0	8.77	1.0	10.0	10.4	12.2
5.0	2.0	10.0	8.77	1.0	10.3	10.5	12.3
10.0	2.0	10.0	8.77	1.0	9.9	10.4	12.2
2.0	2.0	5.0	4.57	1.0	10.0	10.5	12.2
2.0	2.0	7.5	6.70	1.0	9.9	10.3	12.2
2.0	2.0	10.0	8.77	1.0	10.0	10.4	12.2
2.0	2.0	20.0	16.5	1.0	9.9	10.4	12.3
2.0	0.5	10.0	8.77	1.0	10.1	10.5	12.2
2.0	1.0	10.0	8.77	1.0	10.0	10.4	12.3
2.0	2.0	10.0	8.77	1.0	10.0	10.4	12.2
2.0	4.0	10.0	8.77	1.0	9.9	10.4	12.3
2.0	2.0	10.0	8.77	0.2	4.1	3.7	3.8
2.0	2.0	10.0	8.77	0.5	6.6	6.9	7.5
2.0	2.0	10.0	8.77	1.0	10.0	10.4	12.2
2.0	2.0	10.0	8.77	2.0	13.4	15.1	19.0

*[H$^+$] at different [HClO$_4$], computed from equivalent conductance measurements.

dielectric constant of the medium (changing the solvent composition by the addition of methanol) at [H$^+$] = 0.03 mol dm^{-3} and increased with decrease in the dielectric constant at [H$^+$] = 0.1 mol dm^{-3}. The plots of log k_{obs} versus 1/D were linear with negative and positive slopes at low and high [acid], respectively.

Activation parameters

The rates were measured at different temperatures and the activation parameters were computed from the Arrhenius plots (log k_{obs} versus 1/T and log (k_{obs}/T) versus 1/T, both in the absence and presence of Cl$^-$ (Table 5).

Mechanism of oxidation

Chloramine-T (RNClNa, where R = $CH_3C_6H_4SO_2$) is a strong electrolyte in aqueous solution and the probable reactive species in the acid solutions are RNHCl, $RNCl_2$, HOCl and possibly H_2OCl^+ in the absence of Cl$^-$ and Cl_2 in the presence of Cl$^-$ at high [H$^+$] (ref. 1, 7).

121683
25/10/...

Table 5—Kinetic and Thermodynamic Parameters for the Uncatalysed and Catalysed Oxidations of Amino Acids by CAT

orders observed in	In the absence of Cl			In the presence of Cl^- at					
	Ala	Val	Phe	[Low acid]			[High acid]		
				Ala	Val	Phe	Ala	Val	Phe
$[\text{Substrate}]_0$	1.0	1.0	1.0	1.0	1.0	0.9	0	0	0
$[H^+]$	−1.0	−1.0	−1.0	−1.0	−1.0	−1.0	0	0	0
$[CAT]_0$	2.0	2.0	2.0	2.0	2.0	2.0	1.0	1.0	1.0
$[Cl^-]$	—	—	—	0.4	0.64	0.3	0.54	0.64	0.7
Ea, kJ mol^{-1}	67.7	88.8	50.3	71.1	51.1	69.5	74.6	64.9	72.3
log A	7.3	10.9	4.5	8.5	5.3	8.3	9.9	8.2	9.5
$\Delta H^‡$, kJ mol^{-1}	65.2	86.2	47.8	68.6	48.5	67.0	72.1	62.4	69.6
$\Delta S^‡$, JK^{-1} mol^{-1}	−105.9	−36.4	−159.9	−82.9	−144.2	−86.7	−56.5	−87.9	−62.8
$\Delta G^‡$ kJ mol^{-1}	97.3	97.3	96.3	93.7	92.2	93.3	89.2	89.0	88.6

The following common mechanistic schemes have been proposed to explain the observed kinetics for the oxidation of Ala, Val and Phe by CAT in the absence and presence of Cl under varying conditions of acidity.

(a) In the absence of Cl

The second order dependence in [CAT], first order in [substrate] and inverse first order in $[H^+]$ may be explained through Scheme 1 which involves the following steps: (i) rapid deprotonation of amino acid cation; (ii) rapid formation of acyl hypochlorite[5] by the interaction of the oxidising species RNHCl and the carboxylate group of the amino acid; (iii) slow abstraction of hydride ion from the intermediate in the rate limiting step; and (iv) rapid decomposition of the intermediate to the products.

$$SH^+ \overset{K_1}{\rightleftharpoons} S + H^+ \qquad \text{(fast)}$$

$$S + 2RNHCl \xrightarrow{k_2} S' + 2RNH_2 \qquad \text{(slow)}$$

$$S' \xrightarrow{k_3} \text{Products} \qquad \text{(fast)}$$

Scheme 1

Scheme 1 leads to rate law (3)

$$-\frac{d[CAT]}{dt} = k_2[CAT]^2[S] = \frac{K_1 k_2 [CAT]^2 [SH^+]}{[H^+]}$$

or

$$k_{obs} = \frac{K_1 k_2 [SH^+]}{[H^+]} = k_2[S] \qquad \ldots (3)$$

In accord with the above rate law, the plots of k_{obs} versus $1/[H^+]$ and k_{obs} versus [S] were linear

(b) In the presence of chloride ion

(i) At $[H^+] = 0.03$ mol dm^{-3}:

At low $[H^+]$, effect of added Cl^- is kinetically insignificant since orders in [CAT], [substrate] and $[H^+]$ remain unaltered. Hence a mechanism (Scheme 2) similar to Scheme 1 may be operative.

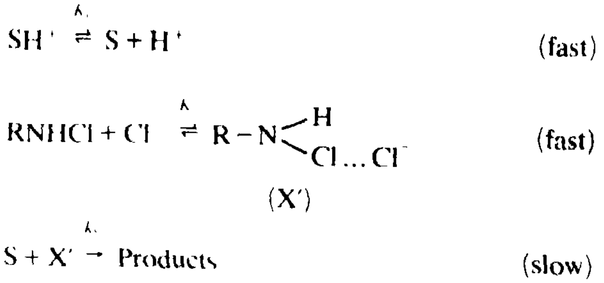

$$SH^+ \overset{K_1}{\rightleftharpoons} S + H^+ \qquad \text{(fast)}$$

$$RNHCl + Cl^- \overset{K_4}{\rightleftharpoons} R-N\begin{matrix} H \\ Cl\ldots Cl^- \end{matrix} \qquad \text{(fast)}$$

$$(X')$$

$$S + X' \xrightarrow{k_5} \text{Products} \qquad \text{(slow)}$$

Scheme 2

The corresponding rate law is given by Eq. (4).

$$-\frac{d[CAT]}{dt} = \frac{K_4^2 k_5 [S][RNHCl]_0^2 [Cl^-]^2}{\{1 + K_4[Cl^-]\}^2}$$

or

$$k_{obs} = \frac{K_4^2 k_5 [S][Cl^-]^2}{\{1 + K_4[Cl^-]\}^2}$$

$$= \frac{K_1 K_4^2 k_5 [SH^+][Cl^-]^2}{[H^+]\{1 + K_4[Cl^-]\}^2} \qquad \ldots (4)$$

The plot of k_{obs} versus [S] was linear in accordance with rate law (4).

(ii) At $[H^+] = 0.10$ mol dm^{-3}:

At high $[H^+]$ the catalytic effect of Cl^- is significant. It affects both the rate and kinetics of oxidation. The order in $[CAT]_0$ changes from second to first order and the rate becomes independent of [S] and $[H^+]$. At high $[H^+]$, CAT is present mostly in protonated form which interacts with Cl^- to give Cl_2. The latter in turn interacts with the substrate in fast steps to yield products. The mechanism similar to the ones proposed with arginine[3] and histidine[2] account for the observed results.

The proposed mechanisms are also supported by the moderate values of kinetic and thermodynamic parameters. The plots of $\Delta H^\ddagger$ versus $\Delta S^\ddagger$ were linear in all the three cases with isokinetic temperatures of 310, 323 and 303 K respectively in the absence of Cl^-, at low and high $[H^+]$. These isokinetic temperatures are closer to the temperature employed in the present investigation (303 K). Almost the same value of $\Delta G^\ddagger$ with all the three amino acids shows the operation of a similar mechanism while the negative $\Delta S^\ddagger$ indicates the formation of more ordered activated complexes.

The observed effects of dielectric constant of the medium on the rates of reactions are in conformity with Laidler-Eyring equation[9] or Amis concept[10].

Acknowledgement

One of the authors (RVR) is grateful to the Mangalore University for the award of a research fellowship.

References

1 Gowda B T & Mahadevappa D S, *J chem Soc Perkin Trans*, **2** (1983) 323 and references therein.

2 Gowda B T & (Mrs) Rao R V, *Indian J Chem*, **25A** (1986) 908; *Oxidn Commn*, **10** (1987) 31; *J chem Soc Perkin Trans*, **2** (1988) 1.

3 Gowda B T, Sherigara B S, Mahadevappa D S & Rangappa K S, *Indian J Chem*, **24A** (1985) 932.

4 Gowda B T & Sherigara B S, *Indian J Chem*, **25A** (1986) 960; *Oxidn Commn*, **9** (1986) 165.

5 *International Encyclopedia of Chemical Science* (Van Nostrand, New York) 1976.

6 Feigl F, *Spot tests in organic analysis* (Elsevier, Amsterdam) 1958.

7 Campbell M M & Johnson G, *Chem Rev*, **78** (1978) 65.

8 Gopalakrishnan G & Hogg J L, *J org Chem*, **50** (1985) 1206.

9 Laidler K J, *Chemical kinetics* (McGraw Hill, New York) 1965.

10 Amis E S, *Solvent effects on reaction rates and mechanism*, (Academic Press, New York) 1966.

Indian Journal of Chemistry
Vol. 27A, January, 1988, pp. 44-47

Synthesis & X-Ray Study of 4,4′-Bis(isoamylamino)biphenyl

N K SHARMA* & ASHA TIKU
Department of Chemistry, University of Jammu, Jammu (Tawi) 180 004
and
K N GOSWAMI & TARSAIM RAJ
Department of Physics, University of Jammu, Jammu-Tawi 180 001

Received 17 *March* 1987, *accepted* 18 *May* 1987

4,4′-Bis(isoamylamino)biphenyl has been synthesised and solid/solid modifications in this compound have been observed microscopically. Rotation and Laue photographs of the compound have been taken. Orientations (β) of crystallite and variation of orientations (β) as a function of temperature up to 95°C have been determined.

It has long been recognized that the distinctive feature of thermotropic liquid crystals formed by pure compounds is the rod-like or lath-like shape of the molecules. Mesophases composed of large plate-like molecules are also known to occur[1]. X-ray studies[2,3] indicate that some nematics are composed of groups of about 10^2 molecules called cybotactic groups. The molecular centres in each cybotactic group are arranged in layers.

In the present investigation, synthesis and X-ray studies of 4,4′-bis(isoamylamino)biphenyl have been undertaken. It is found that molecules are oriented in layers similar to that in a cybotactic group[2,3]. The crystalline order in solid state at room temperature and at higher temperatures has been investigated

Materials and Methods

4,4′-Bis(isoamylamino)biphenyl (I) was synthesised as follows: A mixture of recrystallised benzidine (18.4 g, 0.1 mol), isoamyl alcohol (150 ml) and Raney nickel[4,5] (15 g) was refluxed under constant stirring for about 15 hr. The reaction mixture was filtered, the filtrate concentrated and the residue consisting of the desired compound was purified by recrystallization from pure ethanol (charcoal. NMR (60 MHz, $CDCl_3$; TMS internal reference): δ 1.0 (9H, *t*), 1.6 (9H, *m*), 3.18 (3H, *t*), 6.78 (4H, *t*) and 7.36 (4H, *t*); MS: *m/z* 324 (M^+) (Calc: 326.56).

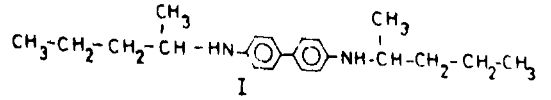

I

Melting point and different solid/solid transitions were observed with the help of a polarizing microscope provided with a microheating stage.

X-Ray study on crystals of 4,4′-bis(isoamylamino)biphenyl was carried out by rotation and Laue photographs. Flat shaped crystals were grown out of ethanol. The crystals were mounted on the goniometer head of rotation and Laue camera. The X-ray radiation used was unfiltered CuK radiation for Laue and filtered radiation CuK (Ni foil) for rotation camera. In Laue method, crystal to film distance was kept at 3.5 cm. Orientations (β) of crystallite were calculated and variation of orientations (β) as a function of temperature up to 95°C was found. Liquid crystal in solid phase undergoes phase transformations similar and work is reported by Vainshtein *et al.*[6] and Chandrasekher *et al.*[7].

Results and Discussion

4,4′-Bis(isoamylamino)biphenyl (I) showed solid/solid modifications at 48-49° and 85°C (see Fig. 1a, b). The compound melts sharply at 113°C confirming its purity. Liquid crystalline properties are suppressed due to its higher melting point, which is attributed to branching of the methyl group[8]. The thermal motion prevents the existence of an ordered liquid crystal after melting occurs.

The X-ray photographs taken either with Laue or rotation method are characterized by rings (Figs 2 and 3). A preferential orientation of the molecules is evident from rotation photograph (Fig. 2). Inner rings reflect layer structure of the molecules in the crystal, while the outer rings represent the higher degree of order within the layers. The Laue photograph (Fig. 3) at room temperature of the same crystal for which the rotation photograph has been taken shows a number of rings indicating high crystalline nature of the substance. Intensities of reflections have been measured by visual estimation after comparison with a standard scale. The standard scale

Fig. 1—(a) Microphotograph at 22°C (× 100); and (b) microphotograph of the same portion at 95°C (× 100)

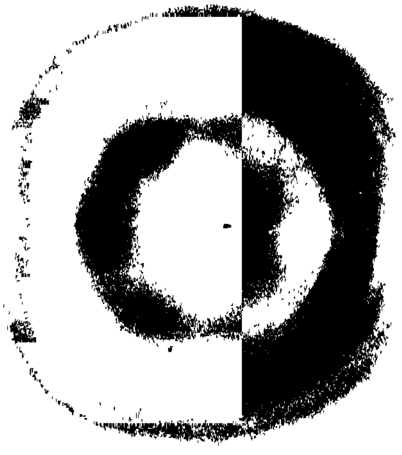

Fig. 2—Protation photograph of the sample at room temperature

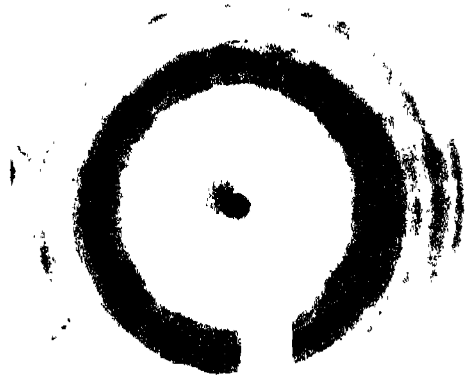

Fig. 3—Laue photograph of the same crystal at room temperature

was prepared by exposing the film for various periods of time and developing it under conditions similar to one for X-ray films. Intensities of strong spots were estimated by multiple film technique. X-ray lines with *d*-values were plotted versus their corresponding intensities at room temperature[9,10]. The *d*-values were calculated based on measurements made precisely by a device to 0.01 mm by interpolation. The high value of intensities of the lines extending over large values of diffraction angles indicate a high degree of crystalline order existing in the crystal at room temperture. The intensities of the diffraction rings show that the molecules are oriented preferentially in some directions. The orientation angles of the molecules have been measured by the relation given by de Vries[11].

$$\cos\beta = \frac{d}{L}$$

where L is the length of the molecule which in present case is 16.6 Å. Table 1 gives the *d*-values and tilt angle of the different planes in the crystal at room temperature. The X-ray patterns of oriented samples allow the direct measurement of the tilt angle. it is seen from the analysis of the photographs that molecules have tilted as well as stretched conformation.

Temperature dependence

Temperature dependence of the orientation of the layers of molecules has been analysed by heating the crystals to different temperatures. The heating was done by blowing warm air over the sample and a thermometer was kept very close to it, so that the precise temperature of the sample could be measured. The accuracy of measurement was ±0.5°. Photographs of sample heated from room tempera-

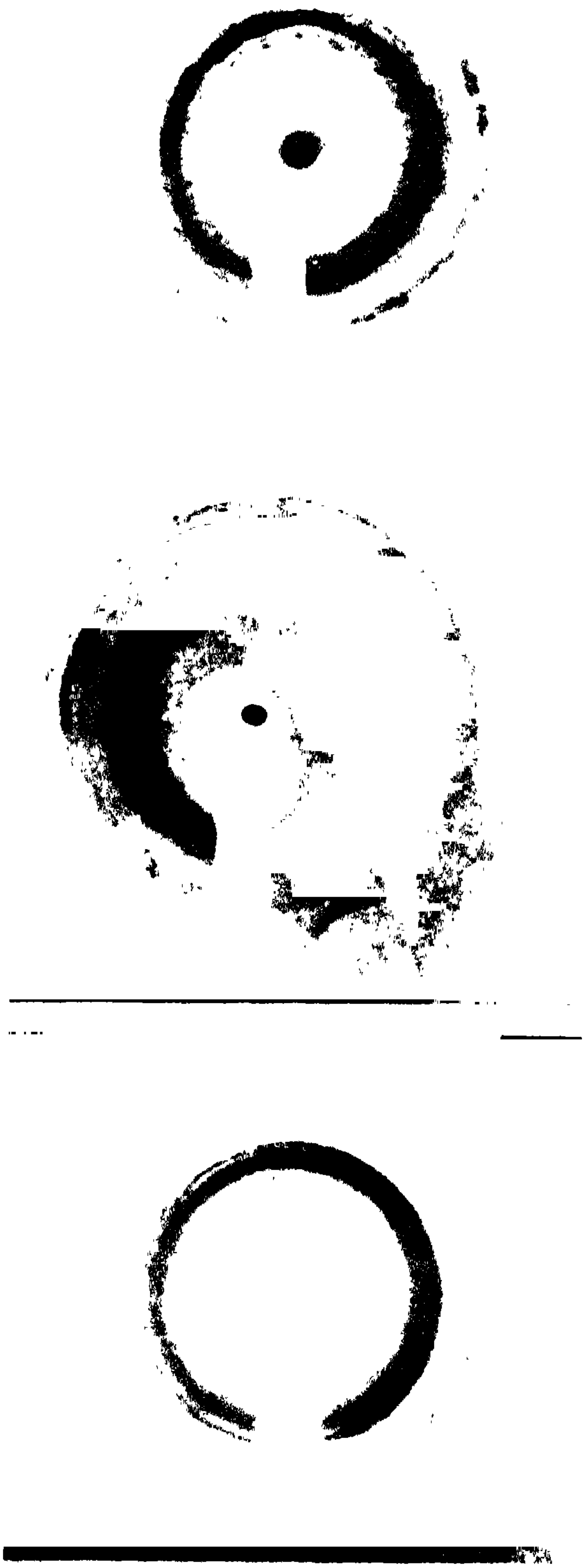

Fig. 4—Photographs of the sample (a) heated at 54°, (b) 71° and (c) 95°

Table 1—Inclination Angles and *d*-Values at 22°C

Sl No.	*d*-values at 22°C in Å	Inclination angle in degree
1	4.848	73.02
2	8.157	60.59
3	11.448	46.44
4	13.521	35.50
5	15.235	26.10
6	14.919	16.05
7	15.969	13.59
8	16.143	0
9	16.676	0

Table 2—Orientation of Layers at Various Temperatures

Temp (°C)	*d*-values	Inclination angle in degrees
22	4.848	73.02
	8.157	60.59
	11.448	46.44
	13.521	35.50
54	4.848	73.02
	7.307	63.89
	9.595	9.595
	10.855	49.23
71	4.848	73.02
	7.307	63.89
	9.595	9.595
	10.855	49.23
95	4.235	75.27
	7.204	64.34
	10.142	52.41

ture to 54°, 71° and 95°C are shown in Figs 4a-c respectively. Orientations (β) of layers at the above temperatures are given in Table 2.

It is evident from the data in Table 2 that for different *d*-values at different temperatures, β varies with temperature. The results are in agreement with the observations of Diele *et al.*[10].

At higher temperatures the crystalline patterns slowly become diffuse. Some of the rings shift their positions and merge with other rings. This indicates that at higher temperatures the crystalline order of the crystals decreases sharply. A comparison of *d*-values (interplanar distances) and intensities of reflections at 22°C (room temperature) and at 95°C indicates that *d*-values and intensities of reflection from a crystal (Fig. 4c) at 95°C are found to be different from those of crystal at 22°C (Fig. 3). This suggests that at 95°C a new phase may emerge. This is further substantiated by the fact that reflections from the new phase are diffused indicating that new phase is probably not well crystalline. As there is large variation in *d*-values and intensities of reflections of the phase at higher temperatures, it is presumed that a new phase may have nucleated. High temperature effects may not bring a change in inter planar distances and their corresponding intensities.

Acknowledgement

One of the authors (AT) wishes to thank CSIR, New Delhi for the award of a senior research fellowship.

References

1 Zimmer Z E & White J L, *Molec Cryst Liq Cryst*, **38** (1977) 177.

2 Chistyakov I G & Chalkowaky W M, *Molec Cryst Liq Cryst*, **7** (1969) 269.

3 de Vries A, *Molec Cryst Liq Cryst*, **10** (1970) 219.

4 Rice & Kohn, *J Am chem Soc*, **77** (1935) 4052.

5 Sharma N K, Weissflog W, Richter L, Diele S, Walther B, Sackmann H & Demus D, *Advances in liquid crystal research and applications*, edited by Lajos Bata (Pergamon Press, Oxford), 1980.

6 Vainshtein B K, Kosterin E A & Kamenchuck L M, *Advances in liquid crystal research and applications*, edited by Lajos Bata (Pergamon Press, Oxford), 1980.

7 Chandrasekhar S, Sadashiva B K & Suresh K A, *Pramana*, **9** (1977) 471.

8 Kelkar H & Hatz R, *Hand book of liquid crystals* (Verlag Chemie, Weinheim), 1980.

9 Doucet J, Levelut A M & Lambert M, *Acta Cryst*, **B33** (1977) 1710.

10 Diele S, Demus D, Echtermeyer A, Preukschas U & Sackmann H, *Acta Physics Polonica*, **755** (1979) 125.

11 de Vries A, *Proceedings of the International Conference on liquid crystals*, Bangalore 1973, Pramana Supplement I, P. 93, edited by Chandrasekhar S.

Indian Journal of Chemistry
Vol. 27A, January, 1988, pp. 48-51

Mixed Ligand Complexes of Copper(II) with L-Asparagine as Primary Ligand & Imidazole, Histamine & L-Histidine as Secondary Ligands

M SIVASANKARAN NAIR*
Department of Chemistry, Madurai Kamaraj University P G Extension Centre, Palaymkottai 627 002
and
B SIVASANKAR & K RENGARAJ
Department of Chemical Engineering, Anna University, A C College Campus, Madras 600 025

Received 17 *November* 1986; *revised and accepted* 11 *May* 1987

The formation constants of the mixed ligand complexes of Cu(II) with L-asparagine as the primary ligand (A) and imidazole, histamine and L-histidine as the secondary ligands (B) have been computed at 37°C and $I = 0.15$ mol dm^{-3} ($NaClO_4$). Copper(II)-asparagine (A)-imidazole (B) system shows the presence of CuAB and $CuAB_2$ mixed species in solution. The MABH and MAB types of mixed species are found to be present in Cu(II)-asparagine (A)-histamine/L-histidine (B) systems. However, the results obtained for the Cu(II)-asparagine (A)-imidazole (B) system show that imidazole prefers to add on to CuA (A = asparagine) binary complex rather than to the aquo complex of Cu(II). In this system, asparagine functions as a terdentate ligand, while in all other systems it binds the metal in a glycine-like manner. Histidine appears to bind in a histamine-like mode in Cu(II)-asparagine (A)-histidine (B) system. The extra proton in the MABH species in Cu(II)-asparagine (A)-histamine/histidine (B) systems resides in the secondary ligand (B).

The exchangeable portion of Cu(II) in blood plasma is shown to exist mainly as mixed ligand complexes asparaginato(histidinato)-, asparaginato(threoninato)-, and histidinato(threoninato)-copper(II)[1,2]. Consequently, considerable attention has been paid to structure elucidation of these mixed ligand complexes in aqueous solution[3,4]. The aqueous titration-colorimetric studies carried out by Baxter and Williams[4] at 25°C and $I = 3.00$ *M* $NaClO_4$ throw some light on the structures of these complexes. However, the same authors have opined that these high ionic strength solutions do not serve as real media for complexes occurring *in vivo*. The above studies showed that asparagine acted as intermediate between tri- and bi-dentate ligand in Cu(II)-asparagine (A)-histidine/threonine (B) mixed ligand systems. Again, histidine has been shown to coordinate to Cu(II) in the presence of asparagine and threonine with two planar amine-Cu(II) bonds and a longer axial carboxylate-Cu(II) bond. The question as to whether the carboxylate group of histidine is involved in bonding or not can easily be answered by a comparison of stability constants of histidine (with imidazole N, primary amino N and the carboxylate O atoms as the donor groups) and histamine (with imidazole N, and primary amino N atoms as the donor groups) complex systems. Further, imidazole being unidentate, investigations on the imidazole complex systems would be rewarding. With this background information, the present paper reports the results of potentiometric studies on the Cu(II)-asparagine (A)-histidine/histamine/imidazole (B) mixed ligand systems under biological conditions.

Materials and Methods

Solutions of all the ligands (Fluka, puris) dried *in vacuo* over P_2O_5 were always prepared afresh in doubly-distilled water. The methods of preparation and determination of $Cu(ClO_4)_2$ has been described elsewhere[5].

Potentiometric measurements were carried at 37°C under nitrogen atmosphere with 0.15 mol dm^{-3} ($NaClO_4$) as background electrolyte. The equipment and electrode standardisation procedures have been described elsewhere[6]. Calculations were made with the help of MINIQUAD-75 computer program[7] on an IBM-370 computer. Various models were fitted to the data and the model selected was that which gaves the best statistical fit. At high *p*H values, hydroxo complexes were often present. Since these data could not be fitted satisfactorily to any simple model, points above the onset of systematic drift in residuals were omitted. During the computation of stabilities of mixed ligand complexes, the stability constants for the binary complexes of Cu(II) with the ligands A and B estimated under identical conditions[8] were treated as non-refinable parameters. The charges of all the complexes reported in this paper are omitted for clarity.

Table 1 — Overall Formation Constants of Binary Complexes of Cu(II) with Asparagine, Imidazole, Histamine and Histidine

[Temp. = 37°C; I = 0.15 mol dm^{-3} NaClO$_4$]

Parameter	Asparagine[a]	Imidazole[b]	Histamine[b]	Histidine[b]
$\log\beta_{HB}$	8.51(3)	6.55(2)	9.39(8)	8.96(3)
$\log\beta_{H_2B}$	11.16(4)	—	15.34(1)	14.96(5)
$\log\beta_{H_3B}$	—	—	—	17.37(9)
$\log\beta_{MBH}$	—	—	13.46(4)	14.38(4)
$\log\beta_{MB}$	7.89(5)	4.21(9)	9.24(18)	10.27(2)
$\log\beta_{MB_2H_2}$	—	—	—	27.41(21)
$\log\beta_{MB_2H}$	—	—	21.82(6)	23.96(3)
$\log\beta_{MB_2}$	*14.33(6)*	*7.55(14)*	*16.16(4)*	*18.49(4)*
$\log\beta_{MB_3}$	—	10.73(16)	—	—
$\log\beta_{MB_4}$	—	12.91(24)	—	—

Standard deviations are given in the parentheses; asparagine becomes *primary ligand* (A) *in the mixed ligand systems.* (a) present investigsation; and (b) reference 8

Table 2 — Stability Constants for Copper(II)-Asparagine (A)-Imidazole, Histamine or Histidine (B) Mixed Ligand Systems

[Temp. = 37°C; I = 0.15 mol dm^{-3}, NaClO$_4$]

Parameter	Imidazole	Histamine	Histidine
$\log\beta_{MABH}$	—	21.36(13)	22.03(12)
$\log\beta_{MAB}$	12.45(1)	16.89(8)	17.12(3)
$\log\beta_{MAB_2}$	15.61(2)	—	—
pK^{H}_{MABH}	—	4.47	4.91
$\log K^{MA}_{MABH}$	—	13.47	14.14
$\log K^{MBH}_{MABH}$	—	7.90	7.65
$\Delta\log K_{MABH}$	—	+0.01	−0.24
$\log X_{MABH}$	—	—	2.32
$\log K^{MA}_{MAB}$	4.56	9.00	9.23
$\log K^{MB}_{MAB}$	8.24	7.65	6.85
$\Delta\log K_{MAB}$	+0.35	−0.24	−1.04
$\log X_{MAB}$	—	3.49	1.42
$\log K^{MAB}_{MAB_2}$	3.61	—	—
$\log K^{MB}_{MAB_2}$	8.06	—	—
$\Delta\log K_{MAB_2}$	+0.17	—	—

Results and Discussion

The protonation constants of imidazole, histamine and histidine designated as ligands (B) and the stability constants of the parent binary complexes of Cu(II) at 37°C and I = 0.15 mol dm^{-3} (NaClO$_4$) used for the computations of mixed ligand complex systems are reported elsewhere[8]. However, such data for the Cu(II)-L-asparagine (A) binary system estimated under identical experimental conditions are reported in Table 1. The logβ values obtained for 1:1 and 1:2 Cu(II)-L-asparagine complexes (Table 1) compare favourably with the values expected[3,9] for glycine-like *mode of binding of asparagine.*

The Cu(II)-asparagine (A)-histamine/histidine(B) systems showed the presence of two mixed complexes of the type MABH and MAB while Cu(II)-asparagine (A)-imidazole (B) system showed complexes of stoichiometry MAB and MAB$_2$. It may be mentioned that Baxter and Williams[4] also reported the MABH (logβ = 23.32) and MAB (logβ = 18.59) types of complexes for Cu(II)-asparagine (A)-histidine (B) mixed system at 25°C and I = 3.00 mol dm^{-3} (NaClO$_4$) and these values are in good agreement with the values obtained in the present investigation (Table 2) after giving allowance for the ionic strength and temperature changes.

Protonation in MABH complexes of Cu(II)-asparagine (A)-histamine/histidine (B) systems seem to occur at histamine or histidine moiety i.e. ligand (B). It may be noted that Cu(II)-asparagine (A) binary system does not have protonated species. A comparison of log K^{MA}_{MABH} values of 13.47 and 14.14 respectively of Cu(II)-asparagine (A)-histamine/histidine (B) systems (Table 2) with the $\log\beta_{MBH}$ values of 13.46 and 14.38 respectively for the Cu(II)-histamine/histidine (B) binary systems indicate that the extra proton in the MABH complex species in these systems resides in the respective secondary ligand (B). It has been reported that the site of protonation in MBH, MB$_2$H$_2$ or MB$_2$H binary complexes in Cu(II)-histamine/histidine (B) systems is the primary amino group of the ligand (B). A similar protonation site may be assigned to MABH complexes also since there is a close agreement between the stabilities of binary and mixed ligand complexes. A comparison of $\log\beta_{MABH}$ values of 22.03 and 21.36 for Cu(II)-asparagine (A)-histidine (B) and Cu(II)-asparagine (A)-histamine (B) respectively shows thast in the formation of MABH in the former system the carboxylate group is also taking part in binding. Baxter and Williams' results also agree with these observations[4]. Baxter and Williams indicate that the amino acid side group CO(NH$_2$) of asparagine is either weakly localized in the vicinity of one of the long axial bonds of Cu(II) or that there is a mixture of bi- and tri-dentate binding in Cu(II)-asparagine complexes. But our results show that asparagine in Cu(II)-asparagine (A)-histamine/histidine (B) mixed systems binds the metal in a glycine-like mode. This is because the log K^{MBH}_{MABH} values of 7.90 and 7.65 respectively for the above two systems are comparable with the logβ value of 7.89 for Cu-asparagine (A) complex, where asparagine binds the metal in a glycine-like mode. Thus the MABH complexes in Cu(II)-asparagine (A)-histamine/histidine (B) systems would have a square planar structure involving amino and carboxylate groups of asparagine (A) resulting in a five-membered chelate ring, and imidazole N of histamine or histidine (B), the fourth square planar position being filled by the solvent water molecule in the system with B = histamine and carboxylate group in the system with B = histidine. In both the cases, the extra proton resides on the primary amino group of histamine or histidine (B) secondary ligand. These structural features for the MABH species in the mixed system with B = histidine would result in one five and one seven membered chelate ring.

In order to explain the stabilities of MABH species, the parameters Δlog K_{MABH} and log X_{MABH} were derived[10]. On statistical grounds one expects a Δlog K value of -0.6 and log X value of $+0.6$. Values higher than these indicate greater stabilities of mixed complexes as compared to the binary analogues. The values obtained (Table 2) for both these parameters for Cu(II)-asparagine (A)-histamine/histidine (B) systems follow this trend.

The log K^{MA}_{MAB} value of 9.00 for Cu(II)-asparagine (A)-histamine (B) system is very close to the logβ value of 9.24 for the Cu(II)-histamine (B) complex indicating identical mode of binding of histamine in both the binary and mixed complexes. Similarly, the log K^{CuB}_{CuAB} value of 7.65 in this system compares favourably with the logβ_{CuA} value of 7.89 for Cu(II)-asparagine system indicating similar mode of binding of asparagine in both the binary and mixed complexes, i.e. in a glycine-like mode. Thus the CuAB species in this system would have a square planar structure involving primary amino and imidazole nitrogens of histamine and N-amino and O-carboxylate groups of asparagine. Such a representation would result in one six and one five membered chelate ring.

The log K^{MA}_{MAB} value of 9.23 for Cu(II)-asparagine (A)-histidine (B) system is one log unit lesser than the logβ_{CuB} value of 10.27 for Cu(II)-histidine (B) binary system where histidine is terdentate[8], but it compares favourably with logβ_{CuB} value of 9.24 for Cu(II)-histamine (B) system showing that histidine binds the metal in the MAB mixed species in a histamine-like manner. Again if histidine were terdentate in the MAB mixed species also as in the CuB histidine binary complex, one could expect a comparable value of log K^{MB}_{MAB} ($=$ logβ_{MAB} $-$ logβ_{MB}) and logβ_{MA}. But, the value obtained for the former parameter is nearly one log unit lesser than the latter (Tables 1 and 2). This lesser value does not imply that asparagine is monodentate in the mixed species because the value expected in such a case should be closer to 2 or 4 log units depending on its coordination via carboxyl or primary amino group[3]. So asparagine should be bidentate in the mixed species also as in the Cu(II)-asparagine (A) binary species. The lower log K^{MB}_{MAB} values are due to the fact that for computing it the logβ_{MB} value used is that for the terdentate binding of histidine in its binary species though it is bidentate in the mixed species, MAB as pointed out elsewhere in the paper. All these considerations indicate that the MAB species in Cu(II)-asparagine (A)-histidine (B) system would have a square planar structures as that in the Cu(II)-aspragine (A)-histamine (B) system. It may be mentioned that Baxter and Williams[4] described the MAB species in the Cu(II)-asparagine (A)-histidine (B) system to be six-coordinated where both the ligands were terdentate.

The parameter Δlog K_{MAB} obtained for Cu(II)-asparagine (A)-histamine (B) system is higher than the statistically expected values[10] indicating the enhanced stabilities of the MAB mixed species. However, the value obtained for this parameter in the Cu(II)-asparagine (A)-histidine (B) is less than the statistically expected value of -0.6 indicating thast the mixed ligand complex formation is less preferred. But, if one takes into account that there is a difference in the mode of coordination of histidine in the binary species where it is terdentate and MAB mixed species where it is bidentate, it becomes clear that the resulting computed value

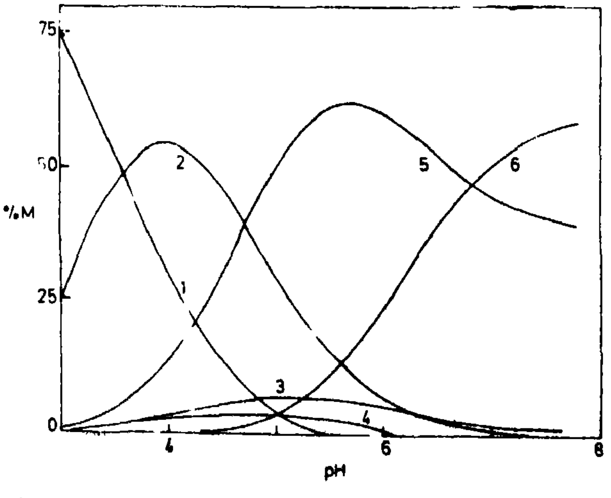

Fig. 1 — Species distribution for Cu(II)-asparagine (A)-imidazole (B) system at metal:A:B ratio of 1:1:2. [(1) unbound metal (2) MA; (3) MA_2; (4) MB; (5) MAB; and (6) MAB_2. The species MB_2, MB_3 and MB_4 are not shown because of their very low concentrations]

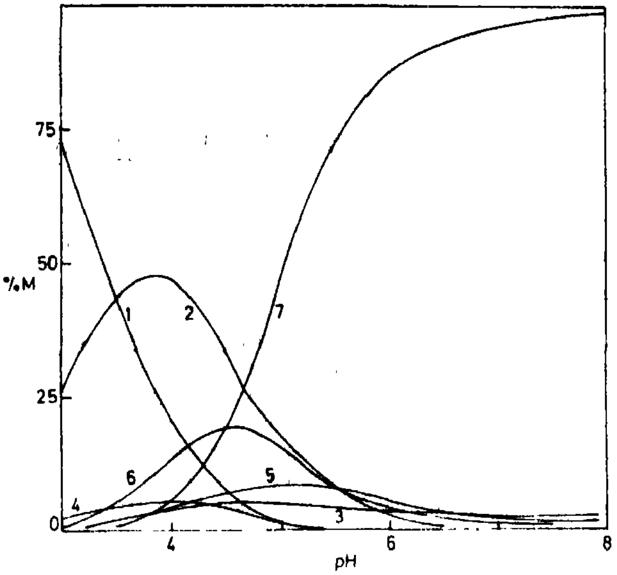

Fig. 2—Species distribution for Cu(II)-asparagine (A)-histamine (B) system at metal:A:B ratio of 1:1:1. [(1) unbound metal; (2) MA; (3) MA_2; (4) MBH; (5) MB; (6) MABH; and (7) MAB]. The species MB_2H and MB_2 are not shown because of their very low concentrations]

of $\Delta\log K_{MAB}$ should be greater than the statistically expected value[10]. Similar instances are also reported in literature[6,10].

The log X_{MAB} values obtained for Cu(II)-asparagine (A)-histamine/histidine (B) systems (Table 2) are higher than the statistically expected value of + 0.6 indicating their marked stabilities[10].

The positive $\Delta\log K$ values of 0.35 and 0.17 respectively obtained for MAB and MAB_2 complexes Cu(II)-asparagine (A)-imidazole (B) system indicate that the ligand imidazole (B) prefers to add on to Cu(II)-asparagine (A) binary complex rather than to the aquo complex of Cu(II). Again, the magnitude of these values indicate that the MAB species is relatively more stable than MAB_2 species in this system. The literature data[5] show that relative stabilities of $CuAB_2$ and CuAB mixed ligand species of Cu(II)-primary ligand (A)-imidazole (B) are highly influenced by the size of the chelate ring formed by the primary ligand (A) i.e. the $CuAB_2$ complexes would be more stable than CuAB if the primary ligand (A) forms a five-membered chelate ring and the reverse would be the trend if the primary ligand (A) forms a six-membered chelate ring or more than one chelate ring. In the light of this observation the higher stability observed for CuAB compared to that of $CuAB_2$ in the Cu(II)-asparagine (A)-imidazole (B) system may be accounted by considering the terdentate mode of binding of asparagine resulting in two five-membered rings. The terdentate binding of asparagine in CuAB and $CuAB_2$ complexes becomes more clear if it is noted that log K^{CuB}_{CuAB} and log K^{CuB}_{CuAB2} values (Table 2) are 0.6 log units higher than $\log_{CuA}$ value of 7.89 in the Cu(II)-asparagine (A) binary system, where asparagine binds the metal in a glycine-like mode.

The distribution of various binary and mixed complexes (as percentages of total metal) as a function of *p*H has been computed for all the systems under study. Formation of MABH complexes in the Cu(II)-asparagine (A)-histamine/histidine (B) systems are favoured in the *p*H range 3.5-6 and with rise in *p*H the formation of the MAB species favoured. The high statistical stability of the mixed ligand complex formation is also reflected in species distribution plots. For e.g. in the Cu(II)-asparagine-histamine system, ca. 95% of the total metal is present in the form of MAB mixed species, though on statistical grounds the MAB formation is expected to be only 50%. The species distribution plots obtained for the Cu(II)-asparagine (A)-imidazole (B) and Cu(II)-asparagine (A)-histamine (B) systems are given in Figs. 1 and 2. The diagram for Cu(II)-asparagine (A)-histidine (B) system showed the same qualitative features as in Figs 1 and 2.

References

1 Sarkar B & Kruck T P A, *The biochemistry of copper*, edited by J Pesiach, P Aisem & W E Blumberg (Academic Press, New York), 1966.

2 Sarkar B in Vol 12 of *Metal ions in biological systems* edited by H Sigel (Marcel Dekker, New York and Basel), 1981.

3 Sillen L G & Martel A E, *Stability constants of metal ion complexes*: Special Publication Nos 17 & 25 (The Chemical Society, London), 1964 & 1971.

4 Baxter A C & Williams D R, *J chem Soc Dalton Trans*, (1975) 1757.

5 Nair M S, Santappa M & Murugan P K, *Inorg Chem*, **21** (1982) 142.

6 Nair M S, Pillai M S & Ramalingam S K, *J chem Soc Dalton Trans*, (1986) 1.

7 Gans P, Vacca & Sabatini A, *Inorg chim Acta*, **18** (1976) 237.

8 Nair M S, Santappa M & Natarajan P, *J chem Soc Dalton Trans*, (1980) 1312.

9 Sigel H, *IUPAC coordination chemistry*-20 edited by D Banerjea (Pergamon Press, Oxford) 1980, p 27.

10 Nair M S, *J chem Soc Dalton Trans*, (1982) 561.

Indian Journal of Chemistry
Vol. 27A, January, 1988, pp. 52-55

Pd(II) & Pt(IV) Complexes with Some Bi-, Tri- & Tetra-dentate Ligands

N RAMA RAO[†] & M C GANORKAR[*][†]
Department of Chemistry, Nizam College, Osmania University, Hyderabad 500 001

Received 1 *December* 1986; *revised and accepted* 26 *May* 1987

Palladium(II) and platinum(IV) halides react with dehydroacetic acid (DHA) and its schiff bases derived from benzoylhydrazine (DBH), thiosemicarbazide (DTS), 2-aminoethanethiol (DHA 2-AET) and ethylenediamine (DHAEN) to form stable complexes. The molar conductance, magnetic moment and spectral data of the complexes suggest square-planar and octahedral stereochemistries around Pd(II) and Pt(IV) ions, respectively. Analytical data reveal that metal to ligand stoichiometry is 1:1 (except for DHA complex). Molecular weight determinations show that all the complexes except Pd(II)-DTS and Pd(II)-DHA2-AET complexes are monomeric. Pd(II)-DTS and Pd(II)-DHA2-AET are dimers. The presence of coordinated water in Pt(IV) complexes has been substantiated by thermal studies (TG & DT).

The complexing behaviour of Pd(II) and Pt(IV) ions with heterocyclic systems containing nitrogen and sulphur atoms has been extensively studied because of the antitumour activity associated with these complexes[1-5]. However, the chelating ability of oxygen heterocyclic compounds towards these ions has received very little attention.

Dehydroacetic acid [3-acetyl-6-methyl-2*H*-pyran-2,4(3*H*)-dione], henceforth abbreviated as DHA, is one of the oxygen heterocyclics which has been reported to be an excellent chelating agent and possesses fungicidal, bacteriocidal, herbicidal and insecticidal activities[6,7]. We report here the synthesis and characterisation of Pd(II) and Pt(IV) complexes with DHA and its schiff bases derived from benzoylhydrazine (DBH), thiosemicarbazide (DTS), 2-aminoethanethiol (DHA2-AET) and ethylenediamine (DHAEN).

Materials and Methods

All the chemicals used were of AR grade. DHA was a Fluka reagent. Chloroplatinic acid ($H_2PtCl_6 \cdot nH_2O$) was used for the preparation of Pt(IV) complexes.

The ligands DBH, DTS, DHA2-AET and DHAEN were prepared as reported earlier[7-9].

Preparation of Pd(II) complexes

To a hot solution of $PdCl_2$ (1 mmol) in absolute ethanol (25 ml) containing a few drops of HCl, the respective ligand (1 mmol; 2 mmol in case of DHA) solution in ethanol (50 ml) was added dropwise with constant stirring. An yellowish coloured product separated out immediately; the reaction mixture was digested on a water-bath for 30 min. The solid complexes were filtered off, washed with ethanol followed by pet. ether (60 to 80°) and dried *in vacuo.*

Preparation of Pt(IV) complexes

An aqueous solution of chloroplatinic acid (1 mmol) was added to a solution of the respective ligand (1 mmol; 2 mmol in case of DHA) in ethanol (50 ml). The yellow coloured products were precipitated instantaneously; these were digested for 30 min on a water-bath. The complexes were filtered, washed with water, ethanol followed by pet. ether (60-80°) and dried *in vacuo.*

Elemental, TG and DT analyses, magnetic susceptibility, IR and electronic spectral measurements of the complexes were carried out as reported earlier[10]. Far IR spectra of the complexes were recorded on a Polytech FIR-30 instrument in nujol mull in the range 650-100 cm^{-1}. Molecular weight determinations of the complexes were carried out by the Rast method[11] using diphenyl as the solvent.

Results and Discussion

All the Pd(II) and Pt(IV) complexes are yellowish in colour and stable towards air and moisture. They decompose at higher temperatures. They are insoluble in water and common organic solvents but soluble in DMF, DMSO and dioxane.

Analytical data (Table 1) reveal that metal to ligand stoichiometry is 1:1 in the complexes of BDH, DTS, DHA2-AET and DHAEN while that in the complexes of DHA is 1:2. The molar conductance values of these complexes (4.5-31.0 ohm^{-1} cm^2 mol^{-1}) in 10^{-3} *M* DMF solutions show their non-electrolytic nature. But in the case of Pt(IV)-DHAEN complex, the Λ_M value is 75 ohm^{-1} cm^2 mol^{-1} suggesting its 1:1 electrolytic behaviour. Molecular weight measurements (Table 1) indicate that all the complexes except

---

[†] Present address: The Birla Institute of Scientific Research, Asmangadh Palace, Malakpet, Hyderabad 500 036

Table 1—Characterisation Data of Pd(II) & Pt(IV) Complexes

Compound	Found (Calc.), %						Mol. Wt
	M	C	H	N	S	Cl	Found (Calc.)
[Pd(DHA)$_2$]	23.95	43.47	3.04	—	—	—	425.71
	(24.16)	(43.60)	(3.18)				(440.40)
[Pd(Cl)(DBH)]	24.67	42.28	2.93	6.61	—	8.27	441.20
	(24.93)	(42.17)	(3.05)	(6.56)		(8.31)	(426.90)
[Pd(DTS)]$_2$	30.71	31.08	2.55	12.23	9.17	—	681.36
	(30.80)	(31.27)	(2.61)	(12.16)	(9.26)		(690.80)
[Pd(DHA2-AET)]$_2$	32.20	36.17	3.26	4.44	9.52	—	646.55
	(32.11)	(36.21)	(3.32)	(4.22)	(9.66)		(662.80)
[Pd(DHAEN)]	22.78	46.36	3.92	6.11	—	—	473.19
	(22.91)	(46.51)	(3.88)	(6.03)			(464.40)
[Pt(Cl)$_2$(DHA)$_2$]	32.41	31.89	2.30	—	—	11.75	610.87
	(32.52)	(32.00)	(2.33)			(11.82)	(600.09)
[Pt(Cl)$_3$(DBH)]	33.11	30.48	2.17	4.91	—	18.02	571.39
	(33.27)	(30.69)	(2.22)	(4.77)		(18.13)	(586.59)
[Pt(Cl)$_2$(DTS)(H$_2$O)]	37.11	20.49	2.06	7.95	6.23	13.74	526.45
	(37.33)	(20.65)	(2.10)	(8.03)	(6.12)	(13.56)	(523.09)
[Pt(Cl)$_2$(DHA2-AET)(H$_2$O)]	38.19	23.41	2.40	2.93	6.35	14.01	515.68
	(38.33)	(23.58)	(2.55)	(2.75)	(6.29)	(13.93)	(509.09)
[Pt(Cl)(DHAEN)(H$_2$O)]Cl	31.05	33.25	3.44	4.67	—	11.62	637.85
	(30.38)	(33.64)	(3.11)	(4.36)		(11.05)	(642.09)

Pd(II)-DTS and Pd(II)-DHA2-AET complexes are mononuclear species. The values in case of Pd(II)-DTS and Pd(II)-DHA2-AET complexes are very close to those expected for dinuclear complexes. All the complexes were found to be diamagnetic.

The IR spectrum of the ligand, DHA, is characterised by strong bands at 3030, 1710, 1640 and 1260 cm^{-1} which are attributed to vO – H (hydrogen-bonded), vC = O (lactone carbonyl), vC = O of C$_3$-acetyl and vC – O (phenolic), respectively. The absence of vO – H (phenolic) peak in the spectra of metal complexes indicates the deprotonation of phenolic OH and participation of phenolic oxygen in coordination[12]. This is further confirmed by an upward shift in vC – O (phenolic) to the extent of 20-25 cm^{-1}. The vC = O at C$_3$-position goes downward by 15-20 cm^{-1} in the spectra of complexes, revealing its involvement in complexation[12]. No change is observed in vC = O (lactone carbonyl) and vC – O – C modes, indicating their non-involvement in coordination. The new absorption bands of medium intensity at 530 and 560 cm^{-1} are assigned to vPd – O and vPt – O, respectively[13]. A strong peak observed at 320 cm^{-1} in Pt(IV)-DHA is assigned to vPt – Cl.

The broad peaks at 3375 and 3360 cm^{-1}, and a sharp peak at 3500 cm^{-1} are due to intramolecularly H-bonded vO – H and free vO – H, respectively[7,9], in the spectra of DBH, DTS and DHA2-AET. The disappearance of these bands in the spectra of complexes indicates the cleavage of H-bond with subsequent deprotonation and participation of phenolic oxygen in coordination. The lowering of vC = O of hydrazide moiety from 1630 cm^{-1} in DBH to 1610 cm^{-1} in the complexes suggests its participation in complexation[14]. The absence of a band due to vC = S at 1175 cm^{-1} in DTS and the appearance of a new band at 1620 cm^{-1}, which is a characteristic of a vC = N absorption, in the complexes indicate the conversion of ligand from thione to thiol form during complexation[15]. The absence of vS – H bands in the range 2600-2500 cm^{-1} in the complexes of DTS and DHA2-AET shows the deprotonation of SH and participation in coordination[16] of sulphur. This is further supported by the lowering of vC – S to the extent of 15-20 cm^{-1} from the ligand position at 640 cm^{-1}. A downward shift in vC = N of azomethine groups by 20-30 cm^{-1} in the complexes suggests that nitrogen atom of azomethine group is involved in complexation[17]. Broad absorption in the range 3400-3200 cm^{-1} in the spectra of Pt(IV)-DTS and Pt(IV)-DHA2-AET complexes is due to vO – H of coordinated water. The medium to strong absorption bands at 510-560, 420-460, 375-410 and 310-330 cm^{-1} are assigned to vM – O, vM – N, vM – S and vM – Cl modes, respectively[18,19].

No band is observed in the range 2900-2850 cm^{-1} in the spectra of complexes of DHAEN, suggesting the cleavage of intramolecularly H-bonded O – H[20] with subsequent deprotonation and coordination through phenolic oxygen. A red shift in vC = N of azomethine groups by 20-25 cm^{-1} from 1650 cm^{-1} in the ligand shows the involvement of both the nitrogen

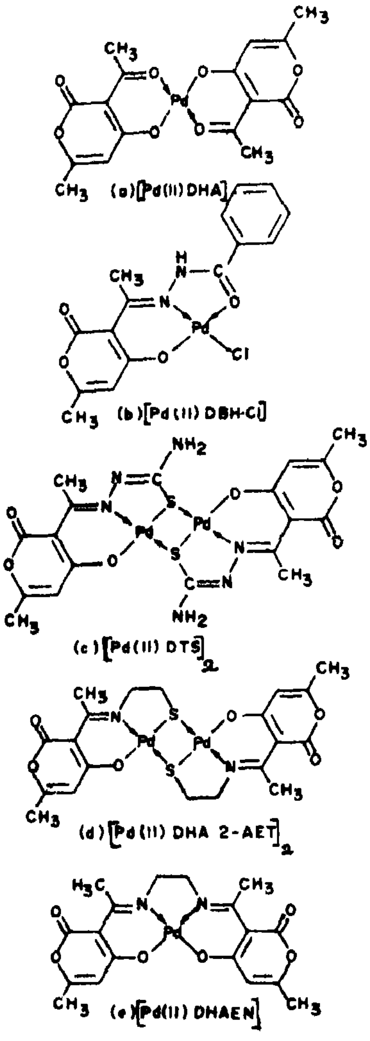

I(a-e). STRUCTURES OF Pd(II) COMPLEXES

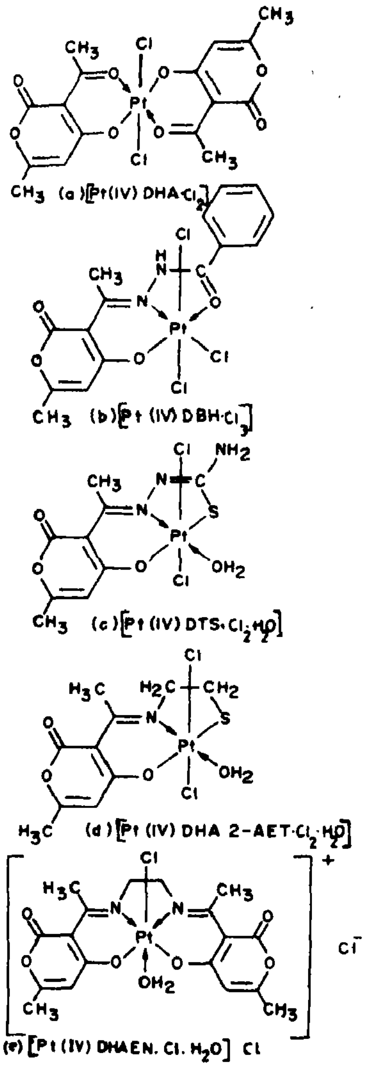

II(a-e) STRUCTURES OF Pt(IV) COMPLEXES

atoms in coordination[17]. The presence of a broad band at 3400 cm^{-1} in Pt(IV)-DHAEN is due to νOH of coordinated water. The νM−O, νM−N and νPt−Cl modes are observed at 505-530, 465-470 and 330 cm^{-1} respectively[13,18].

From the IR studies of the complexes, it has been concluded that DHA, DBH, DTS/DHA2-AET and DHAEN act in monobasic bidentate (O:O donors), monobasic tridentate (O:N:O donors), dibasic tridentate (O:N:S donors) and dibasic tetradentate (O:N:N:O donors) manner, respectively.

The presence of coordinated water in Pt(IV)-DTS, Pt(IV)-DHA2-AET and Pt(IV)-DHAEN complexes was further established by T G and D T analyses. In TG analysis, the percent mass loss is equivalent to one coordinated water molecule per mole of complex and occurs as a single step process in the temperature ranges 140-150, 162-170 and 150-165° in the complexes of DTS, DHA2-AET and DHAEN, respectively. The mass losses in the ranges 210-220 and 190-210°C approximately correspond to loss of sulphur atoms present in the complexes of DTS and DHA 2-AET. In DT analysis, the endothermic peaks at 150 and 220°C in DTS complexes, at 170 and 210°C in DHA2-AET complex and at 165°C in DHAEN complex have been observed. The endothermic peaks at 150, 170 and 165°C are attributed to the presence of coordinated water molecules while the endotherms at 220 and 210°C are due to the extrusion[19] of sulphur atoms in the ligands. Above 300°C, the complexes are decomposed into metal oxides.

Electronic spectra of the complexes

The electronic spectra of Pd(II) complexes exhibit three bands in the ranges 17391-17543, 25000-27777 and 31250-32258 cm^{-1} which are assigned to $^1A_{2g} \leftarrow {}^1A_{1g}$, $^1B_{1g} \leftarrow {}^1A_{1g}$ and $^1E_g \leftarrow {}^1A_{1g}$ transitions, respectively[16,19]. The spectra of Pt(IV) complexes show three absorption bands in the ranges 16393-18000, 23500-26000 and 27000-31250 cm^{-1} which are attributed to ${}^1T_{1g} \leftarrow {}^1A_{1g}$, ${}^3T_{1g} \leftarrow {}^1A_{1g}$ and ${}^3T_{2g} \leftarrow {}^1A_{1g}$ transitions, respectively[21,22].

On the basis of conductance, magnetic moment and spectral data, it is suggested that Pd(II) complexes have square-planar structures (I a-e) and Pt(IV) complexes have octahedral structures (II a-e).

Preliminary studies on the physiological activity of Pd(II) and Pt(IV) complexes with these ligands have been carried out and promising results have been obtained. This part of the study will be published separately in a relevant journal.

Acknowledgement

One of the authors (N R R) is highly indebted to CSIR, New Delhi, for financial assistance.

References

1 Cleare M J & Hoeschele J D, *Platinum Metal Rev*, **17** (1973) 2.
2 Saha N & Kar S K, *J inorg nucl Chem*, **40** (1977) 195.
3 Singh P P, Seth J N & Khan S A, *Inorg nucl Chem Lett*, **11** (1975) 525.
4 Rosenberg B, Van Camp L, Trosko J E & Mansour V N, *Nature*, **222** (1969) 385.
5 Rosenberg B & Van Camp L, *Cancer Res*, **30** (1970) 1799.
6 Surya Rao D, Subba Rao B L, John V T & Ganorkar M C, *Nat Acad Sci Lett*, **1** (1978) 402.
7 Surya Rao D, Sadasiva Reddy C, John V T & Ganorkar M C, *Curr Sci*, **49** (1980) 511.
8 Rama Rao N, Raju V J T, Venkateswar Rao P & Ganorkar M C, *Nat Acad Sci Lett*, **8** (1985) 343.
9 Rama Rao N, Venkateswar Rao P, Venkat Reddy G & Ganorkar M C, *Indian J Chem*, in Press (1986).
10 Rama Rao N, Venkateswar Rao P, Raju V J T & Ganorkar M C, *Indian J Chem*, **24A** (1985) 877.
11 Mann F G & Saunders B C, *Practical organic chemistry* (Longmans, London), 1961, 435.
12 Rama Rao N, Surya Rao D & Ganorkar M C, *Indian J Chem*, **21A** (1982) 839.
13 Nakamoto K, *Infrared spectra of inorganic and coordination compounds* (Wiley Interscience, New York), 1970, 167, 159, 214.
14 Syamal A & Kale K S, *Indian J Chem*, **16A** (1978) 46.
15 Tyaga Raju V T, Ranbaore Vilas, Atre Vasudha & Ganorkar M C, *J Indian chem Soc*, **59** (1982) 199.
16 Rastogi V K, Katiyar A K, Saxena R C & Kotnak A K, *J Indian chem Soc*, **60** (1983) 694.
17 Shukla P R & Takrao Renu, *Indian J Chem*, **20A** (1981) 305.
18 Sandhu S S, Tandon S S & Singh H, *Transition Met Chem*, **5** (1980) 333.
19 Sandhu S S, Tandon S S & Singh H, *Indian J Chem*, **22A** (1983) 867.
20 Rana A K & Shah J R, *J Indian chem Soc*, **58** (1981) 1100.
21 Sinha V K, Srivastava M N & Nigam H L, *Indian J Chem*, **22A** (1983) 348.
22 Syamal A & Gupta B K, *Indian J Chem*, **22A** (1983) 620.

Indian Journal of Chemistry
Vol. 27A, January, 1988, pp. 56-57

Solvent Effect on the Dipole Moments of Some N-Substituted Maleimides

MAGDI M NAOUM*, MOHAMED M ABDEL-MOTELEB & SAMIA M WAHBA
Department of Chemistry, Faculty of Science, University of Cairo, Giza, Egypt

Received 10 *November* 1986; *revised and accepted* 29 *June* 1987

Dipole moments of six N-substituted maleimides have been determined in benzene and dioxane at 30°C. The apparent solution moments obtained in benzene are found to be significantly higher than those determined in dioxane indicating a strong solute-solvent interaction in the former case.

Solute-solvent interactions in the maleimide molecule and its N-substituted derivatives have been intensively studied by Bryce-Smith *et al.*[1,2] using the NMR technique. The large upfield shifts of the ethylenic protons for the maleic anhydride and maleimide molecules were attributed to a 1:1 exospecific association of the solute and the benzene molecules. So, it seemed worthwhile to determine the dipole moments of some N-aryl derivatives of maleimide in benzene and another non-polar solvent, namely dioxane, in order to compare molecular interactions of maleimides with different non-polar solvents.

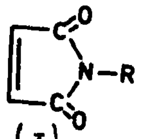

(I)

(a) R = C_6H_5; (b) R = 2-ClC_6H_4; (c) R = 4-ClC_6H_4.
(d) R = 4-$NO_2C_6H_4$; (e) R = 2-$CH_3C_6H_4$; (f) R = 1-naphthyl.

N-Arylmaleimides (Ia-f) were prepared according to the procedure originally developed by Searle[3]. The products prepared were crystallized twice from ethanol and dried *in vacuo*. The melting points and spectral analyses of the compounds were in satisfactory agreement with the literature values[3].

Benzene and dioxane (BDH) were purified according to recommended procedures[4]. Dilute solutions of the maleimides Ia-f in benzene and dioxane were prepared with weight fractions ranging from 10^{-3} to 10^{-2}. The dielectric constants, densities, and refractive indices were measured at 30°C, and the calculations of dipole moments were made as described earlier[5].

On the basis of precisions in the measurements of dielectric constants (±0.0005), densities (±0.0001), refractive indices (±0.0001), and solution concentrations (±0.02%), the dipole moment values obtained are believed reliable to ±0.03 D.

Polarization and dipole moment data of N-arylmaleimides (Ia-f) in benzene and dioxane at 30°C are summarized in Table 1. The average values of the dipole moments obtained by the Hedestrand[6] and the Guggenheim[7] methods in both solvents and the dipole moment difference ($\Delta\mu$) are collected in Table 2.

As is observed from Table 2, the dipole moments of compounds Ia-f are markedly higher in benzene than those in dioxane. These findings confirm specific association between the maleimide and the benzene molecules. The order in which the difference ($\Delta\mu = \mu_{benzene} - \mu_{dioxane}$) decreases is: $I_d > I_b > I_a > I_c > I_e > I_f$.

NMR spectral measurements made by Bryce-Smith *et al.*[8] on solutions of N-substituted maleimides in carbon tetrachloride and benzene showed large solvent-induced chemical shifts ($\Delta = \delta_{CCl_4} - \delta_{C_6H_6}$) for the solute ethylenic protons. Their results were confirmed by UV spectral evidence[9] which showed that complexation occurred with the aromatic solvent.

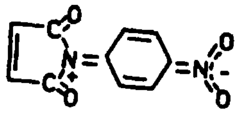

It is well known that the ethylenic double bond in the imide ring of the maleimide molecule is an electron deficient site, mainly due to the presence of the two active electron-acceptor CO groups in the same ring. The electrophilic character of the ethylenic bond might be affected by the nature and location of the substituent present in the phenyl group (Ib-Ie). Thus, for the *p*-nitrophenyl derivatives (Id), the electron deficiency of the ethylenic bond is increased owing to the *p*-quinonoid structure formation in which the lone pair of electrons on the imide nitrogen atom are given to the double bond connecting the phenyl group. This in turn leads to a stronger interaction between the ethylenic bond and the π-electron cloud of the benzene molecule, so that $\Delta\mu$ for this compound

Table 1 — Polarization Data from Measurements on N-Arylmaleimides (Ia-f) at 30°C

Comp.	$D^{P}2$ (cm^3)	Hedestrand				Guggenheim		
		$P_{2\infty}$	α	β	μ	$(\Delta/W_2)_{W_2\to 0}$	γ	μ
				In Benzene				
Ia	63.21	163.98	3.65	0.206	2.23	3.188	0.460	2.26
Ib	72.96	242.28	4.91	0.256	2.88	4.43	0.484	2.92
Ic	78.83	304.27	6.42	0.218	3.33	5.87	0.547	3.36
Id	72.56	1024.03	23.74	0.334	6.84	23.17	0.569	6.84
Ie	57.83	129.93	2.36	0.229	1.88	2.13	0.224	1.92
If	78.87	175.36	2.86	0.256	2.18	2.38	0.471	2.23
				In Dioxane				
Ia	50.45	96.38	1.97	0.170	1.49	1.712	0.257	1.49
Ib	56.54	114.77	2.11	0.283	1.69	1.713	0.398	1.69
Ic	58.38	220.23	4.98	0.171	2.82	4.962	0.024	2.90
Id	63.01	615.37	15.71	0.198	5.50	15.501	0.205	5.50
Ie	46.30	102.61	1.98	0.219	1.59	1.643	0.338	1.58
If	61.84	133.02	2.12	0.134	1.87	1.934	0.190	1.87

would be greater than that for the parent unsubstituted phenyl compound (Ia) as is experimentally observed. Also, the measured μ of this compound in benzene would be (as is the case) greater than that measured in dioxane. On this basis, the difference $\Delta\mu = \mu_{benzene} - \mu_{dioxane}$ can be wholly attributed to the π-interaction with the benzene molecule.

For the *p*-chloro derivatives (Ic), the mesomeric effect associated with the lone pair of electrons on the chlorine atom is slightly more than to be outweighed by the inductive effect. Consequently, the electrophilic character of the ethylenic bond would be deaccentuated with respect to that of the N-phenylmaleimide (Ia). This is borne out by the observation that Δμ of the *p*-chloro derivative is only 0.48 D compared to 0.75 D for Ia.

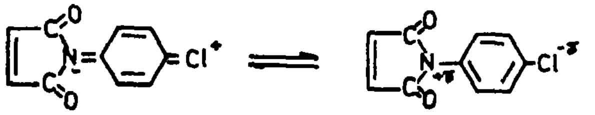

Owing to steric considerations, the phenyl ring would be more or less non-planar with the imide ring for the compound 2-chlorophenyl maleimide (Ib), and consequently, the inductive effect will be the only factor leading to a residual negative charge on the chlorine atom and an equivalent positive charge on the imide nitrogen. As a consequence of such effect, the electrophilic character of the ethylenic bond will increase, so that stronger specific interaction with the benzene molecule might be anticipated; that is to say, Δμ for the 2-chloro derivative would be much higher than that for the 4-chloro derivative. This is in harmony with the results obtained, the values of Δμ of the 2- and 4-chloro derivatives being 1.21 and 0.48 D, respectively.

Table 2 — Average Dipole Moments Measured in Benzene and Dioxane and Their Difference (Δμ)

Compound	$\mu_{dioxane}$	$\mu_{benzene}$	$\Delta\mu$
Ia	1.49	2.24	0.75
Ib	1.69	2.90	1.21
Ic	2.86	3.34	0.48
Id	5.50	6.84	1.34
Ie	1.58	1.90	0.32
If	1.88	2.20	0.32

Conversely, the electron donating character of the methyl substituent in Ie, and the steric interactions of the 2-methylphenyl and 1-naphthyl substituents in Ie and If, respectively, which lead to the non-planarity with the rest of the molecule, decrease the extent of the residual positive charge on the imide nitrogen. Consequently Δμ is expected to be smaller for Ie and If as can be seen from Table 2.

References

1 Bryce-Smith D, Connett B E & Gilbert A, *J chem Soc*, **B** (1968) 816.
2 Bryce-Smith D & Hems A, *J chem Soc*, **B** (1968) 812.
3 Searle N E, *US Patent*, 2,144,536, July 6, 1948; Wahba S M M, Ph D Thesis, Cairo University, 1983.
4 Weissberger A & Proskauer F, *Organic solvent, physical constants and methods of purification* (The Clarendon Press, Oxford), 1955.
5 Tourky A R, Rizk H A & Girgis Y M, *J phys Chem*, **64** (1964) 739.
6 Hedestrand G, *Z phys Chem*, **B2** (1929) 428.
7 Guggenheim E A, *Trans Faraday Soc*, **45** (1949) 714.
8 Bryce-Smith D & Hems A, *Tetrahedron Lett*, (1966) 1895.
9 Brand W G, *Trans Faraday Soc*, **49** (1953); Andrews L J & Keefer R M, *J Am chem Soc*, **75** (1953) 3776.

Indian Journal of Chemistry
Vol. 27A, January, 1988, pp. 58-59

Polarographic Reduction of Furfural Semicarbazone

R VENUGOPAL SETTY†, V SURYANARAYANA RAO & S BRAHMAJI RAO*

Department of Chemistry, Sri Krishnadevaraya University, Anantapur 515 003

Received 31 *December* 1986; *revised* 25 *March* 1987; *accepted* 20 *April* 1987

Polarographic reduction of furfural semicarbazone in acid media is diffusion-controlled and occurs via protonation, at different sites in the heterocyclic ring. While protonation at C-3 leads to the ring-cleaved product, protonation at C-5 gives reduction product with furan ring in tact.

Zuman and Fleet[1] studied the polarographic reduction of a wide variety of semicarbazones of carbonyl compounds except that of furfural semicarbazone. This and many of its derivatives such as nitrofurfural semicarbazone find wide applications in the manufacture of antiseptic ointments. Semicarbazones have also been used in our laboratories for the polarographic determination of transition metal ions. This prompted us to undertake the title investigation.

The furfural semicarbazone was prepared[2] in the laboratory and recrystallised from aq. ethanol, m.p. 200-201° (lit m.p. 202°). All other chemicals used were of AR grade and wherever necessary purified using standard procedures. Polarograms were recorded at 30° ± 0.1°C employing DC pen recording polarograph (ELICO Private Limited, Hyderabad). A Lingane type of H-cell with SCE in the narrow limb was employed and the d.m.e. had the following characteristics: $\tau = 3.0$ s; $m = 1.93$ mg S^{-1}, $h = 85$ cm at 0.0 V (vs SCE in water).

The effect of varying *p*H on the $E_{1/2}$ in buffered solutions (sodium acetate + hydrochloric acid, *p*H 1 to 3; sodium acetate + acetic acid, *p*H 4 to 7; and ammonium chloride + ammonia solution, *p*H 8 to 10) has been studied. A single wave is observed in the *p*H range 1 to 10 and $E_{1/2}$ varies linearly with *p*H in the range 1 to 7 (Table 1). The effects of the height of mercury column and concentration of the depolariser on wave height indicate that the wave is diffusion-controlled. Semi-logarithmic analysis of the polarogram shows the irreversible nature of the wave. As is expected, the reduction of semicarbazone occurs at more positive potentials than that of furfural. It is known that semicarbazones undergo four-electron reductive cleavage in general. But many instances are reported[3,4-7] where the limiting current does not correspond to the number of electrons consumed in the reductive process. Such systems have been classified into four types.

Table 1—Effect of *p*H on $E_{1/2}$ and Wave Height

*p*H	$-E_{1/2}$ (V vs SCE)	Wave height (cm)	α_n
1	0.72	11.6	1.03
2	0.80	14.2	1.03
3	0.88	15.0	1.03
4	0.96	14.5	1.03
5	1.05	14.2	1.03
6	1.12	12.2	1.03
7	1.22	6.9	1.03
8	1.63	10.5*	—
9	1.65	9.0*	—
10	1.68	8.5*	—

*Waves are ill-defined and approximate values are given.

Table 2—Effect of Varying Hydrochloric Acid Concentration on $E_{1/2}$ and Wave Height in Unbuffered KCl Solutions

[KCl] = 0.1 *M*; [FAS] = 1×10^{-3} *M*; [HCl] = 1×10^{-2} *M*; total volume = 25 ml

Volume of HCl (ml)	*p*H (measured)	$-E_{1/2}$ (V vs SCE)	Wave height (cm)
1.0	3.99	0.94	1.8
1.5	3.71	0.94	3.8
2.0	3.56	0.94	5.4
2.5	3.44	0.94	7.2
3.0	3.37	0.94	9.1
4.0	3.24	0.94	11.7
5.0	3.10	0.94	15.8
7.0	2.96	0.94	16.4
8.0	2.89	0.92	16.5
10.0	2.79	0.91	16.2
15.0	2.62	0.89	15.8

(i) Where the maximum value of the limiting current is not reached due to the protonation equilibrium not being fully attained under the experimental conditions; (ii) where the semicarbazide derivatives ($RR'CHNHNHCONH_2$) are formed in increasing proportion during reduction; (iii) where a substituent such as $-NH_2$, a group in the depolariser is susceptible to facile protonation; and (iv) where simultaneous reduction of bi- and mono-protonated forms is possible.

---

†Lecturer in Chemistry, SCNR Government College, Proddatur, AP.

In the present study the limiting current in buffered solutions is less than that observed in acid solutions. The protonation as mentioned in (i) above thus plays a significant role since the substrate under investigation can undergo protonation at different sities in the heterocyclic ring and each protonated form might have a different susceptibility[8] to reduction.

Gharst and Schmir[9] reported that furan derivatives substituted at 2-position are susceptible to protonation at C-3 and C-5. However, species protonated at C-5 alone preserves the furan ring in tact to a larger extent, while that at C-3 brings about cleavage of the furan ring to give an aliphatic product in aqueous acid solutions. The aliphatic intermediate ($OHC.CH_2.CH_2.CH_2.CH=NH$) in acid solutions undergo hydration and is transformed into the electro-inactive [$OHC.CH_2.CH_2.CH_2.C(OH)NH_2^+$] species[10]. It is possible this aliphatic aldehyde wave is responsible for the diminished limiting current in buffered solution. The observed polarogram in acid solutions (pH > 3) is therefore ascribed to the reduction of the species protonated at 5-position (route-B in Scheme 1).

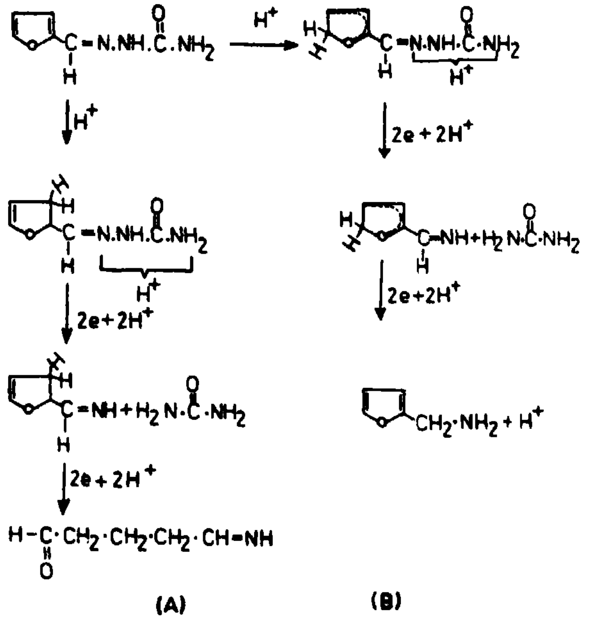

Scheme 1

In strongly acidic solutions, the wave heights are high (Table 2). This is ascribed to the polarographic reduction of species protonated at 3-position. The larger currents are due to the further reduction of the aliphatic aldehyde formed (route-A in Scheme 1).

The authors are thankful to the authorities of Sri Krishnadevaraya University, Anantapur for providing facilities. One of the authors (RVS) is grateful to the Principal, Government College, Anantapur and the Director of Higher Eduction, Hyderabad for deputation.

References

1 Zuman P & Fleet B, *Topics in organic polarography*, (Plenum Press, New York) 1970, 369.
2 Vogel A I, *A text book of practical organic chemistry*, (ELBS Longmans Green, London) Sect III, 74.2, p 344.
3 Kitajev Yu P & Budnikov G K, *Z Obsch Chim*, **33** (1963) 1396.
4 Haas J W, Storey J D & Lynch C C, *Anal Chem*, **34** (1962) 145.
5 Asahi Y, *Chem Pharm Bull*(Tokyo), **11** (1963) 930.
6 Lund H, *Acta Chem Scand*, **13** (1959) 249.
7 Coulson D M, *Anal Chim Acta*, **19** (1958) 284.
8 Zuman P & Fleet B, *Topics in organic polarography*, (Plenum Press, New York) 1970, 384.
9 Garst, John E & Schmir Gaston L, *J org Chem*, **39** (1974) 2920.
10 Zuman P & Fleet B, *Topics in organic polarography*, (Plenum Press, New York) 1970, 386.

Indian Journal of Chemistry
Vol. 27A, January, 1988, p. 60

Reaction of Dianion from Benzil-4,4'-dimethyldianil with Molybdenum Hexacarbonyl Leading to a Dianilinostilbene Complex

(Mrs) GEETA SINGH & K N MEHROTRA*
Department of Chemistry, Banaras Hindu University,
Varanasi 21 005

Received 19 *January* 1987; *revised and accepted* 5 *March* 1987

Substituted tetracarbonyl-[1, 2-di-(4-methylanilino)stilbene]-molybdenum-4,4'-dimethyldianil (**1**) with sodium in THF and motion of benzil-4,4'-dimethyldianil (**1**) with sodium in THF and molybdenum hexacarbonyl.

The cyclisation reaction of dianil dianions with carbon disulphide[1], ethyl chloroformate[1], 1, 4-, 1, 5-alkanes[2] and dichlorophosphate[3] prompted us to investigate the reaction of the dianion of benzil-4, 4'-dimethyldianil with molybdenum hexacarbonyl.

Benzil-4,4'-dimethyl dianil (**1**) and sodium in dry THF were heated to reflux for 5 hr under nitrogen atmosphere. Unreacted sodium pieces were removed by filtration and a solution of molybdenum hexacarbonyl in dry THF was added to the filtrate dropwise. The mixture was heated under reflux for 6 hr, worked up as usual and the crude compound was purified by washing with *n*-hexane. This compound was characterised as tetracarbonyl-[1, 2-di-(4-methylanilino)-stilbene]molybdenum (0) complex (**2**) on the basis of elemental analyses and spectral data. The complex **2**, (80%), m.p. 152° (Found N, 4.16; Mo, 15.63, $C_{32}H_{26}N_2MoO_4$ requires N, 4.68; Mo, 16.05) exhibited in its IR spectrum in nujol peaks at 3265 (νNH), 2010, 1925, 1910, 1850 (νC ≡ 0)[4], 1610(νC = C) cm^{-1}. Its UV/visible spectrum in ethanol displayed maxima at 370 (ε5927) and 579 nm (ε 15805) assignable to $d \leftarrow d$ and $b_2^{\bullet} \rightarrow b$ metal to ligand charge transfer transitions, respectively. The PMR spectrum of the complex **2** exhibited signals at δ 2.26 (*m*, 6H, $2XCH_3$), 3.92 (*s*, 2H, NH, D_2O exchangeable), 7.39 (*m*, 18H, arom). The complex **2** was diamagnetic, monomeric (mol. wt: found 586) (cryscopic method in benzene, calc 598); MS: *m/z* 598 (M^+).

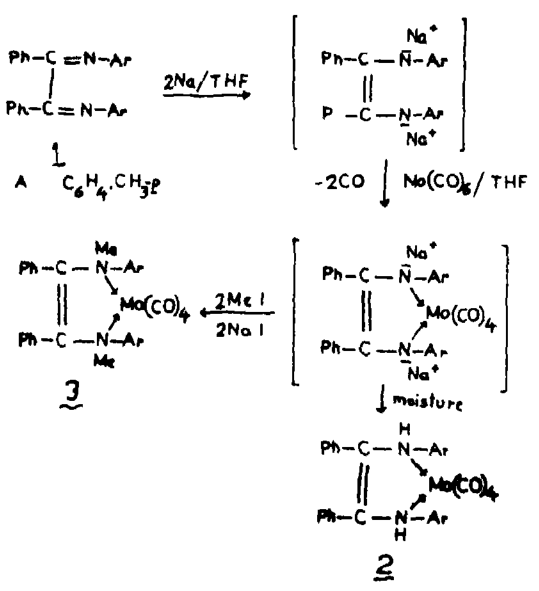

Without isolating complex (**2**), dropwise addition of methyl iodide to the reaction mixture followed by usual work-up led to a solid which was characterised as tetracarbonyl-[N, N'-dimethyl-1, 2-di-(4-methylanilino)stilbene]molybdenum(0) complex (**3**), yield 70%, m.p. 128-30° (Found N, 4.07; Mo, 15.20, $C_{34}H_{30}N_2MoO_4$ requires N, 4.47; Mo, 15.33); MS: *m/z* 626 (M^+); IR (nujol): 2010, 1980, 1920, 1850 (νC≡O)[4], 1600 (νC = C) cm^{-1}; UV/visible (ethanol): 365, 570 nm; PMR ($CDCl_3$): δ 2.22 (*m*, 12H, $4XCH_3$), 6.60 (*m*, 18H, arom). The complex **3** was also diamagnetic and monomeric (mol. wt found 626) (cryscopic method in benzene).

The synthesis involves an initial formation of dianion[1], by the electron transfer from sodium to dianil. The dianion reacts with molybdenum hexacarbonyl to give $Mo(CO)_4L$ dianion (L represents benzil-4,4'-dimethyldianil). The dianion during washing is converted into $Mo(CO)_4LH_2$. Due to strong back bonding from molybdenum to ligand, the ions of ligand may not participate in the formation of complex **2**. This is supported by the conversion of **2** into **3** on the addition of methyl iodide. Additional support to this view is provided by the observed intense solvatochromic CT band (579 nm) in the visible region in these complexes. Similar bands have been reported earlier[4].

We are thankful to the CSIR, New Delhi for the award of poolship to (Mrs) Geeta Singh.

References

1 Mehrotra K N & Singh G, *Synthesis*, (1980) 1001.
2 Singh G & Mehrotra K N, *Heterocycles*, **16** (1981) 1341.
3 Mehrotra K N, Singh I S & Roy J, *Synthesis*, (1985) 81.
4 Balk R W, Stufkens D J & Oskam A, *Inorg chim Acta*, **28** (1978) 133.

Indian Journal of Chemistry
Vol. 27A, January, 1988, pp. 61-62

NMR Study of Brominated Yttrium Acetylacetonate

G SHANKAR & S K RAMALINGAM*
School of Chemistry, Madurai Kamaraj University,
Madurai 625 021

Received 20 *October* 1986; *revised* 15 *January* 1987; *accepted* 9 *April* 1987

Bromination of Y(acac)$_3$ by NBS (where acac = acetylacetone and NBS = N-bromosuccinimide) in chloroform medium yields a bromo product. Analysis of the CMR and PMR spectra based on symmetry consideration helps in fixing the exact number of diketone rings that undergo flipping as two.

We have previously reported[1-3] the unusual phenomenon of ring flipping upon bromination of lanthanide-β-diketonates/β-ketoesters by N-bromosuccinimide (NBS). The near and far IR spectra of the reaction products exhibited bands at 1780 (νC = C), 1700 (νCO) acetyl, 1200 (νC − O) and 180 cm^{-1} (νM − Br) indicating molecular rearrangement. As it is impossible to decide the exact number of flipped diketone rings in the product from IR data only, we envisaged that the changes in the environment of ligand protons and carbons as a result of rearrangement would be reflected in ^{1}H and ^{13}C NMR chemical shifts of the reaction product, leading to identification of number of flipped rings. The results of such a study are reported in this note.

For convenience, the following nomenclature is introduced; M(AA)$_3$ refers to tris-chelate with unflipped bromoacetylacetone ring and O, O coordinating sites; M(AA)$_2$(AB) refers to chelate in which only one ring is flipped with O and Br coordinating sites; M(AA)(AB)$_2$ refers to chelate with two flipped rings; and M(AB)$_3$ refers to chelate in which all the three bromoacetylacetone rings undergo flipping with O and Br becoming the coordinating sites.

The 200 MHz PMR spectrum of Y(acac)$_3$·2H$_2$O in DMSO-d_6 exhibits only one signal due to the methyl protons at δ 1.77 (ref. 4)[4], the other signals appearing at 3.35 (H$_2$O) and 5.32 (γ − CH) [O_h or D_3 geometry neglecting water molecules]. The 50.32 MHz ^{13}C NMR spectrum of this chelate displays signals at δ 27.16 (CH$_3$)[5], 100.72 (CH) and 188.52 (C=O). The above tris-chelate of the type M(AA)$_3$ has a C_3 axis which renders each atom in each ligand ring environmentally equivalent and hence the chemical shifts inherent for a given ligand molecule would appear as such without an increase in number.

Table 1—Total Number of PMR and CMR Signals Expected and Observed for Different Configurations (Water Signals excluded)

Structure	Symmetry	Expected		Observed	
		PMR	CMR	PMR	CMR
M(AA)$_3$	C_3	1	3	—	—
M(AA)$_2$(AB)	NO C_3 NO C_2	4	11	—	—
*M(AA)(AB)$_2$ (*cis/trans*)	C_2	3	8	3	8
M(AB)$_3$ (facial)	C_3	2	5	—	—
M(AB)$_3$ (meridional)	Asymmetric	6	15	—	—

*M(AA)(AB)$_2$ in *cis* or *trans* form or even as an equilibrium mixture will have the same C_2 symmetry and hence the same number of signals.

Since the molecule M(AA)$_2$(AB) has no C_3 and C_2 axes, there will be two separate chemical shifts, one for the (AA)$_2$ part and the other for the (AB) part. In the chelate M(AA)(AB)$_2$, which can exist in *cis* and *trans* forms, the C_2 axis renders the two unsymmetrical bidentate ligands environmentally equivalent. Thus PMR or CMR chemical shifts of AB will not show an increase in the number of signals. Also the NMR spectra of the *cis* and *trans* forms will not be different.

Considering now the molecule M(AB)$_3$, which is an unsymmetrical octahedral tris-chelate, it can exist in facial and meridional forms. Facial form of M(AB)$_3$ has a characteristic C_3 symmetry making (AB)$_3$ interchangeable and hence environmentally equivalent. On the contrary, the meridional isomer is totally asymmetric and all the three ligand moieties (AB)$_3$ are environmentally non-equivalent. The spectra will therefore show an increased number of NMR signals. Thus 200 MHz PMR spectrum of Y(acac-Br)$_3$·H$_2$O in DMSO-d_6 exhibits signals at δ 1.84 (CH$_3$, six-membered ring), 2.58 (CH$_3$CO), 2.83 (CH$_3$, five-membered ring) and 3.5 (H$_2$O). The 50.32 MHz ^{13}C NMR spectrum of this chelate in DMSO-d_6 exhibits signals at δ 24.29 (CH$_3$, six-membered ring), 29.70 (CH$_3$CO), 29.89 (CH$_3$, five-membered ring), 100.74 (C − O, five-membered ring), 178.39 (C=O of CH$_3$CO), 179.61 (C=O, five-membered ring), 186.07 and 186.47 (C − Br in two different rings).

Employing a dynamic model developed by Ramalingam *et al*[6], it is possible to carry out various symmetry operations on an octahedral complex and to examine the changes in the ligand environment for different arrangements. The above discussion centres around this model and the details of such an observation are summarised in Table 1.

It is clear from Table 1 that for a chelate of the type $M(AA)(AB)_2$, the observed and expected signals agree. Thus it may be concluded that the bromo product obtained as a result of bromination of lanthanide-β-diketonates/β-ketoesters contains two flipped rings with O and Br in coordinating sites and one unflipped ring with O and O coordinating sites.

The authors are thankful to Dr. P R Srinivasan of DuPont, USA for PMR and CMR spectra. GS is thankful to the CSIR, New Delhi for the award of a senior research fellowship.

References

1 Shankar G & Ramalingam S K, *Trans Met Chem*, **9** (1984) 449.

2 Shankar G & Ramalingam S K, *Indian J Chem*, **25A** (1986) 94.

3 Shankar G & Ramalingam S K, *Indian J Chem*, **25A** (1986) 1012.

4 Dyer J R, *Applications of absorption spectroscopy of organic compounds* (Prentice Hall of India) 1984, p. 91.

5 Abraham R J & Loftus P, *Proton and Carbon-*13 *NMR Spectroscopy* (Heyden & Son, London) 1978, p. 42.

6 Ramalingam S K, Raman M, Rajaram V & Paulraj K, *Chem Edn*, **1** (1984) 29.

Indian Journal of Chemistry
Vol. 27A, January, 1988, pp. 63-65

Pyridinium Hydrobromide Perbromide as a Brominating Agent for Metal *β*-Diketonates

S ABDUL SAMATH, M RAMAN & S K RAMALINGAM*
Department of Inorganic Chemistry, Madurai Kamaraj University, Madurai 625 021

Received 30 *January* 1987; *revised* 18 *May* 1987; *accepted* 3 *June* 1987

Pyridinium hydrobromide perbromide is tried as a brominating agent for the bromination of many metal acetylacetonates. While the Cr(III) and Co(III) compounds undergo easy *γ*-bromination at room temperature, those of Co(II), Cu(II), Zn(II) and UO_2(VI) undergo chelate ring cleavage to give $[MBr_4](PyH)_2$.

The reagent pyridinium hydrobromide perbromide ($PyHBr_3$) used extensively in organic syntheses, for example, in the bromination of hindered steroid ketones[1], has surprisingly escaped the attention of inorganic chemists. In the only instance reported in a Russian work[2], it has been employed to prepare 1,5-dibromoacetyleacetone starting from cupric acetylacetonate though not for the bromination of chelate itself. We report herein bromination of acetylacetonates of Cr(III), Co(III), Co(II), Cu(II), Zn(II) and oxouranium (VI) using $PyHBr_3$.

$PyHBr_3$, m.p. 130° and the metal acetylacetonates were prepared by standard methods[1,3-5].

Bromination of acetylacetonates of Cr(III) and Co(III) was carried out as follows: To an ethanolic solution of the metal (II) acetylacetonates (0.01 mol) was added dropwise an ethanolic solution of $PyHBr_3$ (0.03 mol) with vigorous stirring. Within minutes the product precipitated out, which was filtered, washed with warm chloroform and dried *in vacuo*; yield 60% gmol. The compound analysed for [M(Br acac)$_3$] (Table 1).

Analogous reaction was attempted with the acetylacetonates of Co(II), Cu(II), Zn(II) and oxouranium (VI) in ethanol/dichloromethane/chloroform. In all these cases the solids obtained analysed for $[MBr_4]$ $(PyH)_2$ (Table 1). The compounds are hygroscopic, insoluble in benzene, chloroform, carbon tetrachloride etc., and are soluble in water, acetone, DMSO and DMF.

Preparation of brominated Co(III) chelate in acetic acid resulted in the formation of $[Co Br_4]$ $(PyH)_2$ probably due to the instability of the Co(III) chelate in this medium[6].

The filtrate, however, in the case of Cu(II) upon treatment with more of Cu(II) salt precipitated bis (1,5-dibromoacetylacetonate)copper (II) (Table 1). Attempts to prepare similar dibromo compounds of the other metal ions were unsuccessful. No solid product could be obtained from the red solutions which became dark brown and eventually black and unworkable.

Pyridinium hydrobromide perbromide ($PyHBr_3$) brominates the kinetically inert Cr(III) and Co(III) acetylacetonates to yield the usual 3-brominated solid products. In contrast, metal (II) chelates of

Table 1—Analytical and Conductance Data of $[MBr_4](PyH)_2$ and Bromo Complexes

Compound	Colour	Found (calc) %					(a) Λ_M (mho cm^{2}mol^{-1})
		M	C	H	N	Br	
$[CuBr_4](PyH)_2$	Green	11.9 (11.6)	22.5 (22.1)	2.5 (2.2)	5.3 (5.2)	59.2 (58.9)	169
$[CoBr_4](PyH)_2$	Blue	11.4 (10.9)	22.4 (22.2)	2.5 (2.3)	5.5 (5.2)	60.1 (59.5)	165
$[ZnBr_4](PyH)_2$	Pale yellow	12.4 (12.0)	22.3 (22.01)	2.4 (2.2)	5.3 (5.1)	59.2 (58.7)	171
$[UOBr_4](PyH)_2$	Yellow	36.6 (36.01)	16.4 (16.02)	1.7 (1.6)	3.9 (3.74)	43.1 (42.7)	178
$[Cu(Br_2acac)_2]$	Red	9.4 (9.3)	20.9 (20.8)	1.6 (1.7)	—	6.1 (62.3)	—
[Co(Br acac)$_3$]	Green	9.7 (9.9)	30.5 (30.4)	3.2 (3.04)	—	40.7 (40.5)	—
[Cr(Br acac)$_3$]	Green	8.6 (8.9)	30.82 (30.75)	3.21 (3.07)	—	41.2 (40.9)	—

(a) Conductances were measured in acetone on a Toshniwal bridge type CL 01/02 A; 1:2 electrolytes in acetone have conductances in the range of 155-240 ohm^{-1} cm^2 mol^{-1} (see ref. 8).

Table 2—PMR Data[a] of Brominated Products

Compound	Solvent	Pyridinium protons			Methyl protons	γ-CH
		NH	Ring	CH		
$[ZnBr_4](PyH)_2$	DMSO-d_6	8.3	8.8	9.1	—	—
$[UO_2Br_4](PyH)_2$	DMSO-d_6	7.9	8.4	9.0	—	—
$[Co(acac)_3]$	$CDCl_3$	—	—	—	2.18	5.52
$[Co(Br\,acac)_3]$	$CDCl_3$	—	—	—	2.17	—

(a) PMR spectra recorded on a 90 MHz Perkin-Elmer R 32 instrument; chemical shifts in δ scale downfield from TMS internal reference.

Co(II), Cu(II), Zn(II) and oxouranium (VI) on reaction with $PyHBr_3$ undergo chelate ring cleavage yielding altogether different solid end products, viz. $[MBr_4]\ (PyH)_2$. However, treatment of the resulting solution in the case of copper (II) with excess metal salt yields the 1,5-dibromoacetylacetone chelate.

The acetylacetonates of Cr(III) and Co(III) in their IR spectra exhibit bands[7] at 1580 ($\nu C=O$), 1500 (νC-H), 1190 (δ C-H), 785 cm^{-1} (π C-H); the spectra of the brominated products are conspicuous by the absence of these bands, indicating bromination at position-3. This is corroborated by the PMR spectrum of Co(III) product, which did not display any signal assignable to the proton at position-3 (Table 2).

The IR spectrum of $PyHBr_3$ exhibits characteristic bands at 3040-3070 ($\nu N\text{-}H^+$), 1630 (δ N-H) and 750 cm^{-1} (pyridine ring def). The spectra of the bromo compounds derived from metal (II) acetylacetonates display bands in the region 3040-3070 ($\nu N\text{-}H^+$), 1620-30 (δ N-H), 1590-1600 (ν C=N) and 745-760 cm^{-1} (pyridine ring def), confirming the presence of pyridinium moiety in the brominated products. The data also indicate that no carbonyl function is present in the products and that the electrophilic substitution has yielded an unusual product wherein there is no diketone of the starting material. Obviously this means that ring cleavage has taken place in these cases to give $[M\ Br_4]\ (PyH)_2$. The conductance data[8] favour their 1:2 electrolytic nature (Table 1); this together with the solubility characteristics are in accord with an ionic formulation.

Further the UV/vis spectra of the products derived by the bromination of metal (II) acetylacetonates exhibit three characteristic absorption bands. In the case of Co(II) product the bands occurring at the higher wavelength region are assignable to $^4T_{1g}(F) \rightarrow {}^4T_{1g}(P)$ and $^4T_{1g}(P) \rightarrow {}^4A_{2g}$ transition (Table 3). This implies a ^4T ground state for the metal ion and a tetrahedral environment around it.

Table 3—UV Data[a] of Brominated Products

Compound	Absorption maxima (cm^{-1})
$PyHBr_3$	35710, 38460, 41660
$[CuBr_4](PyH)_2$	15900, 17400, 20180
$[CoBr_4](PyH)_2$	16100, 19600, 21970
$[Cu(Br_2acac)_2]$	18600, 19800, 21970
$[Co(Bracac)_3]$	29850, 33890, 38460
$[Cr(Br(acac)_3]$	29400, 33300, 37040

(a) UV spectra were recorded on a Perkin-Elmer 402 spectrophotometer.

The PMR spectra of the bromination products of Zn(II) and oxouranium (VI) acetylacetonates (Table 2), provide further evidence for the formation of $[MBr_4]\ (PyH)_2$. Not only the signals due to the 3-methylene protons and the 2,5-dimethyl protons of the acetylacetone are absent, but also the aromatic signals due to the pyridinium ring appear.

An interesting side light is the bromination taking place at 1,5-methyl groups of acetylacetone of the Cu(II) chelate giving a 1,5-dibromo chelate (Table 1). The use of $PyHBr_3$ as a brominating agent appears advantageous over N-bromosuccinimide (NBS) because bromination using $PyHBr_3$ is faster and occurs at room temperature instead of prolonged boiling with NBS[9,10]. However the nature of the end products with $PyHBr_3$ unlike NBS, is dictated by the nature of the central metal ion.

SAS thanks the CSIR, New Delhi for the award of a junior research fellowship. The authors thank the USIC, Madurai Kamaraj University for recording of spectra and CDRI, Lucknow for elemental analyses.

References

1 Fieser L F & Fieser M, *Reagents for organic synthesis*, (John Wiley, New York), 1967, pp 967.

2 Ziemanis A & Kalvina L, *Chem Abstr*, Vol **90** (1979) 71757w

3 Charles R G & Pawlikoshi M A, *J phys Chem*, **62** (1958) 440

4 Fernalis W C, *Inorganic synthesis*, Vol 5 (McGraw Hill, New York) 1957, pp 130, 188

5 Nakomora Y & Kawaguchi S, *Bull chem Soc Japn*, **38** (1965) 954.

6 Banerjee D & Dutta Chaudhuri S, *J inorg nucl Chem*, 33 (1971) 515.

7 Kazuo Nakomoto, *Infra red & Raman spectra of inorganic & coordination compounds* (Wiley-Interscience, New York) 1977.

8 Geary W, *J coord chem Rev*, **7** (1971) 81.

9 Shankar G, Paulraj K, Balasubramanian V & Ramalingam S K, *J Indian Inst Sci*, **65(B)** (1984) 291.

10 Mehrothra R C, Bohra R & Gaur D P, *Metal β-diketonates and allied derivatives* (Academic Press, London) 1978, pp 31.

Indian Journal of Chemistry
Vol. 27A, January, 1988, pp. 66-67

Trivalent Nickel Complexes Containing Uninegative Bidentate Ligands & Bromine

(Miss) MINATI BARAL, B K KANUNGO & B PRADHAN*
Department of Chemistry, Regional Engineering College,
Rourkela 769 008

Received 4 *December* 1986; *revised and accepted* 25 *May* 1987

A series of trivalent nickel complexes of the types [Ni(AA)Br_2], [Ni$(AA)_2$Br].$2H_2O$, [Ni(AA) (BB)Br] and [Ni(AA) (BB)Br].$2H_2O$, where (AA)/(BB) is acetylacetonate (acac)/diethyldithiocarbamate (et_2dtc)/pyridine carboxylate (pyca)/dimethylglyoximate (dmg), have been isolated by oxidation of the suitable Ni(II) complex by bromine. The complexes have been characterised on the basis of their analytical, molar conductance, magnetic susceptibility, molecular weight, infrared and electronic spectral data.

Studies on Ni(III) compounds have been limited. Among the documented examples[1-6], the majority of complexes are of the type NiX_3 $(PR_3)_2$. The geometries of a few compounds have also been established through crystal structure studies[6]. It is known that the kinetic and thermodynamic stability of Ni(III) can be increased through adduct formation. In the present study attempts have been made to stabilise Ni(III) in ligand fields of varying strengths. We report here preparation and characterisation of Ni(III) complexes of the types [Ni(AA)Br_2].$2H_2O$, [Ni(AA) (BB)Br] and [Ni(AA) (BB)Br].$2H_2O$ where AA/BB are uninegative bidentate ligands, viz., acetylacetonate, diethyldithiocarbamate, pyridinecarboxylate, dimethylglyoximate. Earlier, Mishra and Ramana Rao[7] have reported some penta-coordinate complexes of Ni(III).

Preparation of complexes: [*Ni*(*acac*)$_2$*Br*].$2H_2O$ *and* [*Ni*(et_2*dtc*)Br_2]

Bromine solution in CCl_4 was added to a suspension of Ni$(acac)_2$.$2H_2O$ or Ni$(et_2dtc)_2$ in CCl_4 with constant stirring for about 0.5 hr by a magnetic stirrer, when the supernatant liquid changed to reddish brown. The products were suction filtered, washed with CCl_4, ether and dried *in vacuo*.

[*Ni*(et_2*dtc*) (*acac*)*Br*], [*Ni*(et_2*dtc*) (*pyca*)*Br*] *and* [*Ni*(et_2*dtc*) (*dmg*)*Br*].$2H_2O$

The mixed chelate complexes of Ni(II), viz., Ni(et_2dtc) (acac), Ni(et_2dtc) (pyca) and Ni(et_2dtc) (dmg).$2H_2O$ were prepared by reacting equimolar amounts of $NiCl_2$.$6H_2O$ and the ligands in ethanol medium followed by addition of ammonia solution. Bromination of these compounds was carried out as reported above. The complexes were suction filtered, washed with CCl_4, ether and dried *in vacuo*.

Nickel, sulphur and bromine were estimated as Ni$(dmg)_2$, $BaSO_4$ and AgBr, respectively[8]. The molar conductance values were measured in $\sim 10^{-3}$ *M* nitrobenzene medium using a Systronics direct reading conductivity meter - 304. The low values of molar conductance (3.8-7.3 ohm^{-1} cm^2 mol^{-1}) suggest the non-electrolytic nature of the compounds. The IR spectra were recorded in KBr on a Perkin-Elmer-577 spectrophotometer. Electronic spectra were recorded in nujol mull on an Elico CL-54D spectrophotometer. Magnetic susceptibilities were measured at room temperature by Gouy's method. Molecular weights were measured by Rast's method using biphenyl as the solvent. The oxidation state of nickel in the complexes was confirmed iodometrically by reacting the compounds with acidified KI and estimating the liberated iodine by standard $Na_2S_2O_3$ solution. Each atom of nickel was found to liberate 0.98 atom of iodine.

The elemental analyses, molar conductance, and molecular weight data of the complexes are consistent with their formulations (Table 1). Molecular weight measurement indicates that the compound [Ni(et_2dtc)Br_2] is dimeric whereas other complexes are monomeric (Table 1). The magnetic moment values of the compounds indicate the presence of one unpaired electron corresponding to low-spin Ni(III) state $(d)^7$ with $^2A_{1g}$ as the ground term[9]. The $\mu_{eff.}$ values for the three compounds, viz., [Ni$(acac)_2$Br].$2H_2O$, [Ni(et_2dtc) (pyca)Br] and [Ni(et_2dtc) (dmg)Br].$2H_2O$ are within the range expected for one unpaired electron (1.87-2.30 B.M.) whereas the values for other two compounds, viz., [Ni(et_2dtc)Br_2] and [Ni(et_2dtc) (acac)Br] are anomalously low (1.25 and 1.47 B.M.). The anomalous values may be due to an antiferromagnetic interaction as reported by Gore and Busch[10]. In addition, dimeric nature of the compound [Ni(et_2dtc)Br_2] might be responsible for further lowering of magnetic moment value.

Infrared spectra bands of the compounds indicate the uninegative bidentate coordination of all the ligands. For dithiocarbamate, the bands due to $\nu(C=N)$ and $\nu_{as}(C-S)$ appearing at 1500-1510 and 995-1000 cm^{-1}, respectively, suggest that it is bonded to the metal ion through both the sulphur atoms[11,12]. In the complexes containing acetylacetonate, bands due to $\nu(C \overset{...}{=} O)$ and $\nu(C \overset{...}{=} C)$ were obtained at 1600-1630 and 1540-1560 cm^{-1}, respectively, indicating coordination of the ligands through

Table 1—Analytical, Molecular Weight, Magnetic Moment and Electronic Spectral Data of Ni(III) Complexes

Compound (colour; M.P., °C)	Found (Calc.) %			Mol. wt Found (calc.)	μ_{eff} (B.M.)	λ_{max} (cm^{-1})
	Ni	S	Br			
[Ni(et$_2$dtc)Br$_2$]	16.2	17.5	43.0	745.9	1.25	22727, 13157, 11627
(Green; 230)	(16.0)	(17.4)	(43.6)	(366.8)		
[Ni(acac)$_2$Br].2H$_2$O	15.3	—	20.8	435.24	2.3	37037, 23809, 20618, 17064
(Greenish blue; 222)	(15.7)		(21.2)	(372.86)		
[Ni(et$_2$dtc)(acac)Br]	15.3	16.2	21.1	397.54	1.47	36714, 23809, 20618, 17064
(bottle green; 220)	(15.2)	(16.5)	(20.7)	(386.00)		
[Ni(et$_2$dtc)(pyca)Br]	14.8	15.7	18.9	486.13	1.87	37037, 24390, 20833, 17241
(Black; 225)	(14.4)	(15.9)	(19.5)	(409.00)		
[Ni(et$_2$dtc)(dmg)Br].2H$_2$O	13.5	14.1	18.6	672.99	2.0	36714, 23255, 20833, 17241
(Maroon; 250)	(13.4)	(14.6)	(18.3)	(593.9)		

both the oxygen atoms[13]. In the compound containing picolinate group, the band due to free carboxyl group at 1710 cm^{-1} was found to be absent. Other bands due to $\nu_{as}(COO^-)$ and pyridine ring (1620, 1610, 1580 cm^{-1}) were found to be present indicating the coordination of the ligand through nitrogen and oxygen atoms as suggested by Fowles *et al.*[14,15]. The νOH band due to dimethylglyoxime observed at 1670 cm^{-1} in the [Ni(et$_2$dtc)(dmg)Br].2H$_2$O complex supports its coordination through both the nitrogen atoms[15]. In the case of the two compounds containing water, a broad peak due to νOH appeared at ~3200 cm^{-1} and another peak due to δ(O−H) was observed at 1600-1620 cm^{-1} indicating the presence of water in the compounds[16]. However, absence of band at ~830 cm^{-1} in each of these compounds suggests that the water molecules are not coordinated to the metal ion.

The nujol mull electronic spectral data of the present compounds, except [Ni(et$_2$dtc)Br$_2$], show essentially the same features. The electronic absorption maxima found at ~37000, ~24000, ~20800 and ~17000 cm^{-1} (Table 1) are consistent with the assignment of penta-coordinate geometry to these low-spin Ni(III) compounds as observed by Meek *et al.*[17] also. The compound [Ni(et$_2$dtc)Br$_2$] exhibits electronic spectral bands at 22727, 13157 and 11627 cm^{-1} which indicate octahedral geometry with D_{4h} symmetry[10]. Dimerisation by coordination through both the sulphur atoms of dithiocarbamate may be occurring in this compound resulting in six-coordination. Although the assignment of correct geometry can be made only after X-ray structure determination, there will be significant distortion from the idealized geometry due to the Jahn-Teller effect.

References

1 Kreisman P, Marsh R, Peer J R & Gray H B, *J Am chem Soc*, **90** (1968) 1067.

2 Stein L, Neil J M & Alms G R, *Inorg Chem*, **8** (1969) 2472; Allen G C & Warren K D, *Inorg Chem*, **8** (1969) 1895.

3 Owen D A & Hawthorne M F, *J Am chem Soc*, **92** (1970) 3194.

4 Bour J J & Steggerda J J, *Chem Commun*, (1967) 85.

5 Barefield E K, *Chem Commun*, (1970) 552, 1718.

6 Stallick J K & Ibers J A, *Inorg Chem*, **9** (1970) 453.

7 Mishra B P & Ramana Rao D V, *J Inst Chemists (India)*, **52** (1980) 155.

8 Vogel A I, *A text book of quantitative inorganic analysis*, (ELBS & Longman, London) 1973.

9 Dyer G & Meek D W, *J Am chem Soc*, **89** (1967) 3983; Figgis B N & Lewis J, *Progr inorg Chem*, **6** (1964) 196.

10 Gore E S & Busch D H, *Inorg Chem*, **12** (1973) 1.

11 Nelson S M, *Ann Rep* (Chemical Soc, London) Sec A, 71.

12 Golding R M, Harris C M, Jessop K J & Tennat W, *Aust J Chem*, **25** (1972) 2567.

13 Graddon D P, *Coord Chem Rev*, **4** (1969) 1.

14 Drew M G B, Fowles G W A, Mathews R W & Walton R A, *J Am chem Soc*, **91** (1968) 7769.

15 Fowles G W A, Mathews R W & Walton R A, *J chem Soc A*, (1968) 1108.

16 Nakamoto K, *Infrared and Raman spectra of inorganic and coordination compounds* (John Wiley, New York) 1978, 156.

17 Meek D W, Alyea E C, Stallick J K & Ibers J A, *J Am chem Soc*, **91** (1969) 4920.

Indian Journal of Chemistry
Vol. 27A, January, 1988, pp. 68-70

Nickel(II) & Cobalt(II) Complexes of N,N-Diethylpyridine-2-carboxamide

PAMELA LYALL & GURDEV SINGH*
Department of Chemistry, Panjab University,
Chandigarh 160 014

Received 24 *February* 1987; *revised and accepted* 1 *April* 1987

The nickel(II) and cobalt(II) complexes of N,N-diethylpyridine-2-carboxamide (PDEA) have been prepared and characterized on the basis of molar conductance, magnetic moment, infrared and electronic specral data. A distorted octahedral geometry is proposed for all the complexes.

Pyridine-2-carboxamides are versatile polydentate ligands having capacity to bind metals in different modes utilizing some or all the donor sites. Substitution at the amide N would, however, result in a steric interaction of the substituent protons with the ring protons in a coordinated ligand. The concomitant hindered C-N bond rotation would, thus, render the amide N almost inactive[1,2]. As a part of our programme on the study of transition metal complexes of some derivatives of pyridine carboxamides, we report here some new complexes of N,N-diethylpyridine-2-carboxamide with bivalent nickel and cobalt.

The ligand was prepared by the reported[3] method. Infrared spectra were recorded on a PE-621 spectrophotometer. Room temperature magnetic moments of the complexes were determined by Gouy's method using $Hg[Co(CNS)_4]$ as the calibrant. Absorption spectra of solutions and diffuse reflectance spectra of solids were obtained on "Specord UV Vis" or "Beckmann DB" and "UNICAM SP 700A UV VISIBLE" spectrophotometers respectively.

The complexes were prepared by mixing ethanolic solutions of the respective metal salts with the ligand or its ethanolic solution in stoichiometric ratios. Where immediate precipitation did not occur, dried ether was added to effect the separation. The complexes were filtered, washed with ethanol and ether and dried *in vacuo*. All the complexes were isolated as light coloured solids.

Analytical data (Table 1) of all the complexes except two suggest the general formula $MX_2.2PDEA.nH_2O$, the exceptions being the cobalt(II) nitrate complex $Co(NO_3)_2 1.5PDEA.3H_2O$ and the nickel(II) nitrate complex $(Ni(NO_3)_2PDEA.2H_2O$. All complexes are stable towards light and heat. Most of them are not affected on heating upto 120°C. The complexes

Table 1 — Analytical Data of the Complexes

Complex	Colour (m.p.,°C)*	Found (Calc.)				
		Metal (%)	Anion (%)	C (%)	H (%)	N (%)
$[Co(PDEA)_2(NCS)_2]$	Peach (170)**	10.91 (11.1)	12.19 (12.05)	49.05 (49.71)	5.65 (5.28)	15.75 (15.80)
$[Co(PDEA)_2(BF_4)_2].4H_2O$	Pink (220-21)	8.96 (8.92)	– –	37.39 (36.37)	5.66 (5.45)	– –
$Co_2(PDEA)_3(NO_3)_4.6H_2O$	Pink (90-91)	11.62 (11.70)	– –	36.4 (35.7)	5.4 (5.3)	13.8 (13.88)
$[Co(PDEA)_2Br_2]$	Ochre yellow (165-66)	9.92 (10.26)	28.4 (27.8)	41.17 (41.7)	5.37 (4.8)	9.8 (9.73)
$[Co(PDEA)_2I_2]$	Yellow (206-7)	8.53 (8.81)	37.4 (37.9)	36.05 (35.8)	4.15 (4.18)	9.81 (9.73)
$[Ni(PDEA)_2(NCS)_2]$	Pale blue (240)	11.2 (11.06)	12.4 (12.06)	49.36 (49.8)	5.61 (5.28)	15.66 (15.8)
$[Ni(PDEA)(NO_3)_2(H_2O)_2]$	Blue (120-4)	14.67 (14.8)	– –	30.32 (30.22)	5.06 (4.5)	14.15 (14.10)
$[Ni(PDEA)_2I_2]$	Yellow (240)	8.76 (8.77)	37.55 (37.98)	35.67 (35.89)	4.0 (4.18)	8.28 (8.37)
$[Ni(PDEA)_2(BF_4)_2].2H_2O$	Blue (225)	9.44 (9.45)	– –	38.7 (38.4)	5.18 (5.12)	– –

*Melting points are uncorrected.
**Decomposition occurs

Table 2 — Magnetic Moment, Molar Conductance and Electronic Spectral Data of the PDEA Complexes with Cobalt(II) and Nickel(II)

S.No.	Complex	μ_{eff} (B.M.)	Molar conductance (ohm $^{-1}$ cm^2 mol $^{-1}$)	Electronic spectral bands (kK)	
				Solid State	Solution
1.	$[Co(PDEA)_2(NCS)_2]$		25.9^{a}; 237.4^{b}; 134.3^{c}; 33.9^{d}		
	Peach isomer	4.7		19.0, 17.4, 10.0, 6.0	21.0^{*}, 19.0^{*}, 17.8^{*}, 16.0^{a}
	Mixture(?)$^{4'}$	4.8		19.0, 17.4, 10.0, 7.7, 6.7, 5.9	
	Blue isomer	4.8		19.4, 17.4, 16.0, 10.0, 8.0, 6.4	
2.	$[Co(PDEA)_2(BF_4)_2].4H_2O$	4.8	62.5^{a}; 22.4^{c}	28.5, 21.0, 9.1 (broad)	19.5^{c}
3.	$[Co(PDEA)_3][Co(NO_3)_4(H_2O)_2].4H_2O$**	4.9	39.1^{a}; 124.2^{c}	19.0, 15.6^{*}, 8.7, 6.5	21.2^{*}, 19.4^{a}
4-	$[Co(PDEA)_2Br_2]$	5.5	240.1^{b}; 186.5^{c}; 85.4^{d}	18.8, 10.0, 6.1	17.3, 15.0, 13.0^{c}
5.	$[Co(PDEA)_2I_2]$	5.1	61.5^{a}; 263.3^{b}; 123.1^{d}	18.1, 10.0, 7.7, 5.9	19.5^{a}; ca. 16.0^{c}
6.	$[Ni(PDEA)_2(NCS)_2]$	3.2	26.5^{d}	20.1, 17.2, 15.2, 10.0, 5.9	—
7.	$[Ni(PDEA)(NO_3)_2(H_2O)_2]$	3.3	60.9^{a}; 160.3^{c}	17.4^{*}, 14.4, 9.1	25.0, 15.0^{c}
8.	$[Ni(PDEA)_2I_2]$	3.2	63.2^{a}; 165.0^{c}	25.0, 17.3^{*}, 14.8, 8.0, 6.5	24.0^{a}, 15.8^{a}, 15.5^{c}
9.	$[Ni(PDEA)_2(BF_4)_2].2H_2O$	3.5	53.3^{a}; 177.3^{c}	17.4, 14.8, 11.1	—

Medium: a - ethanol; b - water; c - acetonitrile; d - nitromethane; *Shoulder; **One of the three possible structures.

are soluble in almost all common organic solvents, but dissolution is accompanied by change in colour which indicates dissociation or solvolysis. Molecular weight determinations were consequently not carried out. The molar conductance values were inconsistent showing electrical behaviour varying from non-ionic to ionic(1:2), thus corroborating the occurrence of dissociation or solovolysis. On the basis of IR data of NCS and NO_3 groups (discussed later) it would be reasonable to assume that the compounds are non-ionic. The only exception is the $Co(NO_3)_2 1.5PDEA.3H_2O$ complex which behaves as a 1:1 electrolyte in all the solvents studied.

The infrared spectra of all the complexes reveal that PDEA, which contains three potential donor atoms, behaves as a bidentate ligand coordinating through its pyridine ring nitrogen and carbonyl oxygen atoms. The three characteristic vibrational modes of the heterocyclic and aromatic parts of the ligand, 1,6a and 16a show the expected upward shifts[4,5] on complex formation. These together with the lowering of free ligand band at 1620 cm^{-1}, assignable to νC=O, provide evidence for the assignment of probable coordination sites. The two thiocyanate complexes show C-N stretching bands within the generally accepted range (2105-2040 cm^{-1}) characteristic of terminally N-bonded NCS groups[6]. In the complex $Co(PDEA)_2(NCS)_2$, νC-N can be seen as a very strong band at 2070 cm^{-1} while in $[Ni(PDEA)_2(NCS)_2]$ νC-N appears as a pair of very closely spaced bands at 2085 and 2080 cm^{-1} and suggests that the N-coordinated NCS groups are probably *cis* to each other. Strong bands observed at 1420 and 1295 cm^{-1} in both the nitrate complexes, $Co_2(PDEA)_3(NO_3)_4.6H_2O$ and $[Ni(PDEA)(NO_3)_2(H_2O)_2]$, undoubtedly suggest monodentate nature of nitrato groups.

The observed magnetic moments (Table 2) are quite comparable to those expected for distorted octahedral geometry. The diffuse reflectance spectra have been recorded in the 30-5 kK region. In the cobalt(II) thiocyanate complex, which is peach coloured at room temperature, the two closely spaced bands at 19 and 17.4 kK (Fig.1) merging with the stronger ligand absorptions at higher energy can be assigned to the $^4T_{1g}(P) \leftarrow {}^4T_{1g}(F)$ transition in an approximately octahedral crystal field. The intense band seen at 10 kK and a weak but sharp band at 6 kK may be attributed to the split components of the $^4T_{2g}(F) \leftarrow {}^4T_{1g}(F)$ transition. This compound turns bluish even on the application of slight pressure as in grinding. The spectrum of the blue form shows two intense absorptions at 16 and 8 kK. While the positions and band contours differ from those of the octahedral peach isomer, they compare well with the spectra of some five-coordinat-

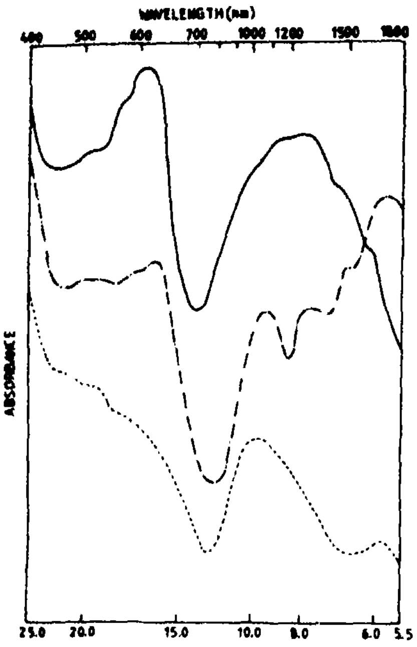

Fig. 1—Diffuse reflectance spectra of the $[Co(PDE)_2(NCS)_2]$ complex {(——) blue isomer; (– – –) mixture; (-----) peach isomer}

ed complexes whose structures have been determined by X-ray analysis[8,9].

All the other cobalt(II) complexes show the diffuse reflectance spectra consistent with that expected for a distorted octahedral environment. The solution spectra, however, are different indicating that the molecular entities in the solid and solution states do not remain essentially the same. The solution spectrum of the cobalt(II) nitrate complex in acetonitrile, however, is similar to the solid state spectrum, indicating that in this case the species are unchanged. The facts that this complex is a 1:1 electrolyte containing unidentate nitrate groups, and its electronic spectrum indicates a distorted octahedral geometry can best be explained on the basis of a cationic-anionic binuclear species of the type, $[CoL_3][Co(NO_3)_4(H_2O)_2].4H_2O$ or $[CoL_2(NO_3)_2][CoL(NO_3)_2(H_2O)_2].4H_2O$ or $[CoL_2(H_2O)_2][CoL(NO_3)_4].4H_2O$.

The diffuse reflectance spectra of the nickel(II) complexes bear a close resemblance in profile and band positions to those of octahedral nickel(II) complexes, except that there is considerable splitting of bands. The low energy bands at 5.9 and 10 kK may be arising due to the splitting of the $^3T_{2g}$ state in O_h symmetry and may be assigned to the transition from $^3A_{2g}$ level to the split components of $^3T_{2g}$ level. Of the group of bands observed at 15.2, 17.2 and 20.4 kK, the former two can be ascribed to the splitting of the $^3T_{1g}(F)$ state, while the latter may arise from a spin-forbidden band due to $'E_g('D)$ or $^1A_1('G)$ state[10]. In the nickel(II) iodide complex, the low energy v_1 band is split into two components and the v_2/v_1 ratio (1.8-1.9), being greater than the usual values for octahedral complexes, suggest a tetragonally distorted octahedral configuration for the complex. The spectra of the other two complexes also are typical of octahedral nickel(II) complexes.

References

1 Nonoyama M & Yamasaki K, *Inorg chim Acta*, **3** (1969) 585.
2 Uhlig E & Neugenbauer V, *Z anorg Chem*, **351** (1967) 286.
3 Swain A P & Naegle S K, *J Am chem Soc*, **79** (1957) 5250.
4 Nagaño K, Kinoshita H & Hirakawa A, *Chem pharm Bull, Japan*, **12** (1964) 1198.
5 Gill N S, Nuttall R H, Scaife D E & Sharp D W A, *J inorg nucl Chem*, **18** (1961) 79.
6 Chamberlain M M & Bailar Jr J C, *J Am chem Soc*, **81** (1959) 6412.
7 Curtis N F & Curtis Y, *Inorg Chem*, **4** (1965) 804.
8 Lions F, Dance L G, Lewis J, *J chem Soc(A)*, (1967) 565.
9 Ciampolini M & Speroni G P, *Inorg Chem*, **5** (1966) 45.
10 Rowley D A & Drago R S, *Inorg Chem*, **6** (1967) 1092.

Indian Journal of Chemistry
Vol. 27A, January, 1988, pp. 71-72

Anionic Complexes of Organotin(IV) with Onium Hydrochlorides

T N SRIVASTAVA*, M A SIDDIQUI & S K SRIVASTAVA
Chemistry Department, University of Lucknow, Lucknow 226 007

Received 17 *March* 1987; *revised and accepted* 11 *May* 1987

Some anionic complexes of the types $[RNH]^+[Ph_3SnCl_2]^-$ and $[RNH]^+[Ph_2SnCl_3]^-$ of Ph_3SnCl and Ph_2SnCl_2 respectively with onium hydrochlorides (RN = pyridine, aniline, quinoline, α- and β-naphthylamines and β- and γ-picolines) have been prepared and characterised. The complexes show appreciable antimicrobial activity.

Organotin(IV) halo or pseudohalo anions of tetraalkylammonium salts have been reported by several workers[1-9]. Denny Cook[10] isolated the anionic complexes of Sn(IV) halides with pyridinium salts. Similar reactions of organotin(IV) halides with onium salts have not been examined. This communication describes the interaction of organotin(IV) chlorides with $[RNH]^+Cl^-$[RN = aniline ($C_6H_5NH_2$), pyridine (C_5H_5N), quinoline (C_9H_7N), α- and β- naphthylamine (α-, β- $C_{10}H_9N$) and β- and γ-picoline (β- and γ-C_6H_7N)].

All operations were carried out under dry nitrogen atmosphere. Ph_3SnCl, Ph_2SnCl_2 and onium hydrochlorides were prepared by standard methods. Typical experiments for preparation of the complexes are as follows:

Preparation of $[C_5H_5NH]^+[Ph_3SnCl_2]^-$

To a solution of Ph_3SnCl (1.16 g, 3 mmol) in absolute methanol (~ 20 ml) was added a solution of C_5H_5NHCl (0.35 g, 3 mmol) in the same solvent (~ 20 ml) and the mixture refluxed for ~ 5 hr. After cooling, the solution was concentrated under reduced pressure, treated with excess pet ether (50-80°) and triturated. The crystalline solid which separated out was filtered off, washed several times with pet ether (60-80°) and recrystallised from absolute methanol.

Preparation of $[C_5H_5NH]^+[Ph_2SnCl_3]^-$

The complex was precipitated by adding a solution of C_5H_5NHCl (0.35 g, 3 mmol) in dry methanol (~ 20 ml) to a well stirred solution of Ph_2SnCl_2 (1.03 g, 3 mmol) in the same solvent (~ 20 ml). The mixture was stirred for 2-3 hr, filtered, the resulting solid washed with dry methanol and dried *in vacuo*.

Table 1—Analytical Data of Anionic Complexes of Organotin(IV)

Complex	m.p. °C	Found % (Calc)				Molar conductance (ohm⁻¹cm²mol⁻¹)	Mol wt found (calc)
		Sn	C	H	N		
$[C_5H_5NH]^+[Ph_3SnCl_2]^-$	156	23.7	54.7	4.2	2.7	103.4	239.6
		(23.6)	(55.1)	(4.1)	(2.5)		(500.7)
$[C_5H_5NH]^+[Ph_2SnCl_3]$	152	25.9	45.6	3.4	3.2	111.3	227.3
		(26.4)	(45.4)	(3.5)	(3.1)		(459.2)
$[C_6H_5NH_3]^+[Ph_3SnCl_2]$	78	23.5	56.0	4.3	2.7	99.6	321.8
		(23.0)	(55.9)	(4.4)	(2.7)		(514.7)
$[C_6H_5NH_3]^+[Ph_2SnCl_3]$	180	24.8	45.5	3.7	2.7	90.5	278.4
		(25.0)	(45.6)	(3.8)	(2.7)		(473.2)
$[C_9H_7NH]^+[Ph_3SnCl_2]$	135	21.3	58.7	4.0	2.4	100.2	305.9
		(21.5)	(58.8)	(4.1)	(2.5)		(550.7)
$[α\text{-}C_{10}H_9NH]^+[Ph_3SnCl_2]$	90	21.0	60.0	4.3	2.3	94.8	313.7
		(21.0)	(59.5)	(4.4)	(2.4)		(564.7)
$[β\text{-}C_{10}H_9NH]^+[Ph_3SnCl_2]^-$	150	20.9	58.1	4.5	2.5	84.6	274.1
		(21.0)	(59.5)	(4.4)	(2.4)		(564.7)
$[β\text{-}C_5H_4NHCH_3]^+[Ph_3SnCl_2]$	130	22.8	56.2	4.4	2.7	99.8	252.7
		(23.0)	(55.8)	(4.4)	(2.7)		(515.7)
$[β\text{-}C_5H_4NHCH_3]^+[Ph_2SnCl_3]$	117	25.0	45.5	3.7	3.0	94.5	249.6
		(24.9)	(45.5)	(3.8)	(2.9)		(474.2)
$γ\text{-}C_5H_4NHCH_3]^+[Ph_3SnCl_2]^-$	162	23.1	56.0	4.4	2.8	102.5	274.3
		(23.0)	(55.8)	(4.4)	(2.7)		(515.7)
$γ\text{-}C_5H_4NHCH_3]^+[Ph_2SnCl_3]$	155	25.0	45.0	3.7	2.8	96.6	266.5
		(24.9)	(45.5)	(3.8)	(2.9)		(474.2)

C_5H_5NH = pyridine, $C_6H_5NH_2$ = aniline, C_9H_7NH = quinoline; α- and β-$C_{10}H_9NH_2$ = α- and β-naphthylamines; and β- and γ-C_6H_7N = β- and γ-picolines

All complexes are white crystalline solids, insoluble in common organic solvents. The complexes are thermally stable and have sharp melting points. The analytical data of the complexes, listed in Table 1, are consistent with proposed 1:1 stoichiometry. The molecular weights of the complexes, determined cryoscopically in nitrobenzene, correspond to 1:1 electrolytic behaviour. The molar conductances of the complexes in absolute methanol at room temperature lie in the range of 84.6-111.3 mho cm^2 mol^{-1} supporting their 1:1 electrolytic nature.

The IR spectra of the complexes of pyridinium[10,11], β-, γ-picolinium[12] and quinolinium[13] cations, recorded in KBr in the region 4000-200 cm^{-1}, exhibit peaks at 1610, 1525, 1480 and 1370 cm^{-1}, respectively assignable to coupled $\nu C=C$ and $\nu C=N$ modes. The bands around 1325, 1215, 1200 and 1055 cm^{-1} in these complexes, respectively are attributed to C-H in-plane deformation, without of-plane modes appearing in the region 740 ± 5 and 690 ± 5 cm^{-1}. A band near 1020 cm^{-1} is due to ring breathing mode. The νN-H and δN-H are identified in the ranges 3040-3400 and 1500-1535 cm^{-1} respectively[10,13,14]. The complexes containing anilinium and α- and β-naphthylaminium[15] cations display, in their IR spectra peaks at 1615 ± 5 and 1300 cm^{-1} due to $-NH_3^+$ asymmetric and symmetric deformation modes respectively. A peak identified at 815 cm^{-1} may be due to NH_3^+ rocking mode.

The ν_sSn-Cl and ν_{as}Sn-Cl modes appearing at 365 and 340 cm^{-1} respectively in organotin(IV) halides undergo shift to lower wavenumbers in the complexes and appear at 335 and 260 cm^{-1} respectively. The marked decrease in νSn-Cl is attributed[16] to the increased coordination number of tin atom.

The PMR spectrum of a typical complex $[C_5H_4NHCH_3]^+$ $[Ph_2SnCl_3]^-$ was recorded in DMSO-d_6. The complex exhibits two groups of signals: multiplets due to phenyl protons in the range δ7.23-8.30 ppm; and a singlet for methyl protons of the base at δ2.23 pm. The spectrum and its integration correspond to the proposed formulation of the compound.

On the basis of the spectral data a trigonal bipyramidal geometry around tin atom in the complex anion is proposed.

Antimicrobial activity of complexes was evaluated against five fungi (*Candida albicans, Cryptococcus neoformans, Sporotrichum schenckii, Trichophyton mentagrophytes* and *Aspergillus fumigatus*) and five bacteria (*Streptococcus faecalis, Klebsiella pneumonie, Escherichia coli, Pseudomonas aeruginosa* and *Staphylococcus aureus*) by two-fold serial dilution method[17]. Most of the complexes are significantly active against *Strept. faecalis, Staphyoaureus* and *T. mentagrophytes.*

Financial assistance from the UGC, New Delhi in support of the present work is gratefully acknowledged.

References

1 Thayer J S & Strommen D P, *J organometal Chem*, **5** (1966) 383.
2 Bertazzi N, Alonza G, Silvestri A & Consiglic C, *J organometal Chem*, **37** (1972) 281.
3 Kupchick E J & Yammitsky G F, *Synth React Inorg Met Org Chem*, **9**(4) (1979) 345.
4 Hobbs L, Smith A & Peter J, *J organometal Chem*, **206** (1984) 59.
5 Sau A C, Carpino L A & Holmes R R, *J organometal Chem*, **197** (1980) 181.
6 Bhattacharya S N & Saxena A K, *Indian J Chem*, **19A** (1980) 222.
7 Ng S W & Zuckermann J J, *J organometal Chem*, **234** (1982) 257.
8 Wassef M A & Hessein S, *Commun Fac Sci, Univ Ankara Ser B*, **27**(11) (1981) 141.
9 Wharf A, Lobas J Z & Onyszchuk M, *Can J Chem*, **48** (1970) 2787.
10 Cook D, *Can J Chem*, **39** (1961) 2009.
11 Chadha R K & Kalsotra B L, *J Indian chem Soc*, (1983) 101.
12 Spinner E, *J chem Soc*, (1963) 3860.
13 Kalsotra B L & Parkangi C, *Inorg chim Acta*, **28** (1978) 185.
14 Gainusu I, Varnely C & Protesta M, *Rev Chem Minor*, **10** (1973) 671.
15 Stone P J, Craig J C & Thomson H W, *J chem Soc*, (1958) 52.
16 Wharj F & Shriver D F, *Inorg Chem*, **8** (1969) 914.
17 Srivastava T N & Tandon S K, *Indian J appl Chem*, **27** (1964) 116.

Indian Journal of Chemistry
Vol. 27A, January, 1988, pp. 73-75

Synthesis & Structural Studies of Oxovanadium(IV), Manganese(II), Iron(II), Cobalt(II), Nickel(II) & Copper(II) Complexes of N-(4-Methyl-8-acetoumbelliferonylidene)-N'-(isonicotinoyl)hydrazine

P VENKATESWAR RAO
Department of Chemistry, Nizam College, Hyderabad 500 001
and
N RAMA RAO & M C GANORKAR*
The Birla Institute of Scientific Research, Asmangadh Palace, Malakpet, Hyderabad 500 036

Received 27 *November* 1986; *revised and accepted* 26 *May* 1987

Complexes of N-(4-methyl-8-acetoumbelliferonylidene)-N'-(isonicotinoyl)hydrazine [MAUINH] with oxovanadium(IV), Mn(II), Fe(II), Co(II), Ni(II) and Cu(II) have been synthesised and characterised on the basis of analytical, conductivity, magnetic moment, TG and DT, infrared, electronic and ESR spectral data. Metal to ligand ratio in all the chelates has been found to be 1:1. Infrared spectral data show that the ligand behaves in a dibasic tridentate manner in all the complexes except in Mn(II) complex where it acts as a monobasic tridentate ligand with O:N:O donor sequence. In Fe(II), Co(II) and Cu(II) complexes, the lactone carbonyl of the ligand (MAUINH) participates in coordination forming polymeric octahedral complexes. The Mn(II) complex has been assigned a dimeric octahedral structure with two chlorides acting as bridging centres between the metal ions. The Ni(II) and oxovanadium(IV) complexes have been assigned dimeric square-planar and square-pyramidal stereochemistries respectively.

In view of the promising physiological properties of coumarin and its derivatives[1-5], we report here the synthesis and characterisation of a new ligand, N-(4-methyl-8-acetoumbelliferonylidene)-N'-(isonicotinoyl)hydrazine (MAUINH), and its complexes with oxovanadium(IV), Mn(II), Fe(II), Co(II), Ni(II) and Cu(II).

4-Methyl-8-acetylumbelliferone was prepared by the reported method[6]. Isonicotinoyl hydrazide was a Fluka reagent. All the other chemicals used were of AR grade and the solvents were purified before use.

The ligand, MAUINH (I), was prepared by mixing 8-acetyl-4-methyl umbelliferone (4.36 g, 0.02 mol) with isonicotinic acid hydrazide (2.78 g, 0.02 mol) in 100 ml of ethanol. The *p*H of the reaction mixture was adjusted to 7-8 and it was refluxed for about two hours. On keeping the reaction mixture overnight, a light yellow crystalline product precipitated which was filtered, washed with ethanol and pet. ether (60-80°) and dried *in vacuo*.

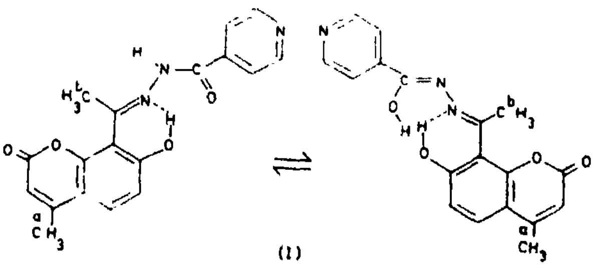

(I)

The compound was recrystallised from dimethylformamide, m.p. 273°C.

[Found: C, 64.16; H, 4.60; N, 12.49. $C_{18}H_{15}N_3O_4$ requires: C, 64.10; H, 4.45; N, 12.46%]. IR: 3250 (νNH), 3200-2800 (H-bonded νOH)[7], 1720 (νC=O lactone), 1680 (νC=O amide), 1600 (νC=N)[8], 1490 (νC−O phenolic)[9], 1060 (νN−N) and 1020 cm^{-1} (νC−O−C); PMR(DMSO-d_6): δ 2.3 (3H, *s*, a-CH_3), 3.7 (3H, *s*, b-CH_3), 6.5 (1H, *s*, C_3−H), 6.8-7.0 (1H, *d*, C_5−H), 7.6-8.0 (1H, *d*, C_6−H)[10], 8.3-8.5 (1H, *s*, ArOH) and 12.7 (1H, *s*, enolic OH).

Preparation of the complexes

The metal complexes were prepared by mixing the ethanolic solutions of the ligand (0.01 mol) with the metal chlorides (0.01 mol); the *p*H of the reaction mixture was adjusted to ~ 8 and it was refluxed for 2-3 hr on a water bath. The metal chelates precipitated on refluxing the reaction mixture. The metal chelates thus precipitated were filtered, washed thoroughly with ethanol, followed by pet. ether (60-80°) and dried *in vacuo*.

All the physicochemical studies were carried out as described earlier[6]. The far infrared spectra of some of the complexes were recorded on a Polytech-FIR-30 IR spectrophotometer.

All the metal chelates are coloured, stable towards air and moisture, decompose at high temperatures and insoluble in common organic solvents, but sparingly soluble in DMF, DMSO and dioxane. The molar conductance values of these complexes (7-20 mhos cm^2 mol^{-1}) in DMF (10^{-3} *M*) show their non-electrolytic nature. The analytical data (Table 1) suggest that the metal to ligand stoichiometry is 1:1.

The absence of a broad band due to hydrogen bonded νOH in the spectra of all the complexes suggests the cleavage of intra-molecularly hydrogen bonded −OH of the ligand with subsequent deprotonation and coordination through phenolic oxygen[7]. This is further supported by an upward shift in νC−O (phenolic) to the extent of 15-20 cm^{-1} (ref. 11). In all

Table 1—Characterisation Data of the Complexes

Complex	Found (Calc.), %				μ_{eff} (B.M.)	Electronic spectral data		
	Metal	C	H	N		λ_{max} (cm^{-1})	*Dq* (cm^{-1})	LFSE ($kJ\ mol^{-1}$)
$[\mathrm{Vo\ MAUINH}]_2$	12.71 (12.67)	53.89 (53.74)	3.41 (3.23)	10.55 (10.45)	1.42	12800, 17000, 24000	1280	61.24
$[\mathrm{Mn\ MAUINH\cdot Cl\cdot H_2O}]_2^*$	12.41 (12.36)	48.28 (48.60)	3.52 (3.60)	9.48 (9.45)	5.16	8500, 15625, 27770	850	0
$[\mathrm{Fe\ MAUINH\cdot 2H_2O}]_n$	13.12 (13.08)	50.68 (50.60)	4.06 (3.98)	9.96 (9.84)	5.10	10500, 28400	1050	50.24
$[\mathrm{Co\ MAUINH\cdot 2H_2O}]_n$	13.62 (13.70)	50.10 (50.24)	4.02 (3.95)	9.90 (9.77)	4.60	8750, 18400	734.6	70.30
$[\mathrm{Ni\ MAUINH}]_2$	15.00 (14.91)	55.06 (54.86)	3.39 (3.30)	10.56 (10.67)	Diamagnetic	18520, 25000	1852	543.63
$[\mathrm{Cu\ MAUINH\cdot 2H_2O}]_n$	14.69 (14.62)	49.52 (49.70)	3.98 (3.91)	9.75 (9.67)	1.86	15850, 27800	1585	113.75

*Satisfactory Cl analysis was obtained

the complexes, except Mn(II) complex, the ligand coordinates in its enolic form as shown by a strong band at 1580 cm^{-1}, which is diagnostic of azine ($>C=N-N=C<$) group[12], and the absence of the characteristic frequencies of νC=O (amide). The presence of a band at 1240-1270 cm^{-1} suggests the participation of C−O (enolic) in complexation. In the spectra of Fe(II), Co(II) and Cu(II) complexes, a downward shift in νC=O (lactone) frequency to the extent of 30 cm^{-1} suggests its involvement in coordination[13]. A negative shift in νC=N to the extent of 20 cm^{-1} indicates the coordination of azomethine nitrogen[14]. This is further supported by an upward shift of 20 cm^{-1} in νN−N. The appearance of a broad crest in the region 3500-3200 cm^{-1} and a non-ligand band around 840 cm^{-1} in the spectra of Mn(II), Fe(II), Co(II) and Cu(II) complexes suggests the presence of coordinated water, which is further corroborated by TG and DT analyses.

In the spectrum of Mn(II) complex the appearance of bands characteristic of νNH and νC=O (amide) and the absence of the band due to νC−O (enolic) suggest the coordination of the ligand in its keto form. The νC=O (amide) undergoes a negative shift to the extent of 30 cm^{-1} which is a conclusive evidence of its coordination to the metal ion. A band observed at 240 cm^{-1} in the far infrared spectrum is due to νM−Cl vibration which indicates the presence of a chloride bridge. This is supported by a low magnetic moment value and analytical tests[15]. The presence of enolic oxygen bridge in Ni(II) and oxovanadium(IV) complexes is substantiated by a positive shift in νC−O (enolic) (> 25 cm^{-1})[9,12]. A band at 980 cm^{-1} in the spectrum of oxovanadium(IV) complex can be assigned to νV=O. New bands observed in the region 300-600 cm^{-1} in the spectra of all the complexes are attributable to νM−N and νM−O vibrations[16].

Thermogravimetric analysis shows a single step mass loss equivalent to one mole of coordinated water per mole of the complex in Mn(II) and Fe(II) complexes and two moles of water per mole of complex in the case of Co(II) and Cu(II) complexes. This is further confirmed by one endothermic peak in DT analysis which occurs at 178, 192, 202 and 150°C for the Mn(II), Fe(II), Co(II) and Cu(II) complexes, respectively.

The room temperature magnetic moment values are given in Table 1. The magnetic moment values of oxovanadium(IV) and Mn(II) complexes are low when compared to the spin-only value, which may be due to the presence of antiferromagnetic interaction between the metal ions. This can be attributed to the dimeric nature of these complexes[9]. The magnetic moment values of Fe(II) and Co(II) complexes are well within the range of high spin octahedral complexes[17].

The electronic spectral data are shown in Table 1. The electronic spectrum of oxovanadium(IV) complex exhibits three main absorption bands which are assigned to the three transitions $^2B_2 \rightarrow {}^2E$; $^2B_2 \rightarrow {}^2B_1$ and $^2B_2 \rightarrow {}^2A_1$ respectively in a square-pyramidal geometry[18]. The Mn(II) complex shows weak absorption bands which are not of any help in deciding the geometry. The first absorption band in Fe(II) complex is assigned to $^5T_{2g} \rightarrow {}^5E_g$ transition and the other one to a charge-transfer transition. The Co(II) complex displays two main absorption bands which are assigned to $^4T_{1g}(F) \rightarrow {}^4T_{2g}(F)(\nu_1)$ and $^4T_{1g}(F) \rightarrow {}^4T_{1g}(P)(\nu_3)$ transitions, respectively. The ligand field parameters calculated[18] for this complex are as follows: $B' = 699.6$ cm^{-1}; $\beta = 0.72$ and $\beta° = 28\%$. These values show a

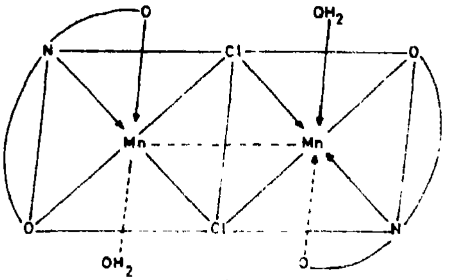

(II)

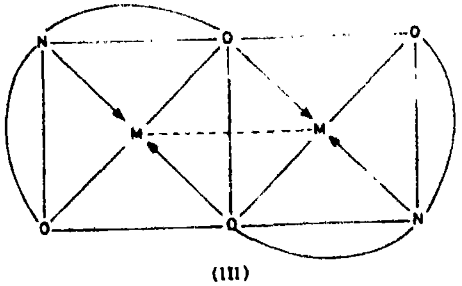

(III)
M=Ni or V=O

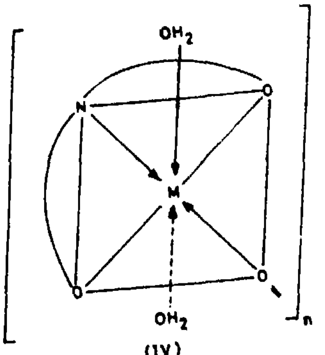

(IV)
M=Fe,Co and Cu

strong M – L covalent bonding in this complex. The Ni(II) complex shows two main absorption bands, which are assigned to $^1A_{1g}\rightarrow{}^1A_{2g}$ and $^1A_{1g}\rightarrow{}^1B_{1g}$ transitions, respectively in a square-planar disposition. The first absorption band in Cu(II) complex can be assigned to $^2E_g\rightarrow{}^2T_{2g}$ transition and the other to a charge-transfer. The *Dq* and LFSE values (Table 1) show that the Cu(II) and Ni(II) complexes are more stabilised than the other complexes.

The ESR spectra of oxovanadium(IV) and Cu(II) complexes were recorded in the powder form at room temperature. The $g_\parallel$, $g_\perp$ and g_{av} values for these complexes are 2.004, 1.957 and 1.972; 2.145, 2.056 and 2.085 respectively[19].

Based on the above data, it is proposed that the Fe(II), Co(II) and Cu(II) complexes are polymeric with octahedral geometries (IV) and Mn(II) complex is a chloride-bridged dimer in an octahedral stereochemistry (II). Ni(II) and oxovanadium(IV) complexes are dimeric with enolic oxygen bridged structures in square-planar and square-pyramidal geometries respectively (III).

Two of the authors (PVR & NRR) are highly grateful to the CSIR, New Delhi for the financial assistance.

References

1 Seshadri T R & Varadarajan S, *Proc Indian Acad Sci*, **35A** (1952) 75.
2 Annoni G, *Riv Geronotol Geriat*, **6** (1957) 243.
3 Di Maggio G, *Biochim Appl*, **5** (1958) 45.
4 Kakimoto S & Yamamoto K, *Pharm Bull*, **4** (1956) 4.
5 Agrawal Mamta, Bansal S B & Singhal O P, *J Indian chem Soc*, **58** (1981) 200.
6 Venkateswar Rao P, Rama Rao N, Tyaga Raju V J & Ganorkar M C, *Indian J Chem*, **25A** (1986) 482.
7 Rana A K & Shah J R, *J Indian chem Soc*, **58** (1981) 1100.
8 Biradar N S, Raythatha R H & Mahale V B, *Curr Sci*, **45**(4) (1976) 125.
9 Syamal A & Gupta B K, *J Indian chem Soc*, **59** (1982) 697.
10 Syamal A & Maurya M R, *Indian J Chem*, **23A** (1984) 950.
11 Rastogi V K, Katiyar A K, Saxena R C & Kotnak A K, *J Indian chem Soc*, **60** (1983) 694.
12 Teotia M P, Gurtu J N & Rana V B, *Indian J Chem*, **20A** (1981) 520.
13 Tyaga Raju V J, Ranabore Vilas, Atre Vasudha & Ganorkar M C, *J Indian chem Soc*, **59** (1982) 199.
14 Iskander M F, Sayed L E & Lasheen M A, *Inorg chim Acta*, **16** (1976) 147.
15 Atre Vasudha, Jaya Tyaga Raju V, Jeeva Ratnam K & Ganorkar M C, *Indian J Chem*, **23A** (1984) 691.
16 Nakamoto K, *Infrared spectra of inorganic and coordination compounds* (Wiley Interscience, New York) 1970, 159, 167, 214, 310.
17 Figgis B N & Lewis J, *Progr inorg Chem*, **6** (1964) 37, 210.
18 Lever A B P, *Inorganic electronic spectroscopy* (Elsevier, Amsterdam) 1968, 290-320.
19 Emeleus H J & Sharpe A G, *Advances in inorganic chemistry and radiochemistry* (Academic Press, New York) 1970, 237, 330.

Indian Journal of Chemistry
Vol. 27A, January, 1988, pp. 76-77

Nicotine Complexes of Zinc(II) Cadmium(II) & Mercury(II)

S MURALIDHARAN & M R UDUPA*
Department of Chemistry, Indian Institute of Technology
Madras 600 036
and
K S NAGARAJA
Department of Chemistry, Loyola College (Autonomous) Madras 600 034

Received 27 *January* 1987; *revised and accepted* 25 *May* 1987

Complexes of nicotine(nic), $M(nic)_nX_2$($M = Zn$ or Cd; $n = 2$, $X = Cl$, Br, I or NCS; $M = Hg$, $n = 1$, $X = Cl$, Br or I) have been prepared. The conductivity measurements indicate that the complexes are nonionic. The complexes have been characterised on the basis of analytical, IR and PMR spectral, and thermal studies

Nicotine(I) is the alkaloid present in the tobacco plant and it is toxic[1]. Eventhough some of the addition compounds of nicotine with metal salts have been reported[2-4], no systematic characterization of the complexes has been carried out. We have recently reported[5] nicotine complexes of cobalt(II), nickel(II) and copper(II). We report in the present note, preparation and characterization of the complexes formed by nicotine with zinc(II), cadmium(II) and mercury(II).

Nicotine was a BDH (England) sample and was used without further purification.

Preparation of dichlorobis(nicotine)zinc(II), $Zn(nic)_2Cl_2$:

Anhydrous zinc chloride (0.65g, 5 mmol) and nicotine (1.62g, 10 mmol) were dissolved in acetone (20 cm^3) separately and mixed. MeOH(40 cm^3) was added to the solution and it was stirred. The precipitated complex was filtered, washed with acetone and dried. Other complexes were prepared by the similar procedure using appropriate metal salts as the starting materials.

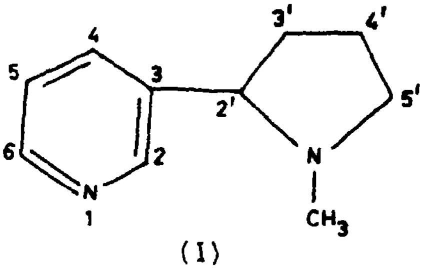

(I)

The elemental analyses of the complexes were carried out on a Hewlett Packard CHN 185 analyzer. The conductivity measurements were made using a Toshniwal conductivity bridge CL01/02A. The IR. far IR and ^1H NMR spectra were recorded on Perkin Elmer 257, Polytec IR 30 and Varian EM 390 spectrometers, respectively. The NMR spectra were recorded in DMSO-d_6 using TMS as the internal reference. The thermogravimetric studies were carried out on a Stanton recording thermobalance in air at a linear heating rate of 6°C min^{-1}.

The analytical data of the complexes are reported in Table 1. The complexes are insoluble in common organic solvents and are sparingly soluble in dimethylformamide and dimethyl sulphoxide. The molar conductance values in DMF (~ 30 $ohm^{-1}cm^2mol^{-1}$) suggest[6] that the anions are involved in bonding to the metal ions.

The neat IR spectrum of nicotine exhibits medium absorption bands at 1580 and 1310 cm^{-1} which are assigned[7] to ν(C=N) of pyridine and ν(C—N) of $—NCH_3$ group of pyrrolidine respectively. A positive

Table 1—Elemental Analyses Data of Nicotone Complexes

Complex	Found (Calc.),%				
	C	H	N	X	M
$[Zn(nic)_2Cl_2]$	52.7(52.1)	6.4(6.1)	12.5(12.2)	15.8(15.4)	14.7(14.2)
$[Zn(nic)_2Cl_2]$	52.7(52.1)	6.4(6.1)	12.5(12.2)	15.8(15.4)	14.7(14.2)
$[Zn(nic)_2Br_2]$	43.1(43 7)	5.3(5.1)	10.9(10.2)	29.8(29.1)	11.2(11.9)
$[Zn(nic)_2I_2]$	37.8(37.3)	4.8(4.4)	8.6 (8.7)	39.9(39.4)	10.8(10.2)
$[Zn(nic)_2(NCS)_2]$	52.9(52.2)	5.1(5.6)	16.9(16.6)	22.3(23.0)	12.2(12.9)
$[Cd(nic)_2Cl_2]$	47.5(47.3)	5.2(5.6)	11.3(11.0)	13.2(14.0)	22.9(22.1)
$[Cd(nic)_2Br_2]$	40.8(40.3)	4.1(4.7)	9.2 (9.4)	26.1(26.8)	18.2(18.8)
$[Cd(nic)_2I_2]$	34.1(34.8)	4.6(4.1)	8.8 (8.1)	36.1(36.8)	16.8(16.3)
$[Cd(nic)_2(NCS)_2]$	47.2(47.8)	5.7(5.1)	15.9(15.6)	20.5(21.0)	20.5(20.3)
$[Hg(nic)Cl_2]$	27.6(27.7)	3.2(3.3)	6.9 (6.5)	16.9(16.4)	46.8(46.2)
$[Hg(nic)Br_2]$	20.8(20.3)	2.9(2.4)	5.9 (5.4)	30.1(30.6)	38.9(38.4)
$[Hg(nic)I_2]$	19.1(19.5)	2.7(2.3)	4.9 (4.5)	41.9(41.4)	32.9(32.5)

Table 2—Thermogravimetric Data of Nicotine Complexes

Complex]	Loss of nicotine		Formation of metal oxide	
	Temp. range (°C)	Found (Calc.) (%)	Temp. range (°C)	Found (Calc.) (%)
$[Zn(nic)_2Cl_2$	240-360	70(70.4)	460-700	82(82.3)
$[Zn(nic)_2Br_2]$	240-380	59(59.1)	440-680	85(85.2)
$[Zn(nic)_2I_2]$	220-360	50(50.4)	440-660	87(87.4)
$[Zn(nic)_2(NCS)_2]$	220-380	64(64.1)	460-660	83(83.9)
$[Cd(nic)_2Cl_2]$	260-320	64(63.9)	440-580	75(74.7)
$[Cd(nic)_2Br_2]$	240-300	54(54.4)	420-560	78(78.5)
$[Cd(nic)_2I_2]$	240-300	47(46.9)	420-560	81(81.4)
$[Cd(nic)_2(NCS)_2]$	220-300	58(58.7)	440-540	77(76.8)
$[Hg(nic)Cl_2]$	—	—	200-380	50(50.1)
$[Hg(nic)Br_2]$	—	—	180-380	58(58.6)
$[Hg(nic)I_2]$	—	—	160-360	65(64.3)

shift (~ 20 cm^{-1}) in $\nu(C=N)$ in the complexes is observed. Further, the bands at 604 cm^{-1} due to inplane ring deformation and at 405 cm^{-1} due to out-of plane ring deformation are shifted[8] to about 640 and 420 cm^{-1} respectively on coordination to metal ions. Thus involvement of pyridine nitrogen in coordination is inferred. The positions of the rest of the bands in the metal complexes are not different from those of nicotine. The $\nu(C—N)$ mode of $—NCH_3$ group of pyrrolidine ring is shifted to 1300 cm^{-1} in the case of mercury complexes from the free ligand value (1310 cm^{-1}). In the mercury complexes both the pyridine and pyrrolidine nitrogens may be involved in bonding to the metal atom. The bands around 250, 230 and 180 cm^{-1} in the zinc, cadmium and mercury complexes respectively are attributed[9] to $\nu(M—N)$. The bonding through nitrogen of the thiocyanate group is indicated[10] by the bands observed at 2060, 840, and 470 cm^{-1}; it is confirmed by the observation of a new band around 240 cm^{-1} due to $\nu(M—NCS)$.

^1H NMR spectral studies on nicotine and its metal complexes have been made to confirm the mode of coordination. The signals exhibited by protons in nicotine are accounted for on the basis of the assignments made by Pitner *et al.*[11]. The positions of the signals observed (δ, ppm) along with the assignment are as follows: 1.7(C_3); 1.8, 1.9(C_4); 2.2($—NCH_3$); 2.3, 3.3, 4.0(C_5); 3.0, 3.1 (C_2); 7.3(C_5); 7.6, 7.7(C_4) and 8.5 (C_2 and C_6). In the complexes of zinc and cadmium with nicotine, the signals due to protons attached to C_2 and C_6 are observed at 8.4 and 8.2δ, respectively. This shift from the value of δ 8.5 for free nicotine suggests the involvement of pyridine nitrogen in coordination. The signal due to $-NCH_3$ protons remains unchanged. In the case of mercury(II) complexes a signal is observed at 8.2 δ corresponding to the protons at C_2 and C_6. Further, the signal observed at 2.2δ due to $—NCH_3$ protons in the spectrum of free nicotine is shifted in the mercury complexes. Thus, the coordination through both the pyridine and pyrrolidine nitrogen atoms in the case of mercury complexes is inferred.

$M(nic)_2X_2$ (M = Zn or Cd; X = Cl, Br, I or NCS) show two stages of thermal decomposition (Table 2). The first step corresponds to the formation of metal halides in the range 240-300°C. In the second stage the metal oxide is formed in the temperature range 440-600°C. The thermogravimetric curves of $Hg(nic)X_2$ show a single stage decomposition wherein the ligand is lost with the formation of mercury(II) oxide.

Zinc(II), cadmium(II) and mercury(II) complexes are tentatively assigned tetrahedral geometry, attained on coordination by two pyridine nitrogen atoms drawn from two nicotine molecules and two halogen atoms or thiocyanate groups. In the case of mercury(II) complexes, the metal atom is surrounded by halogen atoms and two nitrogen atoms of pyridine and pyrrolidine moiety of a nicotine molecule.

References

1 Swan G A, *An introduction to the alkaloids* (Blackwell, Oxford), 1967.

2 Smith C R, *J Am chem Soc*, **71** (1949) 2844.

3 Babak S F & Kagramanova G B, *Zhur obshch Khim.* **24** (1954) 1690.

4 Burkat S E, *Zhur obshch Khim*, **23** (1953) 1401.

5 Muralidharan S, Nagaraja K S & Udupa M R, *Indian J Chem*, **26A** (1987) 348.

6 Geary W J, *Coord Chem Rev*, **7** (1971) 81.

7 Asianian D, Lautie A, Mankai Ch & Balkanski M, *J chim Phys*, **72** (1975) 1052.

8 Sabatini A & Sacconi L, *J Am chem Soc*, **86** (1964) 17.

9 Adams D M, *Metal ligand and related vibrations* (Edward Arnold, London), 1967.

10 Emeleus H J & Sharpe A G, *Advances in inorganic chemistry and radiochemistry* (Academic Press, New York), 1975, 231.

11 Pitner T P, Edwards W B, Bassfield R L & Whidby J F, *J Am chem Soc*, **100** (1978) 246.

Indian Journal of Chemistry
Vol. 27A, January, 1988, pp. 78-79

Mixed Ligand Chelates of Chromium(III)

SARBESHWAR MISHRA & K M PUROHIT*

Department of Chemistry, Regional Engineering College,
Rourkela 769 008(Orissa)

Received 5 *March* 1987; *revised and accepted* 11 *May* 1987

Mixed ligand complexes of chromium(III) of the types [Cr(acac)$_2$L] and [Cr(acac)L$_2$], where acacH = acetylacetone, and LH = oxine (OxH), picolinic acid(pycaH) and anthranilic acid(abH), have been synthesised and characterised by elemental analyses, molar conductance, room temperature magnetic moment, infrared and electronic spectral data. The complexes are paramagnetic and non-electrolytic in nature, and they have been assigned octahedral geometries.

In continuation of our earlier studies on mixed ligand complexes[1-3] of chromium(III), we now report in this note the preparation and characterisation of some mixed ligand complexes of chromium(III) containing two different uninegative bidentate ligands posessing O-O and N-O donor atoms.

All the chemicals used were of AR grade and they were used as such. Tris(acetylacetonato)chromium(III) was prepared as per the known method.

Preparation of [*Cr*(*acac*)$_2$*L*]

Tris(acetylacetonato)chromium(III) and ligand LH(LH = oxine, picolinic acid or anthranilic acid) were taken in 1:1 molar, ratio in ethanol, and were refluxed for six hours The volume was reduced and kept for overnight when the compounds separated out. These were filtered, washed with ethanol, ether and dried *in vacuo* over fused $CaCl_2$.

Preparation of [*Cr*(*acac*)*L*$_2$]

These compounds were obtained by the same method as mentioned above by reacting Cr(acac)$_3$ and oxine, picolinic acid or anthranilic acid in 1:2 molar ratio.

The characterisation data of the complexes are recorded in Table 1. The elemental analyses were carried out by standard methods. The analytical data of the complexes are consistent with the formulation of the compounds. The low molar conductance values (Λ_M = 0.8 to 1.0 mho) of $10^{-3}M$ solutions of the mixed chelates in DMSO, measured on a direct reading conductivitymeter (Systronic 303), suggest that they are non-electrolytes. The magnetic susceptibility measurements employing Gouy's balance with Hg[Co(NCS)$_4$]as the calibrant indicate that all the complexes are paramagnetic with three unpaired electrons as expected for the d^3 system of chromium(III).

Table 1—Characterisation Data of Mixed Ligand Complexes of Chromium(III)

Complex	M.P. (°C)	% Found (Calc.)			μ_{eff} (B.M.)
		Cr	C	H	
[Cr(acac)$_2$(OX)]	160	12.97 (13.19)	57.95 (57.86)	4.98 (5.07)	3.87
[Cr(acac)$_2$(Pyca)]	143	13.83 (13.97)	52.04 (51.61)	4.75 (4.83)	3.77
[Cr(acac)$_2$(ab)]	120	13.12 (13.46)	51.08 (52.85)	4.97 (5.18)	3.65
[Cr(acac)(OX)$_2$]	195	11.49 (11.84)	62.45 (62.87)	4.18 (4.32)	3.81
[Cr(acac)(Pyca)$_2$]	165	13.02 (13.16)	51.89 (51.64)	3.62 (3.79)	3.69
[Cr(acac)(ab)$_2$]	130	12.13 (12.29)	52.80 (53.90)	4.05 (4.49)	3.72

The infrared spectra of the complexes were recorded in KBr on a Perkin Elemer model 337 spectrophotometer. The bands due to $\nu C{\cdots}O$ and $\nu C{\cdots}C$ were observed around 1600 and ~ 1520 cm^{-1}, respectively, as expected, indicating the presence of coordinated acetylacetone as a uninegative bidentate ligand[4]. Charles *et al.*[5] have reported that in several metal-oxine complexes, νC-O is observed at 1120 cm^{-1}, the position of the band slightly varying with the nature of the metal. In the present investigation the presence of a strong band at ~ 1120 cm^{-1} clearly indicates coordination of oxine group through nitrogen and oxygen atoms and its behaviour as a uninegative bidentate ligand[6-7]. Picolinic acid(pycaH) exhibits an absorption band in the region 1750-1700 cm^{-1} due to $C{\cdots}O$ of the free COOH group[8]. This band disappeared in the IR spectrum of the Cr(III) complexes. Other bands due to ν_{as} COO$^-$ and pyridine ring appeared around ~ 1650 cm^{-1}, as observed by Fowles *et al.*[9] also. These observations suggest that picolinic acid is coordinated to metal ion through oxygen and nitrogen atoms as a uninegative bidentate ligand[10,11]. IR spectrum of sodium anthranilate exhibits four absorptions at 3436, 3330, 1521 and 1398 cm^{-1}, the first two have been assigned to ν_{as} and ν_s N-H modes while the latter two have been attributed to ν_{as} and ν_sCOO$^-$ modes, respectively[12]. The negative shifts in ν_{as}NH, ν_sNH, ν_sCOO$^-$ and positive shift in ν_{as}COO$^-$ in the complexes as compared to the values in free ligand suggest bidentate behaviour of the ligand[13]. The formation of Cr-O and Cr-N bonds was indicated by the νCr-O and νCr-N modes appearing at ~ 410 and ~ 470 cm^{-1}, respectively.

The electronic spectra of these complexes exhibit two absorption bands in the regions 18500-19000 and 23200-23400 cm^{-1}. These can be assigned to $^4A_{2g} \rightarrow {}^4T_{2g}$ and $^4A_{2g} \rightarrow {}^4T_{1g}$ transitions, respectively, which are typical of octahedral coordination[14]. Thus, the complexes reported here are mixed ligand, spin-free, six coordinated, octahedral complexes of chromium(III).

The authors are grateful to Prof. D.V. Ramana Rao for valuable suggestions and encouragement and to Prof. S. Misra, Principal, Regional Engineering College, Rourkela for experimental facilities. Thanks are due to CDRI, Lucknow for recording the infrared and electronic spectra of the complexes.

References

1 Purohit K M & Ramana Rao D V, *Indian J Chem*, **22A** (1983) 520.

2 Purohit K M & Ramana Rao D V, *J Indian chem Soc*, **60** (1983) 1009.

3 Purohit K M & Ramana Rao D V, *J Inst of Chemists(Ind)*, **58** (1986) 159.

4 Graddon D P, *Coord Chem Rev*, **4** (1969) 1.

5 Charles R C, Freiser H, Friedel R, Hilland L E & Johnston W D, *Spectrochim Acta*, **8** (1956) 1.

6 Purohit K M & Ramana Rao D V, *J Indian chem Soc*, **57** (1980) 363.

7 Pradhan B & Ramana Rao D V, *J Indian chem Soc*, **55** (1978) 226.

8 Drew M G B, Fowles G W A, Mathews R W & Walton R A, *J Am chem Soc*, **91** (1968) 7769.

9 Fowles G W A, Mathews R W & Walton R A, *J chem Soc(A)*, (1968) 1108.

10 Purohit K M & Ramana Rao D V, *J Indian chem Soc*, **58** (1981) 78.

11 Pradhan B & Ramana Rao D V, *Indian J Chem*, **20A** (1981) 751.

12 Sandhu S S, Manhas B S, Mittal M R & Parmar S S, *Indian J Chem*, 7 (1969) 286.

13 Aggarwal R C, Bala R & Prasad R L, *Indian J Chem*, **22A** (1983) 568.

14 Lever A B P, *Inorganic electronic spectroscopy*, (Elsevier, Amsterdam), 1968, 277.

Indian Journal of Chemistry
Vol. 27A, January, 1988, pp. 80-81

Anionic Complexes of Nickel(II)

C M DANI
Research and Control Laboratory
Rourkela Steel Plant, Rourkela 769 011
and
A K DAS*
Bonaigarh College, Bonaigarh, Orissa

Received 22 *September* 1986; *revised* 6 *April* 1987
rerevised and accepted 18 *May* 1987

Eight anionic complexes of nickel(II) having the compositions, $[LH_2][NiCl_4]$ and $[LH_2][NiCl_2Br_2]$, where L = ethylenediamine, *o*-phenanthroline, bipyridyl or *o*-phenylenediamine have been prepared and characterised. Tetrahedral stereochemistry around nickel(II) has been proposed for these anionic complexes.

Several reports[1-10] have been made earlier on the isolation and characterisation of anionic complexes of different transition metal ions involving different cations. Eight complexes having the general formulae $[LH_2][NiCl_4]$ and $[LH_2][NiCl_2Br_2]$, where L = ethylenediamine(en), *o*-phenanthroline(ophen), bipyridyl(bipy) or *o*-phenylenediamine(opd), have been prepared and characterised in the present investigation.

All the chemicals used were of A R grade (BDH).

Preparation of the complexes of the type $[LH_2][NiCl_4]$

To an ethanolic solution (0.01 mol) of ethylenediamine, bipyridyl, *o*-phenanthroline or *o*-phenylenediamine, dil. HCl was added till the solution became acidic (*p*H ~ 5). The resulting solution was then added to an ethanolic solution of nickel chloride) (0.01 mol) and refluxed for half an hour. The solution was slightly evaporated over a waterbath and kept overnight. The crystalline coloured compound that separated was filtered, washed repeatedly with ethanol, ether and finally dried *in vacuo*.

Preparation of anionic complexes of the type $[LH_2][NiCl_2Br_2]$

To an ethanolic solution of ethylenediamine, bipyridyl, *o*-phenanthroline or *o*-phenylenediamine (0.01 mol), dil. HBr was added till the solution became acidic (*p*H ~ 5). The resulting solution was then added to an ethanolic solution of nickel chloride (0.01 mol) and refluxed for half an hour. The solution was evaporated slightly over a waterbath and kept overnight. The crystalline coloured compound that separated was filtered, washed repeatedly with ethanol, ether and finally dried *in vacuo*.

The relevant physical and analytical data are recorded in Table 1.

Analytical data are in good agreement with the proposed formulations of the complexes. All the complexes are crystalline and coloured having high melting points (> 250°C). The molar conductance values in methanol (120.7 – 142.3 ohm^{-1} cm^{2}mol^{-1}) indicate 1:1 electrolytic nature of the complexes. The magnetic moment values of the complexes lie in the range 3.51-3.88 B.M., which definitely suggest[11] tetrahedral environment around nickel(II) ion. The higher magnetic moment values of the complexes than the spin-only value may be attributed to large orbital contribution to the magnetic moment in the tetrahedral stereochemistry.

Table 1—Analytical and Physical Data of Anionic Complexes of Nickel(II)

Compound	Found (Calc.), %						μ_{eff},
(Colour)	Ni	Cl	Br	C	H	N	(B.M.)
$[enH_2][NiCl_4]$	21.85	53.18	—	8.78	3.20	9.90	3.88
(Green)	(22.36)	(54.02)		(9.14)	(3.80)	(10.66)	
$[enH_2][NiCl_2Br_2]$	15.98	19.80	45.10	6.12	2.20	7.35	3.76
(Green)	(16.70)	(20.17)	(45.47)	(6.82)	(2.84)	(7.96)	
$[ophenH_2][NiCl_4]$	14.04	34.46	—	36.90	2.21	6.85	3.62
(Blue)	(14.64)	(35.39)		(37.61)	(2.61)	(7.31)	
$[ophenH_2][NiCl_2Br_2]$	12.82	14.20	31.84	29.88	1.90	5.20	3.80
(Light blue)	(11.98)	(14.48)	(32.63)	(30.52)	(2.12)	(5.93)	
$[bipyH_2][NiCl_4]$	15.42	39.12	—	33.04	2.22	7.36	3.51
(Blue)	(16.36)	(39.53)		(33.45)	(2.78)	(7.80)	
$[bipyH_2][NiCl_2Br_2]$	12.21	15.24	35.02	26.24	1.90	5.84	3.68
(Green)	(13.11)	(15.84)	(35.70)	(26.80)	(2.23)	(6.25)	
$[opdH_2][NiCl_4]$	19.72	44.78	—	22.90	2.80	8.48	3.67
(Pink)	(18.90)	(45.67)		(23.18)	(3.22)	(9.01)	
$[opdH_2][NiCl_2Br_2]$	14.21	16.98	39.60	17.65	1.85	6.39	3.60
(Reddish brown)	(14.69)	(17.75)	(40.01)	(18.02)	(2.50)	(7.00)	

Involvement of cations in the complexes is well substantiated by the IR spectra of some of the complexes. The IR spectra of the complexes, [enH$_2$][NiCl$_2$Br$_2$] and [opdH$_2$][NiCl$_2$Br$_2$] exhibit bands in the range 3100-3260 and 2780-2850 cm^{-1} which may be assigned[12] to the first overtone or combination bands of the deformation vibration in the region 1600-1500 cm^{-1} and CH$_2$,CH and NH$_3^+$ stretching vibrations respectively. Besides, a band at 2575 cm^{-1}, attributed to combination bands involving fundamentals of NH$_3^+$ deformation vibration, has been observed in the IR spectrum of the complex, [opdH$_2$][NiCl$_2$Br$_2$]. The broad bands at 2775 and 2795 cm^{-1} in the complexes [ophenH$_2$][NiCl$_2$Br$_2$] and [bipyH$_2$][NiCl$_4$] respectively may be assigned[12] to N-H$^+$ stretching frequencies. The ν(Ni—Cl) and ν(Ni—Br) bands are observed in the ranges 265-290 and 238-240 cm^{-1}, respectively, indicating[13-15] metal-halogen bonding in the complexes.

In general, tetrahedral nickel(II) complexes display two characteristics electronic spectral bands around 15.8 kK and 7.0-8.0 kK corresponding to $^3T_1(F)\rightarrow{}^3T_1(P)(\nu_3)$ and $^3T_1(F)\rightarrow{}^3A_2(F)$ (ν_2) transitions, respectively. The electronic spectra of the present complexes in methanol display spectral bands in the region 15,800-16,200 cm^{-1} which may be assigned[16] to $^3T_1(F)\rightarrow{}^3T_1(P)(\nu_3)$ transition in a tetrahedral field. The other band (ν_2) could not be detected due to the limitations of the instrument used. The present complexes have μ_{eff} values ranging between 3.51 and 3.88 B.M. indicating the presence of two unpaired electrons with a large orbital contribution, as expected for a tetrahedral nickel(II) complex[11,17].

In view of the above spectral behaviour and high magnetic moment values, tetrahedral stereochemistry has been proposed[18] for these anionic complexes of nickel(II).

The authors are grateful to the authorities of Rourkela Steel Plant for experimental facilities.

References

1 Gill N S & Nyholm R S, *J chem Soc*, (1959) 3997.
2 Horrocks (Jr) W D, Templeton J H & Zalkin A, *Inorg Chem*, 7 (1968) 2203.
3 Brown D H, Forrest K P, Nuttal R H & Sharp D W A, *J chem Soc(A)*, (1968) 2146.
4 Cotton F A, Goodgame D M L & Goodgame M, *J Am chem Soc*, **83** (1961) 1771, 4690.
5 Foster D & Goodgame D M L, *Inorg Chem*, **4** (1965) 1712.
6 Clark R J H & Dunn T M, *J chem Soc*, (1963) 1198.
7 Turco A, Peaile C & Nicotine M, *Proc chem Soc*, (1961) 213.
8 Norbury A H, *Adv inorg Chem and Radiochem*, **17** (1975) 231.
9 Furlani C & Morpurgo G, *Zh phys Chem*, **23** (1961) 93.
10 Figgis B N, Lewis J, Mabbs F E & Webb G A, *J chem Soc(A)*, (1966) 1411.
11 Figgis B N & Lewis J, *Prog inorg Chem*, **6** (1964) 37.
12 Sathpathy K C & Sahoo B, *J inorg nucl Chem*, **32** (1970) 549.
13 Edward H C M, Woodward L A, Gall M J & Ware M J, *Spectrochim Acta*, **26A** (1970) 287.
14 Sabatini A & Sacconi L, *J Am chem Soc*, **86** (1964) 17.
15 Ferraro J R, *Low frequency vibrations of inorganic and coordination compounds* (Plennum Press New York) 1971.
16 Lever A B P, *Inorganic electronic spectroscopy* (Elsevier, London) 1968.
17 Miller J R, *Adv inorg Chem Radiochem*, **4** (1962) 150.
18 Buffagni S, Vallerina L M & Quagliano J V, *Inorg Chem*, **3** (1964) 480.

Indian Journal of Chemistry
Vol. 27A, January, 1988, pp 82-84

Complexometric Titration of Thallium(III) using Hydrazine Sulphate as Demasking Agent

A NITYANANDA SHETTY & R V GADAG
Department of Chemistry, Karnataka Regional Engg. College,
Surathkal, Srinivasnagar 574 157
and
M R GAJENDRAGAD*
Department of Chemistry, Mangalore University,
Mangalagangothri 574 199

Received 12 *January* 1987; *revised and accepted* 20 *April* 1987

A simple and selective complexometric method is proposed for the determination of thallium(III) using hydrazine sulphate as demasking agent. In the presence of diverse metal ions, thallium(III) is complexed with excess EDTA and the EDTA is back titrated (*p*H 5-6, hexamine) with zinc sulphate solution, using xylenol orange as indicator. Hydrazine sulphate solution is then added, the mixture shaken well and allowed to stand for 2-3 min to release EDTA from the Tl-EDTA complex. The EDTA so released is titrated with standard zinc sulphate solution. Reproducible and accurate results are obtained in the range 4-80 mg of thallium with relative error ±0.3% and coefficient of variation (n = 6) not more than 0.42%

The reduction of thallium(III) by hydrazine sulphate in the presence of EDTA and other complexons has been studied by spectrophotometric and kinetic methods[1-2]. The redox reaction was used for the estimation of Tl(III) by potentiometric method[3], hydrazine sulphate being used as a reducing agent. Tl(III) has been also used for the determination of reductants like hydrazine sulphate by EDTA titrations[4] and by iodate methods[5]. However, no reference is found in literature about complexometric determination of Tl(III) using hydrazine sulphate as a demasking agent. The present note describes the determinatioin of Tl(III) in its salts and alloys using hydrazine sulphate as a reducing and demasking agent. The distinct advantage of the proposed method is that the release of EDTA is instantaneous and quantitative at room temperature itself and the method requires no heating unlike the triazole method.

Hydrazine sulphate (1%) solution was prepared from AR grade hydrazine sulphate by dissolving the crystals in deionised water.

Thallic chloride solution was prepared from AR grade thallous nitrate as follows. A known weight of thallous nitrate was dissolved in water, oxidized to Tl(III) by alkaline bromine, purified by precipitation as $Tl(OH)_3$, dissolved in 2 *N* HCl, made up to known volume[6] and standardised by the chromate method[7].

Zinc sulphate solution (0.02 *M*) was prepared from AR grade zinc sulphate crystals and standardised by gravimetric method[7].

EDTA solution (~0.04 *M*) was prepared by dissolving the disodium salt in deionised water.

An aqueous solution of xylenol orange indicator (0.5%) was used in the present study.

Procedure

An aliquot of the stock solution containing 4-80 mg of Tl was treated with excess of EDTA solution. The solution was diluted with 20 ml of distilled water, followed by the addition of solid hexamine to adjust the *p*H to 5-6. The EDTA was titrated against the standard zinc sulphate solution to the sharp colour change of xylenol orange to pink. 1% aqueous solution of hydrazine sulphate (1 ml for every 4 mg of Tl) was then added, the reaction mixture shaken well, allowed to stand for 2-3 min and the released EDTA was titrated against the standard zinc sulphate solution as before. The second titre value corresponds to the thallium in the aliquot taken.

Analysis of thallium complexes

A number of Tl(I) complexes with some sulphur donor ligands were prepared by the reported method[8,9], and their purities checked by their elemental analyses. About 0.3 g of complex was decomposed by evaporation to nearly dryness with aqua regia. The residue was then cooled, dissolved in 3 ml of 2 *N* HCl, volume made up to 250 ml with deionised water. Aliquots of 25 ml were used for titration as per the recommended procedure.

Effect of excess of hydrazine sulphate

Preliminary experiments showed that addition of hydrazine sulphate in 1:2 molar ratio [hydrazine sulphate:Tl(III)] was sufficient for the quantitative release of EDTA from the Tl-EDTA complex. However, no adverse effects were noticed on adding excess of the reagent. Even a ten-fold excess of the reagent did not affect the results. In order to ensure complete reduction of Tl(III) to Tl(I), we kept hydrazine sulphate:Tl(III) ratio as 2:1; the Tl(I) ion formed as a result of reduction was masked by the excess of the hydrazine sulphate.

To check the accuracy and precision of the method, determination of thallium was carried out under

Table 1—Precision and Accuracy in the Determinatiion of Thallium(III)

Tl(mg)		Recovery* (%)	Coeff. of variation (%)
Taken	Found		
4.08	4.08	100.00	0.39
8.16	8.14	99.76	0.42
12.24	12.27	100.25	0.03
16.32	16.31	99.94	0.11
20.40	20.40	100.00	0.08
32.64	32.59	99.85	0.15
40.80	40.78	99.95	0.14
61.20	61.26	100.10	0.22
81.60	81.66	100.07	0.12

*Average of six readings.

Table 2—Determination of Thallium in Presence of Diverse Metal Ions

(Thallium present in solution = 20.40 mg)

Metal ions	Quantity added (mg)	Tolerance (mg)	Tl found (mg)	Recovery* (%)
Pb(II)	30	200	20.34	99.71
Cu(II)	20	160	20.37	99.85
Ni(II)	25	80	20.41	100.05
Cd(II)	20	100	20.44	100.20
Co(II)	40	180	20.42	100.10
Bi(III)	26	205	20.41	100.05
Fe(III)	10	80	20.42	100.10
Hg(II)	15	100	20.39	99.95
Al(III)	20	100	20.39	99.95

*Average of five readings

optimised conditions. The results presented in Table 1 indicate that the method is accurate besides being precise.

Effect of foreign ions

The effect of diverse metal ions present as co-ions in the solution on the accuracy and precision of the method for determination of Tl(III) was examined by estimating 20 mg of Tl(III) in the presence of cations like Pb(II), Cu(II), Ni(II), Cd(II), Co(II), Bi(III), Fe(III) and Hg(II). These ions did not interfere in the determination. Al(III) interfered at room temperature as its complexation with EDTA is kinetically slow. However, its interference could be avoided by heating the mixture to 80°C just before the back titration. But cations like Cr(III), Mn(II), Sn(II), Sn(IV), Pd(II), Ga(III) and In(III) interfered. The results relating to non-interfering cations are summarised in Table 2.

Application

In order to confirm the utility of the proposed method, it was used for the determination of thallium in its complexes with mercapto ligands and also in mixtures of thallium(III). Tl(III) complex with 4-amino-5-mercapto-3-methyl-1,2,4-triazole (Found: Tl, 61.38%, Calc. 61.27%). Tl(III) complex with 4-benzylidene-3-ethyl-5-mercapto- 1,2,4-triazole (Found: Tl, 46.82%, Calc. 46.97%). Tl(III) complex with 5-amino-2-mercapto-1,3,4-thiadiazole (Found: Tl, 60.89%, Calc. 60.73%). Tl(III) complex with 4-amino-3,5-dimercapto-1,2,4-triazole (Found: Tl, 58.01%, Calc. 58.13%). The method was also used for determining the compositions of alloys containing thallium. The results are summarised in Table 3.

Table 3—Determinatiion of Thallium in Artificial Mixtures

Metal ions	Quantity added (%)	Thallium† present (%)	Thallium* found (%)
Pb + Bi	33.3 + 55.2	11.5	11.51
Pb + Bi + Cd	35.8 + 44.3 + 11.0	8.9	8.89
Hg	59.5	40.5	40.56

*Average of 3 readings; †By difference.

Mechanism of demasking

Of the many possible mechanisms of demasking metal-EDTA complexes, the one involving change in the oxidation state of the metal seems to be the most plausible. Thallium forms a stable complex with EDTA in its trivalent state[10] (log *K*, 22.5), but shows little tendency for complexation in monovalent state[11]. Even if Tl(I) forms a complex with EDTA, it may do so only in basic medium (*p*H 8-9), but complete decomposition of Tl(I)-EDTA complex takes place in acidic medium (*p*H 5-6)[12]. Therefore, the redox system Tl(I)-Tl(III) can be conveniently employed in the acidic medium for its complexometric determination. Hydrazine sulphate is a powerful reducing agent in both acidic and basic media and is also a good complexing reagent. In the acidic medium, as employed in the present work, effective reduction of Tl(III) to Tl(I) takes place by a 4 electron process. The reaction involved can be represented as follows:

$$N_2H_4 \rightarrow N_2 + 4\,H^+ + 4\,e^-$$

$$2\,Tl^{3+} + 4\,e^- \rightarrow 2\,Tl^+$$

Hydrazine sulphate thus selectively demasks Tl(III)-EDTA complex through reduction of Tl(III) to Tl(I) and releases EDTA quantitatively and instantaneously at room temperature itself. Besides changing the oxidation state of thallium, hydrazine sulphate forms stable complex with the Tl(I) so formed. This is indicated by the fact that chloride and chromate tests with the solution are negative.

The authors are thankful to Prof. B S Basavarajaiah and Prof. T Ramachandran, Principals and Prof. S B Akki, Head of the Chemistry Department, Karnataka Regional Engineering College, for providing laboratory facilities.

References

1 Vekshin U V, Pechurova N I, Spitsyn V I, *Zh neorg Khim*, **21** (1976) 972

2 Vekshin U V, Pechurova N I, Spitsyn V I, *Zh neorg Khim*, **22** (1977) 3044

3 Prague Busev A I, *Anal chim Acta*, **27** (1962) 493.

4 Szekers Keliner A, *Chem Anal*, **55** (1966) 77.

5 Verma Krishna K & Rawat Rameshwar, *Chem Anal (Warsaw)*, **25** (1980) 729.

6 Agarwal R C & Srivastava A K, *Indian J Chem*, **4** (1966) 359

7 Vogel A I, *A text book of quantitative inorganic analysis*, 4th Edn (Longmans, London). 1978, 482 & 488.

8 Gadag R V & Gajendragad M R, *Indian J Chem*, **16A** (1978) 703.

9 Gadag R V & Gajendragad M R, *Curr Sci*, **48** (1979) 839.

10 Saito K & Jerry H, *J chem Soc*, (1976) 4701.

11 Prabil R, *Talanta*, **14** (1967) 613.

12 Ioan Al Crisan & Maria Paniti-Bolyai, *Ser Chem*, **12** (1967) 39.

Indian Journal of Chemistry
Vol. 27A, January, 1988, pp. 85-86

Rapid Determination of Manganese by Differential Pulse and Alternating Current (Ist harmonic) Polarography

RASHMI LAKHANI, S S DESHPANDE & A P JOSHI*
Department of Chemistry, Nagpur University, Nagpur 440 010

Received 24*th February* 1987, *revised* 13*th April* 1987, *accepted* 12 *May* 1987

Manganese(II) in trace amounts has been determined by differential pulse polarography (DPP) and alternating current (Ist harmonic) polarography (ACP) in 0.01 *M* LiCl and TEA + NaOH (0.1 *M* each) supporting electrolytes respectively. Manganese(II) gives well-defined, diffusion-controlled, reversible waves with E_p of − 1.472 V and − 0.452 V versus Ag/AgCl (saturated KCl). Linear calibration plots are obtained from 10 ppb to 10 ppm and from 50 ppb to 10 ppm in DPP and ACP respectively, the minimum determinable limits being 10 ppb and 50 ppb respectively. Effect of various metal ions, which commonly occur with Mn(II) has also been studied. The DPP in TEA (0.2 *M*) + NaOH (0.1 *M*) medium has been successfully used for the determination of Mn(II) in high speed steel, coal ash and pharmaceutical products.

Many techniques such as stripping voltammetry[1,2], a.c. polarography[3,4] and dpp[5-7] have been employed for the microdetermination of Mn(II). Presently we hve used differential pulse polarography and a.c. (Ist harmonic) polarography (ACP) for the determination of Mn(II) at ppb level.

A Metrohm-E-506 polarocord with attached cell assembly was used for recording the polarograms. Electrode assembly consisted of a dropping mercury electrode (d.m.e.) as an indicator electrode, Ag/AgCl (saturated KCl) as a reference electrode and Pt metal as an auxiliary electrode. All chemicals used were of AR grade. Stock solutions (0.5 *M*) of the supporting electrolyte were prepared in triply distilled water; working solutions (0.1, 0.05, 0.01 *M*) were prepared by suitable dilutions.

Stock solution of Mn(II) was prepared in triply distilled water using $MnSO_4.4H_2O$ (AR) and standardized. The working solution contained 150 μg of Mn(II)/25 μl. All usual precautions of trace analysis were observed.

Procedure employed in DPP of Mn(II)

Lithium chloride (2.5 ml, 0.1 *M*) was taken in the cell and to this was added the maxima suppressor triton-X-100 (1 ml, 0.001%). The volume was made upto 25 ml. To this, Mn(II) solution (25 μl) was added. The solution was completely deaerated by passing dry N_2 for 15 min and the polarogram recorded against the blank under the following conditions: scan range = − 1.2 to − 2.2 V; scan rate = 4 mV/s; t_{drop} = 0.8; mm/t_{drop} = 1.0; and pulse modulation amplitude = 10 mV.

Procedure employed in ACP of Mn(II)

Triethanolamine (TEA) and aqueous NaOH (2.5 ml, 1 *M* each) were taken in the cell and polarogram recorded under the conditions mentioned in differential pulse polarography with a.c. frequency of 75 Hz and phase angle of 0°.

Differential pulse polarography (DPP)

A variety of supporting electrolytes (neutral, organic and inorganic salts) were employed for recording differential pulse polarograms. Following electrolytes were studied for this purpose: KCl (0.1 *M* to 0.01 *M*); NaOAc (0.1 *M* to 0.01 *M*) NH_4Cl (0.1 *M* to 0.01 *M*), KNO_3(0.1 *M* to 0.01 *M*), trisodium citrate (0.2 *M* to 0.05 *M*); disodium tartrate (0.2 *M* to 0.05 *M*); Na-oxalate (0.1 *M* to 0.01 *M*); Na-succinate (0.1 *M* to 0.01 *M*); Na-salicylate (0.1 *M* to 0.01 *M*); LiCl (0.1 *M* to 0.01 *M*) and sodium dihydrogen phosphate (0.1 *M* to 0.01 *M*).

Amongst these, LiCl solution (0.01 *M*) was found to be most suitable as it gave smooth base line, symmetric, reversible, diffusion-controlled peaks with evenly rising steps, and higher current values and high reproducibility.

The presence of Triton-X-100 (4×10^{-5}%) was found to give improved base line and peak symmetry as compared to others and hence was used as the maximum suppressor.

Current-concentration relationship was found to be linear in three concentration ranges: 10 ppb to 100 ppb, 0.1 ppm to 1.0 ppm, and 1 ppm to 10 ppm. The minimum determinable limit was found to be 10 ppb.

Amongst the various ions studied for interference study Zn(II), Cd(II) and Cu(II) could be tolerated upto a ratio of 1:25, Pb(II) upto 1:20 while Co(II), Mo(VI) tolerated upto 1:10 and V(V) upto 1:5 only. Iron(III) and Cr(III) interfered seriously in the determination of Mn(II). However, interference due to Fe(III) and Cr(III) could be overcome by using 0.2 *M* TEA + 0.1 *M* NaOH as the supporting electrolyte in which Mn(II), Fe(III) and Cr(III) peaks were well separated with peak potentials corresponding to − 0.476 V, − 1.316 V and − 0.998 V respectively. Linear calibration plots of Mn(II) in the range of 0.1 ppm to 10 ppm were also obtained in TEA + NaOH medium. The recording parameters for this particular supporting electrolyte were as follows: scan range − 0.2 to − 1.7 V; scan rate = 6 mV/s; t_{drop} = 0.8, mm/t_{drop} = 1; and pulse modulation amplitude = 40 mV.

Table 1—Determination of Mn(II) in High Speed Steel and Coal Ash Samples

[High speed steel contains 0.27 g% Mn(II)]

Sample	Wt of Mn(II) (g%)			
	DPP Method		ACP Method	
	A	B	A	B
	High speed steel samples (BCS)*			
1	0.2717	0.2634	0.285	0.270
2	0.2751	0.2746	0.270	0.260
Coal ash samples (wt of Mn(II) mg/g coal ash)				
1 Ramkrishna Godavari Valley coal field (AP)†	0.160	0.156	0.158	0.154
2 Bhatadi coal field, Wardha (M S)✦	0.048	0.0487	0.049	0.050

(A) Calibration method, (B) standard addition method
* RMD:1.98%; † RMD:1.273%; and ✦ RMD:1.175%

The method developed using TEA + NaOH was further extended for the determination of Mn(II) in high speed steel, coal ash and pharmaceutical products.

Determination of Mn(II) in high speed steel by DPP

Steel sample (0.3 g) was treated with 25% H_2SO_4 (50 ml) and the solution warmed gently till hydrogen evolution ceased. The contents were cooled and H_2O_2 (100 ml) was added to oxidize any carbide residue. The solution was boiled to expel excess of H_2O_2, cooled and the volume made upto 100 ml with triply distilled water[8]. The polarograms were recorded in TEA + NaOH medium with 1 ml and 2 ml aliquots of sample solution. The amount of Mn(II) was computed from calibration plots and ascertained by standard addition method. The results are presented in the Table 1.

Determination of Mn(II) in coal ash by DPP

To a weighed quantity of coal ash were added 1:1 HCl (25 ml) + conc. HNO_3 (1 ml) and heated to dissolve ash and to expel acid. This procedure was repeated two-three times and finally the volume was made upto 25 ml with triply distilled water. The polarograms were recorded in TEA + NaOH supporting electrolyte with 1 ml to 2 ml aliquots of the sample solution. The concentration of Mn(II) was determined by referring to the calibration curve and ascertained by standard addition method. The results are given in Table 1.

Determination of Mn(II) in drugs by DPP

Cyltab, a vitamineral tablet (Dupher-Interfran Ltd) was analysed for Mn(II) content. Total 5 tablets were taken in a beaker. Hydrochloric acid (10 ml) and a few drops of H_2SO_4 were added to these and volume was made upto 25 ml with triply distilled water. The contents were heated for 3-4 hr, cooled, filtered and the filtrate evaporated to dryness. The residue was dissolved in triply distilled water (25 ml). An aliquot (1 ml) from this was placed in the cell and the polarogram recorded in TEA + NaOH medium. The amounts of Mn(II)/tablet were found to be 0.3531 mg and 0.35 mg by calibration and standard addition method respectively (literature, 0.355 mg/tablet).

Alternating current (Ist harmonic) polarography (ACP)

A variety of electrolytes (alkaline, neutral complexing agents and buffers) were tried as background electrolytes for Mn(II) analysis. The current response and peak symmetry were observed to be the best in TEA + NaOH with relatively lower current value. The supporting electrolytes studied were: KCl (0.5 *M* to 0.01 *M*); Na-succinate (0.1 *m* to 0.01 *M*); KNO_3 (0.1 *M* to 0.01 *M*); NH_4OH + NH_4 succinate (0.1 *M* each); NH_4OH (0.1 *M*) + citric acid (0.05 *M*); NH_4OH (0.1 *M*), tartaric acid (0.1 *M*); and TEA (0.1 *M*) + NaOH (0.1 *M*).

Calibration plots obtained for Mn(II) in TEA + NaOH medium were linear in the Mn(II) concentration range of 50 ppb to 10 ppm. The lowest determinable limit was 50 ppb with relative mean deviation of 1.13%.

Amongst the number of diverse ions studied for interference studies, Cu(II), Co(II), Ni(II), Pb(II) and Zn(II) could be tolerated upto the ratios 1:10, 1:5, 1:7, 1:3 and 1:7 ratios respectively while Cd(II), Fe(III) and Cr(III) could be tolerated upto a ratio 1:25 only. The results of determination of Mn(II) in high speed steel, and coal ash using a.c. polarography are presented in Table 1.

The authors are grateful to Alexander von Humboldt Foundation, West Germany for the donation of a Metrohm polarograph. One of the authors (SSD) is grateful to UGC, New Delhi for the award of a junior research fellowship.

References

1 O'Halloran R J, *Anal chim Acta*, **140** (1982) 51.
2 Trojonek A & Opekar F, *Anal chim Acta*, **126** (1981) 15.
3 Sister Yu D, *Polarografia V tokh Analyze Kishinev* (1979) 42. *Chem Abstr*, No. 101458q, Vol: 91 1979.
4 Zabeski J & Stoch A, *Chem Anal*, **18** (1973) 951.
5 Igarashi K, Motsunaga K, Abe K, Kudo J, Fukase S & Yanado M, *Hakkaido Diagaku Suisangakubu Kenkyu Iho*, **34** (1983) 30. *Chgem Abstr*, 132919k, Vol: 99, 1983.
6 Wisser K & Woehrle G, *Mikrochim Acta*, **5** (1980) 129.
7 De Galen L, Enkelum C, Jongerius C *et al.*, *Fresenius Z anal chem*, **264** (1973) 173. *Chem Abstr*, 26834f Vol: 79, 1973.
8 Gholse S B, Deshmukh B K & Anokar P J, *J Indian chem Soc*, **62** (1984) 466.

Indian Journal of Chemistry
Vol. 27A, January, 1988, pp. 87-88

BOOK REVIEWS

Homogeneous and Heterogeneous Photocatalysis, edited by E Pelizzetti & N Serpone (D. Reidel Publishing Company, P.O. Box 17, 3300 AA Dordrecht, Holland), 1986, pp 711 + xvi, Price $ 119.00.

Photocatalysis, a relatively young field, is fast becoming an overwhelming area of considerable interest for its potentiality in solar energy conversion and storage, and given the short time that has elapsed, the progress made has been enormous.

An ever increasing number of photoreactions have been carried out using a great variety of semiconductor materials. Whatever the regimen used, the main steps which can be envisaged in a photocatalytic process are: (i) photogeneration of electron-hole pairs and their trapping by suitable reducible-oxidisable species to prevent recombination; (ii) chemical transformation of these species into suitable products and their separation (desorption); and (iii) regeneration of the photocatalysts. All such reactions are characterised by low yields, the reason being the difficulty of efficiently performing one or more of the above described stages.

The book under review contains papers presented at the "NATO Advanced Research Workshop on Homogeneous and Heterogeneous Photocatalysis" held at Maratea (Italy) during 1985. The latest developments in some of the intriguing aspects of photocatalysis are well documented in this book, which concludes with a summary of three-panel discussions held at the end of the workshop.

A good number of papers directly deal with the important role played by relay and photosensitiser species and their requirements for effecting a variety of photoinduced electron transfer processes during the conversion of solar energy into fuels. The transition metal complexes appear to be the most suitable chemical molecules in the design of useful relays and photosensitisers. Even if, at the end, it proved impractical to convert solar energy into fuels, the rewards for the development of photosensitisers and relays are enormous because these species can generate a wealth of novel and fascinating chemistry.

Charge injection into irradiated semiconductors and attempts to identify the factors that should be controlled to optimise the cage escape efficiency, have afforded new methods for effecting photocatalytic oxidations. The advantages afforded by this method may include: (i) high chemoselectivity, (ii) controlled secondary reactions of primary reactive intermediates, and (iii) the possibility of restricting the number of electrons exchanged photocatalytically.

The applications of laser photolysis technique to monitor directly the dynamics of fundamental processes such as charge carrier trapping and recombination and flash excitation technique (to determine the rate of interfacial charge transfer from the conduction and valence band of the particle to species present at the surface or in solution) throw more light in a qualitative manner in elucidating the nature and reactivity of charge carriers in colloidal semiconductor particles.

The book describes some of the latest developments in designing efficient photocatalysts being used in advanced researches. Materials like *in situ* generated catalyst-coated colloidal CdS particles in polymerised surfactant vesicles; synthesis of semiconductor clusters of 20-30Å diameter; addition of promoters like Nb and Mg cations on TiO_2 particles and a new class of low band gap materials such as linear chain Pt(II) double salts for the production of fuel gas through cleavage of water, are open for further exploitation.

The reduction of nitrogen on illuminated titanium dioxide surfaces is perhaps the most interesting of many catalytic reactions. Evidences are found to show that photoexcitation of TiO_2 produces reactive centres capable of reducing and possibly oxidising chemisorbed nitrogen. Also, species resembling adsorbed hydrogen peroxide which have the capability of interacting with dinitrogen in a consecutive thermal process are reported. The photochemical studies using iron oxides as a catalyst to dissociate water and the possibility of subsequent reaction of hydrogen with carbon dioxide and nitrogen molecules to produce organic molecules and nitrogen containing molecules is a worthwhile attempt under photo conditions.

Clay minerals are not photocatalysts by themselves. But their usage in this field as catalyst support or as adsorbents for running complex photochemical reactions involving molecular species are illustrated well with examples.

Mention has also been made in this book to solve the environmental problems caused by the discharge of toxic minerals into the aquatic and atmospheric ecosystems through heterogeneous photocatalysis.

Even though, the book strikes a balance in an attempt to consider various available semiconductor catalysts, one can immediately notice the ommission of the newly emerging hybrid catalyst such as $Ti_xFe_yO_z$; CdS_xSe_{1-x}, etc. These hybrid catalysts can be effectively used as selective catalysts. Additional information on the newer catalysts of *p*-type materials (GaAs, *p*-GaP, InP) as well as some of the mechanistic pathways to synthesise organic compounds under heterogeneous conditions as is available under homogeneous conditions would have been useful additions to this book.

Nevertheless, this book is a very useful work in print and generates a sense of completeness as it deals with fundamental aspects as well as several diversified practical applications. Some of the research in the applied area is at the stage of technological transfer to industry. I am sure this book will be invaluable for all research workers in the area of photocatalysis.

V Vishwanathan
Catalysis Section (I & PC)
Regional Research Laboratory
Hyderabad 500 007

Organometallic Compounds of Iron, edited by G R Knox (Chapman and Hall Chemistry Source Book) (Chapman and Hall, New York), 1985, pp. xi + 477.

Organometallic Chemistry has been one of the fastest growing chemical topic over the last two decades mainly due to the innumerable industrial, agricultural and other applications. Potential applications of organometallic compounds in new areas are also being constantly discovered and developed. In such a fast growing field any up-to-date source book is a welcome addition to the literature. The new addition to the handbooks on organometallic compounds, which unlike its predecessors "Gmelin's Handbook on Organometallic Chemistry" and "Dictionary of Organometallic Compounds", both of which cover the entire realm of organometallic chemistry and are being constantly used by researchers in this area as the primary source for basic information on all the important type of compounds including reference to the original literature, the present book covers only the organometallic compounds of iron in a form ideally suited for use as a personal reference book.

The book under review is one of the first volume to be published by Chapman and Hall and the information contained has been derived from its earlier multivolume publication "Dictionary of Organometallic Chemistry". The organometallic compounds of iron collected in this book cover the literature till mid-1983. The 2222 compounds selected for the book covering all types of organoiron compounds can be referenced in terms of three types of index: name index, molecular formula index and a CAS registry number index. In addition, each compound is identified in terms of an entry number with a graphical structural representation of the compound. This allows rapid location of the compound of interest which would have been difficult with formula index only.

In the main body of the book the compounds have been arranged in order of molecular formula accompanied by the corresponding entry numbers. For each compound the molecular formula, IUPAC name, molecular weight, physical description, stability, solvent for crystallization, solubility, melting point, toxicity are given along with the structural diagram and selected references indicating the nature of information available therein. All organoiron chemists, I believe, would feel indebted to Prof. Knox for compiling such a concise data bank. This book will be a very valuable addition to the personal library of all organoiron chemists. Organometallic chemists working with other metals would be eagerly looking forward to such books on elements of their interest.

B Majee
Department of Chemistry
University of North Bengal
Raja Rammohunpur (Darjeeling) 734 430

Indian Journal of Chemistry
Vol. 27 A, February 1988, pp. 89-93

Solvent & *p*H Effects on Photochemistry & Photostability of Two Possible Laser Dyes, 7-Amino-3-(2′-benzoxazolyl)quinoline and 6-Amino-2-(2′-benzimidazolyl)indole

T MUKHERJEE*, K N RAO & J P MITTAL
Chemistry Division, Bhabha Atomic Research Centre, Trombay, Bombay 400085

Received 14 *May* 1987; *revised and accepted* 6 *July* 1987

Absorption and emission spectra of two heterocyclic dyes, viz. 7-amino-3-(2′-benzoxazolyl)quinoline (7-ABQ) and 6-amino-2-(2′-benzimidazolyl)indole (6-ABI) have been studied in a number of solvents and in aqueous ethanol of different *p*H. The photodamage in different solvent systems has been evaluated and compared. Highest photostability has been obtained in ethanol-water and ethanol-glycerol mixtures. Aqueous surfactant solution and nonpolar solvents accelerate the photodamage

The photophysical and photochemical characteristics as well as photochemical stability of a dye system employed in a dye laser determine the ultimate suitability and reliability of a dye in dye laser[1,2]. Estimate of stability of a number of dyes and the dependence of stability on a number of physicochemical parameters have been discussed by various authors[3-8], with little or no attention to the solvent effect on photostability. Since solvent parameters like dielectric constant, viscosity, hydrogen bonding, donor-acceptor properties, *p*H, temperature etc. affect the optical properties of a dye molecule in solution, the choice of appropriate solvent plays a significant role in photodecomposition process[9-12].

We have earlier shown[12] the feasibility as laser dyes of two heterocyclic dyes, viz. 7-amino-3-(2′-benzoxazolyl)quinoline (7-ABQ) and 6-amino-2-(2′-benzimidazolyl)indole (6-ABI).

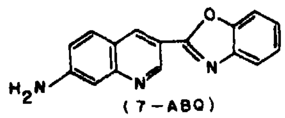

(7-ABQ)

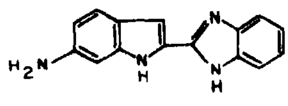

(6-ABI)

In this paper, we have studied the effect of different solvents on the photodecomposition of these two dyes. A comparison of their stability characteristics with those of coumarin 1 and coumarin 120 dyes has also been made. The effect of *p*H on the absorption and emission characteristics is also reported, with possible dye laser applications.

Materials and Methods

The dyes 7-ABQ and 6-ABI were kindly synthesised by Prof. S. Seshadri, Department of Chemical Technology, Bombay University, and were purified by repeated crystallisations from ethanol. All solvents were generally spectrograde (E. Merck) or GR grade (Sarabhai). Further purification was done in some cases to obtain fluorescence-free solvents. Water was re-distilled from alkaline permanganate and acidic dichromate.

The UV-visible absorption spectra were recorded on a Hitachi 200-10 recording spectrophotometer and fluorescence excitation and emission spectra on an AMINCO-Bowman 4-8202B spectrophotofluorometer fitted with a R-136 photomultiplier tube. Fluorescence life-time was measured using a single photon counting instrument (Edinburgh Instruments' 199 M system, UK), fitted with an LSI 11/23 computer (Plessey, UK) and approptiate deconvolution-fit programmes. A Rayonet photochemical reactor (Southern New England Ultraviolet Co., USA) was used for photolysis, using 350 nm 'blakc-light' lamps, and a merry-go-round (4 rpm) for uniform irradiation. An Elico LI-10 *p*H-meter with a Toshniwal combination electrode was used for *p*H measurements.

Results and Discussion

The photophysical characteristics of 7-ABQ and 6-ABI have earlier been shown[12] to be quite comparable to those of coumarin 1. Since the main absorption bands in ethanol appear at 340 nm for 7-ABQ and 332 nm for 6-ABI, the two dyes undergo photodecomposition when irradiated with photons of appropriate energy (say N_2-laser, 337.1 nm). Under identical irradiation

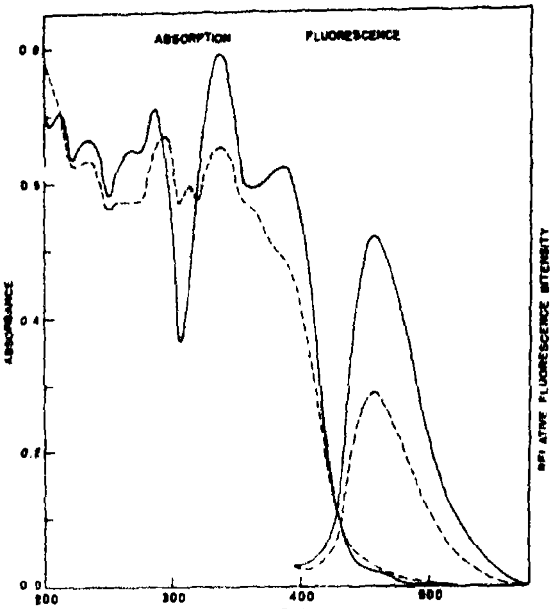

Fig. 1 - Absorption and fluorescence spectra of 7-ABQ in ethanol [(—) Before photolysis, and (---) after 1 hr photolysis]

conditions, the photodecomposition was found to be ~21.5% for 7-ABQ and ~30% for 6-ABI.

Figures 1 and 2 show the absorption and fluorescence spectra of ethanolic solutions of 7-ABQ and 6-ABI respectively before and after photolysis. The solvent systems empolyed, the absorption and fluorescence characteristics and the relative photodecomposition rates with respect to ethanol for 7-ABQ and 6-ABI are given in Tables 1 and 2 respectively. Photobleaching was apparent from the decrease in intensity of the absorption band at the absorbance maximum without significant change in the shape of absorption spectra in most solvents. The photodamage in ethanol was not so extensive[10] as has been observed for coumarin 1 and coumarin 120, the stability being more marked in 7-ABQ. In the case of 6-ABI, the loss in fluorescence intensity in the irradiated solutions, compared to the smaller loss in absorbance, clearly indicates the presence of a photoproduct of 6-ABI, which absorbs in the same region, but is either non-fluorescent or weakly fluorecent or acts as a quencher of the dye fluorescence. The decomposition products show very little absorption at wavelengths greater than the initial absorption.

That the dye structure and its interaction with the solvent is the most significant factor in governing the photostability is evident from the fact that both 7-ABQ and 6-ABI undergo severe photodamage in DMF or DMSO (Tables 1 and 2) in which the coumarin 1 and coumarin 120 have good photostability[10]. The stability is significant in aqueous ethanolic solutions as well as ethanol-glycerol (1:1) solutions, although 7-ABQ is less stable in ethanol-glycol (1:1) than in ethanol. While DMSO has been a traditional solvent for dyes, and is a good triplet quencher, its use is associated with some inherent health and safety problems[13]. The stability of these dyes in ethanol-water system is much less pronounced as compared to that of coumarins[10]. Since the positive charge on the amino nitrogen atom cannot be localised as effectively as in the case of coumarins, the effect of the solvent polarity is much less pronounced.

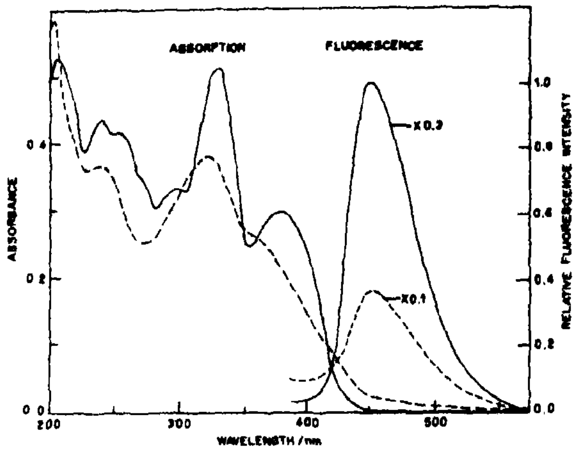

Fig. 2 Absorption and fluorescence spectra of 6-ABI in ethanol [(—) Before photolysis, and (---) after 1 hr photolysis].

The photobleaching of 7-ABQ and 6-ABI is very fast in 5% aqueous Triton X-100 which itself is a triplet quencher and a deaggregating agent. The effect is similar to that observed in the case of coumarins[10] and rhodamine 6G[9]. The photodecomposition pattern of 7-ABQ and 6-ABI in ethanol-CCl_4, ethanol-benzyl alcohol, ethanol-benzene, ethanol-methyl isobutyl ketone, acetonitrile etc. is similar to that of coumarins in the corresponding solvents[10] and hence does not need any discussion.

Effect of pH

Tables 1 and 2 also indicate the effect of *p*H on the absorption, fluorescence and photostability of 7-ABQ and 6-ABI respectively in aqueous ethanolic solution. The effect is more marked in 7-ABQ and 6-ABI than in coumarins, due to the presence of $-NH_2$ group in both 7-ABQ and 6-ABI and additional imino nitrogen atom in 6-ABI. On acidifying solutions of 7-ABQ and 6-ABI, large red shifts (~50 nm) are observed in the absorption spectra, while the colourless solutions of the two dyes turn deep yellow on adding a drop of HCl. The process is found to be quantitatively reversible. Figure 3 shows the effect of *p*H

Table 1—Solvent Effects on Absorption, Fluorescence and Photodecomposition Characteristics of 7-ABQ

([7-ABQ] = 3.65×10^{-5} mol dm^{-3})

Solvents[a,b]	Before photolysis		After photolysis		Relative photobleaching rate (w.r.t. EtOH)
	λ^{abs}_{max} (nm)	λ^{fl}_{max} (nm)	λ^{abs}_{max} (nm)	λ^{fl}_{max} (nm)	
EtOH	387, 340	457	~387(sh), 340	457	1.00
MeOH	386, 340	458	~386(sh), 344	459	1.54
EtOH-i-PrOH	388, 341	459	~388(sh), 340	459	1.18
EtOH-t-BuOH	388, 342	459	~388(shp, 340)	459	1.59
EtOH-Glycol	386, 342	460	~368(sh), 337	461	1.24
EtOH-Glycerol	385, 342	461	383, 338	462	0.50
EtOH-BzOH	~390(sh)	460	~390(sh)	460	2.81[c]
EtOH-Benzene	382, 342	460	~366(sh), ~328(sh)	458	1.94[c]
EtOH-CCl_4 (9:1)	389, 344	464	n	456	c
EtOH-MBK	386, 343(sh)	458	n	456	c
Triton X-100 (5% aqueous)	388, 344	456	n	457	2.80[d]
Acetone	362	445	n	444	3.60[d]
MeCN	365, 335	442	317	442	2.42[c]
DMF	384, 341	457	~385(sh), ~367(sh), ~342(sh, 327	457	2.31[c]
DMSO	~390(sh), 342	466	336	466	2.13[c]
Pentane	n	418	n	n	n
Cylcohexane	360, 333	395, 410(sh)	n	n	n
EtOH-H_2O (1:2)	367, 336	462	364, 329	462	0.99
EtOH-H_2O (*p*H 1.8)	432, 345	505	404, 334	505	2.66[c]
EtOH-H_2O (*p*H 6.9)	378, 337	462	360(sh), 330, 313	462	0.56
EtOH-H_2O (*p*H ~13)	373, 339	465, ~540(sh)	305	465, ~540(sh)	n

[a] Proportion is 1:1 (v/v) unless specified.

[b] EtOH (ethanol), MeOH (methanol), i-PrOH (isopropanol), t-BuOH (t-butanol, BzOH (benzyl alcohol), MBK (methyl isobutyl ketone), MeCN (acetonitrile), DMF (dimethylformamide), DMSO (dimethyl sulphoxide).

[c] Very fast photo-decomposition rate

[d] Solubility very poor.

[n] Cannot be ascertained

[sh] shoulder

on the absorption and fluorescence spectra of 7-ABQ. The difference in absorption spectra for solutions of 7-ABQ at *p*H 6.9 and ~13 is very marginal, while there is a red shift of ~60 nm (from ~380 nm to ~440 nm) for the main absorption peak. On the other hand, the fluorescence quantum yield at *p*H 13 is nearly one-tenth of that at *p*H 6.9, indicating that there must be an intermediate excited state having pK_a^* between these two *p*H values. The fluorescence red shift is approximately equal to the absorption red shift and may be result of shift in the ground state energy level due to protonation. Excitation at all the absorption maxima gave qualitatively similar fluorescence spectra. Figure 4 shows the effect of *p*H on the absorption spectrum of 6-ABI. The *p*H-effect on 6-ABI is similar to that on 7-ABQ and all the above arguments hold good for 6-ABI also.

The ground state equilibria of the two dyes can be represented as shown in Scheme 1.

From the variation of absorbance as a function of *p*H, the ground state pK_a values were estimated

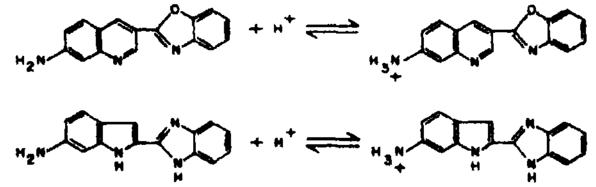

SCHEME 1

to be ~4.15 and ~3.45 for 7-ABQ and 6-ABI respectively. Following Förser's cycle[14], one can write.

$$pK_a - pK_a^* = \frac{\Delta E - \Delta E'}{2.3RT} = 2.1 \times 10^{-3} \Delta \bar{\nu} \qquad \ldots (1)$$

where $\Delta \bar{\nu}$ = difference in frequency (in cm^{-1}) of the zero-zero bands. The corresponding pK_a^* values could now be calculated and are found to be 10.4 (for 7-ABQ) and 9.7 (for 6-ABI), indicating that both the molecules become more basic in the excited state than the ground state. The two excited state structures showing enhanced basicity can therefore be written as shown in Scheme 2,

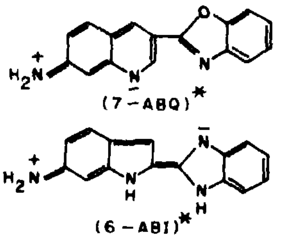

SCHEME 2

although other charge-separated structures may be equally possible.

An interesting situation arises in terms of photostability. 7-ABQ is reasonably photo-resistant at *p*H 6.9, as compared to that in ethanol (Table 1), whereas there is significant deterioration in stability on photolysis of a solution of *p*H 1.8. This is more significant, since the total light absorption at *p*H 1.8 is lower than that at *p*H 6.9. Thus, in order to attain a red-shifted tuning range at acidic *p*H, one has to sacrifice photostability as well as fluorescence intensity. The fluorescence decay time (Fig. 5) changes from 5.18 ns in ethanol[12] to 5.7 ns in ethanol-water (*p*H 7) and 5.4 ns in ethanol-water (*p*H 2). Thus change in fluorescence life-time is insignificant.

On the other hand, there is an improvement in photostability (Table 2) on acidifying a 6-ABI solution in 1:1 ethanol-water to *p*H 1.8. Since the overall number of photons absorbed under the photolysis band (Fig. 4) is comparable, the extra stability for the acidic solution appears to be an inherent property of 6-ABI structure. The fluorescence decay time (Fig. 5) changes from 6.1 ns in ethanol[12] to 6.7 ns in ethanol-water (*p*H 7) and 3.64 ns in ethanol-water (*p*H 2), thus favouring the acidic solutions. However, the loss in fluorescence efficiency in the acidic solution appears to disfavour its use for red shifted tuning.

Thus, use of neutral solution for both 7-ABQ and 6-ABI is recommended for better photostability as well as fluorescence considerations.

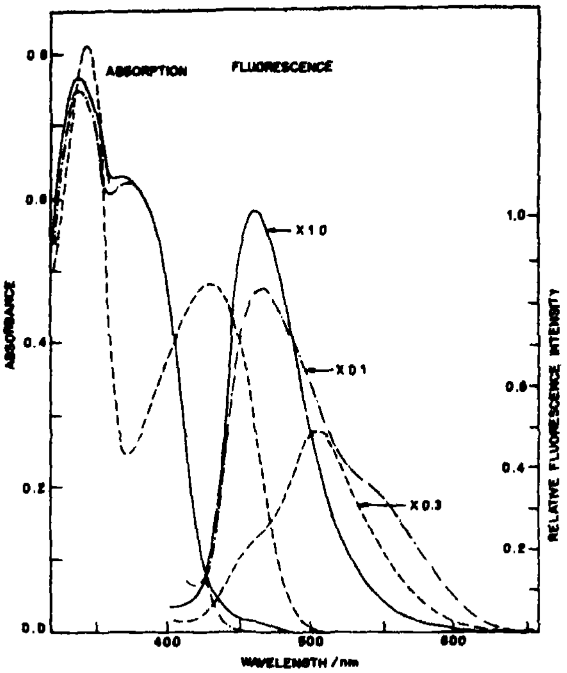

Fig. 3—Absorption and fluorescence spectra of 7-ABQ in ethanol-water mixture (1.1) [(—) *p*H 6.9; (---) *p*H 1.8; (-·-·-) *p*H ~13].

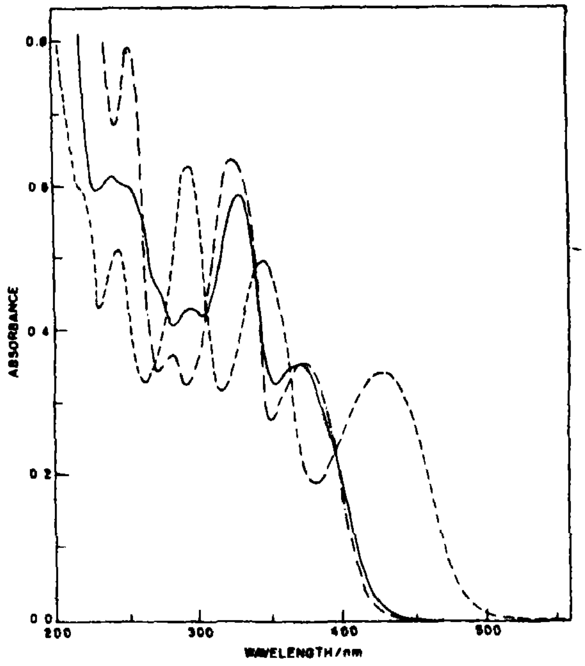

Fig. 4—Absorption spectra of 6-ABI in ethanol-water mixture (1:1) [(—) *p*H 7.2; (---) *p*H 1.8; and (-·-·-) *p*H ~13].

Table 2—Solvent Effects on Absorption, Fluorescence and Photodecomposition Characteristics of 6-ABI

([6-ABI] = 3.65×10^{-5} mol dm^{-3})

Solvents[a,b]	Before photolysis		After photolysis		Relative photobleaching rate (w.r.t. EtOH)
	λ_{max}^{abs} (nm)	λ_{max}^{fl} (nm)	λ_{max}^{abs} (nm)[sh]	λ_{max}^{fl} (nm)	
EtOH	382, 331	449	~381(sh), 325	449	1.00
MeOH	377, 329	450	~377(sh), 324	450	1.00
EtOH-i-PrOH	381, 331	449	~382(sh) 318	446	1.50
EtOH-t-BuOH	379, 331	449	~379(sh), 316	448	1.44
EtOH-Glycol	379, 330	455	~379(sh), 329	455	0.90
EtOH-Glycerol	378, 332	452	377, 330	450	0.27
EtOH-BzOH	388	466	~388(sh)	464	1.54
EtOH-Benzene	379, 330	n	~379(sh), 312	n	2.17[c]
EtOH-CCl_4 (9:1)	380, 331	468	~380(sh), 329	464	2.36[c]
EtOH-MBK	381	448	~381(sh)	n	3.08[c]
Triton X-100 (5% aqueous)	415, 334	475	~415(sh), 332(sh)	485	1.93[c]
Acetone	369	438	~369(sh)	446	2.21[c]
MeCN	368,329	433	~368(sh), 325	440	1.32
DMF	379, 335	448	~379(sh), 313	448	2.86[c]
DMSO	399, 336, 294	369	399, 332, 292	472	1.22
Pentane	i, n	425	n	n	n
Cyclohexane	i, n	425	n	n	n
EtOH/H_2O (1:2)	370, 330	456	~370(sh), 322	456	1.06
EtOH-H_2O (*p*H 1.8)	433, 347, 295	506	432, 347, 294	506	0.22
EtOH-H_2O (*p*H 7 2)	371, 329	454	~371(sh), 321	454	0.86
EtOH-H_2O (*p*H ~13)	377, 326	450	~377(sh), 327	452	1.06

[a] Proportion is 1:1 (v/v) unless specified.

[b] EtOH (ethanol), MeOH (methanol), i-PrOH (isopropanol), t-BuOH (t-butanol, BzOH (benzyl alcohol), MBK (methyl isobutyl ketone), MeCN (acetonitrile), DMF (dimethylformamide), DMSO (dimethyl sulphoxide)

[c] Very fast photo-decomposition rate

[i] Solubility very poor.

[n] Cannot be ascertained

[sh] shoulder

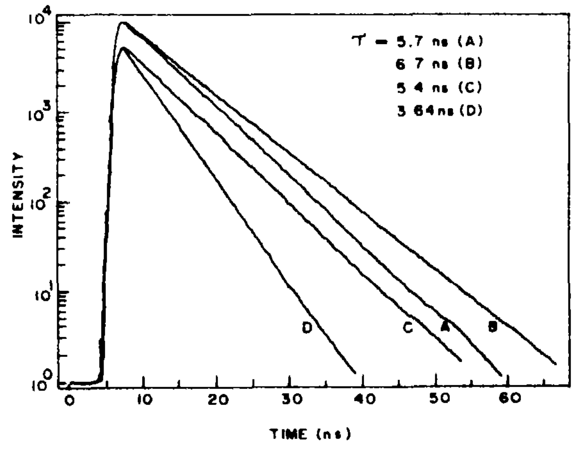

Fig 5—Fluorescence decay profiles of 7-ABQ and 6-ABI in aerated ethanol-water (1:1) solution. [(A) 7-ABQ (*p*H 7), τ = 5.7 ns; (B) 6-ABI (*p*H 7), τ = 6.7 ns, (C) 7-BAQ)*p*H 2), τ = 5.4 ns; and (D) 6-BAI (*p*H 2), τ = 3.64 ns; χ^2 in each case is about 1.1.

References

1 Drexhage K H, in *Topics in applied physics, Dye lasers*, Vol 1, edited by F Schäfer, (Springer-Verlag, Berlin-Heidelberg-New York) 1977.
2 Nair L G, *Progr Quant Elect*, 7 (1982) 153.
3 Reynolds G A R & Drexhage K H, *Opt Commun*, **13** (1975) 222.
4 Schimitschek E J, Trias J A, Hammond P R & Atkins R L, *Opt Commun*, **11** (1974) 353.
5 Schimitschek E J, Trias J A, Hammond P R, Henry R A & Atkins R L, *Opt Commun*, **16** (1976) 313.
6 Jones II G, Bergmark W R & Jackson W R, *Opt Commun*, **50** (1984) 320.
7 Fletcher A N & Bliss D E, *Appl Phys*, **B16** (1978) 289.
8 Fletcher A N, *Appl Phys*, **B31** (1983) 19.
9 Rosenthal I, *Opt Commun*, **24** (1978) 164.
10 Mukherjee T, Rao K N & Mittal J P, *Indian J Chem*, **25A** (1986) 993.
11 Mukherjee T, Rao K N & Mittal J P, *Indian J Chem*, **26A** (1987) 12.
12 Mukherjee T, Rao K N & Mittal J P, *Indian J Chem*, **25A** (1986) 509.
13 Sax N I, *Dangerous properties of industrial material*, (Van Nostrand-Reinhold, New York) 1979, p. 613.
14 Birks J B, *Photophysics of aromatic molecules*, (Wiley-Interscience, London) 1970.

Indian Journal of Chemistry
Vol. 27A, February 1988, pp. 94-97

Spectroscopic Studies on 4-(*p*-Dimethylamino)benzylidene/phenylimino-3-methyl-1-phenyl-2-pyrazolin-5-ones

ANWAR S EL-SHAHAWY*, MAHER M GIRGIS & ZARIEF H KHALIL
Chemistry Department, Faculty of Sciences, Assiut University, Assiut, Egypt

Received 19 *January* 1987; *accepted* 12 *June* 1987

Electronic absorption spectra of 4-(*p*-dimethylamino)benzylidene/phenylimino-3-methyl-1-phenyl-2-pyrazolin-5-ones have been studied in polar and nonpolar solvents. HMO and PPP calculations have been undertaken to investigate the first $\pi^* \leftarrow \pi$ transition and the effect of replacement of carbon atom in 4-(*p*-dimethylamino)benzylidene-3-methyl-1-phenyl-2-pyrazolin-5-one(I) by nitrogen atom as in 4-(*p*-dimethylamino)-phenylimino-3-methyl-1-phenyl-2-pyrazolin-5-one(II). The electron densities at various positions for the two compounds have been calculated by the SCF calculations

Pyrazolone dyes have found wide applications as photosensitisers[1], dyestuffs[2] and analytical[3] and chemotherapeutic reagents[4]. Little attention has been focussed on the electronic absorption spectra of such compounds. Effect of substitution at the phenyl group of 4-arylidene-3-methyl-1-phenyl-2-pyrazolin-5-one on their spectral behaviour has been studied earlier[5]. In the present paper attempts have been made to correlate experimental absorption spectra with the theoretical ones based on HMO and PPP calculations.

Materials and Methods

4-(*p*-Dimethylamino)benzylidene/phenylimino-3-methyl-1-phenyl-2-pyrazolin-5-ones (I and II) were prepared by refluxing equimolar ratios of 3-methyl-1-phenyl-2-pyrazolin-5-one[6] and *p*-dimethylaminobenzaldehyde or N,N-dimethyl-*p*-nitrosoaniline in ethanol containing piperidine as a catalyst[1]. The separated solid products were recrystallized from ethanol. The purity of the compounds (I and II) was checked by elemental analyses: Compound I, m.p. 185° (Found: C, 74.6; H, 6.2; N, 13.7. $C_{19}H_{19}N_3O$ requires C, 74.7; H, 6.3; N, 13.8%). Compound II, m.p. 165° (Found: C, 70.5; H, 5.9; N, 18.2. $C_{18}H_{18}N_4O$ requires C, 70.6; H, 5.9; N, 18.3%).

Stock solutions (10^{-3} *M*) of I and II were prepared by dissolving the accurately weighed amount of the dyes in the appropriate volume of spectral grade solvent (BDH or E. Merck). Working solutions were obtained by accurate dilution.

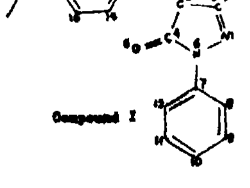

Compound I

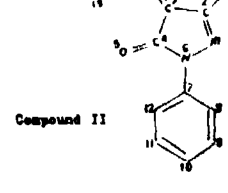

Compound II

The electronic absorption spectra at 27°C were recorded on a Shimadzu UV-200 S double beam spectrophotometer, using 1 cm matched silica cell.

Results and Discussion

Electronic absorption spectra in different solvents and mixed solvents

The λ_{max} and ε_{max} values of the absorption bands of I and II in different solvents used are collected in Tables 1 and 2 respectively.

The plots $\Delta\bar{\nu}$ as a function of $(D-1)/D+1)^7$ for compounds I and II are nonlinear, therefore the band shift is governed by other factors such as solvent-solute interaction, in addition to the dielectric constant of the medium.

The CT bands of I and II are affected by the polarity of the solvent. The observed red shift can be explained by the increase of H-bond strength in 1:1 molecular complex between solute and solvent. The values of formation constant (K_f) of complexes of I and II in ethanol were determined from the spectral behaviour in mixed solvents (see Figs. 1-4) using the relations previously described[8-10].

The values of K_f, ΔG (free energy change of formation) and *n* (the number of EtOH molecules which are complexed with the solute molecule) indicate the formation of 1:1 molecular complexes via a weak intermolecular H-bond (Table 3). The value of K_f is dependent on both the solute and the solvent used.

Theoretical calculations

The HMO and SCF (PPP) calculations were done

Table 1—λ_{max} and ε_{max} Values of Different Bands of I in Different Organic Solvents

λ_{max} (nm)	$\varepsilon_{max} \times 10^{-3}$	λ_{max} (nm)	$\varepsilon_{max} \times 10^{-3}$
	Cyclohexane		
420*	74.16	263	34.58
407	55.00	258	38.74
326	4.25	254	38.58
313	4.75	248	35.74
275(sh)	20.75	243	31.41
	Carbon tetrachloride		
425*	66.24	330(sh)	3.07
407	45.00	264	24.92
	Dioxane		
428*	53.17	325	3.19
407	37.15	310	3.90
		255	29 74
	Chloroform		
442*	88.90	310(sh)	5 51
407	45.12	278(sh)	26.66
	Isopropanol		
450*	48.06	310(sh)	2.20
439(sh)	46.20	262(sh)	18.00
325	1.15	248	24 39
	Ethanol		
460*	70.20	310(sh)	11.01
439(sh)	62.30	270(sh)	33.43
326(sh)	7.47	251	44.84
	Dimethyl Sulphoxide		
465*	84.78	310(sh)	11 23
439(sh)	73.02	275(sh)	31.75
325(sh)	5.73		

*Intramolecular charge transfer band

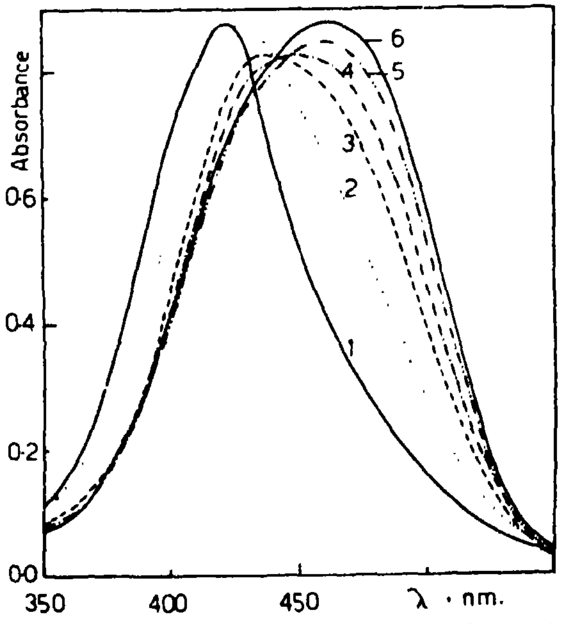

Fig. 1—Electronic absorption spectra of 1.25×10^{-5} *M* solution of I in EtOH-CCl_4 mixtures at 27°C containing [(1) 0.00; (2) 1.20; (3) 4.63; (4) 8.07; (5) 14.08; and (6) 17.17 *M* ethanol]

Table 2—λ_{max} and ε_{max} Values of Different Bands of II in Different Organic Solvents

λ_{max} (nm)	$\varepsilon_{max} \times 10^{-3}$	λ_{max} (nm)	$\varepsilon_{max} \times 10^{-3}$
	Cyclohexane		
481*	52.81	264	37.39
437	48.15	259	45.02
323(sh)	8.90	253	50.84
290(sh)	18.33	249	51.35
277	23.50	244	47.06
	Carbon tetrachloride		
488*	40 25	297(sh)	12.80
439	32.16	267	22.98
325	8.57		
	Dioxane		
500*	47.24	295(sh)	16.90
439	28.89	258	40.38
325	10.05		
	Chloroform		
512*	56.52	297	17 85
438	30 85	256	33.81
325(sh)	11.82		
	Isopropanol		
513*	51.49	295(sh)	15.70
439	26.76	249	41.35
325(sh)	9.70		
	Ethanol		
518*	50.83	297(sh)	12 96
439	25.12	248	37.86
325(sh)	8.21		
	Dimethyl Sulphoxide		
532*	58.89	297(sh)	20.50
445	23.00	261	41.61
325(sh)	14.75		

*Intramolecular charge transfer band.

Table 3—Commutative Data[1] Obtained for Compounds (I and II) in Mixed Solvents

Compound	System	total energy kJ mol^{-1}	n	log K_f	K_f	$-\Delta G$ kJ mol^{-1}
I	C_6H_{12}-EtOH	16.553	1	0.350	2.24	2.027
	CCl_4-EtOH	11.286	1	0.000	1.00	0.000
	$CHCl_3$-EtOH	5.768	1	0.295	1 97	1.705
	H_2O-EtOH	−7.085	2	0.140	1.38	0.792
II	C_6H_{12}-EtOH	11.035	1	0 43	2 69	2.487
	CCl_4-FtOH	8.444	1	0.288	1.94	1.668
	$CHCl_3$-EtOH	2.383	1	0.424	2.65	2.449
	H_2O-EtOH	−8.402	2	0.600	3.98	3.474

(1) at 27°C

as described before[11,12]. From HMO calculations, the eigenvalues of HOMO and LUMO for I ($\varepsilon_{HOMO} = -13.4613$; $\varepsilon_{LUMO} = -10.1985$ eV) and II ($\varepsilon_{HOMO} = -13.3697$; $\varepsilon_{LUMO} = -10.8881$ eV) were calculated. It is clear that replacement of nitrogen at-

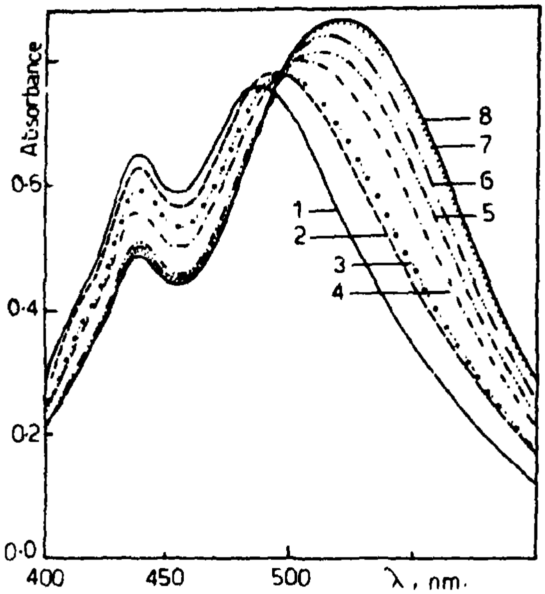

Fig. 2—Electronic absorption spectra of 1.69×10^{-5} *M* solution of II in EtOH-CCl_4 mixtures at 27°C containing [(1) 0.00; (2) 0.86; (3) 1.72; (4) 5.15; (5) 8.58; (6) 11.16; (7) 14.59, and (8) 17.17 *M*ethanol]

Table 4—Electronic Densities of Compounds I and II

Atom	Electron densities I	Electron densities II
1	1.055240	1.029710
2	0.951071	0.956169
3	1.003720	0.502054
4	0.700429	0.749450
5	1.373800	1.346350
6	1.905610	1.906320
7	0.980526	0.980498
8	1.018840	1.018880
9	0.999075	0.999074
10	1.014040	1.014070
11	0.999076	0.999075
12	1.018830	1.018880
13	0.981616	1.529970
14	1.015420	1.003760
15	0.998515	1.003900
16	1.020490	1.024070
17	0.978463	0.975959
18	1.020480	1.024070
19	0.998518	1.003900
20	1.966290	1.958410

om in I by CH to produce II decreases ϵ_{LUMO} and the calculated first $\pi^* \leftarrow \pi$ transitions for I and II are adjacent (380 and 500 nm respectively) and they are comparable with the experimental first $\pi^* \leftarrow \pi$ transitions appearing at 407 and 439 nm respectively.

The SCF-eigenfunctions of LUMO and HOMO are mainly located over 4-dimethylaminobenzylide-

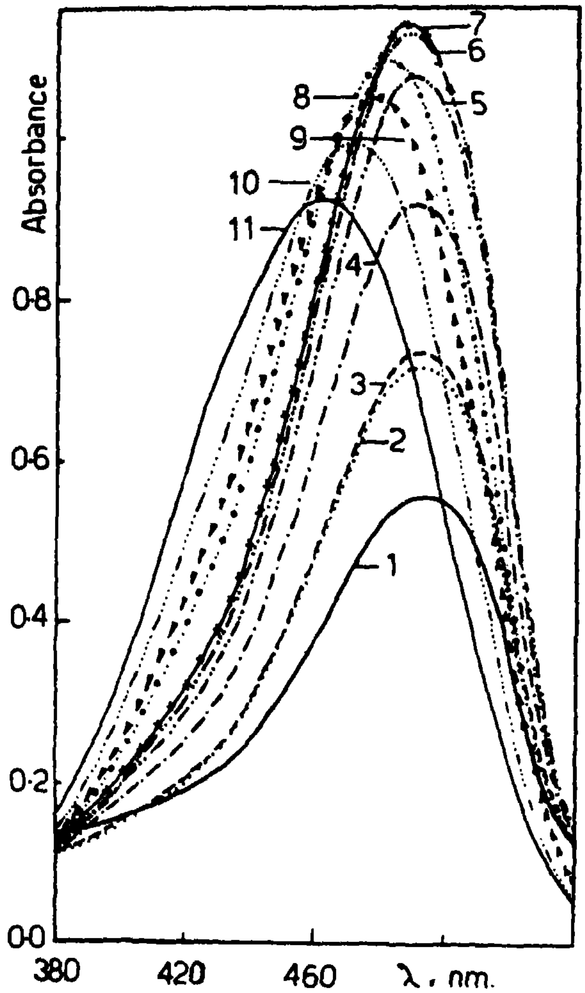

Fig. 3—Electronic absorption spectra of 1.31×10^{-5} *M* solution of I in EtOH-H_2O mixtures at 27°C containing [(1) 1.20; (2) 1 46; (3) 1.80; (4) 2.06; (5) 2.92, (6) 3.78; (7) 4.63, (8) 8.07, (9) 10 08; and (11) 17.17 *M*ethanol]

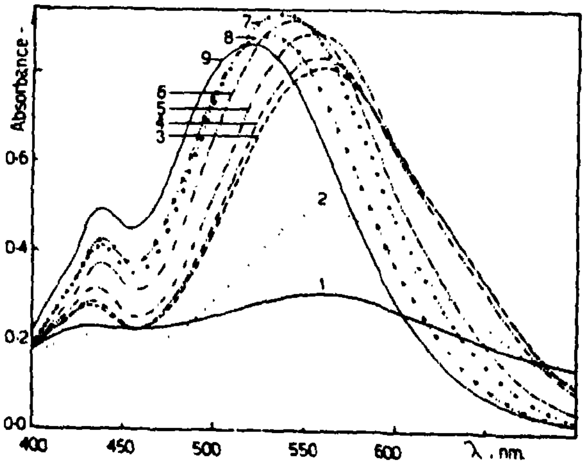

Fig. 4—Electronic absorption spectra of 1.69×10^{-5} *M* solution of II in EtOH-H_2O mixtures at 27°C containing [(1) 1.72; (2) 2.57; (3) 3.43; (4) 4.29; (5) 5.15; (6) 6.01; (7) 11.16; (8) 14.76; and (9) 17.17 *M*ethanol]

ne part in I and over 4-dimethylaminophenylimino part in II. The local symmetry of LUMO and HOMO for the two compounds is B_2, therefore, the first $\pi^* \leftarrow \pi$ transitions for I and II are allowed. This leads to high molar extinction coefficients ($\varepsilon_I = 55 \times 10^3$ and $\varepsilon_{II} = 48.5 \times 10^3$ mol^{-1} cm^2). Also, it is noticed that the contribution of C-13 in HOMO is smaller than that in LUMO. This explains that the variation in the energy of the HOMO is smaller than the variation in the energy of LUMO after the replacement of C-13 by N (as in II).

The electron densities of compounds (I) and (II) were calculated and are presented in Table 4. It is clear from the data in Table 4 that the oxygen atom in I is more negative than that in II. Therefore the energy of the intermoecular H-bond in I is higher than that in II in the different mixed solvents (Table 4). It is concluded that the oxygen atom in position-5 is the negative pole of the intermolecular H-bonding between the solute and the solvent.

References

1 Elderfield R C, *Heterocyclic compounds*, Vol 5 (John Wiley, New York Chapman & Hall, London) 1957, pp 132.

2 Sandoz Ltd. (by Hermann Egli & Richard Kern), *Ger Pat*, 1, 112, 965 (21 Dec, 1957); *Chem Abstr*, **56** (1961) 4995.

3 Trofimov N V, Nekhaev N N, Kanaev N A & Busev A I, *Zh analit Khim*, **37** (1982) 1445.

4 Schoen K (to Endo Laboratories, Inc.), *U S Pat*, 3, 244, 593 (5 April 1966); *Chem Abstr*, **65** (1966) 3885.

5 Mahmoud M R, El-Kashef H S & Abd El-Hamide R, *Spectrochim Acta*, **37A** (1981) 519.

6 Vogel A I, *Practical organic chemistry* (Longmans, London) 1974, 998.

7 Abd El-Mottaleb M S A & Khalil Z H, *Z phys Chim*, **260** (1979) 650.

8 El-Ezaby M S, Salem I M, Zewail A H & Issa R M, *J chem Soc* (*B*), (1970) 1293.

9 Gangaly T & Banerjee, *Spectrochim Acta*, **34A** (1978) 617.

10 Foster R, *Molecular association*, Vol. 1 (Academic Press, London) 1975.

11 El-Shahawy A S, Harfoush A A & Idriss K A, *Spectrochim Acta*, **41A** (1985) 1463.

12 El-Shahawy Anwar, *Bull Sci Ass Univ*, **11** (1982) 47.

Indian Journal of Chemistry
Vol. 27 A, February 1988, pp 98-100

Mode of Lithium Addition to Alumina on Reducibility of Nickel-Alumina

S NARAYANAN* & K UMA

Catalysis Section, Regional Research Laboratory, Hyderabad 500 007

Received 5 *May*, 1987; *revised* 8 *June*, 1987; *accepted* 23 *June* 1987

Modification of γ-alumina by single step and multiple-step addition of lithium before impregnating with nickel improves hydrogen and oxygen uptake. Multiple-step impregnation of lithium helps metal reduction more effectively than the single step impregnation due to increased chances of formation of $LiAl_5O_8$ species and decreased interaction between nickel and modified alumina. The formation of Li-O-Ni kind of species may be responsible for the low reducibility of nickel on modified alumina calcined at 1073 K

Reducibility of supported nickel oxide depends to a great extent onthe nature of the support used. In the case of alumina support the hydroxyl groups which are responsible for its acidity can be eliminated to some extent by calcination at temperatures higher than 873 K. This reduces the nickel-support interaction in the case of nickel impregnated alumina support and helps the reducibility of nickel ions[1]. Alkali and alkaline earth ions are usually used as additives to control the acidity of support and metal-support interaction[2-6]. The extent and type of metal-support interaction affect the degree of reduction of metal ions. Concentration of additives, calcination temperature, order and method of addition of additives play an important role in reduction and dispersion characteristics of a metal. Houalla *et al.*[5] did not find any appreciable effect on dispersion of nickel in the addition of lithium to NiO-supported on γ-Al_2O_3. However, our investigation revealed[7] that lithium addition upto 2 wt% improves reducibility, dispersion and metal area of nickel supported on γ-Al_2O_3. Higher than 2 wt% of lithium addition to γ-Al_2O_3 does not help reduction and this has been explained on the basis of electronic interaction of the type Li-O-Ni between lithium and nickel[7]. As an extension of our earlier paper[7], the mechanism of addition of lithium to alumina in modifying reduction properties of nickel has now been investigated.

Materials and Methods

Harshaw γ-alumina (Al-111-61E) with pore volume 0.65 cm^3g^{-1}, crushed and particles of 1000-1400 μm cross-section was used as a support for preparing the three sets of catalysts, following the flow chart (Fig. 1). Incipient wetness impregnation was used for introducing lithium and nickel with nitrate salt solutions. After impregnation with nickel the catalysts were dried, calcined at 723 K for 5 hr, reduced in a flow of hydrogen at the same temperature for 5 hr, cooled to room temperature and passivated[8] with a mixture of nitrogen and air. The experimental set up for adsorption measurements and the calculation procedure has been described earlier[1]. Acidity was measured by non-aqueous titration method[7]. Auto pore 9200 mercury penetration porosimeter was used to measure total pore area and average pore diameter. X-ray diffraction measurements were done using philips PW 1051 diffractometer with nickel-filtered CuK_α (λ = 1.540 Å) radiation. Metal contents were estimated by atomic absorption spectroscopy.

Results and Discussion

The characteristics of alumina and lithium modified alumina are given in Table 1. The total pore area decreases by the addition of lithium, irrespective of the mode of preparation. It may be due to blocking of narrow pores by lithium[7], which can readily, because of small ionic radius, diffuse into the alumina lattice. This results in increase in average pore diameter whether lithium is added in a single step or multiple steps. Whereas the surface physical properties do not significantly depend on the method of lithium addition, acidity of alumina is decreased, the effect being more pronounced for lithium addition by multiple impregnation.

Hydrogen and oxygen uptake by nickel alumina and nickel on lithium modified aluminas (both single and multiple steps) are given in Table 2. Lithium is added to γ-Al_2O_3 and is calcined at 723 K and 1073 K for 5 hr to modify its properties. γ-Al_2O_3 without lithium also is calcined at the same temperature and time before adding nickel, for a comparison of the reduction properties under identical conditions.

Comparison of catalysts G, I and K shows that lithium addition by whichever method has certainly improved hydrogen as well as oxygen uptake. However,

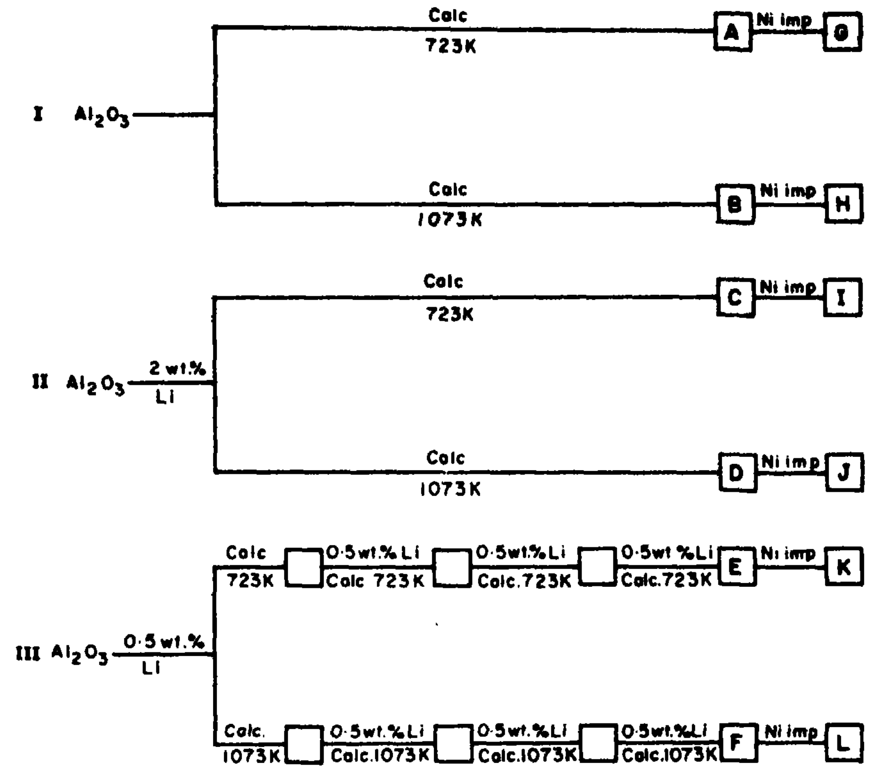

Fig. 1—Flow chart for preparing nickel-alumina catalysts. [Calc-calcination, imp-impregnation.]

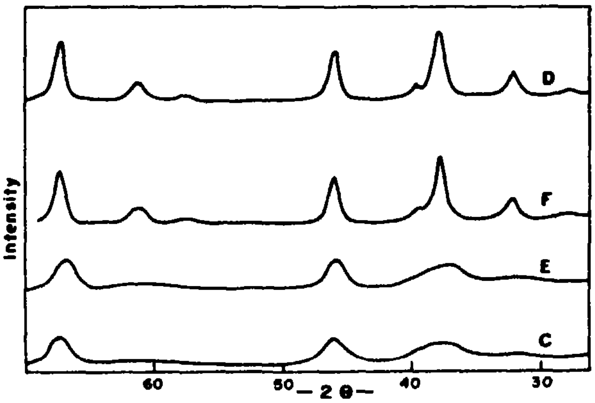

Fig. 2—X-ray diffraction patterns of 2 wt% lithium-modified aluminas calcined at different temperatures [(C) Single step, 723 K; (D) single step, 1073 K; (E) multiple-steps, 723 K; and (F) multiple-steps, 1073 K]

multiple-step impregnation of lithium to alumina before loading nickel seems to be more effective in increasing the reducibility of nickel ions than that achieved by single step impregnation. Relatively higher oxygen uptake compared to hydrogen uptake due to multiple step impregnation of lithium is an indication that more nickel is in bulk than on the surface.

X-ray diffraction patterns of lithium-modified aluminas calcined at 723 K and 1073 K are given in Fig. 2. The starting material Harshaw γ-alumina is amorphous and therefore the characteristic peaks at 2 θ values of 37.6, 45.8 and 66.8° have been identified[7-9] with $LiAl_5O_8$ species. The formation of $LiAl_5O_8$ species reduces the chances of interaction between nickel and alumina. This should help reducibility and

Table 1—Characteristics of Alumina and Lithium-modified Aluminas

Sample	Total pore area ($m^2 g^{-1}$)	Av. pore diam (nm)	Acidity (meq of nBA)
A	265	7.4	0.431
C	226	8.9	0.336
E	243	9.0	0.261
B	218	10.3	0.230
D	176	11.7	–
F	181	12.0	0.202

Table 2—Adsorption Data on Nickel Catalysts

Catalyst	H_2 uptake (μmol g^{-1}Ni)	O_2 uptake (μmol g^{-1}Ni)	Reduction (%)
G	200	718	9
I	270	1708	21
K	357	4762	57
H	1630	4654	56
J	908	7862	94
L	457	4938	59

hence hydrogen uptake if the concentration of metal atoms on the surface also increases. The formation of $LiAl_5O_8$ and the consequential increase in nickel ion reducibility are more when lithium (2 wt%) is introduced by the multiple-step impregnation process. Calcination at 723 K for 5 hr after each dose of lithium addition helps in the diffusion of more lithium into alumina lattice leading to better interaction and hence the increased formation of $LiAl_5O_8$. With the increased formation of $LiAl_5O_8$ the interaction between the support and nickel decreases further, thereby increasing the reducibility and hydrogen uptake. The decrease in acidity of γ-Al_2O_3 (Table 1) on the addition of lithium also supports this, since the hydroxyl groups responsible for acidity are also responsible for interaction[1,7,10] and are used up in spinel formation.

Hydrogen and oxygen uptake of nickel catalysts H, J and L prepared using alumina and lithium-modified aluminas calcined at 1073 K are higher than those for catalysts G, I and K which differ only in the calcination temperature (723 K) of support. It is also clear from Table 2 that both surface and bulk nickel availability has increased. Of all the catalysts, catalyst H shows the highest hydrogen uptake and catalyst J the highest oxygen uptake. The hydrogen uptake by catalyst L is the least even though it is still higher than the calcined samples at 723 K with or without lithium (G, I and K). The reducibilities of catalysts K, H and L are about the same (56-59%). It may be that calcination of alumina without lithium at 1073 K decreases the interaction between nickel and alumina due to dehydroxylation, as has been observed by us earlier[1]. This helps reducibility to some extent and also makes more surface nickel available for hydrogen uptake. Relatively the bulk metallic nickel contents also increase. The oxygen uptake of catalyst J is due to easy reducibility of nickel made possible by lithium addition and calcination. Addition of lithium also neutralizes the hydroxyl groups responsible for acidity[10] and interaction by forming $LiAl_5O_8$ (Table 1 and Fig. 2). This effect is in addition to the dehydroxylation process due to calcination. The decreased interaction, because of this, helps reduction which is almost complete (94%). During the process of reduction, it is likely that more nickel ions are reduced forming large metal crystallites due to agglomeration and less surface nickel atoms. This would probably explain the low hydrogen uptake which is a surface phenomenon.

If the lithium addition and calcination is expected to improve the reducibility as we have seen in the case of catalyst J, the multiple impregnation and calcination steps involved in the preparation of catalyst L should also have the same effect. On the contrary, both hydrogen and oxygen uptake is less than that on catalyst J, and reducibility is only 59%. It is important to have an optimum interaction between the metal ion and OH groups of support to get a reasonable dispersion without agglomeration. The relatively low hydrogen uptake and reducibility of catalyst L may be explained as follows: In the multiple-step modification of alumina, 2 wt% lithium is added in four steps and each step is followed by calcination at 1073 K for 5 hr. It is expected that at each step, lithium diffuses into the pores of alumina and interacts forming $LiAl_5O_8$ species. Calcination helps both the formation of $LiAl_5O_8$ as well as dehydroxylation of OH groups. During each calcination step, naturally, more and more narrow pores are closed exposing only the wide pores (Table 1). The acidity also decreases due to loss of OH groups. It is believed that lithium addition at first few steps results in $LiAl_5O_8$ spinel. Thereafter, there may not be enough OH groups or small pores available for lithium to interact or diffuse into the support. Due to the decreased or relatively no interaction, lithium stays on the surface of alumina as Li_2O. During impregnation steps using this modified alumina with nickel, it is likely that the metal interacts with Li_2O at least partially to form Li-O-Ni species as evidenced earlier[7]. The interacting species makes less nickel available for reduction and for hydrogen adsorption. This explains the low reducibility and low hydrogen uptake of catalyst L prepared by multiple step lithium addition followed by calcination at 1073 K for 5 hr.

Acknowledgement

K. Uma thanks the CSIR, New Delhi for a senior research fellowship.

References

1 Narayanan S & Uma K, *J chem Soc, Faraday Trans* 1, (1985) 2733
2 Tanabe K. *Solid acids and bases* (Academic Press, New York) 1970.
3 Houalla M, Delanny F & Delmon B, *J phys chem*, **85** (1981) 1704.
4 Lopez J M P, Ceckiewicz S, Defosse C, Grange P & Delmon B, *Appl Catal*, **12** (1984) 331.
5 Houalla M, Lemaitre J & Delmon B, *J chem soc, Faraday Trans* 1, (1982) 1389.
6 Machida M, Eguchi K & Arai H, *Chem Lett*, (1986) 151.
7 Narayanan S & Uma K, *J chem Soc, Faraday Trans* 1, (1987) 733.
8 Bartholomew C H & Farrauto R J, *J Catal*, **45** (1976) 41.
9 Levy R M & Bauer D J, *J Catal*, **9** (1967) 76.
10 Brenner A & Burwell (Jr) R L, *J Catal*, **52** (1978) 353.

Indian Journal of Chemistry
Vol. 27A, February 1988, pp. 101-103

Oxygen Chemisorption & X-Ray Diffraction Studies on Molybdena-Titania Catalysts

B MAHIPAL REDDY

Catalysis Section, Regional Research Laboratory, Hyderabad 500007

Received 7 *May* 1987; *revised and accepted* 10 *June* 1987

A series of titania-supported molybdena catalysts with various Mo loadings ranging from 2 to 12 wt% have been prepared and characterized by means of low temperature oxygen chemisorption (LTOC) and X-ray powder diffraction methods. X-ray data indicate that the amount of anatase and rutile forms of titania support undergo changes with increase in Mo concentration. The LTOC results suggest the formation of monolayer MoO_2 patches at about 6 wt% Mo and the anataserutile phase transformations are also found to correlate with this loading on the support.

Titania is an important catalyst material not only because of its effectiveness in photoassisted reactions but also in the enhancement of activity and selectivity of transition and noble metals when used as a support[1,2]. The structural transformations of vanadia – titania catalysts have been extensively investigated by several workers using XRD, EPR, ESCA and other techniques[3,4]. Similar studies on molybdena-titania catalysts are very limited. In the present investigation an attempt is made to characterize the MoO_3-TiO_2 catalysts having various amounts of molybdena in their unreduced and reduced states. In particular, the effect of loading on the structure of the support as well as the dispersion of active component on support surface have been looked into using low temperature oxygen chemisorption (LTOC) and XRD techniques. The LTOC technique has recently been proved to be an important method for measuring specific catalytic surface areas of supported molybdenum oxides and sulfides[5,6].

Materials and Methods

Titonium dioxide (Harshaw-Ti-0720; surface area 169 m^2g^{-1}; pore volume 0.36 ml g^{-1}) supported catalysts with Mo loadings ranging from 2 to 12 wt% were prepared by incipient wetting technique. An appropriate amount of ammonium heptamolybdate (spectroscopic grade, JT Baker, USA) corresponding to the desired Mo loading on the support was dissolved in that volume of water which corresponded exactly to the total pore volume of the quantity of support used for impregnation. The ammonium heptamolybdate solution thus prepared was added to the support, well mixed for 30 min and then allowed to stand for 1 hr. The impregnated samples thus prepared were dried at 120°C for 16 hr and calcined at 540°C for 12 hr in an open air furnace.

LTOC measurements were performed at − 78°C on catalysts, prereduced in a flow of hydrogen (35 ml/min) at 500°C for 6 hr, in a specially designed cell attached to a static volumetric high vacuum system. The details of experimental procedure have been given elsewhere[7]. After the chemisorption experiment BET surface area of the catalyst was determined by N_2 adsorption at − 196°C and the sample was saved after evacuation for XRD measurements. The X-ray diffractograms were recorded on a Philips PW 1051 diffractometer using Ni-filtered CuK_α radiation.

Results and Discussion

Oxygen uptake values and BET surface areas of the reduced MoO_3-TiO_2 catalysts as a function of Mo loading are presented in Fig. 1. Oxygen uptake (g^{-1} catalyst) increases linearly as a function of Mo loading upto about 6 wt% Mo and thereafter levels off with further loading. On the other hand, BET surface areas of the reduced catalysts decrease linearly with Mo loading upto 12 wt%. The saturation in oxygen uptake at 6 wt% Mo loading is indicative of completion of monolayer coverage of the active support surface by Mo oxide phase. A similar trend in oxygen uptake capacities and BET surface areas were also observed on $MoO_3-Al_2O_3$ (ref. 6), MoO_3-C (ref. 8) and MoO_3-ZrO_2 (refs. 9, 10) catalyst systems at different Mo loading. The initial increase and subsequent levelling off in oxygen uptake capacities of the catalysts as a function of Mo loading on different supports are interpreted in terms of Hall's patch model[11]. Based on this model, it is proposed that at low Mo loading small two-dimentional patches of Mo oxide and Mo in octahedral coordination are formed on the support surface. The same structure, however, remains on the support surface as small patches of MoO_2 with coordinately unsaturated Mo sites (CUS) upon reduction in hydrogen. The CUS are the locations on which oxygen chemisorption takes place at low temperatures[12]. As the Mo loading increases the number of these MoO_2 patches increases with attendant increase in the number CUS upto the monolayer level. Hence, oxygen uptake increases linearly with Mo loading upto the monolayer level. Beyond monolayer level these patches grow three-dimensionally, thus decreasing the dispersion of Mo oxide on the support surface. This growth in size of small patches rather in number is expected not to add new CUS per unit of Mo as a function of Mo loading. Therefore, saturation in oxygen uptake beyond monolayer is observed. An important point to note here is that the LTOC technique clearly indicates the Mo loading where the monolayer formation attains completion.

X-ray diffractograms of the unreduced and reduced $MoO_3 - TiO_2$ catalysts are shown in Figs 2 and 3 respectively. In accord with its X-ray profile, the pure TiO_2 support used in this study contains about 85% anatase and 15% rutile phases of TiO_2 but badly crystallized ones. The most intense peaks at 25.3°(2 θ) corresponding to diffraction by planes (101) of anatase and at 27.4°(2 θ) corresponding to the diffraction by planes (110) of rutile are detected in all the samples[13]. The other prominent observable peaks in the spectra are the triplet at 37.4°(2 θ) due to diffraction by planes (103), (004) and (112), as well as the doublet at 53.9°(2 θ) due to the diffraction by planes (105) and (211) of anatase, but these are not well-defined indicating lack of good crystallinity. No XRD lines due to MoO_3 phase and also due to compound formation between MoO_3 and TiO_2 are observed in the spectra.

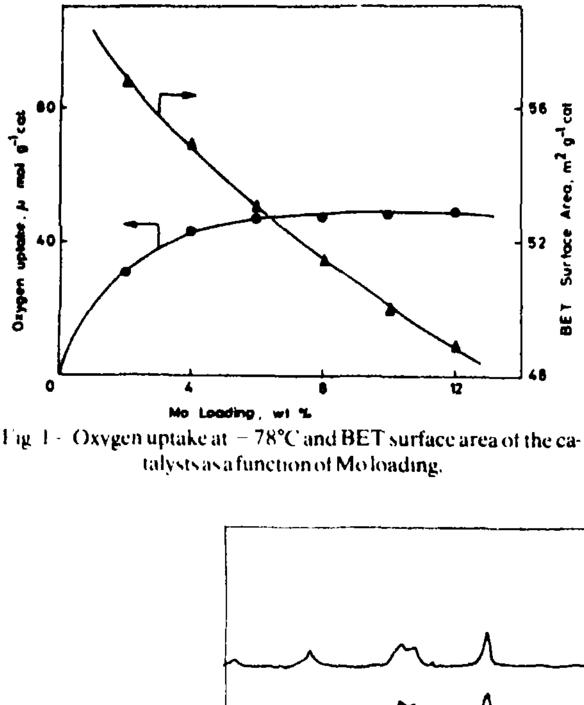

Fig. 1 - Oxygen uptake at − 78°C and BET surface area of the catalysts as a function of Mo loading.

As can be seen from Fig. 3 the prominant peak at 25.3° due to the anatase phase is predominant in all the spectra. The intensity of the peaks are due to rutile phase decreases with Mo loading upto 6 wt% Mo, where the formation of monolayer is observed from LTOC data (Fig. 1), and then starts rising slowly with further Mo loading upto 12 wt%. However, in the case of unreduced samples (Fig. 2) no definite trend in transformation of anatase − rutile phase can be seen in the XRD. This is an interesting observation in this study, but the real significance of these results are not clearly known at present. Bond *et al.*[3] have investigated some of the physicochemical properties of $V_2O_5 - TiO_2$ catalysts using a number of anatase and rutile containing catalysts differing in calcination temperatures and concentration of impurities such as Na^+ and SO_4^{2-}. They reported that during the transformation of anatase to rutile, the vanadia phase was reduced and became incorporated in the rutile structure as $V_xTi_{(1-x)}O_2$ (rutile solid solution). According to Vejux and Courtine[4] the simultaneous reduction of

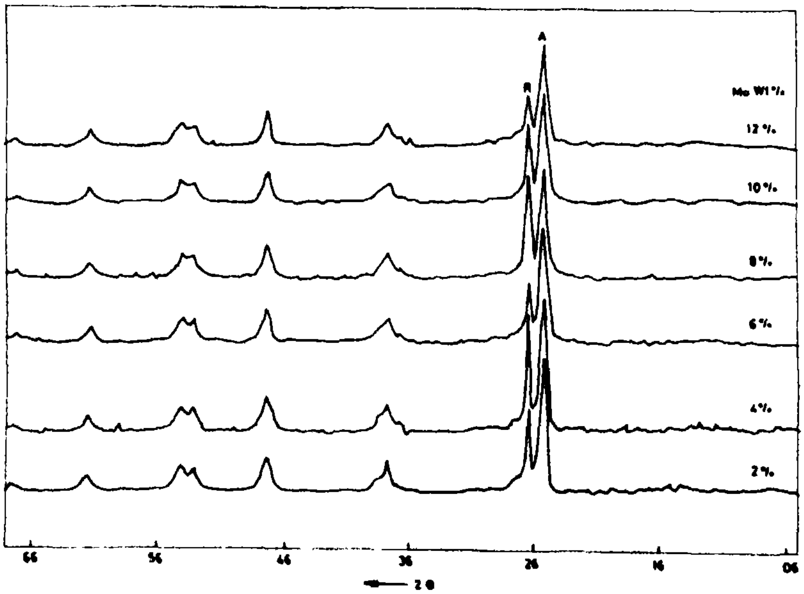

Fig. 2 — X-Ray diffractograms of unreduced $MoO_3 - TiO_2$ catalysts.

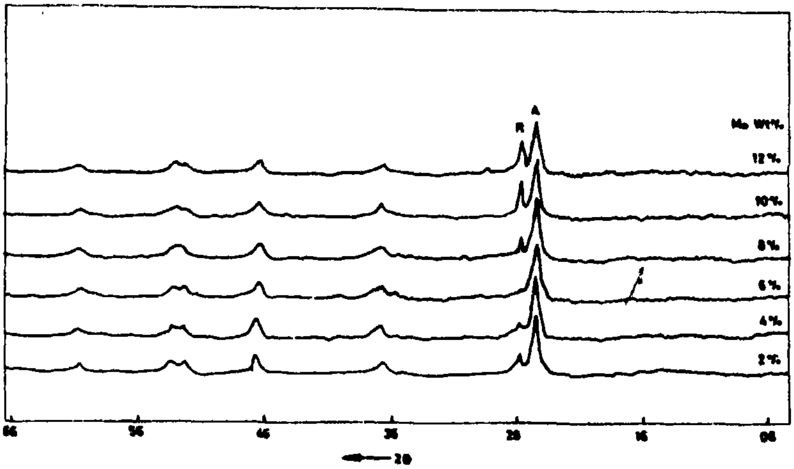

Fig. 3 — X-Ray diffractograms of reduced $MoO_3 - TiO_2$ catalysts.

V_2O_5 and transformation of anatase into rutile are topotactic reactions activated by the remarkable fit of the crystallographic patterns of V_2O_5 and anatase phase of TiO_2. With respect to MoO_3, Bordes *et al.*[14] have claimed that the (110) and (010) planes of MoO_3 can be 'anchored' on the (010) and (001) planes of anatase, thus suggesting facile growth of reduced MoO_3 layers on these faces of TiO_2 crystallites. Chary *et al.*[15] in their recent study on $V_2O_5 - TiO_2$ catalysts have also observed this anomalous occurrence of the anatase-rutile phase transformation, classically observed at much higher temperature than 500°C employed in the present study. The similar detailed studies on $MoO_3 - TiO_2$ catalysts are scarce in the literature. However, it is worth assuming at present that a similar mechanism operates in the $MoO_3 - TiO_2$ catalyst system, and the present results can also be explained with the help of same concepts proposed for $V_2O_5 - TiO_2$ catalysts. Vanadium pentoxide and MoO_3 form layer structures on the anatase phase of TiO_2 support surface because of the remarkable fit of their crystallographic planes[13]. Thus the present X-ray study on the MoO_3 catalysts once again points to the existence of so called 'interfacial synergetic effect' — a catalysis of the topotactic reduction of MoO_3 and a significant lowering of the activation energy for the anatase-rutile transformation which develops concurrently and cooperatively with loading.

Acknowledgement

Thanks are due to Dr B Rama Rao, Head X-ray Section, for his help in obtaining XRD data.

References

1 Vannice M A, *J Catal*, **74** (1982) 199.

2 Wainwright M S & Forster N R, *Catal Rev*, **19** (1979) 211.

3 Bond G C, Sarkany A J & Parfitt G D, *J Catal*, **57** (1979) 476.

4 Vejux A & Courtine P, *J Solid State Chem*, **23** (1978) 93.

5 Weller S W, *Acc chem Res*, **16** (1983) 101.

6 Reddy B M, Chary K V R, Subrahmanyam V S & Nag N K, *J chem Soc Faraday Trans I*, **81** (1985) 1655, and references therein.

7 Nag N K, Chary K V R, Reddy B M, Rao B R & Subrahmanyam V S, *Appl Catal*, **9** (1984) 225.

8 Reddy B M & Subrahmanyam V S, *Appl Catal*, **27** (1986) 1.

9 Reddy B M, Chary K V R, Rao B R, Subrahmanyam V S, Sunanda C S & Nag N K, *Polyhedron*, **5** (1986) 191.

10 Reddy B M & Subrahmanyam V S, *React Kinet Catal Lett*, **31** (1986) 429.

11 Hall W K, in *Proc 4th Climax International conference on chemistry and uses of molybdenum*, edited by H F Barry & P C H Mitchell (Climax Molybdenum Co, Michigan) 1982, 224.

12 Nag N K, *J Catal*, **92** (1985) 432.

13 Arco M D, Holgado M J, Martin C & Rives V, *J Catal*, **99** (1986) 19.

14 Bordes E, Jung S J & Courtine P, in *Proc 9th Iberoamerican symposium on catalysis*, edited by M F portela, 1984, 983.

15 Chary K V R, Reddy B M, Nag N K, Sunanda C S, Rao B R & Subrahmanyam V S, *Advances in catalysis science and technology*, edited by T S R Prasada Rao (Wiley-Eastern, Delhi) 1985, 661, and references therein

Indian Journal of Chemistry
Vol. 27 A, February 1988, pp. 104-109

Adsorption of Sodium Oleate as Surfactant at the Interfacial Surface in Benzene-Water Emulsions

S SHARAN SINGH* & N NATH PANDEY
Department of Chemistry, Bhagalpur University, Bhagalpur 812 007
and
R PRATAP SINGH
Department of Chemistry, Bhagalpur College of Engineering, Bhagalpur

Received 27 *January* 1987; *revised and accepted* 30 *April* 1987

Adsorption of sodium oleate as surfactant on dispersed droplets in benzene-water emulsions has been studied. The amount a of the surfactant adsorbed per cm^2 of the droplet surface area at the corresponding equilibrium surfactant concentration C_s in the aqueous serum has been calculated in each case. The adsorption of the surfactant on the droplet surface does not reach saturation value even when $C_s >$ CMC(III) [third critical micelle concentration value]. The area corresponding to the adsorption of one oleate ion on the emulsion droplet surface (σ_B) and the molar energy of adsorption (E_{ad}) have been calculated using the three-parameter modified BET equation. The number of adsorbed surfactant layers, as determined on the basis of calculated σ_B values, indicates a multilayer adsorption with $\nu_{max} \sim 3$, having a total adsorbed layers thickness of the order of 10^2 Å corresponding to the saturation adsorption. Further, the magnitude of E_{ad} (~ 2 kcal mol^{-1}) indicates that the surfactant ions are held at the emulsified droplet surface by forces akin to those involved in physical adsorption.

It is well known that surfactants adsorb on droplets in oil-water emulsions due to their amphipathic nature forming mono- or multi-molecular layers The present paper aims at determining the amount of sodium oleate adsorbed per unit area on the interface in benzene-water emulsions and also estimating the effective number of layers in the adsorbed sheath in order to decide whether the adsorption in the system studied is monomolecular or multi-molecular. Further, an attempt has been made to characterise the interfacial adsorbed layers vis-a-vis the micro environment of the dispersing phase around the adsorbing droplets.

Materials and Methods

Benzene as disperse phase and sodium oleate used as emulsifier were B D H (India) and B D H (England) products, respectively, while the continuous phase in each case was doubly distilled conductivity water (Specific conductance 10^{-6} Ohm^{-1} cm^{-1} at 30 ± 0.1°C). Before use, benzene was purified and its purity was checked by measuring its density as well as refractive index which compared well with the corresponding literature[1] values. Sodium oleate used was purified[2] by recrystallisation from ethanol-water mixture and dried to constant weight.

The required amount of sodium oleate was weighed and suspended in a known volume of conductivity water at room temperature and the suspension was heated (~50°C) till the turbidity disappeared. The clear solution was cooled in a thermostat to the experimental temperature (30 ± 0.1°C) avoiding excess shaking and prolonged heating in order to prevent foaming and losses due to evaporation. Measured volume of the sodium oleate solution, as prepared above and taken in a clean dry Corning glass jar, was first saturated with benzene and then a known volume of benzene was added and emulsified using a high speed mechanical stirrer in order to get a benzene-water-sodium oleate emulsion of desired phase-volume ratio.

The emulsion so obtained was transferred to a cylindrical separating funnel and allowed to cream at 30 ± 0.1°C for 72 hr. The separated clear serum was taken out and its specific conductivity (K_s) was determined at 30 ± 0.1°C using a Toshniwal conductivity bridge type CL01/01A with a dipping cell (cell constant = 1.1). From the conductivity data, the sodium oleate concentration (C_s) in the serum was determined by interpolation of a K_s vs C_s calibration curve.

The emulsion droplet diameters were measured by a 'Censico' Research Trinocular Microscope, Model TN-I-phot-35 mm having Hertel and Reuss (West German) achromatic objective (100 ×) and paired huyghenian eyepiece (15 ×). The ocular

Table 1—Adsorption Isotherm Data for Benzene/Water Emulsions with Sodium Oleate as Surfactant at Temperature = 30 ± 0.1°C

$C \times 10^2$ (mol lit^{-1})	$\bar{r}$ (μ)	$K_s \times 10^4$ (ohm^{-1}cm^{-1})	$C_s \times 10^2$ (mol lit^{-1})	$a \times 10^9$ (mol cm^{-2})	$C \times 10^2$ (mol lit^{-1})	$\bar{r}$ (μ)	$K_s \times 10^4$ (ohm^{-1}cm^{-1})	$C_s \times 10^2$ (mol lit^{-1})	$a \times 10^9$ (mol cm^{-2})
		$\phi = 0.30$					$\phi = 0.35$		
3.285	2.8	8.40	2.656	1.370	3.285	3.0	8.20	2.569	1.300
4.106	2.6	10.90	3.310	1.610	4.106	2.8	10.30	3.175	1.614
4.927	2.5	12.05	3.886	2.024	4.927	2.7	11.90	3.774	1.927
5.748	2.5	12.50	4.471	2.483	5.748	2.6	12.37	4.292	2.343
6.569	2.5	13.0	4.957	3.134	6.569	2.5	12.0	4.728	2.849
		$\phi = 0.40$					$\phi = 0.45$		
3.285	3.0	7.90	2.463	1.233	3.285	3.2	7.70	2.352	1.216
4.106	2.9	10.00	3.083	1.483	4.106	3.0	9.30	2.942	1.423
4.927	2.8	11.70	3.683	1.742	4.927	3.0	11.45	3.544	1.690
5.748	2.7	12.25	4.187	2.107	5.748	2.9	12.20	4.043	2.014
6.569	2.6	12.60	4.620	2.534	6.569	2.8	12.48	4.416	2.456
		$\phi = 0.50$					$\phi = 0.55$		
3.285	3.3	7.40	2.280	1.106	3.285	3.4	7.10	2.178	1.026
4.106	3.2	9.20	2.880	1.308	4.106	3.3	8.60	2.733	1.236
4.927	3.1	11.10	3.440	1.537	4.927	3.2	10.80	3.289	1.430
5.748	3.0	12.10	3.940	1.808	5.748	3.1	11.93	3.780	1.664
6.569	2.9	12.40	4.340	2.155	6.569	3.0	12.27	4.200	1.938
		$\phi = 0.60$							
3.285	3.5	6.60	1.975	1.019					
4.106	3.4	8.10	2.519	1.999					
4.927	3.3	9.70	3.050	1.376					
5.748	3.2	11.30	3.525	1.581					
6.569	3.1	12.10	3.951	1.804					

micrometer was calibrated with the help of an Erma (Japan) objective micrometer. For each emulsion sample, diameters of about two hundred emulsion droplets were measured and the average droplet diameter was determined from the histogram plots[3].

Results and Discussion

In order to get adsorption isotherms for benzene-water-sodium oleate emulsions studied at 30 ± 0.1°C, the amounts (a) of the surfactant adsorbed per cm^2 of the droplet surface at the corresponding equilibrium surfactant concentrations in the serum (C_s) were calclated by the following equation,

$$a = \frac{(1-\phi)(C-C_s)\bar{r}}{3000\phi} \qquad \ldots (1)$$

where ϕ is the phase-volume ratio, C is the concentration (mol litre^{-1}) of sodium oleate in the aqueous sodium oleate solution used as dispersing phase for emulsion preparation and $\bar{r}$ is the average droplet radius. The values of C varied from 3.28×10^{-2} to 6.57×10^{-2}, and ϕ varied from 0.3 to 0.6. In view of the fact that the first, second and third CMC (critical micelle concentration) values for aqueous sodium oleate solutions are 1.7×10^{-4}, 6×10^{-4} and 2.1×10^{-3} mol litre^{-1}, respectively, at 26°C, and these do not appreciably differ from the corresponding values[4] at 30°C, the standard sodium oleate solutions used for preparing emulsions were always post-micellar such that at equilibrium the values of C_s (Table 1) remained greater than the third CMC.

Table 1 reveals that eventhough C_s is greater than CMC (III), the adsorption of the surfactant on the droplet surface does not reach saturation value. This is an interesting observation in view of the earlier finding that the adsorption of surfactants from aqueous solutions on solid adsorbents, attains a saturation value[5] at CMC.

Using $a - C_s$ data (Table 1), we plotted the Langmuir type adsorption isotherms for various benzene-water-sodium oleate emulsions according to equation[6],

$$\frac{1}{a} = \frac{A}{C_m} \cdot \frac{1}{C_s} + \frac{1}{C_m} \qquad \ldots (2)$$

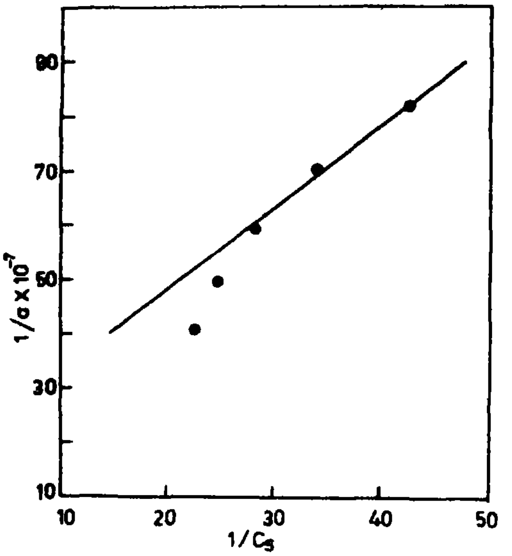

Fig. 1—Plot of $1/a$ versus $1/c_s$ for benzene-water emulsions with sodium oleate as surfactant and $\phi = 0.45$ at 30 ± 0.1°C

where C_m is the surfactant adsorbed (mol cm^{-2}) at effective monolayer adsorption and is a system constant, and A is another constant having the same units as C_s. A representative curve according to Eq. (2) is shown in Fig. 1. These isotherms are linear showing deviations only for higher C_s values. Utilising C_m, as calculated from the intercept of the linear portion (Fig. 1) in each case, we calculated the corresponding area σ_L occupied by one adsorbed surfactant ion by the following equation,

$$\sigma_L = [C_m N]^{-1} \quad \ldots (3)$$

where N is the Avogadro number.

The values of σ_L so obtained (Table 2) are rather too small than the value ($\sigma \sim 20$sq Å) required for an oleate ion in a packed adsorbed monolayer[7]. This indicates that the adsorption of the surfactant in benzene-water-sodium oleate emulsions is probably multimolecular and the linearity of the $1/a$ vs $1/C_s$ curves over the low concentration range (Fig. 1) is a consequence of the compensating effect of various assumptions used in deriving the Langmuir isotherm[8]. For higher C_s values in such systems, the hydrophilic and hydrophobic interactions become quite significant such that the consequent deviations do not compensate each other and the plots of $1/a$ vs $1/C_s$ show nonlinearity.

In order to verify the multimolecular adsorption in benzene-water-sodium oleate emulsions, the BET (Brunauer, Emmet and Teller) adsorption isotherms were plotted according to the 3-parameter equation[9],

Table 2—Values of σ_L, σ_B and E_{ad} for Benzene/Water Emulsions with Sodium Oleate as Surfactant for Varying ϕ at Temperature = 30 ± 0.1°C

ϕ	σ_L (SqÅ)	σ_B (SqÅ)	E_{ad} (kcal mol^{-1})
0.30	1.992	19.1	2.3
0.35	2.407	19.0	2.4
0.40	2.490	20.2	2.5
0.45	3.030	20.0	2.3
0.50	3.321	21.3	2.2
0.55	3.155	21.9	2.1
0.60	3.736	21.3	3.2

$\bar{\sigma}_B = 20.4$ SqÅ, $\bar{E}_{ad} = 2.3$kcal mol^{-1}

$$\frac{1}{a}\left[\frac{C_s}{C_s' - C_s}\right] = \frac{K}{a_m} + \left[\frac{1-K}{a_m}\right]\frac{C_s}{C_s'} \quad \ldots (4)$$

where a_m is the amount adsorbed in g mol cm^{-2} for complete monolayer converge, K is a constant associated with the energy of adsorption. and C_s' represents a characteristic value of C_s equal to the critical surfactant concentration in serum for which the saturation adsorption is achieved. The values of a and the corresponding C_s for each ϕ were taken from Table 1, while C_s' was treated as an adjustable parameter with 0.068 mol $litre^{-1}$ as its best value obtained by the iteration method.

The BET adsorption isotherms, typical once for $\phi = 0.30$ and $\phi = 0.60$ being shown in Fig. 2, reveal that the plots are satisfactorily linear for each ϕ, indicating that the adsorption in the systems studied is multyimolecular. The slopes and intercepts of these isotherms were used to calculate the values of a_m and K in each case. Using a_m, we calculated the areas σ_B (Table 2) corresponding to the adsorption of one oleate ion on the droplet surface from the equation,

$$\sigma_B = [a_m N]^{-1} \quad \ldots (5)$$

while using K, we calculated the values of molar energy of adsorption[10], $E_{ad} = (\psi - \lambda)$, from the equation,

$$K = e^{-(\psi - \lambda)/RT} \quad \ldots (6)$$

Here ψ is the energy required to remove one adsorbed molecule from otherwise free adsorbent surface, λ is the latent heat of vaporisation per

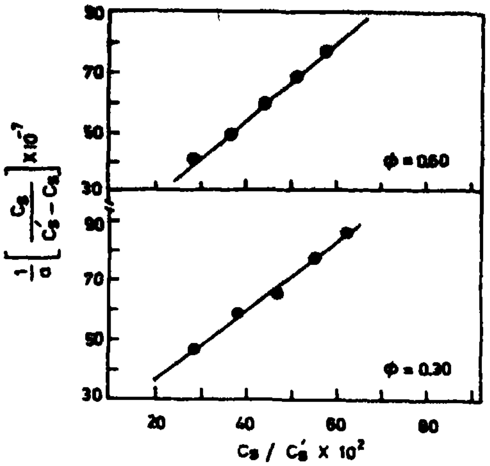

Fig. 2—Plot of $1/a\ [C_s/C_s'-C_s]$ versus C_s/C_s' for benzene-water emulsions with sodium oleate as surfactant at 30 ± 0.1°C

molecule of adsorbate, R is the molar gas constant at T is the temperature in K.

The calculated values of σ_B do not vary widely, giving an average $\bar{\sigma}_B$ value of 20.4 SqÅ, which compares favourably with area (20.5 SqÅ) occupied[11] by one oleate ion in tightly packed condensed films formed on air-water interface. This leads to the conclusion that the adsorbed surfactant ions in the first layer on the drop surface in benzene-water-sodium oleate emulsions are tightly packed. Thus, a value of σ_B less than ~20 SqÅ for lower ϕ (Table 2) implies a corrugated compact film surface due to the penetration of additional surfactant ions in the ordered array of the adsorbed ions in the first layer (Fig. 3), while σ_B greater than ~20 SqÅ for higher ϕ, indicates loose packing in the adsorbed layer. It may be mentioned here that Bromberg[12] observed $\sigma_B < 20.5$ SqÅ and Fisher and Harkins[13] observed $\sigma_B > 20.5$ SqÅ in earlier investigations on benzene-water-sodium oleate emulsions. The existence of rough, corrugated surfaces of solubilised micelles have also been postulated[14] earlier.

Since the value of C_s' equal to 0.068 mol litre^{-1} of serum as used in Eq. (4) represents the critical serum concentration at which the saturation adsorption is achieved, it corresponds to the critical solute concentration for saturation adsorption on solid adsorbents from solutions. In case the solute is a small molecule and the adsorbent is a solid, such critical concentration is the concentration for maximum dissolution[15] of solute, while it is CMC[5] if the solute is a surfactant molecule and the adsorbent is a solid. In the systems investigated here, the solute is a surfactant, adsorbent is the liquid droplet surface and $C_s \gg$ CMC. Consequently, C_s' for such systems appears to represent an effective concentration at maximum dissolution of sodium oleate in its aqueous solution. Such concentration at maximum dissolution could not be verified experimentally as the post micellar aqueous sodium oleate solutions show a tendency for gel formation.

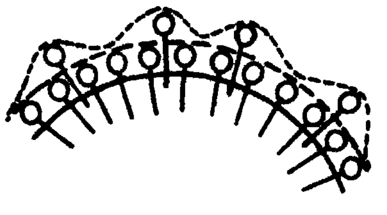

Fig. 3—Formation of first adsorbed layer of surfactant ions at the oil-water interface in emulsions with tight but uneven packing giving corrugated surface

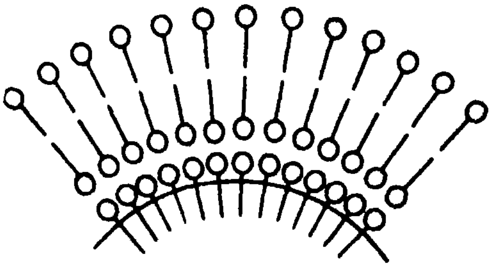

Fig. 4—Adsorbed multilayer formation by radial approach of surfactant ions on drop surface

The values of E_{ad} (Table 2) are of the order of ~2 kcal and do not appear to vary significantly with ϕ. This may be due to the nature of the adsorbing surface remaining unaltered eventhough the average droplet radius $\bar{r}$ varies slightly with ϕ and C. The values of E_{ad} (~2 kcal) rule out strong interactions of the chemisorption type which have energies greater than 10 kcal and are obviously the outcome of the hydrophobic interactions involving forces of smaller magnitude.

If radial approach of oncoming surfactant ions is visualised for layer formation on drop surface (Fig. 4), the distance between the adjacent surfactant tails l in successive layers increases with the increase in the number of layers and ultimately the layer formation ceases when the forces responsible become too weak. In view of the fact that the polar head groups in odd number layers point out towards the aqueous medium, it is highly probable that the adsorbed sheath ends with an odd number. To verify this, the number of layers (ν) was calculated using the following equation,

$$\nu = \frac{N\bar{r}\sigma_B(1-\phi)(C-C_s)}{3000\,\phi} \qquad \ldots(7)$$

Table 3—Values of ν and ν_{max} for Benzene/Water Emulsions with Sodium Oleate as Surfactant at Temperature = 30 ± 0.1°C

ϕ	ν					ν_{max}
	$C=3.285$ (mol lit^{-1})	$C=4.106$ (mol lit^{-1})	$C=4.927$ (mol lit^{-1})	$C=5.748$ (mol lit^{-1})	$C=6.569$ (mol lit^{-1})	
0.30	1.576	1.852	2.329	2.856	3.606	3.758
0.35	1.527	1.847	2.205	2.682	3.260	3.276
0.40	1.500	1.805	2.119	2.564	3.083	3.194
0.45	1.465	1.714	2.036	2.427	2.959	3.133
0.50	1.418	1.678	1.971	2.319	2.764	3.207
0.55	1.354	1.630	1.886	2.195	2.557	3.192
0.60	1.307	1.538	1.766	2.028	2.314	3.164

The values of ν for different emulsions with $1.975 \times 10^{-2} < C_s < C_s'$ are given in Table 3.

Table 3 reveals that ν is always more than 1 and varies with ϕ for constant C and vice versa. It is interesting to calculate the maximum number of adsorbed layers (ν_{max}) for each ϕ with $C_s = C_s'$; for this Eq. (7) was modified to,

$$\nu_{max} = \frac{N\bar{r}'\sigma_B(1-\phi)(C-C_s)}{3000\phi} \qquad \ldots (8)$$

where $\bar{r} = 2.5\mu$ was obtained from $\bar{r}$ vs (C/ϕ) curves for the systems studied. It represent the limiting value of $\bar{r}$ which does not change with ϕ or with further increase in C. The value of C corresponding to C_s' was obtained from C vs C_s curve for each ϕ. The calculated values of ν_{max} (Table 3) are in the range $3 < \nu_{max} < 4$ indicating that, the most probable value of maximum number of complete adsorbed layers for the systems studied is 3. The incomplete formation of the fourth adsorbed layer may be due to the uncertainties involved in Eq. (8). Thus, the expectation that the most probable ν_{max} value, on the basis of radial approach of oncoming surfactant ions for adsorbed layer formation, should be an odd number appears to be justified.

Again, if the formation of the second and the subsequent surfactant ion layers on emulsified droplets is considered as the consequence of the interplay of the coheisve force (f_c) and the repulsive force (f_r) between the adjacent surfactant ions, the $\nu_{max} \sim 3$ indicates that for the third adsorbed layer ($f_c - f_r$) is minimum. For the fourth layer, $f_c = f_r$ and, as such, there is an equal probability for the surfactant ions to stay in or move out from this layer.

The total film thickness (l_T) for sodium oleate as surfactant was calculated using Eqs 9 and 10, for ν_{max} = odd integers,

$$l_T = (l_{COO^-} + l_{C\text{-}C}) + (\nu_{max} - 1)[l_{COO^-} + 1_{HC} \cdot \tfrac{1}{2}(l_p + l_h)] \qquad \ldots (9)$$

and for ν_{max} = even integers,

$$l_T = (l_{COO^-} + l_{C-C} + \tfrac{1}{2} l_p) + (\nu_{max} - 1)[l_{COO^-} + l_{HC} + \tfrac{1}{2}(l_p + l_h)] - \tfrac{1}{2} l_h \qquad \ldots (10)$$

where $l_{COO^-} = l_{C-O} \cos\theta/2$

and $l_{HC} = 16\, l_{C-C} + l_{CH_3} + l_{C=C}$

Here l_{C-O} is the C – O bond length, θ is the $\mathrm{C}{<}^{\mathrm{O}^-}_{\mathrm{O}}$ bond angle, l_{C-C} is the C – C bond length. $l_{C=C}$ is the C = C bond length, l_{CH_3} is the projection of the C – H bond on the axis of the hydrocarbon chain, l_p is the distance between the two polar heads and l_h is the distance between the two hydrocarbon chains of a bilayer. The value of l_T for $\nu_{max} = 3$ was found to be ~ 83Å using the standard values of C – O, C – C, C = C, C – H bond lengths[16] and $\theta = 124.5°$, $l_p = 20$Å and $l_h \sim 5$Å. It is satisfying to note that earlier workers[17] have also determined the film thickness for benzene-water emulsions with 5% sodium oleate as emulsifier and found that the value is of the order of 100Å.

Acknowledgement

One of the authors (NNP) is thankful to Prof K D Banerji, Head of the Department of Chemistry, Bhagalpur University, Bhagalpur for providing laboratory facilities.

References

1 Timmermans J, *Physicochemical constants of pure organic compounds*, (Elsevier, New York) 1950, 140.

2 Attwood D, Currie L R J & Elworthy P H, *J colloid interface Sci*, **46** (1974) 256.

3 Schwarz N & Bezemer C, *Kolloid-Z*, **146** (1956) 139.

4 Zimmels Y & Lin I J, *Colloid Polym Sci*, **252** (1974) 597.

5 Jungermann E, *Cationic surfactants*, Vol 4 (Marcel Dekker, New York) 1970, 348.

6 Rosen M J, *Surfactants and interfacial phenomena*, (John Wiley, New York) 1978, 37.
7 Adam N K, *Nature*, **180** (1957) 50.
8 Betts J J & Pethica B A, *Trans Faraday Soc*, **56** (1960) 1515.
9 Gu T, *J colloid interface Sci*, **85** (1982) 602.
10 Moelwyn-Hughes E A, *Physical chemistry*, (Pergamon Press, London) 1961, 968.
11 Adam N K, *The physics and chemistry of surfaces*, (Oxford University Press, London), 1941, 50.
12 Bromberg A V, *Kolloid Zhur*, **9** (1947) 23.
13 Fischer E K & Harkins W D, *J phys Chem*, **36** (1932) 98.
14 Stigter D & Mysels K J, *J phys Chem*, **59** (1955) 45.
15 Fu Y, Hansen R S & Bartell F E, *J phys Colloid Chem*, **52** (1948) 374.
16 Rao C N R, George M V & Mahanty J, *A handbook of chemistry and physics*, (Affiliated East West Press, New Delhi) 1970, 227.
17 Kremnev L Ya & Soskin S A, *J gen Chem* (*USSR*), **16** (1946) 2000; *chem Abstr*, **41** (1947) 6791i.

Indian Journal of Chemistry
Vol. 27A, February 1988, pp. 110-114

Accurate Kinetic Parameters from Thermogravimetric Data

K N SOMASEKHARAN
Department of Inorganic & Physical Chemistry, Indian Institute of Science, Bangalore 560012

Received 5 *March* 1987; *accepted* 23 *June* 1987

An accurate expression for the analysis of thermogravimetric data and a matching algorithm are given. It is demonstrated with theoretical data that the computer program yields the most accurate kinetic parameters at all values of E^*/RT. Verification with the program reveals that serious computational errors exist in the published literature.

There are many thermal decomposition reactions of interest, in whith the reactant is in a solid phase. With the advent of modern thermoanalytical techniques, collecting kinetic data on solid state reactions has become a major endeavour in chemistry[1]. It is increasingly popular to collect dynamic data, which are obtained under a fixed heating rate—a condition which may be closely realized in modern thermal analyzers. In this paper an accurate kinetic expression for the analysis of thermogravimetric data and a matching algorithm are given.

Theory

The mathematical model most frequently used for the kinetic description of thermogravimetric data is given by expression (1)

$$\frac{d\alpha}{dt} = kf(\alpha) \qquad \ldots (1)$$

It can be readily shown[2] that

$$g(\alpha) = \frac{A}{q}\int_0^{\mathrm{T}} \exp(-E^*/R\mathrm{T})\,d\mathrm{T} \qquad \ldots (2)$$

Due to the fact that the temperature integral has no analytical closed form, approximations abound in the literature.

One of the most widely used approximations is by Coats and Redfern[3]; their solution may be generalized by expression (3)

$$g(\alpha) = \frac{\mathrm{T}^2 AR}{qE^*}\left[1 - \frac{2R\mathrm{T}}{E^*}\right]\exp(-E^*/R\mathrm{T}) \qquad \ldots (3)$$

Because of the statistical superiority of linearizing $\ln[g(\alpha)/\mathrm{T}^2]$ versus $1/\mathrm{T}$, Coats-Redfern equation is given in the rearranged form (4)

$$\frac{g(\alpha)}{\mathrm{T}^2} = \frac{AR}{qE^*}\left[1 - \frac{2R\mathrm{T}}{E^*}\right]\exp(-E^*/R\mathrm{T}) \qquad \ldots (4)$$

A more exact solution to Eq. (2) may be obtained using the Schlömilch, van Tets or a semiconvergent series:

$$\frac{g(\alpha)q}{\mathrm{T}^2 p^*(x)} = \frac{AR}{E^*}\exp(-E^*/R\mathrm{T}) \qquad \ldots (5)$$

where $x = E^*/R\mathrm{T}$; the $p^*(x)$ may be evaluated using any one of the series given in the Appendix. With the advent of and ready access to computers and programmable calculators, this new kinetic expression is readily tractable.

Algorithm

Since $p^*(x)$ is a function of E^* as well as of T, a simplified form of the kinetic expression (Eq. 6),

$$\frac{g(\alpha)q}{\mathrm{T}^2} = \frac{AR}{E^*}\exp(-E^*/R\mathrm{T}) \qquad \ldots (6)$$

is employed first to get an estimate of E^*. This value of E^* is used in the subsequent step of the least-squares linearization of $\ln[g(\alpha)q/\mathrm{T}^2 p^*(x)]$ versus $1/\mathrm{T}$.

Instead of assigning the value of unity to $p^*(x)$ in the first step of the computation, a dummy value of 30 kcal/mol for E^* may be employed in the first iterative step. Convergence being extremely fast, no more than two iterations will be required.

Results

To verify the accuracy of the model, theoretical data points were first generated using Eq. (2), where the temperature integral was evaluated by numerical integration (for typical data, see Table 1). These values were verified against the Schlömilch, van Tets and a semi-convergent series; all four agreed. Double precision (16 digits) was used wherever necessary.

These theoretical data points were then used in the computation of kinetic parameters. Typical results are given in Table 2.

Discussion

Most approximations in the literature give reasonably good estimates of the energy of activation; the error mostly accumulates in the estimation of the pre-exponential factor. From the literature, it appears that E^* has no independent relevance in solid state kinetics; E^* attains significance only in association with A. That is why compensation parameters like $E^*/\log A$ are being tried to characterize solid state reactions[4,5]. For this, the pre-exponential factor also has to be determined accurately. The new model does this.

Table 1—Theoretical Data and the Kinetic Parameters used in Computing them

α	T_1	T_{10}	T_{100}
0.1000	716.008	661.300	446.496
0.2000	730.785	671.471	458.261
0.3000	740.326	677.982	463.902
0.4000	747.798	683.052	468.310
0.5000	754.264	687.417	472.119
0.6000	760.272	691.455	475.651
0.7000	766.241	695.451	479.155
0.8000	772.687	699.747	482.933
0.9000	780.787	705.119	487.671
E^*, kcal mol^{-1}	50.00	30.00	10.00
A, sec^{-1}	1.667×10^{11}	1.667×10^{7}	1.667×10^{3}
q, deg min^{-1}	1	10	100
g(α)	$-\ln(1-\alpha)$	$[-\ln(1-\alpha)]^{1/2}$	$[-\ln(1-\alpha)^{1/3}$

The accuracy of even the Coats-Redfern equation steadily decreases as the value of x decreases. The present method yields accurate values of the kinetic parameters even at low values of x.

Conclusions

The reported kinetic parameters widely differ in the literature; for example, the estimates of the activation energy for the decomposition of calcium carbonate varies between 26 and 377 kcal/mol. Procedural factors (systematic errors) have been implicated in these variations; very little is said about the random errors in data collection, handling and processing. As we now have a program that yields accurate results, we have analyzed some of the published experimental data.

(1) The experimental data reported on the dehydration of zinc oxalate dihydrate[6] appear reasonable, but the reported results[7] differ significantly from the correct values computed by our program (for example, see Table 3). Serious computational errors are evident in reference (7). Since the mechanism for this reaction is arrived at, based on the magnitudes of the incorrectly computed correlation coefficients, these conclusions reported in literature[7] are also not valid.

(2) Another example where both the data and results are reported is for the thermal decomposition of magnisium hydroxide[8]. The reported E^* and R_{xy} match the correct values; but the pre-exponential factors differ significantly from the correct values (Table 4).

(3) Finally, we have used the two sets of theoretical data reported in the literature[9]. Our program generated the exact kinetic parameters

Table 2—Kinetic Parameters Computed from the Theoretical Data in Table 1, Using Various Approximations

	E^*, kcal mol^{-1}	A, sec^{-1}	Error in A, %	Relative computer time
Theoretical	50.00	1.667×10^{11}	—	—
By Eq. (3)	52.89	1.224×10^{12}	634.0	1.0
By Eq. (6)	49.92	1.492×10^{11}	10.5	1.0
By Eq. (4)	49.92	1.587×10^{11}	4.80	1.0
By Eq. (5)	50.00	1.667×10^{11}	0.000	1.2
Theoretical	30.00	1.667×10^{7}	-	
By Eq. (3)	32.61	1.234×10^{8}	640.0	
By Eq. (6)	29.90	1.414×10^{7}	15.2	
By Eq. (4)	29.90	1.556×10^{7}	6.66	
By Eq. (5)	30.00	1.667×10^{7}	0.000	
Theoretical	10.00	1.667×10^{3}	—	
By Eq. (3)	11.73	1.262×10^{4}	657.0	
By Eq. (6)	9.870	1.220×10^{3}	26.8	
By Eq. (4)	9.870	1.505×10^{3}	9.72	
By Eq. (5)	10.00	1.670×10^{3}	0.180	

Table 3—Kinetic Parameters for the Dehydration of $ZnC_2O_4 \cdot 2H_2O$ from DTA Data[a], using Various Mechanistic Equations

Mechanism[b]	E^*, kcal mol^{-1}		A, sec^{-1}		R_{xy}	
	Reported[c]	Correct	Reported[c]	Correct	Reported[c]	Correct
1	59.04	46.28	1.34×10^{29}	1.581×10^{21}	0.9844	−0.9884
2	64.37	52.86	5.92×10^{31}	2.566×10^{24}	0.9909	−0.9951
3	71.42	61.85	9.08×10^{34}	3.364×10^{28}	0.9964	−0.9995
4	66.65	55.78	2.38×10^{32}	2.047×10^{25}	0.9932	−0.9973
5	40.60	35.11	1.95×10^{18}	8.544×10^{15}	0.9989	−0.9986
6	18.49	16.76	5.38×10^{7}	2.342×10^{6}	0.9980	−0.9984
7	11.83	10.66	1.07×10^{4}	1.312×10^{3}	0.9980	−0.9983
8	33.18	27.89	1.77×10^{15}	5.808×10^{11}	0.9938	−0.9981
9	34.82	30.10	1.00×10^{16}	5.958×10^{12}	0.9962	−0.9994

a Taken from ref 6; b mechanisms are referred to in the same sequence as in ref. 7; c as reported in ref. 7.

Table 4—Kinetic Parameters for the Decomposition of Magnesium Hydroxide from TG Data[a], using Various Mechanistic Equations

Mechanism[b]	E^*, kal mol^{-1}		A, sec^{-1}	
	Reported[a]	Present	Reported[a]	Correct
1	86.493	86.49	5.6×10^{25}	4.455×10^{25}
2	91.462	91.45	1.6×10^{27}	1.259×10^{27}
3	97.231	97.22	3.9×10^{28}	2.997×10^{28}
4	93.374	93.36	1.7×10^{27}	1.317×10^{27}
5	50.332	50.37	1.3×10^{14}	1.161×10^{14}
6	23.878	23.98	1.2×10^{5}	1.535×10^{5}
7	15.157	15.22	8.9×10^{1}	14.53×10^{1}
8	45.900	45.94	1.6×10^{12}	1.535×10^{12}
9	47.324	47.36	3.5×10^{12}	3.286×10^{12}

a Taken from ref. 8· b mechanisms are given in the same sequence as in ref. 7.

Table 5—Kinetic parameters Computed from the Theoretical Data of Gyulai and Greenhow

	q, deg min^{-1}	E^* kcal mol^{-1}	A, sec^{-1}	$-R_{xy}$
Theoretical[a]	2	60.00	1.667×10^{12}	—
Computed	—	59.99	1.667×10^{12}	1.0000
Theoretical[a]	4	60.00	1.667×10^{12}	—
Computed	—	65.56	4.246×10^{13}	0.9931

a Taken from ref. 9.

from the first set; but the second set gave disagreement (see Table 5). Verification of these theoretical data against three approximations and numerical integration (Table 6) revealed that there was an error in the published[9] theoretical data.

Appendix

The solution to Eq. (2) is given by expression (7)

$$g(\alpha)=\frac{AE^*}{qR}\,p(x) \qquad \ldots (7)$$

where

$$p(x)=\int_x^{\infty}\frac{e^{-u}}{u^2}\,du \qquad \ldots (7a)$$

$$=\frac{e^{-x}}{x^2}\,p^*(x) \qquad \ldots (7b)$$

(1) The Rainville function[10] and the semi-convergent series given by Arfken[11] are identical in the evaluation of $p^*(x)$:

$$p^*(x)=\sum_{n=0}^{\infty}(-1)^n\frac{n(n+1)!}{x^n} \qquad \ldots (8)$$

The first ten terms were employed in the present computations.

(2) The first six terms of the Schlömilch series[12] used are:

$$p^*(x)=1-\frac{2}{(x+1)}+\frac{4}{(x+1)(x+2)}-\frac{10}{(x+1)\ldots(x+3)}+\frac{30}{(x+1)\ldots(x+4)}-\frac{108}{(x+1)\ldots(x+5)} \qquad \ldots (9)$$

(3) The first five terms of the van Tets series[13] are:

$$p^*(x)=\frac{(x+1)}{(x+3)}-\frac{6}{(x+1)\ldots(x+3)}$$

Table 6—Verification of the Theoretical Data of Gyulai and Greenhow

Temp*	α				
	Gyulai & Greenhow*	Rainville/Arfken	Schlömilch	Van Tets	Numerical
843.394	0.1	0.145900	0.145900	0.145900	0.145901
851.134	0.2	0.199344	0.199344	0.199344	0.199345
861.933	0.3	0.299096	0.299096	0.299096	0.299097
870.386	0.4	0.398904	0.398904	0.398904	0.398905
877.696	0.5	0.498768	0.498767	0.498768	0.498769
884.486	0.6	0.598707	0.598707	0.598707	0.598709
891.225	0.7	0.698682	0.698682	0.698682	0.698684
898.507	0.8	0.798883	0.798882	0.798883	0.798884
907.648	0.9	0.899203	0.899203	0.899203	0.899204

*from ref. 9.

Table 7—Ratio of Approximate to True Value of $p^*(x)$

x	Rainville/ Arfken[a]	Schlömilch[b]	Van Tets[c]
10.0000	0.997798	0.999929	1.000096
15.0000	0.999956	0.999989	1.000013
20.0000	0.999997	0.999997	1.000003
25.0000	1.000000	0.999999	1.000001
30.0000	1.000000	1.000000	1.000000
35.0000	1.000000	1.000000	1.000000
40.0000	1.000001	1.000001	1.000001
45.0000	1.000001	1.000001	1.000001
50.0000	1.000002	1.000002	1.000002

a Ten terms; b six terms; c five terms.

$$+\frac{30}{(x+1)\ldots(x+4)}-\frac{108}{(x+1)\ldots(x+5)}+\frac{810}{(x+1)\ldots(x+6)} \qquad \ldots(10)$$

(4) Numerical integration of the temperature integral, followed by division with $(RT^2/E^*)\exp(-E^*/RT)$ will yield the value of $p^*(x)$:

$$\int_0^T \exp(-E^*/RT)dT=\frac{RT^2}{E^*}\exp(-E^*/RT)p^*(x) \qquad \ldots(11)$$

Numerical integration of the temperature integral is accomplished in 700 weighted increments.

All the three series give excellent estimates of $p^*(x)$, at high values of x. Expectedly, the Schlömilch and van Tets series yield better estimates at low values of x (Table 7). Chen has suggested[14] that the use of one-half the last term would reduce the possible error. It is in this rounded off (rather than truncated) form that the van Tests series is used in the program; the rounding off improves the accuracy—the deviation at $x=10$ reduces from 9.6×10^{-3}% to 1.2×10^{-3}%. For values of x lower than 10, the program estimates $p^*(x)$ by the numerical method.

Symbols

α = the fraction decomposed
A = pre-exponential factor
E^* = energy of activation
k = $A\exp(-E^*/RT)$
q = the linear heating rate, dT/dt
R = gas constant
T = temperature, absolute
t = time
x = E^*/RT
$f(\alpha)$ = a continuous function, describing the dependence of $d\alpha/dt$ on α
$g(\alpha)$ = the integral of $1/f(\alpha)$
$p^*(x)$ = see Appexdix for definition.

Acknowledgements

This work is partly supported by the CSIR, New Delhi. Extensive discussions with and helpful suggestions by Prof S K Rangarajan are gratefully acknowledged.

References

1 Wendlandt W W, *Thermochim Acta*, **50** (1981) 1.

2 Brown M E & Phillpotts C A R, *J chem Educ*, **55** (1978) 556.

3 Coats A W & Redfern J P, *Nature*, (London), **201** (1964) 68.

4 Somasekharan K N & Kalpagam V, *Thermochim Acta*, **107** (1986) 379.

5 Zsako J, *J thermal Anal*, **9** (1976) 101.

6 Krishnan K, Ninan K N & Madhusudanan P M, *Thermochim Acta*, **71** (1983) 305.

7 Krishnan K, Ninan K N & Madhusudanan P M, *Thermochim Acta*, **89** (1985) 295.

8 Fong P H & Chen D T Y, *Thermochim Acta*, **18** (1977) 273.

9 Gyulai G & Greenhow E J, *J thermal Anal*, **6** (1974) 279.

10 Rainville E D, *Special functions*, (Macmillan, London) 1960, p. 44.

11 Arfken G, *Mathematical Methods for Physicists*, 2nd ed. (Academic Press, New York) 1970, p. 472.

12 Schlömilch O, *Vorlesungen über hoheren Analysis*, 2nd ed. (Braunschweig) 1874, p 266; as quoted in van Krevelen D W, van Heerden C & Huntgens F J, *Fuel*, **30** (1951) 253.

13 van Tets A, *Thermochim Acta*, **17** (1976) 372.

14 Chen R, *J Compt Phys*, **4** (1969) 415.

Indian Journal of Chemistry
Vol. 27 A, February 1988, pp. 115-122

Effect of Surfactants on Kinetics of Alkaline Fading of Crystal Violet & Acid-catalyzed Inversion of Sucrose

JAYATI DATTA, ABHIJIT BHATTACHARYA & KIRON K KUNDU*
Department of Chemistry, Jadavpur University, Calcutta 700 032

Received 13 *March* 1987; *accepted* 25 *June* 1987

The kinetics of (i) alkaline fading of Crystal Violet (CV^+) [$=\overset{+}{C}\{-\phi N(CH_3)_2\}_3$] and (ii) acid-catalysed inversion of sucrose have been investigated in aqueous media in the presence of cationic surfactant cetyltrimethylammonium bromide (CTAB), anionic surfactant sodium dodecyl sulphate (SDS) and neutral surfactant Triton X-100 (TX). At [surfactant] above and below their cmcs CTAB accelerates the rate of alkaline fading of the dye, being active specially above its cmc; SDS strongly inhibits the reaction well below its cmc; and TX is only feebly catalytic. The rate enhancement and inhibition are rationalized in terms of various factors like dye-surfactant complexation, double layer effect around micelles of CTAB or formation of mixed micelles by SDS and also possible shift of monomer ⇌ dimer equilibrium of CV^+. In contrast, the surfactants show hardly any effect on the acid-catalyzed inversion of sucrose which, as expected, occurs only in the aqueous phase due to strong hydrophilicity of both sucrose and hydrogen ions, throughout the surfactant concentration ranges employed.

Recently Kundu and coworkers have studied the medium effects on the kinetics of alkaline fading of Crystal Violet (CV^+) [$=\overset{+}{C}\{-\phi N(CH_3)_2\}_3$][1a] and acid-catalyzed inversion of sucrose (Suc)[1b] in a host of aquo-organic solvents with varying acid-base characters. The results indicated that the kinetics of these reactions were amply guided by the relative solvation of the reactants, viz. CV^+ and OH^- or Suc and H^+ respectively in these solvents. It is well known[2-19] that surfactants often affect the kinetics of various types of organic reactions particularly above their critical micelle concentrations (cmc). The surfactant molecules may interact with the reactant molecules and thus change their solvation behaviour variously. Despite extensive investigations on the role of surfactant, there appears to be little understanding of the effect of the surfactants on the structural aspects of reactant organic substrates, the possible specific surfactant-substrate interactions, vis-a-vis their effects on miceller catalysis in general.

In the present paper we report our results of investigations on the effects of cationic surfactant, cetyltrimethylammonium bromide (CTAB), the anionic surfactant sodium dodecyl sulphate (SDS) and the non-ionic surfactant Triton X-100 (TX) on the kinetics of alkaline fading of CV^+ as well as H^+-catalyzed hydrolysis of Suc both above and below the respective cmc regions of the surfactants. Notably Dyunstee and Grunwald[4] have studied the kinetics of alkaline fading of CV^+ in the presence of CTAB and SDS at one concentration far above the cmc of the respective surfactants. However, in view of the fact that dyes having a triphenylcarbonium ion (e.g. CV^+) are usually prone to undergo complexation[20] with these surfactants it was considered extremely useful to extend these reaction kinetics even to the pre-micellar concentration (pmc) region and analyze the results of spectral scans for such solutions. This may help in understanding the catalytic effects of micelles free from those unrelated to micellization. Besides, since the complexation processes might induce shift in cmc's[21a] of the surfactants, as OH^- often does[21b], the determination of their cmc's in presence of CV^+, sucrose and OH^- was considered equally useful.

Materials and Methods

The Crystal Violet chloride (E Merck), TX (Reidel) and sucrose (AR, Glaxo) were used as received. CTAB and SDS (both AR, BDH) were purified by the methods described earlier[22a] and their purity verified from surface tension (γ) measurement of their solutions by the absence of any minima in γ-concentration profiles[22b]. The cmc values of the samples in pure water were found to be $8\text{-}9 \times 10^{-4}$ mol dm^{-3} for CTAB, 8×10^{-3} mol dm^{-3} for SDS and 2.2×10^{-4} mol dm^{-3} for TX, which agree fairly well with the respective literature data[22]. Sodium hydroxide (GR, E Merck) and HCl (AR, Glaxo) were used as such. All solutions were prepared in triply distilled water and all the experiments were carried out at 25°C.

The rate constants for alkaline fading of CV^+ were determined by following the decrease in its absorbance at 590 nm[23] in the presence of various surfactants at four different concentrations of

NaOH employing a Systronic spectrophotometer [model MK (II) – 106]. While the CV$^+$ concentration was kept fixed at 0.65×10^{-5} mol dm^{-3}, the range of surfactant concentration employed were 1.2×10^{-4}-5.7×10^{-3} for CTAB; 2.5×10^{-5}-6.0×10^{-4} for TX and 1×10^{-5}-7.3×10^{-2} mol dm^{-3} for SDS. The required NaOH concentrations were of the order of 10^{-3} mol dm^{-3} (ranging from 0.55×10^{-3}-1.36×10^{-3} mol dm^{-3}) for CTAB and TX as also for water, whereas for SDS the NaOH concentration was of the order of 1 mol dm^{-3} (ranging from 0.3-0.7 mol dm^{-3}), except for the three initial concentrations of SDS (1×10^{-5}-3.5×10^{-5}) where about 10^{-2} mol dm^{-3} NaOH (ranging from 0.5×10^{-2} to 1.3×10^{-2} mol dm^{-3}) was required.

The rate constants for the inversion of Suc were obtained by observing the angle of rotation of monochromatic sodium (D) light, with the help of a Hilger standard polarimeter (MK III) (Watts Microptic, England). These observations were made with a 10% sucrose solution in the presence of surfactant concentrations varying from 1.2×10^{-4}-5.7×10^{-3} for CTAB, 2.5×10^{-5}-6.0×10^{-4} for TX and 1.2×10^{-5}-7.3×10^{-2} mol dm^{-3} for SDS. For the infinity readings the reaction mixtures were kept overnight. All these measurements were performed at 25°C.

The cmc values of CTAB and SDS in the presence of the substrates were determined from the measurement of conductance of solutions using a Phillips PR 9500/90 conductivity bridge, while those of TX in the presence of substrates were obtained by measuring the surface tension (γ) of solutions by drop weight method using a stalagmometer. In such measurements the substrate concentrations were kept constant at the values at which the kinetics of their respective solutions were followed. Because, in the presence of 1 mol dm^{-3} NaOH the conductance of the SDS – NaOH mixed solutions would not change appreciably, the cmc of SDS in the presence of 1 mol dm^{-3} NaOH was also estimated from γ-values.

Spectra of the dye-surfactant solutions covering a range of 460 to 630 nm were taken at a fixed CV$^+$ concentrations [0.85×10^{-5} for CTAB and TX and 0.65×10^{-5} mol dm^{-3} for SDS] varying the [surfactant] in the range of 1.5×10^{-4}-5.0×10^{-3} for CTAB, 2.0×10^{-5}-2.0×10^{-3} for TX and 1×10^{-5}-6.4×10^{-2} mol dm^{-3} for SDS.

Results

Alkaline fading of Crystal Violet:

As is well known[1,24] coloured CV$^+$ in aqueous solution remains in equilibrium with the colourless

Table 1—Rate Constants (k_{sf}) of Alkaline, Fading of Crystal Violet in Presence of Various Surfactants at Different Concentrations and 25°C

[Concentrations in mol dm^{-3} and k_{sf} in dm^3 mol^{-1} s^{-1}]

CTAB		SDS		TX	
$C_{sf} \times 10^3$	k_{sf}	$C_{sf} \times 10^2$	$k_{sf} \times 10^3$	$C_{sf} \times 10^4$	k_{sf}
5.70	5.7	7.28	6.3	6.0	0.8(0.7)
4.80	7.2	6.30	6.8	4.0	0.8(0.7)
3.80	8.3	5.39	7.9	2.0	0.8(0.7)
2.90	8.3	4.54	7.8	1.0	0.8(0.7)
1.90	7.7	3.59	8.7	0.5	0.8(0.7)
1.35	6.3	2.70	8.6	0.25	0.8(0.7)
0.95	5.0	1.80	8.5		
0.75	1.5(1.3)	0.90	9.3		
0.48	0.6(0.5)	0.35	5.2(1.7)		
0.24	0.2(0.2)	0.27	4.5(1.6)		
		0.18	4.2(1.4)		
		0.13	3.7(1.2)		
		0.09	2.1(0.7)		
		0.06	2.8(0.9)		
		0.004	55(27)		
		0.002	153(82)		
		0.0012	187(100)		

$(k^0_{H_2O})^{25°C} = 0.19$ dm^3 mol^{-1} sec^{-1} (see ref. 1a)

Data in parentheses refer to k^0_{sf} as obtained by use of Eq. (3)

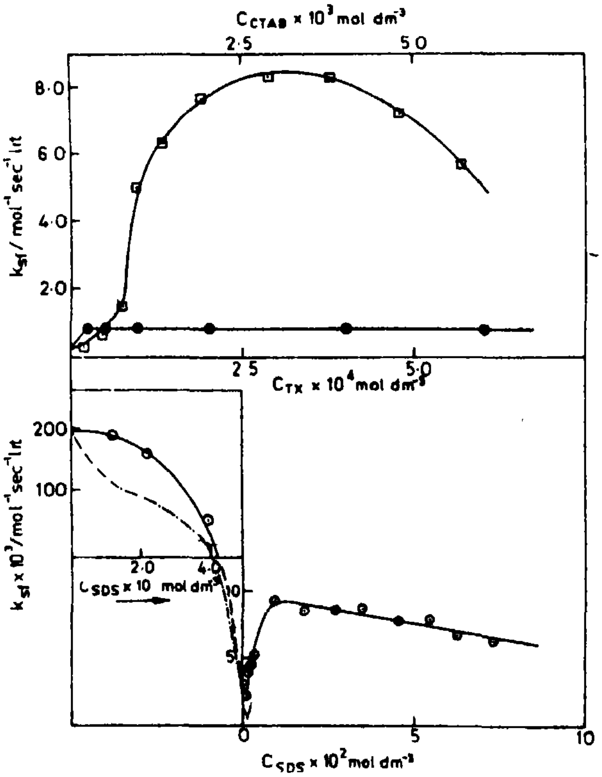

Fig. 1—Variation of rate constants (k_{sf}) for alkaline fading of Crystal Violet in presence of SDS (○), TX (●) and CTAB (□) of varying concentrations at 25°C [-·-·-·- curve represent the variation of k^0_{sf} with SDS concentration]

carbinol (CVOH) (Eq. 1). In the presence of alkali, the backward reaction becomes practically insignificant as compared to the forward one, i.e. fading of CV^+ and the decoloration reaction could be followed spectrophotometrically.

$$CV^+ + OH^- \rightleftharpoons CVOH \qquad \ldots (1)$$

The rate of reaction (1) would be given by Eq. (2)

$$\frac{d[CV+]}{dt} = k_{sf}[CV^+]^{m}[OH^-]^{n} = k_1[CV^+]^{m} \ldots (2)$$

where *m* and *n* are the orders with respect to CV^+ and OH^- respectively, k_1 is the pseudo-unimolecular rate constant; and k_{sf} the second order rate constant in the presence of surfactants. The k_{sf} values, as also the *m* and *n* values were obtained following standard procedures[1a,24] and determining the pseudo-first order rate constants at four different $[OH^-]$. The k_{sf} values are given in Table 1.

Notably, as the reaction is essentially between two oppositely charged ions, a considerable primary salt effect arising out of electrostatic interactions between the charged species present in the solution would be involved[24]. The rate constant free from such effect (k_{sf}) could be obtained using Bronsted-Bjerrum equation[24] (see Eq. 3).

$$\log k_{sf} = \log k^0_{sf} + 1.02\, z_1 z_2 \mu^{1/2}(1 + \mu^{1/2})^{-1} \qquad \ldots (3)$$

where z_1 and z_2 are charges on the reactant ions and μ is the ionic strength of the solution.

Admittedly, application of Eq. (3) to micellar solutions above cmc region is not permissible in view of the uncertainties in the degree of aggregation of surfactant molecules in the presence of OH^- and CV^+. However, since we are specially interested in pmc region, the k^0_{sf} values for such regions employing Eq. (3) were computed and the values are presented in Table 1 and plotted versus [surfactant] in Fig. 1. Notably the $k^0_{sf} - C_{SDS}$ profile (Fig. 1) is more or less similar to that of $k_{sf} - C_{SDS}$ profile, although correction of the ionic strength effect in the pmc region of the SDS shifts the $k^0 - C_{SDS}$ profile slightly downward, as the concentration of NaOH used in that region is of the order of 0.01 mol dm^{-3}. But for CTAB and TX, the effect is fairly insignificant as the concentration of NaOH used is of the order of 0.001 mol dm^{-3}.

The spectra of the dye in aqueous as well as surfactant added solutions at different concentrations of CTAB, TX and SDS are shown in Fig. 2a-c. Because of similarity of such curves in the cases of CTAB and TX only a few representative curves are shown in Fig. 2(b) and (c). The conductance (L) or surface tension (γ) values for the respective surfactants at varying concentrations, in the presence of fixed $[CV^+]$ (0.65×10^{-5} mol dm^{-3}) or [NaOH] (1.0 mol dm^{-3}) are given in Table 2. The cmc values thus obtained are presented in Table 3.

Inversion of sucrose

The reaction for the acid-catalyzed inversion of sucrose[1b] can be represented by Eq. (4)[1b]

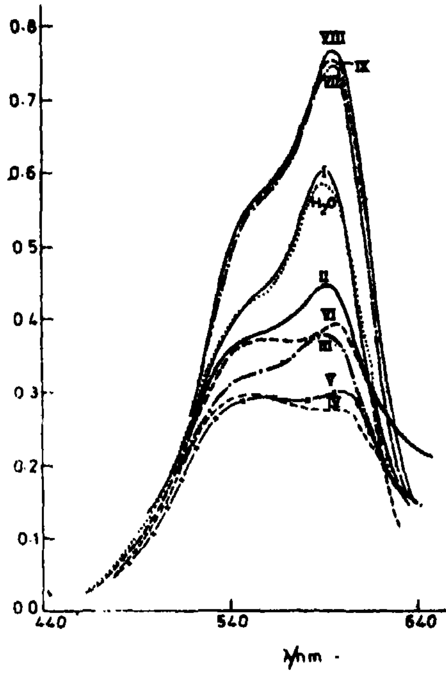

Fig. 2a—Spectra of CV^+ [0.65×10^{-5} mol dm^{-3}] at 25°C in presence of SDS at various concentrations [I = 1.16×10^{-5}, II = 6.96×10^{-5}, III = 9.28×10^{-5}, IV = 6.96×10^{-4}, V = 9.28×10^{-4}, VI = 1.04×10^{-3}, VII = 2.65×10^{-3}, VIII = 4.41×10^{-3}, 1.77×10^{-2}, IX = 4.4×10^{-2}; 5.3×10^{-2} and 6.4×10^{-2} mol dm^{-3} SDS]

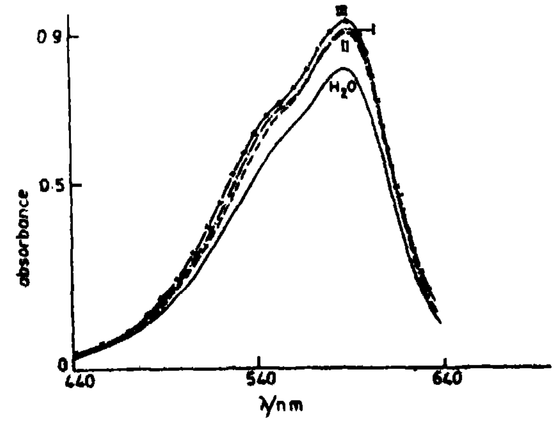

Fig. 2b—Spectra of CV^+ [0.85×10^{-5} mol dm^{-3}] at 25°C in presence of CTAB at various concentrations [I = 2.85×10^{-3}, II = 1.90×10^{-3}, III = 0.24×10^{-3} mol dm^{-3} CTAB]

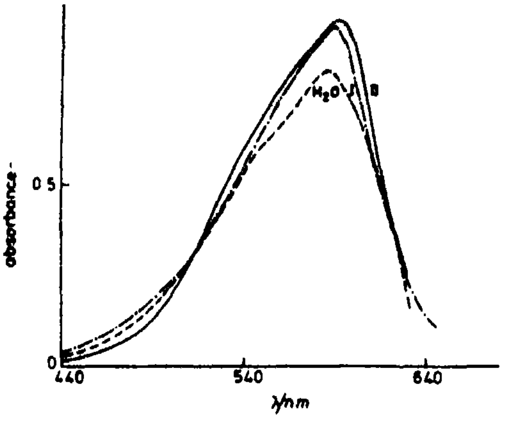

Fig. 2c—Spectra of CV^+ [0.85×10^{-5} mol dm^{-3}] at 25°C in presence of TX at various concentrations [I = 1.36×10^{-4}, II = 16.26×10^{-4} mol dm^{-3} TX]

Table 2—Conductance (L) and/or Surface Tension (γ) of CTAB, SDS and TX Solutions of Different Concentrations in Presence of Crystal Violet (0.65×10^{-5} mol dm^{-3}), Sucrose (10%) and/or Sodium Hydroxide (1 mol dm^{-3}) at 25°C

[C_s in mol dm^{-3}, L values in mhos; γ in dyne/cm^1]

CTAB + Crystal Violet		SDS + Crystal Violet		SDS + NaOH	TX + Crystal Violet	
$C_s \times 10^2$	$L \times 10^4$	$C_s \times 10^2$	$L \times 10^3$	γ	$C_s \times 10^3$	γ
0.86	6.50	8.15	5.26	29.80	1.94	32.35
0.57	5.71	5.43	4.17	30.25	1.30	33.20
0.48	3.23	4.52	3.85	30.25	1.08	33.50
0.29	3.44	2.72	2.17	30.30	0.65	34.00
0.25	3.45	2.41	2.19	—	0.43	34.20
0.19	2.94	1.81	1.49	30.15	0.22	34.80
0.16	2.70	1.51	1.59	—	0.11	37.20
0.12	1.76	1.21	1.16	30.10	0.06	39.70
0.085	2.22	0.91	0.87	30.00		
0.048	1.18	0.45	0.57	30.40		
0.024	0.63	0.30	—	30.50		
		0.23	0.29	31.50		
		0.18	—	34.00		
		0.10	—	37.50		
		0.05	—	42.40		

CTAB + Sucrose		SDS + Sucrose		TX + Sucrose	
0.71	4.9	6.79	3.43	1.96	36.87
0.59	4.1	5.66	2.82	1.30	36.92
0.48	3.5	4.53	2.56	1.10	36.90
0.36	3.1	2.26	1.63	0.94	36.97
0.30	2.7	1.70	1.22	0.65	36.70
0.24	2.3	0.85	0.83	0.40	36.60
0.18	1.9	0.57	0.64	0.20	36.20
0.12	1.9	0.28	0.034	0.16	34.93
0.06	1.2	0.17	0.022	0.10	34.60
0.03	0.7				

Table 3—CMC Values (in mol dm^{-3}) of CTAB, SDS and TX Solutions in Presence of Crystal Violet (0.65×10^{-5} mol dm^{-3}), Sucrose (10%) and/or Sodium Hydroxide (1 mol dm^{-3}) at 25°C

Surfactant	cmc values in presence of		
	CV^+	*Suc*	*NaOH*
CTAB	9.0×10^{-4}	8.0×10^{-4}	—
SDS	4.4×10^{-2}	8.0×10^{-3}	2.4×10^{-3}
TX	2.3×10^{-4}	2.2×10^{-4}	—

Literature values of Cmc's (mol dm^{-3}) of the surfactants in water (a) CTAB: 8-9 × 10^{-4}; (b) SDS: 8-9 × 10^{-3} and (c) TX: 2-4 × 10^{-4} [vide ref 21a and relevant references therein]

Table 4—Rate Constants (k_i) for Acid-Catalyzed Inversion of Sucrose in Presence of Surfactants at Different Concentrations at 25°C

[C_s in mol dm^{-3}; k_i in min^{-1}]

CTAB		SDS		TX	
$C_s \times 10^4$	$k_i \times 10^3$	$C_s \times 10^3$	$k_i \times 10^3$	$C_s \times 10^4$	$k_i \times 10^3$
1.24	2.4	1.16	2.2	0.28	2.0
2.38	2.6	2.24	1.9	0.54	2.2
4.79	2.2	4.56	2.0	1.09	2.9
9.50	2.3	9.05	2.0	2.16	2.6
19.0	2.6	18.10	2.0	4.32	2.3
26.5	2.0	27.15	1.9	6.49	2.3

$(k_i)_{H_2O} = 1.9 \times 10^{-3}$ min^{-1} (see ref. 1b)

$$C_{12}H_{22}O_{11} + H_2O \overset{H^+}{\rightleftharpoons} 2\,C_6H_{12}O_6 \qquad \ldots (4)$$

At constant [H^+] the reaction follows pseudo-first order kinetics which could be studied polarimetrically. The values of the rate constants (k_i) were obtained as usual[1b] from the slopes of the first order linear plots of $-\ln(R_t - R_\infty)$ versus t where R_t and R_∞ represent the angle of rotation at time t and final (infinity) time respectively. The k_i values obtained at [HCl] = 0.25 mol dm^{-3} are given in Table 4.

The cmc values of the detergents in the presence of 10% sucrose solution were also estimated from respective conductance (L) or surface tension values (given in Table 2) and are presented in Table 3.

Discussion

Kinetics of alkaline fading

Figure 1 shows that with addition of CTAB at concentrations well below its cmc, the k_ψ value increases, though rather slowly, from k_{H_2O} (the k-values in water)[1a] up to its cmc. Beyond cmc, the k_ψ values increase steadily with increase in [surfactant] eventually showing a broad maximum around [CTAB] = 3.3×10^{-3} mol dm^{-3}. As for TX the k_{st} value increases by about four times the k_{H_2O} value and then remains the same even beyond cmc of TX. The magnitude of increase in k_{st} is small as compared to that observed above cmc of CTAB. The addition of SDS, on the other hand, retards the rate of reaction at a galloping rate for concentrations well below the cmc of the surfactant (inset in Fig. 1). The decreasing trend in k_{st} values continues up to $C_{SDS} \approx 1 \times 10^{-3}$ mol dm^{-3}. The rate constant then increases, at first steeply and then slowly, to pass through a maximum at the original cmc of SDS (8×10^{-3} mol dm^{-3}). Beyond this there is again a very slow decrease in k_{st} values.

Cmc in presence of CV⁺

When CV^+ (0.65×10^{-5} mol dm^{-3}) is added to SDS, its cmc value increases from 8×10^{-3} to 4.4×10^{-2} mol dm^{-3}, contrary to that observed in the presence of salts[21b]. This seemingly unusual shift in cmc indicates a strong dye-surfactant interaction. The cmc values of CTAB and TX on the other hand, remain unperturbed in the presence of CV^+ pointing to the not-so-strong dye-surfactant interaction. For understanding the observed kinetic behaviour as well as shift in cmc value of SDS, analysis of the spectra (Fig. 2a-c) should be of particular use.

Spectral analysis

The cationic dye molecules (monomeric) are known to exist in equilibrium with their oligomers (mostly dimers)[21a,25]. Aqueous solutions of CV^+, as also the solutions containing the surfactants, show a prominent peak around 590 nm (Fig. 2a-c) presumably due to the monomeric species. An additional peak around 550 nm, prominent in presence of SDS only, probably arises out of the existence of the dimers.

For SDS, depending on its concentration the spectra exhibit extensive variations (Fig. 2a). Three distinct regions are discernible. At very low [SDS], the spectra in general and the peak heights around 590 nm in particular begin decreasing. The feeble dimer shoulder around 550 nm broadens as more SDS is added. The monomer: dimer peak height ratio falls from a value $\gg 1$ to around unity at about 6.96×10^{-4} mol dm^{-3} SDS (Fig. 2a, curve IV) where a maximum broadening of the dimer shoulder along with maximum lowering in absorbance at 590 nm is observed. Beyond this [SDS] the dimer shoulder again gradually recedes away to a hump as feeble as that in pure water. The monomeric peak intensity increases again, eventually surpassing the absorbance value in water till 4×10^{-2} mol dm^{-3} SDS. Notably, this is the cmc of SDS in the presence of CV^+ (vide Table 3). The monomer : dimer peak height ratio in this region again rises to a value exceeding that in pure water. Ultimately, above this cmc the spectra as well as absorbance at 590 nm become invariant as is also the monomer:dimer peak height ratio.

Plots of variation of the peak absorbance λ value (λ = 590 nm or 550 nm) versus log [dye]/[surfactant] which are known[21a] to indicate the types of interactions prevailing at any particular [dye]: [surfactant] ratio are shown in Fig. 3 in the case of SDS. Similar plots, resembling a 'potential well', have been observed for other cationic dye molecules as well[21a]. The right hand side of the curves are assumed to be guided[21a] chiefly by coulombic interactions, indicating that ion-ion interactions are prevailing at low [SDS]. Thus observed increase in [dimer] up to 6.96×10^{-4} mol dm^{-3} SDS indicates that the negatively charged surfactant ions induce dimerization of the dye cations[21,25] via electrostatic forces. As these dipositive dimeric species are stabilized by increased coulombic interactions with SDS anions, the $2\,CV^+ \rightleftharpoons (CV)_2^{2+}$ equilibrium is shifted gradually in favour of the dimer. At higher [SDS] (left hand side of Fig. 3), hydrophobic effect becomes prominent. Submicellar aggregates of SDS are formed gradually and ion-ion interactions (acting in cooperation with hydrophobic forces) become less important[21a]. The observed increase in absorbance 590 nm values and a declining trend in 550 nm shoulder (Fig. 2a, curves V-VIII) then indicate breaking down of dimeric dye units to monomeric cations and their stabilization via hydrophobic interactions with SDS oligomers. Above 4.4×10^{-2} mol dm^{-3} SDS, as the monom-

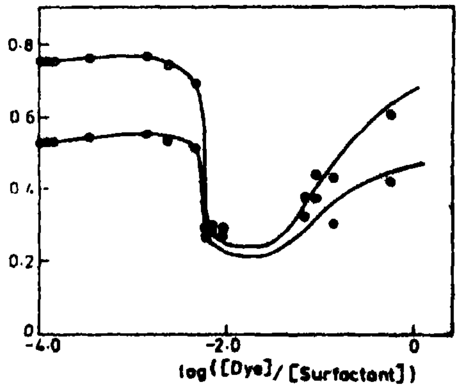

Fig. 3—Plots of absorbance λ [λ = 590 nm or 550 nm] values against log [Dye]/[Surfactant] for fixed dye concentrations of 0.65×10^{-5} mol dm^{-3} and varying SDS concentrations ranging from $\approx 1 \times 10^{-5}$ to 6.4×10^{-2} mol dm^{-3} [○ = OD at 590 nm; ● = OD at 550 nm]

eric dye species are incorporated in the extended SDS-dye mixed micelles[26], essential constancy of the forces involved lead to the plateau of curves in Fig. 3 and practically invariant absorbance values (Fig. 2a curve IX). Only a slight variation could be expected in micellar dilution. The non-availability of the surfactant molecules, engaged in SDS-dye interactions, for micellar aggregation also accounts for the increase in cmc value of SDS from 8×10^{-3} to 4.4×10^{-2} mol dm^{-3} in the presence of the dye.

In the case of CTAB, however, the coulombic forces are repulsive in nature and do not cooperate with hydrophobic forces, while non-ionic TX molecules exert only hydrophobic effects. Expectedly then, the conversion of monomer to dimer is not induced by these surfactants. On the other hand, these two are expected to form complexes with the monomeric dye species via hydrophobic[27] and/or charge transfer[20] interactions and thus shift the monomer ↔ dimer equilibrium in favour of the monomer. This is what has been observed (Fig. 2b and c), as the absorbance values, in general, and those at 590 nm in particular, increase, the dimer hump gets feebler. But this rather inappreciable change in absorbance values, in comparison to that observed in the presence of SDS and the constancy of cmc values even in the presence of CV^+, seems to corroborate the view that dispersion and charge transfer interactions are very weak in nature as compared to ion-ion interactions[21]. However, as micelles are formed, the large hydrophobic moieties may have sufficient dispersive interactions[27] resulting from collective effect of large number of molecules incorporated.

Effect of varying [OH^-] *on cmc*

While cmc values of CTAB and TX are not changed by addition of 10^{-3} mol dm^{-3} NaOH, the cmc decreases to a value 2.4×10^{-3} mol dm^{-3} for SDS in the presence of 1 mol dm^{-3} NaOH (vide Table 3). Since these are [OH^-] employed in kinetic studies, it is expected that apart from its role as reactant, OH^- also alters the interactions present in SDS solutions. Unfortunately, the estimation of cmc of SDS in the presence of both CV^+ and OH^- is forbidden by the chemical reaction that sets in. However, it appears justified to assume that in presence of OH^- the dye-surfactant mixed micelles will be formed at concentration less than 4×10^{-2} mol dm^{-3} but above 2.4×10^{-3} mol dm^{-3} SDS.

Catalytic effect of surfactants

Having established the types of interactions operative in dye-surfactant solutions, the analysis of the k_{st} – [surfactant] profiles appears rewarding. In the case of CTAB, the initial slow rise in k_{st} values is attributable to increase in [dye monomer] on the addition of CTAB. When micellization starts, the dye (CV^+) molecules, instead of being incorporated within the micellar pseudophase[5], possibly adhere to the outer surface, despite coulombic repulsion, through dispersive type interactions. More explicitly, these organic dye cations (CV^+) construct the inner Helmholtz plane (IHP)[28] of the micellar 'microelectrodes', through dispersion interactions in competition with the little hydrated hydrophobic micellar counter ion Br^-. Now the approach of hydrophilic reagent OH^- from the bulk to the outer Helmholtz plane (OHP) of these positively charged microelectrodes will obviously depend on the potential difference $(\phi_{IHP} - \phi_b)$[15,29], where ϕ_{IHP} and ϕ_b are the potentials at the IHP of the micelle and at the bulk respectively (Fig. 4). Thus with increased addition of CTAB, ϕ_{IHP} increases which facilities more OH^- ions to approach to the microelectrode-water interface and the result is the linear increase in k_{st} values with [CTAB].

Admittedly, the presence of Br^- ions, which are known to get specifically adsorbed[28] on Hg-surface and possibly on these microelectrode surfaces as well, will hinder the specific adsorption of CV^+ forming IHP and also the approach of hydrophilic OH^- towards IHP, usually defined as micelle-water interphase[8], to some extent, so that the desired increase of k_{st} values as discussed above, may be substantially restricted. The observed broad hump at 3.3×10^{-3} mol dm^{-3} CTAB may be attributed to the completion of the process of accommodating CV^+ molecules at the IHP's of the micelles and mere dilution[30] through more micelle formation at still higher [CTAB]. In the case of neutral surfactant TX, ϕ_{IHP} is not at all altered by the addition of TX above cmc and the situation remains the same as at pmc. The rate constants are thus held constant throughout, after an initial enhancement due probably to increased dye monomer contribution.

In the case of SDS, at very low [surfactant] the rate constant is almost identical to that in pure water (inset in Fig. 1), where absorbance$_{590}$ values are also nearly the same (Fig. 2a). As more SDS is added, the [monomeric dye] is decreased substantially resulting in a rapid decrease in k_{st} values, as observed up to $C_{SDS} = 6.96 \times 10^{-4}$ mol dm^{-3}. From this concentration up to cmc (4.4×10^{-2} mol dm^{-3} of SDS in the absence of NaOH), the concentration of "monomeric dye-SDS oligomer" in-

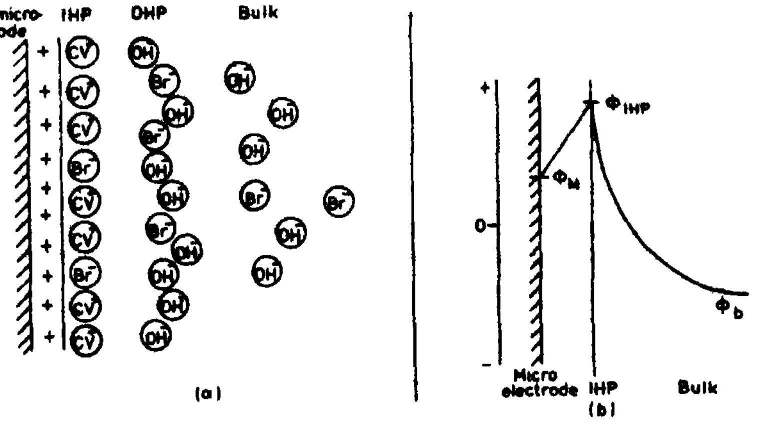

Fig. 4—Distribution of (a) ions and (b) potential around micellar 'micro-electrodes' of CTAB

teracted product increases. While the increased number of monomeric species should enhance the rate of reaction, the negative charge of the SDS oligomers present in these complexes would retard the same by repelling the neucleophile, OH^- ion. Thus the k_{sf} values increase again in this region but the extent of increase is small as compared to the fall and even as the absorbance$_{590}$ values surpass the value in water, the k_{sf} values remain much less than k_{H_2O}. The width of this region, upto which k_{sf} goes on increasing, is however uncertain owing to micelle formation inthe presence of OH^-. From kinetic data, the hump almost at the original cmc of SDS seems to suggest that mixed micelle formation in the presence of 1 mol dm^{-3} NaOH occurs at this concentration. Beyond cmc hardly any dye molecule is left behind. Further addition of SDS is likely to cause simple micellar dilution and hence a very slow decrease in k_{sf} values as has been observed. Obviously the interphase or Stern layer model put forward in the case of CTAB is not applicable here as the reactant CV^+ molecules are the part of the micro-electrode itself and the situation here refers to the pseudophase model[5,18]. Unfortunately, the limitation in using high CV^+ concentrations set by high extinction coefficient of the dye forbid detailed analysis of the suitability of the model.

The results presented above point to following interesting features. (i) It is demonstrated that the surfactants may have significant interactions with the dye molecules even at the pmc region. (ii) In contrast to the popular belief that the kinetic effects involving the surfactants are important only well above their cmc, significant effects might be present in the pmc region as well. In fact, in the present study the decreasing trend in k_{sf} values caused by the addition of SDS was almost over before the micelles were formed. For TX also, although very little, the effect on k_{sf} observed was achieved at pmc. (iii) When the rate of any reaction is affected by micelles, depending on the type and magnitude of the interaction between the organic molecules and the surfactants, either the 'pseudophase model' or 'interphase model' may be operating. Thus for strong coulombic type of reactant-surfactant interactions extending up to the formation of mixed micelles the pseudophase model seems to be valid, as in the case of SDS. In the case of others involving non-coulombic type interactions, the 'interphase model', better defined by the double layer property of micellar micro-electrodes, is applicable, as was found for CTAB.

In the case of kinetics of inversion of sucrose the rate constants (k_i) practically remain unaltered from that in pure water by the addition of surfactants in both pmc and cmc regions. If one considers that H_3O^+ ions interact differently with the cationic and anionic surfactants and are expected to occupy the 'Stern layer' of SDS micelles, and be repelled by that of CTAB micelles this result appears rather perplexing. On the other hand, this is quite expected in view of the fact that sucrose molecules, with so many hydrophilic groups, undergo strong H-bonded interaction with water molecules, as no electrostatic sucrose-surfactant interaction is being expected. The hydrophobic part of the substrate molecule being well shielded by the hydrophilic OH^- groups, the weak hydrophobic interaction operative between the sucrose-surfactant organic moieties is not able to overcome the effect of hydrophilic bonding and the substrate sucrose molecules remain in the bulk phase. As a result, the reaction occurs chiefly in aqueous phase and the k_i values remain constant. Further support to this observation is obtained from the fact that cmc's of the surfactants remain unaltered in the presence of sucrose. Thus the observed kinetic results with sucrose point out that in such catalysis under investigation, the reaction site is of primary importance.

Acknowledgement

Thanks are due to Dr K Das for helpful discussions and to the CSIR, New Delhi for the award of a research associateship to one of them (JD).

References

1 (a) Mondal U, Sen S, Das K & Kundu K K, *Can J Chem*, **64** (1986) 300; (b) Mondal U, Das K & Kundu K K, *Can J Chem*, **64** (1986) 1638.

2 Fendler J H & Fendler E J, *Catalysis in micellar and macromolecular systems* (Academic Press, New York) 1975.

3 (a) Cordes E H & Dunlap R B, *Acc chem Res*, **2** (1969) 329; (b) Cordes E H ed *Reaction kinetics in micelles* (Plenum Press, New York) 1973; (c) Cordes E H & Geitler C, *Prog bioorg Chem*, **1** (1973) 2; (d) Cordes E H, *Pure appl Chem*, **50** (1978) 617; (e) Albrizzio J, Archila J, Rodulfo T & Cordes E H, *J org Chem*, 37 (1972) 871.

4 Duynstee E F J & Grunwald E, *J Am chem Soc*, **81** (1959), 4540, 4542.

5 Bunton C A, (a) *Pure Appl Chem*, **49** (1977) 969; (b) *Prog Solid State Chem*, **8** (1973) 239; (c) In *solution chemistry of surfactants*, Vol. 2, edited by K L Mittal (Plenum Press, New York) 1977; (d) *Catal Rev Sci-Eng*, **1** (1979) 20; (e) Bunton C A, Carrasco N, Huang S K, Paik C H & Romsted L S, *J Am chem Soc*, **100** (1978), 5420; (f) Bunton C A, Romsted L S & Smith H J, *J org Chem*, **43** (1978), 4299; (g) Bunton C A, Romsted L S & Savelli G, *J Am chem Soc*, **101** (1979), 1253; (h) Al-Lobedan H, Bunton C A & Romsted L S, *J phys Chem*, **85** (1981), 2123; *J org Chem*, 47 (1982) 3528; (i) Al-Lohedan H, Bunton C A & Moflet J R, *J phys Chem*, **87** (1983) 332; (j) Bunton C A, Mhola M M, Moffet J R, Monaners D & Savelli G, *J org Chem*, **49** (1984) 426.

6 Berezin I V, Martiner K & Yatsimerskii A K, *Russ chem Rev*, **42** (1973) 787.

7 Martiner K, Yatsimerskii A K, Vbevashov A & Berzin I V in *Micellisation solubilization and micro-emulsions*, Vol. 2, edited K L Mittal (Plenum Press, New York) 1977, pp. 489.

8 (a) Broxton T J, *Aust J Chem*, **34** (1981) 2313; **35** (1982) 2557; **36** (1983) 2203; **37** (1984) 47; (b) Broxton T J & Sango D B, *Aust J Chem*, **36** (1983) 711.

9 Romsted L S in *Micellization, solubilization and micro-emulsions*, Vol. 2 edited by K L Mittal (Plenum Press, New York) 1977, pp. 509.

10 Nome F, Rubira A F, Franco C & Ionesku L G, *J phys Chem*, **86** (1982) 1881.

11 Dougherty S J & Berg J C, *J Colloid Interface Sci*, **48** (1974) 110; **49** (1975) 135.

12 Brown J M & Darwent J R, *J Chem Soc Chem Commun*, (1969) 171.

13 Dash A C, Dash B & Mahapatra P K, *J chem Soc Dalton*, (1981) 2063, (1983) 1503 and other relevant references therein.

14 Gern L H, *Can J Chem*, **63** (1985) 578.

15 (a) Lelivre J & Gaboriaud R, *J chem Soc Faraday Trans I*, **81** (1985), 335; (b) Gaboriaud R, Charbit G & Dorion F, in *Surfactants in solutions*, Vol. 2, edited by K L Mittal (Plenum Press, New York) 1984, 949.

16 (a) Funasaki N, *J phys Chem*, **83** (1979) 237, 1988; (b) Funasaki N & Murata A, *Chem pharm Bull*, **28** (1980) 805.

17 (a) Quina F H, Chaimovich H, *J phys Chem*, **83** (1979) 1844; (b) Chaimovich H, Bonilha J B S, Politi M J & Quina F H, *J phys Chem*, **83** (1979) 1851; (c) Quina F H. Politi M J, Cuccovia I M, Martins-Franchetti S M & Chaimovich H in *Solution behaviour of surfactants theoretical and applied aspect*, Vol. 2, edited by K L Mittal & F J Fendler, (Plenum Press, New York) 1982, pp. 1125.

18 (a) Cipiciani A, Linda P, Savelli G & Bunton C A, *J phys Chem*, **87** (1983) 5262; (b) Bunton C A, Frankson J & Romsted L S, *J phys Chem*, **84** (1980) 2607; (c) Bunton C A, Hamed F H & Romsted L, *J phys Chem*, **86** (1982) 2103; (d) Bunton C A, Huang S K, *J org Chem*, **37** (1972) 1790; **40** (1976) 41; (e) Bunton C A, Chan S, Huang S K, *J org Chem*, **39** (1974) 1262.

19 Fendler E J & Fendler J H, *Adv phys-org Chem*, **8** (1970) 27.

20 (a) Hayashi H, *Bull chem Soc*, Japan **34** (1961) 119; (b) Rohatgi-Mukherjee K K, Choudhuri R & Bhowmick B B, *J colloid interface Sci*, **106** (1985) 45.

21 (a) Moulick S P, Ghosh S & Das A R, *Colloid polym Sci*, **257** (1979) 645; (b) Evans D N & Ninham B N, *J phys Chem*, **87** (1983) 5020, 5025.

22 (a) Suzuki C H, *Bull chem Soc Japan*, **44** (1971) 2630; (b) Mukherjee P, Cardinal J R, *J phys Chem*, **82** (1978) 1620.

23 *International Critical Tables*, Vol. VII (McGraw Hill, New York) 1930.

24 Carsaro G, *J chem Educ*, **41** (1964) 48.

25 Levshin L V & Gorshkov V K, *Opt Spectrosc*, **10** (1961) 401.

26 Corkill J M, Goodman J F & Tate J R, *Trans Faraday Soc*, **60** (1964) 986.

27 (a) Ben Naim A, *Hydrophobic interactions*, (Plenum Press, New York) (1980); Franks F, Pedlay M D & Reid D S, *J chem Soc Faraday Trans-I*, **72** (1976) 359; (c) Clark A H, Franks F, Padley H D & Reid D S, *J chem Soc Faraday Trans I*, (1977) 290; (d) *The hydrophobic interactions*, *Faraday Soc Symp* (1982); Hertz H G & Leiter A, *Zeit physik Chem Neue Folge*, 33 (1982) 451.

28 Bockris J O'M & Reddy A K N, *Modern electrochemistry*, Vol. 2 (Plenum Press, New York) 1970.

29 Treiner C, Lebesnerais A & Micheletti C, in *Adv Chem Ser* edited by W F Furter, no. 177 (American Chemical Society, Washington) 1979, pp. 109.

30 Bunton C A & Wolfe B, *J Am chem Soc*, **95** (1973) 3742; (b) Bunton C A, Minch M J, Hidalgo J & Sepulveda L, *J Am chem Soc*, **95** (1973) 3262; (c) Buist G J, Bunton C A, Robinson L, Sepulveda L & Stam M J, *J Am chem Soc*, **92** (1970) 4072.

Indian Journal of Chemistry
Vol. 27A, February 1988, pp. 123-125

Kinetics of Oxidation of Some α-Hydroxy Acids by Sodium N-Bromobenzenesulphonamide

ABHA MATHUR, VINITA SHARMA & KALYAN K BANERJI*
Department of Chemistry, University of Jodhpur, Jodhpur 342001

Received 27 *April* 1987; *revised* 15 *June* 1987; *accepted* 1 *July* 1987

Oxidation of lactic, glycollic, mandelic and 2-hydroxy-2-methylpropanoic acids by sodium N-bromobenzenesulphonamide (BAB) gives the corresponding carbonyl compounds by oxidative decarboxylation. The reaction is first order each in [BAB] and [substrate] and is catalysed by hydrogen ions. Addition of parent sulphonamide does not affect the reaction rate. The observed dependence of rate on acidity suggests that both $PhSO_2NHBr$ and its protonated form are reactive oxidant species. Oxidation shows the absence of a primary kinetic isotope effect. The value of solvent isotope effect, $k(H_2O)/k(D_2O)$ is 3.99 at 303 K. The activation parameters for the reaction have been evaluated. The possible reaction mechanisms are discussed.

The kinetics of oxidation of α-hydroxy acids by many oxidants have been studied[1-5]. Being bifunctional compounds, their oxidation can proceed by many possible routes. In continuation of our studies[6] on kinetics and mechanism of oxidation of organic substrates by sodium N-bromobenzenesulphonamide (bromanine-B or BAB), we report herein the results of kinetics and mechanism of oxidation of lactic acid (LA), glycollic acid (GA), mandelic acid (MA) and 2-hydroxy-2-methylpropanoic acid (HMPA) by BAB in aqueous acetic acid solutions.

Materials and Methods

The hydroxy acids were commercial products and were used as such. Their aqueous solutions were standardized by alkalimetric titrations. BAB was prepared in the laboratory. Perchloric acid (Merck, 60%) was used as a source of hydrogen ions. Purified acetic acid was used as the solvent. α-Deuteriomandelic acid (isotopic purity 92 ± 5%; PMR[3]) was prepared by the method of Kemp and Waters[2].

Product analysis

The product analysis was carried out under kinetic conditions, i.e. [substrate] $\gg$ [BAB]. In a typical experiment, HMPA (5 g, 0.05 mol) was added to BAB (2.8 g, 0.01 mol) and made upto 100 ml in 1:1 (v/v) acetic acid-water in the presence of 1.0 mol dm^{-3} perchloric acid. The reaction mixture was allowed to stand for nearly 10 hr for completion of the reaction, treated with an excess (250 ml) of a saturated solution of 2,4-dinitrophenylhydrazine in 2 mol dm^{-3} HCl and kept overnight in a refrigerator. The precipitated 2,4-dinitrophenylhydrazone (DNP) was filtered off, dried, weighed, recrystallized from ethanol and weighed again. The DNP was found identical (m.p. and mixture m.p.) with an authentic sample of DNP of acetone. The yields of DNP were 2.18 g (94%) and 2.02 g (87%) before and after recrystallization respectively. In similar experiments with the other hydroxy acids the yields of DNPs of corresponding carbonyl compounds were 82-91% after recrystallization. The overall reaction corresponds to Eq. (1).

$$R_2C(OH)COOH + PhSO_2NBr^- \rightarrow R_2C=O + PhSO_2NH_2 + CO_2 + Br^- \quad \ldots(1)$$

Kinetic measurements

The kinetic runs were followed iodometrically upto 70% reaction under pseudo-first order conditions ([substrate] $\gg$ [BAB]) at constant temperature (± 0.1 K) in reaction flasks blackened from outside. The pseudo-first order rate constants were determined from the linear ($r > 0.990$) plots of log [BAB] against time. The solvent used was 1:1 (v/v) acetic acid-water. The linear regressions were carried out by the least squares method using a Workhorse II (HCl) microcomputer.

Results

The reaction is first order each in [BAB] and [substrate]. Further the pseudo-first order rate constants do not depend on the initial [oxidant]. The reaction is catalysed by perchloric acid (Table 1).

The α-deuteriomandelic aq. acid (PhCD(OH)-COOH)and mandelic acid undergo oxidation by almost similar rates, indicating the absence of a primary kinetic isotope effect. Addition of one of the product of oxidation, i.e. benzenesulphonamide (BSA) does not affect the rate. The rate varies from

15.0 to $14.7 \times 10^{-5} s^{-1}$ in BSA concentration range of 0.0 to 15.0×10^{-3} mol dm^{-3} under the condition: [substrate] = 0.2 mol dm^{-3}, [H$^+$] = 0.5 mol dm^{-3}; and temp. = 303 K.

The rate of oxidation of HMPA was determined in D_2O (overall deuterium content, 95%). The rates of oxidation in pure water and D_2O are: $10^5 k_1 = 10.7$ and 2.68 s^{-1} respectively at [HMPA] = 0.2 mol dm^{-3}, [H$^+$] = 0.2 mol dm^{-3}, [BAB] = 0.005 mol dm^{-3} and temp. 303 K. The value of solvent isotope effect, $k(H_2O)/k(D_2O)$ is 3.99 at 303 K.

Bromamine-B undergoes dissociation, protonation, hydrolysis, disproportionation etc. in an aqueous acid solution[7]. These reactions have been studied quantitatively and various equilibrium constants have been determined[8]. The pk of the free acid[8], $PhSO_2NHBr$, is 4.95 at 298 K. The absence of any effect of added BSA suggests[6] that $PhSO_2NHBr$ is the reactive oxidising species.

Table 1—Rate Constants for Oxidation of Lactic Acid and Glycollic Acid by BAB at 303 K.

10^3[BAB] (mol dm^{-3})	[Hydroxy Acid] (mol dm^{-3})	[H$^+$] (mol dm^{-3})	$10^5 k_1$(s^{-1})	
			LA	GA
2.0	0.10	0.5	7.40	5.53
3.5	0.10	0.5	7.63	5.21
5.0	0.10	0.5	7.47	5.40
10.0	0.10	0.5	7.52	5.40
15.0	0.10	0.5	7.37	5.32
5.0	0.05	0.5	3.80	2.75
5.0	0.20	0.5	15.0	10.7
5.0	0.30	0.5	22.3	16.1
5.0	0.50	0.5	37.5	27.0
5.0	0.10	0.2	4.52	3.21
5.0	0.10	0.7	9.53	6.61
5.0	0.10	1.0	12.4	8.70
5.0	0.10	1.3	15.5	10.9
5.0	0.10	1.5	17.7	12.0
5.0	0.10	1.7	19.3	13.3
5.0	0.10	2.0	22.5	15.8
5.0	0.10	2.2	24.7	17.0
5.0	0.10	2.5	27.3	18.7

A plot of [H$^+$] against the observed rate is linear with a non-zero intercept, indicating[9] that (i) the pre-equilibrium between the protonated and unprotonated forms is rapid, (ii) the equilibrium constant is small and (iii) both the forms are active, the protonated form, $PhSO_2NH_2Br$, being more reactive. Experimental evidences for the formation of such protonated species have been presented[10] in structurally related compound, chloramine-T.

The above situation leads to the experimental rate law (2)

$$k_1 = k_2 + k_3[H^+] \qquad \ldots(2)$$

The values of k_2 and k_3 were determined from the linear plots (r = 0.9965 to 0.9999) of k_1 against [H$^+$] at different temperatures. The specific rate constants of the uncatalysed and acid-catalysed reactions were obtained from the relation $k = k_2$/[hydroxy acid] and $k' = k_3$/[hydroxy acid] respectively, and the activation parameters were evaluated (Table 2). α-Hydroxy acids can be oxidised like alcohols[1] or may undergo oxidative decarboxylation[5].

The absence of a kinetic isotope effect confirms that the C − H bond is not cleaved in the rate-determining step. The relative ease of oxidation of HMPA shows that the oxidative decarboxylation is energetically more favourable and the α-hydrogen is not involved in oxidation at all.

D_3O^+ is a stronger acid[11] than H_3O^+ and the rate of an acid-catalysed reaction is expected to be faster in D_2O than in H_2O. However, labile hydrogens like those present in hydroxyl and carboxyl groups undergo rapid exchange in D_2O and if the O − H bond is

Table 2—Rate Constants and Activation Parameters for Acid-independent and Acid-dependent Oxidation of Hydroxy Acids by BAB

Compound	$10^4 k$(dm^{3}mol^{-1}s^{-1})				$\Delta H^\ddagger$ (kJmol^{-1})	$\Delta S^\ddagger$ (Jmol^{-1}K^{-1})	$\Delta G^\ddagger$ (kJmol^{-1})
	298	303	308	313K			
			Acid-independent oxidation				
LA	1.49	2.91	3.72	5.67	63.3	−104	94.4
GA	1.05	1.91	2.81	4.50	70.9	−81	95.3
HMPA	3.10	5.10	7.36	11.1	62.5	−102	92.7
MA	7.28	11.8	16.4	24.2	58.3	−108	90.6
			Acid-dependent oxidation				
LA	6.20	9.55	14.0	20.7	59.2	−106	91.1
GA	4.01	6.80	9.75	15.2	64.8	−91	92.1
HMPA	11.7	17.5	25.2	35.6	54.7	−116	89.5
MA	19.5	28.4	38.8	52.4	48.1	−134	88.2

cleaved either in the rate-determining step or in a step prior to it, O – H/O – D isotope effect comes into play. This cancels the rate-enhancing effect of D_2O and may result in an 'inverse' solvent isotope effect. In the present reaction an 'inverse' solvent isotope effect has been observed indicating that – OH group and/or – COOH group are involved in the rate-determining step.

The above results indicate the possible mechanisms for the reaction as outlined in Schemes 1-4. Scheme 4 involves the formation of an acyl hypobromite derivative in the rate-determining step. This is unlikely since a protonated species cannot act as a nucleophile[12]. In the reactions of formic acid and oxalic acid with BAB[13], where the formation of acyl hypobromites has been invoked, an inverse dependence on acidity is observed. On this basis also the mechanism depicted in Scheme 4 is ruled out.

The present data, however, do not enable us to identify the most probable mechanisms amongst Schemes 1 to 3. Though there is no kinetic evidence for the formation of a hypobromita ester in the slow step (Scheme 3), a similar mechanism has been suggested for the oxidation of alcohols[14] and α-hydroxy acids[4] by N-bromoamides. Schemes 1 and 2 involve oxidative decarboxylation in the rate-determining steps and the difference between these two mechanisms is subtle. Similar mechanisms can be written for the uncatalysed path involving $PhSO_2NHBr$ instead of its protonated form.

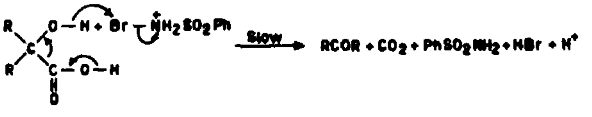

SCHEME 1

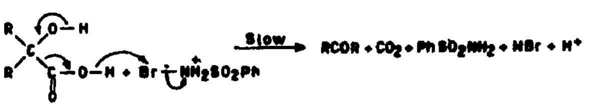

SCHEME 2

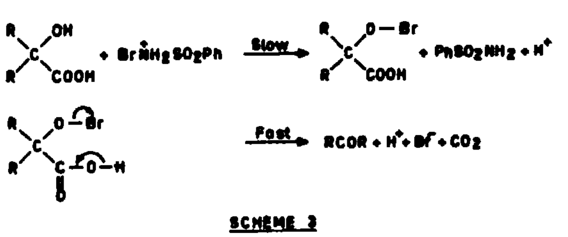

SCHEME 3

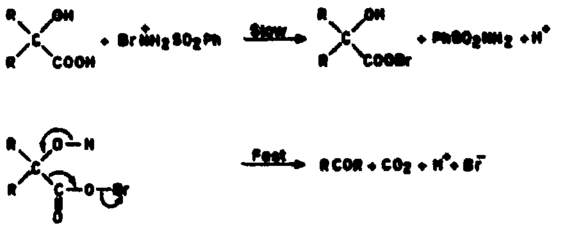

SCHEME 4

Acknowledgement

Thanks are due to the authorities of University of Jodhpur for the award of a fellowship to AM and to the CSIR, New Delhi, for the award of a senior fellowship to VS.

References

1 Banerji K K, *Tetrahedron*, **29** (1973) 1401; Banerji K K, *J chem Res* (*S*), (1978) 193; (*M*) 2561.
2 Kemp T J & Water W A, *J chem Soc*, (1964) 1194.
3 Banerji K K, *Indian J Chem*, **17A** (1979) 90; Mathur A K & Banerji K K, *Indian J Chem*, **20B** (1981) 529; Jain A L & Banerji K K, *J Indian Chem Soc*, **59** (1982) 694.
4 Bishnoi M L, Negi S C & Banerji K K, *Indian J Chem*, **25A** (1986) 660; Pink J M & Stewart R, *Can J Chem*, **49** (1971) 654; Natarajan R & Venkatasubramanian N, *Indian J Chem*, **13** (1975) 261.
5 Sengupta K K, *Bull chem Soc Jpn*, **42** (1969) 298; Krishna B & Tiwari K C, *J chem Soc*, (1961) 3097; Levesley P & Waters W A, *J chem Soc*, (1955) 217.
6 Kothari S & Banerji K K, *Can J Chem*, **63** (1985) 2726; Kothari S, Sharma V & Banerji K K, *J chem Res* (*S*), (1985) 234; (*M*) (1985) 2371.
7 Banerji K K, Mahadevappa D S & Jayaram B, *J Sci Ind Res*, **45** (1987) 65.
8 Hardy F E & Johnston J P, *J chem Soc Perkin Trans* 2, (1973) 742.
9 Gupta K S & Gupta Y K, *J chem Educ*, **61** (1984) 972.
10 Narayanana S S & Rao V R S, *Radiochem Acta*, **32** (1983) 211.
11 Collins C J & Bowman N S, *Isotope effects in chemical reactions* (Van Nostrand, New York) 1970, 267.
12 March J, *Advanced organic chemistry*, (Academic Press, New York) 1977, 399.
13 Mathur A & Banerji K K, *Indian J Chem*, **26A** (1987) 774.
14 Mukherjee J & Banerji K K, *J org Chem*, **46** (1981) 2323.

Indian Journal of Chemistry
Vol. 27 A, February 1988, pp. 126-128

Flexibly Bridged Binuclear Ruthenium (II) Complexes of Dithiobis(β-diketones)†

(Mrs) SARADA GOPINATHAN, (Mrs) S S DESHPANDE & C GOPINATHAN*
Inorganic Chemistry Division, National Chemical Laboratory, Pune 411 008

Received 3 *March* 1987; *revised and accepted* 1 *June* 1987

Binucleating dibasic tetradentate chelating ligands of the type H(β-dik)S-S(β-dik)H[β-dik = 2,4-pentanedione (HAcac), 1-phenyl-1,3-butanedione (HBa) and 1,3-diphenylpropanedione (HDbm)] react with Ru-H/Ru-Cl bond of the complexes $RuHClCO(PPh_3)_3$ and $[RuClCO(PPh_3)_2(CH_3CHCN)]_2$ to yield novel chelated compounds of the type $[RuClCO(PPh_3)_2]_2(\beta\text{-dik})_2S_2$ (I), $[RuHCO(PPh_3)_2]_2(\beta\text{-dik})_2S_2$ (II) and $[RuCO(PPh_3)_2(CH_3CHCN)]_2(\beta\text{-dik})_2S_2$ (III). These complexes are characterised by elemental analyses, IR and PMR spectra, and molecular weight determinations. In the presence of acrylonitrile, the binuclear chloro complexes (I) form cationic species with a large anion like ClO_4^-. Phosphine substitution reaction in these complexes using pyridine and substituted pyridines fails to give expected products. Attempts to prepare mercapto derivatives by S − S bond cleavage with methyllithium lead to decomposition of the complex.

Square planar binuclear complexes of rhodium (I) with aromatic azine derivatives as bridging ligands have recently been reported by us[1]. The X-ray crystal studies of the complex $Rh_2(CO)_2$(Salazine) reveal that rhodium atoms are linked through a pair of oxyanion and azomethine nitrogen atoms of salicylaldazine ligand. Several binuclear complexes of dithiobis(β-diketones) containing titanium (IV) and organotin (IV) have been synthesised and characterised by us[2]. This paper describes the preparation and some reactions of binuclear ruthenium (II) derivatives of the above dithio ligands.

Materials and Methods

The reactions were carried out under dry N_2 atmosphere. Solvents and other liquid reagents were carefully purified, dried, freshly distilled and degassed before use. Benzoylacetone and dibenzoylmethane were purified by recrystallisation. The ruthenium complex $RuHCOCl(PPh_3)_3$ (ref. 3) and dithiobis(β-diketones) were prepared by reported methods[2,4].

The IR spectra were recorded on a Perkin-Elmer 599 spectrophotometer and PMR spectra on a Bruker FT-90 instrument. Molecular weights were determined using a Wescan vapour pressure osmometer.

(a) *Reactivity of Ru − H bond in* $RuHCOCl(PPh_3)_3$

Dithiobis(acetylacetone) (0.0524 g; 0.0002 mol) was dissolved in benzene-ethanol (2:1, v/v) and to this was added $RuHCOCl(PPh_3)_3$ (0.380 g; 0.0004 mol) and the mixture refluxed for 6 hr. The clear solution upon concentration and cooling gave green crystalline solid which was washed with hexane and dried *in vacuo* at 60°; yield 0.324 g (75%). Other two chlororuthenium compounds were prepared similarly.

(b) *Reactivity of Ru − Cl bond in* $RuHCOCl(PPh_3)_3$

Sodio derivative of dithiobis(acetylacetone) was prepared from oil-free sodium hydride (0.0096 g; 0.0004 mol) and dithiobis(acetylacetone) (0.0525 g; 0.0002 mol) in ether (25 ml) by stirring at room temperature. The dry sodio derivative was suspended in THF and $RuHCOCl(PPh_3)_3$ (0.380 g; 0.0004 mol) added to it and stirred for 20 hr. The THF solution was evaporated to dryness *in vacuo* and extracted with benzene. The benzene extract on concentration gave a brown microcrystalline product which was washed with hexane and dried *in vacuo* at 60°, yield 0.302 g (70%). Derivatives of other two ligands were prepared similarly.

(c) *Formation of cationic complexes*

A solution of $[RuCOCl(PPh_3)_2]_2(Acac_2S_2)$ (0.819 g; 0.0005 mol) in acrylonitrile (25 ml) was treated with anhydrous silver perchlorate (0.208 g; 0.001 mol) and the contents stirred for 3 hr. The precipitate of AgCl was filtered off and the solution concentrated under reduced pressure to obtain a crystalline solid. This was washed with pet. ether (40-60°) and dried *in vacuo* at 60°; yield 0.562 g (60%).

Results and Discussion

Dithiobis(β-diketones) react with RuH-

---

†NCL Communication No. 4219

Table 1 — Analytical Data for Dithiobis(β-diketone)ruthenium(II) Complexes

Sl No.	Complex	m.p. (°C)	Found (Calc.) (%) C	H	P	S
1	$[RuClCO(PPh_3)_2]_2(Acac)_2S_2$	130	61.10 (61.57)	4.20 (4.43)	7.45 (7.54)	3.72 (3.91)
2	$[RuClCO(PPh_3)_2]_2(Ba)_2S_2$	155	64.35 (64.05)	4.23 (4.35)	6.95 (7.03)	3.42 (3.64)
3	$[RuClCO(PPh_3)_2]_2(Dbm)_2S_2$	132	66.18 (66.20)	4.08 (4.27)	6.38 (6.57)	3.12 (3.40)
4	$[RuHCO(PPh_3)_2]_2(Acac)_2S_2$	110	64.15 (64.27)	4.26 (4.75)	7.59 (7.89)	4.02 (4.08)
5	$[RuHCO(PPh_3)_2]_2(Ba)_2S_2$	170	66.40 (66.65)	4.38 (4.64)	7.19 (7.31)	3.62 (3.79)
6	$[RuHCO(PPh_3)_2]_2(Dbm)_2S_2$	115	68.56 (68.71)	4.42 (4.66)	7.20 (7.08)	3.15 (3.53)
7	$[RuCO(PPh_3)_2(CH_3CHCN)]_2(Acac)_2S_2$	142	64.25 (64.50)	4.65 (4.81)	7.06 (7.39)	3.68 (3.83)
8	$[RuCO(PPh_3)_2(CH_3CHCN)]_2(Ba)_2S_2$	135	66.56 (66.73)	4.45 (4.70)	6.56 (6.88)	3.32 (3.56)
9	$[RuCO(PPh_3)_2(CH_3CHCN)]_2(Dbm)_2S_2$	110	68.23 (68.66)	4.24 (4.61)	6.31 (6.44)	3.10 (3.33)

Table 2—Infrared and PMR Data for Dithiobis(β-diketone)ruthenium (II) Complexes

Sl No.*	IR ν(cm^{-1})				PMR chemical shift δ ppm		
	(CO)	(dik)	(RuH)/(C≡N)	(S–S)	(Ru–H	CH_3	Other resonances
1	1950	1580, 1550		450		2.03, 2.17	
2	1960	1590. 1560		450		1.30, 1.20	6.70-8.10 (ArH)
3	1950	1540, 1520		450			6.00-8.50 (ArH)
4	1905	1550	1945	445	– 14.40	2.00, 1.90	6.88-7.77 (ArH)
5	1910	1580, 1540	1930	445	– 14.10 – 14.40	1.28	6.60-8.30 (ArH)
6	1910	1540, 1510	1940	440	– 13.70, – 16.20		6.22-8.44 (ArH)
7	1935	1580, 1560	2220	440		2.30	7.30-8.00 (ArH) 0.85*d* (CH_3), 2.3*m* (CH)
8	1910	1540	2220, 2180	445		1.24	7.00-8.10 (ArH) 0.90*d* (CH_3), 2.35*m* (CH)
9	1910	1540, 1510	2220, 2180	445			6.80-8.20 (ArH) 0.87 (CH_3), 2.3*m* (CH)

*Sl nos refer to compounds listed in Table 1.

$COCl(PPh_3)_3$ in boiling ethanol-benzene (1:2, v/v) to afford chelated diruthenium complexes of the formula $[RuClCO(PPh_3)_2]_2(\beta\text{-dik})_2S_2$ (I) as crystalline solids. Disodium derivatives of the ligands react with $RuHClCO(PPh_3)_3$ or $[RuClCO(PPh_3)_2(CH_3CHCN)]_2$ in benzene to yield chlorine-free binuclear complexes of the types (II) and (III) respectively. The complexes are greenish yellow to brown solids, soluble in benzene, toluene and chloroform (Table 1). Molecular weight determinations by vapour pressure osmometry using toluene as the solvent suggests them to be binuclear having two hexacoordinated ruthenium atoms. The chloro complexes react with perchlorate ion in the presence of acrylonitrile giving cationic complexes of the formula $\{RuCO(PPh_3)_2(CH_2=CHCN)]_2(\beta\text{-dik})_2S_2\}^{2+}[ClO_4]_2^-$. The S – S bond cleavage reaction in these complexes using methyllithium results in decomposition of the complex molecule.

The IR spectra of dithiobis(Acac/Ba)$_2$S$_2$ exhibit strong band in the 1560 cm^{-1} region (Table 2), attributable to a strongly conjugated chelated carbonyl group[4]. Absence of a band in the region 780-800 cm^{-1} implies the absence of a hydrogen attached to the carbon joining the two C=O groups. The IR spectrum of (Dbm)$_2$S$_2$ exhibits νC=O at 1660 and 1690 cm^{-1}, indicating the presence of free carbonyl groups. The presence of a medium intensity band at 770 cm^{-1} is characteristic of CH out-of-plane bending mode. The presence of two medium intensity bands at ~420 and 450 cm^{-1} in these three dithiobis(β-diketone) derivatives may be associated with the S – S linkage[5] (Table 2).

The IR spectra of the ruthenium (II) complexes (I-

III) exhibit chelated β-diketone bands at 1520 and 1570 cm^{-1} (Table 2). The ν (S−S) is observed around 440 cm^{-1} as a weak band. The ν(C≡O) in the chlororuthenium complexes is shifted to higher frequency region (~1960 cm^{-1}) (Table 2) as compared to the hydrido derivatives (~1910 cm^{-1}) which can be attributed to decreased Ru−C *dπ-pπ* back bonding as a result of increased electronegativity of chloride ligand compared to that of the hydride. The hydrido complexes (II) exhibit ν(Ru−H) at ~1940 cm^{-1} as a medium band. The ν(C≡N) mode in cyanoethylruthenium derivatives (III) appears almost at normal position (~2220 cm^{-1}), indicating non-involvement of the cyano group in the coordination.

The PMR spectra of the dithio ligands $(HAcac)_2S_2$ and $(HBa)_2S_2$ display methyl resonances at δ 2.40 and 2.26 ppm respectively. The enolic protons resonate at δ 16.96 and 17.06 ppm respectively. This low field shift compared to the starting β-diketone [HAcac = 2.00 (CH_3), 15.56 (OH); BHa = 2.00 (CH_3), 16.3 (OH)] is attributed to the anisotropic effect of dithio moiety. Absence of signal due to enolic protons in the ruthenium complexes suggests replacement of the enolic protons. An upfield shift has been observed for the methyl resonances in these complexes (Table 2).

The ligand $(HDbm)_2S_2$ exhibits methine proton resonance at δ 6.53 ppm. Absence of enolic protons in the lower magnetic field indicates that the ligand exists in the keto form. However, enolization is evident from the reaction of this ligand with ruthenium hydrido/chloro complex to give a chelated ruthenium (II) complex. All these evidences suggest a binuclear structure (IV) for the complexes.

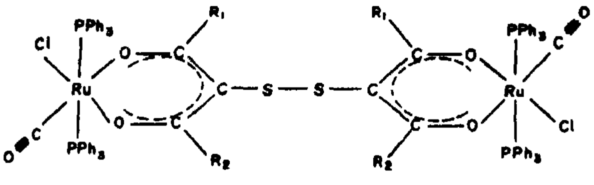

IV

The cationic complexes {[RuCO$(PPh_3)_2(CH_2=CHCN)]_2(\beta\text{-dik})_2S_2\}^{2+}[ClO_4]_2^-$ show an increase in ν(C≡N)[6] (2280 cm^{-1}) compared to the acrylonitrile ligand (2230 cm^{-1}). This increase in ν(C≡N) is attributed to the coordination through the nitrile nitrogen atom. The complexes show characteristic bands due to the perchlorate ion ClO_4^- (T_d) at 1100 (bs), 938 (m) and 620 (s) cm^{-1}. The PMR spectra display multiplets at δ 5.6-6.2 ppm due to vinylic protons. A small downfield shift of δ 0.2 ppm has been observed for the methyl resonance of β-diketone part of the cationic complexes which could possibly be due to strong metal-ligand interaction.

References

1 Gopinathan S, Pardhy S A, Gopinathan C, Puranik V, Tavale S S & Guru Row T N, *Inorg chim Acta*, **111** (1986) 1333.

2 Awasarkar P A, Gopinathan S & Gopinathan C, *Synth React Inorg Met-Org Chem*, **15** (1985) 133.

3 Robinson S D, Levison J J, Ahmed N & Uttley M F, *Inorganic syntheses*, Vol. 15 (McGraw Hill, New York), 1974.

4 Jones R D G & Power L F, *Aust J Chem*, **24** (1971) 735.

5 Dewar D H, Fergusson J E, Hentschel P R, Wilkins William P P, *J chem Soc (A)*, (1964) 688.

6 Gopinathan S, Deshpande S S & Gopinathan C, *Z anorg allg chem*, **527** (1985) 203.

Indian Journal of Chemistry
Vol. 27A, February 1988, pp. 129-132

Synthesis & Reactions of Some Cyclobutadiene Complexes of Cobalt

JASIM U AHMAD, SHARIFF E KABIR & SAYED S ULLAH*
Department of Chemistry, Jahangirnagar University, Savar, Dhaka (Bangladesh)

Received 13 *April* 1987; *revised and accepted* 15 *June* 1987

Optimum conditions for the stepwise synthesis of the cyclobutadiene complexes $C_4H_4Co_2(CO)_6$(I) and $C_4H_4Co(CO)_2HgCo(CO)_4$(II) have been established. Their common iodine derivative, $C_4H_4Co(CO)_2I$(III), on reaction with PPh_3, CH_3MgI and $Hg[Co(CO)_4]_2$ gives the substitution product $C_4H_4Co(CO)PPh_3I$(V), methyl derivative $C_4H_4Co(CO)_2CH_3$(X) and the heteronuclear complex $C_4H_4Co_2Hg(CO)_5PPh_3$(VIII), respectively. The reaction of $C_4H_4Co_2(CO)_6$(I) with triphenylmethyl tetrafluoroborate gives the butadienyl salt $[C_4H_4Co(CO)_3]^+$(IV). When (III) is reacted with PPh_3 and $AgPF_6$, a mixture of phosphine substituted butadienyl salt $[C_4H_4Co(CO)_2(PPh_3)]PF_6$(VI), and the phosphine substituted iodo derivative (V) is obtained. Appropriate reaction schemes have been proposed on the basis of IR and PMR evidences.

Although free cyclobutadiene has, at best, a transient existence[1], it can be stabilized with various transition metals to give rise to many interesting complexes. Ever since its stabilization in the form of cyclobutadienetricarbonyliron in the mid sixties[2], a vast amount of literature has been produced on various complexes of cyclobutadiene[3]. We report in this paper the details of the synthesis of cyclobutadienehexacarbonyldicobalt(I) and its reactions with various reagents. Although the preparation of (I) was reported in a communication[4] some years ago, there was no mention of the suitable reaction conditions. As we required (I) as a precursor for further work, we have attempted to find the optimum reaction conditions for its preparation. A preliminary report of the reaction of (I) with triphenylmethyl tetrafluoroborate has appeared[5].

Materials and Methods

Preparation of 3,4-*Dichlorocyclobutene*

3,4-Dichlorocyclobutene was prepared by the method described in the literature[6]. A higher percentage of dichlorocyclobutene was obtained in the pyrolysate of the Diels-Alder adduct by lowering the pyrolysis temperature from 200° to 190°. The isomer dichlorobutadiene and dichlorocyclobutene were conveniently separated by column chromatography [SiO_2, solvent pet ether (b.p. 30-40°)] instead of spinning band column distillation. The purity of dichlorocyclobutene (55% yield; m.p., − 5°) was checked spectroscopically; PMR: δ6.28 (2H, *d*) and 5.15 (2H, *d*). Thin film IR was identical with the reported values[7].

Reaction of dichlorocyclobutene with sodium tetracarbonylcobaltate

The sodium salt was prepared by the vigorous stirring together of Na/Hg (1.501 g) and $Co_2(CO)_8$ (9.998 g) for 10 hr in THF (150 ml). After completion of salt formation, the grey yellow solution was washed with fresh mercury. Then it was treated with dichlorocyclobutene (2.502 g) under varying experimental conditions. Optimum yield of $C_4H_4Co(CO)_2$—$Co(CO)_4$, complex(I), was obtained by stirring the reaction mixture at 70° for 12 hr. After completion of the reaction, THF was removed *in vacuo*. The viscous reaction mass was extracted 2-3 times with pet ether (b.p. 30-40°). The pet ether extract was chromatographed on neutral alumina and eluted with ethyl acetate (5%) in pet ether. The first band gave a brown oil (0.208 g) which is thought to be the intermediate 'A' (Scheme 1). The second band (yellow), on removal of the solvent, gave bright yellow crystals (m.p. 55°) of $C_4H_4Co(CO)_2$—$HgCo(CO)_4$(II), (0.998 g); IR: νCO at 2065, 2035, 2005 and 1960 cm^{-1}; PMR: (C_6D_6) δ3.40(*s*) (Found: C, 22.8; H, 0.7. $C_{10}H_4Co_2HgO_6$ requires: C, 22.3; H, 0.75%); it also gave the tests for Hg. The third band (orange red) gave $C_4H_4Co(CO)_2$—

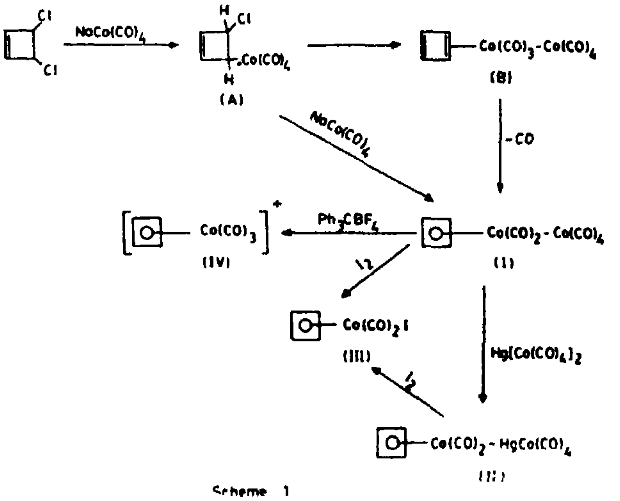

Scheme 1

$Co(CO)_4$(I) (1.113 g) as bright red crystals (m.p. 34°); IR: νCO at 2968, 2038, 2025, 1960 and 1940 cm^{-1}; PMR: $(C_6D_6)\delta 3.7(s)$. Its mass spectrum showed $(M^+—CO)$ and subsequent loss of five carbonyl groups. The fourth band, which was eluted with ethyl acetate, gave $Hg[Co(CO)_4]_2$ as orange crystals (0.512 g; m.p., 82°).

If the reaction was carried out at room temperature for a longer period (72 hr), the yield of (II) increased while that of (I) decreased.

Reaction of 'intermediate A' with $NaCo(CO)_4$

The above 'intermediate A' (0.090 g) was stirred with a solution $NaCo(CO)_4$ in THF (30 ml) for 12 hr. The reaction was monitored by IR which showed the formation of complex (I). After removal of the solvent, the residue was chromatographed as above to get $C_4H_4Co(CO)_2—Co(CO)_4$(I).

Reaction of $C_4H_4Co(CO)_2—Co(CO)_4$(I) and $Hg[Co(CO)_4]_2$

The complex (I) (0.050 g) and $Hg[Co(CO)_4]_2$ (0.101 g) were stirred in 30 ml of cyclohexane. IR monitoring clearly showed the formation of (II) and $Co_2(CO)_8$. After 48 hr, $C_4H_4Co(CO)_2—HgCo(CO)_4$ (0.056 g) was isolated by chromatography.

Reaction of $C_4H_4Co(CO)_2—Co(CO)_4$(I) with iodine

To a solution of complex (I) (1.022 g) in 75 ml of chloroform, iodine (0.201 g in 50 ml chloroform) was added dropwise over a period of 30 min and the reaction mixture was stirred for another 40 min and brought to room temperature. Chloroform was removed and the reaction mass was extracted with ether. Removal of ether gave $C_4H_4Co(CO)_2I$(III), (0.981 g, 92%) [IR: ν(CO) 2070(s) and 2040(s) cm^{-1}; PMR: δ4.70] as dark red crystals, m.p. 84°.

Reaction of $C_4H_4Co(CO)_2I$(III) with PPh_3

Complex (III) (0.210 g) and PPh_3 (0.220 g) were allowed to react in THF at room temperature for 12 hr. After removal of the solvent and crystallization from ether $C_4H_4Co(CO)(PPh_3)I$(V) (0.190 g) was obtained as dark red crystals (m.p. 192°); ν(CO): 2005 (s) cm^{-1}; PMR: δ4.25(*s*) (Found: C, 52.9; H, 3.6. $C_{23}H_{19}CoIOP$ requires: C, 52.3; H, 3.6%).

Reaction of $C_4H_4Co(CO)_2I$(III) with $AgPF_6$ and PPh_3

$C_4H_4Co(CO)_2I$ (0.245 g), $AgPF_6$ (0.204 g) and PPh_3 (0.205 g) were stirred in 40 ml of THF at room temperature for 6 hr. The solvent was removed and the reaction mass extracted with dichloromethane. On addition of ether to the dark red dichloromethane solution, a yellow precipitate was formed. This was washed and dissolved in acetonitrile and reprecipitated with ether to get $[C_4H_4Co(CO)_2PPh_3]PF_6$(VI) (0.112 g) as a pale yellow solid; ν(CO): 2090(s) and 2055(s) cm^{-1}; PMR: δ5.18 (4H, *s*) and 7.38 (15 H, *m*) (Found: C, 50.0; H, 3.7. $C_{24}H_{19}CoF_6O_2P_2$ requires: C, 50.2: H, 3.3%). The filtrate on removal of the solvent and subsequent crystallization from other (−70°) gave $C_4H_4Co(CO)PPh_3I$(V) as dark red crystals (0.102 g).

Reaction of $C_4H_4Co(CO)PPh_3I$(V) with $AgPF_6$ and PPh_3

$C_4H_4Co(CO)PPh_3I$ (0.081 g), $AgPF_6$ (0.152 g) and PPh_3 (0.121 g) in 50 ml THF were refluxed for 50 hr. The solvent was removed *in vacuo* and the residue extracted with dichloromethane. When the extract was treated with ether, a very small amount of yellow precipitate was formed. IR showed a band at 1940 cm^{-1} and also presence of some $C_4H_4Co(CO)PPh_3I$. The PMR spectrum showed, in addition to the signal due to $C_4H_4Co(CO)PPh_3I$ at δ4.25(*s*), another peak at δ4.90(*s*) which is ascribed to $[C_4H_4Co(CO)(PPh_3)_2]PF_6$.

Reaction of $C_4H_4Co(CO)PPh_3I$(V) with $Hg[Co(CO)_4]_2$

$C_4H_4Co(CO)PPh_3I$ (0.051 g) and $Hg[Co(CO)_4]_2$ (0.102 g) were stirred in hexane (50 ml) for 12 hr. The product was then chromatographed on neutral alumina eluting with ethyl acetate. A yellow band gave $C_4H_4Co(CO)PPh_3—HgCo(CO)_4$(VIII) as a pale yellow solid: IR: νCO at 2060, 2010, 1005 and 1910 cm^{-1}; PMR: δ2.95 (*s*).

Reaction of $C_4H_4Co(CO)_2—HgCo(CO)_4$(II) with I_2

To a chloroform (50 ml) solution of compound (II) (0.401 g), iodine solution (0.09 g in 30 ml chloroform) was added dropwise at −70° in 30 min with stirring. After that, solvent was removed and the reaction mass was chromatographed on alumina and eluted with pet. ether (b.p. 30-40°); a little unreacted $C_4H_4Co(CO)_2HgCo(CO)_4$ was separated thus. A brown red band which started moving a little from the top was scooped out and extracted with ether to get dark red crystals of $C_4H_4Co(CO)_2I$(III). The reaction residue contained HgI_2 which could be sublimed at red hot temperature as yellow solid which turned red on etching; tests for Hg gave positive results.

Reaction of $C_4H_4Co(CO)_2I$(III) with CH_3MgI

To a solution of $C_4H_4Co(CO)_2I$ (0.40 g), CH_3MgI (from 0.120 g CH_3I) in diethyl ether was added dropwise at −60° in 30 min. The reaction solution turned grey. After 30 min, water was added to the solution to decompose excess CH_3MgI and the reaction mass was extracted with ether. The ether extract was dried over $MgSO_4$. Removal of the solvent left a very small amount (0.05 g) of a brown oil. This was filtered through neutral alumina in pentane solution to retain unreacted $C_4H_4Co(CO)_2I$. Removal of pentane resulted in a pale yellow and very volatile oil; IR: vCO at 2045 and 2010 cm^{-1}; PMR: δ3.60(*s*) and 0.90 (*s*).

Reaction of $C_4H_4Co_2(CO)_6(I)$ with triphenylmethyl tetrafluoroborate

The complex(I) (0.342 g) and triphenylmethyl tetrafluoroborate (0.304 g) were stirred together in 25 ml of dichloromethane. After 6 hr, the reaction mass was filtered, dry diethyl ether was added to the filtrate when an yellow precipitate was obtained. This was dissolved in dichloromethane and an aqueous solution of NH_4PF_6 (0.165 g) was added to get $[(C_4H_4Co(CO)_3]PF_6$ (0.12 g, 35%) as pale yellow solid; IR: vCO at 2150(m) and 2105(s) cm^{-1}; PMR: (acetone-d_6) δ6.08 (Found: C, 25.2; H, 1.65. $C_7H_4CoF_6O_3P$ requires: C, 24.75; H, 1.2%).

Results and Discussion

The reaction of 3,4-dichlorocyclobutene with $NaCo(CO)_4$ prepared from $Co_2(CO)_8$ and sodium amalgam in tetrahydrofuran yields, in addition to $C_4H_4Co_2(CO)_6$(I), another complex $C_4H_4Co(CO)_2$—$HgCo(CO)_4$(II) (m.p. 55°, yellow crystals) under varying experimental conditions. PMR signal for the cyclobutadiene proton in (II) does not vary significantly (δ3.4) from that of complex(I) (δ3.7). The slight upfield shift may indicate the electron donating nature of the $HgCo(CO)_4$ group. The formation of (I) is thought to take place via an intermediate metal-carbon σ-complex as shown in Scheme 1.

Although we have no firm evidence for the intermediates A and B, spectroscopic evidence points towards the presence in solution of, at least, one intermediate, probably 'A'. In the process of isolation by chromatography the first fraction was found to be a brown and very unstable oil having two sharp v(CO) bands at 2078 and 2005 cm^{-1} characteristics of a $Co(CO)_4$ moiety attached to a ligand. It could not be due to $Hg[Co(CO)_4]_2$ since this was isolated at a later stage under much enhanced conditions of solvent polarity.

The PMR in C_6D_6 shows three signals at δ6.7 (2H, *m*) 4.9 (1H, broad singlet) and 2.2 (1H, *m*). The signal at δ6.7 can be assigned to the olefinic protons, the signal at δ4.9 can be due to the CHCl group; in the precursor, $C_4H_4Cl_2$, such protons occur at δ5.15. The signal at δ2.2 is thought to be due to the metal-bonded CH: a characteristic upfield shift will be expected in this case. In one instance it was also possible to observe another compound along with 'A' which could be the intermediate 'B' (Scheme 1). Its PMR along with signals due to 'A' showed two triplets at δ8.0 (2H, *t*) and 5.85 (2H, *t*) [v(CO) 2078, 2020, 2005, and 1940 cm^{-1}]. The signal at δ8.0 could be due to protons of the olefinic bond attached to the metal atom.

Furthermore, when 'A' was separately treated with $NaCo(CO)_4$, it gave the complex $C_4H_4Co(CO)_2$—$Co(CO)_4$(I). The formation of complex (II) can be rationalized as being a further reaction of (I) with $Hg[Co(CO)_4]_2$ present in the reaction medium. And this was found to be the case when these components were reacted separately (Scheme 1). Complex(I) reacts with I_2 quantitatively to give cyclobutadienecobaltdicarbonyliodide[8](III). We have found that complex(II) also reacts with I_2 to give a quantitative yield of (III). Compound $C_4H_4Co_2(CO)_6$(I) reacts with triphenylmethyl tetrafluoroborate to give the cationic species $[C_4H_4Co(CO)_3]^+$(IV), isolated as the hexafluorophosphate salt. The spectroscopic properties (IR and PMR) of this cation are similar to those of the isoelectronic cation $[C_4H_4Fe(CO)_2NO]^+$ (ref. 9).

Complex (III) is amenable to carbonyl substitution by triphenylphosphine as well as to formation of a cationic species formed by triphenylphosphine displacement of iodide in the presence of a halide acceptor ($AgPF_6$) (Scheme 2). Compound (V) is an air-stable dark red crystalline solid (m.p. 192°). It PMR signal at δ4.25(*s*) shows an upfield shift due to substitution by a σ-donor.

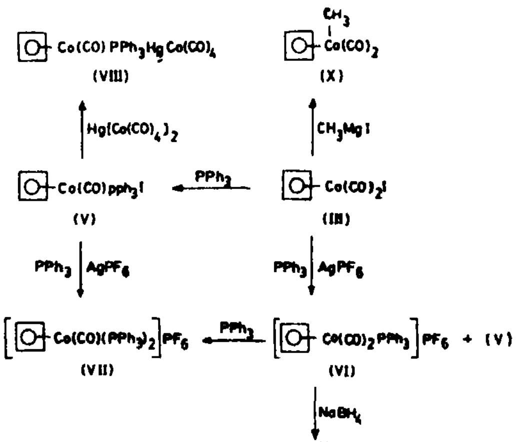

Scheme 2

The cationic compound(VI) is an air-stable pale yellow solid which shows PMR signals at δ7.40 (15H, *m*) and 5.18 (4H, *s*) thus exhibiting the effect of phosphine substitution.

Attempts to prepare the analogous cationic cyclobutadienetricarbonylcobalt complex according to the equation:

$$C_4H_4Co(CO)_2I + AgPF_6 \xrightarrow{CO} [C_4H_4Co(CO)_3]PF_6$$

were unsuccessful. The cationic complex(VI) undergoes further substitution by triphenylphosphine, although very slowly, to give rise to the monocarbonylbisphosphine substituted cationic complex $[C_4H_4Co(CO)(PPh_3)_2]PF_6$(VII). Its IR and PMR indicate effects of further phosphine substitution.

The phosphine substituted monocarbonyl iodide complex(V) reacts with $Hg[Co(CO)_4]_2$ to give a phosphine substituted dicobalt complex $C_4H_4Co(CO)PPh_3HgCo(CO)_4$(VIII). Nucleophilic attack on the cationic complex(VI) with sodium borohydride indicates the formation of a neutral complex in very small amounts. There was no evidence for a hydride peak in the PMR spectrum, but it may be that the amount of resulting complex $C_4H_4CoH(CO)_2PPh_3$(IX) was much too small for the sensitivity of 90 MHz instrument.

The dicarbonyliodide complex(III) is also amenable to nucleophilic attack by methylmagnesium iodide affording $C_4H_4Co(CO)_2CH_3$(X). The neutral complex(X) is a very volatile pale yellow oil and has been characterised only on the basis of IR and PMR evidences (see experimental section). This reactivity of (III) is compatible with its ability to undergo substitution by triphenylphosphine.

The reactions of (III) described above are summarised in Scheme 2.

ν(CO) of the complexes

It is interesting to note that by examining the ν(CO) (Fig. 1) of the parent complex(I) and some of its derivatives, it is possible to assign the various ν(CO) modes.

It may be seen that the ν(CO) frequencies of the three complexes in the region 2000-1900 cm^{-1} are lowered in accordance with the presence of a σ-donor attached to the $C_4H_4Co(CO)_2$ moiety. This is expected because σ-donating substituent is directly attached to the cobalt and hence changes in ν(CO) should be more pronounced here. Based on this observation, it can be assumed that the ν(CO) frequencies exhibited in the region 2000-1900 cm^{-1} are due to the carbonyl groups in the $C_4H_4Co(CO)_2$ fragment and the frequencies in the region 2100-2000 cm^{-1} are due to $Co(CO)_4$ or $HgCo(CO)_4$ moieties.

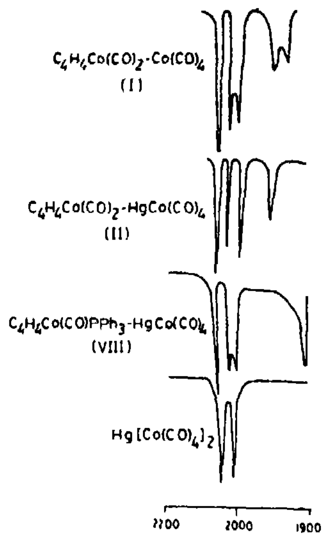

Fig. 1—ν(CO) frequencies of complexes(I), (II), (VIII) and $Hg[Co(CO)_4]_2$ showing the effect of a σ-donor substituent

Acknowledgement

Part of this work was done at the laboratory of Prof P L Pauson, Department of Pure and Applied Chemistry, Strathclyde University. One of us (S S U) thanks the Association of Commonwealth Universities for a fellowship.

References

1 Emerson G F, Watts L & Pettit R, *J Am Chem Soc*, **87** (1965) 131.

2 Watts L, Fitzpatrick J D & Pettit R, *J Am Chem Soc*, **87** (1965) 3253.

3 Efraty A, *Chem Rev*, **77** (1977) 691.

4 Amiet R G & Pettit R, *J Am Chem Soc*, **90** (1968) 1050.

5 Harter P, Pauson P L & Ullah S S, *J organomet Chem*, **247** (1983) C27.

6 Pettit R & Henery J, *Org Synthesis*, **50** (1970) 36.

7 Avran M, Marica E, Dinulescu I, Farcasiu M, Elian M, Matusu G & Nenitzescu C D, *Chem Ber*, **97** (1964) 372.

8 Bruce R & Maitlis P M, *Can J Chem*, **45** (1967) 2017.

9 Efraty A, Bystrek R, Geaman J A, Sandhu S S, Huang M H A & Harber R H, *Inorg Chem*, **13** (1974) 1269.

Indian Journal of Chemistry
Vol. 27 A, February 1988, pp. 133-136

New Schiff Bases Derived From 2-Benzoylpyridine & Their Complexes with Transition Metals

R L DUTTA* & KUNTALA DE
Department of Chemistry, University of Burdwan, Burdwan 713 104

Received 30 *April* 1987; *revised and accepted* 22 *June* 1987

Seven new schiff base ligands have been synthesised by condensation of 2-benzoylpyridine with phenylhydrazine (**1**), 2,4-dinitrophenylhydrazine (**2**), ethylenediamine (**3**), isonicotinoylhydrazine (**4**), quinaldinoylhydrazine (**5**), anthraniloylhydrazine (**6**) and benzildihydrazide (**7**). The ligands have been characterised by elemental analyses and IR and PMR spectra. Coordination complexes of ligands (**1**) and (**3**) with Ni(II), Co(II), Cu(II), Zn(II) and Hg(II) have been synthesised and characterised. While **1** acts as a bidentate N,N donor, **3** functions as a quadridentate N,N,N,N donor. Ligand(**1**) forms complexes of the type $[Ni(L)_2Cl_2]H_2O$; $[Co(L)Cl_2]$; $[Cu(L)Cl_2]$; $[Hg(L)Cl_2]$; $[Hg(L)(CH_3COO)_2]$ and $[Zn(L)Cl_2]$. Complexes of ligand (**3**) (L′) are of the type $[Ni(L')Cl_2]$; $[Ni(bipy)(L')]SO_4 . 6H_2O$; $[Co(L')Cl_2]$; and $[Cu(L')Cl_2]H_2O$. Magnetic moments, electronic spectra and infrared spectra have been examined in most cases.

Coordination chemistry of acyl, aroyl and heteroaroyl hydrazones and related ligands and their metal complexes has recently been reviewed by Dutta and Hossain[1]. Recently Dutta and Hossain[2] reported the preparation of 2-benzoylpyridine benzoyl and salicyloyl-hydrazones and their metal (II) complexes. The title investigation is in continuation of this work from our laboratory. Several hydrazones of 2-benzoylpyridine have been synthesised as new schiff base ligands and coordination complexes of Ni(II), Co(II), Cu(II), Hg(II) and Zn(II) with two of these ligands are also reported herein.

Materials and Methods

Benzoylpyridine was obtained from Sigma Chemicals. Commercial phenylhydrazine was distilled twice under reduced pressure immediately before use. Isonicotinic acid hydrazide was a BDH product. Quinaldinoylhydrazine, anthraniloylhydrazine and benzildihydrazine were synthesised following standard procedures[3].

Preparation of ligands: Benzoylpyridine phenylhydrazone (**1**)

Benzoylpyridine (2 g) was dissolved in anhydrous ethanol (8 ml), treated with freshly distilled phenylhydrazine (1.2 g), refluxed for 6 hr and the reaction mixture was allowed to stand at room temperature for 1 hr. The crystalline solid obtained was purified by recrystallisation from hot ethanol to have **1** as a colourless crystalline solid, m.p. 147°; yield 2 g.

Benzoylpyridine 2,4-*dinitrophenylhydrazone* (**2**)

This was obtained as a yellow crystalline solid by refluxing 2,4-dinitrophenylhydrazine (0.5 g) and benzoylpyridine (0.5 g) in methanol (60 ml) for 6 hr, m.p. 222°; yield 0.75 g.

Bis(benzoylpyridine)ethylenediimine (**3**)

This was prepared by refluxing benzoylpyridine (2 g) in dehydrated ethanol (5 ml) and ethylenediamine (1 g) for 8 hr. On cooling in ice colourless crystals separated out, which were purified by recrystallisation from ethanol m.p. 93°; yield 2 g.

Benzoylpyridine isonicotinoylhydrazone (**4**)

It was prepared by refluxing isonicotinic acid hydrazide (0.8 g) and benzoylpyridine (1.3 g) in methanol (20 ml) for 25 hr. The crude product was recrystallised from methanol, m.p. 195°; yield 1.6 g.

Benzoylpyridine quinaldinoylhydrazone (**5**)

This was obtained by refluxing benzoylpyridine (0.6 g) and quinaldinoylhydrazine (0.6 g) in ethanol (15 ml) for 6 hr. The product was finally recrystallised from hot ethanol, m.p. 187°; yield 0.9 g.

Benzoylpyridine anthraniloylhydrazone (**6**)

It was obtained by refluxing anthraniloylhydrazine (1.5 g) and 2-benzoylpyridine (2 g) in ethanol (15 ml). Cream coloured crystals were obtained after recrystallisation from hot ethanol, m.p. 182°; yield 2.2 g.

Bis(benzoylpyridine) benzildihydrazone (**7**)

Benzildihydrazide (0.5 g) and 2-benzoylpyridine (1.1 g) were taken in anhydrous ethanol (15 ml) and refluxed for 20 hr. The separated crystals were purified by recrystallisation from hot ethanol, m.p. 175°; yield 1 g. This compound was hygroscopic.

Synthesis of complexes: $[Ni(L)_2Cl_2]H_2O$

Anhydrous $NiCl_2$ (0.2 g) was dissolved in methanol (3 ml) and to this was added a solution of ligand (**1**) (0.82 g) in acetone (20 ml). The solution was refluxed for 3 hr, cooled to room temperature and the separated dark brown crystals were filtered, washed thoroughly with acetone and dried and stored over silica gel.

$[Co(L)Cl_2]$

This was obtained as dark brown mass by the procedure described above using $CoCl_2, 6H_2O$ (0.2 g) and the ligand (**1**) (0.34 g).

$[Cu(L)Cl_2]$

This was obtained as a brown coloured product by reacting $CuCl_2$ (1 g) and the ligand (**1**) (0.2 g) in ethanol (10 ml) at 15° under magnetic stirring.

$[Hg(L)Cl_2]$ and $[Zn(L)Cl_2]$

These were obtained by refluxing the respective metal chlorides and the ligand (**1**) in 1:1.5 (metal-ligand) ratio for 2-4 hr. The products were recrystallised from hot ethanol.

$[Hg(L)(CH_3COO)_2]$

A clear solution of $Hg(CH_3COO)_2$ (0.2 g) in ethanol (6 ml) was obtained by adding a few drops of acetic acid to the acetate salt. Ligand (**1**) (0.4 g) in ethanol (10 ml) was then added to this solution and refluxed for 4 hr when a yellow solid separated out, which was filtered.

$[Ni(L')Cl_2]$

This was obtained by refluxing a solution of $NiCl_2$ (0.1 g) in methanol (0.5 ml) with a solution of the ligand (**3**) (L′) (0.25 g) in acetone (10 ml) for 1.5 hr. A red compound that separated out was filtered hot, washed with acetone and dried over silica gel.

$[Co(L')Cl_2]$ and $[Cu(L')Cl_2]H_2O$

A brown coloured product $[Co(L')Cl_2]$ was obtained by stirring at 20°C, a solution containing $CoCl_2, 6H_2O$ (0.1 g) in acetone (2 ml) and the ligand (**3**)(L′)(0.2 g) also in acetone (10 ml). Using $CuCl_2$ the corresponding bluish green Cu(II) complex was obtained.

$[Ni(L')(bipy)]SO_4, 6H_2O$

$NiSO_4, 6H_2O$ (0.2 g) was dissolved in methanol (3 ml) by warming. To this was added a solution of ligand (**3**) (0.35 g) in anhydrous ethanol (5 ml) and the mixture was heated on a steam-bath for 15 min. 2,2′-Bipyridyl (0.15 g) was then added and the solution allowed to stand at room temperature (20°C) for seven days. The pink crystals were filtered and washed with ice-cold ethanol.

Physical measurement

The IR spectra were recorded at CDRI, Lucknow and IACS, Calcutta. The PMR spectra were run in $CDCl_3$ on EM—360 60 MHz NMR spectrometer at CDRI, Lucknow; chemical shifts are expressed in δ (ppm) downfield from TMS internal reference. The mull spectra of the complexes were recorded at RSIC, Madras. Room temperature magnetic susceptibilities were determined by Guoy method using $CuSO_4, 5H_2O$ as the calibrant. Diamagnetic corrections were obtained using Pascal's constant[4a]. Conductances of $10^{-3}M$ solutions of the complexes in methanol or nitromethane were measured with the help of a Philips conductivity bridge.

Results and Discussion

Elemental analyses (C, H, N) of all the ligands (Table 1) are consistent with their formulae. The IR spectra of the ligands exhibit $\nu C=N$ at 1600 cm^{-1}. Additionally the ligands (**4, 5** and **6**) display $\nu C=O$ (amide-1)[5] modes at 1680, 1685 and 1650 cm^{-1} respectively. The νNH_2 of the ligand (**6**) appears at 3340 and 3460 cm^{-1}, while νNH is observed at 3050 cm^{-1}. The PMR spectra of the ligands are compatible with the assigned structures. As expected, the PMR spectra of the ligands (**3**) and (**7**) do not exhibit any hydrazinic proton downfield of 10 ppm. The hydrazinic protons of the ligands **1, 2, 4, 5** and **6** appear at 11.75, 13.8, 9.7, 10.0 and 10.25 ppm respectively[6]. Significant downfield shift of the hydrazinic proton in the case of **2** is likely to be due to the presence of electron withdrawing nitro groups. The NH_2 protons of **6** appear at 5.35 ppm, while the CH_2 protons of **3** are seen at 2.45 ppm. The aromatic protons are observed[7] in the range 6.8 to 8.8 ppm.

Complexes of ligand (**1**)

The dark brown $[Ni(L)_2Cl_2]H_2O$ loses lattice held water quite easily at 110°C without any change in colour. Conductance value (105 $ohm^{-1}cm^2mol^{-1}$) in methanol indicates some solvolysis of coordinated chloride. The magnetic moment (3.13 B M) is in the range of octahedral Ni(II) complexes[8]. The $\nu C=N$ mode shifts to lower wavenumber ($\Delta\nu = 5$ cm^{-1}) as compared to that of the free ligand[9]. The electronic spectrum of the complex displays bands at 28.5 and 20 kK. These two transitions may be assigned to $^3A_{2g} \rightarrow {}^3T_{1g}(P)(\nu_3)$ and $^3A_{2g} \rightarrow {}^3T_{1g}(F)(\nu_2)$ respectively. The magnetic moment predicts[4b] value around 11.9 kK for $^3A_{2g} \rightarrow {}^3T_{2g}$ transition [without applying any correction to the free ion spin orbit coupling constant of 315 cm^{-1} of Ni(II)].

Table 1—Characterisation Data of the New Schiff Bases and Their Complexes

Compound	Colour	Found (Calc.)%					μ_{eff} (B M)
		M	N	C	H	Cl/SO$_4$	
Ligand 1	Colourless	—	15.3(15.3)	78.8(79.1)	5.4(5.5)	—	—
Ligand 2	Yellow	—	19.3(19.3)	59.4(59.5)	3.6(3.5)	—	—
Ligand 3	Colourless	—	14.3(14.3)	79.0(80.0)	5.7(5.6)	—	—
Ligand 4	Colourless	—	18.6(18.5)	71.5(71.5)	4.6(4.6)	—	—
Ligand 5	Yellow brown	—	16.0(15.9)	75.4(75.0)	4.7(4.5)	—	—
Ligand 6	Cream	—	17.7(17.7)	72.0(72.1)	5.0(5.0)	—	—
Ligand 7	Yellow	—	14.8(14.8)	80.0(80.0)	5.2(4.9)	—	—
[Ni(L)$_2$Cl$_2$]H$_2$O	Dark brown	8.3 (8.46)	12.1(12.1)	61.6(62.2)	5.0(4.6)	10.3(10.2)	3.1
[Co(L)Cl$_2$	Dark brown	14.6 (14.61)	10.6(10.4)	54.2(53.6)	4.0(3.7)	17.6(17.6)	5.0
[Co(L)Cl$_2$]	Brown	15.68(15.6)	10.4(10.3)	—	—	17.1(17.4)	—
[Hg(L)(CH$_3$COO)$_2$]	Yellow	34.6 (34.0)	6.8 (7.0)	45.0(44.6)	3.6(3.5)	—	—
[Hg(L)Cl$_2$]	Yellow	36.8 (36.3)	7.9 (7.7)	39.0(39.6)	3.0(2.7)	13.3(13.0)	—
[Zn(L)Cl$_2$]	Yellow	15.7 (15.9)	10.2(10.2	53.5(52.7)	4.0(3.6)	17.5(17.3)	—
[Ni(L′)Cl$_2$]	Red	11.5 (11.3)	11.0(10.8)	*	*	14.0(13.6)	3.0
[Ni(L′)bipy]SO$_4$,6H$_2$O	Pink	7.2 (7.2)	10.4(10.4)	*	*	11.6(11.8)	3.0
[Co(L′)Cl$_2$	Brown	11.6 (11.3)	10.8(10.8)	*	*	14.0(13.6)	2.45
[Co(L′)Cl$_2$]H$_2$O	Bluish green	11.8 (11.7)	10.3(10.3)	*	*	13.2(13.1)	2.07

Abbreviation: Ligand 1 = L; Ligand 3 = L′. * These samples do not keep well on standing and hence were not analysed for C,H.

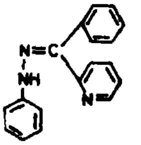
Ligand-1

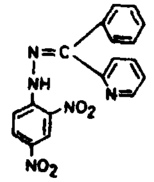
Ligand-2

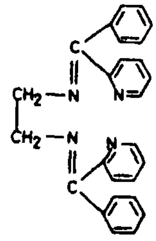
Ligand-3

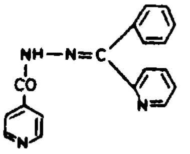
Ligand-4

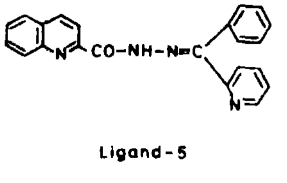
Ligand-5

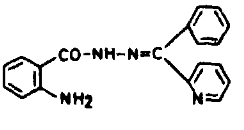
Ligand-6

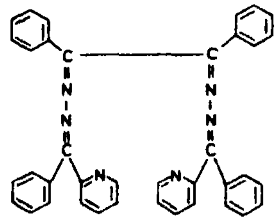
Ligand-7

The complex [Co(L)Cl$_2$] is also dark brown and has a conductance value of only 18 ohm^{-1}cm^{2}mol^{-1} in methanol indicating insignificant solvolysis of the coordinated chloride. The νC = N mode of this complex is shifted to lower wavenumber (Δν = 10 cm^{-1}).

The magnetic moment (5 B.M.) is in the range of high spin octahedral Co(II) and close to that of a five-coordinate high spin complex[4c]. The composition of the complex indicates a monomeric four coordinate or a dimeric chloro-bridged 5-coordinate or a chloro-bridged polymeric six-coordinate structure. Its electronic spectrum exhibits bands at 25, 16.66, 14.6, 13.88 and 6.45 kK. This spectrum appears to favour a five-coordinate geometry[10] rather than a tetrahedral or a high spin octahedral geometry. The magnetic moment is too high for a tetrahedral Co(II) complex (c.f. [CoCl$_4$]$^{2-}$, 4.59 B.M.), particularly in view of the presence of a bidentate N,N ligand inside the coordination zone. The electronic spectra of high spin six-coordinate[10] Co(II) complexes usually show two or three well-defined bands in the range of 8 to 20 kK with ν_2/ν_1 ratio of 2.1 to 2.2. Ready solubility in solvent like methanol also rules out a polymeric structure. The corresponding [Cu(L)Cl$_2$] is a non-electrolyte in nitromethane. Unfortunately the sample readily becomes sticky on exposure to humid atmosphere and hence its magnetic moment and electronic spectrum could not be recorded.

Zn(II) and Hg(II) chlorides give complexes of similar type; [Zn(L)Cl$_2$] and [Hg(L)Cl$_2$]. Both show low conductance in methanol. The νC = N modes are shifted to lower wavenumbers (Δν = 5-10 cm^{-1}) as compared to the free ligand. The two spectra are very similar and match with the IR spectra of the Co(II) complex indicating a five-coordinate chloro-bridged dimeric structure.

A comparison of IR spectra of [Hg(L)Cl$_2$] and [Hg(L)(CH$_3$COO)$_2$] reveal the ν_{as} and ν_s modes of the acetato complex at 1630 and 1360 cm^{-1} respectively. Monodentate coordination of the acetate group results in the ν_{as} mode appearing at higher energy and the ν_s at lower energy compared to ν_{as} and ν_s modes of the uncoordinated acetate group[12a] (1582 and 1425 cm^{-1}).

Ligand (**2**) appears to be rather inactive towards complexation presumably due to the presence of the two electron withdrawing nitro groups as substituents in the aromatic ring.

Complexes of ligand (**3**)

The red coloured [Ni(L′)Cl$_2$] has a magnetic moment of 3.0 B.M., typical of pseudo-octahedral complex. The νC = N mode appears at 1585 cm^{-1} as compared to that of ligand (**3**) at 1615 cm^{-1}. The conductance behaviour of the complex (Λ_M = 94 ohm^{-1}cm^{2}mol^{-1}) in nitromethane apparently indicates its 1:1 electrolytic nature on a monomer basis. The conductance also is consistent with a dimeric chloro-bridged six-coordinate structure. Dissociation of coordinated chloride even in nitromethane leading to substantially high conductivity has been reported in literature[13]. Poor keeping quality of the complex prevented running the solid state electronic spectra.

The mixed ligand complex [Ni(L′)(bipy)]SO$_4$.6H$_2$O is pink and has a magnetic moment of 3.0 B.M. The three electronic transitions appear at 31.6, 19.0 and 12.2 kK. The ν_2/ν_1 ratio is close to 1.56 which indicates a pseudo-octahedral structure[8,12]. The 10 *Dq* value thus comes out to be 12.2 kK. This complex has a conductance of 240 ohm^{-1}cm^{2}mol^{-1} in water, which compares well with data for bi-bivalent electrolytes[14] in the same solvent (c.f. MgSO$_4$, 266 at 25°C). Interestingly, the conductance in methanol (in which the compound is quite soluble) has a value of about 94 ohm^{-1}cm^{2}mol^{-1}, strongly suggesting ion-pair formation in methanol. The infrared spectrum of this complex displays broad, high intensity bands around 3380 and 1120 cm^{-1} due to lattice water and ionic sulphate[12b], respectively.

Co(II) complex [Co(L′)Cl$_2$] undergoes solvolysis in methanol (Λ_M = 107 ohm^{-1}cm^{2}mol^{-1}). Several preparations give a magnetic moment of around 2.5 B.M. This anomalous magnetic moment indicates an equilibrium[4d] between high spin and low spin octahedral forms. Since the complex has poor keeping quality its electronic spectrum could not be recorded satisfactorily.

The magnetic moment (2.07 B.M.) of copper(II) complex, [Cu(L′)Cl$_2$]H$_2$O is in the range of usual six-coordinate Cu(II) complexes.

References

1 Dutta R L & Hossain Md M, *J scient ind Res*, **44** (1985) 635.

2 Dutta R L & Hossain Md M, *Indian J Chem*, **23A** (1984) 30.

3 Dutta R L & Sarkar A K, *J inorg nucl chem*, **43** (1981) 57.

4 Dutta R L & Syamal A, *Elements of magnetochemistry* (S Chand & Co, New Delhi) 1982, (a) 9, (b) 134, (c) 135, (d) 139.

5 Dutta R L & Das B R, *Indian J Chem*, **23A** (1984) 654.

6 Dutta R L & Das B R, *Indian J Chem*, **23A** (1985) 493.

7 Dyer J R, *Application of absorption spectroscopy of organic compounds* (Prentice Hall, New Delhi) 1984.

8 Sacconi L, *Transition metal chemistry*, Vol 4 (Marcel-Dekker, New York) 1968, 199.

9 Dutta R L & Hossain Md M. *Indian J Chem*, **22A** (1983) 203.

10 Lever A B P, *Inorganic electronic spectroscopy* (Elsevier, Amsterdam) 1968, 320.

11 Cotton F A & Wilkinson G W, *Advanced inorganic chemistry* 3rd Edn (Wiley Eastern) 1972, 882.

12 Nakamoto K & McCarthy P J, *Spectroscopy & structure of metal chelate compounds* (John Wiley, New York) 1963 (a) 269, (b) 258.

13 Bennett M A & Wild J D, *J chem Soc*, (A) (1971) 536.

14 Conway B E, *Electrochemical data* (Elsevier, Amsterdam) 1952, 145.

Indian Journal of Chemistry
Vol. 27A, February 1988, pp. 137-140

Chelating Ion-Exchanger Containing Benzoylacetanilide Group: Part 1—Separation of Titanium(IV)

SWAPAN MAJEE, CHANDRIMA RAY & JYOTIRMOY DAS*
Department of Chemistry, University of Burdwan, Burdwan 713 104

Received 26 *December* 1986; *revised and accepted* 22 *June* 1987

A macroreticular polystyrene based chelating resin with 1,3-diketo group in the form of benzoylacetanilide has been synthesized and characterised. The resin is stable towards fairly strong acids and alkalis. The sorption patterns of U(VI), Ti(IV), Fe(III), Al(III), Co(II), Cu(II), Ni(II), Ca(II), Mg(II), Na(I) and K(I) have been studied with respect to variation in *p*H. The selective absorption of Ti(IV) at *p*H 2.1 has been utilised for the separation and determination of the metal ion in synthetic mixtures and in bauxite. Fairly strong H_2SO_4 (6 *N*) is required for the recovery (> 96%) of Ti(IV) from the resin.

Various chelating ion-exchange resins have been developed and used in the last two decades for the preconcentration of metal ions found in sea water and industrial wastes. Many such resins containing iminodiacetate[1], derivatives of hydroxylamine[2], hydroxyquinoline[3], thioglycolates[4,5], dithizone[6], oximes[7,8] and 1-nitroso-2-naphthol[9] as chelating groups have been extensively used in the separation of metal ions.

However, no resin containing diketo compounds as chelating agents has yet been reported though acetylacetone, benzoylacetone and 1,3-diketoanilides have been found to be very selective reagents for several metal ions, particularly those having hard acid character.

In the present study a new resin containing benzoylacetanilide group has been developed; it has been characterised and studied for the separation of titanium(IV) from different metal ions.

Materials and Methods

An atomic absorption spectrophotometer (Shimadzu AA-646) and a double beam UV-visible specrophotometer (Beckmann-26) were used for measurement of concentrations of the metal ions. Infrared measurements were carried out in KBr matrix on a Beckmann Acculab-10 spectrophotometer. Gravity flow columns were constructed of glass with appropriate reservoirs.

Synthesis of the resin

Styrene-DVB polymer (Beads, 80-100 mesh) containing 8% DVB (Thermax Private Ltd, Poona, India) was nitrated using a mixture of concentrated sulphuric and nitric acids. The polystyrene beads (5 g) were swollen in $CHCl_3$ and then charged in small portions over a period of one hour into a stirred mixture of sulphuric acid (25 ml, sp. gr. 1.84) and nitric acid (10 ml, sp. gr. 1.5) at 70°C. After stirring the reaction mixture at this temperature for further 30 min, it was poured into ice-water and the nitrated resin was washed repeatedly with water until free from acid.

The wet nitrated product was mixed with tin (20 g), industrial ethanol (50 ml) and sufficient amount of conc. hydrochloric acid and refluxed for 12 hr. Conc. HCl was added from time to time, until tin dissolved completely. The aminopolystyrene-tin complex thus obtained was filtered off, washed with water and treated with excess 2 *N* sodium hydroxide to produce free aminopolystyrene.

Finally, the aminated product was condensed with ethylbenzoylacetate (6 g for every 4.5 g of the resin). This condensation was carried out by refluxing the mixture in toluene medium at 110°-115°C for 24 hr. The resin was then filtered and washed thoroughly with deionised water. Finally, it was washed with dilute hydrochloric acid followed by deionised water until free from acid. The resin was air-dried.

Several buffer solutions of different *p*H values were required for the control of acidity during absorption of the metal ions on the resin as well as washing. Sodium chloride-hydrochloric acid buffers were used for the *p*H range 0.5-4.0 while sodium acetate-acetic acid buffers were used for the *p*H range 4.0-6.0. For studying the exchange behaviour of metal ions above *p*H 6.0-7.5, buffers were prepared from KH_2PO_4 and Na_2HPO_4.

Concentrations of the metal ions before and after elution from the resins were determined by standard methods. Titanium(IV), uranium(VI) and copper(II) were determined spectrophotometrically, titanium(IV) was determined with hydrogen peroxide in acid medium[10], uranium(VI) with hydrogen peroxide in alkaline medium[10] and copper(II) with sodium diethyldithiocarbamate[10]. Aluminium(III), iron(III), cobalt(II), sodium(I) and potassium(I) were determined by atomic absorption spectrophotometry. Nickel(II) was determined gravimetrically with dimethylglyoxime[11]. Calcium(II) and magnesium(II) were determined by titration with EDTA using Eriochrome black-T as the indicator[11].

Ion-exchange capacity of the resin for metal ions was studied by batch and column operation methods. In batch operation, 0.5 g of the air-dried resin was stirred on a magnetic stirrer for 24 hr with an excess of the desired metal ion solution of known strength (~ 0.1 *M*) at a known *p*H (Buffer); the mixture was filtered and the resin was thoroughly washed with the same buffer until free from the metal ions. The sorbed metal ions were then completely eluted by sulphuric acid of suitable strength. The whole process was repeated with buffers of different *p*H. The eluted metal ions were determined following the standard methods.

It was found that 50 ml 4 *N* sulphuric acid were sufficient for eluting cobalt(II), copper(II), iron(III), calcium(II), magnesium(II) and nickel(II) while 50 ml of 6 *N* sulphuric acid were required for titanium(IV) and uranium(VI). The exchange capacities of the metal ions at different *p*H are shown in Fig. 1.

In column operation, a glass column of 30 cm length and 1 cm inner diameter was packed with ~ 20 g of air-dried resin (initially swollen with 2 *N* hydrochloric acid for 24 hr). The bed was thoroughly washed with 1 *N* hydrochloric acid and then with deionised water to make the column free from acid. The flow rate was adjusted to 0.5-1.0 ml per minute. The solution of the metal ion (50 ml) was passed through the column, washed with water and finally the sorbed metal ions were eluted with sulphuric acid of appropriate strength as discussed earlier and determined by appropriate methods.

Separation procedure

For the separation of titanium(IV) from a mixture containing Cu(II), Co(II), Ca(II), Ni(II), Mg(II), Al(III), Ti(IV) and U(VI), the resin column was equilibrated with a buffer solution of *p*H 2.1. The *p*H of the solution containing the mixture of metal ions was adjusted to 2.1 and it was percolated through the resin column, washed thoroughly with the same buffer and eluted with 150 ml 6 *N* sulphuric acid.

It was found that over 96% titanium could be recovered if the normality of the eluting sulphuric acid was 6 *N* and the volume was 150 ml. Recovery was less, when diluted acid was used.

Separation and determination of titanium in bauxite

The resin has been successfully used for the separation and determination of titanium in bauxite. About 0.15 g bauxite ore (British Chemical Standard) was fused with Na_2CO_3 and treated using standard procedure[12]. Finally, the solution was diluted to 250 ml. After passing 10 ml or 20 ml of this solution through the column at *p*H 2.1, only titanium was absorbed on the resin, rest of the metal ions such as aluminium(III), alkali metals, etc., passed out of the resin column. The resin column was then washed with the same buffer (NaCl-HCl) and finally titanium(IV) was eluted with 200 ml of 6 *N* sulphuric acid and collected in a 250 ml volumetric flask. Finally, the column was again washed and washings collected in the same flask. The results are given in Table 1.

Results and Discussion

Characterisation of the resin

The resin was characterised on the basis of its water regain value, IR spectrum, stability towards acids and alkalis, elemental analysis and metal ion exchange capacity.

A sample of dry resin was immersed in deionised water for 48 hr. The resin was then centrifuged, air-dried and weighed. It was then dried at 100°C for 48 hr and weighed again. Water regain, calculated from the difference in weights, was found to be 0.35 g/g.

The resin was found to be stable in 6 *N* sulphuric acid and in 4 *N* sodium hydroxide, because no appreciable changes in its nitrogen content and sorption capacity for titanium were found.

Estimation of nitrogen and amino group

Small amounts of the air-dried resin of the nitrated polystyrene, aminopolystyrene and the chelating resin containing diketo group (all belonging to the same batch) were perfectly dried by heating at 80°C for 48 hr and then keeping *in vacuo* over phosphorus pentoxide. Nitrogen in each case was deter-

Table 1—Determination of Titanium in Bauxite Ore

Bauxite soln passed through the resin column (ml)	Ti present (mg)	Ti found* (mg)	Extraction of titanium (%)	% TiO_2 in bauxite	% TiO_2 in bauxite (reported)
10	0.2226	0.2172	97.45	2.18	2.25
20	0.4452	0.4320	97.04	2.18	2.25

*Mean of three determinations.

mined by micro Duma's method. The amino group content of aminopolystyrene was determined by titration in nonaqueous medium[13].

The nitrogen content and the capacity for Ti(IV) remained unchanged after treatment with sulphuric acid of concentration of 6 *N* or less and sodium hydroxide of concentration 2 *N* or less. The small value of water regain of the resin indicated that its sorption capacity may not be very high, but experiments showed that the resin had a moderate capacity for titanium.

The nitrogen content of the nitrated polymer was found to be 5.53%. After reduction, the percentage of nitrogen of the amino resin was found to be 7.1% as total nitrogen and 5.23% as amino nitrogen (from the estimation of amino group) with 1.87% nitrogen as unconverted nitro group. The nitrogen content of the final resin was found to be 5.84%.

Infrared spectrum of the resin recorded in KBr showed a band at 1500 cm^{-1} indicating the presence of – CONH group.

In order to study the cation retention effect of the residual nitro and amino groups of the resin, the capacities of both nitropolystyrene divinylbenzene and aminopolystyrene divinylbenzene were studied and these were found to be negligible.

The function of the diketo group was well established. Chelation of the type,

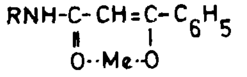

$$\mathrm{RNH{-}\underset{\underset{O\cdots}{\|}}{C}{-}CH{=}\underset{\underset{Me\cdots O}{|}}{C}{-}C_6H_5}$$

(R = resin matrix, Me = metal equivalent) is assumed to take place, on the basis of the drop in *p*H, when the resin is shaken with a metal ion solution.

Metal absorption capacity and separation

The capacity of metal absorption (titanium) on resin column was slightly lower than the same for batch operation (Fig. 1, dotted line). Fig. 1 shows that the resin exhibits high selectivity for titanium(IV). Absorption of Ti(IV) starts at *p*H ~ 1.3 followed by a sharp rise with a peak at *p*H 2.1, though the total amount absorbed is not very high. Complete precipitation of titanium bis-benzoylacetanilide[14] for gravimetric determination has been reported to occur in the *p*H range 0.9-2.0. Uranium(VI) is also absorbed in lower amounts at *p*H 0.5-3.0 and then the curve rises. Among the other metals studied, viz., iron(III), copper(II), cobalt(II) and nickel(II), only iron(III) is absorbed in small amounts in the working range for titanium(IV). Sodium(I), potassium(I), calcium(II), magnesium(II) and aluminium(III) are not at all absorbed. Thus, a clean separation of titanium(IV) from copper(II) and cobalt(II) is possible. Separation of titanium from calcium(II), magnesium(II), aluminium(III) and iron(III) is also possible. Some examples of separation of titanium(IV) in synthetic mixture are shown in Table 2.

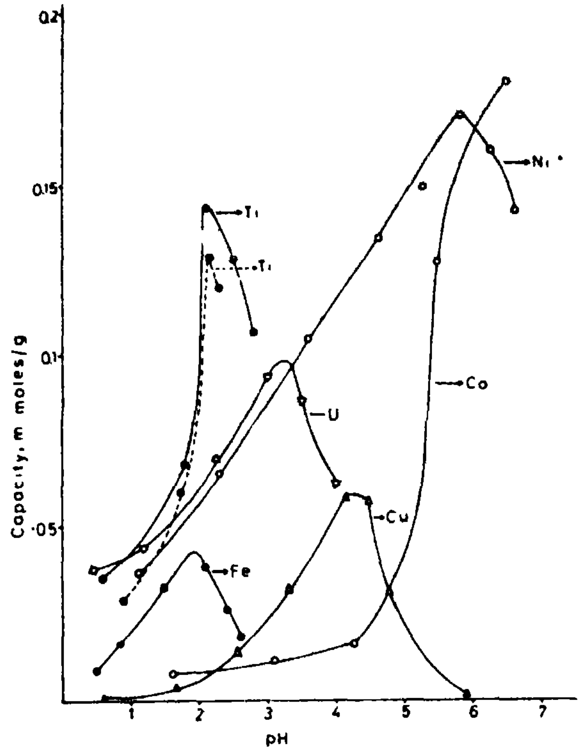

Fig. 1—Exchange capacity of the benzoylacetanilide resin for different metal ions as a function of *p*H [—, total exchange capacity; ....., exchange capacity in the resin column]

Table 2—Separation of Titanium from Diverse Ions
[Ti(IV) taken, 41 mg]

Diverse ions	(mg)	Ti(IV) recovered (%)
Co(II)	100	98.50
Ni(II)	50	
Cu(II)	100	
U(VI)	50	97.77
Al(III)	100	
Na(I)	100	
K(I)	100	
Fe(III)	50	97.77
Ni(II)	50	
Co(II)	100	
Fe(III)	50	98.50
Al(III)	100	
Ca(II)	100	
Mg(II)	100	

The rates of absorption of the metal ions were also determined. The time taken for 50% uptake of titanium(IV), uranium(VI), nickel(II), cobalt(II), iron(III) and copper(II) varied between 1.5 and 3 hr.

Acknowledgement

The authors are grateful to M/s Thermax Private Ltd, Poona, for supplying the polystyrene DVB resin beads as gift sample.

References

1 Hirsch R F, Gancher E & Russo F R, *Talanta*, **17** (1970) 483.
2 Vernon F & Eccles H, *Analyt chim Acta*, 77 (1975) 145.
3 Sugawara K F, Weetall H H & Schucker G D, *Analyt Chem*, **46** (1974) 489.
4 Moyer E M & Fritz J S, *Analyt Chem*, **48** (1976) 1117.
5 Philips R J & Fritz J S, *Analyt Chem*, **50** (1978) 1504.
6 Tanaka H, Chikuma M, Harad A, Veda T & Yube S, *Talanta*, **23** (1976) 489.
7 Sugii A, Ogawa N & Hashizume H, *Talanta*, **26** (1979) 189.
8 Bhattacharyya S & Das H R, *Indian J Chem*, **22A** (1983) 134.
9 Ghosh J P & Das H R, *Talanta*, **28** (1981) 274.
10 Sandell E B, *Colorimetric determination of traces of metals* (Interscience, New York), 1959, p. 870, 915, 443.
11 Vogel A I, *A text book of quantitative inorganic analysis* (Longman, London), 1978, p. 420, 320.
12 Kodama K, *Methods of quantitative inorganic analysis* (Interscience, New York), 1964, p. 328.
13 Fichen G E & Lane E S, *Analyt chim Acta*, **16** (1957) 207.
14 Sarkar A K & Das J, *Analyt Chem*, **39** (1967) 1608.

Indian Journal of Chemistry
Vol. 27 A, February 1988, pp. 141-144

Notes

Deduction Rules for Spectroscopic Properties of One-electron Diatomic Systems

B JOULAKIAN†

Laboratoire de Spectrométrie Ionique et Moléculaire (associé au C.N.R.S. n°171), Université Lyon I bât. 205, 43 Bd du 11 Novembre 1918 69622 Villeurbanne Cedex, France

Received 16 *January* 1987; *revised and accepted* 12 *May* 1987

The possibility of deducing wavefunctions energies, dipole and quadrupole moments from a given one-electron diatomic system to a series of others is considered.

In spite of the growing interest in stripped one-electron diatomic systems in the study of low energy collision phenomena[1-3], the possibility of deducing results for these systems from already existing rules has been rarely exploited; and that too, only for the electronic energy values[4,5].

To present briefly the basic idea which permits the obtention of deduction rules for the energy and all other spectroscopic properties from a reference one, we write, following Aubert *et al.*[6], the one-electron two-centre Schrödinger equation in prolate spheroidal coordinates ($1 \leqslant \lambda \leqslant \infty$; $-1 \leqslant \mu \leqslant 1$; $0 \leqslant \phi \leqslant 2\pi$) in separated form:

$$\left\{\frac{\mathrm{d}}{\mathrm{d}\mu}(1-\mu^2)\frac{\mathrm{d}}{\mathrm{d}\mu}-\frac{m^2}{1-\mu^2}-R(Z_a-Z_b)\mu-\mathscr{A}+P^2\mu^2\right\} \times M(\mu,\phi)=0 \qquad \ldots(1a)$$

$$\left\{\frac{\mathrm{d}}{\mathrm{d}\lambda}(\lambda^2-1)\frac{\mathrm{d}}{\mathrm{d}\lambda}-\frac{m^2}{\lambda^2-1}-R(Z_a-Z_b)\lambda+\mathscr{A}-P^2\lambda^2\right\} \times K(\lambda)=0 \qquad \ldots(1b)$$

where R is the internuclear distance, Z_a and Z_b being the nuclear charges, $\mathscr{A}$ the characteristic value of an invariant operator $A(6)$ and m the eigenvalue of L_z.

The electronic wavefunction for a given one-electron diatomic molecule at a given internuclear distance R, and for a given state ν (where ν stands for the triplet $\{nlm\}$ in the united-atom limit) may be considered as the product of $M(\mu,\phi)$ and $K(\lambda)$ [Eq. (2)]:

$$\psi(Z_a,Z_b,\nu,R,r)=M(\mu,\phi)\,K(\lambda) \qquad \ldots(2)$$

The electronic energy is given by:

$$E(Z_a,Z_b,\nu,R)=-\frac{2P^2}{R}$$

where P is an energy parameter.

Equations (1) and (2) show that the solutions for all systems, for which the two quantities $R(Z_a-Z_b)$ and $R(Z_a+Z_b)$ are simultaneously identical, are the same. We can then write

$$\Psi(Z_a,Z_b,\nu,R)=\Psi'(Z'_a,Z'_b,\nu,R') \qquad \ldots(3)$$

and

$$P(R)=P(R')$$

if

$$\left.\begin{array}{l}(Z_a+Z_b)R=(Z'_a+Z'_b)R' \\ (Z_a-Z_b)R=(Z'_a-Z'_b)R'\end{array}\right\}\text{ simultaneously} \qquad \ldots(4)$$

Here primed quantities are related to the second system.

Finally the conditions (4) are equivalent to:

$$\frac{Z_a}{Z'_a}=\frac{Z_b}{Z'_b}=\frac{R'}{R} \qquad \ldots(5)$$

The purpose of this note is essentially to show the utility of Eq. (3) for systems satisfying condition (5), firstly, in avoiding unnecessary calculations, and secondly, in testing new calculation procedures.

Calculations

The deduction rules given in Table 1 have been checked by determining the solutions in prolate spheroidal coordintes of the two centre one-electron problem in the following forms:

(i) For the homonuclear case ($Z_a=Z_b=Z$):

$$\Psi(Z,m,q,R,r)=\{(\lambda^2-1)(1-\mu^2)\}^{1/2} \times \mathrm{e}^{im\psi}\,\Phi(Z,m,q,R,r) \qquad \ldots(6)$$

with

$$\Phi(Z,m,q,R,r)$$

$$=\sum_{i=1}\mathrm{e}^{-\alpha_i\lambda}\sum_{j=0}\lambda^j\sum_{k=0}C_{ijk}\mu^k(\mathrm{e}^{-\beta_i\mu}+(-1)^q\mathrm{e}^{\beta_i\mu})$$

---

†Present address:

B. Joulakian
Département de Physique
Ecole Nationale d'Ingénieurs de Sfax
B.P.W
3038 SFAX
Tunisie

Table 1 — Some Rules to Deduce Spectroscopic Properties for a One-electron Diatomic System with Nuclear Charges[a] at Fixed Internuclear Distance[b], from Same Properties Known for a One-electron Diatomic System with Nuclear Charges (Z_a and Z_b) at Fixed Internuclear Distance (R)

Definition	System 1 (Z_a, Z_b, R)	System 2 (Z'_a, Z'_b, R')	Relation between 1 and 2
Electronic Energy	E_1	E_2	$E_2 = (Z_a/Z_a)^2 E_1$
Total energy $\varepsilon = E + \frac{Z_a Z_b}{R}$	ε_1	ε_2	$\varepsilon_2 = (Z_a/Z_a)^2 \varepsilon_1 + \frac{Z'_a}{R'}(Z_b - Z_b)$
Wavefunction	$\Psi_1(Z_a, Z_b, \nu, R)$	$\Psi_2(Z'_a, Z'_b, \nu, R')$	$\Psi_1 = \Psi_2$
Av. value of dipole moment $D = z$	$\langle D \rangle_1$	$\langle D \rangle_2$	$\langle D \rangle_2 = (Z_a/Z'_a) \langle D \rangle_1$
Av. value of electric *quadrupole moment* $Q = (3z^2 - r^2)/2$	$\langle Q \rangle_1$	$\langle Q \rangle_2$	$\langle Q \rangle_2 = (Z_a/Z'_a)^2 \langle Q \rangle_1$

(a) $Z_a = Z_a(R/R')$ and $Z_b = Z_b(R/R')$, (b) $R' = R(Z_a/Z_a)$

Table 2 — Tests Results (in a.u.) for the Rules Given in Table 1 for Homonuclear System He_2^{3+}

Designation of states	H_2^+ (R = 10)	He_2^{3+} (R = 5)		
		Deduced from H_2^+	Approx. calc.	Exact direct calc.[b]
		Negative of electronic energy		
$X^2\Sigma_g$	0.600579	2.402316	2.402315	2.402316
$(1)^2\Sigma_g$	0.273117	1.092468	1.092462	1.092468
$(2)^2\Sigma_g$	0.204711	0.818844	0.818840	0.818844
$(3)^2\Sigma_g$	0.144536	0.578144	0.578133	0.578144
$(1)^2\Sigma_u$	0.599901	2.399604	2.399600	2.399604
$(2)^2\Sigma_u$	0.200586	0.802344	0.802320	0.802344
$(3)^2\Sigma_u$	0.184887	0.739548	0.739902	0.739548
		Dipole transition moments[a]		
$\langle X^2\Sigma_g \lvert D \rvert (1)^2\Sigma_u \rangle$	4.9535	2.47675	2.47665	2.47675
$\langle X^2\Sigma_g \lvert D \rvert (2)^2\Sigma_u \rangle$	0.4785	0.23925	0.23925	0.23926
$\langle X^2\Sigma_g \lvert D \rvert (3)^2\Sigma_u \rangle$	0.6495	0.32475	0.32471	0.32465
$\langle (1)^2\Sigma_u \lvert D \rvert (1)^2\Sigma_g \rangle$	0.6985	0.34925	0.34901	0.34925
$\langle (1)^2\Sigma_u \lvert D \rvert (2)^2\Sigma_g \rangle$	0.4808	0.24040	0.24030	0.24040
$\langle (1)^2\Sigma_g \lvert D \rvert (3)^2\Sigma_g \rangle$	0.0016	0.0008	0.0008	0.0008
		Quadrupole transition moments[a]		
$\langle X^2\Sigma_g \lvert Q \rvert X^2\Sigma_g \rangle$	11.9745	2.99363	2.99320	2.99363
$\langle X^2\Sigma_g \lvert Q \rvert (1)^2\Sigma_g \rangle$	6.1274	1.53185	1.53172	1.53185
$\langle X^2\Sigma_g \lvert Q \rvert (2)^2\Sigma_g \rangle$	4.4491	1.11226	1.11226	1.11226
$\langle (1)^2\Sigma_u \lvert Q \rvert (1)^2\Sigma_u \rangle$	12.1405	3.03513	3.03530	3.03513
$\langle (1)^2\Sigma_u \lvert Q \rvert (2)^2\Sigma_u \rangle$	4.7114	1.17785	1.17788	1.17785
$\langle (1)^2\Sigma_u \lvert Q \rvert (3)^2\Sigma_u \rangle$	7.1538	1.78846	1.78820	1.78846

(a) D and Q are defined in Table 1. (b) In column 4 the results are obtained with the improved basis. The agreement is perfect between columns 2 and 4.

where $q = 0$ or 1 for gerade or ungerade states respectively.

(ii) For the heteronuclear case $(Z_a \neq Z_b)$:

$$\Psi(Z_a, Z_b, m, R, r) = \{(\lambda^2 - 1)(1 - \mu^2)\}^{1/2} e^{im\phi} \Phi(Z_a, Z_b, m, R, r) \qquad \ldots(7)$$

with

$$\Phi(Z_a, Z_b, m, R, r) = \sum_{i=1} e^{-\alpha_i \lambda} \sum_{j=0} \lambda^j \sum_{k=0} \mu^k (C_{ijk} e^{-\beta_i \mu} + D_{ijk} e^{\beta_i \mu})$$

This type of functions has been used by several authors[7-9]. Recently Wells and Wilson[10] applied this type of functions to diatomic, multiply charged systems. Taking the parameters α_i and β_i [Eqs. (6) and (7)]

Table 3—Test Results (in a.u.) for Rules given in Table 1 for Heteronuclear System $BeHe^{5+}$

Designation of states	HeH^{2+} (R = 8)	$BeHe^{5+}$ (R = 4) Deduced from HeH^{2+}	Approx. calc.	Exact direct calc.
		Negative of electronic energy		
$X^2\Sigma$	2.125035	8.500140	8.50012	8.500140
$(1)^2\Sigma$	0.753140	3.012320	3.01244	3.012320
$(2)^2\Sigma$	0.652661	2.610644	2.61038	2.610644
$(1)^2\Pi$	0.623179	2.492716	2.49263	2.492716
$(2)^2\Pi$	0.390719	1.562876	1.56194	1.562876
$(3)^2\Pi$	0.316854	1.267416	1.26751	1.267416
		Dipole permanent and transition moments		
$\langle X^2\Sigma\|D\|X^2\Sigma\rangle$	3.9956	1.9978	1.9971	1.9978
$\langle X^2\Sigma\|D\|(1)^2\Sigma\rangle$	0.0228	0.0114	0.0113	0.0114
$\langle X^2\Sigma\|D\|(2)^2\Sigma\rangle$	0.27062	0.1353	0.1350	0.1353
$\langle (1)^2\Pi\|D\|(1)^2\Pi\rangle$	3.8542	1.9271	1.9263	1.9271
$\langle (1)^2\Pi\|D\|(2)^2\Pi\rangle$	0.8050	0.4025	0.4033	0.4025
$\langle (1)^2\Pi\|D\|(3)^2\Pi\rangle$	0.5744	0.2872	0.2866	0.2872
		Qudrupole permanent and transition moments		
$\langle X^2\Sigma\|Q\|X^2\Sigma\rangle$	15.9652	3.9913	3.9914	3.9913
$\langle X^2\Sigma\|Q\|(1)^2\Sigma\rangle$	0.1727	0.0432	0.0430	0.0432
$\langle X^2\Sigma\|Q\|(2)^2\Sigma\rangle$	2.1382	0.5346	0.5345	0.5346
$\langle (1)^2\Pi\|Q\|(1)^2\Pi\rangle$	13.4754	3.3689	3.3689	3.3689
$\langle (1)^2\Pi\|Q\|(2)^2\Pi\rangle$	5.5272	1.3818	1.3818	1.3818
$\langle (1)^2\Pi\|Q\|(3)^2\Pi\rangle$	3.1993	0.7998	0.7999	0.7998

(a) D and Q are defined in Table 1.

as constants independent of *R*, they could factorize the internuclear distance (*R*) from the expressions of the matrix elements of the kinetic and potential energy operators. In this way, they did not have to repeat the calculations of these matrix elements for different value of *R*. This, as they observed, was an acceptable approximation for a reduced range of *R* values. They also observed that as the nuclear charge (*Z*) increased, the range of *R* for which accurate results could be so obtained was reduced.

In Tables 2 and 3 are presented numerical test values obtained for the electronic energies and dipole and quadrupole transition moments of He_2^{3+} and $BeHe^{5+}$ by a direct calculation and by applying the deduction rules to presently known results for the ionic systems H_2^+ and HeH_2^+ respectively.

One of the interests in these passage rules is the role that they can play in the improvement of the wavefunctions of given states for which no reliable reference values exist or for very excited states for which very large basis sets are necessary. For example, if the expected value of the quadrupole moment of He_2^{3+} for a $\pi^2\Delta_g$ state is not equal to the quarter of the corresponding exact H_2^+ value, we should go back and improve our He_2^{3+} $^2\Delta_g$ wavefunctions. As a matter of fact, we used this criterion to improve our variational direct calculations of He_2^{3+} and $BeHe^{5+}$ (see Tables 2 and 3, column 4).

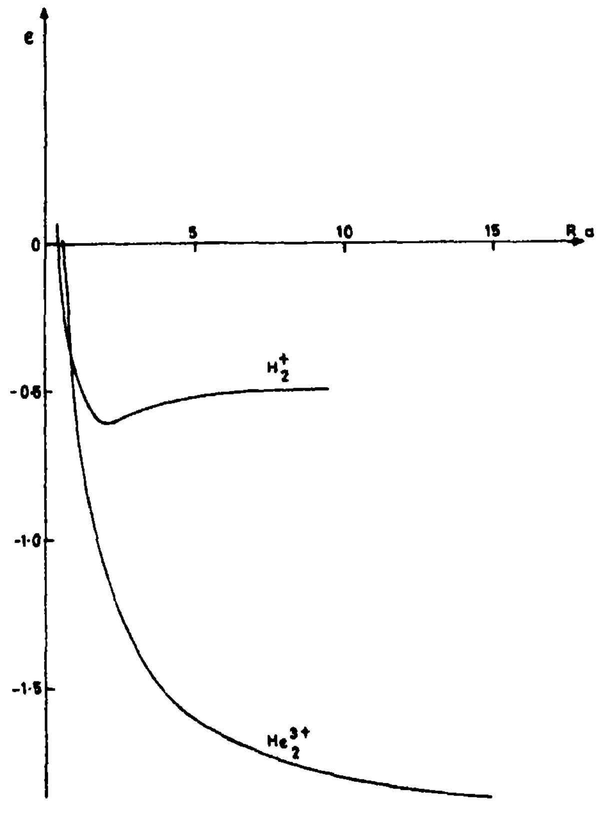

Fig. 1—Potential energy curves of the ground states of H_2^+ and He_2^{3+}

The deduction of solutions for heavier monoelectronic diatomic systems from existing ones is very useful for the determination of zero order properties of these systems, but one needs an extensive data set for the basic systems including accurate values for large *R*. Extensive tables, for the energy, can be found for H_2^+ in literature[11] from which one may deduce results for any other homonuclear systems. Such tables also exist for HeH^{2+} in literature[12] from which one may deduce results for heteronuclear systems corresponding to $Z_a/Z_b = 0$.

Figure 1 shows the potential energy curve for the ground states of He_2^{3+} deduced from that of H_2^+. The predicted curve explains the unstable nature of this system.

References

1 Ponomarev L I & Puzynina T P, *J.E.T.P. Sov Phys*, **25** (1967) 846.
2 Errea L F, Mendez L & Riera A, *J chem Phys*, **82** (1985) 4537.
3 Olson R E & Salop R E, *Phys Rev (A)*, **16** (1977) 531.
4 Power J D, *Phil Trans R Soc*, **A274** (1973) 664.
5 Helfrich & Hartman H, *Theoret Chim Acta (Berl)*, **16** (1970) 263.
6 Aubert M, Bessis N & Bessis G, *Phys Rev*, **A10** (1974) 51.
7 Wilson S, *J Phys*, **B 16** (1983) L429.
8 Henriet A & Masnou-Seeuws F, *Chem Phys Lett*, **101** (1983) 535.
9 Bishop D M & Cheung L M, *J chem Phys*, **78** (1983) 1396.
10 Wells B H & Wilson S, *J Phys*, **B 19** (1986) 17.
11 Madsen M & Peek J M, *Atomic Data*, **2** (1971) 171.
12 Winter T G, Duncan M D & Lane N F, *J Phys*, **B 10** (1976) 285.

Indian Journal of Chemistry
Vol. 27A, February 1988, pp. 145-147

Improved Calculation of Binding Energies of Molecules in Singlet Ground States

S C RAKSHIT* & B HAZRA
Chemistry Department, University of Burdwan,
Burdwan 713 104

Received 12 *March* 1987; *revised and accepted* 20 *May* 1987

The molecular binding energies in singlet ground states can be calculated fairly accurately by a semiclassical equation [SC Rakshit & Bani Mukherjee, *Indian J Chem*, **22A** (1983) 273]. The present note gives an improved method of calculation involving extensions in two directions, viz., a modification of the k_n parameter of the semiclassical equation proposed earlier and secondly the inclusion of *d*-orbitals in the CNDO charge density calculation.

In earlier publications[1,2] from our laboratory, it was shown how a semiclassical expression, based on CNDO formalism, can lead to extremely good binding energy values of the singlet state molecules and ions. We have carried out further work on this aspect and propose here some modifications of our earlier approach which enable one to obtain even more improved values of binding energies.

In the previously reported method[2], one uses parametrised k_n values, a table for which was given for valence shell orbitals numbering upto thirtyone. Modification of k_n values involving curve fitting techniques[7] may be effected to arrive at an analytic expression for k_n, viz., $k_n = A + B/n - \lambda \ln n$, where $A = 0.0487$, $B = 0.1851$, $\lambda = 0.0109$ and n indicates the number of valence shell orbitals.

The employment of this expression for the value of k_n in the original Eqs (3) and (5) of the previously reported paper[2] shows even better results (Table 1) and has allowed us to extend calculations to the valence shell orbital number 44. However, its use for molecules with valence shell orbital number upto 50 is also possible. For still higher valence shell basis set, the calculated k_n values are to be slightly altered.

The second modification is to examine the effect of including the *d*-orbitals in the calculation of binding energies[2] where chlorine, sulphur and phosphorus atoms are present in the molecules.

Table 1—Binding Energies of Different Molecules

Molecule	Binding energy (eV) from ref. 2	Binding energy (eV) based on the modified k_n values		Thermodynamic binding energy (eV)
		Eq. 3	Eq. 5	
Water	-9.05	-9.52	-9.58	-9.59
Ammonia	-12.42	-12.997	-12.317	-12.16
Phosphine	-9.85	-9.32	-10.00	-9.93
Hydrogen sulphide	-6.70	-6.68	-7.36	-7.04
Carbon dioxide	-15.5	-16.43	–	-16.66
Methane	-16.05, -16.73	-16.44	-17.12	-17.26
Ethane	-28.13, -28.81	-29.00	-29.68	-29.33
Propane	-41.24, -41.92	-41.96	-41.28	-41.50
n-Butane	–	-54.30	-53.62	-53.69
n-Pentane	—	-66.77	-66.09	-65.89
n-Hexane	—	-78.71	-78.03	-78.082
n-Heptane	—	—	-89.95	-90.26
Isobutane	—	-54.36	-53.679	-53.68
2-Methylbutane	—	—	-66.12	-65.97
2,2-Dimethylpropane	—	—	-66.2	-66.09
2-Methylpentane	—	—	-78.06	-78.15
3-Methylpentane	—	—	-78.07	-78.011
3-Methylpentane (S)	—	—	-78.053	-78.118
2,2-Dimethylbutane	—	—	-78.16	-78.26
2,3-Dimethylbutane	—	—	-78.13	-78.18
Methyl formate	-32.27	-32.83	-32.15	-32.70
Ethyl formate	43.90, -46.21	–	-44.958	-44.87

Table 1 Contd.

Table 1—Binding Energies of Different Molecules—*Contd.*

Molecule	Binding energy (eV) from ref. 2	Binding energy (eV) based on the modified k_n values		Thermodynamic binding energy (eV)
		Eq. 3	Eq. 5	
Methyl acetate	−45.89	—	−45.99	−45.93
Ethyl acetate	—	−57.71	−57.03	−57.48
Ethyl propionate	—	−69.78	—	−69.84
Acetamide	−36.99	—	−36.46	−36.18
Propionamide	−48.40	—	−49.02	−48.35
Methanol	−19.42, −20.39	−20.64	−21.32	−21.14
Ethanol	−34.30, −32.59	−33.51	—	−33.46
n-Propanol	—	−46.04	−45.36	−45.69
n-Butanol	—	−58.61	−57.93	−57.93
Amyl alcohol	—	−70.76	−70.08	−70.23
Isopropanol	−47.66, −45.28	−46.01	—	−46.11
t-Butyl alcohol	−58.92	−58.65	−57.97	−58.36
t-Amyl alcohol	—	−69.72	−70.40	−70.74
Glycol	−38.12	−37.77	—	−37.81
Formaldehyde	−15.46	−16.03	−15.35	−15.73
Diethyl ketone	—	−65.97	−65.286	−65.30
Methyl *n*-butyl ketone	—	—	−78.38	−78.08
Oxalic acid	−37.24	−36.87	−37.55	−37.25
Urea	−32.23	−32.46	−31.775	−32.29

Table 2—Calculated Binding Energies with Inclusion of *d*-Orbitals

Molecule	Thermodynamic binding energy (eV)	Binding energy (eV) from ref. 2	Binding energy (eV) (*d*-basis set included)
Methyl chloride	−16.32	−14.86	−15.99
Dichloromethane	−15.36	−14.53	−15.065
Dichloroacetic acid	−31.62	−32.38	−30.62
Ethyl chloride	−28.52	−28.31	−28.28
Carbon tetrachloride	−13.51	−12.14	−13.08
Chloroform	−14.46	−10.97	−14.017
Phosphorous trichloride	−10.14	−7.41	−12.445, −11.73 (Eq. 5)
Phosphine	−9.93	−9.85	−9.60
Hydrogen sulphide	−7.04	−6.70	−7.08

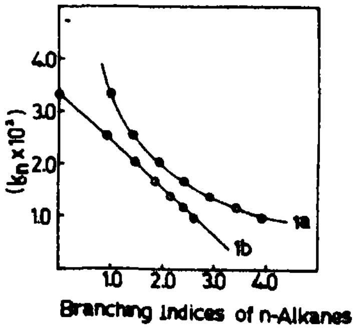

Fig. 1—Relation between ($k_n \times 10^2$) and branching indices of Randic (a), Bonchev & Trinajstic (b)

The basic CNDO expression then provides more dependable values of diatomic exchange energies and of the atomic charge densities which form the core of the semiclassical expression[2]. Table 2 lists the binding energies of some molecules after taking into account the effect of *d*-orbitals. The improvement in binding energies on incorporation of the *d*-orbitals in the basis set is evident. It may be worthwhile to point out that the improvement is achieved even without the use of the correction factor (viz., 0.05 a.u.) of Eq. (3) of the earlier paper[2].

A third aspect to which attention may be drawn is the smooth variation of the k_n values vis-a-vis the topological branching indices of the homologous alkanes as defined by Randic[3]. It, however, displays a linear variation against the information theory based graphical indices proposed by Bonchev and Trinajstic[4] [Figs. 1(a) and 1(b)]. This dependence of k_n and hence of binding energies on branching indices will be dealt with in a forthcoming publication.

References

1 Rakshit S C & Mukherjee B, *Indian J Chem*, **20A** (1981) 1103.

2 Rakshit S C & Mukherjee Bani, *Indian J Chem*, **22A** (1983) 273.

3 Randic M, *J Am chem Soc*, **97** (1975) 6609.

4 Bonchev D & Trinasjstic N, *J chem Phys*, **67** (1977) 4517.

5 *Handbook of chemistry*, edited by N B Lange (Mc Graw Hill, N.Y.) 1961.

6 *Handbook of chemistry & physics*, edited by R C Weast (C R C Press, Florida) 1979, C-730, C-722, C-723.

7 Demidovich B P & Maron I A, *Computational mathematics* (MIR Publishers, Moscow) 1976.

Indian Journal of Chemistry
Vol. 27 A, February 1988, pp. 148-150

Simple & Two Dimensional Hückel Molecular Orbital Treatments of Conjugated Polyolefins & Polyacetylenes

LALJI DIXIT & SANTANU BHATTACHARJEE
Indian Institute of Petroleum, Dehra Dun
and
R P SEMWAL[*,†]
Department of Chemistry, SGRR College, Dehra Dun

Received 5 *January* 1987; *revised and accepted* 27 *June* 1987

The simple and two dimensional Hückel molecular orbital (HMO) theory has been applied to sixteen polyacetylenes (C_2H_2 to $C_{16}H_2$) and polyolefins (C_2H_4 to $C_{16}H_{18}$), all of which are conjugated systems. Energy levels, delocalization energies, bond orders and π-bond polarizabilities of all the systems have been calculated. The π-π* transitions for the systems bear an excellent linear relationship with the highest occupied molecular orbital (HOMO) and the lowest unoccupied molecular orbital (LUMO) energy differences.

One of the latest extensions of the Hückel molecular orbital (HMO) theory[1,2] has been introduced by Cyvin[3-6]. Using two-dimensional HMO approach, he has extended the use of the HMO theory to *sp*-hybridized carbon atoms in addition to the sp^2-hybridized carbon atoms. Hence, the extended theory covers systems with acetylenic $C \equiv C$ bonds. The purpose of the present work is to apply Cyvin's approach to bigger conjugated hydrocarons and to determine their molecular structural parameters, viz., bond length, bond order, bond polarizability, delocalization energy and spectroscopic (π-π*) transitions. The systems studied are conjugated polyolefins C_nH_{2n+2} (n = 1 to 8) and polyacetylenes $C_{2n}H_2$ (n = 1 to 8).

The simple Hückel molecular orbitals (HMOs) were constructed by taking linear combination of atomic orbitals (LCAOs) for 2*p* orbitals in two dimensions, perpendicular and independent of each other. Total π-energy (E_π) was obtained by adding the energies of the π′ and π″ systems.

$$E_\pi = E_{\pi'} + E_{\pi''}$$

The bond orders obtained separately in the π′ and π″ systems, say P' and P'', are additive. Thus, the total π-bond order (P) of a given CC bond is,

$$P = P' + P''$$

The range of P is $0 < P \leq 2$; $P = 2$ corresponds to the pure triple bond, $C \equiv C$. Coulson's[7] empirical formula that relates the bond order (P) with internuclear distance (r) is given by the equation,

$$r = 1.536 - \frac{0.192\,P}{P + 0.765\,(1 - P)}$$

On the basis of expanded range ($0 < P \leq 2$) and comparison of results obtained from Coulson's formula with the modern structural data, Cyvin[3] revised the above formula as,

$$r = 1.557 - \frac{0.220\,P}{P + 0.750\,(1 - P)}$$

Using both the formulae, we have determined bond lengths of all the CC bonds in the present systems and compared them with the experimental data available from literature (Table 1). Cyvin's formula is found to give better results than the Coulson's formula. The delocalization energy (D) was obtained by subtracting $2(\alpha + \beta)$ for every double bond and $4(\alpha + \beta)$ for every triple bond from E_π. The conventional HMO theory has been used in calculating total π-electronic polarizability (by considering only ij-ij parts of every system) and π-energy levels (Table 1)[‡]. For the sake of comparison, the relative positions of all the energy levels are shown in Fig. 1. Total polarizabilities of the systems have been calculated by the one-dimensional δ-function model of Frost[8]. For the lower systems, the theoretical and experimental values of total polarizability are in close agreement while they differ very much for the higher ones; this is due to one dimensional nature of the model and approximations involved in the theory.

The coefficient of correlation (C) between individual π-bond orders and observed bond distances is 0.951 and the equation of the line correlating these two physical properties is

$$a = C - b - 1/P$$

where $b = 0.138$ and $a = 1.172$. On the basis of this line (say ideal line) and a set of four lines corresponding to different types of hybridized carbon atoms involved in the bond formation, bond lengths have been predicted (Table 1).

The HMO theory treats the σ-part of a system as a constant and focuses on the π-part, whereas

---

[†] This work is part of the Ph.D. thesis to be submitted by RPS. Details of these calculations and computer programme can be obtained from him at the address: 162A, Chukhuwala, Dehra Dun

[‡] Only a few molecules are chosen

Table 1—Calculated Values of Molecular Structural Parameters (*r* in Å)

Sl. No.	Molecule	Delocalization Energy, D	Total π-Electron Energy	Total π-bond Polarizability	Total Polarizability by δ-funct method (in 10^{-25} cm³)*	Exp. value of total poloriz. (in 10^{-25} cm³)*	Bond	Bond Order (P)	Bond length, *r* by Coulson's formula	Bond length, *r* by Cyvin's formula	Expt. Value of Bond length, *r**	Prediction by graph of expl. value of *r*	*r*, by ideal line
1	C_2H_4	0.000 β	2α + 2β	0.000	34.984	23.7[13]*	C=C	1.000	1.344	1.337	1.337[16,17]	—	—
2	C_2H_2	0.000 β	4α + 4β	0.000	34.984	32.7[13]	C≡C	2.000	1.205	1.205	1.205[18]	—	—
3	C_4H_6	−0.472 β	4α + 4.472β	0.537	62.103	—	C=C	0.894	1.360	1.355	1.341[19]	—	—
							C−C	0.447	1.437	1.443	1.463[19]	—	—
4	C_4H_2	−0.844 β	8α + 8.944β	1.074	62.103	52.33[13]	C≡C	1.789	1.246	1.228	1.217[20]	—	—
							C−C	0.894	1.360	1.355	1.384[20]	—	—
15	$C_{16}H_{18}$	−3.644β	16α + 19.644β	4.509	223.701	—	$C{=}C_a$	0.852	1.366	1.368	—	1.352	1.364
							$C{=}C_b$	0.785	1.377	1.379	—	1.368	1.374
							$C{=}C_c$	0.707	1.390	1.393	—	1.388	1.388
							$C{=}C_d$	0.698	1.392	1.895	—	1.388	1.388
							$C{-}C_e$	0.506	1.426	1.427	—	1.455	1.419
							$C{-}C_f$	0.558	1.416	1.419	—	1.448	1.410
							$C{-}C_g$	0.574	1.414	1.416	—	1.440	1.408
							$C{-}C_h$	0.579	1.413	1.415	—	1.445	1.407
16	$C_{16}H_2$	−7.288 β	32α + 39.288β	9.018	223.701	434.0[13]	$C{\equiv}C_{a'}$	1.704	1.255	1.238	—	1.221	1.231
							$C{\equiv}C_{b'}$	1.570	1.270	1.255	—	1.230	1.252
							$C{\equiv}C_{c'}$	1.414	1.288	1.275	—	1.239	1.276
							$C{\equiv}C_{d'}$	1.396	1.291	1.278	—	1.240	1.279
							$C{-}C_{e'}$	1.012	1.342	1.335	—	—	1.337
							$C{-}C_{f'}$	1.116	1.327	1.318	—	—	1.320
							$C{-}C_{g'}$	1.148	1.323	1.313	—	—	1.315
							$C{-}C_{h'}$	1.158	1.322	1.312	—	—	1.310

*Figures in parenthesis indicate references to literature

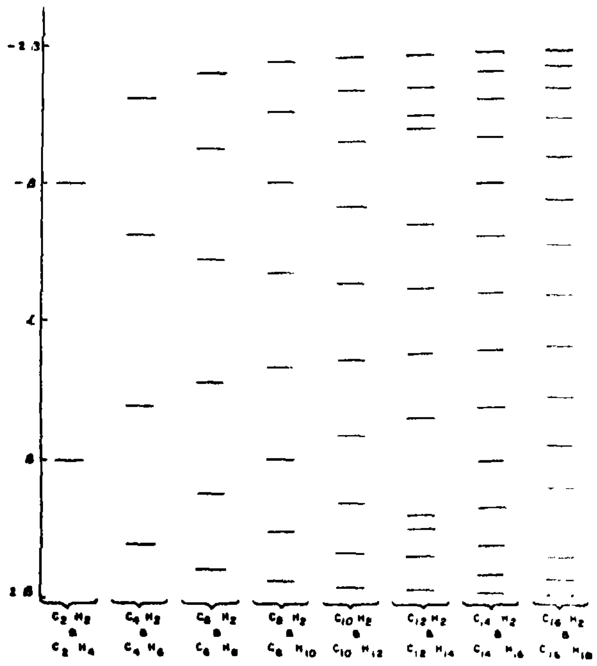

Fig. 1—Relative positions of HMO π-energy levels of polyolefins and polyacetylenes

in many systems the σ-hybridization affects the bond length[9,10] and the π-electron effects are negligible[11]. All α and β are assumed to be equal, which may not be so. These anomalies can be removed if equivalent hybrid orbitals be formed by the judicious choice of linear combinations.

π-π* *Transitions in the conjugated polyenes*

Non-conjugated olefins have overlapping bands due to π-π* transitions; as a result of conjugation these bands extend towards longer wavelengths. If the π-system is extended, say by adding another double bond, the original bonding and antibonding levels split into two levels each with a consequent reduction in the energy of transition. Associating the first intense absorption ($^1A \rightarrow {}^1B$) in Platt's terminology[12] with the transition of an electron from the highest occupied MO (HOMO) to the lowest unoccupied MO (LUMO), we looked for a correlation between the observed frequency and the corresponding HMO energy difference. The energy levels of linear polyenes are given in analytic form,

Table 2—Absorption Bands and the Energy Differences of Polyenes

	Present work			Literature		
	λ_{max} (nm)	ν (cm $^{-1}$)	HMO (Δm)	λ_{max}† (nm)	ν (cm $^{-1}$)	HMO (Δm)
Ethylene	174	57471	2.00	162(12)*	61500	2.000
Butadiene	217	46083	1.24	217(13)*	46080	1.236
Hexatriene	266	37594	0.89	251(13)*	39750	0.890
Octatetraene	302	33112	0.695	304(14)*	32900	0.695
Decapentaene	334	29940	0.57	—	—	—
Dodecahexaene	364	27472	0.48	364(21)*	27472	0.480
Tetradecaheptaene	390	25641	0.42	—	—	—
Hexadecaoctaene	410	24390	0.37	—	—	—

†For eicosadecane, $H-(CH=CH)_{10}-H$, $\lambda_{max}=447$ nm (21)*

*Figures in parenthesis indicate references to literature

$$x_j = -2\cos\frac{j\pi}{n+1};\ j = 1,2,3\ \ldots\ldots\ldots\ldots\ n$$

where n is the number of π-centers. The corresponding energy difference is given by the relation,

$$\Delta E = 4\beta\sin\frac{\pi}{2(n+1)}$$

The simple polyenes are known through hexadecaoctaene. Table 2 lists the frequency of the $^1A \rightarrow {}^1B^{\circ}$ absorption band and the HMO energy difference for each of these polyenes. The plot of these data showed a good linear relationship.

We also found that the following relation between Δm and ν(cm^{-1}) holds with a correlation coefficient of 0.9924,

$$\Delta\nu(\mathrm{cm}^{-1}) = -0.847 + 4.77\times10^{-5}\,\Delta m$$

References

1 Hückel E, *Z Phys*, **70** (1931) 204.
2 Streitwieser (Jr) A, *Molecular orbital theory for organic chemists* (Wiley, New York) 1961.
3 Cyvin S J, *J molec Struct*, **86** (1982) 315.
4 Cyvin S J, *Kgl Norske Videnskab Selskabs Skr*, **4** (1982) 1; *Chem Abstr*, **97** (1982) 133779k.
5 Cyvin S J, *Tetrahedron Lett*, **22** (1981) 2709.
6 Cyvin S J, Cyvin B N & Brunvoll J, *Kgl Norske Videnskab Selskabs Skr*, **5** (1982) 1.
7 Coulson C A, *Proc Roy Soc*, **169A** (1939) 413.
8 Frost A A, *J chem Phys*, **47** (1967) 3707.
9 Mulliken R S, *Tetrahedron*, **6** (1959) 68.
10 Hansen-Nygaard L & Bak B, *J chem Phys*, **33** (1960) 418.
11 Benstein H J, *J phys Chem*, **63** (1959) 565; Brown M G, *Trans Faraday Soc*, **55** (1959) 694.
12 Platt J R, Klevens H B & Price W C, *J chem Phys*, **17** (1949) 466.
13 Amos A T & Crispin R J, *J chem Phys*, **63** (1975) 1890.
14 Price W C & Walsh A D, *Proc Roy Soc*, **174A** (1940) 220; 185A (1946) 182.
15 Woods G F & Schwartzman L H, *J Am chem Soc*, **71** (1949) 1396.
16 Allen (Jr) H C & Plyler E K, *J Am chem Soc*, **80** (1958) 2673.
17 Bartell L S, Roth E A, Hollowell C D, Kuchitsu K & Young J W, *J chem Phys*, **42** (1965) 2683.
18 Christensen M T, Eaton D R, Green B A & Thompson H W, *Proc Roy Soc*, **238A** (1965) 15.
19 Kuchitsu K, Fukuyama T & Morino Y, *J molec Struct*, **1** (1968) 463.
20 Tanimoto M, Kuchitsu K & Morino Y, *Bull chem Soc Japan*, **44** (1971) 386.
21 Sondheimer F, Ben-Efraimd A & Wolovsky R, *J Am chem Soc*, **83** (1961) 1675.

Indian Journal of Chemistry
Vol. 27A, February 1988, pp. 151-152

Cobalt-60 Gamma Radiolysis of Tris(oxalato)cobalt(III) Ion in Oxygenated Aqueous Solution

B K SHARMA*
Department of Chemistry, University of Delhi, Delhi 110 007
and
PURSHOTTAM SARAN
Department of Chemistry, Zakir Husain College, Delhi 110 006

Received 18 *March* 1987; *revised* 25 *May* 1987; *accepted* 23 *June* 1987

Radiolysis of the tris(oxalato)cobalt(III) ions in oxygenated neutral aqueous solution has been studied. It is observed that CO_2^- radical ion reduces the complex ion while $C_2O_4^-$ and O_2^- radical ions do not. Evidence that $C_2O_4^-$ does not dissociate into CO_2^- and CO_2 is also presented.

Tris(oxalato)cobalt(III) ions in deoxygenated aqueous media[1-4] undergo radiolytic degradation by reducing species such as hydrated electrons, hydrogen atom and $C_2O_4^-$ radicals. Memetea and Paun[2,3] have reported that CO_2^- species reduce the complex ion only when all the dissolved oxygen in aqueous solution has been used up. The present investigation has been undertaken to identify the actual reducing species in the oxygenated aqueous medium.

Potassium tris(oxalato)cobalt(III) was prepared by Sorensen's method[5]. All the operations were carried out in the dark. Gamma rays from ^{60}Co source were used. Triply distilled water was used in the preparation of all the solutions. The solutions were irradiated in a special type of pyrex glass vessel, fitted with pyrex stopper, and consisting of an inlet and outlet for maintaining oxygen atmosphere.

The dose rate was determined as 0.8×10^{17} eV min^{-1} cm^{-3} using Fricke dosimeter, taking $G_{Fe(III)}$ as 15.6. The radiation-induced decomposition of the complex in aqueous solution was studied spectrophotometrically at 420 nm using a Beckmann model DU spectrophotometer fitted with quartz cells having 1 cm path length. The absorbance was reproducible upto the third place of decimal. The concentration of $[Co(C_2O_4)_3]^{3-}$ ion was determined from a calibration curve. Accumulation of Co(II) was determined by extraction with isobutyl methyl ketone[6].

Figure 1 depicts the degradation of oxygenated solution containing 3.2×10^{-3}, 5.5×10^{-3} and 1×10^{-2} mol dm^{-3} complex ion in the presence of 1×10^{-2} mol dm^{-3} sodium oxalate and sodium formate. It is evident that the rate of reduction decreases in the presence of oxygen and the *G* (−complex) comes out to be 1.7. This may be due partly to scavenging of e_{aq}^- and H by O_2, producing O_2^-. It is worth noting that *G* (−complex) is independent of initial solute concentration at low doses. During the initial stage of radiolysis, where there is low concentration of H_2O_2, a decrease in the rate of radiolytic reduction of complex ion alone predicts that O_2^- does not act as a reducing agent like CO_2^-. Further the radiolysis of 5.5×10^{-3} mol dm^{-3} oxygenated solution of the complex ion in the presence of 1×10^{-2} mol dm^{-3} sodium oxalate gives a *G* (−complex) value of 1.7 (calculated from the initial portion of the curve in Fig. 2d). It is interesting to note that same *G* (−complex) value was found in oxygenated solution in the absence of sodium oxalate.

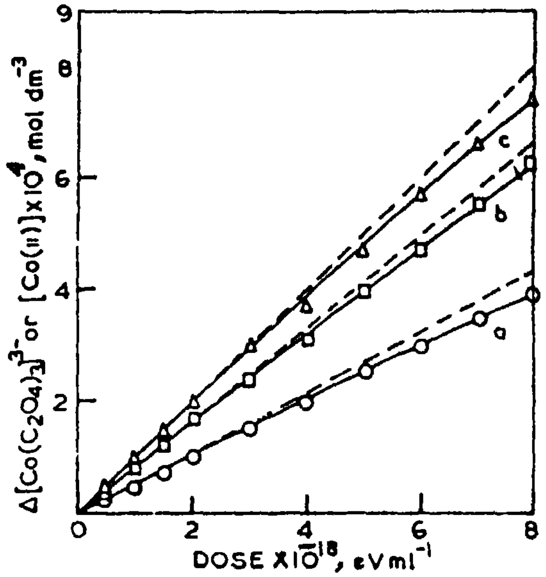

Fig. 1—Radiolytic degradation of 3.2×10^{-3} mol dm^{-3} deoxygenated solution of tris(oxalato) cobalt(III) in aqueous medium (○—○) and of the above solution of the complex in the presence of 10^{-2} mol dm^{-3} sodium oxalate (□ – □) and sodium formate (△ – △). (Similar curves were obtained when the [complex ion] were 5.5×10^{-3} and 1×10^{-2} mol dm^{-3})

In contrast, *G* (−complex) value of 3.3 or 4.9 have been obtained for the radiolysis of the complex alone and in the presence of 1.0×10^{-2} mol dm^{-3} sodium oxalate respectively in deoxygenated solution (Fig. 1). Thus the radiolysis of the complex ions in oxygenated solution and in solution

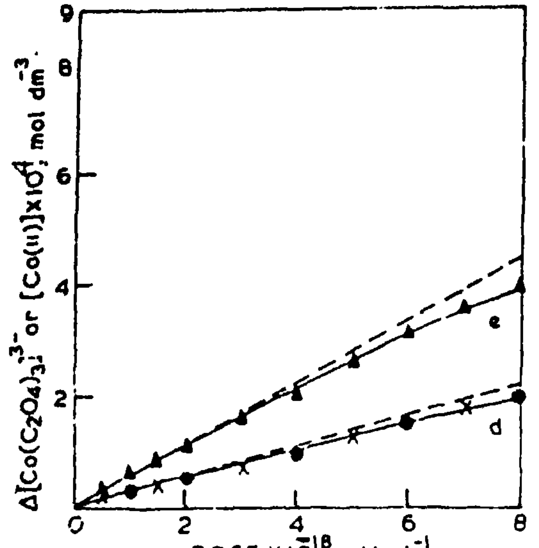

Fig. 2—Radiolytic degradation of 3.2×10^{-3} mol dm^{-3} oxygenated solution of tris(oxalato)cobalt(III) (× — ×) and of the above solution in the presence of 1×10^{-2} mol dm^{-3} sodium oxalate (●—●) and sodium formate (▲—▲) (Similar curves were obtained when the [complex ion] were 5.5×10^{-3} and 1×10^{-2} mol dm^{-3})

containing oxalate ions reveal that $C_2O_4^{\cdot -}$ ion radicals produced during the radiolysis (reaction-1) do not reduce the complex ion but may react with O_2 to give $O_2^{\cdot -}$ radical ion (reaction-2) which would give H_2O_2 by the reaction-2b. Moreover $C_2O_4^{\cdot -}$ ion radical does not seem to be dissociated to give $CO_2^{\cdot -}$ and CO_2 (reaction-2a), since if had it been so, then G (− complex) would have been 3.4 instead of 1.7.

$$C_2O_4^{2-} + OH \rightarrow C_2O_4^{\cdot -} + OH^- \quad \ldots (1)$$

$$C_2O_4^{\cdot -} + O_2 \rightarrow 2CO_2 + O_2^{\cdot -} \quad \ldots (2)$$

$$C_2O_4^{\cdot -} \rightarrow CO_2^{\cdot -} + CO_2 \quad \ldots (2a)$$

$$O_2^{\cdot -} + O_2^{\cdot -} \xrightarrow{2H_2O} H_2O_2 + O_2 + 2OH^- \quad \ldots (2b)$$

After a sufficient dose, the rate of decomposition of the complex decrease because e_{aq}^- and H are partially scavenged by accumulated H_2O_2.

Radiolytic degradation of oxygenated aqueous solutions of the complex ions in the concentration range of 3.2×10^{-3}-1×10^{-2} mol dm^{-3} is enhanced by the presence of 1×10^{-2} mol dm^{-3} formate ions as the G (− complex) value is found to be 3.4 (Fig. 2e). In deoxygenated aqueous solution and in the presence of 1×10^{-2} mol dm^{-3} sodium formate, G (− complex) value comes out to be 6.0 (Fig. 1c). It can be explained on the basis of the reactions (3) and (4)

$$HCOO^- + OH \rightarrow CO_2^{\cdot -} + H_2O \quad \ldots (3)$$

$$[Co(C_2O_4)_3]^{3-} + CO_2^{\cdot -} \rightarrow [Co(C_2O_4)_2]^{2-} + CO_2 + C_2O_4^{2-} \quad \ldots (4)$$

The lower G (− complex) value in the presence of oxygen is because of the disappearance of a fraction of $CO_2^{\cdot -}$ species in accordance with reaction (5)

$$CO_2^{\cdot -} + O_2 \xrightarrow{k} CO_2 + O_2^- \quad \ldots (5)$$

where $k = 2.4 \times 10^9$ mol $dm^{-3} \cdot s^{-1}$. $CO_2^{\cdot -}$ radical may react with water to give HCHO, CH_4, CH_3OH etc. However, in the presence of oxygen, reaction (5) would be much more favoured and facile since the rate constant for this reaction is 2.4×10^9 mol dm^{-3} s^{-1}. Thus under the present experimental conditions the reaction of $CO_2^{\cdot -}$ with water will be negligible, i.e. $CO_2^{\cdot -}$ radicals produced by formate ions seem to undergo reactions (4) and (5) and not reaction (4) alone. If it had been so, then the G (− complex) value would have been (1.7 + 2.7) = 4.4 and not 3.4, the observed value. A comparison of the results of radiolysis of oxygenated solutions of the complex ion in the presence of oxalate and formate ions, clearly reveals that while the $C_2O_4^{\cdot -}$ ion radicals are completely scavenged by oxygen to give CO_2 and O_2^- and do not reduce the complex ion, the $CO_2^{\cdot -}$ ion radicals do so partly. It can thus be inferred that $O_2^{\cdot -}$ radicals do not reduce the complex and also no dissociation of $C_2O_4^{\cdot -}$ occurs.

One of the authors (P S) is thankful to the UGC, New Delhi for the award of a research project.

References

1 Murgulescu I G, Oncescue T, Paun J & Mihalcea I, *Rev Rouma Chim*, **12** (1967) 573.

2 Paun J, Memetea T & Store E, *Radiochem Radioanal Lett*, **22(2)** (1975) 101.

3 Memetea T & Paun J, *Rev Rouma Chim*, **19** (1974) 1689.

4 Sharma B K & Saran P, *Radiat Eff Lett*, **87** (1985) 141.

5 *Inorganic Syntheses*, Vol 1, edited by H S Booth (McGraw Hill, New York), 1939, pp. 37.

6 Katakis D & Allen A, *J phys Chem*, **68** (1964) 1359.

Indian Journal of Chemistry
Vol. 27 A, February 1988, pp. 153-155

Synthesis & Characterisation of Organotin(IV) Complexes of Acetoin & Benzoin Semicarbazones & Thiosemicarbazones

(Miss) PURNIMA DIXIT & J P TANDON*
Department of Chemistry, University of Rajasthan,
Jaipur 302 004

Received 13 *April* 1987; *revised and accepted* 7 *July* 1987

Condensation of benzoin and acetoin with semicarbazide hydrochloride and thiosemicarbazide leads to the formation of corresponding schiff bases. These, when reacted with dimethyltin dichloride and dibutyltin oxide, lead to the formation of substitution products of the type, R_2SnL (where R = Me or Bu and LH_2 = ligand molecule). The resulting complexes have been characterized on the basis of elemental analysis, molecular weight determination and conductivity measurements. The mode of bonding of the ligands with the metal atom has been deduced on the basis of IR, ^1H NMR and electronic spectral studies. All the ligands have been found to behave as bifunctional tridentate donors.

Extensive work has been carried out on the coordination chemistry of organotin(IV) derivatives, but only a little work has so far been reported on the tin(IV) complexes with bifunctional tridentate schiff bases[1,2]. Semicarbazones and thiosemicarbazones are important nitrogen and oxygen/sulphur donor ligands and their organotin(IV) complexes show significant biological activity[3,4]. In view of this, it was considered of interest to synthesize and characterize organotin(IV) complexes of acetoin and benzoin semicarbazones and thiosemicarbazones. Results of these studies are reported in the present note.

All the reactions were carried out under strictly anhydrous conditions. Semicarbazones and thiosemicarbazones were prepared by refluxing benzoin (3.90 g, 3.44 g) or acetoin (4.77 g, 6.85 g) with semicarbazide hydrochloride (2.06 g, 6.05 g), in presence of sodium acetate (2.50 g,7.37 g), or thiosemicarbazide (1.40 g, 7.08 g) in 1:1 molar ratio in ethanol (150 ml) for 2-3 hr. These were purified by recrystallization from the same solvent and analysed before use. The ligands synthesized are: (I) acetoin semicarbazone, white creamy solid m.p. 175°C, yield 90%; (II) acetoin semicarbazone white creamy solid, m.p. 142°C, yield 90%; (III) benzoin semicarbazone, white solid, m.p. 191°C, yield 92%; (IV) benzoin thiosemicarbazone, light yellow solid, 130°C, yield 95%.

Tin was estimated as tin oxide gravimetrically. Nitrogen was estimated by the Kjeldahl's method and sulphur as $BaSO_4$ by the Messenger's method.

Electronic spectra were recorded in methanol on a Pye Unicam SP-8-100 spectrophotometer. IR spectra were recorded on a Perkin-Elmer 577 grating spectrophotometer in KBr. ^1H NMR spectra were recorded on a 60 MHz RB-12 spectrometer in DMSO-d_6 using TMS as an internal standard. The conductances of 10^{-3} *M* solutions of the complexes in DMF were measured with a Systronics conductivity bridge (type 305, at 30 ± 1°C). The molecular weights were determined by the Rast's Camphor method.

Synthesis of organotin(IV) complexes

To a weighed amount of dimethyltin dichloride were added the calculated amounts of the ligand and triethylamine in 1:1:2 molar ratio using dry THF as the reaction medium under perfectly anhydrous conditions. The colour of the contents immediately changed with the precipitation of triethylamine hydrochloride. The solution was stirred for an hour on a magnetic stirrer and precipitate of triethylamine hydrochloride was filtered off. The excess of the solvent was removed fromt he filtrate and the compound so obtained was dried *in vacuo* at 35 ± 5°C. The complexes were then repeatedly washed with dry cyclohexane so as to ensure their purity.

For the synthesis of complexes with Bu_2SnO, a weighed amount of dibutyltin oxide was added to the calculated amount of ligand in 1:1 molar ratio using dry benzene as the reaction medium. The contents were refluxed for 7-8 hr under absolutely dry conditions and the liberated H_2O was removed azeotropically with benzene. The resulting product was then isolated as described above. Their synthesis, analysis and physical properties are recorded in Table 1.

The reaction of dimethyltin dichloride or dibutyltin oxide with the schiff base in 1:1 molar ratio can be represented as follows:

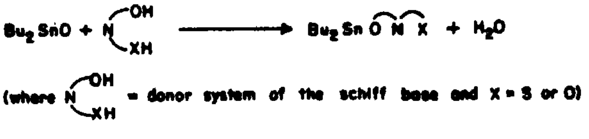
Me_2SnCl_2 + N OH XH
triethylamine
Me_2Sn O N X + $2(C_2H_5)_3N{\cdot}HCl$
Bu_2SnO + N OH XH
Bu_2Sn O N X + H_2O
(where N OH XH = donor system of the schiff base and X = S or O)

Table 1—Synthesis, Analysis and Physical Properties of Tin Complexes

Tin compound (g)	Ligand (g)	Complex, Colour and State	Yield (g) (Calc.)	M.P. (°C)	Found (Calc.) (%) Sn	N	S	C	H	Molec. wt. Found (Calc.)
Me_2SnCl_2 (1.22)	$C_5H_{11}OSN_3$ (0.80)	$C_7H_{15}OSN_3Sn$ Orange yellow solid	0.42 (0.48)	154	38.0 (38.5)	13.2 (13.65)	10.00 (10.40)	26.92 (27.3)	4.30 (4.88)	290 (307.69)
Me_2SnCl_2 (1.06)	$C_5H_{11}O_2N_3$ (0.70)	$C_7H_{15}O_2N_3Sn$ Orange yellow solid	0.40 (0.42)	81	39.9 (40.69)	14.01 (14.40)	—	28.4 (28.8)	4.97 (5.14)	279 (291.69)
Me_2SnCl_2 (0.74)	$C_{15}H_{15}OSN_3$ (0.96)	$C_{17}H_{19}OSN_3Sn$ Off white solid	0.72 (0.76)	340	27.0 (27.49)	9.11 (9.73)	7.10 (7.41)	46.98 (47.26)	4.02 (4.40)	423 (431.69)
Me_2SnCl_2 (0.56)	$C_{15}H_{15}O_2N_3$ (0.68)	$C_{17}H_{19}O_2N_3Sn$ Yellow solid	0.49 (0.54)	187	27.0 (27.55)	9.97 (10.1)	—	48.79 (49.08)	4.21 (4.57)	402 (415.69)
Bu_2SnO (1.33)	$C_5H_{11}OSN_3$ (0.81)	$C_{13}H_{27}OSN_3Sn$ White creamy solid	0.71 (0 75)	90	29.9 (30.30)	10.11 (10.72)	7.99 (8.17)	39.24 (39.83)	6.26 (6.89)	380 (391.69)
Bu_2SnO (1.46)	$C_5H_{11}O_2N_3$ (0.8)	$C_{13}H_{27}O_2N_3Sn$ Light yellow solid	0.69 (0.74)	65	31.1 (31.59)	11.01 (11.18)	—	41.0 (41.52)	7.07 (7.19)	366 (375.69)
Bu_2SnO (0.45)	$C_{15}H_{15}OSN_3$ (0.51)	$C_{23}H_{31}OSN_3Sn$ Light yellow solid	0.41 (0.49)	74	22.9 (23.02)	7.87 (8.14)	5.97 (6.21)	53.10 (53.52)	5.97 (6.01)	505 (515.69)
Bu_2SnO (1.21)	$C_{15}H_{15}O_2N_3$ (1.06)	$C_{23}H_{31}O_2N_3Sn$ Light yellow solid	0.96 (1.01)	144	23.22 (23.75)	7.98 (8.41)	—	54.98 (55.23)	5.99 (6.20)	485 (499.69)

All the complexes are coloured solids, monomeric and soluble in methanol, THF, DMF and DMSO and are susceptible to hydrolysis. Their conductance measurements in dry DMF (10-15 ohm^{-1} cm^2 mol^{-1}) show that they are non-electrolytes in nature.

The electronic spectra of ligands and their tin(IV) complexes were recorded in methanol. In the spectra of ligands, a band observed at ~276 nm may be attributed to π-π^* transition of $>C=N$ moiety; it gets shifted to ~300 nm in the spectra of the metal complexes showing the coordination of azomethine nitrogen to the tin atom. Further, two bands due to π-π^* transitions of ligands at ~236 and ~212 nm remain almost unchanged in the complexes.

The IR spectra of the ligands show a broad and strong band in the region 3200-2800 cm^{-1} attributable to ν(OH) and ν(NH) modes. It disappears in the spectra of the metal complexes showing thereby the deprotonation of these functional groups. Two sharp peaks at ~3300 cm^{-1} and 3420 cm^{-1} due to $\nu(NH_2)$ remain unaltered in the metal complexes[5]. One strong band in all the ligands at 1600 ± 5 cm^{-1} due to ν(C=N) gets split into two sharp bands at 1620 ± 10 cm^{-1} and ~1590 cm^{-1} on complex formation. The band at 1620 ± 10 cm^{-1} in the metal complexes, indicates the coordination of the azomethine nitrogen to the tin atom[6] whereas the other one is due to uncoordinated azomethine group.

Bands due to ν(C=O) and ν(C=S) modes in the ligands are observed at 1680 and 1020 cm^{-1}, respectively. These disappear in the spectra of the complexes suggesting thereby enolisation of the ligands and their chelation through alcoholic oxygen or thiolic sulphur[7]. This view is corroborated by the observation of the bands due to νC−O and νC−S modes at lower frequencies in the complexes

Further, some new bands observed in the far IR region of the metal complexes at ~565, 415 and 325 cm^{-1} are assigned to ν(Sn−O)[8], ν(Sn←N)[9] and ν(Sn−S)[10] modes respectively.

^1H NMR spectra

To substantiate further the bonding in these complexes, ^1H NMR spectra of acetoin thiosemicarbazone (a), benzoin-semicarbazone (b) and their tin derivatives (c and d) were recorded in DMSO-d_6. The chemical shift values (δ, ppm) of different protons are discussed below:

The signal due to NH proton of the ligands (a) and (b) appears at δ 10.7 and 10.8 ppm respectively; it disappears in the spectra of corresponding metal complexes. Further, broad signals observed at δ 3.9 (a) and 3.6 (b) due to OH protons in the ligands are not observed in the spectra of the corresponding tin complexes showing thereby the chelation of the ligand moeity through deprotonated alcoholic oxygen. Sharp singlets at δ 4.8 (a) and 4.6 (b) ppm due to NH_2 protons remain un-

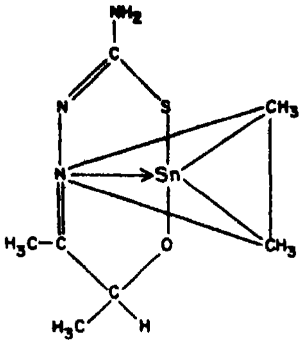

(1)

changed in the complexes showing the non-involvement of NH_2 group in complexation. A doublet due to methyl protons at δ 1.9 (a) and multiplet due to aromatic protons δ 7.7 (b) undergo deshielding in the complexes indicating the coordination of $>C=N$ nitrogen to the metal atom. Further, new signelts are observed at δ 1.3 (c) and 1.1 (d) in the complexes due to the CH_3 protons of $Sn-Me_2$ groups.

Thus, on the basis of the above spectral studies, a penta-coordinated trigonal bipyramidal structure (1) may be proposed for the tin complexes with acetoin thiosemicarbazone as ligand.

References

1 Saxena A & Tandon J P, *Polyhedron*, **3** (1984) 681.
2 Saxena A & Tandon J P, *Polyhedron*, **4** (1985) 1085.
3 Saxena A & Tabndon J P, *J antifung antibact agents Japan*, **9** (1981) 413.
4 Saxena A & Tandon J P, *Cancer Lett*, **19** (1983) 73.
5 Singh P K, Koacher J K & Tandon J P, *J inorg nucl Chem*, **43** (1981) 1755.
6 Samual B, Snaith R, Summerford C & Wade K, *J chem Soc* (A) (1970) 2019.
7 Kato S, Hori A, Shiotone H & Mizuta M, *J organometal Chem*, **82** (1974) 223.
8 Obafemi C A, Obaleye J A & Akanni M S, *Synth react inorg met org Chem*, **16** (1986) 777.
9 Saxena A, Tandon J P, Molloy K C & Zuckerman J J, *Inorg chim Acta*, **63** (1982) 71.
10 Domazetis G, Magee R J & James B D, *J inorg nucl Chem*, **43** (1981) 1351.

Indian Journal of Chemistry
Vol. 27A, February 1988, pp. 156-159

Fe(III) Complexes of 2-Mercaptocarboxylic Acids

L D DAVE[*] & V PANDIT RAO[†]
University Department of Chemistry, Bhavnagar University,
Bhavnagar 364 002

Received 17 *November* 1986; *revised and accepted* 25 *June* 1987

Fe(III) complexes of four 2-mercaptocarboxylic acids, HL (R.SH CH.COOH; R = CH_3, C_2H_5, C_3H_7 and C_4H_9) have been prepared and characterised on the basis of elemental and thermal analysis, molecular weight, magnetic moment and electronic, IR and Mössbauer spectral studies. *All the complexes are* polymeric in nature. The ligand with R = CH_3 forms a tris chelate, $[FeL_3]_n$, whereas the other three ligands form bis chelates, $[FeL_2X]_n$, where X = Cl^- or NO_3^-.

Literature survey revealed that complexes of 2-mercaptocarboxylic acids with only a few metal ions have been prepared[1-7]. Therefore, we thought it worthwhile to investigate the reactions of Fe(III) with 2-mercaptocarboxylic acids. The acids chosen were 2-mercaptopropionic acid, HMP; 2-mercaptobutyric acid, HMB; 2-mercaptovaleric acid, HMV; and 2-mercaptocaproic acid, HMC.

The 2-mercapto acids used in this study were prepared by the known procedure[8]. For preparing the complexes, equimolar amounts of the metal salt (ferric chloride or nitrate, AR) solution in water and the ligand solution in methanol were mixed and stirred continuously at room temperature till a brown solid was obtained. It was filtered and washed repeatedly with hot distilled water to remove excess of metal ion solution. It was then washed with acetone to remove the unreacted ligand. 2-Mercaptopropionic acid formed the complex only when the *p*H was raised to 5.0. Preparation of complexes with other 2-mercapto acids did not require any *p*H adjustment. The Fe(III) complexes of 2-mercaptovaleric and 2-mercaptocaproic acids were recrystallised from chloroform.

Magnetic susceptibility measurements were carried out using the Gouy method at room temperature. The molecular weight measurements were done by the Rast method using biphenyl as the solvent (m.p., 71°C). Electronic spectra of the complexes were recorded in chloroform solution on a Toshniwal spectrophotometer. Infrared spectra of ligands (neat) and the complexes (KBr pellet) were recorded on a Perkin-Elmer spectrophotometer model 283 in the range 4000-250 cm^{-1}. The Mössbauer spectra were recorded on a electromechanical constant velocity spectrometer. The source was 5.2 mc $^{57}Co(Pd)$.

The complexes obtained were reddish-brown solids which were insoluble in water and common organic solvents. They, however, showed a regular gradation in solubility in chloroform and DMF. The complexes of HMP and HMB were insoluble even in hot chloroform while those of HMV and HMC were soluble in hot chloroform and DMF.

The elemental analyses (Table 1) show that HMP forms a tris chelate, $Fe(MP)_3$, whereas the other three ligands form bis complexes having general formula FeL_2X, where L = HMB or HMV or HMC and X = Cl^- or NO_3^-. The compounds were found to be non-electrlytes in $CHCl_3$ and DMF. The molecular weight measurements gave large values in the range 5,000-10,000 for the $Fe(MV)_2X$ and $Fe(MC)_2X$ complexes. The complexes of HMP and HMB were insoluble even in biphenyl. Thus, it is concluded that these complexes are polymeric in nature. Thermal analysis (DTA & TGA) of all the complexes in air showed the absence of water; the complexes were stable upto 160°C.

Characteristic absorption band for νS-H, appearing at 2550 cm^{-1} in the IR spectra of the ligands, was lowered to 2380 cm^{-1} in the spectra of the complexes. This indicates that the sulphur of -SH group coordinates to metal without getting deprotonated. A broad band occurring in the spectra of ligands in the range 3300-2700 cm^{-1} was assigned to νOH of the hydrogen bonded entity SH....O. It was observed around 3140 cm^{-1} in the spectra of complexes. The out-of-plane O-H deformation mode was observed in all the complexes at 700-680 cm^{-1} while it was found at 720 cm^{-1} in the ligands. The ν_{as} COO and ν_s COO modes of the ligands occurring at 1420 and 1610 cm^{-1}, respectively, got shifted to 1405 and 1600 cm^{-1} respectively in the spectra of the complexes.

From the above discussion, it appears that all the mercapto acids behave as monobasic bidentate ligands in which -SH is not deprotonated. In all the complexes νM-O band is found near 400

[†] Present address: Birla Institute of Scientific Research, Asmangadh Palace, Malakpet, Hyderabad 500 036

Table 1 — Analytical Data of Fe(III) Complexes with 2-Mercaptocarboxylic Acids

Complex	Found (Calc.) %					Mol.wt.	μ_{eff} (B.M.)
	C	H	S	Cl	Metal		
$Fe(MP)_3$	29.00 (29.12)	3.96 (4.04)	25.84 (25.88)	—	15.10 (15.05)	—	2.90
$Fe(MB)_2Cl$	29.32 (29.16)	4.33 (4.25)	19.43 (19.44)	10.59 (10.77)	16.85 (16.96)	—	2.95
$Fe(MV)_2Cl$	33.87 (33.58)	5.33 (5.03)	18.02 (17.91)	9.82 (9.93)	15.60 (15.63)	10050	3.00
$Fe(MC)_2Cl$	37.58 (37.37)	5.81 (5.70)	16.58 (16.61)	9.30 (9.21)	14.42 (14.49)	8100	3.20
$Fe(MB)_2NO_3$	26.69 (26.95)	4.13 (3.93)	17.90 (17.98)	—	15.58 (15.69)	—	3.16
$Fe(MV)_2NO_3$	31.08 (31.26)	4.73 (4.68)	16.70 (16.67)	—	14.42 (14.54)	10000	3.20
$Fe(MC)_2NO_3$	34.72 (34.96)	5.53 (5.34)	15.58 (15.53)	—	13.51 (13.56)	7020	3.17

cm^{-1} while vM-S mode appears at 320 cm^{-1} indicating that sulphur is taking part in complex formation. These bands are of medium intensities; no bands were observed in low frequency region of ligand IR spectra. Fe-Cl bands were not observed upto 250 cm^{-1}; in polymeric compounds the briding vM-Cl frequencies have been shown to occur below 250 cm^{-1} (ref.9). Hence, it is concluded that chloride acts as a bridging centre between the two iron atoms. In nitrato complexes the presence of spectral bands at ~1270(s), ~1485(s), ~970(s), ~820(m), 710(w) and 745(w) suggests[10-12] that NO_3 groups behave as bidentate and bridging centres. The N-O stretching frequencies at 1485, 1270 and 970 cm^{-1} indicate[13] the presence of bridging nitro groups. The bands at 300 and 280 cm^{-1} in nitrate complexes are assigned[14,15] to the M-O stretching vibrations of nitrate.

The magnetic moments of all the solid complexes are in the ranges 3.1-3.2 BM. This indicates a condensed system for all these complexes due to antiferromagnetic coupling either directly through a metal-metal bond or through super-exchange via oxygen, sulphur or chlorine atoms (structures I and II).

The complexes with propionic, butyric and valeric acids were not soluble enough in $CHCl_3$ for spectral study. Electronic spectra of $Fe(MC)_2$ Cl/NO_3, taken in chloroform, exhibited three absorption bands at 470 nm ($\varepsilon = 354$), 550 nm (133) and 640 nm (25) which may be assigned to transitions ^4E_g, $^4A_{1g} \leftarrow {}^6A_{1g}$, $^4T_{2g} \leftarrow {}^6A_{1g}$ and $^4T_{1g} \leftarrow {}^6A_{1g}$, respectively. These occur as shoulders on a broad C T band and hence have higher intensities.

Mössbauer spectra of $Fe(MP)_3$, $Fe(MB)_2X$ and $Fe(MV)_2X$ ($X = Cl^-$ or NO_3^-) were recorded at room temperature. This isomer shifts, δ mm/sec (relative to sodium nitroprusside), quadrupole splittings, ΔE_Q (mm/sec) and internal field, H (kG) of five complexes are given in Table 2. All the complexes, show hyperfine splitting with six peaks; this could be due to the development of an internal magnetic field due to spin-ordering leading to ferromagnetic or antiferromagnetic exchange.

Sometimes hyperfine splitting is observed even in paramagnetic substances because of large spin relaxation times as compared to nuclear precession. rates[16]. In the present studies, the observed magnetic moments are lower than even the "spin-only" values suggesting the presence of antiferromagnestism. The consequent ordering of spins would give rise to strong internal field which would cause Zeeman splitting of nuclear bands. The higher level with $I = 3/2$ as well as the ground level with $I = 1/2$ will further split into four ($M_I = +3/2, +1/2, -1/2, -3/2$ and two ($M_I = +1/2, -1/2$) levels[17] giving six lines ($\Delta M_I = \pm 1$ or 0). Hyperfine splitting is known to occur in polymeric complexes, but it usually occurs at low temperatures[18]. Room temperature Mössbauer spectra generally give a doublet which develops structures at low temperatures. Our compounds are probably the first to exhibit hyperfine structure at room temperature. The isomer shift in all the complexes is of an order compatible with an oxidation number +3 for iron in the complexes. Hence, no reduction of Fe(III) to Fe(II) through reaction with S-H bond seems to have occurred. IR spectra do not show any band due to S-S bond, but show a distinct, weak, S-H stretching

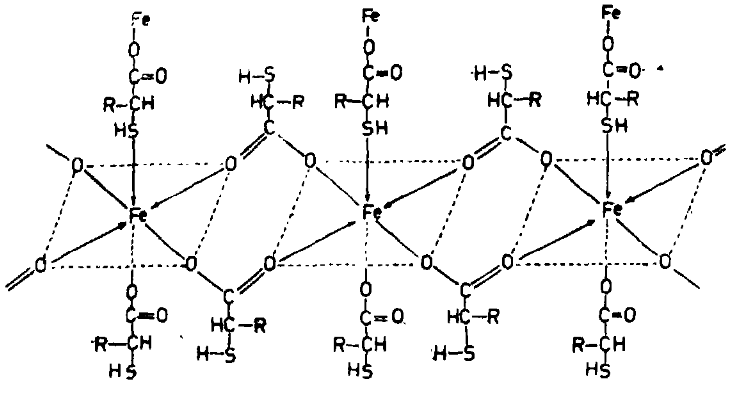

(I), $Fe(MP)_3$

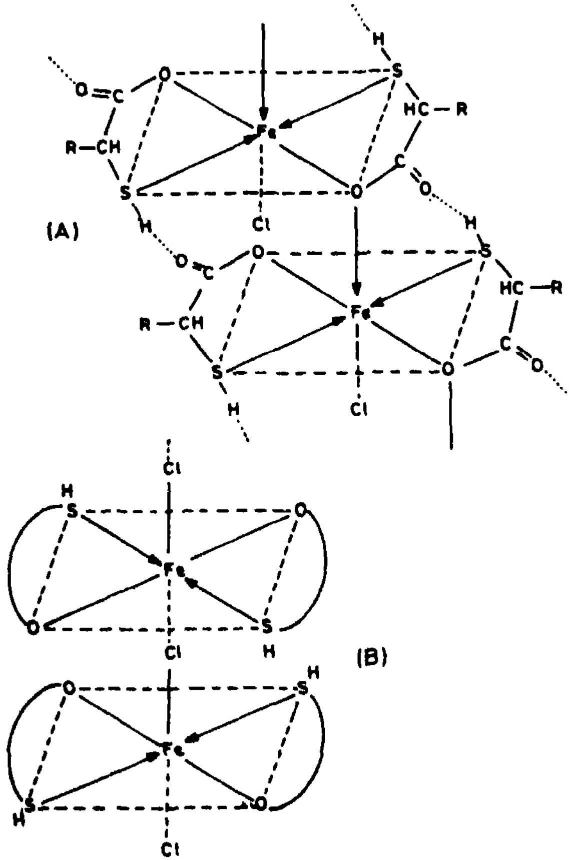

(II), FeL_2X, Where L=MB,MV,MC & X = Cl or NO_3

Table 2 — Mössbauer Parameters for Iron Complexes

Complex	δ (mm/sec)	ΔE_q (mm/sec)	H (kG)
$Fe(MP)_3$	0.54	1.64	635.2
$Fe(MB)_2Cl$	0.35	1.86	544.5
$Fe(MV)_2Cl$	0.29	2.00	544.5
$Fe(MB)_2NO_3$	0.64	1.64	594.0
$Fe(MV)_2NO_3$	0.68	1.50	598.1

vibration. The isomer shift value, suggestive of *s*-electron density in the vicinity of the nucleus, is quite different for $[Fe(MP)_3]_n$ compared to those for other complexes. It suggests a different structure for $[Fe(MP)_3]_n$ from those of other complexes (structure I). The isomer shifts are lower for chloro complexes compared to those for the corresponding nitrato complexes. This would suggest greater *s*-electron density near the Fe nucleus in the chloro complexes. The more electronegative nitro groups seem to draw electrons away from the Fe nucleus.

The nuclear quadrupole splitting indicates asymmetry around the nucleus. Fe(III), being a symmetric ion ($t_{2g}^3e_g^2$), should not have valency contributions to ΔE_q and hence the asymmetry may arise mainly from lattice-related causes only. Since the near neighbours around Fe(III) are different (O,S,Cl), such a quadrupole splitting is expected.

The internal field calculations gave quite high values. It is highest (635 kG) for $[Fe(MP)_3]_n$, again pointing to a different structure for it. The observation of hyperfine splitting in the complexes confirms antiferromagnetic coupling and polymeric nature of the Fe(III) complexes.

The authors are grateful to the Director, CSMCRI, Bhavnagar, for permitting them to use the scientific equipment and the library of the Institute. The authors are also thankful to Prof R G Kulkarni, Physics Department, Saurastra University, Rajkot for facility to record Mössbauer spectra.

References

1 Srivastava S K, Srivastava P C & Nigam H L, *Indian J Chem*, **10** (1972) 223.

2 Union Francaise commercial et. Industrelle, Er.(1953) 1036; *Chem Abst*, **52** (1958) 17631.

3 Hane Schwarzkoft, *Ser*, **501** (1957) 1958.

4 Saxena R S, Singh P & Mittal M C, *Indian J Chem*, 7 (1969) 1149.

5 Bhattacharya P K & Reddy M V, *Indian J Chem*, 7 (1969) 282.

6 Srivastava S K, Pandeya K B & Nigam H L, *Indian J Chem*, **12** (1974) 530.

7 Srivastava S K, Pandeya K B & Nigam H L, *Indian J Chem*, **13** (1975) 498.

8 Nicolet B H & Bate L F, *J Am chem Soc*, **49** (1927) 2064.

9 Postmus C, Ferraro J R, Quattrochi A & Nakamoto K, *Inorg Chem*, **8** (1969) 1851.

10 Addision C C, Logan N & Wallwork S C, *Quart Rev*, **25** (1971) 289.

11 Curtis N F & Curtis Y M, *Inorg Chem*, **4** (1965) 804.

12 Bannister E & Cotton F A, *J chem Soc*, (1960) 2276.

13 Field B D & Hardy C J, *Quart Rev*, **18** (1964) 361.

14 Topping G, *Spectrochim Acta*, **21** (1965) 1743.

15 Nuttal R H & Tylor D W, *Chem Commun*, (1968) 1417.

16 Wertheim G K, *Mössbauer effect principles and applications* (Academic Press, New York) 1964.

17 Mathur H B, *Spectroscopy in inorganic chemistry*, Vol 1, Edited by C N R Rao & John R Ferraro (Academic Press, NY) 1970, 362.

18 Greenwood N N & Gibbs T C, *Mössbauer spectroscopy* (Champman and Hall Ltd, London) 1971, 206.

Indian Journal of Chemistry
Vol. 27 A, February 1988, pp. 160-162

Synthesis & Characterisation of Oxovanadium(IV), Manganese(II), Iron(II), Cobalt(II), Nickel(II) & Copper(II) Complexes of N-(4-Methyl-8-acetoumbelliferonylidene)-N'-(salicyloyl)hydrazine

P VENKATESWAR RAO
Department of Chemistry, Nizam College, Hyderabad 500 001
&
N RAMA RAO & M C GANORKAR*
The Birla Institute of Scientific Research, Asmangadh, Palace, Malakpet, Hyderabad 500 036

Received 27 *November* 1986; *revised and accepted* 26 *May* 1987

Complexes of oxovanadium(IV), Mn(II), Fe(II), Co(II), Ni(II) and Cu(II) with a new ligand, N-(4-methyl-8-acetoumbelliferonylidene)-N'-(salicyloyl)hydrazine (MAUSH), have been synthesised and characterised on the basis of analytical, conductivity, thermal, magnetic moment and infrared and electronic spectral data. The analytical data show that the stoichiometry of the complexes is 1:1 (metal to ligand). All the complexes have the general composition $[ML.xH_2O]_n$ where L = MAUSH, x = 0, 1 & 2 and n = 2,3,4, . . . n except in the case of Co(II) where the complex formed is $[Co(MAUSH).2H_2O]_2$. Oxovanadium(IV), Mn(II), Fe(II), Cu(II) and Ni(II) complexes are polymeric in nature; the first four complexes are assigned octahedral geometries while Ni(II) complex is assigned a square-planar geometry. Co(II) complex has been assigned a dimeric octahedral stereochemistry with enolic oxygen acting as bridging centre. Ligand field parameters like *Dq* and LFSE have been calculated.

In continuation of our earlier studies on some transition metal complexes of benzoyl hydrazones, which are potential fungicides[1], we report here the synthesis and structural studies of some dimeric and polymeric transition metal complexes with N-(4-methyl-8-aceto umbelliferonylidene)-N'-(salicyloyl)hydrazine (MAUSH).

4-Methyl-8-acetylumbelliferone was prepared by the reported procedure[2]. Salicylhydrazide was synthesised using the reported method[3]. All the other chemical used were of AR grade and the solvents were used after purification.

The ligand, N-(4-methyl-8-acetoumbelliferonylidene)-N'-(salicyloyl)hydrazine (MAUSH) (I) was prepared by refluxing one mole of 4-methyl-8-acetylumbelliferone with one mole of salicylhydrazide in methanol for about one hour at *p*H ~ 7. The yellow powdery substance that separated out was filtered, washed with methanol and petroleum ether (60-80°) and dried *in vacuo*. It was recrystallised from dimethylformamide, m.p. 284°C.

[Found: C, 64.80; H, 4.58; N, 7.98. $C_{19}H_{16}N_2O_5$ requires: C, 64.77; H, 4.55; N, 7.95%]. IR: 3300-2900 (νNH and H-bonded νOH)[4], 1720 (νC = O lactone), 1630 (νC = O amide), 1600 (νC = N)[5], 1520 (νC − O phenolic of salicyl hydrazide), 1480 (νC − O phenolic of AMU)[6], 1060 (νN − N) and 1020 cm^{-1} (νC − O − C)[2]; PMR(DMSO-d_6): δ 2.3 (3H, *s*, a − CH_3), 3.1 (3H, *s*, b − CH_3), 5.85 (1H, *s*, C_3 − H), 6.5-6.65 (1H, *d*, C_5 − H), 7.3-7.8 (1H, *d*, C_6 − H)[7], 8.2-8.5 (2H, *d*, ArOH) and 12.2 (1H, *s*, enolic OH).

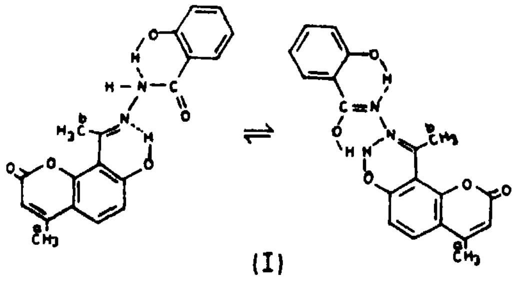

(I)

Preparation of the complexes

For the preparation of the metal chelates, hot ethanolic solutions of the respective metal chloride (0.01 mol in 20 ml) and the ligand (0.01 mol, 3.52 g in 50 ml) were mixed and the *p*H of the reaction mixture was adjusted to ~ 8; the contents were refluxed for about three hours on a water bath. During the refluxion the metal chelates separated out. The metal chelates thus separated were filtered, washed successively with ethanol and petroleum ether (60-80°) and dried *in vacuo*. In the preparation of Fe(II) and oxovanadium(IV) complexes, aqueous ethanolic solutions of ferrous ammonium sulphate and vandyl sulphate were used respectively.

Analytical and physicochemical measurements were carried out as reported earlier[8].

All the metal chelates are distinctly coloured, stable towards air and moisture, insoluble in common organic solvents but partially soluble in DMF, DMSO and dioxane, and decompose at high temperatures. The analytical data (Table 1) of the metal complexes show that all the metal chelates have 1:1 (metal to ligand) stoichiometry. Molar conductance values of the complexes (7.8-20 mhos cm^2 mol^{-1}) in DMF (10^{-3} *M*) at 30°C suggest their non-ionic character. All the complexes except the Co(II) complex have a general composition $[ML.xH_2O]_n$ where L = MAUSH, x = 0, 1 & 2, n = 2, 3, 4 . . . n.

Infrared spectra of all the complexes show the absence of νC = O (amide, carbonyl), present at 1630

Table 1—Characterisation Data of the Complexes of MAUSH.

Complex	Found (Calc.) %				$\mu_{eff.}$ (B.M.)	Electronic spectral data		
	Metal	C	H	N		λ_{max} (cm^{-1})	*Dq* (cm^{-1})	LFSE (kJ mol^{-1})
$[VO\ MAUSH \cdot H_2O]_n$	11.74 (11.70)	52.50 (52.43)	3.73 (3.70)	6.48 (6.43)	1.84	13000, 17500, 23300, 27750	1300	62.20
$[Mn\ MAUSH \cdot 2H_2O]_n$	12.40 (12.45)	51.68 (51.72)	4.05 (4.11)	6.32 (6.35)	5.90	8350, 15700, 25000, 27777	835	0
$[Fe\ MAUSH \cdot 2H_2O]_n$	12.60 (12.64)	51.64 (51.60)	4.16 (4.07)	6.38 (6.33)	5.20	10500, 27000	1050	50.24
$[Co\ MAUSH \cdot 2H_2O]_n$	13.28 (13.23)	51.40 (51.25)	4.13 (4.08)	6.37 (6.29)	4.20	8950, 18100, 28000	908.7	86.95
$[Ni\ MAUSH]_n$	14.41 (14.35)	55.66 (55.79)	3.53 (3.45)	6.89 (6.85)	Diamagnetic	18800, 25700	1880	552.30
$[Cu\ MAUSH \cdot 2H_2O]_n$	14.15 (14.12)	50.65 (50.72)	3.89 (4.03)	6.17 (6.23)	1.94	15000, 25000	1500	107.65

cm^{-1} in the ligand, and the presence of a new band characteristic of νC – O (enolic) at 1230-1250 cm^{-1} indicating that the ligand undergoes tautomeric change to its enol form in metal chelate formation. The spectra of all the complexes except that of Ni(II) complex show a broad crest in the region 3550-3200 cm^{-1} which can be attributed to the presence of coordinated water. This is well supported by a non-ligand band at 830-840 cm^{-1} region. The spectra of all the complexes except that of Co(II) complex display downward shift of 40 cm^{-1} in νC = O (lactone) frequency which confirms participation of C = O (lactone) in coordination[2]. A negative shift in νC = N to the extent of 20 cm^{-1} in all the metal chelates suggests participation of azomethine group in complexation. This is further supported by an upward shift in νN – N to the extent of 20 cm^{-1}. The magnitude to this positive shift (10-20 cm^{-1}) indicates the monodentate linkage[9] of $>N-N<$ residue. A positive shift in νC – O (phenolic) to the extent of 10-15 cm^{-1} indicates its involvement in complexation[2]. The absence of νC = O (amide), present at 1630 cm^{-1} in the ligand, and the appearance of a new band at 1230-1235 cm^{-1} in the spectra of all the chelates, except that of Co(II) complex, indicates the participation of C – O (enolic) group in coordination[7]. The non-participation of C – O (phenolic) of salicylhydrazide moiety in coordination is supported by the presence of a crest in the region 3200-2800 cm^{-1} which is due to the hydrogen-bonded νOH. The νC – O (phenolic) at 1520 cm^{-1} also remains unaltered. In donor systems comparable to MAUSH, a shift in νC – O (phenolic) of > 25 cm^{-1} has been interpreted by some earlier workers to indicate the formation of a phenoxo bridge in magnetically condensed complexes. Such a positive shift is not observed in νC – O (phenolic) of these complexes. But in the spectrum of Co(II) complex the shift in νC – O (enolic) is > 25 cm^{-1} (from 1230 to 1260 cm^{-1}). Hence, the formation of enolic oxygen bridge is proposed. A strong band at 980 cm^{-1} is assigned to νV = O[10]. New bands observed in the region 400-600 cm^{-1} are assignable to νM – O and νM – N vibrational modes[11]. From the infrared spectral data it has been concluded that the ligand behaves in a dibasic tetradentate manner with O:N:O:O donor sequence in all the complexes except in the Co(II) complex where it acts as a dibasic tridentate ligand with O:N:O donor sequence.

Thermogravimetric analysis was carried out to ascertain the presence of coordinated water in these metal chelates. It shows a mass loss of one mol of coordinated water per mol of complex in the case of oxovanadium(IV) and Fe(II) complexes while in the case of Mn(II), Co(II) and Cu(II) complexes the mass loss is two mol of coordinated water per mol of complex.

The magnetic moments of oxovanadium(IV) and Cu(II) complexes agree well with the proposed stereochemistries[10]. Mn(II) and Fe(II) complexes have high-spin octahedral geometries[12]. The Co(II) complex possesses a low magnetic moment value of 4.20 B.M. which is characteristic of magnetically dilute octahedral complexes due to their metal-metal interactions[13]. Ni(II) complex is orange in colour and diamagnetic.

The electronic spectral data of the complexes are given in Table 1. The oxovanadium(IV) complex shows three spectral bands which are assigned to three transitions $^2B_2 \rightarrow {}^2E$; $^2B_2 \rightarrow {}^2B_1$ and $^2B_2 \rightarrow {}^2A_1$ respectively in an octahedral environment; another band is present which is assigned to a charge-transfer transition[10]. The Mn(II) complex exhibits weak absorption bands which are not of any help in assigning the geometry[14]. The Fe(II) complex displays two electronic spectral bands which are assigned to the $^5T_{2g} \rightarrow {}^5E_g$ transition and a charge-transfer transition respectively. The Co(II) complex exhibits three spectral bands

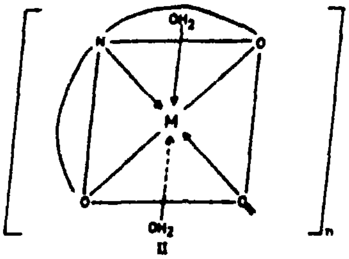

II

M = Mn, Fe, Cu and V=O (with one coordinated water)

which are assigned to the transitions ${}^4T_{1g}(F) \rightarrow {}^4T_{2g}(\nu_1)$ and ${}^4T_{1g}(F) \rightarrow {}^4T_{1g}(P)(\nu_3)$ and charge-transfer respectively in an octahedral field[14,15]. The electronic spectral parameters of the Co(II) complexes are as follows[14]: $Dq = 908.7\ \mathrm{cm}^{-1}$, $B' = 699\ \mathrm{cm}^{-1}$, $\beta = 0.72$, $\beta^{\circ} = 28\%$. The reduction in the Racah parameter from the free ion value of 971 cm^{-1} and in β° value of 28% testify to the presence of strong M−L covalent bonding in these complexes. Two main spectral bands observed in Ni(II) complex are assigned to ${}^1A_{1g} \rightarrow {}^1A_{2g}$ and ${}^1A_{1g} \rightarrow {}^1B_{1g}$ transitions[14]. The Cu(II) complex exhibits a broad band which is assigned to ${}^2E_g \rightarrow {}^2T_{2g}$ transition[14]; another band is observed due to charge-transfer transition. The Dq and LFSE values of these complexes have been calculated[14,16] (Table 1) and they show that the Cu(II), Ni(II), Co(II) and oxovanadium(IV) complexes are more stabilised than the other complexes.

On the basis of the above data it is proposed that oxovanadium(IV), Mn(II), Fe(II), Cu(II) and Ni(II) complexes are polymeric with the first four complexes in octahedral (II) and Ni(II) complex in square-planar geometries (III). The Co(II) complex has been assigned a dimeric octahedral stereochemistry (IV).

The authors are thankful to the Principal, Nizam College, Hyderabad, for providing laboratory facilities. Two of the authors (PVR & NRR) are grateful to the CSIR, New Delhi for the financial assistance.

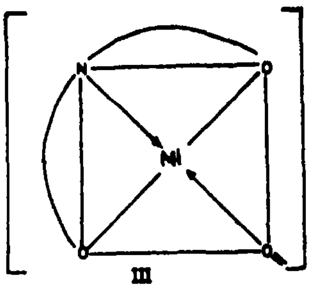

III

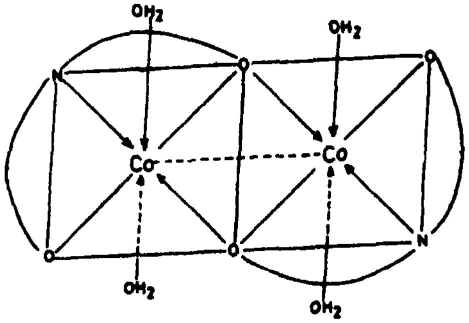

IV

References

1 Surya Rao D & Ganorkar M C, *J Indian chem Soc*, **58** (1981) 217.
2 Tyaga Raju V J, Ranbaore Villas, Atre Vasudha & Ganorkar M C, *J Indian chem Soc*, **59** (1982) 199.
3 Ito M, *Chem Abstr*, **58** (1963) 11346.
4 Rama A K & Shah J R, *J Indian chem Soc*, **58** (1981) 1100.
5 Dutta R L & Das B R, *Indian J Chem*, **23A** (1984) 654.
6 Syamal A& Kumar D, *Indian J pure appl Phys*, **21A** (1983) 87.
7 Syamal A & Maurya M R, *Indian J Chem*, **23A** (1984) 950.
8 Venkateswar Rao P, Rama Rao N, Tyaga Raju V J & Ganorkar M C, *Indian J Chem*, **25A** (1986) 482.
9 Aggarwal R C, Singh N K & Singh R P, *Inorg chim Acta*, **32** (1979) 187.
10 Das R C, Misra M K & Bohidar P N, *J Indian chem Soc*, **60** (1983) 286.
11 Kokot S, Harris C M & Sinn E, *Aust J Chem*, **25** (1972) 45.
12 Holm R H *et al.*, *Prog inorg Chem*, **7** (1986) 83.
13 Syamal A & Kumar D, *Transition met Chem*, **7** (1982) 118.
14 Lever A B P, *Inorganic electronic spectroscopy* (Elsevier, Amsterdam) 1968, 292-355.
15 Syamal A & Gupta B K, *J Indian chem Soc*, **59** (1982) 697.
16 Hubeey James E, *Inorganic chemistry* (Harper & Row, New York) 1978, 360.

Indian Journal of Chemistry
Vol. 27A, February 1988, pp. 163-165

Complexes of Cu(II), Ni(II), Co(II), Fe(II), Mn(II), Zn(II) & Oxovanadium(IV) with Schiff Base Derived from 2-Hydrazinopyridine & 6-Chloro-4-hydroxy-3-acetylcoumarin

(Miss) L NALANDA SHARADA & M C GANORKAR*
Department of Chemistry, Osmania University,
Hyderabad 500 007

Received 1 *December* 1986; *revised and accepted* 18 *May* 1987

Cu(II), Ni(II), Co(II), Fe(II), Mn(II), Zn(II) and oxovanadium(IV) complexes of the schiff base derived from 2-hydrazinopyridine and 6-chloro-4-hydroxy-3-acetylcoumarin have been synthesized and characterised on the basis of elemental analysis, conductivity, magnetic moment, infrared, electronic and ESR spectral data. All the chelates except oxovanadium(IV) chelate are octahedral in nature. Oxovanadium(IV) chelate is found to have square-pyramidal structure.

In continuation of our earlier work on some transition metal complexes derived from active organic molecules[1-3], we report here the synthesis and characterization of a few more transition metal complexes of schiff base derived from 2-hydrazinopyridine and 6-chloro-4-hydroxy-3-acetylcoumarin (Cl-HACPyH).

All the chemicals used were of AR grade. The schiff base was prepared by refluxing for 1 hr a mixture of 2-hydrazinopyridine and 6-chloro-4-hydroxy-3-acetylcoumarin in 1:1 molar ratio in methanol. The product obtained was crystallised from DMF (m.p. 215-216°C).

Preparation of metal chelates

Hot methanolic solutions of metal chloride and the ligand were mixed in 1:2 molar ratio with continuous stirring and the contents were refluxed for about an hour. The product thus obtained was filtered and washed with hot methanol and pet. ether and dried *in vacuo* (60-80°).

In the case of oxovanadium(IV) and Fe(II) complexes, vanadyl sulphate and aqueous ethanolic solution of ferrous ammonium sulphate respectively were used.

The complexes were analysed for metal, carbon, hydrogen, nitrogen and chlorine and the analytical data are given in Table 1. Magnetic susceptibility measurements were carried out by the method described earlier[1]. IR spectra were recorded on a Perkin-Elmer instrument.

Table 1 — Analytical Data of Complexes of Cl-HACPyH

Complex (molecular formula)	Found (Calc) %				
	Metal	C	H	N	Cl
Cu(II)(Cl-HACPyH)$_2$	8.80	53.30	3.00	11.60	9.70
(Cu $C_{32}H_{22}N_6O_6Cl_2$)	(8.81)	(53.29)	(3.05)	(11.65)	(9.71)
Ni(II)(Cl-HACPyH)$_2$	8.30	53.55	3.00	11.74	9.70
(Ni $C_{32}H_{22}N_6O_6Cl_2$)	(8.20)	(53.65)	(3.07)	(11.73)	(9.78)
Co(II)(Cl-HACPyH)$_2$	8.20	53.60	3.00	11.72	9.75
(Co $C_{32}H_{22}N_6O_6Cl_2$)	(8.23)	(53.64)	(3.07)	(11.73)	(9.77)
Fe(II)(Cl-HACPyH)$_2$	7.83	53.74	3.05	11.55	9.75
(Fe $C_{32}H_{22}N_6O_6Cl_2$)	(7.85)	(53.86)	(3.08)	(11.78)	(9.82)
Mn(II)(Cl-HACPyH)$_2$	7.70	53.59	3.00	11.75	9.72
(Mn $C_{32}H_{22}N_6O_6Cl_2$)	(7.72)	(53.94)	(3.09)	(11.79)	(9.83)
Zn(II)(Cl-HACPyH)$_2$	9.10	53.17	3.00	11.60	9.70
(Zn $C_{32}H_{22}N_6O_6Cl_2$)	(9.05)	(53.16)	(3.04)	(11.62)	(9.69)
Oxovanadium(IV)– (Cl-HAClyH)	10.55	40.40	2.30	8.65	7.35
(V $C_{16}H_{11}N_3ClO_7S$)*	(10.72)	(40.38)	(2.31)	(8.83)	(7.46)

*Satisfactory analysis for sulphur was also obtained.

Electronic and ESR spectra were recorded in nujol mull and as powder at room temperature on UV visible spectrophotometer DMR-21 and EPR spectrometer JOEL-JES-F3X respectively.

The analytical data indicate that all the complexes, except the oxovanadium complex, have 1:2 (M:L) stoichiometry. In oxovanadium(IV) complex, the metal:ligand stoichiometry is 1:1. The complexes are soluble in DMF, DMSO and dioxane.

The molar conductance values of 1×10^{-3} *M* solutions of the complexes in DMF (5-32 mho cm^{2}mol^{-1}) show them to be non-electrolytes.

4-Hydroxycoumarins are known to exist in two tautomeric forms, namely, the lactone and the chromone forms. In the case of Cl-HACPyH, two tautomeric forms I and II are possible. The forms I and II can be differentiated with the help of νC=O mode. The νC=O (lactone) absorbs above 1700 cm^{-1} while the νC=O (chromone) appears around 1650 cm^{-1}.

The IR spectrum of Cl-HACPyH shows a sharp intense band at 3000-3200 cm^{-1}, which can be assigned to νOH having strong H-bond interaction. A band at 1650-1670 cm^{-1} is assigned to νC=O vibration indicating the presence of chromone form in Cl-HACPyH. Two bands occurring at 1600 and 1270 cm^{-1} are assigned to νC=N (azomethine) and νC-O (phenolic). The bands observed in the region 1560-1430 cm^{-1} are due to νC=N and νC=C of the pyridine moiety.

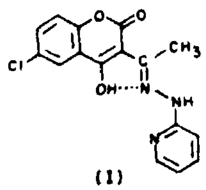

(I)

Lactone form

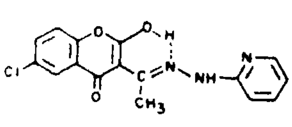

(II)

Chromone form

The free ligand band in the region 3200-3000 cm^{-1}, which is assigned to νOH having strong H-bond interaction, is absent in the spectra of all the complexes. The disappearance of the broad band is attributed to the deprotonation of the phenolic group and subsequent bonding through the oxygen[4]. Bonding through the oxygen is further evidenced by an upward shift in νC-O (phenolic)[5] by 20 cm^{-1}. The spectra of oxovanadium(IV), Fe(II) and Cu(II) complexes show νC=O in the region 1710-1700 cm^{-1} indicating the presence of lactone form of the ligand. The IR spectra of Mn(II), Co(II), Ni(II) and Zn(II) complexes show νC=O mode around 1650 cm^{-1} thus indicating the presence of chromone form of the ligand in these complexes. The >C=N- of the hydrazone moiety shows a positive shift[6] by 10-20 cm^{-1} which is assignable to coordination through the nitrogen[7]. Considerable changes have been noticed in the range of 1560-1430 cm^{-1} which are consistent with the participation of nitrogen of the pyridine ring in coordination. In the case of oxovanadium(IV) complex the non-ligand bands of medium intensity observed at 1020, 1040, 610-660 cm^{-1} can be attributed to bridging mode of SO_4 group. A strong band at 900 cm^{-1} is assigned to νV=O. On the basis of IR data it can be concluded that the ligand Cl-HACPyH acts as a monobasic tridentate ONN donor system preferring the chromone form to coordinate with Mn(II), Co(II), Ni(II) and Zn(II) ions and the lactone form to coordinate with oxovanadium(IV), Fe(II) and Cu(II). The non-ligand bands observed in the region 600-400 cm^{-1} are assigned to νM-N and νM-O respectively[8,9].

The magnetic moment and electronic spectral data of the complexes are presented in Table 2. The magnetic moment and electronic spectral data are indicative of octahedral geometry for Cu(II), Ni(II), Fe(II) and Co(II) complexes10 – 12.

Table 2 — Magnetic and Electronic Spectral Data of the Complexes of Cl-HACPyH

Complex	μ_{eff} (B.M)	Electronic spectral bands (cm^{-1}) and their assignments
Cu(II)(Cl-HACPyH)$_2$	1.73	15385 ($^2E_g \rightarrow {}^2T_{2g}$) 21052 (Charge transfer)
Ni(II)(Cl-HACPyH)$_2$	2.85	10752 ($^3A_{2g} \rightarrow {}^3T_{2g}$) 16392 ($^3A_{2g} \rightarrow {}^3A_{1g}(F)$) 22222 ($^3A_{2g} \rightarrow {}^3T_{1g}(P)$)
Co(II)(Cl-HACPyH)$_2$	4.24	8474 ($^4T_{1g} \rightarrow {}^4T_{2g}$) 21276 ($^4T_{1g}(F) \rightarrow {}^4T_{1g}(P)$)
Fe(II)(Cl-HACPyH)$_2$	5.09	10869 ($^5T_{2g} \rightarrow {}^5E_g$)
Mn(II)(Cl-HACPyH)$_2$	5.9	16600-22727
Oxovanadium(IV) (Cl-HACPyH)	1.8	12000 ($b_2 \rightarrow e$) 20000 ($b_2 \rightarrow a$) 25000 (Charge-transfer)

The $\mu_{eff.}$ value of Co(II) complex is somewhat higher, which may be due to orbital contribution. The Mn(II) complex shows a $\mu_{eff.}$ value of 5.9 B.M. which is indicative of five unpaired electrons[13]. The weak electronic spectral bands of Mn(II) complex observed in the range of 16600-22700 cm^{-1} are, however, not of much help in deciding the transitions. On the basis of analytical and magnetic moments data octahedral stereochemistry is proposed for Mn(II) also.

The oxovanadium(IV) complex possesses magnetic moment value of 1.8 B.M. which is well within the range expected for a single electron. Three bands are observed in its electronic spectrum at 12000, 20000 and 25000 cm^{-1} which are assigned to $b_2 \rightarrow e$, $b_2 \rightarrow a$ and charge-transfer transitions, respectively. These bands are consistent with a square-pyramidal geometry. Zn(II) complex is found to be diamagnetic.

ESR spectrum of Cu(II) shows g_{av} = 2.068. The small g_{av} value indicates strong interaction between the ligand and metal ion. In the case of oxovanadium(IV) complex the ESR spectrrum reveals the g_{av} value to be 1.9793 which is suggestive of a single electron and square-pyramidal geometry.

One of the author (LNS) is thankful to the CSIR, New Delhi, for the award of Junior and Senior Research Fellowships.

References

1 Venkat Reddy G, Surya Rao D & Ganorkar M C, *Indian J Chem*, **20A** (1981) 194.
2 Tyaga Raju V J, Ranbaore Vilas, Atre Vasudha & Ganorkar M C, *J Indian chem Soc*, **2** (1982) 199.
3 Atre Vasudha, Vankat Reddy G, Sharada L N & Ganorkar M C, *Indian J Chem*, **21A** (1982) 934.
4 Biradar N S, Mahale V B & Havinale B R, *Curr Sci*, **45**(1) (1976) 6.

5 Rastogi V K, Katiyar A K, Saxena R C & Kotnak, *J Indian chem Soc*, **60** (1983) 694.

6 Shukla P R & Takroo Renu, *Indian J Chem*, **19A** (1980) 137.

7 Patel M M, Patel M R, Patel M N & Patel Ratilal P, *Indian J Chem*, **20A** (1981) 623.

8 Nakamoto K, *Infrared spectra of inorganic and coordination compounds* (Wiley Interscience, New York) 1970, 159, 214, 173-175.

9 Narang K K & Agarwal A, *Inorg chim Acta*, **9** (1974) 137.

10 Lever A B P, *J chem Soc*, (1965) 1821.

11 Lever A B P, *Inorganic electronic spectroscopy* (Elsevier, New York) 1968, 320.

12 Figgis B N & Lewis J, *Progr inorg Chem*, **6** (1964) 157.

13 Holm R H, Everette (Jr) G W & Chakravorthy A, *Progr inorg Chem*, **7** (1966) 120.

Indian Journal of Chemistry
Vol. 27 A, February 1988, pp. 166-168

Some Three-coordinate Complexes of Cadmium (II)

I S AHUJA*, SHAILENDRA TRIPATHI & C L YADAVA†
Chemistry Department,
Banaras Hindu University, Varanasi 221005

Received 30 January 1987; revised and accepted 5 June 1987

Coordination compounds of cadmium(II) chloride, bromide and iodide with 2-, 3- and 4-cyanoanilines (CA) have been prepared and characterized by electrical conductance, molecular weight and infrared spectral measurements down to 180 cm^{-1}. The 1:1 cadmium(II) halide complexes with the cyanoanilines isolated in the present study are tentatively assigned neutral, monomeric three-coordinate structures in the solid state.

Although empirical formulae of cadmium(II) complexes of the types CdL_2X_2 and $CdL'X_2$ (L = monodentate ligand, L' = a bidentate ligand and X = Cl, Br or I) might suggest 4-coordination around the metal atom, they are generally 6-coordinate polymeric structures built from chains of octahedra with halogen bridges[1]. Some 1:1 complexes, e.g., $CdLX_2$ are known but these have either halogen-bridged dimeric tetrahedral structures or polymeric octahedral structures involving extensive bridging through halogens[2-5]. We now report the preparation of some cadmium(II) chloride, bromide and iodide complexes with 2-, 3- and 4-cyanoanilines which have been characterized by electrical conductance, molecular weight and infrared spectral measurements down to 180 cm^{-1}. Most of the complexes isolated have 1:1 stoichiometries (metal:ligand) and are considered as neutral species having monomeric, three-coordinate environments around cadmium(II) in the solid state.

Cadmium(II) halide complexes with the cyanoanilines were prepared by allowing an excess of the respective ligand to react with a hot solution of the cadmium(II) salt in ethanol. The mixtures were concentrated by evaporation on a water bath and the complexes which crystallized out on cooling were suction-filtered, washed with ethanol and dried at ~100°C in an air oven. Stoichiometries of the complexes isolated were established by gravimetric estimations of metal and halogen. Conductivity measurements were made on freshly prepared ~*M*/1000 solutions in absolute ethanol and in distilled water by means of a Philips conductivity bridge Model PR 9500. The infrared spectra in the rock salt region were recorded as nujol mulls supported between sodium chloride plates on a Perkin-Elmer spectrophotometer model 783. Infrared spectra in the range 650-180 cm^{-1} were recorded as nujol mulls supported between caesium iodide plates on a Perkin-Elmer spectrophotometer model 983. Apparent molecular weights were determined in distilled water at 37°C with a Mechrolab Inc vapour pressure osmometer model 301 A. Calibrations were carried out using glucose in the range 0.005-0.010 *M*. ΔR readings were recorded at intervals of 2 min each. The solutions were approximately 0.005 *M*. The values reported here are the means of three determinations in each case.

The cadmium(II) halide complexes with 2-, 3- and 4-cyanoanilines isolated in the present study (Table 1) are quite stable and soluble in water and ethanol. Molar conductances of ~*M*/1000 solutions indicate them to be non-electrolytes in ethanol but 1:2 electrolytes in aqueous solutions[6]. No infrared bands were observed in their spectra which could be attributed to water or ethanol thus establishing them to be anhydrous and free from coordinated or lattice water/ethanol.

Cyanoanilines possess two potential donor sites: (i) amino nitrogen, and (ii) the nitrile group. Further, the nitrile group may be involved in coordination through either the nitrogen or the triple bond. Coordination through nitrogen of the nitrile group invariably results in an increase[7] in νCN by at least 30 cm^{-1}. A decrease in νCN frequency is generally interpreted as resulting from coordination of the cyano group through its triple bond[8,9].

In practically all the cadmium(II) complexes studied here the νCN of the uncoordinated cyanoanilines at ~2240 cm^{-1} remains essentially unchanged thereby suggesting that the cyano group of these ligands does not participate in coordination. In the free cyanoanilines the asymmetric and symmetric NH stretching vibrations occur at ~3440 and 3360 cm^{-1}, respectively. In the cadmium(II) halide complexes these bands are lowered by ~130 cm^{-1} indicating weakening of the NH bonds[10] resulting from the electron drainage from the nitrogen atom on account of its coordination to cadmium(II).

Cadmium(II) being a d^{10} ion does not show

---

†Chemistry Department, Kamla Nehru Institute of Physical and Social Sciences, Sultanpur 228118.

Table 1 – Analytical, Melting Point, Molar Conductance, Apparent Molecular Weight and Selected Infrared Spectral Data (cm^{-1}) of Cadmium(II) Halide – Cyanoaniline Complexes

Compound (m.p., °C)	Found (Calc) %		Molar conductance (Ω^{-1} cm^2 mol^{-1})		App. molec. wt. Found (Calc.)	νCN	ν_{as}NH	ν_sNH	νCd – Cl
	Metal	Halogen	Ethanol	Water					
$Cd(2\text{-}CA)Cl_2$ (>280)	37.2 (37.2)	23.5 (23.6)	19	160	103 (301)	2240	3310	3240	227
$Cd(3\text{-}CA)Cl_2$ (>280)	37.1 (37.2)	23.4 23.6)	18	160	92 (301)	2245	3320	3240	225
$Cd(4\text{-}CA)Cl_2$ (220)	37.1 (37.2)	23.5 (23.6)	12	160	97 (301)	2240	3320	3200	223
$Cd(2\text{-}CA)Br_2$ (>280)	28.7 (28.7)	41.2 (41.0)	15	160	120 (390)	2242	3310	3260	–
$Cd(3\text{-}CA)_2Br_2$ (>280)	22.2 (22.0)	31.6 (31.5)	11	150	–	2240	3320	3260	–
$Cd(4\text{-}CA)_2Br_2$ (>280)	22.1 (22.0)	31.6 (31.5)	13	160	–	2240	3320	3240	–
$Cd(2\text{-}CA)I_2$ (220)	22.9 (23.1)	52.6 (52.5)	10	160	170 (483)	2235	3320	3220	–
$Cd(3\text{-}CA)_4I_2$ (185)	13.2 (13.4)	30.5 (30.3)	10	160	–	2230	3330	3230	–
$Cd(4\text{-}CA)I_2$ (200)	23.3 (23.1)	52.0 (52.5)	10	160	170 (483)	2240	3360	3250	–

d→*d* transitions and, therefore, information regarding the stereochemistry of cadmium(II) complexes cannot be derived from their UV and visible reflectance spectra. However, some information about their structures can be derived from the positions and multiplicities of the metal-halogen stretching frequencies in these complexes[11,12]. The 1:2 cadmium(II) halide complexes with cyanoanilines may be assigned monomeric tetrahedral structures with terminal Cd – X bonds or halogen-bridged polymeric octahedral structures. The 1:1 (metal:ligand) complexes may be assigned (i) 6-coordinate polymeric octahedral structures with only bridging halogens, (ii) 4-coordinate, halogen-bridged dimeric tetrahedral structures involving two sets of Cd – X vibrations – (a) terminal, and (b) bridging (the frequency of bridging metal-halogen vibrations is usually ~ 70 cm^{-1} lower than that of the corresponding terminal metal-halogen bonds[12]), or (iii) monomeric, three-coordinate structures with only terminal halogens.

Apparent molecular weights of the complexes determined by osmometric method are found to be one-third of their formula weights suggesting that these complexes are 1:2 electrolytes in aqueous solutions. This is in accord with their molar conductance behaviour discussed earlier. The low frequency infrared spectra of the 1:1 cadmium(II) chloride-cyanoaniline complexes exhibit absorptions at ~ 220 cm^{-1} assignable to Cd – Cl stretching modes[12], consistent with the presence of only terminally bonded[12] chlorines in the chloro complexes. Thus, the apparent molecular weight determinations and the presence of only one band due to νCd – Cl mode strongly suggest that the 1:1 cadmium(II) chloride complexes with 2-, 3- and 4-cyanoanilines have monomeric structures with three-coordinated planar environments around the cadmium(II) ions in the solid state. Molecular weights of 1:1 cadmium(II) bromide complex with 2-cyanoaniline and the cadmium(II) iodide complexes with 2- and 4-cyanoanilines also correspond to the presence of three species in aqueous solutions suggesting monomeric, three-coordinated environments around cadmium(II) in these complexes as well. However, the νCd – Br and νCd – I modes expected[1,12] at ~ 150 and ~ 100 cm^{-1}, respectively, could not be recorded as these fall outside the range of the far infrared spectrophotometer used in these studies.

We thank Prof. D W A Sharp, University of Glasgow, for recording the far infrared spectra and the UGC, New Delhi, for the award of a research associateship to one of us (C L Y).

References

1 Coates G E & Ridley D, *J chem Soc*, (1964) 166; Constable E C, *Coord Chem Rev*, **45** (1982) 329; **52** (1983) 1.

2 Schmauss G & Specker H, *Naturwissenchaften*, **54** (1967) 248; Schmauss G & Specker H, *Z anorg allg Chem*, **363** (1968) 113.

3 Evans R C, Mann F G, Peiser H S & Purdie D, *J chem Soc*, (1940) 1209; Cass R C, Coates G E & Hayter R G, *J chem Soc*, (1955) 4007.

4 Ahuja I S, Brown D H, Nuttall R H & Sharp D W A, *J inorg nucl Chem*, **27** (1965) 1105.

5 Ahuja I S & Rastogi P, *J inorg nucl Chem*, **32** (1970) 2665; Ahuja I S & Singh Raghuvir, *Inorg chim Acta*, **7** (1973) 565.

6 Geary W J, *Coord Chem Rev*, **7** (1971) 81.

7 Hathaway B J & Holah D J, *J chem Soc*, (1964) 2400.

8 Farona M F & Brewer N J, *J Am chem Soc*, **88** (1966) 3735.

9 Ford P C & Clarke R E, *J chem Soc, Chem Commun*, (1968) 1109.

10 Jangbauer M A & Curran C, *Spectrochim Acta*, **21** (1965) 641.

11 Cass R C, Coates G E & Hayter R G, *J chem Soc*, (1955) 4007.

12 Adams D M, Chatt J, Davidson J M & Gerratt J, *J chem Soc*, (1963) 2189; Deacon G B & Green J H S, *Chem Commun*, (1966) 629; Deacon G B, Green J H S & Harrison D J, *Spectrochim Acta*, **24A** (1968) 1921.

Indian Journal of Chemistry
Vol. 27A, February 1988, pp. 169-170

Synthesis & Characterization of a Neutral, Monomeric, Dinuclear Tetrahedral Manganese(II) Species

I S AHUJA*
Chemistry Department, Banaras Hindu University, Varanasi 221 005
and
C L YADAVA
Chemistry Department, Kamla Nehru Institute of Physical & Social Sciences, Sultanpur 228 118

Received 6 *March* 1987; *revised and accepted* 2 *July* 1987

A 2:3 manganese(II) bromide complex with 2-benzoylpyridine has been prepared and characterized from the results of molar conductance, molecular weight, room temperature magnetic moment, electronic and infrared spectral studies. The compound is monomeric and may have a dinuclear structure with a high-spin tetrahedral environment around each manganese(II) in the solid state.

Neutral, monomeric mononuclear manganese(II) complexes of the type MnL_2X_2, where L = a monodentate ligand and X = Cl, Br, I or NCS, which exhibit tetrahedral environments around manganese(II), are well known[1-10]. However, no report has yet been made on *monomeric dinuclear* manganese(II) species exhibiting tetrahedral coordination around the metal ion. Herein we report the synthesis of a 2:3 manganese(II) bromide complex with 2-benzoylpyridine, a potentially bidentate ligand. The complex isolated has been shown, from molar conductance, molecular weight, room temperature magnetic moment, electronic and infrared spectral measurements (down to 200 cm^{-1}), to possess a neutral, monomeric dinuclear structure exhibiting high-spin tetrahedral environment around each manganese(II) in the solid state.

The manganese(II) bromide complex with 2-benzoylpyridine was prepared by mixing together hot solutions of the metal salt and excess of the ligand in ethanol. The complex, which crystallized out on cooling, was suction-filtered, washed with ethanol and dried at ~100°C in an air oven. Mn_2(2-Benzoylpyridine)$_3Br_4$, m.p. 157°C (Found: Mn 11.3, Br 33.0 Calc.: Mn 11.2; Br 32.7%).

Conductivity measurements were made on freshly prepared ~*M*/1000 solutions in ethanol and DMF with a Philips conductivity bridge model PR 9500. Molecular weight measurements were carried out by Rast's method using camphor as the solvent. Electronic spectrum of the complex was recorded in nujol in the range 200-800 nm on a Hitachi UV/Visible spectrophotometer model 320 against nujol as a reference. Infrared spectra of the uncoordinated ligand and its manganese(II) complex were recorded in nujol on a Perkin-Elmer spectrophotometer model 783. Magnetic susceptibility was measured at room temperature by the Faraday's method with a Cahn R G Electrobalance Model 7550 using $Hg[Co(NCS)_4]$ as the standard.

The manganese(II) bromide complex with 2-benzoylpyridine, isolated in the present study, is orange coloured and soluble in ethanol and DMF, in each of which solvents it behave as an electrolyte[11]. No absorption bands were observed which could be attributed to water or ethanol in the infrared spectrum of the complex thus supporting it to be anhydrous and free from coordinated or lattice water/ethanol.

2-Benzoylpyridine possesses two potential donor sites: (i) pyridine ring nitrogen, and (ii) oxygen of the carbonyl group, and may coordinate through both or either of these sites. The infrared spectrum of the complex investigated herein shows absorption bands at 1650 and 1620 cm^{-1} due to νCO indicating thereby the presence of two types of benzoylpyridine coordination[12] (uncoordinated 2-benzoylpyridine shows νCO at 1654 cm^{-1}). Moreover, pyridine ring vibrations at 990, 603 and 401 cm^{-1} undergo significant positive shifts[13] and appear at 1012, 637 and 424 cm^{-1}, respectively. The observed frequencies of νCO and the pyridine ring vibrations strongly suggest the presence of two types of 2-benzoylpyridine molecules[13] in the complex: (i) terminally pyridine ring nitrogen bonded, and (ii) pyridine ring nitrogen as well as oxygen (carbonyl) bonded bidentate ligand acting as a bridge between two manganese(II) ions.

The room temperature magnetic moment value (6.12 B.M.) of the present compound is consistent with the presence of high-spin manganese(II)[14]. Because of the additional stability of the half-filled *d* shell, manganese(II) generally forms high-spin complexes. Since the high-spin manganese(II) complexes have an orbitally non-degenerate ^6S ground state term, the spin-only magnetic moment of ~5.92 B.M. is independent of temperature and stereochemistry. All the excited states of d^5 system have different spin multiplicities from those of the ground state term and transitions to them are spin-forbidden[15]. Because of the weak spin-orbit interactions, very weak absorption bands which are ~ 100 times weaker than the spin-allowed transitions[15] are observed. Electronic spectra of tetrahedrally coordinated manganese(II) differ[15] remarkably from the octahedral ones in (i) the number of bands, (ii) weakness of the bands, and (iii) variations in the widths of bands. Further, tetrahedral manganese(II) complexes are greenish-yellow or orange coloured[16] whereas octahedral complexes are pale-pink or almost white. Moreover, the molar absorbance values for tetrahedral geometry are[15] in the range $1.0-4.0$ while those for octahedral ones are in the range 0.01—0.04. Energy level diagrams for tetrahedrally coordinated manganese(II) indicate that three sets of absorptions, each set comprising three closely-spaced bands occur[16] in the ranges 20000-25000, 25000-28000 and 28000-50000 cm^{-1} representing transitions to the excited states ^4G, ^4D and ^4F, respectively. Because of the low Δ values of tetrahedral complexes, resolution of the first two sets of closely-spaced peaks is not observed. The overlapping of bands in the third set is also severe which makes their Gaussian analysis rather difficult. Moreover, this third set of bands occurs in the region where solvent absorptions, absorptions due to the organic groups and the charge transfer bands become pertinent and tend to obscure[16] the relatively weak $d \rightarrow d$ bands. Distinction between the ligand field and charge transfer bands cannot be made sharply if there is extensive mixing of the metal and ligand wave functions in the molecular orbitals of the complex. The observed bands in the electronic spectrum of the complex studied herein (20400, 28570 and 40000 cm^{-1}) are consistent[15-17] with the three respective transitions, ^4G, ^4D and ^4F.

The frequencies of the observed absorption bands in the electronic spectrum and the orange colour of the complex are consistent with a tetrahedrally coordinated manganese(II), as octahedral manganese(II) complexes are either pale-pink or almost colourless and exhibit[15-17] a strong absorption band at ~ 25000 cm^{-1}. In addition, the value of 10 Dq for tetrahedral manganese(II) complexes is much smaller than that for octahedral ones. The values for 10 Dq (5600 cm^{-1}) and B (728 cm^{-1}) in the present study are consistent with tetrahedral environments around manganese(II)[15-18].

The 650-200 cm^{-1} region infrared spectrum of the present complex exhibits a strong band at 225 cm^{-1} which is identified as νMn-Br mode consistent with terminally bonded metal-bromine bonds with tetrahedral environments[19] around the metal(II) ions. The observed molecular weight (530, 528) as determined by the Rast's method suggests partial fragmentation of the dinuclear species (mol. wt. 970) into mononuclear one in molten camphor. Thus, the room temperature magnetic moment value, colour, molecular weight, electronic spectrum, ligand field parameters, presence of terminally as well as bridging 2-benzoylpyridine molecules and the νMn-Br mode of the present complex strongly suggest that it is a neutral, dinuclear tetrahedral manganese(II) species (structure I).

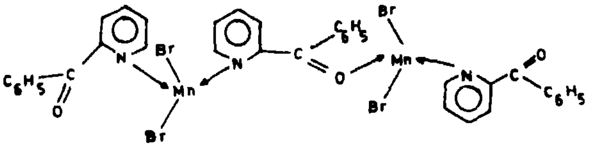

(STRUCTURE I)

We thank Dr P C Misra, Physics Department, BHU, Varanasi, for help in recording the UV/Visible spectrum.

References

1 Goodgame D M L & Cotton F A, *J chem Soc*, (1965) 3735.
2 Jorgensen C K, *Inorganic chemistry* (Academic Press, New York) 1963.
3 Colton R & Canterford J H, *Halides of the first row transition metals* (Wiley, New York) 1969.
4 Kemmitt R D W, *The chemistry of manganese, technetium and rhenium*, Edited by R D W Kemmitt & R D Peacock in *Pergamon Press texts in inorganic chemistry*, Vol 22, Chapter 37 (Pergamon Press, Oxford) 1975.
5 Dowsing R D, Gibson J F, Goodgame M & Hayward P J, *J chem Soc*, Sec A (1969) 187.
6 Dowsing R D, Gibson J F, Goodgame D M L, Goodgame M & Hayaward P J, *J chem Soc*, Sec A (1969) 1242.
7 Ahuja I S, Singh Raghuvir & Yadava C L, *J coord Chem*, **12** (1982) 59.
8 Ahuja I S & Yadava C L, *Nat Acad Sci Lett*, **9** (1986) 317.
9 Ahuja I S & Yadava C L, *Synth react inorg met-org Chem*, **16** (1986) 105.
10 Ahuja I S & Yadava C L, *Indian J Chem*, **25A** (1986) 186.
11 Geary W J, *Coord chem Rev*, 7 (1971) 81.
12 Paul R C, Shreenathan B R & Chadha S L, *J inorg nucl Chem*, **28** (1966) 1225.
13 Singh Raghuvir, Ahuja I S & Yadava C L, *J molec Struct*, **98** (1983) 175.
14 Kettle S F A, *Coordination compounds* (ELBS, Thomas Nelson, London) 1975.
15 Cotton F A & Wilkinson G, *Advanced inorganic chemistry. A comprehensive treatise* 3rd Edn, (Wiley Eastern, New Delhi) 1976.
16 Cotton F A, Goodgame D M L & Goodgame M, *J Am chem Soc*, **84** (1962) 167.
17 Dunn T M, *Some aspects of crystal field theory*, Edited by T M Dunn, D S McClure & R G Pearson (Harper & Row, New York) 1965.
18 Figgis B N, *Introduction to ligand fields* (Wiley Eastern Ltd, New Delhi) 1976.
19 Clark R J H, in *Halogen chemistry*, Vol 3, Edited by V Gutmann (Academic Press, New York) 1967.

Indian Journal of Chemistry
Vol. 27 A, February 1988, pp. 171-173

Synthesis & Characterization of Pyrazinamide Complexes with Some Uranyl Salts

I S AHUJA*, C L YADAVA† & SHAILENDRA TRIPATHI

Chemistry Department, Banaras Hindu University,
Varanasi 221 005

Received 12 *March* 1987; *revised and accepted* 5 *June* 1987

Complexes of uranyl chloride, nitrate, sulphate and acetate with pyrazinamide have been prepared and characterized on the basis of analytical data, molar conductance, electronic and IR spectral measurements down to 200 cm^{-1}. *It is shown that* pyrazinamide, though a potentially tetradentate ligand, acts only as a monodentate ligand in the present complexes bonding through one of the pyrazine ring nitrogens. Tentative stereochemistries are assigned in each case.

Although uranyl complexes with pyrazine derivative like methylpyrazine, quinoxaline and 2,3-dimethylquinoxaline have been studied earlier[1], there is no report on the uranyl complexes with pyrazinamide, a potentially tetradentate ligand. The present note describes the preparation and characterization of the complexes formed by pyrazinamide with uranyl chloride, nitrate, sulphate and acetate.

Pyrazinamide was purchased from M/s Ega Chemie, West Germany and used as such. The uranyl chloride, nitrate and acetate complexes were prepared by mixing together ethanolic solutions of the respective uranyl salt and excess of pyrazinamide. The mixtures were concentrated on a water bath and then allowed to stand. The uranyl sulphate complex was prepared by adding the ligand solution in methanol to a hot solution of uranyl sulphate in the same solvent. The complexes, which crystallized out on standing, were suction-filtered, washed with ethanol (or methanol) and dried in an air oven at ~80°C. Stoichiometries of the solid complexes were established by uranium and anion (except acetate) estimations gravimetrically. C, H and N contents of the acetate complex were determined by microanalysis.

$UO_2(Pyrazinamide)_2Cl_2$: [Found: U, 40.5; Cl, 12.0. Calc. U, 40.4; Cl, 12.1%]. $UO_2(Pyrazinamide)_2(NO_3)_2$: [Found: U, 29.4; NO_3, 19.5. Calc. U, 29.4; NO_3, 19.3%]. $UO_2(Pyrazinamide)_2SO_4$: [Found: U, 39.0; SO_4, 15.8. Calc. U, 38.8; SO_4, 15.6%]. $UO_2(Pyrazinamide)_4(OAc)_2$: [Found: U, 27.1; C, 32.8; H, 4.41; N, 19.1. Calc. U, 26.9; C, 32.6; H, 4.19; N, 19.0%].

Conductivity measurements were carried out on freshly prepared ~*M*/1000 solutions in ethanol with a Philips conductivity bridge model PR 9500. Electronic spectra of the complexes were recorded as nujol mulls in the range 200-600 nm on a Hitachi UV/visible spectrophotometer model 320. IR spectra of the uncoordinated ligand and the complexes were recorded as nujol mulls supported between sodium chloride plates (rock salt region) and thin polyethylene sheets (650-200 cm^{-1}) on a Perkin-Elmer spectrophotometer model 783 equipped with caesium iodide optics.

Analytical data indicate that uranyl chloride, nitrate and sulphate complexes have 1:2 (metal:ligand) stoichiometries but uranyl acetate has 1:4 stoichiometry. Comparison of the IR spectra of these complexes with that of the uncoordinated ligand facilitated the assignment of bands due to the uranyl moiety and the coordinated anionic groups. Strong bands due to nitrato, sulphato and acetato groups in the range 1600-1000 cm^{-1} superimposed and masked some of the bands due to the organic moiety. No absorption bands were observed which could be attributed to water or ethanol thus establishing these complexes to be anhydrous and free from coordinated or lattice water/ethanol. All the complexes are soluble in methanol and ethanol. The sulphate and acetate complexes behaved as non-electrolytes (1.6 and 2.9 Ω^{-1} cm^2 mol^{-1}, respectively) while the chloride and nitrate complexes behaved as electrolytes[2] (42 and 45 Ω^{-1} cm^2 mol^{-1}, respectively).

Pyrazinamide possesses four potential donor sites—two tertiary nitrogen atoms in the ring at 1- and 4-positions, carbonyl oxygen and NH_2 group. Owing to the fixed orientation in space, the two nitrogens cannot coordinate simultaneously to the same metal ion. However, one cannot rule out the possibility of coordination of any two sites in the ligand molecule to different metal ions (bidentate bridging ligand) resulting in polymeric structures.

Significant IR absorption bands due to the amido group in pyrazinamide are: νNH (3420 and 3300 cm^{-1}), νCO (1665 cm^{-1}) and νCN (1090 cm^{-1}). In complexes with uranyl salts the carbonyl frequency (1665 cm^{-1}) of the uncoordinated pyrazinamide did not undergo any shift. Similarly, the νNH and νCN frequencies of the uncoordinated pyrazinamide remained unperturbed or underwent slight positive shifts. This trend in the NH, CO and CN stretching modes indicates clearly that the amido group of pyrazinamide is inert towards coordination in these complexes. Although the pyrazine part of the pyrazinamide possesses two potential donor sites, their geometry precludes chelation but favours coordination of the two donor sites to different metal ions thus leading to the formation of polymeric chain structures. IR spectral studies have shown that in metal complexes where pyrazine is bonded through only one of its nitrogen atoms, medium intensity bands appear in the regions ~470, 1000 and 1250 cm^{-1}. Such bands are absent in uncoordinated pyrazine as well as in ligand-bridged polymers of long chain length. Weak bands, however, appear in metal complexes where the chain length is short. The intensity of these bands has been considered as a measure of chain length in metal complexes with this ligand[3-6].

---

†Chemistry Department, Kamla Nehru Institute of Physical & Social Sciences, Sultanpur 228 118

IR spectra of the uranyl complexes with pyrazinamide showed additional medium intensity bands at ~470, 1000 and 1250 cm^{-1} indicating clearly that pyrazinamide molecules were terminally bonded monodentate ligands[3-6]. In addition to the ligand bands shifted/modifed on account of coordination, IR spectra of the uranyl complexes showed strong bands at ~920 cm^{-1} due to ν_3 vibration of the uranyl group. The ν_1 mode of the uranyl group is IR-forbidden in the free uranyl ion which has a linear OUO arrangement. Absence of a band assignable to this mode at ~850 cm^{-1} implied that the linearity of the OUO group was maintained in all these complexes. The doubly degenerate OUO bending mode, ν_2, was observed at ~260 cm^{-1} in these complexes.

Electronic spectra of all the uranyl complexes studied herein are almost identical with slight splitting and shifting of band positions. All the complexes exhibit three absorptions[7] in the regions ~525, 425 and 250 nm. Of the three absorptions, the first band (~525 nm) is attributed to the transition from apical oxygen to *f* orbitals of the uranyl moiety. The other two bands at ~425 and 250 nm are the consequences of transitions from π-orbitals to *f* orbitals of the uranyl ion. Electronic spectra of the complexes studied are consistent with the vibronic structure of the triatomic entity of the $[UO_2]^{2+}$ group in these complexes.

The far IR spectrum of the 1:2 uranyl chloride complex with pyrazinamide shows a strong band at 250 cm^{-1} which is assigned as νU−Cl mode[8,9] in analogy with bands observed for monomeric 6-coordinated complexes of uranium(VI) containing terminally bonded chlorines. The 1:2 uranyl chloride complex with pyrazinamide is, therefore, tentatively assigned a monomeric, hexa-coordinated structure with four ligand atoms (two nitrogens from terminally ring nitrogen bonded pyrazinamide molecules and two terminally bonded chlorine atoms) forming an equatorial ring perpendicular to the linear uranyl group.

IR spectrum of the 1:2 uranyl nitrate complex with pyrazinamide shows the presence of coordinated nitrato groups[10-13] The doubly degenerate IR-active fundamentals of ionic nitrates, ν_3 at ~1360 cm^{-1} and ν_4 at ~720 cm^{-1}, are split up into their components (ν_3 to ν_1 1550 cm^{-1} and ν_4 1280 cm^{-1}; and the ν_4 to ν_3 755 cm^{-1} and ν_5 713 cm^{-1}). Moreover, additional bands appear at 1035 cm^{-1} and 809 cm^{-1} which are assigned to ν_2 and ν_6 modes, respectively, of the coordinated nitrato groups. Further, IR spectrum of this complex shows bands in the combination tone region, 1785 and 1738 cm^{-1} (separation 47 cm^{-1}) characteristic of bidentate chelating nitrato ligands[10-13]. Considering that the nitrato groups act as bidentate chelating ligands and that the pyrazinamide molecules are terminally bonded monodentate ligands, it is suggested that the 1:2 uranyl nitrate-pyrazinamide complex is monomeric containing eight-coordinated uranium(VI). The six ligand atoms (two nitrogens of the two pyrazinamide molecules and four oxygen atoms of two bidentate chelating nitrato groups) form a hexagonal equatorial ring around the linear uranyl group.

IR spectrum of the 1:2 uranyl sulphate complex shows the presence of coordinated sulphato groups[14,15]. The strong broad band expected at ~1120-1080 cm^{-1} due to triply degenerate SO stretching mode, ν_3, in ionic sulphates splits up into its components at 1050, 1130 and 1230 cm^{-1} in the IR spectrum of this complex, masking the ligand bands in this region. The triply degenerate OSO bending mode, ν_4, which occurs as a sharp well-defined band at ~610 cm^{-1} in sulphates with T_d symmetry, also splits up into its components at 602, 625 and 650 cm^{-1} in this complex. In addition to these, ν_1 and ν_2 modes, both IR-forbidden in uncoordinated sulphates, appear at 990 and 480 cm^{-1}, respectively. The frequencies due to coordinated sulphato groups are consistent with those normally associated with bidentate chelating sulphato groups[14,15] and the complex is considered to have monomeric hexa-coordinated uranium(VI) with four ligand atoms (two nitrogen atoms from the two terminally bonded monodentate pyrazinamide molecules and two oxygens of the bidentate chelating sulphato group) forming an equatorial ring around the linear OUO group.

IR spectrum of the 1:4 uranyl acetate-pyrazinamide complex shows absorption bands at 1587, 1470 and 685 cm^{-1} which are assigned to ν_{as}OCO, ν_sOCO and δOCO modes, respectively, due to coordinated acetato groups. These fundamental frequencies are consistent with the exclusive presence of terminally bonded monodentate acetato ligands[14]. From considerations of both terminally bonded monodentate pyrazinamide molecules and acetato groups, the present complex is considered to have monomeric, eight-coordinated uranium(VI) with six ligand atoms (four nitrogen atoms of the four pyrazinamide molecules and two oxygen atoms of the two acetato ligands) forming an equatorial ring around the linear uranyl group.

We thank Dr. P C Misra, Department of Physics, BHU, for help in recording the UV/visible reflectance spectra and the UGC, New Delhi, for the award of a Research Associateship to one of us (CLY).

References

1 Ahuja I S, Tikoo P K, Singh Raghuvir & Sriramulu R, *Indian J Chem*, **19A** (1980) 171.
2 Geary W J, *Coord Chem Rev*, **7** (1971) 81.
3 Lever A B P, Lewis J & Nyholm R S, *J chem Soc*, (1962) 1235; (1963) 3156, 5042; (1964) 4761.
4 Ahuja I S & Rastogi P, *J chem Soc*, **A** (1970) 2161.
5 Ahuja I S & Singh Raghuvir, *Indian J Chem*, **15A** (1977) 562.
6 Singh P P & Seth J N, *J inorg nucl Chem*, **37** (1975) 593.
7 Kim Bong I L, Miyakoe C & Imoto S, *J inorg nucl Chem*, **37** (1975) 963.
8 Day J P & Venanzi L M, *J chem Soc*, **A** (1966) 1363.
9 Ahuja I S & Singh Raghuvir, *Trans met Chem*, **2** (1977) 32.
10 Curtis N F & Curtis Y M, *Inorg Chem*, **4** (1965) 804.
11 Lever A B P, Mantovani E & Ramaswamy B S, *Can J Chem*, **49** (1971) 1957.
12 Ahuja I S, Singh Raghuvir & Singh Rajindar, *Spectrochim Acta*, **32A** (1976) 547.
13 Ahuja I S, Singh Raghuvir & Rai C P, *J molec Struct*, **49** (1978) 201.
14 Nakamoto K, *Infrared and Raman spectra of inorganic & coordination compounds* (John Wiley, New York) 1977.
15 Ahuja I S & Singh Rajindar, *Inorg nucl chem Lett*, **9** (1973) 545.

Indian Journal of Chemistry
Vol. 27A, February 1988, pp. 174-175

Lanthanide(III) Nitrate Complexes of the Schiff Base Vanillideneanthranilic Acid

JESSY CHACKO & GEETHA PARAMESWARAN*
Department of Chemistry, University of Calicut
Malapuram 673 635

Received 2 *July* 1986; *revised* 10 *March* 1987;
rerevised and accepted 12 *May* 1987

The complexes formed by the lanthanide(III) nitrates with the schiff base vanillideneanthranilic acid (H_2L) have been isolated and characterised. These compounds have the formula $[Ln(HL)_2(NO_3)(H_2O)]$ where Ln = La, Ce, Pr, Nd, Sm, Eu and Gd. The structures of the complexes have been established on the basis of IR, PMR and electronic spectroscopy and thermal analysis. The IR spectral data reveal that the ligand acts in a monovalent bidentate manner in the chelates.

Coordination compounds formed by schiff bases with *d*-transition elements have been extensively studied[1]. A survey of literature shows that corresponding compounds of lanthanide elements have been much less studied[2-8]. No systematic studies have been carried out on the reactions of the schiff base vanillideneanthranilic acid with lanthanides. In continuation of our earlier work[9-12] on vanillideneanthranilic acid complexes of *d*-transition metal ions, we report here the results of our studies on some new lanthanide(III) complexes of this schiff base.

Vanillideneanthranilic acid was prepared as reported earlier[9] (M.P., 173°C). La(III), Ce(III), Pr(III), Nd(III), Sm(III), Eu(III) and Gd(III) nitrates, supplied by BDH, were used as such. All the other chemicals were of reagent quality.

An ethanolic solution (0.01 mol) of vanillideneanthranilic acid was mixed with an ethanolic solution of lanthanide(III) nitrate (0.01 mol) and the mixture was stirred magnetically. After 5 min, dilute ammonia (1:20) was added till the solution became turbid. Soon a flocculent mass was obtained, which was stirred for 5-6 h. The precipitate was filtered, washed with hot ethanol and dried *in vacuo* over P_2O_5.

The lanthanides were determined by conversion into the corresponding oxides. Microanalyses for carbon, hydrogen and nitrogen were performed at the Central Drug Research Institute, Lucknow.

Conductance measurements were made with a Toshniwal conductivity bridge. Infrared spectra were recorded in nujol and KBr in the region 4000-200 cm^{-1} on a Perkin Elmer 257 spectrophotometer. Electronic spectra of the complexes were recorded in ethanol on a Carl Zeiss DMR-21 UV-Vis spectrophotometer. NMR spectra were obtained in DMSO-d_6 with TMS as an internal standard, using a Varian EM-390 NMR spectrometer. Thermal analyses were conducted on a Stanton recording thermobalance Model TR-1, in an atmosphere of static air. The heating rate was 4K min^{-1} and chart speed was 6 in h^{-1}.

Table 1—Analytical Data of Complexes

Complexes	Found (Calc.), %			
	C	H	N	M
$La(LH)_2(NO_3)(H_2O)$	47.62	3.52	5.64	18.33
	(47.44)	(3.45)	(5.53)	(18.29)
$Ce(LH)_2(NO_3)(H_2O)$	47.56	3.62	5.71	18.32
	(47.37)	(3.45)	(5.52)	(18.42)
$Pr(LH)_2(NO_3)(H_2O)$	47.42	3.58	5.67	18.41
	(47.32)	(3.44)	(5.52)	(18.51)
$Nd(LH)_2(NO_3)(H_2O)$	46.96	3.49	5.52	18.71
	(47.11)	(3.43)	(5.49)	(18.86)
$Sm(LH)_2(NO_3)(H_2O)$	46.68	3.35	5.49	19.31
	(46.74)	(3.40)	(5.45)	(19.50)
$Eu(LH)_2(NO_3)(H_2O)$	46.55	3.32	5.35	19.58
	(46.64)	(3.39)	(5.44)	(19.67)
$Gd(LH)_2(NO_3)(H_2O)$	46.25	3.31	5.36	20.18
	(46.33)	(3.37)	(5.40)	(20.22)

All the complexes are solid reddish-yellow compounds. These compounds are finely divided powders which decompose above 120°C without melting. The compounds could not be recrystallised due to their insolubility in common solvents. The results of the analyses of these compounds are presented in Table 1. The analytical data are in good accord with their formulation as $[Ln(HL)_2(NO_3)(H_2O)]$ where H_2L is the schiff base vanillideneanthranilic acid.

All the chelates are non-conducting (ΛM = 0.5-4.8 $ohm^{-1}cm^2mol^{-1}$) in nitrobenzene at 28 ± 2° which indicates their non-electrolytic nature.

The medium intensity band at 2700 cm^{-1} in the IR spectrum of the ligand may be due to intramolecularly H-bonded νOH; this band remains largely unaffected in the chelates providing evidence for the uninegative bidentate nature of the ligand in these complexes. The band appearing in the region 3300-3100 cm^{-1} is assigned to ν(− OH) of coordinated water. The free ligand band at 1620 cm^{-1}, assignable to νC = N, undergoes shift to lower wavenumbers (1570-1590 cm^{-1}) in the complexes indicating participation of the nitrogen atom of the azomethine group in coordination[13-16].

The asymmetric and symmetric stretching vibrations of the carboxylate group occur at 1590-1630 and 1440-1450 cm^{-1}, respectively, showing a Δν value of 140-190 cm^{-1}. these observations suggest that the present compounds contain monodentate carboxylate group[15,17,18]. The IR spectrum shows bands around 1290, 1030 and 745 cm^{-1} corresponding to the ν_1, ν_2 and ν_3 vibrations of unidentate nitrate group[19]. The formation of M—N and M—O bonds is further supported by the appearance of ν(M—N) and ν(M—O) in the regions 400-600 and 350-440 cm^{-1} respectively in the spectra of the chelates[20].

The NMR spectrum of vanillideneanthranilic acid in DMSO-d_6 is characterised by four signals at δ9.5, 8.7, 7.2 and 3.8 and they have been attributed to the various proton resonances due to —OH, —HC=N, phenyl and methoxy groups respectively. In the spectra of the complexes, the resonance due to the —OH group does not disappear but the resonance due to the azomethine proton shifts to upfield due to shielding effect and merges with proton signal at 7.3δ. These observations suggest that the azomethine nitrogen coordinates with Ln(III).

The electronic spectrum of the ligand shows one absorption maximum due to $n \rightarrow \pi^*$ transition at $\approx$ 330 nm. The spectrum below 300 nm ($\pi \rightarrow \pi^*$) region has not been investigated. The very broad band observed in the visible region with absorption maximum around $\approx$ 380 nm in all the complexes may be assigned to the very strong ligand to metal charge-transfer transition.

The thermogravimetric studies of lanthanide(III) chelates show mass loss corresponding to one water molecule around 160°C. Above this temperature, the complexes undergo continuous decomposition and oxidation to give the stable oxides.

References

1 Holm R H, Everett (Jr) G W & Chakravorty A, *Progress in inorganic chemistry*, Vol. 7 (Interscience, New York), 1964,83.

2 Dutt N K & Nag K, *J inorg nucl Chem*, **30** (1968) 2493.

3 Yamada S, Yamanonchi K & Kuma H, *Bull chem Soc Japan*, **44** (1971) 1448.

4 Isobe T, Kida S & Misumi S, *Bull chem Soc Japan*, **40** (1967) 1867.

5 Yamada S, Yamanonchi K & Kuma H, *Synth React inorg met org Chem*, **1** (1971) 9.

6 Butter E, Lorenz B & Hayer E, *J prakt Chem*, **34** (1966) 30.

7 Durham D A & Hart F A, *J inorg nucl Chem*, **31** (1969) 145.

8 Smith G D, Conghlin C N, Mozhar-ul-Haque & Hart F A, *Inorg Chem*, **12** (1973) 2654.

9 Chacko J & Parameswaran G, *J therm Anal*, **29** (1984) 3.

10 Chacko J & Parameswaran G, *Indian J Chem*, **24A** (1985) 977.

11 Chacko J & Parameswaran G, *J Indian chem Soc*, **63** (1986) 774.

12 Chacko J & Parameswaran G, *J Indian chem Soc*, **57** (1980) 95.

13 Olszewski E J & Martin D F, *J Inorg nucl Chem*, **26** (1964) 1577.

14 Dutta R L & Sengupta G P, *J chem Soc*, **48** (1971) 33.

15 Nakamoto K, *Infrared spectra of inorganic and coordination compounds* (John Wiley, New York) 1966.

16 Sacconi L & Campigli U, *Inorg Chem*, **5** (1966) 606.

17 Curtis N F, *J chem Soc*, **7A** (1968) 1579.

18 Dey K & Ray K C, *J Indian chem Soc*, **50** (1973) 66.

19 Ueno K & Martell A E, *J phys Chem*, **60** (1956) 1270.

20 Nakamoto K, *Spectroscopy and structure of metal chelate compounds* (John Wiley, New York) 1968.

Indian Journal of Chemistry
Vol. 27 A, February 1988, pp. 176-178

Analysis of Chromium(III) by a Kinetic Method

S A CHIMATADAR, G S GOKAVI, S T NANDIBEWOOR & J R RAJU*

Department of Chemistry, Karnatak University,
Dharwad 580 003

Received 5 *February* 1987; *revised and accepted* 26 *June* 1987

Catalysis by chromium(III) of the cerium(IV) oxidation of arsenic(III)/allyl alcohol in acid medium has been utilized to propose a kinetic method of analysis of chromium(III). The analysis can be carried out either titrimetrically or spectrophotometrically. Interferences by different ions have been studied. The method enables analysis of chromium(III) in the range of 10-40 μg per ml.

Methods of analysis of chromium(III) usually involve its oxidation to chromium(VI) state followed by a titrimetric or colorimetric procedure[1]. The complexometric method for the estimation of chromium(III) involves prolonged boiling with EDTA and back titration of the latter[2]. A recent micro method[3] of estimation of chromium(III) utilizes conversion of the metal to its pyridylazoresorcinol (PAR) complex in presence of triethanolamine and spectrophotometric estimation of the complex. Micro amounts of chromium(VI) have been determined by kinetic methods[4,5]. No direct method, however, is found feasible for chromium(III). Chromium(III) catalyses several redox reactions[6,7] but such reactions have rarely been used for its analysis by a kinetic procedure. In this work, we report a kinetic method for the analysis of chromium(III) based on its catalysis of cerium(IV) oxidation of arsenic(III) and allyl alcohol.

Reagent grade chemicals were used and doubly distilled water was used for preparing solutions. The cerium(IV) stock solution was prepared by dissolving cerium(IV) ammonium sulphate in dilute sulphuric acid and it was standardised with iron(II) solution. The iron(II) solution was obtained by dissolving iron(II) ammonium sulphate in dilute sulphuric acid. The arsenic(III) stock solution was prepared by dissolution of arsenic(III) oxide in 1 mol dm^{-3} sodium hydroxide and the solution was standardised with potassium iodate. Allyl alcohol was purified according to a known procedure[7] and its solution was made by dissolution of a known weight of the alcohol in water. The stock solutions were diluted as required. The catalyst, chromium(III), was used in the form of chromium(III) potassium alum.

Table 1—Cr(III) Catalysed Ce(IV)-As(III) Reaction

[Cr^{III}] × 10^4, mol dm^{-3}	$k_1 \times 10^4$, s^{-1}	
	Titrimetry*	Spectrophotometry**
0.0	1.7	1.1
1.0	2.8	2.1
2.0	3.2	2.6
4.0	4.8	3.6
6.0	5.9	4.4
8.0	7.3	4.9
10.0	—	5.1

*[Ce^{IV}] = 0.01, [As^{III}] = 0.05, [H_2SO_4] = 0.40 mol dm^{-3}; 30°C
**[Ce^{IV}] = 0.001, [As^{III}] = 0.005, [H_2SO_4] = 0.10 mol dm^{-3}; 26°C

Table 2—Cr(III) Catalysed Ce(IV)-Allyl Alcohol Reaction

[Cr^{III}] × 10^4, mol dm^{-3}	$k_1 \times 10^4$, s^{-1}	[Cr^{III}] × 10^4, mol dm^{-3}	$k_1 \times 10^4$, s^{-1}
0.00	0.28	3.0	8.2
0.10	1.6	4.0	10.5
0.50	3.8	5.0	11.8
1.0	5.1	6.0	13.4
2.0	5.6	8.0	14.0
3.0	8.2	9.0	14.5

[Alc] = 0.05, [Ce^{IV}] = 0.001, [$HClO_4$] = 0.50 mol dm^{-3} 50% acetic acid-water (v/v) solution; 26°C

The kinetics of chromium(III) catalysed cerium(IV) oxidation of arsenic(III) in the aqueous medium were followed both spectrophotometrically and titrimetrically under different conditions mentioned in Table 1. The applicability of Beer's law at 430 nm in case of the absorption of cerium(IV) under the reaction conditions in the concentration range of 5.0×10^{-4}-3.0×10^{-3} mol dm^{-3} was verified and ε was found to be 300 using a Bausch and Lomb spectronic 2000 instrument. In the titrimetric procedure of following the kinetics of the cerium(IV) oxidation of arsenic(III) catalysed by chromium(III), excess of added iron(II) ammonium sulphate solution was titrated against standard cerium(IV) solution. The second reaction, i.e. chromium(III) catalysed cerium(IV) oxidation of allyl alcohol in 50% acetic acid-water (v/v) was followed spectrophotometrically by measuring the absorption due to cerium(IV) at 430 nm. The applicability of Beer's law was earlier tested and ε found to be 345 at 430 nm under the experimental conditions. Kinetic studies were

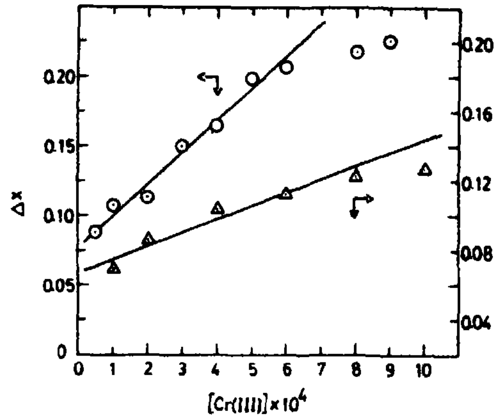

Fig. 1—Calibration curve for chromium(III) analysis by kinetic method in case of the cerium(IV) oxidation of allyl alcohol (⊙) and arsenic(III) (Δ) (conditions as stated in text)

carried out under pseudo first order conditions with the concentration of the reductant (arsenic(III)/allyl alcohol) in excess over that of the oxidant. All measurements were carried out at constant acidity using sulphuric acid in the arsenic(III) oxidation and perchloric acid in the oxidation of allyl alcohol. The pseudo first order rate constants, at constant acidities, were found from the slopes of log (a-x) vs time plots which were linear over 80% reaction or more.

The chromium(III) catalysed cerium(IV) oxidation of arsenic(III) has been studied in detail and the mechanism discussed[6]. The products, cerium(III) and arsenic(V), result via the intervention of a reactive chromium(IV) species (Scheme 1). The active oxidant is understood to be a cerium(IV) acid sulphate complex[6], $H_3Ce(SO_4)_4^-$. The catalysed reaction is very sensitive to acid concentration[6]. Likewise, the chromium(III) catalysis of cerium(IV) oxidation of allyl alcohol under the conditions studied leads to cerium(III) and acrylic acid, again via the formation of a reactive chromium(IV) species (Scheme 2). Here also the active oxidant is understood to be $H_3Ce(SO_4)_4^-$ and the reaction is sensitive to acid concentration[7].

$$\begin{aligned}
&Ce(IV) + Cr(III) \rightleftharpoons Ce(III) + Cr(IV)\\
&Cr(IV) + As(III) \rightarrow Cr(III) + As(IV)\\
&Ce(IV) + As(IV) \rightarrow Ce(III) + As(V)
\end{aligned}$$

Scheme 1

$$\begin{aligned}
&Cr^{3+} + H_2CCHCH_2OH \rightleftharpoons Cr^{3+} - H_2CCHCH_2OH\\
&Cr^{3+} - H_2CCHCH_2OH + Ce^{4+} \rightarrow H_2CCHCHOH + Ce^{3+}\\
&\qquad\qquad\qquad\qquad\qquad\qquad + Cr^{3+} + H^+\\
&H_2CCHCHOH + Ce^{4+} \rightarrow H_2CCHCHO + Ce^{3+} + H^+\\
&H_2CCHCHO + Ce^{4+} + H_2O \rightarrow H_2CCHC(OH)_2 + Ce^{3+} + H^+\\
&H_2CCHC(OH)_2 + Ce^{4+} \rightarrow H_2CCHCOOH + Ce^{3+} + H^+
\end{aligned}$$

Scheme 2

Table 3—Cr(III) Analysis (Kinetic Method)

Cr(III), μg/ml Taken	 Found	 S.D
4.16	4.11	±0.02
13.0	12.9	±0.03
16.6	16.6	±0.05
23.9	24.2	±0.10

In both the reactions, cerium(IV) is the oxidant and its concentration is measured. Furthermore, the chromium(III) catalyst was found to be regenerated at the end of the reaction[6,7].

In both reactions, the pseudo first order rate constant (k_1) is not only a linear function of the catalyst concentration (Tables 1 and 2) but also depends on the acid concentration. Nevertheless, at constant acidity, the rate constant (k_1) in both cases is a linear function of the concentration of the catalyst only (Tables 1 and 2). In view of this fact, a kinetic method of measurement of chromium(III) concentration becomes available. For this purpose, a calibration curve of pseudo first order constant (k_1) vs concentration of chromium(III) can be constructed from data such as those of Tables 1 and 2 under a known set of conditions of concentration of oxidant, substrate, acid, temperature, etc. The reaction is then repeated under similar conditions in presence of the solution of unknown chromium(III) concentration and the value of rate constant k_1 is used to get the concentration of chromium(III) from the calibration curve. Alternatively, under the conditions of the reaction, after a definite interval of time, say 10 min, one of the concentrations, that of cerium(IV), is measured both in presence and absence of a known amount of catalyst. Such data again lead to a calibration curve as that shown in Fig. 1 and the unknown concentration of chromium(III) can be obtained from such a graph.

For routine measurements, the latter procedure is recommended. However, as shown in Fig. 1, for concentrations higher than 8.0×10^{-4} mol dm^{-3} of chromium(III), under the given conditions of the reactions of Tables 1 and 2, deviations from linearity occur and the method is no longer satisfactory

Method recommended for analysis

A set comprising known concentrations of cerium(IV), arsenic(III), sulphuric acid and chromium(III) [e.g. 1.0×10^{-3}, 5.0×10^{-3}, 0.10 and 1.0×10^{-4} mol dm^{-3} respectively] is thermostated and mixed. The reading (OD or titre) is taken at the 10th minute. With the same concentrations of the reactants and acid, chromium(III) is varied, the reading at the 10th minute being taken in each case. Taking the difference in OD between the catalysed and uncatalysed reactions as Δx, a calibration curve of Δx vs [Cr(III)] is plotted (Fig. 1). This plot is used for determining unknown concentrations of chromium(III). The results of such a method of analysis are shown in Table 3.

Interference by a few metals was also tested for the chromium(III) analysis. Apart from the reductants which reduce cerium(IV) and the oxidants which oxidise arsenic(III)/allyl alcohol, it was found that Fe^{3+}, Cu^{2+}, Zr^{4+} have no effect, whereas Ag^{+} and Mn^{2+} interfere. In the analysis, the role of acid is significant and it is necessary that the same concentration and sample of acid be used for satisfactory results. The method enables analysis of chromium(III) in the range of 10-40 µg per ml.

References

1 Vogel A I, *Textbook of quantitative inorganic analysis*, IVth edition (ELBS, Longman, NY) 1978, 361.

2 Schwarzenbach G & Flaschka H, *Complexometric titrations*, 2nd edition (Methuen, London) 1969, 218.

3 Hoshino H & Yotsuyanagi T, *Analyt Chem*, **57** (1985) 625.

4 Uma P, Kanta Rao P & Sastri M N, *Indian J Chem*, **24A** (1985) 539.

5 Wen-Bin Q I & Li-Zhong Zhu, *Talanta*, **33** (1986) 694.

6 Chimatadar S A, Nandibewoor S T, Sambrani M I & Raju J R, *J Chem Soc Dalton Trans*, (1987) 573.

7 Gokavi G S, *Kinetics and mechanism of some oxidation reactions*, Ph D Thesis, Karnatak University, Dharwad, 1987

Indian Journal of Chemistry
Vol. 27A, February 1988, pp. 179-180

Trace Level Determination of Zinc by Differential Pulse Anodic Stripping Voltammetry

S S DESHPANDE & A P JOSHI*
Department of Chemistry, Nagpur University, Nagpur 440010

Received 8 *January* 1987; *revised and accepted* 29 *June* 1987

Trace amount of Zn(II) has been determined by differential pulse anodic stripping voltammetry in 0.03 *M* sodium acetate supporting electrolyte. Linear calibration plots are obtained in the range of 0.1 ppb to 1 ppb and 2 ppb to 10 ppb with the minimum determinable limit of 0.1 ppb. The method is relatively free from interference by other metal ions. The method developed has been extended for Zn(II) assay in tap water, plant tissues, human blood, coal ash and pharmaceutical products.

Zinc(II) has been determined by a variety of techniques such as neutron activation analysis[1], spectrophotometry[2], atomic absorption spectroscopy[3] and polarography[4-8].

Presently a differential pulse anodic stripping voltammetric method has been developed. Determination of trace amounts of Zn(II) has been extended to samples, such as plant tissues, human blood, coal ash, pharmaceutical products and tap water samples.

The voltammetric measurements were made on a Metrohm polarecord E-506 with attached cell assembly on a stand E-505. The electrode system consisted of a hanging mercury drop electrode (HMDE), Ag/AgCl (satd, KCl) as a reference electrode and Pt-metal electrode as an auxiliary electrode. Total volume of the system was maintained at 25 ml. Nitrogen gas was bubbled through the solution for 15 min. All chemicals used were of AR grade. Stock solutions (0.5 *M*) of all supporting electrolytes were prepared in triply distilled water, working solutions were prepared by suitable dilutions. Standard Zn(II) solution was prepared by dissolving known weight of $ZnSO_4.7H_2O$ (GR, proanalyse). All usual precautions of trace analysis were observed.

Procedure

Sodium acetate solution (0.3 *M*, 2.5 ml) was taken in the cell and the volume was made upto 25 ml with triply distilled water. To this was added a standard solution of zinc (25 μl containing 250 ng of zinc) and the voltammogram was recorded with the instrumental settings as follows: (A blank was also similarly recorded): pre-electrolysis potential = -1.2 V; scan range = -1.2 V to -0.2 V; scan rate = 4 mV/s; enrichment time = 60 sec; quiescent time = 10 sec; $mm/t_{drop} = 1$; $t_{drop} = 0.8$; electrode surface area = 1.82 mm^2; pulse amplitude = 10 mV; and Zn(II) conc. = 10 ppb.

These optimum conditions for recording voltammograms were obtained after many trial runs. For example a variety of electrolytes (alkaline, neutral, organic and inorganic salts and buffers) of different concentrations were tried as supporting electrolytes. Peak response and height current signal value were the best in 0.03 *M* Na-acetate as compared to those obtained in other supporting electrolytes.

Current-concentration relationship was found to be linear from 0.1 ppb to 10 ppb of Zn(II). Calibration plots were obtained in two ranges 0.1 ppb to 1 ppb and 2 ppb to 10 ppb. Minimum determinable limit was found to be 0.1 ppb of Zn(II). The values of RMD, SD and CV for determination of 0.1 ppb Zn(II) and 2 ppb Zn(II) are 2.33%, 0.23, 3.15 and 0.822%; 0.22, 1.011 respectively.

The effect of presence of some cations on determination of 2 ppb Zn(II) showed that Ga(III), Pb(II) and Cu(II) could be tolerated upto the ratios of 1:100; beyond this concentration ratio the peak distortion and suppression were observed. Nickel(II), Cd(II) and Tl(I) could be tolerated upto 1:200, 1:500 and 1:1000 respectively while Fe(III), Mn(II), As(III) and Co(II) could be tolerated upto 1:120, 1:25, 1:60 and 1:50 respectively.

Determination of Zn(II) in tap water

Three tap water samples (500 ml each) were collected and to each was added 1500 ng, 750 ng and 375 ng of Zn(II) respectively along with a few drops of HNO_3. The contents were evaporated to dryness and volume was made upto 10 ml with triply distilled water. An aliquot (1 ml) from this solution was used for Zn(II) recovery experiment. The concentration of Zn(II) was computed from calibration plots and was ascertained by standard addition method. The recovery was found to be 97.9%, 96.66% and 93.33% respectively.

Determination of Zn(II) in plant tissues

Coriander plant tissue was taken for Zn analysis. It was dried under IR lamp and powdered and a known weight of tissue powder was ashed at 600°C for 2 hr. The ash was dissolved in minimum quantity of 1 *N* hydrochloric acid, triply distilled water (100 ml) followed by 5 ml of 1 *N* ammonium citrate. The contents were shaken vigorously with 10 ml of 0.1% dithiozone in chloroform. The chloroform layer was separated and the extraction procedure was repeated 2-3 times with 5 ml fractions of the reagent. The complexed Zn(II) in chloroform layer was shaken with 0.5 *N* hydrochloric acid, the aqueous layer collected evaporated to dryness, the residue was taken in 25 ml of 0.03 *M* Na-acetate and voltammogram was recorded against the reagent blank.

The concentration of Zn(II) was computed from calibration plots and ascertained by standard addition method. The Zn(II) concentration was found to be 5.05 mg/kg and 5.046 mg/kg by calibration and standard addition methods, respectively.

Determination of Zn(II) in coal ash

Coal ash samples obtained from Bhatadi Coal Fields, Wardha (Maharashtra) and Rawanwara Pench, Madhya Pradesh were analysed for Zn(II).

To a weighed quantity of coal ash was added conc. HCl (10 ml) and the contents were heated. The precipitated silica was filtered off, the filtrate evaporated to dryness and final volume was made upto 10 ml with triply distilled water. Aliquots (1 ml and 2 ml) were used for analysis. The average Zn(II) content in Bhatadi coal and Rawanwara coal ash samples was found to be 0.8306 mg/kg, 0.82 mg/kg and 1.8 mg/kg, 1.806 mg/kg by calibration and standard addition methods respectively.

Determination of Zn(II) in human blood

Heparinized human blood sample was analysed for Zn(II) content. The blood sample (5 ml) was refluxed with $H_2SO_4 + HClO_4 + HNO_3$ (4 ml + 2 ml + 4 ml) for 3-4 hr till colourless solution was obtained. It was filtered, the filtrate evaporated to dryness and residue was taken up in water and the volume was made upto 15 ml by adding triply distilled water. An aliquot (3 ml) was taken for analysis by the standard procedure. The average Zn(II) content was found to be 1.155 μg% and 1.153 μg% by calibration and standard addition method respectively.

Determination of Zn(II) in pharmaceutical product

Becadexamine (Glaxo) tablets were analysed for Zn(II) content. To conc. HCl (10 ml) was added one tablet of Becadexamine and to this were added, few drops of H_2SO_4, and the volume was made upto 25 ml. The contents were heated strongly for 3-4 hr, cooled, filtered and the filtrate evaporated to dryness. The residue was dissolved in triply distilled water (500 ml). An aliquot from this solution was used for analysis. The concentration of Zn(II) was found to be 11.5 mg/tablet and 11.46 mg/tablet by calibration and standard addition methods respectively against the manufacturers value of 11.35 mg Zn(II)/tablet.

The method is highly sensitive, precise, rapid with minimum determinable limit of 0.1 ppb of Zn(II) and very useful for the routine analysis of zinc(II).

The authors are grateful to Alexander von Humboldt Foundation of West Germany for the donation of Metrohm polarograph. One of the authors (SSD) is grateful to the UGC, New Delhi for the award of a junior research fellowship.

References

1 Olmez K, Kowalczyk G S & Harrison G H, *J radional nucl Chem*, **94** (1985) 391.
2 Linxi-Jian, *Fen Hsi Hua Hsueh*, **9** (1981) 198.
3 Hennon G, Bode K & Pelzer J, *Z Chem*, **23** (1983) 424.
4 Zhang Y, *Gantie*, **18** (1983) 51.
5 Schieckmann F & Umland F, *Fresenius Z Anal Chem*, **314** (1983) 21.
6 Alevato S de J & Rebello A de L, *Talanta*, **28** (1981) 909.
7 Sviridenko V G, Lin D G & Lapitskaya S K, *Khim Khim Tekhnol*, **26** (1983) 1178.
8 Alexander P W & Marpang, *Talanta*, **28** (1981) 909.

Indian Journal of Chemistry
Vol. 27 A, February 1988, pp. 181-182

BOOK REVIEWS

Symmetry Through the Eyes of a Chemist by Istvan Hargittai & Magdolna Hargittai (VCH Verlagsgesellschaft mbH, D-6940 Weinheim, Federal Republic of Germany), 1986; pp 458 + xii; Price DM 156.00.

The vast majority of scientists, and chemists are no exception, rarely take more than a superficial interest in subjects outside their immediate areas of specialisation. The stress upon specialisation in and compartmentalisation of different branches of science may serve to some extent the purpose of maintaining a set of well-established norms, on the basis of which scientific research is evaluated and judged. However, one obvious shortcoming of this rigorous but somewhat blinkered approach is that very often the interdisciplinary unifying aspects of fundamental concepts are lost sight of and only particular applications highlighted. It is, therefore, always a matter of considerable surprise and delight when one comes across a book which retains the rigour that is dear to a specialist's heart but also gives a much broader perspective than what is normally encountered.

The concept of symmetry is as fundamental as that of space and time: it is amenable to formalised mathematical representation, can stimulate epistemological enquiries, and is considered to be an important element of aesthetic appeal. The book under review makes the universal nature of symmetry abundantly clear through striking examples drawn from natural phenomena as well as from the creative arts.

For the down-to-earth chemist the book provides all the important practical applications of symmetry, more than adequately illustrated and explained. There are excellent chapters on molecular shapes and geometry, molecular vibrations, electronic structures of atoms and molecules, chemical reactions, space-group symmetries and symmetries in crystals. Top quality figures make all these topics easy to read and understand. To give one example, the use of Projection Operator is neatly explained pictorially along with the standard mathematical manipulation. A number of significant and up to date references are given at the end of each chapter. Although no special background in mathematics would seem necessary to appreciate the content of the book, a short chapter outlining elementary group theory and matrix algebra has been included for the mathematically uninitiated.

For readers already at home with character tables, glide planes etc., it will probably be a revelation and joy to know about the underlying symmetry in Bela-Bartok's music, M.C. Escher's painting and Hungarian author Figyes Karinthy's short stories. The book will be useful to students and teachers for its sound appreciation of the applications and occurrences of symmetry. I would rate this book as the best currently available among those on similar subjects.

S Bhaduri
Alchemie Research Centre
Thane 400 061

The Art of Scientific Writing by Hans F. Ebel, Claus Bliefert and William E. Russey (VCH Verlagsgesellschaft mbH, Weinheim, FRG), 1987, pp. 493 + XIX.

"......Scientific knowledge is distinguished from other intellectual artefacts of human society by the fact that its contents are consensible. By this I mean that each message should not be so obscure or ambiguous that the recipient is unable either to give it whole-hearted assent or to offer well-founded objections" —John Ziman in *Reliable Knowledge.*

Unambiguous exchange of information among scientists is thus basic to the growth of scientific knowledge. If this is so, the formal mode of this exchange, scientific writing, should be a subject of serious attention for all scientists. However, scientists generally pay little attention to scientific writing as a tool of their trade and some even consider it as a necessary evil to be faced at the end of a given set of experiments. This situation needs to be changed and an obvious way to do so, in the Indian context, is to include scientific writing as a subject of study at the graduate level for the would-be scientists. Alternatively, successful completion of a short course in scientific communication should be made a mandatory requirement at the Ph.D. level. The book under review could form the core of such a course, if it ever materialises.

The authors of the present book consider all stages in scientific writing—from a student note book to a professional paper and even a book In Part I, termed as Scientific Writing: Aims and Forms, they deal with different types of basic scientific writing, viz., reports, theses, research papers and books. In Part II, termed as Scientific Writing: Materials, Tools and Methods, they deal with mechanics of manuscript preparation, nomenclature, units and numbers, equations and formulas, figures, tables and references, etc. In addition, there are over 100 pages of appendices dealing with such diverse topics as oral presentation, copyright, ISSN, ISBN, indexes, abbreviations, proof reading and common units and constants. Most of the examples chosen are from chemistry reflecting the academic background of the authors, but the conclusions drawn are valid for scientific writing in other fields also.

Any written communication may be considered in terms of its two components: the message and the medium. In scientific writing, English language has by now become the accepted medium of exchange of information among scientists of different nationalities. Therefore, scientific writing has to be considered in terms of the peculiarities of scientific message as well as those of the English language. The authors of the book under review deal more than adequately with the unique features of the scientific message like need to communicate detailed data and procedures, which may be verified by the recipients of the message. The characteristic format of scientific writing, its specialised vocabulary, graphic aids, tables, etc. are covered in detail. The authors have taken pains to point out sources of ambiguity in the presentation of data, tabular as well as graphic. However, they have paid less attention to some other common sources of ambiguity in scientific writing arising from a mishandling of the medium of communication. Lack of precision and accuracy in the usage of words, lack of proper organisation of information, and wordiness often inhibit the effective communication of the message. Careless grammatical constructions may not only confuse the meaning but also lead to hilarious interpretations.

Nevertheless, the authors do provide some good tips on handling English language in an appendix entitled, "Aspects of Scientific English". Two points worth noting are the authors' criticism of tendency towards nominification, i.e., conversion of an expression of action (verb form) to the noun form, and excessive use of passive voice in scientific writing. The reason for writing "distillation was carried out on the residue" instead of "the residue was distilled" may be the desire of the author to sound scholarly. There is no justification of such a nominification which results in a longer and less readable expression. But a similar stand cannot be taken against the use of passive voice. There may be occasions when passive form is quite appropriate. The expression, "The solution was poured..." is more appropriate than "I poured the solution....". An impersonal style and objective presentation are well known and valued features of scientific writing.

The book is very well produced and free from printing and other errors, though use of the expression "comprised of" at a couple of places and that of "comprise" when the authors intend "constitute" (p. 198: "the digits that comprise it.....", referring to registry number) should have been avoided in a book of this type. However, there is no doubt that this is a very valuable book; it is strongly recommended to all would-be and practising scientists. The wealth of information it contains makes it useful for others also who are not active scientists but are interested in science communication, like science editors, publishers and printers.

B C Sharma

Indian Journal of Chemistry
Vol. 27A, March 1988, pp. 183-187

Molecular Branching Topology & Quantum Mechanical Quantities

S C RAKSHIT*, M BANERJEE & BIREN HAZRA
Chemistry Department, University of Burdwan, Burdwan 713104

Received 12 *March* 1987; *revised and accepted* 17 *July* 1987

Topological branching indices of *n*-alkanes and their isomers have been shown to lead to standard curves when some quantum mechanical properties, such as binding energies, two-electron exchange integrals (CNDO), charge densities, etc are plotted against them. These curves can be used to obtain the values of molecular level quantities for an unexplored alkane without resorting to quantum treatment. Either the graphs or the regression equations may be used for this purpose. This method has been extended to calculate the quantum mechanical properties of some primary alcohols, carboxylic acids and silanes also. Tentative reasons have been suggested for the link between the specific quantum quantities and the branching indices, The validity of the treatment, when the alkanes are substituted by alcohols or carboxylic acids, has also been justified.

The degree of molecular branching in the members of a homologous series of a general formula or in the isomers of a given molecular composition is a topic of considerable importance in graph theory. Different methods have been employed to set up measures, called branching indices[1-4], using the topological parameters of the molecular graphs. Randic[4] has shown that a function of the degrees of vertices of the molecular graph of the straight-chain and branched alkane isomers produces a numerical order that runs parallel to an ordering of the alkanes based on their topological matrices when the vertex labelling is done in a unique way. This unique labelling can be done either by a few trials for not too big molecules or by use of a computer programme, developed by Randic[5], for bigger molecules.

Bonchev and Trinajstic[3] have used information theory in conjunction with distance matrices of the molecules to set up information theoretic graphical indices of molecular branching. Besides these two, a few more branching indices have been proposed.

It has been shown[4] that the experimental values of many physical and thermodynamic properties, such as melting points, boiling points, vapour pressure, enthalpies of formation, etc., when plotted against Randic branching indices (RBI) of the alkane isomers, either give a smooth curve or, in some cases, even yield linear graphs. We thought it worthwhile to explore the relation between the branching indices proposed by Randic (RBI) and Bonchev and Trinajstic (BTBI) and some molecular level properties.

Theoretical

Interestingly enough, the response was found to be positive in cases of some important quantum-mechanically derived quantities like binding energies and diatomic electron-electron exchange energy of CNDO molecular orbital method.

The binding energies of molecules and ions in the singlet sigma state may be calculated with a satisfactory accuracy by a semiclassical method[6]. This semiclassical expression is virtually the CNDO expression for energy in which some parameters of the latter are substituted by their effective classical analogues. A further improvement in accuracy has been made possible by a recent modification[7] of k_n of the original formulation[6]. The binding energy (in eV) is given by Eq. 1,

$$E_{\text{bin}} = \frac{1}{2}\left[\left\{\sum_i \frac{q_i^2}{2r_i} + \sum_{i<j}\sum \frac{q_i q_j}{r_{ij}}\right\} - \sum_{A<B}\left\{\frac{1}{2}(1+k_n n)\sum_{\mu}^{A}\sum_{\nu}^{B} P_{\mu\nu}^2 \gamma_{AB}\right\} \pm \Delta U_D\right] \times 27.2 \quad \ldots(1)$$

where the symbols have their usual significances as given by Pople[8] in his original valence shell basis treatment.

Eq. (1) may be written as[6],

$$E_{\text{bin}}(\text{eV}) = \frac{1}{2}(Q + E_{\text{ex}} + k_n n . E_{\text{ex}} \pm 0.05) \times 27.2 \quad \ldots(2)$$

where Q is the electrostatic work of charging and assembling the atoms as these exist in the molecule and is calculated from CNDO charge distribution data. E_{ex} is the total diatomic electron-electron exchange integral, 'n' represents the number of valence shell basis orbitals and k_n, a calibrated quantity connected with resonance energy, is obtained from Eq. 3,

$$k_n = A + (B/n) - \lambda \ln(n) \qquad \ldots(3)$$

The topological branching indices of Randic[4] and of Bonchev and Trinajstic[3] are given by (for alkanes) Eqs 4 and 5, respectively,

$$RBI = \sum_{i<j} (v_i v_j)^{-1/2}, \text{for all ijth bonds} \qquad \ldots(4)$$

where v_i and v_j are the degrees of vertices in the carbon-carbon chain without the H-attaching bonds in the molecular graphs.

$$BTBI = \bar{I}_D = -\Sigma \frac{2k_i}{N(N-1)} \log_2 \frac{2k_i}{N(N-1)} \qquad \ldots(5)$$

where $\bar{I}_D$ = mean information content for a distance in the distance matrix for alkane chain, k_i = the number or times a particular distance 'i' occurs in the probability scheme based on the distance matrix and N^2 equals the total number of elements in the matrix.

Results and Discussion

When the molecular level properties of Eq. (2) are plotted against RBI values of a homologous series of alkanes, interesting graphs are obtained. Extremely good straight lines result for plots of (i) binding energies (ii) total diatomic electron exchange energies and (iii) quantity Q of Eq. (2) (Fig. 1). The plots of binding energies against RBI for a set of alkane isomers are also linear (Fig. 2).

The linear graphs (drawn for the first few members) offer the unique advantage of serving as standard curves for predicting the binding energies of unexplored alkanes and their two electron diatomic exchange energies obviating the need of onerous molecular orbital computation. For the sake of graphic demonstration, quantum mechanical value of binding energy of an arbitrarily chosen alkane (*n*-octane) is indicated by the point P (Fig. 1). The binding energy and the diatomic exchange energy of *n*-hexane of the C_6-alkane isomer series are denoted by the points P and R (Figs 2a, 2b) respectively. However, to demonstrate the general predictability for the alkanes, a comprehensive Table 1 is provided, the data of which are based on the regression equation of the method of least squares, with correlation coefficient $r = 0.9995$ The equation is,

$$y = 24.413x + 6.425 \qquad \ldots(a)$$

where x represents the Randic branching index and y, the binding energy.

The binding energy value for the alkane *n*-eicosane involving a basis set of 122 atomic orbitals (much beyond the limit of the present day programmes available for 80 orbital basis set of the conventional CNDO technique) has been elegantly obtained by the use of the regression equation (Table 1). The importance of the graphical method, apart from its simplicity, is further emphasised by the fact that for calculat-

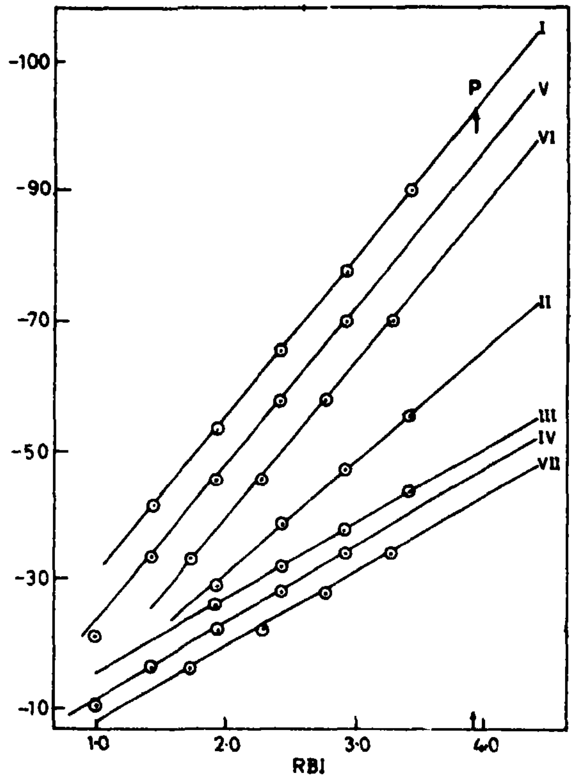

Fig. 1 — Plots of calculated molecular level properties against RBI values [Curves I, V and VI: B.E. of *n*-alkanes, alcohols and carboxylic acids respectively; curves III, IV and VII: $10 E_{ex}$ of *n*-alkanes, alcohols and carboxylic acids respectively; curve II: 10^{-5} Q of *n*-alkanes; prediction for point P: *n*-octane (RBI = 3.914), lit. B.E. (eV) = − 102.43, graphical B.E. (eV) = − 101.98].

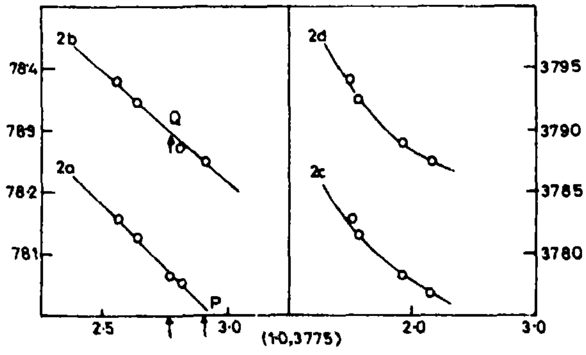

Fig. 2 — Plots of calculated molecular level properties of *n*-hexane and its isomers against RBI and BTBI [Curve 2a: − B.E. vs RBI; curve 2b: $-10^3 E_{ex}$ vs RBI; curve 2c: − B.E. vs BTBI; curve 2d: $-10^3 E_{ex}$ vs BTBI; prediction for point P (hexane): lit B.E. = − 78.09 eV, graphical B.E. = − 78.02 eV; prediction for point R (2-methylpentane): calc. $E_{ex} = -3788 \times 10^{-3}$ a.u., grapical $E_{ex} = -3789 \times 10^{-3}$ a.u.]

Table 1 — Values of Binding Energies for *n*-Alkanes

Molecule (*n*-Alkane)	Randic branching indices	Calc. B.E. (eV) using Eq. 2	Value of B.E. (eV) predicted* from regression Eq. (a)	Thermo-dynamic B.E. (eV)	Standard error
Ethane	1.00	−29.68	−30.839	−29.33	
Propane	1.414	−41.28	−40.95	−41.50	
n-Butane	1.914	−53.62	−53.158	−53.69	
n-Pentane	2.414	−66.09	−65.365	−65.887	
n-Hexane	2.914	−78.033	−77.570	−78.082	
n-Heptane	3.414	−89.95	−89.778	−90.255	
n-Octane	3.914	−100.998	−101.98	−102.43	
n-Nonane	4.414	—	−114.19*	−114.62	
n-Decane	4.914	—	−126.39*	−126.80	
n-Undecane	5.414	—	−138.60*	−139.03	0.697
n-Dodacane	5.914	—	−150.81*	−151.17	
n-Tridecane	6.414	—	−163.02*	−163.35	
n-Tetradecane	6.914	—	−175.22*	−175.53	
n-Pentadecane	7.414	—	−187.43*	−187.72	
n-Hexadecane	7.914	—	−199.64*	−199.90	
n-Heptadecane	8.414	—	−211.84*	−212.08	
n-Octadecane	8.914	—	−224.05*	−224.27	
n-Nonadecane	9.414	—	−236.26*	−236.45	
n-Eicosane	9.914	—	−248.46*	−248.63	

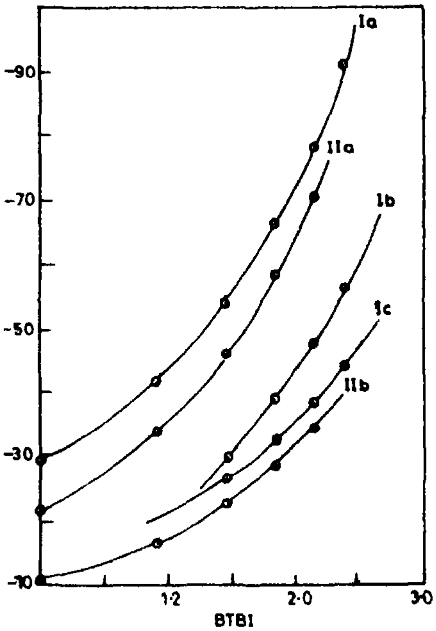

Fig. 3 — Plots of calculated molecular level properties against BTBI [Curve Ia: B.E. of *n*-alkanes; curve IIa: B.E. of alcohols; curve Ic: 10 E_{ex} of *n*-alkanes; curve IIb: 10 E_{ea} of alcohols; curve Ib: 10^{-5} Q of *n*-alkanes]

ing binding energy of even *n*-heptane, with just 44 atomic orbitals as the basis, around 15 min of a fairly fast computer are required. It is easy to comprehend the time and cost involved in CNDO calculations when 122 basis orbitals are involved, as in the case of *n*-eicosane.

In Fig. (3) are displayed the plots of the B.E., 10 E_{ex} and Q against BTBI (relation-5). In all cases (except for Q) the curves are smooth, though not always linear. Although extrapolation is permissible for the unexplored alkanes, RBI linear curves decidedly have an advantage over the BTBI curves in this respect.

This convenient way of obtaining quantum mechanical quantities of unexplored alkanes and their isomers from standard curves can be extended to domains of some other homologous series deemed to be derived from the alkanes. The homologous series of the normal aliphatic alcohols (RCH_2OH) and carboxylic acids (RCOOH) have been chosen for this study and both quantum mechanical calculations have been done and graphs have been drawn for them. The rationale behind this extension is explained below.

The molecular graph in a normal alkane is of the type 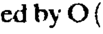, where the vertices (all carbon atoms) are of degrees either 2 or 1. The terminal vertices have the degree value 1. If one such terminal atom be replaced by O (as in the formation of alcohol), this new vertex may be considered as that of a pseudo C-atom having the unaltered degree 1. Hence, the branching index (RBI) of the new chain remains the same as that of the original alkane. The BTBI branching index, based on information theoretic graphical scheme, should also remain unchanged if the O-atom plays the role of a pseudo C-atom. It is in this perspective that the previous molecular level properties (viz. binding energies, etc.) are plotted as functions of the RBI or BTBI.

The results obtained for primary alcohols and the carboxylic acids are represented graphically in Figs 1 and 3. All the curves faithfully mimic the pattern of the corresponding *n*-alkane series. The linear curves, as in the earlier cases, serve as standards for evaluating the corresponding molecular level properties. Alternatively, one may use the regression equations (b) and (c) to predict the values of the binding energies of the primary alcohols and of the carboxylic acids, respectively. Tables 2 and 3 exhibit such data with the correlation factors, the regression equations appearing at the head of each table.

While comparing the data predicted for the alcohols and the acids with the thermodynamic data, one ought to remember that the latter intrinsically include the effect of the possible polymeric forms of the species due to hydrogen bonding in the vapour state[11]. However, as the percentage of the polymeric species is expected to be rather low, the effect on the overall thermodynamic value is negligible. The binding energy calculated with the help of Eq. (2) refers to that of the single species in the vapour state.

While the potential uses of such graphs are evident, a suitable explanation is needed to account for the linear variation of the quantum molecular properties with the topology based property, viz., the branching index. A rigorous explanation cannot be offered at this stage, but plausible reasons for linearity are not difficult to divine.

Actual computation shows that the main contribution to E_{bin} in Eq. (2) comes from E_{ex} which essentially involves a series of integrals over diatomic overlap functions and distance parameter $r_{\mu\nu}$. The binding energy of an alkane may be thought to be proportional to the total overlap integral comprising a series of definite integrals representing $\Phi_{Csp^3} - \Phi_{Csp^3}$ overlaps and $\Phi_{Csp^3} - \Phi_{H1s}$ overlaps. That is,

$$E_{\mathrm{bin}} = \mathrm{k}[\mathrm{S}_{(\mathrm{n}'-\mathrm{alkane})}]$$

$$= \mathrm{k}[(\mathrm{n}'-1)\mathrm{S}_{\mathrm{C-C}} + (2\mathrm{n}'+2)\mathrm{S}_{\mathrm{C-H}}] \quad \ldots (6)$$

(where n′ = number of carbon atoms)

Table 2—Binding Energies of Primary Alcohols (correlation coefficient, $r = 0.9996$) Obtained by the Regression Eq. $y = 24.998x - 2.712$ ...(b)

Molecule	Branching index (Randic)	Calc. value of binding energy (eV) Eq. 2	Value of B.E. (eV) predicted from regression Eq. (b)	Thermodynamic value of the heat of atomisation (eV)	Standard error
Methanol	1.00	−21.32	−22.286	21.14	
Ethanol	1.4142	−33.51	−32.64	33.46	
n-Propanol	1.9142	−45.361	−45.139	45.67	
n-Butanol	2.4142	−57.927	−57.638	57.92	0.570
n-Pentanol	2.9142	−70.08	−70.137	70.229	
n-Hexanol	3.4142	−82.28	−82.636	—	
n-Heptanol	3.9142	—	−95.135	95.495	
n-Octanol	4.4142	—	−107.634	107.77	

Table 3—Binding Energies of Carboxylic Acids (correlation coeff. = 0.9997); Obtained by the Regression Eq., $y = 24.249x - 8.967$ ...(c)

Molecule	Branching index (Randic)	Calc. value of B.E. (eV) Eq. 2	Value of B.E. (eV) predicted from regression Eq. (c)	Thermodynamic value of the heat of atomisation (eV)	Standard error
Acetic acid	1.7321	−33.363	−33.034	33.61	
Propionic acid	2.2701	−45.48	−46.08	45.76	
Butyric acid	2.7702	−58.149	−58.207	58.44	
Valeric acid	3.270	−70.905	−70.327	70.71	
Caproic acid	3.7701	−82.206	−82.45	–	0.416
Heptylic acid	4.270	—	−94.576	–	
Caprylic acid	4.770	—	−106.70	–	
Pelargonic acid (Nonanoic)	5.27	—	−118.82	–	
Capric acid	5.77	—	−130.94	131.64	

The overlap integral involving two, ith and jth carbon atoms of degrees 1 and 2, respectively, will have an S_{C-C}, deemed to be a geometric mean (positive) of two real number contributions,

$$(S_C . \tfrac{1}{2} S_C)^{1/2} = (1.2)^{-1/2} S_C = (v_i . v_j)^{-1/2} S_C$$

related to the graphical degree values as in RBI. Similarly if k and l atoms be of degrees 2 and 3 respectively (as is possible in a branched hydrocarbon containing tertiary C-atoms) each,

$$S_{C-C} = (\tfrac{1}{2} S_C \tfrac{1}{3} S_C)^{1/2} = (2.3)^{-1/2} S_C = (v_k v_l)^{-1/2} S_C$$

This equality to geometric mean is based on an assumption that carbon atoms of topological degrees 1, 2 and 3 respectively, contribute an effective multiple of S_C, each consistent with the corresponding connectivity number. It implicitly neglects the overlap contributions coming from the classically unconnected *C*-atoms, which are really small, notwithstanding the fact that the exchange integral involves all possible pairs of orbitals.

The remaining part of contribution to E_{bin} due to all S_{C-H}'s (Eq. 6) increases additively by a constant amount as, n′, the number of C-atoms in the chain, increases.

It is thus possible to conceive of a linear dependence of the exchange integrals and binding energies upon the RBI index values and, in practice, this turns out to be the case (Fig. 1).

The reason why such quantum properties fail to show linear dependence on BTBI is that the latter branching index, unlike RBI, is not merely a sum of two vertex properties, but depends on a more elaborate probability scheme.

The reasons for linear variation of the binding energies with the branching indices (RBI) of the alcohol set is easily understood if we accept the truth of the Eq. (6). Taking the diatomic exchange energies to be the determinant and assuming that such exchange energies are proportional to diatomic overlap integrals, the binding energies of alcohols derived fromthe corresponding alkanes can be written, following Eq. (6), as

$$E_{bin} = k[(n'' - 1)S_{C-C} + S_{C-O} + (2n'' + 1)S_{C-H} + S_{O-H}] \quad \ldots(7)$$

where, n″ + 1 = n′ = total number of C-plus O-atoms in the primary alcohol. The difference of Eqs (6) and (7) leads to,

$$E_{bin(alkane)} - E_{bis(alcohol)} = k[(S_{C-C} - S_{C-O}) + (3S_{C-H} - S_{O-H})] \quad \ldots(8)$$

for all *n*′-alkanes and the corresponding alcohols. This means a constant difference, ΔE_{bin}, between an alkane and the alcohol irrespective of the value of n′. We ought to expect not only linearity for the alcohol graphs but also parallel runs for the sets of alkanes and alcohols (cf. Fig. 1, curves I and V, and curves III and IV).

Referring to Mulliken *et al.*[9], data on diatomic overlap enable us to calculate $(S_{C-C} - S_{C-O})$ and $(3S_{C-H} - S_{O-H})$ of Eq. (8) and hence k from the known values of binding energies of the LHS.

Keeping in view the increasing attention received by silanes and their derivatives and the fact that molecular orbital studies on silanes are rather limited, we have calculated the binding energies of the first four normal silanes[12] by the present method. Following the procedure adopted for the alkane series and including the *d*-orbitals of the silicon atom in the basis set for the CNDO charge and exchange energy computation, we have obtained binding energies of silanes (Si 1 to 4):

Molecule	Branching index (Randic)	Binding energy (eV)
SiH_4	0	− 10.73
Si_2H_6	1.00	− 21.067
Si_3H_8	1.4142	− 30.11
Si_4H_{10}	1.9142	− 38.256

As in the case of alkanes, the binding energies of the silanes, quite expectedly, turn out to be a linear function of the branching indices.

References

1 Wiener H, *J Am chem Soc*, **69** (1947) 17; **69** (1947) 2636; *J phys Chem*, **52** (1948) 425.
2 Hosoya H, *Bull chem Soc Jpn*, **44** (1971) 2332.
3 Bonchev D & Trinajstic N, *J chem Phys*, **67** (1977) 4517.
4 Randic M, *J Am chem Soc*, **97** (1975) 6609.
5 Randic M, *J chem Phys*, **60** (1974) 3920.
6 Rakshit S C & Mukherjee Bani, *Indian J Chem*, **22A** (1983) 273.
7 Rakshit S C & Hazra B, *Indian J Chem* (communicated).
8 Pople J A & Segal G A, *J chem Phys*, **43** (1965)S 136; **44** (1966) 3289.
9 Mulliken R S, Ricke C A, Orloff D & Orloff H, *J chem Phys*, **17** (1949) 1248.
10 Pople J A & Beveridge D L, *Approximate molecular orbital theory* (McGraw Hill, NY) 1970.
11 Pauling Linus, *The nature of the chemical bond* (Cornell University Press, Ithaca) 1967.
12 Cotton F A, *Advanced inorganic chemistry* (Wiley Eastern, New Delhi) 1969.

Indian Journal of Chemistry
Vol 27A, March 1988, pp. 188-191

A Study of Quantitative Structure—Property Correlations (QSPC) Applying an Unusual Additivity Scheme

S SINGH, B K MISHRA & R K MISHRA*
Department of Chemistry, Sambalpur University, Jyoti Vihar 768 019

Received 15 *May* 1987; *revised* 27 *July* 1987; *rerevised and accepted* 14 *September* 1987

An additivity scheme based on a bond parameter (χ) and a distance parameter ($I_{D,1}^{W}$) is suggested to model the entropies of some aliphatic and aromatic hydrocarbons. The model equation obtained is: $S^\circ = \alpha\chi + \beta I_{D,1}^{W} + \gamma$.

A graph theoretical approach to additivity schemes makes use of the topological indices[1]. Graph and information theoretical indices have been recently developed as quantitative structural characteristics of molecules to predict different thermodynamic properties[2-5].

Gutman[6] introduced an index M_1 based on the degrees of the vertices (V_i) in the hydrogen suppressed graph, G, for a molecule (Eq. 1),

$$M_1 = \sum_{i=1}^{n} V_i^2 \qquad \ldots (1)$$

Randic[7] also defined two parameters considering h (the path length between the vertices) to be either zero or 1. The first index (when h = 0) is the same as the Gutman's M_1 index. The second index of Randic, M_2 (when h = 1), which he termed as χ (a bond parameter), is given by Eq. 2,

$$M_2 = \chi = \sum_{q} (V_i V_j)^{-\frac{1}{2}} \qquad \ldots (2)$$

where V_i and V_j denote the degrees of the two end points of an edge in the hydrogen suppressed graph G and the summation is extended over all q edges.

Trinajstic *et al.*[3] have introduced an index, $I_{D,1}^{W}$, which evolves from the distance matrix, for the modeling of the thermodynamic properties of the molecules. The partition of the total topological distance in the molecule, W, into distances of different lengths d can be used as a basis of the definition of an information measure of the distance matrix,

$$I_D^W = W \log_2 W - \Sigma K_d \, d \log_2 d \qquad \ldots (3)$$

where the distance of value d appears K_d times in the W partition. This index is normalised by the following process to obtain a new index, $I_{D,1}^{W}$,

$$I_{D,1}^{W} = 2\, I_D^W / N(N-1) \qquad \ldots (4)$$

where N = total number of carbon atoms in the molecule.

In this paper we have studied the QSPC of a series of hydrocarbons (including aromatic and aliphatic molecules) taking entropy (S°) as the dependent variable and χ and $I_{D,1}^{W}$ as the independent variables. This type of additivity scheme is rather unusual one. χ (a bond parameter) is taken from the adjacency matrix and $I_{D,1}^{W}$ (a distance parameter) is taken from the distance matrix. The bonding pattern of a molecule can be well explained by taking together both adjacency and distance matrices. The former explains the connection of a vertex with its adjacent vertices whereas the letter explains the correlation of a vertex with all other vertices of the molecule. Till now, the parameters χ and $I_{D,1}^{W}$ have been used only individually in the linear and nonlinear equations for the study of QSPC.

The topological information index ($I_{D,1}^{W}$) and the connectivity index (χ[8]) of the training set compounds have been calculated by standard methods. The training set is classified according to the number of π-bonds present. Each set ($\pi = 0,1,2,3,4$) has been fitted into the model Eq. 5,

$$S^\circ = \alpha\chi + \beta I_{D,1}^{W} + \gamma \qquad \ldots (5)$$

S° is the entropy of the given substance in its thermodynamic reference state at the temperature 298 K. All the data are taken from the literature[9].

Results and Discussion

Trinajstic *et al.*[3] have introduced the index $I_{D,1}^{W}$ in the study of QSPC of some aromatic compounds. Another variable they have added is N_C which lacks the power to differentiate between the isomers. To get a good model they had to take re-

Table 1—Values of x, $I_{D,1}^{W}$, S°_{obs}, S°_{cal} for the Training Set $\pi = 0$

Compounds	(x)	$I_{D,1}^{W}$	S°_{obs} (kcal/mol)	S°_{cal} (kcal/mol)	Difference
Methane	0	0	44.50	44.00	0.50
Ethane	1	0	54.85	57.40	2.55
Propane	1.4142	1.9988	64.51	65.09	0.58
n-Butane	1.9142	4.0750	74.10	74.01	0.09
2-Methylpropane	1.7320	3.7527	70.42	71.22	0.80
n-Pentane	2.4142	6.2892	83.27	83.08	0.19
n-Hexane	2.9142	8.6384	92.45	92.29	0.16
n-Heptane	3.4142	11.1108	101.64	101.64	0.00
n-Octane	3.9142	13.6949	110.82	111.10	0.28
2-Methylheptane	3.7700	12.9345	108.81	108.36	0.05
3-Methylheptane	3.8081	12.4918	110.32	108.40	1.92
4-Methylheptane	3.8081	12.3465	108.35	108.24	0.11
3-Ethylhexane	3.8461	11.9120	109.51	108.28	1.23
2,2-Dimethylhexane	3.5607	11.7085	103.06	104.24	1.18
2,3-Dimethylhexane	3.6807	11.5842	106.11	105.71	0.40
2,4-Dimethylhexane	3.6639	11.7390	106.51	105.66	0.85
2,5-Dimethylhexane	3.6259	12.1817	104.93	105.62	0.69
3,3-Dimethylhexane	3.6213	11.1198	104.70	104.42	0.28
3,4-Dimethylhexane	3.7187	11.2998	107.15	105.91	1.24
2-Methyl-3-ethylpentane	3.7187	11.1503	105.43	105.76	0.33
3-Methyl-3-ethylpentane	3.1213	10.6797	103.48	97.25	6.23
2,2,3-Trimethylpentane	3.4814	10.5128	101.62	101.90	0.28
2,2,4-Trimethylpentane	3.4165	10.9635	101.62	101.51	0.11
2,3,3-Trimethylpentane	3.5040	10.3642	103.14	102.04	1.10
2,3,4-Trimethylpentane	3.5534	10.8299	102.99	103.20	0.21
2,2,3,3-Tetramethylbutane	3.2500	9.7432	94.34	97.97	3.63
n-Nonane	4.4142	16.3801	120.00	120.67	0.67
n-Decane	4.9142	19.1575	129.19	130.35	1.16
n-Undecane	5.4142	22.0194	138.37	140.11	1.74

course to nonlinear equations and in some cases to addition of variables. Connectivity index, x, can quantitatively differentiate the positional isomers and it is chosen for this purpose in the present study.

In the first set, i.e., when $\pi = 0$ for C_8 systems, 18 compounds have $N_C = 8$ and for that the variable N_C does not seem to be appropriate in the study of QSPC. Eq. 6 seems to be a good model to predict the entropy of the saturated hydrocarbons on the basis of x and $I_{D,1}^{W}$. From Eq. 6, it is observed that x has a greater contribution to the QSPC for entropy of saturated hydrocarbons. The predicted and observed values of S° for saturated hydrocarbons are given in Table 1.

$$S^\circ = 13.402 + 1.070\ I_{D,1}^{W} + 43.995 \qquad \ldots (6)$$

$$(n = 29, r = 0.997, f = 0.017)$$

Neither x nor $I_{D,1}^{W}$ have different values for *cis* and *trans* isomers. Eq. 7 explains the correlations of x and $I_{D,1}^{W}$ with S° for compounds with one π-bond. Though the correlation coefficient is found to be highly significant ($r = 0.998$) a remarkable extent of deviation has been observed in predicted and observed S° values of *cis* and *trans* isomers. Table 2 shows the observed and predicted values of S° for compounds with one π bond.

$$S^\circ = 17.438\ x + 0.229\ I_{D,1}^{W} + 45.791 \qquad \ldots (7)$$

$$(n = 35, r = 0.998, f = 0.014)$$

For the compounds having two π-bonds, Eq. 8 has been obtained to predict the S° values (Table 3).

$$S^\circ = 13.300\ x + 1.097\ I_{D,1}^{W} + 47.534 \qquad \ldots (8)$$

$$(n = 22, r = 0.997, f = 0.019)$$

For a hypothetical molecule C_1 (π bond = 0, CH_4: neutral) when π bond character increases, the S° value increases linearly. Due to limited experimental data, studies on aliphatic compounds with π bond = 3 and 4 could not be done.

Eq. 9 shows the correlation of S° with x and $I_{D,1}^{W}$ for π bond = 3 systems (Table 4) and more precisely for aromatic systems when π bond = 3. The intercept in Eq. 9 (23.739) is much smaller in comparison to these in Eqs 6-8. This may be ascribed to the aromaticity of the system with π bond = 3. For π bond = 4 system (Eq. 10), another

Table 2—Values of x, $I^W_{D,1}$, S°_{obs}, S°_{cal} for the Training Set $\pi = 1$

Compounds	(x)	$I^W_{D,1}$	S°_{obs} (kcal/mol)	S°_{cal} (kcal/mol)	Difference
Ethene	0.5000	0	52.54	54.50	1.96
Propene	0.9856	1.9988	63.80	63.43	0.37
1-Butene	1.5236	4.075	73.48	73.29	0.19
cis-2-Butene	1.4880	4.075	71.90	72.67	0.77
trans-2-Butene	1.4880	4.075	70.86	72.67	1.81
2-Methylpropene	1.3535	3.7527	70.17	70.25	0.08
1-Pentene	2.0236	6.2892	83.08	82.51	0.57
cis-2-Pentene	2.0260	6.2892	82.76	82.56	0.20
trans-2-Pentene	2.0260	6.2892	81.81	82.56	0.75
2-Methyl-1-butene	1.9142	5.7515	81.73	80.48	1.25
3-Methyl-1-butene	1.8963	5.7515	79.70	80.17	0.47
2-Methyl-2-butene	1.6969	5.7515	80.90	76.69	4.21
1-Hexene	2.5236	8.6384	92.25	91.77	0.48
cis-2-Hexene	2.5260	8.6384	92.35	91.81	0.54
cis-3-Hexene	2.5640	8.6384	90.73	92.48	1.75
2-Methyl-1-pentene	2.4142	7.9777	91.32	89.72	1.60
3-Methyl-1-pentene	2.4343	7.7662	90.42	90.02	0.40
4-Methyl-1-pentene	2.3794	7.9777	89.58	89.11	0.47
2-Methyl-2-pentene	2.4040	7.9777	90.45	89.54	0.91
cis-3-Methyl-2-pentene	2.4267	7.7662	90.45	89.89	0.56
trans-3-Methyl-2-pentene	2.4267	7.7662	91.26	89.89	1.37
cis-4-Methyl-2-pentene	2.3987	7.9777	89.23	89.44	0.21
trans-4-Methyl-2-pentene	2.3987	7.9777	88.02	89.44	1.42
2-Ethyl-1-butene	2.4749	7.7662	90.01	90.72	0.71
2,3-Dimethyl-1-butene	2.2969	7.3199	89.39	87.52	1.87
3,3-Dimethyl-1-butene	2.1969	7.0853	83.79	85.72	1.93
2,3-Dimethyl-2-butene	2.2500	7.3199	86.67	86.70	0.03
1-Heptene	3.0236	11.1108	101.43	101.06	0.37
1-Octene	3.5236	13.6949	110.61	110.37	0.24
1-Nonene	4.0236	16.3801	119.80	119.71	0.09
1-Decene	4.5236	19.1575	128.98	129.06	0.08
1-Undecene	5.0236	22.0194	138.16	138.43	0.27
1-Dodecene	5.5236	24.9592	147.34	147.83	0.49

Table 3—Values of x, $I^W_{D,1}$, S°_{obs}, S°_{cal} for the Training Set $\pi = 2$

Compounds	(x)	$I^W_{D,1}$	S°_{obs} (kcal/mol)	S°_{cal} (kcal/mol)	Difference
Ethyne	0.3333	0.9988	47.997	51.96	3.96
Propadiene	0.7071	1.9988	58.30	59.13	0.83
Propyne	0.7887	1.9988	59.30	60.21	0.91
1,2-Butadiene	1.2196	4.0750	70.03	68.22	1.81
1,3-Butadiene	1.1498	4.0750	66.62	67.29	0.67
1-Butyne	1.3493	4.0750	69.51	69.95	0.44
2-Butyne	1.2500	4.0750	67.71	68.62	0.91
1-Pentyne	1.8493	6.2892	79.10	79.03	0.07
2-Pentyne	1.8107	6.2892	79.30	78.51	0.79
3-Methyl-1-butyne	1.7320	5.5715	76.23	76.88	0.65
1,2-Pentadiene	1 7576	6.2892	79.70	77.81	1.89
cis-1,3-Pentadiene	1.6532	6.2892	77.50	76.41	1.09
trans-1,3-Pentadiene	1.6523	6.2892	76.40	76.40	0.00
1,4-Pentadiene	1.633	6.2892	79.70	76.15	3.55
2,3-Pentadiene	1.372	6 2892	77.60	77.47	0.13
3-Methyl-1,2-butadiene	1.6035	5.7515	76.40	75.17	1.23
2-Methyl-1,3-butadiene	1.5505	5.7515	75.44	74.46	0.98
1-Hexyne	2.3493	8.6384	88.27	88.25	0.02
1-Heptyne	2.8493	11.1108	97.25	97.62	0.37
1-Octyne	3.3493	13.6949	106.63	107.10	0.47
1-Nonyne	3.8493	16.3801	115.82	116.70	0.88
1-Decyne	4.3493	19.1575	125.00	126.40	1.40

Table 4—Values of x, $I^W_{D,1}$, S°_{obs}, S°_{cal} for the Training Set $\pi = 3$

Compounds	(x)	$I^W_{D,1}$	S°_{obs} (kcal/mol)	S°_{cal} (kcal/mol)	Difference
Benzene	2.000	6.8039	64.34	66.78	2.44
Ethylbenzene	2.9713	10.6048	86.15	8673	0.58
1,2-Dimethylbenzene	2.8273	10.0075	84.13	83.84	0.47
1,3-Dimethylbenzene	2.8214	10.1545	85.49	83.39	2.10
1,4-Dimethylbenzene	2.8214	10.2892	84.23	83.13	1.10
Methylbenzene	2.4107	8.5047	76.42	75.04	1.38
n-Propylbenzene	3.4713	12.9856	95.74	96.18	0.44
Isopropylbenzene	3.354	12.2267	92.87	94.35	1.48
1,3,5-Trimethylbenzene	3.232	11.7199	92.15	91.90	0.25
n-Butylbenzene	3.9713	15.576	104.91	105.24	0.33

Table 5—Values of x, $I^W_{D,1}$, S°_{obs}, S°_{cal} for the Training Set $\pi = 4$

Compounds	(x)	$I^W_{D,1}$	S°_{obs} (kcal/mol)	S°_{cal} (kcal/mol)	Difference
Ethenylbenzene (Styrene)	2.6076	10.6048	82.48	82.48	0.00
Isopropenylbenzene	3.0142	12.2262	91.70	91.95	0.25
o-Methylstyrene	3.0243	11.9792	91.70	92.45	0.75
m-Methylstyrene	3.0183	12.2267	93.10	92.04	1.06
p-Methylstyrene	3.0183	12.4579	91.70	92.13	0.43

fall has been observed in the intercept value and this may be ascribed to the presence of styrene system (see Table 5).

$$S^\circ = 28.070\,x - 1.925\,I^W_{D,1} + 23.739 \qquad \ldots (9)$$

(n = 10, r = 0.992, f = 0.017)

$$S^\circ = 21.792\,x + 0.375\,I^W_{D,1} + 21.688 \qquad \ldots (10)$$

(n = 5, r = 0.990, f = 0.009)

To have a generalised equation, π-character was included in the variables and an equation was obtained (Eq. 11). The coefficient of π reveals that with increasing π value the entropy of the system decreases to the extent of 3.611 units per π bond.

$$S^\circ = 2.692\,x + 3.212\,I^W_{D,1} - 3.611\pi + 58.480 \qquad \ldots (11)$$

(n = 101, r = 0.987, f = 0.023).

References

1 Balaban A T, *Steric fit in QSAR, lecture notes in chemistry* (Springer Verlag, Berlin), 1979.

2 Bonchev D, Knop J V & Trinajstic N, ***Math Chem*, 6** (1979) 21.

3 Mekenyan O, Bonchev D & Trinajstic N, *Int J quantum Chem*, **18** (1980) 369.

4 Bonchev D, Kamenski D & Kamenski V, ***Bull Math Bio*, 38** (1976) 119.

5 Bonchev D & Trinajstic N, *Int J quantum Chem* (*Quantum Chemistry Symp*), **12** (1978) 293.

6 Gutman I, *J chem Phys*, **62** (1975) 3399.

7 Randic M, *J Am chem Soc*, **97** (1975) 6609.

8 Murry J W, Kier B L & Hall H L, *J medni Chem*, **19** (1976) 573.

9 *Handbook of physics and chemistry* (CRC Press, Ohio) 1975-76.

Indian Journal of Chemistry
Vol 27A, March 1988, pp 192-197

Hot Atom Chemistry in Oxyanion Targets: Part 3†—Some Theoretical Aspects of Reincorporation of Parent Form in Permanganates

SHUDDHODAN P MISHRA* & (Miss) JYOTI SINGH
Nuclear and Radiochemistry Laboratory, Department of Chemistry, Banaras Hindu University, Varnasi 221005

Received 14 *April* 1987; *revised* 22 *June* 1987; *accepted* 27 *July* 1987

An attempt is made to advance qualitative and quantitative interpretations for the observed data on retention of recoil ^{56}Mn in potassium and ammonium permanganates in the light of following physical models; (a) extreme back-diffusion model, (b) billiard-ball collision model and (c) hot zone model.

The solid state reactions occurring during energy loss of (n, γ) produced recoils have been studied in mixed and pure complexes and results obtained are described by a few basic mechanisms: (i) correlated recombination (primary retention); (ii) direct substitution; (iii) multi-step process involving ligand vacancy exchange followed by combination; and (iv) replacement reactions (billiard ball)[2-5]. A good success for the hot atom behaviour of such complex ionic crystals appears to have been obtained by the atomic collision dynamics[5] using computer simulation technique. An analysis of the position of defects which escape the collapse of close pairs might help to elucidate the thermal annealing and solid state exchange processes observed in complex ionic compounds[4]. However, similar calculations are not available in the case of oxyanions. In the present paper, initial retention and maximum retention after annealing of ^{56}Mn in potassium and ammonium permanganate targets are considered to arise mainly from the secondary effects produced during the process of attenuation of recoil energy and the results are discussed in the light of some known models, viz. back-diffusion, billiard ball collision and hot zone[6-8].

Materials and Methods

Potassium or ammonium permanganate (300 mg) was subjected to thermal neutron activation upto 20 hr using a 300 mCi (Ra-Be) neutron source having an integral flux of 3.2 × 10^6n cm^{-2}s^{-1}. The lower valent and parent forms of manganese were separated using the precipitation technique as described earlier[1]. The radioactivities were counted with the help of an end-window G.M. counter under conditions of constant geometry and necessary corrections applied. Irradiation was also performed at 77K and same procedures were adopted for separation and measurement of radioactivities. Isothermal annealing was accomplished in an electronically controlled oven (±0.5°C).

Theoretical computations of various data were performed at the Banaras Hindu University Computer Centre using the ICL 1904 Computer.

Results and Discussion

Experimentally observed results: (*a*) *Solid* $KMnO_4$ *target*

(i) Initial retention of ~12% was obtained[1] for room temperature activation. However, an initial retention of 20-25% was obtained by reactor irradiation[9-11].

(ii) Similar initial retention (~12%) was obtained on irradiation at 77K in contrast to higher value (~25%) obtained by Van Herk and Aten[12]. In the case of alkali bromates, Sasaki and Shiokawa[13] have also concluded that the retention is constant below room temperature but increases in the higher temperature regions. However, as the material activated at liquid nitrogen was dissolved in water at room temperature, annealing at this temperature is expected to be nearly complete[14]. At this stage, it appears that annealing between 77K and 298K is practically unaffected by radiation dose of the order used in the present work.

(iii) A maximum retention of ~80% was observed after isothermal annealing[1], which is compatible with the result (~78%) of Teeling *et al.*[11].

(*b*) *Solid* NH_4MnO_4 *target*

For this compound, initial retention both for room temperature (298K) and low temperature (77K) irradiation was ~4% (see ref. 1) and maxi-

---

† For Part 2, see ref. 1

Table 1—Back-diffusion Parameters for a few Selected ^{56}Mn Recoil Energies of (n, γ) Activated Permanganates

Recoil energy E_0 (ev)	Hard sphere radius R (Å)	Distance of closest approach c (Å)	Retained fraction F_0 (%)	Probability of particular recoil energy P	Retained fraction $F_0' = P \cdot F_0$ (%)
38.9	0.697	1.574	45.168	0.036	0.935
52.0	0.661	1.552	50·.613	0.021	0.865
111.2	0.570	1.456	63.314	0.010	1.380
189.2	0.508	1.374	70.873	0.022	0.446
213.7	0.494	1.360	72.458	0.035	0.116
245.9	0.478	1.339	74.215	0.011	1.314
292.4	0.458	1.320	76.291	0.009	3.120
356.6	0.436	1.300	78.535	0.007	0.942
476.8	0.404	1.289	81.569	0.008	5.547
502.2	0.398	1.287	82.082	0.020	6.123

Cumulative back-diffusion retention $= \sum_{i=1}^{280} P_{(i)} \cdot F_{0(i)} = 58.2\%$

mum retention by isothermal annealing was ~ 60% (ref. 1).

Interpretation of experimental results in the light of some models: (*a*) *Extreme back-diffusion model*[6]

Successful explanation of retention in potassium chromate[15], metalloporphines[16] and cobalt complexes[17] has been offered by this model. The required maximum probability of reformation is equal to $(1-F_d)$, where F_d the probability of damage is given by Eq. (1)

$$F_d = \frac{2Rc}{B_L^2} \qquad \ldots (1)$$

In Eq. (1) R represents the hard sphere collision radius, c the distance of closest approach and B_L the bond length between manganese and oxygen atom in permanganate which is 1.63Å. Further, the fractional per cent retention, F_0 (theoretical) is calculated using the relation (2)

$$F_0 = 100(1-F_d) \qquad \ldots (2)$$

For a particular recoil energy with probability P,

$$F_0' = P \cdot F_0 \qquad \ldots (3)$$

Hence, theoretical cumulative per cent retention in permanganate is given by Eq. (4)

$$\text{Cumulative \% retention} = \sum_{i=1}^{280} P_{(i)} F_{0(i)} \qquad \ldots (4)$$

where $P_{(i)}$ is the probability of the particular ith recoil energy which takes part in the parent reformation process.

Values of R, c, % F_0, P and % F_0' (Table 1) have been calculated for all recoil energies (E_0) of ^{56}Mn (viz, 25-502 eV). In the above recoil energy range of 25-502 eV in all, 280 values corresponding to each parameter are obtained, but only a few selected values are reported in Table 1. It is noticed from Table 1 that both R and distance of closest approach (c) decrease with increase in recoil energy as expected from the calculations of Wiles and Wong[6].

Presently we have calculated the % cumulative retention, taking into account the probability factor and the value is found to be ~58% (Table 1). This value lies between the value of initial retention (~12%) and maximum retention (~80%)[1] after annealing for potassium permanganate which is in close agreement with the values of Wiles and Wong[6] for other oxyanions. Nonetheless, Wiles and Wong[6] have reported a value of % F_0 of ~ 75% for MnO_4^- at a recoil energy of 400 eV. These authors have not taken into account the contributions at all recoil energies. One interesting and noteworthy result of NH_4MnO_4 system is that the maximum retention after annealing (~60%)[1] is quite close to the value of cumulative retention of ~58% (Table 1) calculated presently on the basis of back-diffusion mechanism. Since the 100% degree of ordering cannot be achieved, the experimental values are expected to be somewhat different from the calculated values, and a proper comparison should be done only at the end of back-diffusion, i.e. after final annealing where possible.

(*b*) *Billiard ball collision model*[7]

The idea was further developed by Miller *et al.*[18] and later by Capron and Oshima[19] to explain their results for multicomponent systems, such as CCl_4-Br system. A more rigorous theoretical treatment of the billiard ball collision model in solids

Table 2—Billiard Ball Collision Parameters for a few Selected ^{56}Mn Recoil Energies of (n, γ) Activated Permanganates

Recoil energy E_0 (eV)	Bohr's screened potential $V(c) \times 10^{13}$ (Volt)	Soft sphere collision parameter b (Å)	†$P_a \times 10^2$	††P_m
38.9	0.776	1.568	4.749	0.452
52.0	0.911	1.547	4.334	0.506
111.2	1.864	1.450	3.417	0.633
189.2	3.426	1.367	2.855	0.709
213.7	3.831	1.353	2.727	0.725
245.9	4.476	1.332	2.582	0.742
292.4	5.149	1.313	2.408	0.763
356.6	5.972	1.294	2.107	0.785
476.8	6.406	1.285	1.921	0.816
502.2	6.507	1.283	1.870	0.821

†P_a: Probability of collision of the projectile atom with the target atoms

††P_m: Probability of the recoil atom entering a molecule.

Table 3—Billiard Ball Collision Contribution to Initial Retention for a few Selected ^{56}Mn Recoil Energies of ($n\gamma$) Activated Permanganates

Recoil energy E_0 (eV)	$\varepsilon = 30$ eV					
	$E_c = 50$ eV			$E_c = 100$ eV		
	$\Delta \times 10^{11}$	R_{bil} (%)	$R'_{bil} = R_{bil} \cdot P$ (%)	$\Delta \times 10^{11}$	R_{bil} (%)	$R'_{bil} = R_{bil} \cdot P$ (%)
38.9	6.116	1.661	0.034	31.113	0.339	0.007
52.0	5.315	1.941	0.033	17.606	0.601	0.010
111.2	4.395	2.304	0.050	10.399	0.983	0.021
189.2	4.134	2.301	0.014	9.046	1.056	0.007
213.7	4.094	2.269	0.035	8.856	1.053	0.016
245.9	4.054	2.230	0.039	8.673	1.046	0.018
292.4	4.013	2.159	0.088	8.486	1.024	0.042
356.6	3.974	2.062	0.025	8.316	0.987	0.012
476.8	3.931	1.878	0.128	8.129	0.909	0.062
502.2	3.925	1.843	0.137	8.101	0.894	0.067

$$\text{Cumulative billiard ball retention} = \sum_{i=1}^{280} R_{bil(i)} \cdot P_{(i)}$$

$= 2.01\%$ when $\varepsilon = 30$ eV, $E_c = 50$ eV

$= 0.93\%$ when $\varepsilon = 30$ eV, $E_c = 100$ eV

$= 1.02\%$ when $\varepsilon = 15$ eV, $E_c = 50$ eV

$= 0.45\%$ when $\varepsilon = 15$ eV, $E_c = 100$ eV

after n successive collisions was later given by Wong and Wiles[7].

Presently, we have calculated the values of different parameters of billiard ball collision model[7], i.e. $V(c)$, b, P_a, P_m, Δ and billiard ball retention for various values of ε (15 and 30 eV) when E_c is 50 or 100 eV for all 280 recoil energies of ^{56}Mn (25-502 eV). Values of the above parameters are reported in Tables 2 and 3 for only a few selected recoil energies and for $\varepsilon = 30$ eV when $E_c = 50$ and 100 eV. It is evident that soft sphere collision parameter b (Table 2) decreases with increase in recoil energy, a trend expected from the theory.

Further, cumulative billiard-ball retention (Table 3) is calculated using the relation

Theoretical cumulative retention

$$= \sum_{i=1}^{280} R_{bil(i)} P_{(i)} \qquad \ldots (5)$$

A maximum cumulative value of billiard ball retention of ~2.01% (Table 3) is obtained for $\varepsilon = 30$ eV and $E_c = 50$ eV, and this value is approximately double that at $\varepsilon = 30$ eV and $E_c = 100$ eV. Similar results and trends were also observed by Wong and Wiles[7] for different recoil atoms in a few solid compounds including manganese carbonyls. So far, billiard ball contribution towards initial retention, for permanganates, has not been reported and the present results could be taken a novel effort in this direction.

(*c*) *Hot zone model*[8]

This model[8], which explains the chemical effects of nuclear recoil in solids, is based upon Seitz and Koehler's[20] view of the slowing-down of energetic atoms and makes use of the concept of the displacement spikes. Basically, the underlying mechanism is dependent on the loss of a part of energy of the recoil atoms via elastic collisions with the surrounding atoms and the appearance of the remaining energy as heat in small zones. The life-time of these zones is so short that the displaced atoms cannot return to their original lattice position and thus, form the displacement spikes. Aten[21] and Harbottle[22] have put forward the evidence of specific effects in the hot zone.

Taking into account all ^{56}Mn recoil energies, various relevant parameters of hot zone model[8] are calculated.

Values of velocity of recoil atom (V), number of collisions (n), probability factor (n_j) and average energy (ΔT) are listed in Table 4 for a few selected ^{56}Mn recoil energies out of 280 ranging from 25-502 eV. An inspection of Table 4 reveals that for the maximum recoil energy of 502.2 eV in the targets studied, the recoil atom with an initial velocity (V) of 4.16×10^{14}Å s^{-1} dissipates an average energy (ΔT) of 173.6 eV in the first collision and in about 6.95 collision comes down to ~ 25 eV.

Tables 5 and 6 gives the values of mean free path (L_s), mean maximum range ($\bar{r}$), diffusion distance (l), radius of hot zone (r_m), critical radius (r) and time of thermalisation (t) at selected recoil energies for potassium and ammonium permanganates respectively. For all recoil energies and for both the targets; the value of $L_s > r$ (Tables 5 and 6). Hence, manganese atoms will definitely be outside the region in which the rate processes, during the existence of the hot zone, contribute to recombination. These recoil manganese atoms, created outside the hot zone, participate little in the hot zone reactions. Consequently, the contributions of hot zone reactions towards initial retention are low indeed. Furthermore, a comparison of values of mean free path (L_s) and critical radii (r) for both the targets ($KMnO_4$ and NH_4MnO_4) reveals that L_s and r for $KMnO_4$ are greater than those for NH_4MnO_4. Values of mean atomic radius (r_s), thermal diffusion coefficient (D), diffusion distance (l), radius of hot zone (r_m) and time of thermalisation (t) are also greater for $KMnO_4$ than those for NH_4MnO_4 at all recoil energies (Tables 5 and 6). This is due to the reduction of the recoil fragments by ammonium ions in NH_4MnO_4 (see ref. 1). It is evident that (r_m) increases with increase in recoil energy in both the targets (Tables 5 and 6). Since, the existence of hot zone is very short lived (~ 10^{-12}s), the reactions are quenched before reaching completion due to rapid cooling and solidification of the hot zone. These reactions may, however, be reinitiated on heating as is apparent from the increase of retention on thermal annealing.

The time (t) required for recoil ^{56}Mn atoms, with an energy 502.2 eV, to come down to ~ 25 eV after collision is calculated to be 5.45×10^{-13} and 3.47×10^{-13}s for $KMnO_4$ and NH_4MnO_4 respectively (Table 5 and 6). Thus, the enormous loss of energy of the recoil atom, in both the targets, in spheres of radii equal to their mean free path (L_s) (31.6 and 20.8Å) produces a high local temperature in the crystal within very

Table 4—Calculated Values of a few Hot Zone Parameters during Thermalisation of Recoil Manganese Atoms in Permanganates for a Few Selected Recoil Energies

Recoil energy E_0 (eV)	Velocity of recoil atom $V \times 10^{-14}$ (Å sec^{-1})	Number of collisions n	Probability factor n_j	Average Energy ΔT (eV)
38.9	1.078	2.49	3.88	13.45
52.0	1.162	1.33	4.29	17.98
111.2	1.295	0.13	4.96	38.45
189.2	1.471	0.97	5.88	65.40
213.7	1.538	1.31	6.23	73.88
245.9	1.725	2.12	7.27	84.99
292.4	2.041	3.17	9.09	101.09
356.6	3.039	5.36	15.45	123.27
476.8	3.278	5.75	17.10	164.81
502.2	4.161	6.95	23.49	173.61

Table 5—Relevant Parameters of Hot Zone during Thermalisation of Recoil Manganese Atoms in $KMnO_4$ for a few Selected Recoil Energies

Mean atomic radius (r_s) = 1.57Å
Thermal diffusion coefficient (D) = 0.618×10^{-3} cm²/s

Recoil energy E_0 (eV)	Mean free path L_s (Å)	Mean maximum range $\bar{r}$ (Å)	Diffusion distance l (Å)	Radius of the hot-zone r_m (Å)	Critical radius r (Å)	Time of thermalisation $t \times 10^{13}$ (sec)
38.9	10.14	39.45	9.24	9.79	6.26	2.34
52.0	10.69	41.17	7.12	10.32	6.58	1.23
111.2	11.55	43.85	2.44	11.13	7.07	0.12
189.2	12.70	47.36	7.24	12.16	7.70	0.84
213.7	13.14	48.68	8.69	12.54	7.93	1.12
245.9	14.37	52.38	12.07	13.56	8.56	1.76
292.4	16.50	58.63	16.96	15.20	9.58	2.56
356.6	18.80	78.80	31.58	19.88	10.62	4.17
476.8	25.45	83.82	35.24	20.92	13.13	4.47
502.2	31.63	103.12	49.67	24.54	15.39	5.45

Table 6—Relevant Parameters of Hot Zone during Thermalisation of Recoil Manganese Atoms in NH_4MnO_4 for a few Selected Recoil Energies

Mean atomic radius (r_s) = 1.35Å
Thermal diffusion coefficient (D) = 0.457×10^{-3} cm²/s

Recoil energy E_0 (eV)	Mean free path L_s (Å)	Mean maximum range $\bar{r}$ (Å)	Diffusion distance l (Å)	Radius of the hot-zone r_m (Å)	Critical radius r (Å)	Time of thermalisation $t \times 10^{13}$ (sec)
38.9	6.45	25.11	5.88	9.23	5.38	1.49
52.0	6.80	26.21	4.53	9.75	5.66	0.78
111.2	7.35	27.91	1.53	10.52	6.08	0.07
189.2	8.09	30.15	4.61	11.50	6.62	0.54
213.7	8.36	30.99	5.53	11.86	6.82	0.71
245.9	9.15	33.34	7.68	12.84	7.36	1.12
292.4	10.50	37.32	10.80	14.40	8.24	1.63
356.6	11.20	50.17	20.10	18.84	9.01	2.65
476.8	16.20	53.36	22.43	19.83	11.30	2.84
502.2	20.77	65.65	31.62	23.27	13.24	3.47

short periods mentioned above. For low recoil energies, this loss is quick and thus hot spots are created which merge to form the hot zone within around 10^{-12}s. With decrease in recoil energy, the collision cross-section becomes very large so that the remainder of its kinetic energy will be dissipated within a compact volume whose radius is of the order of its mean free path. This energy is transferred to the lattice by collisions which takes place in very quick succession and these collisions produce, within a volume mentioned above, a hot spot, i.e., a region, where the recoil manganese atoms and the displaced secondary atoms attain kinetic energies of the order of 25 eV in coming to rest or where a oxygen atom receives a little less than the threshold energy for displacement. The diameters of these hot volumes, may be ascribed to the mean maximum range ($\bar{r}$) of ^{56}Mn recoil atom in both targets and are found to be 103.1 and 65.6Å, at 502.2 eV recoil energy, in $KMnO_4$ and NH_4MnO_4 respectively (Tables 5 and 6).

Conclusions

(1) Back-diffusion mechanism seems to be successful, in the case of permanganates, so far, as maximum retention after annealing is concerned. However, it does not account for the initial retention at room temperature.

(2) Billiard ball substitution contribution to the initial retention is low. So, the rest is considered to be due to other hot or chemical processes beyond the scope of the idealised billiard ball concept.

(3) In hot zone mechanism, the mean free path of recoil manganese atom, for recoil energies 25-502 eV, is greater than the critical radius for both the targets ($KMnO_4$ and NH_4MnO_4). Therefore, the probability of thermalization of these recoil atoms within the critical volume to contribute to

parent reformation becomes very less. Hence, the contribution of hot zone towards initial retention appears to be very low.

(4) Experimental results at 77K reveals that thermal diffusion induced reactions leading to parent réformation (up to room temperature) are absent. Hence, retention values of about 12% and 4% in both the targets are purely due to hot processes (failure of bond rupture followed by quick correlated recombination + billiard ball + hot zone + epithermal 'ion-molecule' reactions) and dissolution induced reactions.

(5) Increase in retention on thermal annealing above room temperature is due, mainly, to radical reactions or exchange processes which may also involve some intermediate species.

Thus, detailed computations based on existing physical models show that separate contributions of different mechanisms to the retention are quite reasonable and a success lies in considering these in a cumulative fashion.

Acknowledgement

One of us (J S) is thankful to the CSIR, New Delhi, for the award of a senior research fellowship.

References

1 Part 2: Mishra S P & Singh J, *J radional nucl Chem Letts,* **105** (1986) 107.

2 Rössler K, Otterbach J & Stocklin G, *J phys Chem,* **76** (1972) 2499.

3 Müller H, Bekk P & Bicheler U, *Radiochim Acta,* **36** (1984) 115.

4 Rössler K & Robinson M T, *Atomic collisions in solids,* edited by S Datz, B R Appleton & C D Moak (Plenum Press, New York and London) Vol 1 (1975) 237.

5 Robinson M T, Rössler K & Torrens Ian M, *J chem Phys,* **60** (1974) 680.

6 Wiles D R & Wong W H, *Can J Chem,* **45** (1967) 1813.

7 Wong W H & Wiles D R, *Can J Chem,* **46** (1968) 3201.

8 Harbottle G & Sutin N, *J Phys Chem,* **62** (1958) 1344.

9 Apers D J & Harbottle G, *Radiochim Acta,* **1** (1963) 188.

10 Shiokawa T & Sasaki T, *Bull chem Soc Japan,* **43** (1970) 801.

11 Teeling M T A, Aten (Jr) A H W & Boersma J, *J inorg nucl Chem,* **42** (1980) 1535.

12 Van Herk (Jr) G & Aten (Jr) A H W, *Radiochim Acta,* **17** (1972) 214.

13 Sasaki T & Shiokawa, *Bull chem Soc Japan,* **43** (1970) 2835.

14 Cogneau M A, Apers D J & Capron P C, *Radiochim Acta,* **8** (1967) 143.

15 Maddock A G & DeMaine M M, *Can J Chem,* **34** (1957) 441.

16 Rosenberg H E & Sugihara T T, *Chemical effects of nuclear transformation,* (IAEA, Vienna) Vol II (1965) 151.

17 Moddock A G & Todesco A B J B, *Proc Inst Intern Am Conf Radiochem Pan Am Union,* (1965) 237.

18 Miller J M, Gryder J W & Dodson R W, *J chem Phys,* **18** (1950) 579.

19 Capron P C & Oshima Y, *J chem phys,* **20** (1952) 1403.

20 Seitz F & Koehler J S, *Solid state physics,* edited by Seitz & D Turnbull (Academic Press, New York) Vol II (1956) 305.

21 Aten (Jr) A H W, *Phys Rev,* **71** (1947) 641.

22 Harbottle G, *J chem Phys,* **22** (1954) 1083.

Indian Journal of Chemistry
Vol 27A, March 1988, pp 198-203

Current Efficiency, Dielectric Measurements & Ion Mobility Studies of Anodic Oxide Films Formed on Tantalum in Aqueous Electrolytes

R K NIGAM*, K C KALRA & PARVEEN KATYAL
Department of Chemistry, Maharashi Dayanand University, Rohtak 124001

Received 6 *April* 1987; *revised* 10 *July* 1987; *accepted* 27 *July* 1987

Current efficiencies, dielectric constants and ion mobilities of variously formed anodic oxide films on tantalm in the presence of various electrolytes such as citric, tartaric, acetic and hydrochloric acids have been evaluated. The current efficiencies of such films are unity upon an electrolyte concentration of 100 mol m^{-3}. However, at higher electrolyte concentration, the experimental mass-gain of the tantalum sample during anodization is greater than that expected for the anodic formation of Ta_2O_5 on tantalum, implying that mass-gain is probably due to the incorporation of anions into the films. The capacitances of such films depend on the concentration as well as nature of the aqueous electrolyte. The addition of chloride ions has been found to inhibit film growth, the effect being pronounced with increase in concentration of chloride ions. Only tantalum ions are mobile during the growth of tantalum oxide films

The kinetics of growth of anodic oxide films formed on tantalum in aqueous electrolytes, and their breakdown characteristics have been reported recently by the authors[1-3]. The present investigation is an extension of our earlier work[1-3], and has been undertaken in view of conflicting results[4-15] of studies on current efficiences, dielectric measurements and ionic mobilities of such anodic films.

Materials and Methods

Tantalum specimens (32×10^{-4} m^2 in area and 0.25 mm thick) with small tags were cut from tantalum sheets (purity 99.9%) mechanically and were chemically polished and anodically polarized in aqueous electrolytes (at a particular current density) as described earlier[1]. Increase in weight of the tantalum specimen due to its anodic oxidation to tantalum oxide was used to calculate current efficiency. The capacitance and $\tan\delta$ measurements of the oxide films were made using an electrolytic capacitor bridge (BPL, India) at 1 KHz [$\tan\delta$, known as loss tangent or dielectric loss is the ratio of the voltage drop across the hypothetical series equivalent resistance (R_S) and capacitance (C_S). Also $\tan\delta = WC_SR_S$ where $W = 2\pi F$, F being the frequency]. Special care was taken to prevent the tags dipping into the electrolyte.

For ionic mobility measurements, two 0.25 mm thick tantanum specimens of different area, one of 169 mm^2 area (sample-I) and the other 100 mm^2 area (sample-II) were anodized upto identical formation voltage in 100 mol m^{-3} aqueous citric acid at a current density of 30 A m^{-2} and then paired together to get Ta, Ta_2O_5, Ta sandwitch geometry. Perfect sealing of samples I and II was ensured by applying lacomite and Edward hard vacuum grease on the joints and the surfaces, except the outer surface of the sample II in the manner described earlier[13]. The effective geometric surface area after sealing was 1×10^{-4}m^2.

All measurements were made in a well-stirred, electronically controlled, thermostatic bath maintained at 298K (± 0.5). The results reported are the mean of five repeat experiments. All the chemicals used were of AR(BDH) grade. The density of tantalum oxide film was taken as 793 kg m^{-3} as reported by Young[15].

Results and Discussions

Current efficiency

The data for the experimental mass-gain (as a result of anodic oxidation), the calculated mass-gain due to oxidation (when current efficiency is unit) and the current effciency (η) for the growth of oxide films in 10, 50, 100, 500 and 1000 mol m^{-3} aqueous citric acid at a current density of 50 A m^{-2} (when a particular amount of charge was passed) are reported in Table 1.

At each electrolyte concentration current efficiency was found to be the same irrespective of the charge passed. The experimental and calculated mass-gains are close to each other upto an electrolyte concentration of 100 mol m^{-3} (i.e. current efficiency is close to unity) implying that the entire current passed is ionic (and no fraction is electronic) and has been used for the film formation. However, the experimentally observed mass-gains were greater than those calculated by about

Table 1—Experimental and Calculated Mass-Gains and Current Efficiencies for Formation of Oxide Films on Tantalum in Aqueous Electrolytes at Different Charges

Electrolyte	Concentration (mol m^{-3})	Charge C × 10^3	Mass-gain (kg × 10^9)		Current efficiency
			Exp.	Calc.	
Citric acid	10	8320	681	690	0.987
do	50	4000	330	332	0.994
do	100	9280	764	769	0.993
do	500	4320	380	358	1.051
do	1000	8640	801	716	1.118
Tartaric acid	100	4000	331	332	0.997
do	1000	17760	1680	1472	1.141
Acetic acid	100	18400	1520	1526	0.996
do	1000	9440	862	783	1.101
Hydrochloric acid	100	4800	393	398	0.987
do	1000	9920	889	882	1.082

6 and 12% respectively at 500 and 1000 mol m^{-3} citric acid concentrations. The data in tartaric, acetic and hydrochloric acids as electrolytes also showed similar trends (Table 1). The data indicate an excess equivalent to 14, 10 and 8% respectively over the calculated mass-gain due to oxidation in 1000 mol m^{-3} tartaric, oxalic and hydrochloric acids. Experimental error and formation of higher oxides of tantalum have been ruled out as the possible causes for the observed mass-gain since experiments were repeated five times and the excess mass-gain obtained was highly reproducible ($\pm 2 \mu g$), and in literature formations of no other stable tantalum oxide, except Ta_2O_5 has been reported. The only possibility is the incorporation of anions into the oxide film and this is substantiated by the results reported in our earlier communication[2] that the breakdown voltage of the films is affected by the incorporation of anions (and not cations) from these electrolytes. Further, the incorporation of anions such as P, Cl, S and F into the oxide film has been reported by other workers[4,5] and this also suggests that the enhanced mass-gain is most probably due to the incorporation of anions into the oxide films.

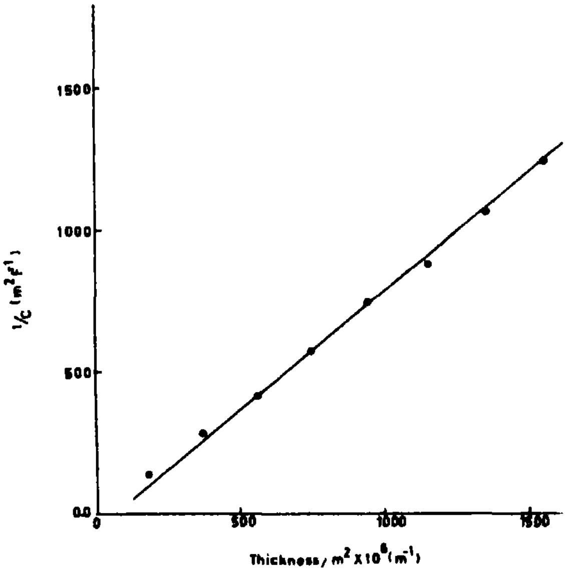

Fig. 1—Plot of 1/C per m^2 versus thickness per m^2 for anodic oxide films in aqueous citric acid.

Dielectric measurements

Capacitance data for the oxides films formed upto various formation voltages (V) in 100 mol m^{-3} aqueous citric acid at a current density 50 A m^{-2} were obtained. The plot of reciprocal capacitance (1/C) per m^2 versus thickness per m^2 calculated using Faraday's law, is linear (Fig. 1), indicating that the film is uniformly formed with constant field and 1/C can be taken as a measure of thickness of the oxide film formed in aqueous electrolyte. The effect of concentration of the electrolyte was studied by forming films of varying voltages in 10, 100 and 1000 mol m^{-3} citric acid. The plots of 1/C per m^2 versus V at each electrolyte concentration are linear (Fig. 2) and show a higher value of 1/C for a film formed at lower electrolyte concentration. The plots of tanδ versus V for these films are given in Fig. 3. As expected tanδ decreases with the increase in voltage of formation at each electrolyte concentration. The values of tanδ are higher at lower electrolyte concentration. The capacitance data were also obtained for the films formed in 100 mol m^{-3} tartaric, acetic, oxalic and hydrochloric acids and the plots of 1/C per m^2 versus V are linear and their

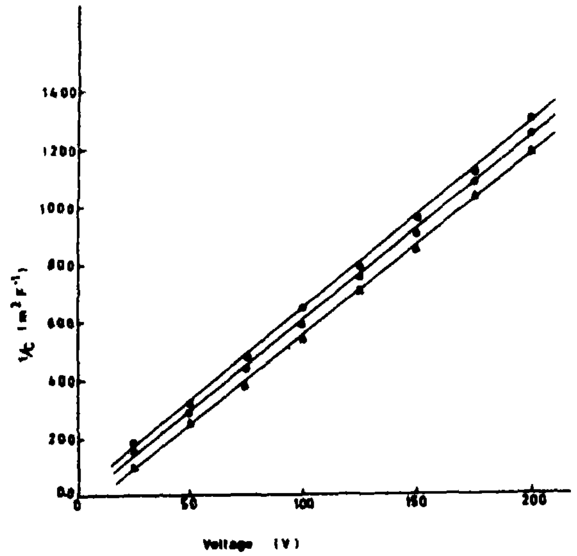

Fig. 2—Variation fo 1/C per m² with voltage of formation (V) for anodic oxide films on tantalum at varying concentrations of aqueous citric acid [(●) 10 mol m^{-3}; (⊙) 100; (△) 1000]

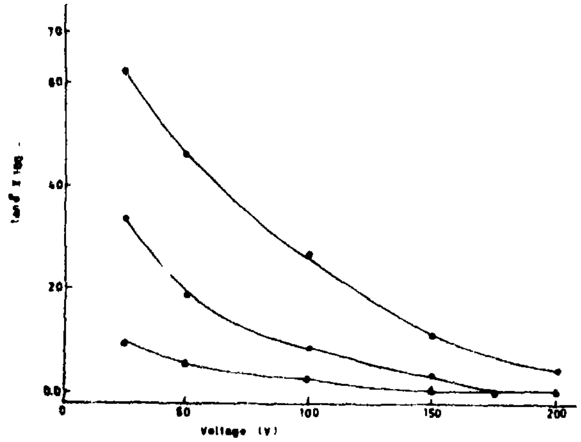

Fig. 3—Variation of dielectric loss factor (tan δ) with voltage of formation for anodic oxide films on tantalum at varying concentrations of aqueous citric acid. [(●) 10 mol m^{-3}; (○) 100; (△) 1000].

slopes obtained by the method of least squares are reported in Table 2. The typical data for a 50V film (Table 2) show dependence of capacitance on the nature of the electrolyte.

The dielectric constants were calculated using the capacitance formulae for a parallel plate capacitor in the manner described below:

The capacitance (C) is defined by Eq. (1)

$$C = \frac{\varepsilon A \varepsilon_0}{d} \qquad \ldots (1)$$

where ε is the dielectric constants of the oxide film, ε_0 is the permitivity of the free space ($8.85 \times 10^{-12} Fm^{-1}$), A is the area of the specimen (used as a counter electrode) and d is the thickness of the oxide film. At a constant current density, d increases linearly with voltage and becomes equal to βV where β is the anodization constant. Substituting βV for d in Eq. (1) we get

$$C = \frac{\varepsilon A \varepsilon_0}{\beta V} \qquad \ldots (2)$$

putting $A = 1$ m² and rearranging Eq. (2), we get

$$\frac{1}{C} = \frac{\beta V}{\varepsilon \varepsilon_0} \qquad \ldots (3)$$

The plot of 1/C versus V is linear with the slope $= \beta/\varepsilon\varepsilon_0$. If the anodization constant is known then from the slope ε can be calculated. Anodization constants were calculated from the anodization data using Faraday's law and are reported in Table 2. Using the slopes of 1/C per m² versus V plots and the anodization constants (Table 2), the dielectric constants were calculated. The results reported in Table 2 show dependence of dielectric constant on the nature as well as the concentration of the electrolyte.

Table 2—Dielectric Measurement Data for Variously Formed Tantalm Oxide Films in Aqueous Electrolytes

Electrolyte	Concentration (mol m^{-3})	Capacitance of a 50V film ($F \times 10^6$)	Anodiation constant (β) ($mV^{-1} \times 10^{10}$)	Slope of 1/C versus V plots ($F^{-1} m^2 V^{-1}$)	Dielectric constant
Tartaric acid	100	10.4	15.72	6.17	28.8
Acetic acid	100	10.9	16.31	6.16	28.9
Oxalic acid	100	10.6	15.48	6.05	28.9
Hydrochloric acid	100	10.8	16.00	6.22	29.1
Citric acid	10	10.2	15.95	6.25	28.8
do	100	11.2	15.92	6.20	29.0
do	1000	12.3	15.85	6.12	29.3

The effect of chloride ions on the capacitance of Ta_2O_5 formed in 100 mol m^{-3} citric acid was studied by measuring the capacitances of the films in the mixed solutions of hydrochloric and citric acids in the molar ratios of 1:1200, 1:120, 1:12 and 1:2.4. The capacitance of the film increased with the increase in the amount of chloride ions. The plots of 1/C per m^2 versus voltage of film formation are linear (Fig. 4). The slopes of these linear plots decrease from 6.20 to 5.30, 4.30, 3.95 and 3.45 $m^2F^{-1}V^{-1}$ when the concentration of hydrochloric acid is increased successively. The corresponding dielectric constants are found to increase from 29.0 to 33.9, 41.8, 45.6 and 52.2, respectively.

Direct anodization of tantalum was also carried out in all the mixed solutions. It is found, though the maximum film formation voltage is 365V in citric acid yet the films could be formed only upto 340, 320, 280 and 220V respectively in the respective mixed solutions containing chloride ions in increasing concentration. It appears that during the growth of tantalum oxide film in the presence of chloride ions tantalum metal combines with chloride ions giving an adsorbed film of tantalum chloride ($TaCl_5$) which then undergoes partial dissolution providing Ta^{+5} ions in solution. The released tantalum ions can combine with the chloride ions in the solution giving rise to a stable chloro-complex of tantalum (of the type $Ta_5Cl_a^{(a-5)-}$) which does not dissociates and thus prevents further participation of chloride ions in the anodic charge transfer. At higher chloride ion concentration, the chlorocomplex of tantalum is formed more efficiently, thereby inhibiting the growth of oxide film. A similar observation has been recorded earlier[12].

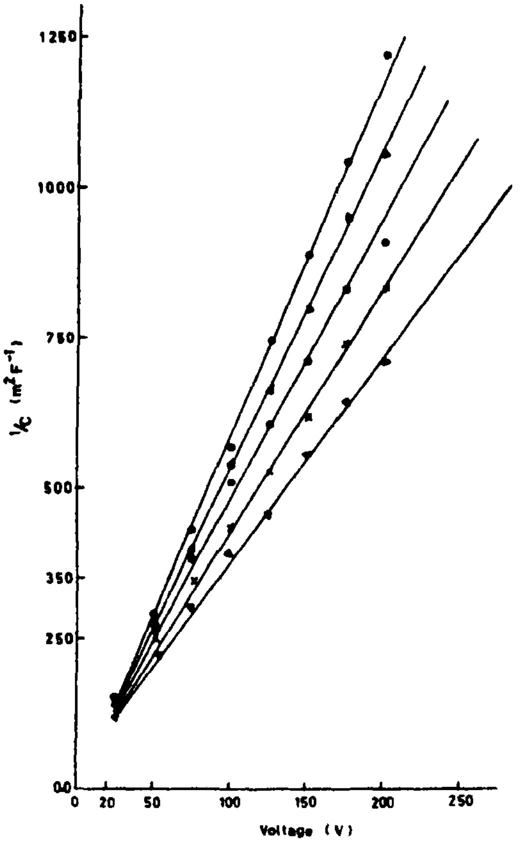

Fig. 4—Effect of chloride ion concentration on anodic oxide film growth on tantalum. [(○) 100 mol m^{-3} citric acid; mixed solution of hydrochloric acid and citric acid in the molar ratios of (▲) 1:1200; (●) 1:120 (×) 1:12; (△) 1:2.4].

The rate of film dissolution was studied next by measuring the capacitance of a 50 V film (formed in 100 mol m^{-3} citric acid) in 5,400 and 10,800 mol m^{-3} aqueous hydrofluoric acid solutions at various intervals of time (t) and the plots of 1/C per m^2 versus t are shown in Fig. 5. The film dissolves more readily in 10,800 mol m^{-3} than in 5,400 mol m^{-3} HF; for instance, the time periods required to dissolve half of the film in 10,800 and 5,400 mol m^{-3} HF are 205 and 275 sec., respectively. The rate of dissolution is very fast upto a stage when half the flim dissolves and thereafter it slows down. Similar trends in the rate of dissolution are found for a 100 V film (Fig. 5), and since this film has larger thickness, it requires larger time to reduce to half its original thickness. It is most likely that when Ta_2O_5 film is put in concentrated hydrofluoric acid, a surface layer of tanta-

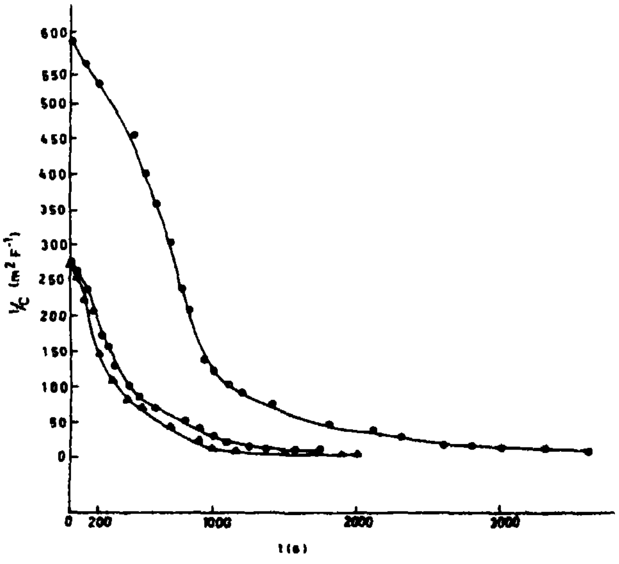

Fig. 5—Rate of dissolution of anodically formed film on tantalum in hydrofluoric acid. [(○) 100V in 5400 mol m^{-3} hydrofluoric acid; (●) 50V in 5400 mol m^{-3} hydrofluoric acid; and (△) 50V in 10800 mol m^{-3} hydrofluoric acid].

lum fluoride (TaF_5) is formed which dissolved completely in conc HF and hence causes dissolution of the film.

Ion mobility studies

The specimens I and II were anodized at film formation voltages of 30, 40 and 50V in 100 mol m^{-3} citric acid at a current density of 30 A m^{-2} and their capacitances before sealing were measured and found to be 1.92, 1.44, 1.15 (for specimen I) and 1.14, 0.85, 0.68 F × 10^{-6} (for specimen II) at the above film formation voltages respectively. In the combined assembly the capacitance of both specimens I and II are the same (0.57, 0.43, 0.34 × 10^{-6}F at 30, 40 and 50V respectively) and the values are in proportion to their reduced areas of 1 × 10^{-4}m^2, and the assembly acts as one unit (area 1 × 10^{-4}m^2). The tag of the specimen I in each of the paired assembly was connected to the positive terminal of the constant current generator and the specimen II which was earlier anodized upto 30, 40 and 50V paired assemblies was further anodized upto 60, 70 and 80V, respectively. The capacitances of these paired systems were again measured taking samples I and II in the circuit respectively. The capacitances of specimens I and II were again found to be the same (0.30, 0.26 and 0.22 × 10^{-6}F at 60, 70 and 80V respectively) and this ensured complete sealing of I and II and no possibility of the electrolyte creeping through the oxide. The magnitudes of capacitances were further reduced due to further formation of the film. The assemblies were dismantled by dissolving lacomite in acetone and washing with conductivity water. The capacitances of separated specimens I and II were measured as also those of the outer and inner surfaces of both the specimens after applying lacomite to the other side. The capacitances of the specimen I after separation (1.90, 1.42, 1.17 × × 10^{-6}F at 30, 40 and 50V, respectively) and before sealing were identical indicating that specimen-I remained unaffected. The capacitances per m^2 for both the inner and outer surfaces of the specimen-I were 0.56, 0.42 and 0.35 × 10^{-2}F m^{-2} at film formation voltages of 30, 40 and 50V respectively while the corresponding values for the inner surface of the specimen-II were 0.57, 0.43 and 0.34 × 10^{-2}F m^{-2}. The magnitudes of capacitance per m^2 for the specimen I compare well with those of the inner surface of the specipen-II. This implies that the sandwitched oxide film is not affected. Further anodization of the separated specimen-I increases the film formation voltage immediately and the film formation voltage attains the voltage of the film already present on it (Fig. 6). This shows that there is no possibility of oxygen ion moving through the electrolyte to specimen-I to produce layers inside the existing oxide layers. The normal rate of anodization compare well with the anodization rate during this experiment. This indicates that the field of Ta_2O_5 film between specimens I and II of this experiment remains unchanged and tantalum ions produced at specimen I are transported to specimen-II through the tantalum oxide (where the field is constant) and then to solution to produce fresh layer on the outer surface of the specimen-II. Thus it can be concluded that only tantalum ions are mobile during the growth of Ta_2O_5 film.

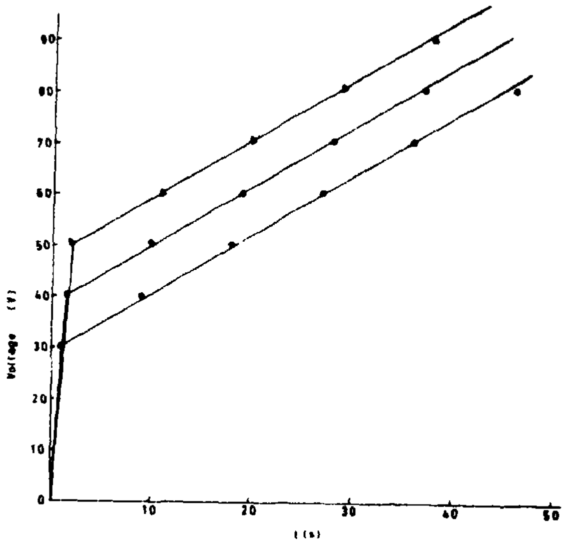

Fig. 6—Plot of variation of voltage of formation versus time of anodization for tantalum oxide films of various thicknesses [(⊙) 30V; (●) 40V, (△) 50V].

Acknowledgement

One of the authors (PK) thanks the CSIR, New Delhi for the award of a junior research fellowship.

References

1 Nigam R K, Kalra K C & Katyal P, *Indian J Chem*, **25A** (1986) 1080.
2 Nigam R K, Kalra K C & Katyal P, *Indian J Chem*, **26A** (1987) 17.
3 Nigam R K, Kalra K C & Katyal P, *Indian J Chem*, 26A (1987) 819.
4 Randall J J Jr, *Electrochim Acta*, **20** (1975) 663.
5 Anfuku F, Iwakura C, Yoneyama H & Tamura H, *Denki Kogaku*, **46** (1978) 19.
6 Nigam R K & Chaudhary R S, *Indian J Chem*, **11** (1973) 356.
7 Amsel G, Cherki C, Feiullade G & Nadai J P, *J phys Chem solids*, **30** (1969) 2117.

8 Cherki C, *Electrochim Acta,* **16** (1971) 1227.
9 Young L, *Anodic oxide films,* (Academic Press, New York) 1961.
10 Klerer J, *J electrochem Soc,* **112** (1965) 896.
11 Vijh A K, *Corr Science,* **11** (1971) 161.
12 Vijh A K, *Oxide and oxide films,* Vol 2 edited by J W Diggle (Marcel Dekker, New York) 1973.
13 Nigam R K & Chaudhary R S, *Electrochim Acta,* **16** (1971) 1719.
14 Amsel G & Samuel D, *J phys chem Solids,* **23** (1962) 1707.
15 Young L *Proc Roy Soc London,* **A244** (1958) 41.

Indian Journal of Chemistry
Vol. 27A, March 1988, pp 204-206

Permeability of Nitrogen, Oxygen, Argon & Helium through Porous Medium (Fuel Cell Grade Asbestos + 5% Polyvinyl Alcohol)

R L BLOKHRA
Department of Chemistry, Himachal Pradesh University, Summer Hill, Shimla 171005

Recieved 22 *May* 1987; *revised and accepted* 10 *August* 1987

The permeability coefficients of nitrogen, oxygen, argon and helium through a separator made of fuel cell grade asbestos + 5% PVA are reported. The results show that the rate of gaseous flow (N^v) depends linearly on the force applied, ΔP. However, the plots of N^v versus ΔP do not pass through the origin, and give positive intercepts. This has been interpreted in terms of slip flow. It is also observed that the Darcy's permeability coefficient varies non-linearly with the molecular weight of the gases.

The literature on transport phenomena such as permeation, osmosis and diffusion of liquids across both natural and artificial membranes is voluminous[1,2]. The studies on gas permeation through membranes/separators have gained importance only after the discovery of polymeric membranes. Several mechanisms for permeation of gases through membranes have been proposed[3]. Studies of gas permeation is important from the view point of improving the performance of fuel cells and batteries[4], in most of which, the electrochemical reaction is either the evolution of gas or its utilization. Further, most of the devices use separators and sometimes porous electrodes. Thus the study of permeation of gases through such components may help in understanding gas management problems in these devices. In the present study, a porous separator made from fuel cell grade asbestos (FCGA) + 5% polyvinyl alcohol (PVA) has been used to measure the permeability coefficients of N_2, O_2, Ar and He gases at 25 ± 0.5°C. The results are analyzed from the view point of Hagen-Poiseuille's law[7].

Materials and Methods

The FCGA + 5% PVA separator was prepared in the laboratory. The sample used was 10 mil thick and had an exposed diameter of 2.0 cm. Compressed nitrogen, oxygen, argon and helium gases (Matheson and Fisher Scientific Co, USA), were used as such.

The separator holder consisted of two blocks of plexiglass (16 cm^3 each) having a hole (diam., 2.0 cm) in the middle with an outlet and inlet ports on top of each block. The porous material was placed between these blocks and cell leakage was prevented using rubber gaskets and silicon rubber cement (GE-RTV). The cell was tested for any leakage by immersing in water and passing gas at a pressure twice that used in the experiments.

The rate of flow of gas was measured with a gas bubble flow meter, model No. 823-1 (Mast Development Co, Davenport, Towa). The time required for the flow of gas bubble through a fixed calibrated distance and volume was measured with the built-in electronic stop watch (accuracy ± 0.001 s). The pressure difference (ΔP) across the separator during gas flow was never more than 3.0 psi. This pressure was measured with a gauge (accuracy 2%). The pressure readings could be kept constant by a fine needle value. The time used for calculating rate of gas flow was the mean average of six determinations. The mean average never differed by more than 1.0%.

Results and Discussion

The rates of flow nitrogen, oxygen, argon and helium through the separator are given in Table 1.

The molar flux of gases (N^v) through the porous medium is given by Eq. (1) as suggested by Hagen-Poiseuille[5]

$$N^v = -\frac{R^2}{8\mu}\cdot\frac{\bar{p}}{R_g\cdot T}\cdot\frac{\Delta P}{\Delta Z} \qquad \ldots(1)$$

where R is the radius of the capillary, R_g is the gas constant, ΔP is the pressure difference, p is the mean pressure, μ is the viscosity of the gas, and ΔZ is the thickness of the separator through which the gas passes. For a porous medium, its obstructing character is to be taken into account in order to calculate the flux. Replacing the geometric factor, $R^2/8$ in Eq. (1) with an effective

Table 1—Rate of Flow of Gases through FCGA + 5% PVA Separator

Pressure difference (Atm) × 10^2	10^4 × Flow rate (mol cm^{-2} s^{-1})			
	Nitrogen	Oxygen	Argon	Helium
3.40	0.31	0.29	0.27	0.56
6.80	0.45	0.43	0.41	1.04
10.21	0.65	0.59	0.55	1.37
13.61	0.85	0.75	0.68	1.72
17.01	1.04	0.92	0.84	2.15
20.41	1.18	1.09	1.03	2.50

Table 2—Slopes and Intercepts of Plots of N^v Versus ΔP for Flow N_2, O_2, Ar and He across FCGA + 5% PVA, Darcy Permeability Coefficients (B_k) and Slip Frictional Coefficients (β)

Gas	10^4 × Slope (mol cm^{-2}s^{-1}atm^{-1})	10^4 × Intercept (mol cm^{-2}s^{-1})	10^{20} × B_k (m^{3}s^{-2})	10^{-9} × β (Ns m^{-3})
N_2	5.31	0.11	5.84	5.33
O_2	4.73	0.12	6.02	5.13
A	4.38	0.11	6.07	3.93
H_e	11.24	0.21	13.70	3.30

coefficient, B_k the Darcy permeability coefficient, we get[7]:

$$N^v = -\frac{B_k}{\mu} \cdot \frac{\bar{p}}{R_g \cdot T} \cdot \frac{\Delta P}{\Delta Z} \qquad \ldots (2)$$

In accordance with Eq. (2), the molar flux should be directly proportional to ΔP and B_k can be estimated from the slope of plots of N^v versus ΔP. Since ΔP is very small, $\bar{p}$ can be taken as unity. The plots of N^v versus ΔP are linear, but these do not pass through the origin, and in each case we get aq. positive intercept. The slopes and the intercepts of these plots are given in Table 2.

The intercept values which are much higher than the experimental error, indicate that N^v of the gases through the separator is greater than that predicted by the Hagen-Poiseuille's law. In the derivation of the normal Poiseuille's law, resistance to the forward movement of the gas due to the presence of a stagnant layer adjacent to the walls of the pores is presumed. Therefore, the higher intercept value may be attributed to the absence of the stagnant layer and to the presence of slip flow at the pore walls. The slope value is given by the relation: Slope = $(B_k/\mu R_g . T)\Delta Z$. Taking $R_g = 0.0806$ l atm k^{-1} mol^{-1}, T = 298 K, ΔZ = 10 mil and μ (298 K) = 204.8 (O_2), 177.0 (N_2), 196.2 (He) and 200.0 (Ar) micropoise, the values of the Darcy's permeability coefficients have been estimated and are given in Table 2.

The values of Darcy coefficients show that for the FCGA + 5% PVA separator, the permeability decreases non-linearly with increase in molecular weight of the gas. Oxygen has approximately the same permeability coefficient as nitrogen gas. Such a behaviour has been observed earlier[3] in microporous separators.

The positive intercept (Table 2) has been termed as slip flux[6]. If we take into account this slip flux, the $N^{v,ext}$ may be given by Eq. (3)[5]:

$$N^{v,ext} = -\left(\frac{B_k}{\mu} + \frac{R}{2\beta}\right) \cdot \frac{\bar{p}}{R_g\,T} \cdot \frac{\Delta P}{\Delta Z} \qquad \ldots (3)$$

where $N^{v,ext}$ is the extended viscous flow and β is slip friction coefficient which determines the value of the fluid velocity at the wall. A estimation of β is made by fitting an equation to the plots of $(N_v.R_g \cdot T, \Delta Z)/\Delta P$ versus $\bar{p}$ (see reference 7). According to Knudson, a minimum should be observed with a positive intercept[7]. The protion of the plot with a positive slope shall refer to the region where Poiseuille's law holds good and the portion having the negative slope would refer to the Knudson flow. In the present case, these plots give negative slopes for all the gases indicating the occurrence of Knudson flow and hence of slip flux (β). The slopes for N_2, O_2, Ar or He have been estimated by a regression analysis and the values are: -1.91×10^{-9}, -1.98×10^{-9}, 2.57×10^{-9} and -3.10^{-9}m^{4}N^{-1}s^{-1} respectively. From the values of these slopes, the Dracy permeability coefficient, B_k, or the slip frictional coefficient, β has been estimated by Eq. (4).

$$\beta = \frac{R}{2(\text{slope} - B_k/\mu)} \qquad \ldots (4)$$

These values are given in Table 2. The lower β values in case of argon and helium may be attributed to the ideal behaviour of these gases and absence of intermolecular forces of attraction and repulsion.

The author is thankful to National Research Council, USA, for financial support during author's stay at NASA-Lewis Research Centre, Cleveland, Ohio, USA, where the experimental work was carried out by the author.

References

1 Lakshminarayanaiah N, *Transport phenomena in membranes*, (Academic Press, New York) 1969.

2 Stern S A, *Industrial processing with membranes*, edited by

R E Lacey & S Loeb (Wiley Interscience, New York) 1972.

3 Sun-tak Hwang & Kammermeyer K, *Membranes in separation*, (John Wiley, New York) 1976.

4 Post R E, *Evaluation of potassium titnate as a component of alkaline fuel cell matrices—NASA*, Technical Memorandum NASA TN-8341 (1976).

5 Cunningham R E & Williams R J J, *Diffusion in gases and porous media*, (Plenum Press, New York) 1980, 40.

6 Barrer R M, *Diffusion in and through solids*, Cambridge University Press, London) 1951.

7 Cunningham R E & Williams R J J, *Diffusion in gases and porous media*, (Plenum Press, New York) 1980, 76.

Indian Journal of Chemistry
Vol. 27A, March 1988, pp. 207-210

Kinetics & Mechanism of Oxidation of Sulphanilamide by Peroxomonophosphoric Acid

G P PANIGRAHI* & R C PAICHHA
Department of Chemistry, Berhampur University, Berhampur 760 007

Received 18 *November* 1986; *revised* 30 *April* 1987; *rerevised and accepted* 10 *August* 1987

Oxidation of sulphanilamide by peroxomonophosphoric acid (PMPA) in the *p*H range 0-7 is first order both in [PMPA] and [sulphanilamide]. Dependence in [H^+] is complex and rate-*p*H profile shows rate maximum around *p*H 1.1. The observed data have been rationalised in terms of an electrophilic attack by neutral PMPA species namely H_3PO_5 on the amino group of sulphanilamide.

The title investigation forms a part of a broad programme from our laboratory on peroxomonophosphoric acid oxidation of aminobenzoic acids[1], aminopyridine[2], aniline[3], sulphanilic acid[4] etc.

Materials and Methods

All the chemicals were of AR grade. All solutions were prepared in conductivity water. PMPA was prepared by acid hydrolysis of $K_4P_2O_8$ (ref. 5) and its concentration checked frequently by iodometry. The self decomposition was found negligible in the *p*H region examined. The acidity was adjusted by adding appropriate amounts of perchloric acid or standard buffers[6]. Sulphanilamide (EGA-CHEMIE, W. Germany) was used after checking its purity.

The kinetics was followed upto three half-lives under pseudo-first order conditions in the temperature range 35-50°C by measuring the rate of disappearance of PMPA iodometrically, in acetic acid-acetate buffer medium (*p*H 4-5) containing a drop of ammonium molybdate solution[7]. The rate constants were computed by the usual method and were found to be reproducible within ± 7-10%. Dissociation constant (K_h) for the conjugate acid was measured by *p*H-metric titration of hydrochloride of sulphanilamide. *p*H values were reproducible within ± 0.05 *p*H units.

Results

Good agreement (within 10%) was noticed in the first order rate constant values calculated upto three half-lives for each run and those obtained from the slopes of the linear plots of log[PMPA] versus time. No change in the values of first order rate constants was noticed even in repeating experiments with varying [PMPA] but constant [sulphanilamide] and *p*H (Table 1). At fixed [PMPA] and [acid] with [sulphanilamide] varying, the k_1 values (Table 1) increased with increase in [sulphanilamide] and k_2 ($= k_1$/[sulphanilamide]) was constant indicating order in sulphanilamide to be one.

Table 1—Rate Constants for the Oxidation of Sulphanilamide in Aqueous Medium by Peroxomonophosphoric Acid (PMPA)

Temp. °C	*p*H (± 0.02)	10^3 [Sulphanilamide] (mol dm^{-3})	10^4 [PMPA] (mol dm^{-3})	$10^4 k_1$ (s^{-1})	$10^2 k_2$ (dm^3 mol s^{-1})
35	0.85	2.903	2.573	2.04	
	0.85	2.903	5.1	1.99	
	0.85	2.903	6.3	1.85	
	0.85	2.903	7.6	1.95	
	1.12	1.742	4.105	1.24	7.16
	1.12	2.915	4.105	2.24	7.69
	1.12	5.772	4.105	3.92	6.79
	1.12	5.8	4.105	4.09	7.04
	1.12	8.7	4.105	6.51	7.4
	1.12	11.6	4.105	9.25	7.9
40	1.12	2.903	4.105	2.52	8.68
45	1.12	2.903	4.105	4.42	15.22
50	1.12	2.903	4.105	4.91	16.90

Since the rates were not influenced by added salts, no attempt was made to maintain the ionic strength constant during the rate measurement. The plot of k_{obs} versus *p*H (varied from 0 to 7) at 45 and 50°C, showed rate maximum around *p*H 1.1 indicating participation of different species of PMPA resulting from dissociation as well as involvement of protonation equilibria of sulphanilamide.

Addition of acrylamide did not affect the kinetic results or produce any turbidity indicating that no radical intermediate is involved in the oxidation of sulphanilamide by PMPA.

Under the condition [sulphanilamide] ≫ [PMPA], one mol of PMPA was found to consume one mol of sulphanilamide. However, the product of oxidation could not be isolated. It may be concluded that sulphonamide derivative of hydroxylamine is formed since the NH_2 group is converted into NHOH when heterolytic oxidation occurs. Further the reaction mixtures were almost colourless. Formation of condensation products like azo or azoxy derivatives would have resulted in coloured mixtures. This is at variance with the observations of Srivastava *et al.*[8] who identified the corresponding azoxy derivative in the oxidation of sulphanilamide with peroxodisulphate ion.

Plots of log k_2 ($p\mathrm{H} = 1.1 \pm 0.02$) versus 1/T (T varied in the range 308 to 323 K) were linear. The energy of activation E_a and entropy of activation $\Delta S^{\ddagger}$ were calculated from the linear plots and the values were found to be 34.1 kJ mol^{-1} and -213 J K^{-1}mol^{-1} respectively in the *p*H range 2.0 to 5.0.

Discussion

Based on the kinetic results, the rate law can be expressed by Eq. (1) at constant acidity

$$\text{Rate} = k'[\text{Sulphanilamide}]_T[\text{PMPA}] \quad \ldots(1)$$

where k' is the second order rate constant and the subscript T denotes total concentration. The rate maximum at *p*H 1.1 may arise from contribution of proton dissociation equilibria for both the oxidant and substrate. The PMPA is known to undergo dissociation as shown by Eqs (2-4) (ref. 9).

$$H_3PO_5 \rightleftharpoons H_2PO_5^- + H^+ \; (K_1 = 8\times10^{-2} \text{ at } 25°\text{C}) \quad \ldots(2)$$

$$H_2PO_5^- \rightleftharpoons HPO_5^{2-} + H^+ \; (K_2 = 4.2\times10^{-6}) \quad \ldots(3)$$

$$HPO_5^{2-} \rightleftharpoons PO_5^{3-} + H^+ \; (K_3 = 1.6\times10^{-13}) \quad \ldots(4)$$

The proton dissociation constants[9] suggest that in the *p*H region 0-2 PMPA exists as H_3PO_5 and $H_2PO_5^-$, former being present in significant concentration over the latter. It is reasonable to expect that in the *p*H range 0-1, it is H_3PO_5 species which is most important and hence any reaction in this region is due to neutral H_3PO_5. This is consistent with the idea put forth by Secco and Venturini[10] who demonstrated higher reactivity of H_3PO_5 over $H_2PO_5^-$ in terms of greater leaving group ability of H_3PO_4 over $H_2PO_4^-$. Equilibrium given by Eq. (4) is of little significance.

Sulphanilamide is also likely to be protonated in this *p*H region and equilibrium (5) may be important.

$$BH^+ \overset{K_h}{\rightleftharpoons} B + H^+ \quad \ldots(5)$$

where $B = (p)H_2NC_6H_4SO_2NH_2$

However, the value of K_h is not available and hence it has been measured by *p*H-metric titration of sulphanilamide hydrochloride. The K_h value comes out to be $\sim 1\times10^{-3}$. This suggests substantial protonation of sulphanilamide below *p*H 3. As has been established in our earlier work[1-4] oxidations by PMPA are basically polar in nature and nucleophiles are oxidised with ease. In the present case the amino group gets protonated (Eq. 5) and it is the unprotonated sulphanilamide molecule which undergoes oxidation with PMPA. However, the protonated species is not capable of reacting with PMPA presumably due to reduced nucleophilicity as indicated by very slow reactivity at high [H$^+$] ($p\mathrm{H} < 1$). The observed rate maximum at *p*H 1.1 can be rationalised as follows:

As *p*H increases, the equilibrium concentration of neutral sulphanilamide increases and it is this species which undergoes oxidation. Similarly with increase in *p*H, H_3PO_5 concentration decreases from a high value and $H_2PO_5^-$ slowly accumulates and in significant amount after *p*H 2. Therefore, initial increase in rate with increase in *p*H from 0 to 1.1 is due to increase in neutral sulphanilamide concentration and this species is oxidised by H_3PO_5 only because of its higher nucleophilicity. As no $H_2PO_5^-$ species is available in significant amount at *p*H 1.1, one cannot expect any reaction between sulphanilamide and $H_2PO_5^-$ below *p*H 1.1. As *p*H increases beyond 1.1, $H_2PO_5^-$ slowly starts accumulating and hence one can expect oxidation of sulphanilamide by both H_3PO_5 and $H_2PO_5^-$.

In view of the experimental results obtained, the reaction steps involving oxidation of sulphanilamide may be visualised as shown in Scheme 1.

$$BH^+ \overset{K_h}{\rightleftharpoons} B + H^+$$

$$H_3PO_5 \overset{K_1}{\rightleftharpoons} H_2PO_5^- + H^+$$

$$B + H_3PO_5 \xrightarrow{k_1} \text{Product} + H_3PO_4$$

$$B + H_2PO_5^- \xrightarrow{k_2} \text{Product} + H_2PO_4^-$$

Scheme 1

These steps lead to rate law (6)

$$-\frac{d[\text{PMPA}]_T}{dt} = k_1[B][H_3PO_5] + k_2[B][H_2PO_5^-] \quad \ldots (6)$$

Equilibrium concentration can be expressed by the following relationships in terms of their total concentrations, since whole of PMPA in the *p*H range studied would be present as H_3PO_5 and $H_2PO_5^-$ only.
From Eq. (5), we get,

$$[B] = \frac{K_h[B]_T}{K_h + [H^+]} \quad \ldots (7)$$

From Eqs 2 and 3,

$$[H_3PO_5] = \frac{[H^+]}{K_1 + [H^+]}[\text{PMPA}]_T \quad \ldots (8)$$

and

$$[H_2PO_5^-] = \frac{K_1}{K_1 + [H^+]}[\text{PMPA}]_T \quad \ldots (9)$$

Substituting Eqs 7-9, in the rate expression (6) we get Eq. (10)

$$-\frac{d[\text{PMPA}]_T}{dt} = \frac{k_1 K_h[H^+] + k_2 K_h K_1}{(K_h + [H^+])(K_1 + [H^+])}[B]_T[\text{PMPA}]_T \quad \ldots (10)$$

Equation (10) is similar to Eq. (1) where

$$k' = \frac{k_1 K_h[H^+] + k_2 K_h K_1}{(K_h + [H^+])(K_1 + [H^+])}$$

Validity of the rate expression (Eq. 10) consequently of the oxidation steps represented by Eq. (5) and the last two steps in Scheme 1 would require that plot of k' $(K_h + [H^+])$ $(K_1 + [H^+])$ versus $[H^+]$ should be linear with a positive slope and positive intercept. To test this, K_1 reported by Battaglia and Edwards[9] and K_h values determined by us were used to evaluate the left hand side term. In fact such a plot was linear with a positive slope but almost negligible intercept. As the rate expression (Eq. 10) suggests the slope and intercept should be a measure of k_1 (oxidation brought by H_3PO_5) and k_2 (oxidation by $H_2PO_5^-$) respectively. However, zero intercept signifies that the second term in Eq. (10) i.e. $k_2 K_1 K_h$ is equal to zero. Since K_1 and K_h are finite, it implies k_2 shall be either zero or negligibly small. Hence the contribution to the rate of oxidation by $H_2PO_5^-$ species is not very significant. It can therefore be concluded that oxidation of sulphanilamide is only affected by H_3PO_5 but not by any of the charged PMPA species. In the same way it can be concluded that protonated sulphanilamide, is also inert towards the oxidant species. Consequently the reaction step which should rightfully represent the oxidation process is

$$B + H_3PO_5 \xrightarrow{k_1} \text{Product} + H_3PO_4 \text{ (see Scheme 1)}$$

This mechanism of the reaction in essence would be a polar one involving electrophilic attack on the lone pair of nucleophilic amino group in the rate-limiting step forming a bimolecular S_N2 transition state (A).

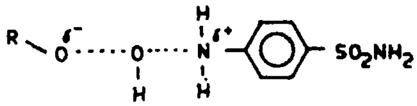

(A)

where $R = H_2PO_3$ or HPO_3^-

This is supported by the observed kinetic data and large negative entropy of activation which indicates a large structured unit with much decreased rotational and vibrational degrees of freedom[11].

The mechanism postulated here is different from that of the oxidation of sulphanilamide by $S_2O_8^{2-}$ proposed by Srivastava and others[8] which essentially involved a radical process. These workers observed that the rate increased upto a *p*H of 5.34 only beyond which the rate remained constant and no sharp maximum was reported.

Acknowledgement

One of us (RCP) wishes to thank the UGC, New Delhi, for grant of a teacher fellowship under Faculty Improvement Programme.

References

1 Panigrahi G P & Panda A K, *Bull chem Soc (Japan)*, **54** (1981) 1554.

2 Mahapatro S N, Panda A K & Panigrahi G P, *Bull chem Soc (Japan)*, **54** (1981) 2507.

3 Panigrahi G P, Panda A K & Mahapatro S N, *J org Chem*, **46** (1981) 4000.

4 Panigrahi G P & Nayak R N, *React Kin Catal Lett (Hung)*, **21** (1982) 283.

5 Crutchfield M M, *Peroxodiphosphoric acid in peroxide reaction mechanisms*, Edited by J O Edwards (Interscience, New York) 1961, p. 41.

6 Lange N A, *Handbook of chemistry*, (McGraw-Hill, New York) 1962, p 791.

7 Kapoor S & Gupta Y K, *J chem Soc (Dalton)*, (1976) 473.

8 Srivastava S P, Mittal A K & Gupta V K, *Indian J Chem*, **20A** (1981) 806.

9 Battaglia C J & Edwards J O, *Inorg Chem*, **4** (1965) 552.

10 Secco F & Venturini M, *J chem Soc (Dalton)*, (1977) 634.

11 Moore W J, *Physical chemistry*, (Orient Longmans, New Delhi) 1969, 298.

Indian Journal of Chemistry
Vol. 27A, March 1988, pp. 211-213

Kinetics of Co-oxidation of Ethylene Glycol & Propan-2-ol by Acid Bromate

P NARASIMHA CHAR, S SONDU, B SETHURAM & T NAVANEETH RAO*
Department of Chemistry, Osmania University, Hyderabad 500 007

Received 24 *April* 1987; *revised* 22 *July* 1987; *accepted* 10 *August* 1987

Acid bromate oxidation of a mixture of ethylene glycol and propan-2-ol proceeds much faster than that of the either of the two substrates taken alone. The products of oxidation are aceton and formic acid. The order in $[BrO_3^-]$ is unity and in [ethylene glycol] and [propan-2-ol] it is fractional. The rate increases with increase in $[H^+]$ and percentage of acetic acid in the reaction medium. The amount of acetone formed from propan-2-ol during a particular time period in the presence of ethylene glycol is nearly twice that formed in its absence. A mechanism involving formation of a termolecular complex involving ethylene glycol, propan-2-ol and bromate and decomposition of this complex in the rate-determining step is proposed. The nature of the complex formed has not been ascertained.

Recently we have reported the co-oxidation of 1,2-glycols and aliphatic esters by periodate in basic medium[1]. Preliminary studies in the present investigation have shown that the rate constant of acid bromate oxidation of a mixture of ethyleneglycol (EG) and propan-2-ol is almost twice that of the sum of the rate constants of .the individual substrates under identical conditions. This indicates that co-oxidation is taking place. Detailed kinetic investigation of acid bromate coordination of EG + propan-2-ol is therefore called for in order to arrive at a suitable mechanism.

Materials and Methods

Potassium bromate, sulphuric acid and mercuric accetate were of AR grade (BDH) and were used as such. Acetic acid (AR, BDH), ethyleneglycol (EG) and propan-2-ol (AR) samples were purified before use.

All the experiments were carried out in aqueous medium under pseudo-first order conditions using ten-fold excess of substrates over the oxidant and the kinetics were followed iodometrically. Mercuric acetate was used as a scavenger for Br^- formed as one of the products. The rate constants were calculated by the least squares method.

Acetone and formic acid were identified as the reaction products by their characteristic tests. One of the oxidation products, viz. acetone was estimated colorimetrically by measuring the absorbance of the coloured complex formed by the addition of salicylaldehyde and KOH solution and comparing it with the standard Beer's law plot. The results indicated that 1 mol of acetone was formed for every mol of bromate consumed in the presence of EG in accordance with Eq. (1).

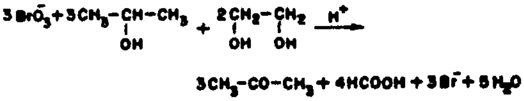

$$3BrO_3^- + 3CH_3-\underset{OH}{\underset{|}{C}H}-CH_3 + 2\underset{OH}{\underset{|}{C}H_2}-\underset{OH}{\underset{|}{C}H_2} \xrightarrow{H^+} 3CH_3-CO-CH_3 + 4HCOOH + 3Br^- + 5H_2O \qquad ....(1)$$

Results and Discussion

The kinetic results are summarised below:

(i) Under the conditions [substrate] $\ll$ $[BrO_3^-]$ the order in $[BrO_3^-]$ was unity (Fig. 1A).

(ii) The orders in [EG] and [propan-2-ol] were both fractional (Figs 1B and 1C).

(iii) The rate increased with increase in $[H^+]$ and the order in $[H^+]$ was two, indicating the involvement of two protons in this process (Table 1).

(iv) The rate increased with increase in percentage of acetic acid in the reaction medium and the plot of $\log k_{obs}$ versus 1/D was linear with a positive slope (Fig. 1D) indicating that probably a positive ion and a dipole are involved in the rate-determining step.

Second order dependence of rate on $[H^+]$ indicates that two protons are involved in the reaction and the probability is the protonation of BrO_3^- (see Eq. 2).

$$BrO_3^- + 2H^+ \rightleftharpoons BrO_2^+ + H_2O \qquad \ldots (2)$$

This shows that BrO_2^+ is the reactive species. Such a reactive species has also been proposed by earlier workers[2] in the bromate oxidation.

(v) Linear plots of $1/k_{obs}$ versus 1/[EG] and 1/[propan-2-ol] with definite intercepts on Y-axes indicates the involvement of the substrates in complex with Br (V).

(vi) The first order rate constant ($k_{obs} \times 10^4$ s^{-1}) under the conditions $[BrO_3^- = 5.00 \times 10^{-3}$

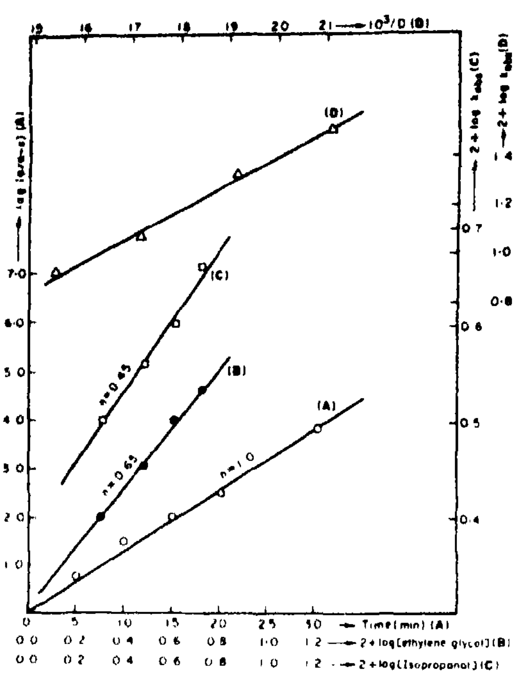

Fig. 1—(A) Plot of log($a/a-x$) versus time ($[BrO_3^-] = 5.00 \times 10^{-3}$ mol dm^{-3}; [propan-2-ol] = 2.50×10^{-2} mol dm^{-3}; [ethylene glycol] = 2.50×10^{-2} mol dm^{-3}; [H_2SO_4] = 1.00 mol dm^{-3} [mercuric acetate] = 0.100 mol dm^{-3}; temp = 313K)

(B) Plot of log k_{obs} versus log[ethylene glycol] ([EG] = 2.00×10^{-2} to 5.00×10^{-2} mol dm^{-3}; [propan-2-ol] = 5.00×10^{-2} mol dm^{-3}; other conditions same as in (A)).

(C) Plot of log k_{obs} versus log[propan-2-ol] ([Propan-2-ol] = 2.00×10^{-2} to 3.00×10^{-2} mol dm^{-3}; [EG] = 5.00×10^{-2} mol dm^{-3}).

(D) Plot of log k_{obs} versus 1/D

mol dm^{-3}, [propan-2-ol] = 2.50×10^{-2} mol dm^{-3}, [EG] = 2.50×10^{-2} mol dm^{-3}, [H_2SO_4] = 1.00 mol dm^{-3}, [mercuric acetate] = 0.100 mol dm^{-3} are 7.29, 7.31, 7.25 and 7.33 at [$NaClO_4$] = 0.05, 0.10, 0.15 and 0.20 mol dm^{-3} respectively indicating that $NaClO_4$ has no effect on the reaction rate.

In the oxidation of 1,2-glycols by acid bromate the formation of a complex between the substrate and oxidant is well established. However, no such complex has been observed between bromate and propan-2-ol[3]. The fact that there is no interaction between propan-2-ol and EG as such and the fractional order dependence of rate on [EG] and [propan-2-ol] indicate that both the substrates are involved in the formation of some sort of complex with the oxidant. The kinetic evidence for such a complex comes from the plot of $1/k_{obs}$ versus 1/[substrate] which gives clear intercept on $1/k_{obs}$ axis. The exact nature of the complex is difficult to decide at this stage. No induced polymerisation of acrylonitrile was observed when it was added to the reaction systems. The experimental observation that the rate constant of acid bromate oxidation of a mixture of two substrates is twice that of the individual substrates under identical conditions suggests that co-oxidation is taking place. In order to see whether the rate enhancement due to co-oxidation results in the formation of more of the reaction products for a certain time interval, we have estimated one of the products, i.e. acetone colorimetrically. The results indicate that under the conditions [BrO_3^-] = 5.00×10^{-3} mol dm^{-3}, [H_2SO_4] = 1.00 mol dm^{-3}, [$Hg(OAc)_2$] = 0.10 mol dm^{-3}, temp = 313K, [EG] = 0.25 mol dm^{-3} and [propan-2-ol] = 0.24 mol dm^{-3} the amounts of acetone formed in presence and absence of EG is 0.414 mmol and 0.218 mmol (for 20 ml of reaction mixture in 30 min) respectively, thus providing additional support for the occurrence of co-oxidation of the two substrates. Based on the above experimental observations the probable mechanism is shown in Scheme 1.

Table 1—Effect of Varying [H^+] on Rate Constants of Br(V) Oxidation of Ethylene Glycol + Propan-2-ol

[BrO_3^-] = 5.500×10^3 mol dm^{-3}; [ethylene glycol] = 2.50×10^{-2} mol dm^{-3} [propan-2-ol] = 2.50×10^{-2} mol dm^{-3}; [$Hg(OAc)_2$] = 0.100 mol dm^{-3}; temp = 318K

[H^+] mol dm^{-3}	k_{obs} (10^{-4}) s^{-1}	[H^+] mol dm^{-3}	k_{obs} (10^{-4}) s^{-1}
0.594	1.79	1.94	16.6
0.788	4.19	2.15	28.3
1.11	7.67	3.35	66.5

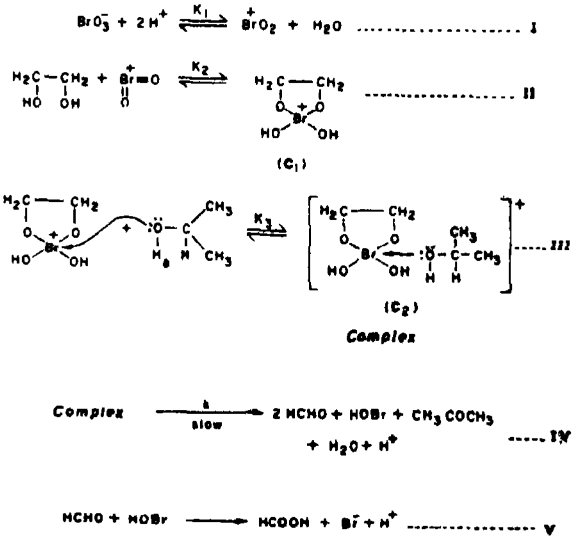
$BrO_3^- + 2H^+ \underset{}{\overset{K_1}{\rightleftharpoons}} \overset{+}{Br}O_2 + H_2O$ I
K₂
(C₁)
...... II
K₃
(C₂)
Complex
...... III
Complex
k
slow
2 HCHO + HOBr + CH₃COCH₃ + H₂O + H⁺ IV
HCHO + HOBr → HCOOH + Br⁻ + H⁺ V

SCHEME 1

Scheme 1 leads to rate law (3)

$$\frac{-2.303\, d \log[\mathrm{BrO_3^-}]}{dt} = k_{obs} = \frac{k K_1 K_2 K_3 [\mathrm{EG}]\,[\text{ProPan-2-ol}]\,[\mathrm{H^+}]^2}{\{1+K_1[\mathrm{H^+}]^2\}\{1+K_2[\mathrm{EG}]+K_3[\text{ProPan-2-ol}]+K_1K_2[\text{ProPan-2-ol}][\mathrm{EG}]\}} \quad \ldots(3)$$

Rate law (3) envisages first order dependence in [Br(V)] and fractional order dependence in both [EG] and [propan-2-ol] in keeping with the observed results. It also explains the increase in rate with increase in $[\mathrm{H^+}]$. The reciprocal of the Eq. (3) after simplification leads to Eq. (4) which

$$\frac{1}{k_{obs}} = \left[\frac{1+K_1[\mathrm{H^+}]^2}{k K_1 [\mathrm{H^+}]^2}\right]\left[\frac{1}{K_2[\mathrm{EG}]}+1\right]\left[\frac{1}{K_3[\text{ProPan-2-ol}]}+1\right] \quad \ldots\ldots\ldots\ldots\ldots(4)$$

predicts linear plots with same intercepts for (i) $1/k_{obs}$ versus 1/[EG] at fixed [propan-2-ol] and $[\mathrm{H^+}]$ and (ii) $1/k_{obs}$ versus 1/[propan-2-ol] at fixed [EG] and $[\mathrm{H^+}]$. Such plots have been realised in the present work.

The K_1 and K_2 values calculated from the oxidation of EG alone with Br(V) were found to be 0.24 and 22.9 respectively. The K_2 values calculated from the slope and intercept of the plot of $1/k_{obs}$ versus 1/[EG] at higher [propan-2-ol] (Eq. 4) is found to be 22.6 which is in excellent agreement with the value (22.9) obtained for the individual oxidation of EG indicating the validity of the rate law and hence the proposed mechanism. The K_3 value calculated in a similar fashion was 5.00. Substitution of these values in Eq. (3) gives the k value as 3.29×10^{-2} mol dm^{-3}s^{-1}.

References

1 Swarnalakshmi N, Uma V, Sethuram B & Navaneeth Rao T, *Indian J Chem*, **23A** (1984) 646.

2 Vijayalakshmi & Sundaram E V, *Indian J Chem*, **20A** (1981) 300.

3 Natarajan R & Venkatasubramanian N, *Tetrahedron Lett*, **57** (1969) 5021; **30** (1970) 785.

Indian Journal of Chemistry
Vol. 27A, March 1988, pp. 214-216

2,2,2-Trifluoroethoxy Derivatives of Chromium(III) : Synthesis & Coordination Chemistry

S L CHADHA* & KAMINI UPPAL
Department of Chemistry, Panjab University, Chandigarh 160 014

Received 17 *March* 1987; *revised and accepted* 10 *August* 1987

New trifluoroethoxy derivatives of chromium(III) formulated as $Cr(OCH_2CF_3)_3.THF$, $CrCl(OCH_2CF_3)_2.THF$ and $CrCl_2(OCH_2CF_3).2THF$, have been synthesised and characterised. With ligands (L), they form adducts of the types $Cr(OCH_2CF_3)_3.L$, $CrCl(OCH_2CF_3)_2.2L$ and $CrCl_2(OCH_2CF_3).2L$ for which the magnetic moment data indicate the presence of antiferromagnetic interaction. Their electronic spectra are consistent with octahedral coordination of chromium(III). On the basis of IR and NMR data, it is proposed that the complexes contain bridging trifluoroethoxy groups and the ligands are probably *cis* to each other. Mass spectral data are in favour of a dimeric structure.

Whereas many metal alkoxides have been synthesised[1], the corresponding trifluoroethoxy derivatives are relatively unknown and of these the trifluoroethoxy derivatives of chromium(III) have not been reported so far. The alkoxide group is known to display a great propensity to bridge two or more metal atoms[2]; therefore, a tendency to form strong polynuclear molecular clusters dominates the structural chemistry of metal alkoxides[3]. This brings about coordinative saturation which precludes ligation. The alkoxy ligands containing electronegative atoms are expected to not only increase the sensitivty of the central metal atom to nucleophilic attack but also to weaken the alkoxy-bridged polymers and may thus enable coordination by a strong ligand. Here, we report the preparation of 2,2,2-trifluoroethoxy derivatives of chromium(III) and their stable adducts with tetrahydrofuran (THF), dimethyl sulphoxide (DMSO), tetramethylurea (TMU), γ-picoline N-oxide (γ-Pic-N-O), α-, β- and γ-picolines (α-,β-,γ-pic).

Materials and Methods

All the reagents were purified by standard methods before use. All preparations and manipulations were done on a vacuum line, occasionally flushing it with dry oxygen-free nitrogen.

Preparation of tris(2,2,2-trifluoroethoxy)-chromium(III)tetrahydrofuranone

To a known amount of lithium metal in benzene was added 2,2,2-trifluoroethanol slightly in excess than that required for 1:1 molar ratio and the contents were stirred until the whole of lithium dissolved. To this was added tetrahydrofuran suspension of anhydrous chromium trichloride (molar ratio of $CrCl_3$: Li, 1:3) and the contents were stirred and simultaneously refluxed for 8 hr in order to ensure the completion of the reaction. To this was added dry ether when lithium chloride precipitated which was removed by filtration; the filtrate was concentrated by removing ether *in vacuo* when a solid was obtained. It was washed with petroleum ether (40-60°) to remove any trace of alcohol an dried *in vacuo* to get a green solid which was found on analysis to be $Cr(OCH_2CF_3)_3.THF$. All attempts to free it from coordinated tetrahydrofuran failed as it decomposed on heating or distillation under reduced pressure.

Chlorobis(2,2,2-trifluoroethoxy)chromium (III) tetrahydrofuranoate, $CrCl(OCH_2CF_3)_2.THF$ and dichloro(2,2,2-trifluoroethoxy)chromium(III) bis-tetrahydrofuranoate, $CrCl_2(OCH_2CF_3).2THF$ were prepared in a similar manner as mentioned above except that the molar ratio of $CrCl_3$:Li was 1:2 and 1:1, respectively, and the products obtained were green hygroscopic solids. The adducts were prepared by dissolving the alkoxides in the liquid ligands and stirring the contents for ~ 4-5 hr followed by precipitation of adducts by addition of ether, petroleum ether (40-60°) and dichloromethane. The adducts with solid ligands (γ-picoline N-oxide) were prepared by adding the alkoxide to the solution of the ligand in chloroform.

Chromium and fluorine were estimated volumetrically[4,5] while chlorine was estimated gravimetrically[6]. Magnetic susceptibility measurements were carried out by Gouy's method. Infrared spectra of complexes were recorded in nujol on a Perkin Elmer 621 spectrophotometer. The diffuse reflectance spectra of the compounds were recorded on a Hitachi spectrophotometer model 330 in the region 1500-200 nm. NMR spectra of the compounds were recorded on a Varian EM 390 spectrometer at

Table 1—Analytical and IR Spectral Data of 2,2,2-Trifluoroethoxy Derivatives of Chromium(III)

Compound†	Found(Calc.),%					(C-O)t	(C-O)b
	Cr	Cl/F^a	C	H	N		
$Cr(OR_f)_3$.THF	11.98(12.35)	39.89(40.61)^a				1060	1010
$CrCl(OR_f)_2$.THF	14.00(14.54)	9.12(9.93)	29.2(30.14)	3.8(3.76)		1080	1045
$CrCl_2(OR_f)$.2THF	13.97(14.20)	19.27(19.39)	32.95(32.78)	5.00(4.91)			1020
$CrCl(OR_f)_2$.2DMSO	11.54(11.77)	7.98(8.04)				1050	1010
$Cr(OR_f)_3$.TMU	11.08(11.18)	36.34(36.77)^a				1060	1030
$CrCl(OR_f)_2$.2TMU	9.99(10.04)	6.21(6.85)	35.11(35.10)	5.53(5.85)	10.90(11.70)	1050	1020
$CrCl_2(OR_f)$.2TMU	11.32(11.45)	15.51(15.63)					1030
$Cr(OR_f)_3$.γ-pic-N-O	11.73(11.35)	37.15(37.33)^a	31.27(31.44)	2.67(2.83)	3.06(3.05)	1070	1065
$CrCl(OR_f)_2$.2γ-pic-N-O	10.12(10.32)	7.00(7.05)				1075	1025
$CrCl_2(OR_f)$.2γ-pic-N-O	11.26(11.81)	16.02(16.13)	38.43(38.18)	3.26(3.63)	6.66(6.36)	—	1035
$Cr(OR_f)_3$.α-pic	11.54(11.76)	37.65(38.68)^a	30.64(32.57)		2.88(3.16)	1080	1020
$CrCl(OR_f)_2$.2α-pic	10.98(11.02)	7.25(7.52)				1085	1030
$Cr(OR_f)_3$.β-pic	11.33(11.76)	37.93(38.68)^1				1080	1025
$CrCl(OR_f)_2$.2β-pic	11.00(11.02)	7.43(7.52)				1090	1035
$CrCl_2(OR_f)$.2β-pic	12.26(12.74)	17.22(17.40)					1030
$Cr(OR_f)_3$.γ-pic	10.69(11.76)	37.88(38.68)^a	31.00(32.57)	2.74(2.94)	3.5(3.16)	1050	1015
$CrCl_2(OR_f)$.2γ-pic	12.31(12.74)	17.15(17.40)					

†$OR_f = OCH_2CF_3$. All compounds are green solids which decompose at their melting points; t & b = terminal, bridging respectively; THF = tetrahydrofuran, TMU = tetramethylurea. Pic-N-O = picoline-N-oxide, Pic = picoline.

Table 2—Electronic Spectral and Magnetic Moment Data of 2,2,2-Trifuloroethoxy Derivative of Chromium(III) and Their Adducts

Compound	λ_{max} (kK)			Δ(kK)	B'(kK) (free ion = 1.03 kK)	$\beta = B'/B$	$\mu_{eff.}$(B.M.)
	A	B	C				
$Cr(OR_f)_3$.THF	16.6	23.5	45.45	16.6	0.70	0.67	3.32 (297K)
$CrCl(OR_f)_2$.THF	16.9	23.8	—	16.9	0.69	0.67	3.53 (300K)
$CrCl_2(OR_f)$.2THF	16.6	23.3	—	16.9	0.67	0.65	3.63 (300K)
$Cr(OR_f)_3$.TMU	16.8	25.0	37.73	16.8	0.76	0.74	—
$CrCl(OR_f)_2$.2TMU	16.6	23.6	—	16.6	0.71	0.69	3.52 (299K)
$CrCl_2(OR_f)$.2TMU	16.6	23.5	—	16.6	0.70	0.67	—
$Cr(OR_f)_3$.α-pic	17.1	25.6	36.40	17.1	0.71	0.69	3.38 (297K)
$CrCl(OR_f)_2$.2α-pic	16.6	23.8	—	16.6	0.75	0.72	3.50 (299K)
$CrCl(OR_f)_2$.2β-pic	16.6	23.7	—	16.6	0.72	0.70	—
$CrCl_2(OR_f)$.2β-pic	16.9	23.8	—	16.9	0.69	0.67	3.64 (300K)
$CrCl_2(OR_f)$.2γ-pic	16.9	24.0	—	16.9	0.72	0.70	3.65 (300K)
$Cr(OR_f)_3$.γ-pic-N-O	—	—	—	—	—	—	3.40 (299K)

$R_f = CH_2CF_3$; A = $^4A_{2g} \rightarrow {}^4T_{2g}$; B = $^4A_{2g} \rightarrow {}^4T_{1g}(F)$; C = $^4A_{2g} \rightarrow {}^4T_{1g}(P)$

90 MHz; TMS was used as internal reference. Mass spectra of the compounds were recorded on a 'VG micromass 7075 instrument'.

Results and Discussion

The analytical data of the compounds support their proposed formulations (Table 1). They are green hygroscopic solids and are insoluble in common nonpolar solvents, a fact which supports their polymeric nature. They are reasonably soluble in polar/donor solvents. They react with a variety of oxygen and nitrogen donor ligands (L) to form adducts, the analyses of which indicate (Table 1) the stoichiometries $Cr(OCH_2CF_3)_3$.L, $CrCl(OCH_2CF_3)_2$.2L and $CrCl_2(OCH_2CF_3)$.2L for them. These adducts are also insufficiently soluble in non-polar solvents as also in nitromethane and acetonitrile which precludes the determination of their molecular weights.

The observed magnetic moment values (Table 2) at room temperature are slightly lower than the spin-only value for the high spin d^3 ion (3.88 B.M.) and this is suggestive of the antiferromagnetic interactions[7] of two or more chromium atoms through the bridging OCH_2CF_3 groups in these compounds. An increase in the magnetic moment is observed when the alkoxy groups are replaced by chloride ion and this is similar to the results obtained for $Cr(OMe)_3$ compared to $CrCl(OMe)_2$ and $CrCl_2(OMe)$[8]. The reflectance spectra of the present compounds show bands at 16 ± 0.8 and 24 ± 1 kK due to the transitions $^4A_{2g} \rightarrow {}^4T_{2g}$ and $^4A_{2g} \rightarrow {}^4T_{1g}(F)$, respectively and a third spin-allowed transition $^4A_{2g} \rightarrow {}^4T_{1g}(P)$ is observed only in some cases at 37 ± 0.5 kK (Table 2). In addition, the ligand field splitting parameter (Δ), inter-electronic repulsion parameter or Racah parameter (B) and covalency factor (β) have been calculated and are given in Table 2; values of these are consistent with an octahedral geometry for these compounds[9].

The IR spectra of $Cr(OCH_2CF_3)_3.THF$ and $CrCl(OCH_2CF_3)_2.THF$ and their adducts show bands at 1090-1050 and 1040-1010 cm^{-1} which have been assigned to the νC-O modes of the terminal and bridging $-OCH_2CF_3$ groups[1,10,11] respectively (Table 1). The symmetric and assymmetric ν(C-O-C) vibrations of the coordinated THF[12] molecules appear at 870, 910 and 1025 cm^{-1}. The compound $CrCl_2(OCH_2CF_3).2THF$ and its adducts, however, show only one band (1035-1020 cm^{-1}) and its position compares well with that of the bridging alkoxy groups which suggests that the terminal $-OCH_2CF_3$ groups are absent in these compounds. The spectra also show shifting of ligand vibrations in these complexes when compared to those of the pure ligands which indicates coordination of the ligands to chromium[13,14]. For example, the displacement of the characteristic bands of picolines to higher spectral region on complex formation was comparable to that of their reported adducts with other acceptors; the lowering of νS = O, νN-O and νC = O modes of DMSO, amine-oxides and amides respectively in the complexes of these ligands is in accord with the earlier results on the adducts of these ligands. In the bis-(picoline-N-oxide) (ligand, 1255 cm^{-1}; adducts 1215, 1200 cm^{-1}) complexes ν(N-O) appears as a doublet which suggests that the ligands are in *cis* positions.[15] The bands around 560-450 cm^{-1} in these compounds are assigned to Cr-O stretching vibrations confirming the existence of covalent bonds between Cr and $-OCH_2CF_3$ ligand while the bands around 360-325 cm^{-1} have been assigned to ν(Cr-Cl) vibrations.[9]

^1H NMR spectrum of $Cr(OCH_2CF_3)_3.THF$ in D_2O solution at room temperature shows two signals; a quartet at δ 4.2 ppm and a singlet at δ 2.2 ppm. The signal at 4.2 ppm (10H) is due to the overlapping of $-CH_2$ protons of $-OCH_2CF_3$ group (δ for CH_2 protons of CF_3CH_2OH = 3.9 ppm) and ethereal protons of THF and the signal at 2.2 ppm (4H) is due to other CH_2 protons of THF (δ for CH_2 protons of free THF = 3.75 and 1.85 ppm). The observation of a single peak for $-OCH_2CF_3$ group may be attributed to an exchange of terminal and bridging $-OCH_2CF_3$ groups. The ^{19}F NMR spectrum of $Cr(OCH_2CF_3)_3.THF$ gives a single fluorine resonance[16,17] at δ 78 ppm.

The mass spectra of $Cr(OCH_2CF_3)_3.THF$ (1), $CrCl(OCH_2CF_3)_2.THF$(2) and $Cr(OCH_2CF_3)_3.\alpha$-picoline (3) do not show any peak corresponding to the dimeric or the monomeric species. However, the spectra of the compounds give rise to strong z/e peaks corresponding to dichromium species. The peaks at z/e 220 and 148 in (1) may be assigned to the species $[F_2C\text{-}Cr\text{-}O\text{-}Cr\text{-}CF_2]^+$ and $[CH_2\text{-}Cr\text{-}O\text{-}Cr\text{-}CH_2]^+$, respectively. Peak at z/e 148 in (2) may be assigned to $[CH_2\text{-}Cr\text{-}O\text{-}Cr\text{-}CH_2]^+$ and at z/e 205 and 148 in (3) may be assigned to the species $[F_2H_2C\text{-}Cr\text{-}O\text{-}Cr\text{-}CH_2F]^+$ and $[H_2C\text{-}Cr\text{-}O\text{-}Cr\text{-}CH_2]^+$, respectively. These observations, therefore, tentatively suggest a 2,2,2-trifluoroethoxybridged dimeric structure for these compounds.

Acknowledgement

We thank the CSIR, New Delhi for financial support.

References

1 Bradley D C, Mehrotra R C & Gaur D P, *Metal alkoxides* (Academic Press, London), 1978.

2 Cavell K J, Connor J A, Pilcher G, Ribeiro De Silva M A, Ribeiro de Silva M D M C, Skinner H A, Virmani Y & Zafaran Moattar M T, *J chem Soc Faraday Trans*, 77 (1981) 1585.

3 *Advances in inorganic chemistry and radiochem* (Academic Press, New York) Vol 15, edited by D C Bradley, H J Emeleus & A G Sharpe, (1972) 259.

4 Sharma V, *Preparation, characterisation and reactions of 2,2,2-trichloroethoxides of some transition metals*, Ph D Thesis, Panjab University, Chandigarh, 1986.

5 Singh S, *Chemistry of some novel fluoro sulphates*, Ph D thesis, Panjab University, Chandigarh, 1982.

6 Vogel A I, *A text-book of inorganic quantitative analyses*, (Longman Green, London), 1961.

7 Dubicki L, Kakos G A & Winter G, *Aust J Chem*, **21** (1968) 1461.

8 Brown D A, Cunningham D & Glass W K, *J chem Soc* (*A*), (1968) 1563.

9 Agarwal S K & Mehrotra R C, *Inorg chim Acta*, **112** (1986) 177.

10 Chadha S L, Sharma V & Uppal K, *Indian J Chem*, **25A** (1986) 625.

11 Chadha S L, Singh T, Uppal K & Jaswal C M, *Indian J Chem*, **24A** (1985) 781.

12 Crouch P C, Fowles G W A, Marshall P R & Walton R A, *J chem Soc A*, (1968) 1636.

13 Chadha S L, Sharma V, Jaswal C M, Taneja S P & Raj D, *Z anorg allg Chem*, **536** (1986) 164.

14 Chadha S L, Sharma V & Sharma A, *J chem Soc, Dalton Transactions*, (1987) 1253.

15 Hubert-Pfalzgraf L G & Reiss J G, *Inorg chim Acta*, **47** (1981) 7.

16 Hubert Pfalzgraf L G & Reiss J G, *Inorg chim Acta*, **41** (1980) 111.

17 Gerlach J N & Gard G L, *Inorg Chem*, **9** (1970) 1865.

Indian Journal of Chemistry
Vol. 27A, March 1988, pp. 217-221

Synthesis & Spectral Studies of Complexes of Co(II), Ni(II), Cu(II), Zn(II), Ru(II), Pd(II) & Pt(II) with 2,3-Disubstituted Quinazolin-(3H)-4-ones

B PRABHAKAR, K LAXMA REDDY & P LINGAIAH*
Department of Chemistry, Kakatiya University, Warangal 506 009

Received 20 *April* 1987; *revised* 22 *July* 1987; *rerevised and accepted* 7 *September* 1987

Complexes of Co(II), Ni(II), Cu(II), Zn(II), Ru(II), Pd(II) and Pt(II) with 2-methyl-3-(2′-hydroxybenzylamino)-quinazolin-(3H)-4-one (MHBQ) and 2-phenyl-3-(2′-hydroxybenzylamino)-quinazolin-(3H)-4-one (PHBQ) have been synthesized and characterized by analytical, conductivity, magnetic and infrared, electronic, PMR and ESR spectral data. Based on analytical data, the stoichiometry of the complexes is found to be 1:2 (metal to ligand). The infrared and PMR spectral data of the metal complexes indicate that MHBQ and PHBQ act as uninegative tridentate ligands towards Co(II), Ni(II), Cu(II) and Ru(II) and as uninegative bidentate ligands towards Pd(II), Pt(II) and Zn(II). The electronic spectral data suggest that all the Co(II), Ni(II) and Ru(II) complexes are octahedral, Cu(II) complexes are tetragonal, Pd(II) and Pt(II) complexes are square-planar and Zn(II) complexes are tetrahedral.

Quinazolin-(3H)-4-ones possess four coordinating sites: (i) oxygen of the phenolic −OH, (ii) oxygen of the carbonyl function, (iii) nitrogen of the benzylamino group and (iv) nitrogen of the quinazolin ring (structure-I). These ligands may, therefore, act as monodentate, bidentate or tridentate ligands[1,2]. In order to find out the nature of interaction of these ligands with different metal ions and in continuation of our earlier work[3-5] on complexes of 2,3-disubstituted quinazolin-(3H)-4-ones, we report here the synthesis of Co(II), Ni(II), Cu(II), Zn(II), Ru(II), Pd(II) and Pt(II) complexes of 2-methyl-3-(2′-hydroxybenzylamino)quinazolin-(3H)-4-one (MHBQ) and 2-phenyl-3-(2′-hydroxybenzylamino)quinazolin-(3H)-4-one (PHBQ). The complexes have been characterized on the basis of analytical data, conductivity measurements, magnetic susceptibility measurements and infrared, electronic, electron spin resonance (ESR) and proton magnetic resonance spectra (PMR).

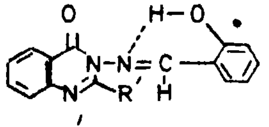

R′=CH_3(MHBQ)
R′=Ph (PHBQ)
I

Materials and Methods

Anthranilic acid, hydrazine hydrate, salicylaldehyde, acetic anhydride and other solvents used in this work were BDH reagents of AR grade. The metal salts like nickel(II) chloride, cobalt(II) acetate and zinc(II) acetate were the products of M/s Chempure Chemicals Limited, Bombay. Palladium(II) chloride, platinum(II) chloride and ruthenium(III) chloride were obtained from Johnson Mathey Chemicals, London. The ligands MHBQ and PHBQ were prepared as reported in literature[6] and their purities checked by TLC and melting point determinations. The complex $RuCl_2(DMSO)_4$ was prepared by literature method[7].

Preparation of the complexes

In the preparation of all the Co(II), Ni(II), Cu(II) and Zn(II) complexes the following general procedure was adopted. The aqueous metal salt solution (0.1 *M*) was added drop-wise to a solution (0.3 *M*) of the ligand in acetone with constant stirring. In all the cases, the ligand concentration was kept in slight excess over that required by 1:3 (metal-ligand) molar ratio. The reaction mixture was refluxed on a water bath for 60-90 min. The complex separated out on cooling. It was filtered off and washed several times with hot acetone until the washings were free from excess ligand. The complexes were finally dried *in vacuo* over fused calcium chloride.

Ruthenium(II) complexes

The complex, dichlorotetrakis(dimethyl sulphoxide)ruthenium(II) $[RuCl_2(DMSO)_4]$ is a convenient starting material for the preparation of a variety of mixed ligand ruthenium(II) complexes. It was prepared using the method of Wilkinson *et al.*[7] The complex, $[RuCl_2(DMSO)_4]$ (0.2 g), was suspended in toluene (30 ml) and refluxed for one hour with the appropriate ligand in acetone (30 ml). In all the cases, 1:4 (metal to ligand) ratio was maintained. During the period of refluxing, the whole suspension dissolved, resulting in a clear solution which was then evaporated under reduced pressure to remove the excess of solvent. The residue was treated with diethyl ether when the solid complex precipitated. This was filtered off, washed several times with diethyl ether, dried and recrystallized from acetone-ether to get the pure complex. Finally the complexes were dried *in vacuo* over fused calcium chloride.

Palladium(II) and platinum(II) complexes

To Pd(II)/Pt(II) salt solution, was added the ligand in acetone (50 ml) drop by drop with constant stirring. In all the cases the ligand concentration was kept in slight excess over that required by 1:3 (metal to ligand) molar ratio. The reaction mixture was refluxed on a water bath for about 40 min. The complex separated out in neutral medium on cooling. It was filtered and washed several times with hot water and acetone until the washings were free from the excess ligand and chloride ions. The complexes were dried *in vacuo* over fused calcium chloride.

The analytical data (C, H, N) for the ligands and their metal complexes were obtained from the Micro-analytical Laboratory, Calcutta University, Calcutta. The metal contents of the complexes were determined using standard procedures after heating these to decomposition. Molar conductivities of the complexes in DMF were measured using a Digisun digital conductivity meter, model DI-909. Magnetic susceptibilities were measured at room temperature by the Gouy method using Hg[Co(SCN)$_4$] as the calibrant. Diamagnetic corrections were applied using Pascal's constants. Infared spectra of the ligand and the complexes in the region 4000-200 cm^{-1} were recorded in nujol on a Perkin-Elmer infrared spectrophotometer model-283. Electronic spectra of the complexes were recorded in DMF on a Shimadzu multipurpose recording spectrophotometer model-MPS-5000. The solid state ESR spectra of Cu(II) complexes at liquid nitrogen temperature were recorded on a Varian E-4, X-band instrument at RSIC, IIT, Bombay. 100 MHz PMR spectra of the ligands and their Ru(II), Pd(II), Pt(II) and Zn(II) complexes were recorded in DMSO-d_6 on a Jeol instrument at I.I.Sc., Bangalore.

Results and Discussion

All the complexes are stable at room temperature, non-hygroscopic, insoluble in water and some common organic solvents, but are soluble in DMF and DMSO. The analytical data of the complexes (Table 1) indicate that the metal to ligand ratio is 1:2. The molar conductances of 1×10^{-3} *M* solutions of the complexes in DMF are in the range 5-20 ohm^{-1} cm^2 mol^{-1} indicating their nonionic nature[8].

Table 1—Analytical and Physical Data of the Complexes

Complex	Colour	m.p. (°C)[a]	Analysis (%)[b]			
			M	C	N	H
[Co(MHBQ)$_2$]	Brown	290	9.43 (9.09)	62.54 (62.03)	13.68 (13.30)	3.90 (3.10)
[Co(PHBQ)$_2$]	Brown	286	7.83 (7.21)	68.29 (67.92)	11.38 (11.08)	3.79 (3.12)
[Ni(MHBQ)$_2$]	Brown	295	9.44 (9.07)	62.54 (62.25)	13.68 (13.06)	3.90 (3.10)
[Ni(PHBQ)$_2$]	Dark Brown	295	7.85 (7.23)	68.29 (67.63)	11.38 (11.03)	3.79 (3.02)
[Cu(MHBQ)$_2$]	Brown	300	10.17 (9.90)	62.03 (61.86)	13.57 (13.12)	3.87 (3.22)
[Cu(PHBQ)$_2$]	Green	310	8.47 (8.09)	67.83 (67.02)	11.30 (10.89)	3.77 (3.12)
[Zn(MHBQ)$_2$]	Colourless	280	10.46 (10.03)	61.83 (61.02)	13.52 (13.08)	3.86 (3.20)
[Zn(PHBQ)$_2$]	Colourless	278	8.72 (8.23)	67.65 (67.09)	11.27 (10.82)	3.76 (3.19)
[Ru(MHBQ)$_2$]	Green	285	—	58.44 (58.08)	12.78 (12.43)	3.65 (3.22)
[Ru(PHBQ)$_2$]	Snuff	290	—	64.53 (64.02)	10.75 (10.20)	3.58 (3.07)
[Pd(MHBQ)$_2$]	Dark Yellow	270	—	58.00 (57.18)	12.68 (11.17)	3.62 (3.05)
[Pd(PHBQ)$_2$]	Snuff	272	—	64.12 (63.65)	10.68 (9.98)	3.56 (3.20)
[Pt(MHBQ)$_2$]	Snuff	270	—	51.13 (50.92)	11.18 (10.96)	3.19 (3.00)
[Pt(PHBQ)$_2$]	Snuff	275	—	57.6 (56.55)	9.60 (9.01)	3.27 (3.00)

[a]All the complexes decomposes above the temperature cited.
[b]Calculated values in parenthesis.

2-Substituted-3-aminoquinazolin-(3H)-4-ones, which are structurally similar to the present ligands, are reported to coordinate in a bidentate manner through oxygen of the carbonyl group and nitrogen of the amino group[9]. In the IR spectra of the present ligands, a strong band appearing around 1680 cm^{-1}, attributed to ν(C=O), is shifted to lower wave numbers by 35-50 cm^{-1} in the spectra of all the complexes except in the complexes of Zn(II), Pd(II) and Pt(II), indicating that the carbonyl oxygen is involved in coordination[10]. However, the complexes of Zn(II), Pd(II), Pt(II) exhibit a band at 1680 cm^{-1}, indicating the non-involvement of carbonyl oxygen in complex formation. The appearance of ν(−OH) in the lower region (3200-3100 cm^{-1}) than expected (3600-3400 cm^{-1}) in the spectra of both the ligands can be attributed to the hydrogen bonding of OH with nitrogen of the benzylamino group[11]. The disappearance of this band in all the metal complexes indicates complex formation by deprotonation of OH group.

The ligands MHBQ and PHBQ have two C=N groups, one belonging to quinazolin ring and the other to benzylamino group. The IR absorptions at 1640 and 1610 cm^{-1} are assigned to $\nu(C=N)$ of quinazolin ring and benzylamino group, respectively[12]. The band at 1640 cm^{-1} remains unchanged in the spectra of the metal complexes, but the one at 1610 cm^{-1} undergoes shift to lower wave numbers ($\Delta\nu = 40$-50 cm^{-1}) indicating that the nitrogen of benzylamino group is involved in coordination with the metal ion[12]. The absence of a $\nu(S=O)$ band in the region 1050-1100 cm^{-1} in all Ru(II) complexes indicates that DMSO is not coordinated with the metal ion[13]. The participation of oxygen and nitrogen in coordination in all the complexes is further supported by the appearance of $\nu(M-O)$ and $\nu(M-N)$ at 400 and 500 cm^{-1}, respectively, in the far infrared region[14,15] (Table 2).

Electronic spectra

The electronic spectral data of the complexes along with their assignments are presented in Table 3.

All the ligands exhibit strong bands around 33000 cm^{-1} with a shoulder at 29000 cm^{-1}, assignable to $\pi^* \leftarrow \pi$ and $\pi^* \leftarrow n$ transitions, respectively. Electronic spectra of Co(II) complexes display three bands around 8000, 16000 and 19500 cm^{-1} which are characteristic of octahedral geometry around Co(II)[5]. Electronic spectra of Ni(II) complexes exhibit three bands around 9000, 15000 and 24000 cm^{-1} which are characteristic of octahedral geometry around Ni(II)[16]. The octahedral geometry of Co(II) and Ni(II) complexes is further supported by the value of ν_2/ν_1 ratio which lies around 2.0 and 1.60, respectively[16]. Various ligand field parameters, such as the ligand field splitting energy (10 *Dq*), Recah inter-electronic repulsion parameter (*B*), covalency factor (β) and ligand field stabilization energy (LFSE) have been calculated for all the Co(II) and Ni(II) complexes[17]. The calculated 10 *Dq* values of Co(II) and Ni(II) complexes suggest for these ligands a place between water and ammonia in the spectrochemical series. The *B*-values for the complexes are lower than the free ion value which is an indication of orbital overlap and delocalization of *d*-orbitals. The β-values obtained are less than unity suggesting considerable amount of covalent character of the metal-ligand bonds. The β values for Co(II) complexes are less than those for the Ni(II) complexes indicating the greater covalent nature of Co(II) complexes.

Table 2—Some IR Spectral Bands (cm^{-1}) of 2,3-Disubstituted Quinazolin-(3H)-4-ones and Their Complexes

Compound	$\nu(C=O)$	$\nu(C=N)$	$\nu(OH)$	$\nu(M-O)$	$\nu(M-N)$
MHBQ	1680	1610	3150	—	—
PHBQ	1670	1610	3200	—	—
$[Co(MHBQ)_2]$	1630	1560	—	400, 430	480
$[Co(PHBQ)_2]$	1640	1560	—	410, 430	480
$[Ni(MHBQ)_2]$	1620	1570	—	420, 450	500
$[Ni(PHBQ)_2]$	1640	1560	—	410, 430	490
$[Cu(MHBQ)_2]$	1640	1570	—	400, 450	500
$[Cu(PHBQ)_2]$	1640	1570	—	410, 440	480
$[Zn(MHBQ)_2]$	1640	1560	—	400, 430	—
$[Zn(PHBQ)_2]$	1620	1550	—	400, 420	—
$[Ru(MHBQ)_2]$	1630	1575	—	400, 450	500
$[Ru(PHBQ)_2]$	1620	1570	—	390, 420	490
$[Pd(MHBQ)_2]$	1630	1565	—	380, 430	—
$[Pd(PHBQ)_2]$	1620	1570	—	410, 440	—
$[Pt(MHBQ)_2]$	1630	1580	—	400, 450	—
$[Pt(PHBQ)_2]$	1630	1570	—	400, 450	—

The electronic spectra of Cu(II) complexes exhibit one broad band around 16000 cm^{-1}. This is characteristic of tetragonal geometry around Cu(II)[18]. The two spin-allowed *d-d* transitions are observed in the Ru(II) complexes at 19200 and 24500 cm^{-1} which are characteristic of octahedral geometry[19]. The absence of splitting of lower energy band in the electronic spectra of Ru(II) complexes indicates that there is no tetragonal distortion. The bands observed for the Pd(II) complexes at 15000 and 20000 cm^{-1} indicate for them square-planar geometry[20,21]. Electronic spectra of Pt(II) complexes show two bands around 20000 and 24000 cm^{-1} which are characteristic of square-planar geometry[22].

Magnetic moments

The experimental and calculated magnetic moments of the complexes are given in Table 3.

The values obtained for all the complexes of Co(II) and Ni(II) are in the respective expected ranges for octahedral geometry[23,24]. The Cu(II) complexes possess magnetic moment value (1.82 B.M.) corresponding to one unpaired electron. All the Ru(II), Pd(II), Pt(II) and Zn(II) complexes are diamagnetic in nature.

PMR spectra

The aromatic protons in the PMR spectra of ligands appear in the region[25] δ 7.0-8.5 ppm. The methyl protons of MHBQ appear at δ 2.8 ppm. The signal due to the proton present on benzylamine carbon atom is overlapped by the signals of

Table 3—Magnetic Moment and Electronic Spectral Data and Relevant Ligand Field Parameters of Complexes

Complex	μ_{eff} (B.M.)	ν_1(cm^{-1})	ν_2(cm^{-1})	ν_3(cm^{-1})	ν_2/ν_1	10 *Dq* (cm^{-1})	*B*(cm^{-1})	β	LFSE (kcal mol^{-1})
[Co(MHBQ)$_2$]	4.99 (5.01)^b	8000	16000	19500	2.00	8000	766.7	0.68	18.29
[Co(PHBQ)$_2$]	5.03 (5.01)	8200	16100	19600	1.96	7900	740.0	0.65	18.05
[Ni(MHBQ)$_2$]	3.20 (3.15)	9050	15100	24000	1.67	6050	796.7	0.76	20.76
[Ni(PHBQ)$_2$]	3.28 (3.16)	9000	15000	24200	1.67	6000	813.3	0.78	20.57
[Cu(MHBQ)$_2$	1.82 (1.81)	—	16000^a	—	—	—	—	—	—
[Cu(PHBQ)$_2$]	1.83 (1.82)	—	16000	—	—	—	—	—	—
[Ru(MHBQ)$_2$]	—	—	19200	24500	—	—	—	—	—
[Ru(PHBQ)$_2$]	—	—	19100	24450	—	—	—	—	—
[Pd(MHBQ)$_2$]	—	—	15000	20000	—	—	—	—	—
[Pd(PHBQ)$_2$]	—	—	15200	20000	—	—	—	—	—
Pt(MHBQ)$_2$]	—	—	20000	24000	—	—	—	—	—
[Pt(PHBQ)$_2$]	—	—	20100	24050	—	—	—	—	—

For Co(II) complexes: $\nu_1 = {}^4T_{1g}(F) \rightarrow {}^4T_{2g}(F), \nu_2 = {}^4T_{1g}(F) \rightarrow {}^4A_{2g}(F), \nu_3 = {}^4T_{1g}(F) \rightarrow {}^4T_{1g}(P)$

For Ni(II) complexes: $\nu_1 = {}^3A_{2g}(F) \rightarrow {}^3T_{2g}(F), \nu_2 = {}^3A_{2g}(F) \rightarrow {}^3T_{1g}(F), \nu_3 = {}^3A_{2g}(F) \rightarrow {}^3T_{1g}(P)$

For Cu(II) complexes: $\nu_2 = {}^2E_g \rightarrow {}^2T_{2g}$

For Ru(II) complexes: $\nu_2 = {}^1A_{1g} \rightarrow {}^1T_{1g}, \nu_3 = {}^1A_{1g} \rightarrow {}^1T_{2g}$

For Pd(II) complexes: $\nu_2 = {}^1A_{2g} \rightarrow {}^1A_{2g}, \nu_3 = {}^1A_{1g} \rightarrow {}^1B_{1g}$

For Pt(II) complexes: $\nu_2 = {}^1A_{1g} \rightarrow {}^1B_{1g}, \nu_3 = {}^1A_{1g} \rightarrow {}^1E_g$

[a] Broad band indicates the overlapping of different transitions

[b] Calculated values in parenthesis

aromatic protons. In complexes,this signal is shifted to δ 9.6 indicating a decrease in the electron density at benzylamine carbon atom, which also supports the participation of nitrogen of benzylamino group in coordination[26]. A signal present at δ 10.5 in both the ligands indicates that hydroxyl proton is hydrogen bonded. The disappearance of this signal in the complexes confirms complex formation after deprotonation.

ESR spectra

The $g_\parallel$ and $g_\perp$ values have been found to be 2.24 and 2.06 respectively for Cu(II) complex of MHBQ by Kneubuhl's method[27] from which |g| is calculated. The trend $g_\parallel > g_\perp$ is characteristic of tetragonal geometry with $d_{x^2-y^2}$ as the ground state. The axial symmetry parameter (*G*) for the complexes is found to be greater than 4. This shows the absence of interaction between copper centers in the solid state[28]. The ESR spectrum of Cu(II)-MHBQ complex is magnetically dilute in the solid state as evidenced by the presence of four peaks in the $g_\parallel$ region. The $g_\parallel$ value is 2.24 and $A_\parallel$ value is 195 G. Further, the $g_\perp$ region is split with $g_y = 2.07$ and $g_x = 2.05$ suggesting a rhombic structure.

Based on their stoichiometry, conductance, magnetic and IR, electronic, PMR and ESR spectral data, the complexes have been assigned structures IIa and IIb.

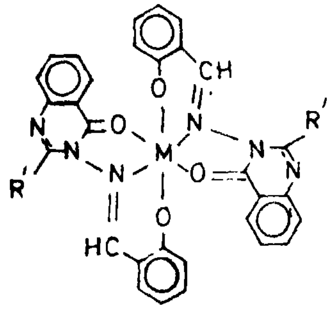

II(a) M = CO(II), Ni (II), Cu (II) and Ru (II)

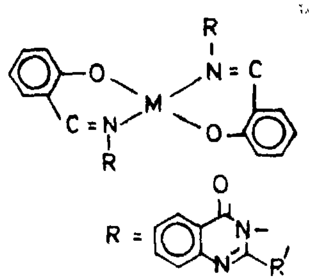

II (b) M = Pd(II), Pt(II) and Zn (II)

Acknowledgement

One of the authors (BP) is greateful to the CSIR, New Delhi for the award of a JRF.

References

1 Singh B, Lakshmi & Agarwala U, *Inorg Chem*, **8** (11) (1969) 2341.
2 Agarwala U & Agarwala Lakshmi, *J inorg nucl Chem*, **34** (1972) 241.
3 Laxma Reddy K, Lingaiah P & Veera Reddy K, *Polyhedron*, **5(10)** (1986) 1519.
4 Laxma Reddy K, Sri Hari S & Lingaiah P, *Indian J Chem*, **23A** (1984) 780.
5 Laxma Reddy K, Sri Hari S & Lingaiah P, *Indian J Chem*, **23A** (1984) 172.
6 Ravishankar Ch, *Studies in synthesis, biological and pharmacological evaluation of some* 6,8-*dibromoquinazolin*-(3*H*)-*one derivatives*, Ph.D. Thesis, Kakatiya University, Warangal, 1984.
7 Evans I P, Spencer A & Wilkinson G, *J chem Soc, Dalton Trans*, (1973), 204.
8 Greay M J, *Coord Chem Rev*, 7 (1971) 81.
9 Laxma Reddy K, Sri Hari S & Lingaiah P, *J Indian chem Soc*, **60** (1983) 1020.
10 Sahu R, Agarwal R S & Kushwaha S S S, *J Indian chem Soc*, 7 (1982) 853.
11 Sammour A, Fammy A F M & Mahmoud M, *Indian J Chem*, **13** (1973) 272.
12 Prabhakaran C P & Patel C C, *J inorg nucl Chem*, **34** (1972) 3485.
13 Raynolds W L, *Prog inorg Chem*, **12** (1970) 1.
14 Inomata T & Moriwaki T, *Bull chem Soc Japan*, **46** (1978) 1148.
15 Agarwala R C & Rao D S S V, *Indian J Chem*, **21A** (1982) 735.
16 Seetharama Rao T, Laxma Reddy K, Swamy S J & Lingaiah P, *Indian J Chem*, **24A** (1985) 942.
17 Lever A B P, *J chem Educ*, **45** (1966) 711.
18 Nishida Y & Kida S, *Coord Chem Rev*, **27** (1979) 275.
19 Preti C, Tosi G & Zannihi P, *J inorg nucl Chem*, **41** (1979) 485.
20 Ray Hem Lata, Pandeya K B & Singh R P, *Indian J Chem*, **12** (1974) 532.
21 Gray H B & Ballahusen C J, *J Am chem Soc*, **85** (1963) 260.
22 Singh P P, Srivastava A K & Khan Sushil A, *Aust J Chem*, **28** (1975) 267.
23 Carlin Richard L, In *Transition metal chemistry*, Vol. 1 (Marcel Dekker, New York) 1965, 20.
24 Khulbe R C, Bhoon Y K & Singh R P, *J Indian chem Soc*, **9** (1981) 940.
25 Mookkerjee M N, Singh R V & Tandon J P, *Indian J Chem*, **21A** (1982) 388.
26 Sakata K, Hashimoto M, Tagani M & Marakani Y, *Bull chem Soc, Japan*, **53** (1980) 2262.
27 Kheubuhl F K, *J chem Phys*, **33** (1960) 1074.
28 Procter I M, Hathaway B J & Nicholis P, *J chem Soc*, A (1968) 1678.

Indian Journal of Chemistry
Vol. 27A, March 1988, pp. 222-224

Synthetic & Structural Studies on the Polymeric Complexes of Terephthaloyl-bis-(N-phenylhydroxamic Acid) (TPHA) & Sebacyl-bis-(N-phenylhydroxamic Acid) (SPHA) with Co(II), Ni(II), Cu(II) & Zn(II)

K N MUNSHI*, V W KHARCHE† & H D JUNEJA
Department of Chemistry, Nagpur University, Campus, Nagpur 440 010

Received 9 *March* 1987; *revised* 16 *July* 1987; *rerevised and accepted* 7 *September* 1987

Polymeric complexes of terephthaloyl-bis-(N-phenylhydroxamic acid) (TPHA) and sebacyl-bis-(N-phenylhydroxamic acid) (SPHA) with Co(II), Ni(II), Cu(II) and Zn(II) have been prepared by the reaction of the corresponding ligands with transition metal ions in dimethylformamide medium. Polymers formed have been characterised by their elemental analysis. Thermal stabilities of the polymers have been investigated by carrying out differential thermal analysis and thermogravimetric analysis. The structures of the polymeric complexes are assigned on the basis of their reflectance and infrared spectral and magnetic susceptibility data.

Hydroxamic acids are an important class of reagents and form complexes with various metal ions[1-4]. In the present paper, preparation of terephthaloyl-bis-(N-phenylhydroxamic acid) (TPHA) and sebacyl-bis-(N-phenylhydroxamic acid) (SPHA) and their polymeric complexes with Co(II), Ni(II), Cu(II) and Zn(II) have been reported for the first time. Besides the synthesis and examination of their thermal stability, present work describes structural characterisation of these polymeric complexes on the basis of elemental analysis, infrared and reflectance spectra and magnetic susceptibility measurements.

Materials and Methods

All the chemicals used as starting materials in the synthesis of ligands and coordination polymers were of chemically pure quality. If required, these were further purified by standard procedures.

Preparation of ligands

Terephthaloyl-bis-(N-phenylhydroxamic acid) (TPHA) and sebacyl-bis-(N-phenylhydroxamic acid) (SPHA) were prepared by the modified method of Priyadarshini and Tandon[5] based on the Schotten-Baumann reaction. N-Phenylhydroxylamine (0.25 *M*), ethanol (50 ml), sodium bicarbonate (0.5 *M*) and distilled water (25 ml) were taken in a 250 ml beaker. To this, acid dichloride (0.1 *M*) dissolved in diethyl ether (100 ml) was added over a period of 45 min with constant stirring. A granular solid separated which was filtered and triturated with saturated solution of sodium bicarbonate to remove any acidic impurities. The products were obtained in low yields (60 to 70%) and were crystallized with difficulty from dimethylformamide (DMF) (m.p. SPHA 152° and TPHA 232°). TPHA melted with decomposition. TPHA [Found: C, 68.55; H, 4.81; N, 7.80; Calc. for $C_{20}H_{16}O_4N_2$: C,.68.96; H, 4.80; N, 7.81%]. SPHA [Found: C, 67.60; H, 7.39; N, 7.30; Calc. for $C_{22}H_{28}O_4N_2$: C, 68.76; H, 7.29; N, 7.29%].

Preparation of polymers

The ligand (0.01 *M*), metal acetate (0.01 *M*), and DMF (50 ml) were heated on a waterbath for 2 hr. The insoluble polymers formed were filtered and throughly washed several times with dimethylformamide and ethanol till free from unreacted reactants.

The polymers were obtained as amorphous powders and were found to be insoluble in almost all the common organic solvents. The elemental analyses and proposed compositions for these polymers are given in Table 1.

Carbon, hydrogen and nitrogen were estimated usuing a Coleman's analyser.

IR spectra were recorded on a specord IR-75 instrument in the range 4000-400 cm^{-1} using nujol mull.

A single beam Carl-Zeiss USU-2-p-spectrophotometer was used for recording reflectance spectra of polymers and magnesium carbonate was used as a reference sample. A DTA apparatus fabricated at IIT, Bombay was used for recording differential thermograms of the polymers. The heating rate was maintained at 7°/min. A Stanton-Redcroft thermogravimetric balance with an automatic recorder (BARC, India) was used for thermogravimetric analysis. The analysis was carried out in air with 100 mg of a sample taken in a platinum crucible. The

---

†Present address: Chemistry Department, Sindhu Mahavidyalaya, Nagpur.

Table 1—Elemental Analyses and Decomposition Temperatures of Ligands and Polymers

Proposed composition (Dec. Temp., °C)	Found (Calc.), %				Colour	$\mu_{eff.}$ (B.M.)
	C	H	N	M		
$[Co(a)]_n$ (290)	58.65 (58.98)	3.56 (3.44)	6.78 (6.88)	14.40 (14.48)	Brown	3.91
$[Ni(a)(H_2O)_2]_n$ (300)	55.00 (54.21)	4.16 (4.01)	6.55 (6.32)	13.23 (13.26)	Yellow	3.44
$[Cu(a)]_n$ (260)	57.20 (58.32)	3.64 (3.40)	6.88 (6.80)	14.88 (15.43)	Yellowish green	1.88
$[Zn(a)]_n$ (270)	58.10 (58.06)	3.22 (3.39)	6.82 (6.77)	15.62 (15.82)	White	–
$[Co(b)]_n$ (355)	58.75 (58.61)	5.71 (5.87)	6.20 (6.32)	14.45 (13.30)	Light pink	4.67
$[Ni(b)(H_2O)_2]_n$ (320)	56.65 (56.15)	5.74 (5.85)	6.76 (6.27)	12.24 (12.26)	Light green	3.39
$[Cu(b)]_n$ (375)	58.80 (58.99)	6.10 (5.81)	6.22 (6.26)	13.88 (14.19)	Dirty green	1.83
$[Zn(b)]_n$ (330)	58.50 (58.74)	5.99 (5.79)	6.23 (6.23)	14.39 (14.55)	White	–

(a = TPHA, b = SPHA)

heating rate was maintained at 3°C/min. Magnetic susceptibilities of polymers were determined by Gouy's method.

Results and Discussion

An IR band around 2800 cm^{-1} has been assigned to O – H stretching vibration in this type of hydroxamic acids[6]. In the present case this band appears at 3170 cm^{-1} in SPHA and TPHA ligands. Bands appearing at 1615 and 1595 cm^{-1} in SPHA may be due to the resonating structures of N – N-(– C = O)-OH moiety. In the case of TPHA it appears at 1600 cm^{-1}. An intense band appearing at 3275 cm^{-1} is due to free N – H stretching whereas the band appearing at 895 in SPHA and 890 cm^{-1} in TPHA is assigned to N – O stretching vibration.

The hydroxamic acids generally form five membered chelates with metal ions coordinating through $\rangle$N – O and > C = O oxygens.

As is anticipated, the band due to O – H group disappears in polymers. The band due to carbonyl group is shifted towards lower frequency side indicating the formation of $C = O \rightarrow M$ coordinate bond. The N – O band in polymer is found to have been shifted slightly to higher frequency side with increase in its intensity. Medium bands appearing in the region of 520 to 565 cm^{-1} are assigned to M – O bonding in polymers[7].

Reflectance spectra and magnetic properties

A band appearing around 18.69 kK in Co(II)-TPHA and around 18.60 kK in Co(II)-SPHA polymers may be assigned to ${}^4A_2 \rightarrow {}^4T_1\ (P)$ transition in tetrahedral field[8].

Magnetic data of Co(II)-TPHA and -SPHA polymers also support the tetrahedral geometry of these complexes. A band appearing at 25.64 kK in Ni(II)-SPHA and at 28.00 kK in Ni(II)-TPHA polymer is due to ${}^3A_{2g} \rightarrow {}^3T_{1g}(P)$ transition. The magnetic moment value also confirms the octahedral geometry of the complexes.

Broad bands around 15.38 kK and 12.66 kK in Cu(II) polymers of SPHA occur due to $d_{yz}, d_{xz} \rightarrow d_{x^2-y^2}$ and $d_{z^2} \rightarrow d_{x^2-y^2}$ transitions respectively[9].

In TPHA-Cu(II) polymer, however, only one band is observed around 15.88 kK which may be due to $d_{yz}, d_{xz} \rightarrow d_{x^2-y^2}$ transition. Thus, in both the cases, the square planar geometry is predicted[10].

Thermal studies of polymers

Co(II) and Cu(II) complexes of TPHA show a large exotherm in the range 310-400°C (390-520°C for SPHA complexes) while the range for Ni(II), Zn(II) complex is 310°-340°C (360°-500°C for SPHA complexes). In addition to this, Co(II) and Cu(II) complexes of TPHA show a sharp exotherm at ~ 230°C (250°C for SPHA complexes) while for Ni(II) complex it occurs at ~ 300°C (310°C for SPHA complex). Zn(II)-TPHA complex shows no such sharp exotherm.

It has been observed in the case of Co(II) and Cu(II) polymers that this sharp exotherm is not associated with mass loss in TGA. In Ni(II) polymer

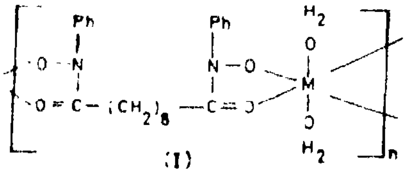

(I)

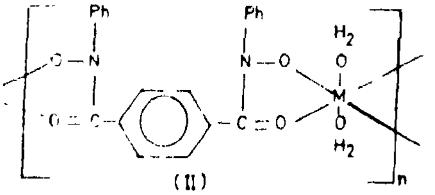

(II)

this exotherm is almost merged with the large exotherm.

Decomposition temperature of the polymers are given in Table 1.

On the basis of above studies, structures (I) and (II) are proposed for Ni-SPHA and Ni-TPHA polymers respectively. In case of Co(II), Cu(II) and Zn(II) complexes of SPHA and TPHA water of coordination is absent.

References

1 Das J & Shome S C, *Anal chim Acta*, **24** (1961) 37.
2 Luitwick G D & Ryan D E, *Can J Chem*, **32** (1954) 949.
3 Ryan D E & Armour C A, *Can J Chem*, **35** (1965)-1454.
4 Ryan D E & Lutwick G D, *Can J Chem*, **31** (1953) 9.
5 Priyadarshini U & Tandon S G, *J chem Engg Data*, **12** (1967) 143.
6 Shukla J P, Agrawal Y K & Kuchya K P, *J Indian chem Soc*, **51** (1954) 437.
7 Nakamoto, *Infrared spectra of inorganic and coordination compounds* (John Wiley, New York), 1970, 270.
8 Lever A B P, *Inorganic electronic spectroscoy* (Elsevier, New York), 1968, 383.
9 Wentworth R A D, *Inorg Chem*, **5** (1966) 496.
10 Lever A B P, *Inorganic electronic spectroscopy* (Elsevier, New York), 1968, 356.

Indian Journal of Chemistry
Vol. 27A, March 1988, pp. 225-230

Synthesis & Characterization of Nitrato & Acetato Complexes of Dioxouranium(VI) with Disalicylaldehyde Acyl Hydrazones

S DAS & R A LAL*
Department of Chemistry, Pachhunga University College, North-Eastern Hill University, Aizawl 796 001, Mizoram

Received 20 *November* 1986; *revised* 26 *May* 1987; *re-revised and accepted* 21 *July* 1987

Dioxouranium(VI) complexes of disalicylaldehyde oxaloyldihydrazone (H_4A_2), malonoyldihydrazone (H_4B_2), succinoyldihydrazone (H_4C_2), glutaroyldihydrazone (H_4D_2), adipoyldihydrazone (H_4E_2) and phthaloyldihydrazone (H_4F_2) have been synthesized from the reaction of uranyl nitrate hexahydrate and uranyl acetate dihydrate with the title ligands in alcoholic medium. The complexes have the compositions $[(UO_2)_2(H_2L_2)(H_2O)_4(NO_3)_2].2H_2O$ and $[(UO_2)_2(H_2L_2)(C_2H_5OH)_2(CH_3COO)_2].C_2H_5OH$ where $H_4L_2 = H_4A_2$, H_4B_2, H_4C_2, H_4D_2, H_4E_2 and H_4F_2. The complexes have been characterized on the basis of elemental analyses, TGA, DTA, molar conductance, infrared and Raman spectral data.

Metal complexes of acylhydrazones have received great attention during recent years because of their pharmacological applications[1,2], unusual magnetic properties and diverse structural features[3]. Although some complexes of acyldihydrazones with 3*d* metal ions[4-6] and a few of pyridyldihydrazone complexes with actinides[7] have been reported, those of acyldihydrazones with actinides are almost non-existent. This is probably due to the fact that in dihydrazones two hydrazone units are joined together through methylene chains of varying length or phenyl or pyridyl group making the system more complex. Dihydrazones, which react in keto (I), keto-enol (II) and enol (III) forms depending upon the mode of preparation of the complexes, nature of the solvent, the *p*H of the reaction medium, the nature of metal salt and the molar ratio of the reactants, give rise to polymeric complexes through both ligand bridging (because of their flexibility) and oxo-bridging.

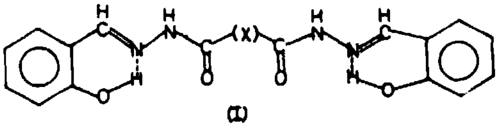
(I)

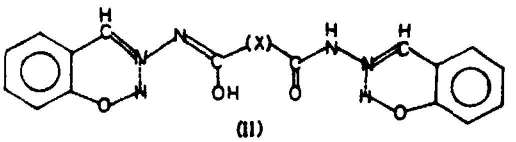
(II)

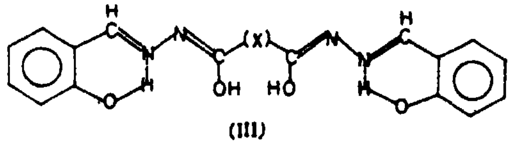
(III)

We report here the preparation and characterization of dioxouranium(VI) complexes with some disalicylaldehyde acylhydrazones (IV).

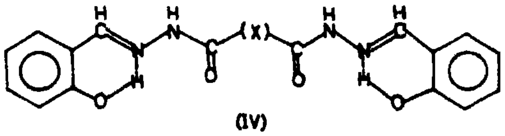
(IV)

X = $-(CH_2)_n-$

n	H_4L_2	*Ligand*
0	H_4A_2	Disalicylaldehyde oxaloyldihydrazone
1	H_4B_2	Disalicylaldehyde malonoyldihydrazone
2	H_4C_2	Disalicylaldehyde succinoyldihydrazone
3	H_4D_2	Disalicylaldehyde glutaroyldihydrazone
4	H_4E_2	Disalicylaldehyde adipoyldihydrazone

X = $-C_6H_4-$ H_4F_2 Disalicylaldehyde phthaloyldihydrazone

Materials and Methods

Uranyl nitrate hexahydrate, uranyl acetate dihydrate, diethyl esters of oxalic, malonic, succinic, glutaric, adipic and phthalic acids, hydrazine hydrate and salicylaldehyde were BDH reagents of AR or equivalent grade. Acyldihydrazines, viz., oxaloyl, malonoyl, succinoyl, glutaroyl, adipoyl and phthaloyl dihydrazines were prepared by reacting the corresponding diethyl esters (1 mol) with hydrazine hydrate (2 mol). The dihydrazones were prepared by reacting warm or refluxing dilute solutions of the above acid dihydrazides (1 mol) with salicylaldehyde (2 mol) and were collected as described elsewhere[8].

Uranium in the complexes was determined by standard literature method[9]. The ligands in the complexes were determined in 5*M* H_2SO_4 with standard $KMnO_4$ using a calibration curve[5]. Nitrogen was determined by microanalytical method. Nitrate was determined as nitron nitrate. Water and ethanol contents were determined by heating the samples in an electric oven maintained at 80 and 180°C and estimating the loss in weight. The IR spectra were recorded in KBr in the range 4000-180 cm^{-1} on a Perkin-Elmer-983 spectrophotometer. Raman spectra of $(UO_2)_2(H_2A_2)(NO_3)_2 \cdot 6H_2O$ and $(UO_2)_2(H_2A_2)(CH_3COO)_2 3C_2H_5OH$ complexes were recorded on a Raman spectrophotometer (Ramalog 1403) using rotating sample technique in order to avoid the decomposition of the samples. The molar conductances of the complexes at 10^{-3} *M* dilution in ethanol and DMF were measured using an Elico conductivity cell. Thermal studies of the complexes were carried out in an atmosphere of air, under static conditions, heating the specimen at the rate of 10°C/min in the range 0-800°C, using heated alumina as the standard reference material.

Preparation of the complexes

The following general procedures were used for the isolation of the complexes:

(i) Uranyl nitrate hexahydrate (0.1 *M*) was dissolved in ethanol. The ligand (2 g), powdered well in an agate morter, was taken in 50 ml ethanol and stirred well to get a homogeneous slurry. Uranyl nitrate solution was added to the ligand slurry with gentle stirring maintaining the metal: ligand molar ratio 3:1. The mixture was refluxed for 2 hr. In the case of H_4A_2 and H_4F_2, the complexes precipitated immediately but in the cases of other ligands, a solution was obtained. The solution, on concentration (~ 70 ml) followed by addition of ether, precipitated a semi-solid. This was extracted with benzene and stirred well for about half an hour and kept overnight. The complex so obtained was washed with ethanol-benzene mixture, benzene and dried over anhydrous calcium chloride.

(ii) Uranyl acetate dihydrate was dissolved in ethanol containing one drop of acetic acid to get a 0.1 *M* solution. Any undissolved material was filtered off. Uranyl acetate solution was added to the ligand slurry (2 g) obtained as above with gentle stirring maintaining the metal:ligand molar ratio at 3:1. The mixed solution, after refluxing for one hour, precipitated the complex which was isolated as above.

Results and Discussion

The results of elemental analyses (Table 1) are consistent with 2:1 (metal:ligand) stoichiometry and accordingly, the general formulae $(UO_2)_2(H_2L_2)(NO_3)_2$ $6H_2O$ and $(UO_2)_2(H_2L_2)(CH_3COO)_2 3C_2H_5OH$. All the complexes are amorphous powders and their colours vary from dull yellow, yellow, dull orange,

Table 1—Analytical and Melting Point Data of Dioxouranium(VI) Complexes of Acyldihydrazones

S. No.	Complex	Colour (m.p./d.p., °C)	Found (Calc.) %				
			U	N	Ligand	NO_3	H_2O/C_2H_5OH
1	$(UO_2)_2(H_2A_2)(NO_3)_2 6H_2O$	Brown (>250*)	43.01 (43.43)	7.47 (7.66)	29.51 (29.56)	10.97 (11.31)	9.97 (9.85)
2	$(UO_2)_2(H_2A_2)$ $(CH_3COO)_2 3C_2H_5OH$	Brown (>250*)	42.82 (42.50)	3.11 (3.21)	28.75 (28.93)	—	11.27 (12.32)
3	$(UO_2)_2(H_2B_2)(NO_3)_2 6H_2O$	Red brown (170)	42.69 (42.88)	7.61 (7.57)	30.01 (30.45)	10.98 (11.17)	9.48 (9.78)
4	$(UO_2)_2(H_2B_2)$ $(CH_3COO)_2 3C_2H_5OH$	Brown (>250)	41.69 (41.98)	4.77 (4.94)	29.99 (29.81)	—	11.97 (12.17)
5	$(UO_2)_2(H_2C_2)(NO_3)_2 6H_2O$	Brown (165)	42.05 (42.35)	7.38 (7.47)	31.09 (31.32)	11.00 (11.03)	9.51 (9.61)
6	$(UO_2)_2(H_2C_2)$ $(CH_3COO)_2 3C_2H_5OH$	Orange (>250*)	41.87 (41.46)	4.62 (4.88)	30.78 (30.66)	— —	11.98 (12.02)
7	$(UO_2)_2(H_2D_2)(NO_3)_2 6H_2O$	Dull orange (160)	42.03 (41.83)	7.29 (7.38)	31.98 (32.16)	10.89 (10.00)	9.18 (9.47)
8	$(UO_2)_2(H_2D_2)$ $(CH_3COO)_2 3C_2H_5OH$	Dark orange (>250)	40.66 (40.96)	4.93 (4.82)	31.72 (31.50)	— —	11.98 (11.88)
9	$(UO_2)_2(H_2E_2)(NO_3)_2 6H_2O$	Orange (185)	41.01 (41.32)	6.98 (7.29)	32.76 (32.99)	10.65 (10.76)	9.29 (9.38)
10	$(UO_2)_2(H_2E_2)$ $(CH_3COO)_2 3C_2H_5OH$	Orange (>250)	40.07 (40.48)	4.82 (4.76)	31.99 (32.31)	— —	11.68 (11.73)
11	$(UO_2)_2(H_2F_2)(NO_3)_2 6H_2O$	Yellow (>250*)	40.59 (40.61)	7.32 (7.17)	34.00 (34.13)	10.27 (10.58)	9.08 (9.22)
12	$(UO_2)_2(H_2F_2)$ $(CH_3COO)_2 3C_2H_5OH$	Dull yellow (>250)	39.72 (39.80)	4.49 (4.68)	33.29 (33.44)	— —	9.78 (9.87)

*Decompose.

orange, red brown to brown. The nitrato complexes of the ligands $H_4B_2 - H_4E_2$ are partially soluble in ethanol, methanol and acetone and completely so in DMF, but are insoluble in water and other organic solvents like ether, chloroform, carbon tetrachloride and benzene. Acetato complexes of these ligands are soluble in donor solvents like DMF and DMSO only. The nitrato complexes of H_4A_2 and H_4F_2 are only sparingly soluble in DMF and DMSO while acetato complexes are not soluble at all. The molar conductances of the nitrato complexes of H_4B_2 to H_4E_2 ligands lie in the ranges 154-190 and 145-167 ohm^{-1} cm^2 mol^{-1} in methanol and DMF respectively indicating their 1:2 electrolytic behaviour[10]. Such high values of molar conductances are due to solvolysis of the complexes in coordinating solvents, methanol and DMF[11]. The molar conductance values (4.9 to 15.5 ohm^{-1} cm^2 mol^{-1}) of acetato complexes indicate their non-electrolytic nature in DMF[10]. This is, most probably, due to strong coordination by acetato group.

The nitrato and acetato complexes show mass loss corresponding to two water and one ethanol molecules at 80°C indicating their lattice-held nature. The complexes show mass loss corresponding to four water and two ethanol molecules at 180°C indicating their coordinated nature. In the nitrato complexes of H_4B_2 to H_4E_2, we could get satisfactory results by heating the samples although they started melting. The TGA curve of the acetato complex No. 6 (see Table 1 for numbering) shows mass loss corresponding to three ethanol molecules in the temperature range 70-160°C after which the complex remains stable up to 300°C. The DTA curve of the acetato complex shows a broad endothermic peak in the region 70-220°C with a minimum at 160°C giving additional evidence for the presence of ethanol molecules. The loss of one ethanol molecule in the temperature range 70-120°C indicates that it is held in the lattice while the loss of two ethanol molecules in the temperature range 120-160°C indicates that they are coordinated to the uranyl ion. The complex starts decomposing beyond 300°C and attains stability in weight after 550°C indicating the formation of U_3O_8. DTA curve shows that the complex decomposes in two distinct steps, losing two CH_3CO and two $-N_2HCOCH_2$ groups in the range 300-380°C and two phenyl rings in the range 380-550°C. Compared to acetato complex (No. 6), the nitrato complex (No. 5) gives no indication of its stability at any stage once the decomposition has commenced after loss of coordinated water molecules upto 250°C. The decomposition of the complex starts after 250°C and two exothermic peaks are observed in the temperature ranges 250-380 and 380-630°C. The TGA curve shows loss of weight corresponding to two and four water molecules in the temperature ranges 70-120°C and 120-250°C respectively. DTA curve shows one endothermic peak from 70 to 120°C and another between 120 and 250°C corresponding to lattice held and coordinated water molecules respectively. The complex decomposes above 250°C and shows maxima at 335 and 445°C in the ranges 250 to 380°C and 380 to 630°C which corresponds to loss of two nitro and two $-N_2HCOCH_2-$ groups and two phenyl groups, respectively.

The IR spectra of the ligands show bands due to amide I and $C=N$ stretching vibrations in the 1700-1600 cm^{-1} region. Recently, Paolucci, *et al.*[7] have reported the existence of tautomeric keto-enol phenomenon in the solid state in dihydrazones of pyridine dicarboxylic acid on the basis of the presence of two bands at ~ 1700 and 1685 cm^{-1} in their IR spectra. In the present study, we have observed only one band at 1666 cm^{-1} in the spectrum of H_4E_2 and at 1655 cm^{-1} in H_4F_2 while in the other ligands two bands at ~ 1674 and 1666 cm^{-1} are observed. The presence of bands in the 1674-1655 cm^{-1} region rules out the possibility of the existence of tautomeric keto-enol equilibria in ligands and suggests that the ligands exist primarily in the keto form. The positions of the bands indicate the involvement of intermolecular and intramolecular hydrogen bonding. The appearance of amide I band at as low position as 1655 cm^{-1} indicates that the hydrogen bonding is stronger in H_4F_2 than that in the other ligands which is also confirmed by the appearance of νOH and νNH bands at as low positions as 3149 cm^{-1}.

The amide I bands of the complexes 1, 3, 6 and 8 show a negative shift of 12-51 cm^{-1} and appear as medium to strong bands in the 1662-1621 cm^{-1} region indicating coordination of the ligand through $>C=O$ group to the uranyl ion. However, the IR spectra of the other complexes in the region 1700-1600 cm^{-1} are difficult to interpret due to weakening of amide I band and negative shift by about 50-60 cm^{-1} in $\nu C=O$ mode. As a result, amide I band either appears as a shoulder to the $\nu C=N$ band or merges with it. Similar observations have been made by Iskander *et al.*[6] in the copper(II) and nickel(II) complexes of some acyldihydrazone ligands. Such a negative shift and weakening of amide I band may be attributed to strong bonding between oxygen of carbonyl group and uranyl ion. The complexes show bands in the 1590-1500 cm^{-1} region which may be due to $\nu C-O$ and amide II modes. The bands in the region 1573-1552 cm^{-1} in the IR spectra of the ligands undergo splitting and suffer positive as well as negative shifts on complex formation and appear in the 1590-1564 cm^{-1} and 1550-1520 cm^{-1} regions respectively. The bands in the 1550-1520 cm^{-1} region are due to the negative shift of amide II band by 2-55 cm^{-1} and the coordination of $>C=O$ group to the uranyl ion suggesting the exist-

Table 2—Important Spectral Bands of Acyldihydrazones and Their Dioxouranium(VI) Complexes

S. No.	Ligand/Complex	$\nu C=O$	$\nu C=N$	Amide II + $\nu(C-O)$ (phenyl)	$\nu(C-O)$	Anion vibrations
	H_4A_2	1674s 1666s	1624s	1572s 1525s	1271s	—
	H_4B_2	1673s 1666s	1623s 1612s	1572s 1553s	1269s	—
	H_4C_2	1673s 1666s	1623s	1572s	1270s	—
	H_4D_2	1673s 1666s	1623s 1609s	1552s	1275s	—
	H_4E_2	1666s	1623s 1612s	1555s	1278s 1261m	—
	H_4F_2	1655s	1623s 1612s	1573s 1554s	1279s 1265s	—
1	$(UO_2)_2(H_2A_2)(NO_3)_2$ $6H_2O$	1662m	1603m	1564s 1542m	1305m 1261w	1384s, 821w, 1746w
2	$(UO_2)_2(H_2A_2)$ $(CH_3COO)_2 3C_2H_5OH$	—	1605s	1590s 1542s	1306m 1273w	1554s, 1411w
3	$(UO_2)_2(H_2B_2)(NO_3)_2$ $6H_2O$	1621s	1583s	1572s 1547s 1530s	1314m 1273m	1383s, 825w, 1709s
4	$(UO_2)_2(H_2B_2)$ $(CH_3COO)_2 3C_2H_5OH$	—	1605s	1564s 1537s	1307m	1547s, 1409m
5	$(UO_2)_2(H_2C_2)(NO_3)_2$ $6H_2O$	—	1601s	1550s	1283s	1384s, 853w, 1780w
6	$(UO_2)_2(H_2C_2)(NO_3)_2$ $(CH_3COO)_2 3C_2H_5OH$	1653m	1602s	1574m 1541w	11307w	1547m**, 1394m
7	$(UO_2)_2(H_2D_2)(NO_3)_2$ $6H_2O$	—	1602s	1688m 1550m	1283m	1384s, 825w, 1761w
8	$(UO_2)_2(H_2D_2)$ $(CH_3COO)_2 3C_2H_5OH$	1657m	1610s	1566s	1306m 1268m	1566s**, 1401m
9	$(UO_2)_2(H_2E_2)(NO_3)_2$ $6H_2O$	—	1602s	1566m 1550m	1282s	1384vs, 840w, 1767w
10	$(UO_2)_2(H_2E_2)$ $(CH_3COO)_2 3C_2H_5OH$	—	1606s	1564s 1542s	1305m	1564s**, 1395m
11	$(UO_2)_2(H_2F_2)(NO_3)_2$ $6H_2O$	—	1628s	1570s 1520m	1262m	1391vs, 826w*, 1702w
12	$(UO_2)_2(H_2F_2)$ $(CH_3COO)_2 3C_2H_5OH$	—	1631s	1569s	1262m	1569s**, 1391s

*Masks ligands bands; **overlaps with the C – O or amide II band of the ligand.

ence of the ligands in the keto form(I) in the complexes. The $\nu C-O$ band is present in the region 1590-1564 cm^{-1} signifying a positive shift by about 11-35 cm^{-1}. Such high shift of $\nu C-O$ band is considered diagnostic of binuclear or polynuclear complexes through oxobridging. The multiplicity of the $\nu C=N$ bands (1624-1609 cm^{-1}) exhibited in the IR spectra of the ligand is lost upon complexation. Further, they suffer negative shift by about 10-40 cm^{-1} in all the complexes except in those of H_4F_2 complexes. The negative shift of $\nu C=N$ band is attributed to a decrease in the π-bond character of the $>C=N$ group as a result of nitrogen to metal coordination.

However, the IR spectra of the phthalamido complexes show a positive shift in the $\nu C=N$ mode. This fact can be understood in terms of the drainage of the electron density, attributed to the replacement of methylene groups by phenyl group between two hydrazone units, from the phenyl ring of salicylaldimine group to the uranyl ion through the azine group nitrogen atom increasing carbon and nitrogen bond order as has been reported in thiosemicarbazonato complexes[12]. In other complexes the drainage of π-electron density occurs through oxygen atoms. From the above discussion, it is evident that the ligands act as dibasic hexadentate and bond to uranyl ion through phenolic oxygen, carbonyl oxygen and azine group nitrogen. On examining the spectra of the ligands and their complexes below 600 cm^{-1}, the new bands appearing in the ranges 590-497, 496-421 and 413-300

cm^{-1} are tentatively assigned to $\nu(U-O)$ (phenolic), $\nu(U-O)$ (carbonyl) and $\nu(U-N)$ respectively.

The IR spectra of all the uranyl complexes studied here show strong absorption in the region 938-907 cm^{-1} masking weak to medium ligand bands and weak to medium to strong absorption in the 871-851 cm^{-1} region respectively assigned to ν_3 and ν_1 vibrations of the uranyl group. In uranyl complexes $(UO_2)_2(H_2L_2)(NO_3)_2\,6H_2O$ and $(UO_2)_2(H_2L_2)(CH_3COO)_2\,3C_2H_5OH$ (where $H_4L_2 = H_4C_2$, H_4E_2) the assignment of ν_1 is a little doubtful as bands of weak to medium intensity occur in the IR spectra of the uncoordinated ligands also in the 864-853 cm^{-1} region. However, H_4F_2 complexes show a strong band at ~855 cm^{-1} which can not be assigned to ligand bands. The forbidden vibrations may become allowed as a result of particular symmetry of the ligand field around uranyl group in the complexes rather than slight bending of this group. The ν_3 band in some complexes (Table 2) is resolved into a doublet[7,13-15]. The Raman spectra of the complexes $(UO_2)_2(H_2A_2)(NO_3)_2\,6H_2O$ and $(UO_2)_2(H_2A_2)(CH_3COO)_2\,3C_2H_5OH$ in the range 1000-800 cm^{-1} show a strong band centred at 864 and 860 cm^{-1} respectively, but do not show band corresponding to ν_3. The doubly degenerate OUO bending mode is observed as a medium to strong band in the 245-212 cm^{-1} region and it masks the ligand bands occurring in this region.

The IR spectra of the acetato complexes show ν_sCOO mode in the region 1412-1391 cm^{-1} and ν_{as}COO mode at 1564-1547 cm^{-1}; but in some complexes the latter band is masked by either amide II or $\nu C-O$ band. The positions of the COO bands are in agreement with the bidentate coordination of acetato group with uranyl ion. Keeping in view the difference between the solubility, decomposition temperature (melting point) of the nitrato and acetato complexes and the separation (180-138 cm^{-1}) between ν_{as}COO and ν_sCOO modes, the bridging nature of the acetato groups is more probable in the present complexes[16]. The IR spectra of the nitrato complexes show a strong band in the region 1392-1384 cm^{-1} (masking ligand band) and a weak band in the region 853-821 cm^{-1} suggesting that nitrato group is present either in ionic or weakly coordinated form[18]. The IR spectra of the nitrato complexes in the region 1800-1700 cm^{-1} show combination bands (diagnostic of the type of nitrato group present). A single band attributable to $(\nu_1 + \nu_4)$ mode is observed which indicates that strong coordination by nitrato group is unlikely[17]. Considering the compositions of the complexes, their solubility behaviour in the common organic sovlents, high melting points/decomposition points, the dibasic hexadentate nature of the ligand and the presence of oxo and ligand bridging, both the nitrato and acetato dioxouranium(VI) complexes may tentatively be assigned oxo-bridged polymeric structures (V and VI) involving nine coordinate uranium atom.

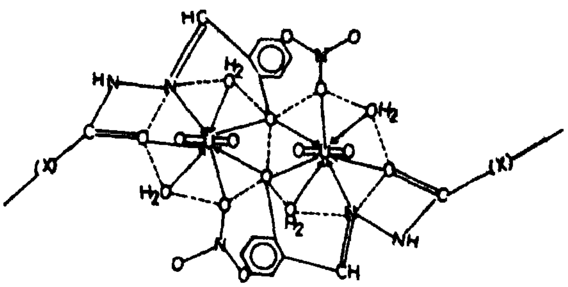

(V)

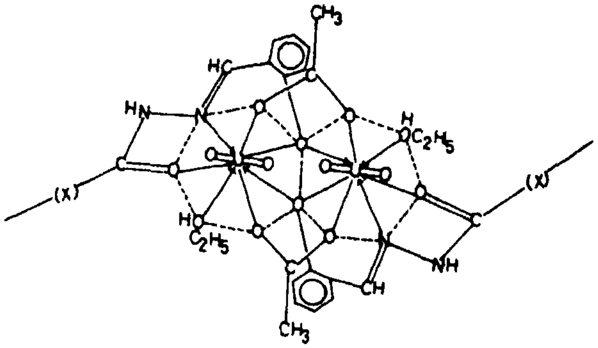

(VI)

References

1 Merchant J R & Chothia D S, *J mednl Chem*, **13** (1970) 335; Redda K, Coreto L A & Knans E E, *J mednl Chem*, **22** (1979) 1079.
2 Katyal M & Dutta Y, *Talanta*, **22** (1975) 151.
3 Nardelli M, Pelizzi C & Pelizzi G, *Transition Met Chem*, **2** (1977) 35; Pelizzi C, Pelizzi G & Predieri G, *J organoletal Chem*, **263** (1984) 9; Lorenzini C, Pelizzi C, Pelizzi G & Predieri G, *J chem Soc Dalton Trans*, (1983) 721; (1983) 2155; Aruffo A A, Murphy T, Johnson D K, Rose N & Schoemaker M F, *inorg chim Acta*, **67** (1982) L25.
4 Arora D L, Lal K, Gupta S P & Sahni S K, *Indian J Chem*, **24A** (1985) 980.
5 Narang K K & Lal R A, *Transition Met Chem*, **1** (1976) 260; **2** (1977) 100; **3** (1978) 272; *Curr Sci*, **46** (1977) 401; **47** (1978) 793.
6 El-Sayed L & Iskander M F, *J inorg nucl Chem*, **38** (1976) 2209.
7 Paolucci G, Stelluto S & Sitran S, *Inorg chim Acta*, **110** (1985) 19.
8 Lal R A, Srivastava K N & Das S, *Synth React inorg met-org Chem*, (Communicated); Lal R A, Das S & Thapa R K, *Inorg chim Acta*, (In press).
9 Vogel A I, *A text book of quantitative inorganic analysis*, (ELBS and Longmans, London), 1973.
10 Geary W J, *Coord Chem Rev*, **7** (1971) 81.
11 Livingstone S E & Oluka J E, *Transition Met Chem*, **3** (1978) 261; Saha N & Bhattacharya D, *Indian J Chem*, **21A** (1982) 574.
12 Saxena A & Tandon J P, *Polyhedron*, **3** (1984) 681.

13 Bullock J I, *J inorg nucl Chem*, **29** (1967) 2257.

14 Hornig D F, *J chem Phys*, **16** (1948) 1063; Flint C D & Tanner P A, *Polyhedron*, **2** (1968) 43.

15 Panattoni C, Graziano R, Croatto U, Zarli B, Bombieri G, *Inorg chim Acta*, **2** (1968) 623.

16 Long G J, Robinson W T, Toppmeyer W P & Bridges D L, *J chem Soc, Dalton Trans*, (1973) 573.

17 Curtis N F & Curtis Y M, *Inorg Chem*, **3** (1965) 804; Lever A B P, Mantovani E & Ramaswamy B S, *Can J Chem*, **49** (1976) 1957; Speca A N, Pytleeski L L, Owens C & Karayamis, *J inorg nucl Chem*, **38** (1976) 1119.

18 Ramakrishnan & Soundarajan S, *Mh Chem*, **107** (1976) 1095; Viçentini G & De Oliverra, *J inorg nucl Chem*, 37 (1975) 2018.

Indian Journal of Chemistry
Vol 27A, March 1988, pp 231-234

Mixed-Ligand Complexes of Fe(II) & Cu(II) with Alizarin Maroon as a Primary Ligand & 5-Sulphosalicylic Acid as a Secondary Ligand

M M SELEIM, K A IDRISS*, M S ABU-BAKR & M K HASSAN
Department of Chemistry, Faculty of Science, Assiut University, Assiut, Egypt

Received 9 *March* 1987; *revised* 22 *June* 1987; *accepted* 27 *July* 1987

Reactions of Fe(II) and Cu(II) with alizarin maroon (azm) as a primary ligand and 5-sulphosalicylic acid (ssa) as a secondary ligand have been studied spectrophotometrically and potentiometrically in 20% (v/v) ethanol and dioxane at an ionic strength $I = 100$ mmol dm^{-3} NaClO$_4$ and temperature $= 25 \pm 0.1$°C. Based on the spectrophotometric studies, a method for the determination of Fe(II) and Cu(II) is proposed. The stability constants of the mono and mixed ligand complexes of Fe(II) and Cu(II) have been evaluated. The difference in stability constants, $\Delta \log K_M = \log K^{M}_{M}{}^{(azm)}_{(azm)(ssa)} - \log K^{M}_{M\,(ssa)}$ is found to be positive showing an astatistical increase in the values of mixed ligand stability constants.

In continuation of our work on the complexation equilibria of mixed ligand complexes in solution[1,2], we report here the spectrophotometric and potentiometric study of the reaction of Fe(II) and Cu(II) with alizarin maroon (3-amino-1,2-dihydroxyanthraquinone) as a primary ligand and 5-sulphosalicylic acid as a secondary ligand. The *p*H-titration technique of Irving and Rossotti[3,4] and its modified form[5,6] were employed in the present study to determine the stability constants of the ternary complexes Fe(II)-azm-ssa and Cu(II)-azm-ssa. The measurements were carried out at 25 ± 0.1°C and at an ionic strength of 0.1 mol dm^{-3} (NaClO$_4$) in 20% (v/v) ethanol or dioxane. The absorption spectra of the mixed ligand complexes were also investigated. The fundamental conditions for the spectrophotometric determination of Fe(II) and Cu(II) complexes usign Fe(II)-azm-ssa and Cu(II)-azm-ssa ternary systems were established.

Materials and Methods

All the chemicals used were of AR grade. Dioxane was purified by recommended procedure[7]. A stock solution of azm (10^{-3} mol dm^{-3}) was prepared by dissolving an accurately weighed amount of the reagent in ethanol or dioxane. A solution of ssa (10^{-3} mol dm^{-3}) was prepared by dissolving the requisite amount of the pure reagent in deionised water. Fe(II) perchlorate was prepared from Fe(II) carbonate and perchloric acid. Cu(II) perchlorate was a Fluka reagent. The stock solutions of Fe(II) and Cu(II) (5×10^{-3} mol dm^{-3}) were prepared and standardised as recommended[8]. Standard solutions of NaOH (0.1 mol dm^{-3}) and HClO$_4$ (2.5×10^{-2} mol dm^{-3}) were prepared by accurate dilutions. Buffer solutions and solutions of diverse ions used for interference studies were prepared as mentioned elsewhere[9].

All *p*H-metric titrations were carried out at 25 ± 0.1°C using on Orion (M 501 A) digital *p*H-meter with a combined glass calomel electrode. The ionic strength of solutions was kept constant at 0.1 mol dm^{-3} (NaClO$_4$) All the measurements were carried out in 20% (v/v) ethanol or dioxane-water medium (20%, v/v), *p*H values were corrected for partially aqueous media as described previously[10]. The absorption spectra of solutions were recorded on a Pye-Unicam SP 8000 spectrophotometer in the range 350-750 nm using 1-cm mathed stoppered quartz cells.

Results and Discussion

Spectrophotometric studies

Recent work from this laboratory[11,12] on the acid-base properties of azm in aqueous solution or in water-ethanol (or dioxane) mixture indicated that the predominant form of this reagent within the *p*H range 3.0-6.0 is the monocationic species (H_3A^+) which undergoes stepwise ionisation on increasing the *p*H of the solution. The visible spectrum of azm exhibits an absorption band at $\lambda = 410$-420 nm in the *p*H range 3.5-6.0. This band shifts to longer wavelengths on adding the metal ion solutions. The spectra of Fe(II) and Cu(II)-azm 1:1 complexes measured with reagent blank as reference are characterised by an absorption band with λ_{max} near 620 and 630 nm respectively. The solution containing equimolar concentrations of azm and ssa undergoes a change in colour, from yellow to pink-violet when mixed with

Fe(II) or Cu(II) solution. The spectrum of the reaction mixture measured against a blank solution containing the same concentration of the two ligands shows an apparent decrease in the absorption at 410 nm and the appearence of a new band at 580 nm for Fe(II) and 540 nm for Cu(II) ternary system. This band is unambiguously due to the formation of a mixed-ligand complex of the metal ion with maximum colour development being attained at *p*H 5.8 for Fe(II) and at 5.4 for Cu(II) ternary systems.

Stoichiometry of the complexes

Job's method of continuous variation[13,14] was applied to find out the composition of the ternary complexes. The results indicate that the overall ratio of metal ion:azm:ssa is 1:1:1. The stoichiometric ratio of the complexes was also confirmed by applying the mole ratio method[15].

The reaction of Fe(II) or Cu(II) with azm and ssa can be represented by Eqs,

$$M^{2+} + H_3A^{+} \rightleftharpoons [M(HA)]^{+} + 2H^{+}$$

$$[M(HA)]^{+} + H_2L^{-} \rightleftharpoons [M(HA)L]^{2-} + 2H^{+}$$

where H_2L^{-} is the mononegative charged species of the secondary ligand.

Table 1—Validity of Beer's Law

Metal ion	Metal ion per 25 ml (μg)	Metal ion (ppm) in the final conc.	Molar Absorptivity
	20% (v/v) Ethanol		
Fe(II)	5.0-40.0	0.20-1.60	10,000
Cu(II)	20.0-60.0	0.80-2.40	7,500
	20% (v/v) Dioxane		
Fe(II)	15.0-70.0	0.60-2.80	12,000
Cu(II)	10.0-45.0	0.40-1.80	7,000

Spectrophotometric determination of Fe(II) and Cu(II)

An aliquot of the test sample containing 5-70 μg of Fe(II) or 10-60 μg of Cu(II) was transferred to a 25 ml calibrated flask and subsequently azm (5 ml, 10^{-3} mol dm^{-3}) added. The *p*H was adjusted to 5.8 for Fe(II) and 5.4 for Cu(II) and ssa (5 ml, 10^{-3} mol dm^{-3}) was added. The solution was diluted to the required volume with deionized water and the required amount of ethanol or dioxane. After thoroughly mixing the reaction mixture, the absorbance was measured at 580 nm for Fe(II) and 540 nm for Cu(II) against a reagent blank similarly prepared but containing no metal ion.

Effect of masking agents and foreign ions

The addition of EDTA as a masking agent causes an apparent decrease in the absorbance values and consequently could not be used. On the other hand, addition of fluoride ions as a masking agent upto 200-fold molar excess over Fe(II) or Cu(II) had no effect on the sensitivity of the proposed method. The effect of diverse ions at levels of 1-14 mg per 25 ml on the determination of metal ions was examined by the recommended procedure. There was no interference from 14 mg (200-

Table 2—Negative Logarithms of Acidity Constants of the Ligands and Logarithms of the Stability Constants of Their Binary Complexes with Fe(II) and Cu(II)

[Ionic strength = 0.1 mol dm^{-3} NaClO$_4$; temp. = 25°C]

	$pK^{H}_{H_2L}$	pK^{H}_{HL}	M(II)	$\log K^{M}_{ML}$	$\log K^{ML}_{ML_2}$	$\log \beta^{M}_{ML_2}$
			20% (v/v) Ethanol			
azm†	9.10	11.20*	Fe(II)	6.20	5.05	11.25
			Cu(II)	5.20	4.56	9.76
ssa	3.10	12.60	Fe(II)	5.10	4.70	9.80
			Cu(II)	4.96	4.57	9.53
			20% (v/v) Dioxane			
azm††	9.50	11.50*	Fe(II)	6.40	5.40	11.80
			Cu(II)	5.49	4.59	10.08
ssa	2.90	11.40	Fe(II)	5.85	5.50	11.35
			Cu(II)	5.15	4.38	9.63

†$pK^{H}_{H_3L^{+}} = 6.75$

††$pK^{H}_{H_3L^{+}} = 7.55$

*Ref. 11.

Table 3—Logarithms of the Equilibrium Constants of the Ternary M-azm-ssa Systems and Some Related Data

[Ionic strength = 0.1 mol dm^{-3} NaClO$_4$; temp. = 25°C]

Metal ion	$\log\beta^{M}_{M(azm)(ssa)}$	$\log K^{M(azm)}_{M(azm)(ssa)}$	$\log K^{M(ssa)}_{M(ssa)(azm)}$	$\Delta\log K$	$\log X$
		20% (v/v) Ethanol			
Fe(II)	11.75	5.55	6.65	0.75	2.45
Cu(II)	10.80	5.60	5.84	0.64	2.21
		20% (v/v) Dioxane			
Fe(II)	13.10	6.70	7.25	0.85	3.05
Cu(II)	11.33	5.84	6.18	0.69	2.95

fold excess) of Li$^+$, Na$^+$, Ba^{2+}, Cl^{-1}, I$^-$, NO$_3^-$ and SO$_4^{2-}$ or 8 mg (100 fold excess) of Mg^{2+}, Ca^{2+}, Al^{3+}, Br$^-$, CO$_3^{2-}$, SO$_3^{2-}$ and HPO$_4^{2-}$. Among the anions investigated, CN$^-$ causes a serious negative error even when present in only ~ 20-fold excess.

The validity of Beer's law was examined. Calibration graphs obtained were linear over the range 1×10^{-5}-1×10^{-4} mol dm^{-3} of Fe(II) or Cu(II). The moalr absorptivities of the ternary systems are given in Table 1. Ten identical samples each with a final metal ion concentration of 1×10^{-5} mol dm^{-3} were tested according to the recommended procedure and their absorbances were measured. The relative standard deviation was found to be less than 0.004 absorbance unit.

Potentiometric studies

The proton-association constant $pK^{H}_{H_2A}$, and the dissociation constant $pK^{H}_{H_2A}$ of azm in ethanol-water and dioxane-water medium (20%, v/v) were determined using Irving-Rossotti pH-titration technique[3,4] (Table 2). The details regarding the potentiometric method have been reported earlier[12]. The values of the dissociation constants of 5-sulphosalicylic acid (ssa) were also determined potentiometrically under the same experimental conditions. The metal-ligand titration curves exhibit two inflections at $m = 2$ and $m = 4$ (m = nol of base added per mol of metal ion) indicating the formation of [M(HA)]$^+$ and [M(HA)$_2$] binary complexes.

The formation constants corresponding to the equilibria (1 and 2) were calculated and the values are given in Table 2.

$$M + 2\,azm \rightleftharpoons M(azm)_2 \quad \beta^{M}_{M(azm)_2} \qquad \ldots(1)$$

$$M + 2\,ssa \rightleftharpoons M(ssa)_2 \quad \beta^{M}_{M(ssa)_2} \qquad \ldots(2)$$

Potentiometric titration curves for ternary systems containing M(II)-azm and ssa exhibit two inflections at $m = 3$ and $m = 4$. The divergence of mixed ligand curves from binary curves indicates that the deprotonation of azm or ssa in the ternary systems occurs at a lower pH. This means that the ternary complexes are more stable than the corresponding binary systems. The values of the formation constant of the general equilibrium

$$M + azm + ssa \rightleftharpoons M(azm)(ssa) \quad \beta^{M}_{M(azm)(ssa)} \qquad \ldots(3)$$

are given in Table 3.

One way to quantify the stability of ternary complexes is according to equation (4)[16], i.e., by comparing the differences in stability, e.g., for the reaction between M(ssa) and (azm).

$$\begin{aligned}\Delta\log K_M &= \log K^{M(ssa)}_{M(ssa)(azm)} - \log K^{M}_{M(azm)}\\ &= \log K^{M(azm)}_{M(azm)(ssa)} - \log K^{M}_{M(ssa)} \qquad \ldots(4)\end{aligned}$$

The other approach commonly used to quantify the stability of a ternary complex is based on the equilibrium constant, X, as defined by equation (5)[17,18]; $\log X$ may be calculated according to Eq. (6).

$$X = M(azm)(ssa)]^2/[M(azm)_2][M(ssa)_2] \qquad \ldots(5)$$

$$\begin{aligned}\log X = {} & 2\log\beta^{M}_{M(ssa)(azm)}\\ & -\left(\log\beta^{M}_{M(azm)_2} + \log\beta^{M}_{M(ssa)_2}\right)\\ & = \left(\log K^{M(azm)}_{M(azm)(ssa)} - \log K^{M(ssa)}_{M(ssa)_2}\right)\\ & + \left(\log K^{M(ssa)}_{M(ssa)(azm)} - \log K^{M(azm)}_{M(azm)_2}\right)\end{aligned} \qquad \ldots(6)$$

The calculated values of log X are listed in Table 3. The values obtained show an astatistical increase in the stability of the mixed ligand complexes (logX_{stat} = 0.6)[18,19].

The higher stability of the complexes formed in dioxane (20%, v/v) may be due to the fact that the protonation and the stability constant values are more sensitivie to the dielectric constant of the medium. In dioxane-water mixtures of low dielectric constant, these values were expected to be significantly higher than those for the aqueous-ethanol medium. This may also be ascribed to the predominant basic property of dioxane[20].

The higher stability of Fe(II) chelates may be due to the resonance stabilisation energy derived through the coordination with ligands having aromatic ring system[21].

References

1 Idriss K A, Seleim M M, Hassan M K, Abu-Bakr M S & Sedaira H, *Analyst*, **110** (1985) 705.

2 Idriss K A, Seleim M M, Saleh M S & Hashem E Y, *Polyhedron*, **5** (1986) 1525.

3 Irving H M & Rossotti H S, *J chem Soc*, (1953) 3397.

4 Irving H M & Rossotti H S, *J chem Soc*, (1954) 2904.

5 Chidambaram M V & Bhattacharya P K, *J inorg nucl Chem*, **32** (1970) 3271.

6 Chidambaram M V & Bhattacharya P K, *Indian J Chem*, **9** (1971) 1294.

7 Vogel A I, *A text book of practical organic chemistry* (Longmans Green, London) 1956, 177.

8 Scott W & Furman, *Standard methods of chemical analysis*, 6th Edn (Van Nostrand, New York) 1962.

9 Idriss K A, Seleim M M, Abu-Bakr M S & Saleh M S, *Analyst*, **107** (1982) 12.

10 Douheret G, *Bull Soc Chim Fr*, (1967) 1412.

11 Idriss K A, Awad A M, Seleim M M & Abu-Bakr M S, *Bull Soc Chim Fr*, (1981) 180.

12 Idriss K A, Seleim M M, Abu-Bakr M S & Saleh M S, *Indian J Chem*, **21A** (1982) 395.

13 Job P, *Ann Chim (Rome)*, **10** (1928) 113.

14 Sharif F G & Awad A M, *J inorg nucl Chem*, **24** (1962) 79.

15 Yoe G H & Jones A L, *Ind Engng Chem, Anal Ed*, **16** (1944) 111.

16 Fischer B E & Siegl H, *Inorg Chem*, **18** (1979) 425.

17 Martin R B & Prados R, *J inorg nucl Chem*, **36** (1974) 1665.

18 Dewit R & Watters J J, *J Am chem Soc*, **76** (1954) 3810.

19 Kida S, *Bull chem Soc Japan*, **29** (1958) 805.

20 Sahai R, Agrawal & Kushwaha S S S, *J Indian chem Soc*, **59** (1982) 1121.

21 Irving H & Williams R J P, *J chem Soc*, (1983) 3206.

Indian Journal of Chemistry
Vol. 27A, March 1988, pp. 235-236

Notes

Internal Pressure & Free Volume of Potassium Chloride Solutions in Water-Dimethylformamide Mixtures

S O PILLAI* & S NATARAJAN
Department of Physics, Anna University, Madras 600025

Received 18 *May* 1987; *revised* 8 *July, accepted* 6 *August* 1987

Internal pressure and free volume have been calculated for potassium chloride solutions in water-DMF mixtures from ultrasonic velocity measurements at different concentrations and temperatures. For any given solution, at a given concentration, variation of internal pressure and free volume obeys the equation $\pi_i V_f^{*} = K$ in conformity with the results reported by Suryanarayana and Kuppusami [*J Accous Soc India*, **8** (1980) 29; **9** (1981) 6].

Whatever be the model chosen for the liquid state, the cohesive forces are of primary importance. Though the origin of these cohesive forces is known, all theories of liquids have failed to assess correctly these forces in totality in a simple and elegant way. However, one can estimate their magnitude from thermodynamic considerations. Such an estimate is provided by the internal pressure. In this note we have estimated the internal pressure and free volume of solutions of potassium chloride in DMF-water mixtures.

Dimethylformamide (Baker analysed) after drying over anhydrous potassium carbonate (24 hr), was purified by vacuum distillation over CaO. Doubly distilled water was used in the preparation of potassium chloride solutions.

Solutions of KCl at different concentrations in DMF-water (20:80 v/v) are prepared on molal scale. Solutions were also prepared in DMF-water (40:60 v/v).

Measurement of ultrasonic velocity

Ultrasonic interferometer, model M-77 (Mittal Enterprises, New Delhi) was used for measuring ultrasonic velocities of solutions of KCl at different temperatures: 30°, 35°, 40° and 45° ± 0.05°C.

Density

The densities of the solutions were measured at these temperatures using a specific gravity bottle of 20ml capacity.

Viscosity

The viscosities of the solutions at these temperatures were obtained using Oswald's viscometer.

Calculation of free volume and internal pressure of KCl solutions

Having measured the required parameters u, ρ and η of the solutions, the free volume, V_f and the internal pressure (π_i) were computed from Eqs (1) and (2) respectively[2,3].

$$V_f = \left[\frac{uM_{eff}}{K\eta}\right]^{3/2} \qquad \ldots (1)$$

$$\pi_i = \alpha RT\left[\frac{K\eta}{u}\right]^{1/2} \frac{\rho^{2/3}}{M_{eff}^{7/6}} \qquad \ldots (2)$$

where ρ = density, u = ultrasonic velocity, η = viscosity, M_{eff} = effective molecular weight of the me-

Table 1—Free Volume and Internal Pressure of Potassium Chloride Solutions in 20% and 40% DMF-Water Mixtures

KCl (m)	$V_f \times 10^2$ ml				π_i (atm)			
	30°	35°	40°	45°	30°	35°	40°	45°
				DMF-Water (20:80%)				
0	1.682	2.089	2.444	2.892	25513	24112	23212	22259
0.25	1.654	2.059	2.441	2.942	25649	24194	23191	22086
0.50	1.782	2.203	2.546	3.036	24992	23625	22843	21846
0.75	1.893	2.290	2.680	3.198	24454	23298	22426	21443
1.0	1.811	2.239	2.590	3.055	24776	23444	22646	21779
				DMF-Water (40:60%)				
0	1.378	1.742	2.096	2.530	23946	22468	21406	20385
0.25	1.338	1.678	2.004	2.402	24174	22740	21725	20735
0.50	1.389	1.765	2.074	2.514	23869	22355	21467	20408
0.75	1.388	1.759	2.114	2.553	23848	22322	21314	20293
1.0	1.429	1.803	2.113	2.544	23604	22159	21243	20298

Table 2—Values of Arbitrary Constants *a*, *b*, *c* and *d* of Eqs (3) and (4)

KCl (*m*)	$a \times 10^{-5}$	$b \times 10^3$	$c \times 10^{10}$	$d \times 10^3$
		DMF-Water (20:80%)		
0.25	5.262	9.971	1.463	38.392
0.50	3.785	8.785	3.769	35.522
0.75	3.476	8.760	4.746	34.957
1.0	2.785	7.986	3.545	32.641
		DMF-Water (40:60%)		
0.25	5.364	10.230	0.979	39.008
0.50	5.651	10.444	0.861	39.553
0.75	6.217	10.762	0.589	40.627
1.0	4.794	10.060	1.246	38.451

dium given by $\Sigma M_i x_i$ where M_i and x_i are the molecular weight and the molfraction of the individual constituents, respectively and α, the packing factor in liquids being equal to 2 for cubic packing. The experimental errors in the determination of V_f and π_i were respectively ± 0.15% and 0.5%.

The values of V_f and π_i for KCl solutions in 20% and 40% (v/v) DMF-water mixtures are given in Table 1. It is observed that in pure aqueous solutions[4] both potassium and chloride ions are contributing to a fall in the internal pressure while in the case of DMF-water mixtures with a progressive increase in DMF content more and more K^+ ions are solvated heavily and only anions are left comparatively less solvated. Hence, though there is, in general, a trend of progressive fall in internal pressure with the increase in KCl concentration, a progressive increase in DMF immobilises the effect of K^+ ions and what is observed is only due to the concentration of chloride ions.

At all the concentrations of KCl, increase in temperature decreases the internal pressure and increases the free volume[5]. The plots of both V_f and π_i versus temperature are slightly non-linear, but the trend is the same in all the cases.

The variations of internal pressure and free volume with temperature at any given concentration can be expressed by Eqs (3) and (4) respectively.

$$\pi_i = a \exp(-bT) \qquad \ldots (3)$$

$$V_f = c \exp(dT) \qquad \ldots (4)$$

where *a*, *b*, *c* and *d* are arbitrary constants dependent on concentration (Table 2).

The plots of $\log \pi_i$ versus $\log V_f$ for given concentrations at different temperatures are linear and parallel satisfying the linear Eq. (5) propased by Suryanarayana and co-workers[4,5],

$$\pi_i V_f^x = K \qquad \ldots (5)$$

In Eq (5) *K* is a constant and x_{rms} value is computed to be 0.256 ± 0.007 and K_{rms} value is 1454 ± 185. *K*-values vary considerably between 20% DMF and 40% DMF and do not have much of a significance, in conformity with the results reported by Suryanarayana and Kuppusami[4,5]. *x* was found to be 0.288 in aqueous solutions.

The authors thank Prof C V Suryanarayana, Emeritus Scientist, Alagappa College of Technology, Anna University, Madras for useful discussions.

References

1 Suryanarayana C V, *J Acoust Soc India*, **5(4)** (1977) 111.

2 Suryanarayana C V & Kuppusamy J, *J Acoust Soc India*, **4(3)** (1976) 75.

3 Samuel Glasstone, *Theoretical chemistry*, (Van Nostrand, New York) 1944.

4 Suryanarayana C V & Kuppusamy J, *J Acoust Soc India*, **9(1)** (1981) 4.

5 Dhanalakshmi A, *J Acousl Soc India*, **8** (1980) 29.

Indian Journal of Chemistry
Vol. 27A, March 1988, pp. 237-239

Absorption & Fluorescence Spectra of Phenosafranin in Aqueous Solutions in Presence of Alkylamines

BENOY B BHOWMIK* & SHARMILA ROY
Physical Chemistry Laboratory, Jadavpur University,
Calcutta 700032

Received 8 *May* 1987; *revised and accepted* 3 *August* 1987

While the absorption spectra of phenosafranin (PFS) in aqueous solutions are not appreciably perturbed in the presence of alkylamines, indicating no molecular interaction between PSF and amines, the fluorescence of PSF is quenched in the presence of all the alkylamines studied. The Stern-Volmer constants (K_{sv}) for fluorescence quenching are correlated with the ionization potentials of the amines. The results have been interpreted in terms of charge-transfer interaction between PSF as an electron acceptor and the alkylamines as electron donors.

Photovoltage generation in systems consisting of phenosafranin (PSF) and a series of alkylamines in aqueous solution increases with decreasing ionization potentials of the amines confirming the charge-transfer (CT) interaction between PSF and amine in one of the intermediate steps[1]. One of the mechanistic steps in the photovoltage generation of PSF-EDTA system involves CT interaction between PSF (electron acceptor) and EDTA (electron donor) and this has been confirmed spectrophotometrically[2]. The CT interaction of amines as electron donors with some dyes such as methylene blue, thionine and toluidine blue has been reported[3,4]. The fluorescence quenching of acridine dye by amines in aqueous solutions[5] and of acridine orange[6] by N,N-dimethylaniline, nitrobenzene, *s*-trinitrobenzene and tetracyanoethylene has been reported and explained in terms of exciplex formation[5] and CT interaction, respectively.

To confirm the possible molecular interactions between PSF and alkylamines, presently the absorption and fluorescence spectra of PSF have been studied in aqueous solution containing different alkylamines and the results are reported here.

Phenosafranin (PSF) (Sigma Chemicals, USA) was purified chromatographically, recrystallized from ethanol-water and its purity checked. All the alkylamines used (BDH/E Merck/Fluka) were of AR grade and were fractionally distilled before use.

Absorption spectra were recorded on a Perkin-Elmer model 200 spectrophotometer with a pair of matched silica cells of 1 cm optical pathlength. Fluorescence spectra were recorded on a Perkin-Elmer MPF-44B spectrofluorimeter (excited at 520 nm, the absorption maximum of PSF dye in aqueous solution) with automatic recorder using silica cell of 1 cm optical pathlength. The photomultiplier tube (model R 446F of Hamamatsu Corporation, Japan) was sensitive to both the red and blue regions of the visible spectrum. All measurements were done with freshly prepared solutions.

The UV-visible spectra of PSF in aqueous solution are slightly perturbed in the presence of alkylamines with a little shift in the absorption maximum. There is no specific interaction between PSF and amines as the spectrophotometric data do not yield any equilibrium between them. Therefore, the marginal change of absorption spectra of PSF in presence of amines can only be explained on the basis of medium effect, i.e, the change of refractive index of solution.

Figure 1 shows the fluorescence spectra of PSF in aqueous solution containing different concentrations of triethylamine. The fluorescence spectra of PSF in the presence of other alkylamines are similar except for the variation of fluorescence intensity quenching. By measuring the decrease in relative quantum yield of PSF (excited at 520 nm) at varying concentrations of the amines, the Stern-Volmer quenching constant, K_{sv} has been calculated using the relation[7] (1).

$$\frac{\phi_f^0}{\phi_f} = 1 + K_{sv}\,[\text{Amine}] \qquad \ldots(1)$$

where ϕ_f^0 and ϕ_f are the relative quantum yields of fluorescence of PSF alone and in the presence of amine respectively. The plots of ϕ_f^0/ϕ_f against [amine] are linear in all cases with unit intercept, and from the slope, K_{sv} values have been calculated. The values are: 1.88, 2.07, 2.11, 2.19, 2.67, 3.20, 3.56, 3.89 and 4-.56 $mol^{-1}dm^3$ for ethylamine, *n*-butylamine, *s*-butylamine, *t*-butylamine, dimethylamine, diethylamine, trimethylamine, triethanolamine and triethylamine respectively. According to the electron transfer mechanism for

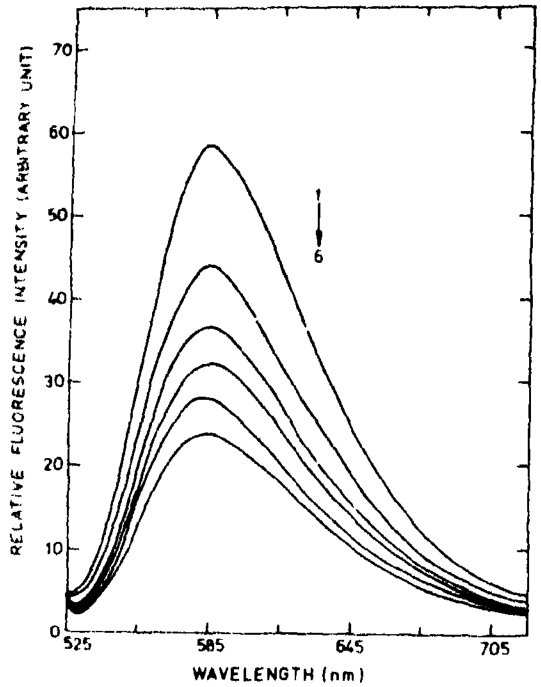

Fig. 1 – Fluorescence spectra of PSF in aqueous solution containing different concentrations of triethylamine at 25°C. [PSF] = (1.17×10^{-5} mol dm^{-3}); and [Triethylamine] mol dm^{-3}); (1) 0.00, (2) 1.0×10^{-1}, (3) 2.0×10^{-1}, (4) 3.0×10^{-1} (5) 4.0×10^{-1}, and (6) 5.0×10^{-1}).

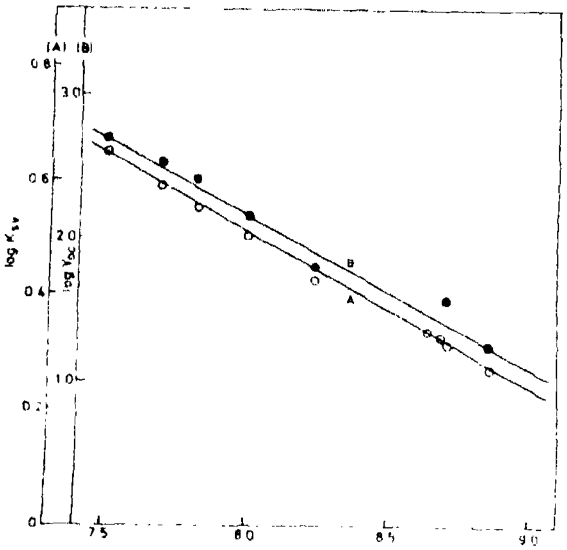

Fig. 2 – (A) Plot of log K_{sv} versus ionization potentials of the amines and (B) plot of log V_{oc} versus ionization potentials of the amines (V_{oc} values taken from literature[1]).

quenching[8] we should expect that a fluorescer which is an electron acceptor, is quenched by an electron donor or vice versa and that the quenching constant should increase with decreasing ionization potential of the electron donating quencher when a same fluorescer is quenched by different electron donor quenchers. The results presented herein are consistent with this electron transfer or CT mechanism of quenching. A good correlation between log K_{sv} versus ionization potentials of the amines is shown in Fig. 2 (IP of amine were taken from literature[9]).

The generation of photovoltage in PSF-amine systems also supports the CT interaction between excited PSF and amine molecule[2] as an intermediate step before photochemical change occurs for photovoltage generation. Hence open-circuit photovoltage (V_{oc}) of these systems is expected to increase with decrease in ionization potential of the amine (V_{oc} values were taken from literature[1]). This is found to be so (Fig. 2). The possible mechanism for the quenching of PSF by amine in aqueous solution may be represented as shown in Scheme 1.

$$D + h\nu \rightarrow D^{*}$$

$$D^{*} \rightarrow D + h\nu_{f}$$

$$D^{*} \rightarrow D + \text{heat}$$

$$D^{*} + NR_3 \rightleftharpoons (D \ldots NR_3^{+}) \rightleftharpoons (D^{-} \ldots N\overset{+}{R}_3) \rightarrow D + NR_3$$

Scheme 1

where D represents PSF dye, R represents alkyl or hydrogen and ($D^{-} \ldots NR_3^{+}$) represents exciplex (CT complex in excited state). The K_{sv} values have been measured at comparatively higher concentrations of amines and no curvature is obtained in the Stern-Volmer plots, thus ruling out ground state complex formation[10] in these systems, which is further verified by absorption spectra. Thus, the present spectral studies of PSF-amine systems show a good correlation with the photogalvanic effects of these systems in photoelectrochemical cells[1].

Financial assistance and maintenance grant by the CSIR, New Delhi to one of the authors (SR) is gratefully acknowledged.

References

1 Bhowmik B B & Roy S, *Energy*, **12** (1987) 519.
2 Rohatgi-Mukherjee K K, Bagchi M & Bhowmik B B, *Indian J Chem*, **25A** (1985) 1002.
3 Murthy A S N & Bharadwaj A P, *Proc Indian Acad Sci (Chem Sci)*, **89** (1980) 463.
4 Murthy A S N & Bharadwaj A P, *J chem Soc Farad Trans II*, **78** (1982) 1811.

5 Rohatgi-Mukherjee K K, *Fundamentals of photochemistry*, (Wiley Eastern, India) 1978 pp 193.

6 Komiyama T, Miwa T & Koizuimi M, *Bull chem Soc Japan*, **39** (1966) 2597.

7 Stern O & Volmer M, *Physik Z*, **20** (1919) 183.

8 Leonhardt H & Weller A, *Z phys Chem* (*Nouv Folge*), **29** (1961) 277;

9 (a) Watanabe K, Nakayama T & Mottl J, *J Quant Radiat Transfer*, **2** (1962) 369.

(b) *Hand book of chemistry and physics*, edited by R C Weast, (The Chemical Rubber, Cleveland, Ohio), 1971-72, pp E 62.

10 Encinas M V, Rubio M A & Lissi E A, *J Photochem*, **18** (1982) 137.

Indian Journal of Chemistry
Vol. 27A, March 1988, pp. 240-241

Electronic Spectra & Ionisation Equilibria of Thymol

MANNAM KRISHNAMURTHY
Department of Chemistry, Andhra University, P.G. Extension Centre, Nuzvid 521 201
and
SNEH K DOGRA*
Department of Chemistry, Indian Institute of Technology, Kanpur 208 016

Received 12 *May* 1987; *revised and accepted* 13 *July* 1987

Electronic absorption and fluorescence spectra of thymol in different solvents indicate that thymol in S_0 and S_1 states acts as a proton donor in solvents having proton accepting ability. Both anion and cation of thymol are non-fluorescent at room temperature. Thymol cation becomes very basic upon excitation.

Table 1—Electronic Spectral Data of Thymol at 298 K

Solvent	λ_a, nm (log ε)*		λ_f, nm (ϕ_f)
Cyclohexane	282 (3.22)	216 (3.73)	289 (0.14)
	274 (3.23)	202 (4.10)	
	267 sh		
Ether	283 (3.35)	217 (3.73)	293 (0.21)
	273 (3.37)		
Acetonitrile	284 (3.37)	217 (3.86)	295 (0.18)
	273 (3.38)		
Methanol	284 (3.37)	218 (3.85)	298 (0.20)
	274 (3.39)	204 (4.37)	
Water (*pH* 7)	285 (3.30)	218 sh	300 (0.19)
	273 (3.32)	201 (4.87)	
Water (*pH* 12)	291 (3.58)	240 (3.87)	non-fluorescent
		210 (4.24)	
H_2SO_4 (H_0 −7)	340 (3.31)	231 sh	non-fluorescent
	328 (3.32)	211 (4.39)	

*Molar absorptivity (ε) in $dm^3 \ mol^{-1} \ cm^{-1}$.

Thymol[5-methyl-2-(1-isopropyl)phenol], an anthelmintic and antiseptic compound[1], is an integral part of the well known acid-base indicator, thymolphthalene. It has been found that in S_0 state, phenols[2] and aromatic phenolic compounds act as proton acceptors as well as proton donors, depending upon the nature of solvents, but in the S_1 state these behave as proton donors. This is because charge migrates from the OH group to the aromatic ring, thereby rendering the hydroxyl proton more labile and phenolic compounds more acidic in S_1 state. The title investigation is in continuation of our earlier work on photoluminescence and prototropic behaviour of phenol-like compounds[3-5]. In addition, the proton transfer nature of thymol is verified by studying its electronic spectra in different sovlents. Usefulness of thymol as an acid-base fluorescent indicator has also been studied.

Thymol (Aldrich Chemicals, USA) was recrystallised from methanol. Other solvents were purified before use. Calculations were made as reported in a recent papers[3].

The absorption maxima (λ_a), molar absorptivities (ε), fluorescence maxima (λ_f) and quantum yields (ϕ_f) of thymol in different solvents are listed in Table 1. The absorption spectrum in cyclohexane is nicely structured and with increasing solvent polarity the fine structure is lost. In cyclohexane, the vibronic structure can be explained by a vibrational frequency of $\sim 10^3$ cm^{-1}. This is further consistent with the earlier findings that the vibrational frequency of this magnitude is observed in benzene and naphthalene, but in condensed ring systems with three or more rings, the vibrational frequency is of the order of 1.4×10^3 cm^{-1}. With increase in polarity and H-bonding ability of the solvent, a small red shift is observed in the long wavelength absorption maximum of thymol. The loss in the fine structure is due to the interaction of solvents, the latter will be predominant in solvents of high polarity. The dispersive forces between the solute and the solvent as well as the proton donor ability of thymol can be accounted for by the small red shift in the absorption spectrum from non-interacting solvent, cyclohexane to more polar solvent, water. In comparison to the absorption maximum of phenol (270 nm[6]) in aqueous solutions, the one of thymol is red shifted by 3 nm, indicating the possible mesomeric effect from the methyl and the isopropyl groups.

The fluorescence maximum of thymol from cyclohexane to water is red shifted by 11 nm, indicating that thymol acts as a proton donor in S_1 state. This is consistent with the literature that charge migration takes place from OH group to the ring. However, in contrast to the absorption maximum of thymol, the fluorescence maximum is slightly blue-shifted by 2-10 nm as compared to those of phenol and cresols[7,8]. This may be explained as follows: The methyl or the isopropyl group is an electron donating and due to mesomeric effect, these can lower the energy of S_1 state, if present individually. The methyl group at position-5 is *meta* to the −OH group and thus does not offer greater interaction[6], whereas, the isopropyl group is *ortho* to the $-OH$ group but *para* to the methyl group. Thus it may happen that charge cloud interaction of the methyl and isopropyl groups may cancel each other and the net effect may be either negligible or very small. The fluorescence spectral results support this. Moreover, due to steric hindrance by the bulky isopropyl group, the OH group may not be in the same plane as benzene ring and may slightly be rotated. This minimises the interaction of the lone pair on OH group with the benzene ring. The near constancy of the fluorescence quantum yields in various solvents also support the above point.

The effect of acidity on spectral characteristics of thymol in aqueous solutions is studied from H_0-10 to *p*H 14. The constancy of absorption maximum of thymol from H_0 -4 to *p*H 8 is attributed to the neutral species. The red shift in absorption maximum in basic solutions is due to the dissociation of the $-OH$ group, leading to the formation of anion. In acidic solutions with H_0 more negative than -6, the absorption maximum is largely red-shifted. Such large shifts are not uncommon if the protonation is on the ring carbon atom of aromatics[9,10].

The fluorescence intensity of the neutral species of thymol is almost constant between *p*H 1 and 7 and keeps on decreasing on either side. This could be due to the formation of a non-fluorescent anion and cation in basic and in acidic solutions respectively, as has been observed in early works[1,9,11]. On the basis of the above observations prototropic equilibria of thymol can be given as shown in Scheme 1.

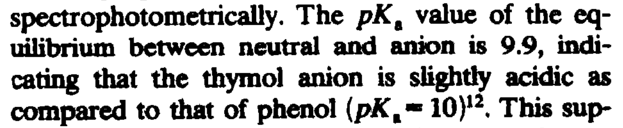

Scheme 1

The pK_a values in the S_0 state are calculated spectrophotometrically. The pK_a value of the equilibrium between neutral and anion is 9.9, indicating that the thymol anion is slightly acidic as compared to that of phenol ($pK_a = 10$)[12]. This supports the view that the two alkyl groups do not change the charge density at the $-OH$ group. The pK_a for thymol cation is found to be -5.1, indicating that thymol is more basic than benzene and toluene (pK_a values are -10.2 and -6.8, respectively[10]). The pK_a values in the S_1 state are derived from the fluorimetric titration and also using Förster cycle method[13] and absorption maxima. Fluorimetric titration could give only the S_0 state pK_a (9.9) for the equilibrium between neutral thymol and its anion [spectrophotometric pK_a $(S_0) = 9.9$]. This is due to the fact that the equilibrium is not established in the S_1 state, because of the shorter lifetimes of the conjugate acid-base species. However, the pK_a (S_1) value of 8.4 obtained by Försters method indicates that the phenol becomes more acidic upon excitation in agreement with earlier results[8]. Though there is no good agreement of the pK_a (S_1) values, for the equilibrium between cation and neutral, obtained by the two methods (0.0 by fluorimetric titration and 6.8 by Förster cycle method) these results do indicate that thymol becomes very basic upon excitation, owing to the redistribution of the electronic charge density of the ring upon excitation.

We are thankful to the Department of Science and Technology, Govt of India, for financial support.

References

1 *The Merck Index*, edited by M Windholz (Merck & Co, Rahway, New Jersey) 1976, pp. 1214.

2 Ireland J F & Wyatt P A H, *Advances in physical organic chemistry*, Vol. 12, edited by V Gold & D Sathell, (Academic Press, New York) 1976, pp. 162.

3 Krishnamurthy M & Dogra S K, *J Photochem*, **32** (1986) 235; *Chem Phys*, **103** (1986) 325; *Spectrochim Acta*, **42A** (1986) 793; *J chem Soc Perkin Trans* 2, (1986) 1247; *Photochem Photobiol*, **44** (1986) 571: *Indian J Chem*, **26A** (1987).

4 Phaniraj P, Krishnamurthy M & Dogra S K, *Indian J Chem*, **25A** (1986) 513.

5 Krishnamurthy M, Iyer K A & Dogra S K, *J Photochem* (In press).

6 Herrington C F G & Kynaston W, *Trans Faraday Soc*, **53** (1957) 138.

7 Bertok W, Lucchesi P S & Snider N S, *J Am chem Soc*, **84** (1962) 1842.

8 Wehry E L & Rogers L B, *J Am chem Soc*, **87** (1965) 4234.

9 Flurry Jr R L & Wilson R K, *J phys Chem*, **71** (1967) 587.

10 Mason S F & Smith B E, *J chem Soc A*, (1969) 325.

11 Colpa J P, MacLean C & Markor E L, *Tetrahedron*, **19** (1963) suppl 2, 65.

12 Mackor A, Hofstra A & van der Waals J M, *Trans Faraday Soc*, **54** (1958) 186.

13 Förster Th, *Z Elektrochem*, **54** (1950) 531.

Indian Journal of Chemistry
Vol. 27A, March 1988, pp. 242-243

Hydrolysis of 1-*p*-Anisyl-2,2-dimethylbutyl Chloride: Special Salt Effects

M R NAIR* & V R SHAJI
Department of Chemistry, University of Kerala,
Trivandrum 695 034

Received 5 *March* 1987; *accepted* 11 *May* 1987

The effect of lithium perchlorate, tetramethylammonium bromide, sodium nitrate and sodium chloride on the rate of hydrolysis of 1-*p*-anisyl-2,2-dimethylbutyl chloride has been investigated in aqueous acetone. The data show the presence of both mass-law and special salt effects for the hydrolytic reaction.

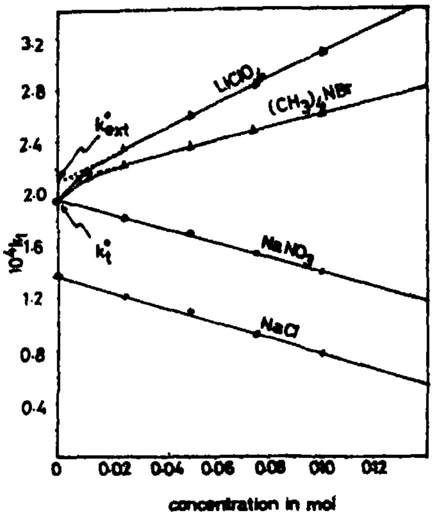

Fig. 1—Plot of [salt] versus k_1 for the hydrolysis of 1-*p*-anisyl-2, 2-dimethylbutylchloride in 80% (v/v) aq. acetone.

Table 1—Effect of Added Salts on Rate of Hydrolysis of 1-*p*-Anisyl-2,2-dimethylbutyl Chloride in 80% aq. Acetone

[RCl] = 0.01 mol dm^{-3}; temp. = 15.0°C

[Salt] 10^2 mol dm^{-3}	$10^4 k_1$ (s^{-1})				
	LiClO$_4$		(CH$_3$)$_4$NBr	NaNO$_3$	NaCl
0.00	1.95^{a}	(1.03)^{b*}	1.95	1.95	1.95
1.25	2.17	—	2.10	—	—
2.50	2.34	(1.52)	2.22	1.82	1.22
5.00	2.59	(1.95)	2.34	1.69	1.08
7.50	2.82	(2.22)	2.47	1.56	0.920
10.00	3.07	(2.44)	2.60	1.39	0.764

(a) At 25°C the value is 5.78, the corresponding values for the *p*-tolyl and phenyl substituted compounds are 0.00196 and 0.0000371.

(b) Values in parentheses are in 90% (v/v) aq acetone.

*At 35°C.

In connection with our studies on the mechanism of solvolytic reactions[1], we have investigated the effect of added LiClO$_4$, (CH$_3$)$_4$NBr, NaNO$_3$ and NaCl on the rate of hydrolysis of the title compound in aqueous acetone.

The dependence of rate in 80% (v/v) aq acetone on concentration of added salts is shown in Fig. 1 (Table 1). At higher concentrations of LiClO$_4$ and (CH$_3$)$_4$NBr a linear relationship is observed between the rate constants and [salt]. The extrapolation of the linear portions of the curves to zero [salt] gives a value of the rate constant (k^0_{ext}) which is more than the measured value (k^0_1), under identical conditions, without the added salts. Since the value obtained for the ratio, k^0_{ext}/k^0_1 in 80% (v/v) aq acetone is only slightly more than unity (1.07), the effect of LiClO$_4$ has been studied in 90% aq acetone. The value of the ratio changes to 1.42. This has been attributed to the fact that as the ionising power of the medium decreases the attraction between ions is increased and that the value of the ratio becomes more[2]. This type of behaviour is typical of the systems which show special salt effects. For certain compounds addition of small amounts of LiClO$_4$ produces an initial steep acceleration followed by a normal linear acceleration. This has been called as special salt effect, and is observed only with systems which yield relatively stable cations[3]. Winstein and coworkers reported this type of behaviour for the acetolysis of several alkylarens sulphonates. To our knowledge this is the first report of special salt effect for the hydrolysis of an aralkyl chloride.

Figure 1 also shows that added NaNO$_3$ decreases the rate of hydrolysis and the relationship between the rate retardation and [NaNO$_3$] is linear and that the value of k^0_{ext} is identical with k^0_1 in the absence of salt. This observation could be explained on the basis of the operation of a salt-induced medium effect superposed on the ubiquitous ionic strength effect. The progressive decrease in the rate with increase in [NaNO$_3$] points to a substantial initial state stabilisation caused by salting-in of the substrate by the organic cosolvent.

With added chloride ions, in addition to salt-induced medium effect, there is the operation of mass-law effect. The k^0_{ext} value is less by about 30% than the k^0_1 in the absence of the salt. This technique of finding the presence of mass-law effect has been described by Schleyer[4].

An essential condition to show mass-law effect is the stability of the carbonium ion. In the system under investigation this condition has been satisfied by the presence of *p*-anisyl group. Winstein and coworkers found a close correspondence between mass-law effect and special salt effect for a number of acetolysis reactions[5]. The presence of special salt effect in solvolytic reactions is a consequence of interference with return from solvent-separated ion pairs and is independent of the nature of the salt. For example in the hydrolysis of *p*-tolyl and phenyl substituted compounds, neither the special salt effect nor the mass-law effect is observed.

References

1 Nair M R & Shaji V R, *Indian J Chem*, **25A** (1986) 74; Nair M R & Raveendran G, *Indian J Chem*, **21A** (1982) 418, **20B** (1981) 258; Nair M R & Nair S V, *Indian J Chem*, **19B** (1980) 1091; **18B** (1979) 341; **16A** (1978) 984; Anantaraman R & Nair M R, *Can J chem*, **44** (1966) 2415.

2 Streitwieser J r A, *Solvolytic displacement reactions*, (McGraw-Hill Book Co, New York) 1962, p 170.

3 Winstein S, Clippinger E, Fainberg A H & Robinson G C, *J Am chem Soc*, **76** (1954) 2597; Winstein S & Robinson G C, *J Am chem Soc*, **80** (1958) 169.

4 Raber D J, Harris J M & Schleyer P V R, *Ions and ion pairs in organic chemistry*, edited by Szware (John Wiley, New York) 1974, p. 255.

5 Winstein S & Fainberg A H, *J Am chem Soc*, **80** (1958) 459.

Indian Journal of Chemistry
Vol. 27A, March 1988, pp. 244-245

Effects of Anionic & Non-ionic Surfactants in Differential Pulse Polarography

VINAY KUMAR*, GARY L BAKER, PATRICK T FARRELL, LINDA M MILEWSKI & SANDRA L ZIMMERMAN

Physical Sciences Department, Northern Kentucky University, Highland Heights, KY 41076

Received 12 *February* 1987; *revised* 2 *June* 1987; *accepted* 2 *July* 1987

The peak heights of the differential pulse polarograms of lead, cadmium, and zinc ions are enhanced by the presence of sodium alkyl ($C_8 - C_{18}$) sulfates. The maximum increase in the peak current is observed with sodium dodecyl sulfate. Like Triton X-100, Triton X-45 and X-165 greatly reduce the peak heights. However, Triton H-55 has only a marginal effect on the peak-height.

Table 1—Effects of Anionic Surfactants on DPP Peak of 20 ppm Pb^{2+} in 0.1 *M* KCl

[Drop time = 1 s; scan rate = 2 mVs^{-1}; modulation amplitude = 25 mV]

[Surfactant] (ppm)	Peak current, $i_p/\mu A$					
	C_8	C_{10}	C_{12}	C_{14}	C_{16}	C_{18}
0	6.27	6.27	6.27	6.27	6.27	6.27
10	6.49	6.90	6.99	6.36	6.31	6.29
20	6.63	6.88	7.51	6.38	6.36	6.33
30	6.86	6.89	7.95	6.32	6.35	6.40
40	6.85	7.04	8.28	6.41	6.35	6.39
50	6.81	6.95	7.84	6.40	6.35	6.40
70	6.79	6.85	7.77	6.39	6.35	6.40

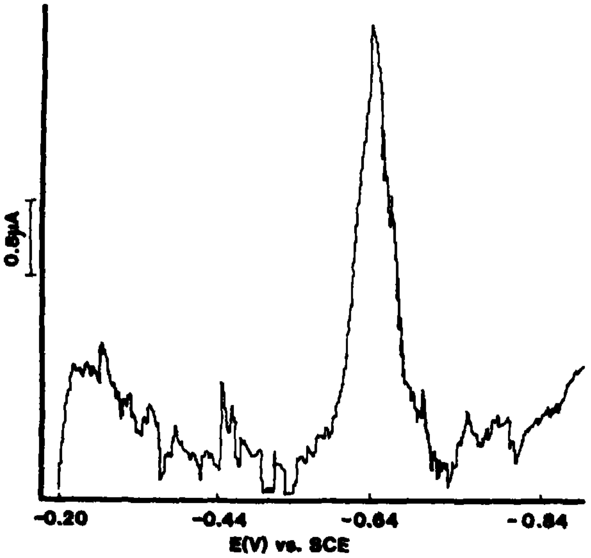

Fig. 1—Differential pulse polarogram of 10 ppm Cd^{2+} in 0.1 *M* KCl in the presence of 30 ppm sodium tetradecyl sulfate [Scan rate = 2 mVS^{-1}; and modulation amplitude = 25 mV]

Adsorption of surfactants or adsorbed reactants has been reported to cause enhancement of waves in differential pulse polarography[1,2]. According to Jacobsen and Lindseth[1], the presence of a surfactant with a charge opposite to that of the depolarizer increased the rate of the electron transfer in differential pulse polarography and this resulted in an increase inthe peak current of the reducible substance. However, these authors also reported[1] that anionic surfactants like sodium dodecyl sulfate and Benax did not affect the peak height of uncomplexed cations like copper, lead and cadmium. To resolve this apparent contradiction, in the present study the role of sodium dodecyl sulfate has been reexamined, and its behaviour is compared with that of other members of the homologous series, viz. sodium octyl, decyl, tetradecyl, hexadecyl, and octadecyl sulfates on the differential pulse polarographic (DPP) peaks of reducible substances like lead, cadmium and zinc ions. In addition, this note also discusses the effects of Triton X-45, X-165, and H-55. Unlike Triton X-100, these non-ionic surfactants have been rarely used in the DPP studies.

The differential pulse polarograms of surfactants were obtained in 0.1 *M* KCl and 0.1 *M* $KClO_4$ as supporting electrolytes at 20 ± 1°C (unless otherwise stated) employing a Princeton Applied Research model 174 polarographic analyzer, and recorded with a Houston Omnigraph model 2000 XY recorder. The dropping mercury electrode (DME) had the following characteristics (measured in 0.1 *M* KCl, open circuit) at a corrected mercury height of 49.0 cm; 2.578 mg/s, and t = 3.54 s. A silver-silver chloride electrode (sat. KCl) and a platinum wire served as the reference and auxiliary electrodes respectively. Dissolved oxygen was removed by bubbling oxygen-free nitrogen through the solutions cell for 10 min, and passing it over the solution during the polarographic measurements.

Stock solutions (1000 ppm) of sodium octyl (C_8-), decyl (C_{10}-), dodecyl (C_{12}-), tetradecyl (C_{14}-), hexadecyl (C_{16}-), and octadecyl (C_{18}-) sulfates were prepared by dissolving the surfactant in doubly distilled water.

Among the sodium alkyl sulfates only sodium decyl and dodecyl sulfates gave rise to tensammetric peaks, the heights of which increased with increase in [surfactant]; however, at higher [surfactant] the calibration curve was non-liner. Our results are in agreement with those of Jacobsen and Lindseth[1].

Table 2—Effects of Non-ionic Surfactants on DPP Peak of 10 ppm Cd^{2+} in 0.1 *M* KCl

[Experimental conditions same as in Table 1]

[Surfactant] (ppm)	Peak current, $i_p/\mu A$			
	Triton X-45	Triton X-100	Triton X-165	Triton H-55
0	5.40	5.40	5.40	5.40
10	5.25	4.25	5.35	5.32
20	5.20	4.10	5.55	5.30
30	5.10	3.50	5.30	5.30
40	4.35	1.80	5.00	5.34
50	0.70	0.30	4.80	5.35
60	0.45	0.18	4.50	5.32
80	0.20	—	4.20	5.32
90	—	—	2.45	5.32
100	—	—	1.82	—
120	—	—	0.80	—
150	—	—	0.18	—

The non-ionic surfactants Triton X-100, X-45, and X-165 do not give tensammetric peaks in the potential range of +0.10V to −3.0V.

Effects of anionic surfactants

Differential pulse polarographic (DPP) waves of lead, cadmium and zinc ions are affected in the presence of sodium alkyl sulfates. The DPP data for the lead ion are given in Table 1. The peak current (i_p) increases with increase in [surfactant]. However, at a [surfactant] of about 40 ppm, a saturation limit is reached. The magnitude of increase in peak currents in the presence of sodium octyl, decyl, tetradecyl, hexadecyl, and octadecyl sulfates is relatively small. However, sodium dodecyl sulfate is more strongly adsorbed on the electrode, and causes a considerable increase in the peak current. For example, at a C_{12}-alkyl sulfate concentration of 40 ppm, the increase in the peak current amounts to about 32%. According to some earlier reports[3-6] the negative charge of the surfactant probably facilitates the approach of the depolarizer to the electrode surface. The magnitude of increase in peak currents follows the order: $C_8 > C_{10} > C_{12} > C_{14} > C_{16} > C_{18}$. The effectiveness of C_{14}, C_{16} and C_{18} alkyl sulfates is limited by the turbidity that results on the addition of these surfactants to the depolarizer solutions in 0.1 *M* KCl. The turbidity formation also causes a slight distortion of the DPP peak (Fig. 1). The distortion is also noticed in 0.1 *M* NaCl as the supporting electrolyte. In the case of C_{16} and C_{18} alkyl sulfates, a probable cause of the turbidity formation is the presence of micelles[7]. This conclusion seems reasonable because only in the case of C_{16} and C_{18} alkyl sulfates, the surfactant concentrations utilized in this study exceeded their cmc's[7].

The addition of sodium alkyl sulfates does not affect the peak potentials in the case of lead, cadmium and zinc ions, indicating that depolarizer can very easily penetrate the adsorbed surfactant layer.

Effects of non-ionic surfactants

The peak currents of cadmium, zinc and lead ions are decreased by the presence of Triton X-45, X-100, and X-165. The DDP data for cadmium ion are given in Table 2. Initially, there is a very slight decrease in the peak current; however, as the [surfactant] approaches 80-150 ppm level, the DPP peak almost disappears. The peak potential for the cadmium ion in 0.1 *M* KCl is −0.64V (vs SCE) and remains unaffected by the addition of surfactants. Addition of Triton H-55 has only marginal effect on the peak height of the uncomplexed cadmium ion.

References

1 Jacobsen E & Lindseth H, *Anal Chim Acta*, **86** (1976) 123.
2 Anson F C, Flanangan J B, Takahashi K & Yamada A, *J electroanal Chem*, **67** (1976) 253.
3 Gundersen N & Jacobsen E, *J electroanal Chem*, **20** (1969) 13.
4 Frumkin A N, Fedorovich N N & Ivanova R, *Can J Chem*, **37** (1959) 253.
5 Jacobson E & Kalland G, *Anal Chim Acta*, **30** (1964) 240.
6 Frumkin A N, *Trans Faraday Soc*, **55** (1969) 156.
7 Kumar V & Gilbert T W, *J electroanal Chem*, **40** (1972) 419.

Indian Journal of Chemistry
Vol. 27A, March 1988, pp. 246-249

Kinetics of Interaction of Nickel (II) & Cobalt (II) with α-Amino-β-methylbutyric Acid

H C MALHOTRA* & AMITABH K JAIN
Department of Chemistry, University of Delhi, Delhi 110 007

Received 26 *March* 1987; *revised and accepted* 23 *June* 1987

The kinetics of interaction of Ni(II) and Co(II) with α-amino-β-methylbutyric acid (valine) have been investigated under the condition $[M(II)] \gg [\text{valine}]$ by stopped flow technique at 25 ± 0.05°, 30 ± 0.05°, 35 ± 0.05° and 40 ± 0.05°C in the *p*H range 6.34-7.42 and ionic strength of 0.1 mol dm^{-3} (KNO_3). The overall rate constants have been resolved into specific rate constants k_1 and k_2 corresponding to interaction with zwitterionic form and monoanionic form of the amino acid respectively.

Fast reaction techniques have made possible the systematic study of metal complexation kinetics. The kinetic data thus obtained can yield information about the detailed mechanism by which the ligand enters the first coordination sphere of metal ion. Study of complexation reaction of α-amino-β-methylbutyric acid (valine) which is a terminal part of certain proteins, nucleic acids and metalloenzymes[1], can provide useful information about the behaviour of these biochemicals. The title investigation is an attempt in this direction.

Valine (LOBA CHEMIE), KNO_3 (Sarabhai, G R), bromothymol blue (BDH, AR), $Co(NO_3)_2 \cdot 6H_2O$ and $Ni(NO_3)_2 \cdot 6H_2O$ (all E Merck) were used as such. The *p*H was adjusted using 2,6-lutidine (Merck-Schuchardt) and HCl (Glaxo, A R).

The reactions were followed spectrophotometrically using a stopped flow spectrophotometer (Aminco-Morrow) at 620 nm by *p*H indicator method[3] employing bromothymol blue. All the reactions were carried out at $\mu = 0.1$ mol dm^{-3} (KNO_3), neglecting the effects of metal ions (10^{-2} mol dm^{-3}) on ionic strength. All runs were made under pseudo-first order conditions using excess of metal ions over ligand.

Blank experiments in which indicator and metal ion solutions or indicator and ligand solutions were mixed showed no absorbance change at 620 nm to interfere with the results.

The total absorbance change was kept small so that the relative voltage change (ΔV) could be observed on the oscilloscope.

The kinetic study was carried out in the *p*H range of 6.34-7.42, since protonated form of valine is more significant[2,3] in the *p*H range of 6.00-7.50.

In general, the interaction of Ni(II) and Co(II) with valine follows the overall differential Eq. (1)

$$\text{Rate} = \frac{-d[M(II)]}{dt} = \frac{-d}{dt}[\text{valine}] = k_{obs}[M(II)][\text{valine}] \qquad \ldots (1)$$

Since [M(II)] is in large excess over [valine], [M(II)] term can be absorbed in k_{obs}.

Under this condition Eq. (1) can be written as

$$\text{Rate} = k'_{obs}[\text{valine}] \qquad \ldots (2)$$

The applicability of Eq. (2) was confirmed by the linear plots of k'_{obs} and concentrations of reactants (Fig. 1). Second order rate constants (k_{obs}) were calculated using the relation: $k_{obs} = k'_{obs}/[M(II)]$. k_{obs} values thus obtained are reported in Table 1.

The interaction of valine with Ni(II) and Co(II) can be visualised as shown in Scheme 1[3],

$$\begin{tikzcd}
LH^+ + M^{2+} \arrow[r, "k_1^T"] \arrow[d, shift left] & ML^{2+} + H^+ \\
L + M^{2+} \arrow[r, "k_2^T"] \arrow[u, shift left, "K_a^T"] & ML^{2+}
\end{tikzcd}$$

Scheme 1

Scheme 1 shows that

$$k_{obs} \cdot \frac{K_a^T + [H^+]}{[H^+]} = k_1^T + \frac{k_2^T K_a^T}{[H^+]} \qquad \ldots (3)$$

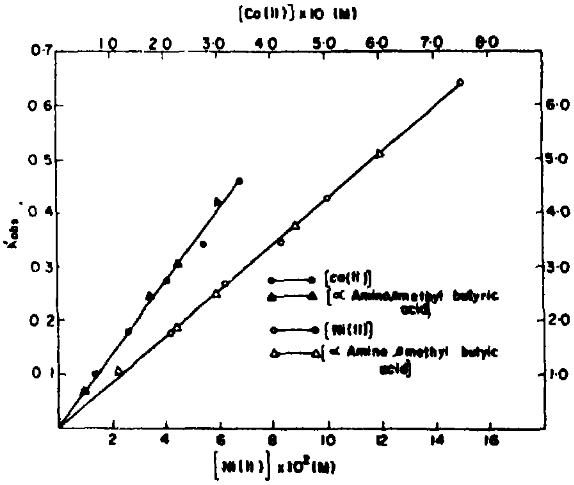

Fig. 1—Plot of k'_{obs} versus concentration of reactants

Table 1—Second Order Rate Constants for Interaction of Ni(II) and Co(II)* by α-Amino-β-Methyl Butyric Acid at Different *p*H and Temperatures

[Ni(II)] = 1.25×10^{-2} mol dm^{-3}; [Co(II)] = 1.86×10^{-2} mol dm^{-3}; [Valine] = 1.81×10^{-3} mol dm^{-3}; $\mu = 0.1$ mol dm^{-3} (KNO_3)

*p*H	k_{obs} (dm^{3}mol^{-1}s^{-1})
Temp = 25 ± 0.05°C	
6.48 (6.50)	4.62 (1.55×10^3)
6.72 (6.71)	6.16 (2.06×10^3)
6.94 (6.96)	9.24 (3.10×10^3)
7.14 (7.17)	13.86 (4.65×10^3)
7.37 (7.42)	25.20 (8.09×10^3)
Temp = 30 ± 0.05°C	
6.42 (6.46)	7.92 (2.86×10^3)
6.65 (6.67)	8.82 (3.38×10^3)
6.89 (6.93)	13.86 (5.66×10^3)
7.09 (7.12)	27.72 (8.12×10^3)
7.32 (7.38)	39.90 (13.30×10^3)
Temp = 35 ± 0.05°C	
6.38 (6.40)	14.70 (4.96×10^3)
6.66 (6.71)	20.20 (6.89×10^3)
6.86 (6.88)	26.50 (9.31×10^3)
7.05 (7.07)	36.92 (11.64×10^3)
7.29 (7.31)	55.51 (20.69×10^3)
Temp = 40 ± 0.05°C	
6.34 (6.35)	18.48 (6.70×10^3)
6.57 (6.58)	30.81 (10.64×10^3)
6.79 (6.80)	42.64 (14.90×10^3)
6.99 (6.96)	55.86 (20.69×10^3)
7.20 (7.21)	77.51 (31.04×10^3)

*Values in parentheses for Co(II) interaction

In accordance with Eq. (3), a plot of $k_{obs}(K_a^T + [H^+])/[H^+]$ versus $[H^+]^{-1}$ should be linear. This is found to be so (Fig. 2). The values of k_1^T and k_2^T evaluated from intercepts and slopes of the linear plots respectively are given in Table 2. The value of K_a^{25} (2.45×10^{-10}) was taken from literature[4]. At temperatures employed in the present investigation, the corrected values of K_a^T have been evaluated using the thermodynamic relation (4).

$$\log K_a^{T_2} = \frac{\Delta H^{\neq}}{4.6} \frac{(T_2 - T_1)}{T_1 T_2} + \log K_a^{T_1} \qquad \ldots (4)$$

The values at different temperatures are $K_a^{30} = 3.31 \times 10^{-10}$; $K_a^{35} = 4.43 \times 10^{-10}$ and $K_a^{40} = 5.88 \times 10^{-10}$. The values of activation parameters corresponding to metal ion-zwitterion and metal ion-monoanion interaction are reported in Table 3.

Table 2—k_1^T and k_2^T for Interaction of Ni(II) and Co(II) with Valine at Different Temperatures

Temp (°C)	k_1^T (dm^{3}mol^{-1}s^{-1})	k_2^T (dm^{3}mol^{-1}s^{-1})
	Ni(II)-Valine	
25 ±0.05	2.14	3.66×10^3
30 ±0.05	3.95	5.25×10^3
35 ±0.05	7.45	5.87×10^3
40 ±0.05	7.36	12.48×10^3
	Co(II)-Valine	
25 ±0.05	0.85×10^3	1.02×10^5
30 ±0.05	1.32×10^3	1.39×10^5
35 ±0.05	2.78×10^3	2.90×10^5
40 ±0.05	4.13×10^3	3.80×10^5

Table 3—Activation Parameters for Interaction of Ni(II) and Co(II) with Valine for k_1 and k_2 Paths

$\Delta H_1^{\neq}$ (kJ mol^{-1})	$\Delta H_2^{\neq}$ (kJ mol^{-1})	$\Delta S_1^{\neq}$ (J K^{-1}mol^{-1})	$\Delta S_2^{\neq}$ (J K^{-1}mol^{-1})
	Ni(II)-Valine		
87.9	33.5	33.9	−80.3
	Co(II)-Valine		
79.0	17.0	59.9	−108.4

A general mechanism for complex formation involves a rapid ion formation between the metal ion and ligand followed by loss of a water molecule from inner coordination sphere of the metal ion[5] and an attack by the ligand. This can be represented as shown in Scheme 2.

$$M(H_2O)_6{}^{2+} + L^{n-} \overset{K_{os}}{\rightleftharpoons} (H_2O)_5M(H_2O)L^{(2-n)+}$$

$$(H_2O)_5M(H_2O)L^{(2-n)+} \xrightarrow{k_0} (H_2O)_5ML^{(2-n)+} + H_2O$$

Scheme 2

Scheme 2 leads to the rate law (5).

$$\frac{d[ML^{(2-n)+}]}{dt} = k_0[(H_2O)_5M(H_2O)L^{(2-n)+}]$$
$$= k_0 K_{os}[M(H_2O)_6{}^{2+}][L^{n-}] \qquad \ldots (5)$$

Sound absorption and temperature jump[6] data have been used to determine the value of k_0, considering the expressions derived by Eigen[6] on kinetic consideration and by Fuoss[7] on statistical grounds. Thus K_{os} can be theoretically determined by Eq. (6)

$$K_{os} = \frac{4\pi Na^3}{3000} e^{-U(a)/kT} \qquad \ldots (6)$$

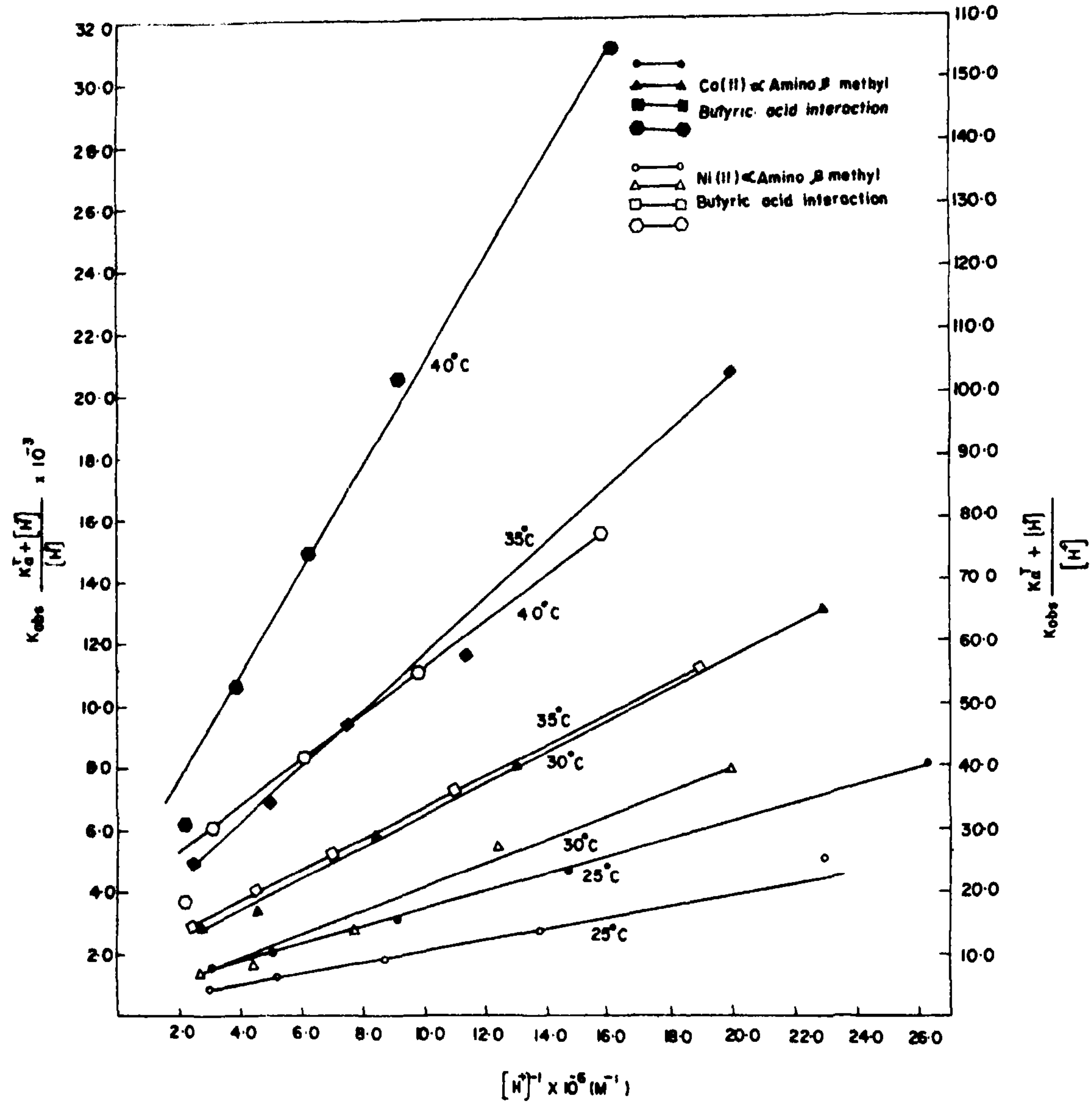

Fig. 2—Plot of $k_{obs}\cdot(K_a^H+[H]^+)/[H^+]$ versus $[H^+]^{-1}$ for Ni(II) and Co(II) interaction with valine at different temperatures

Table 4—k_0 Values for Interaction of Ni(II) and Co(II) with Valine at Different Temperature

Temp (°C)	$k_0 \times 10^{-3}$ (s^{-1})	Temp (°C)	$k_0 \times 10-5$ (s^{-1})
Ni(II)-Valine		Co(II)-Valine	
25 ±0.05	1.84	25 ±0.05	0.51
30 ±0.05	2.65	30 ±0.05	0.70
35 ±0.05	2.96	35 ±0.05	1.46
40 ±0.05	6.30	40 ±0.05	1.91

$\Delta S_0^{\neq}(\mathrm{Ni}) = 59.0$ kJ mol^{-1}; $\Delta S_0^{\neq}(\mathrm{Ni}) = -4.4$(J K^{-1} mol^{-1})
$\Delta H_0^{\neq}(\mathrm{Co}) = 65.7$ kJ mol^{-1}; $\Delta S_0^{\neq}(\mathrm{Co}) = -21.6$(J K^{-1} mol^{-1})

where $U(a) = (Z_1Z_2e^2/aD) - (Z_1Z_2e^2K/D\ (1+Ka))$ and $K^2 = (8\pi Ne^2/1000DkT)\ \mu$, a = distance of closest approach of two ions and other symbols have their usual significance. If the value[8] of a is taken as 5Å then the value of K_{os} can be approximated to 1.98 mol dm^{-3} at all temperatures. From Table 2 it can be seen that at all the temperatures and for both metal ions k_1^T is negligible compared to k_2^T leading to the verification of the fact that protonated form of amino acid does not react. It can now be assumed that $k_2 = k_0 K_{os}$ or $k_0 = k_2/K_{os}$. The values of k_0 are reported in Table 4. The values of activation parameters are also reported in Table 4. The values of $\Delta H_0^{\ast}$ and $\Delta S_0^{\ast}$ compare well with the expected values[6] of water exchange as determined for amino acids by temperature jump and sound absorption methods, though our values have been calculated using stopped flow apparatus, i.e. the theory presented above accomplishes well for this case.

One of the authors (AKJ) is thankful to UGC (New Delhi) for award of junior research fellowship.

References

1 Roberts F Colman, *Peptide and Protein Rev*, **1** (1983) 41; Irwin M Chaiken, Danial M Abercombie, Tatsuhiko Kaumera & Reginald Paul Sequeria, *Peptide and Protein Rev*, **1** (1983) 139.

2 Roche T S & Wilkins R G, *J Am chem Soc*, **96** (1974) 5082.

3 Cassatt J C & Wilkins R G, *J Am chem Soc*, **90** (1968) 6045.

4 Sillen L G & Martell A E, *Stability constants of metal ion complexes*, Special publication No 17, W1, (Chemical Society, London) 1964.

5 Basolo F & Pearson R G, *Mechanism of inorganic reactions*, (Wiley, New York) 1967.

6 Eigen M, *Z Phys Chem*, **1** (1954) 176.

7 Fuoss R M, *J Am chem Soc*, **80** (1958).

8 Burgees J, *Metal ions in solution*, (Ellis Horwood & John Wiley, England) 1978.

Indian Journal of Chemistry
Vol. 27A, March 1988, pp. 250-251

Ru(III)-catalysed Decomposition of Ni(III) in Aqueous Sulphuric Acid Medium: A Kinetic & Ionic Strength Effect Study

G KRISHNA REDDY, T RAYAPA REDDY &
V JAGANNADHAM*

Department of Chemistry, Nizam College, Hyderabad 500 001

Received 24 *April* 1987; *revised* 13 *July* 1987; *accepted* 6 *August* 1987

Ru(III)-catalysed decomposition of Ni(III) ion in aqueous sulphuric acid medium at varying ionic strengths is overall second order, first order each in [Ru(III)] and [Ni(III)]. The reactive species of Ni(III) ion is inferred to be $Ni(OH)^{2+}$ in aqueous sulphuric acid.

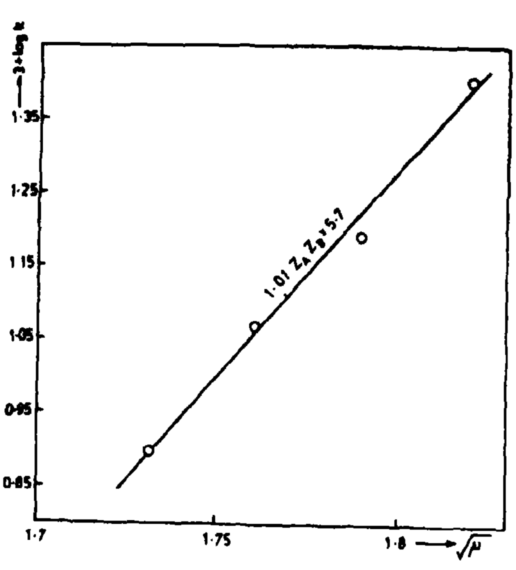

Fig. 1—Plot of log k versus $\sqrt{\mu}$

In continuation of the earlier work on Ni(III) ion oxidations of some organic[1-3] and inorganic[4,5] compounds from our laboratory the authors attempted to study some catalysed oxidations using Ru(III) chloride as a catalyst. Preliminary observations on Ru(III)-catalysed Ni(III) oxidation of aliphatic secondary alcohols indicated self-decomposition of Ni(III) in aqueous sulphuric acid in the absence of alcohol. In this note we present preliminary results on the decomposition of Ni(III) in the presence of Ru(III).

All the chemicals used were of AR grade. Experimental procedures employed were the same as reported earlier[1-5]. Ruthenium(III) chloride was a commercial product from John Mathew Chemical Co., (U.K.) and NiO(OH) was prepared according to literature procedure[6].

Under the conditions $[Ni(III)] = 1.00 \times 10^{-3}$ mol dm^{-3} $[Ru(III)] = 1.6 \times 10^{-4}$ mol dm^{-3}, $[H_2SO_4] = 1.00$ mol dm^{-3}, and temp. = 50°C, the plot of log [Ni(III)] versus time was linear indicating unit dependence in [Ni(III)]. Under these conditions the observed first order rate constants (k/min^{-1}) varied from 6.67×10^{-3} at $[Ru(III)] = 1.6 \times 10^{-4}$ mol dm^{-3} to 2.72×10^{-2} at $[Ru(III)] = 6.4 \times 10^{-4}$ mol dm^{-3} at $\mu = 3.00$ mol dm^{-3}. From the plot of log k versus log [Ru(III)] the order in [Ru(III)] was found to be unity. Hence, at constant $[H_2SO_4]$ the rate law comes out to be

$$\text{Rate} = k'[\text{Ni(III)}][\text{Ru(III)}]$$

The observed first order rate constants (k/min^{-1}) increased from 4.00×10^{-4} at $[H^+] = 0.250$ mol dm^{-3} to 6.67×10^{-3} at $[H^+] = 1.00$ mol dm^{-3} at $\mu = 3.00$ mol dm^{-3}. From the plot of log k versus log $[H^+]$ the order in $[H^+]$ was found to be two. Therefore the reactive species of Ni(III) is assumed to be $Ni(OH)^{2+}$ (Eq. 1)

$$NiO(OH) + 2H^+ \rightleftharpoons Ni(OH)^{2+} + H_2O \quad \ldots(1)$$

Hence, it may be concluded that both $Ni(OH)^{2+}$ and Ru(III) are participating in the rate-determining step. In order to further confirm that the reactive species of Ni(III) is $Ni(OH)^{2+}$, Ru(III)-catalysed decomposition of Ni(III) was carried out at different ionic strengths using K_2SO_4 for adjusting the ionic strength. The rate increased with increase in ionic strength (Fig. 1). The rates at different ionic strengths followed the linear equation[7](2)

$$\log k = \log k_0 + 1.01\, Z_A Z_B \sqrt{\mu} \quad \ldots(2)$$

where k and k_0 are the rate constants at ionic strength μ and zero respectively and Z_A and Z_B are the charges of the ions participating in the rate-determining step. The slope ($1.01\, Z_A Z_B$) of 5.7 ($r = 0.994$) of the plot in Fig. 1 confirms that the charge on Ni(III) species is +2 if the charge on ruthenium is +3. Hence, in the present study, the effect of ionic strength on Ni(III) decomposition provides yet additional evidence[4,8] for the participation of $Ni(OH)^{2+}$ as the reactive species in aqueous acid medium. Based on the foregoing results the mechanism of Ru(III)-catalysed decomposition of Ni(III) can be depicted as shown in Scheme 1.

$$\mathrm{NiO(OH)} + 2\mathrm{H}^+ \xrightarrow{\text{fast}} \mathrm{Ni(OH)}^{2+} + \mathrm{H_2O}$$

$$\mathrm{Ni(OH)}^{2+} + \mathrm{Ru(III)} \xrightarrow[\text{slow}]{k} \mathrm{Ru(IV)} + \mathrm{Ni(OH)}^+$$

$$2\,\mathrm{Ru(IV)} + \mathrm{H_2O} \xrightarrow{\text{fast}} 2\,\mathrm{Ru(III)} + 2\mathrm{H}^+ + \frac{1}{2}\mathrm{O_2}$$

or

$$2\,\mathrm{Ru(IV)} \rightleftharpoons \mathrm{Ru(V)} + \mathrm{Ru(III)}$$

$$\mathrm{Ru(V)} + \mathrm{H_2O} \xrightarrow{\text{fast}} \mathrm{Ru(III)} + 2\mathrm{H}^+ + \frac{1}{2}\mathrm{O_2}$$

Scheme 1

One of the author (G K R) is grateful to the CSIR, New Delhi for the award of a senior research fellowship.

References

1 Reddy T R, Murthy G S S & Jagannadham V, *Oxidation Communs*, **9** (1986) 83.

2 Reddy T R, Murthy G S S & Jagannadham V, *Oriental J Chem*, **2** (1986) 92.

3 Reddy G K & Jagannadham V, *Indian J Chem*, **26A** (1987) 331.

4 Reddy T R, Murthy G S S & Jagannadham V, *Bull Soc Chim Belgs*, **94** (1985) 565.

5 Reddy T R, Murthy G S S & Jagannadham V, *Indian J Chem*, **25A** (1986) 1120.

6 Glemser O & Einerhand J, *Z Anorg Chem*, **261** (1950) 26.

7 Laidler K J, *Chemical kinetics*, (McGraw Hill, New York), 1965, pp. 220.

8 Morliere P & Patterson L K, *Inorg Chem*, **20** (1981) 1458.

Indian Journal of Chemistry
Vol. 27A, March 1988, pp. 252-253

Kinetics & Mechanism of Oxidation of Dimethyl Sulphoxide by Chromic Acid in Aqueous Acid Medium

S VENKATESWARA RAO & V JAGANNADHAM*

Department of Chemistry, Nizam College (Osmania University), Hyderabad 500 001

Received 5 *May* 1987; *revised* 15 *June* 1987; *accepted* 26 *June* 1987

The title reaction shows first order dependence each on [oxidant] and [substrate]. The reaction is acid-catalysed and shows fourth order dependence in [H^+]. The rate is affected to a small extent by added sulphate ions and are dependent upon solvent polarity. Added Mn(II) retards the rate while the rate is enhanced if 1,10-phenanthroline is also present along with Mn(II). The sole reaction product is identified as dimethyl sulphone.

In continuation of earlier work from our laboratory on chromic acid oxidations[1,2], we report herewith results of hitherto unreported title investigation.

All the chemicals used were of AR grade. Sulphuric acid was used as a source of H^+ ions. The course of the reaction was followed by estimating unreacted Cr(VI) iodometrically. The product was identified as dimethyl sulphone (m.p. 109°). However difficulty was experienced to calculate the stoichiometry of the reaction.

Oxidation of DMSO (0.1 mol dm^{-3}) by chromic acid (0.001 mol dm^{-3}) was carried out in aqueous sulphuric acid medium at constant acidity (2.0 mol dm^{-3}) and ionic strength at 317 K. Under the conditions [DMSO] $\gg$ [Cr(VI)], the plot of log[Cr(VI)] versus time was linear indicating first order dependence in [Cr(VI)]. The order in [DMSO] was also unity as revealed by the slope of the linear plot of log k' versus log [DMSO], where k' is the pseudo-first order rate constant.

The rates of oxidation of DMSO were affected to a small extent by added salts, indicating that the reaction may be involving an ion and a dipole.

The k' value at constant ionic strength increased from 3.00×10^{-3} min^{-1} at 1.0 ml dm^{-3} H_2SO_4 to 5.1×10^{-2} min^{-1} at 2.0 mol dm^{-3} H_2SO_4. The plot of log k' versus log[H^+] was linear, the slope of which revealed the order in [H^+] to be four. This is in accord with the overall hydrolytic and protolytic equilibrium (1) which Cr(VI) undergoes in acid medium.

$$Cr_2O_7^{2-} + 4H^+ \rightleftharpoons 2\,HCrO_3^+ + H_2O \qquad \ldots(1)$$

Further k' values increased with decrease in dielectric constant (D) from 5.1×10^{-2} min^{-1} at 2.0 mol dm^{-3} H_2SO_4 in pure water to 1.46×10^{-1} min^{-1} in 20% (v/v) acetic acid. In accordance with Amis' equation[3], the plot of log k' versus 1/D was linear with a positive slope ($r = 0.986$), indicating the reaction to be positive ion-dipole type. Hence in the present reaction the active oxidant species of Cr(VI) is considered to be $HCrO_3^+$ (see also references 1a, 1b and 1e).

Added Mn(II) ions retarded the rate of oxidation. When the concentration of Mn(II) ions was equal to or more than 0.012 mol dm^{-3} the rate of oxidation was diminished to one third (1.84×10^{-2} min^{-1}) from that (5.1×10^{-2} min^{-1}) in the absence of Mn(II) ions. This result is expected if Mn(II) ions catalyse the disproportion of the intermediate valence states of chromium, i.e. Cr(IV) of Cr(V)[4]. However added 1,10-phenanthroline (0.001 mol dm^{-3}) in the presence of Mn(II) ions catalysed the rate of oxidation. This may be due to the fact that the Cr(VI) or *in situ* product of Cr(VI), i.e. Cr(IV) or Cr(V) and Mn(II) may compete for the added ligand to form a complex. In this process Mn(II) may be more effective and thus is removed completely in the form of a complex and the disproportionation of Cr(VI) or Cr(IV) or Cr(V) is not diminished resulting in the higher rate of oxidation.

The rate enhancement in the presence of 1,10-phenanthroline (0.001 mol dm^{-3}) may be explained by assuming that chromic acid forms a complex with 1,10-phenanthroline just like picolinic acid[5] and such a complex is supposed to be more effective as an oxidant than chromic acid alone. The complex formation also diminishes the disproportionation of Cr(VI), thus leading to enhancement of rate.

Based on the above discussion and observed product analysis the mechanism for the reaction can be written as shown in Scheme 1.

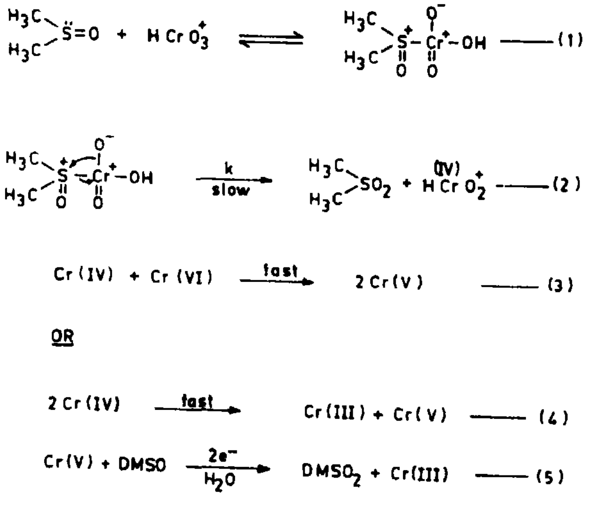

Scheme 1

From Scheme 1 it is clear that the reaction involves two-electron transfer which is confirmed by the absence of polymerisation when acrylonitrile monomer is added to the reaction mixture. The determination of stoichiometry was found difficult because of the steps 2-5. The same type of difficulty was also experienced by Hasan and Rocek[6] during Cr(VI) oxidation of isopropanol. However the stoichiometry was found to be 1:1 in the presence of 1,10-phenanthroline.

The authors are grateful to Prof T Navaneeth Rao and Prof B Sethuram, for their encouragement.

References

1 Musala Reddy P, Jagannadham V, Sethuram B & Navaneeth Rao T, (a) *Indian J Chem*, **21A** (1982) 483; (b) *Indian J Chem*, **21A** (1982) 608; (c) *Z phys Chem* (*Neue folge*), **127** (1981) 251; (d) *Bull Soc Chim Belgs*, **91** (1982) 707; (e) *Oxidation Commun*, 3 (1983) 1; (f) *React Kinet & Catal Lett*, **19** (1982) 243; (g) *React Kinet & Catal Lett*, **21** (1982) 437.

2 Satyanarayana Reddy T & Jagannadham V, *Proc natl Acad Sci India*, **56A** (1986) 129.

3 Amis E S, *J chem Edn*, **30** (1953) 351.

4 Chang Y W & Fotto Weistheimer, *J Am chem Soc*, **82** (1960) 1401.

5 Peng T Y & Roček J, (a) *J Am chem Soc*, **98** (1976) 1026; (b) **99** (1977) 7622.

6 Hasan F & Roček J, *J Am chem Soc*, **94** (1972) 3181.

Indian Journal of Chemistry
Vol. 27A, March 1988, pp. 254-255

Dipole Moments & Structure of Some Hydrazonomalononitriles

MAGDI M NAOUM*, MOHAMED M ABDEL-MOTELEB
& ZAGHLOL E KANDEEL
Department of Chemistry, Faculty of Science,
University of Cairo, Giza, Egypt

Received 9 *December* 1986; *revised and accepted* 1 *June* 1987

The dipole moments of N-methyl-N-phenylhydrazonomalononitrile (Ia) and its four derivatives (Ib-e) having electron donating substituent (Ib) and electron withdrawing substituents (Ic-Ie) have been determined in dioxane at 30°C. The results obtained when compared with those calculated by the method of vector summation of bond moments indicate that these compounds exist, most probably, as zwitterions. The data have also been used to investigate the effect of substituents on the extent of formation of zwitterion.

The abnormal stability of the hydrazonomalononitrile [$H_2N-N=C(CN)_2$] and its unexpectedly high dipole moment[1] was considered as an evidence for the existence of such group of compounds in a zwitterion form. With this in mind, five N-methyl-N-arylhydrazonomalononitriles (Ia-e) have been prepared and their dipole moments measured in dioxane at 30°C. Compounds Ia-e have limited solubility in either benzene or cyclohexane.

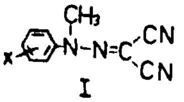

I

[(a) X = H, (b) X = *p*-CH_3O, (c) X = *p*-Br, (d) X = *m*-NO_2, (e) X = *p*-COOH

The hydrazonomalononitriles (Ia-c) were prepared as described previously[2], and crystallized twice from ethanol after treatment with charcoal and their purity was checked by TLC and analytical data.

Dilute solutions of hydrazones (Ia-e) in purified dioxane[3] with weight fractions ranging from 10^{-3} to 10^{-2} were prepared and the dielectric constants, densities, and refractive indices were measured at 30°C. The dipole moment of the solute (μ_2) was calculated by refractivity method, where the molar deformation polarization was obtained by extrapolating the measured refraction for the sodium D-line to infinite wavelength; the molecular polarization of solute at infinite dilution was taken as the average of that determined graphically and those calculated from Hedestrand's[4] and Palit-Banerjee's[5] equations. A computer programme was used to calculate observed moments from measured data†. On the basis of precision of ±0.0005 in dielectric constants, ±0.0001 in densities and refractive indices, and ±0.02% in solution concentrations, the dipole moment values obtained were believed reliable to ±0.05 D.

For the deduction of the probable structure of parent compound, N-methyl-N-phenylhydrazonomalononitrile (Ia), a configuration, presented in structure (II), has been assumed from which the various conformations are produced by rotating the $C_6H_5N(CH_3)-$ group about the $N-N=$ bond by an angle ϕ between zero and 360° with respect to the initial configuration. The angle $\phi = 0°$ represents the case where the phenyl group is initially in the plane of the rest of the molecule, while the methyl group is tetrahedrally oriented out of plane. The fixed set of reference axes, required for the calculation of the total dipole moment of Ia in its various hypothetical conformations applying the vector summation method of bond moments, are taken for convenience as shown in structure (II). It has its origin at the nitrogen atom of the $C_6H_5N(CH_3)-$ group, the y-axis along the $N-N=$ bond, and x-axis in the plane of the rest of the molecule. Also indicated in structure (II), are the bond moments and valence bond angles as taken from the literature[6,7]. The computer programme developed in Basic V 3.5 to output the calculated moments from bond moments and valence bond angles, as a function of the angle of rotation, ϕ was developed†. The dipole moments of the various conformations of compounds (Ia-e), calculated this way, are listed in Table 1.

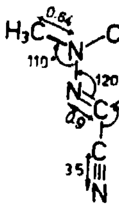

II

When compared with the observed dipole moment value of 7.46 D (Table 1) of Ia, none of those calculated for the various conformations ($\phi = 0$ to 360°) are in close agreement with the measured one. Such a considerable difference between observed and calculated moments leads one to suggest the existence of Ia in a highly polar form, i.e. the zwitteri-

---

†The detailed computer programme can be had from the authors on request.

Table 1—Measured and Calculated Dipole Moments of Compounds Ia-e as a Function of Angle (ϕ) between 0 and 360°

Compound	Substituent	μ_{obs}	μ_{calc} (D) at ϕ between 0 and 360°					
			ϕ = 0	60	120	180	240	300
Ia	H	7.46	3.13	3.10	2.74	2.38	2.43	2.83
Ib	*p*-CH_3O	6.59	2.78	2.96	3.05	2.95	2.77	2.68
Ic	*p*-Br	5.36	4.71	4.20	2.65	0.97	2.33	4.01
Id	*m*-NO_2	4.67	4.67	4.17	2.62	0.90	2.29	3.97
Ie	*p*-COOH	5.74	3.58	3.36	2.53	1.77	2.19	3.12

on, as represented in structure (III), which is in accordance with the structure suggested by Ciganek[1] for the hydrazonomalonitrile (IV).

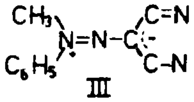
III

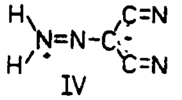
IV

As is expected, the electron donating substituent OCH_3 in the phenyl ring of Ia (i.e. Ib), will favour the formation of zwitterion. On the other hand, increase in electron withdrawing character of the substituent will decrease the extent of the electromeric shift leading to the zwitterion formation. This was found to be the case; a considerable difference was observed between the measured and the highest value of the caculated moments ($\Delta\mu = \mu_{obs} - \mu_{maxcalc}$) for the *p*-$CH_3O$ derivative (Ib) ($\Delta\mu = 3.54$ D). Such a deviation was found to be relatively small ($\Delta\mu = 0.65$ D) in the case of Ic bearing the electron withdrawing Br atom, and negligible in the *m*-nitro derivative (Id).

Finally, the relatively high $\Delta\mu$ value (= 2.16 D) in the case of compound bearing an electron withdrawing substituent *p*-COOH, such as in Ie, can be attributed to the formation of another zwitterion as represented by structure (V).

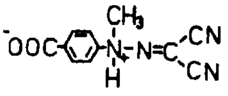
V

References

1 Ciganek E, *J org Chem*, **30** (1965) 4198.

2 Kandeel Z E, Ph.D. thesis, Cairo University, Faculty of Science, 1981.

3 Weisberger A & Proskauer R, *Organic solvents and methods of purifications* (The Clarendon Press, Oxford), 1953.

4 Hedestrand G, *Z phys Chem*, **2B** (1929) 424.

5 Palit S R & Banerjee B C, *Trans Faraday Soc*, **47** (1951) 1299.

6 Smyth C P, *Dielectric behaviour and structure* (McGraw-Hill, London), 1955.

7 Soundarajan S, *Trans Faraday Soc*, **53** (1957) 159.

Indian Journal of Chemistry
Vol. 27A, March 1988, pp. 256-257

^{13}C & ^{19}F NMR Studies of *para*-Substituted Monothio-β-diketones & Their Zn(II) Complexes

B R DUBEY, R K BANSAL & A K RAI*
Department of Chemistry, University of Rajasthan,
Jaipur 302 004

Received 6 April 1987, revised and accepted 24 July 1987

^{13}C NMR spectra of four *para*-substituted monothio-β-diketones and their zinc(II) complexes together with ^{19}F NMR spectra of 4'-fluoromonothiodibenzoylmethane and its zinc(II) complex are reported. The *para*-substituted monothiodibenzoylmethanes exist in solution as mixtures of rapidly interconverting *Z*-enol and *Z*-enethiol tautomers with a predominance of enol form. On complexation, the carbonyl and the methine carbons experience downfield shifts (from TMS) whereas the thiocarbonyl carbon shows an upfield shift. This suggests that the electrons are delocalised in both the chelate rings of the complex leading to the "quasi-aromatic" character.

The ^{13}C NMR spectra of monothio-β-diketones and their metal complexes have proved to be of immense help in the elucidation of their structures. However, studies are mainly confined to ^{13}C and ^{19}F NMR spectra of fluoro alkyl groups[1-3], esters[4,5] and aryl groups[6,7], and no systematic ^{13}C NMR studies of the substituted monothiodibenzoylmethanes and their complexes have been done so far. In the present note, we are reporting the ^{13}C NMR studies of four *para*-substituted monothiodibenzoylmethanes and their zinc(II) complexes together with the ^{19}F NMR studies of 4'-fluoromonothiodibenzoylmethane and its Zn(II) complex.

p-Halo- and *p*-methyl-substituted monothiodibenzoylmethanes were prepared by the literature method[8]. For the preparation of zinc(II) complexes, a general method was followed which has been reported in an earlier publication[9]. The ^{13}C NMR spectra of the crystallised ligands and their complexes were recorded in chloroform on a JEOL FX-90-Q NMR spectrometer at 22.49 MHz using the $CHCl_3$ signal at δ 77.2 ppm as an internal standard. All the spectra were run over 5000 Hz spectral width using 8K data points and a pulse width of 5 μs. The ^{19}F NMR spectra were run in $CDCl_3$ at 84.25 MHz over a 15,150 Hz sweep width using 8K data points and a pulse width of 18 μs. ^{19}F signal of C_6F_6 at δ −162.5 ppm was used as an external standard.

The assignments of the chemical shift values to the thiocarbonyl carbon (C-1), methine carbon (C-2), enol carbon (C-3) and phenyl ring (B) carbons (Ca'...Cd') have been made on the basis of the literature reports[6,7] (see structure I). The phenylring (A) carbon (Ca...Cd) signals have been assigned on the basis of a previous report[7] and substituent chemical shift effects[10]. The chemical shifts of different carbons in the zinc(II) complexes have also been assigned in a similar manner. These assignments were checked by off-resonance experiments and low intensity of the signals of quarternary carbons. The chemical shift values are presented in Table 1.

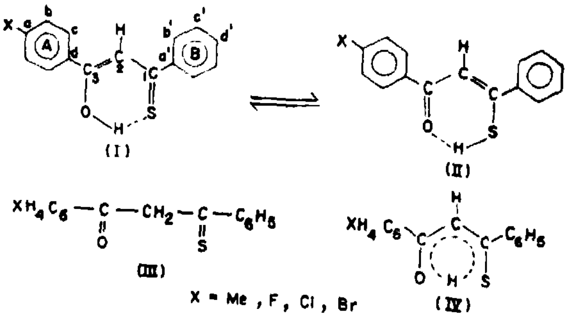

The monothio-β-diketones have been shown to exist in solution exclusively or preponderantly as equilibrium mixtures of the tautomeric *Z*-enol(I) and *Z*-enethiol(II) forms, which interconvert very rapidly (on the NMR time scale) by intramolecular chelate proton transfer[11,12]; this has been confirmed by recent dynamic proton NMR studies by Duus *et al.*[13]. The enolic form predominates in this equilibrium mixture and its percentage further increases on substitution in ring(A) because of the conjugative effect[14]. No evidence has been found for the existence of the thioxoketone tautomeric form(III). The existence of a "quasi-aromatic structure"(IV), similar to that found in β-diketones, has been ruled out for these compounds[14]. In the present studies, the distinct carbon signals are found for thiocarbonyl carbon (C-1), enol carbon (C-3) and methine carbon (C-2), but no signal is observed for methylene carbon corresponding to the structure(III). These results clearly support the earlier observations that monothio-β-diketones exist as equilibrium mixtures of *Z*-enol(I) and *Z*-enethiol(II) tautomers.

In the present studies, it is found that *p*-fluorosubstituent affects the chemical shift of the thiocarbonyl carbon most whereas this effect is less pronounced in the *p*-chloro- and *p*-bromo-substituted analogues. In *p*-halobenzenes, the mesomeric effect outweighs the inductive effect[15]. It is

Table 1—^{13}C Chemical Shifts (δ ppm) and Coupling Constants (Hz) of Some Substituted Monothiodibenzoylmethanes and Their Zinc(II) Complexes ($CHCl_3$, TMS, 27°C)

Compound	C−S	C−O	C−H	Substituted phenyl carbons				Phenyl carbon				CH_3
				Ca	Cb	Cc	Cd	Ca′	Cb′	Cc′	Cd′	
$FC_6H_4C(OH)CHCSC_6H_5$	201.4	178.7	110.3	164.6	115.9	129.5	131.8	145.0	126.7	128.4	131.0	..
(J_{C-F})				(277.2)	(22.0)	(9.7)	(2.4)					
$Zn(FC_6H_4COCHCSC_6H_5)_2$	188.8	186.3	115.1	153.1	115.5	130.2	135.8	147.1	127.2	128.2	131.0	..
(J_{C-F})				(270.0)	(22.0)	(9.7)	(2.4)					
$ClC_6H_4C(OH)CHCSC_6H_5$	203.6	178.2	110.3	138.9	128.7	128.8	134.2	145.4	126.9	128.6	129.3	..
$Zn(ClC_6H_4COCHCSC_6H_5)_2$	188.6	187.0	114.8	138.9	128.6	129.5	137.9	146.9	127.0	128.1	130.2	..
$BrC_6H_4C(OH)CHCSC_6H_5$	203.5	178.3	110.1	134.6	132.1	128.5	131.4	145.3	126.7	128.2	127.4	..
$Zn(BrC_6H_4COCHCSC_6H_5)_2$	203.1	189.1	115.1	130.1	130.4	129.9	128.5	131.9	127.3	128.5	127.8	..
$CH_3C_6H_4C(OH)CHCSC_6H_5$	204.1	179.4	110.3	143.5	129.5	127.2	132.7	145.6	126.8	128.3	130.9	21.6
$Zn(CH_3C_6H_4COCHCSC_6H_5)_2$	190.3	184.8	115.6	143.7	129.3	127.4	137.3	147.5	127.2	128.4	130.0	21.8

also known that among the halogens the mesomeric effect of fluorine is strongest because of its smallest size, and that of bromine is least. It is, therefore, obvious that thiocarbonyl carbon will be expected to be most shielded in *p*-fluorosubstituted ligand as compared to the other ligands.

The carbons of ring(A) experience shielding effect on substitution, which is most pronounced for Ca and Cb, whereas phenyl ring (B) carbons are not, as expected, appreciably affected. Further, coupling with fluorine is observed in the *p*-fluoro ligand and values of the coupling constants are consistent with the reported values[10].

In ^{19}F NMR spectrum of 4′-fluoromonothiodibenzoylmethane, a singlet is observed at δ −104.3 ppm using the signal of C_6F_6 at δ −162.9 ppm as the external reference. Joshi *et al.*[16], however, reported this value as δ 30 ppm with reference to CF_3COOH.

The ^{13}C NMR spectrum of Zn(II) complex is found to be quite interesting. As expected, C-1 experiences a pronounced upfield shift while C-3 shows downfield shift. This clearly indicates that the thiocarbonyl and enol-carbons undergo changes in the opposite directions, the former acquires more single bond character while the latter shifts towards more double bond (carbonyl) character[17]. This indicates that in contrast to the liands, the chelate rings in the complex possibly acquire a "quasi-aromatic character" through delocalisation of electrons, which is in conformity with the earlier report[18]. The methine carbon experiences a downfield shift as per expectation.

The ^{19}F signal of Zn(II) complex of 4′-fluoromonothiodibenzoylmethine is observed at δ −103.84 ppm (ligand: −104.31) thereby showing the equivalence of the two chelate rings as expected in a square planar structure (structure V).

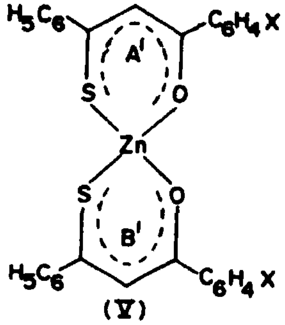

(V)

One of the authors (BRD) thanks the UGC, New Delhi for the award of a Teacher Research Fellowship, Prof. J.P. Tandon, Head of the Department for providing all necessary facilities and Sri Suman Gupta for recording NMR spectra.

References

1 Haworth D T & Das M, *J fluorine Chem*, **26(3)** (1984) 331.
2 Haworth D T & Das M, *J fluorine Chem*, **20** (1982) 487.
3 Das M & Haworth D T, *J inorg nucl Chem*, **43** (1981) 2317 and references therein.
4 Duus F & Hansen P E, *Org magn Reson*, **22(1)** (1984) 16.
5 Haworth D T & Das M, *J inorg nucl Chem*, **43** (1981) 2313.
6 Das M & Haworth D T, *Inorg chim Acta*, **64** (1982) L115.
7 Haworth D T & Das M, *Inorg nucl Chem Lett*, **16** (1980) 529.
8 Saini S K, Gupta V D & Mehrotra R C, *J Indian chem Soc*, **59** (1982) 1424.
9 Dubey B R & Rai A K, *Indian J Chem*, **24A** (1985) 294.
10 *Sadtler standard carbon-13 NMR spectra* (Sadtler Research Laboratories, Philadelphia, Pa) 1979.
11 Duus F & Anthonsen J W, *Acta chem scand*, **B31** (1977) 40.
12 Duus F, *J org Chem*, **42** (1977) 3123.
13 Berg U, Sandstrom J, Carlsen L & Duus F, *J chem Soc Perkin Trans II*, (1983) 1321.
14 Carlsen L & Duus F, *J chem Soc Perkin II*, (1980) 1768.
15 Das M & Livingstone S E, *J chem Soc Dalton*, (1975) 452.
16 Joshi K C, Pathak V N & Kumawat K R, *J chem Soc Perkin I*, (1977) 1127.
17 Wilkie C A & Haworth D T, *J inorg nucl Chem*, **40** (1978) 195.
18 Singh Y P & Rai A K, *Indian J Chem*, **23A** (1984) 350.

Indian Journal of Chemistry
Vol. 27A, March 1988, pp. 258-260

Structural Studies of Cu(II) & Ni(II) Complexes with a Chiral Schiff Base

L D DAVE, CHERIAN MATHEW*,
VARUGHESE OOMMEN & P K KRISHNAN NAMBOORI

University Department of Chemistry, Bhavnagar University,
Bhavnagar 364 002

Received 7 *October* 1986; *revised* 9 *January* 1987; *re-revised and accepted* 14 *May* 1987

Cu(II) and Ni(II) complexes of the schiff base derived from 6-ethoxy-2-hydroxynaphthaldehyde and isopropylenediamine [N,N'-bis(6-ethoxy-2-hydroxynaphthalidene)isopropylenediamine] have been prepared and characterised by elemental analysis, magnetic and spectral data. Circular dichroism spectral data show that the Cu(II) complex has a non-planar structure and the Ni(II) complex has a planar structure.

Investigations on metal complexes of chiral schiff bases have got a boost due to the fast development of circular dichroism and other spectrophotometric techniques. Divalent metal ion complexes of quadridentate schiff base ligands derived from the reaction of diamines with 2,5-dihydroxyacetophenone, 2,5-dihydroxypropiophenone and 2,5-dihydroxybenzophenone were assigned square-planar structure[1,2]. If the diamine involved in the schiff base condensation is made optically active $\pi \rightarrow \pi^*$ transitions in the chromophoric part of the ligands may couple and produce exciton components of opposite handedness in case of deviation from planarity of the coordination sphere in the complexes[3-5]. Circular dichroism spectral studies on Cu(II) complexes of the above ligands show that they have got a psuedotetrahedral structure[6]. This prompted us to undertake synthesis and characterization of Cu(II) and Ni(II) complexes of the chiral schiff base N,N'-bis(6-ethoxy-2-hydroxynaphthalidine)isopropylenediamine(I).

Isopropylenediamine was resolved by standard procedure described by Dwyer *et al.*[7] This was treated with 6-ethoxy-2-hydroxynaphthaldehyde when yellow crystalline schiff base was instantaneously obtained. It is soluble in almost all common organic solvents. It was recrystallised from chloroform (m.p. 93°C).

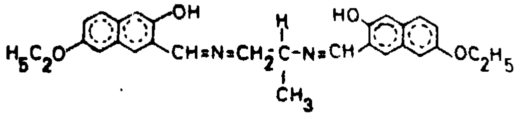

(I)

The metal complexes were prepared by mixing hot equimolar solutions of ligand in methanol and copper nitrate/nickel nitrate in water. The Ni(II) complex was formed at $pH \approx 6$. The complexes were digested on a waterbath and extracted several times with chloroform. Finally, the complexes were recrystallised from chloroform. The copper complex is dark-green in colour while the nickel complex is reddish-yellow.

Carbon, hydrogen and nitrogen were estimated by micro-analytical methods. Copper and nickel were estimated gravimetrically as CuO and $Ni(DMG)_2$. Analytical data: Cu(II) complex: Found: C, 64.95; H, 5.23; N, 5.29; Cu, 12.00. Calc.: C, 65.46; H, 5.30, N, 5.26; Cu, 11.94%; Ni(II) complex: Found: C, 65.81; H, 5.29; N, 5.24; Ni, 11.13. Calc.: C, 66.06; H, 5.35; N, 5.32; Ni, 11.14%.

Elemental analyses show that the complexes have 1:1 (M:L) ratio. Thus, the ligand behaves in a quadridentate dibasic manner. Molecular weights of the complexes determined ebullioscopically in chloroform revealed their monomeric nature. Conductivity measurements showed the covalent nature (2.2-2.7 mhos cm^2 mol^{-1}) of these complexes.

Room temperature magnetic moment obtained using Gouy method for Cu(II) complex was found to be 2.2 B.M. The excess over that required for one unpaired electron may be due to spin-orbit coupling. The Ni(II) complex was found to be diamagnetic.

IR spectra of both the complexes are similar. A band observed at 3480 cm^{-1} in the spectrum of ligand, assigned to $\nu O-H$, is not observed in the spectra of the complexes suggesting the involvement of oxygen atom of the hydroxyl group in coordination after deprotonation of OH. The band observed at 1580 cm^{-1} in the ligand spectrum due to $\nu C=N$ is shifted to 1630 cm^{-1} in the complexes suggesting the involvement of the azomethine group ($>C=N$) in complexation through the nitrogen atom. $\nu M-N$ and $\nu M-O$ modes were observed at 530 and 420 cm^{-1} respectively.

The absorption spectrum of the Cu(II) complex showed only one band at 562 nm which is typical of square-planar complexes. The spectrum of the Ni(II) complex showed three weak bands[8] at 557, 686 and 712 nm due to the transitions ${}^1E_g \leftarrow {}^1A_{1g}$, ${}^1A_{2g} \leftarrow {}^1A_{1g}$ and ${}^1B_{1g} \leftarrow {}^1A_{1g}$, respectively.

Polycrystalline state EPR spectrum of the Cu(II) complex showed the anisotropic character of the

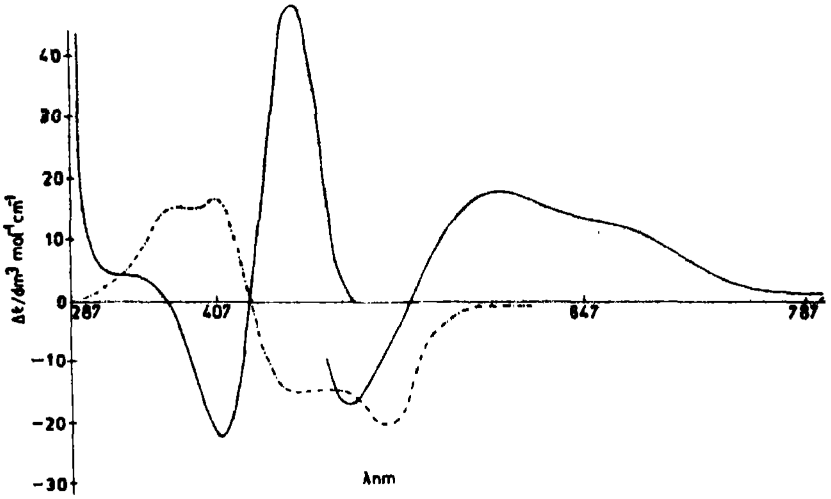

Fig. 1—CD Spectrum of Cu(II) complex (——) in chloroform and of the ligand (------) in chloroform

complex. The solution spectrum in a mixture of $CHCl_3$ and acetone at room temperature showed four g_{iso} bands. The two bands at higher field showed superhyperfine splitting due to nitrogen. g_{iso} and A_{iso} values have been calculated to be 2.092 and 89.13G respectively. The solution spectrum at liquid nitrogen temperature gave three values for the *g*-tensor, g_x (2.02), g_y (2.07) and g_z (2.185). The g_{av} value calculated was found to be exactly the same as the g_{iso} value (2.092) obtained from room temperature spectrum. The first band in the $g_{\parallel}$ region showed the splitting due to nitrogen. $A_{\parallel} = 200G$, $A_0 = 89.13$ G, $A_x^{('' } = 7.0G$ and $A_y^{('' } = 9.0$ G were also calculated from the spectra. Since three *g*-factors are observed, the molecule is rhombic with the unpaired electron in the $d_{x^2-y^2}$ orbital with the ground state term $^2B_{1g}$. The values $g_{\parallel}/A_{\parallel} = 109.25$ and $A_{\parallel}$ are in the range expected for square planar complexes.

NMR spectrum of the Ni(II) complex showed a signal at τ 8.6 which could be due to the two $-CH_3$ groups in the ethoxy moiety attached to the naphthyl ring. The $-CH_2$ groups attached to the $-CH_3$ group broaden the $-CH_3$ peak due to *J-J* coupling. The signal due to $-CH_2$ group was found at τ 3.7. This signal was deshielded by the presence of oxygen atom. The peak at τ 8.3 could be due to the $-CH_3$ group attached to the asymmetric carbon atom of the diamine. This was not split, confirming that this $-CH_3$ group is chemically isolated from other protons as is evident from the proposed structure. Two sharp peaks observed at τ 7.0 and 7.1 are assigned to the $\geq CH$ group of the aldehyde through which the diamine group is attached to the naphthyl ring. The $-CH_2$ group in the diamine part gave a signal at τ 6.4. The signals due to aromatic protons were observed as strong peaks at τ = 3.1, 2.65 and 2.80. The proton attached to the asymmetric carbon atom in the coordination sphere gave signal at τ 2.7. It is highly deshielded and this deshielding could be due to its position in the coordination sphere.

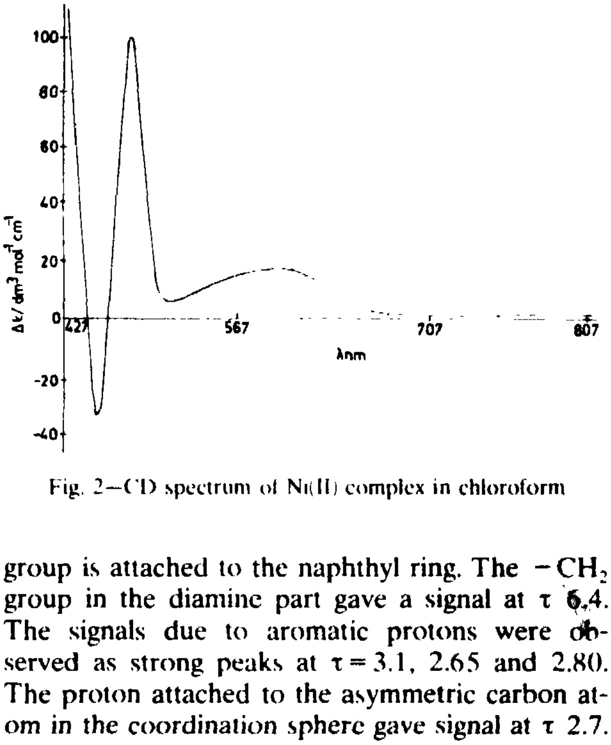

Fig. 2—CD spectrum of Ni(II) complex in chloroform

The circular dichroism (CD) spectrum of the ligand is typical of exciton coupling in a gauche conformation with negative optical factor for the low energy component. The observed fine structure in the CD spectrum could be due to an overlayed $n \rightarrow \pi^*$ transition as shown below:

$$>\overset{\frown}{C{=}N:} \longrightarrow >C{=}N:$$

In the CD spectrum of the Cu(II) complex of the schiff base, transition region of the chromophore is observed at the same energy level as in the spectrum of schiff base (Fig. 1); furthermore, it exhibits a CD spectrum typical of exciton coupling. This indicates a tetrahedral distortion of the Cu(II) coordination sphere. The low energy exciton component of the complex has a positive optical factor whereas that of the ligand has a negative optical factor. This suggests that the absolute configuration of the ligand part in the complex is opposite to that of the free ligand. The CD spectrum of the complex shows an envelope in the $\pi \rightarrow \pi^*$ region, indicating the copper complex to be non-planar. Hence the CD spectrum of the Cu(II) complex suggests a psuedotetrahedral, i.e., a deformed square-planar structure for the complex. However, the electronic and EPR spectra clearly point to a square-planar strucutre for Cu(II) complex. The distortion from square-planar towards tetrahedral structure suggested by the CD spectrum must, therefore, be small. In the spectrum of Ni(II) complex (Fig. 2), the transition regions of the chromophore of the ligand and the complex are at different energies suggesting the absence of tetrahedral distortion of the Ni(II) coordination sphere. There is no envelope in the $\pi \rightarrow \pi^*$ region in the CD spectrum suggesting a planar structure for Ni(II) complex. Like in the case of Cu(II) complex, the absolute configuration of the ligand part in the complex is opposite to that of the free ligand since the low energy exciton component of the complex has a positive optical factor whereas that of the ligand has a negative optical factor as is evident from the CD spectra of the two. Hence, it is concluded that the Ni(II) complex is square-planar.

Two of the authors (CM & VO) thank CSIR, New Delhi and Bhavnagar University, respectively, for financial assistance.

References

1 Dave L D & Mohankumar V B, *Indian J Chem*, **12A** (1974) 984.

2 Dave L D & Prasad B G S, *Indian J Chem*, **12A** (1974) 1002.

3 Larsen E, *Acta chem scand*, **23** (1969) 2158.

4 Jensen H P & Warsen E, *Acta chem scand*, **25** (1971) 1439

5 Bernth N, Larsen E & Larsen S, *Tetrahedron*, **37** (1981) 2477.

6 Jensen H P, *Indian J Chem*, **23A** (1984) 475.

7 Dwyer F P, Garvani F L & Schulmann, *J Am chem Soc*, **81** (1959) 290.

8 Lever A B P, *Inorganic electronic spectroscopy* (Elsevier, New York) 1968, 343.

Indian Journal of Chemistry
Vol. 27A, March 1988, pp. 261-263

Synthesis & Characterisation of Ternary Complexes of Copper(II) with 2-Hydroxy-1-naphthaldehyde & α-Amino Acids

B V MRUDULA RAO, G VENKATANARAYANA
& P LINGAIAH*
Department of Chemistry, Kakatiya University,
Warangal 506 009

Received 8 *April* 1987; *revised and accepted* 3 *August* 1987

The ternary complexes of Cu(II) with 2-hydroxy-1-naphthaldehyde (A^1) and some α-amino acids have been synthesized and characterized by analytical, conductivity, thermal, magnetic, infrared, electronic and ESR spectral data. Based on analytical and thermal data, the stoichiometry of the complexes is found to be 1:1:1. The infrared spectral data of the ternary complexes (1) [Cu A^1 gly]; (2) [Cu A^1 α-ala]; (3) [Cu A^1 β-ala]; (4) [Cu A^1 val]; (5) [Cu A^1 leu]; (6) [Cu A^1 ϕ-ala]; (7) [Cu A^1 ser] and (8) [Cu A^1 threo] indicate that the ligands act as bidentate ones while in the complexes (9) [Cu A^1 his H_2O]; (10) H[Cu A^1 asp.H_2O] and (11) [Cu A^1.glut.H_2O], the amino acids act as tridentate ligands. The electronic spectra of the Cu(II) complexes suggest that complexes 1-8 are square-planar while complexes 9-11 are tetragonal. Various parameters like $g_{\parallel}$, $g_{\perp}$, α^2 and λ have been calculated from ESR spectral data.

In continuation of our earlier work on mixed ligand complexes of copper(II) and dioxouranium(VI)[1,2], we report here the preparation and characterisation of ternary complexes of Cu(II) with O^-, O^- donor ligand 2-hydroxy-1-naphthaldehyde (A^1) and O^-, N-donors glycine (gly), DL-α-alanine (α-ala), DL-β-alanine (β-ala), L-valine (val), L-leucine (leu), DL-phenylalanine (ala), DL-serine (ser), DL-threonine (threo), L-histidine (hist), L-aspartic acid (asp) and L-glutamic acid (glut).

The ligand 2-hydroxy-1-naphthaldehyde was obtained from Sigma Chemical Company (USA) while α-amino acids were obtained from Loba Chemical Company and were recrystallized before use. Their purities were checked by TLC and melting point determination.

The following general procedure was adopted for the synthesis of ternary complexes of Cu(II) with 2-hydroxy-1-naphthaldehyde (A^1) and the α-amino acids:

The solutions of 2-hydroxy-1-naphthaldehyde (0.02 mol) in methanol and of amino acid (0.02 mol) in water were simultaneously added to a methanolic solution of copper acetate (0.01 mol) with constant stirring. The *p*H of the resulting solution was adjusted (6-7) by adding sodium acetate. The reaction mixture was refluxed on a water bath for about 30 min. On cooling the reaction mixture, the solid complex separated out, which was filtered and washed with hot water and methanol to remove the excess ligand and the metal ion. The complexes so obtained were dried *in vacuo* over fused anhydrous calcium chloride.

The analytical data (C, H and N) for the solid complexes were obtained from the Micro-analytical Laboratory, Calcutta University, Calcutta. The metal contents in the complexes were determined by standard procedures[3]. The conductivity measurements were made in DMF using a Digital Conductivity bridge model-304. The magnetic susceptibility measurements were made at room temperature by Gouy method using $Hg[Co(NCS)_4]$ as the calibrant. Diamagnetic corrections were made using Pascal's constants. The thermal data of the complexes were obtained using a Stanton thermobalance. The infrared spectra of the ligands and complexes (4000-200 cm^{-1}) were recorded on a Perkin-Elmer infrared spectrophotometer model-283. The electronic spectra of the complexes were recorded in DMF on a Shimadzu Multipurpose spectrophotometer model MPS-5000. The ESR spectra of the complexes were recorded in solid state at room temperature on a varian V_3 Q spectrometer.

All the complexes are non-hygroscopic, stable at room temperature, insoluble in water and common organic solvents, but soluble in DMF and DMSO. The molar conductances of 1×10^{-3} *M* solutions of the complexes of 1-9 (see Table 1) were low (10-15 ohm^{-1} cm^2 mol^{-1}) indicating them to be non-electrolytes. The values for the complexes (10) and (11) were in the range 40-60 ohm^{-1} cm^2 mol^{-1} indicating that they were 1:1 electrolytes[4]. The elemental analysis and conductivity data of the complexes support the formulation of complexes shown in Table 1.

All the complexes except (9) to (11) were thermally stable upto 225°C indicating that they were not hydrated. This was confirmed by the absence of endothermic peak in the DTA curves of these complexes in the temperature range 150-200°C. The complexes (9) to (11) showed an endothermic peak in the temperature range 160-190°C indicating the presence of coordinated water[5]. The amount of water present in these complexes was confirmed by the thermogravimetric curves. These curves showed a mass loss in the temperature range 150-200°C which corresponded to one water molecule. All the complexes decomposed in a

Table 1—Elemental Analyses, Electronic Spectral and Magnetic Moments of Copper(II) Complexes

S. No	Complex	m.p. (°C)	Found (Calc.), %				ν_{max} (cm^{-1})	Magnetic moment (B.M.)
			Metal	C	H	N		
1	[Cu A^{1} gly]	280	19.88 (20.66)	50.96 (50.56)	3.88 (3.57)	4.36 (4.52)	15625 20533	1.88 (1.85)
2	[Cu A^{1} α-ala]	265	19.04 (19.71)	51.03 (52.08)	4.13 (4.03)	3.95 (4.34)	15625 24570	1.87 (1.83)
3	[Cu A^{1} β-ala]	275	19.18 (19.71)	51.37 (52.08)	3.86 (4.03)	4.21 (4.34)	15504 24570	1.88 (1.85)
4	[Cu A^{1} val]	270	17.64 (18.13)	53.77 (54.76)	4.36 (4.85)	4.27 (4.99)	15337 20618	1.90 (1.86)
5	[Cu A^{1} leu]	265	16.85 (17.44)	55.18 (55.96)	5.16 (5.21)	4.02 (3.84)	15455 20471	1.87 (1.85)
6	[Cu A^{1} O-ala]	255	15.03 (15.48)	61.04 (61.46)	3.97 (4.17)	3.28 (3.41)	15503 20672	1.82 (1.85)
7	[Cu A^{1} ser]	275	18.54 (18.54)	49.27 (49.62)	3.59 (3.84)	3.94 (4.14)	15552 24390	1.84 (1.86)
8	[Cu A^{1} threo]	250	17.62 (18.03)	50.56 (51.05)	4.33 (4.25)	3.68 (3.97)	15576 24570	1.86 (1.85)
9	[Cu A^{1} hist.H$_2$O]	255	15.67 (16.15)	49.04 (48.78)	3.74 (4.07)	10.44 (10.67)	16000*	1.90 (1.81)
10	H[Cu A^{1} asp.H$_2$O]	275	16.15 (16.57)	46.16 (46.93)	4.03 (3.65)	3.38 (3.65)	15625*	1.82 (1.82)
11	H[Cu A^{1} glut.H$_2$O]	265	15.36 (15.95)	48.35 (48.17)	4.13 (4.27)	3.22 (3.1)	15576*	1.89 (1.83)

*Broad band indicates the overlapping of different transitions.

single step in the temperature range 250-500°C corresponding to the loss of ligand moiety. The final products of decomposition as computed from the pyrolysis corresponded in each case to metallic oxide.

The presence of characteristic bands of the two ligands in the IR spectra of the complexes indicate the formation of ternary complexes. The bands observed at 3360(b) and 1725 cm^{-1} in the infrared spectrum of 2-hydroxy-1-naphthaldehyde are assigned to stretching vibrations of phenolic hydroxyl and ν(C=O) of aldehyde group, respectively. The disappearance of the former band and a shift in latter towards lower frequency region (35-50 cm^{-1}) in all the ternary complexes confirms the involvement of phenolic oxygen, with deprotonation, and carbonyl oxygen in the coordination. The bands around 3265 and 3120 cm^{-1} observed in the IR spectra of free amino acids are assigned to ν_{as} (NH$_2$) and ν_s (NH$_2$) respectively[6-8]. In the ternary complexes, a shift of the NH$_2$ stretching vibrations to lower frequency side ($\Delta\nu = 50$-80 cm^{-1}) shows the complex formation through amino nitrogen. Further, the free ligands display a band at 1515 cm^{-1} due to the bending vibration of NH$_2$ group. In the complexes this band undergoes a negative shift to an extent of 40-50 cm^{-1}, confirming the involvement of amino group in coordination. The ν_{as}COO and ν_sCOO modes of the carboxylate anion in the IR spectra of free amino acids occur in the regions 1630-1600 and 1420-1400 cm^{-1}, respectively. These bands are shifted towards the lower frequency region by 25-30 and 30-40 cm^{-1}, respectively in the ternary complexes indicating the participation of carboxylic oxygen in coordination. Further, the disappearance of the ν(O−H) of the carboxylic group, appearing at 2600 cm^{-1} in the IR spectra of free amino acids, confirms its involvement in coordination[9].

The amino acids containing hydroxyl group, like serine and threonine, show an additional broad band centred at 2800 cm^{-1} due to the ν(O−H). The lower position of this band indicates the involvement of this group in hydrogen bonding with the nitrogen of the amino group. The non-disappearance of this band in their ternary complexes confirms the non-involvement of hydroxyl oxygen in coordination with the central metal ion.

In the IR spectrum of free histidine, broad bands observed at 3230 and 3160 cm^{-1} may be assigned to the asymmetric and symmetric stretching of the amino and imino grops. A shift of these bands towards the lower region to an extent of 30-20 cm^{-1} in the ternary complex is observed;

Table 2—ESR Spectral Data of Copper(II) Complexes

S. No.	Complex	$g_\parallel$	$g_\perp$	$\lvert g \rvert$	α^2	$-\lambda$ (cm^{-1})
1	[Cu A^1 gly]	2.25	2.08	2.13	0.603	249
2	[Cu A^1 α-ala]	2.23	2.07	2.12	0.556	230
3	[Cu A^1 β-ala]	2.25	2.08	2.14	0.645	267
4	[Cu A^1 val]	2.22	2.11	2.15	0.684	283
5	[Cu A^1 leu]	2.22	2.10	2.14	0.642	266
6	[Cu A^1 O-ala]	2.23	2.07	2.12	0.551	228
7	[Cu A^1 ser]	2.23	2.10	2.14	0.647	268
8	[Cu A^1 threo]	2.22	2.10	2.14	0.648	268
9	[Cu A^1 hist.H_2O]	2.14	2.08	2.10	0.472	195
10	H[Cu A^1 asp.H_2O]	2.18	2.06	2.10	0.461	191
11	H[Cu A^1 glut.H_2O]	2.23	2.07	2.12	0.554	229

this indicates the involvement of amino and imino nitrogens in coordination with the metal ion.

In the complexes (9), (10) and (11) additional bands are observed around 3600-3200, 1630-1600 and 800-700 cm^{-1}, due to the presence of coordinated water and these are assigned to ν(OH), δ(HOH) and ρ(HOH), respectively[10]. Further, in the far infrared spectra all the complexes show vibrations of ν(Cu−N) and ν(Cu−O) around 500 and 400 cm^{-1} respectively[11-14].

The electronic spectra of the copper(II) complexes (1)-(8) show strong bands around 15500 and 25000 cm^{-1} which may be assigned to ${}^2B_{2g} \leftarrow {}^2B_{1g}$ and ${}^2E_g \leftarrow {}^2B_{1g}$ transitions respectively (characteristic of square planar geometry)[15], while the remaining complexes, (9)-(11), each show a broad absorption band around 16000 cm^{-1}. Tetragonal copper(II) complexes are expected to show the transitions ${}^2A_{1g} \leftarrow {}^2B_{1g}$, ${}^2B_{2g} \leftarrow {}^2B_{1g}$ and ${}^2E_g \leftarrow {}^2B_{1g}$, but bands due to these transitions usually overlap to give one broad absorption band[16]. The broad band observed in the present complexes around 16000 cm^{-1} suggests that it has tetragonal configuration around copper(II) ion. Further, all the complexes show bands above 26000 cm^{-1} which are attributed to charge transfer[17].

All the complexes are found to be paramagnetic (Table 1) showing the presence of one unpaired electron. The small excess over the spin-only value (1.73 B.M.) observed in the present complexes may be due to spin-orbit coupling. The μ_{eff} for these complexes have also been calculated and the experimental values are in good agreement with the calculated ones.

The ESR spectra of Cu(II) complexes in solid state at room temperature exhibit two peaks, one intense absorption at high field and the other with lower intensity at low field. From these peaks the values of $g_\parallel$ and $g_\perp$ have been calculated using Kneubuhl's method[18]. All the complexes show an isotropic ESR spectra with $g_\parallel > g_\perp$ (Table 2), characteristic of $d_{x^2-y^2}$ ground state[19]. The $g_\parallel$ obtained for these Cu(II) complexes is less than 2.3 indicating that the metal-ligand bond is of covalent character[20]. The α^2 values for all the complexes fall in the range 0.4-0.6 indicating the presence of appreciable in-plane covalency[21].

The spin-orbit coupling constant (λ) for all the complexes is found to be less than that of the free metal ion ($\lambda_0 = -828$ cm^{-1}) suggesting considerable mixing of ground and excited terms. The $\lvert g \rvert$ values are also useful for calculating the magnetic moments (μ) of the complexes and the calculated values are in agreement with the experimental ones[22].

Two of the authors (B V M and G V N) thank CSIR, New Delhi, for the award of research fellowships.

References

1 Ravindar V, Venkatanarayana G, Mrudula Rao B V, Swamy S J & Lingaiah P, *Indian J Chem*, **23A** (1984) 336.

2 Mrudula Rao B V, Swamy S J & Ligaiah P, *Indian J Chem*, **24A** (1985) 887.

3 Vogel A I, *A text book of quantitative inorganic analysis* (Longman, London) 1968, 358.

4 Geary W J, *Coord Chem Rev*, 7 (1971) 81.

5 Nikolaev A V, Myachina L I & Logvinenko V A, *Thermal analysis*, (Academic Press, New York), **2** (1969) 779.

6 Tsuboi M, Onishi K, Nakagawa I, Shimanouchi T & Mizushima S, *Spectrochim Acta*, **12** (1958) 253.

7 Fukushima K, Onishi K, Shimanouchi T & Mizushima S, *Spectrochim Acta*, **14** (1959) 236.

8 Sen D N, Mizushima S, Kurran C & Quagliano J V, *J Am chem Soc*, 77 (1955) 211.

9 Young R P, *J heterocyclic Chem*, **9** (1972) 371.

10 Nakamato K, *Infrared and Raman spectra of inorganic and coordination compouns* (Wiley, New York), 1978, 227.

11 Adams D M, *Metal ligand and related vibrations* (Arnold, London), 1967.

12 Prabhakaran C P & Patel C C, *J inorg nucl Chem*, 37 (1975) 1901.

13 Djordjevic C, *Spectrochim Acta*, **17** (1961) 448.

14 Behnke G T & Nakamato K, *Inorg Chem*, **6** (1967) 443.

15 Werden B C, Billing E & Gray H B, *Inorg Chem*, **2** (1963) 97.

16 Nishida Y & Kida S, *Coord Chem Rev*, **27** (1979) 275.

17 Hatzield W J & Wyman R, *Transition metal chemistry*, Edited by R C Carlin (Marcel Dekker, N.Y.) 1968.

18 Kneubuhl F K, *J chem Phys*, **33** (1960) 1074.

19 Ballhausen C J, *Introduction to ligand field theory* (McGraw-Hill, New York) 1962, 134.

20 Kivelson D K & Neiman R, *J chem Phys*, **35** (1961) 149.

21 Satyanarayana M & Sastry Siva Rama, *Indian J Chem*, **13A** (1975) 611.

22 Laxma Reddy K, Sri Hari S & Lingaiah P, *Indian J Chem*, **23A** (1984) 172.

Indian Journal of Chemistry
Vol. 27A, March 1988, pp. 264-266

Stabilities & Thermodynamic Functions of the Complexes of Dimethyltin(IV) Ion with Some Amino Acids

KH AJIT SINGH, (Miss) G SINGH & V D GUPTA*

Department of Chemistry, Faculty of Science, Banaras Hindu University, Varanasi 221 005

Received 20 *April* 1987; *revised and accepted* 2 *July* 1987

Proton-ligand and dimethyltin(IV) complex formation constants of glycine, DL-alanine and DL-methionine have been determined potentiometrically at 20°, 30° and 40°C and constant ionic strength ($\mu = 0.1$ *M*-sodium chloride). The stability constants of the complex species (ML) formed in the *p*H range 3.5-5.5 have been determined. The values of changes in free energy (ΔG), enthalpy (ΔH), entropy (ΔS) and heat capacity (ΔC_p) accompanying the complex formation have also been determined.

Despite the significance of organotin(IV) derivatives from the environmental point of view[1], the information about the stability of the complexes of dialkyltin(IV) ions in solution is still meagre[2-4]. The present note describes the results of our investigations on complexes formed by the dimethyltin(IV) ion in solution with glycine, DL-alanine and DL-methionine at various temperatures; formation of only one type of complexes, $(CH_3)_2SnL$, is anticipated[2]. The stability constants were computed in 75% (v/v) dioxan-water medium to avoid hydrolysis, the evidences of which have already been produced in an earlier publication[4].

Experimental details are the same as described earlier[4]. Glycine used was an Aldrich Chemical Company product, DL-alanine and DL-methionine were EGA-Chemie reagents and dimethyltin dichloride was an Alfa product. Preliminary titrations were carried out on a high precision Beckman *p*H meter (model ϕ 71). The ionic strength was adjusted to 0.1 *M* with AR grade sodium chloride. The combined electrode used was a Beckman electrode (39820, S 311 A) and its linearity was checked before and after the experiments. The *p*H-meter was calibrated at *p*H 4.00 with 0.05 M potassium hydrogen phthalate. Correction factors[3,5] [$\log_{10} U_H = 0.08$ at 20°C, 0.13 at 30°C and 0.17 at 40°C] were applied to the observed *p*H values to obtain the correct *p*H in dioxan-water media.

Table 1—Acid Dissociation Constants of Glycine, DL-Alanine and DL-Methionine

Amino acid	Temp. (±0.1°C)	Acid dissociation constants			
		From slope & intercept		From $\bar{n}_H$ and *p*H	
		pK_1	pK_2	pK_1	pK_2
Glycine	20°C	3.04	10.36	3.10±0.08	10.30±0.01
	30°C	2.903	10.25	3.08±0.08	10.24±0.03
	40°C	2.47	8.80	2.57±0.09	8.75±0.02
DL-Alanine	20°C	2.77	10.10	2.82±0.01	10.04±0.07
	30°C	2.73	9.49	2.81±0.04	9.48±0.016
	40°C	1.908	9.41	2.08±0.05	9.35±0.04
DL-Methionine	20°C	3.11	10.48	3.22±0.03	10.44±0.03
	30°C	2.92	10.08	3.16±0.09	10.14±0.016
	40°C	2.86	9.37	3.05±0.06	9.32±0.01

The first and second acid dissociation constants of the amino acids were computed by two methods: (i) slope and intercept method due to Irving and Rossotti[6,7] and (ii) from *p*H and $\bar{n}_H$ (the degree of proton-ligand complex formation) using the method of Hartley, Burgees and Alcock[8]. pK_1 and pK_2 values calculated from the two methods were in good agreement, but the values obtained from the second method were used for the calculation of stability constants, as this method enabled us to calculate pK_1 and pK_2 values at different $\bar{n}_H$ values. The apparatus and procedure were checked by determining the dissociation constants of glycine at 25°C. The values found ($pK_1 = 2.46$, $pK_2 = 9.79$) agreed well with those previously reported[9] ($pK_1 = 2.41$, $pK_2 = 9.76$). The degree of formation of the complexes, and the free ligand exponent, *pL*, were calculated by literature procedure[10]. Stability constants of the complexes were directly read from $\bar{n}-pL$ plots[3,4]; these were also computed by Irving and Rossotti's curve fitting method[6,11] and by the use of Henderson's or Hasselbalch's equation[6] over a limited range. The curve fitting method helped us refine the log K_1 values obtained from $\bar{n}$-*pL* plot. The experimental $\bar{n}(pL)$ data were fitted with the normalised curves calculated for 1:1 complexes. When best fits were obtained, the regions in which the experimental $\bar{n}(pL)$ data fitted the calculated curve were carefully chosen for the calculation of log K_1 using Henderson's or Hasselbalch's equation[6],

$$\log \frac{\bar{n}}{1-\bar{n}} = \log K_1 + \log[L]$$

Stoichiometric formation constants calculated from the above mentioned methods were in good

Table 2—Formation Constants of Dimethyltin(IV) Amino Acid Systems

Amino acid	Temp. (± 0.1°C)	log K_1			log β_1
		From half $\bar{n}$ method	From curve fitting method	From Henderson's or Hasselbalch's equation	
Glycine	20°C	7.75	7.74	7.75 ± 0.02	11.31 ± 0.07
	30°C	7.71	7.68	7.67 ± 0.02	11.35 ± 0.07
	40°C	6.85	6.88	6.88 ± 0.03	10.68 ± 0.11
DL-Alanine	20°C	8.03	8.02	7.98 ± 0.08	11.54 ± 0.28
	30°C	7.67	7.68	7.68 ± 0.08	11.36 ± 0.29
	40°C	6.92	6.90	6.93 ± 0.05	11.73 ± 0.19
DL-Methionine	20°C	7.72	7.73	7.70 ± 0.04	11.26 ± 0.14
	30°C	7.24	7.22	7.18 ± 0.03	10.86 ± 0.11
	40°C	7.08	7.01	7.006 ± 0.08	10.806 ± 0.30

Table 3—Thermodynamic Parameters

System	$-\Delta G$(kcal mol^{-1})			$-\Delta H$(kcal mol^{-1})	ΔS(cal deg^{-1} mol^{-1})
	$-\Delta G_{293}$	$-\Delta G_{303}$	$-\Delta G_{313}$		
Dimethyltin dichloride-glycine	15.16	15.73	15.29	11.44	13.15
Dimethyltin dichloride-DL-alanine	15.75	15.36	16.20	9.80	18.66
Dimethyltin dichloride-DL-methionine	15.09	15.05	15.47	8.80	21.19

agreement but the values of log K_1 obtained from Henderson's or Hasselbalch's equation were used for the calculation of thermodynamic formation constants (log β_1), as this method enabled us to calculate log K_1 values from different values of $\bar{n}$ along with the mean deviations. The thermodynamic stability constant (log β_1) was calculated from the equation[4,12,13]:

$$\log \beta_1 = \log K_1 + 4 \log[1/\gamma \pm]$$

log $[1/\gamma \pm]$ values (0.89, 0.92 and 0.95 at 20°C, 30°C and 40°C respectively) determined by Harned and Oven[14] for HCl in dioxan-water mixture (75% v/v) at constant ionic strength ($\mu = 0.1$ M−NaCl), were used for the calculation of log β_1. The change in free energy was calculated from the equation $-\Delta G = 2.303$ RT log β_1, where R = gas constant, T = absolute temperature. The other thermodynamic functions; ΔH, ΔS and ΔC_p, were calculated by plotting log β_1 vs T^{-1}. Values of ΔH and ΔS were calculated from the slope and intercept respectively[3].

Values calculated for the proton-ligand and dimethyltin(IV) complex formation constants are given in Tables 1 and 2. In the pH range 3.5-5.5, $\bar{n}$ values never rose above one and the experimental data in this range were interpreted for the formation of 1:1 complexes in all the cases. Equilibrium was always established very slowly, possibly owing to the slow dissociation of the complexes, ML, which would tend to be formed at the point where alkali was introduced into the solution[15].

Replacement of the methylene-hydrogen atoms in glycine is seen to produce a small increase in the values of pK_1 and pK_2. This is the expected consequence of electron repulsion by the alkyl groups[15]. In the present study, we note that despite the increased basicity of the nitrogen in H_2L (DL-alanine and DL-methionine) compared with that in glycine, there is little variation in the stabilities of the complexes studied. This may be attributed to (i) similarity in the structures of the amino acids, (ii) primarily steric origin of the differences in the values of pK_1 and pK_2 and (iii) probability that the conformational factors involved in the formation of complexes do not significantly influence the log K_1 values. This observation is in accord with the earlier report of Irving and Pettit[15] on the stabilities of complexes of bivalent cobalt, nickel, copper and zinc ions with some amino acids.

DL-Methionine, in contrast to glycine and DL-alanine, is expected to form a more stable complex since it contains a sulphur atom. But, on the contrary, the results obtained give a weak indication of sulphur-metal bonding. This is also in accord with earlier observation that in the complexes of uranyl and thorium ions with amino acids, there is weak bonding between the metal ions and the sulphur atom but relatively stronger bonding between the ions and oxygen donors[16].

Within the *p*H range 3.5-5.5, the straight lines with zero slopes, obtained by plotting $\frac{\bar{n}}{(1-\bar{n})[L]}$ against $\frac{(2-\bar{n})[L]}{(1-\bar{n})}$ supported the formation of 1:1 complexes[7]. The plots of log β_1 against T^{-1} are linear which indicate that the values of ΔC_p are equal to zero[3,4,17]. Values of ΔH and ΔS, calculated from the slopes and intercepts respectively of the above mentioned straight lines, are shown in Table 3 along with the values of ΔG.

Two of the authors (KAS and GS) are grateful to the Education Ministry, Govt. of Manipur and the CSIR, New Delhi, respectively for financial assistance.

References

1 Barnes J M & Magos L, *Organometal chem Rev*, **3** (1963) 137.
2 Tobias R & Yasuda M, *Inorg Chem*, **2** (1963) 207.
3 Singh G, Singh B & Gupta V D, *J Indian chem Soc*, **60** (1983) 987.
4 Singh G & Gupta V D, *Indian J Chem*, **24A** (1985) 440.
5 Bachlas B P, Rai A K & Gupta B P, *Mh Chim*, **108** (1977) 41.
6 Rossotti F J C & Rossotti H S, *Acta chem scand*, **9** (1955) 1166.
7 Ramamoorthy S & Santappa M, *Bull chem Soc Japan*, **41** (1968) 1330.
8 Hartley F R, Burgess C & Alcock R M, *Solution equilibria* (Ellis Hardwood limited, West Sussex, England) 1980.
9 Perrin D D, *J chem Soc*, (1958) 3125.
10 Irving H M & Rossotti H S, *J chem Soc*, (1954) 2904.
11 Sillen L G, *Acta chem scand*, **10** (1956) 186.
12 Mathur H B & Rao B, *J inorg nucl Chem*, **33** (1971) 2919.
13 Irving H & Rossotti H S, *J chem Soc*, (1953) 3397.
14 Harned H S & Oven B B, *The physical chemistry of electrolytic solution* (Reinhold, New York) 1958.
15 Irving H & Pettit L D, *J chem Soc*, **1** (1963) 1546.
16 Nourmand M & Meissam N, *J chem Soc Dalton Trans*, (1983) 1529.
17 Mcauley A & Nancollas G H, *J chem Soc*, (1961) 2215.

Indian Journal of Chemistry
Vol. 27A, March 1988, p. 267

Formation Constants of Binary Complexes of Lanthanides with 2-Hydroxymethylbenzimidazole

A NAGENDRAM, K L OMPRAKASH,
A V CHANDRA PAL* & M L N REDDY
Department of Chemistry, Osmania University,
Hyderabad 500 007

Received 19 *March* 1987; *revised and accepted* 16 *July* 1987

Proton-ligand and metal-ligand formation constants of binary complexes of La(III), Pr(III), Nd(III), Gd(III), Dy(III) and Y(III) with 2-hydroxymethylbenzimidazole have been determined *p*H-metrically in 50% v/v aq dioxane medium at 30°, 40° and 50°C and $I = 0.1$ M ($NaClO_4$). The thermodynamic parameters of complex formation have been evaluated. Stabilities (log β_2 values) of the chelates increase with decrease in ionic radius of the metal [Dy(III) > Gd(III) > Y(III) > Nd(III) > Pr(III) > La(III)].

In continuation of our studies on the complexing tendencies of benzimidazoles[1-3], we report herein the formation constants of binary complexes of the type ML_2 [where M = La(III), Pr(III), Nd(III), Gd(III), Dy(III), Y(III) and L = 2-hydroxymethylbenzimidazole (HMB)] in 50% v/v aq dioxane medium and I = 0.1 M($NaClO_4$).

The proton-ligand and metal-ligand formation constants for binary systems were determined using Irving-Rossotti *p*H titration technique[4]. The general experimental details were the same as discussed earlier[1-3]. The *p*H meter readings (B) in the aq dioxane media were corrected by the method of Van Uitert and Haas[5].

From the proton-ligand formation curves ($0.1 < \bar{n}_H < 1.8$) the proton-ligand formation constants log K_{OH} and log K_{NH} evaluated at 30° (12.59 and 5.03), 40° (12.12 and 4.74) and 50°C (11.46 and 4.52) are in accordance with the values reported by Lane and Durham[6].

From the formation curve ($\bar{n}$ vs *p*L), it is found that the log K_1 and log K_2 do not differ much from one another and hence they have been evaluated by the least-square treatment[4] of Eq. (1)

$$\frac{\bar{n}}{(\bar{n}-1)(L)} = \frac{(2-\bar{n})(L)}{(\bar{n}-1)}\beta_2 - K_1 \qquad \ldots (1)$$

Calculations using this method resulted in negative values of K_1 (positive intercept) and hence only log β_2 values are reported in Table 1.

Lane and Quinlan[7] have reported the formation of only 1:1 complexes of La(III) with 2-hydroxymethylnaphthimidazole. The formation of 1:2 complexes of Ln(III) with HMB in the present investigation is quite reasonable because of the lesser steric hindrance of benzimidazole moiety as compared to a naphthimidazole moiety.

Table 1—Formation Constants (log β_2) and Thermodynamic Parameters of Ln – HMB Chelates in 50% v/v aq dioxane medium

[$I = 0.1$ M($NaClO_4$)]

Temp (K)	Dy(III)	Gd(III)	Y(III)	Nd(III)	Pr(III)	La(III)
			log β_2			
303	16.79	16.55	16.47	16.11	15.89	15.36
313	16.63	16.44	16.38	16.01	15.81	15.30
323	16.48	16.35	16.30	15.92	15.74	15.25
			$-\Delta G$ (kJ mol^{-1} at 303 K)			
	97.1	96.0	95.5	93.4	92.2	89.1
			$-\Delta H$ (kJ mol^{-1})			
	28.9	18.8	16.3	17.5	15.3	9.8
			ΔS (JK^{-1} mol^{-1} at 303 K)			
	226.1	254.6	261.5	250.0	253.0	261.5

The order of stabilities (log β_2) of Ln(III) – HMB complexes [Dy(III) > Gd(III) > Y(III) > Nd(III) > Pr(III) > La(III)] is almost in the increasing order of their Z^2/r values indicating that the metal-ligand bond is primarily ionic.

The thermodynamic parameters, ΔG, ΔH and ΔS of formation of Ln – HMB complexes have been evaluated using well known equations and are presented in Table 1. The stabilities are found to decrease with increase in temperature suggesting that the interaction of Ln(III) ions with the ligand is exothermic in nature.

One of the authors (A N) is grateful to the CSIR, New Delhi, for the award of a senior research fellowship.

References

1 Omprakash K L, Chandra Pal A V & Reddy M L N, *Indian J Chem*, (a) **21A** (1982) 322; (b) **22A** (1983) 546.
2 Omprakash K L, Goverdhan Reddy K, Chandra Pal A V & Reddy M L N, *Indian J Chem*, **23A** (1984) 79.
3 Goverdhan Reddy K, Omprakash K L, Chandra Pal A V & Reddy M L N, *Indian J Chem*, **24A** (1985) 161.
4 (a) Irving H & Rossotti H S, *J chem Soc*, (1954) 2904; (b) (1953) 3397.
5 Van Uitert L G & Haas C G, *J Am chem Soc*, **75** (1953) 451.
6 Lane T J & Durham H B, *Inorg Chem*, **2** (1963) 632.
7 Lane T J & Quinlan K P, *J Am chem Soc*, **82** (1960) 2997.

Indian Journal of Chemistry
Vol. 27A, March 1988, pp. 268-270

Atomic Absorption Spectrophotometric Determination of Palladium After Separation by Coprecipitation of Its 2-Mercaptobenzimidazole Complex with Microcrystalline Naphthalene

M SATAKE, G KANO, S USAMI[*] & B K PURI[†]
Faculty of Engineering, Fukui University, Fukui 910, Japan

Received 23 *October* 1986; *revised and accepted* 21 *May* 1987

A highly sensitive and fairly selective atomic absorption spectrophotometric method has been developed for the determination of palladium after coprecipitation of its 2-mercaptobenzimidazole with microcrystalline naphthalene in the *p*H range 0.0-3.5 and 1-3*N* hydrochloric acid by shaking for a few seconds. Beer's law is obeyed in the concentration range of 3-80 μg of palladium in 10 ml of DMF solution (244.7 nm). Ten replicate determinations of a sample solution containing 50 μg of palladium gave a mean absorbance of 0.140 with a standard deviation of 0.0021 and a relative standard deviation of 1.5%. The method has been applied for the determination of palladium in various synthetic samples corresponding to standard alloys.

The reagent 2-mercaptobenzimidazole (2-MBI) has been used in the determination of a few metal ions by different techniques[1-5]. A method involving solid-liquid separation after liquid-liquid extraction has already been developed and applied to the separation and determination of certain metal ions[6-8]. Although, this method has many advantages over the usual liquid-liquid extraction[9], it is inconvenient as it is carried out at a high temperature, is time-consuming and cannot be applied for the extraction of thermally unstable complexes[10]. Recently, we have developed a better method involving separation of metals after coprecipitation of their metal complexes with microcrystalline naphthalene[11-14]. Herein, we report atomic absorption spectrophotometric (AAS) determination of palladium after coprecipitation of its 2-mercaptobenzimidazole complex with microcrystalline naphthalene.

Preliminary observations reveal that palladium reacts with this reagent to form a slightly water soluble and non-extractable complex. However, in the presence of sodium tetraphenylborate (TPB) this metal complex is insoluble in water and highly stable at room temperature but decomposes rapidly above 60 °C. The complex, therefore, cannot be extracted into molten naphthalene. This metal complex is also non-extractable into many of the non-aqueous organic solvents due to its poor solubility but can be coprecipitated from a large volume of the aqueous phase (~600 ml) with a very small amount of naphthalene (0.4 g) by shaking for a few seconds. The interference of various ions has been studied and the method has been employed for the trace determination of palladium in various synthetic samples.

A solution of palladium nitrate (AR) was prepared in doubly distilled water containing a few drops of nitric acid and standardized by known methods[15]. A solution (0.1%) of 2-MBI was prepared in ethanol, while solutions of TPB (1%) and naphthalene (20%) were prepared in water and acetone, respectively. A buffer solution of *p*H 1.5 was prepared by mixing 1*M* hydrochloric acid and 1*M* sodium chloride. A Perkin-Elmer model 403 atomic absorption spectrophotometer was used. It was fitted with a palladium hollow cathode lamp (244.7 nm); slit setting 4 (7A); current 10 mA; burner height from the top of the burner head 11 mm; acetylene flow 35 (pressure 0.5 kg/cm^2) and air flow 55 (pressure 2.1 kg/cm^2); and Toa-Dempa, HM-5A *p*H meter.

General procedure

To an aliquot of a sample solution containing 3-80 μg of palladium were added 2-MBI solution (0.1%, 2 ml), TPB solution (1%, 1 ml) and buffer (*p*H 1.5, 1 ml), mixed well and allowed to stand for 15 min for the precipitation of the metal complex. To this was added a 20% solution (2 ml) of naphthalene in acetone in a fast stream and the solution shaken vigorously for 30 sec. The solid mass was filtered off, dissolved in DMF and made upto volume in a 10 ml standard flask. This solution was aspirated into an air acetylene flame at 244.7 nm using a hollow palladium cathode lamp.

Reaction conditions were established by taking 50 μg of palladium. The Pd-2MBI complex was quantitatively coprecipitated with naphthalene in the *p*H range of 0-3.5 and 1-3*N* hydrochloric acid solution. Addition of 0.5-5.0 ml of HCl-NaCl buffer (*p*H 1.5) had no effect on the coprecipitation of the complex, therefore, 2 ml of buffer solution were used.

---

[*] Department of Industrial Chemistry, Faculty of Engineering, Toyama University, Toyama 930, Japan.

[†] Department of Chemistry, Indian Institute of Technology, Hauz Khas, New Delhi 110 016.

The effect of various electrolytes (0.001-0.1 *M*) on the coprecipitation of Pd-2-MBI complex was studied. Coprecipitation was 80% in the absence of these electrolytes, 87% in the presence of KNO_3, KCl and $NaClO_4$, 92% in the presence of sodium acetate and 100% in the presence of sodium tetraphenylborate (TBP). Therefore, 1 ml of 1% TPB solution was used in all experiments. Absorbance remained constant in the presence of 0.1 to 5.0 ml of the 2-MBI solution (0.1%). Hence to provide a safety margin 2 ml of 2-MBI solution (0.1%) were used throughout this study. Absorbance increased with the increase in volume of naphthalene upto 0.5 ml of 20% naphthalene solution and thereafter remained constant between 0.5 and 3.0 ml; therefore 2 ml of 20% naphthalene solution were used for coprecipitation of the metal complex. The coprecipitation was very rapid, being practically complete in less than 10 sec, and a shaking time of 30 sec giving an ample safety margin. A minimum standing time of 15 min at 25°C is recommended, although the reaction is complete in less than 5 min. Coprecipitation was quantitative if the volume of the aqueous phase did not exceed 600 ml. Evidently the technique is very good for the preconcentration of palladium from a large volume of the aqueous phase (600 ml) in a small volume of the organic phase (5 to 10 ml). The developed conditions have been utilized for the determination of palladium at low concentration in various synthetic samples where direct atomic absorption method is not possible.

The metal complex-naphthalene is insoluble in many non-aqueous organic solvents and water-miscible organic solvents like propylene carbonate, dioxane and DMSO but dissolves easily in acetone and DMF. Acetone being volatile is not preferred for AAS measurements. Therefore, DMF was preferred. The sensitivity for 1% absorption is 0.14 μg/ml in DMF while it is 0.27 μg/ml in water. Naturally the present method is more sensitive than the direct method. Sensitivity can be further improved by carrying out the coprecipitation from a large volume of the aqueous phase.

Under the optimum conditions developed, a calibration curve was constructed at 244.7 nm. It was found to be linear over thes concentration range 3.0-80.0 μg of palladium in 10 ml of DMF solution. Ten replicates determinations of a sample containing 50 μg of palladium gave a mean absorbance of 0.140 with a standard deviation of 0.0021 and a relative standard deviation of 1.5%.

Table 1 — Determination of Palladium in Synthetic Mixtures

Composition (%)	Amount taken (μg)	Amount of Pd[*] (μg)
Pt-Rh alloy		
Pt:80; Rh:19; Pd:0.25; Cu:0.25; Fe:0.5	Pt:3500; Rh:800; Pd:10; Cu:10; Fe:10	10 ± 0.2
	Pt:3000; Rh:1300, Cu:10; Fe:15; Pd:4	4.1 ± 0.3[†]
	Pt:3200; Rh:1000; Cu:50; Fe:48; Pd:2	1.9 ± 0.2[†]
Pt-Ni alloy		
Pt:50; Ni:40; V:7 5; Pd:2.5	Pt:500; Ni:500; V:80; Pd:20	19.8 ± 0.3
	Pt:550; Ni:450; V:100; Pd:2	2.1 ± 0.2[†]
	Pt:530; Ni:470; V:97; Pd:3	3.0 ± 0.2[†]
Pt-Ir alloy		
Pt:55; Ir:28; Rh:7; Pd:3.5; Fe:3.5; Cu:3	Pt:700; Ir:300; Rh:80; Pd:40; Fe:40; Cu:40	39.8 ± 0.5
	Pt:800; Ir:250; Rh:70; Fe:50; Cu:25; Pd:4	4.1 ± 0.2[†]

[*] Mean of five determinations, ± r.s.d.

[†] The coprecipitated mixture of Pd-2-MBI and naphthalene was dissolved in 5 ml of DMF using column attached with glass funnel.

Effect of diverse ions

Diverse ions were added individually to the sample solution containing 50 μg of palladium at *p*H 1.5 following the general procedure. The following (the amounts shown in parentheses) did not interfere: NaCl, $CH_3COONa.3H_2O$, KCl and $NaClO_4$ (2 g each); Na_2SO_4 and sodium citrate (1 g each); NH_4Cl (500 mg); KH_2PO_4 and EDTA (100 mg each); KSCN, $Na_2C_2O_4$, NH_4F, malonic acid and ethylenediamine (1 mg each); KI and thiourea (500 μg each); KCN (100 μg) and $Na_2S_2O_3.5H_2O$ (10 μg); Mg^{2+}, Ca^{2+}, Cd^{2+}, Pb^{2+}, Al^{3+} and Zn^{2+} (500 mg each); Cu^{2+} and Ni^{2+} (100 mg each); Mn^{2+}, Fe^{3+} and Co^{2+} (50 mg each); Mo^{6+} (10 mg), Rh^{3+}, Pt^{4+} and Ir^{3+} (5 mg each); V^{5+} (1 mg); Hg^{2+} (500 μg; could be tolerated upto 2 mg using KCl as the masking agent); Bi^{3+} and Os^{8+} (100 μg each; these could be tolerated upto 300 μg if the coprecipitation was carried out from 2*N* HCl); and Ru^{3+} (50 μg; but could be tolerated upto 200 μg using 400 μg of thiourea as the making agent at *p*H 3.2).

Preliminary observations reveal that Cd^{2+}, Rh^{3+}, Pt^{4+}, Zn^{2+}, Hg^{2+}, Cu^{2+}, Ru^{3+}, Os^{8+}, Ir^{3+}, Fe^{3+}, Ni^{2+}, Co^{2+}, Pb^{2+}, Mn^{2+}, Mo^{6+}, W^{6+}, V^{5+}, Bi^{3+} and Al^{3+} do not react with the reagent under these conditions hence these are not coprecipitated along with palladium.

Determination of palladium in synthetic samples

Various synthetic mixtures were prepared containing palladium along with other metals (Table 1). Since no standard samples of palladium were available, the compositions of the mixtures were adjusted in such a manner that these corresponded to the standard samples like Oakay and Palau. "Real" samples in case available, could be decomposed with aqua regia to obtain the desired oxidation states, Pd^{2+}. An aliquot of the solution was taken and palladium was determined by the general procedure (Table 1).

References

1 Lomakina L N & Alimarin I P, *Vest Mosk Gos Univ Ser Khim*, (1966) 79.
2 Bera B C & Chakrabarthy M M, *Analyt Chem*, **38** (1966) 1419.
3 Majumdar A K & Chakrabartty M M, *Anal chim Acta*, **20** (1959) 379.
4 Busev A I & Minh-Chau M, *Zh analit Khim*, **17** (1962) 1092.
5 Busev A I, Bairenko N L & Khoang M I, *Zh analit Khim*, **18** (1963) 1094.
6 Lin J L, Puri B K, Satake M & Endo M, *Mikrochim Acta*, **III** (1984) 87.
7 Nagahiro T, Uesugi K, Satake M & Puri B K, *Bull chem Soc, Japan*, **58** (1985) 1115.
8 Nagahiro T, Satake M & Puri B K, *Indian J Chem*, **25A** (1986) 99.
9 Puri B K & Gautam M, *Talanta*, **25** (1978) 484.
10 Puri B K, Gupta A K, Rao A L J & Satake M, *Croatica Chemica Acta*, **58** (1985) 91.
11 Nagahiro T, Satake M, Lin J L & Puri B K, *Analyst*, **109** (1984) 163.
12 Hussain M F, Puri B K, Bansal R K & Satake M, *Analyst*, **109** (1984) 1291.
13 Ishida K, Puri B K, Satake M & Mehra M C, *Talanta*, **32** (1985) 207.
14 Mehra M C, Nagahiro T & Satake M, *Microchem J*, **83** (1986) 198.
15 Vogel A I, *A textbook of quantitative inorganic analysis* (Longmans, London) 1969.

Indian Journal of Chemistry
Vol. 27A, March 1988, pp. 271-273

Extraction & Spectrophotometric Determination of Rhenium with Thiocyanate & Hydroxamic Acids

INDRANI SHARMA & A K CHAKRABURTTY*
Department of Chemistry, Jadavpur University,
Calcutta 700032

Received 21 *November* 1986; *revised* 16 *July* 1987; *accepted* 3 *August* 1987

The sensitivity and selectivity of Re(VII) estimation by the standard thiocyanate method can be improved by adding salicyl, cinnamoyl and anthranilo hydroxamic acids and subsequently extracting the mixed ligated complexes with methyl isobutyl ketone and determining Re(VII) in the organic layer spectrophotometrically against reagent blank. The λ_{max}, optimum ranges, molar absorptivities and Sandell's sensitivity are respectively 450 nm, 0.67-3-20 μg/ml, 4.8×10^4, 0.0038 μg/cm^2 for salicyl; 455 nm; 0.62-3.60 μg/ml, 4.9×10^4, 0.0037 μg/cm^2 for cinnamoyl; 470 nm, 0.27-1.60 μg/ml, 8.6×10^4, 0.0021 μg/cm^2 for anthranilo-hydroxamic acids. Most of the ions closely associated with rhenium do not interfere, excepting Mo(VI) and the platinum metal ions. The extractive separations of these interfering ions have also been worked out.

The thiocyanate method for the spectophotometric determination of rhenium[1] has undergone several modifications[2-6] and improvements have also been brought about using additional organic ligands like thiourea[7], 2-mercapto-benzo-γ-thiophene[8], hexamethylphosphoramide (HMPA)[9], impipramine[10] and chloropramazine[11]. Though some of these methods are sufficiently sensitive, they suffer from serious interferences due to other metal ions present in the system[7,8]. The method using HMPA[9] although quite selective is not sensitive enough. Other methods recommend too many steps. The present work describes the use of salicyl, cinnamoyl- and anthranilo-hydroxamic acids in conjunction with thiocyanate in enhancing the sensitivity and reducing interferences due to other ions.

A Hitachi 20-200 spectrophotometer and an Elico-L1 10 *p*H-meter were used respectively for spectrophotometric and *p*H measurements. All the chemicals used were of AR (Glaxo/BDH), GR (E Merck) or high purity grade and standardized when required. All the solvents used were doubly distilled.

Salicyl-(I)[12]-, cinnamoyl-(II)[13]- and anthranilo-(III)[14]-hydroxamic acids were prepared and recrystallised in the laboratory. Solutions of these acids were prepared in doubly distilled ethanol (for I and II) and 3:1 water-ethanol mixture (for III).

Stannous chloride solution was prepared by dissolving the salt in conc hydrochloric acid and subsequently diluting with water Ammonium thiocyanate solution was prepared in doubly distilled water and required strength obtained by proper dilutions.

A standard solution of rhenium (VII) was prepared by dissolving potassium perrhenate (HP, Johnson and Mathey) in water and standardized by internal electrolysis method[15]. Dilute solutions of rhenium (VII) were prepared by proper dilutions.

General Procedure

To an aliquot (0.75 ml) of perrhenate solution (20 ppm) was added conc hydrochloric acid (1.5 *M*-2.0 *M* final acidity) and stannous chloride (0.2 *M*, 1.0 ml for I, 0.5 ml for II 1.5 ml for III) followed by ammonium thiocyanate (2 *M*, 1 ml) and 5.5 ml of respective hydroxamic acids (0.2 *M*) (I, II or III). The total volume was made upto 10 ml (1.5 ppm of Re). The complexes formed were extracted with methyl isobutyl ketone (MIBK, 4 ml) after shaking vigorously for 3 min, the extraction being repeated twice with 2 ml portions of the solvent. The separated organic layers were dried over anhydrous sodium sulphate, transferred into 10 ml volumetric flasks and sodium sulphate was rinsed with MIBK. All the extracts with a single hydroxamic acid were collected in the same volumetric flask and the volume was made upto the mark with MIBK. Rhenium (VII) in these extracts was determined spectrophotometrically against reagent blanks. The optimum conditions for estimation with different hydroxamic acids are summarized in Table 1.

The absorption spectra of the systems against the respective reagent blanks showed two maxima in each case: 370, 450 nm for system I; 380, 455 nm for II; and 410, 470 nm for system III. The system without hydroxamic acids showed maximum absorbance at 430 nm.

The peaks at 450, 455 and 470 nm for stystms I-III respectively were found suitable for spectrophotometric estimation of rhenium as slight changes in the concentration of acid or stannous chloride produced sharp changes in the absorption maximum of the extracts at 370, 380 and 410 nm for systems I-III respectively.

Table 1—Optimum Conditions for Estimation of Rhenium using Different Hydroxamic Acids

Reagent	Acid range (M)	Amount (in ml) of		
		$SnCl_2$ (0.2 M)	Thiocyanate (2 M)	Hydroxamic Acid (0.2 M)
Thiocyanate	0.5-2.0	0.5-1.5	1.0-2.0	—
Thiocyanate + SHA	1.2-2.4	0.8-1.2	1.8-2.2	4.5-6.5
Thiocyanate + CHA	1.0-1.8	0.2-0.7	1.0-1.5	4.0-5.0
Thiocyanate + AHA	0.8-1.5	1.0-1.8	0.8-1.2	4.0-5.0

SHA = Salicylhydroxamic acid; CHA = cinnamoylhydroxamic acid; and AHA = anthranilohydroxamic acid

Table 2—Results of Spectrophotometric Studies

Reagent	Amount of Re(VII)		Beer's Law range (ppm)	Optimum range (μg·ml)	$\varepsilon \times 10^4$ (mol $^{-1}$/cm $^{-1}$)	Sandell's sensitivity (μg/cm^2)
	Taken (ppm)	Extracted* (ppm)				
Thiocyanate	4.0	0.80	1.00-10.00	1.20-9.45	1.8	0.0090
Thiocyanate + SHA	4.0	1.60	0.45-8.45	0.67-3.20	4.8	0.0038
Thiocyanate + CHA	4.0	1.82	0.27-8.90	0.62-3.60	4.9	0.0037
Thiocyanate + AHA	4.0	3.1	0.09-4.00	0.27-1.60	8.6	0.0021

*After a single extraction with MIBK

The results of the comparative study of optimum ranges, extinction coefficients, sensitivities and amount of the metal separated as mixed ligated complexes after a single extraction are summarized in Table 2. Systems I-III show increased sensitivity by a factor of 2-3 over the simple thiocyanate system and the sensitivities follow the order: III > II > I. The extractabilities of these mixed ligated metal complexes are found greater than those of the metal thiocyanate complexs[2-6]. These complexes are quite stable, their absorbances remaining unchanged even after 48 hr. Although the system II and I show lesser sensitivities, yet show greater tolerance against foreign ions (Table 3).

In general, the systems I-III were not at all influenced by the presence of Al(III), Ba(II), Be(II), Ca(II), Cr(III), Cu(II), Ga(III), Ge(III), Au(IV), In(III), Pb(IV), Mn(II), Mg(II), Hg(II), Ni(II), Ag(I), Zn(II) sulphate, chloride and quite high concentration of As(III), Cd(II), bromide, phosphate, oxalate and EDTA (= > 0.5 g/10 ml). The tolerance limits of these systems with some of the interfering ions are summarized in Table 3. The platinum metal ions, molybdate, nitrate and iodide seriously interfere with the determinations.

All the platinum metal ions, viz. Ru(III), Os(III), Rh(II), Ir(IV), Pd(II) and Pt(IV) in the presence of stannous chloride and hydrochloric acid form yellow to reddish brown chloro complexes[16], which are extractable in MIBK thereby causing interferences in the rhenium estimation. However, interferences due to platinum metals could be removed as follows: The solution containing these and Re(VII) was acidified with hydrochloric acid (final acidity 3.5 M) and to this was added stannous chloride (2 M, 7.5 ml). The mixture was then shaken with butyl acetate. The non-aqueous layer was rejected. This process was repeated till the aqueous layer turned light yellow to colourless depending upon rhenium concentration. Estimation of Re(VII) in this layer was carried out by the general procedure described earlier.

Table 3—Tolerance of the Systems against Foreign Ions

Ions	Tolerance in (mg/10 ml) for system		
	I	II	III
Bismuth (IV)	4.5	4.0	3.2
Cerium (IV)	0.25	0.25	0.02
Cobalt (II)	2.5	3.05	1.50
Iron (III)	0.60	0.80	0.20
Titanium (IV)	0.25	0.30	0.80
Uranium (III)	0.80	1.0	0.15
Tungsten (VI)	0.15	0.15	0.12
Zirconium	6.0	6.0	6.0
Selenium (III)	8.4	0.4	0.2
Tellurium (III)	0.4	0.4	0.2
Vanadium (V)	0.5	0.45	0.32

Ten determinations were done for each system. The relative mean errors and relative mean deviations were 0.09% and 0.10% for system I, 0.08% and 0.12% for system II, 0.05% and 0.15% for system III respectively.

Determination of Re(VII) in the presence of Mo(VI) was carried out in the following way:

To a synthetic mixture containing molybdenum (VI) (4 mg), vanadium (V) (1 mg), tungsten (VI)

(1 mg), iron (II), manganese (II), cobalt (II), copper (II), and nickel (II) (each 5 × 10^{-2} mg) and rhenim (VII) (5 × 10^{-4} mg) was added a 10 ml fraction of 1% (w/v) solution of tribenzyl amine in chloroform (acidity approximately 2 *M* HCl)[17] and shaken vigorously for 5 min. Molybdenum (VI), tungsten (VI) and vanadium (V) remained in the aqueous phase. The extraction was repeated thrice with smaller fractions of the extractant. From the non-aqueous phase, rhenium was back extracted into water by making it ammoniacal.

The relative mean errors and relative mean deviations were: 0.06% and 0.15% for system I; 0.07% and 0.12% for system II; and 0.05% and 0.15% for system III. (computed for 10 estimations).

One of the authors (IS) acknowledges her gratitude to the CSIR, New Delhi, for the award of a junior and subsequently a senior research fellowship.

References

1 Geilmann W & Bode H, *Z anal Chem*, **128** (1948) 489.

2 Hoffman J I & Lundell G E E, *J Res natl Bur Stand*, **23** (1939) 407.

3 Kojima M & Okubo I, *Tokyo Kogyo Shikenshu Holeokus*, **61** (1966) 372.

4 Lazarev A I & Lazarev V I, *Zhur anal Khim*, **22** (1967) 1210.

5 Pavlova M, *Zhur anal Khim*, **25** (1970) 123.

6 Tarayan V M & Mushegyan L G, *Am Khim Zh*, **26** (1973) 118.

7 Savariar C P & Hariharan T P, *Mikrochim Acta*, (1975) 477.

8 Savariar C P & Hariharan T P, *J Indian chem Soc*, **55** (1978) 349-51.

9 Mitra Monidipa & Mitra B K, *Talanta*, **28** (1978) 899.

10 Nayak Anant M, Manjappa S, Ramappa P G & Yathirajan H S, *Fresenius Z Anal Chem*, **309** (1981) 396.

11 Ramappa P G, Gowda H Sanke & Manjappa S, *J Inst Chem*,**84** (1982) 271-2

12 Bhaduri A S, *Z anal Chem*, **151** (1956) 109.

13 Thiele & Pickard, *Ann*, **309** (1899) 194.

14 Scott & Ward, *J org Chem*, **7** (1942) 575.

15 Majumdar A K & Bhowal G, *Anal chim Acta*, **48** (1969) 192.

16 Sandell E B, *Colorimetric methods of estimation* (Interscience, New York) 1959.

17 Yathirajan V & Kakkar L R, *Anal chim Acta*, **82** (1970) 555.

Indian Journal of Chemistry
Vol. 27A, March 1988, pp. 274-276

Separation & Determination of Trace Amounts of Nickel in Industrial Waste Water using a Liquid Chelating Exchanger & Atomic Absorption Spectrophotometry

SANTI RANI DAN (BISWAS) & ARABINDA K DAS*

Department of Chemistry, University of Burdwan,
Burdwan 713 104

Received 3 *February* 1987; *revised and accepted* 3 *July* 1987

Nickel present in industrial waste water has been separated by a liquid β-diketo chelating exchanger ($RCOCH_2COCF_3$; $R = C_9H_{19}$) followed by its determination by flame atomic absorption spectrophotometry. Preparation of the chelating exchanger, extraction conditions, effect of diverse ions and composition of the extracted species have been discussed.

Flame and flameless atomic absorption spectrophotometry (AAS) has been used for nickel determination by several authors[1-5]. Interferences in nickel determination by air-C_2H_2 flame have been reported by Sundberg[6]. Effective separation of nickel from other transition metals by the use of liquid ion-exchanger was described by De *et al.*[7] The utility of preconcentration for the determination of trace amounts of nickel in natural water by AAS has been mentioned earlier[8]. In the present note we propose a method for the separation of trace amounts of nickel by extraction with a new β-diketo liquid chelating exchanger[9] ($RCOCH_2COCF_3$; $R = C_9H_{19}$) in chloroform medium and subsequent determination of nickel by AAS. The nickel content in Tumla nallah water (Durgapur) has been monitored by the present method.

β-Diketo liquid chelating exchanger ($RCOCH_2COCF_3$; $R = C_9H_{19}$) was prepared in two steps[10]. The parent compound is a C_{10}-isomeric monocarboxylic acid, Versatic-10 (Shell Chemical Co., London). After esterification of this acid, the resulting ethyl ester was condensed with trifluoroacetone (Fluka, Switzerland) in presence of sodium ethoxide. The liquid exchanger was separated and purified. The physical characteristics of the chelating exchanger are: mol. wt., 263; density, 0.918 g/c.c. at 33°C; IR 1698-1700 cm^{-1} ($\nu C = O$ of diketo group); NMR, -0.72 τ (enolic $-OH$, intramolecularly hydrogen bonded). A 0.1 *M* solution in chloroform was used in the present work.

Stock solution of nickel(II) was prepared by dissolving $NiCl_2.6H_2O$ (E. Merck) in doubly distilled water and it was standardised complexometrically[11]. The solution was diluted so that the final nickel concentration was 80 ppm.

Stock solutions of diverse ions were prepared from pure samples of various metal salts. All the reagents used were of AR grade.

Absorbance measurements were made with a Shimadzu atomic absorption spectrophotometer (model 646) having background correction system using a D_2-lamp. The following conditions were maintained: nickel hollow cathode lamp current = 9 mA, burner height = 5 mm, wavelength = 232 nm, slit width = 1.9 Å, air flow rate = 10 litre/min, acetylene flow rate = 2.3 litre/min, working concentration range 2.0 to 10.0 ppm nickel.

The *p*H values were measured with a Sambros digital *p*H meter (model 335).

General procedure

To a solution containing 80 μg nickel in a 50 ml separatory funnel, dilute ammonia was added to adjust the *p*H to about 9.0; 2 ml of tris-buffer solution (*p*H = 9.0) were added and volume of the solution was made up to 10 ml. 1 ml of 0.1 *M* liquid chelating exchanger in chloroform was added, contents were shaken for 1 min and allowed to settle for 6 min. The organic phase was transferred to another separatory funnel and the aqueous phase was washed twice with 5 ml portions of chloroform. The resulting chloroform extract was stripped back into 0.1 *N* HCl. The aqueous phase was taken and volume was made upto 10 ml in a volumetric flask. The absorbance value of the resulting solution was measured by AAS in air-C_2H_2 flame using 232 nm wavelength. The amount of nickel was then computed from the calibration curve.

Preliminary studies were carried out to find out optimum conditions for the separation and estimation of Ni(II) by the present method. The effect of *p*H on the amount of extraction of nickel with chelating exchanger was studied by verying *p*H of the solution. It was found that in the *p*H range 8.9-9.4, nickel was rapidly and effectively extracted from aqueous medium.

The effect of various solvents on extraction of nickel by the chelating exchanger was studied at a definite *p*H. Most quantitative extraction of nickel occurred with chloroform, the percentage of extraction being 97.14%. Hence, it was used in the present work.

The amount of extraction of nickel was measured by varying the concentration of liquid chelating exchanger from 0.075 *M* to 0.600 *M* in chloroform. It was found that extraction increased with increasing exchanger concentration and was complete at 0.2 *M* concentration of the excahgner. Nickel was completely stripped back from chloroform layer into hydrochloric acid solution of different strengths, e.g., 0.1 *N* to 3.0 *N*. So, a 0.1 *N*HCl solution was used as the stripping agent.

The time of shaking for extraction was varied from 5 min to 1 min. It was found that 1 min was sufficient for quantitative extraction. However, 30 sec was enough for completion of back-extraction. In both the cases, a period of 5 min was allowed for the attainment of the equilibrium.

Effect of foreign ions

Since the method has been developed for determination of nickel in industrial waste water, a study of the effects of foreign species commonly present in industrial waste was made. Known amounts of various ions were added and their effect on the estimations of Ni(II), within an error of ± 2% was noted. The results are as follows: 1000 ppm of Na(I), K(I), Li(I); 2000 ppm of Ba(II), Sr(II), Ca(II); 150 ppm of Cu(II); 100 ppm of Cd(II), Zn(II); 80 ppm of Pb(II); 50 ppm of Mn(II), Bi(III); 30 ppm of Sn(II), Al(III), Cr(III); 8 ppm of Mg(II); and 4 ppm of Co(II), Fe(III), Ti(IV) did not affect the estimation of Ni(II). 1000-fold excess of Cl , 500-fold excess of F^-, NO_3^-,SO_4^{2-} and 200-fold excess of PO_4^{3-} did not interfere. The determination was also possible in presence of more than one foreign ion. The method was actually tested for nickel(II) extraction in the following synthetic mixtures: (a) Ba(II) 100 ppm + Zn(II) 80 ppm; (d) Ca(II) 500 ppm + Cu(II) 100 ppm + Bi(III) 30 ppm; (e) Na(I) 500 ppm + Zn(II) 50 ppm + Mg(II) 8 ppm; (f) Sr(II) 500 ppm + Cr(III) 20 ppm + Pb(II) 500 ppm.

Nature of the extracted species

The extracted species may be considered to be bis-chelated as the plot of log *D* against the concentration of liquid chelating exchanger gave a straight line with a slope of 2.0. Thus, the extraction mechanism of nickel may be represented as:

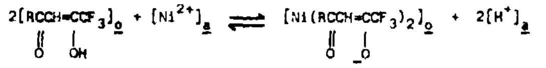

$$2[\underset{\underset{O}{\|}}{RC}\underset{\underset{OH}{|}}{CH}{=}CCF_3]_{\underline{o}} + [Ni^{2+}]_{\underline{a}} \rightleftharpoons [Ni(\underset{\underset{O}{\|}}{RC}\underset{\underset{\_O}{|}}{CH}{=}CCF_3)_2]_{\underline{o}} + 2[H^+]_{\underline{a}}$$

where *o* and *a* are respectively organic and aqueous phases.

Table 1—Recovery of Nickel Added to Tumla Nallah Water

Nickel (µg/litre)		Percent recovery*
Amount added	Amount found	
0	9.9	–
10.0	20.0	100.5
20.0	29.7	99.3
30.0	39.8	99.7

*Average of two determinations

Applications

The estimation of nickel was made in Tumla nallah which carries the industrial effluents of Durgapur industrial area. Water samples were collected in clear polyethylene containers. and stored as described earlier[12]. 1-2 litre of water sample was taken each time for pretreatment and the *pH* was adjusted to 4 with conc. nitric acid, followed by the addition of 5 ml of conc. nitric acid. The total volume was reduced to ~ 40 ml by keeping on a hot plate. To this, 5 ml conc. hydrochloric acid was added and then the mixture was again heated on the hot plate for 15 min. The solution was cooled and filtered *in vacuo*. The filtrate was transferred to a 50 ml volumetric flask and made upto the mark. A 25 ml aliquot was taken, nickel was separated by the proposed method and finally the AAS method was applied to determined the nickel content. The results of the determination of nickel in industrial waste water of Tumla nallah at Durgapur at different sampling stations by the recommended procedure are: sample 1 (9.9 µg/litre), sample 2 (14.3 µg/litre), sample 3 (8.8 µg/litre), sample 4 (11.6 µg/litre), sample 5 (17.8 µg/litre), sample 6 (12.0 µg/litre).

To the aliquots of a sample of Tumla nallah water various amounts of nickel were added and the metal was estimated by the present method (Table 1). The percentage of recovery ranges from 99 to 101 indicating a good reproducibility of the present method.

The authors thank Shell Chemical Co:, London for gift samples of Versatic-10. One of the authors (SRD) is grateful to the CSIR, New Delhi for sponsoring the project.

References

1 Itsuki K, Komuro H & Nagasawa T, *Bunseki Kagaku*, **19** (1970) 1282.
2 Dipierro S & Tessari G, *Talanta*, **18** (1971) 707.
3 Mikhaibva T P & Lushmikova L G, *Zavod Lab*, **37** (1971) 1069.

4 Pearton D C G & Mallett R C, *Nat inst met repub s afr Rep*, **1435** (1972) 20; *Chem Abstr*, **78** (1973) 23593v.

5 Sakata M & Shimoda O, *Bunseki Kagaku*, **31** (1982) T81

6 Sundberg L L, *Analyt Chem*, **45** (1973) 1460.

7 De A K & Roy U S, *Sep Sci*, **6** (1971) 25.

8 Fujino O, Matsui M & Shigematsu T, *Mizu shori Gijutsu*, **20** (1979) 201; *Chem Abstr*, **91** (1979) 128795j.

9 Dan (Biswas) S R & Das A K, *Proc 4th national symposium, Indian Society of Analytical Scientists*, 1987.

10 Vogel A I, *A textbook of practical organic chemistry including qualitative organic analysis* (Longmans Green, London) 1959, 383, 863.

11 Bassett J, Denny R C, Jeffery G H & Mendham J, *Vogel's textbook of quantitative inorganic analysis including elementary instrumental analysis* (ELBS and Longman) 4th Edn, 1978, 322.

12 Das A K, *Indian j environ Hlth*, **22** (1980) 130.

Indian Journal of Chemistry
Vol. 27A, March 1988, pp. 277-278

BOOK REVIEWS

Conducting Polymers: Special Applications, edited by L. Alcacer (D. Reidel Publishing Company, Dordrecht, Holland) 1987, pp. 220 + vi, Price $ 69.00

The discovery in 1977 that polyacetylene can be "doped" with acceptors such as iodine to yield metallic organic polymers sparked off a frenzy of activity in the study of electrically conducting conjugated polymers. While a fundamental understanding of these materials remains incomplete, they are no longer merely a laboratory curiosity. Numerous industries and special applications' laboratories have begun investing heavily in research on conducting polymers, and rapid advances have been made in improving the conductivity, stability, and processability of these materials. Nevertheless, this highly interdisciplinary area of science is still in its infancy, and is likely to remain a frontier area of research and development during the coming decade.

"Conducting Polymers: Special Applications" is a timely publication containing the proceedings of a workshop held in Sintra, Portugal on this subject. The workshop, which was sponsored by the U.S. Army Research, Development and Standardisation Group (U.K.) in July 1986, successfully combined basic research activities on ionic and electronically conducting polymers with applications of these materials in industry. Reports on the panel discussions held during the workshop have also been included in this volume.

The book contains several papers on syntheses and characterisation of new conducting polymers, while two additional papers describe preparation and properties of non-crystalline solid electrolytes based on poly(ethylene oxide)-alkali halide complexes. It may be mentioned that the latter materials are of potential use as separators in solid state batteries. Papers on conductive porphyrin-, phenothiazine-, and phthalocyanine-based polymeric systems have also been included. The book also covers the current techniques employed to improve the orientation, organization, and crystallinity of polymeric thin films, and highlights research efforts geared towards improving the stability and processability of these materials. Additionally, electrochemical and spectroscopic studies of conducting polymers, and their potential applications in the fabrication of catalytic electrodes, lightweight batteries, and new sensor systems, have been adequately covered in this book. Finally, readers will also be benefitted by the inclusion of numerous up-to-date references in this volume.

The book is recommended for libraries and for those engaged in research on conducting polymers.

Pushpito K Ghosh
Alchemie Research Centre
Thane Belapur Road
Thane 400 601

Structure Reports for 1984, Volume 51A, Metals and Inorganic Sections, General Editor: G. Ferguson, Section Editor: J. Trotter (D. Reidel Publishing Co.) 1987, pp. 384 + vi, Price $ 75.00.

"Structure Reports" are the successor volumes of Strukturbericht and have been published every year since 1940-41. These volumes are prepared under the guidance of a Commission of the International Union of Crystallography. The volume under review continues the objective of these reports and presents critical accounts of all cyrstallographic structure determinations reported during 1984 using diffraction techniques. Section A deals with metals and inorganic compounds while Section B covers organic compounds, including organometallic compounds and metal complexes with organic ligands.

Ideally, reports are prepared in such a way that no further structural information would be gained by consulting the original paper. However, in view of the increasing amount of literature covering structural studies appearing in recent years, starting with volume 37, tables of atomic coordinates have been omitted except for simple structures in order to keep the volumes to fairly uniform and convenient size. Further, all interatomic distances are not given, but only significant ones are discussed in the description of the structure. The arrangement within individual reports usually is: name, formula, paper(s) reported, unit cell dimensions, space group, brief details of structure analysis, atomic positions, interatomic distances and angles (if given in full), description and discussion of structure (with diagrams if appropriate), and additional references. Editorial comments, if any, are enclosed in square brackets. Every effort is made to avoid jargon, so that the information is readily understood by a non-crystallographer.

The arrangement in metals section is roughly alphabetical and that in inorganic section is in the order of increasing complexity of composition, related substances and related structures being kept together as far as possible. The metal section includes alloys, intermetallic compounds and also metal chalcogenides, borides, nitrides, phosphides etc. The inorganic compounds are grouped under the following categories: elements, hydrides, carbonyls, phosphorus-nitrogen and sulphur-nitrogen compounds, halides, cyanides, oxides, double oxides, hydroxides, sulphides, borates, carbonates, nitrates, phosphates, arsenates, sulphates, perchlorates, iodates, silicates and silicate minerals. Incomplete structural data and compounds described in preliminary communications are separately tabulated. The subject index, formula index and author index are available at the end of the volume.

The phenomenal increase in the number of structural studies in recent years, published in a large number of journals, makes it extremely difficult for scientists to keep track of the work done in any particular area. "Structure Reports" is an extremely valuable source book useful to the X-ray crystallographer, structural chemist, metallurgist, material scientist and, in fact, to any scientist who generates or uses structural information. This volume and, indeed, all the volumes deserve a place in any good scientific library.

H Manohar
Department of Inorganic & Physical Chemistry
Indian Institute of Science
Bangalore 560 012

Mössbauer Spectroscopy Applied to Inorganic Chemistry, edited by G J Long, (Plenum, New York), 1984, pp. 667 + xvii, Price $ 92.50.

This book is one of a new series of the books on modern inorganic chemistry. It contains eighteen chapters. The first two chapters deal with introduction, historical background and basic concepts of Mössbauer spectroscopy. The remaining sixteen chapters are written by senior research scientists specializing in different fields. It is presumed that the editor has selected these specialists—the choice seems to be rather arbitrary and is limited to specialists from four countries only.

On the part of the reader, a reasonable background/acquaintance with Mössbauer effect is assumed. There are markedly different styles in presenting the wealth of information provided in various chapters. This has made the task of the editor rather difficult in normalising different aspects in a cooperatively written textbook. For example, the chapter on isomer or chemical shift comprises just twenty pages although this is the unique parameter, easily available to chemists from the analysis of Mössbauer spectral data. May be the reader is expected to have referred to the classic books on isomer shifts published earlier. What have appealed to me most are the chapters on relaxation phenomena, spin equilibrium in complexes, one dimensional magnetism, etc., because these are written in a clear and concise way and these are generally not treated in any textbook. But keeping in view the high price of the book, I wonder how many Departmental libraries will be able to afford the book.

S K Date
National Chemical Laboratory
Pune 411 008

Indian Journal of Chemistry
Vol. 27A, April 1988, pp. 279-280

Communication

Structure of Conducting Polyaniline

AKHEEL A SYED* & MARAVATTICKAL K DINESAN
Department of Post-Graduate Studies & Research in Chemistry, University of Mysore, Mysore 570 006
and
K N SOMASEKHARAN*
Department of Inorganic & Physical Chemistry, Indian Institute of Science, Bangalore 560 012

Received 22 *December* 1987; *accepted* 9 *March* 1988

Reagent analysis for the peroxodisulphate oxidation of aniline in acid medium establishes that 2.5 electrons per aniline unit are involved in the oxidative condensation of aniline to give conducting polyaniline.

Polyaniline, which is obtained as an insoluble precipitate on oxidation of aniline chemically or electrochemically, in acid medium, has reestablished itself as a useful conducting polymer[1-8]. Neither product analysis[9] nor MO calculations[10] have succeeded in establishing the structure of the conducting polymer. Reagent analysis has been resorted to, in the present work, for elucidating its structure.

In a series of polymerization reactions, aniline (40 mmol) in acid solution (100 ml; $pH = 0$) was oxidized with varying amounts of peroxodisulphate by stirring the reaction mixture for 60 min. The precipitate was separated by filtration and was washed with copious amounts of acid ($pH = 0$). The soluble oligomers were removed from the filtrate by repeated extraction with *n*-butanol. Unreacted peroxodisulphate in the filtrate was then estimated iodometrically[11]. The results are summarized in Table 1. At lower peroxodisulphate/aniline ratios (i.e. ≤ 2.5 equiv/mol), no peroxodisulphate was detected in the filtrate.

The peroxodisulphate anion is one of the strongest oxidizing agents, the standard redox potential being 2.01 V in aqueous solution. Redox decomposition of $S_2O_8^{2-}$ provides under mild conditions the radical anion, $SO_4^{\cdot -}$. Both $S_2O_8^{2-}$ and $SO_4^{\cdot -}$ appear to be very effective electron transfer oxidizing agents[12]. When the transfer is exergonic, the reaction occurs at or near diffusion-controlled rates[12]. Oxidation of aniline, under these conditions, proceeds by the reaction sequence shown in Scheme 1. Thus peroxodisulphate oxidation of aniline in acid medium yields the salt of poly(emeraldine) which is conducting.

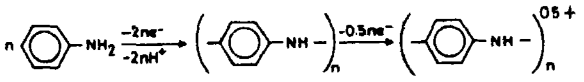

Chemical analyses of the precipitate manifest the presence of counteranions. The formulae deduced from chemical analyses data are as follows: $(C_6H_5N)(SO_4)_{0.23}(H_2O)_{0.78}$ in sulphuric acid medium; and $(C_6H_5N)(Cl)_{0.52}(SO_4)_{0.01}(H_2O)_{0.82}$ in hydrochloric acid medium. It is evident that the medium/supporting electrolyte imposes the corresponding anion in the conducting polymer. The anion content suggests the structure of poly(emeraldine) salts as shown in Scheme 2.

Gravimetric determination demonstrates that the anion in the matrix can be exchanged in acid media.

Table 1—Determination of Stoichiometry of Peroxodisulphate-Aniline Reaction[a]

Sl No	Medium	Amount of peroxodisulphate (m equiv)			Peroxodisulphate/ aniline[b] (equiv/mol)
		Taken	Unreacted[b]	Consumed[b]	
1	H_2SO_4 + 1*M* Na_2SO_4	110	7.12	102.9	2.57 ± 0.005
2	H_2SO_4 + 1*M* Na_2SO_4	120	19.1	100.9	2.52 ± 0.057
3	H_2SO_4 + 1*M* Na_2SO_4	160	57.7	102.3	2.56 ± 0.006
4	H_2SO_4 + 1*M* Na_2SO_4	200	93.1	106.9	2.67 ± 0.017
5	H_2SO_4	120	16.0	104.0	2.60 ± 0.012
6	HCl	120	15.9	104.1	2.60 ± 0.022

[a] 40.0 mmol aniline in 100 ml solution, at $pH = 0$
[b] Average of 5 replicates

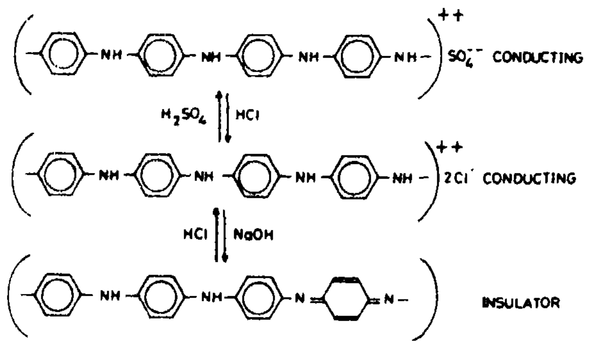

Known amounts of poly(emeraldine sulphate), on treatment with excess 1 *M* hydrochloric acid for 1 hr, yields poly(emeraldine chloride). The gravimetric ratio of 0.9457 (±2%) for the dried chloride/sulphate is in conformity with the results of reagent analyses and chemical analyses.

Supporting evidence for the structure comes from solid state ^{13}C NMR spectra. The spectrum of the deprotonated species exhibits three broad signals centered at 124.7, 144.6 and 160.3 ppm. The high-field peak originates from the proton-bonded carbons (2,3,5,6) of the benzenoid rings, whereas the low-field peak is from the 1,4 carbons of the quinonoid rings; the broad signal around 144.6 ppm is from the 2,3,5,6 carbons of the quinonoid rings and the 1,4 carbons of the benzenoid rings. After curve resolution, and integration, the observed intensities are in the ratio 6.00 : 4.87 : 1.01, which matches the expected intensity ratio of 6 : 5 : 1 for this structure. For the structure with alternate benzenoid and quinonoid rings, the expected intensity ratio is 6 : 9 : 3.

References

1 Noufi R, Nozik A J, White J & Warren L F, *J electrochem Soc*, **129** (1982) 2261.
2 Kobayashi T, Yoneyama H & Tamura H, *J electroanal Chem*, **177** (1984) 281.
3 Paul E W, Ricco A J & Wrighton M S, *J phys Chem*, **89** (1985) 1441.
4 MacDiarmid A G, Chiang J -C, Halpern M, Huang W -S, Mu S -L, Somasiri N L D, Wu W & Yaniger S I, *Mol Cryst Liq Cryst*, **121** (1985) 173.
5 Genies E M, Syed A A & Tsintavis C, *Mol Cryst Liq Cryst*, **121** (1985) 181.
6 Syed A A, Genies E M & Santier C, in *Materials for solid state batteries*, edited by B V R Chowdari & S Radhakrishna (World Scientific Publishing Co, Singapore) 1986, 435.
7 Genies E M, Pernault J M, Santier C, Syed A A & Tsintavis C, *Springer Ser solid-state Sci*, **63** (1985) 211.
8 Kitani A, Kaya M & Sasaki K, *J electrochem Soc*, **133** (1986) 1069.
9 Hjertberg T, Salaneck W R, Lundstrom I, Somasiri N L D & MacDiarmid A G, *J Polym Sci : Polym Lett Edn*, **23** (1985) 503.
10 Stafstrom S, Sjogren B, Wennerstrom O & Hjertberg T, *Synth Met*, **16** (1986) 31.
11 Kolthoff I M & Belcher R, *Volumetric analysis*, Vol 3 (Interscience, New York) 1957, 287-289.
12 Minisci F, Citterio A & Giordano C, *Acc chem Res*, **16** (1983) 27.

Indian Journal of Chemistry
Vol. 27A, April 1988, pp. 281-285

Porphyrin-sensitised Photodecomposition of Thymine in Aqueous Triton X-100 Solution

V V LOBKO[†]
Institute of Spectroscopy, USSR Academy of Sciences, Troitzk, Moscow Region, USSR
and
L V SHASTRI, T MUKHERJEE & J P MITTAL[*]
Chemistry Division, Bhabha Atomic Research Centre, Bombay 400 085, India

Received 16 *December* 1986; *revised* 10 *September* 1987; *accepted* 21 *September* 1987

Hematoporphyrin (Hp) and protoporphyrin (disodium salt) sensitise the photodecomposition of thymine, in aqueous solutions of Triton X-100, under CW excitation ($\lambda = 320$-490 nm). A number of products have been detected by HPLC. The effect of addition of ascorbate ion (AA), tryptophan (TRP) and sodium azide (NaN_3) on the yields of the most prominent photoproduct has been studied. From this, the involvement of type-I mechanism in the observed photodecomposition of thymine, i.e. electron transfer from thymine to the excited sensitisers has been suggested.

The photoradiation therapy of malignant tumours, based on the photosensitised destruction of transformed cells, is of great interest at present[1-3]. It is well known that the therapeutic effect is due to comparatively selective accumulation of the sensitiser hematoporphyrin derivative (HpD) in tumours. As a rule the activation of HpD in cells is achieved by coherent or incoherent CW red light which can penetrate rather well into tissues and be absorbed by HpD molecules.

The mechanism of toxic action of the excited molecules of HpD on the cells is still not clear. It is known[3-6] that the CW excitation of hematoporphyrin (Hp) and HpD in solutions produces a series of reactive intermediates ($^1O_2$, $O_2^{\bullet -}$, $OH^\bullet$). The role of these species in the cytotoxic action has not yet been clearly defined[1-3].

The role of light intensity in the decomposition of thymine sensitised by Hp and HpD has been studied earlier[7] by analysing the thymine photoproducts by high performance liquid chromatography (HPLC) technique. It has been shown[7] that with $I \geq 10^4$ WCm^{-2} (337.1 nm), Hp and HpD were excited by two quantum mechanism, resulting in thymine products whose quantum yields were proportional to I^2. However, such dependence could not be observed at CW excitation of the sensitisers. In the latter case, the main products of thymine were somewhat dependent on the scavengers of the intermediates ($H^\bullet$, $OH^\bullet$, $^1O_2$). However, for both CW and high-power pulsed excitation of Hp and HpD the resulting products of thymine were almost the same[7].

The purpose of the present investigation was to study the effect of different quenchers on the efficiency of formation of thymine photoproducts in order to understand the mechanism of sensitised decomposition of thymine by Hp and HpD under CW excitation. Thymine, being a constituent of nucleic acids, is a potential "target" which can be acted upon by the excited molecules of HpD in the cells, leading to the destruction of the former[8,9]. The available aqueous solution of HpD ("Photofrin" medicine) is a composite mixture of porphyrins and so it would be rather difficult to interpret the experimental results. In our experiments, therefore, pure Hp and sodium salt of protoporphyrin-IX (Na_2-PP) were used.

Materials and Methods

Hematoporphyrin (Hp) was synthesised and purified at the Physical Institute, USSR Academy of Sciences (Minsk). Protoporphyrin-IX sodium salt (Sigma), sodium azide (Reachim, USSR) and tryptophan (Reachim, USSR) were certified pure compounds and were used as such.

Fresh porphyrin solutions were prepared as follows. In a 2% solution of Triton X-100 (TX-100) in phosphate buffer (0.1 mol dm^{-3}, *p*H 7.4; 100 ml), thymine was dissolved to a concentration of 10^{-2} mol dm^{-3}. Porphyrins were added to an aliquot (4 ml) of this solution to get a concentration of 8×10^{-5} mol dm^{-3} as determined spectrophotometrically. All the solutions were prepared in triply distilled water. Before irradiation the solutions were filtered through 0.2 micron membrane filters. The samples were irradiated in quartz test tubes of 1.5 cm internal diamter or in quartz cells of 0.2 cm path length. The test tubes containing the sample (4 ml) were irradiated in a Rayonet photochemical reactor (Southern New England Ultra Violet Company, USA), fitted with 16 "black phosphor" coated low pressure Hg lamps (output range 320-380 nm approximately, with a peak at 350 nm) in a cylindrical geometry, giving about 1×10^{16} photons $cm^{-2}s^{-1}$. The cells with 0.25 ml of sample were irradiated by light in the wavelength range 330-490 nm using a mercury quartz lamp and a set of appropriate glass filters.

[†] Present address: Institute of Medical Polymers, Moscow Nauchnii Proezd 10, USSR

High pressure liquid chromatography (HPLC) was employed to separate thymine photoproducts. Preliminary qualitative results were obtained with a Laboratory Data Control Chromatograph (USA) equipped with a C-6 column (length 250 mm, i.d. 4.6 mm, spherisorb C-6, 5 μm). The elution rate of triply distilled water was 0.75 ml min^{-1}. The quantitative measurements were carried out using a Spectra Physics Chromatograph (USA) (SP 8700 solvent delivery system, SP 8750 organizer, SP 8400 UV/vis detector and SP 4100 computing integrator) with a RP-18 column (C-18, 10 μm Lichrosorb, 250 mm length, 4.6 mm i.d.). The rate of elution by 3% methanol in triply distilled water was ~1 ml min^{-1}. In both cases the detection of thymine products was performed at $\lambda = 206$ nm, but other wavelengths were used whenever necessary.

Results and Discussion

In the present experiments, the aim was to study the effect of different quenchers on the efficiency of formation of thymine photoproducts in order to understand the mechanism of the photochemical reactions between excited porphyrins and thymine.

Figure 1 shows the absorption spectrum of thymine-Hp solution, showing that in experiments reported below, excitation light was exclusively absorbed by the porphyrin. Thus direct excitation of thymine to its excited state or energy transfer from the exicited porphyrin to thymine are improbable. Any photosensitisation leading to thymine photoproducts must therefore involve an indirect mechanism.

Figure 2 shows a HPLC chromatogram of the Hp-thymine mixture irradiated by 330-490 nm light. The first and last intense peaks correspond to Hp and thymine respectively. Although the peaks 1-3 (Fig.2) correspond to the decomposition products of thymine photosensitised by Hp, no attempt was made to unambiguously identify these peaks[10]. As is evident from Fig.2, peak 3 is the most intense at 206 nm. The integrated area of peak 3 is higher than those of peaks 1 and 2 by about 24 and 2 times respectively. Peak 4 is attributed to an admixture of thymine with 5-hydroxymethyluracil.

The products obtained in the photo-sensitised oxidation of thymine by 2-methyl-1,4-naphthoquinone (menadione) in aqueous oxygenated solutions have been analysed earlier[10]. Although all the photoproducts were not identified unambiguously, it was observed that the photoproducts

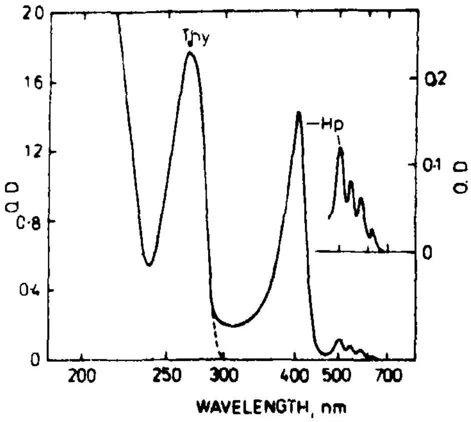

Fig. 1—Absorption spectrum of mixture of thymine (2.1×10^{-3} mol dm^{-3}) and Hp (1.1×10^{-4} mol dm^{-3}) in 2% TX-100 aqueous solution [The dashed line corresponds to the absorption tail of thymine in the absence of Hp]

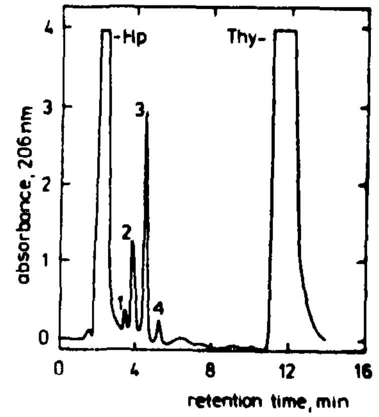

Fig. 2—HPLC of the mixture of thymine and Hp after irradiation with 330-490 nm CW light [The sample volume is 0.25 ml, the absorbed light dose is 5 J. Peaks 1,2,3 correspond to the products of sensitized decomposition of thymine]

were more or less similar to those produced by the gamma radiolysis of oxygenated solutions of thymine. Furthermore, employing ^{14}C-labelled thymine in the photo-sensitisation experiments, it was shown that the prominent peaks seen in HPLC with UV absorbance detector set at 229 nm correlated well with the major photoproducts of sensitised oxidation of thymine as estimated by the tracer technique[10].

In our experiments, the products were also monitored at several other wavelengths including 229nm[10] at which the extinction coefficients of both saturated and unsaturated pyrimidines would have comparable values. In these analyses also, the peak 3 was found to be the most intense in HPLC showing that this peak corresponded to a prominent product from the photo-sensitised damage of thymine. However, since the sensitivity for detection at 206nm was better than that at 229nm, the chromatograms were routinely monitored at 206nm.

The yields of products, determined from the corresponding integrated absorption peaks, increased linearly with absorbed light energy at least upto 20 J, when the sample volume was 0.25 ml. Similar products with almost the same yield were formed when thymine was sensitised by Na_2-PP.

When Hp is excited to the first singlet excited state (S_1), intersystem crossing to the first long-lived triplet states (T_1) occurs[11] with a high quantum efficiency of 0.92. So it may be assumed that the triplet state of Hp takes part in the sensitised photodecomposition of thymine. However, it is known[3,12] that the triplet state energy of many porphyrins, including Hp and Na_2-PP, is effectively transferred to molecular oxygen ($^3O_2$) forming chemically active singlet $^1O_2$. The reaction rate constant of $^1O_2$ with thymine is rather low[13], e.g. $k \leqslant 1\times10^6$ dm^{3}mol^{-1}s^{-1}. If $^1O_2$ was to participate in the modification of thymine, the quencheres of $^1O_2$ must affect the yield of thymine products. Therefore, ascorbate ion (AA), tryptophan (TRP) and sodium azide (NaN_3) were used as quenchers of $^1O_2$.

The results of measurements of the relative efficiency of product 3 formation are given in Figs. 3 and 4. It can be seen that for both Hp and Na_2-PP, the yield of the product 3 is most sensitive to the addition of AA. The relative yield decreases to half when AA concentration is 1×10^{-4} mol dm^{-3}. In presence of 1×10^{-3} mol dm^{-3} AA, the yield of product 3 is almost zero, but the yield of the product 1 increases by 2.5-3 times and the integrated area under peak 2 decreases by ~35% due to its narrowing. This means that peak 2 corresponds to at least two thymine products. When the concentration of tryptophan is upto 5×10^{-4} mol dm^{-3}, it is an effective quencher of the sensitised decomposition of thymine. At higher concentrations (upto 1.5×10^{-3} mol dm^{-3}) thymine product yield remains practically constant (Fig.3). Tryptophan has qualitatively the same effect on the yield of all thymine products.

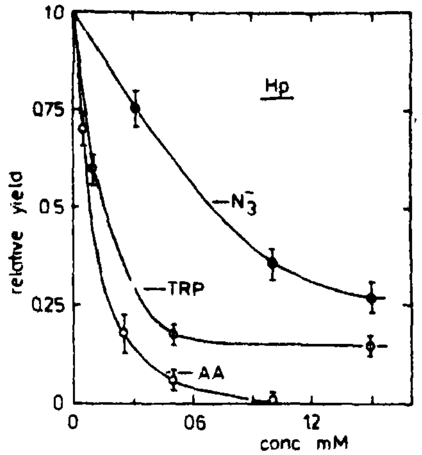

Fig. 3—Effect of addition of AA, TRP and N_3^- on the yield of thymine product 3 sensitised by Hp [The sample volume is 0.25 ml and the absorbed light dose is 5 J]

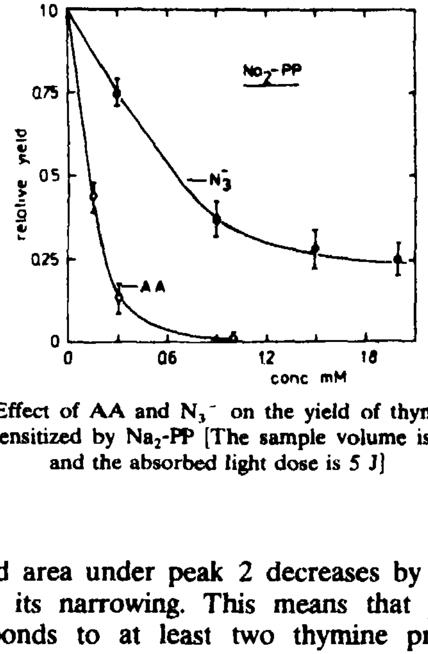

Fig. 4—Effect of AA and N_3^- on the yield of thymine product 3 sensitized by Na_2-PP [The sample volume is 0.25 ml and the absorbed light dose is 5 J]

Sodium azide was found to be the least effective quencher of thymine photoproducts formation (Figs. 3 and 4). For example, at a concentration of $5\text{-}7\times10^{-4}$ mol dm^{-3} sodium azide, the relative yield of product 3 slowly decreases and reaches a value of 0.25 when the azide concentration is 2×10^{-3} mol dm^{-3}. The yields of the other thymine products decrease likewise.

Product 3, the integral absorption of which at 206 nm is 60-70% of all the thymine decomposition products, cannot be explained by the participation of $^1O_2$. As far as the quenching efficiency of product 3 formation is concerned, the quencher molecules follow the order: AA > TRP > NaN_3. But this result does not agree with the rates of $^1O_2$ quenching by these molecules[13] ($k = 8.3 \times 10^6$, 2.5×10^8 and 2.3×10^9 dm^3 mol^{-1} s^{-1} for AA, TRP and NaN_3 respectively) since NaN_3 and AA are the most and least effective quenchers of $^1O_2$ respectively.

It may be assumed that the sensitised formation of thymine product 3 in the absence of AA occurs in agreement with type-I mechanism which includes an electron transfer from thymine to the excited triplet state of Hp. With addition of AA the yield of thymine product 3 decreases due to the competition between thymine and AA as electron donors (AA is a very good electron donor[14]) for the triplet state of the porphyrins.

The assumption qualitatively agrees with other results[15,16] on the relative role of type-I and type-II photoreactions sensitised by Hp and HpD. For example, it has been shown[15] that at Hp concentration of 5×10^{-5} mol dm^{-3}, photo-oxidation of TRP in the presence and in the absence of sodium dodecyl sulphate micelles occurs in accordance with the type-I mechanism. In this experiment the electron, however, is assumed to be transferred from the triplet state of Hp to tryptophan.

In the lysis of phosphatidylcholine liposomes sensitised[16] by Hp and HpD, it was found that for small Hp concentrations ($\leqslant 1 \times 10^{-6}$ mol dm^{-3}) the lysis of liposomes could be explained by the participation of singlet oxygen (type-II mechanism), whereas, at higher concentrations (15×10^{-5} mol dm^{-3}) the destruction of liposomes by type-I mechanism prevailed. Methylene blue[17] and 2-methyl-1,4-naphthoquinone[10] also sensitise photodecomposition of thymine by an electron transfer to the excited triplet states of the sensitisers.

The results of the present experiments show that in aqueous solutions containing TX-100 micelles the role of $^1O_2$ in the decomposition of thymine is not important. This is in agreement with an observation[18] that guanine is the only base of nucleic acids which can be modified to a great extent by $^1O_2$. Under modified conditions, however (thymine adsorbed on the surface of silica gel)[19], thymine can be affected by $^1O_2$.

In the presence of *n*-butanol, an effective scavenger of H$^\bullet$ and OH$^\bullet$ radicals, peak 1 decreased by half when *n*-butanol concentration was 6×10^{-2} mol dm^{-3} and could not be observed when *n*-butanol concentration was 0.18 mol dm^{-3}. Thus OH$^\bullet$ radicals are probably involved in the formation of the product 1. In a concentration range of upto 0.18 mol dm^{-3} the integral absorption under peak 2 remained constant and that under peak 3 increased by ~ 1.5 times.

On the addition of $^1O_2$ quenchers, not only there was a decrease in the yield of the main thymine product 3 but also an increase in the yield of some products; e.g. ascorbic acid favoured the formation of product 1.

Thus the effect of quenchers on the yield of thymine photoproducts 1,2 does not allow us to make unambiguous conclusions about the mechanism of their formation.

The experimental results obtained here enable us to conclude that: (i) Hp and Na_2-PP under CW excitation sensitise the decomposition of thymine in aqueous solution of TX-100 leading to formation of products 3-4; (ii) product 3 which is dominant at 206 nm is apparently formed by type-I mechanism with an electron being transferred from thymine to the excited triplet state of the sensitisers; and (iii) the role of $^1O_2$ in the thymine modification at the porphyrin concentration of 8×10^{-5} mol dm^{-3} is negligible.

Acknowledgement

The authors express their deep appreciation to Dr J T Kunjappu for experimental assistance, to Drs K V S Rama Rao and O A Tiflova for useful discussions and to Dr R M Iyer for his keen interest and encouragement.

References

1 Kessel D, *Photochem Photobiol*, **39** (1984) 851.

2 Van den Bergh H, *Chem Brit*, **22** (1986) 430.

3 *Primary photoprocesses in biology and medicine*, edited by R V Bensasson, G Jori, E J Land & T G Truscot (Plenum Press, New York) 1985.

4 Hariharan P V, Courtney J & Eleczkos, *Int J Radiat Biol*, **37** (1980) 691.

5 Buettner G R & Oberley L W, *FEBS Lett*, **121** (1980) 161.

6 Cox G S, Whitten D G & Giannotti C, *Chem Phys Lett*, **67** (1979) 511.

7 Kozlov A A, Lobko V V, Matveetz YuA, Nikogosyan D N & Letokhov V S, *Lasers in the Life Sciences* (In Press).

8 Boye E & Moan J, *Photochem Photobiol*, **31** (1980) 223.

9 Blazek E R & Hariharan P V, *Photochem Photobiol*, **40** (1984) 5.

10 Wagner J R, Cadet J & Fischer G J, *Photochem Photobiol*, **40** (1984) 589.

11 Bonnett R, Lambert C, Land E J, Scourides P A, Sinclair R S & Truscott T G, *Photochem Photobiol*, **38** (1983) 1.

12 *Singlet oxygen reactions with organic compounds and polymers*, edited by B Ranby & J E Rabek (John Wiley, New York) 1979.

13 Wilkinson F & Brummer J G, *J phys Chem Ref Data*, **10** (1981) 809.

14 Buettner G R & Need M J, *Cancer Lett*, **25** (1985) 297.

15 Sconfienza C, Van De Vorst A & Jori G. *Photochem Photobiol*, **31** (1980) 351.

16 Grossweiner L I, Patel A S & Grossweiner J B, *Photochem Photobiol*, **36** (1982) 159.

17 Knowles A, *Photochem Photobiol*, **13** (1971) 473.

18 Simon M I & Vunakis H V, *J molec Biol*, **4** (1962) 488.

19 Choughuley A S U & Chadha M S, *Proceedings of Symposium* (1975) *on 'singlet molecular oxygen* (BARC, Bombay) pp *153*.

Indian Journal of Chemistry
Vol. 27A, April 1988, pp. 286-289

Molybdena Dispersion in Nickel Promoted Molybdena Hydrodesulfurisation Catalysts

M O ALIAS & V SRINIVASAN*
Department of Chemistry, Indian Institute of Technology, Madras 600 036, India

Received 25 *May* 1987; *revised* 3 *August* 1987; *accepted* 5 *October* 1987

To determine molybdena dispersion on oxidic nickel molybdena catalysts, a method of specific irreversible adsorption of 1-butene has been applied. A pulse flow technique has been used to measure the amount of 1-butene adsorption at 100°C. The results show that Ni in a nickel-molybdena catalysts increases the dispersion of molybdena species on the catalyst and, therefore, the activity of the catalyst. The catalyst systems chosen do not suggest that the molybdena species form a monolayer on the surface of alumina used; bulk MoO_3 might reasonably be expected. However, changes in dispersion of Mo phase are quite probable, as is evident from 1-butene adsorption. When the same amount of molybdenum oxide (0.13 g) is incorporated per gram of each nickel-molybdena catalyst, the mode of dispersion of molybdena phase is different for different catalysts as revealed by variation of 1-butene adsorption on different catalysts. Hence an attempt has been made to estimate molbdena surface.

Active surface area of a catalyst is an important factor in assessing its performance, and on various catalysts active surface areas range from minute fraction of the total surface area to almost the total surface area of the catalyst. Although physical techniques such as electron diffraction[1] and ion scattering[2] may be useful for the determinatioin of active surface area, the potential of specific chemisorption has been appreciated since the classic use, by Emmett and Brunauer[3,4] of CO and CO_2 chemisorption to establish the surface composition of iron synthetic ammonia catalysts. Hydrogen chemisorption has been used for determining the metal surface of supported catalyst[5,6]. The adsorption of CO and of other gases on various metals supported on silica gel has been reported[7]. Although selective chemisorption has been most widely applied to supported metals, it can also be applied, with discretion, to supported transition metal oxide (or sulfide) catalysts. A generic problem with this class of catalysts is the lability of many transition metal compounds with respect to bulk oxidation or reduction under the condition of the chemisorption test. Chromia is a notable exception; the thermodynamic stability of bulk (but not surface) Cr_2O_3 permits Cr_2O_3-Al_2O_3 to be studied by the chemisorption[8,9] of either O_2 or H_2 at temperatures as high as 500°C. Bridges and coworkers[10] analysed the surface composition of a series of chromia-alumina catalysts by chemisorption of O_2 and CO on these catalysts. Mac Iver and coworkers[11,12] elucidated the mechanism of catalytic cracking by investigating 1-butene chemisorption on silica-alumina catalyst.

Ready susceptibility of molybdena catalysts to bulk oxidation and reduction has hindered the development of a chemisorption system that may permit discrimination between pure chemisorption and bulk phase reaction. However, Massoth[13] made an attempt to use 1-butene chemisorption for the measurement of molybdena dispersion. Ben Yaccov[14] also applied this method to characterise dispersion of molybdenum. Variation of hydrodesulfurisation (HDS) activity is influenced by Mo dispersion in molybdena catalysts[15,16]. The method used in the present study for the determination of molybdena dispersion on the oxide catalysts utilizes the specific irreversible adsorption of 1-butene.

Materials and Methods

Catalysts were prepared by conventional method of impregnating alumina with solutions of ammonium paramolybdate and nickel nitrate (AR, BDH). Low surface area α-alumina support ($6\ m^2g^{-1}$) was used in order to highlight the activity of active molybdena species. Concentrations of solutions were adjusted to give nine catalysts covering the range of composition from $r = 0$ to 0.54 ($r =$ Ni/Ni + Mo). Of these catalysts, seven catalysts were prepared by co-impregnation. After co-impregnation, the samples were dried in an oven at 110°C for 3 hr and finally calcined at 500°C for 6 hr. The remaining two catalysts were prepared by successive impregnation. Both these catalysts had Ni/Ni + Mo atomic ratio of 0.47. In one case (Cat. No. 9) the alumina was impregnated first with a solution of ammonium paramolybdate and dried in an oven at 110°C for 3 hr. After calcining for 6 hr at 500°C the powder was impregnated with nickel nitrate solution and dried in an oven for 3 hr at 110°C. The dried sample was then calcined at 500°C for 6 hr. The other sample

Table 1—Butene Adsorption Results on Nickel-Molybdena Catalysts (Oxidic State)

Sl No.	Catalyst*	Ni/Ni + Mo (r)	Surface area m^2g^{-1} (BET, N_2)	Amount of 1-butene adsorbed $\mu molg^{-1}$	Area of molybdena phase (m^2g^{-1})†
1	13 Mo-Al_2O_3	0.0	7.2	5.89	1.4
2	0.3 Ni-13 Mo-Al_2O_3	0.04	4.3	7.20	1.7
3	3 Ni-13 Mo-Al_2O_3	0.31	9.1	7.50	1.8
4	3.9 Ni-13 Mo-Al_2O_3	0.37	7.5	9.08	2.1
5	6 Ni-13 Mo-Al_2O_3	0.47	10.2	11.80	2.8
6	6.7 Ni-13 Mo-Al_2O_3	0.50	8.5	9.00	2.1
7	8 Ni-13 Mo-Al_2O_3	0.54	9.3	7.00	1.6
8	6 Ni-13 Mo-Al_2O_3‡	0.47	5.5	4.57	1.1
9	6 Ni-13 Mo-Al_2O_3**	0.47	12.3	5.21	1.2

*Notation used is such that 6 Ni-13 Mo-Al_2O_3 denotes NiO 6 wt % and MoO_3 13 wt %. Carrier used was α-alumina having surface area, 6 m^2g^{-1} (BET, N_2).

†Area of molybdena phase = number of molecules in the amont of 1-butene adsorbed multiplied by cross-sectional area of butene molecule (39 Å^2).

‡Ni was impregnated first.

**Mo was impregnated first.

(Cat. No. 8) was prepared in a similar way, but the order of impregnation was reversed. Surface areas of all catalysts were determined by BET method using N_2 as adsorbate at − 196°C (Table 1).

Determination of molybdena dispersion

A pulse flow technique[17-19] was employed for measuring the amount of 1-butene chemisorption. Flow method is fast and dynamic technique free from the disadvantages of the static high vacuum adsorption procedure. The catalyst tube was made out of 10 inch × 1/4 inch stainless steel tube. This could be maintained at the desired temperature by temperature control system which consisted of sunvic energy regulator, variable transformer, electric furnace and a thermocouple. The gas monitoring unit (model 90P3) consisted of a thermal conductivity detector (TCD) with signal processing equipment. A recorder having 10 inch full scale range with 0.1 mV/inch output was used to record the cell output. The temperature-regulated detector cell was operated at 150 mA and 180°C. The gas distribution system served two purposes; it provided the necessary gases for adsorption and pretreatment of the catalyst. A gas sampling valve allowed the injection of a certain amount of 1-butene gas (0.25 ml) into argon carrier gas stream. Gas flow could be adjusted by pressure regulators and needle valve, and was measured by calibrated rotameter.

A catalyst charge of 0.37 g was loaded into the catalyst tube. The catalyst was held in place in the tube by small plugs of glass wool. The catalyst tube was connected to the adsorption system through the use of 'Swage lok' fittings. A constant stream of pure argon (15 cm^3/min) was allowed to flow first to the reference side of the conductivity cell. Argon gas from the reference channel was passed over the catalyst sample and then through the measuring channel of the conductivity cell. The catalyst was heated to the adsorption temperature (100°C) using an electric furnace, the temperature being kept constant with the temperature control system. After all the air was flushed out by two-hour pretreatment in argon, 1-butene was injected as a pulse into the argon stream in front of the catalyst bed. A part of the gas was adsorbed by the catalyst. The amount of 1-butene remaining in the argon stream was measured by the thermal conductivity detector. The difference between the amount injected and the amount recorded gave the amount of 1-butene adsorbed on the catalyst sample.

Based on the findings of Massoth[13] that 1-butene polymerised at room temperature and that the catalyst underwent partial reduction at 175°C, we chose a temperature of 100°C for the adsorption study, where both of these phenomena were not observed.

HDS activity measurements

Catalytic activity measurements were made using microcatalytic reactor under pulse flow conditions[20]. Analysis of product stream was accomplished with a gas chromatograph. Before the actual microreaction, the catalyst placed in the reactor was reduced in pure H_2 at a flow rate of 20 ml/min for 4 hr, at 400°C. In thiophene desulfurisation reaction, the reactant H_2 also served as the carrier gas. A large number of thiophene pulses of 5 μl was introduced at 10-min intervals in order to have steady state catalyst activity; on further injections no significant charge in activity occurred. The activities were calculated as fractional conversion of thiophene using the data obtained from the analysis of the product stream. All conversions were normalised to 0.38 g of catalyst which was the average weight of all catalysts. The reaction temperature was 400°C.

Results and Discussion

The promotional effect of nickel in nickel-molybdena hydrodesulfurisation catalysts was clearly observed during the activity study (Fig. 1, curves a and b). The determination of Mo dispersion on the surface of the catalysts was essentially an attempt to understand this promotional effect. The results obtained from 1-butene adsorption measurements indicated that the effect of nickel was to increase the dispersion of molybdena species in the catalyst and therefore to increase its activity. A discussion of these results is given in the sequel.

1-Butene adsorption experiments with all catalysts were performed in the oxidic state. The pulse flow method used here utilized the specific irreversible adsorption of butene. This is in accordance with the following facts. The area corresponding to the effluent pulse is directly proportional to the amount of adsorbate issuing from the catalyst bed. If the pulse area obtained when flowing through the packed catalyst bed was less than that obtained with a completely empty column, it would imply that irreversible adsorption had occurred[21]. Similar behaviour was observed in all adsorption experiments.

Adsorption of 1-butene on alumina carrier was found to be negligibly small, therefore, adsorption of 1-butene involved Mo phase only, and the amount of butene adsorbed per gram catalyst was by itself a measure of dispersion of molybdenum. Since the primary interest was only in the trend in dispersion as a function of nickel rather than in dispersion itself, this much information was considered quite sufficient for the present work. The plot of 1-butene adsorption against nickel concentration for various Ni-Mo catalysts (Fig. 1, curve c) demonstrates that dispersion of molybdenum phase is dependent on nickel content. The dispersion increases upto 6 wt % NiO (Cat. No. 5) and then decreases. The 1-butene adsorption results in Fig. 1, curve (c) are directly proportional to the reaction results in Fig. 1 curves (a) and (b). This suggests that there is a linear relation between the dispersion of molybdena and activity. 1-Butene adsorption is thus a good measure of active sites for hydrodesulfurisation, i.e. molybdenum sites. The catalyst No. 5 containing 6 wt % NiO (r = 0.47) shows maximum dispersion of Mo and hence the maximum activity.

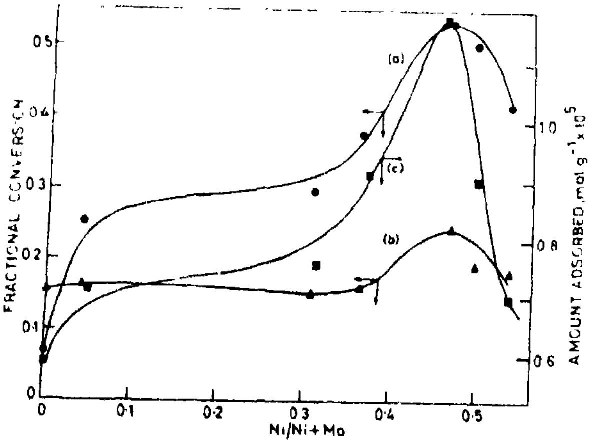

Fig. 1—(a, b) Theophene desulfurisation as a function of Ni concentration in nickel-molybdena catalysts at 400°C [(a), initial state; (b) steady state (14th pulse) and (c), butene adsorption on oxidic nickel molybdena catalyst as a function of nickel content

It was postulated by Schuit and Gates[22] that the role of promoter cobalt was to increase the dispersion of Mo on the catalyst and therefore to increase its activity. But results by Ben Yaacov[14] showed that dispersion of Mo was independent of cobalt. Therefore, he could not attribute the activity increase to dispersion of molybdenum, since cobalt did not effect disperson of the oxidic catalysts.

Massoth[13] found that the amount of 1-butene retained on the support was small, whereas, that on the catalyst was substantial, representing a butene-to-molybdena ratio of 0.63. If all the molybdena were available on the surface for adsorption of butene and taking a cross-sectional area for MoO_4^{2-} of 25 Å^2 the ratio of molecular area of adsorbed butene to surface molybdena would be 0.64, close to that found experimentally. Therefore, Massoth suggested that all of the molybdena existed as a monolayer on the alumina surface. But the present study does not suggest that the molybdena species forms a monolayer on the surface of the alumina used, because of the following reasons.

For the alumina used for the preparation of catalysts, the number of O^{2-} ions (6.74 Å^2) (ref. 23) exposed on the surface is 0.873×10^{20} per gram. Because three O^{2-} ions on the surface combine with one molybdenum atom[24] the maximum amount of molybdenum required to cover the surface of the alumina carrier completely with a monolayer of molybdenum oxide-carrier interaction species is 0.291×10^{20} molybdenum atoms per gram alumina. But the molybdenum actually incorporated in molybdena catalysts exceeds this calculated amount. For example, 13 wt % MoO_3 in Mo-Al_2O_3 corresponds to 6.22×10^{20} molybdenum atoms per gram alumina. Hence it is suggested that molybdenum cannot form a monolayer and bulk MoO_3 might reasonably be expected to result in these catalysts. However, changes in dispersion of Mo phase is always quite probable, as evident from 1-butene adsorption results. During the structural investigation performed with molybdena catalyst in oxidic state, Kabe and coworkers[24] found that the nature of Mo phase on alumina in the oxidic state depended on MoO_3 content incorporated. Todo and coworkers[25] reported the dispersion behaviour of molybdena in Co-Mo-Al_2O_3 catalysts. Two states of MoO_3 could be identified in these catalysts prepared with an alumina carrier having a surface area of 224 cm^2/g (BET, N_2); one was fairly well dispersed MoO_3 and another was a massive phase of MoO_3.

It is quite apparent from the present study that when the same amount of molybdenum oxide (0.13 g) is incorporated per gram of each Ni-Mo catalyst, the mode of dispersion of MoO_3 phase is different for different catalysts as revealed by variation of 1-butene adsorption on different Ni-Mo catalysts. An attempt can probably be made to estimate the amount of molybdena surface assuming all the butene molecules to be adsorbed on the Mo phase and considering the molecular area for butene to be 39 $Å^2$ (Table 1), assuming the molecules to be lying flat on the surface[13].

For the actual calculation of specific metal surface area by chemisorption, the chemisorbate cross-section should be known. In the absence of an absolute calibration of the adsorbate cross-section the amount of chemisorption still provides a relative measure of active surface. This idicates that even if the specific mechanism of chemisorption on a certain active species carrier combination is not known, the amount of chemisorption can still be used as a reliable measure of dispersion of active species.

It seems unusual to discuss chemisorption (ratio of adsorbate to adsorbent) only in terms of molecular sizes. While this is true for physical adsorption, one must treat chemisorption in terms of the stoichiometry of adsorbate-adsorbent interactions. In spite of these criticisms, 1-butene chemisorption has been used to characterise Mo dispersion by taking into consideration the molecular area of butene[13]. 1-Butene chemisorption is, however, a good way to characterise the dispersion of the Mo.

In conclusion the principal benefit obtained by Ni incorporation to molybdena catalyst appears to be better dispersion of molybdenum phase, which is an important factor in improving the catalytic activity. Results indicate that the dispersion of molybdena is dependent on nickel content. 1-Butene adsorption varies with Ni content and is maximum at which activity is maximum. Hence it is reasonable to attribute increase in activity with dispersion of molybdena.

Acknowledgement

This work was supported by the CSIR, New Delhi.

References

1 Yamaguchi S, *J chem Phys*, **27** (1957) 1114.
2 Rubin S, Passell T O & Belley L E, *Analyt Chem*, **29** (1957) 736.
3 Emmett P & Brunauer S, *J Am chem Soc*, **59** (1937) 310, 1553.
4 Emmett P & Brunauer S, *J Am chem Soc*, **62** (1940) 1732.
5 Burchtein R Kh & Frumkin A N, *Trans Faraday Soc*, **28** (1932) 273.
6 Spenadel L & Boudart M, *J phys Chem*, **64** (1960) 204.
7 Reyerson L H & Swearingen L E, *J phys Chem*, **31** (1927) 88.
8 Weller S W & Voltz S E, *J Am chem Soc*, **76** (1954) 4695.
9 Voltz S E & Weller S W, *J Am chem Soc*, **76** (1954) 4701.
10 Bridges J M, Mac Iver D S & Tobin H H, *Proc Int Congr* Catalysts: 2nd Congr Paris, 1960 (Technip Press, Paris), 1961.
11 Mac Iver D S, Zabor R C & Emmett P H, *J phys Chem*, **63** (1959) 484.
12 Mac Iver D S, Tobin H H & Barth R T, *J Catal*, **2** (1963) 485.
13 Massoth F E, *J Catal*, **30** (1973) 204.
14 Ben Yaacov R, *Ph.D. Thesis*, University of Houston, Texas, 1975.
15 Houalla M, Kibby C L, Petrakis L & Hercules D M, *J Catal*, **83** (1983) 50.
16 Badilla Ohlbaum R & Chadwick D, *Stud Surf Sci Catal*, **7** (1981) 1126.
17 Gruber H L & Ramser J H, 136th ACS Meetings, Atlantic City, N J, September, 1959, Abstracts, pp 22-I.
18 Hughee T R, Houston R J & Sieg R P, *Ind Eng Chem, Process Res Dev*, **1** (1962) 96.
19 Gruber H L, *Analyt Chem*, **34** (1962) 1828.
20 Bassett D W & Habgood H W, *J phys Chem*, **64** (1960) 769.
21 Eberly (Jr) P E, *J phys Chem*, **65** (1961) 68.
22 Schuit G C A & Gates B C, *AIChEJ*, **19** (1973) 417.
23 Peri J B, *J phys Chem*, **69** (1965) 211.
24 Kabe T, Yamadaya S, Oba M & Miki Y, *Int chem Eng*, **12** (1972) 366.
25 Todo M, Muramatsu K, Kurita M, Ogawa K, Sato T, Ogawa M & Kotera Y, *Bull Japan Petrol Institute*, **14** (1972) 89.

Indian Journal of Chemistry
Vol. 27A, April 1988, pp. 290-296

Water Sorption & Ion Exchange Properties of Hydrous Oxides

B VENKATARAMANI & A R GUPTA*
Chemistry Division, Bhabha Atomic Research Centre, Trombay, Bombay 400 085

Received 23 *March* 1987; *revised and accepted* 11 *August* 1987

Water sorption and ion exchange properties of hydrous titanium oxide (HTiO), thorium oxide (HThO), magnetite (MAG) and bismuth oxide (HBiO) have been studied. Water sorption isotherms have been analysed by D'Arcy and Watt equation. Monolayer formation on the surfaces, with one type of Langmuir sites having specific binding energy, is observed for HTiO and HThO The total number of water sorption sites are nearly equal to the number of OH groups as deduced from chemical analyses, except for freshly precipitated HTiO, where very weak sites, other than hydroxyl groups participate in the monolayer formation. These weak groups are eliminated by aging HTiO in alkaline solution. In general amorphous hydrous oxides have three types of surface groups: (i) hydroxyl groups that are most acidic which participate in ion exchange and serve as strong water sorption sites; (ii) hydroxyl groups which do not participate in ion exchange, but still serve as strong water sorption sites; and (iii) surface grups which serve as very weak water sorption sites (such groups are present in freshly prepared samples). Aging of the samples in alkali eliminates these very weak water sorption sites and produces extra hydroxyl groups belonging to categories (i) and (ii). Of the total number of surface OH groups, only a fraction is sufficiently acidic and participates in ion exchange reaction. MAG and HBiO have very small number of hydroxyl groups and exhibit multilayer formation typical of hydrophobic surfaces.

Water sorption isotherms have been used as a probe to characterise the surface hydroxyl groups of oxides[1,2]. Techniques like infrared (IR), heat of immersion, temperature programmed desorption (TPD), NMR etc., have been used to elucidate the nature of the surface hydroxyl groups and state of sorbed water on crystalline and mostly dehydroxylated surfaces[1-10]. However, due to the absence of well defined morphology, it has not been possible, even with these techniques, to fully characterise the state of water on amorphous oxides[7-10]. Amorphous hydrous oxides are generally preferred for ion exchange studies. With a view to characterise the surface of such amorphous oxides, we have studied their water sorption characteristics in relation to their ion sorption properties. Hydrous titanium oxide (HTiO), thorium oxide (HThO), bismuth oxide (HBiO) and magnetite (MAG) chosen for the present study have varying acidities and ion sorption properties[11].

Langmuir isotherm, BET equation[1] and D'Arcy and Watt equation[12] have been used to analyse the water sorption data. Gupta[13] has shown that the last mentioned equation yields more information about ion-water interaction in Dowex 50W type ion exchange resins. The same equation has been used to derive information on water-sorption site interaction in hydrous oxides and correlate it with their ion exchange characteristics and chemical compositions.

Materials and Methods

Hydrous titanium oxide (HTiO)

Titanium sponge was dissolved in conc. H_2SO_4 and HTiO was precipitated by the addition of excess of NaOH at about 370K. The gelatinous precipitate was digested for 2 hr at 370K, allowed to cool and age at room temperature in alkaline solution for 0, 2, 7 and 15 days (samples are designated B0, B2, B7 and B15 respectively). The samples were washed free from alkali, dried in air, rewashed and finally stored as air-dried samples.

Portions of the samples were treated with 0.01 mol dm^{-3} $HClO_4$ to remove sodium, washed free of acid and resuspended in water. This process was repeated till *p*H of water in contact with the oxide was neutral. Air-dried samples were crushed and sieved. Acid treated samples were designated B0T, B2T, B7T and B15T, T indicating treatment.

HTiO was also prepared by homogeneous precipitation by boiling a natural Ti(IV) sulphate solution with urea (40 g/g Ti). The final *p*H was about 7. The precipitate was allowed to age in the mother liquor for 2 days at room temperature and processed as described above. The oxide was designated H. The *p*H of the water in contact with this material was about 3. The oxide was used as such without further chemical treatment.

Hydrous thorium oxide (HThO)

HThO was precipitated from a hot (about 370K) acidic solution of Th(IV) nitrate with either 1 mol dm^{-3} NH_4OH or NaOH and aged in the mother liquor for 2 days at room temperature. The samples were designated TH1 and TH2 respectively.

Hydrous magnetite (MAG)

It was prepared by two methods: (i) by the method of Benton and Horsfall[14] by oxidising a precipit-

Table 1—Chemical and Surface Characteristics of Hydrous Oxides

Oxide	Prepn condition		Chemical composition	Surface groups[1], mmol/g		Water sorbed[2] (a_w = 1) (mmol/g)	Surface sites[2] (n_s) (mmol/g)	OH groups condensed[2] at 773K (TG) (mmol/g)	Binding energy parameter[2] K_1	Surface area[2] (N_2 ads.) (m^2/g)
	Method	Aging (days)		(OH)+(ONa)	SO_4 or NO_3					
			Hydrous Titanium Oxide							
B0	NaOH	0	$TiO_{1.49}(OH)_{0.82}(ONa)_{0.20}$	10.91	—	11.89	16.72*	7.78	1.9	260 (20)[3]
B2	NaOH	2	$TiO_{1.20}(OH)_{1.30}(ONa)_{0.30}$	12.88	—	9.67	13.30	7.70	3.4	310 (1)[3]
B7	NaOH	7	$TiO_{1.57}(OH)_{0.48}(ONa)_{0.38}$	8.96	—	6.78	7.72	2.80	10.1	—
B15	NaOH	15	$TiO_{1.53}(OH)_{0.55}(ONa)_{0.39}$	9.69	—	6.56	6.94	0.50	18.6	30 (1)[3]
H	Homog. pptn.	2	$TiO_{1.47}(OH)_{0.99}SO_{4\,0.07}$	10.42	0.74	6.67	8.52	9.02	4.2	165
			Hydrous Thorium Oxide							
TH1	NH_4OH	2	$ThO_{0.05}(OH)_{3.87}(NO_3)_{0.03}$	12.88	0.10	3.78	4.13	—	—	—
TH2	NaOH	2	$ThO_{0.89}(OH)_{2.17}(ONa)_{0.03}(NO_3)_{0.05}$	7.59	0.17	5.89	7.12	6.32	6.3	70
			Magnetite							
MAG1	$FeSO_4 + KNO_3$ (ref. 14)	2	Crystalline pure Fe_3O_4	—	—	0.56†	0.22‡	—	58.4	25
MAG2	$FeCl_3 + FeSO_4$ (ref 15)	2	$Fe_3O_4 + \alpha\text{-}Fe_2O_3$	—	—	1.66†	0.73‡	—	54.1	105
			Hydrous Bismuth Oxide							
Bis1	NH_4OH	2	Crystalline pure Bi_2O_3	—	—	0.83†	0.82‡	—	82.3	10

(1) Based on chemical analysis
(2) Values for acid-treated HTiO samples
(3) Surface areas of as-prepared HTiO samples given in bracket.
*Contribution also from C term (2.72×10^{-2})
†at a_w = 0.55
‡Values for D term (multilayer sites)
MAG1 = 0.34, MAG2 = 1.52, Bis1 = 0.07 mmol/g.

ate of ferrous hydroxide in boiling KNO_3 solution (designated MAG 1) and (ii) by mixing acidic ferric chloride and ferrous sulphate in the ratio 1 : 2 and precipitating magnetite with 1 mol dm^{-3} NaOH (ref. 15) (designated MAG 2).

Hydrous bismuth oxide (HBiO)

It was precipitated from a hot (about 370K) acidic solution of Bi(III) nitrate using excess of 1 mol dm^{-3} NH_4OH (designated Bis 1).

Characterisation of the hydrous oxides

The hydrous oxides were characterised by their elemental analyses, X-ray analysis and *p*H titration. Chemical compositions of various oxide sample are presented in Table 1.

X-ray diffraction analysis showed that all HTiO and HThO samples were amorphous. MAG 1 was pure magnetite while MAG 2 was a mixture of Fe_3O_4 and α-Fe_2O_3. Bis 1 was crystalline.

Oxide sample (0.4 g) in 50 ml of 0.1 mol dm^{-3} $NaNO_3$ was titrated against 0.1 mol dm^{-3} NaOH under constant stirring, measuring the *p*H 10 min after the addition of alkali. The *p*H-titration curves were analysed to evaluate the dissociation constants, $pK^*_{a_1}$, of the surface OH groups following the method of Schindler and Gamsjaeger[16].

Surface area

Surface area of the oxides were determined by three point measurement using N_2 as adsorbent in Quantasorb Instrument (Japan). The oxides were degassed at 573K for 4 hr prior to N_2 adsorption. To that extent, measured surface areas do not represent true surface areas of the samples, being the surface areas of samples heated to 573K. Surface area values are listed in Table 1.

Thermal analysis

Thermogravimetric (TG) and differential thermal (DT) analyses of the water sorbed oxides ($a_w = 0.95$) were done using a Stanton thermobalance.

Infrared spectra

IR spectra of the vacuum-dried HTiO were taken in KBr on a Perkin-Elmer grating infrared spectrophotometer model 577. However, all the samples, including the HTiO dried at 773K for 4 hr to constant weight, showed water peaks in the spectra, presumably due to the absorption of moisture by KBr itself.

Water sorption

Water sorption experiments were done at room temperature (298 ± 1K) in an isopiestic set-up consisting of a vacuum desciccator attached to a vacuum pump.

While preparing completely dry samples for experiments it was observed that heating the air-dried samples *in vacuo* at350-360K was not sufficient to dehydrate the sample completely. TG experiments showed negligible loss of water beyond 773K. Equilibrating the oxide samples *in vacuo* over conc. H_2SO_4, led to dehydration of the samples to the same extent as drying at 773K. Hence, samples dried *in vacuo* over conc. H_2SO_4 were taken as completely dry samples. The advantage of this approach is that the physical characteristics of the oxides are not altered as in drying at high temperatures (HTiO samples changed their colour to yellowish brown on drying at ~373K or over conc. H_2SO_4. They became colourless on water sorption).

Water sorption isotherms were determined using LiCl and H_2SO_4 solutions of known concentrations. The water activity at equilibrium was computed from their equilibrium concentrations[17]. Though equilibrium was established in about 6 days, the samples were equilibrated for much longer time (upto 15 days) for low water activities.

Results and discussion

Water sorption isotherms and their analysis

Water sorption isotherms of different hydrous oxides are shown in Fig. 1. Absence of hysteresis loops for all the oxides indicated that water sorption was reversible and the oxide surfaces were completely hydroxylated[5]. Water sorption on HTiO and HThO were of Langmuir type indicating formation of only monolayer on the surface, while MAG and Bis 1 samples exhibited multilayer formation.

The equilibrium water sorption data on oxides were analysed by D'Arcy and Watt equation[12] (Eq. 1):

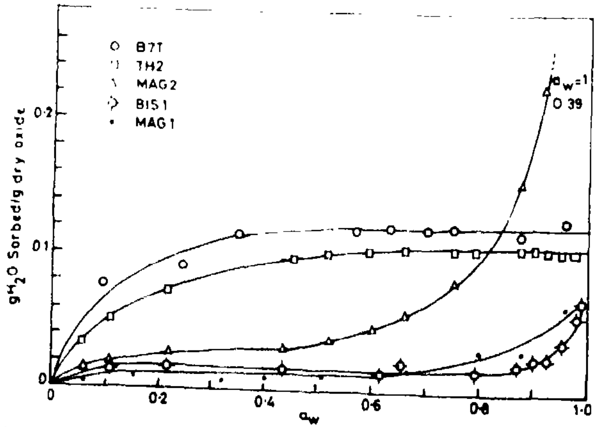

Fig. 1—Water sorption isotherms of hydrous oxides [The points are experimental data. The solid line is calculated from parameters of D'Arcy and Watt equation]

$$W = \sum_{i=0}^{l} \frac{K_i' K_i a_w}{1 + K_i a_w} + Ca_w + \frac{k' k a_w}{1 - k_i a_w} \quad \ldots (1)$$

where W is the weight of water sorbed by 1 g of the oxide, $K_i' = mn_i/N$, n_i is the number of primary sites of type i; m is the molecular weight of water, N is the Avogadro's number, K_i is a constant which is related to the binding energy of ith site for water; K_0 and K_0' both equal zero (i = 0), l = n − j is the number of different types of primary sorption sites for water described by a Langmuir isother, C(= m Kp_0/N) is a constant for the linear approximation of Langmuir sorption of specific sites; k′ = mD/N, where D is the number of sites for secondary (or multilayer) sorption and k is a constant which is related to the attraction between water molecules in the multilayer.

A computer programme based on non-linear least square analysis was used for fitting the equation to water sorption data of various hydrous oxides.

In all the cases, there was no improvement in the fit with i = 2. In fact, K_i was the same for both i = 1 and i = 2, indicating only one type of primary sorption site (which follow Langmuir isotherm) for water on all oxides.

The binding energy parameter, K_i, gives values for Langmuir sites of ith type on the oxide. As K_i values do not appear to be unique (other combinations of K_i and n_i can give similar fits), it is more appropriate to discuss the results in terms of a range of values for K_i. The ranges in which K_i values fall are 1-5, 5-10, 10-20 and 20 and above.

The various parameters (n_i, K_i, C, D) evaluated from the water sorption data for various oxides, using Eq. (1) are given in Tables 1 and 2.

Effect of precipitating agent and aging

Aging HTiO in alkaline solution has a marked effect on the development and nature of the surface hydroxyl groups. Aging in alkali promotes condensation of hydroxo groups and the oxolation process and hence the total surface hydroxyl groups decrease as a result of aging (Table 1). Similar observation on the formation of compact HTiO with strong hydroxo bridges on aging has been made by Komarnenin *et al.*[18]

Though aging decreases water sorption sites, (Table 1), it increases the ion exchange capacity of HTiO, as reflected by the increase in the amount of Na^+ exchanged by the acid-treated material at *p*H 11.0.

The binding energy parameter, K_i of the surface hydroxyl groups increases markedly on aging HTiO. In the acid-treated B0 sample (or B0T), i.e. zero time for aging, weak sites that could be approximated to linear Langmuir isotherm (C term) are also available (Table 1), which were eliminated on aging the sample in alkaline solution (absence of C term for acid treated B2 sample or B2T).

Presence of sulphate ion in homogeneously precipitated HTiO (sample H) (Table 1) is due to the fact that the hydrolysis of Ti(IV) is not complete as reflected in the *p*H-titration curves (Fig. 2).

Table 2—Surface Characteristics of Na^+-form of Hydrous Oxides

Oxide	Na^+ present (m mol/g)	Water sorbed (a_w = 1) (m mol/g)	Surface sites (n_i) (m mol/g)	Binding energy parameter (K_i)	Other type of sites
HTiO					
As prepared					
B0	2.14	11.89	16.47	3.1	—
B2	2.97	8.22	10.93	4.0	—
B15	4.02	8.89	9.59	13.0	—
Exchanged					
B0TEX1	1.18*	10.83	17.85	1.9	—
B0TEX2	1.58†	13.06	6.58	8.8	0.14‡
B15TEX1	1.00*	6.11	6.52	14.4	0.007§ mmol/g
B15TEX2	2.16†	7.11	6.72	11.5	0.29§ mmol/g
HThO					
Exchanged					
TH1EX	0.12†	3.47	3.92	—	—
TH2EX	0.22†	4.72	5.87	5.5	—

**p*H = 9.0; †*p*H = 11.0; ‡C term; §D term (multilayer sites)

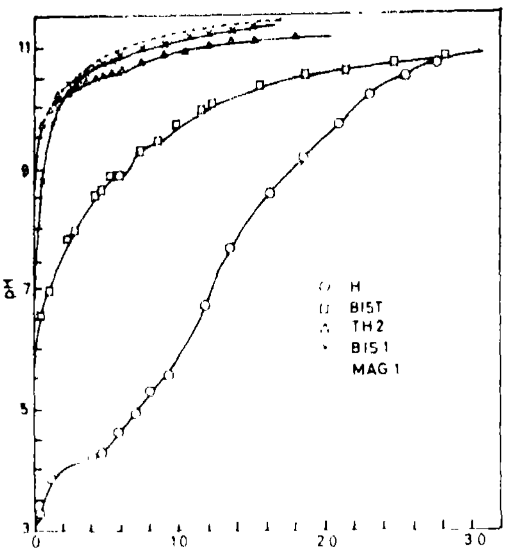

Fig. 2 – pH-titration curves of hydrous oxides

When mild alkali (NH_4OH) is used to precipitate HThO, the final product is nearly a hydroxide (OH/Th ratio nearly 4 for TH1). Oxolation process is promoted when strong alkali (NaOH) is used for precipitation (OH/Th ratio nearly 2 for TH2) (Table 1). Though oxolation process decreases the number of OH groups, it increases the water sorption and ion exchange capacity of HThO. Unlike TH1, where only a fraction of OH groups take part in water sorption (Table 1), all OH groups participate in water sorption in TH2. Hence, analysis of water sorption data was done only in the case of TH2 to get a meaningful picture of the sorption process.

Nature of the sorption sites

The number of sorption sites (n_i) as deduced from the water sorption data, or from chemical analysis of HTiO were in good agreement (Table 1), except BOT. This indicates that surface hydroxyl groups act as water sorption sites, though in the case of BOT some other weak water sorption sites are also present (C term in BOT).

Attempts to estimate the total surface hydroxyl groups on HTiO by measuring the water loss due to condensation of hydroxyl groups at high temperature (773K-TG data) and maximum water uptake (at $a_w = 1$) did not yield consistent results (Table 1). The values were less than n_i evaluated from Eq (1) and chemical anlayses. As water loss continued upto 773K and beyond, probably dehydroxylation of HTiO was not complete. Similar difficulty in estimating total surface hydroxyl groups on poorly crystalline TiO_2 by heating at high temperature, has been reported by Omori *et al*[7] and Morishige *et al.*[10]

The number of hydroxyl groups taking part in ion exchange process (Table 2) are much less than the total number of hydroxyl groups (n_i) on HTiO surfaces (Table 1). This implies that there are two types of hydroxyl groups on HTiO surface: (i) having definite pK_a^* value of 8.1 ± 0.05 (see below) and (ii) having weakly acidic strength. They may differ in their water sorption behaviour (different K_i values), but due to cooperative hydrogen bonding phenomenon in the formation of monolayer, they exhibit a single binding energy and become indistinguishable from water sorption point of view.

Doremieux-Morin *et al*[9] based on NMR study of the state of water on different forms of TiO_2 concluded that two types of water sorption sites exist on amorphous TiO_2: one bicoordinated to Ti in the matrix and the other attached directly to Ti atom. According to these authors[9] the lattice OH groups (the former type) sorb water stronger than those on Ti atoms (the latter type). Presumably, the stronger OH groups take part in ion exchange process.

Taking sample TH2 as the representative sample of HThO, it is seen that reasonably consistent estimate of surface OH groups could be obtained from water sorption data (n_i) and chemical analysis (Table 1). Unlike HTiO, TG data also give a reasonably good estimate of the surface OH groups on HThO. Two types of water sorption surface sites, viz (i) and (ii) mentioned above are also present on HThO but the fraction of type (i) sites are too small [as reflected in the low ion exchange capacity (Table 2)] compared to HTiO.

Small number of surface sites having high binding strength were present on MAG and HBiO (Table 1). Similar low water sorption on magnetite and mixture of iron oxides has been reported by Morimoto *et al.*[19] Comparing the values of n_i and D for MAG, it appears that nearly 2 water molecules are associated with each surface site in the monolayer, in conformity with the observation of Morimoto *et al*[19]. The poor water sorption and multilayer formation indicate that these oxides surfaces are hydrophobic in nature[1].

Surface area

HTiO samples (Na^+-containing) gave very low surface area values (Table 1). Bonsack[20] attributes this to the blocking of pores by surface Na^+. However, the acid-treated (Na^+-free) HTiO samples give larger surface areas (Table 1). Even these do not represent the true surface of HTiO samples on which water sorption has been studied due to preheating of samples prior to N_2 sorption measurements.

Water is not a recommended adsorptive for surface area determination[21] primarily due to multilayer effects. However, in cases, as in the present study, when well defined monolayers are formed (with complete absence of multilayer) by the sorption of one water molecule on one sorption site, water sorption isotherms are expected to give reliable values for the surface area. The surface areas calculated based on water sorption data (650-900 m^2/g, based on 0.16 nm^2 per molecule of water[9]) are comparable to those expected of amorphous HTiO. Besides, these surface area determinations do not involve pre-heat treatment of the samples and are not influenced by the presence of Na$^+$ or other impurities (see below and Table 2).

Surface area of HThO, sample TH2 (Table 1), was in the range reported in literature[4] for precipitated thorium oxide. Similarly the surface area of MAG (Table 1) was also in reasonable agreement with the literature value[22], for material prepared by the precipitation technique.

Ion exchange property

Hydrous oxides possess cation exchange property (in alkaline solution) as a result of the *p*H-dependent dissociation of the surface hydroxyl groups. Analysis of *p*H-titration curves (Fig. 2) in alkaline solution gives an estimate of the dissociation constant, $pK^*_{a_2}$, the value of which reflects the acidic strength of the surface hydroxyl groups. The $pK^*_{a_2}$ was found to be 8.1 ± 0.05 for all the HTiO preparations. Aging in alkaline solution increased only the ion exchange capacity but did not alter the $pK^*_{a_2}$. This is because only a fraction of the total surface hydroxyl groups take part in ion exchange reaction in solution—a conclusion reached by Yates *et al*[23] also. The surface acidity constants ($pK^*_{a_2}$) for HThO, MAG and HBiO were similar (10.5). Accordingly their ion exchange capacities are much lower than the total number of hydroxyl groups as deduced from water sorption.

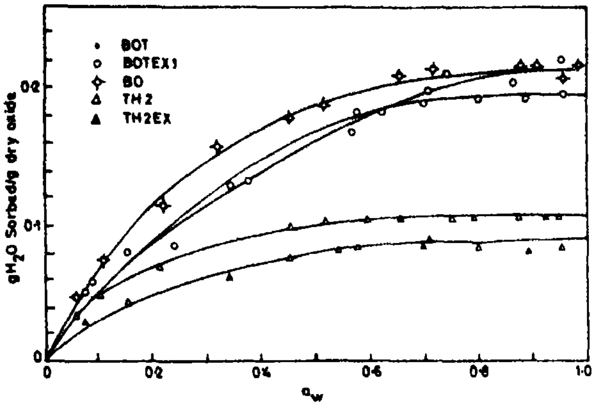

Fig. 3—Effect of sorbed sodium on the sorption of water on HTiO and HThO [The points are experimental data. The solid line is calculated from parameters of D'Arcy and Watt equation]

The water sorption isotherms on Na$^+$-form of the hydrous oxides are given in Fig. 3 and the relevant parameter deduced from the analysis of the isotherms are given in Table 2. Ion exchange reactions were carried out at *p*H 9.0 and 11.0, and the samples designated with a suffix "EX" in Table 2. As the number of surface groups participating in ion exchange are less, the shape of the isotherm, amount of water sorbed and the sorption site density of H$^+$-form (Table 1) and Na$^+$-form (Table 2) of the oxides hardly differ, except for changes in the bindig energy. A small contribution from the C and D terms in the case of Na$^+$-exchanged HTiO (Table 2) presumably reflects the binding of more than one water molecules by the –ONa sites. Even these marginal effects are not seen in Na$^+$-exchanged HThO, because very low amounts of Na$^+$ are present in these samples due to very low ion exchange capacity.

Acknowledgement

The authors wish to thank Shri S K Roy and Shri T S Krishnamoorthy for their help in surface area measurements.

References

1 Zettlemoyer A C, Micale F J & Klier K, in *Water—Comprehensive treatise*, Vol. 5 (edited by F Franks) (Plenum Press, New York) 1975, pp. 249.
2 Texter J, Klier K & Zettlemoyer A C, in *Surface and membranes Science*, Vol. 12 (edited by D A Cadenhead & J F Danielli) (Academic Press) 1978, pp. 327.
3 Parfitt G D, in *Surface and membrane science*, Vol. 11 (edited by D A Cadenhead & J F Danielli) 1976, pp. 181.
4 Brey (Jr) W S & Lawson K D, *J phys Chem*, **68** (1964) 1474.
5 Fuller (Jr) E L, Holmes H F & Secoy C H, *J phys Chem*, **70** (1966) 1633.
6 Holmes H F, Fuller (Jr) E L & Secoy C H, *J phys Chem*, **72** (1968) 2293.
7 Omori T, Imai J, Nagao M & Morimoto T, *Bull chem Soc (Japan)*, **42** (1969) 2198.
8 Primet M, Pichat P & Mathieu M V, *J phys Chem*, **75** (1971) *1216*.
9 Doremieux-Morin C, Enriquez M A, Sanz J & Fraissard J, *J Colloid Interf Sci*, **95** (1983) 502.
10 Morishige K, Kanno F, Ogawava H & Sasaki S, *J phys Chem*, **89** (1985) 4404.
11 Fuller M J, *Chromatogr Rev*, **14** (1971) 45.
12 D'Arcy R L & Watt I C, *Trans Faraday Soc*, **66** (1970) 1236.
13 Gupta A R, *Indian J Chem*, **24A** (1985) 368.
14 Benton D P & Horsfall G A, *J Chem Soc*, (1962) 3899.
15 Venkataramani B, Venkateswarlu K S & Shankar J, *J Colloid Interf Sci*, **67** (1978) 187.
16 Schindler D W & Gamsjaeger H, *Killoid Z Z, Polymers*, **250** (1972) 759.

17 (a) Robinson R A, *Trans Faraday Soc*, **41** (1945) 756.
  (b) Robinson R A & Stokes R H, *Electrolyte solutions* (Butterworths; London) 1969.

18 Komarneni S, Breval E & Roy R, *J Non Crystalline Solids*, **79** (1986) 195.

19 Morimoto T, Yokota Y & Nagao M, *J Colloid Interf Sci*, **64** (1978) 188.

20 Bonsack J P, *J Colloid Interf Sci*, **44** (1973) 430.

21 Sing K S W, in *Characterisation of powder surface*, (edited by G D Parfitt &K S W Sing) (Academic Press) 1976, Chap. 1, pp. 1.

22 Tewari P H, Campbell A B & Lee W, *Canad J Chem*, **50** (1972) 1642.

23 Yates D E, Griesser F, Cooper R & Healy T W, *Austr J Chem*, **30** (1977) 1655.

Indian Journal of Chemistry
Vol. 27A, April 1988, pp. 297-302

Solubilities of Amino Acids in Methanol + Water Mixtures at Different Temperatures

B P DEY & S C LAHIRI*
Department of Chemistry, University of Kalyani, Kalyani 741 235

Received 19 *December* 1986; *revised* 6 *July* 1987; *rerevised and accepted* 7 *September* 1987

The solubilities of amino acids in methanol + water mixtures have been determined at three different temperatures to understand the thermodynamics of transfer of amino acids from water to methanol + water mixtures. The results have been interpreted in terms of structural changes in the solvent mixtures.

The importane of the systematic studies of the solubilities of electrolytes and non-electrolytes in different solvent system is well known due to their wide applications in almost all branches of science and technology.

The importance and usefulness of amino acids in biological processes led us to study the solubilities of amino acids in methanol + water mixtures (0-100%) at different temperatures. Inspite of the similarities, there are wide differences in the behaviour of the amino acids and each of them has a distinct character of its own. The thermodynamics of transfer of amino acids may be coupled with the thermodynamics of the ionization of amino acids to determine the single ion thermodynamics of the cations and anions of the amino acids. Moreover, the entropy of transfer of amino acids can be used as structural probe to understand the structural changes taking place in $MeOH + H_2O$ mixtures in presence of the amino acids. The results of our investigations on the solubilties of amino acids in methanol + water mixtures at different temperatures are reported in this paper.

Materials and Methods

Purification of amino acids, methanol and determination of the solubilities of amino acids at 288 ± 0.01, 293 ± 0.01 and 298 ± 0.01 K were carried out in the way described in our earlier communications[1-3]. The accuracy of the solubility values was: 0.3-0.6% upto 45 wt % of methanol and 0.5-0.8% at higher percentage of methanol.

Results and Discussions

The free energies of solvation of amino acid at different temperatures are given by Eq. 1,

$$\Delta G^\circ = -2.303\, RT \log C_s \qquad \ldots (1)$$

where C_s is the solubility of amino acid in molar unit.

The free energies of transfer (ΔG_t°) of amino acid from water to mixed solvents are given by Eq. 2,

$$\Delta G_t^\circ = \Delta G_s^\circ(RH^\pm) - \Delta G_w^\circ(RH^\pm) \qquad \ldots (2)$$

where $\Delta G_s^\circ(RH^\pm)$ and $\Delta G_w^\circ(RH^\pm)$ represent the free energies of solvation of amino acids in mixed solvents and water respectively.

The activity coefficients of the amino acids in different solvents are not known; these have been taken to be unity for the saturated solutions in the different solvent mixtures.

The enthalpies of solvation of amino acids (ΔH°) have been obtained from the slope of the plots of log C_s against 1/T assuming ΔH° to be constant in the temperature range 288-298 K. In view of the limitations of the method, the accuracy of ΔH° values has been estimated to be ± 0.5 kJ mol^{-1} upto 45 wt% of methanol and 1.0 kJ mol^{-1} at higher percentages. The ΔS° values have been calculated from the relation $\Delta G^\circ = \Delta H^\circ - T\Delta S^\circ$.

The solubility values and the thermodynamic parameters of the amino acids in methanol + water mixtures are given in Tables 1 and 2. The ΔG_t°, ΔH_t° and $T\Delta S_t^\circ$ vs % org. solv. profiles of Glycine are shown in Fig. 1.

The replacement of a H atom in acetic acid and propionic acid by a $-NH_2$ group results in an increase in the acidic nature in glycine and alanine. It also leads to an appreciable decrease in solubility. The amino acids, we studied, are derived by the replacement of hydrogen in glycine and alanine by different hydrophobic groups.

The replacement of H in alanine by OH, $-CONH_2$ and $-C_6H_5$ leads to the decrease in the solubility of the resulting amino acids almost to the same extent whereas the replacement of H

Table 1—Solubility and Free Energy of Transfer of Amino Acids in MeOH + H_2O Mixtures at 288, 293 and 298 K

Wt% of MeOH	$1/\varepsilon \times 10^2$	288 K		293 K		298 K	
		C_s (mol dm^{-3})	ΔG_t°(kJ mol^{-1})	C_s (mol dm^{-3})	ΔG_t°(kJ mol^{-1})	C_s (mol dm^{-3})	ΔG_t°(kJ mol^{-1})
				Glycine			
0	1.27	3.025	0	3.180	0	3.325 (3.333)	0
8.0	1.33	2.850	0.14	3.020	0.13	3.175	0.12
16.0	1.40	2.675	0.30	2.860	0.26	3.025	0.24
25.2	1.48	1.175	2.26	1.267	2.24	1.3625	2.21
34.4	1.57	1.0125	2.62	1.115	2.56	1.225	2.48
44.7	1.69	0.875	2.97	0.910	3.05	0.950	3.11
54.2	1.84	0.1225	7.68	0.140	7.61	0.1575	7.56
64.1	2.01	0.875	8.48	0.100	8.43	0.1150	8.34
75.9	2.25	0.0675	9.11	0.080	8.97	0.1050	8.56
87.9	2.57	0.016	12.55	0.025	11.81	0.04	10.95
100	2.96	0.0065	14.71	0.009	14.30	0.0115	14.04
				α-Alanine			
0	1.27	1.64	0	1.78	0	1.87 (1.868)	0
8.0	1.33	1.50	0.21	1.62	0.22	1.70	0.24
16.0	1.40	1.31	0.53	1.42	0.55	1.49	0.56
25.2	1.48	0.87	1.51	0.89	1.68	0.91	1.78
34.4	1.57	0.375	3.53	0.405	3.60	0.425	3.67
44.7	1.69	0.345	3.73	0.375	3.79	0.40	3.82
54.2	1.84	0.155	5.64	0.1695	5.72	0.1825	5.76
64.1	2.01	0.1425	5.85	0.1585	5.89	0.1675	5.98
75.9	2.25	0.020	10.55	0.0215	10.75	0.024	10.79
87.9	2.57	0.010	12.20	0.013	11.98	0.016	11.80
100	2.96	0.005	13.87	0.007	13.49	0.009	13.22
				L-Valine			
0	1.27	0.718	0	0.736	0	0.755	0
8.0	1.33	0.676	0.15	0.689	0.16	0.70	0.18
16.0	1.40	0.632	0.31	0.641	0.33	0.65	0.37
25.2	1.48	0.493	0.90	0.499	0.94	0.505	0.99
34.4	1.57	0.213	2.92	0.216	2.98	0.22	3.05
44.7	1.69	0.196	3.11	0.203	3.13	0.21	3.17
54.2	1.84	0.162	3.46	0.182	3.40	0.195	3.35
64.1	2.01	0.0269	7.87	0.0302	7.78	0.035	7.60
75.9	2.25	0.0182	8.80	0.0209	8.67	0.0245	8.49
87.9	2.57	0.000398	17.96	0.000501	17.76	0.000625	17.58
100	2.96	0.000229	19.28	0.000309	18.94	0.000425	18.54
				L-Leucine			
0	1.27	0.174	0	0.180	0	0.186	0
8.0	1.33	0.160	0.19	0.163	0.21	0.170	0.22
16.0	1.40	0.140	0.51	0.144	0.54	0.148	0.56
25.2	1.48	0.113	1.03	0.119	1.01	0.124	1.00
34.4	1.57	0.0513	2.92	0.055	2.89	0.059	2.84
44.7	1.69	0.0495	3.01	0.0525	3.00	0.057	2.93
54.2	1.84	0.0460	3.18	0.049	3.17	0.054	3.06
64.1	2.01	0.0178	5.45	0.0204	5.30	0.0235	5.12
75.9	2.25	0.0131	6.19	0.0158	5.91	0.0185	5.71
87.9	2.57	0.0041	8.97	0.00525	8.61	0.0068	8.20
100	2.96	0.00366	9.25	0.00468	8.89	0.0062	8.42

(*—Contd.*)

Table 1—Solubility and Free Energy of Transfer of Amino Acids in MeOH + H_2O Mixtures at 288, 293 and 298 K—*Contd.*

Wt% of MeOH	$1/\varepsilon \times 10^2$	288 K		293 K		298 K	
		C_s (mol dm^{-3})	ΔG_t°(kJ mol^{-1})	C_s (mol dm^{-3})	ΔG_t°(kJ mol^{-1})	C_s (mol dm^{-3})	ΔG_t°(kJ mol^{-1})
				L-Asparagine			
0	1.27	0.218	0	0.221	0	0.226	0
8.0	1.33	0.172	0.56	0.175	0.58	0.177	0.61
16.0	1.40	0.0765	2.40	0.0782	2.54	0.08	2.58
25.2	1.48	0.0342	4.43	0.0355	4.46	0.0363	4.54
34.4	1.57	0.0130	6.75	0.0135	6.82	0.0141	6.88
44.7	1.69	0.00614	8.55	0.00617	8.73	0.0062	8.91
54.2	1.84	0.00295	10.30	0.00315	10.37	0.00335	10.44
64.1	2.01	0.00170	11.62	0.00191	11.59	0.00215	11.54
75.9	2.25	0.00118	12.51	0.00132	12.49	0.00155	12.35
87.9	2.57	0.00046	14.75	0.000537	14.67	0.00065	14.50
100	2.96	0.00027	16.02	0.000347	15.74	0.00045	15.41
				L-Phenylalanine			
0	1.27	0.174	0	0.177	0	0.180	0
8.0	1.33	0.165	0.12	0.167	0.14	0.169	0.15
16.0	1.40	0.0794	1.88	0.0796	1.95	0.08	2.01
25.2	1.48	0.0687	2.22	0.0703	2.25	0.072	2.27
34.4	1.57	0.0295	4.25	0.0308	4.26	0.032	4.28
44.7	1.69	0.026	4.56	0.0275	4.53	0.029	4.52
54.2	1.84	0.0218	4.96	0.0234	4.92	0.026	4.79
64.1	2.01	0.0073	7.59	0.00831	7.50	0.0092	7.37
75.9	2.25	0.00608	8.03	0.00692	7.90	0.0082	7.65
87.9	2.57	0.0044	8.81	0.00513	8.63	0.0062	8.34
100	2.96	0.00114	12.05	0.00141	11.77	0.0018	11.41
				L-Serine			
0	1.27	0.453	0	0.461	0	0.47	0
8.0	1.33	0.427	0.14	0.432	0.17	0.438	0.18
16.0	1.40	0.243	1.49	0.248	1.51	0.253	1.53
25.2	1.48	0.205	1.90	0.210	1.92	0.217	1.92
34.4	1.57	0.1245	3.09	0.131	3.08	0.136	3.07
44.7	1.69	0.0913	3.83	0.0975	3.79	0.103	3.77
54.2	1.84	0.0525	5.16	0.0575	5.08	0.063	4.98
64.1	2.01	0.0186	7.64	0.0209	7.54	0.024	7.37
75.9	2.25	0.0073	9.90	0.00851	9.73	0.01	9.54
87.9	2.57	0.0026	12.38	0.00309	12.20	0.00375	11.97
100	2.96	0.0008	15.08	0.00105	14.84	0.00135	14.50
				L-Histidine			
0	1.27	0.258	0	0.264	0	0.272	0
8.0	1.33	0.253	0.04	0.259	0.05	0.266	0.06
16.0	1.40	0.161	1.12	0.166	1.14	0.171	1.15
25.2	1.48	0.145	1.37	0.150	1.39	0.155	1.39
34.4	1.57	0.111	2.02	0.116	2.01	0.122	1.98
44.7	1.69	0.0437	4.25	0.0468	4.22	0.0505	4.17
54.2	1.84	0.0145	6.90	0.0162	6.80	0.0188	6.62
64.1	2.01	0.0113	7.48	0.0135	7.25	0.016	7.02
75.9	2.25	0.00115	12.96	0.00151	12.58	0.002	12.17
87.9	2.57	0.000824	13.75	0.00112	13.31	0.0015	12.88
100	2.96	0.000483	15.03	0.000646	14.66	0.0009	14.45

by β-imidazole group of $-\mathrm{CH}\langle\begin{smallmatrix}\mathrm{CH_3}\\ \mathrm{CH_3}\end{smallmatrix}$ group decreases the solubility to a greater extent. However, the solubility is highest in the case of glycine in water, methanol and methanol + water mixtures. The hydrophobic interactions appear to be one of the reasons for the changed solubility of the amino acids in water.

Both enthalpies and entropies of transfer of the amino acids show minima in the water-rich regions. The presence of maxima or minima in the water-rich regions is generally observed and the location of the extrema is generally in the region 8 wt%-44 wt% of methanol depending on the nature of the solute. An increase in the size of amino acid shifts the extrema towards the media richer in water. However, the extrema in the enthalpies and entropies of transfer do not always coincide.

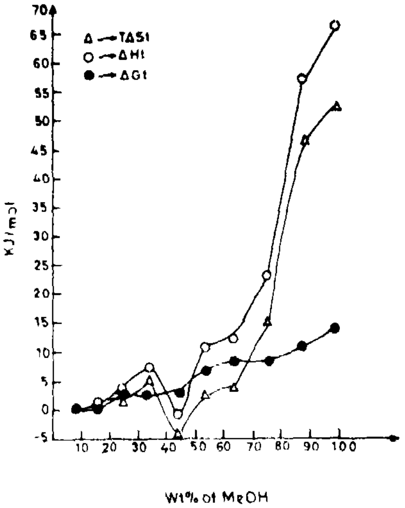

Fig. 1—Plots of thermodynamic parameters of glycine against wt % of methanol

The structural changes associated with the addition of cosolvent (methanol) to water result in enthalpy and entropy changes. The addition of methanol first strengthens the three dimensional water structure. Structure formation appears to be maximum at 0.2-0.3 mole fraction of methanol after which structural collapse begins. The excess thermodynamic properties of mixing of MeOH + H_2O mixtures show[4] a maximum in exothermic enthalpy of mixing at about $X_2 = 0.2$, a minimum in $T\Delta S$ at $X_2 = 0.3$ and a maximum in the positive free energy of mixing at $X_2 = 0.5$ (X_2 = mole fraction of methanol). It is expected that structural changes associated with the dissolution of amino acids in the solvent mixtures would be well reflected in the changes in enthalpy and entropy values.

The amino acids are chacracterised by the presence of hydrophilic centres (CO_2^-, NH_3^+) and hydrophobic centre (R) leading to two different types of hydration. Thus, both hydrophilic and hydrophobic interactions compete for water structure organization. The addition of amino acid to water leads to the rupture of the tetrahedral structure of water. When two non-polar regions (of amino acids) come close together, these regions are shielded to a greater extent from interaction with water molecules leading to the collapse of some of the quasi-crystalline water structure and a gain in entropy. The addition of amino acid to methanol also leads to a structural collapse as would be apparent from the large positive entropy values. However, in MeOH + H_2O mixtures, the maximum in the structure formation (entropy minimum) appears to be in the region of 44 wt% of methanol in case of glycine, but with the introduction of hydrophobic groups in the amino acids, the maximum (in terms of structure formation i.e. entropy minimum) shifts towards the lower methanol % region. The cooperative structure formation appears to be maximum at about 25 wt% of methanol in case of alanine and valine but about 16 wt% in case of other amino acids studied. The minima in the enthalpy changes are 44 wt% for glycine, 25 wt% for alanine and valine, 16 wt% for leucine and 8 wt% for other amino acids studied. Since the nature of the reacting groups is the same for all the amino acids, the changes in thermodynamic properties can be attributed to specific solvation effects and hydrophobic effects[5-7]. Specific solvation effects are dependent mainly on the composition of the solvent mixture, being greatest for strongly solvated amino acid, the hydrophobic effect on the other hand increase with the size of the solute molecules and is maximum where maximum enhancement of the water structure occurs i.e. in the region of 0.2-0.3 mole fraction of methanol. The specific solvation effect and the hydrophobic effect act in the opposite directions[5-7]. The hydrophobic effect increases with the increase in the size of the solute and shifts the point of maximum structure formation towards the media richer in water.

The peculiar behaviour of glycine as compared to those of other amino acids is apparent from the study of the variation of ΔG_t° at different temperatures with the solvent composition. For glycine, ΔG_t° values decrease with increase in temperature upto 34.4 wt% of methanol beyond which ΔG_t° values increase with increase in temperature, but a reverse behaviour is observed for other amino acids where ΔG_t° values increase with increase in temperature when the percentage of organic solvent is low. But inversion takes place

Table 2—Thermodynamic Parameters for Solvation of Amino Acids in MeOH + H_2O Mixtures at 298 K

Wt% of MeOH	ΔG_t°(kJ mol^{-1})	ΔH_t°(kJ mol^{-1})	$T\Delta S_t^\circ$(kJ mol^{-1})
		Glycine	
0	−2.98	6.85	9.83
8.0	−2.86	6.68	9.54
16.0	−2.74	7.98	10.72
25.2	−0.77	10.55	11.32
34.4	−0.50	13.95	14.45
44.7	0.13	5.74	5.61
54.2	4.58	17.55	12.97
64.1	5.36	19.14	13.78
75.9	5.58	30.31	24.73
87.9	7.97	63.82	55.85
100	11.06	73.07	62.01
		α-Alanine	
0	−1.55	9.48	11.03
8.0	−1.33	9.40	10.73
16.0	−0.99	9.14	10.13
25.2	0.23	3.21	2.98
34.4	2.12	4.73	2.61
44.7	2.27	6.07	3.80
54.2	4.21	11.66	7.45
64.1	4.43	11.96	7.53
75.9	9.24	12.76	3.52
87.9	10.25	33.50	23.25
100	11.67	41.48	29.81
		L-Valine	
0	0.77	3.51	2.74
8.0	0.88	2.39	1.51
16.0	1.07	1.91	0.84
25.2	1.69	1.59	−0.10
34.4	3.75	2.39	−1.36
44.7	3.87	4.63	0.76
54.2	4.05	9.57	5.52
64.1	8.30	17.55	9.25
75.9	9.19	20.74	11.55
87.9	18.28	31.91	13.63
100	19.24	43.08	23.84
		L-Leucine	
0	4.17	4.79	0.62
8.0	4.39	3.99	−0.40
16.0	4.73	3.67	−1.06
25.2	5.17	6.38	1.21
34.4	7.01	9.57	2.56
44.7	7.10	10.37	3.27
54.2	7.23	11.17	3.94
64.1	9.29	19.14	9.85
75.9	9.88	23.93	14.05
87.9	12.37	35.10	22.87
100	12.39	36.69	24.30
		L-Asparagine	
0	3.68	2.71	−0.97
8.0	4.29	1.91	−2.38
16.0	6.26	3.03	−3.23
25.2	8.22	3.99	−4.23
34.4	10.56	5.90	−4.66
44.7	12.59	7.02	−5.57
54.2	14.12	8.78	−5.34
64.1	15.22	14.04	−1.18
75.9	16.03	19.15	3.12
87.9	18.18	23.93	5.75
100	19.09	35.10	10.01
		L-Phenylalanine	
0	4.25	2.39	−2.06
8.0	4.40	1.60	−2.80
16.0	6.26	2.07	−4.19
25.2	6.52	3.19	−3.33
34.4	8.53	5.58	−2.95
44.7	8.77	7.66	−1.11
54.2	9.04	11.97	2.93
64.1	11.62	15.95	4.33
75.9	11.90	20.74	8.84
87.9	12.59	23.93	11.34
100	15.66	31.91	16.25
		L-Serine	
0	1.87	2.55	0.68
8.0	2.05	1.75	−0.30
16.0	3.40	2.87	−0.53
25.2	3.79	3.83	0.04
34.4	4.94	5.74	0.80
44.7	5.64	7.98	2.34
54.2	6.85	12.76	5.91
64.1	9.24	17.55	8.31
75.9	10.41	22.33	11.92
87.9	13.84	25.53	11.69
100	16.37	33.50	17.13
		L-Histidine	
0	3.23	3.68	0.45
8.0	3.29	3.51	0.22
16.0	4.38	3.99	−0.39
25.2	4.62	4.63	0.01
34.4	5.21	6.54	1.31
44.7	7.40	10.21	2.81
54.2	9.85	20.74	10.89
64.1	10.25	23.93	13.68
75.9	15.40	38.29	22.89
87.9	16.11	41.48	25.37
100	17.38	43.07	25.69

at different percentages for different amino acids. Inversion takes place at 87.9 wt% for alanine, 44.7 wt% for valine, 44.7-54.2% for leucine, beyond 25.2 wt% for serine, beyond 34.4 wt% for L-phenylalanine at 64.1 wt%, for L-asparagine. For L-histidine, the variation of ΔG_t° with temperature is almost negligible at low percentages of methanol and inversion takes place beyond 25.2 wt%. Explanation for this behaviour is difficult to offer.

References

1 Dey B P, Dutta S & Lahiri S C, *Indian J Chem*, **21A** (1982) 886.
2 Pal A, Dey B P & Lahiri S C, *Indian J Chem*, **25A** (1986) 322.
3 Dey B P & Lahiri S C, *Indian J Chem*, **25A** (1986) 136.
4 Franks F & Ives D J G, *Quart Rev*, **20** (1966) 1.
5 More J P, Fauve J, Avedikian L & Juillard J, *J soln Chem*, **3** (1974) 403.
6 Dollet N & Juillard J, *J soln Chem*, **5** (1976) 77.
7 Pointud Y & Juillard J, *J chem Soc Faraday Trans I*, **73** (1977) 1907.

Indian Journal of Chemistry
Vol. 27A, April 1988, pp. 303-307

Thermodynamic & Optical Studies on Binary Liquid Mixtures

T M AMINABHAVI*, L S MANJESHWAR & R H BALUNDGI
Department of Chemistry, Karnatak University, Dharwad, 580 003
and
S B HALLIGUDI
Central Salt and Marine Chemicals Research Institute, Bhavnagar 364 002

Received 8 *June* 1987; *revised and accepted* 14 *September* 1987

Excess molar volume (V^E) and excess molar refractivity (R^E) have been calculated at 20 ± 0.01°C from density and refractive index data on three binary mixtures of bromobenzene with cyclohexane, carbon tetrachloride and ethyl acetate. The validity of the existing mixing rules in the prediction of excess molar refractivity is discussed. The data are also used to predict density and refractive index increments of the mixtures. Results are discussed in terms of thermodynamic interactions between the mixing components.

As a part of our earlier work on interactions in binary solvent mixtures[1-3], we now report data on density and refractive index for three binary mixtures of bromobenzene with cyclohexane, carbon tetrachloride and ethyl acetate at 293.1K. These data have been used to calculate the excess molar volume (V^E) and excess molar refraction (R^E) of mixing. The latter quantity has been calculated using the existing mixing rules discussed elsewhere[4]. The results are discussed in terms of thermodynamic interactions with respect to the nature of mixing components.

Materials and Methods

The solvents used were of spectral grade and were found to be free from any impurity as revealed by gas chromatography. The purity of the solvents were further checked by measuring their densities and refractive indices and comparing these with the literature values. Agreement between the two sets of values was within ± 0.0005 units.

Solvent mixtures were made by weight in special air-tight stoppered bottles; the volume fractions were calculated from the weights and densities of pure components[5]. The possible error in the calculation of volume fraction (ϕ) was estimated to be less than 0.0001. All the physical properties were studied on the same day on which mixtures were prepared.

Densities were measured with a precision density meter, model DMA 02C (Anton Paar K.G., Austria) adopting the procedure described earlier[6]. Refractive indices of pure solvents and solvent mixtures were measured with a Bausch and Lomb precision refractometer equipped with mercury and sodium light sources. The precision of the instrument as quoted by the manufacturer is ± 0.00003 units. The initial calibration of the instrument was made at 293.1K using the standard glass test piece provided by the manufacturer. Samples were applied to the prism surfaces of the refractometer and readings were taken by using sodium (589 nm) and the mercury green (546 nm) and blue (436 nm) lines. Experimental densities and refractive indices are given in Table 1.

Results and Discussion

The experimentally measured densities were used to predict the excess molar volume using[1] Eq (1)

$$V^E(\text{cm}^3/\text{mol}) = \frac{M_1\phi_1 + M_2\phi_2}{\rho} - \frac{M_1\phi_1}{\rho_1} - \frac{M_2\phi_2}{\rho_2} \quad \ldots (1)$$

where ρ_1, ρ_2 and ρ are the densities of components 1, 2 and their mixtures respectively; M_1 and M_2 are the molecular weights of components 1 and 2, and ϕ_1 and ϕ_2 their volume fractions, respectively.

Excess molar refraction was calculated using Eq. (2)

$$R^E(\text{cm}^3/\text{mol}) = R - R_1\phi_1 - R_2\phi_2 \quad \ldots (2)$$

where R_1, R_2 and R are respectively the molar refractions of components 1, 2 and their mixtures. A large number of refractive index mixture rules have been proposed in the literature[4]. However, the Lorentz-Lorenz[7,8] rule is usually preferred because it is supported by a plausible theory; other rules such as Eykman[9], Gladstone-Dale[10], Newton[11] and Oster[12] are at least as good as the Lorentz-Lorenz rule. The Eykman rule is often superior from the experimental viewpoint[13]. In this paper one of our goals is to

Table 1—Densities and Refractive Indices of Binary Mixtures

Volume fraction (ϕ_1)	Density (g/cm³)	Refractive index for 589 nm	Refractive index for 546 nm	Refractive index for 436 nm
(I) Bromobenzene (1)-cyclohexane (2)				
1.0	1.49132	1.55891	1.56373	1.58422
0.9	1.42122	1.54580	1.55010	1.56943
0.8	1.35118	1.53193	1.53587	1.55380
0.7	1.27835	1.51804	1.52188	1.53850
0.6	1.20780	1.50451	1.50809	1.52344
0.5	1.13591	1.49092	1.49420	1.50813
0.4	1.06268	1.47742	1.48041	1.49348
0.3	0.99320	1.46430	1.46734	1.47880
0.2	0.92222	1.45304	1.45392	1.46402
0.1	0.85093	1.43820	1.44051	1.44931
0.0	0.77880	1.42627	1.42810	1.43580
(II) Bromobenzene (1)-ethyl acetate (2)				
1.0	1.49131	1.55891	1.56363	1.58421
0.9	1.43780	1.54070	1.54519	1.56420
0.8	1.38109	1.52229	1.52643	1.54408
0.7	1.32104	1.50182	1.51670	1.52352
0.6	1.26440	1.48518	1.48871	1.50550
0.5	1.20534	1.46670	1.46983	1.48330
0.4	1.14491	1.44792	1.45081	1.46281
0.3	1.08484	1.42928	1.43181	1.44240
0.2	1.02724	1.40969	1.41190	1.42101
0.1	0.96534	1.39172	1.39360	1.40140
0.0	0.90072	1.37230	1.37377	1.38033
(III) Bromobenzene (1)-carbon tetrachloride (2)				
1.0	1.49131	1.55891	1.56355	1.58416
0.9	1.50442	1.55010	1.55462	1.57420
0.8	1.51577	1.54091	1.54533	1.56460
0.7	1.52728	1.53193	1.53601	1.55368
0.6	1.53650	1.52192	1.52582	1.54231
0.5	1.54853	1.51222	1.51580	1.53133
0.4	1.55426	1.50143	1.50469	1.51888
0.3	1.56791	1.49148	1.49455	1.50777
0.2	1.57692	1.48113	1.48400	1.49612
0.1	1.58544	1.47112	1.47370	1.48460
0.0	1.59430	1.46002	1.46241	1.47222

present an experimental argument supporting the superiority of the mixing rules. Expressing Eq. (2) in terms of mixing rules we get for Lorentz-Lorenz relation (3);

$$R^E_{(LL)} = \left(\frac{n^2-1}{n^2+2}\right)(V_m) - V_1\left(\frac{n_1^2-1}{n_1^2+2}\right)\phi_1 - V_2\left(\frac{n_2^2-1}{n_2^2+2}\right)\phi_2 \quad \ldots (3)$$

for Gladstone-Dale relation (4);

$$R^E_{(GD)} = (n-1).(V_m) - V_1(n_1-1)\phi_1 - V_2(n_2-1)\phi_2 \quad \ldots (4)$$

for Eykman relation (5);

$$R^E_{(EYK)} = \left(\frac{n^2-1}{n+0.4}\right)(V_m) - V_1\left(\frac{n_1^2-1}{n_1+0.4}\right)\phi_1 - V_2\left(\frac{n_2^2-1}{n_2+0.4}\right)\phi_2 \quad \ldots (5)$$

for Oster relation (6);

$$R^E_{(OST)} = \left[\frac{(n^2-1)(2n^2+1)}{n^2}\right](V_m) - V_1\left[\frac{(n_1^2-1)(2n_1^2+1)}{n_1^2}\right]\phi_1 - V_2\left[\frac{(n_2^2-1)(2n_2^2+1)}{n_2^2}\right]\phi_2 \quad \ldots (6)$$

for Newton relation (7);

$$R^E_{(NWT)} = (n^2-1)(V_m) - V_1(n_1^2-1)\phi_1 - V_2(n_2^2-1)\phi_2 \quad \ldots (7)$$

where $V_m = [(M_1\phi_1 + M_2\phi_2)/\rho]$ and $V_1 = (M_1/\rho_1)$ and $V_2 = (M_2/\rho_2)$ are the molar volumes of mixture, components 1 and 2 respectively.

The excess quantities as calculated from Eq. (1) and Eqs (3-7) are fitted to a polynomial of the type (8)

$$X^E = a + b(\phi_2 - \phi_1) + c(\phi_2 - \phi_1)^2 \quad \ldots (8)$$

to evaluate the coefficients *a*, *b* and *c* from least-squares fitting of the data. Here X^E refers to either V^E or R^E.

The values of the computed coefficients for R^E are compiled in Table 2 together with the error analysis.

Density and refractive index increments have been[2,3] calculated from Eqs. (9) and (10), respectively

$$\left(\frac{\partial\rho}{\partial\phi_1}\right)_{P,T} = \frac{(\rho_1-\rho_2)-\rho.D}{(1+A_{12}\phi_1\phi_2)} \quad \ldots (9)$$

Table 2—Least-squares Fittings of Eq. (8) and Statistical Errors[a] for Excess Molar Refraction

λ (nm)	Coefficients Eq. (8)	R^E(LL) Eq. (3)	R^E(GD) Eq. (4)	R^E(EYK) Eq. (5)	R^E(OST) Eq. (6)	R^E(NWT) Eq. (7)
		(I) Bromobenzene(1)-cyclohexane(2)				
589	*a*	−0.024	−0.038	0.081	0.415	−0.092
	b	−0.233	−1.001	−1.704	−11.929	−4.474
	c	0.278	1.109	1.536	11.156	4.791
	$10^4\,\sigma$	4.10	5.22	3.00	10.82	8.00
546	*a*	0.010	0.023	0.025	0.148	0.081
	b	−0.401	−1.374	−1.521	−11.314	−5.627
	c	0.359	1.294	1.423	10.826	5.405
	$10^4\,\sigma$	4.20	5.41	2.98	10.10	6.00
436	*a*	0.012	0.030	0.033	0.198	0.106
	b	−0.337	−1.394	−1.501	−12.056	−6.094
	c	0.287	1.298	1.383	11.464	5.822
	$10^4\,\sigma$	4.51	6.41	3.11	10.00	7.98
		(II) Bromobenzene(1)-ethyl acetate(2)				
589	*a*	0.067	0.165	−0.165	−0.732	0.476
	b	0.628	−0.178	0.078	−7.190	−3.710
	c	−0.790	−0.165	0.022	7.607	2.689
	$10^4\,\sigma$	4.91	6.10	3.62	9.42	8.48
546	*a*	0.023	-0.069	−0.158	−0.731	0.267
	b	0.610	−0.245	0.089	−7.436	−4.668
	c	−0.704	0.045	0.007	7.889	4.043
	$10^4\,\sigma$	4.12	5.14	3.19	10.11	9.22
436	*a*	−0.076	−0.133	−0.178	−0.876	−0.350
	b	0.710	−0.254	0.284	−7.586	−5.260
	c	−0.683	0.302	−0.216	7.951	5.392
	$10^4\,\sigma$	4.66	5.86	3.42	10.01	8.96
		(III) Bromobenzene(1)-carbon tetrachloride(2)				
589	*a*	−0.029	−0.039	−0.057	−0.201	−0.063
	b	−0.183	−0.634	−0.709	−5.325	−2.612
	c	0.213	0.673	0.048	5.524	2.673
	$10^4\,\sigma$	4.91	5.86	3.98	8.78	7.69
546	*a*	−0.019	−0.018	−0.032	−0.063	0.002
	b	−0.202	−0.692	−0.774	−5.775	−2.836
	c	0.221	0.708	0.803	5.819	2.825
	$10^4\,\sigma$	4.88	6.10	3.48	9.68	8.99
436	*a*	−0.017	−0.013	0.007	0.163	0.022
	b	−0.198	−0.773	0.881	−6.872	−3.326
	c	0.213	0.780	0.886	6.665	3.282
	$10^4\,\sigma$	4.44	6.08	3.07	10.08	8.80

[a] standard error $\sigma = \{\Sigma[\text{exptl-calc}]^2/\text{number of observations}\}^{1/2}$

$$\left(\frac{\partial n}{\partial \phi_1}\right)_{P,T} = \frac{(n^2+2)^2\{[(P_1-P_2)+B_{12}(\phi_2-\phi_1) + dB_{12}/d\phi_1(\phi_1\phi_2)]-P\cdot D\}}{6n(1+A_{12}\phi_1\phi_2)} \qquad \ldots (10)$$

where

$$D = [A_{12}(\phi_2-\phi_1)+\frac{dA_{12}}{d\phi_1}(\phi_1\phi_2)] \qquad \ldots (11)$$

The procedure to evaluate these quantities has already been outlined earlier[2,14].

Dependence of refractive index on volume fraction is shown in Fig. 1. As expected, refractive index is higher for mercury blue line than that for the green wavelength. The lowest refractive indices are

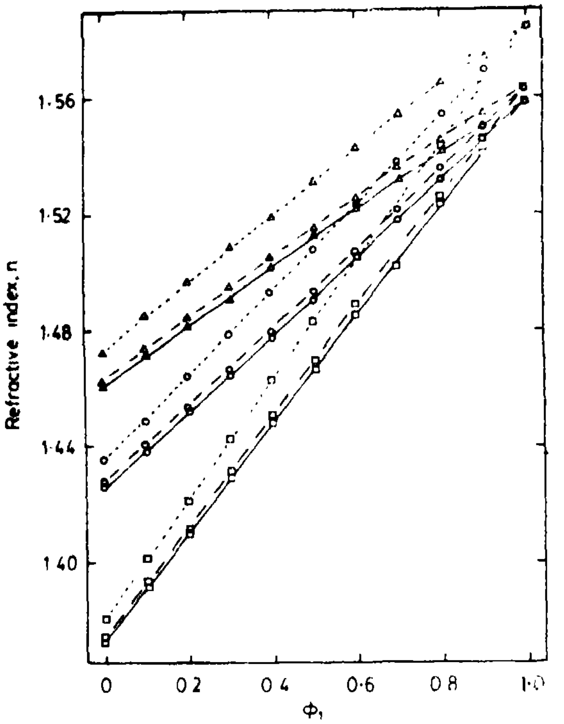

Fig. 1—Refractive index versus volume fraction for bromobenzene(1)-carbon tetrachloride(2) (△), bromobenzene(1)-cyclohexane(2) (O), and bromobenzene(1)-ethyl acetate(2) (□), [---- 436 nm; – – 546 nm and —— 589 nm]

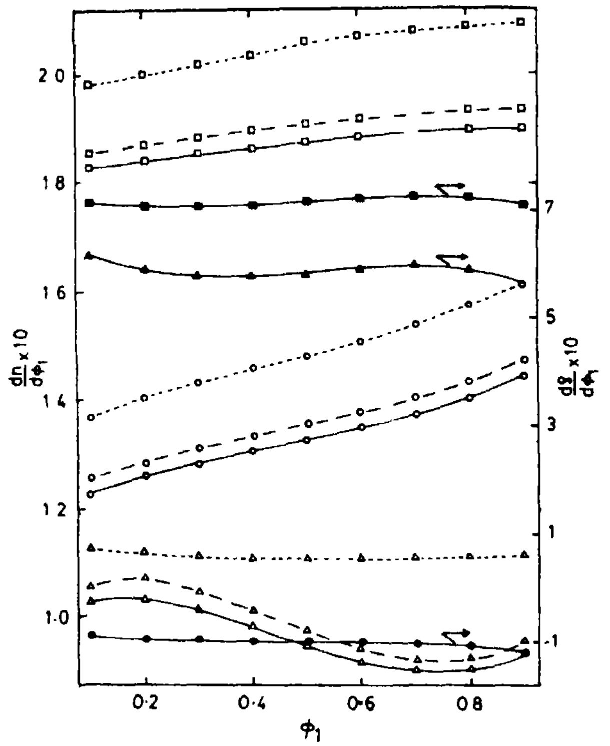

Fig. 2—Refractive index increment (left scale) and density increment (right scale) versus volume fraction. [Symbols for refractive index increment are the same as in Fig. 1] Symbols for density increment: bromobenzene(1)-cyclohexane(2) (●); bromobenzene(1)-carbon tetrachloride(2) (▲); and bromobenzene(1)-ethyl acetate(2) (■)]

observed for sodium line. As is evident from Fig. 1, the plots of the three systems slightly deviate from linearity.

The computed density and refractive index increments, evaluated from Eqs (9) and (10), are plotted as a function of ϕ_1 in Fig. 2. Smaller values of refractive index increments are observed for bromobenzene (1)-carbon tetrachloride (2) system as compared to bromobenzene (1)-cyclohexane (2) and bromobenzene (1)-ethyl acetate (2) systems. Refractive index increments exhibit the same trend as that of refractive index, i.e. the increment is higher for mercury blue line than that for green line. However, sodium yellow line exhibits highest refractive index increments. The density increment is negative and small for bromobenzene (1)-cyclohexane (2) system; but for the remaining two systems it is positive and also large.

The curves for density and refractive index increments (Fig. 2) exhibit widely differing behaviours. for bromobenzene (1)-carbon tetrachloride (2) system, refractive index increment at 589 and 546 nm shows a sigmoid behaviour; but at 436 nm, almost a rectilinear behaviour exists. Even the density increment for this system has a flattened sigmoid shape.

for all the systems, the shape of refractive index increment curve for the mercury blue line is different from those for the curves at 589 and 546 nm, for which identical behaviour is seen.

Excess molar volumes as calculated from Eq. (1) are plotted in Fig. 3 as a function of ϕ_1. For mixtures of bromobenzene with either carbon tetrachloride or cyclohexane, the excess molar volume is negative. Due to the presence of vacant 3*d*-orbitals in bromine atom of bromobenzene it acts as an electron acceptor towards both carbon tetrachloride or cyclohexane which act as electron donors. This suggests that weak donor-acceptor type complexes with attractive interactions are formed in solution thereby giving negative V^E values. On the otherhand, in the case of bromobenzene (1)-ethyl acetate (2) mixture, V^E curve shows both negative and positive values. Such systems are very rare in literature. Ethyl acetate, being highly polar, its polarity seems to be affected by the addition of bromobenzene. Presence of methyl and ethyl groups in ehtyl acetate may be the cause of this anomaly. In the mixture, when methyl group comes closer to bromine atom of bromobenzene an attractive force exists between bro-

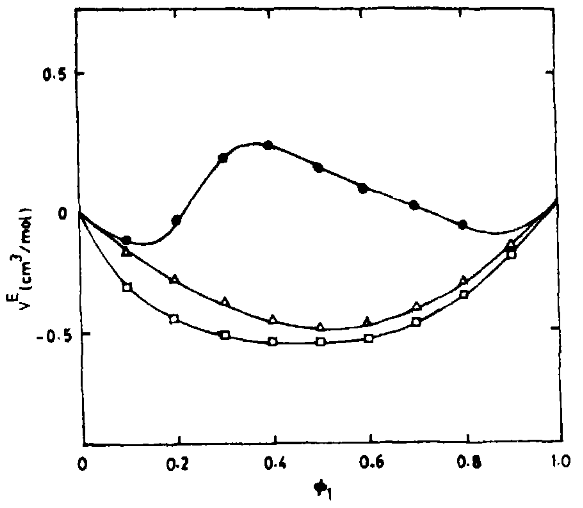

Fig. 3—Excess molar volume versus volume fraction. [bromobenzene(1)-ethyl acetate(2) (●); bromobenzene(1)-cyclohexane(2) (□); and bromobenzene(1)-carbon tetrachloride(2) (△)]

mine and oxygen atom of ethyl acetate. On the otherhand, when the carboxylate moiety comes close to bromine atom then the Br---O type weak bond formed may be broken giving positive V^E. This happens around $\phi_1 = 0.25$ to 0.65 and above $\phi_1 = 0.65$, negative V^E is observed.

From the results of Table 2 it is seen that the standard error (σ) involved in fitting Eykman relation (Eq. 5) is very small as compared to those of the other relations, viz. Eqs (3), (4), (6) and (7). However, the errors for R^E(LL) are also significantly smaller but somewhat larger than those for Eykman; for Oster's mixing rule the error involved is large. The errors for Gladstone-Dale and Newton relations are more or less the same although in majority of cases small deviations are observed for Newton's relation. This analysis indicates that Eykman relation gives the best results, whereas Lorentz-Lorenz and Gladstone-Dale relations are quite satisfactory. Newton's relation is better than Oster's relation but not comparable in its performance to either Eykman, Lorentz-Lorenz or Gladstone-Dale relations. Although Lorentz-Lorenz relation has a sound theoretical foundation than that of Eykman, the latter seems to fit the data much satisfactorily.

Acknowledgement

T M Aminabhavi thanks Prof. P E Cassidy of Southwest Texas State University for facilities provided during the preparation of this manuscript and Mrs. Sue Hall for typing. This work is originated from the Ph.D. thesis of Mrs Lata S Manjeshwar submitted to Karnatak University.

References

1 Aminabhavi T M, Manjeshwar L S & Balundgi R H, *Indian J Chem*, **25A** (1986) 465.
2 Aminabhavi T M, Manjeshwar L S & Balundgi R H, *Indian J Chem*, **25A** (1986) 820.
3 Aminabhavi T M, Manjeshwar L S & Balundgi R H, *J chem Engg Data*, **32** (1987) 50.
4 Aminabhavi T M, *J chem Engg Data*, **29** (1984) 54.
5 Gokavi G S, Raju J R, Aminabhavi T M, Balundgi R H & Muddapur M V, *J chem Engg Data*, **31** (1986) 15.
6 Aminabhavi T M & Munk P, *Macromolecules*, **12** (1979) 1186.
7 Lorentz H A, *Wied Ann*, **9** (1880) 641.
8 Lorenz L, *Wied Ann*, **11** (1880) 70.
9 Eykman J F, *Rec Trav Chim*, **14** (1895) 185.
10 Gladstone J H & Dale T P, *Phil Trans*, **153** (1863) 317.
11 Kurtz S S & Ward A L, *J Franklin Inst*, **222** (1936) 563.
12 Oster G, *Chem Rev*, **43** (1948) 319.
13 Abdel-Azim A A & Munk P, *J phys chem*, **91** (1987) 3910.
14 Aminabhavi T M, *J chem Engg Data*, **32** (1987) 406.

Indian Journal of Chemistry
Vol. 27A, April 1988, pp. 308-313

Kinetics & Mechanism of Thallium(III) Oxidation of Benzilic, Phenyllactic & 2-Hydroxyisobutyric Acids in Acid Perchlorate Solution & Comparison with Other Substituted Glycollic Acids

DINESH KUMAR, PUSHPA GUPTA & YUGUL K GUPTA*
Department of Chemistry, University of Rajasthan, Jaipur 302 004

Received 7 *July* 1987; *revised and accepted* 5 *October* 1987

Oxidation of benzilic acid (HBA), phenyllactic acid (HALA) and 2-hydroxyisobutyric acid (HIBA) with Tl(III) occurs via the formation of atleast three complexes between the metal ion and the organic acids. Rate law could be derived and verified only when limiting rates at large [organic acid] are obtained. Under the conditions two complexes seemed to exist in all the cases. For HBA and HIBA the two complexes differ by one proton, and in the case of HALA, the two differ by two protons. The rate constants (s^{-1}) for the deprotonated reactive complexes are $(8.5 \pm 6) \times 10^{-3}$, $(5.7 \pm 0.4) \times 10^{-4}$ and $(1.0 \pm 0.1) \times 10^{-4}$ for HBA, HALA and HIBA respectively at 70° and $I = 1.5$ mol dm^{-3}.

Formation of a complex followed by intramolecular electron transfer is an established mechanism for the oxidation of most organic compounds with thallium(III). However, a paper[1] on the oxidation of α-hydroxy acids reported no complex formation and this prompted us to reinvestigate these systems. The results of oxidation of glycollic[2] (HGA), mandelic[3] (HMA) and lactic[3] (HLA) acids have already been reported from this laboratory, and the present paper describes the results of Tl(III) oxidation of benzilic (HBA), phenyllactic (HALA) and 2-hydroxyisobutyric (HIBA) acids. The present study was made with a limited objective of obtaining evidence for complex formation between Tl(III) and the hydroxy acids and compare the results with those reported earlier.

Several redox studies[4] on benzilic acid with a number of oxidants have been reported but the complex formation has been found only with cerium(IV)[4a]. Phenyllactic acid is fairly resistant to oxidation[5] and hence only a few oxidation studies[6] have been made. Similarly 2-hydroxyisobutyric acid has received but little attention[7].

Materials and Methods

Benzilic acid (E. Merck), phenyllactic acid (Koch-Light, puriss) and 2-hydroxyisobutyric acid (Fluka AG) were used as such. Their solutions were prepared in doubly distilled water and standardized with a NaOH solution. The kinetics were followed iodometrically[2,3] at 70 ± 0.1°C unless mentioned otherwise. Since such systems are known to have complex rate dependence on [substrate], initial rates were obtained by the plane mirror method[8] with a precision of ± 8%.

Stoichiometry and products

The stoichiometry of HBA-Tl(III) reaction was determined from time to time simultaneously estimating both thallium(III) (iodometrically) and HBA (cerimetrically). The latter procedure involved addition of known volume of reaction mixture to a known excess of Ce(IV) in 1.0 mol dm^{-3} $HClO_4$, and then estimating unused Ce(IV) using a standard solution of Fe(II) after rendering the solution about 1.0 mol dm^{-3} in H_2SO_4. One mol of Tl(III) reacted with one mol of HBA. Reaction mixtures after about 6 hr of heating at 70° yielded a small quantity of a solid, m.p. 45-50°, which was characterised as benzophenone (m.p. 49°) by direct comparison (m.m.p. and co-IR).

Stoichiometry for the other two acids was determined by mixing excess Tl(III) and the organic acid, and allowing them to react in the presence of a large concentration (2.0 mol dm^{-3}) of $LiClO_4$ (large ionic strength) for about 10-12 hr. Excess Tl(III) was estimated iodometrically. The products were found to be $C_6H_5COCH_3$ and CH_3COCH_3 for HALA and HIBA respectively, characterised by their characteristic 2,4-DNP derivatives. Separate experiments with the ketones showed that they were not oxidized by Tl(III) under these conditions. The stoichiometry was compatible with Eq. (1).

$$R_1R_2COHCOOH + Tl(III) \rightarrow R_1COR_2 + CO_2 + 2H^+ + Tl(I) \quad \ldots(1)$$

Intermediate product in oxidation of benzilic acid

A white precipitate was formed if [HBA] > 0.01 mol dm^{-3} and [Tl(III)] > 0.002 mol dm^{-3}. This on drying was found to melt at 110-20°. The solid on analysis indicated Tl(III) and HBA in the ratio of 1:3. The filtrate did not show the presence of Tl(III) but HBA was found to be present. The IR spectrum of the solid was devoid of peaks at 3450 and 1745 cm^{-1}, characteristic of vOH and vC = O respectively, indicating that the solid complex between HBA and Tl(III) was formed involving OH and CO groups of HBA. In a separate experiment it was observed that some Tl(III) always reacted with HBA and this was confirmed by the presence of Tl(I) and benzophenone in the filtrate.

Potentiometry

Redox potentials of Tl(III)/Tl(I) couples were measured with and without organic acids in 3.0 ml dm^{-3} $HClO_4$ and $I = 4.0$ mol dm^{-3} ($LiClO_4$) at 30° against saturated calomel electrode to obtain information about complex formation between Tl(III) and organic acids by Ahrland's method[9]. Concentrations of organic acids were varied from 2.0×10^{-4} mol dm^{-3} to 50×10^{-4} mol dm^{-3} at four different concentrations (5×10^{-4} to 12×10^{-4} mol dm^{-3}) of Tl(III) and fixed [Tl(I)] = 5.0×10^{-4} mol dm^{-3}. Three complexes of HBA with $\beta_1 = (9.0 \pm 0.5) \times 10^4$, $\beta_2 = (5.5 \pm 0.8) \times 10^9$ and $\beta_3 = (5.8 \pm 1.0) \times 10^{13}$, three complexes with HALA with $\beta_1 = (2.6 \pm 0.5) \times 10^4$, $\beta_2 = (4.0 \pm 1.0) \times 10^7$ and $\beta_3 = (4.0 \pm 1.5) \times 10^9$ and three complexes with HIBA with $\beta_1 = (5.0 \pm 0.5) \times 10^2$, $\beta_2 = (4.3 \pm 0.9) \times 10^4$ and $\beta_3 = (2.2 \pm 1.2) \times 10^6$ were indicated.

Spectrophotometry

Though the absorption spectra were quite complicated, there was ample qualitative evidence for complex formation from the spectra at different concentrations of the organic acids. Spectra of mixtures of Tl(III) and HALA are given in Fig. 1. Attempts were made to determine formation constants by Yatsimirskii's method[10] but without success.

Results

Thallium(III) dependence

Since the reaction is complicated by the formation of atleast three complexes of Tl(III) with the organic acids, the correct dependence of rate of [Tl(III)] could be known only when [organic acid] was large. There is additional limitation in the case of benzilic acid on account of the formation of a white turbidity in the presence of large [HBA]. Thus [Tl(III)] was varied in the range 5.0×10^{-4} to 4.0×10^{-3} mol dm^{-3} with [HBA] = 9.0×10^{-3} mol dm^{-3}. For the other two organic acids, [Tl(III)] was varied in the concentration range $(1.0\text{-}10.0) \times 10^{-3}$ mol dm^{-3} at 0.04 mol dm^{-3} HALA or HIBA. The order in each case was one with respect to Tl(III).

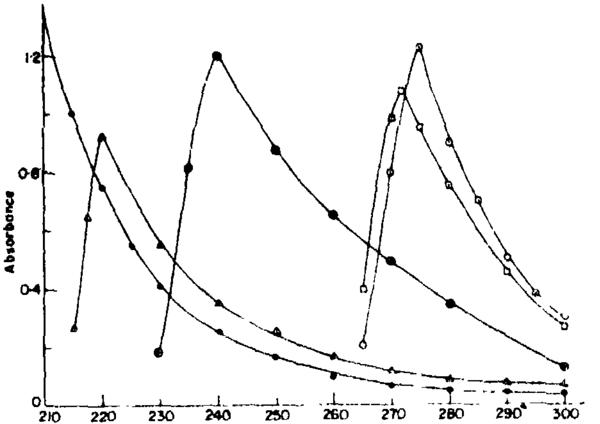

Fig. 1 — Absorption spectra of mixtures of Tl(III) and HALA ([Tl(III)] = 5.0×10^{-4} mol dm^{-3}; [$HClO_4$] = 0.5 mol dm^{-3}; 30° [HALA] = 0, 0.0; Δ, 5×10^{-4} mol dm^{-3}; (⊗), 5.0×10^{-3} mol dm^{-3}; □, 5.0×10^{-2} mol dm^{-3}; ○, 1.0×10^{-1} mol dm^{-3})

Table 1 — Initial Rates at Different [Benzilic Acid] in Tl(III) HBA Reaction

[$HClO_4$] = 0.35 mol dm^{-3}; I = 0.35 mol dm^{-3}

10^3[HBA] (mol dm^{-3})	10^7 Initial rate (mol dm^{-3}) at [Tl(III)] = 1.8×10^{-3} mol dm^{-3}			10^7 Initial rate (mol dm^{-3}) at [Tl(III)] (mol dm^{-3}) and 70°	
	65°	70°	75°	2.7×10^{-3}	0.9×10^{-3}
1.0	8.0	14	19	22	9.0
2.0	17	25	30	31	12.5
3.0	23	33	38	46	17.5
4.0	35	40	44	60	19
5.0	40	46	51	63	21
6.0	41	48	56	64	22
7.0	41	47	57	68	23
8.0	41	48	56	69	23
9.0	41	48	56	69	23

Organic acid dependence

[HBA] was varied at three [Tl(III)] and three temperatures. The results given in Table 1 show that the rates increase and attain limiting values with the increase in [HBA]. The pseudo-first order rate constants in the region of limiting rates were 2.3×10^{-3}, $(2.7 \pm 0.05) \times 10^{-3}$ and 3.1×10^{-3} s^{-1} at 65°, 70° and 75° respectively and at [$HClO_4$] = 0.35 mol dm^{-3}. [HIBA] was varied at three [Tl(III)] and the results given in Table 2 show initial increase in rate, which attains a maximum value and then decreases to a minimum value and finally increasing to a limiting value with increase in [HIBA]. The pseudo-first order rate constants in the region of limiting rates were in the range of $(4.4 \pm 0.4) \times 10^{-5}$ s^{-1} at 70° and [$HClO_4$] = 0.5 mol dm^{-3}. The results of variation of [HALA] given in Fig. 2 also show a complex behaviour and the pseudo-first order rate constants in the limiting rate region were 1.32×10^{-5}, $(1.75 \pm 0.05) \times 10^{-5}$ and 2.4×10^{-5} s^{-1} at 65°, 70° and 75° respectively and [HClO$_4$] = 0.5 mol dm^{-3}. All these results show complex formation between Tl(III) and the organic acid. Complexes of Ce(IV), with HBA[4], HALA[12] and HIBA[12] have already been reported.

Hydrogen ion dependence

The dependence of rate on [H$^+$] was studied by varying [HClO$_4$] at I = 1.5 mol dm^{-3} (LiClO$_4$). The results are given in Table 3 at three temperatures. The rate decreases with the increase in [H$^+$]. A plot of (rate)$^{-1}$ versus [H$^+$] is linear with a non-zero intercept, conforming to the empirical rate law (2) at fixed [Tl(III)] and [organic acid] in the case of HBA and HIBA

$$-d[\text{Tl(III)}]/dt = A/(B + [\text{H}^+]) \qquad \ldots (2)$$

and to the rate law (3) in case of HALA

$$-d[\text{Tl(III)}]/dt = A/(B + [\text{H}^+]^2) \qquad \ldots (3)$$

Table 2 — Initial Rates at Different [HIBA] [HClO$_4$] = 0.5 mol dm^{-3}; 70°; I = 0.5 mol dm^{-3}

10^3[HIBA] (mol dm^{-3})	10^8 Initial rate (mol dm^{-3} s^{-1}) at [Tl(III)] (mol dm^{-3})		
	2.0×10^{-3}	3.0×10^{-3}	4.0×10^{-3}
1.0	2.3	5.6	—
2.0	8.3	7.0	2.0
3.0	10	—	—
4.0	–	8.7	4.2
6.0	13	10	6.0
8.0	18	12	8.0
10.0	20	15	11
12.0	—	19	
16.0	13.5	13	18
20.0	8.3	10.5	17
25.0	4.8	8.6	9.2
30.0	9.4	12	14
40.0	9.4	12.5	16
50.0	9.6	13	17
60.0	9.4	13	18
8.0	9.4	13	17

Effect of varying ionic strength

The results of variation of ionic strength from 0.20 to 1.5 mol dm^{-3} (LiClO$_4$) are given in Table 4. The rate significantly increases with increase in ionic strength in the case of HLA, HALA and HIBA, but slightly in the case of HBA. No such significant effect has been noticed in other metal ion oxidations of lactic, phenyllactic and 2-hydroxyisobutyric acids. Only in the case of Tl(III) oxidation of 4-methylquinoline-2-hydrazine[15] significant positive effect of ionic strength has been reported.

Discussion

The most significant observation of the present investigation is the limiting rates at large [organic acid]. Kinetic results for HALA indicate formation of atleast three complexes, also supported by potentiometric measurements. In the case of HBA, formation of only one complex is indicated kinetically, though potentiometry provides evidence for the formation of three complexes. Formation of solid in the case of Tl(III) and HBA in the ratio of 1:3 also indicates the formation of atleast one complex.

The reactivity of the complexes increases with increase in the content of HBA. In the case of HIBA and HALA, atleast three complexes are indicated kineti-

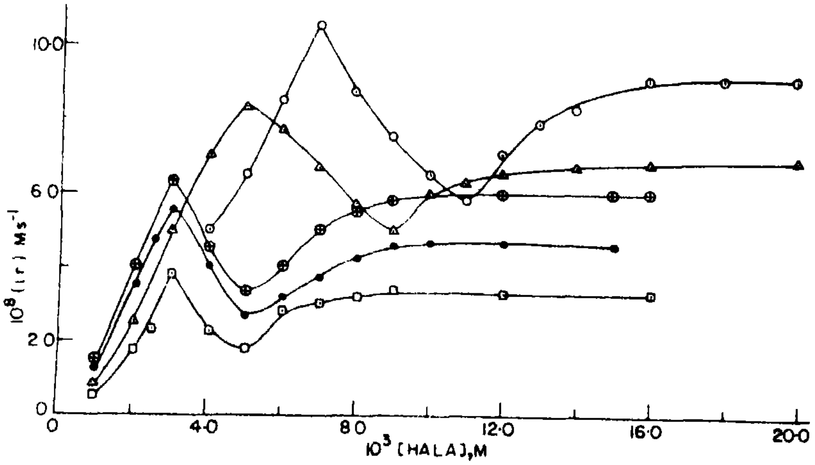

Fig. 2—Plot of initial rate (ir) versus [HALA] at [HClO$_4$] = 0.5 mol dm^{-3}; (□, 45°; 70°; ⊗, 75°), [Tl(III)] = 2.5×10^{-3} mol dm^{-3}; ○, 70° [Tl(III)] = 5.0×10^{-3} mol dm^{-3}; and △, 70°, [Tl(III)] = 4.0×10^{-3} mol dm^{-3})

Table 3 — Initial Rates at Different [$HClO_4$] in Oxidation of α-Hydroxy Acids by Tl(III) (I = 1.5 mol dm^{-3})

[$HClO_4$] (mol dm^{-3})	10^7 Initial rate (mol dm^{-3} s^{-1}) at								
	65°	70°	75°	65°	70°	75°	65°	70°	75°
	HBA[a]			HALA[b]			HIBA[c]		
0.30	—	—	—	6.7	9.0	16	1.2	1.5	2.4
0.35	37	50	60	—	—	—	—	—	—
0.50	28	41	48	3.8	6.0	8.6	—	1.33	—
0.75	25	29	35	1.7	3.0	4.2	0.96	1.25	1.9
1.00	16	22	28	1.2	1.8	2.4	0.79	1.04	1.6
1.25	13	18	21	0.83	1.2	1.8	—	0.96	—
1.50	11	15	18	—	—	—	0.67	0.83	1.4

(a) [HBA] = 5.0×10^{-3} and [Tl(III)] = 1.8×10^{-3} mol dm^{-3}
(b) [HALA] = 2.0×10^{-3} and [Tl(III)] = 2.5×10^{-3} mol dm^{-3}
(c) [HIBA] = 6.0×10^{-2} and [Tl(III)] = 2.0×10^{-3} mol dm^{-3}

Table 4 — Effect of Varying Ionic Strength on Rate of Oxidation of HBA, HALA and HIBA at 70°C

[$LiClO_4$] (mol dm^{-3})	10^7 Initial rate (mol dm^{-3} s^{-1}) for		
	HBA[a]	HALA[b]	HIBA[c]
0	46	0.6	1.7
0.2	—	2.2	—
0.5	47	—	4.0
0.7	-	—	—
1.0	50	—	7.0
1.20	—	10	
1.25	53	—	—
1.50	55	—	9.6

(a) [Tl(III)] = 1.75×10^{-3} mol dm^{-3}, [HBA] = 5.0×10^{-3} mol dm^{-3}, [$HClO_4$] = 0.35 mol dm^{-3}
(b) [Tl(III)] = 2.5×10^{-3} mol dm^{-3}; [HALA] = 2.0×10^{-2} mol dm^{-3}, [$HClO_4$] = 0.30 mol dm^{-3}
(c) [Tl(III)] = 2.0×10^{-3} mol dm^{-3}; [HIBA] = 6.0×10^{-2} mol dm^{-3}, [$HClO_4$] = 0.50 mol dm^{-3}

cally. The first and third complexes (probably 1:1 and 1:3) are reactive, and the second one (probably 1:2) is either not reactive or less reactive than the other two. The potentiometric results also indicate formation of three complexes in both these cases.

Another significant observation from the mechanistic point of view is [H^+] dependence of the rate under the condition when the latter is independent of [organic acid]. Since the latter situation indicates complete complexation of Tl(III), H^+ dependence cannot be connected with Tl(III). It is also not connected to the organic acid since the acid dissociation constants of the organic acids[14] are of the order of ~ 10^{-4}. Only deprotonation of the complex (with maximum ligand to metal ion ratio) can explain these results. It is probably the unreactive protonated penultimate and reactive deprotonated ultimate complexes which are responsible for H^+ dependence. Since the complexes are not exactly defined, it is best to treat kinetic data quantitatively for the ultimate and penultimate complexes. For HBA, HIBA and HALA mechanism shown in Scheme 1, can be proposed under the condition of limiting rates.

$$Tl(BA)_2(HBA)^+ \overset{K}{\rightleftharpoons} Tl(BA)_3 + H^+ \qquad \ldots (4)$$

$$Tl(BA)_3 \xrightarrow{k} \text{products} \qquad \ldots (5)$$

$$Tl(IBA)_2(HIBA)^+ \overset{K}{\rightleftharpoons} Tl(IBA)_3 + H^+ \qquad \ldots (6)$$

$$Tl(IBA)_3 \xrightarrow{k} \text{products} \qquad \ldots (7)$$

$$Tl(ALA)(HALA)_2 \overset{K}{\rightleftharpoons} Tl(ALA)_3 + 2H^+ \qquad \ldots (8)$$

$$Tl(ALA)_3 \xrightarrow{k} \text{products} \qquad \ldots (9)$$

Scheme 1

Rate law (10) can be obtained for HBA and HIBA.

$$-d[Tl(III)]/dt = kk[Tl(III)]_T/(K + [H^+]) \qquad \ldots (10)$$

Rate law (11) holds for HALA

$$-d[Tl(III)]/dt = kK[Tl(III)]_T(K + [H^+]^2) \qquad \ldots (11)$$

Rate laws (10) and (11) are similar to the rates given by Eqs (2) and (3), respectively. Plots of (rate)$^{-1}$ versus [H^+] for HBA and HIBA, and (rate)$^{-1}$ versus [H^+]^2 for HALA should be linear with non-zero intercepts, from which k and K could be calculated. Indeed such plots are linear and values of k and K calculated are given in Table 5. Deprotonation constant appears to be independent of temperature. Such deprotonated complexes are reported to be reactive in Ce(IV)[12] oxidations too.

Table 5 — k and K at Different Temperatures for Oxidation of α-Hydroxy Acids by Tl(III) at I = 1.5 mol dm^{-3}

Organic acid	$10^4 k$ (s^{-1})			K (mol dm^{-3})		
	65°	70°	75°	65°	70°	75°
HBA	65 ± 4	85 ± 6	111 ± 8	0.15	0.17	0.16
HALA	4.4 ± 0.1	5.7 ± 0.4	10 ± 0.6	0.12	0.14	0.14
HIBA	0.7 ± 0.03	1.0 ± 0.1	1.4 ± 0.06	1.3	1.2	1.5

A comparison of the kinetic results of oxidation of benzilic acid, mandelic acid (HMA), lactic acid (HLA), glycollic acid (HGA), phenyllactic acid and 2-hydroxyisobutyric acid can now be made. The salient features of these reactions are given in Table 6. One difficulty in making quantitative comparison arises because of considerable enhancement in the rates with increase in ionic strength in the case of HLA, HALA and HIBA and the difficulty in the choice of an ionic strength. For I = 1.5 mol dm^{-3}, the rate constants are in the order HBA > HMA > HLA > HALA > HIBA > HGA. The order of reactivity in [$HClO_4$] = 0.5 mol dm^{-3} and I = 0.5 mol dm^{-3} would be HBA > HMA > HGA ≈ HIBA > HLA > HALA (Table 6). If one takes into account the trend in the decrease in the rate constant with the decrease of ionic strength, the reactivity pattern at zero ionic strength is likely to be HBA > HMA > HGA > HALA > HLA > HIBA.

The tendency of complex formation between Tl(III) and the organic acid is given by β_n values or by the ratio [organic acid]/[Tl(III)] to obtain limiting rates. This order is HBA > HALA ≈ HMA > HIBA ≈ HLA > HGA. This is in line with the electron withdrawing properties of the phenyl group and consequent decrease in the electron density at oxygen and release of proton from OH group when Tl(III) coordinates to the organic acid. Hence, once Tl(III) is completely converted into a ligand-saturated complex, it is the intramolecular electron transfer only which determines the overall rate since Ks are not very different for different organic acids. In all these acids it is the C – C bond rupture that is rate-controlling and this is facilitated[15,16] by the substitution of R_1 and R_2 by phenyl group. Thus the rates for HBA and HMA are significantly larger than those for other acids.

The acid dissociation constants given in Table 6 run almost parallel to the tendency of complex formation. Although there is some effect of ionic strength[17] on the acid dissociation constants, it cannot explain the significant increase in the rate. In the case of HBA and HIBA, K slightly decreases with the increase in ionic strength, but there is no change in the case of lactic acid.

A strict comparison of the results with those of the earlier paper[1] cannot be made since the earlier study has been made in acetate medium and the rate constants decrease with increase in [Tl(III)]. Although this is not unexpected in a situation where a number of intermediate metal-ion substrate complexes are formed, the earlier report does not include intermediate complex formation at all.

Table 6 — Comparison of Some Constants for Different Substituted Glycollic Acids

Organic acid	$10^4 k^a$ (s^{-1})	K (mol dm^{-3})	$10^4 K^b$	[Org. Acid]^c / [Tl(III)]	β_n^d
Benzilic acid^h	85(26)^e	0.17	17.8	3.3	5.8×10^{13}
Mandelic acid^i	55(16.7)^f	0.23	11.0	10	2.3×10^9
Glycollic acid^j	0.69(0.46)^g	1.1	6.17	40	—
Lactic acid^i	12.5(0.3)^g	0.17	4.4	20	4.4×10^3
2-Hydroxyisobutyric acid^h	1.0(0.44)^g	1.2	3.8	15	2.2×10^6
Phenyllactic acid^h	5.7(0.18)^g	0.14	8.32	4.0	4.0×10^9

(a) At ionic strength = 1.5 mol dm^{-3} and 70°
The figures in parentheses are pseudo-first order rate constants obtained from limiting rates
(b) Acid dissociation constants determined[16] in dioxan-water mixture (4:1 v/v) at 31°.
(c) Approximate minimum ratio when the rates become limiting.
(d) Gross formation constant of Tl(III)-organic acid complex determined potentiometrically
(e) [$HClO_4$] = 0.35 mol dm^{-3} = I
(f) [$HClO_4$] = 0.30 mol dm^{-3} = I
(g) [$HClO_4$] = 0.50 mol dm^{-3} = I
(h) This work
(i) ref. 3
(j) ref. 2

References

1 Mohanty S B, Acharya R C, Nanda C N & Rout M K, *J Indian chem Soc*, **43** (1976) 59.

2 Gupta Pushpa, Sharma P D & Gupta Y K, *J chem Soc Dalton Trans*, (1984) 1867.

3 Gupta Pushpa, Sharma P D & Gupta Y K, *Indian J Chem*, **23A** (1984) 392.

4 (a) Sengupta K K, Chatterji A K & Moulik S P, *Bull chem Soc, Japan*, **43** (1970) 3841;

(b) Vaidyanathan K & Venkatasubramanian N, *Indian J Chem*, **11** (1973) 1146;

(c) Pocker Y & Davies B, *J Am chem Soc*, **95** (1973) 6216;

(d) Ackett P & Barker I R L, *J chem Soc, Perkin Trans*, (1973) 965,

(e) Khandual N C & Nayak P L, *J Indian chem Soc*, **50** (1973) 786;

(f) Paddila J & Herran J, *Bal Inst Quim Univ nacl, auton, Mexico*, (1956) 83,

(g) Grover V K & Gupta Y K, *J inorg nucl Chem*, **31** (1969) 1403

5 Kay H D & Raper H S, *Biochem J*, **16** (1922) 465

6 (a) Sengupta K K, Chatterji A K, Pal B B & Sasmal S S, *Z physik Chem*, **72** (1970) 330,

(b) Grover V K & Gupta Y K, *Austr J Chem*, **23** (1970) 757;

(c) Behera J N, Rout G B & Mahendra K, *J Indian chem Soc*, **46** (1969) 400;

(d) Singh H & Prasad M, *J Chinese chem Soc*, **27** (1980) 119

7 (a) Nazar A F M & Wells C F, *J chem Soc Dalton Trans*, (1980) 119,

(b) Sengupta K K, Maiti S, Chatterji U & Samanta T, *Trans Metal Chem*, **7** (1982) 89;

(c) Singh H, Govil J C & Saxena S C, *J Indian chem Soc*, **58** (1981) 951;

(d) Tapodi H P, Shankar R & Bakore G V, *Indian J Chem*, **19A** (1980) 330;

(e) Sengupta K K, Chatterji A K, Shankar T & Sengupta S, *Indian J Chem*, **13** (1975) 1024;

(f) Sengupta K K, Khumarai D K & Mukherji D C, *J Indian chem Soc*, **52** (1975) 467;

(g) Pocker Y & Davies B C, *J Am chem Soc*, **95** (1973) 6216.

8 Latshaw M, *J Am chem Soc*, **47** (1925) 793.

9 (a) Ahrland S, Chatt J, Davies N K & Williams A A, *J chem Soc*, (1958) 276;

(b) Ahrland S, Grenthe I, Johanson L & Noren B, *Acta chem Scand*, **17** (1963) 1567.

10 Yatsimirskii K B, *Z Neorg Khim*, **1** (1956) 2306; Beck M T, *Chemistry of complex equilibria*, (Von Nostrand Reinhold, London) 1970, p 86.

11 Grineva A V & Presnyak N T, *Zhur Obsch Khim*, **32** (1962) 316; **38** (1968) 1957; Lee A G, *Chemistry of thallium* (III) (Elsevier, London) 1971, p. 88.

12 Amjad U S, McAuley A & Gomwalk U D, *J chem Soc, Dalton Trans*, (1977) 82.

13 Banthia U S, Joshi B C & Gupta Y K, *Indian J Chem*, **23A** (1984) 413.

14 Heilburn I & Banbury H M, *Dictionary of organic compounds*, Edited by Eyre and Spottiswoode, Vol. 1, 1953, p. 252.

15 Kemp T J & Waters W A, *J chem Soc*, (1964) 1169.

16 Wiberg K B, Oxidation in organic chemistry, Part A (Academic Press, New York) 1965, p. 207.

17 Grover V K & Gupta Y K, *Bull chem Soc, Japan*, **43** (1970) 2445.

Indian Journal of Chemistry
Vol 27A, April 1988, pp. 314-317

Kinetics & Mechanism of Bromination of Phenols by N-Bromoacetamide: Effect of Substituents on Decomposition of Intermediate Adduct

S VENKATESHWARLU & V JAGANNADHAM*
Department of Chemistry, Nizam College (Osmania University), Hyderabad 500 001

Received 24 *February* 1987; *revised* 13 *July* 1987; *accepted* 24 *August* 1987

Rates of reactions of phenol and substituted phenols with HOBr, produced *in situ* by the hydrolysis of N-bromoacetamide (NBA) are measured in aqueous methanol iodometrically in the presence of excess acetamide (AA). A mechanism involving an intermediate six-membered cyclic transition state between phenol and HOBr (formation constant K) which decomposes in a slow step with a rate constant (k) has been proposed. Activation/thermodynamic parameters for all the steps, i.e. k, K and K_h (K_h is the hydrolysis constant of NBA) have been evaluated in the temperature range 303 to 323 K and discussed. The sole reaction product has been identified as the corresponding o-bromophenol.

Considerable work has been reported using N-halo compounds as oxidising or brominating agents[1-6]. One such N-halo compound, N-bromoacetamide (NBA) has also received considerable attention[7-9]. The study of the brominating agents in aromatic substitution reactions had been the subject of much interest in recent times[1-3,10-16]. We have recently studied the kinetics of oxidation of dimethyl sulphoxide, benzaldehydes and mandelic acids by NBA[9]. The oxidation of benzaldehydes was reported to proceed via a six-membered transition state formed from aldehyde hydrate and HOBr, resulting in large negative entropies. Title investigation is an extension of our earlier work.

Materials and Methods

All the chemicals used were of AR grade. N-Bromoacetamide (E Merck, GR) was used as such. All the phenols used were distilled or recrystallised. The reaction between NBA and phenol took place almost instantaneously in the presence of any mineral acid and hence kinetics could not be followed titrimetrically. However added acetamide rendered the reaction amenable to titrimetric investigation. Therefore, the reactions were carried out in the absence of mineral acid and in the presence of excess of acetamide (AA) (0.1 mol dm^{-3}) in 40% aq. methanol. The course of the reaction was followed by estimating unreacted NBA iodometrically. The product of the reaction (taking 4-nitrophenol as a representative phenol) was identified as 2-bromo-4-nitrophenol by its m.p. 113° (lit. m.p. 114°).

Addition of acrylonitrile to the reaction mixture did not show any polymerisation ruling out the possibility of a free radical mechanism for the oxidation process. Stoichiometry of reaction was carried out for 45 min under the conditions [NBA] $\gg$ [phenol]. The stoichiometry was found to be 1:1 (NBA: phenol) in accord with the reaction: $C_6H_5OH + CH_3CONHBr \rightarrow BrC_6H_4OH + CH_3CONH_2$. The reason for restricting the time factor to 45 min was to avoid any other side reaction.

Results and Discussion

Kinetic results and mechanism

Under the conditions [NBA] $\ll$ [phenol] the plot of log [NBA] versus time was linear indicating unit order dependence in [NBA]. Psuedo-first order rate constants (k') were calculated under varying [phenol]. Also the plot of log k' versus log [phenol] was linear with a slope of 0.40 indicating the order in [phenol] to be fractional. The rates were unaffected by added Na_2SO_4 indicating that the reaction may be between two dipoles.

The rates of reactions decreased with increase in [AA] indicating a shift of the prehydration equilibrium reaction towards left during the production of HOBr as shown in step (1) of Scheme 1.

The mechanism shown in Scheme 1 is supported by the following observations. Since in the present work, no mineral acid was used, HOBr is the reactive oxidant species. This contention gets further support from the following facts: HOBr in aqueous soloution is known to be a weak acid[17a] ($K_a = 2 \times 10^{-9}$ at 25°). Comparatively, water is a much weaker acid[17b] than HOBr since self-ionisation constant of water is 1×10^{-14} at 25°. Therefore the existence of H_2OBr^+ is ruled out even in the presence of mineral acid[12]. Since the order in [phenol] is fractional, a rapid reversible formation of an adduct between phenol and HOBr which could be a six-membered cyclic encounter pair is envisaged, which decomposes in a slow step to give products. Encounter pair formation is not uncommon in liter-

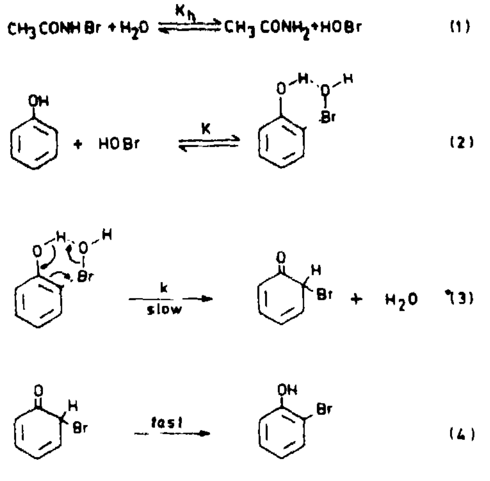

SCHEME 1

ature[11]. The formation of dienone intermediate (step 3 in Scheme 1) from the encounter pair is also a frequently observed phenomenon[12]; flow NMR technique[16] has been used in the bromination of phenols in aqueous acetic acid solutions to detect the dienone intermediate. Also such dienone intermediate has been isolated when 2,6-di-*t*-butylphenol was reacted with bromine[18]. Fractional order dependence in [phenols] in the reaction with N-halo compounds are also very common in literature[1,10].

Scheme 1 leads to the rate law (5)

$$\text{Rate} = \frac{kKK_h[\text{NBA}][\text{Phenol}]}{(K_h + [\text{AA}])(1 + K[\text{Phenol}])} \quad \ldots (5)$$

or

$$\frac{-2.303\, d\log[\text{NBA}]}{\text{dt}} = k'$$

$$= \frac{kKK_h[\text{Phenol}]}{(K_h + [\text{AA}])(1 + K[\text{Phenol}])} \quad \ldots (6)$$

where k' is the observed psuedo-first order rate constant, k the first order rate constant for the decomposition of the adduct, K, the formation constant of the adduct, and K_h the hydrolysis constant of NBA. Equation (5) accounts for the first order dependence of rate in [NBA], fractional order dependence in [phenol] and decrease in rate with increase in [AA]. Taking the reciprocal of Eq. (6), we get

$$\frac{1}{k'} = \frac{1}{kK[\text{Phenol}]} + \frac{1}{k} + \frac{[\text{AA}]}{kKK_h[\text{Phenol}]} + \frac{[\text{AA}]}{kK_h} \quad \ldots (7)$$

or at constant [AA]

$$\frac{1}{k'} = \frac{1}{[\text{Phenol}]}\left[\frac{K_h + [\text{AA}]}{kKK_h}\right] + \frac{K_h + [\text{AA}]}{kK_h} \quad \ldots (8)$$

A plot of $1/k'$ versus 1/[phenol] is linear (Fig. 1A) with a slope $= (K_h + [\text{AA}])/kKK_h$ and an intercept $= (K_h + [\text{AA}])/kK_h$. The ratio of intercept and slope gives the value of K; the adduct formation constant (step 2). At constant [phenol]

$$\frac{1}{k'} = [\text{AA}]\left[\frac{1 + K[\text{phenol}]}{kKK_h[\text{phenol}]}\right] + \frac{1 + K[\text{phenol}]}{kK[\text{phenol}]} \quad \ldots (9)$$

Hence, a plot of $1/k'$ versus [AA] should be linear. This is found to be so (Fig. 1B) with a slope $= (1 + K[\text{phenol}])/kKK_h$ [phenol] and intercept $= (1 + K[\text{phenol}])/kK$ [phenol]. The ratio of intercept and slope then gives the value of K_h, the hydrolysis constant for step (1).

With K and K_h thus determined, decomposition rate constant (k) of the adduct for step-3, could be obtained by substituting either K or K_h or both, wherever necessary. All the four values for k obtained from the two plots coincided very well, strongly supporting the proposed mechanism.

Effect of dielectric constant

The absence of added salt effect indicated that the reaction occurred between two dipoles, i.e. phenol and HOBr. In order to further confirm this, the reaction was carried out in MeOH-water mixture of different compositions. According to coulombic energy approach[19] Amis obtained Eq. (10) for the reaction that occurs between two dipoles,

$$\log k_D = \log k_\infty - \frac{2\mu_1\mu_2}{kTDr^3} \quad \ldots (10)$$

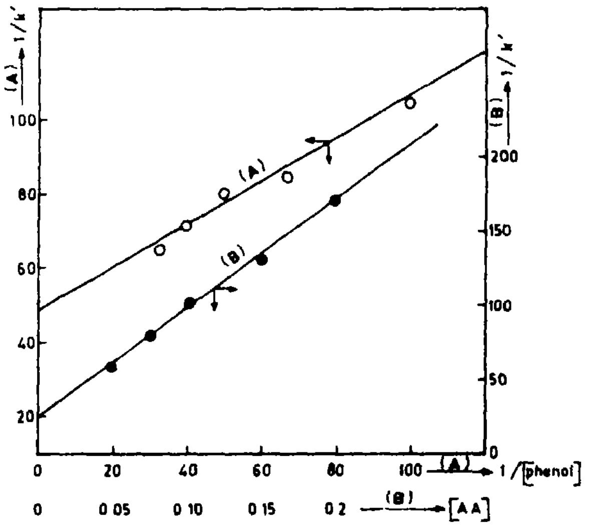

Fig. 1—(A) Plot of $1/k'$ versus 1/[phenol] ([NBA] = 1.00×10^{-3} mol dm^{-3}; [Hg(OAc)$_2$] = 0.005 mol dm^{-3}; [AA] = 0.100 mol dm^{-3}; MeOH: H$_2$O = 40:60 (v/v); temp. = 313 K); (B) Plot of $1/k'$ versus [AA] (Conditions same as in A above, except [AA] was varied from 0.050 mol dm^{-3} to 0.200 mol dm^{-3})

Table 1—Effect of Substituents on r, K_h and Thermodynamic Parameters

[NBA] = 1.00×10^{-3} mol dm^{-3}, [Hg(OAc)$_2$] = 0.005 mol dm^{-3}, [Phenol] = 0.010 mol dm^{-3}, MeOH: H_2O = 40:60 (v/v); [AA] = 0.02-0.2 mol dm^{-3}; temp. = 313 K

Substituent	σ^+	r^* (Å)	K_h	ΔH_h (kJ mol^{-1})	ΔS_h (J mol^{-1} K^{-1})
H	0.00	186	0.032	39.4	−9.50
4-NO_2	—	—	0.034	29.4	−41.7
3-NO_2	—	—	0.031	—	—
4-CH_3	−0.07	170	0.038	27.2	−48.0
3-CH_3	−0.31	161	0.033	—	—
4-Cl	0.40	226	0.028	·	—
3-Cl	0.11	215		—	—

*r values were determined at [AA] = 0.100 mol dm^{-3}

Table 2—Effect of Substituents on K, k and Thermodynamic/Activation Parameters

[NBA] = 1.00×10^{-3} mol dm^{-3}, [Hg(OAc)$_2$] = 0.005 mol dm^{-3}; [Phenol] = 0.01-0.05 mol dm^{-3}; MeOH: H_2O = 40:60 (v/v) [AA] = 0.100 mol dm^{-3}; temp. = 313 K

Substituent	K	ΔH (kJ mol^{-1})	ΔS (J mol^{-1} K^{-1})	$k \times 10^4$ (s^{-1})	E_a (kJ mol^{-1})	ΔH^* (kJ mol^{-1})	ΔS^* (J mol^{-1} K^{-1})
H	90.0	32.2	4.00	14.7	11.3	8.67	−271
4-NO_2	70.8	36.2	8.04	5.90	44.7	42.1	−172
3-NO_2	51.3	18.9	−48.0	4.65	33.2	30.6	−211
4-CH_3	63.9	31.4	−8.22	15.6	20.5	17.9	−241
3-CH_3	56.2	45.1	−35.5	22.0		·	—
4-Cl	55.6	20.1	44.2	7.32	24.2	21.6	236

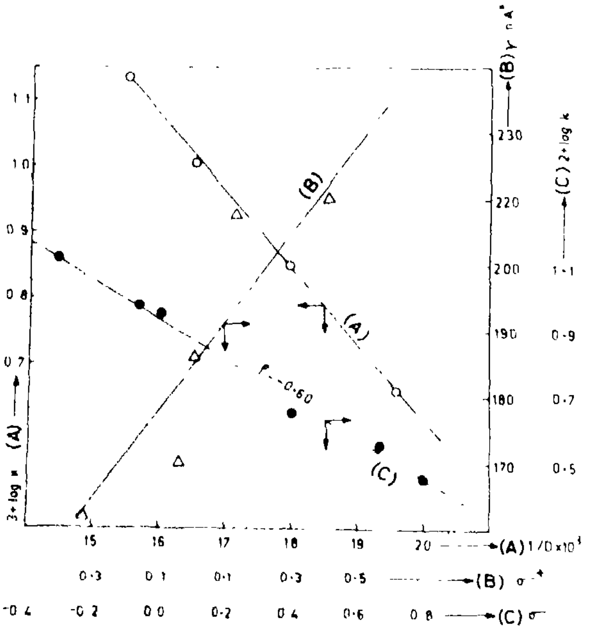

Fig. 2—(A) Plot of log k versus 1/D; (B) plot of r versus σ^+, and (C) plot of log k versus σ (Conditions same as in Table 1 for plots A and B and same as in Table 2 for plot C)

where k_D and k_∞ have their usual significance and μ_1, μ_2 are the dipole moments of the two molecules[20,21]; k is the Boltzman constant, T, the absolute temperature, D, the dielectric constant of the medium and r is the distance of closest approach of the two dipoles in the transition state. According to Eq. (10), decrease in dielectric constant (i.e. increase in methanol content in MeOH-water mixture) of the medium should decrease the rate for a reaction between two dipoles. This is found to be so in the present study (Fig. 2A). From the slope of such a plot, r-value was calculated knowing μ_1, μ_2, k and T. The r-values were obtained in a similar way for all the phenols. It is interesting to see that the r-values correlated well with Hammett's σ^+ values (Table 1; Fig. 2B), assuming *meta* substituents as *para* and vice versa. This indicates that the bromination occurs at position *ortho* to −OH (in Table 1 the σ^+ values of *meta* substituents are given for *para* and vice versa).

Effect of substituents

Though the values of K_h did not change (Table 2) the values of K and k were found to change with substituents in phenol. The invariance of K_h towards substituents in phenol shows that hydrolysis of NBA is not influenced by substituents in phenol.

From Table 2 it is clear that the values of formation constants (K), do not vary much for different phenols, and do not follow any sequence; K is maximum for parent phenol. The decomposition rate constants (k) of the adducts vary systematically (Table 2). Assuming bromination at carbon atom *ortho* to −OH group, the Hammett plot was found to be good with ρ = −0.60; r = 0.986 (Fig. 2C) taking

σ-values of *meta* substituents as *para* and vice versa. Negative ρ-value supports electrolophilic aromatic substitution reaction.

Effect of temperature

The values of K_h, K and k increased with increase in temperature and various thermodynamic parameters were evaluated and the values are presented in Tables 1 and 2. The ΔS_h values for hydrolysis of NBA are negative. This is because of (i) consumption of a free water molecule during hydrolysis of NBA and (ii) change in entropy of hydration of a proton is -105 J mol^{-1} K^{-1} (ref. 24). In principle hydration also involves loss of free movement of water molecules. Similar observation was reported earlier in the decomposition of adducts derived from α-hydroxyalkyl radicals and nitrobenzenes[25] where a proton generated is extensively hydrated.

The ΔS values for adduct formation are also negative (Table 2). This is because of the formation of a bulky cyclic transition state which accounts for decrease in number of molecules in going from reactants to the transition state which may be sufficiently polar to be solvated.

Since in step-3 of Scheme 1 free water molecule is generated, the $\Delta S^{\neq}$ values are expected to be positive. The actual values observed in the present study are largely negative. This can be explained as follows: Since the activation energies are not large, the low decomposition rate constants (k) at 313 K result from the strongly negative activation entropies. These values can be interpreted in terms of loss in entropy due to solvation of developing 2-bromocyclohexadiene-1-one (step 3). The observed $\Delta S^{\neq}$ values (Table 2) are highly negative and are comparable to that of hydration of proton transfer to solvent (-105 J mol^{-1} K^{-1})[24]. On analogy, the hydration of 2-H, which undergoes intramolecular migration to oxo group to give 2-bromophenol, is suggested.

Isokinetic phenomena

Isokinetic plots for the steps (1-3) in Scheme 1 are linear with isokinetic hydrolysis temperature ($\beta_h = 325$ K), isokinetic activation tèmperature ($\beta_{eq} = 278$ K) and isokinetic activation temperature ($\beta^{\neq} = 296$ K). According to isokinetic phenomenon[26] the values of β_h, β_{eq} and $\beta^{\neq}$ are intrepreted as follows. The values of β_h is close to the experimental temperature range 303-323 K which means that the hydrolysis step may be influenced by both enthalpy and entropy changes. Also it is clear that the variation in ΔH_h values (from 27 to 40 kJ) and ΔS_h values (from -9 to -4.8 J mol^{-1} K^{-1}) are comparable. The value of β_{eq} is 278 which is well below the experimental temperature range 303-323 K. This means that the formation of the cyclic adduct (step 2) is largely influenced by entropy changes. Finally the value of $\beta^{\neq}$ is again well below the experimental temperature range. Therefore the discussion as that for β_{eq} holds good for $\beta^{\neq}$.

Acknowledgement

The authors are grateful to Prof. T Navaneeth Rao, and Prof. B Sethuram, for constant encouragement. One of the authors (S V) thanks the Management, Sardar Patel College for providing necessary facilities to carry out this work.

References

1 Radhakrishnamurti P S & Damodar Rao B V, *Indian J Chem*, **20A** (1981) (a) 473, (b) 1002.
2 Radhakrishnamurti P S & Sahu S N, *Indian J Chem*, **15A** (1977) 785.
3 Sivakamasundari S & Ganesan R, *Int J Chem Kinet*, **12** (1980) 837.
4 Radhakrishnamurthi P S, Sasmal B M & Patnaik D P, *Indian J Chem*, **23A** (1984) 948.
5 Singh B, Pandey L, Sharma J & Pandey S M, *Tetrahedron*, **38** (1982) 169.
6 Filler R, *Chem Rev*, **63** (1963) 21.
7 Mukherjee J & Banerji K K, *J Org Chem*, **46** (1981) 2323.
8 Sharma V & Banerji K K, *J chem Research*, (1985) 3551 & references cited therein.
9 Venkateswarlu S & Jagannadham V, *React Kinet Catal Lett*, **27** (1985) 293; *Oxidn Commns*, **8** (1985) 149; *Z Physik Chem* (leipzig) (accepted).
10 sharma S, Rajaram J & Kuriacose J C, *Indian J Chem*, **15B** (1977) 274.
11 Gilow H M & Ridd John H, *J Chem Soc Perk II* (1973) 1321.
12 Rao T S, Mali S I & Dangat V T, *Tetrahedron*, **34** (1978) 205.
13 Rao T S & Mali S I, *J Univ Poona Sci Tech*, **48** (1976) 149.
14 Srinivasan C & Chellamani A, *React Kinet Catal Lett*, **18** (1981) 187.
15 De la Mare P B D & Hilton, *J Chem Soc*, (1961) 997.
16 Fyfe Colin A & Van Veen L (Jr), *J Am Chem Soc*, **99** (1977) 3366.
17 Cotton F A & Wilkinson G W, *Advances in inorganic chemistry*, Wiley Eastern, 2nd Edn. p (a) 569, (b) 197.
18 De la Mare P B D, el Dusouqui, Tillett J C & Zeltner M, *J chem Soc* (1964) 5306.
19 Amis Edward S & Hinton James F, *Solvent effects on chemical phenomena*, Vol I, Academic Press, New York, 1973, p. 265.
20 The dipole moments for phenols are taken from Balaiah V & Uma M, *Indian J Chem*, **10** (1972) 395; McClellan V A L, *Tables of experimental dipole moments*, W H Freeman & Co., San Francisco, 1963.
21 The dipole moment of HOBr is not available in literautre. It was estimated by using the equation $\mu_{HBr}/\mu_{HCl} = \mu_{HOBr}/\mu_{HOCl}$. Here the authors assumed that the ratios of dipolements of HBr[22], HCl[22] and HOBr, HOCl[23] are equal. In this way $^{\mu}$HOBr was calculated to be 1.00 D.
22 Linus Pauling, *The nature of chemical bond*, Oxford & IBH Co., III Ed., p. 78, 90.
23 Gills H E, Anderson W D, Lovas F J D & Suenram R D, *J Mol Spectroscopy*, **103** (1984) 466.
24 Buschmann H J, Butkiewicz & Knoche W, *Ber Bunsenges Phys Chem*, **86** (1982) 129.
25 Jagannadham V & Steenken S, *J Am Chem Soc*, **106** (1984) 6542.
26 Exner O, *Collect Czech Chem Commun*, **37** (1972) 1425.

Indian Journal of Chemistry
Vol. 27A, April 1988, pp. 318-322

Studies on Metal-Vitamin B$_6$ Systems: Part II—Reaction of Iron(III)-Pyridoxol Complexes with Vitamins & Amino Acids

SUMITRA SEN, S GANGOPADHYAY, B K SEN & P BANDYOPADHYAY*
Department of Chemistry, University College of Science, Calcutta 700 009

Received 3 *March* 1986; *revised* 3 *July* 1987; *accepted* 21 *August* 1987

By reacting iron(III)-pyridoxol complex, [Fe(Pyr)(OH)$_2$(H$_2$O)], with different vitamins and amino acids, stable mixed ligand complexes have been prepared. These are characterised by analytical, molar conductance, magnetic susceptibility, thermogravimetric, spectral, potentiometric and polarographic studies and their tentative structures have been proposed.

In a previous communication from this laboratory[1], we reported the isolation and characterisation of several iron(III)-pyridoxol complexes. All the complexes contained only one vitamin B$_6$ per metal atom. These complexes have now been found to react further with vitamins and amino acids to produce mixed ligand chelates of sufficient stability. Existence of such complexes was never considered before and formation of such chelates of iron with vitamins and amino acids present in biological systems is of considerable importance from the chemical and therapeutic viewpoints. In the present paper, we describe the preparation and properties of complexes of pyridoxol containing iron species with glycine, alanine, proline, thiamine (vitamin B$_1$) and nicotinic acid. These mixed complexes are characterised by elemental analysis, conductance, magnetic moment, pyrolytic, spectral, potentiometric and polarographic studies.

Materials and Methods

Glycine, alanine and proline hydrochlorides were prepared by dissolving the corresponding amino acids (BDH) in conc. hydrochloric acid and evaporating the solutions *in vacuo*. Glycine sulphate was similarly prepared by dissolving calculated quantity of glycine (BDH) in aqueous sulphuric acid and drying *in vacuo*. Pyridoxol hydrochloride (E. Merck) was recrystallised from ethanol and stored in a dark bottle at 0°C. Thiamine hydrochloride (IDPL) was recrystallised from methanol and stored similarly. Nicotinic acid (BDH) was used directly. Fe(Pyr)(OH)$_2$(H$_2$O) was prepared by the method described earlier[1]. Magnetic susceptibilities of all the compounds were measured at 303 K in a Gouy balance. The electronic spectra were recorded on a Hilger's UVISPEK spectrophotometer and the infrared spectra were recorded on Beckmann IR 20, Pye-Unicam and Perkin-Elmer instruments. Conductance measurements of solutions were done with a Philips RCL bridge. Pyrolytic decompositions of the solid compounds were studied in a manual thermobalance, constructed in the laboratory, at a heating rate of 5°C per minute in the temperature range 50-800°C. 100 mg of the sample was used in each experiment. Potentiometric measurements were made on an ECIL expanded scale *p*H cum potentiometer. Silver-silver chloride electrode was fabricated in the laboratory. The saturated calomel electrode (SCE) used for measuring the chloride ion concentrations was connected to the reference cell through a double bridge of agar-sodium perchlorate (2*M*). The potentiometer was previously calibrated with solutions of known $[Cl^-]$ under identical conditions. Polarographic experiments were carried out with a Cambridge pen recording polarograph.

General method of preparation and general properties

For preparing vitamin derivatives, Fe(Pyr)(OH)$_2$(H$_2$O) (200-300 mg) was added to a methanolic solution (100-150 mg, 15-20 ml) of the ligand and the contents were stirred for 2-3 hr. For preparing the amino acid complexes, the mixture was kept for 12 hr. Deep red solution obtained in each case, was separated by filtration from the unreacted starting compound and the filtrate was dried *in vacuo*. Glycine sulphato complex was prepared in aqueous medium.

Fe$_2$(Pyr)$_3$(OH)$_3$(H$_2$O)$_2$ was obtained by dissolving 200 mg of Fe$_2$(Pyr)$_3$(OH)$_2$(H$_2$O)$_3$Cl in 5 ml of 4*N* aqueous ammonia and subsequently precipitating the desired product by adding ethanol. The precipitate was filtered, washed with aqueous etha-

Table 1—Analytical and Physicochemical Data of the Mixed Ligand Iron-Pyridoxol Complexes

Compound	Found % (Calc.)				μ_{eff} (B.M.)	Λ (ohm^{-1}cm^2 mol^{-1})		ν_{max}, kK (ε in parenthesis)
	Fe	N	Cl	Others		Water	DMSO	
$Fe_2(Pyr)_2(NH_2CH_2COO)_2Cl_2$	16.6 (16.8)	8.6 (8.4)	9.9 (10.2)	—	4.35	266	36	31.65(13650), 34.01(12952), 40.00(12126), 45.45(27556)
$Fe_2(Pyr)_2(NH_2CH_2COO)_2(H_2O)_2SO_4$	15.5 (15.4)	8.1 (7.7)	—	4.50* (4.40)	4.28			33.90(13519), 34.50(12713)(sh) 45.45(19225)
$Fe_2(Pyr)_2(CH_3CHNH_2COO)_2Cl_2$	15.9 (16.1)	8.3 (8.1)	9.2 (10.2)	—	4.36	230	30	31.45(11140), 34.01(12776), 40.00(11578), 45.45(24596)
$Fe_2(Pyr)_2(C_4H_8NCOO)_2Cl_2$	15.0 (15.0)	7.6 (7.5)	9.3 (9.5)	—	4 42	204	20	31.75(15772), 33.90(15954), 40.00(15954), 45.05(30638)
$Fe_2(Pyr)_2(Thia)(OH)_3(H_2O)_2Cl_2$	13.1 (12.8)	9.6 (9.7)	8.0 (8.2)	3.80* (3.68) 37.7** (38.6) 4.90*** (5.05)	4.33	198	43	31.75(13774), 40.00(22698), 45.45(37245)
$Fe_2(Pyr)_3(OH)_2(H_2O)_3Cl$	15.3 (15.1)	5.8 (5.7)	4.67 (4.80)	—	5.04	122	23	30.96(19404), 34.25(15503), 39.22(15811), 45.25(43121)
$Fe_2(Pyr)_3(OH)_3(H_2O)_2$	16.6 (15.9)	6.43 (6.00)	—	—	5.00	—	—	—
$Fe_2(Pyr)_2(Nic)(OH)_3(H_2O)_2$	17.1 (17.0)	6.57 (6.39)	—	—	4.16	36	2	—

*S, **C, ***H

Pyr, Thia, Nic represent deprotonated pyridoxol, thiamine andnicotinic acid respectively.

nol and dried. The analytical data of the compounds with their magnetic moments, molecular conductance and absorption maxima are shown in Table 1. The compounds are, in general, soluble in water, methanol and DMSO. The glycine sulphato complex is insoluble in organic solvents while $Fe_2(Pyr)_3(OH)_3(H_2O)_2$ is insoluble in all these solvents.

Results and Discussion

Nearly all the compounds were obtained by the reaction of $Fe(Pyr)(OH)_2(H_2O)$ with the ligands, which are weak acids. The most probable reaction is, therefore, the replacement of the hydroxyl groups of the iron complex by the ligand anion formed on deprotonation which simultaneously forms a chelate. Microscopic examination, solubility in different solvents and fractional extraction with solvents confirmed that the products were really stoichiometric compounds and not mixtures. The compositions of some of the products directly indicate that they are polymers. The degree of polymerization was not determined and the indicated dimeric formulations are only tentative. All other products, being obtained in the same way, are assumed to contain similar polymeric structures. The physicochemical data agree quite well with these polymeric formulations.

Conductance data

The three amino acid complexes formed by glycine, alanine and proline exhibit very low conductivities in freshly prepared aqueous solutions, which increase with time to reach constant values corresponding to four ions for one dimeric complex molecule (Table 1); the constant values reported are for the solutions kept overnight. In DMSO, the values do not change with time and are less than those expected for two ions for one dimer. These facts agree with a chlorine bridged dimeric non-electrolytic structure of the molecules which slowly hydrolyse in aqueous solution as follows:

$$Fe_2Cl_2(Pyr)_2(AA)_2 + 4H_2O \xrightarrow[\text{slow}]{} 2[Fe(H_2O)_2(Pyr)(AA)]^+ + 2Cl^-$$

where AA stands for amino acid anion.

The molar conductivity of the glycine sulphato complex, $Fe_2(Pyr)_2(NH_2CH_2COO)_2(H_2O)_2SO_4$, in water is the time-independent but is a function of concentration. Concentrated solutions show 1:1 electrolytic behaviour whereas on dilution values corresponding to1:2 electrolyte are obtained. This can be explained by considering a sulphate

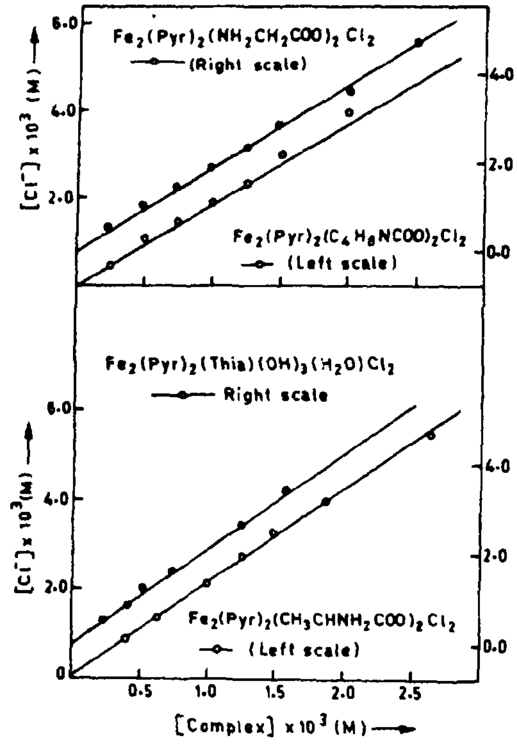

Fig. 1—Plots of measured $[Cl^-]$ against total complex concentration.

bridged dimer remaining in hydrolytic equilibrium with an ionic species as shown below:

$$(Fe_2SO_4)(Pyr)_2(NH_2CH_2COO)_2(H_2O)_2 + 2H_2O \rightleftharpoons 2[Fe(Pyr)(NH_2CH_2COO)(H_2O)_2]^+ + SO_4^{2-}$$

The nicotinate derivative is a non-electrolyte both in water and DMSO. The diferritris(pyridoxol) species and the thiamine derivative are 1:1 and 1:2 electrolytes respectively in both the solvents. Their structures are discussed later.

Potentiometric data

To prove that the increase in conductivity of aqueous solutions of amino acid complexes is really due to the increase in Cl^- ions, the equilibrium chloride ion concentrations of such solutions (which were allowed to attain equilibrium by keeping them overnight) were mesured potentiometrically using Ag−AgCl electrode. Solutions of different analytical concentrations of each complex were used and the measured $[Cl^-]$ were plotted against the total complex concentrations. Straight line plots with slopes of 2 were obtained in each case (Fig. 1) indicating that two Cl ions were liberated by every molecule of the dimeric complex.

Magnetic properties

With the exception of the tris(pyridoxol) compounds, all these complexes exhibit $\mu_{eff.}$ values of ~4.36 B.M. The tris(pyridoxol) derivative exhibits a higher value (~5.0 B.M.). It is significant that these values are uniformly much lower than the $\mu_{eff.}$ values (5.4-5.7 B.M.) exhibited by the monomeric iron(III)-pyridoxol complexes described earlier[1]. The dimeric diol bridged iron(III) compounds are known to have low magnetic moments due to weak antiferromagnetic coupling between two high spin ions[2]. The magnetic moment approaches the full high spin values (5.9 B.M.) only at higher temperatures. The low magnetic moment values of iron(III) complexes thus support the existence of bridged dimeric structures. Interestingly, the hexacoordinated chlorine bridged dimers like $Fe_2(Pyr)_2(AA)_2Cl_2$ are possibly the first such groups of compounds to exhibit low magnetic moments.

Electronic spectra

The salient electronic spectral bands (along with their intensity values) of these complexes in aqueous medium are recorded in Table 1. All the spectra, excepting that of the thiamine derivative, are characterised by the presence of the 34 kK band (acid band) indicating the presence of the protonated ring nitrogen of pyridoxol[3]. As noted earlier in the case of pyridoxol derivatives, the *d-d* transition band of Fe(III) ion is observed at 21 kK only in a limited range of acidity. Ths is observed in the spectrum of $Fe_2(Pyr)_2(NH_2CH_2COO)_2Cl_2$. Other bands are due to the intra-ligand transitions in different molecules.

Infrared spectra

The IR spectra of these mixed ligand complexes are too complicated to allow precise assignments of all the bands. However, a few conclusions could be derived by comparing these with the spectra of simple pyridoxol systems described earlier[1]. That the pyridoxol moiety acts as a bifunctional ligand coordinating through phenolic −OH group and the viscinal $-CH_2OH$ group in the present complexes also is shown by a composite band at 1015 ± 5 cm^{-1} and a band at 920 ± 10 cm^{-1}. That the sulphate group in the sulphato complex is present as a bridging group[4] is established by comparing the spectrum of the sulphato derivative with that of the corresponding chloro derivative. The presence of a strong band at 1100 cm^{-1} and two shoulders at 1170 and 1050 cm^{-1} in the former compound is indicative of a bridged SO_4^{2-} group.

Thermogravimetric studies

Thermograms were recorded for the glycine and alanine complexes. No structural information could be obtained from them except that the compounds are thermally unstable right from ~50°C and that both the organic ligands and $FeCl_3$ are eliminated according to the equations,

$$3\ Fe_2(Pyr)_2(NH_2CH_2COO)_2Cl_2 \xrightarrow[\text{(loss: 84.0\%)}]{\text{ligands} + 2\ FeCl_3} 2\ Fe_2O_3$$

$$3\ Fe_2(Pyr)_2(CH_3CHNH_2COO)_2Cl_2 \xrightarrow[\text{(loss: 84.6\%)}]{\text{ligands} + 2\ FeCl_3} 2\ Fe_2O_3$$

Polarographic studies

The glycine and the thiamine derivatives undergo polarographic reduction in two steps, the first of which corresponds to Fe(III)/Fe(II) reduction. The $E_{0.5}$ values for the first wave are −0.550 V (vs SCE) for the glycine complex and −0.651 V for the thiamine complex. This reduction is reversible for both the complexes and from the plot of log $i/(i_d - i)$ against E, the number of Faradays consumed per mol of the depolarizer was found to be 0.98 and 0.93 for glycine and thiamine complexes respectively. The second waves were irreversible and the $E_{0.5}$ and n values were −1.450 V, 0.81 (glycine compound) and −1.40 V, 0.84 (thiamine compound). A comparison of the $E_{0.5}$ values for the first wave of these complexes with that for the simple pyridoxol derivative (−0.476 V)[1] indicates that these mixed ligand derivatives are more stable than the simpler pyridoxol derivative. The diffusion current constant values of the mixed ligand compounds (0.80 for glycine and 0.92 for thiamine) are somewhat less than that for Fe(PyrH)Cl_3 (0.96). These lower values are in conformity with the larger size of the mixed ligand depolarizer particles.

Structures of the complexes

The structure (I) of dihydroxopyridoxoliron(III) has been discussed in the earlier communication[1]. The result of the reaction of (I) with acidic reactants like amino acid hydrochlorides or sulphate is the neutralisation of the hydroxyl groups present in the complex and their replacement by deprotonated ligand which simultaneously forms a chelate. In methanolic medium, the chloro complexes are stable and hence chlorine bridged dimers(II) are produced. In aqueous solution, the chloro complexes are hydrolysed and since the medium is acidic, the hydroxyl bridged structures are not formed. The liberated proton attaches itself to the pyridine nitrogen and the resulting structure is represented by (III) which agrees with the electronic spectra (34 kK band) and conductance data.

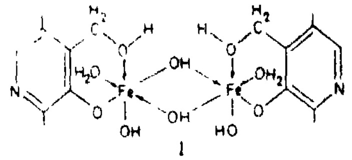
I

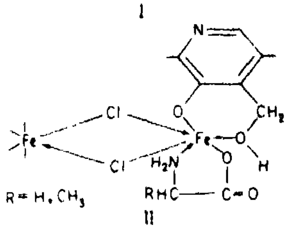

II

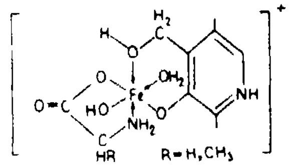

III

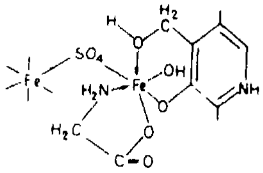
IV

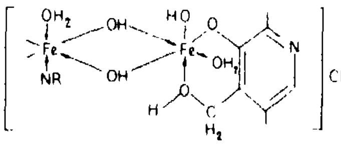

V

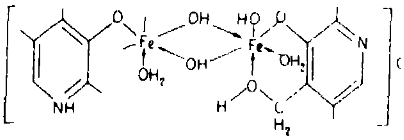

VI

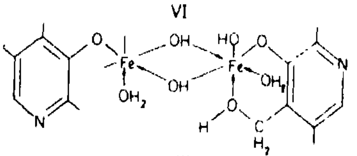
VII

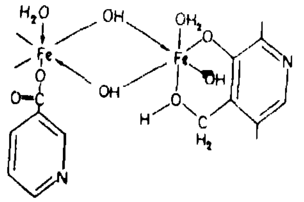
VIII

In the sulphato complex (IV), a pair of chlorine bridges is replaced by a single bridging sulphate which is also stable in aqueous medium, and this is corroborated by the IR data. One additional water molecule attaches to each metal ion to satisfy the coordination number and the coordinated water releases its proton to the pyridine nitrogen as evidenced by the electronic spectrum (acid band).

The trispyridoxol, thiamine and nicotinic acid complexes are formed under similar conditions where the hydrochlorides and nicotinic acid act as weak acids. The acidities of the reaction media for these reactants are not so high as in the cases of amino acid hydrochlorides and this results in the retention of the hydroxyl bridge of the parent complex. Evidently, the type of reaction depends on the acid strength of the reacting ligand. Since only one mole of the acidic ligand reacts with every mole of the dimer, the structures of thiamine, trispyridoxol and nicotinic acid derivative can be represented by (V) to (VIII). The IR, electronic spectral and conductance data agree with them. $Fe_2(Pyr)_3(OH)_3(H_2O)_2$ (VII) is obtained by raising the *p*H of the solution of $[Fe_2(Pyr)_2(PyrH)(OH)_3-(H_2O)_2]Cl$ (VI) and, hence, it is represented by the same structure with one HCl remvoed. In structure (V), NR indicates the thiamine residue coordinating through pyrimidine nitrogen.

Acknowledgement

Thanks are due to the UGC, New Delhi, for financial support.

References

1 Gangopadhyay S, Sen S, Sen B K & Bandyopadhyay P, *Indian J Chem*, **20A** (1981) 258.

2 Cotton F A & Wilkinson G, *Advanced inorganic chemistry* (Wiley Eastern, New Delhi), 1978, 516, 866.

3 Stiller E T, Keresztesy J C & Stevens J R, *J Am chem Soc*, **61** (1939) 1237.

4 Nakamoto K, *Infrared and Raman spectra of inorganic and coordination compounds* (Wiley-Interscience, New York), 1978, 240.

Indian Journal of Chemistry
Vol. 27A, April 1988, pp. 323-326

Chemistry of Bis(fluorosulphuryl)amine: Part V—Reactions of Bis(fluorosulphuryl)amine with Antimony(V) Chloride & Protonic Acids

P L DHINGRA, PAMELA LYALL & R D VERMA*
Department of Chemistry, Panjab University, Chandigarh 160014

Received 23 *March* 1987; *revised* 21 *May* 1987; *accepted* 23 *July* 1987

Antimony(V) chloride reacts with bis(fluorosulphuryl)amine, $HN(SO_2F)_2$, to form $SbCl_4N(SO_2F)_2$, the Λ_0 value of which in nitrobenzene indicates that it behaves as a strong Lewis acid. Its 1:1 adducts with triphenylphosphine oxide, formamide, dimethylformamide and N,N-dimethylacetamide have been isolated. These adducts are formed by coordination through oxygen of Lewis base. In the probable structure of the adducts, hexacovalency of Sb(V) and monodentate nature of $N(SO_2F)_2$ is proposed. Addition compounds of some carboxylic acids with $HN(SO_2F)_2$ have also been isolated and characterized on the basis of their elemental analyses, molar conductance, infrared, ^1H and ^{19}F NMR data.

Bis(fluorosulphuryl)amine, $HN(SO_2F)_2$, has been known for quite sometime[1] and several aspects of its chemistry have been reported[2-5]. In continuation of our studies on the chemistry of $HN(SO_2F)_2$ we report herein its reactions with antimony(V) chloride and some carboxylic acids, RCOOH($R = CH_3$, C_2H_5, *n*-C_3H_7, CH_2Cl).

Materials and Methods

Bis(fluorosulphuryl)amine was prepared as described earlier[6]. Antimony(V) chloride, pyridine, diethylamine, 1,10-phenanthroline, formamide, dimethylformamide, and all organic solvents used were purified by standard procedures. Triphenylphosphine oxide and 2,2'-bipyridyl were used as such.

Preparation of $SbCl_4N(SO_2F)_2$ *and its complexes*

$SbCl_4N(SO_2F)_2$ was prepared by treating $SbCl_5$ (10 mmol) with $HN(SO_2F)_2$ (20 mmol) in dry CCl_4 (30 ml) followed by refluxing until evolution of HCl ceased. Excess CCl_4 was removed by distillation, the residual liquid treated with ether and the $SbCl_4N(SO_2F)_2$ obtained as a white crystalline solid was filtered under dry nitrogen, washed with ether and finally dried *in vacuo.*

Complexes of $SbCl_4N(SO_2F)_2$ with triphenylphosphine oxide, formamide, dimethylformamide and N,N-diethylacetamide were prepared by adding an equimolar solution of the respective base in CCl_4 to a suspension of $SbCl_4N(SO_2F)_2$ also in CCl_4 and the reaction mixture stirred at room temperature for 7 hr. Adducts formed were filtered, washed with CCl_4 and finally dried *in vacuo.*

Preparation of adducts of $HN(SO_2F)_2$ *with protonic acids*

Protonic acid was added to ice-cold $HN(SO_2F)_2$ in an equimolar ratio, the reaction mixture stirred for 4 hr, and the solid adduct so formed was washed with CCl_4 and dried *in vacuo.*

Physical measurements

The IR spectra of the compounds were recorded as nujol/hcb mulls or neat liquids between AgCl plates on a Perkin-Elmer model 621 spectrophotometer in the range 4000-200 cm^{-1}.

For measuring equivalent conductances of $SbCl_4N(SO_2F)_2$ at varying concentrations, its stock solution was prepared in nitrobenzene and the stock solution suitably diluted to obtain solutions of desired strengths. Conductance was measured on a Toshniwal Cl01/01 conductivity bridge. Molecular weight in nitrobenzene was determined cryoscopically. The ^1H and ^{19}F NMR were recorded on a Varian model EM-390 instrument using TMS as internal and CCl_3F as external references respectively.

Results and Discussion

Antimony(V) chloride, a strong Lewis acid, is found to form a yellow crystalline hygroscopic compound[7] $SbCl_3[N(SO_2Cl)_2]_2$ with the chloro analogue of bis(fluorosulphuryl)amine. It also forms white crystalline compounds[8] with HSO_3X ($X = Cl, F$).

Antimony(V) chloride in bis(fluoro sulphuryl) amine behaves as a solvo acid, dissolves exothermically and the solution conducts electricity[5]. However, on refluxing, the two components give a highly moisture-sensitive white crystalline solid of composi-

Table 1—Analytical Data

Compound	Found (Calc)%					
	S	C	H	N	Sb	C
$SbCl_4N(SO_2F)_2$	14.17 (14.43)	—	—	3.14 (3.16)	27.92 (27.45)	31.26 (31.97)
$SbCl_4N(SO_2F)_2.(C_6H_5)_3PO$	8.82 (8.87)	29.71 (29.94)	20.4 (20.8)	1.92 (1.94)	17.01 (16.87)	19.81 (19.65)
$SbCl_4N(SO_2F)_2.HCONH_2$	12.89 (13.10)	2.44 (2.46)	0.60 (0.61)	5.70 (5.73)	26.45 (24.92)	28.54 (29.02)
$SbCl_4N(SO_2F)_2.HCON(CH_3)_2$	12.12 (12.39)	6.91 (6.97)	1.35 (1.36)	5.38 (5.42)	23.16 (23.57)	27.06 (27.45)
$SbCl_4N(SO_2F)_2.CH_3CON(C_2H_5)_2$	11.24 (11.45)	12.78 (12.89)	2.30 (2.33)	4.97 (5.01)	21.16 (21.79)	24.93 (25.38)
$CH_3CO_2H.HN(SO_2F)_2$	27.06 (26.55)	9.81 (9.90)	2.01 (2.07)	—	—	—
$C_2H_5CO_2H.HN(SO_2F)_2$	25.86 (25.10)	14.03 (14.12)	2.69 (2.74)	—	—	—
$C_3H_7CO_2H$ $HN(SO_2F)_2$	24.13 (23.79)	17.65 (17.84)	3.29 (3.34)	—	—	—
$CH_2ClCO_2H.HN(SO_2F)_2$	23.12 (23.23)	8.68 (8.71)	1.43 (1.45)	—	—	13.14 (12.88)

tion $SbCl_4N(SO_2F)_2$, m.p. 127°, soluble in acetonitrile, nitromethane and nitrobenzene. Molar conductance values of its millimolar solutions in acetonitrile (152 ohm^{-1}cm^{2}mol^{-1}) and nitrobenzene (35 ohm^{-1}cm^{2}mole^{-1}) suggest 1:1 elecrolytic nature of $SbCl_4N(SO_2F)_2$ in accordance with equilibrium(1)

$$2SbCl_4N(SO_2F)_2 \rightleftharpoons SbCl_4^+ + SbCl_4[N(SO_2F)_2]_2^- \quad \ldots(1)$$

The molecular weight of $SbCl_4N(SO_2F)_2$ in nitrobenzene appeared to be a function of its concentration and varied from 107.4 for a 0.0048 *M* solution to 288.09 for a 0.04 *M* solution in nitrobenzene. A similar behaviour is exhibited by $AgN(SO_2F)_2.C_6H_6$ in benzene[9].

The strong Lewis acid character of $SbCl_4N(SO_2F)_2$ is indicated[8] by the Λ_0 value of 41.66 ohm^{-1}cm^{2}mol^{-1} obtained by extrapolating the plot of C Λ_c versus $1/\Lambda_c$. Its Lewis acid behaviour was further confirmed by carrying out its conductometric titrations against Lewis bases such as diethylamine, pyridine, 1,10-phenanthroline and 2,2′-bipyridyl in nitrobenzene. The plot of relative conductance versus molar ratio of acid/base showed a break in the titration curve at 1:1 acid/base mol ratio in the case of Et_2NH and pyridine, and two breaks at 1:1 and 2:1 acid/base mol ratios in the case of 1,10-phenanthroline and 2,2′-bipyridyl. These observations suggest that $SbCl_4N(SO_2F)_2$ behaves as a monobasic acid.

The IR spectrum of $SbCl_4N(SO_2F)_2$ exhibits bands attributable to the $N(SO_2F)_2$ group[10]. The vibrational bands at 335 and 250 cm^{-1} may be attributed[11] to νSb – Cl.

Adducts with Lewis bases and having the composition $SbCl_4N(SO_2F)_2.L$ ($L = Ph_3PO$, $HCONH_2$, $HCONMe_2$, CH_3CONEt_2) have been isolated and their analytical data are presented in Table 1. $SbCl_4N(SO_2F)_2.(C_6H_5)_3PO$, a white solid, m.p. 143°, is soluble in acetonitrile, nitromethane and nitrobenzene. Its IR spectrum displays characteristic bands attributable to $N(SO_2F)_2$ group. The bands at 340 and 290 cm^{-1} have been assigned[11] to νSb – Cl. In pure triphenylphosphine oxide, νP=O appears at 1192 and νP–C at 1440 and 995 cm^{-1} (ref. 12). The νP=O mode in the complex appears at 985 at νP–C at 1450 and 1005 cm^{-1}, indicating coordination of triphenylphosphine oxide through its oxygen atom[13,14]. Furthermore the magnitude of the lowering ($\Delta\nu = 207$ cm^{-1}) of νP=O may be taken as a measure of the extent of its Lewis acid strength.

Formamide and N,N-diethylacetamide CH_3CONEt_2 react with $SbCl_4N(SO_2F)_2$ to give white solids. The IR spectra of both the solid adducts exhibit all characteristic bands associated with the $N(SO_2F)_2$ group, while νSb – Cl appears as a split band at 345 and 310 cm^{-1} for $SbCl_4N(SO_2F)_2.HCONH_2$. Coordination of Lewis acids to the carbonyl oxygen in amides in preference to nitrogen is already well esta-

Table 2—PMR Data of Carboxylic Acids and Their Adducts of Bis(Fluorosulphuryl)Amine

Complex	Acid	Assignment (ppm)		
			Acid	Complex
$CH_3CO_2H.HN(SO_2F)_2$	CH_3COOH	a	2.13	2.20
	a b	b	11.80	12.85
$C_2H_5CO_2H.HN(SO_2F)_2$	CH_3CH_2COOH	a	1.25	1.55
	a^3 b^2 c	b	2.46	2.98
		c	12.13	12.93
$C_3H_7CO_2H.HN(SO_2F)_2$	$CH_3CH_2CH_2COOH$	a	1.13	1.35
	a^3 b^2 c^2 d	b	1.80	2.08
		c	2.46	2.93
		d	12.21	12.95
$CH_2ClCO_2H.HN(SO_2F)_2$	$ClCH_2COOH$	a	4.15	4.40
	a^2 b	b	11.15	11.85

blished[15,16] and on the basis of hexacovalency of antimony(V)[17], the structure (A) may be proposed for the amide adducts. The expected decrease in $\nu C=O$ in the adduct of formamide (from 1695 to 1670 cm^{-1}) and diethylacetamide (from 1628 to 1618 cm^{-1}) indicates decrease in bond order in C = O as a result of linkage through oxygen. This mode of coordination should result in an increase in $\nu C-N$ and shifts of 20-30 cm^{-1} in $\nu C-N$ to higher wavenumbers have actually been observed.

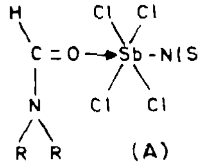

(A)

The yellowish brown $SbCl_4N(SO_2F)_2$. $HCON(CH_3)_2$ complex is a liquid which fumes in air. It is insoluble in ether, carbon tetrachloride, acetonitrile, nitrobenzene and nitromethane. The IR spectrum of the complex displays trends, similar to those observed in the adducts of formamide and diethylacetamide, e.g. decrease in $\nu C=O$ and increase in $\nu C-N$ and by analogy a similar structure may be proposed.

The addition compounds of various protonic acids with bis(fluorosulphuryl)amine are colourless mobile liquids which fume in moist air. They are insoluble in CCl_4, chloroform, benzene and nitrobenzene, but are soluble in dichloromethane and nitromethane. Molar conductance values (72-81 ohm^{-1}cm^{2}mol^{-1}) in nitromethane are suggestive of 1 : 1 electrolytic behaviour of the adducts, which probably arises as a result of equilibrium(2).

$$RCOOH + HN(SO_2F)_2 \rightleftharpoons RCOOH_2^+ + N(SO_2F)_2^- \qquad \ldots(2)$$

This acceptance of a proton by carboxylic acid from $HN(SO_2F)_2$ is corroborated by the expected shifts in the IR spectra of the adducts, where a decrease in $\nu C=O$ and an increase in νOH modes, relative to those observed in the pure carboxylic acids, are discernible. The νOH of the carboxylic acid in the region 3000-2500 cm^{-1} (ref. 18) is shifted to higher wavenumbers in the IR spectra of the adducts and appears in the region 3440-3410 cm^{-1}. The $\nu C=O$ mode which is generally observed in the range 1740-1700 cm^{-1} in pure saturated aliphatic acids and α-halosubstituted aliphatic acids shifts to lower wavenumbers ($\Delta\nu = 90$-145 cm^{-1}) in the adducts, appearing in the region 1610-1570 cm^{-1}. The lowering of $\nu C=O$ mode is accompanied by a concomitant shift of $\nu O-C$ mode to higher frequencies, thus supporting electron donation from the carbonyl oxygen to the proton of $HN(SO_2F)_2$ as shown in equilibrium (2). The characteristic bands appearing around 1480 s, 1380 s, 1250 vs, 1180 vs, 920 vs, 880 s, 830 s, 560 s, 450 m cm^{-1} assignable to $N(SO_2F)_2$ moiety[9] are observed in all the adducts†.

The ^1H NMR of neat carrboxylic acids and their adducts and ^{19}F NMR of the adducts only were recorded. The single sharp signal at 8.60 ppm in neat $HN(SO_2F)_2$ does not appear in its adducts. The hydroxylic proton in carboxylic acids gets deshielded and appears at lower applied field strength in the adducts (Table 2). In addition to this, other multiplets due to the presence of other protons, as reported in the literature have also been observed. The ^{19}F NMR signals in the adducts do not show much change and appear around 58 ppm downfield from Freon-11 as external reference.

---

†Complete IR spectral data can be had from the authors on request.

Thus the ^{1}H and ^{19}F NMR. and IR spectral data, and the molar conductance values suggest that the carboxylic acids studied behave as solvo bases in $HN(SO_2F)_2$, as these compounds can accept a proton from $HN(SO_2F)_2$ thus forming a conjugate acid.

References

1 Appel R & Eisenhauer G, *Chem Ber*, **95** (1962) 246

2 Colburn C B, Hill W E & Verma R D, *J Fluorine Chem*, **17** (1981) 75.

3 Dhingra P L & Verma R D, *Bull chim Soc France*, (1984) 346.

4 Dhingra P L, Singhal R L & Verma R D, *Indian J Chem*, **24A** (1985) 472.

5 Dhingra P L & Verma R D, *Bull chim Soc France*, (1986) 367.

6 Ruff J K & Lustig M, *Inorg Synth*, **11** (1968) 138.

7 Paul R C, Kapoor P, Kapoor R & Verma R D, *J inorg nucl Chem*, **40** (1978) 2001.

8 Paul R C, Kumar R C & Verma R D, *Indian J Chem*, **16A** (1978) 695.

9 Ruff J K, *Inorg Chem*, **4** (1965) 1446.

10 Sawyer J F, Schrobilgen G J & Sutherland S J, *Inorg Chem*, **21** (1982) 4064.

11 Beattie I R, Gilson T, Livingston K, Fawcett V & Ozin G A, *J chem Soc*(*A*), (1967) 712.

12 Dassch L E & Smith D C, *Analyt Chem*, **23** (1951) 853.

13 Cotton F A, Goodgame D M L & Soderberg, *Inorg Chem*, **2** (1963) 1162.

14 Clark J P, Langford V M & Wilkins C J, *J chem Soc*(*A*), (1967) 792.

15 Gerrard W, Lappert M F, Pyszora H & Wallis J W, *J chem Soc*, (1960) 2144.

16 Patnaik P G & Ramiah K V, *Proc Ind acad Sci*, **54** (1961) 69.

17 Paul R C, Sharda S & Seenathan B R, *Indian J Chem*, **2** (1964) 97.

18 Bellamy L J, *Infrared spectra of complex molecules*(Methuen, London) 1959.

Indian Journal of Chemistry
Vol. 27A, April 1988, pp. 327-331

Polymeric Dioxouranium(VI) Complexes with Malonoyldihydrazine

R A LAL* & M N SINGH†
Department of Chemistry, Pachhunga University College, North-Eastern Hill University, Aizawl 796 001
and
R K THAPA
Department of Physics, Pachhunga University College, North-Eastern Hill University, Aizawl 796 001

Received 30 *March* 1987; *revised* 21 *May* 1987; *rerevised and accepted* 13 *July* 1987

Twelve new polymeric uranyl complexes with malonoyldihydrazine (MH) have been prepared and characterized on the basis of various physicochemical data. The complexes have the compositions $UO_2(MH)X_2nH_2O$ and $UO_2(MH)_2X_2nH_2O$ ($X = NO_3^-$, Cl^-, SCN^-, CH_3COO , $1/2SO_4^{2-}$, $1/2C_2O_4^{2}$; n = 0-4). It is shown that MH coordinates in keto form as a bidentate bridging ligand retaining the intramolecular hydrogen bonding of the uncoordinated molecule in all these complexes. The complexes are assigned polymeric structures involving eight coordinated uranium atom with ligand atoms arranged around the linear uranyl group in the equatorial plane.

Complexes of acyl- and aroyl-hydrazines have been reported with transition metal ions and actinides. In metal complexes, acyl- and aroyl-hydrazines exist either in keto or enol form and coordinate to metals through the primary nitrogen and amide groups[1-7]. A literature survey revealed that although some complexes of acyldihydrazines[8] with 3*d* metal ions have been reported, virtually no acyldihydrazine complexes with actinides are known. Surprisingly, acyldihydrazines have been reported to coordinate to the 3*d* metal ions through secondary nitrogen atoms. Therefore, we thought it of interest to study the compounds of acyldihydrazines with uranyl ion. Because of its strong tendency to coordinate in the equatorial plane with 4 to 8 donors[9-11], uranyl ion may rupture the intramolecular hydrogen bonding and make $>C=O$ and $-NH_2$ groups reactive. In the present paper, synthesis and characterization of coordination compounds of malonoyldihydrazine (MH) with dioxouranium(VI) are reported.

Materials and Methods

Uranyl nitrate hexahydrate, uranyl acetate dihydrate, uranyl sulphate, ammonium thiocyanate, barium chloride, diethylmalonate, oxalid acid and hydrazine hydrate used were BDH reagents of A R quality. Methanolic solution of uranyl thiocyanate was obtained by the metathesis reaction of uranyl nitrate with ammonium thiocyanate. A methanolic solution of uranyl chloride was obtained by the interaction of a hot methanolic solution of uranyl sulphate with calculated amount of barium chloride in 1:1 molar ratio. Malonoyldihydrazine (m.p., 153-154°C; lit. 152°C)[2] was prepared by refluxing diethylmalonate and hydrazine hydrate in 1:2 molar ratio; it was recrystallized from water. Uranium in the complexes was estimated by the standard literature procedure[13]. Chloride and thiocyanate were estimated as silver salts. Nitrate was estimated as nitron nitrate[13a]. Hydrazine was estimated volumetrically by KIO_3 after submitting the complexes to acid hydrolysis for ~ 4 hr[13b]. Oxalate was estimated volumetrically by standard $KMnO_4$ in hot 2 *N* sulphuric acid medium. Nitrogen was determined by microanalysis. Thermogravimetric study of the complex $UO_2(MH)_2(NO_3)_2$ was carried out on a manual unit supplied by FCI, Sindri, by heating the sample at the rate of 10°C per minute. The molar conductances of $10^{-3}M$ solutions of the complexes in DMF were determined using an Elico conductivity bridge model CM-82T with a dip-type conductivity cell. IR spectra were recorded in mull in the range 4000-200 cm^{-1} on a Perkin-Elmer 621 spectrophotometer. Raman spectrum of $UO_2(MH)_2(NO_3)_2$ was recorded on a Raman spectrophotometer (Ramalog 1403) in KBr by employing rotating sample technique to avoid decomposition of the sample.

Preparation of the complexes

(*i*) $UO_2(MH)X_2nH_2O$ *and* $UO_2(MH)_2X_2nH_2O$ ($X = NO_3^-$, CH_3COO^-, SCN^-, Cl^-, $1/2SO_4^{2-}$, $1/2C_2O_4^{2-}$; $n = 0, 2\text{-}4$)

These compounds were synthesized by adding ethanolic solution of the uranyl salt (in case of sulphato complex methanolic solution) (0.01 mol) to an ethanolic solution (methanolic solution in sulphato complex) of the ligand, keeping uranyl salt in slight excess for $UO_2(MH)X_2nH_2O$ type complexes and ligand in excess for $UO_2(MH)_2X_2nH_2O$ type complexes. In $UO_2(MH)X_2nH_2O$ type complexes, the solutions were concentrated to two thirds of their original volumes by keeping on a water bath. The resulting solutions were refluxed for 2 and 1 hr for 1:1 and 1:2 (metal:ligand) complexes, respectively. The $UO_2(MH)X_22H_2O$ ($X = 1/2SO_4^{2-}$, CH_3COO^-) complexes precipitated during refluxing while other complexes precipitated only when the solutions were concentrated to half of their original volumes and cooled to room temperature. Addition of ether was necessary for the precipitation of the $UO_2(MH)X_22H_2O$ ($X = NO_3^-$, Cl^-) complexes; a semi-solid was obtained in the case of $UO_2(MH)(SCN)_23H_2O$ complex which on extraction into benzene and stirring vigorously for 1 hr yielded the complex. The complexes were filtered, washed with hot ethanol, ether and dried *in vacuo* over silica gel. $UO_2(MH)(SCN)_23H_2O$ was washed with a mixture of ethanol and ether and finally washed with benzene and dried as above.

---

† S.P. Degree College, Shohratgarh, Basti.

(*ii*) $UO_2(MH)_mC_2O_42H_2O$ ($m = 1, 2$)

Oxalato complexes were obtained by adding uranyl nitrate hexahydrate solution (0.01 mol) in ethanol to a well stirred mixture of oxalic acid and MH as required by stoichiometry, keeping oxalic acid in slight excess. The resulting solutions were concentrated to about half of their original volume and then refluxed on a water bath for 2 hr. This precipitated $UO_2(MH)_2C_2O_42H_2O$ complex. $UO_2(MH)C_2O_42H_2O$ precipitated only on adding ether and keeping the solution overnight. The complexes were filtered and collected as indicated above.

Results and Discussion

The molecular model of the ligand MH shows the existence of intermolecular and intramolecular hydrogen bonding in the solid state. MH possesses an active methylene group flanked by two keto groups on the two sides. It can coordinate to metal ions either in the keto form (A) or in the enol forms (B), (C), (D) or (E).

It has as many as six donor sites and is capable of exhibiting flexidentate behaviour. However, simultaneous involvement of all the donor atoms in coordination is unlikely. The ligand can function as a quadridentate ONNO donor (two carbonyl oxygen and two primary nitrogen atoms) or as a bidentate NN donor (two secondary nitrogen atoms) coordinating to the metal ions in the keto form (A) depending upon whether the intramolecular hydrogen bonding is ruptured by coordination or not. The ligand can also function as a dibasic quadridentate ONNO donor (two enolized carbonyl oxygens and two primary nitrogen atoms) in its enol form (D) or (C). On the other hand, if the ligand coordinates to the metal ions in the keto-enol form (B) or (C), it will function either as a monobasic tetradentate ONNO donor (one enolized carbonyl oxygen, another carbonyl oxygen and two primary nitrogen atoms) or as a monobasic tridentate ONN donor (one enolized carbonyl oxygen, one primary nitrogen and one secondary nitrogen atom) keeping intact hydrogen bonding in half of the molecule.

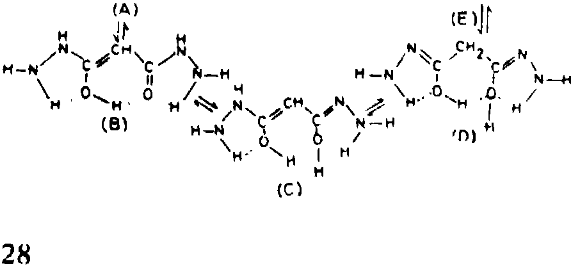

The analytical results indicate that the complexes possess the general formulae $UO_2(MH)X_2nH_2O$ and $UO_2(MH)_2nH_2O$ ($X = NO_3^-$, CH_3COO^-, SCN^-, Cl^-, $1/2SO_4^{2-}$, $1/2C_2O_4^{2-}$; $n = 0$, 2-4). All the complexes are coloured solids insoluble in common organic solvents but dissolve in polar solvents like DMSO and DMF and decompose without melting above 250°C. Insolubility of the complexes in water and common organic solvents coupled with their high decomposition temperatures suggest their polymeric nature in the solid state. The presence of water molecules in the complexes was confirmed by heating the complexes for 4 hr in an electric oven maintained at 110°C and 160°C and passing the vapours through a trap containing anhydrous copper sulphate which turned blue. The mass loss occurred at 110°C in the complexes No. 4, 10 and 12 (Table 1); it corresponded to three, four and two water molecules, probably lattice-held. In the remaining complexes, the mass loss occurring at 160°C corresponded to two water molecules indicating that the water molecules were coordinated.

The molar conductances of nitrate, acetate, chloride and thiocyanate complexes in DMF solution were found to be in the range 120-140 mhos cm^2mol^{-1} while sulphato and oxalato complexes showed molar conductances in the range 55.8-68.0 mhos cm^2mol^{-1} indicating their 1:2 and 1:1 electrolytic nature, respectively in DMF[14]. Although DMF is not an ideal solvent for conductivity measurements, it was chosen because of the insolubility of the complexes in other comon organic solvents. The observed molar conductance values of the complexes probably indicate the breaking of their polymeric structures and ionisation of the coordinated anions in highly coordinating medium (DMF)[15,16].

Table 1—Characterization Data of Uranyl Malonoyldihydrazine Complexes

Sl. No.	Complex	Colour (Dec Temp, °C)	Found (Calc)%					
			U	C	H	N	N_2H_4	Anion
1	$UO_2(MH)(NO_3)_2 2H_2O$	Orange	43.07	6.03	2.14	15.35	11.97	22.75
		(>250)	(42.35)	(6.41)	(2.13)	(14.95)	(11.39)	(22.06)
2	$UO_2(MH)_2(NO_3)_2$	Orange yellow	36.62	10.52	2.45	21.12	19.83	18.48
		(>250)	(36.17)	10.94)	(2.45)	(21.28)	(19.45)	(18.84)
3	$UO_2(MH)(SCN)_2 2H_2O$	Orange	42.50	11.41	2.15	15.62	11.42	21.36
		(>250)	(42.96)	(10.83)	(2.17)	(15.16)	(11.55)	(20.94)
4	$UO_2(MH)_2(SCN)_2 3H_2O$	Dark orange	33.35	13.27	3.11	19.50	18.56	15.95
		(>250)	(33.81)	(13.64)	(3.12)	(19.89)	(18.18)	(16.48)
5	$UO_2(MH)SO_4 2H_2O$	Shining yellow	45.06	6.97	2.29	10.87	11.73	18.40
		(>250)	(44.56)	(6.74)	(2.25)	(10.49)	(11.99)	(17.98)
6	$UO_2(MH)_2SO_4$	Light yellow	38.25	11.12	2.49	18.32	19.86	15.74
		(>250)	(37.78)	(11.43)	(2.54)	(17.78)	(20.32)	(15.24)
7	$UO_2(MH)(CH_3COO)_2 2H_2O$	Dull orange	42.39	15.45	3.23	10.50	10.01	–
		(>250)	(42.81)	(15.11)	(3.24)	(10.07)	(11.51)	
8	$UO_2(MH)_2(CH_3COO)_2$	Yellow	36.24	18.86	3.35	17.50	20.01	–
		(>250)	(36.50)	(18.40)	(3.37)	(17.18)	(19.63)	
9	$UO_2(MH)Cl_2 2H_2O$	Yellow	47.06	7.45	2.39	11.42	13.01	13.58
		(>250)	(46.76)	(7.09)	(2.36)	(11.00)	(12.51)	(13.99)
10	$UO_2(MH)_2Cl_2 4H_2O$	Orange yellow	35.60	10.12	3.59	16.03	18.51	11.02
		(>250)	(35.15)	(10.54)	(3.55)	(16.54)	(18.91)	(10.49)
11	$UO_2(MH)C_2O_4 3H_2O$	Dirty yellow	44.21	11.09	2.55	10.53	11.34	16.57
		(>250)	(43.75)	(11.03)	(2.57)	(10.29)	(11.76)	(16.17)
12	$UO_2(MH)_2C_2O_4 2H_2O$	Yellow	36.60	14.98	3.04	17.41	18.98	13.71
		(>250)	(36.17)	(14.59)	(3.04)	(17.02)	(19.45)	(13.74)

The IR spectra of MH has been discussed by Mashima[17]. It shows a very strong band at 1640 cm^{-1} with a strong shoulder at 1665 cm^{-1}. These bands are due to $-NH_2$ bending and amide I band. The above bands show a positive shift and an unusual increase in the intensity and broadness in the spectra of the complexes appearing in the region 1700-1660 cm^{-1}. The nature of the bands in the 1700-1660 cm^{-1} region in the IR spectra of the complexes eliminates the possibility of the coordination of the ligand in enol form (B), (C), (D) or (E) and suggests that the ligand coordinates to the uranyl ion in keto form (A) in the complexes. There are conflicting reports regarding the involvement of $-CO-NH-NH_2$ group in bonding-whether it coordinates through $>C=O$ and $-NH_2$ groups or through secondary nitrogen atoms. Aggarwal *et al.*[18] and Iskander *et al.*[19] have reported a negative shift in amide I and $-NH_2$ bending vibrations indicating coordination through $>C=O$ and $-NH_2$ groups to the metal ions in the complexes of monoacyl- and aroyl-hydrazines. In aroyldihydrazine complexes with 3*d* metal ions, Ahmad *et al.*[8] reported positive shift in amide I and $-NH_2$ bending vibrations indicating coordination through secondary nitrogen atoms. In the MH complexes presently studied, a positive shift and an unusual increase in the intensity and broadness of the bands at 1665 and 1640 cm^{-1} parallel the observations of Ahmad *et al.*[8]. We, therefore, conclude that the secondary nitrogen atoms are involved in the bonding. The intramolecular hydrogen bonding is weakened in the complexes as compared to that in the uncoordinated ligand, but it is retained. Although coordination of both secondary nitrogen atoms to the same uranyl group would give rise to sterically favoured six-membered chelate ring, it is more reasonable to suggest tentatively, coordination of the secondary nitrogen atoms to different uranyl groups in a bridging manner to give rise to polymeric structures. This view is consistent with the insolubility of the complexes in common organic solvents and their high decomposition temperatures.

The thermogravimetric studies of a representative complex, $UO_2(MH)_2(NO_3)_2$ were carried out. The complex starts showing significant mass loss from 220°C (about 3% at the temperature intervals of 20°C) to 280°C. The most significant decomposition step occurs in the temperature range 280-300°C, the mass loss being about 23%. The total mass loss in the temperature range 220-300°C corresponds to two nitrato groups and four hydrazinic groups. The complex shows insignificant mass loss from 300 to 320°C, beyond which another decomposition step occurs in which the complex loses mass by ~ 3% at 20°C. temperature intervals until a constant weight is attained at > 500°C. Such a thermogravimetric behaviour of the complex indicates the absence of water molecules in the complex and suggests that both the ligand molecules are coordinated, otherwise the complex could have shown mass loss corresponding to one ligand molecule somewhere near its melting point, if it were present in the complex in uncoordinated or hydrogen bonded form.

The *IR* spectra of *all* the uranyl complexes show medium to strong absorptions at 940-895 cm^{-1} assignable to ν_3 vibrations of the uranyl group, but do not show any absorption band around 860 cm^{-1} due to ν_1 mode. The Raman spectrum of the complex $UO_2(MH)_2(NO_3)_2$ shows a very strong broad band centred at 860 cm^{-1}. The absence of band around 860 cm^{-1} in the IR spectra of the complexes and appearance of a strong broad band in the Raman spectra suggests that the linearity of the UO_2 group is maintained in the complexes. The doubly degenerate OUO bending mode (ν_2) is observed between 260 and 245 cm^{-1} in the low frequency IR spectra of these complexes.

The doubly degenerate IR-active fundamental modes at ~ 1360 cm^{-1} and ~ 720 cm of ionic nitrate are split up into their components (ν_3 to ν_1 and ν_4, and ν_4 to ν_3 and ν_5) in the IR spectra of nitrato complexes (Nos. 1 and 2). Additional bands at 1060, 812 and 1055, 810 cm^{-1}, respectively, in the two complexes are assigned as ν_2 and ν_6 modes of the coordinated nitrato groups. The difference between ν_1 and ν_4 for the nitrato complexes presently studied is 180 and 190 cm^{-1}, respectively indicating unidentate behaviour of the nitrate group[21]. Monodentate nature of coordinated nitrato groups is corroborated by two bands in the 1800-1700 cm^{-1} region separated by 15 and 10 cm^{-1} in the two complexes respectively[20,21]. New bands at 2040s; 805m; 430s, 420ssh, and 2050vs; 815m; 480s, 420s cm^{-1} in the thiocyanato complexes (Nos. 3 and 4) assigned to νCN; νCS; δNCS modes are in good agreement with the presence of terminal N-bonded thiocyanato groups[22]. The strong broad band at ~ 1120-1080 cm^{-1} and the sharp well-defined band at ~ 610 cm^{-1}, due to triply degenerate ν_3 and ν_4 modes respectively in the ionic sulphato group, split into their components at 1255s, 1130s, 1065s; 650s, 600ssh, 580vs, and 1220s, 1120s, 1020sbr; 650s, 600ssh, 580vs cm^{-1} in sulphato complexes (Nos 5 and 6). These bands mask the weak ligand bands occurring in these regions. Moreover, the ν_1 band (IR-forbidden in the uncoordinated sulphate) appears at 1000 cm^{-1}. Besides ν_1, ν_3, and ν_4 modes the ν_2 mode is observed as a medium intensity band in the 480-460 cm^{-1} region. The positions of the absorption bands of sulphato group suggest the presence of bidentate chelating sulphato group in these complexes[23]. Acetato complexes (Nos. 7 and 8) show absorption bands at 1610, 1410 and 1605, 1395 cm^{-1} respectively. If coordination occurs symmetrically, both COO stretching bands (the antisymmetric ν_{as} and the symmetric ν_s) are expected to be shifted to lower frequencies as compared to their positions in the free ion (1582 and 1425 cm^{-1}). If the acetato group acts as a monodentate ligand, the two bands are expected to be shifted to higher and lower frequencies respectively. In the present complexes (Nos. 7 and 8) and ν_{as} lies at 1610 and 1605 cm^{-1} and ν_s lies at 1410 and 1395 cm^{-1}, respectively, indicating the presence of monodentate acetato groups in these complexes[24,25]. In the IR spectra of oxalato complexes (Nos. 11 and 12), the antisymmetric and symmetric C = O vibrations are split up into their components (ν_{as}C = O 1690vs, 1660ssh; 1650vs, ν_sCO + δOCO 1465s, 1350s, 1305s for complex No. 11 and ν_{as}C = O 1680 vs, 1650vs; ν_sCO + δOCO, 1480vs, 1470vs, 1410s, 1300vs for complex No. 12) and mask the ligand bands in these regions. IR frequencies associated with oxalato group in these complexes are almost in the same frequency range in which the chelated oxalato groups have been established to absorb[25].

Keeping in view the bidentate bridging nature of MH ligand, terminal monodentate behaviour of nitrato, acetato, chloro and thiocyanato groups and bidentate chelating behaviour of sulphato and oxalato groups and the presence of two coordinated water molecules in the $UO_2(MH)X_2nH_2O$ ($X = NO_3^-$, CH_3COO^-, SCN^-, Cl^-, $1/2SO_4^{2-}$, $1/2C_2O_4^{2-}$, n = 0, 2-4) type complexes, all the complexes are considered to involve eight coordinated uranium with six ligand atoms arranged around the linear uranyl group in an equatorial plane.

References

1 Sorkin E, Roth W & Erlenmeyer H, *Helv chim Acta*, **35** (1952) 1736; Gogorishvilli P V, Karkarashvilli M V & Kalandrishvilli D Z, *Z anorg Khim*, **14** (1969) 1516.

2 Alcock J F, Baker R J & Diamantis A A, *Aust J Chem*; **25** (1972) 239

3 Iskander M F, Zayan S E, Khalifa M A & El-Sayed L, *J inorg nucl Chem*, **36** (1974) 551.

4 Johnson D K, Murphy T B, Rose N J, Godwin W H & Pickart L, *Inorg chim Acta*, **67** (1982) 159.

5 Meltzer R T, Lewis A D, McMillan F H, Genzer J D, Leonard F L & King J A, *J Am pharm Assoc*, **42** (1982) 594.

6 Superiewski J, Bany J & Knipinska J, *Bull Acad polon Sci*, Class II, **3** (1955) 55; *Chem Abstr*, **50** (1956) 7801b.

7 Georgescu I I, Coomarton D, Teodorescu G, Hlevca M & Zaharescu M, *Revue Roum Chim*, **18** (1973) 1159.

8 Dutta Ahmad A, Mandal P K & Roy Chauuhury N, *J inorg nucl Chem*, **28** (1966) 2951; *J inorg nucl Chem*, **31** (1969) 2545.

9 Wells A F, *Structural inorganic chemistry*, 3rd Ed (Oxford University Press, London) 1966; Zachariason W H, *Acta Crystallogr*, **7**)1954) 795.

10 Cattalini C, Croatto U, Degetto S & Tandello E, *Inorg chim Acta*, **5** (1971) 19.

11 Ahuja I S & Singh Rajindar, *Inorg nucl Chem Lett*, **9** (1973) 283; Ahuja I S & Singh R, *Transition Met Chem*, **2** (1977) 32; *J inorg nucl Chem*, **35** (1973) 2075; *Inorg nucl Chem Lett*, **9** (1973) 545; *Spectrochim Acta*, **29A** (1973) 1879.

12 Bulow C & Weidlisch R, *Chem Ber*, **39** (1906) 3373.

13 Vogel A I, *A text book of quantitative inorganic analysis*, (ELBS and Longmans, London), 1973, pp. 539, (a) pp. 583 (b) pp. 380.

14 Geary W J, *Coord Chem Rev*, **8** (1971) 71.

15 Livingstone S E & Oluka J E, *Transition Met Chem*, **3** (1978) 261.

16 Saha N & Bhattacharya D, *Indian J Chem*, **21A** (1982) 574.

17 Mashima M, *Bull chem Soc Japan*, **35** (1962) 2020.

18 Aggarwal R C & Prasad B, *J inorg nucl Chem*, **33** (1971) 3984; Aggarwal R C & Bahadur A, *Indian J Chem*, **7** (1969) 1038.

19 Iskander M F, Zayan S E, Khalifa M A & El-Sayed L, *J inorg nucl Chem*, **36** (1974) 551.

20 Curtis N F & Curtis Y M, *Inorg Chem*, **4** (1965) 804.

21 Yamada S & Takeuchi A, *Bull chem Soc Japan*, **42** (1969) 2549.

22 Burmister J L, *Coord Chem Rev*, **1** (1966) 205; **3** (1968) 225; Bailey R A, Kojak S L, Michelson T W & Miles W N, *Coord Chem Rev*, **6** (1970) 407.

23 Zachariason W H & Plettinger H A, *Acta Crystallogr*, **12** (1959) 526; Van Cleave A B, Caldow G L & Edger R L, *Can J Chem*, **38** (1970) 772.

24 Curtis N F, *J chem Soc*, (1963) 4109; (1964) 2644; (1968) 1584; Scott K L, Weigharett & Sykes A G, *Inorg Chem*, **12** (1973) 655.

25 Nakamoto K, *Infrared spectra of inorganic and coordination compounds*, (Wiley, New York) 1970.

Indian Journal of Chemistry
Vol. 27A, April 1988, pp. 332-335

Stabilities of Proton, Binary & Ternary Lanthanide Complexes of 2-Methyl-8-hydroxyquinoline-5-sulphonic Acid in Various Aquo-Organic Solvents

ANUP KUMAR BANDOPADHYAY & A K CHAUDHURY*
Chemistry Department, University of Burdwan, Burdwan 713 104

Received 25 *January* 1987, *revised* 25 *June* 1987, *accepted* 16 *July* 1987

Proton-ligand formation constants of 2-methyl-8-hydroxyquinoline 5-sulphonic acid have been measured in water and other aquo-organic media containing dioxane, isopropanol, ethanol and methanol as cosolvents. The trends of ${}^{P}K_n^H$ are interpreted in terms of the dielectric constants of the media and proton-solvent interactions. Stabilities of binary complexes of the ligand with La, Pr, Nd, Sm, Gd, Tb, Dy have also been calculated in different media and the trends are discussed in terms of dielectric constants of the media and the ionic radii of the metal ions. Stepwise constants for ternary complex formation with NTA or EDTA as primary ligands have also been computed. The ternary complexes with NTA are more stable than those with EDTA. Thermodynamic parameters of ternary complex formation have also been evaluated.

Although a good amount of work has been done on various quinoline derivatives, survey of literature reveals that systematic investigation on the complex equilibria involving 2-methyl-8-hydroxyquinoline 5-sulphonic acid as a ligand has not been done. We report herein proton-ligand stability constants of the ligand and stability constants of binary complexes with lanthanides and of ternary complexes of lanthanides with nitrilotriacetic acid (NTA) and EDTA as primary ligands and this ligand as secondary ligand in aquo-organic solvents containing dioxane, isopropanol, ethanol or methanol as the organic component. Thermodynamic parameters of the ternary step are also measured.

Materials and Methods

All the reagents used were of AR/GR grade. The ligand was prepared by sulphonation of 2-methyl-8-hydroxyquinoline, recrystallised from hot water and purity checked by elemental analyses. Lanthanide perchlorates were prepared from lanthanide carbonates and estimated gravimetrically as oxalates and volumetrically with EDTA[1]. All solvents were dehydrated and redistilled and dioxane was further purified[2]. Experiments were carried out at 30±0.1°C but for a few ternary systems the measurements were also done at 20±0.1°C and 40±0.1°C. Ionic strength was maintained at 0.1 *M* by adding $NaClO_4$. Experimental procedure and compositions of solutions employed for titration were described in a previous communication[3].

Calculation

As the ${}^{P}K^{H}$ values are widely different they were calculated at two distinct steps with the help of the expression for monoprotic ligands[3]. The metal-ligand (secondary) formation constants β_1 and β_2 of the binary complexes were computed from linear plots[3] of $\bar{n}/(\bar{n}-1)[L](=Y)$ versus $(2-\bar{n})[L]/(\bar{n}-1)(=X)$ in the range $0.3<\bar{n}<1.8$. The mean values and the standard deviations for β_1 and β_2 were calculated by a similar computation method using linear plots of $\bar{n}+(\bar{n}-1)\beta_1[L]/(\bar{n}-2)[L]^2(=Y)$ versus $(3-\bar{n})[L]/(\bar{n}-2)(=X)$ in the region $1.6<\bar{n}<2.8$.

For the ternary complexes $\log K_{MAL}^{MA}$ step constants were calculated as described earlier[3]. The dielectric constants (ε) of aquo-organic solvents were either obtained from literature or calculated from the data given by Hall *et al.*[4] and Akerloff[5].

Results and Discussion

Proton ligand formation constants

Two protonation constants, ${}^{P}K_1^H$ (phenolic OH) and ${}^{P}K_2^H$ (NH^+) were measured. Mol fraction of the cosolvents was kept at 0.24 where the structuredness of water crosses the maximum value for all the media[6,7]. The plots of $\log {}^{P}K_1^H$ and $\log {}^{P}K_2^H$ versus $1/\varepsilon$ (curves not shown) show gradual rise of the former and slight decrease of the latter with increase of $1/\varepsilon$ (Table 1). The same thing happens in water-dioxane and water methanol media where compositions were continuously changed from

30% to 70% (v/v) of the cosolvent (Table 1). The magnitude of increase for $^{P}K_1^H$ falls when concentration of the cosolvent exceeds 50-60% (v/v). This happens because structuredness of water breaks down and water becomes more basic which tends to lower the value of log $^{P}K_1^H$. Such a behaviour was also observed by Kole and Chaudhary[8] for acetylacetone. Gradual and small decrease in $^{P}K_2^H$ is possibly due to less polar nature of N−H bond in NH$^+$ which is affected only to a minor extent by the composition of the solvent mixture.

Table 1—Proton Ligand Formation Constants* of 2-Methyl-8-Hydroxyquinoline 5-Sulphonic Acid in Various Mixed Aqueous Solvents

Solvent composition	Mol fraction co-solvent	1/ε	log $^{P}K_1^H$	log $^{P}K_2^H$
W	0	0.013	9.15	4.78
30% W − W	0.161	0.0154	9.85	4.73
40% M − W	0.232	0.0165	9.98	4.71
50% M − W	0.309	0.0178	10.12	4.69
60% M − W	0.401	0.0195	10.28	4.65
70% M − W	0.501	0.0216	10.45	4.62
30% D − W	0.083	0.0195	10.37	4.67
40% D − W	0.123	0.0234	10.67	4.61
50% D − W	0.174	0.0293	10.90	4.48
60% D − W	0.238	0.0388	11.16	4.30
70% D − W	0.329	0.0561	11.38	4.10
42.5% M − W	0.240	0.01676	10.05	4.70
51.8% E − W	0.240	0.0198	10.40	4.64
58.6% I − W	0.240	0.0254	10.74	4.56
61.2% D − W	0.240	0.0399	11.19	4.32

*Standard deviation of $^{P}K_1^H$ & $^{P}K_2^H$ values are generally ±0.005 and ±0.02 in log units respectively; M, methanol; D, dioxane; W, water; E, ethanol; and I, isopropanol

Stabilities of binary complexes

The values of log β_1, log β_2 log β_3 in different media with constant mol fraction (0.24) of the cosolvent shows the following decreasing order in the values of these constants for a particular metal ion in different media (Table 2): Dioxane-water > isopropanol-water > ethanol-water > methanol-water > water. This is expected as ε increases in the same order. In general, it is found that log β_1, log β_2 or log β_3 values in a particular solvent increase in the order: La > Pr > Nd > Gd > Tb > Dy. This is also the order of decreasing ionic radii. A plot of log β_1 versus $1/r$ (curve not shown) is linear but shows a break at Gd(III). A plot of log β_2 versus 1/ε has features similar to those of $^{P}K_1^H$ versus 1/ε curves. So parallelism exists between metal-ligand and proton-ligand interaction. Although the dielectric constant of the medium has predominant effect, metal ion solvation also has some influence on the stability values. Above mentioned parallelism indicates that metal ions also undergo, like proton, greater solvation by water when structuredness of water breaks down. Solvation by cosolvents at higher concentrations also cannot be ruled out. All these effects tend to lower the β_n values slightly. Hence the magnitude of increase in β_n with increase in 1/ε becomes less with the increase in concentration of the cosolvent.

Stabilities of ternary complexes

Formation of ternary complexes is proved as usual by non-super-imposable nature of the com-

Table 2—Formation Constants* of Binary Complexes of Lanthanides in Different Mixed Aqueous Solvents

Solvent composition	Mol fraction of cosolvent	1/ε	Formation constant	La	Pr	Nd	Sm	Gd	Tb	Dy
Water	0	0.013	log β_1	4.64	4.84	4.95	5.15	5.39	5.46	5.57
			log β_2	8.82	9.33	9.61	9.92	10.34	10.52	10.70
			log β_3	12.05	12 75	13.11	13.61	14.25	14.50	14.69
42.5% M − W	0.24	0.01676	log β_1	5.92	6.03	6.14	6.29	6.36	6.41	6.48
			log β_2	10.68	11.11	11 41	11.76	12.17	12.33	12.48
			log β_3	14.51	15.33	15.70	16.28	16.68	16.93	17.16
51.8% E − W	0.24	0.0198	log β_1	6.25	6.45	6.53	6.64	6.77	6.83	6.91
			log β_2	11.37	11.73	12.09	12.31	12.76	12.91	13.16
			log β_3	15.02	15.70	16.14	16.75	17 34	17.70	18.01
58.6% I − W	0.24	0 0254	log β_1	6.67	6.80	6 88	7.02	7.15	7.24	7.40
			log β_2	12.05	12.50	12.74	13.09	13.41	13.65	13.79
			log β_3	16.24	17.25	17.45	18.01	18.62	18.91	19.46
61.2% D − W	0.24	0.03994	log β_1	7.42	7.58	7.67	7.82	7.97	8.04	8.13
			log β_2	13.41	13.84	14.15	14.64	15.01	15.20	15.39
			log β_3	19.07	19 74	20.94	21.35	21.64	21.96	

*Standard deviation in log β are generally ±0.004 M, E, I, D and W refer to methanol, ethanol, isopropanol, dioxane and water respectively.

posite curve over the ternary complex curves. Here again ternary step constants (Table 3) are in the order: La < Gd < Dy and log K^{MA}_{MAL} < log $K^{ML_2}_{ML_3}$ < log K^{ML}_{ML2} < log K^{M}_{ML} (where A is NTA or EDTA). This is because there is ionic interaction leading to charge neutralisation in ML, ML_2 and ML_3 whereas when MAL is formed the ligand L^- approaches a neutral [M.NTA] or charged [M.EDTA]$^-$ moiety.

In [M.EDTA.L] the metal has to expand its coordination sphere. The sequence log $K^{M.NTA}_{M.NTA.L}$ > log $K^{M.EDTA}_{M.EDTA.L}$ was also observed with all the metals. Similar reasons as above can be advanced to explain this. Moreover EDTA is bulkier than NTA so it offers greater steric hindrance.

Thermodynamic parameters

These were calculated by usual methods[3], ΔG, ΔH and ΔS are found to be negative (Table 4). The ΔH values increase in the order La < Gd < Dy for both NTA and EDTA complexes indicating increasing strength of bonding with the increase of ionic potential of the ion. The ΔH values are more negative for [M.EDTA.L] than those for [M.NTA.L]. This is surprising since a greater steric hindrance is expected with [M.EDTA]$^-$ moiety and also a repulsive effect towards the approaching L^-.

Table 3—Stepwise Formation Constants* of Ternary Complexes of Some Lanthanides in 50% (v/v) Dioxane Water Medium

Temp. (°C)	log *K*			log *K*		
	La	Gd	Dy	La	Gd	Dy
	EDTA complex			NTA complex		
20	3.36	3.55	3.59	3.62	3.81	3.88
30	3.23	3.38	3.42	3.48	3.66	3.71
40	3.08	3.22	3.24	3.37	3.51	3.56

*Standard deviations in log are generally ± 0.004

However the methyl group at 2-position of the ligand plays an important role. For a similar ligand 7-iodo-8-hydroxyquinoline 5-sulfonic acid[9] the stepwise negative enthalpies for the binary complexes increase in the sequence $\Delta H_1 < \Delta H_2 < \Delta H_3$ (exothermic) and values increase from −5.61 kJmol^{-1} for ΔH_1 to −17.74 kJmol^{-1} for ΔH_3. ΔH values for the ternary complexes are more negative for both the EDTA and NTA complexes. So on consideration of enthalpy change it appears that in spite of the steric hindrance due to the primary ligand, bond formation is stronger in the ternary complex formation. This is supported by X-ray structure determination of [La-EDTA] complexes by Hoard *et al.*[10] who found that the central metal ion La although hexacoordinated to EDTA is markedly off centre. This shows that chelation in the ternary step may take place without much of the anticipated hindrance due to the presence of the primary ligand. The higher negative values of ΔH for ternary complexes compared to those for the binary complexes may be also due to less competition faced by ligand at this step from water molecules. The step entropies of binary complex formation in the above system follows the sequence $\Delta S_1 > \Delta S_2 > \Delta S_3$ the range being 79.91 to 15.06 JK^{-1} mol^{-1} (ref. 9). ΔS in the ternary complex formation is negative and comparatively large. This is responsible for lower values of the stability constants of the ternary complexes. It appears that translational entropy gained by ion desolvation at the initial steps of the secondary system are no more available after the primary complexes are formed. On the other hand negatively charged mixed ligand complexes start getting solvated and hence decrease in entropy.

The separation of ΔG and ΔH into electrostatic and cratic component (Table 4)[11,12], shows that the

Table 4—Thermodynamic Parameters* for the Stepwise Formation of Ternary Complexes and the Electrostatic and Cratic Components

[Values of ΔG and ΔH in kJmol^{-1} and ΔS in JK^{-1} mol^{-1}]

	$-\Delta S$	$-\Delta H$	$-\Delta H_e$	$-\Delta H_c$	$-\Delta G$	$-\Delta G_e$	$-\Delta G_c$
La−EDTA	20.04	24.81	1.72	23.10	18.74	2.34	16.40
Gd−EDTA	27.45	27.82	0.75	27.11	19.49	1.00	18.49
Dy−EDTA	30.88	29.08	0.29	28.79	19.71	0.42	19.29
La−NTA	6.49	21.97	3.43	18.54	20.0	4.69	15.31
Gd−NTA	16.40	26.02	2.13	23.89	21.05	2.97	18.07
Dy−NTA	20.42	27.61	1.63	25.98	21.42	2.26	19.16

*Precision of ΔH values, ± 0.84 kJ mol^{-1} and ΔS values, ± 1.05 JK^{-1} mol^{-1}

cratic terms tend to be more negative. So it may be inferred that the covalent nature predominates in the bonding in the ternary step.

References

1 Kolthoff I M, Elving P J & Sandall E B, *Treatise in analytical chemistry*, Part II (Interscience, New York), 1967, 27 & 59.

2 Vogel A I, *A text book of practical organic chemistry* (Longmans) 1961, 117.

3 Bandopadhyay A K & Chaudhuri A K, *Indian J Chem*, **26A** (1987) 853.

4 Frank I, Critchfield J A, Gibson I R & Hall J H, *J Am chem Soc*, **75** (1953) 1991.

5 Akerloff G, *J Am chem Soc*, **54** (1932) 4130

6 Franks F & Ives D J G, *Quart Rev*, **20** (1966) 1.

7 Frank F (Ed.), *Physicochemical processes in mixed aqueous solvents* (Heimann, London) 1967, 60 & 124.

8 Kole N & Chaudhury A K, *J inorg nucl Chem*, **41** (1981) 2471.

9 Kane Y D & Joshi D M, *Curr Sci*, **43** (1974) 332.

10 Hoard J L, Lee B & Lind M D, *J Am chem Soc*, **87** (1965) 1611.

11 Degischer G & Nancollas G H, *J chem Soc (A)*, (1970) 1125.

12 Akerloff G & Short O A, *J Am chem Soc*, **58** (1936) 1241.

Indian Journal of Chemistry
Vol. 27A, April 1988, pp. 336-337

Notes

Application of Refractive Index Mixing Rules in the Analysis of Binary Liquid Mixtures

J D PANDEY, A K SHUKLA, R K SHUKLA & R D RAI*

Department of Chemistry, University of Allahabad,
Allahabad 211 002

Received 6 *January* 1987; *revised* 21 *May* 1987; *rerevised and accepted* 28 *July* 1987

A comparative study of seven mixing rules of refraction has been carried out to test their validity for binary liquid mixtures. All the mixing rules perform well within the limit of experimental error but the performance of Lorentz-Lorenz (L-L) and Gladstone-Dale (G-D) relation is comparatively better than those of others.

The most widely used theoretical rules for predicting refractivity of binary liquid mixtures are due to Lorentz-Lorenz (L-L), Wiener (W), Eykman[1] (EK) and Oster[2] (OS). The Gladstone-Dale (G-D), Argo-Biot (A-B) and Heller's[3] (H) relations are found to follow either Lorentz-Lorenz equation or Wiener's equation for dilute solutions, especially when the refractive indices of both the liquids are nearly the same. Most of the mixing rules do not account for the changes in volume and refractivity on mixing. This problem was attacked recently by Aminabhavi *et al.*[4,5] who pointed out the usefulness of mixing rules in treating the binary refractive index and density data[6].

A similar attempt is made here for 14 binary liquid mixtures whose refractive index data are available in the literature. The following mixture rules were used to calculate the refractive indices of the binary mixtures:

Lorentz-Lorenz (*L-L*) *relation*

$$\left[\frac{n_{12}^2-1}{n_{12}^2+2}\right]\frac{1}{\rho_{12}}=\left[\frac{n_1^2-1}{n_1^2+2}\right]\frac{W_1}{\rho_1}+\left[\frac{n_2^2-1}{n_2^2+2}\right]\frac{W_2}{\rho_2} \qquad \ldots (1)$$

Gladstone-Dale (*G-D*) *relation*

$$\left[\frac{n_{12}-1}{\rho_{12}}\right]=\left[\frac{n_1-1}{\rho_1}\right]W_1+\left[\frac{n_2-1}{\rho_2}\right]W_2 \qquad \ldots (2)$$

Wiener's (*W*) *relation*

$$\left[\frac{n_{12}^2-n_1^2}{n_{12}^2+2n_1^2}\right]=\phi_2\left[\frac{n_2^2-n_1^2}{n_2^2+2n_1^2}\right] \qquad \ldots (3)$$

Heller's (*H*) *relation*

$$\left[\frac{n_{12}-n_1}{n_1}\right]=\frac{3}{2}\phi_2\left[\frac{m_1^2-1}{m_1^2+2}\right] \qquad \ldots (4)$$

Argo-Biot (*A-B*) *relation*

$$n_{12}=n_1\phi_1+n_2\phi \qquad \ldots (5)$$

Eykman's (*Ek*) *relation*

$$\left[\frac{n_{12}^2-1}{n_{12}+0.4}\right]\bar{V}_{12}=\left[\frac{n_1^2-1}{n_1+0.4}\right]\bar{V}_1+\left[\frac{n_2^2-1}{n_2+0.4}\right]\bar{V}_2 \qquad \ldots (6)$$

Oster's (*OS*) *relation*

$$\left[\frac{(n_{12}^2-1)(2n_{12}^2+1)}{n_{12}^2}\right]\bar{V}_{12}=\left[\frac{(n_1^2-1)(2n_1^2+1)}{n_1^2}\right]\bar{V}_1+\left[\frac{(n_2^2-1)(2n_2^2+1)}{n_2^2}\right]\bar{V}_2 \qquad \ldots (7)$$

In Eqs (6) and (7), $\bar{V}_1$, $\bar{V}_2$ and $\bar{V}_{12}$ are the molar volumes of the pure components and mixture respectively as shown below,

$$\bar{V}_1=\frac{M_1X_1}{\rho_1},\quad \bar{V}_2=\frac{M_2X_2}{\rho_2},\quad \bar{V}_{12}=\frac{M_1X_1+M_2X_2}{\rho_{12}}$$

In the above relations M_1, M_2 and X_1, X_2 are the molecular weights and mole fractions of the respective components. Other notations used in the above equations have their usual meanings as given earlier[4].

In the present note, using density and refractive index data[6], we have made an attempt to study the validity of mixing rules for predicting refractivity of binary mixtures containing aliphatic, aromatic and alicyclic liquids. Density of the mixture can be obtained from the experimental value of refractivity intercept (R_I) using Eq. (8),

$$\rho_{12}=2R_I-2n_{12} \qquad \ldots (8)$$

where n_{12} is the refractive index of mixture.

We have computed the refractivities of binary mixtures using mixing rules (Eqs 1-7) and compared these with the experimental values to obtain

Table 1—Average Percentage Deviations (APD) for Various Refractivity Mixing Rules at 25°C

	System	10^3(APD)						
		(L-L) Eq.(1)	(G-D) Eq.(2)	Wiener Eq.(3)	Heller Eq.(4)	A−B Eq.(5)	Eykman Eq.(6)	Oster Eq.(7)
1	*n*-Hexadecane + Benzene	9.8	40.4	202.3	198.3	216.9	14.6	24.0
2	*n*-Tetradecane + 2-Bromobutane	34.6	39.5	77.1	77.0	77.2	177.0	165.6
3	*n*-Tetradecane + *n*-Hexane	19.6	15.2	87.1	9.5	82.7	40.2	15.0
4	4-Methylcyclohexanone + *n*-Hexane	19.9	16.0	74.6	89.8	67.7	35.7	13.8
5	*n*-Hexadecane + *n*-Hexane	22.0	15.1	73.8	91.7	81.5	53.2	16.2
6	*n*-Hexadecane + Carbon tetrachloride	11.9	21.3	115.8	94.7	91.5	58.8	67.6
7	4-Methylcyclohexanone + *n*-Tetradecane	10.4	5.3	66.8	73.9	77.7	240.4	127.6
8	4-Methylcyclohexanone + *n*-Hexadecane	9.4	8.5	94.7	94.4	100.4	367.3	285.0
9	*n*-Hexadecane + 2-Bromobutane	17.6	26.0	59.4	83.1	83.1	432.2	391.5
10	Benzene + *n*-Hexane	40.8	49.1	121.0	96.8	139.7	19.4	97.5
11	Carbon Tetrachloride + *n*-Hexane	51.4	10.7	26.2	20.5	44.6	1418.6	1222.1
12	*n*-Hexadecane + *n*-Tetradecane	8.3	4.1	4.6	4.6	4.5	4.7	5.4
13	2-Bromobutane + *n*-Hexane	37.4	33.2	39.9	32.4	45.2	286.4	229.1
14	Carbon tetrachloride + Benzene	91.6	68.7	50.9	55.2	48.4	1054.0	1051.0

the average percentage deviation which is recorded in Table 1. A look at Table 1 shows that all the relations give good agreement with the experimental values, specially the Lorentz-Lorenz (L-L) and Gladstone-Dale (G-D) relations. The exception is in the case of system no. 12. Since the Lorentz-Lorenz (L-L) relation is based on a sounder theoretical basis, its performance is found to be better. For the systems, 5, 7, 8, 11 and 12, Gladstone-Dale (G-D) relation appears to give quite satisfactory results. Wiener's (W) relation has been found to predict satisfactory agreement generally. The systems 3 & 13 exhibit best performance for Heller's (H) relation, 4 for Oster's (OS) relation, 10 for Eykman (EK) and 14 for Arago-Biot (A-B) relation as evidenced by the small deviations. Ultimately, it was found that (L-L), (G-D) and Wiener's relation provide very good results followed by Heller, Arago-Biot, Oster and Eykman relations. Standard average percentage deviation from minimum to maximum ranges from 4.1×10^{-3} to 1.418.The deviations between the theoretical and observed values of refractive indices for all the systems under present investigation may be reduced if the concept of excess volume (V^E) is taken into consideration in various mixing rules, as suggested by Aminabhavi *et al.*[4,5]

The authors are thankful to Prof. T M Aminabhavi, Karnatak University, Dharwad for valuable suggestions from time to time.

References

1 Eykman J F, *Rec trav chim Pays Bas Belg*, **14** (1895) 185.
2 Oster G, *Chem Rev*, **43** (1948) 319.
3 Heller W J, *J phys Chem*, **69** (1965) 1123.
4 Aminabhavi T M & Munk P, *Macromolecules*, **12** (1979) 1186.
5 Aminabhavi T M, *J chem Engng Data*, **29** (1984) 54.
6 Henc E L & Brewer J G, *J chem Engng Data*, **16** (1971) 313.

Indian Journal of Chemistry
Vol. 27A, April 1988, pp 338-340

Volumetric & Solvation Behaviour of Amino Acids in Some Aqueous Binaries: Part II – Behaviour of – DL – Alanine in Aqueous Solutions of Strong Electrolytes in the Temperature Range 25-45°C

RAJANI K MOHANTY & INDRA N BASUMALLICK*
Department of Chemistry, Visva-Bharati, Santiniketan
and
UTSABANANDA CHAKRABORTY
TDB College, Raniganj

Received 3 *October* 1986; *revised* 12 *June* 1987, *rerevised and accepted* 7 *September* 1987

Apparent molal volumes, apparent molal adiabatic compressibilities and hydration numbers of DL-alanine have been determined at 35 and 45°C in water and in aqueous salt solutions, M^+X^- ($M^+ = Li^+$, K^+, Cs^+, and $X^- = Cl^-$, Br^-, I^-). The expansibilities at 35°C have also been calculated. The results have been combined with those published earlier (obtained at 25°C) and explained in terms of the Bockris and Saluja's model of hydration of the species and the interactions between ions and zwitterions in solution.

In continuation of our earlier work on the solvation behaviour of amino acids in salt solutions[1], we report here the temperature dependence of the limiting values of apparent molal volumes (ϕ_v°), apparent molal adiabatic compressibilities (ϕ_k°) and hydration numbers (n_h) of DL-alanine in 0.4 and 0.8 molal solutions of LiCl, KCl, CsCl, KBr and KI at 35° and 45°C. These results have been combined with that at 25°C from our earlier work[1]. It is expected that such a study will provide additional information on amino acid-electrolyte and electrolyte-water interactions[2-7].

The details of purification and drying of the amino acid and salts are the same as described earlier[1]. The solutions were prepared by weight using deionised doubly distilled water. All measurements and calculations were carried out as done before[1].

The limiting apparent molal volumes (ϕ_v°) and limiting apparent molal diabatic compressibilities (ϕ_k°) of DL-alanine in these salt solutions at 25, 35 and 45°C have been presented in Table 1. The apparent molal expansibilities (E°) at 35°C have also been shown in Table 1. The volumes of transfer ($\phi_{v,tr}^\circ$), the compressibilities of transfer ($\phi_{k,tr}^\circ$) and the hydration number for DL-alanine at 25, 35 and 45°C are given in Table 2.

Volumes and expansibilities

The partial molal volume of an amino acid in water is given by[8],

$$\phi_v^\circ = \phi_v^\circ(int) + \phi_v^\circ(elect)$$

where ϕ_v°(int) is the intrinsic partial molal volume and ϕ_v°(elect) is that due to electrostriction. The

Table 1 – Limiting Apparent Molal Volumes (ϕ_v°), Compressibilities (ϕ_k°) and Limiting Apparent Molal Expansibilities ($E^\circ = d\phi_v^\circ/dT$) of DL-Alanine-Water and in Alkali Halide Solutions at Different Temperatures

Solvent	Salt conc. (mol kg^{-1})	25°C[a]	35°C	45°C	25°C[a]	35°C	45°C	($E^\circ \times 10^2$)[d] (ml mol^{-1} deg^{-1})
Water	0	60.5(0.7)[b]	60.9(0.5)	61.3(0.5)	−23.9(3.5)	−21.0(3.2)	−18.0(2.2)	4.0
Aq. LiCl	0.4	61.1(0.5)	61.5(0.5)	61.9(0.5)	−19.3(1.6)	−17.3(1.8)	−14.4(1.5)	4.0
	0.8	61.6(0.3)	62.0(0.4)	62.4(0.3)	−16.2(1.4)	−13.0(0.8)	−11.9(0,9)	4.0
Aq. KCl	0.4	61.3(0.3)	61.7(0.4)	62.1(0.2)	−18.9(1.3)	−15.8(1.3)	−13.6(1.1)	4.0
	0.8	61.9(0.3)	62.1(0.3)	62.6(0.2)	−16.0(1.4)	−12.9(1.5)	−11.1(0.9)	3.5
Aq. CsCl	0.4	61.2(0.6)	61.4(0.4)	61.9(0.4)	−19.3(2.0)	−16.3(2.0)	−14.0(1.5)	3.5
	0.8	61.6(0.5)	61.9(0.5)	62.4(0.3)	−16.6(1.8)	−13.9(2.4)	−11.6(1.8)	4.0
Aq. KBr	0.4	61.1(0.5)	61.5(0.5)	61.9(0.5)	−19.3(1.8)	−16.3(1.4)	−14.0(1.0)	4.0
	0.8	61.7(0.5)	61.9(0.5)	62.4(0.4)	−16.2(1.5)	−13.4(0.9)	−11.2(0.8)	3.5
Aq. KI	0.4	61.1(0.5)	61.4(0.7)	61.8(0.5)	−19.5(2.1)	−16.3(1.2)	−14.5(1.1)	3.5
	0.8	61.6(0.5)	61.8(0.6)	62.2(0.6)	−16.5(1.4)	−13.4(1.0)	−11.1(0.5)	3.0

Uncertainties in ϕ_v° and ϕ_k° are ± 0.1 ml mol^{-1} and ± 1 × 10^{-4} ml mol^{-1} bar^{-1} respectively.

[a] Data at 25°C taken from ref. 1.

[b] Slope values are given in the parentheses.

[c] The concentration of DL-alanine ranges from 0.09 to 0.97 molal.

[d] ϕ_v° values at different temperatures are fitted to the equation, $\phi_v^\circ = a + bT + CT^2$ and corresponding E° values are obtained using the equation $E^\circ = b + 2\,CT$.

Table 2 – Limiting Apparent Molal Volumes of Transfer ($\phi^{\circ}_{v,tr}$), Compressibilities of Transfer ($\phi^{\circ}_{k,tr}$) of DL-Alanine from Water to Alkali Halide Solutions and Hydration Numbers (n_h) in These Media at Different Temperatures

Solvent	Salt conc. (mol kg^{-1})	$\phi^{\circ}_{v,tr}$ (ml mol^{-1})			$\phi^{\circ}_{k,tr} \times 10^4$ (ml mol^{-1} bar^{-1})			Hydration number (n_h)		
		25°C[a]	35°C	45°C	25°C[a]	35°C	45°C	25°C[a]	35°C	45°C
Water	0	0	0	0	0	0	0	3.2	2.7	2.3
Aq. LiCl	0.4	0.6	0.6	0.6	4.6	3.7	3.6	2.8	2.3	1.9
	0.8	1.1	1.1	1.1	7.7	8.0	6.1	2.5	1.8	1.6
Aq. KCl	0.4	0.8	0.8	0.8	5.0	5.2	4.4	2.7	2.1	1.8
	0.8	1.4	1.2	1.3	7.9	8.1	6.9	2.5	1.8	1.5
Aq. CsCl	0.4	0.7	0.5	0.6	4.6	4.7	4.0	2.8	2.2	1.9
	0.8	1.1	1.0	1.1	7.3	7.1	6.4	2.6	1.9	1.6
Aq. KBr	0.4	0.6	0.6	0.6	4.6	4.7	4.0	2.8	2.2	1.9
	0.8	1.2	1.0	1.1	7.7	7.6	6.8	2.5	1.8	1.5
Aq. KI	0.4	0.6	0.5	0.5	4.4	4.7	3.5	2.8	2.1	1.9
	0.8	1.1	0.9	0.9	7.4	7.6	6.9	2.5	1.8	1.5

[a] Data taken from ref. 1.

temperature dependence of partial molal volume is given by,

$$\frac{d\phi^{\circ}_{v}}{dT} = \frac{d\phi^{\circ}_{v}(\text{int})}{dT} + \frac{d\phi^{\circ}_{v}(\text{elect})}{dT}$$

$$\text{or, } E^{\circ} = E^{\circ}(\text{int}) + E^{\circ}(\text{elect})$$

The temperature dependence of partial molal volumes of small monovalent ions has been discussed elaborately by Millero[2]. The positive values of E° have been explained in terms of the positive contribution from E°(int), as E°(elect) values remain unaltered upto 50°C. In the present case, ϕ°_{v} of DL-alanine has been found to increase slowly with temperature imparting a small positive E° value to it. This behaviour is typical of all nonelectrolytes having a hydrophilic part which prevails over the hydrocarbon part[6].

In salt solutions, the extra factor contributing to volume changes is the zwitterion-ion interaction. Because of such interactions, as emphasized earlier[1], the electrostriction of the solvent molecules by the zwitterions decreases, resulting in a positive volume change (Table 1).

The temperature dependence of ϕ°_{v} of DL-alanine, (E°), in salt solutions is very similar to that in water (Table 1). However, in some cases the salt solution values appear to be slightly less, which may result from the small change in zwitterion-ion interactions due to increased thermal agitation at higher temperatures. Hence, $\phi^{\circ}_{v,tr}$ will remain almost constant for a given salt concentration as indicated in Table 2. As in most of the cases the temperature dependence of ϕ°_{v} i.e. E° values do not alter either with the nature of the salt or its concentration, one may conclude that the zwitterion-ion interactions may not really change much in the temperature range studied here.

Compressibilities and hydration numbers

Partial molal adiabatic compressibilities (ϕ°_{k}) of DL-alanine in water and in salt solutions were found to decrease with decreasing temperature. Similar variation of ϕ°_{k} with temperature has also been observed in other systems too by several workers[9,10]. However, $\phi^{\circ}_{k,tr}$ values (vide Table 2) of DL-alanine from water to aqueous salt solutions go on decreasing with increasing temperature. This means that the relative compressibility decreases with temperature indicating that the hydration sheaths of the amino acid and the ions retained at higher temperature become less and less compressible. This suggests that it is the non-solvational coordinated water (NSCW) molecules or the so-called outer hydration sphere[11] that is affected or dehydrated at higher temperature; and the hydration sheath that remains behind is the solvational coordinated water (SCW) molecules or the inner hydration sphere.

The hydration number of DL-alanine in salt solutions is less than that in water because of the scarcity of water molecules[12] as well as interaction of the ions of the salt with the amino acid. Again, the observed change in hydration number of DL-alanine in water and in salt solutions with temperature is due to the loss of NSCW as has been explained earlier.

One of the authors (UC) is thankful to the UGC, New Delhi for the award of a teacher fellowship and to the authorities of TDB College, Raniganj, for grant of study leave.

References

1 Basumallick I N, Mohanty R K & Chakraborty U, *Indian J Chem*, **25A** (1986) 1089.

2 Millero F J, *Chem Rev*, **71** (1971) 147.

3 Mohanty R K, Basumallick I N, Das A K & Bhowmik S, *J Indian chem Soc*, **LXII** (1986) 301.

4 Bhowmik S & Mohanty R K, *Indian J Chem*, **25A** (1986) 416.

5 Cabani S, Conti G, Matteoli E & Tine M R, *J chem Soc Faraday Trans I*, 77 (1981) 2377.

6 Cabani S, Conti G, Matteoli E & Tine M R, *J chem Soc Faraday Trans I*, 77 (1981) 2385.

7 Kaulgud M & Rao K S M, *J chem Soc Faraday Trans I*, **75** (1979) 2237.

8 Millero F J, Surdo A L & Shin C, *J phys Chem*, **82** (1978) 784.

9 Cabani S, Conti G & Matteoli E, *J sol Chem*, **8** (1979) 11.

10 Nakajima T, Komatsu T & Nakagawa T, *Bull chem Soc Japan*, **48** (1975) 788.

11 Bockris J O M & Saluja P P S, *J phys Chem*, **76** (1972) 2298.

12 Chattopadhyay A K & Lahiri S C, *Electrochim Acta*, **27** (1982) 269.

Indian Journal of Chemistry
Vol. 27A, April 1988, pp. 341-342

Kinetic Study of Oxidation of Iodide Ion by N-Bromoacetamide by Stopped-flow Technique

SEEMA KOTHARI, VINITA SHARMA &
KALYAN K BANERJI*

Department of Chemistry, University of Jodhpur,
Jodhpur 342 001

Received 20 *May* 1987; *revised and accepted* 17 *August* 1987

The oxidation of iodide ion by N-bromoacetamide (NBA) has been studied in buffered solutions in the *p*H range 4.4 to 5.5 by stopped-flow technique. The reaction is first order each in [iodide] and [NBA]. The H^+ ion dependence has the form $k_{obs} = a + b[H^+]$, but reaction is not subjected to general acid-catalysis. Addition of acetamide retards the reaction. A suitable mechanism has been proposed.

Quantitative determination of N-haloamides, including N-bromoacetamide (NBA), is generally carried out by iodometric method[1]. We have also used this method to follow the kinetics of oxidation of several organic compounds by NBA[2]. Surprisingly the kinetics of oxidation of iodide ion by NBA or other N-haloamides do not seem have been studied so far. One of reasons may be that the reaction is too fast to be studied by conventional techniques. This prompted us to undertake the title investigation.

Stopped-flow module (Hi-Tech, model SFL-PTJ-44, UK) coupled with a SU-4DA spectrophotometer and MCS-1 data acquisition system were used. Potassium iodide (GR, Merck) was used as supplied. Phthalate buffer was used to keep constant *p*H. Ionic strength was maintained at 0.3 mol dm^{-3} with sodium perchlorate. Doubly distilled water was used throughout.

The reaction was studied under pseudo-first order conditions, i.e. [iodide] ≫ [NBA] by monitoring the concentration of liberated iodine at 370 nm. The pseudo-first order rate constants, k_{obs}, along with the standard deviations were calculated using a computer programme specially written for the equipment.

The deviations from the linearity of the first order plots in the later stages of the reactions were eliminated by initially adding an excess of acetamide to the reaction mixture.

The reaction of iodide ion and NBA is quantitative and the overall reaction corresponds to Eq. (1)

$$MeCONHBr + 2\,I^- + H^+ \rightarrow MeCONH_2 + Br^- + I_2 \quad \ldots (1)$$

Table 1—Kinetic Data for Oxidation of Iodide Ion by NBA

[Acetamide] = 0.001 mol dm^{-3}; I = 0.3 mol dm^{-3}; temp. = 293 K

10^4 [I^-] (mol dm^{-3})	10^4 [NBA] (mol dm^{-3})	*p*H	k_{obs} (s^{-1})
10.0	2.0	5.00	8.143 ± 0.11
20.0	2.0	5.00	15.80 ± 0.21
36.0	2.0	5.00	28.24 ± 0.17
50.0	2.0	5.00	40.94 ± 0.36
75.0	2.0	5.00	60.87 ± 0.73
100.0	2.0	5.00	81.22 ± 1.03
50.0	4.0	5.00	41.21 ± 0.27
50.0	8.0	5.00	40.73 ± 0.32
50.0	10.0	5.00	40.21 ± 0.45
50.0	2.0	4.40	92.85 ± 0.66
50.0	2.0	4.60	68.05 ± 0.42
50.0	2.0	4.80	48.75 ± 0.32
50.0	2.0	4.90	45.25 ± 0.27
50.0	2.0	5.10	35.16 ± 0.40
50.0	2.0	5.20	32.85 ± 0.19
50.0	2.0	5.50	26.69 ± 0.10

Table 2—Dependence of Reaction Rate on Buffer Concentration

[I^-] 0.005 mol dm^{-3}; [NBA] 0.0002 mol dm^{-3}; [Acetamide] 0.001 mol dm^{-3}; I = 0.3 mol dm^{-3}; *p*H = 5.10; temp. = 293 K

10^2 [Potassium hydrogen phthalate] (mol dm^{-3})	10^2 [NaOH] (mol dm^{-3})	k_{obs} (s^{-1})
1.5	0.8	35.52 ± 0.40
3.0	1.6	37.72 ± 0.73
6.0	3.2	33.32 ± 0.17
12.0	6.4	33.93 ± 0.32
15.0	8.0	34.14 ± 0.56

The reaction was found to be first order each in [iodide] and [NBA]. Further, k_{obs} values were independent of initial [NBA]. The rate increased with decrease in *p*H indicating that the reaction was catalysed by H^+ ions (Table 1).

To ascertain the occurrence of general acid catalysis, the rate of oxidation was obtained at different buffer concentrations and constant *p*H and ionic strength. The rate was independent of [buffer] (Table 2). The rate of reaction was retarded by the addition of acetamide. For example under the conditions: [I^-] = 0.005 mol dm^{-3}; [NBA]: 0.0002 mol dm^{-3}, *p*H = 5.10; I = 0.3 mol dm^{-3}; and temp. = 293 K, the values of k_{obs} (s^{-1}) were 96.63 ± 0.72, 74.35 ± 0.53, 56.83 ± 0.63, 47.62 ± 0.57, 40.24 ± 0.31 and 35.52 ± 0.40 in the presence of 0.0, 2.0, 4.0, 6.0, 8.0 and 10.0 × 10^{-4}

mol dm^{-3} acetamide, respectively.

The retarding effect of the added acetamide suggests a pre-equilibrium in which acetamide is one of the products.

$$\mathrm{MeCONHBr} + \mathrm{H_2O} \overset{K_h}{\rightleftharpoons} \mathrm{MeCONH_2} + \mathrm{HOBr} \quad \ldots (2)$$

If this equilibrium is involved in the oxidation process and hypobromous acid is the reactive oxidising species, then the rate should be an inverse function of [acetamide]. The plots of k_{obs} against [acetamide] was linear ($r = 0.9965$). The value of K_h determined from the slope and intercept of this plot came out to be 0.055 at 293 K. This compares favourably the value of 0.037 obtained at 303 K earlier[3].

The plot of k_{obs} versus $[H^+]$ was linear corresponding to the rate law (3)

$$k_{obs} = a + b[H^+] \quad \ldots (3)$$

The values of a and b determined from the plot were 21 s^{-1} and 18.5×10^5 mol^{-1} dm^3 s^{-1}. The above observation[4] indicates that (i) a rapid equilibrium exists between the protonated and deprotonated forms, (ii) the protonation constant is small, (iii) both the protonated and deprotonated species are kinetically active and (iv) the protonated form is more reactive. Thus the oxidation of iodide ion by NBA follows an acid-independent and another acid-catalysed pathway. It is suggested that hypobromous acid is protonated to give a stronger electrophile and oxidant, $(H_2OBr)^+$, and both HOBr and $(H_2OBr)^+$ are the reactive oxidising species. The formation and participation of hypobromous acidium ion in many electrophilic substitution[5] and oxidation[2] reactions are well documented.

Based on the above results, it is proposed that the rate-determining step involves a halide exchange reaction:

$$(H_2OBr)^+ + I^- \rightarrow (H_2OI)^+ + Br^-$$

The cationic iodine species, thus generated, reacts rapidly with another iodide ion to liberate iodine.

$$[(H_2OI)^+ + I^- \rightarrow H_2O + I_2].$$

References

1 Mathur N K & Narang C K, *Determination of organic compounds with N-bromosuccinimide and allied reagents* (Academic Press, London) 1975, p. 15
2 Sharma V & Banerji K K, *J chem Res* (S) (1985) 340, (M) (1985), 3351 and references cited therein.
3 Bishnoi M L & Banerji K K, *Tetrahedron*, **41** (1985) 6047.
4 Gupta K S & Gupta Y K, *J chem Educ*, **61** (1984) 972
5 Berliner E H, *J chem Educ*, **43** (1966) 124.

Indian Journal of Chemistry
Vol. 27A, April 1988, pp. 343-346

Separation of Polar & Steric Effects: Reactions of *ortho*-Substituted Benzoate & 3-Substituted 2-Naphthoate Ions with Picryl Bromide·

P ANANTHAKRISHNANADAR
Chemistry Department, Anna University, Madras 600 025, India

Received 30 *July* 1986; *revised* 23 *June* 1987; *accepted* 18 *August* 1987

Rate constants for the reactions of *ortho*-substituted benzoate and 3-substituted 2-naphthoate ions with picryl bromide have been determined at 30°, 40° and 50°±0.1°C in 80% methanol-20% water (v/v) mixtures. Electron-donating groups increase the rate, while electron-withdrawing groups decrease the rate. The rate data are analysed through multiple correlations involving electronic and steric terms associated with substituents. The steric term is rate-accelerating.

Although several approaches are known for the treatment of substituent effects in *ortho*-substituted benzene systems, that of Charton[1-3] based on multiple regression analysis of reactivity data in terms of substituent parameters, which measure the electronic and steric effects of substituents, is considered the best. Hence the results in the present study are subjected to Charton's treatment.

All the *ortho*-substituted benzoic acids were either commercial samples or prepared by literature methods. *o*-Methylthiosalicyclic acid, prepared from thiosalicylic acid, was oxidised by hydrogen peroxide to afford *o*-methylsulphonylbenzoic acid. 3-Acetamido-2-naphthoic acid, m.p. 142-43° (Found: C, 68.0; H, 4.7. $C_{13}H_{11}NO_3$ requires C, 68.1; H, 4.8%), 3-methylmercapto-2-naphthoic acid, m.p. 130-31° (Found: C, 66.1; H. 4.7. $C_{12}H_{10}O_2S$ requires C, 66.0; H, 4.6%) and 3-methylsulphonyl-2-naphthoic acid, m.p. 172-73° (Found: C, 57.7; H, 4.1. $C_{12}H_{10}O_4S$ requires C, 57.6; H, 4.0%) were prepared from 3-amino-2-naphthoic acid[5]. All the other 3-substituted 2-naphthoic acids were prepared by literature methods. Picryl bromide was prepared and recrystallized from ethanol, m.p. 123-24°. Purified methanol was used. Triply distilled water was used for dilution. Sodium salts of the acids were prepared in ethanol by the usual procedure.

The solvent used for the kinetic measurement was 80% methanol-20% water (v/v). The temperature was controlled within ±0.1°C. Low concentrations of the reactants (0.01 mol dm^{-3} in both) were found suitable for kinetic runs, which were followed by mixing equal volumes of equimolar solutions of sodium salts of the acids and of picryl bromide and estimating the bromide ion by the Volhard's method.

The activation energies were computed from the linear plots of log *k* against 1/T. The entropies of activation are negative as observed in similar bimolecular reactions (Tables 1 and 2).

With a view to testing the applicability of Taft's linear free energy-polar energy and linear free energy-steric energy relationships[6] in the reactions studied, single parameter correlations were attempted with σ^*_o and Taft's *Es* (*ortho*) values separately. The σ^*_o values of SCH_3 and SO_2CH_3 groups used in the correlations were obtained from literature[7]. In all the correlation equations generated, the correlation coefficients are very poor.

As the one-parameter equations did not help to predict the substituent effect, the results were subjected to analysis involving several substituent parameters as suggested by Charton[1]. The correlations were attempted through Eqs (1) and (2) involving inductive (σ_I), resonance (σ_R) and steric (v) substituent constants. The values of these constants are those compiled by Aslam *et al.*[4]

$$\log k_{ortho} = \alpha\sigma_I + \beta\sigma_R + h \qquad \ldots(1)$$

$$\log k_{ortho} = \alpha\sigma_I + \beta\sigma_R + \phi v + h \qquad \ldots(2)$$

Application of Eq (1) omitting NHAc, OAc and assuming orthogonal configuration of NO_2 generates Eqs (3-6) for the reactivities of *o*-substituted benzoates at 30°, 40° and 50°C respectively.

$$\log k = -2.842 - \underset{(\pm 0.160)}{0.523\,\sigma_I} - \underset{(\pm 0.167)}{0.257\,\sigma_R} \qquad \ldots(3)$$
$$R = 0.812;\ s = 0.111;\ n = 10$$

$$\log k = -2.524 - \underset{(\pm 0.118)}{0.503\,\sigma_I} + \underset{(\pm 0.123)}{0.277\,\sigma_R} \qquad \ldots(4)$$
$$R = 0.880;\ s = 0.082;\ n = 10$$

$$\log k = -2.213 - \underset{(\pm 0.146)}{0.492\,\sigma_I} - \underset{(\pm 0.152)}{0.235\,\sigma_R} \qquad \ldots(5)$$
$$R = 0.819;\ s = 101;\ n = 10$$

A similar treatment of data in the case of 3-substituted 2-naphthoate ions omitting NHAc generates Eqs (6-8) at 30°, 40° and 50°C respectively.

$$\log k = -3.003 - \underset{(\pm 0.156)}{0.499\,\sigma_I} - \underset{(\pm 0.154)}{0.340\,\sigma_R} \qquad \ldots(6)$$

Table 1—Second-order Rate Constants and Activation Parameters for Reaction of *ortho*-Substituted Benzoate Ions with Picryl Bromide in 80% Methanol—20% Water (v/v)

Substituent	$10^3\,k\,(\mathrm{dm^3\,mol^{-1}\,s^{-1}})$			$\Delta H^{\ddagger}$ (kJ mol^{-1}) (at 30°C)	$-\Delta S^{\ddagger}$ (JK^{-1} mol^{-1}) (at 30°C)
	30°	40°	50°C		
H	1.00 ± 0.02	2.30 ± 0.03	4.51 ± 0.03	60.0 ± 3.1	104.8 ± 16.2
F	0.80 ± 0.01	1.90 ± 0.02	3.62 ± 0.03	51.7 ± 3.6	135.9 ± 15.4
Cl	0.85 ± 0.01	2.10 ± 0.02	4.01 ± 0.03	56.4 ± 4.5	117.8 ± 17.1
Br	0.84 ± 0.01	2.00 ± 0.02	3.90 ± 0.02	49.7 ± 5.2	140.0 ± 13.4
I	1.40 ± 0.02	2.72 ± 0.02	6.41 ± 0.04	52.6 ± 5.6	126.5 ± 14.5
Me	1.90 ± 0.02	3.81 ± 0.01	7.72 ± 0.04	53.8 ± 5.4	119.7 ± 21.5
OMe	1.41 ± 0.02	2.70 ± 0.02	5.42 ± 0.03	53.0 ± 3.9	124.8 ± 20.6
NHAc	0.57 ± 0.01	1.02 ± 0.01	2.12 ± 0.02	48.8 ± 4.2	146.3 ± 21.2
SCH_3	1.62 ± 0.03	3.27 ± 0.01	6.51 ± 0.02	42.5 ± 5.3	158.4 ± 18.3
SO_2CH_3	0.72 ± 0.01	1.40 ± 0.02	2.92 ± 0.03	52.2 ± 6.2	133.1 ± 17.5
OAc	0.85 ± 0.01	1.40 ± 0.01	3.31 ± 0.03	50.0 ± 5.8	139.1 ± 16.9
NO_2	0.60 ± 0.01	1.25 ± 0.02	2.62 ± 0.02	40.0 ± 4.2	174.9 ± 17.6

Table 2—Second-order Rate Constants and Activation Parameters for Reaction of 3-Substituted 2-Naphthoate Ions with Picryl Bromide in 80% Methanol-20% Water (v/v)

Substituent	$10^3\,k\,(\mathrm{dm^3\,mol^{-1}\,s^{-1}})$			$\Delta H^{\ddagger}$ (kJ mol^{-1}) (at 30°C)	$-\Delta S^{\ddagger}$ (JK^{-1} mol^{-1}) (at 30°C)
	30°	40°	50°C		
H	0.74 ± 0.02	1.50 ± 0.03	3.01 ± 0.03	58.8 ± 3.2	171.2 ± 20.1
F	0.70 ± 0.01	1.42 ± 0.02	2.91 ± 0.03	55.5 ± 4.0	122.4 ± 17.2
Cl	0.73 ± 0.02	1.38 ± 0.01	2.62 ± 0.02	46.6 ± 3.8	151.5 ± 16.95
Br	0.72 ± 0.01	1.46 ± 0.02	2.91 ± 0.04	53.8 ± 2.9	127.8 ± 21.2
I	0.92 ± 0.02	1.90 ± 0.02	4.46 ± 0.03	62.4 ± 4.2	97.3 ± 11.5
Me	1.41 ± 0.01	3.10 ± 0.01	5.90 ± 0.04	56.4 ± 4.1	113.6 ± 21.5
OMe	0.92 ± 0.01	1.81 ± 0.02	3.82 ± 0.03	54.7 ± 3.8	122.9 ± 22.6
NHAc	0.36 ± 0.02	0.69 ± 0.01	1.41 ± 0.01	52.7 ± 6.1	137.1 ± 21.4
SCH_3	1.10 ± 0.02	2.21 ± 0.01	5.01 ± 0.03	57.4 ± 5.0	112.6 ± 20.6
SO_2CH_3	0.41 ± 0.01	0.71 ± 0.02	1.21 ± 0.01	36.9 ± 5.1	118.5 ± 17.8

$$R = 0.833;\ s = 0.096;\ n = 9$$

$$\log k = -2.686 - 0.590\,\sigma_I - 0.391\,\sigma_R \quad \ldots(7)$$
$$(\pm 0.181)\quad(\pm 0.178)$$
$$R = 0.836;\ s = 0.111;\ n = 9$$

$$\log k = -2.389 - 0.629\,\sigma_I + 0.491\,\sigma_R \quad \ldots(8)$$
$$(\pm 0.219)\quad(\pm 0.216)$$
$$R = 0.816;\ s = 0.134;\ n = 9$$

In equations (3-8) the correlation coefficients are poor. This establishes that Eqs (3-8) also do not explain the substituent effects correctly. It was thought that the poor correlations in the case of *ortho*-substituents might be due to the inclusion of NO_2 substituent which could assume any conformation between coplanar and orthogonal. However, exclusion of NO_2 did not help to improve the correlation. In view of this other correlations were sought in order to accommodate several other substituent parameters which might influence the *ortho*-substituent effect. Thus correlation was attempted through Eq. (2). This generated Eqs (9-11) in the case of *ortho*-substituted benzoate ions omitting NHAc, OAc and assuming NO_2 orthogonal, and Eqs (12-14) in the case of 3-substituted 2-naphthoate ions omitting NHAc group, at 30°, 40° and 50°C respectively.

$$\log k = -2.950 - 0.666\,\sigma_I - 0.366\,\sigma_R + 0.260\,\nu \quad \ldots(9)$$
$$(\pm 0.126)\quad(\pm 0.126)\quad(\pm 0.094)$$
$$R = 0.922;\ s = 0.079;\ n = 10;\ \text{S.L.} > 99.0\%$$

$$\log k = -2.600 - 0.604\,\sigma_I - 0.353\,\sigma_R + 0.183\,\nu \quad \ldots(10)$$
$$(\pm 0.098)\quad(\pm 0.098)\quad(\pm 0.073)$$
$$R = 0.943;\ s = 0.062;\ n = 10;\ \text{S.L.} > 99.0\%$$

$$\log k = -2.302 - 0.611\,\sigma_I - 0.325\,\sigma_R + 0.215\,\nu \quad \ldots(11)$$
$$(\pm 0.127)\quad(\pm 0.127)\quad \pm 0.095)$$
$$R = 0.907;\ s = 0.080;\ n = 10;\ \text{S.L.} > 98\%$$

$$\log k = -3.097 - 0.729\,\sigma_I - 0.514\,\sigma_R + 0.238\,\nu \quad \ldots(12)$$
$$(\pm 0.177)\quad(\pm 0.167)\quad(\pm 0.124)$$
$$R = 0.907;\ s = 0.080;\ n = 9;\ \text{S.L.} \sim 97.5\%$$

$$\log k = -2.781 - 0.822\,\sigma_I - 0.567\,\sigma_R + 0.241\,v \quad \ldots (13)$$
$$(\pm 0.221)\ (\pm 0.196)\ (\pm 0.155)$$
$$R = 0.893;\ s = 0.100;\ n = 9;\ \text{S.L.} \sim 96.0\%$$

$$\log k = -2.489 - 0.874\,\sigma_I - 0.675\,\sigma_R + 0.253\,v \quad \ldots (14)$$
$$(\pm 0.284)\ (\pm 0.252)\ (\pm 0.199)$$
$$R = 0.865;\ s = 0.128;\ n = 9;\ \text{S.L.} < 95.0\%$$

Similar correlations in the case of *ortho* substituted benzoate ions omitting NHAc, OAc and NO_2 produce Eqs (15-17) at 30°, 40° and 50°C respectively.

$$\log k = -3.001 - 0.881\,\sigma_I - 0.528\,\sigma_R + 0.400\,v \quad \ldots (15)$$
$$(\pm 0.135)\ (\pm 0.120)\ (\pm 0.095)$$
$$R = 0.949;\ s = 0.061;\ n = 9;\ \text{S.L.} > 99.0\%$$

$$\log k = -2.627 - 0.702\,\sigma_I - 0.427\,\sigma_R + 0.247\,v \quad \ldots (16)$$
$$(\pm 0.137)\ (\pm 0.121)\ (\pm 0.096)$$
$$R = 0.929;\ s = 0.062;\ n = 9;\ \text{S.L.} \sim 98.5\%$$

$$\log k = -2.336 - 0.751\,\sigma_I - 0.430\,\sigma_R + 0.306\,v \quad \ldots (17)$$
$$(\pm 0.173)\ (\pm 0.154)\ (\pm 0.122)$$
$$R = 0.897;\ s = 0.078;\ n = 9;\ \text{S.L.} \sim 97.0\%$$

The analysis of three-parameter equations (Eqs 9-17) reveals that the improvement in the correlations in the case of *ortho*-substituted benzoate ions by including the steric term is at an adquate significance level (⩾95%) except in one case (50°C including orthogonal NO_2); the overall significance level is adequate (⩾97%) in all the cases. However the improvement in the correlations in the case of 3-substituted 2-naphthoate ions by including the steric term is barely at an adequate significance level (~90%) at 30° and really does not reach an adequate level for 40° and 50°C and the overall significance level is quite good at 30°C [97.5% and just about acceptable for 40°C (~96%) and 50°C (Ca. 95%)].

Using Eqs (15-17) the log *k* values were calculated for *ortho*-nitrobenzoate ion at 30°C with NO_2 group having coplanar or orthogonal orientation. The values are presented in Table 3. The calculated values correspond to a conformer in between the two orientations, since the correlations for orthogonal/coplanar NO_2 based on correlations with 9-substituents indicate clearly that NO_2 adopts an intermediate conformation. Correlations (15-17) are to be preferred to the 10-substituents correlations eventhough acceptable correlations are obtained by assuming NO_2 orthogonal.

In the case of *ortho*-NHAc benzoate and 3-NHAc-2-naphthoate ions, the log *k* values were calculated using the three-parameter equations in which the NO_2 group was omitted. There is considerable discrepancy between the calculated and observed log *k* values (Table 4) and the observed values are less than those calculated in all the cases. This may indicate that the NHAc group is involved in H-bonding with the carboxylate ion, reducing the nucleophilicity of the anion. It is striking that the regression coefficient of the steric term in all the equations is positive. Moreover the 'student t' test for the significance of ϕ gives a significance level greater than 95% in the case of *ortho*-substituted benzoate ions. This indicates that the reactions are subject to steric acceleration. A similar observation was made earlier in the reaction between *o*-substituted benzoate ions and phenacyl bromide[7]. It is believed that bulky *ortho*-substituents can cause considerable desolvation around the carboxylate ion both by steric inhibition to solvation and by desolvation due to steric inhibition of resonance, thereby generating carboxylate ions free from the solvent cloud. This accounts for the steric acceleration.

Table 3—Effect of Conformations on Reactivity of *o*-Nitrobenzoate Ion

Temp. (°C)	log *k* (calc) Coplanar	log *k* (calc) Orthogonal	log *k* (obs)
30	−3.088	−3.451	−3.222
40	−2.794	−3.008	−2.903
50	−2.457	−2.732	−2.582

Table 4—Behaviour of NHAc Group

Temp. (°C)	log *k*		log *k*	
	Calc.	Obs.	Calc.	Obs.
	o-NHAc-benzoate ion		3-NHAc-2-naphthoate ion	
30	−2.789	−3.244	−2.968	−3.444
40	−2.507	−2.991	−2.660	−3.161
50	−2.188	−2.674	−2.341	−2.851

The composition of electronic effect was calculated using Eq. (18). The average values of P_R estimated for the reactivity of *ortho*-substituted benzoate and 3-substituted 2-naphthoate ions are approximately 32.0 and 40.5 respectively. These values suggest that the localised component of the electrical effect is important than the delocalised component in these reactions.

$$P_R = \beta\, 100/\alpha + \beta \quad \ldots (18)$$

In order to assess the magnitude (%) of steric effect, P_S was calculated using expression (19).

$$P_S = \frac{|\phi| 100}{|\alpha| + |\beta| + |\phi|} \quad \ldots (19)$$

The magnitude of the steric effect has been found to be close to 22.0 and 17.0% respectively for the reactivities of *o*-substituted benzoate and 3-substituted 2-naphthoate ions. This indicates that steric effect is significant in these two reaction series.

The plots of $\Delta H^{\ddagger}$ against $\Delta S^{\ddagger}$ are linear. The Exner plots of log k at 40°C versus log k at 30°C are also linear. The existence of good correlations in both the plots shows that the two reaction series obey isokinetic relationships and they follow the same mechanism[8,9].

References

1 Shorter J, *Chem Brit*, **6** (1969) 269.
2 Charton M, *Prog phys org Chem*, **8** (1971) 235.
3 Charton M, *J org Chem*, **40** (1975) 407.
4 Aslam N H, Burden A G, Chapman N B, Shorter J & Charton M, *J chem Soc, Perkin II*, (1981) 500.
5 Dutta P C, Ber., **67** (1934) 1319.
6 Taft R W (Jr), *Steric effects in organic chemistry*, edited by Newman (Wiley New York) 1956, Ch. 13.
7 Ananthakrishnanadar P & Shanmugasundaram A, *Indian J Chem*, **14A** (1976) 805.
8 Ananthakrishnanadar P & Gnanasekaran C, *J chem Soc, Perkin Trans II*, (1978) 671.
9 Leffler J E, *J org chem*, **20** (1955) 1205.

Indian Journal of Chemistry
Vol. 27A, April 1988, pp. 347-349

Kinetics & Mechanism of Aquation & of Silver Ion Catalysed Peroxydisulphate Oxidation of Pentaammineformatocobalt(III) Ion

NIROD KUMAR MOHANTY*,
BISHNU PRASAD PANDA & SANGITA PANI
Post-graduate Department of Chemistry, Sambalpur University, Sambalpur, Orissa

Received 3 *February* 1987;
revised 28 *July* 1987; *accepted* 17 *September* 1987

Kinetics of aquation and of silver ion catalysed peroxydisulphate oxidation of formatopentaamminecobalt(III) ion have been investigated. The course of these reactions is followed spectrophotometrically by observing the disappearance of complex. In case of oxidation, the pseudo-first order rate constant increases with increase in [silver ion] and [peroxydisulphate ion]. The oxidation rate is found to be several fold faster than the aquation rate showing that the oxidation rate is not substitution-controlled. The product of oxidation has been found to be pentaammineaquocobalt(III) ion. The aquation rate is found to be acid-catalysed. Possible mechanism for the oxidation reaction has been suggested to account for the kinetic results.

We have been interested in the kinetic and mechanistic aspects of oxidation of coordinated substrates[1-3]. In this paper we report the kinetics and mechanism of oxidation of coordinated formate in formatopentaamminecobalt (III) ion by peroxydisulphate catalysed by silver ion.

All the chemicals used were of reagent grade and solutions were prepared in conductivity water. Pentaammineformatocobalt(III) perchlorate was prepared by the general method of Gould and Taube[4] and its purity was checked by estimating cobalt[5] and formate[6]. Silver perchlorate solution was prepared by dissolving freshly precipitated silver hydroxide in perchloric acid. Silver and peroxydisulphate were estimated by standard methods.

Oxidation kinetics

The oxidation reaction was initiated by adding requisite volume of pre-equilibrated stock complex solution to a solution containing known amounts of perchloric acid, silver perchlorate (catalyst) and sodium perchlorate (to adjust ionic strength) pre-equilibrated at the desired temperature. To this was added peroxydisulphate solution. The reaction was studied spectrophotometrically under pseudo-first order conditions following decrease in absorbance with time at 240 nm with the help of a Beckman (model 35) spectrophotometer. Ice-cold water was used to quench the reaction. The pseudo-first order rate constants were calculated from slopes of log $(A_t - A_\infty)$ versus time plot where A_t and A_∞ are the absorbances of the solutions at time t and infinity. All the calculations were done by the method of least squares.

Aquation kinetics

The kinetics of acid hydrolysis of the substrate was also followed spectrophotometrically in the temperature range 70-85°C. A blank experiment (absence of acid) with the complex alone indicated that concentration change due to water evaporation was within 3% during the period employed for aquation studies. This change was, therefore, neglected.

Reaction product and stoichiometry

In a typical spectrophotometric run peroxydisulphate was taken 4-5 fold excess over the substrate. The absorbance decreased and after sometime became steady and tallied with the absorbance of $[(NH_3)_5Co(H_2O)]^{3+}$ ion[7]. This observation indicated that the product of oxidation was $[(NH_3)_5Co(H_2O)]^{3+}$. When the absorbance became constant, calculated volume of the reaction mixture was withdrawn and passed over Dowex 50 WX-8 resin when Ag^+ and $[(NH_3)_5Co(H_2O)]^{3+}$ were exchanged. The resulting peroxydisulphate was estimated. This experiment showed that 1 mol of complex reacted with 1 mol of peroxydisulphate. No Co(II) could be detected as one of the products.

Mechanism of aquation

The aquation of pentaammineformatocobalt(III) ion has been studied in the acidity range 0.05 to 0.3 mol dm^{-3} and at constant ionic strength of 0.3 mol dm^{-3}. The pseudo-first order rate constant (k_{obs}) increased with increase in $[H^+]$. The acid-catalysed aquation of various pentaamminecarboxylatocobalt(III) ions have been explained[8-10] by the mechanism shown in Scheme 1.

In accord with Scheme 1, rate-law is given by Eq. (1)

$$-d\ln[\text{complex}]_{\text{total}}/dt = k_{obs} = \frac{k_0 + k_1[H^+]}{1 + k'[H^+]} \qquad \dots(1)$$

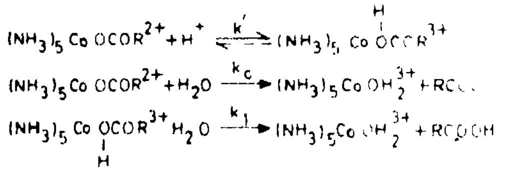

$$(NH_3)_5CoOCOR^{2+} + H^+ \underset{}{\overset{k'}{\rightleftharpoons}} (NH_3)_5Co\overset{H}{\overset{|}{O}}CCR^{3+}$$

$$(NH_3)_5CoOCOR^{2+} + H_2O \xrightarrow{k_c} (NH_3)_5CoOH_2^{3+} + RCOOH$$

$$(NH_3)_5Co\underset{\underset{H}{|}}{O}COR^{3+}\ H_2O \xrightarrow{k_1} (NH_3)_5CoOH_2^{3+} + RCOOH$$

(where RCOOH - carboxylic acid)

Scheme 1

where k_{obs} is the pseudo-first order rate constant and $k'_1 K' = k_1$. However, presently it is observed that the formato complex undergoes aquation by k'_1 path alone. For this the rate law is given by Eq. (2).

$$k_{obs} = k_1 [H^+] \qquad \ldots (2)$$

Eq. (2) predicts that the plot of k_{obs} versus $[H^+]$ should be linear passing through the origin. This is found to be the case. Eqs (1) and (2) can be identical only if the k_0 path is absent and $K'[H^+] \ll 1$, i.e. $K' \ll 1$. The low value of K' for the formato complex may be explained in a manner similar to one suggested by Dash and Nanda[9]. The higher rate of reaction in the K' path compared to the k_0 path is obviously due to the fact that the protonation at the oxygen linked to cobalt(III) produces an electron deficient centre which facilitates the Co – O bond fission. For the formato complex, k_0 appears to be much smaller than k'_1 such that k_0 is not observed as an intercept in the k_{obs} versus $[H^+]$ plot. Basolo *et al.*[8] have also made similar observations for some such systems. The value of k_1 calculated from Eq. (2) and the corresponding activation parameters calculated from transition state equation are collected in Table 1.

Table 1 – Pseudo-first Order Rate Constants for Aquation of Formato Complex

$[Complex] = 2.0 \times 10^{-3}$ mol dm^{-3}; and $I = 0.3$ mol dm^{-3}.

$[H^+]$ (mol dm^{-3})	$10^4\ k_{obs}$ (s^{-1}) at			
	70°	75°	80°	85°C
0.05	0.45	0.74	1.28	2.03
0.10	0.90	1.38	3.04	4 21
0.15	1.11	2.36	4.82	5.20
0.20	1.56	2.68	4.84	7.65
0.25	2.04	3.20	5.86	7.93
0.30	2.32	4.80	8.65	10.40

$10^3\ k_1$ (dm^3 mol^{-1} s^{-1}) = 0.76, 1.49, 2.59 and 3 50 at 70°, 75°, 80° and 85° respectively.

$\Delta H^{\neq} = 107.0$ kJ mol^{-1} and $\Delta S^{\neq} = -6.3$ JK^{-1} mol^{-1}

Mechanism of oxidation

In the absence of Ag^+ the formato complex is not oxidised by peroxydisulphate. Under the conditions: $[Ag^+] = 2 \times 10^{-3}$ mol dm^{-3}, $[S_2O_8^{2-}] = 2 \times 10^{-3}$ mol dm^{-3}, acidity $= 2 \times 10^{-2}$ mol dm^{-3}, $I = 0.3$ mol dm^{-3} and temperature = 40°C, oxidation rate constant comes out to be $1.66 \times 10^{-4} s^{-1}$. The aquation rate constant is $0.99 \times 10^{-4} s^{-1}$ at 70°C and acidity = 0.1 mol dm^{-3} and $I = 0.3$ mol dm^{-3}. A comparison of aquation and oxidation rate constants indicates that the latter reaction is not substitution-controlled. The observed pseudo-first order rate constant, k_{obs} increases with increase in $[Ag^+]$ and $[S_2O_8^{2-}]$ (Table 2). The invariance of rate constant with variation in [complex] indicates that the order with respect to complex is unity. The experimental observations can be explained by assuming a mechanism shown in Scheme 2, which leads to rate-law (5).

Equation (5) predicts that the plot of k_{obs} versus $[Ag^+]$ at constant $[S_2O_8^{2-}]$ and that between k_{obs} versus $[S_2O_8^{2-}]$ at constant $[Ag^+]$ should be linear yielding comparable values of k. Plot between k_{obs} versus $[Ag^+]$ at constant $[S_2O_8^{2-}] = 2.0 \times 10^{-3}$ mol dm^{-3} and $I = 0.3$ mol dm^{-3} yields values of $k = 12.0$, 31.5 and 55.0 mol^{-2} dm^6 s^{-1} at 35, 40 and 45°C respectively while the plot between k_{obs} versus $[S_2O_8^{2-}]$ at constant $[Ag^+] = 2.0 \times 10^{-3}$ mol dm^{-3} and $I = 0.3$ mol dm^{-3} yield $k = 12.5$, 35.3 and 60.0 mol^{-2} dm^6 s^{-1} at 35, 40 and 45°C respectively. The activation parameters are $\Delta H^{\neq} = 123.3$ kJ mol^{-1} and $\Delta S^{\neq} = 178.1$ JK^{-1} mol^{-1}.

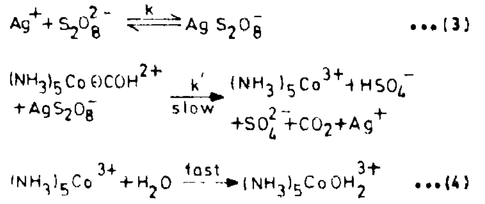

$$Ag^+ + S_2O_8^{2-} \overset{K}{\rightleftharpoons} AgS_2O_8^- \qquad \ldots (3)$$

$$(NH_3)_5CoOCOH^{2+} + AgS_2O_8^- \xrightarrow[slow]{k'} (NH_3)_5Co^{3+} + HSO_4^- + SO_4^{2-} + CO_2 + Ag^+$$

$$(NH_3)_5Co^{3+} + H_2O \xrightarrow{fast} (NH_3)_5CoOH_2^{3+} \qquad \ldots (4)$$

Scheme 2

$$k_{obs} = k[Ag^+][S_2O_8^{2-}] \qquad \ldots (5)$$

(where k - k'K)

Scheme 2 involves formation of $AgS_2O_8^-$ as proposed by Nandwana and Solanki[11]. We presume that both substrate and $AgS_2O_8^-$ form a transition complex during electron transfer which is of inner sphere type formed between Ag^+ and coordinated formate. The substrate and oxidant

Table 2 – Pseudo-first Order Rate Constants for $K_2S_2O_8$ Oxidation of Formato Complex

I (mol dm^{-3})	$10^3[Ag^+]$ (mol dm^{-3})	$10^3[S_2O_8^{2-}]$ (mol dm^{-3})	10^4[complex] (mol dm^{-3})	$10^4 k_{obs}$ (s^{-1}) at		
				35°	40°	45°C
0.1	2.0	2.0	2.0	–	5.8	–
0.2	2.0	2.0	2.0	–	3.45	–
0.3	2.0	2.0	2.0	0.53	1.66	2.58
0.5	2.0	2.0	2.0	–	1.41	–
0.6	2.0	2.0	2.0	–	1.26	–
0.3	1.0	2.0	2.0	0.38	0.81	1.65
0.3	4.0	2.0	2.0	1.01	2.11	4.38
0.3	6.0	2.0	2.0	1.71	3.43	6.91
0.3	8.0	2.0	2.0	1.88	4.55	9.63
0.3	10.0	2.0	2.0	2.52	6.60	13.66
0.3	12.0	2.0	2.0	–	7.80	–
0.3	2.0	1.0	2.0	0.45	0.90	1.79
0.3	2.0	4.0	2.0	1.02	3.10	5.04
0.3	2.0	6.0	2.0	1.71	5.10	7.33
0.3	2.0	8.0	2.0	2.06	5.55	9.84

($AgS_2O_8^-$) being oppositely charged show ionic strength effect; k_{obs} increases with decrease in ionic strength (Table 2). We further believe that in the transition state $S_2O_8^{2-}$ in $AgS_2O_8^-$ removes electrons making silver higher valent (presumably tervalent) and the latter in turn derives both the electrons from coordinated formate. Due to simultaneous removal of electrons the oxidation state of cobalt is preserved[12] (Co^{III} is the product) and a radical ion of the type $(NH_3)_5CoOCO^{\cdot +}$ is not generated by one electron step, a process which[13], in addition to Co^{III}, would have also produced Co^{2+} as the product (which is not detected) via internal electron transfer to Co(III) centre. Dash *et al.* have however found that Ag^+-catalysed peroxydisulphate oxidation of pentaammineoxalato[14] and pentaammineglycinatocobalt(III)[15] ions produce Co^{2+} as the only product. These observations show that nature of the product depends on the nature of substrate.

The activation parameters for the aquation reaction have been calculated using the k_1 values. The k_1 values are associated with the equilibrium constant K'. As K' in case of carboxylatopentaamminecobalt(III) systems does not change appreciably with temperature, the k_1 values are directly used[8-10] to calculate the activation parameters. We have also adopted this method. However. in case of the oxidation reaction, literature survey indicated that data on the association constants (K) between Ag^+ and $S_2O_8^{2-}$ are not available. We have, therefore, calculated the activation parameters for the oxidation reaction using k values.

References

1 Mohanty N K & Rath P C, *J Indian chem Soc*, **60** (1983) 1027.

2 Mohanty N K & Rath P C, *Indian J Chem*, **21A** (1983) 56.

3 Mohanty N K & Nanda R K, *Bull chem Soc (Japan)*, **58** (1985) 3597.

4 Gould E S & Taube H, *J Am chem Soc*, **86** (1964) 1318.

5 Dash A C & Nanda R K, *Inorg Chem*, **12** (1973) 2024.

6 Rath P C & Mohanty N K, *J Indian chem Soc*, **58** (1981) 26.

7 Splinter R C, Harris S J & Tobias R S, *Inorg Chem*, **7** (1968) 898.

8 Monacelli F, Basolo F & Pearson R G, *J inorg nucl Chem*, **24** (1962) 1241.

9 Dash A C & Nanda R K, *Inorg Chem*, **12** (1973) 2024.

10 Andrade C & Taube H, *Inorg Chem*, **5** (1966) 1087.

11 Nandwana R K & Solanki S K, *Indian J Chem*, **21A** (1982) 519.

12 Saffir P & Taube H, *J Am chem Soc*, **82** (1960) 13.

13 Candlin J P & Halpern H, *J Am chem Soc*, **85** (1963) 2518.

14 Nanda R K, Dash A C & Mohanty P, *Indian J chem*, **23A** (1984) 11.

15 Nanda R K, Dash A C & Mohanty P, *J Indian chem Soc*, **61** (1984) 940.

Indian Journal of Chemistry
Vol. 27A, April 1988, pp 350-352

Electro-reduction & Coulometric Determination of Titanium(III) in Calcium Nitrate Tetrahydrate Melt

C K BHASKARE*
Department of Chemistry, Shivaji University, Kolhapur 416004
and
K N GANAGE
Department of Chemistry, S S G M College, Kopargaon 423601

Received 26 *February* 1987, *revised* 19 *June* 1987,
revised and accepted 7 *September* 1987

Polarographic investigation of the Ti(III)/Ti(II) system in calcium nitrate tetrahydrate melt has been carried out at 55°C. The reversibility of the system in the melt has been used successfully for coulometric generation of Ti(II) and its amperometric titration with potassium dichromate. The reduction is a single electron change as shown by the reciprocal of the slope of log $i/(i_d - i)$ vs E plot. L type plots are obtained in amperometric and dead stop titrations.

The electroreduction of metal ions in aqueous melts has evoked considerable interest in recent years because of its theoretical and practical importance. The aqueous melts are intermediate between the aqueous solutions of normal concentration range and anhydrous melts. Lovering[1,2] has reported half wave potentials for different cations in lithium nitrate trihydrate, calcium chloride hexahydrate and calcium nitrate tetrahydrate melts. The studies on Cu(II), Cr(III) and Bi(III) by Delimarskii *et al.*[3] and of Tl(I) and UO_2 ions by Plambeck *et al.*[4,5] have generated important electrochemical data.

The electrochemistry of titanium has been studied to a greater extent in molten LiCl-KCl eutectic mixture[6-8] and in molten NaCl-KCl[9] than in any other melt. In LiCl-KCl eutectic melt, two halfwaves have been reported corresponding to the reductions Ti(III)/Ti(II) and Ti(II)/Ti. The electroreduction of titanium(III) to lower oxidation state in calcium nitrate tetrahydrate melt is of theoretical interest. In the present note we report the results of our studies on polarographic reduction of Ti(III), coulometric generation of Ti(II) and amperometric detection of the end point in the oxidation of Ti(II) to Ti(III).

A double walled, water jacketted borosilicate glass cell was used for the polarographic measurements. Hot water from a thermostat was circulated around the cell to maintain the temperature of the cell at 55 ± 1°C.

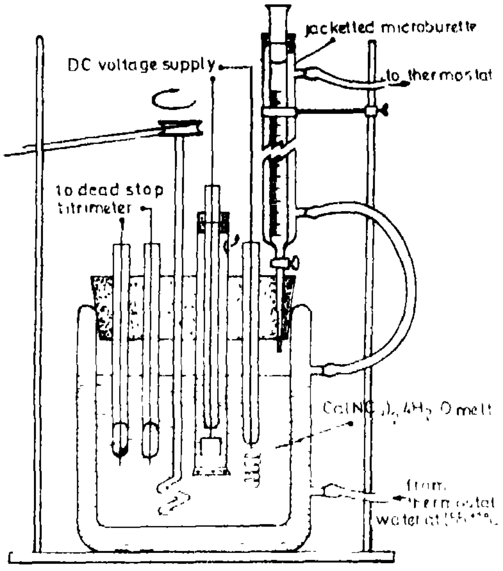

Fig. 1 — Coulometric assembly

A double walled, water jacketted borosilicate glass cell (Fig. 1) was used for coulometric generation of Ti(II) and its biamperometric titration. Hot water was circulated around the cell from a thermostat to maintain the cell at 55 ± 1°C.

The generating electrodes were of platinum, the anode was placed in a fritted glass compartment whereas the cathode was placed in the outer compartment. An externally driven stirrer was used for proper stirring of the viscous melt. The constant current source for coulometry was a stabilized high voltage D.C. power supply (Systronix Type 621). Biamperometric measurements were carried out with a dead stop titrator fabricated in our laboratory.

Calcium nitrate tetrahydrate (BDH, AnalaR) and titanium chloride (May and Baker, England) were used.

Potassium dichromate solution (0.00334 *M*)

0.098 g of $K_2Cr_2O_7$ (BDH, AR) were dissolved in about 40 ml of calcium nitrate melt and volume made upto 100 ml in a volumetric flask with the melt. The contents of flask after attainment of homogeneity were kept in a thermostat at 55°C.

Titanium(III) solution (1.577×10^{-3} *M*)

One ml of 12% $TiCl_3$ was transferred to a 50 ml volumetric flask and about 20 ml calcium nitr-

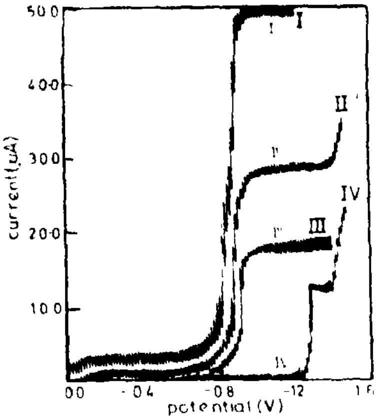

Fig. 2 – Polarograms for reduction of Ti^{3+} (I, II, III) and $Cr_2O_7^{2-}$ (IV) in calcium nitrate tetrahydrate melt.

ate melt was added. The flask was shaken vigorously and finally the volume was made upto the mark with the melt. The solution was shaken to allow attainment of homogeneity and was then standardized by the literature procedure[10]. The flask was kept in a thermostat at 55°C.

Procedure: Polarography

Polarograms of Ti(III) were run using the previously reported procedure on a Sargent-Welch polarograph model XVI with a low scan rate. The solubility of oxygen in the melt was negligible so no special precautions were taken to exclude air[11]. The typical polarographic waves are shown in Fig. 2. The capillary characteristics were, $m = 19$ mg sec^{-1}, $t = 3$ sec, $h = 60$ cm, $A = 0.1072$ cm^2.

Coulometric generation of titanium (II)

A known volume of titanium chloride solution was added to 90 g of melt and the electrode system was inserted into the melt. The salt was mixed properly by stirring and a constant current (10 mA) was passed through the cell for a known interval of time (about 100 sec). The contents of the outer vessel were titrated amperometrically or biamperometrically with 0.00334 *M* dichromate ion. The amperometric titration was carried out at −0.95 V using DME as the cathode and mercury pool as the anode.

The experiment was repeated by passing constant current for a longer duration until it gave constant titration reading, indicated by L shaped biamperometric curve; a similar plot was obtained for the amperometric detection. The amount of Ti(III) was determined using the relation, 1 ml of 0.00334 $M\ K_2Cr_2O_7 = 0.958$ mg of Ti(III).

Polarographic investigations of Ti(III) in calcium nitrate tetrahydrate melt showed that the Ti(III)/Ti(II) couple behaved reversibly when Ti(III) concentrations were between 0.15×10^{-4} and 0.80×10^{-4} *M*. The reciprocal of the slope of the plot of log $i/(i_d - i)$ versus E showed that there was one electron change during the reduction. The reciprocal of the slope of the straight line is 0.070 V as against 0.065 V for one electron change at 55°C. The diffusion coefficient of Ti(III) to Ti(II) reduction in calcium nitrate tetrahydrate melt was found to be 7.586×10^{-6} cm^2sec^{-1}.

The constant current technique has more precision than the controlled potential coulometry for titanium because in the latter technique the concentrations of the electrolysed solutions are lower at the electrode. The titanium(II) species is found to be sufficiently stable in this melt, and this stability has been used for the determination of titanium by amperometric and biamperometric titrations. The current efficiency is found to be 100% in the constant current coulometry. The results of amperometric and biamperometric titrations are reproducible with standard deviations of 0.15 and 0.30, respectively.

Ti(III) can be successfully determined by coulometric generation of Ti(II) and its amperometric titration against dichromate due to reversibility of Ti(III)/Ti(II) system in calcium nitrate tetrahydrate. The amperometric titrations at mercury electrode give more satisfactory results as compared to the biamperometric method. Many transition metals and rare earths undergo reduction under similar experimental conditions so prior separation is necessary.

Though the estimation of titanium can be done by more simple literature procedures, the studies in the molten salt media constitute a new field which needs extensive investigations. The electroreduction of titanium in molten salt is, therefore, important from theoretical point of view rather than analytical.

One of the authors (KNG) is thankful to the CSIR, New Delhi for award of a JRF.

References

1 Lovering D G, *Collin Czech chem Commun*, **37** (1972) 3797, **38** (1973) 1719

2 Lovering D G, *J electroanal Chem*, **50** (1974) 91.

3 Delimarskii Ku K & Shilina G V, *Ukr khim Zh*, **36** (1970) 781.

4 Plambeck J A & Bansal N P, *J electrochem Soc*, **124** (1977) 1036.

5 Plambeck J A & Bansal N P, *Electrochim Acta*, **23** (1978) 1053.

6 Liu L H, Johnson K E & Laitinen H A, *Molten salt chemistry*, edited by M Blander (Interscience, New York) 1964.

7 Laitinen H A & Osteryoung A, in *Fused salts*, edited by B K Sundheim (McGraw Hill, New York) 1964.

8 Baboian R, Hill D L & Bailey R A, *Can J Chem*, **43** (1965) 197.

9 Flengas S N, *Ann N Y Acad Sci*, **79** (1960) 853.

10 Sheffer E R, in *Treatise on analytical chemistry*, edited by I M Kolthaff & P J Elving, Part II, Vol 5 (Interscience New York) 1961.

11 Moynihan C T & Angell C A, *J phys Chem*, **74** (1970) 736.

Indian Journal of Chemistry
Vol. 27A, April 1988, pp. 353-354

Preparation & Characterization of Some New Titanium (IV) Alkyl Acetopyruvates

(Mrs) P PARDASANI, A SINGH, A K RAI &
R C MEHROTRA*
Department of Chemistry, University of Rajasthan,
Jaipur 302 004

Received 2 *April* 1987; *revised* 10 *August* 1987; *accept* 31 *August* 1987

Titanium (IV) derivatives of the type (Ti $(OR)_3$ [MeCOCH-COCOOR^1] and Ti $(OR)_2$ [MeCOCHCOCOOR^1]$_2$ (R = Et, Pr^i, R^1 = Me, Et) have been prepared and characterized by elemental analyses, IR and PMR spectroscopy

Reactions of titanium alkoxides with β-diketones to form derivatives of the type Ti $(OR)_2$ (β-diketonate)$_2$ in which titanium is hexacoordinated having *cis*-octahedral structure, are well known[1]. Like β-diketones, β-ketoesters also form similar derivatives with titanium alkoxides[2-4]. So far no such derivatives of titanium alkoxides with alkyl acetopyruvates (β-ketoesters) have been reported, though reactions of benzoyl pyruvates with titanium tetrachloride have been reported by Podolesov *et al*[5].

Herein we describe the synthesis and characterization of some alkoxytitanium (IV) alkyl acetopyruvates.

All experiments were carried out in moisture-free environment. Benzene was deried over sodium wire and finally by azeotropic dehydration technique. The titanium alkoxides[6,7] and alkyl acetopyruvates[8] were prepared by literature methods.

IR spectra in the range 4000-400 cm^{-1} were recorded on a Perkin-Elemer model 577 grating infrared spectrophotometer and PMR spectra on a Perkin-Elmer R12B spectrometer.

Synthesis of complexes: *General procedure*

To a benzene solution (20 ml) of titanium alkoxide, stoichiometric amount of alkyl acetopyruvate was added and allowed to stand at 40°C for 1 hr. Removal of excess solvent under reduced pressure (60°/0.1 mm) afforded coloured complexes in quantitative yields, the characterisation data of which are recorded in Table 1.

Reactions of titanium alkoxides with alkyl acetopyruvates have been carried out in 1:1 and 1:2 molar ratios in benzene. The reactions were exothermic and mono and bis derivatives $Ti(OR)_3$ [MeCOCHCOCOOR^1]$^{\cdot}$ (I) and Ti $(OR)_2$ [MeCOCHCOCOOR^1]$_2$ (II) (R = Et, Pr^i; R^1 = Me, Et) were isolated. However, tris- and tetrakis-derivatives could not be obtained even after refluxing and continuously removing the liberated alcohol azeotropically. This may be ascribed to the nature of ligands, which do not appear to permit an increase in coordination number beyond six in this class of derivatives[2,3]. These observations are in agreement with reactions of titanium alkoxides with other β-diketones[2,3,9-11].

All these derivatives are yellow to red highly viscous liquids or solids. These products are susceptible to hydrolysis and are soluble in common organic solvents like carbon tetrachloride, benzene, *n*-hexane, chloroform, cyclohexane and monomeric in nature.

Infrared spectra of methyl and ethyl acetopyruvates exhibit strong bands at 1738 cm^{-1}, assignable to vinyl ester grouping[12]. Strong bands at 1640 and 1636 cm^{-1} in methyl and ethyl acetopyruvates, respectively have been assigned to $\nu C=O$ (enolic form)[11-13].

Trisalkoxy and bisalkoxytitanium alkyl acetopyruvates exhibit[3,5,13-21] the following peaks in their IR spectra: a strong band in the region 1750-1725 cm^{-1} assignable to $\nu C=O$ of ester group; strong bands around 1610-1600 cm^{-1} characteristic of $\nu C=O$ mode; strong broad bands in the range 1520-1510 cm^{-1} due to $\nu C \overset{..}{=} C$ coupled with $\nu C \overset{..}{=} O$ mode; strong to medium intensity bands in the regions 615-600 cm^{-1} and 445-435 cm^{-1} due to νTi-O (alkoxy)[22,23] and νTi-O (ligand)[23-29] respectively.

PMR spectrum of methyl acetopyruvate displays signals (δ, ppm, TMS) at 2.38, 4.00 and 6.47 due to CH_3CO, $COOCH_3$, $-CH=$ respectively, while that of ethyl acetopyruvate a three-proton triplet at 1.30 (J = 6Hz) is assigned to $COOCH_2CH_3$, a three-proton singlet at 2.15 to CH_3CO, and a two-proton quartet centred at 4.25 (J = 7Hz) to $COOCH_2CH_3$. The γ-protons are seen at 6.23. Absence of signals due to methylene protons in the alkyl acetopyruvates studied herein, suggest that these exist predominantly in the enol form.

PMR spectral data of some of the trisalkoxy and bisalkoxytitanium alky acetopyruvates exhibit the following characteristic signals: vinylic protons (-CH =) appear in the range 6.30 to 6.37;

Table 1 — Analytical Data of Trisalkoxy & Bisalkoxytitanium(IV) Alkyl Acetopyruvates

Compound	Nature	Ti found (calc) %
$Ti(OEt)_3[MeCOCHCOCOOMe]$	Yellow viscous liquid	14.64 (14.68)
$Ti(OEt)_2[MeCOCHCOCOOMe]_2$	Yellow viscous liquid	11.25 (11.29)
$Ti(OEt)_3[MeCOCHCOCOOEt]$	Yellow-red viscous liquid	14.02 (14.08)
$Ti(OEt)_2[MeCOCHCOCOOEt]_2$	Yellow-red viscous liquid	10.56 (10.59)
$Ti(OPr^i)_3[MeCOCHCOCOOMe]$	Yellow viscous liquid	12.97 (13.01)
$Ti(OPr^i)_2[MeCOCHCOCOOMe]_2$	Yellow semi-solid	10.53 (10.59)
$Ti(OPr^i)_3[MeCOCHCOCOOEt]$	Yellow-red viscous liquid	12.50 (12.53)
$Ti(OPr^i)_2[MeCOCHCOCOOEt]_2$	Yellow-red semi-solid*	9.94 (9.97)

*solidifies on colling.

the methyl protons of the acetyl group are recognized by a singlet in the range 2.11 to 2.20, the methyl protons of methyl ester are identified by a singlet at 3.84; a quartet in the range 4.25-4.35 ($J = 6Hz$) may be assigned to methylene protons of the ester group in ethyl ester; methine protons of the isopropoxy group, $[OC\mathit{H}(CH_3)_2]$ appear as a septet in the range 4.30-5.20 ($J = 6Hz$); and methyl protons of isopropoxy group $[OC\mathit{H}(CH_3)_2]$ and ethoxy group OCH_2CH_3 appear at 1.00-1.50 and 1.39 respectively. However, the appearance of two doublets for methyl protons of isopropoxy group $[OCH(CH_3)_2]$ at 1.28 and 1.29 in the complex $Ti[OCH(CH_3)_2]_2[CH_3COCHCO\text{-}COOCH_3]_2$ may be due to steric interactions which causes isopropoxy methyl protons to be in a different environment.

On the basis of the above preliminary findings, it seems that titanium is hexacoordinated in bis-derivatives (II). However, more definite conclusion regarding their configuration can only be obtained by variable temperature PMR studies.

The authors are grateful to the UGC, New Delhi for financial assistance.

References

1 Mehrotra R C, Bohra R & Gaur D P, *Metal β-diketonates* (Academic Press, London), 1978.

2 Mehrotra R C & Puri D M, *J Less Common Metals*, **3** (1961) 253.

3 Yamamoto A & Kambara S, *J Am chem Soc*, **79** (1957) 4344.

4 Reeves R E & Mazzeno Jr L W, *J Am chem Soc*, **76** (1954) 2533.

5 Podolesov B D, Jordanovska V B, Korunoski M R & Tosev D N, *J inorg nucl Chem*, **36** (1974) 1495.

6 Bradley D C, Mehrotra R C & Wardlaw W, *J chem Soc*, (1952) 2027.

7 Bradley D C, Hancock D C & Wardlaw W, *J chem Soc*, (1952) 2773.

8 Marvel C S & Dreger E E, *Organic Syntheses Collective Vol* 1 (1951) 238.

9 Mehrotra R C, Puri D M & Pandey K C, *J Less Common Metals*, **4** (1962) 393.

10 Mehrotra R C & Puri D M, *J Indian chem Soc*, **39** (1962) 499.

11 Rasmussen R S, Tunnicliff D D & Brattain R R, *J Am chem Soc*, **71** (1949) 1068. Park J D, Brown H A & Lacher J R, *J Am chem Soc*, **75** (1953) 4753.

12 Barnes R B, Gore R C, Liddel U & Williams V Z, *Infrared spectroscopy* (Reinhold, New York), 1944.

13 Nakamoto K, *Infrared spectra of inorganic and coordination compounds* (John Wiley, New York), 1963.

14 Syamal A, *J inorg nucl Chem*, **31** (1969) 1850.

15 Pinchas S, Silver B L & Laulicht I, *J chem Phys*, **46** (1967) 1506.

16 Behnke G T & Nakamoto K, *Inorg Chem*, **6** (1967) 440.

17 Junge H & Musso H, *Spectrochim Acta*, **24A** (1968) 1219.

18 Liang C Y, Schimitschek E J & Trias J A, *J inorg nucl Chem*, **32** (1970) 811.

19 Singh Y P, Saxena S & Rai A K, *Synth react inorg met-org Chem*, **12** (1982) 867.

20 Singh Y P & Rai A K, *Proc Indian acad Sci*, **93** (1984) 177.

21 Singh Y P, Saxena S & Rai A K, *synth react inorg met-org Chem*, **14** (1984) 217.

22 Lynch C T, Mazdiyasni K S, Smith J S & Crawford W J, *Analyt Chem*, **36** (1964) 2332.

23 Barraclough C G, Bradley D C, Lewis J & Thomas I M, *J chem Soc*, (1961) 2601.

24 Nakamoto K, McCarthy P J, Ruby A & Martell A E, *J Am chem Soc*, **83** (1961) 1066.

25 Nakamoto K & Martell A E, *J chem Phys*, **32** (1960) 588.

26 Fay R C & Pinnavaia T J, *Inorg Chem*, **7** (1968) 508.

27 Djordjevic C, *Spectrochim Acta*, **17A** (1961) 448.

28 Gillard R D, Silver H G & Wood J L, *Spectrochim Acta*, **20A** (1964) 63.

29 Mikami M, Nakagawa I & Shimanouchi T, *Spectrochim Acta*, **23A** (1967) 1037.

Indian Journal of Chemistry
Vol. 27A, April 1988, pp. 355-356

Addition Compounds of Dithiophosphinates of Cobalt & Nickel with Acetylpyridines†

R N MUKHERJEE* & B B S SHASTRI
Department of Chemistry, Indian Institute of Technology, Powai, Bombay 400 076

Received 22 *April* 1987; *accepted* 11 *August* 1987

Addition compounds of cobalt and nickel dithiophosphinates with 2-, 3- and 4-acetylpyridine have been prepared. The magentic moments and electronic spectral data are consistent with either MS_4N or MS_4N_2 chromophore. The observed pattern of PMR shifts in cobalt compounds is explained by considering a negative dipolar contribution in addition to contact interaction whereas for the ring protons in the nickel adducts, the shifts are in agreement with σ-delocalisation mechanism.

Isotropic PMR shift has been widely applied as a means to study the properties of paramagnetic transition metal complexes[1,2]. A few reports are available on the addition compounds of metallic dithiophosphinates with pyridine and methylpyridines[3-5]. However, no such studies have been reported with systems having more than one carbon atom in the side chain. To see the effect of two-carbon side chain on the properties of complexes, adducts of diphenyldithiophosphinates of cobalt and nickel, $M(dtpi)_2$ with 2-, 3- and 4-acetylpyridine (2-, 3- and 4-Acpy) have been prepared and characterised by magnetic moments and IR, UV/vis and PMR spectra.

All the chemicals used were chemically pure or of AR grade. A procedure similar to that reported in literature[6] was used to synthesise diphenyldithiophosphinic acid. IR spectra were recorded in KBr on a Pye-Unicam SP 2000 IR spectrophotometer, electronic spectra on a Shimadzu UV 260 spectrophotometer and PMR spectra in $CDCl_3$ on a Varian XL 100 MHz instrument using TMS as the internal standard. Room temperature magnetic measurements were carried out on a Gouy balance using $Hg[Co(SCN)_4]$ as the ;calibrant.

The colour, magnetic moment and analytical data of the complexes are presented in Table 1. All the cobalt complexes were prepared by interacting the mixture of metal chloride and the respective base with the sodium salt of the dithio ligand and the nickel compounds were isolated by treating the corresponding base with $Ni(dtpi)_2$.

The IR spectra of these complexes exhibit $\nu C=C$, $\nu C=N$ and $\nu C=O$ modes around 1470, 1600 and 1700 cm^{-1} respectively. The ν_s P-S and ν_{as} P-S appear around 585 and 650 cm^{-1} respectively. The diadducts of nickel had magnetic moments in the range 3.10-3.20 B.M. and their electronic spectra exhibit bands around 13850 and 21600 cm^{-1}. The monoadduct of nickel having a $\mu_{eff}=3.21$ B.M., exhibits in its electronic spectrum (chloroform) two ligand field bands at 12850 and 21000 cm^{-1} with a shoulder in the intermediate region (18000 cm^{-1}). The electronic spectra of the cobalt compounds display maxima around 14750, 15600 and 17250 cm^{-1} and have μ_{eff} in the range of 4.60-4.70 B.M., as reported for adducts prepared with methylpyridines[5].

The isotropic shifts in the PMR of nickel compounds are predominantly contact in origin[7] whereas both contact and dipolar contributions have been reported[8] for cobalt complexes. The assignments of the various protons could be made on the basis of intensity, line-width and their approach to diamagnetic values upon the addition of more and more ligand. As the actual shifts depends on solution composition, only relative shifts have been discussed. The observed shifts have been normalised to give a value of −10.00 for the α proton. Negative shifts are shifts to lower fields and positive shifts to higher applied fields. The relative isotropic shifts for the present com-

Table 1 —Colour, Magnetic Moment and Analytical Data of Complexes

Complex	Colour	Magenetic moment (B.M.)	Found (Calc.)%	
			M	S
$Co(dtpi)_2$ (2-Acpy)	Blue	4.61	8.52 (8.71)	18.75 (18.90)
$Co(dtpi)_2$ (3-Acpy)	Blue	4.65	8.61 (8.71)	18.72 (18.90)
$Co(dtpi)_2$ (4-Acpy)	Blue	4.68	8.58 (8.71)	18.69 (18.90)
$Ni(dtpi)_2$ (2-Acpy)	Brown	3.21	8.54 (8.68)	18.81 (18.91)
$Ni(dtpi)_2$ $(3\text{-}Acpy)_2$	Green	3 14	7.25 (7.37)	16.01 (16.08)
$Ni(dtpi)_2$ $(4\text{-}Acpy)_2$	Green	3.18	7.30 (7.37)	15.96 (16.08)

---

†Presented at the 74th Session of Indian Science Congress, Bangalore, 1987

Table 2—Relative isotropic Shifts for Ligands Coordinated to Metal Complexes

Ligand	Proton	Relative isotropic shifts	
		Ni (II) adducts	Co (II) adducts
3-Acpy	α-CH	−10.00	−10.00
	β-CH	−3.52	−3.72
	γ-CH	−0.57	−0.65
	$-CH_3$	+0.07	−0.09
4-Acpy	α-CH	−10.00	−10.00
	β-CH	−3.42	−3.57
	$-CH_3$	+0.08	−0.11

plexes are given in Table 2. The solubility of the 2-Acpy adducts of both cobalt and nickel is very poor and hence their PMR spectra could not be recorded.

In the nickel adducts with acetylpyridines, all the ring proton resonances shifted downfield with α = −10.00, β = −3.52 and γ = −0.57 in 3-Acpy and α = −10.00, β = −3.42 in 4-Acpy derivative. There is an attenuation in the shifts with increasing number of intervening bonds between the metal ion and relevant proton. A similar observation was made for other complexes, which is characteristics of σ-delocalisation mechanism[9]. In the acetylpyridine adducts of cobalt, all the ring proton resonances shifted downfield and the relative isotropic shifts were comparable to those observed for the corresponding protons in the nickel complexes. However, the much larger magnitude of actual shifts is not consistent with a pure σ-delocalisation mechanism. This observation can be explained by considering a negative dipolar contribution in addition to contact interaction while positive dipolar contribution has been reported for the acetylacetonate complexes of cobalt[10].

The upfield shifts of methyl protons in 3-and 4-acetylpyridine adducts of nickel dithiophosphinate are small in magnitude (Table 2) to merit any convincing interpretation. It appears that in 4-acetylpyridine the positive spin density on the carbon atom adjacent to the ring is transmitted through the σ-bonded side chain with attenuation. Spin correlation results in negative spin density on the carbon atom attached to β-position of the ring in 3-acetylpyridine. Proximity of this position to the paramagnetic metal ion may lead to more dominant π-delocalisation resulting in reversal of the sign of the spin density on the methyl carbon atom. This would explain the small upfield shift observed for the methyl protons. It would have been of interest to compare our findings with those systems in which saturated carbon-carbon chains are connected to paramagnetic centres through unsaturated framework possessing π-orbitals. Unfortunately, no such studies are available in literature.

References

1 Maitani T, Chikuma M & Tanaka H, *J inorg nucl Chem*, **42** (1980) 1689.

2 Maitani T, Chikuma M & Tanaka H, *J inorg nucl Chem*, **41** (1979) 1121.

3 Mukherjee R N, Venkateshan M S & Zingde M D, *J inorg nucl Chem*, **36** (1974) 547.

4 Mukherjee R N, Venkateshan M S & Zingde M D, *J inorg nucl Chem*, **36** (1974) 1043.

5 Mukherjee R N, Shankar S & Mascarenhas D L, Bull chem Soc Japan, **59** (1986) 3239.

6 Higgins W A, Vogel P W & Craig W G, *J Am chem Soc* **77** (1955) 1864.

7 Maitani T, Chikuma M & Tanaka H, *J inorg nucl Chem*, **41** (1979) 1115

8 Bertini I, Canti G, Luchinat C & Mani F, *J Am chem Soc*, **103** (1981) 7784

9 Boyer A & Fazakerley G V, *J inorg nucl Chem*, **43** (1981) 1955.

10 Happe J A & Ward R L, *J chem Phys*, **39** (1963) 1211.

Indian Journal of Chemistry
Vol. 27A, April 1988, pp. 357-359

Lanthanide(III) Complexes of ONO Donor Schiff Bases Derived from Salicylaldehyde & *o*-Hydroxybenzylamine or *o*-Aminobenzylalcohol†

A SYAMAL* & M R MAURYA
Department of Applied Sciences and Humanities, Kurukshetra University, Kurukshetra 132 119
and
Department of Chemistry, Regional Engineering College, Kurukshetra 132 119

Received 3 *April* 1987; *revised and accepted* 7 *August* 1987

Several new complexes of isomeric schiff bases derived from salicylaldehyde and *o*-hydroxybenzylamine/*o*-aminobenzylalcohol with Pr(III), Nd(III), Sm(III), Gd(III), Tb(III) and Dy(III) have been synthesized and characterized by elemental analysis, molar conductance, IR, electronic spectra and magnetic susceptibility measurements. The schiff bases behave as monobasic tridentate ONO donor and dibasic tridentate ONO donor ligands and form complexes of the type Ln(LH)L.

As water molecules are easily coordinated to lanthanide complexes, the non-aqua lanthanide complexes are less frequently reported. We have undertaken a programme to study the non-aqua lanthanide complexes whose synthesis is effectively promoted by elimination of competition by water molecules through the use of polydentate ligands. In continuation of our earlier[1] work on the non-aqua complexes of Fe(III), Cu(II), V(IV), Mo(V, VI) and W(VI), we now report the synthesis of non-aqua lanthanide(III) complexes of the tridentate ligands (I and II).

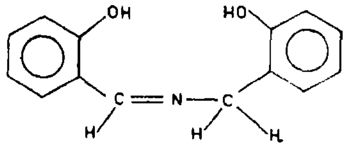

(I)

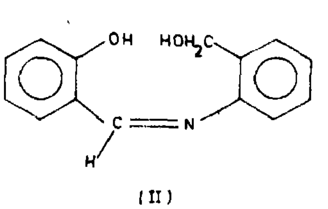

(II)

Lanthanide(III) nitrate hexahydrates were obtained from M/S Indian Rare Earths Ltd. Salicylaldehyde was purchased from Sarabhai M. Chemicals. *o*-Aminobenzylalcohol was purchased from Aldrich Chem. Co. (U.S.A.). *o*-Hydroxybenzylamine was prepared by following the published procedure[2].

The metal contents of the complexes were determined gravimetrically[3] as the metal oxides {Ln_2O_3 where Ln = Nd(III), Sm(III), Gd(III) and Dy(III), Pr_6O_{11} and Tb_4O_7} after decomposing the complexes with conc. HNO_3 and igniting the residue. Nitrogen analyses were done microanalytically. IR spectra were recorded in nujol on a Beckman IR-20 spectrophotometer calibrated with polystyrene. Electronic spectra were recorded on a Beckman DU spectrophotometer in DMF. The molar conductance measurements were carried out on 0.001 *M* solutions in DMF using a Toshniwal conductivity bridge(type C101-02A) and a dip-type cell calibrated with potassium chloride solutions. The magnetic susceptibility measurements were done at room temperature by the Gouy method using $Hg[Co(NCS)_4]$ as the calibrant. The diamagnetic corrections were applied using Pascal's constants[4].

Synthesis of schiff bases—The schiff bases were prepared as described earlier[5].

General method for the synthesis of the complexes—An ethanolic (95%) solution (20 ml) of the appropriate schiff base (0.004 mol) was added with stirring to a 95% ethanolic solution (10 ml) of the respective lanthanide(III) nitrate hexahydrate (0.002 mol) and the mixture was refluxed on a water bath for 2 hr. The resulting yellow solution was treated with 0.5 *N* NH_4OH solution under stirring until the *p*H was adjusted to 5. The yellow precipitate thus obtained was separated by filtration, washed with ethanol and finally dried at 110°C for one hour; yield, 50-60%.

The complexes are insoluble in water and common non-coordinating solvents but are soluble in the coordinating solvents like dimethylformamide. The analytical and magnetic data of the complexes are given in Table 1.

The schiff bases (I and II) react with freshly prepared solutions of lanthanide(III) ions in 1:2 (metal:ligand) ratio and give complexes of the type Ln(LH)L {where Ln = Pr(III), Nd(III), Sm(III), Tb(III) and Dy(III), LH_2 = schiff base (I and II)}. All the complexes are anhydrous and do not contain coordinated H_2O. The analytical data support this view. The complexes have been found to be non-electrolytes (Λ_M = 3.4-12.5 $ohm^{-1}mol^{-1}cm^2$) in dimethylforma-

---

† Presented at the 23rd Annual Convention of Chemists held at Annamalai University, Annamalai Nagar in December, 1986.

Table 1—Analytical and Magnetic Moment Data of Lanthanide(III) Complexes

Compound (colour)	Found (Calc) %		$\mu_{eff.}$, B.M. (Temp, K)
	M	N	
Pr(LH)L (Yellow)	23.7(23.8)	4.5(4.7)	3.50(298)
Nd(LH)L (Dirty yellow)	23.8(24.2)	4.8(4.7)	3.52(298)
Sm(LH)L (Greenish yellow)	24.6(25.0)	4.4(4.7)	1.69(299)
Gd(LH)L (Yellow)	26.0(25.8)	4.4(4.6)	7.91(298)
Tb(LH)L (Yellow)	26.2(26.0)	4.9(4.6)	9.42(301)
DY(LH)L (Yellow)	26.6(26.5)	4.5(4.6)	10.43(300)
Pr(L'H)L' (Yellow)	23.6(23.8)	4.6(4.7)	3.53(301)
Nd(L'H)L' (Dirty yellow)	24.0(24.2)	4.3(4.7)	3.59(299)
Sm(L'H)L' (Greenish yellow)	24.7(25.0)	4.2(4.7)	1.72(298)
Gd(L'H)L' (Yellow)	25.5(25.8)	4.4(4.6)	7.84(300)
Tb(L'H)L' (Yellow)	26.2(26.0)	4.7(4.6)	9.51(299)
Dy(L'H)L' (Yellow)	26.2(26.5)	4.3(4.6)	10.47(302)

Abbreviations: LH_2 = schiff base derived from salicylaldehyde and *o*-aminobenzylalcohol, $L'H_2$ = schiff base derived from salicylaldehyde and *o*-hydroxybenzylamine.

mide. Although there is a possibility of coordination of dimethylformamide, the similarity of electronic spectra of the Sm(III), Gd(III), Tb(III) and Dy(III) complexes in dimethylformamide solution and solid state rules out the coordination of dimethylformamide. Molecular weights of the complexes could not be determined due to their insolubility in a suitable solvent. All the complexes show normal magnetic moment values (Table 1) expected on the basis of their *J* values. Although all the lanthanide(III) complexes could not be studied, the plot of the magnetic moments versus atomic numbers of the lanthanide studied indicated the usual double-humped curve expected for the lanthanides[4].

The free schiff bases exhibit a sharp band at 1615-1657 cm^{-1} due to ν(C=N). On complexation, this band shifts to a lower energy by 10-27 cm^{-1} which might be due to a reduction in the electron density in the azomethine linke owing to the coordination of nitrogen atom to the metal ions[6]. The ν(C—O) (phenolic) occurring at 1530 cm^{-1} in the free schiff bases shifts to higher energy side by 5-10 cm^{-1} indicating the oxygen coordination of these ligands[7]. The ν(C—O) (phenolic) is expected to occur at higher energy in comparison with the ν(C—O) (alcoholic) due to the electron delocalisation towards the benzene ring. The ν(C—O) (alcoholic) mode of the schiff base(II) occurs at 1190 cm^{-1}. In the lanthanide(III) complexes this band shifts to lower energy side by 5-15 cm^{-1} indicating the coordination through the alcoholic oxygen atom of the ligand(II)[5]. The ligands exhibit a medium intensity band at around 2700 cm^{-1} which may be assigned to the intramolecularly hydrogen bonded ν(O—H). In the spectra of lanthanide(III) complexes this band is absent. However, a new broad band appears around 3400 cm^{-1} due to the ν(O—H) of coordinated schiff bases. Thus, it is apparent that the ligands behave as tridentate ones coordinating through ONO donor system. The valence requirement of the metal ion and the infrared data indicate that the two ligands are attached to lanthanide(III) ion in two different forms, viz., one as a monobasic tridentate ONO donor and the other as a dibasic tridentate ONO donor[8].

The electronic spectra of the Nd(III) complexes of the schiff bases (I and II) are identical in dimethylformamide solutions and are different from the reflectance spectra. This difference may be due to the different symmetry of Nd(III) complexes in solid and solution states. The dissimilarity of solution and solid state spectra has been observed for Nd(III) complexes of some schiff bases by other workers[8] also. The electronic spectra of all the other lanthanide(III) complexes are comparable in both solid and solution states. The hypersensitive transition ($^4I_{9/2} \rightarrow {}^4G_{5/2}$, $^4G_{7/2}$) in Nd(III) complexes exhibits a pronounced bathochromic shift (Δν = 110-300 cm^{-1}) in comparison to the spectrum of aquoneodymium(III) complex The electronic spectral band positions of Nd(III) complexes are comparable to those of other octahedral Nd(III) complexes[3,9]. The bathochromic shift of the above hypersensitive band has been used to calculate the nephelauxetic ratio (β) (where $\beta = \nu_{complex}/\nu_{aquo}$) and is in the range 0.9832-0.9884. The covalence factor ($b^{1/2}$) and Sinha metal-ligand covalency parameter (δ%) were calculated using the relations[10]: $b^{1/2} = [1/2(1-\beta)]^{1/2}$ and $\delta\% = 100(1-\beta)/\beta$. The values of $b^{1/2}$ and δ% lie in the ranges 0.0762-0.0919 and 1.174-1.719 respectively and are comparable to those for other similar Nd(III) complexes[8]. The above β, $b^{1/2}$ and δ% values indicate the week covalent character in metal-ligand bonding with a small participation of 4 *f* orbitals in chemical bonding.

The praseodymium(III) complexes exhibit two bands in the visible region at ~16670 (ε = 2.0-2.5) and 22270 (ε = 11.3-11.6) cm^{-1} which are assigned to the hypersensitive transitions $^3H_4 \rightarrow {}^1D_2$ and $^3H_4 \rightarrow {}^3P_0$ respectively[11]; these bands exhibit bathochromic shift (Δν = 170-270 cm^{-1}) in comparison with the spectrum of the aquopraseodymium(III) complex. The other bands due to $^3H_4 \rightarrow {}^3P_1$ and $^3H_4 \rightarrow {}^3P_2$ transitions could not be identified as these are presumably masked by the ligand $n \rightarrow \pi^*$ transition.

The electronic spectra of the schiff bases exhibit three bands at 29410-33330, 36040-36363 and 40000-40820 cm^{-1} due to the $n \rightarrow \pi^*$, hydrogen bonding and association, and $\pi \rightarrow \pi^*$ transitions, respectively. The band due to hydrogen bonding and association is absent in the spectra of the present complexes indicating the coordination of the ligands to the metal ions. The bands due to $n \rightarrow \pi^*$ and $\pi \rightarrow \pi^*$ transitions undergo a red shift to 26800-29600 ($\varepsilon = 10200$-12680) and 37200-39215 ($\varepsilon = 11280$-14280) cm^{-1} respectively in the lanthanide(III) complexes suggesting coordination of the schiff bases to the metal ions. The isomeric schiff bases (I and II) have produced isomeric lanthanide(III) complexes which have comparable chemical, spectral and magnetic properties. The electronic spectra of the dysprosium(III) and samarium(III) complexes of the schiff bases (I and II) are quite comparable and these complexes do not exhibit any band resulting from the 4*f* transitions and only exhibit the $n \rightarrow \pi^*$ and $\pi \rightarrow \pi^*$ transitions [Dy(LH)(L), 26950 ($\varepsilon = 11350$), 38910 ($\varepsilon = 14250$) cm^{-1}; Dy(L'H)(L'), 28990($\varepsilon = 12500$), 38480($\varepsilon = 14600$) cm^{-1}; Sm(LH)(L), 26800($\varepsilon = 10850$), 38760($\varepsilon = 13400$) cm^{-1}; Sm(L'H)(L'), 28735 ($\varepsilon = 11450$), 38315($\varepsilon = 13850$) cm^{-1}]. The similarity in the electronic spectra is expected since these two ions are hole equivalent of each other. Dutta and Das[8] have also reported the absence of *f-f* bands due to the presence of charge-transfer transitions in the Dy(III) and Sm(III) complexes of some schiff bases. Gadolinium(III) and terbium(III) complexes also exhibit only $n \rightarrow \pi^*$ and $\pi \rightarrow \pi^*$ transitions and do not show any band due to 4*f* transitions and this is in line with the electronic spectral properties of other Gd(III) and Tb(III) complexes[12].

On the basis of the above discussion a six-coordinated octahedral structure is suggested for the complexes.

The authors are thankful to the CSIR, New Delhi for financial support of the work and for the award of a Senior Research Fellowship to MRM.

References

1 Syamal A & Kale K S, *Inorg Chem*, **18** (1979) 992; *Transition Metal Chem*, **4** (1979) 298; *Indian J Chem*, **19A** (1980) 438; Syamal A & Maurya M R, *Synth react inorg met org Chem*, **16** (1986) 857.
2 Raiford L C & Clark F P, *J Am chem Soc*, **45** (1923) 1738.
3 Willard H H & Diehl H, *Advanced quantitative analysis*, D Van Nostrand Company Inc, New York) 1965, 311.
4 Dutta R L & Syamal A, *Elements of magnetochemistry*, S Chand and Co, New Delhi) 1982, 9.
5 Syamal A & Singhal O P, *Transition Metal Chem*, **4** (1979) 179; Syamal A & Kumar D, *Synth react inorg met org Chem*, **10** (1980) 63.
6 Maggio F, Pizzino T & Romano V, *Inorg nucl chem Lett*, **10** (1974) 1005.
7 Batley G E & Graddon D P, *Aust J Chem*, **20** (1967) 877.
8 Dutta R L & Das B R, *Indian J Chem*, **23A** (1984) 524.
9 Rajasekar N & Soundarajan S, *J inorg nucl Chem*, **43** (1981) 977.
10 Sinha S P, *Spectrochim Acta*, **22** (1966) 57.
11 Henrie D E, *Coord Chem Rev*, **18** (1976) 119.
12 Hamer A M & Livingstone S E, *Transition Metal Chem*, **8** (1983) 298.

Indian Journal of Chemistry
Vol. 27A, April 1988, pp. 360-361

Some Novel Cationic Mixed Ligand Complexes of Cobalt(III)

N THANKARAJAN* & K MOHANAN
Department of Chemistry,
University of Calicut, Kerala 673635

Received 24 *November* 1986;
revised and accepted 24 *August* 1987

Mixed ammine complexes of cobalt(III) of the type $[Co(NH_3)_3(tridentate)]NO_3$, wherein 'tridentate' denotes the dibasic tridentate schiff base moiety derived from N-acetylacetoneglycine, N-salicylideneglycine or N-(2-hydroxy-1-naphthylidene)glycine, have been prepared using $[Co(NH_3)_5CO_3]NO_3$ as the synthetic intermediate. These diamagnetic complexes have been characterised by elemental analytical, molar conductance, UV, IR and NMR spectral data. The N-(2-hydroxy-1-naphthylidene)glycine complexes containing chloride, bromide, iodide and perchlorate anions instead of nitrate have also been obtained. Infrared spectra of these compounds reveal that hydrogen bonding of the ammine ligands with the anion gets weakened as the size of the latter increases

Although mixed ligand complexes of cobalt(III) have been extensively investigated[1], cationic mixed complexes containing tridentate schiff base as primary ligand have received only scanty attention. Herein we report complexes of the type, $[Co(NH_3)_3(tridentate)]NO_3$, obtained by reacting $[Co(NH_3)_5(CO_3)]NO_3$ with potassium salts of N-acetylacetoneglycine, N-salicylideneglycine and N-(2-hydroxy-1-naphthylidene)glycine. A series of compounds with chloride, bromide, iodide and perchlorate replacing nitrate in the parent compound could be prepared in the case of the complex of N-(2-hydroxy-1-naphthylidene)glycine. These salts permitted a comparative IR spectral study of the hydrogen bond interactions of the anion with the ammine ligands.

All the chemicals used were either BDH (Analar) or E. Merck (GR) reagents. Commercial solvents were distilled and used.

Synthesis of $[Co(NH_3)_3(tridentate)]NO_3$

To $[Co(NH_3)_5(CO_3)NO_3].\frac{1}{2}H_2O$ (2.75 g, 0.01 mol) in refluxing methanol (70 ml) was added slowly a methanolic solution of potassium salt of the ligand (0.01 mol, 50 ml, *p*H adjusted to ~ 5.5). After refluxing for 3 h, the mixture was filtered hot and the filtrate concentrated over a water-bath to about 25 ml. The complex which crystallised on allowing the solution to cool, was filtered and dried *in vacuo*. The complexes were recrystallised from methanol.

Synthesis of $[Co(NH_3)_3(nap{:}gly)]X$ *where* $X = Cl, Br, I$ *or* ClO_4

A saturated aqueous solution (15 ml) of the appropriate salt (KCl, KBr, KI, $NaClO_4$) was added to a concentrated solution of $[Co(NH_3)_3(nap{:}gly)]NO_3$ in methanol (30 ml). The precipitated complex was filtered, washed with water (20 ml) and ether and dried *in vacuo*.

Infrared spectra were recorded in KBr and nujol in the range 4000-400 cm^{-1} on a Pye Unicam SP 3-300 infrared spectrophotometer. ^1HNMR spectra were recorded in DMSO-d_6 on a Varian XL-100 FT NMR specrometer, using TMS as reference. UV spectra were recorded on a Pye Unicam SP 1800, UV-visible spectrophotometer. Molar conductances of 10^{-3} *M* solutions in methanol were measured using a Toshniwal conductivity bridge.

Analytical data of the complexes are in good accord with their formulations (Table 1). All the complexes are diamagnetic and their molar conductances fall within the range expected for uni-univalent electrolytes[2]. These mixed ligand complexes could be recrystallised repeatedly from methanol without any change in composition, and were found chromatographically pure (TLC/silica gel). Cationic nature of the complexes was further confirmed by their quantitative and tenacious adsorption by cation exchange resins.

N-β-Diketoneglycine, N-salicylideneglycine and N-(2-hydroxy-1-naphthylidene)glycine have been shown to exist as β-ketoenamine-, hydroxyimine- and quinoneamine-N-acetic acids respectively[3,4], and to form metal chelates through their ONO donor set. Electronic spectra of the mixed ligand complexes are similar to those of the corresponding $Na[Co(tridentate)_2]$ complexes[3,4], indicating thereby that the tautomeric structure and bonding mode of the chelates ligand moiety, as well as the overall geometry of the metal complexes, remain unaltered in the mixed ligand complexes also.

Signal for the N − H proton of the tridentate ligand (at ~ 13.5 δ) was absent in the ^1H NMR spectra of the complexes, thus confirming deprotonation during metal chelation.

Infrared spectral data are also quite in agreement with the reported[3,4] bonding mode of the tridentate ligand moieties in metal complexes.

Table 1 – Characterisation Data of Cationic Mixed Ligand Cobalt(III) Complexes of N-Acetylacetoneglycine (H_2acac:gly), N-Salicylideneglycine (H_2sal:gly) and N-(2-Hydroxy-1-naphthylidene)glycine (H_2nap:gly)

Complex (yield, %)	Found (Calc.) %			Molar conductance (mho cm^2 mol^{-1})	ν(N – H) cm^{-1}
	C	H	N		
[Co(NH_3)$_3$(acac:gly)]NO_3	25.38	5.25	21.40	90.15	3405
(65)	(25.68)	(5.55)	(21.40)		3500
[Co(NH_3)$_3$(sal:gly)]NO_3	31.50	4.51	19.77	83.12	3415
(62)	(30.94)	(4.62)	(20.05)		3510
[Co(NH_3)$_3$(nap:gly)]NO_3	38.61	4.10	16.89	81.80	3410
(67)	(39.10)	(4.55)	(17.54)		3500
[Co(NH_3)$_3$(nap:gly)]Cl	41.91	4.51	14.71	90.19	3300
(63)	(41.88)	(4.87)	(15.03)		
[Co(NH_3)$_3$(nap:gly)]Br	38.19	4.48	13.91	84.20	3330
(61)	(37.40)	(4.35)	(13.43)		
[Co(NH_3)$_3$(nap:gly)]I	33.80	4.15	11.80	95.19	3370
(58)	(33.62)	(3.91	(12.07)		
[Co(NH_3)$_3$(nap:gly)]ClO_4	35.59	3.97	12.70	97.17	3425
(58)	(35.74)	(4.16)	(12.83)		3520

Breadth and relatively high intensity of ν(N – H) band of the ammine ligands seemed to indicate hydrogen bonding of the ammine with the anion. Spectra of a series in which the nitrate in [Co(NH_3)$_3$(nap:gly)]NO_3 was replaced by other counter anions like chloride, bromide, iodide and perchlorate confirmed occurrence of the above type of hydrogen bonding. Thus, position and appearance of the ν(N – H) band (nujol mull spectra) of the complex salts were found to be dependent on the nature of the anion, changing from a broad band at low frequency for the chloride, to sharper and more resolved bands at higher frequencies with increasing size of the anion. These changes indicate the declining strength of the N – H...X hydrogen bonding in the order $Cl^- > Br^- > I^- > (NO_3)^- > (ClO_4)^-$. Since charge density increases with decreasing size of the anion, the above trend is to be expected[5].

Attempted direct synthesis of the mixed ligand complexes was not successful. This reveals the useful role of labile metal complexes as synthetic intermediates.

References

1 Syamal A & Mandal P K, *Indian J Chem*, **19A** (1980) 812.

2 Geary W J, *Coord Chem Rev*, 7 (1971) 81.

3 Thankarajan N & Mohanan K, *Indian J Chem*, **26A** (1987) 234.

4 Thankarajan N & Mohanan K, *J Indian Chem Soc*, **63** (1986) 861.

5 Chatt J, Leigh G J & Thankarajan N, *J chem Soc* (*A*), (1971) 3168.

Indian Journal of Chemistry
Vol. 27A, April 1988, pp. 362-363

Synthesis & Characterisation of Some Lanthanide Perchlorate Complexes of 4-Nitrosoantipyrine

H JAYASANKAR & P INDRASENAN*
Department of Chemistry, University of Kerala
Trivandrum 695 034

Received 25 *May* 1987; *revised and accepted* 17 *August* 1987

Seven lanthanide perchlorate complexes of 4-nitrosoantipyrine (NAP) of the general formula $[\mathrm{Ln(NAP)_4ClO_4}](\mathrm{ClO_4})_2$ (where Ln = La, Pr, Nd, Sm, Gd, Dy and Y), have been synthesised and characterised by elemental analyses, molecular weights, conductances, magnetic moments and infrared and electronic spectral data. In these nine-coordinated complexes, all the four NAP molecules are coordinated bidentately and one of the perchlorate groups is coordinated monodentately.

As part of our programme on the synthesis and characterisation of solid lanthanide complexes[1-4], we now report herein seven lanthanide perchlorate complexes of 4-nitrosoantipyrine (NAP), in which one of the perchlorate groups is also coordinated. In this respect, these complexes are very interesting. The ligand NAP has two donor sites, namely the ring carbonyl and the nitroso group and, therefore, it is expected to behave like a bidentate ligand forming a stable six-membered ring with the metal ion.

Perchlorates of La, Pr, Nd, Sm, Gd, Dy and Y were prepared from the respective oxides (99.9% pure) as reported earlier[1]. The ligand NAP, was prepared by the literature method[5] and its purity checked by elemental analyses and IR spectral data, m.p. 192° (lit.[5] m.p. 192°).

Solutions containing lanthanide perchlorates (2 mmol) and NAP (8.1 mmol) in minimum quantity of hot ethanol were kept under reflux for 2 hr and cooled to room temperature (28 ± 2°C). To the reaction mixture was added ether in small portions with vigorous stirring. The precipitates obtained were filtered, washed repeatedly with hot benzene and ether and dried *in vacuo* over phosphorus pentoxide. The complexes were analysed for the metal and perchlorate contents by the conventional methods[6,7].

The molar conductances of $10^{-3}M$ solutions of the complexes in nitrobenzene, methanol and acetonitrile were determined at room temperature (28 ± 2°C) on an ELICO M 82T conductivity bridge with a dip-type cell and platinum electrodes (cell constant = 1.56 cm^{-1}). The room temperature magnetic susceptibilities of the complexes were measured by the Gouy method using mercury(II) tetrathiocyanatocobaltate(II) as the calibrant[8]. Molecular weights of the complexes were determined by the Rast method using biphenyl as the solvent[9]. The IR spectra of the ligand and the complexes were recorded in KBr on a Perkin-Elmer 397 IR spectrophotometer in the range 4000-400 cm^{-1}. The electronic spectra of $10^{-4}M$ solutions of the ligand and the complexes in acetonitrile were recorded on a Hitachi 220A UV-visible spectrophotometer.

The analytical, molecular weight, molar conductivity and magnetic data of the complexes are presented in Table 1. All the seven complexes are reddish brown, non-hygroscopic solids. These are soluble in acetone, acetonitrile, nitrobenzene, methanol and ethanol and insoluble in benzene, petroleum ether and ether. The complexes can be represented by the general composition $\mathrm{Ln(NAP)_4(ClO_4)_3}$ (where Ln = La, Pr, Nd, Sm, Gd, Dy and Y, and NAP = 4-nitrosoantipyrine).

The molar conductances of the complexes correspond to 2:1 electrolytes, indicating that one of the perchlorate ions is coordinated to the metal ions. However, slightly higher conductances of Gd and Dy complexes in acetonitrile are probably due to partial substitution for the coordinated perchlorate ions by the solvent molecules (acetonitrile). In fact, these higher values are always much less than those expected for a 3:1 electrolyte.

The room temperature magnetic data show that all the complexes, except those of La and Y, are paramagnetic; La and Y complexes are diamagnetic as expected. The observed magnetic moments are generally found to agree well with the theoretical values calculated by the Van-Vleck formula[10].

The IR spectrum of the free ligand exhibits νC = O and νN = O modes as strong bands at 1680 and 1410 cm^{-1} respectively, which are shifted to 1630 and 1390 cm^{-1}, respectively in the complexes. These shifts to lower wavenumbers indicate that NAP is coordinated to the lanthanide ion through the oxygen atoms of these two groups. Comparatively, smaller shift ($\Delta\nu$ = 20 cm^{-1}) in the νN = O mode on coordination is probably due to its coupling with other stretching vibrations of the ligand[11].

The IR spectra of the complexes exhibit strong, doubly split band with band maxima at 1110 and 1090 cm^{-1} which are assigned to the ν_3 vibration of the monodentately coordinated perchlorate ion having C_{3v} symmetry[12]. Two more additional bands, a medium band at 925 and a strong band at 620 cm^{-1}, which are unsplit and absent in the spectrum of the ligand are

Table 1 – Analytical, Conductance, Magnetic and Molecular Weight Data of Lanthanide(III) Perchlorate Complexes of 4-Nitrosoantipyrine

Complex	Found (Calc)%		Mol wt*	Molar conductivity (ohm^{-1}cm^{2}mol^{-1})			Magnetic moment* (B.M.)
	Metal	Perchlorate		Nitrobenzene	Methanol	Acetonitrile	
$[La(NAP)_4ClO_4](ClO_4)_2$	10.89 (10.64)	22.20 (22.85)	1270 (1305)	71.06	174.39	257.54	0.00 (0.00)
$[Pr(NAP)_4ClO_4](ClO_4)_2$	10.74 (10.78)	22.46 (22.82)	1268 (1307)	73.92	189.40	293.88	3.60 (3.62)
$[Nd(NAP)_4ClO_4](ClO_4)_2$	11.20 (11.01)	22.38 (22.76)	1281 (1310)	77.14	185.09	282.80	3.68 (3.68)
$[Sm(NAP)_4ClO_4](ClO_4)_2$	11.87 (11.42)	22.32 (22.65)	1292 (1317)	75.70	158.20	257.58	1.63 (1.55-1.65)
$[Gd(NAP)_4ClO_4](ClO_4)_2$	11.63) (11.88)	(21.81) (22.53)	1265 (1324)	76.50	218.54	374.94	7.70 (7.94)
$[Dy(NAP)_4ClO_4](ClO_4)_2$	11.76 (12.23)	21.91 (22.46)	1301 (1328)	76.59	214.47	330.90	10.61 (10.60)
$[Y(NAP)_4ClO_4](ClO_4)_2$	7.01 (7.08)	23.50 (23.76)	1205 (1255)	70.24	184.18	288.47	0.00 (0.00)

* Values given in brackets are the theoretical values

assigned to the v_1 and v_4 vibrations, respectively of the perchlorate ion.

The electronic spectrum of the ligand displays three intense absorption bands at 30.86 ($n \rightarrow \pi^*$), 43.10 ($\pi \rightarrow \pi^*$) and 46.29 kK ($\pi \rightarrow \pi^*$). All these bands are red shifted in the spectra of the complexes. The very strong band observed in the visible region with absorption maximum in the region 26.59 – 28.09 kK may be assigned to the strong L → M charge-transfer (CT) transition. Most of the absorption bands due to *f-f* transitions of the lanthanide ions in the visible region are obscured in the complexes and are replaced by broad CT bands (L → M) that spread over the whole visible region.

On the basis of the above discussion and the molecular weights of the complexes (Table 1), the lanthanides in the present series of complexes which are represented by the general formula $[Ln(NAP)_4ClO_4](ClO_4)_2$ are assigned a coordination number of nine.

We are thankful to Prof C G R Nair, for his useful suggestions, and to the University of Kerala for the award of a research fellowship to one of us (H J).

References

1 Giri V & Indrasenan P, *Polyhedron*, **2** (1983) 573.

2 Radhakrishnan P K, Indrasenan P & Nair C G R, *Polyhedron*, **3** (1984) 67.

3 Jayasankar H & Indrasenan P, *Indian J Chem*, **26A** (1987) (in press).

4 Jayasankar H & Indrasenan P, *J less-common Met*, **132** (1987) 43.

5 Nanda B, Padmanavan S, Tripathy B & Mittra A S, *J Indian chem Soc*, **52** (1975) 533.

6 Kolthoff I M & Elving P J, *Treatise on analytical chemistry* Part II, Vol 8 (Interscience, New York), 1963.

7 Kurz E, Kober G & Berl M, *Analyt Chem*, **30** (1958) 1983.

8 Lewis J & Wilkins R G (Eds), *Modern coordination chemistry* (Interscience, New York) 1960.

9 Palmer W G, *Experimental physical chemistry* (The University Press, Cambridge) 1954.

10 Van Vleck J H & Frank N, *Phys Rev*, **34** (1927) 1494.

11 Koppikar D K, Sivapulliah P V, Ramakrishnan L & Soundararajan S, *Structure and bonding*, **34** (1978) 135.

12 Nakamoto N, *Infrared spectra of inorganic and coordination compounds* (Wiley, New York) 1963.

Indian Journal of Chemistry
Vol. 27A, April 1988, pp. 364-365

Mixed Ligand Complexes of Sulphadiazine & Sulphadimidine as Secondary Ligands & Ethylenediaminetetraacetic Acid & Nitrilotriacetic Acid as Primary Ligands: Complexes of Lanthanides(III) & Transition Metal Ions

MOHAMED M SHOUKRY*† & EMAN M SHOUKRY
Department of Chemistry,
Faculty of Science, Cairo University, Giza, Egypt

Received 12 *February* 1987; *revised* 8 *May* 1987;
accepted 3 *September* 1987

The *p*H-metric titrations of the reaction mixtures containing equimolar solutions of metal ion, EDTA or NTA and sulpha have shown the formation of 1:1:1 mixed ligand complexes. The pK_a of sulpha and formation constants of the resulting complexes have been determined at 25°C ($\mu = 0.1$ *M* $NaNO_3$). The stabilities of the lanthanide complexes follow the order: La < Gd < Ho > Yb; while stabilities of transition metal complexes follow the order: Mn < Co < Ni < Cu > Zn. The mode of chelation has been deduced from conductivity measurements.

In pursuit of our research work oriented towards the study of the metal complexes of biologically active ligands[1-6], we report herein the formation constants of the mixed ligand complexes of some lanthanides as La(III), Gd(III), Ho(III) and Yb(III) and some transition metal ions as Cu(II), Zn(II), Ni(II), Co(II) and Mn(II), with EDTA or NTA as primary ligands and sulphadiazine and sulphadimidine as secondary ligands. The mode of chelation of these sulpha drugs has been ascertained from conductivity measurements.

All solutions were prepared in doubly distilled, deionised water. The sulpha drugs used were of pure quality. The lanthanide and transition metal nitrates were BDH products and their solutions were prepared and standardised as previously described[7].

The *p*H meter (Schott) and electrodes (glass-calomel) were calibrated using standard buffer solutions.

The following mixtures (A−C) were prepared for the determination of acid dissociation constant of sulpha drugs and formation constants of the mixed ligand complexes and titrated against 0.15 *M* NaOH: (A) 5 ml of 0.80 *M* $NaNO_3$ + 20 ml of ethanol + 15 ml of water + required weight of sulpha to make 0.00375 *M* solution; (B) 5 ml of 0.80 *M* $NaNO_3$ + 10 ml of 0.015 *M* EDTA (or NTA) + 5 ml of 0.03 *M* metal ion + 20 ml of ethanol; and (C) 5 ml of 0.80 *M* $NaNO_3$ + 20 ml of ethanol + 10 ml of 0.015 *M* EDTA (or NTA) + 5 ml of 0.03 *M* metal ion + required weight of sulpha to make 0.00375 *M* solution. The following mixture (D) was titrated conductometrically against 0.15 *M* NaOH: (D) 20 ml of ethanol + 10 ml of 0.015 *M* EDTA (or NTA) + 10 ml of 0.015 *M* metal ion + required weight of sulpha to make 0.00375 *M* solution.

All titrations were carried out in a special vessel described elsewhere[1], at 25°C in a purified N_2 atmosphere. The solvent composition used was 50% (v/v) aq. ethanol. The *p*H meter readings were corrected to get the actual $[H^+]$ using the method of Van Uitert and Hass[8]. The correction factor at 25°C and $\mu = 0.1$ *M* in 50% (v/v) aq. ethanol was found to be − 0.25.

Calculations were made with the aid of the MINIQUAD-75 computer program[9] on an IBM-4331 computer. The model selected was that which gave the best statistical fit and consistent with chemical logic. The formation of mixed ligand complexes of lanthanide and transition metal ions is assumed to involve equilibria (1-3):

$$HS \rightleftharpoons H^+ + S^- \quad \ldots (1)$$

$$Ln(EDTA)^- + S^- \rightleftharpoons [Ln(EDTA)S]^{2-} \quad \ldots (2)$$

$$M(NTA)^- + S^- \rightleftharpoons [M(NTA)S]^{2-} \quad \ldots (3)$$

The formation constants $K^{Ln(EDTA)}_{Ln(EDTA)S}$ and $K^{M(NTA)}_{M(NTA)S}$ were calculated assuming that the complexes $Ln(EDTA)^-$ and $M(NTA)^-$ are undissociated in

Table 1 − Formation Constants of Mixed Ligand Complexes of Sulphadiazine (SZ) and Sulphadimidine (SM)

System	log*K**	System	log*K**
Sulphadiazine	7.66(0.01)	Ho-EDTA-SM	3.25(0.05)
Sulphadimidine	8.30(0.01)	Yb-EDTA-SM	2.93(0.05)
La-EDTA-SZ	2.00(0.21)	Cu-NTA-SM	2.78(0.01)
Gd-EDTA-SZ	2.70(0.05)	Ni-NTA-SM	1.90(0.02)
Ho-EDTA-SZ	3.23(0.05)	Co-NTA-SM	1.41(0.03)
Yb-EDTA-SZ	2.91(0.05)	Zn-NTA-SM	1.49(0.03)
La-EDTA-SM	1.47(0.30)	Mn-NTA-SM	1.24(0.06)
Gd-EDTA-SM	2.62(0.05)		

*Standard deviations are given in parentheses.

---

†Present address: University of United Arab Emirates, Faculty of Science, Al-Ain, P.O. Box 15551, United Arab Emirates.

the region of formation of mixed ligand complexes.

*p*H titration curve of a 1:1 mixture of Gd(III) and EDTA shows an inflection at $a=2$, (a = number of mols of base added per mol of ligand), indicating the formation of a simple 1:1 complex. The mixed Gd(III)-EDTA-sulpha (1:1:1) solution does not show a sharp inflection at $a=2$, but it reveals two inflections at $a=3$ and 4. Also the mixed ligand titration curve coincides with the Gd(III)-EDTA titration curve between $a=0$ and $a=2$. The formation of the mixed ligand complex is also supported by the fact that the experimental titration curve of the mixed ligand system is quite different from the composite curve obtained by graphical addition of free sulpha curve to 1:1 Gd(III)-EDTA curve.

As expected, the formation constants of the mxied ligand complexes of lanthanides follow the order: La(III) < Gd(III) < Ho(III) > Yb(III) (Table 1).

The conductometric titration curve for the ternary complex of Gd(III) shows initial decrease in conductance and an inflection at $a=2$. This may be ascribed to the neutralisation of H^+ ions resulting from the formation of Gd-EDTA complex. Between $a=2$ and $a=3$, the conductance increases slightly, most likely due to the formation of a ternary complex associated with the release of H^+ ion from the sulpha. Beyond $a=3$, the conductance increases appreciably due to the presence of excess NaOH.

The formation of the mixed ligand complexes of transition metal ions containing NTA and sulphadimidine is ascertained by the fact that the experimental mixed ligand titration curve is quite different from the composite curve. The formation constants of the mixed ligand complexes, follow the order: Mn(II) < Co(II) < Ni(II) < Cu(II) > Zn(II) (Table 1) which is in accord with Irving-Williams order[10] for bivalent metals of 3*d* series.

The trend observed in the conductometric titration of the mixed ligand complexes with NTA is the same as that found in mixed ligand complexes with EDTA, and probably is due to the same causes.

Chelation is, therefore, achieved by a tautomeric shift of the sulphonamide hydrogen to the sulphonyl oxygen. This can explain the chelating ability of sulphonamide when a six-membered stainless chelate ring is formed.

It is interesting to note that the binary complexes of sulpha with the transition and lanthanide metal ions could not be detected in solution, because of the insolubility of sulpha. The formation and stability of the mixed ligand complexes may be attributed to the π back-bonding from $[Ln(EDTA)]^{2-}$ and $[M(NTA)]^-$ to the heteroaromatic nitrogen base (sulpha)[11,12].

References

1 Shoukry M M, Khater M M & Shoukry E M, *Indian J Chem*, **25A** (1986) 488.

2 Rabenstein D L, Isab A A & Shoukry M M, *Inorg Chem*, **21** (1982) 3234.

3 Rabenstein D L, Daignault S A, Isab A A, Arnold A P & Shoukry M M, *J Am chem Soc*, **107** (1985) 6435.

4 Shoukry M M, Darwish N A & Hosny W M, *J Chinese chem Soc*, **33** (1986) 179.

5 Shoukry M M, Mahgoub A E & Hosny W M, *Trans Met Chem*, (In press).

6 Shoukry M M, Khairy E M & Saeed A, *Trans Met Chem*, (In press).

7 Pribil R, *Applied complexometry* (Pergamon Press, London), 1982.

8 Van Uitert L G & Hass C G, *J Am chem Soc*, **75** (1953) 451.

9 Gans P, Sabatini A & Vacca A, *Inorg chim Acta*, **18** (1976) 237.

10 Irving H & Williams R P, *Nature* (London), **162** (1948) 746.

11 Munakata M, Harada M & Niina S, *Inorg Chem*, **15** (1976) 1727.

12 Sigel H, Fischer B E & Prijs B, *J Am chem Soc*, **22** (1977) 4489.

Indian Journal of Chemistry
Vol. 27A, April 1988, pp. 366-367

Spectrophotometric Determination of Traces of Osmium with 4-Sulpho-2-aminobenzenethiol

ANIL K CHAKRABARTY[†]
Department of Chemistry Jadavpur University
Calcutta 700 032

Received 20 *April* 1987; *revised and accepted* 10 *August* 1987

Spectrophotometric method for the determination of ultratrace quantities of osmium(VI) with 4-sulpho-2-aminobenzenethiol is described. Os(VI) forms a violet 1:2 complex with the reagent; it is stable for 3 hr and has λ_{max} at 490 nm. Beer's law is obeyed from 0.5 to 16 ppm of Os with a photometric error of 2.7%. The molar absorptivity and Sandell's sensitivity values are 1.08×10^4 $1.mol^{-1}cm^{-1}$ and 0.175 $\mu g/cm^{-2}$ Os(VI) respectively at 490 nm.

The osmium determination is important due to its well-known association with other Pt-group metals and lack of suitable micro-chemical techniques. The separation process as well as its individual determination, specially in presence of iridium and palladium matrices, is a real problem in both the pure and applied analytical chemistry.

The osmium content of many biological species (0.01-0.1 ppm range) is required to be determined accurately and reasonably rapidly. Although many thio reagents have been proposed[1-4] for the determination of trace amounts of osmium, and they are highly sensitive, they require strict control of several parameters.

In this note, a sensitive and selective method for the determination of osmium in presence of other Pt-group metals is presented. It is based on the formation of a 1:2 complex by Os(VI) with 4-sulpho-2-aminobenzenethiol.

Absorbance measurements were made on Hilger-Uvispek and Perkin-Elmer digital spectrophotometers using 2-cm matched glass cuvettes.

Osmium solution was prepared by dissolving OsO_4 (Johnson & Methey) in 50 ml of 0.2 *M* NaOH and diluted to 100 ml. A standard stock solution (0.1 mg/ml) was prepared from this solution.

4-Sulpho-2-aminobenzenethiol was synthesised as reported earlier[5]. A freshly prepared 1% reagent solution in water was used. All chemicals used were of A R or G R quality.

Procedure

An aliquot of standard osmium (0-400 μg) solution was mixed with 4 ml of 1% reagent solution and 4 ml of 12 *M* hydrochloric acid in a 25 ml volumetric flask The solution was mixed thoroughly and the volume was made up to the mark. A reagent blank was prepared exactly in the same way; it did not absorb in the range of λ_{max} of the complex. A water blank was found almost satisfactory. The absorbance of the violet osmium(VI) complex was measured at 490 nm.

The spectrum was recorded over the wavelength range 400-600 nm. The complex showed maximum absorption at 490 nm in aqueous medium. The reagent showed no absorption in the range. All measurements were made at 490 nm. The Os(VI) complex is formed in the presence of 0.2-3.8 *M* HCl. The optimum acidity range was found to be 1.7-2.9 *M* HCl. Therefore, 4 ml of 12 *M* HCl was used in the estimations.

Effect of reagent concentration and stability of colour—A 1% reagent solution was used to study the effect of reagent concentration on the complexation of osmium. The optimum range was 2.0-6.0 ml of 1% reagent; 3 ml of 1% solution was found sufficient for complete formation of the violet coloured complex.

The complex formation was independent of the mode of addition of variables and it formed immediately on addition of the acid and the reagent solutions. The system is stable for more than 3 h at room temperature (30°C).

Beer's law, optimum range, photometric error, molar absorptivity and sensitivity—The osmium(VI) complex obeyed Beer's law over the range 0.5-16 ppm of Os(VI) at 490 nm. The optimum range of determination obtained from Ringhbom's plot[6] was 2-14 ppm. The relative photometric error was 2.7% (cf. Ayres' plot[7]). The molar absorptivity (Beer's law) and Sandell's sensitivity[8] were 1.08×10^4 $1.mol^{-1}cm^{-1}$ and 0.0175 $\mu g\, cm^{-2}$ Os(VI) at 490 nm, respectively.

Effect of diverse ions—The foreign ions were mixed with 8 ppm of Os(VI) in the final volume and the tolerance limit was set at 0.005 scale unit at 490 nm. A 25-fold excess of Fe(III), Fe(II), Cr(VI), Cr(III), Ni(II), Co(II), Mn(II), Zn(II), Cd(II), Ca(II), Ba(II), Sr(II), Bi(III), Al(III), Sb(III), As(V), Mo(VI), W(VI), U(VI), Nb(V), Ti(IV), Sn(II), Tl(I), Cu(II) and a 15-fold excess of Ru(III), Rh(III), Ir(III), Pt(IV), Pt(II) did not interfere in the normal procedure. Pd(II) did not interfere when present in 1:1 ratio. Fifty-fold excess of EDTA, citrate, oxalate, tartrate, acetate chloride, bromide, iodide, phosphate, iodate, borate, perchlorate, sulphate and nitrate did not interfere. Hg(II), thiocyanate, Ag(I) and cyanide showed strong interference.

[†] Presented at the 56th Annual Session of Natl. Acad. Sci., 1986, Jaipur.

Composition of osmium(VI) complex and stability constant—The composition of the complex was determined by the continuous variation and mole-ratio methods[9,10]. The plot of absorbance against M/M + R (M = metal, R = reagent) ratio showed a 1:2 [OS(VI):thiol] compoition at 490 nm. The composition was verified by mole ratio method using the equimolar solutions and a constant metal concentration.

The instability constant $K' = [(n\alpha c)^n.(\alpha c)]/[c(1-\alpha)]$ and the degree of dissociation $\alpha = A_m - A_s/A_m$ were calculated from the M:R ratio in reagent effect studies for 1:2 osmium(VI) complex. The value of α and thermodynamic stability constant (K) as evaluated by the Harvey-Mannings method[11] came out to be 0.2093 and 8.89 (log K) respectively at 30°C.

The author gratefully acknowledges the CSIR, New Delhi for a position in the Scientist Pool.

References

1 Beamish F E, *The analytical chemistry of noble metals* (Pergamon, Oxford), 1966.
2 Majumdar A K & Bhowal S K, *Anal chim Acta*, **62** (1972) 233.
3 Sandell E E, *Ind Engng Chem Anal Edn*, **16** (1944).
4 Bag S P, Chakrabarti A K & Bhattacharya B, *Indian J Chem*, **21** (1982) 212.
5 Chakrabarti A K, *Indian J Chem*, **21** (1982) 63.
6 Ringbom A I, *Z analyt Chem*, **115** (1938) 332.
7 Ayres G H, *Anal Chem*, **21** (1949) 652.
8 Sandell E B, *Colorimetric determination of traces of metals*, 3rd Ed (Interscience, New York) 1959.
9 Job P, *C R Acad Sci*, **180** (1925) 928; *Ann Chim* (*Paris*), **9** (1928) 113.
10 Yoe J H & Jones A L, *Ind Engg Anal Edn*, **16** (1944) 111.
11 Harvey A E & Manning D L, *J Am chem Soc*, **72** (1950) 4488; **74** (1952) 4744.

Indian Journal of Chemistry
Vol. 27A, April 1988, pp. 368-369

Spectrophotometric Titration of Oxazine Dyes with Iron(II) in Triethanolamine Medium

K VIJAYA RAJU

Department of Engineering Chemistry
Andhra University, Waltair

Received 14 *May* 1987; *revised* 1 *September* 1987
accepted 15 *September* 1987

A convenient spectrophotometric titration method has been developed for the determination of microgram quantities of eleven oxazine dyes using iron(II) as a reductant in alkaline triethanolamine (TEA) media. For a satisfactory titration the reaction media must be 3.75-5.00 *M* in TEA, and 0.5-0.7 *M* in NaOH towards the equivalence point. In these titrations all the dyes are reduced to their leuco bases.

Oxazine dyes find wide use in textile dyeing, histological and cytological investigations as staining agents and as redox indicators. Various titrimetric methods for their determination involve the use of reductants like titanium(III)[1,2], tin(II)[3] or iron(II) in phosphoric acid medium[4]. However, the available methods are not free from drawbacks. Herein is reported a more satisfactory and convenient spectrophotometric titration method for the determination of microgram quantities of eleven oxazine dyes using iron(II) as a reductant in triethanolamine (TEA) medium[5-9].

An approximately 0.0005 *M* solution of iron(II) was prepared from ferrous ammonium sulphate (BDH, AR) and standardised[10]. The iron(II) solution was found to be stable for more than ten days.

Solutions (0.05%) of gallocyanine(GC), celestin blue (CLB), gallamine blue(GB) were prepared in 1 *M* HCl[4] while those of brilliant cresyl blue (BCB), nile blue (NB), capri blue(CPB), sevron blue 5G(SB 5G), alizarine blue S(AB-S), resorcin blue(RB), lacmoid(LM) and meldola's blue (MB) were prepared in water and assayed by titrating against titanium(III) chloride[2,4]. From these standard dye solutions 5×10^{-5} *M* solutions of GC, CLB and GB were prepared in 1 *M* NaOH while those of the remaining dyes were prepared in water for spectrophotometric titrations.

Triethanolamine (GR, Loba) was used (Blank correction must be applied if the presence of oxidising impurities is detected).

A Shimadzu double beam spectrophotometer (UV 140.02) was used in the study, employing matched glass cells of 1 cm path length for recording the absorption spectra and a glass cell of 3 cm pathlength for the spectrophotometric titrations. A few modifications as described by Dikshitulu *et al.*[4] were made in the cell compartment for carrying out the titrations.

Table 1—Spectrophotometric Titration of Oxazine Dyes with Iron(II)

Dye	Recommended λ for titration, nm	Range studied ppm	Standard deviation (%)
MB	405	15.54- 46.62	0.68
LM	405	11.51- 34.52	0.64
AB- S	510	23.58- 70.72	0.51
GC	535	15.01- 45.01	0.71
NB	535	36.64-109.92	0.36
GB	545	16.79- 50.36	0.55
BCB	555	15.89- 47.68	0.73
CB	555	17.29- 51.88	0.62
CLB	555	18.19- 54.56	0.49
RB	620	27.30- 81.88	0.42
SB 5G	685	17.98- 53.92	0.58

Procedure

To the dye solution (5-15 ml) in the titration cell, required amount of TEA (25-35 ml) and sodium hydroxide solution were added to give the strengths of about 3.75-5.0 *M* and 0.50-0.70 *M* respectively towards the equivalence point. The solution was made homogeneous by passing a rapid stream of purified N_2 gas, which also prevented the aerial oxidation of the leuco dye and titrated with iron(II) Solution. . The stirring was stopped and the absorbance noted. The titration was continued till the absorbance became almost constant. The equivalence point was given by the inflection in the plot between the volume of the titrant and the corresponding absorbance.

The accuracy of this method with each dye has been found to be ± 0.9%. The precision[11] in this method was determined by titrating six samples of each dye (concentration approximately in the middle of the optimum range) and the relative standard deviations calculated. The range studied and the relative standard deviation for each dye are given in Table 1. From the absorption spectra of the dyes (overall concentration 3.0×10^{-5} *M*) recorded (400-800 nm) in alkaline TEA media (3.75 *M* in TEA and 0.5 *M* in NaOH), suitable wavelength for carrying out the titration of each dye has been selected and included in the Table 1 [iron(II), iron(III) and leuco bases have negligible absorbance in this region].

Beer's law was obeyed in the concentration range of 15-48 ppm in the case of MB, GC and BCB; 17-55 ppm in the case of CB, CLB and SB 5G; and 11-35 ppm, 23-71 ppm, 36-110 ppm, 16-51 ppm and 27-82 ppm in the case of LM, AB S, NB, GB and RB respectively. All the dye solutions in alkaline TEA media are stable for two days, except LM (one day), where as the leuce bases are stable for 3 hr.

For a rapid and quantitative reduction of the dyes with iron(II), the TEA concentration must be 3.75-5.00 *M* (50-70%, v/v) in addition to the NaOH concentration of about 0.5-0.7 *M* towards the equivalence point. In a similar method proposed by Dikshitulu *et al.*[4] using iron(II) as a reductant in H_3PO_4 medium, it was stated that the reduction of some of the dyes was either extremely slow (e.g. MB, SB 5G, AB S) or proceeded to an intermediate product (e.g. LM). The present method is advantageous over the earlier one in that almost all the oxazine dyes are rapidly and quantitatively reduced to their leuco bases. Attempts to carry out potentiometric titration of these dyes with iron(II) in these media did not succeed because of the lack of clear break in potential during the titration.

Chloride, sulphate, acetate and perchlorate ions do not interfere; however nitrate ion interferes.

The author wishes to express his grateful thanks to the authorities of the University for research facilities.

References

1 Knecht E & Hibbert E, *New reduction methods in volumetric analysis* (Longmans, London), 1925, 53.

2 Conn H J, *Biological stains* (Waverly Press, Inc., U S A) 1961, 291.

3 Cap L & Kotoucek M, *Microchim Acta*, (1968) 1154.

4 Dikshitulu L S A, Vijaya Raju K & Hanumantha Rao V, *Indian J Chem*, **19A** (1980) 1031.

5 Alfaro H, Dolezal J & Zyka J, *Chemist Analys*, **55** (1966) 84.

6 Dolezal J, Lukayte E, Rybacek L & Zyka J, Colin *Czech chem Commun*, **29** (1964) 2597, *Chem Abstr*, **62** (1965) 2235C.

7 Zyka J & Dolezal J, *Micro Chem J*, **10** (1966) 554.

8 Dolezal J, Alfaro H & Jyka J, *Z Analyt Chem*, **224** (1967) 365; *Chem Abstr*, **66** (1967) 4344OY.

9 Dolezal J & Langmyber F J, *Anal chim Acta*, **61** (1972) 73; *Chem Abstr*, **77** (1972) 96169a.

10 Vogel A I, *A text book of quantuative inorganic analysis* (ELBS, London) 1961, 319.

11 Dean R B & Dixon W J, *Analyt Chem*, **23** (1951) 634.

Indian Journal of Chemistry
Vol. 27A, April 1988, pp. 370-372

BOOK REVIEWS

Thin Layer Chromatography with Flame Ionization Detection by Mojmir Ranny (D. Riedel Publishing Company, P. Box 17,3300 AA Dordrecht, Holland), 1987, pp. 198, Price $ 54.0.

The present book by Prof. Ranny is an English translation of the original Czechoslovakian text. It is a detailed exposition of the practice of thin layer chromatography (TLC) with flame ionization detection (FID). The methods of conventional TLC and TLC-FID are very different so much so that the experience of ordinary TLC will have limited application in TLC-FID. The procedures are constantly under imporvement rendering the TLC-FID even today a relatively developing technique. The book is divided into 3 parts: Part I is devoted mainly to methodoly, operational procedures, preparation of chromarods, quantitative evaluation, and reproducibility; Part II deals with specialised applications with particular reference to biology-medicine-pharmacy, food industry, and chemical industry; and Part III presents new perspectives in TLC on chromarods. The book has an impressive bibliography of 328 references.

The author has given practical hints, e.g., the use of manufactured chromarods rather than attempting to prepare them in the laboratory. Suggestions are given for careful mechanical handling of chromarods and their storage. The chapter on operational procedures gives useful suggestions on choice of solvents, elution technique, drying of the eluted rods prior to detection, and finally the FID system itself.

Application of TLC-FID to biology and medicine includes separation and purification of such complex molecules as lipids, steroid compounds, vitamins, alkaloids and purine bases, amino acids, terpenes and resins, pyschotropic substances, antipyretics, analgesics and hypnotics, antibiotics, sulphonamides and sulphanilic acid, and polyamines. In the food industry applications, procedures are outlined for fats, oils and related substances, phospholipids, saccharides, food additives and cosmetics. Applications of TLC-FID to chemical industry include analysis of surfactants and detergents, petroleum industry products, emulsions, polymer industry products, and pesticides and plant-growth regulators.

In the last part of the book (Part III) dealing with further developments and improvements in TLC-FID, the main thurst is towards sample application on rods; improvements in geometry of the FID collector, new thin layers, and new detection systems, such as flame thermionic ionization detector (FTID) and flame emission photometric detector (FEPD).

A promising separation, identification, and quantitative evaluation technique with varied applications, TLC-FID is yet to emerge as a full-fledged analytical method. The present book should inspire chemists, chemical technlogists, and instrumentation engineers, especially those in the inter-disciplinary groups, in bringing about further improvements in the technique of TLC-FID. The book is very well produced and aptly illustrated. It will be extremely useful to research scientists and other practising scientists and technologists who are concerned with the analytical technology of biological, medicinal, pharmaceutical, food and chemical industry products.

B R Sant
CSIR-Polytechnology Transfer Centre,
Hyderabad 500 001

Molten Salt Electrochemistry—An Introduction and Selected Applications, Edited by G Mamantov & R Marassi, NATO ASI Series C: Mathematical and Physical Sciences, Vol. 202 (D. Reidel Publishing Company, P.O. Box 17,3300 AA, Dordrecht, Holland) 1987, pp. 525 + XXV, Price $ 99.0

Studies on molten salts are important from both applied and fundamental points of view thereby necessitating investigations by many diverse techniques. The possible range of molten salts is wide: from the low melting (room temperature) systems like N-(1-butyl)-pyridinium chloride—aluminium chloride; 1-methyl-3-ethylimidozolium halide—aluminium halide to the high melting structurally simple ionic systems like NaCl (801°C) or high melting structurally complex systems like cryolite-alumina (~950°C). Utilization of such high melting systems as solvents and reaction media is being practised in electrowinning, refining, plating and electroforming. Fused salts have been put to a variety of uses owing to their high chemical and thermal stability, low vapour pressure, good electrical conductivity and diffusivity, low viscosity, high heat transfer coefficients, ability to dissolve a variety of materials; wide 'electrochemical window', extremely wide useful temperature range and the very high temperatures which can be reached. These properties make them attractive for a number of applications, such as molten salt batteries and fuel cells, catalysis and conversion of solar energy.

Thus, it is needless to point out that for investigators working in various aspects of molten salts as well as for the new entrants in this field this book is welcome as it creates awareness of the emerging trends.

The articles in this collection embrace a wide cross-section of the latest developments and are based on the plenary lectures delivered at the NATO Advances Study Institute on Molten Salt Chemistry, Camerino, Italy, during Aug. 3-15, 1986. A total of 24 articles are included which are contributed by specialists in various aspects of this subject.

This book includes an excellent review of structural properties of halide melts with special emphasis on the principles, practices, potentialities and limitations of various approaches like X-ray, neutron diffraction, isotopic methods etc. to the chemistry of molten salt.

The importance of thermodynamic properties of melts and the influence of different ionic interactions has been brought out in a lucid manner. Also an overview of the available experimental methods, such as vapour pressure, EMF, cryoscopy, chemical equilibrium, calorimetry, density and volume changes with their attendant advantages and limitations has been added.

A summary of theoretical and experimental studies of transport processes, phenomenology in ionic liquids covering a wide range of viscosity and temperatures and their correlations have been critically examined from various view points. The article on Brillouin scattering used to determine the elastic properties and structural relaxation behaviour of molten alkali nitrates alkali chlorides and some glassforming molten salts is particularly interesting.

Application of optical electronic absorption spectroscopy in the study of chemical reactions in molten salts and in the determination of the coordination geometry of transition metal ions has been outlined. Furthermore, various aspects, such-as experimental techniques at high temperature corrosive molten salt and the qualitative and quantitative information that could be obtained by vibrational spectroscopy and NMR are surveyed.

Recent developments in the field of metal-metal salt solutions and various spectroscopic techniques employed in such studies are covered in a review. A summary of the principles, methodology, electroanalytical chemistry and electrode kinetics; general features of acid-base effects, chemical solubilization of oxides and sulphides, organic reactions and the use of recently developing conducting polymer coated electrode in molten salts have been dealt with in an easily understandable manner.

The ambient temperature organic chloroaluminate ionic liquids, specifically (N-BuPy)Cl-AlCl$_3$ and (MeEt.im)X-AlX$_3$, their synthesis and general properties, transport properties, electronic absorption spectra, electrochemical properties, NMR spectra and their use as unique solvents for studying the inorganic complexes are covered exhaustively. Friedel-Crafts reactions of organic compounds in chloro-aluminate melts and their mechanisms are also presented.

The advantages and disadvantages of employing molten salts for electrodeposition with focus on refractory metals are discussed along with the kinetics and the forms of electrodeposits.

The principles, instrumentation, data analysis and the potentials of X-ray photoelectron spectroscopy (XPS) in solving problems relevant to molten salt systems are highlited with specific examples, like characterisation of surface films produced on Pt, Ni, Rh, W electrodes by seasoning in various melts and elucidation of failure mechanism of β-alumina tubes employed as solid electrolytes for Na—S cell. The possibility of exploiting XPS and AES techniques in molten salt research work has also been pointed out.

The influence of various additives on the chemical and physical properties of the Hall-Heroult electrolyte like phase equilibria, electrical conductivity, vapour pressure, solubility of metal and aluminium carbide in the melt, viscosity, surface tension, melt structure, activity, transport numbers and hence their interdependent effect on Faradaic efficiency of aluminium metal produced have been described. In addition, the complex electrode reactions occurring in the cell have been discussed for better understanding and to enable the aluminium smelters to compromise the bath chemistry and operating conditions and to improve current efficiency.

The good conductivity moltent salts lend themselves to use as electrolytes in conjunction with highly reactive electode materials which cannot be used with aqueous electrolytes. This permtis: (i) the development of batteries having very high specific energy, (ii) employment of high current densities thereby achieving high specific power (>100 W/kg) and (iii) long life with attendant advantages, like high cell voltage, low equivalent weight materials, high utilization of active material, rapid mass transport, low internal resistance etc. The basic thermodynamics of galvanic cells and fundamentals of electrode kinetics are reviewed in this connection. The advantages of molten salts as electrolytes or as active components in practical batteries are discussed. The emerging trends in batteries under development are also described.

All articles are provided with exahustive references.

A perusal of this book will certainly facilitate one to observe the futuristic trend in a number of new research programmes which could usher in several new developments in this important field. The compilation, get-up and finish of this book deserve a special mention. No doubt it will be a valuable addition to the libraries of all industrial and research institutions.

S Viswanathan
Central Electrochemical Research Institute,
Karaikudi 623 006

Indian Journal of Chemistry
Vol. 27A, May 1988, pp. 373-376

On the Utility of Akima's Bivariate Interpolation Method: Rotational Energy Transfer in HF – M (M = Ar, He) and HCl – Ar Collisions

I P DUBEY & S K UPADHYAY*
Department of Chemistry, Harcourt Butler Technological Institute, Kanpur 208 002
and
K RAGHAVAN
Department of Chemistry, Indian Institute of Technology, Kanpur 208 016

Received 14 *July* 1987; *revised and accepted* 31 *August* 1987

We report state-to-state integral inelastic cross-sections for rotational energy transfer in collisions between rigid rotor HF and M (M = Ar, He) and rigid rotor HCl and Ar over a range of initial rotational states and relative translational energies using Akima's bivariate interpolated potential energy surfaces. The cross-sections have been fitted to power gap law in order to compare these with previously reported results. We have also computed the rotational rainbows in HF-He collisions.

Knowledge of potential energy surface (PES) for any system is of fundamental importance for theoretical studies of chemical reactions. *Ab-initio* potential energy (PE) values for different geometries are usually available in the form of table of numbers. However, for dynamical calculations the PES must be known in some convenient analytical or numerically interpolated form which is capable of generating potentials and its derivatives accurately and efficiently at any arbitrary geometry. Various methods for fitting the *ab-initio* PE values have been reviewed by Connor[1] and more recently by Sathyamurthy[2]. Recently, the accuracy of Akima's bivariate method of interpolation[3] in fitting *ab-initio* potential energy surface has been tested[4] and this method has been shown to be comparable in efficiency and reliability to 2D-cubic spline interpolation. Akima's method has also been shown to be fairly insensitive to choice of grids and to be applicable to sudden surfaces like that of LiFH.

We provide here a further test on the utility of Akima's interpolation method on the basis of our studies on non-reactive collisions such as rotational energy transfer (RET) processes. The RET processes were chosen for study because a wealth of information is available on these in the form of state-to-state integral inelastic cross-sections (IICS)[5]. Many fitting laws and scaling relationships have been proposed[6] to compact these cross-sections. The most commonly employed such law is power gap law (PGL) proposed by Brunner *et al.*[7]:

$$\sigma_{J_i \to J_f} \propto (2J_f + 1)\, T_f^{1/2}\, |\Delta E_{if}|^{-\gamma} \qquad \ldots (1)$$

where $\sigma_{J_i \to J_f}$ is the inelastic integral cross-section for transition from initial rotational state (J_i) to final rotational state (J_f), ΔE_{if} the associated energy transferred and T_f is the final collision energy ($= T_i - \Delta H_{if}$ with T_i the initial collision energy).

We have studied the rotational energy transfer in collisions between rigid rotor HF and M (M = Ar, He) and rigid rotor HCl and Ar using Akima's bivariate interpolated surfaces. The results have been analysed in terms of PGL. We have also computed the rotational rainbows in HF-He collisions at $J_i = 1$ and $T_i = 0.492$ eV and compared these with those obtained by Gianturco and Palma[8].

Methods

Akima's interpolation method

Let us consider a function $y = f(x)$ for which the function values y_i are known at specific nodes $x_i = 1,2....$ Interpolation of y_i is achieved by constructing a piecewise function composed of a set of cubic polynomials applicable to successive intervals of x_i. The polynomial representing a portion of the curve between two adjacent x_i is determined by the coordinates and slopes at these two nodes. The slope of the curve at a given node is determined locally by the coordinates of five nodes with the node in question at the centre and two at each side of it as shown in Fig. 1a. The slope of curve at the node 3 for example is determined by Eq. 2,

$$\left(\frac{dy}{dx}\right)_3 = (|m_4 - m_3|m_2 + |m_2 - m_1|m_3) \times (|m_4 - m_3| + |m_2 - m_1|)^{-1} \qquad \ldots (2)$$

where m_1, m_2, m_3 and m_4 are slopes of line segments $\overline{12}$, $\overline{23}$, $\overline{34}$ and $\overline{45}$ respectively. In the special case of

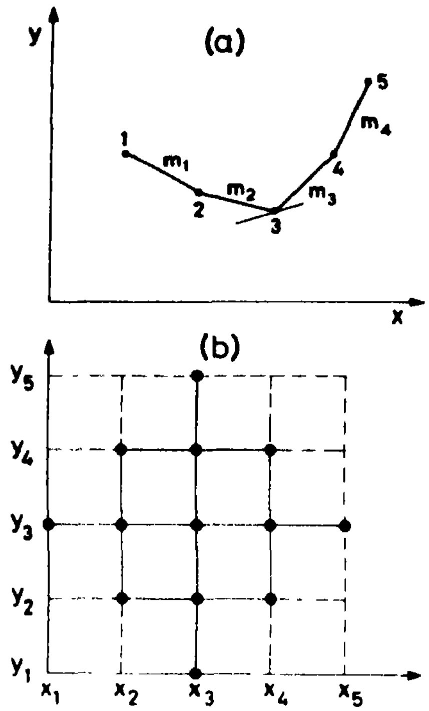

Fig. 1(a)—A schematic diagram illustrating the nodes in Akima's univariate interpolation; (b)—A schematic diagram indicating the 13 grid points involved in the bivariate interpolation at (x_3, y_3)

$m_1 = m_2 \neq m_3 = m_4$, the slope is equated to $\frac{1}{2}(m_2 + m_3)$. Near the end points of curve, two more points estimated outside the end points are used to determine the slope.

When a function z is dependent on two independent variables, x and y, it is constructed from a set of bicubic polynomials in x and y

$$z = \sum_{\alpha,\beta} x^{\alpha} y^{\beta}, \ \alpha = 0,1,2,3; \ \beta = 0,1,2,3 \qquad \ldots (3)$$

Each polynomial is applicable within a rectangle in the xy plane. The polynomial corresponding to a rectangle is determined by the values of the function and its derivatives at the four corner points. The partial derivatives are determined at each point locally with the help of a weighted mean of first- and second-order divided differences which are determined by the coordinates of 13 data points, with the datum point in question at the centre, two on each side of it in x and y directions and one in each diagonal direction as illustrated in Fig. 1b. When interpolation is desired near the boundaries of the defined range, the function values estimated at several points outside the range are used to determine the partial derivatives. Details of the method are given elsewhere[3].

Potential energy surface

For HF-Ar and HF-He systems, the electron gas potentials computed by Detrich and Conn[9] using the electron gas approximation of Gordon and Kim[10] were used to generate the PE values over a R × θ grid where R is the centre of mass separation between HF and M (= Ar, He) and θ is the angle between R and r (r being the internal coordinate of the diatom, HF). For HF-Ar system the grid (23 × 9) consisting of R from 1.0 to 10.0 bohr and θ from 0° to 180° was used, while for HF-He system the grid (21 × 9) consisting of R from 1.0 to 8.0 bohr was used.

For HCl-Ar system, Green's Gordon-Kim[11] potential were used to generate the PE values over a R × θ grid. The grid (19 × 7) consists of R from 1.0 to 12.0 bohr and θ from 0° to 180° was used.

Results and Discussion

We report the results of a quasiclassical trajectory (QCT) study of the rotationally inelastic collisions between a rigid rotor HF and Ar atom for $J_i = 0$, $T_i = 0.3767$ eV; $J_i = 1$, $T_i = 0.39$ eV and 0.65 eV; $J_i = 6$, $T_i = 0.65$ eV. In the case of rigid rotor HF and He atom we have chosen $J_i = 0$, $T_i = 0.3767$ eV; $J_i = 1$, $T_i = 0.492$ eV and $J_i = 20$, $T_i = 0.20$ eV. In case of collisions between rigid rotor HCl and Ar atom the studies have been made at $J_i = 0$, $T_i = 0.0774$ and 0.3767 eV. In our trajectory program we followed the methodology given in ref. 12. The initial rotor state J_i was fixed and for each J_i we varied the impact-parameter b systematically from 0 through b_{max}. All other variables were chosen randomly with the aid of the random number generator subroutine GGUB of IMSL[13]. The individual trajectories were started and terminated at the centre-of-mass separation of 14 a.u. Conservation of total energy and total angular momentum was used to check the accuracy of integration of the trajectory. We computed 50 trajectories at each b and the resulting probabilities of transition $P_{J_i \to J_f}$ were converted to $\sigma_{J_i \to J_f}$ using Eq. 4,

$$\sigma_{J_i \to J_f} = \int_0^{b_{max}} 2\pi \, b \, P_{J_i \to J_f}(b) \, db$$

$$\simeq 2\pi \, b \sum_i b_i \, P(b_i) \qquad \ldots (4)$$

We have shown the plots of $\ln[\sigma_{J_i \to J_f}/2J_f + 1) \, T_f^{1/2}]$ as a function of $\ln|\Delta E_{if}|$ for HF-Ar, HF-He and HCl-Ar systems in Figs 2, 3 and 4, respectively.

The slope (γ) computed from power gap law i.e. the plots of $\ln[\sigma_{J_i \to J_f}/(2J_f + 1) \, T_f^{1/2}]$ as a function of $\ln|\Delta E_{if}|$ are summarised in Table 1. We have also re-

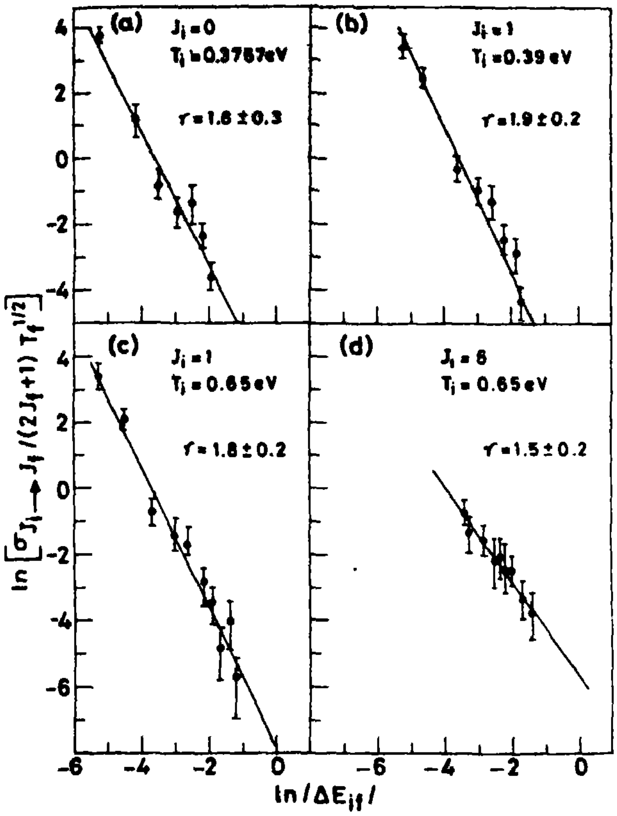

Fig. 2—Power gap law fit for rotationally inelastic integral cross-sections for HF-Ar collisions for different initial rotational states (J_i) and initial collision energies (T_i)

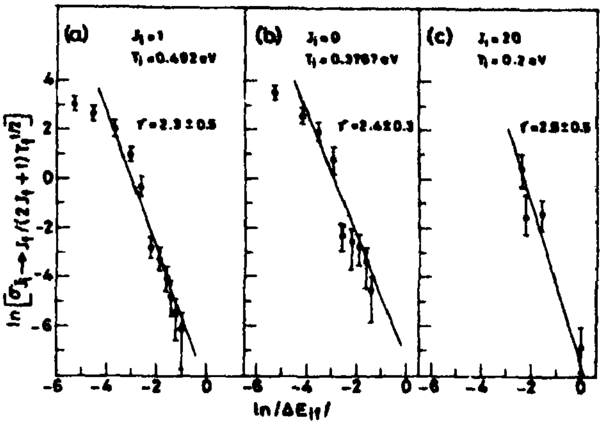

Fig. 3—Power gap law fit for rotationally inelastic integral cross-sections for HF-He collisions for different initial rotational states (J_i) and initial collision energies (T_i)

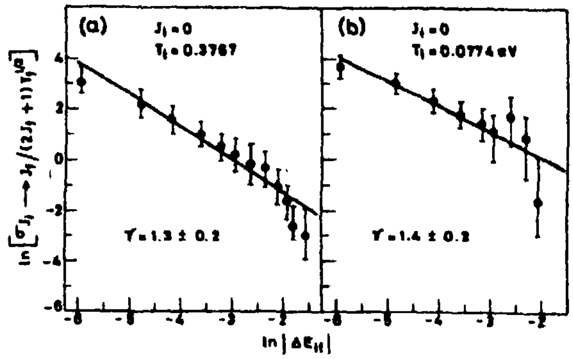

Fig. 4—Power gap law fit for rotationally inelastic integral cross-sections for HCl-Ar collisions for different initial rotational states (J_i) and initial collision energies (T_i)

Table 1—A Summary of γ Values Obtained by PGL Fit of IICS

System	Ref	V_i	J_i	T_i (eV)	γ
HF-Ar	5(a)	1	1	0.17-0.69	1.35
	5(b)	2,4,6	6,10	0.65	1.80 ± 0.1
	Present	—	0	0.3767	1.80 ± 0.3
	study	—	1	0.39	1.9 ± 0.3
		—	1	0.65	1.8 ± 0.2
		—	6	0.65	1.5 ± 0.2
HF-He	5(c)	4	20	0.2	2.4 ± 0.3
	Present	—	20	0.2	2.5 ± 0.5
	study	—	0	0.3767	2.4 ± 0.3
		—	1	0.492	2.3 ± 0.3
HCl + Ar	5(g), 5(h)	0.5	8	0.216	2.0 ± 0.5
		—	8	0.65	1.6 ± 0.2
		—	8	1.3	1.3 ± 0.2
		—	0,4,8	0.65	1.5 ± 0.1
	Present	—	0	0.3767	1.3 ± 0.2
	study	—	0	0.0774	1.4 ± 0.2

ported in Table 1 the computed γ values[5(g)] for these systems based on the available QCT data[5(b),5(c),5(h)]. The γ values computed by us for these systems are in agreement with those reported earlier for HF-Ar, HF-He and HCl-Ar systems.

We have also analysed our results for the presence of rotational rainbows in HF-He collisions at $J_i = 1$ and $T_i = 0.492$ eV in order to compare these with those reported by Gianturco and Palma[8]. We have run 200 trajectories at each impact parameter. The

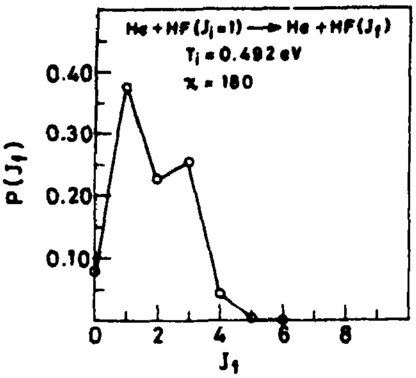

Fig. 5—Rotationally inelastic transition probabilities as a function of the final rotational states for scattering angle χ = 180°.

computed transition probabilities $P(J_f)$ for scattering angle χ = 180° (which occurs almost exclusively at zero impact parameter) as a function of J_f are given in Fig. 5. The rainbow at $J_f = 3$ is qualitatively in agreement with that reported by Gianturco and Palma[8] at the same initial conditions. However, we do not find any rainbow for smaller scattering angles. This may be due to the number of trajectories run being insufficient.

Thus, we have tested the utility of Akima's bivariate interpolation method by computing state-to-state integral inelastic cross-sections for RET in rigid rotor HF-M (M = Ar, He) and rigid rotor HCl-Ar collisions over a range of J_i and T_i using Akima's bivariate interpolated potential energy surfaces. The IICs for RET have been fitted using PGL. γ values obtained from PGL have been found to be in agreement with those based on the available results for these systems. The rotational rainbows in HF-He collisions at $J_i = 1$ and $T_i = 0.492$ eV are also in qualitative agreement with those reported by Gianturco and Palma. We find that Akima's method serves as a valuable method of fitting *ab initio* surfaces.

Acknowledgement

We thank Prof. N. Sathyamurthy for his valuable suggestions. Calculations reported herein were carried out on the DEC-1090 computer at the IIT, Kanpur. This study was supported by a grant from the DST, New Delhi. Thanks are also due to Prof. A K Vasishtha (Director) and Prof. R S Tewari for their encouragements.

References

1 Connor J N L, *Computer Phys Commun*, **17** (1979) 117.
2 Satyamurthy N, *Computer Phys Reports*, **3** (1985) 1.
3 Akima H, *J Asso Comput Mach*, **17** (1970) 589; *Commun Asso Comput Mach*, **15** (1972) 914; **17** (1974) 18; **17** (1974) 26.
4 Upadhyay S K & Sathyamurthy N, *Chem Phys Lett*, **92** (1982) 631.
5(a) Barnes J A, Keil M, Kutina R E & Polayni J C, *J Chem Phys*, **76** (1982) 913.
(b) Thompson D L, *Chem Phys Lett*, **84** (1981) 397.
(c) Thompson D L, *J chem Phys*, **78** (1983) 1763.
(d) Margolies S, Garetz B A & Sathyamurthy N, *J chem Phys*, **79** (1983) 2763.
(e) Scott T P, Smith N & Pritchard D E, *J chem Phys*, **80** (1984) 4841.
(f) Mayne H R & Kiel M, *J phys Chem*, **88** (1984) 883.
(g) Raghavan K, Upadhyay S K, Sathyamurthy N & Ramaswamy R, *J chem Phys*, **83** (1985) 1573.
(h) Polanyi J C & Sathyamurthy N, *Chem Phys*, **29** (1973) 9.
6(a) Brunner T A & Pritchard D E, *Adv chem Phys*, **50** (1982) 589.
(b) Whitaker B J & Brechinganae P, *Chem Phys Lett*, **95** (1983) 407.
(c) Nyeland C, *Chem Phys Lett*, **109** (1984) 603.
7 Brunner T A, Driver R D, Smith N & Pritchard D E, *Phys Rev Lett*, **41** (1978) 856.
8 Giantruco F A & Palma A, *J chem Phys*, **83** (1985) 1049.
9 Detrich J & Conn R W, *J chem Phys*, **64** (1976) 3001.
10 Gordon R G & Kim Y S, *J chem Phys*, **56** (1973) 3122.
11 Green S, *J chem Phys*, **60** (1974) 2654.
12 Pattengill M D, *Atom-molecule collision theory*, edited by R B Bernstein (Plenum, New York) 1979, Chap. 10.
13 International Mathematical and Statistical Libraries, Inc. Houston, Texas, U.S.A.

Indian Journal of Chemistry
Vol 27A, May 1988, pp. 377-379

Calculation of Quantum Chemical Parameters of S – N Ring Systems by Graph Theoretical Techniques

R K MISHRA*, B K MISHRA & S SINGH
Department of Chemistry, Sambalpur University, Jyoti Vihar 768 019

Received 15 *May* 1987; *revised and accepted* 14 *September* 1987

The electronic and structural properties of a series of aromatic rings composed only of sulphur and nitrogen atoms, such as S_3N^+, S_2N_2, $S_3N_2^{2+}$ and S_4N_2, are discussed. The bond orders and charge densities have been calculated using graph theory.

Planar cyclic molecules and ions comprising sulphur and nitrogen atoms are known. In these S – N rings each sulphur atom can be considered to be contributing a pair of electrons to the π-system while each nitrogen provides only one electron[1]. Consider the planar ring $(S_xN_y)^q$, where the charge q could be plus, minus or zero. For such type of systems to be aromatic, the total number of π-electrons $(2x+y-q)$ must be equal to $(4n+2)$. These S – N rings have more π-electrons than the aromatic hydrocarbons with the same ring size and are "electron rich", e.g., $S_3N_3^-$ has 10 π-electrons compared to 6 for benzene as pointed out by Banister[2]. Because these electrons occupy MOs that are non-bonding or mainly antibonding, the bond orders of S – N ring bonds usually turn out to be smaller than those of conjugated hydrocarbon rings of the same size.

Many attempts[3] have been made to rationalise and understand the electronic structure of binary compounds of nitrogen and sulphur, but a larger perspective analogous to that in coordination chemistry, or boron hydride chemistry is still missing[4]. The electronic structure of these materials are discussed *ab initio* and on the basis of density functional theory by Turner[5]. The object of this paper is to study the electronic properties of some simple inorganic ring systems on a qualitative basis using graph theoretical formalism.

Method of Calculation

The molecules under study, i.e., S_3N^+, S_2N_2, $S_3N_2^{2+}$ and S_4N_2 can be represented as bipartite graphs from which characteristic polynomial can be generated by utilising Sachs theorem[6] (Eq. 1),

$$P(G_{VEW}; x) = \sum_{n=0}^{N} \sum_{s \in S_n} (-1)^{c(s)} 2^{r(s)} \prod_{s} h_i^{l(s)} \prod_{s} k_j x^{N-n} \quad \ldots (1)$$

where h and k represent the Hückel parameters[7]. c(s) and r(s) denote the total number of components and total number of rings in the subgraph 's' respectively. S_n is the total number of all Sachs graphs (with n vertices) for a given graph G and l(s) represents the number of loops in any particular vertex weighted graph. From the characteristic polynomial, the eigen values were obtained and utilised to construct the molecular orbitals. The coefficients of the atomic orbitals (C_{km}) have also been evaluated. Rouvray[8] has proved that the topological matrix and Hückel matrix commute with each other and they must have the same eigen vectors. Hence, the eigen vector (C_k) generated from column matrix of 'C_{km}' has been utilised for the calculation of electron probability density 'P' (Eq. 2),

$$P = \sum_{k=1}^{\mu} a_k (C_{km}^2 \varphi_m^2 + 2C_{kl}C_{km}\varphi_l\varphi_m) \quad \ldots (2)$$

where a_k is the occupancy number, φ_l and φ_m are the atomic orbitals (l and m are adjacent atoms), C_{kl} is the corresponding coefficient and the summation extends over all μ occupied orbitals. From the above equation the charge density $(P_{mm} = q_r)$ and the mobile bond order (P_{lm}) have been evaluated (Eqs 3 and 4),

$$P_{mm} = q_r = \sum_{k=1}^{\mu} a_k C_{km}^2 \quad \ldots (3)$$

$$P_{lm} = \sum_{k=1}^{\mu} a_k C_{kl} C_{km} \quad \ldots (4)$$

Results and Discussion

The characteristic polynomials obtained for the molecules S_3N^+(i), S_2N_2(ii), $S_3N_2^{2+}$ (iii) and S_4N_2

Table 1—Bond Orders for Different Molecules

Compds	P_{12}	P_{23}	P_{34}	P_{14}	P_{15}	P_{45}	P_{16}	P_{56}
$(S_3N)^+$	0.5743	0.4588	0.4588	0.5743	—	—	—	—
S_2N_2	0.5720	0.5720	0.5720	0.5720	—	—	—	—
$(S_3N_2)^{2+}$	0.2294	0.5053	1.0513	—	0.2294	0.5053	—	—
S_4N_2	0.1093	0.8044	0.3440	—	—	0.3440	0.1093	0.8044

Table 2—Charge Densities for Different Molecules

Compds	q_1	q_2	q_3	q_4	q_5	q_6
$(S_3N)^+$	1.705	1.386	1.525	1.386		
S_2N_2	1.600	1.386	1.600	1.386		
$(S_3N_2)^{2+}$	0.780	1.660	0.943	0.943	1.660	
S_4N_2	2.574	1.371	1.716	1.333	1.716	1.371

(iv) are given below.

$$P(G_{(i)\,VEW}; x) = x^4 - 3.5x^3 - 10x^2 + 7x \qquad \ldots(5)$$

$$P(G_{(ii)\,VEW}; x) = x^4 + 7x^3 - 3.75x^2 - 56x \qquad \ldots(6)$$

$$P(G_{(iii)\,VEW}; x) = x^5 - 7x^4 - 4.25x^3 + 63x^2 + 43.75x - 60.0 \qquad \ldots(7)$$

$$P(G_{(iv)\,VEW}; x) = x^6 - 7x^5 - 5.75 \times x^4 + 70x^3 + 47.5x^2 - 126.0x - 64.0 \qquad \ldots(8)$$

The characteristic polynomials of (i) and (ii) clearly reflect the presence of non-bonding molecular orbitals. This indicates the instability of the molecules. The quantum chemical parameters such as bond orders and charge densities of the molecules under study were calculated by the graph theoretical principle[8] and are tabulated in Tables 1 and 2 respectively.

Bond orders

Compared to the hydrocarbons, the lower energy atomic orbitals on sulphur and nitrogen pull MO energies down which accommodate bound electrons to a greater extent in the S – N rings. Because these electrons occupy MOs that are nonbonding or mainly antibonding, the bond orders of the S – N ring bonds usually turn out to be smaller than those for conjugated hydrocarbon rings of the same size[1]. The bond orders for the different molecules are given in Table 1.

In the first molecule, $P_{12} = P_{14}$ and $P_{23} = P_{34}$. Further, it is observed that the S – S bond order is less than that of S – N. The bond order of the corresponding aromatic hydrocarbon (C_6H_6) is 0.6 (ref. 1). Hence, the idea given by Trinajstic *et al.*[6] is valid. As expected in case of the second molecule, i.e., disulphur dinitride all the bond orders are equal. This is essentially a square-planar molecule with nearly equal S – N bonds. The third molecule, i.e., the polycation has $P_{12} = P_{15}$ and $P_{23} = P_{45}$, but P_{34} is greater than all the other bond orders. This result shows that the electronic environment of S_1 is different from those of S_3 and S_4. Trinajstic *et al.*[1] have rightly pointed out that the S – S bond exceeds the length of the normal S – S single bond. This study further corroborates the idea given by Trinajstic *et al.* In case of the fourth molecule we found $P_{12} = P_{16}$, $P_{23} = P_{56}$ and $P_{34} = P_{45}$. Though both P_{23} and P_{45} are S – N bonds, still they are not identical. This may be due to the different electronic clouds around S_1 and S_4.

Charge densities (q_r)

The charge densities (q_r) for different molecules are given in Table 2.

q_r values can sometimes be used to predict the position(s) at which substitution reaction takes place in conjugated cyclic molecules. An electrophilic substitution reaction occurs by attack of a positive ion or of a positive end of the polarized species. If one neglects the variation in σ-electron distribution, electrophilic substitution is expected to occur preferentially at positions where the π-electron charge (q_r) is the greatest. In contrast, nucleophilic substitution occurs at the position which has the smallest q_r value[9].

In the first molecule (i) the q_r values clearly reflect the distinct difference between two types of sulphur atoms in the $(S_3N)^+$ ring. The two sulphur atoms (S_2 and S_4) bonded to nitrogen atom are in the same electronic environment whereas S_3 is in entirely different environment. Further, this empirical result indicates the type of substitution reactions that can occur at various positions. In the case of the second molecule (ii) the two nitrogen atoms and the two sulphur atoms are in similar electronic environments. Two distinct types of substitution reactions may occur at the nitrogen

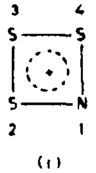

(i)

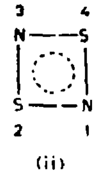

(ii)

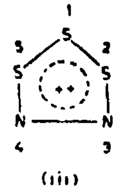

(iii)

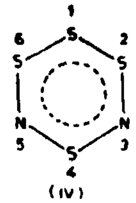

(iv)

and sulphur centres. The third molecule (iii) is very interesting, as of the three sulphur atoms present, S_1 is entirely different from S_3 and S_4. Two different types of substitution reactions are possible at the sulphur centres. But in the case of nitrogen atoms only one type of reaction is possible, since they are in the same electronic environment. In the fourth molecule (iv) there are three distinct types of sulphur charge sites. S_2, S_4 and S_6 are susceptible to nucleophilic substitution whereas S_1 is susceptible to electrophilic substitution. Both the nitrogen centres are susceptible to the same type of substitution reaction.

References

1 Gimare B M & Trinajstic N, *Pure & Appl Chem*, **52** (1980) 1443.

2 Banister A J, *Nature*, **237** (1979) 92.

3 Roesky H W, *Angew Chem*, **91** (1979) 112.

4 Gleiter R, *Angew Chem Int Edn*, **20** (1981) 444.

5 Turner A in *Chemical application of topology and graph theory*, Edited by R B King (Elsevier, Amsterdam), 1983, 141.

6 Trinajstic N, *Croat chem Acta*, **49** (1977) 593.

7 Streitwiesser (Jr) A, *Molecular orbital theory of organic chemistry* (Wiley, New York), 1961.

8 Rouvray D H in *Chemical application of graph theory*, Edited by A T Balaban (Academic Press, London) 1976, 204.

9 Levine I N, *Quantum chemistry* (Allyn and Bacon Inc, Boston) 1983, 484.

Indian Journal of Chemistry
Vol. 27A, May 1988, pp. 380-386

Studies on Some Novel Silica Clathrates

R P GUNAWARDANE
Department of Chemistry, University of Peradeniya, Peradeniya, Sri Lanka

Received 2 *June* 1987; *revised* 31 *July* 1987; *accepted* 15 *September* 1987

Clathrate compounds of silica have been synthesized from aqueous silica solutions in the presence of a wide variety of guest molecules under hydrothermal conditions. Five different clathrasil types namely melanophlogite, dodecasil 3C, dodecasil 1H, deca-dodecasil 3R and nonasil have been crystallized. Nitrogen—containing cyclic organic compounds show greater tendency to form clathrasils. However, most hydrocarbons, ethers, alkali halides and reactive inorganic species fail to crystallize clathrasils. Free diameters of windows of the cages in clathrasils are too small for free movement of the guest species unlike in zeolites. Although the guest species are essential for their formation, the clathrasil frameworks have been found to be stable up to 900-1100°C, even after the removal of guest species by thermal treatment. It appears that the framework topology and the nature of cages in clathrasils depend mainly on the size and shape of the guest species. Factors which affect the formation and stability of these silica clathrates are also discussed.

Clathrosils[1], the clathrate compounds with silica frameworks represent a new class of porous tectosilicates distinct from zeolites[2], in which the guest molecules, unlike in zeolites[3], are entrapped in the cages and are not exchangeable due to the small size of "windows" connecting these cages.

Interest in silica clathrates arose with the chemical investigations[4] and subsequent structure determination[5] of the rare mineral melanophlogite. Melanophlogite contains three-dimensional, tetra-coordinated, electrically neutral network of SiO_4 tetrahedra forming two types of cages, viz. pentagonaldodecahedra, $[5^{12}]$ and tetrakisdecahedra $[5^{12}6^2]$. From the difference in X-ray diffraction Fourier maps it has been concluded that the voids are occupied by the guest molecules such as N_2, CO_2, CH_4 etc. Subsequently, five more clathrasil-types, silica sodalite[6], dodecasil 3C[7], dodecasil 1H[8], deca-dodecasil 3R[9] and nonasil[10] have been reported. They all possess topologically different three-dimensional $[SiO_4]$ frameworks containing different types of cages, in which the guest molecules are enclathrated.

This paper reports the synthesis of different clathrasils using widely different guest species, their characterization and properties. Cage characteristics and the nature of the guest molecules are correlated with the stability of clathrasils. Furthermore, factors which control the formation of different clathrasil frameworks are suggested from the available data.

Materials and Methods

Synthesis

Clathrasils were synthesised using a homogeneous 0.5 *M* silicic acid solution prepared by the hydrolysis of tetramethoxysilane [TMOS, $Si(OCH_3)_4$], in water or in 2 *M* aqueous ethylenediamine solution under continuous and vigorous agitation. The hydrolysis takes place according to Eq. (1)

$$Si(OCH_3)_4 + 4H_2O \rightarrow Si(OH)_4 + 4CH_3OH \quad \ldots (1)$$

Since previous work[1] has shown that methanol has no influence on the crystallization of various clathrasils, no attempt was made to remove methanol from solution. Crystallizations were carried out mostly in silica tubes. However, instances where relatively large amounts of crystalline materials were required, steel autoclaves with teflon reaction vessels were used. The silicic acid solution was filled into thick silica tubes and after addition or condensation of the guest species into the reaction tube by cooling it in liquid nitrogen, the tubes were sealed in air. In general guest species were added in excess (~ 0.2 ml or 20 mg per ml silica solution). Tubes were subjected to thermal treatment at 150-250°C for a period ranging from 1 week to several months. The maximum total pressure generated in the reaction vessels was about 150 bar.

Identification and analysis

Crystalline products were identified by optical microscopy followed by powder X-ray diffraction. In most cases, quick identification of the products was possible with optical microscopy since all known clathrasils have characteristic morphologies. Mass spectroscopic analyses of some clathrasils were performed using BALZERS mass spectrometer and thermogravimetric analyses using a Dupont 1090 thermal analyzer. Some crystals were subjected to chemical analysis by energy diepersive X-ray fluorescence.

Table 1—Results of Synthesis Using Characteristic Guest Species

Guest*	Molar ratio	Products† at temp (°C)			
		160	180	200	240
Pyrrolidine	—	D3C	D3C	D3C	D3C
1-Aminoadamantane	—	DD3R	D1H	D1H	D1H
Pyr, Adam	1:1	DD3R	DD3R	D1H	D1H
Pyr, Adam	1:10	DD3R	DD3R	D1H	D1H
Pyr, Adam	1:20	DD3R	DD3R	D1H	D1H
Pyr, Adam	10:1	D3C	D3C	D3C	D3C
Methylamine	—	Melano	Melano	Melano	D3C
MeNH$_2$, Adam	1:1	DD3R	D1H	D1H	D1H
MeNH$_2$, Pyr	1:1	D3C	D3C	D3C	D3C
Pyr, MeNH$_2$, Adam	1:1:1	D3C	D3C	D3C	D3C
Pyr, MeNH$_2$, Adam	10:1:1	D3C	D3C	D3C	D3C
Pyr, MeNH$_2$, Adam	10:1:10	DD3R	D1H	D1H	D1H
2-Aminopentane	—	Nonasil	Nonasil	—	—
Aminopen, Pyr	1:1	D3C	D3C	D3C	D3C

*Pyr = Pyrrolidine; Adam = 1—aminoadamantane; MeNH$_2$ = methylamine; and aminopen = 2-aminopentane.
†Melano = Melanophlogite; D3C = dodecasil 3C; D1H = dodecasil 1H, DD3R = deca-dodecasil 3R.

Results and Discussion

Clathrasil formation

Five different clathrasil phases namely melanophlogite (melano), dodecasil 3C (D3C) dodecasil 1H (D1H), deca-dodecasil 3R (DD3R) and nonasil have been observed to crystallize depending on the guest species used and the temperature of synthesis (Table 1).

In the absence of guest species aqueous silicic acid solutions afford various crystalline polymorphs of silica such as cristobalite, quartz etc. under hydrothermal conditions. However, when the guest species are added and under certain experimental conditions, the condensation of silica occurs around the guest species forming porous tectosilicates possessing polyhedral cavities or cages (Table 2, Fig. 1). Important structural data of these products are given in Table 3. Types of cages present in different clathrasils as determined[11] by single crystal X-ray diffraction studies are shown in Fig. 2.

For the formation of melano, methylamine acts as an efficient guest in the temperature range 160-200°C (Table 2). Similarly, pyrrolidine and 2-aminopentane act as efficient guest molecules for the formation of D3C and nonasil respectively. 1-Aminoadamantane acts as a very effective guest for the formation of D1H at 180-240°C while at lower temperatures (~ 160°C) DD3R is obtained. Since the crystallization of clathrasils is rapid with these guest species they may be considered as characteristic guests for the formation of different clathrasil frameworks (Table 2).

Although a wide variety of guest species were employed, no new clathrasil frameworks were formed. Attempts to synthesize clathrasils with larger cages, using large guest molecules such as mesotetraphenylporphin, cyclam(15)ane N$_4$, dicyclohexylamine, hexacyclantrisulphate and a fluorescent compound-dimethylpopop were not successful. Furthermore, attempted enclathration of metal complexes such as ferrocene, aminoferrocene, copperpthallocyanin and haemoglobin proved unsuccessful even after six-month thermal treatment. Dodecasil 1H (D1H) possesses the largest cage, [$5^{12}6^{8}$], of inner volume ~ 430Å^3 among the clathrasils so far synthesized. It is apparent that the clathrasils possessing cages bigger than ~ 450 Å^3 are not thermodynamically stable under the present synthesis conditions.

Use of mixture of guests

Mixtures of different guest molecules were also used in order to synthesize new clathrasil frameworks containing only medium and large size cages. These mixtures too yielded only known clathrasils characteristic of individual guest species employed (Table 1). In the presence of mixture of guests there is a greater tendency for the formation of clathrasils containing large cages with large guest molecules. However, this tendency seems to be altered by the presence of a large excess of one guest. Once the nucleation of a particular clathrasil commences, the crystallization of that phase goes to completion making use of all the available silica in solution.

Temperature dependence of clathrasil formation

It has been observed in the present study that the same guest molecule stabilises one clathrasil at lower temperature and another clathrasil at higher temper-

Table 2—Guest Species Successfully Used for Clathrasil Synthesis

Clathrasil*	Guest molecules
Melanophlogite (cubic)	N_2, Kr, Xe, N_2O, CO_2, CH_4, CH_3NH_2
Dodecasil 3C (octahedral)	Kr, Xe, SF_6, CH_3NH_2, $C_2H_5NH_2$, $(CH_3)_2CHNH_2$, $(CH_3)_3CNH_2$, $(CH_3)_3CCH_2NH_2$, $(CH_3)_2NH$, $(C_2H_5)_2NH$, $(CH_3)_3N$, $(CH_3)_2NC_2H_5$, 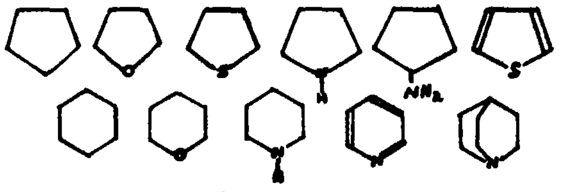
Dodecasil 1H (hexagonal)	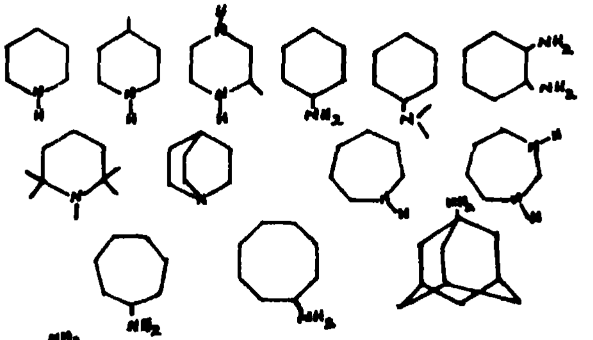
Deca-dodecasil 3R (rhombohedral)	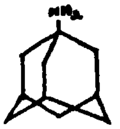
Nonasil (lath-like)	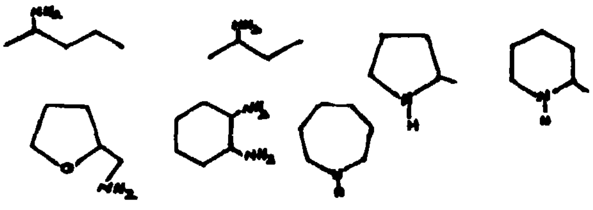

*Characteristic morphologies are indicated within brackets under each clathrasil type.

ature. Some examples are given in Table 4. It is apparent that the guest molecules fit into a relatively smaller cages or larger cages depending on whether the temperatures of formation is lower or higher. For instance, piperidine and 1-azobicyclooctane guest molecules form D3C at lower temperatures occupying $[5^{12}6^4]$ cages with inner volume ~ 250 Å^3 while at higher temperatures these guests occupy larger $[5^{12}6^8]$ cage with inner volume ~430 Å^3 (Table 5). Certain guests (Table 4) which form nonasils at lower temperatures occupying their $[5^86^{12}]$ cages (V~ 290 Å^3), prefer to occupy bigger $[5^{12}6^8]$ cages (V~ 430 Å^3) forming D1H at higher temperatures. Thermal expansions and theirmal vibrations of the free guest molecules are much higher than the expected flexibility of the cages formed by Si-O-Si bonding. As such, at higher temperatures the guest molecules require cages with higher inner volumes.

Properties of clathrasils

From the approximate values of free diameters of the "windows" in different cages (Table 5) it is clear that during synthesis silica framework is formed around the guest species. It is not possible for the guest molecules to enter the cages once the cages are formed. Except DD3R, all other clathrasils have

Table 3—Structural Data of Clathrasils

Clathrasil	Unit cell content of guest-free clathrasil	Space group, cell dimensions	Framework density (D_f)*	Cage type and number per unit cell
Melanophlogite	46 SiO_2	Pm3n $a = 13.78$ Å	19.0	$2[5^{12}]: 6[5^{12}6^2]$
Dodecasil 3C	136 SiO_2	Fd3 $a = 19.46$ Å	18.6	$16[5^{12}]: 8[5^{12}6^4]$
Dodecasil 1H	34 SiO_2	P 6/mmm $a = 13.78$ Å $c = 11.19$ Å	18.5	$3[5^{12}]: 2[4^35^66^3]: 1[5^{12}6^8]$
Deca-dodecasil 3R	120 SiO_2	R3m $a = 13.86$ Å $c = 40.89$ Å	17.6	$6[4^35^66^1]: 9[5^{12}]: 6[4^35^{12}6^18^3]$
Nonasil	88 SiO_2	Fmmm $a = 22.32$ Å $b = 15.06$ Å $c = 13.63$ Å	19.3	$8[5^46^4]: 8[4^15^8]: 4[5^86^{12}]$

*Framework density (D_f) is defined as the number of SiO_4 tetrahedra per 1000 $Å^3$ in the structure.

five-membered ring (d ~ 1.5 Å) and six-membered ring (d ~ 2.5 Å) windows. In addition, nonasil has slightly larger windows with eight-membered rings (d ~ 4.0 Å). Therefore, except for very small gaseous species, the guest molecules cannot move freely through these windows. In this respect clathrasils are different from zeolites and thus have limited industrial applications. Furthermore, as observed in high-silica zeolites[12], clathrasil frameworks are found to be hydrophobic.

Thermal behaviour

All five clathrasil frameworks are found to be stable up to 900°C, as confirmed by X-ray powder diffraction. Calcination of clathrasils can be performed in the temperature range 500-900°C and in this temperature interval guest species are decomposed, oxidized and removed from the host framework without structural damage to the framework. Thus, calcination product at this temperature is a pure silica polymorph having the same framework topology of clathrasils.

In a typical case, e.g. decadodecasil or nonasil, mass loss in TG was slow up to 150°C and became faster in the temperature range 500-700°C and in the temperature range 800-900°C, there was no mass loss. X-ray powder patterns of the end products are almost identical with those of as-synthesized clathrasils. Chemical analysis of the guest-free clathrasils by X-ray fluorescence has shown the presence of only silicon in the framework.

Nevertheless, when the temperature is raised above 900°C in the case of melanophlogite and 1100°C in the case of other clathrasils, phase transformation to thermodynamically stable polymorphs of silica occurs. The transformation product is cristobalite for all the clathrasils, but in hydrothermal experiments the transformation of melanophlogite to quartz has been observed at 300°C and 2 kb.

Factors which affect clathrasil formation

There are a large number of possible guest species which are likely to fit into cages in clathrasile. But only a small number of molecules (Table 2) have been successfully enclathrated to form clathrasils. For instance, methylamine readily forms melano or D3C or dodecasil 3C depending on the temperature. however, alcohols such as CH_3OH, C_2H_5OH, C_3H_7OH and alkyl halides such as CH_3Cl, CH_2Cl_2 and $CHCl_3$ do not act as guest species. Although methane alongwith N_2 or CO_2 readily form melano, it is not possible to synthesize any clathrasil with C_2H_4, C_2H_6, C_3H_8, C_4H_{10}, C_5H_{12} and C_6H_{14}.

Inorganic species such as N_2, CO_2, inert gases and SF_6 act as guests for the formation of clathrasils. however, HCl, HBr, Br_2, Cl_2, SO_2, SO_3, N_2O_4, NH_3 and N_2H_4 do not act as guest species probably due to solvation or reaction in aqueous silicic acid solution.

It has been observed that nitrogen bases have a greater tendency for clathrasil formation and compounds like piperidine, 4-methylpiperidine, 1-azabicyclo[2,2,2]octane and 1-aminoadamantane fit well into the $[5^{12}6^8]$ cage forming D1H within one weak. however, no clathrasils are formed using benzene, toluene or adamantane even after 6 months of thermal treatment. A series of mainly less symmetric amines readily act as guests (Table 2) for the formation of nonasils.

The guest molecules which occupy larger cages may be considered as 'structure-controlling guests'.

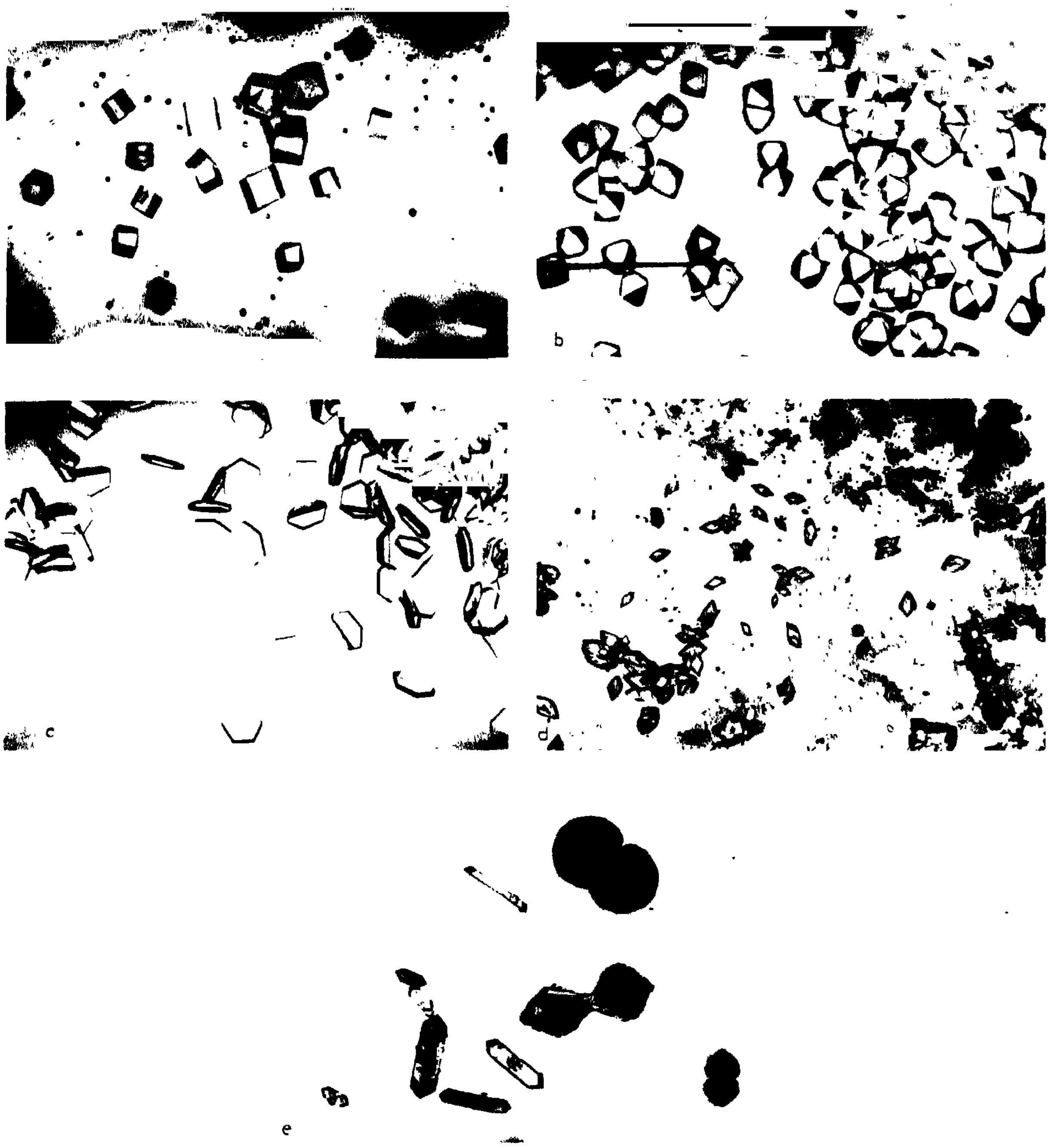

Fig. 1—Morphology of different clathrasils [(a) Melanophlogite, (b) dodecasil 3C, (c) dodecasil 1H; (d) decadodecasil 3R; and (e) nonasil].

In contrast smaller cages are filled with small gaseous molecules (N_2, CO_2 etc.) or they may remain empty depending on the availability of these molecules during synthesis. On the other hand, it has been observed by mass spectroscopy and single crystal X-ray diffraction studies[10] that the small cages $[5^4 6^4]$ and $[4^1 5^8]$, present in nonasils are in fact empty. It is apparent that these cages are too small to accomodate even small gaseous molecules.

It is evident from the available data that the interaction between the guest and the silica framework is mainly by van der Waals forces. It is also possible that lone pairs of the N atoms in the guests interact with the vacant *d*-orbitals of silicon in the framework, facilitating enclathration of the guest molecules. Single crystal X-ray investigations[7,8] have revealed that large guest molecules are not randomly oriented but have preferred orientations within the

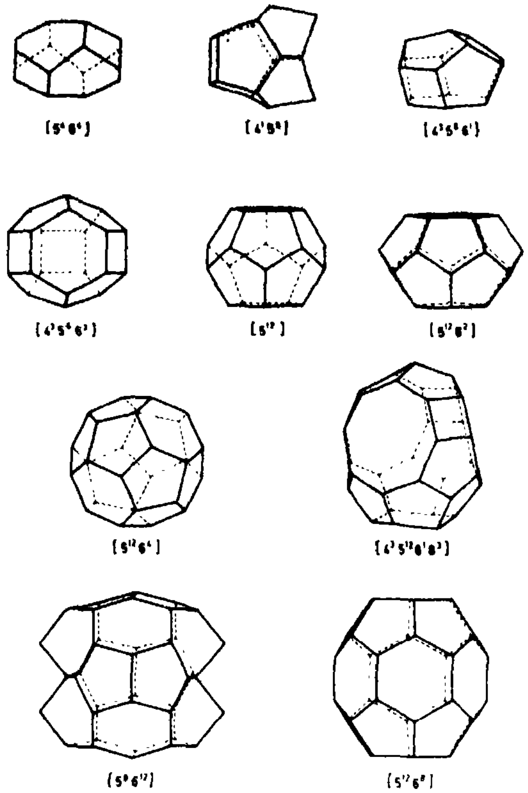

Fig. 2—Cages present in different clathrasils (Silicon atoms are located at the corners of the polyhedra and the oxygen atoms *near the centers of the lines connecting the silicon atoms: e.g.* $[5^{12}6^8]$ means that a 20-hedron consisting of 12 five-membered rings and 8 six-membered rings of $[SiO_4]$ units)

cages. Orientation of some guest species in the clathrasil cages are shown in Fig. 3.

Boron, phosphorus incorporation

It is theoretically possible to replace silicon by other similar cations with tetrahedral coordination such as Ge^{4+} or a combination of B^{3+}, Al^{3+}, Ga^{3+} and P^{5+}.

Attempts have been made to synthesize clathrasils in the presence of small amounts of H_3BO_3 or a mixture of H_3BO_3 and H_3PO_4. In most cases the same clathrasil phases were crystallized. For instance, 1-aminoadamantane crystallized DD3R at 160°C and D1H at 180-240°C in the presence of H_3BO_3 or H_3BO_3 and H_3PO_4. However, pyrrolidine gave nonasil at 160-200°C and D1H at 240°C in the presence of H_3BO_3 as well as in the presence of a mixture of H_3BO_3 and H_3PO_4. Nonasil and D1H thus obtained were subjected to thermal treatment to obtain the guest-free clathrasils which were analysed by X-ray fluorescence. Only silicon has been detected in the framework suggesting that neither boron nor phosphorus has been incorporated into the framework.

Table 4—Effect of Temperature on Clathrasil Formation

Guest	Product* at			
	160°	180°	200°	240°C
Methylamine	Melano	Melano	Melano	D3C
Piperidine	D3C	D3C	D3C	D1H
1-azabicyclooctane	D3C	D3C	D1H	D1H
1-aminoadamantane	DD3R	D1H	D1H	D1H
Hexamethyleneimine	NS	NS	D1H	—
2-(aminomethyl)tetrahydrofuran	NS	NS	D1H	—
1,2-diaminocyclohexane	NS	NS	D1H	—

*D3C = dodecasil 3C; Melano = melanophlogite; D1H = dodecasil 1H; DD3R = deca-dodecasil 3R and NS = nonasil.

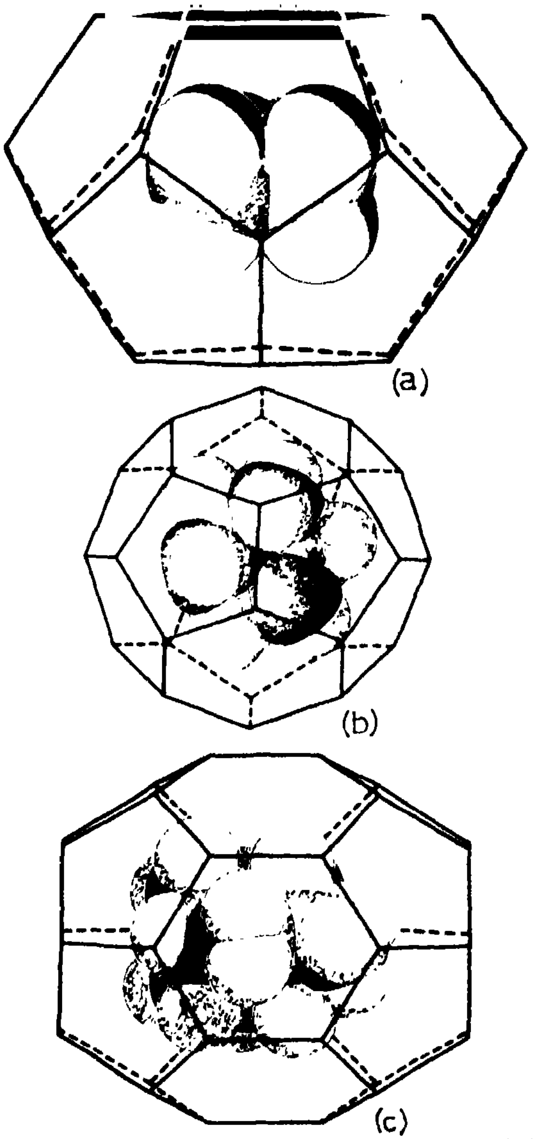

Fig. 3—Orientation of guest molecules in some cages of clathrasils [(a) Methylamine in $[5^{12}6^2]$ cage of melanophlogite; (b) piperidine in $[5^{12}6^4]$ cage of dodecasil 3C; and (c) 1-aminoadamantane in $[5^{12}6^8]$ cage of dodecasil 1H)

Table 5—Cage Characteristics of Clathrasils

Cage type	Shape	Free diameter of 'windows' in Å (approx)	Effective inner volume in $Å^3$ (approx)
$[5^4 6^4]$-8-hedron	Ellipsoid	2.5	25
$[4^1 5^8]$-9-hedron	Sphere	1.5	30
$[4^3 5^6 6^1]$-10-hedron	Sphere	2.5	35
$[4^3 5^6 6^3]$-12-hedron	Sphere	2.5	50
$[5^{12}]$-12-hedron	Sphere	1.5	80
$[5^{12} 6^2]$-14-hedron	Ellipsoid	2.5	160
$[5^{12} 6^4]$-16-hedron	Sphere	2.5	250
$[4^3 5^{12} 6^1 8^3]$-19-hedron	Ellipsoid	4.0	350
$[5^{12} 6^8]$-20-hedron	Ellipsoid	2.5	430
$[5^8 6^{12}]$-20-hedron	Ellipsoid	2.5	290

Attempts to synthesize pure B-P analogues of clathrasils have so far been unsuccessful.

Acknowledgement

Part of the work reported in this paper has been carried out at the Institute of Mineralogy, Kiel University in West Germany with the financial support from the Alexander von Humboldt Stiftung. The author wishes to thank Prof. Dr. F. Liebau and Dr. H. Gies for their assistance in the experimental work.

References

1 Gies H, Liebau F & Gerke H, *Angew Chem* (*Int. Ed*), **21** (1982) 206.
2 Liebau F, *Zeolites*, **3** (1983) 191.
3 Barrer R M, *J Inclusion Phenomena*, **1** (1983) 105.
4 Kropatshewa S K & Makarow J J, *Dokl Akad Nauk USSR*, **224** (1975) 905.
5 Gies H, *Z Kristallogr*, **164** (1983) 247.
6 Bibby D M & Dale M P, *Nature*, **317** (1985) 157.
7 Gies H, *Z Kristallogr*, **167** (1984) 73.
8 Gerke H & Gies H, *Z Kristallogr*, **166** (1984) 11.
9 Gies H, *Z Kristallogr*, (In press).
10 Marler B, Dehnbostel N, Eulert H H, Gies H & Liebau F, *J Inclusion Phenomena*, **4** (1986) 339.
11 Gunawardane R P, Gies H & Liebau F, *Z Anorg Allg Chem*, **546** (1987) 189.
12 Flanigen E M, Bennett J M, Grose R W, Cohen J P, Patton R L, Kirchner R M & Smith J V, *Nature*, **271** (1978) 512.

Indian Journal of Chemistry
Vol. 27A, May 1988, pp. 387-389

Composition of Chromate & Chromate-Phosphate Conversion Coatings on Aluminium using Rutherford Backscattering Spectroscopy

M OKI
Department of Chemistry, University of Port Harcourt, P.M.B. 5323, Port Harcourt, Nigeria

Received 8 *June* 1987; *accepted* 8 *September* 1987

Compositions of chromate and chromate-phosphate conversion coatings formed by natural immersion of aluminium specimens in the respective coating baths have been studied by Rutherford backscattering spectroscopy (RBS). The chromate coating consists mainly of chromium oxide whereas the coating formed from the chromate-phosphate bath consists essentially of chromium phasphate.

Conversion coatings on aluminium and other metals provide an adherent base for subsequent paint application[1]. In addition, the coatings afford some degree of corrosion resistance on the substrate metal[2].

The chromate or chromate-phosphate coatings are usually developed in solutions containing fluoride ions which activate the metal followed by cathodic reduction of Cr(VI) species in solution, in addition to hydrogen evolution reaction.

The present Rutherford backscattering spectroscopy investigation seeks to know the composition of these coatings in order to formulate a general mechanism for their formation. An understanding of the mechanism of formation of the coatings may lead to the formulation of better corrosion resistant coatings.

Materials and Methods

Spade-like electrodes, made of 99.999% pure aluminium (0.002% Cu; 0.004% Fe; 0.003% Si) were electropolished at ~5°C and 20-22V in perchloric acid- ethanol mixture for 5 min. After electropolishing, the specimens were rinsed in distilled water and dried by passing a cold stream of air.

The two conversion coating baths employed had the following compositions: Chromate: 4g CrO_3, 3g $Na_2Cr_2O_7$ and 0.8g NaF, and chromate-phosphate: 100g H_3PO_4, 4g CrO_3 and 1g NaF. The coating baths were made up to 1 litre with distilled water. Conversion coating procedure was performed by fully immersing the electropolished specimens in the individual coating solution for 2 min at 25°C. The specimens were then rinsed in distilled water and dried in air.

Rutherford backscattering spectroscopic (RBS) examination of the two specimens was carried out with a 6 MeV Van de Graaff accelerator at the University of Manchester, UK.

The RBS arrangement and calculations of the elemental compositions of the coatings closely followed those described by Skeldon[3,4]. However, $^4He^+$ ion beams were employed to obtain the spectra in the present study. The specimens were tilted at an angle of 30° to the incident beam in the system with a background vacuum level of approximately 10^{-4}Pa. Scattered particles from the targets were detected at an angle of 165° to the incident beam direction by an annular silicon surface barrier detector. The operating current employed was in the range of 1-15 nA.

Results and Discussions

The RBS spectra for the chromate and chromate-phosphate conversion coated specimens are displayed in Figs. 1 and 2 respectively.

For the chromate specimen (Fig.1) the major peaks identified are from chromium and oxygen, whereas oxygen, chromium and phosphorous are identifiable from Fig.2. The oxygen to the other atom atomic ratios, calculated from the peak yields are: oxygen to chromium ratio 0.53 + 0.03 (Fig.1) and oxygen to chromium ratio 0.160 ± 0.005 (Fig.2) and oxygen to phosphorous ratio 0.187 ± 0.005. In both cases, the ratios are constant throughout the bulk of the coatings, i.e. from the coating/environment interface to the metal/coating interface. The ratios indicate that the atomic compositions of the coatings are: $Cr_{1.59\pm0.09}\cdot O_3$ for the chromate specimen and $Cr_{0.64\pm0.02}\cdot P_{0.75\pm0.002}\cdot O_4$ for chromate-phosphate specimen. For both the coatings the approximated atomic ratios will be Cr_2O_3 and $CrPO_4$ respectively.

In a similar study[5], XPS investigation revealed that the chromate conversion coating was composed mainly of hydrated Cr(III) oxide, with about 10% of the chromium content being in +6 oxidation state. The same investigation showed

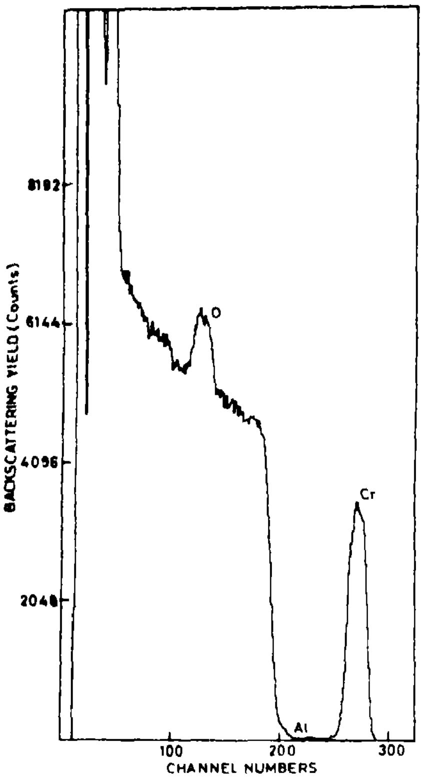

Fig. 1—RBS spectrum for chromate conversion coating developed on aluminium for 2 min

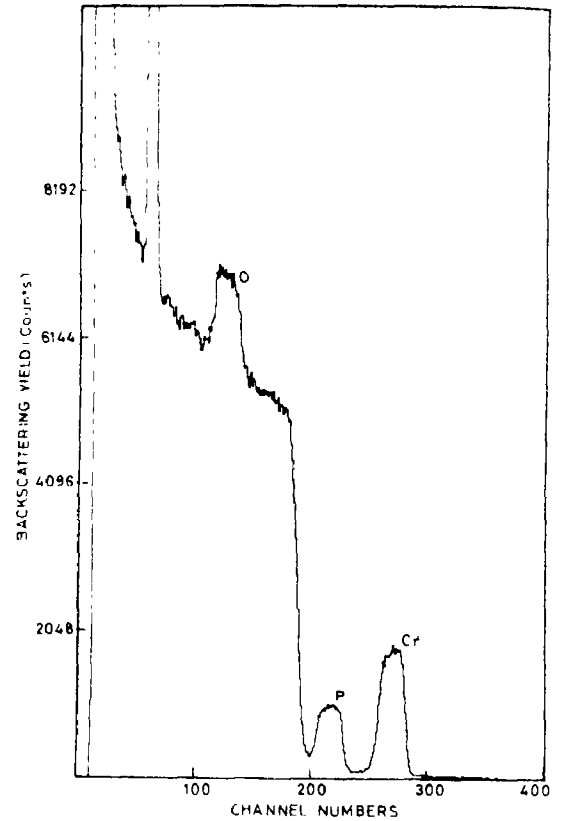

Fig. 2—RBS spectrum for chromate-phosphate conversion coating developed on aluminium for 2 min

that the composition of the specimen treated in the chromate-phosphate bath was hydrated $CrPO_4$. These results are in agreement with the findings of Traverton and Davies[6] who employed XPS techniques with argon etching to study chromate and chromate-phosphate conversion coatings on aluminium. In the present study, there is no indication for the presence of water of hydration. This may be due to the age of the coating – two weeks, prior to analysis. During this period the coatings would have dried up completely. In addition, the water of hydration may have dried up in the high vacuum operating in the Van de Graaff accelerator before analysis was completed.

In Fig.1, a small peak from aluminium is observable at channel number 210. Whereas, in Fig.2, it is not clear whether aluminium is present in the coating. The edge corresponding to scattering from aluminium is overlapped by the phosphorous peak, indicating, the phosphorous yield includes some contribution due to aluminium if the latter were present in the coating. However, in both cases the aluminium yield may be derived from within the coatings and/or from the substrates at spalled or cracked regions. 'Mud-cracking' is a characteristic feature of both coatings[7]. From investigations using Scanning electron Microscopy (SEM) and ultramicrotomy/ Transmission electron Microscopy (TEM) techniques[8], some of the cracks present in the coatings are observed to penetrate to the metal/coating interface. It is likely that the aluminium yield is partly derived from such cracked regions. In addition, during the activation of aluminium substrate by the complexing action of the fluoride species present in the coating baths, cathodic reduction of Cr(VI) to Cr(III) species is accompanied by hydrogen evolution. The liberation of hydrogen, obviously, leads to increase in the *p*H of the solution. The theory[9,10] which supports the hydrogen evolution reaction also indicated the deposition of hydrated aluminium oxide-from Al^{3+} generated during the activation of the substrate by F^-. Such hydrated aluminium oxide may be trapped within the growing coating and this will partly account for the aluminium yields observed.

If the aluminium yield is derived from the coatings and its distribution within the coating thickness assumed to be constant, the aluminium oxygen ratio (from Fig.1) comes out to be 0.074.±0.005. This leads to the composition of $Al_{0.22\pm0.02}$. $Cr_{1.59\pm0.09}$. O_3. On the other hand, the aluminium oxygen ratio in the chromate-phosphate specimens is $<<0.01$. The presence of aluminium species in the coatings agrees with the findings of Abd Rabbo *et al*[11] and that of Traverton and Davies[6] who respectively employed SIMS and XPS techniques to study conversion coatings on aluminium. Such aluminium species are either AlF_3 or AlOF.

From the atomic composition obtained by the RBS technique, the formation of the coatings can proceed through the following steps.

(i) Activation of aluminium substrate achieved by the complexing action of fluoride in the coating baths (Eqs 1 and 2),

$$Al_2O_3 \xrightarrow{F^-} AlOF\text{ (soluble)} \qquad \ldots(1)$$

or

$$Al_2O_3 \xrightarrow{3F^-} AlF_3\text{ (soluble)} \qquad \ldots(2)$$

It has been shown by potential-time measurements for electropolished aluminium 1g/litre NaF solution that fluoride maintains aluminium substrate active at a potential of about -0.9V. This is consistent with activation of substrate by fluoride species in the solution[8].

(ii) The exposed, reactive aluminium surface acts as a source of electrons for the reduction of Cr(VI), in contact with it, to Cr(III) species (Eq.3).

$$Al^\circ + Cr^{6+} \rightarrow Cr^{3+} + Al^{3+} \qquad \ldots(3)$$

When the solubility product for Cr_2O_3 is exceeded, it deposits on the metal via the quilibrium reaction (Eq.4).

$$Cr_2O_3 \rightleftharpoons 2Cr^{3+} + 3H_2O \qquad \ldots(4)$$

However, in the presence of PO_4^{3-} in the chromate-phosphate bath, $CrPO_4$ is deposited in preference to Cr_2O_3. the solubility product of the former is lower than that of the latter. Thus, reaction (5) becomes predominant.

$$CrPO_4 \rightleftharpoons Cr^{3+} + PO_4^{3-} \qquad \ldots(5)$$

The presence of Cr_2O_3 in chromate-phosphate coating was reported by Traverton and Davies[6]. However, they further stated that it might have been generated from $CrPO_4$ during argon sputtering prior to XPS analysis. It is likely that reaction (4) takes place as well; however, the product, Cr_2O_3, is largely converted into $CrPO_4$ in the presence of excess phosphate ions.

Acknowledgement

The author wishes to thank Dr M Skeldon of UMIST, UK, for the provision of time during RBS analysis and Dr G E Thompson for his guidance.

References

1 Wernick S & Pinner R, *The surface treatment and finishing of aluminium and its alloys* (Robert Draper, Teddington) 1972.

2 Katzman H A, Malouf G M, Baner R & Stupian G, *Appl Surf Sci*, **2** (1979) 416.

3 Skeldon P, Shimizu K, Thompson G E & Wood G C, *Surface Interface Anal*, **5** (1983) 252.

4 Skeldon P, Shimizu K, Thompson G E & Wood G C, *Surface Interface Anal*, **5** (1983)247.

5 Asami K, Oki M, Thompson G E, Wood G C & Ashworth V, *Electrochim Acta*, **32**(2) (1987) 337.

6 Treverton J A & Davies N C, *Metals Technology*, **4** (1977) 480.

7 Treverton J A & Amor M P, *Trans Inst Metal Finishing*, **60** (1982) 92.

8 Oki M, *Conversion coatings on aluminium*, Ph D Thesis, UMIST, UK, 1985.

9 Sutton W H, *Pitting corrosion of aluminium*, Ph D Thesis, University of Manchester, UK, 1971.

10 Wood G C, Sutton W H, Richardson J A, Riley T K & Natherbe A C, *Proceeding of U R Evans Conference on Localized Corrosion*, National Association of Corrosion Engineers Houston, Texas.

11 Abd Rabbo M F, Richardson J A & Wood G C, *Corr Sci*, **18** (1978) 117.

Indian Journal of Chemistry
Vol. 27A, May 1988, pp. 390-393

Ionic Conduction through Anodic Oxide Films Formed on Niobium in Oxalic Acid

R K NIGAM*, K C SINGH & SANJEEV MAKEN
Department of Chemistry, Maharshi Dayanand University, Rohtak 124 001

Received 14 *May* 1987; *revised* 29 *September* 1987; *accepted* 7 *October* 1987

Anodic oxidation of niobium is carried out at different current densities and temperatures in 0.1 *N* oxalic acid solution by eliminating the difference of film growth caused by different surface conditions. Tafel slope is found to be independent of temperature, but decreases with increase in current density. Dewald's double barrier theory of ionic conduction has been examined critically and various parameters calculated for Nb_2O_5 films and compared with those of Ta_2O_5 films. A comparison of Nb_2O_5 and Ta_2O_5 film data shows that Dewald theory is applicable to both the systems However, magnitudes of various parameters are quite different in both the cases The large values of parameters *a* and *b* particularly at higher current density set, are difficult to visualize but these large half-distance values are not impossible in amorphous Nb_2O_5 film.

In our earlier work[1,2] on the kinetics of anodic oxidation of tantalum, it was established that Dewald's double barrier theory[3,4] expalined the data more satisfactorily than any other single barrier theory. In order to check, if the anodic oxidation behaviour of tantalum and niobium is similar or not, the kinetics of growth of Nb_2O_5 films, has been presently studied using 0.1 *N* oxalic acid as contacting electrolyte. The data have been examined in terms of Dewald's theory[3,4].

Materials and Methods

The method of preparing niobium specimens (99.9% purity) with 2×10^{-4} m^2 in area was the same as that described elsewhere[1]. To eliminate the surface condition effects, the specimens were treated as described earlier[2] such that the Tafel slope was given by Eq. (1)

$$\tau = \frac{E_1 - E_2}{2.303} \qquad \ldots (1)$$

where E_1 and E_2 are the field strength at i_1 (upto a formation voltage of 30V) and i_2 (upto a formation voltage of 50V) current densities respectively. The values of E_1 and E_2 were calculated for the same formation voltage. The density of Nb_2O_5 film was taken as 4.36 $kgdm^{-3}$ as reported by Holtzberg *et al.*[5] Oxalic acid used for preparation of 0.1 *N* contacting electrolyte was of AR (BDH) grade.

Results and Discussion

The plot of voltage of formation versus time of anodization for the current density pair (100, 10 Am^{-2}) at 294.15K is presented in Fig. 1. Similar plots were obtained at other current density pairs (20, 2 and 60, 6 Am^{-2}) and also at other temperatures (294.15, 304.15, 314.15, 324.15 and 334.15K). Each set of observation was repeated five times and the values of field strengths, E_1 and E_2, at a particular current density pair and temperature

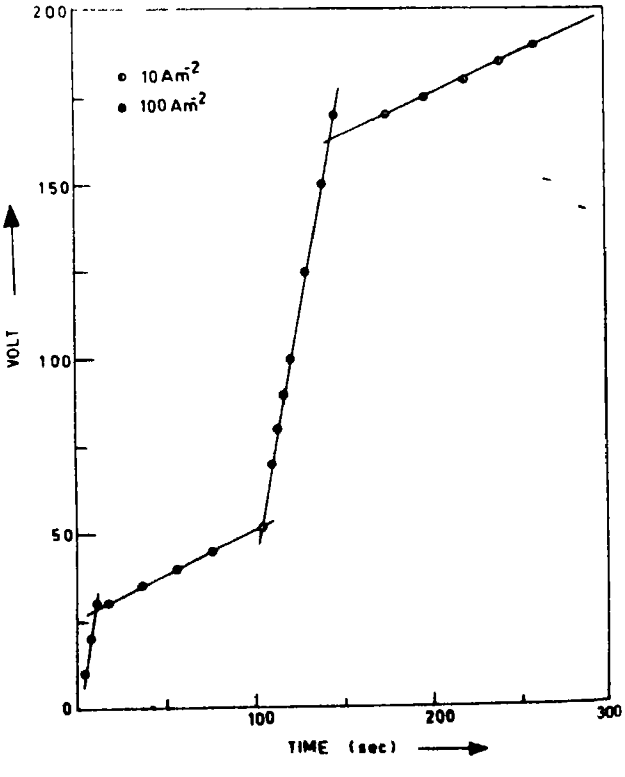

Fig. 1—Typical run for anodization at 294.15K

Table 1—Calculated Values of Field Strengths (E_1 and E_2) for Various Current Density Sets

Temp. (K)	10^{-8} Field strength (Vm^{-1}) at current density sets 20-2		60-6		100-10	
	E_1	E_2	E_1	E_2	E_1	E_2
284.15	4.14	3.87	4.36	4.20	4.62	4.48
294.15	3.94	3.67	4.16	4.00	4.44	4.30
304.15	3.76	3.49	3.98	3.82	4.28	4.14
314.15	3.57	3.30	3.80	3.64	4.12	3.98
324.15	3.40	3.13	3.64	3.48	3.98	3.84
334.15	3.26	2.99	3.50	3.34	3.85	3.71

were calculated and the values are presented in Table 1. The reproducibility in the field values was $\pm 0.005 \times 10^8$ Vm^{-1}. The field strength increases with current density but decreases with temperature for all the current density pairs studied. As in case of tantalum the plots of E versus 1/T irrespective of current density employed are linear and parallel (Fig. 2) indicating that the difference of field at all temperatures for a given current density pair is constant and hence the Tafel slopes are independent of temperature. Now we examine our data in term of Dewald's theory[3]. The expression for change in the field (ΔE), bringing about increase in current density ten times is given by Eq. (2)

$$\Delta E = \Delta E_0 - \frac{1}{\beta}\left[F(\delta) - F(\delta/\theta)\right] \qquad \ldots (2)$$

Here ΔE_0 is the change in the field due to surface charge and its value is 2.303 kT/bq and $F(\delta)$ is a function dependent upon the space charge δ. Equation (2) can be written as

$$2.303\, a/b - \beta \Delta E = F(\delta) - F(\delta/\theta) \qquad \ldots (3)$$

Tafel slope (τ) from Dewald's theory is given by Eq. (4)

$$\tau = \frac{kT}{aq}\left[1 + (a/b - 1)\ln\left(\frac{1+\delta}{\delta}\right)\right] \qquad \ldots (4)$$

Using Equations (4) and (3), the parameters a and b were determined as under:

(i) The values of a and a/b were assumed and hence the value of θ was evaluated.

(ii) $F(\delta) - F(\delta/\theta)$ (r.h.s. of Eq. (3)) was represented graphically as a function of δ.

(iii) The values of 2.303 $a/b - \beta\Delta E$ (l.h.s. of Eq. (3)) at different temperatures were evaluated.

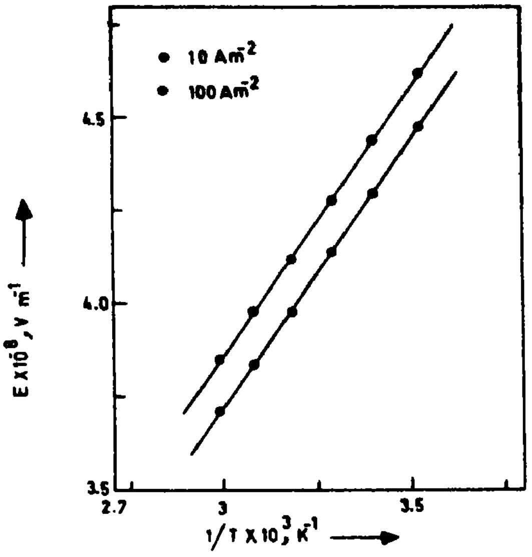

Fig. 2—Plot of E versus 1/T

(iv) From (i) and (iii) by interpolation, the value of $\delta(T)$ was determined.

(v) Using the values of δ, a and a/b, the theoretical value of Tafel slope (τ) was calculated.

Such a calculation was repeated until values of a and b were found such that an agreement with experimental values of Tafel slopes were obtained. There are two widely different values of a/b ratio which allow a quantitative fit to all the data available. The ratio a/b along with absolute values of a and b are presented in Table 2. Only for these values of a/b, it was possible to achieve a temperature-independent Tafel slope. The values of a and b increase with increase in current density; the ratio a/b increase slightly with increase in current density. The correct value of a/b (whether it is ≈ 1.35 or ≈ 0.820) is difficult to decide. Dewald used the values of a/b ratio, which gave minimum values of a and b. Using the same criterion we have chosen $a/b \approx 0.820$, for further calculation of various parameters. The values of δ at different temperatures and for different current density sets, show that δ decreases with increase in temperature (Table 3). The effect of space charge is more clearly observed at a temperature when $\delta > 1$. This effect becomes predominant as the temperature is lowered. The δ value depends mainly on $\exp[-W/kT]$ as shown in Eq. (5)

$$\delta = \beta\gamma n_0 \Delta x$$

$$= \frac{2\pi q}{\nu kT\varepsilon}(N_s \nu_s q)^{a/b} i^{1-a/b} \exp(-W/kT)\,\Delta x \qquad \ldots (5)$$

Table 2—Two Sets of Absolute Values of Parameters *a*, *b* and *a/b*

Current density pair (A m $^{-2}$)	*a* (nm)	*b* (nm)	*a/b*	*a* (nm)	*b* (nm)	*a/b*
2-20	0.540	0.417	1.295	0.400	0.492	0.813
6-60	0.950	0.704	1.349	0.680	0.829	0.820
10-100	1.090	0.805	1.354	0.780	0.948	0.823

Table 3—Values of Space Charge Terms (δ) of Dewald Theory for Different Current Density Sets at Various Temperatures

Temp. (K)	Current density (Am $^{-2}$) set*			Current density (Am $^{-2}$) set†		
	20-2	60-6	100-10	20-2	60-6	100-10
284.15	0.020	0.014	0.008	8.900	11.200	12.80
294.15	0.546	0.486	0.473	3.270	3.6700	3.95
304.15	1.320	1.140	1.120	1.510	1.6250	1.72
314.15	2.500	2.070	2.030	0.720	0.7470	0.78
324.15	4.430	3.440	3.350	0.280	0.2800	0.29
334.15	7.920	5.570	5.400	0.012	0.0005	0.005

**a/b* > 1
†*a/b* < 1

The value of W has been evaluated from the plot of log δ versus 1/T (Fig. 3). These plots were linear for all the current density pairs and the values of W calculated at such current density pairs are given in Table 4. Knowing δ and E, the surface charge field (E_0) was evaluated using Eq. (6)

$$E = E_0 + \frac{1}{\beta}\left[\left(1 + \frac{1}{\beta\gamma n_0 \Delta x}\right)\ln(1 + \beta\gamma n_0 \Delta x) - 1\right] \qquad \ldots (6)$$

The values of E_0/T were computed and plotted against 1/T (Fig. 4). For each current density pair such plots were linear. E_0, the field due to surface charge is given by Eq. (7)

$$E_0 = kT/bq \ln(i/N_s \nu_s q) + \phi/bq \qquad \ldots (7)$$

Here *b* is entrance half-jump distance, N_s is the concentration of ions on the surface, ν_s is the vibrational frequency normal to the barrier and ϕ is the entrance barrier energy. According to Eq. (7) such plots should be linear with a slope = ϕ/bq. From the slopes, the values of ϕ, the entrance barrier energy were obtained and are given in Table 4. Using the relation $U = a\phi/b - W$ the value of *U*, the diffusion barrier energy were calculated and these are reported in Table 4. Both ϕ and *U* seem to increase with current density and magnitude of *U* is smaller than that of ϕ at all the current density sets. This suggests that the rate-determining step would be ionic movement at the metal/oxide interface and not across the film. However, at high field the correct activation energies would be ($\phi - Ebq$) and ($U - Eaq$) instead of ϕ and *U*. Therefore, using average value of field for each current density set, taking charge on each

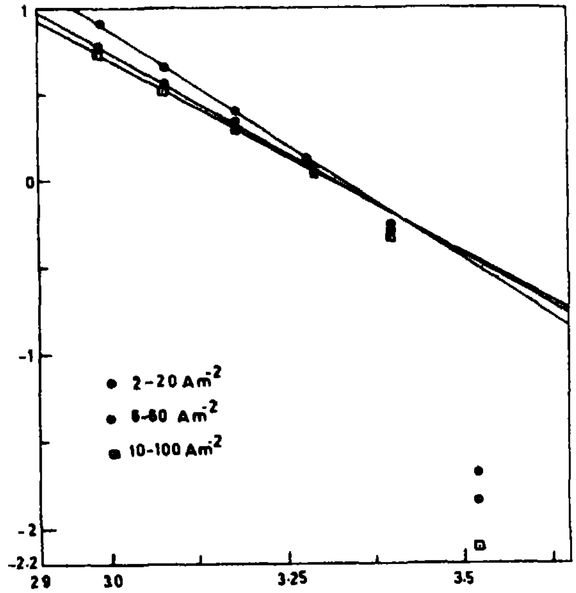

Fig. 3—Plot of log δ versus 1/T when (*a/b* > 1)

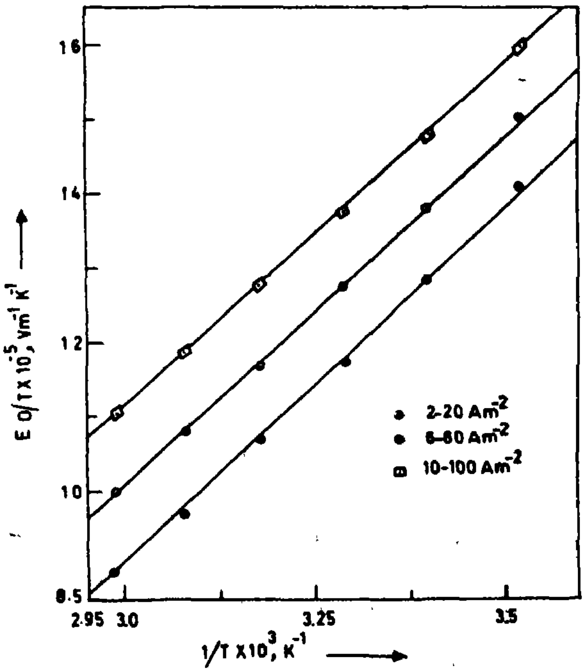

Fig. 4—Plot of E_0/T versus 1/T when (*a/b* > 1)

Table 4—Values of Various Parameters for Oxalic Acid Film from Dewald Theory at Different Current Density Sets

Current density set (Am^{-2})	τ(Vm^{-1})	W$\times10^{-19}$ (J)	$\phi\times10^{-19}$ (J)	U$\times10^{-19}$ (J)	$(\phi-U)\times10^{-19}$ (J)	$(\phi-Ebq)\times10^{-19}$ (J)	$(U-Eaq)\times10^{-19}$ (J)
				$a/b > 1$			
20-2	11.72	0.8671	3.2478	3.3388	−0.0910	2.0619	1.8031
60-6	6.95	0.7631	5.3239	6.4187	−1.0948	3.0134	3.5038
100-10	6.08	0.7439	5.9587	7.3243	−1.3655	3.2824	3.7003
				$a/b < 1$			
20-2	11.72	0.9528	2.9227	1.5946	1.4082	1.5229	0.9157
60-6	6.95	1.1002	5.4723	3.1161	2.3411	2.9288	1.9247
100-10	6.08	1.2146	6.1515	3.8467	2.5917	2.9998	1.9407

niobium atom in Nb_2O_5 film as 5e and using values of ϕ, U, b and a from Table 4, the values of $(\phi-Ebq)$ and $(U-Eaq)$ were computed and are recorded in Table 4. The value of $(\phi-Ebq)$ is greater than that of $(U-Eaq)$ at each current density set and this again suggests that the rate-determining step would involve ionic movement at metal/oxide interface. Though there is a substantial contribution of space charge $(\delta > 1)$ at low temperature yet the rate-controlling step is at the metal/oxide interface. This is a misleading conclusion. It seems that our choice of $a/b \approx 0.820$ is not correct. Next we assumed $a/b \approx 1.35$ and calculated the values of various parameters at different current densities and temperatures adopting the same procedure as given above, and the values of various parameters obtained are recorded in Table 4. The values of W were obtained from the plots of log δ versus 1/T for all the current density pairs. The values of ϕ were obtained from plots of E_0/T versus 1/T at each current density pair.

It can be seen from Table 4, that magnitude of ϕ is smaller than that of U at all current density pairs, thus indicating that the rate-determining step for ionic movement would be within the film and not at the metal/oxide interface. The values of $(\phi-Ebq)$ and $(U-Eaq)$ are not much different from each other suggesting the metal/oxide interface barrier is important for the conduction of ions. With the increase in current density, the value of $(\phi-Ebq)$ is slightly less that of $(U-Eaq)$. This shows that the rate-controlling step also shifts from metal/oxide interface to the diffusion barrier within the film.

Comparison of results of Ta_2O_5 and Nb_2O_5 films

In our earlier work[2] on Ta_2O_5 films, it was found the value of Tafel slope increases with increase in current density. Contrastingly decreases for Nb_2O_5 films. In Ta_2O_5 films a is constant at all current densities while b decreases with increase in current density. In Nb_2O_5 film both a and b increase with increase in current density. The behaviour of ϕ, U and W with current density is the same for Nb_2O_5 films, showing the dual barrier control of ionic movement. But the Ta_2O_5 film the value of $(U-Eaq)$ is consideribly larger than that of $(\phi-Ebq)$, indicating that the space charge (ϕ) plays a dominant role in the conduction of ions in Ta_2O_5 film.

Acknowledgement

One of the authors (SM) thanks the CSIR, New Delhi for the award of a junior research fellowship.

References

1 Nigam R K, Kalra K C & Katyal P, *Indian J Chem*, **25A** (1986) 1080.

2 Nigam R K, Kalra K C & Katyal P, *Indian J Chem*, **26A** (1987) 819.

3 Dewald J F, *J electrochem Soc*, **102** (1955) 1.

4 Bray A R, Jacobs P W M & Young L, *Proc phys Soc, London*, **71** (1958) 405.

5 Holtzberg F, Reisman A, Berry M & Berkenblit M, *J Am chem Soc*, **79** (1957) 2039.

Indian Journal of Chemistry
Vol. 27A, May 1988, pp. 394-397

Solvent Effects on Solvolysis of Transition Metal Complexes: Part III[†]— Kinetics of Aquation of Chloropentaamminecobalt(III) in Aquo-Organic Solvent Media

ANADI C DASH[*], NIMAI C NAIK[‡] & RABINDRA K NANDA[*]
Department of Chemistry, Utkal University, Bhubaneswar 751 004

Received 24 *February* 1987; *accepted* 6 *July* 1987

The kinetics of aquation of chloropentaamminecobalt(III) ion has been investigated in aquo-organic solvent media in the temperature range of 40-55°C and in 0-60 wt% organic cosolvent such as MeOH, EtOH, isopropanol and *t*-butanol. Activation parameters are interpreted in terms of initial state and transition state solvation effects. It apears that the transition state is solvent-stabilised to a greater extent than the initial state. The rate data in isodielectric solvent media involving MeOH, EtOH, isopropanol, *t*-butanol, ethyleneglycol and dioxan ($D = 50$ at 40°C) interestingly point out the differential solvation interaction of these solvents with the substrate, the individuality of the monohydroxylic alcohols being completely lost in the correlation of aquation rate constant (log k_{aq}) with the mol fraction of the organic solvent component.

It has now been realised that solvent structure plays important role in controlling the rate and activation parameters of solvolysis of haloamminecobalt(III) complexes[1]. The interaction of ionic substrates with aquo-organic solvent media is likely to be influenced by the potential H-bonding sites available in the substrate and the solvent. The chloropentaamminecobalt(III) ion [$(NH_3)_5CoCl^{2+}$] is an ideally suited substrate in this regard as it possesses potential hydrophilic NH-centres for H-bonding with aqueous-alcoholic solvent systems. Earlier studies[2] on solvolytic aquation of this substrate have been concerned with the correlation of aquation rate constant with $1/D$ (D= bulk dielectric constant) or Grunwald-Winstein's '*Y*' parameters of the solvent to provide evidence in favour of the dissociative interchange mode (I_d) of activation. We present in this paper the results of a detailed investigation of the energetics of aquation of this substrate in different aquo-organic solvent media with a view to throwing light on the solvation of its initial state and transition state and explore the role, if any, of the structure of the solvent medium in modulating its reactivity.

Materials and Methods

Chloropentaamminecobalt(III) diperchlorate, prepared as mentioned earlier[3], analysed satisfactorily and its spectral parameters were in excellent agreement with those reported in the literature: {λ_{max} nm (ε, dm^3 mol^{-1} cm^{-1}); 532 (50.5) lit λ_{max} 532 (50.5)[4] and 532 (50.8 ± 0.4)[5]}.

Absorption spectra were recorded on a Beckman DU_2 spectrophotometer. Methanol and isopropanol (AR, BDH) were distilled before use. Absolute ethanol was prepared from rectified spirit. Dioxan (AR, BDH) was refluxed for 48 hr over solid caustic soda and distilled. It was again treated with sodium wire, kept overnight and redistilled. *t*-Butanol (AR, BDH) and ethyleneglycol (LR, BDH) were dried over anhydrous potassium carbonate before fractional distillation. All solvents were kept out of contact with atmospheric moisture. Solvent mixtures of desired compositions (weight %) were prepared using measured densities of the organic solvent and water.

The kinetics of aquation were followed by potentiometric titration of the liberated chloride against standard $AgNO_3$ (N/100) and the pseudo-first order rate constant (k_{aq}) was calculated from the gradient of the plots of log ($V_\infty - V_t$) against time. V_∞ was determined by subjecting the mixture (5 cm^3) to base hydrolysis in the presence of alkali and then working up in the usual way.

For most of the solvent systems used and at > 40 Wt % organic cosolvent, the reverse reaction shown in Eq. (1), interfered with the aquation process. Under such condition the equilibrium point was established and the titration data were treated in terms of a first order reaction opposed by a second order reaction[6].

$$(NH_3)_5CoCl^{2+} + H_2O \underset{k'}{\overset{k_{aq}}{\rightleftharpoons}} (NH_3)_5CoOH_2^{3+} + Cl^- \quad \ldots (1)$$

[†] Part II: Dash A C & Dash N, *J chem Soc Faraday Trans* 1 (In press)

[‡] Present address: Deputy Registrar, Utkal University, Bhubaneswar 751 004.

Table 1—Rate Data for Aquation of $(NH_3)_5CoCl^{2+}$ in Aquo-Organic Solvent Mixtures

Wt % of organic cosolvent	$10^6\ k^s_{aq}\ (s^{-1})^{(a)}$ in different solvent and at different temperatures												
	Methanol			Ethanol			Isopropanol			*t*-Butanol			
	40°	45°	50°	40°	45°	50°	40°	45°	50°	40°	45°	50°	55°C
10.0	8.11	16.7	28.5	8.11	15.7	30.3	8.16	16.3	30.9	8.83	15.4	32.7	52.6
20.0	6.63	11.8	24.0	6.92	13.7	25.8	7.52	14.9	28.3	8.22	13.5	30.3	49.2
30.0	5.65	10.4	19.3	6.19	11.2	23.2	6.44	12.5	22.5	6.58	13.0	23.3	43.2
40.0	4.20	7.72	14.2	5.46	10.3	18.9	5.71	11.0	20.4	5.64	12.8	18.9	44.0
50.0	3.26	6.55	10.8	4.86	9.01	16.2	4.52	9.04	16.1	5.84	12.8	20.4	45.1
60.0	—	5.46	7.31	3.83	7.33	14.4	3.54	7.31	13.3	—	—	—	—

(a) $[H^+]_T = 0.01$, $[Complex]_T = 0.005$ mol dm^{-3}

$10^6\ k^s_{aq}\ (s^{-1}) = 10.2$ (40°C), 18.7 (45°C) and 33.7 (50°C) in the absence of organic cosolvent.

All runs were made atleast in duplicate. The mean deviation of k^s_{aq} in most cases was < 2%.

Results and Discussion

Table 1 presents the k^s_{aq} values, corresponding to the forward reaction in Eq (1), in various solvent systems at different temperatures. The plots of log k^s_{aq} against D_s^{-1} (D_s = bulk dielectric constant of the medium) and X_{org} (X_{org} = mol fraction of the organic solvent component) at 40-45°C were linear in the MeOH-, EtOH- and isopropanol-water systems. However, deviations from linearity in the plots were distinct in *t*-butanol-water system beyond 30 wt%. Linearity in the correlation of log k^s_{aq} with *Y*-parameter was good in MeOH-water and EtOH-water systems but was poor in isopropanol and *t*-butanol-water systems (using the data of Robertson and Sugamori[7] for the values of *Y*) (see Fig. 1). Hence individuality of solvent system is evident. Nevertheless, the electrostatic effect mediated by the solvent interaction with substrate appears to be the dominant factor in Co-Cl bond heterolysis. It is interesting to note that the individuality of the monohydroxylic alcohols is completely lost in the plot of log k^s_{aq} versus X_{org} under isodielectric condition (Fig. 2). The data points in ethyleneglycol and dioxan clearly deviate significantly from linearity in opposite direction, indicating the rate- accelerating effect of the former and the rate- retardation of the latter (relative to monohydroxylic alcohols). It is in line with the fact that between ethyleneglycol and dioxan, the former acts as a better solvating agent than the monohydroxylic alcohols.

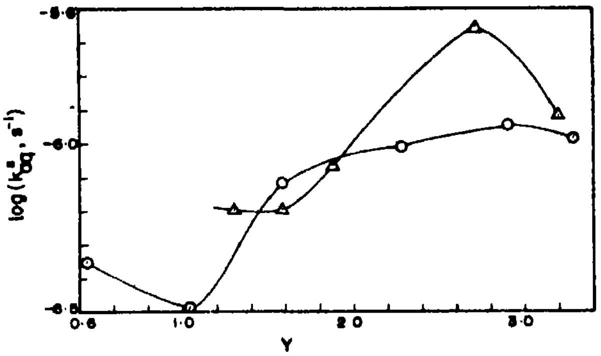

Fig. 1—Plots of log k^s_{aq} versus *Y* at 25°C [(⊙)-Isopropanol-water and (△)-*t*-butanol-water]

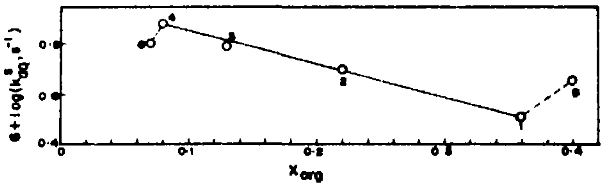

Fig. 2—Correlation of k^s_{aq} of $(NH_3)_5CoCl^{2+}$ with X_{org} at 40°C and isodielectric media (D = 50) [(1) MeOH, (2) EtOH, (3) isopropanol, (4) *t*-butanol, (5) ethyleneglycol and (6) dioxan].

It has been suggested that aquation of $(NH_3)_5CoCl^{2+}$ in fully aqueous and mixed solvent media involves I_d mode of activation in which Cl^- at best is very weakly bound to the cobalt(III) centre in the transition state[8]. Recently volume profile calculations for aquation of $(NH_3)_5CoX^{n+}$ ($X = Cl^-, Br^-, SO_4^{2-}, NO_3^-$, Me_2SO and H_2O) by Palmer and Kelm[9] agree with the fact that the charges of the departing groups are fully developed in the transition state. Their calculations, based upon the additivity principle for the molar volume of the transition state, indicate that the transition state is a D-type one which leads to the formation of the intermediate $(NH_3)_5Co^{3+}$. It then seems reasonable to represent the general scheme of activation as shown in Scheme 1.

In accord with Scheme 1, and assuming that the additivity principle is valid for the transfer free energy of the transition state,

$$[\Delta G_t\,(t.s.)]_{(s-w)} = [\Delta G_t\,(C^{+3})]_{(s-w)} + [\Delta G_t\,(Cl^-)]_{(s-w)}$$

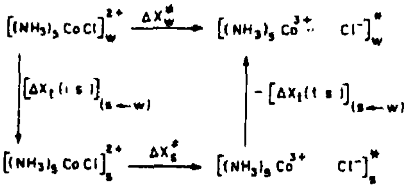
$[(NH_3)_5CoCl]^{2+}_w$
$\Delta X^{\neq}_w$
$[(NH_3)_5Co^{3+}\cdots Cl^-]^{\neq}_w$
$[\Delta X_t(i.s.)]_{(s\leftarrow w)}$
$-[\Delta X_t(t.s.)]_{(s\leftarrow w)}$
$[(NH_3)_5CoCl]^{2+}_s$
$\Delta X^{\neq}_s$
$[(NH_3)_5Co^{3+}\quad Cl^-]^{\neq}_s$

Scheme 1—Interchange dissociative (I_d) mode of activation [i.s. and t.s. denote initial state and transition state respectively: $X = G, H, S$. $[\Delta X_t(i)]_{(s\leftarrow w)}$ refer to the transfer function of the species i, transfer being assumed to take place from water (w) to the mixed solvent (s)]

we get

$$[\Delta G_t(C^{3+}) - \Delta G_t(i.s.)]_{(s\leftarrow w)} = \Delta G^{\neq}_s - \Delta G^{\neq}_w - [\Delta G_t(Cl^-)]_{(s\leftarrow w)} \quad \ldots (2)$$

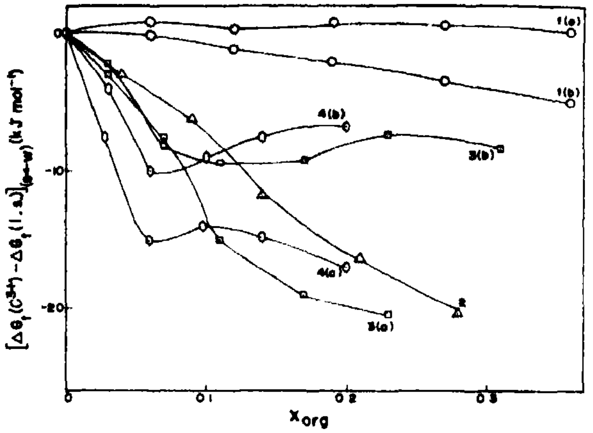

Fig. 3—$[\Delta G_t(C^{3+}) - \Delta G_t(i.s.)]_{(s\leftarrow w)}$ (kJ mol^{-1}) versus X_{org} plots at 25°C [1(a, b), MeOH: based on $\Delta G_t(Cl^-)$ data of (a) Abraham *et al.*[10], (b) Wells[12c]; 2, EtOH: based on $\Delta G_t(Cl^-)$ values of Kundu *et al.*[11]; 3(a, b), isopropanol: based on $\Delta G_t(Cl^-)$ data of Kundu *et al.*[11] and (b) Wells[12c]; 4(a,b), *t*-butanol: based on $\Delta G_t(Cl^-)$ data of (a) Kundu *et al.*[11] (b) Elgy and Wells[12a]]

where $C^{3+} = [(NH_3)_5Co^{3+}]$, $\Delta G^{\neq}_s$ and $\Delta G^{\neq}_w$ denote the free energy of activation in mixed solvent and in water respectively; $[\Delta G_t(i)]_{(s\leftarrow w)}$ is the transfer free energy of the species i when transferred from water (w) to the mixed solvent (s). The values of $\Delta G_t(Cl^-)$ at 298.2K for the solvent systems were taken from literature[10] (directly or by intrapolation/extrapolation to the desired solvent composition), were converted into the mol fraction scale and the values of the relative transfer free energy term at all solvent compositions $[\Delta G_t(C^{3+}) - \Delta G_t(i.s.)]_{(s\leftarrow w)}$ were calculated at 25°C. These were plotted as a function of X_{org} (Fig. 3). It is interesting to note that the relative transfer free energy term is strongly negative at all solvent compositions except in MeOH-water system for which it is less convincing due to the larger disagreement in the data for $[\Delta G_t(Cl^-)]_{(s\leftarrow w)}$ reported by Abraham *et al.*[10], Kundu *et al.*[11] and Wells[12]. Nevertheless it is worth noting that tripositive cobalt(III) centre in the transition state is relatively more stabilised than the dipositive initial state when transfer occurs from water to mixed solvent, $[\Delta G_t(C^{3+})]_{(s\leftarrow w)} < [\Delta G_t(i.s.)]_{(s\leftarrow w)}$. It may be noted, however, that the disagreement in two sets of values of $[\Delta G_t(Cl^-)]_{(s\leftarrow w)}$ in MeOH-water system is perhaps due to different extra thermodynamic assumptions used as pointed out by Blandamer *et al.*[13]. Also it is important to note that different experimental methods of evaluation of $[\Delta G_t(Cl^-)]_{(s\leftarrow w)}$ yield slightly different results for isopropanol-water and *t*-butanol-water solvent systems (see Fig. 3). Nevertheless the nonlinear variation of $[\Delta G_t(C^{3+}) - \Delta G_t(i.s.)]_{(s\leftarrow w)}$ with X_{org} exhibiting minima in the plots (Fig. 3) depict the solvent structural reorganisation in the cospheres of the initial state and transition state of the substrate. The activation parameters are given in Table 2.

The solvent structural changes in the cospheres of the initial state and the transition state are also evident in the activation enthalpy and activation entropy versus X_{org} plots (Fig. 4, curves a and b). The solvent cosphere effects on $\Delta H^{\neq}$ and $\Delta S^{\neq}$ seem to vary with the nature of the organic solvent component in the order: *t*-butanol > isopropanol > EtOH > MeOH. It is worthwhile to note that there exists

Table 2—Activation Parameters[a] for Aquation of $(NH_3)_5CoCl^{2+}$ in Aquo-Organic Solvent Mixtures

Wt% of organic cosolvent	Methanol		Ethanol		Isopropanol		*t*-Butanol	
	$\Delta H^{\neq}$	$\Delta S^{\neq}$	$\Delta H^{\neq}$	$\Delta S^{\neq}$	$\Delta H^{\neq}$	$\Delta S^{\neq}$	$\Delta H^{\neq}$	$\Delta S^{\neq}$
10.0	103 ± 1	−15 ± 5	108 ± 1	+25 ± 2	109 ± 1	+5 ± 4	99.2 ± 2.9	−26 ± 8
20.0	100 ± 2	−23 ± 7	108 ± 2	+ 2 ± 5	109 ± 1	+8 ± 4	84.9 ± 1.7	−71 ± 5
30.0	102 ± 2	−20 ± 5	103 ± 1	−17 ± 2	102 ± 6	−17 ± 17	104 ± 2	−12 ± 5
40.0	101 ± 2	−25 ± 5	102 ± 2	−21 ± 7	104 ± 1	−12 ± 2	115 ± 1	+21 ± 3
50.0	105.9 ± 0.4	−11 ± 2	99.1 ± 0.4	−29 ± 1	109.5 ± 0.4	−2 ± 1	112.9 ± 0.2	+15.1 ± 0.4
60.0	—	—	106.2 ± 0.4	−10 ± 1	114.1 ± 0.4	+16 ± 1	—	—

[a] Units. kJ mol^{-1} for $\Delta H^{\neq}$ and JK^{-1} mol^{-1} for $\Delta S^{\neq}$; $\Delta H^{\neq} = 97.9 \pm 0.8$ kJ mol^{-1} and $\Delta S^{\neq} = -28 \pm 2.5$ JK^{-1} mol^{-1} in aqueous medium.

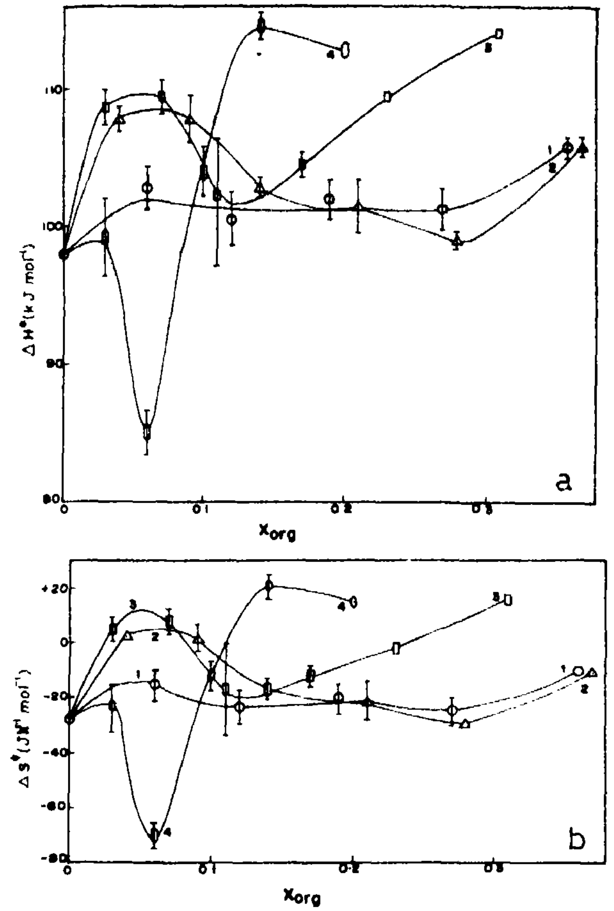

Fig 4—(a) Solvent dependence of activation enthalpy for, aquation of $(NH_3)_5CoCl^{2+}$ [$\Delta H^{\neq}$ (kJ mol^{-1}) versus X_{org} plots for (1) MeOH, (2) EtOH, (3) isopropanol and (4) *t*-butanol].
(b) Solvent dependence of activation entropy for the aquation of $(NH_3)_5CoCl^{2+}$ [$\Delta S^{\neq}$ (JK^{-1} mol^{-1}) versus X_{org} plots for (1) MeOH, (2) EtOH, (3) isopropanol and (4) *t*-butanol]

an isoenthalpy and isoentropy region in MeOH, EtOH and isopropenol-water systems around $X_{org} = 0.12$ to 0.14. The effects of activation enthalpy and entropy on the reaction rate are mutually compensatory. It is reasonably to think that variation in enthalpy and entropy values are associated with the enthalpy and entropy changes, due to H-bond breaking and reformation in the Gurney-cosphere[14] of the initial state and the transition state of the substrate.

Acknowledgement

One of the authors (ACD) is thankful to the CSIR, New Delhi for financial support. This work forms a part of the Ph.D thesis of NCN who is thankful to the UGC, New Delhi for the award of Junior Research Fellowship.

References

1 Blandamer M J & Burgess J, *J Coord Chem Rev*, **31** (1980) 93.
2 Burgess J & Price M G, *J chem Soc(A)* (1971) 3108.
3 Naik N C & Nanda R K, *J inorg nucl Chem*, **36** (1974) 3793.
4 Buckingham D A, Olsen I I, Sargeson A M & Satrapa H, *Inorg Chem*, **6** (1967) 1028.
5 Reynold W L & Barber E S, *Int J Chem Kinetics*, **7** (1975) 443.
6 Frost A A & Pearson R G, '*Kinetics and Mechanism*' (Wiley, 2nd ed) (1961) p 186.
7 Robertson R E & Sugamori N, *J Am Chem Soc*, **91** (1969) 7256.
8 Swaddle J W, *Coord Chem Rev*, **14** (1974) 217.
9 Palmer D A & Kelm H, *Coord Chem Rev*, **36** (1981) 89.
10 Abraham M H, Hill T, Ling H C, Schulz R A & Watt R A C, *J chem Soc Faraday Trans* 1, **80** (1984) 489.
11 Bose K, Das K, Das A K & Kundu K K, *J chem Soc Faraday Trans* 1, **74** (1978) 1051.
12(a) Elgy N C & Wells C F, *J chem Soc Faraday Trans* 1, **79** (1983) 2367 (see Table 3).
(b) Sidahmed I M & Wells C F, *J chem Soc Faraday Trans* 1, **79** (1983) 1035 (see Table 3).
(c) Wells C F, *J chem Soc Faraday Trans* 1, **69** (1973) 984.
13 Blandamer M J, Burgess J, Clark B, Duce P P, Hakin A W, Gosal N, Radulovic S, Guardado P, Sanchez F, Hubbard C D & Abu-Gharib E A, *J chem Soc Faraday Trans* 1, **82** (1986) 1471.
14 Gurney R W, *Ionic processes in solution* (Mc-Graw Hill, New York) 1953.

Indian Journal of Chemistry
Vol. 27A, May 1988, pp. 398-403

Solvent Effects on Reactions of Coordination Complexes: Part IV† – Acid Catalysed Aquation of Oxygen Bonded (αβS)-(Sulphito)(tetraethylenepentamine)cobalt(III) in Aqeous Binary Mixtures of Protic & Dipolar Aprotic Cosolvents—A Flash Photolysis Study on Sulphur Bonded (αβS)(Sulphito)-(tetraethylenepentamine)cobalt(III) Ion

ANADI C DASH* & NEELAMADHAB DASH
Department of Chemistry, Utkal University, Bhubaneswar 751 004
and
SUKUMAR ADITYA* & ANSUMAN ROY‡
Department of Chemical Technology, University College of Science and Technology, 92, A P C Road,
Calcutta 700 009

Received 21 *September* 1987; *accepted* 29 *October* 1987

Medium effects on the acid-catalysed aquation of oxygen-bonded (αβS)(sulphito)(tetren)cobalt(III) has been investigated at 25°C using dimethyl sulphoxide-water, acetonitrile-water and methanol-water media of varying compositions. The O-bonded sulphito species has been generated *in situ* from the corresponding stable S-bonded isomer as a transient by flash photolysis of the latter isomer in solution and the kinetics of its acid-catalysed decay to $(\alpha\beta S)[(tetren)CoOH]^{2+}$ and SO_2 (ms time scale) has been investigated by flash kinetics in the range of $[H^+]_T = (1$ to $20) \times 10^{-4}$ mol dm^{-3}. The protonation constant of $(\alpha\beta S)[(tetren)CoOSO_2]^+$ and the rate constant of aquation of its protonated form have been evaluated at various compositions of the mixed solvent media. It turns out that the reaction medium plays dominant role in mediating the rate of elimination of SO_2 from the protonated O-bonded sulphito complex, although the process is totally intramolecular. The Brønsted correlation between log k_H and pK of $(\alpha\beta S)[(tetren)CoOSO_2H]^{2+}$ is valid with a slope $= -0.58$ irrespective of the solvent media chosen except for acetonitrile-water at mol fraction of acetonitrile > 0.25.

The acid-catalysed aquation of oxygen bonded (αβS)(sulphito)(tetraethylenepentamine) cobalt (III), $(\alpha\beta S)[(tetren)CoOSO_2]^+$ involves fast protonation preequilibrium followed by slow elimination of SO_2 from the protonated substrate without heterolysis of Co – O bond[1] as depicted in Eq. (1):

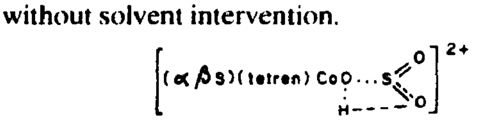

$$\begin{tikzcd}[(tetren)CoOSO_2]^+ + H^+ \arrow[r, shift left, "K_H"] & \arrow[l, shift left] [(tetren)CoOSO_2H]^{2+} \arrow[d, "k_H", "-SO_2"'] \\ {[(tetren)CoOH_2]^{3+}} \arrow[r, shift left, "fast"] & \arrow[l, shift left] H^+ + [(tetren)CoOH]^{2+} \end{tikzcd} \quad ..(1)$$

The rate-controlling step is presumed to involve a transition state (I) in which the proton attached to S-bound oxygen is transferred to the Co – O bond. This process may be totally intramolecular with or without solvent intervention.

I

In the light of these observations, it was considered worthwhile to examine the medium effect on the protonation equilibrium of the dipolar complex ion, (tetren) $CoO^{2+} - SO_2^-$, a species in which the cobalt(III) centre is surrounded by the hydrophobic skeleton of tetren. Unfortunately the oxygen-bonded sulphito complex is highly unstable[1] and has not yet been prepared in the solid state. On the contrary the corresponding sulphur-bonded isomer is highly stable and has been well characterized[1] in the solid state and in solution. In an earlier paper, Aditya and coworkers[2] demonstrated that flash photolysis of a solution of the S-bonded sulphito complex generated the corresponding O-bonded isomer as a transient intermediate which underwent fast acid-catalysed elimination of SO_2 without any other side reaction. We took advantage of this method of generating the O-bonded sulphito complex, $(\alpha\beta S)(tetren)CoOSO_2^+$ from the corresponding stable S-bonded isomer. In this paper attempts have been made to elucidate the role of medium on the rate of acid-catalysed aquation and on the protonation equilibrium of $(\alpha\beta S)[(tetren)CoOSO_2]^+$. The organic solvent components of the mixed solvent media chosen

---

†Part III: Dash A C, Naik N C & Nanda R K, *Indian J Chem*, **27A** (1982) 394.

‡Present address: Chloride India R&D Centre,
Calcutta 700 059

Table 1—Rate Data for Acid-catalysed Aquation of (αβS)[(tetren)CoOSO$_2$]$^+$ at 25.0°C

[(tetren)CoSO$_3^+$]$_T$ = 3.4 × 10^{-4} mol dm^{-3}

Medium	Vol % of O.S.$^{(a)}$	k_{obs} (s^{-1})^b at		10^4[HClO$_4$]$_T$ (mol dm^{-3})		
		1.00	2.00	5.00	10.0	20.0
AN/W	0	165 ± 11	366 ± 25	713 ± 32	1410 ± 290	1690 ± 230
	10.0	186 ± 8	357 ± 25	876 ± 140	1450 ± 150	1980 ± 180
	30.0	423 ± 60	799 ± 50	1620 ± 30	2500 ± 200	
	50.0	1100 ± 280	1650 ± 210	3480 ± 210		
DMSO/W	10.0	274 ± 15	505 ± 45	1100 ± 80	2010 ± 150	3330 ± 500
	30.0	269 ± 28	587 ± 60	1100 ± 82	2030 ± 110	
	50.0	279 ± 39	571 ± 90	1080 ± 200	1650 ± 160	
	70.0	420 ± 40	790 ± 150	1390 ± 140	2030 ± 120	2080 ± 20
MeOH/W	10.0		359 ± 21	950 ± 90	1520 ± 200	2330 ± 400
	30.0		321 ± 28	793 ± 73	1450 ± 110	2400 ± 400
	50.0			535 ± 40	865 ± 72	1740 ± 200
	70.0			910 ± 110	1640 ± 100	3010 ± 100

(a) Vol % refer to organic solvent component

(b) Errors are average deviations from mean of duplicate or triplicate runs

were methanol (MeOH) dimethyl sulphoxide (DMSO), and acetonitrile (AN).

Materials and Methods

Water was triply-distilled. The organic solvents were all spectroscopic grade. The sulphur-bonded (αβS) (sulphito) (tetraethylenepentamine) cobalt (III) perchlorate was prepared and characterized as described earlier[1,2]. Solvent mixtures were prepared by volume and then converted to weight per cent. All other chemicals used were of AR grade. The acidity of the reaction media was controlled by HClO$_4$. No attempt was made to fix ionic strength by addition of any inert electrolyte since added electrolytes at high concentrations are likely to cause structural perturbations in the solvent media.

Flash photolysis of the acidified ([HClO$_4$]$_T$ = (1 to 20) × 10^{-4} mol dm^{-3}) solutions of the S-bonded sulphito complex (3.4 × 10^{-4} mol dm^{-3}) was performed in optical quartz cell of 10 cm path length with air filled quartz lamps discharged at ~ 200J (1/e time ≅ 30 μs). A 150 watt xenon arc lamp was used as the analysing source. The decay kinetics of the transient species, (αβS)[(tetren)-CoOSO$_2$]$^+$, monitored at 390 nm, was recorded on a Iwatsu Digital Storage oscilloscope through IP28 photomultiplier; data captured were then transferred to a strip chart recorder. The voltage out-put versus time (ms) plot was manually smoothened and analysed graphically to yield the pseudo-first order rate constant from the slope of log ($A_t - A_\infty$) versus t (ms) plots. The rate measurements were made at 25°C.

Results and Discussion

The rate data for the acid-catalysed decay of the transient in different solvent media of varying compositions are presented in Table 1. It is worth noting that at low acidities in methanol-water media, the formation of a stable species absorbing at 390 nm could be observed**. The reason for not getting any transient absorption at 390 nm in some of the acetonitrile-water and DMSO-water media at [H$^+$] = 0.01, 0.02 mol.dm^{-3} (see Table 1) may be due to high acid-catalysed decomposition rates of the transient or formation of no transient under these conditions. In accord with the rate and equilibrium steps shown in Eq. (1), the pseudo-first order rate constant is given by Eq. (2),

$$k_{obs.} = \frac{k_H K_H^T [H^+](f_{H^+} f_{CoOSO_2^+} / f_{CoOSO_2H^{2+}})}{1 + K_H^T [H^+](f_{H^+} f_{CoOSO_2^+} f_{CoOSO_2H^{2+}})} \quad ...(2)$$

where K_H^T denotes the thermodynamic protonation constant of (αβS)[(tetren)CoOSO$_2$]$^+$; *f*s are the activity coefficients; and K_H is the SO$_2$ elimination rate constant for the protonated O-bonded sulphito complex. Equation (2) further assumes that the activity coefficient of the transition state of the acid-catalysed path (k_H path) is equal to the activity coefficient of the initial state (i.e. (αβS) [(tetren)CoOSO$_2$H]$^{2+}$ species). This is reasonable considering the net charge of the initial state and the transition state and the low ionic strength of the media (2.34 × 10^{-3} ≤ *I*, mol dm^{-3} ≤ 4.4 × 10^{-3}).

**Further work is in progress to identify the species in methanol-water media at low acidities

Further assuming $f_{H^+} = f_{CoOSO_2^+} = f_+$ and writing $f_{CoOSO_2H^{2+}} = f_{2+}$, Eq. (2) is linearized to yield Eq. (3):

$$k_{obs}^{-1} = k_H^{-1} + (k_H K_H^T)^{-1} \{f_{2+}/([H^+]f_+^2)\} \quad \ldots (3)$$

The activity coefficient (f_i) was calculated from the Debye-Huckel equation,

$$\log f_i = -AZ_i^2\sqrt{I}/(1 + Ba\sqrt{I}) \quad \ldots (4)$$

assuming $a = 5$ Å for both the solvated proton and the cobalt(III) species; the values of the parameters $A = 1.8246 \times 10^6/(DT)^{3/2}$ and $B = 50.29/(DT)^{1/2}$ were computed using the dielectric constant (D) data of DMSO-water and AN-water media[3]. The values of A and B for MeOH-water were chosen from the compilation of Bates and Robinson[4]. The rate data were fitted to Eq. (3) by weighted least squares procedure, the weight of k_{obs}^{-1} being calculated from the error quoted for k_{obs} ($w = [\delta k_{obs}/k_{obs}^2]^{-2}$). Typical plots of k_{obs}^{-1} versus $f_{2+}/([H^+]f_+^2)$ are presented in Fig. 1 and the calculated values of k_H and K_H^T are presented in Table 2. The values of k_H and K_H^T for fully aqueous medium compare reasonably with those reported in our earlier preliminary communication[2] ($k_H = 1.2 \times 10^3$ s^{-1}, $K_H^T = 2 \times 10^3$ dm^3 mol^{-1}).

The plots of log K_H^T versus X_{org} (X = mol fraction of the organic solvent component) (Fig. 2) clearly demonstrate the medium effect on the protonation equilibrium of the O-bonded sulphito complex. Log K_H^T decreases nonlinearly with X_{MeOH} while for AN- and DMSO-water systems minimum in this plot occurs at $X_{AN} = 0.038$ and $X_{DMSO} = 0.032$. Beyond $X_{DMSO} = 0.032$, log K_H^T increases steadily (see curve 3 of Fig. 2). On the other hand at $X_{AN} > 0.038$ log K_H^T increases nonlinearly and tends to attain limiting value at $X_{AN} = 0.2$ (see curve 2, Fig. 2). This behaviour reflects the differential propensities of the mixed solvents to transfer proton from the solvated state to the O-bonded sulphito complex as also the solvation interaction of the protonated and the unprotonated forms of the concerned cobalt(III) substrate in the mixed solvent media. The dielectric constants of the mixed solvent media for any value of X_{Org} are comparable in magnitude. Hence the nature of variation of log K_H^T with X_{Org} is not entirely due to the electrostatics of the protonation reaction. Solvent structural changes also seem to influence K_H^T.

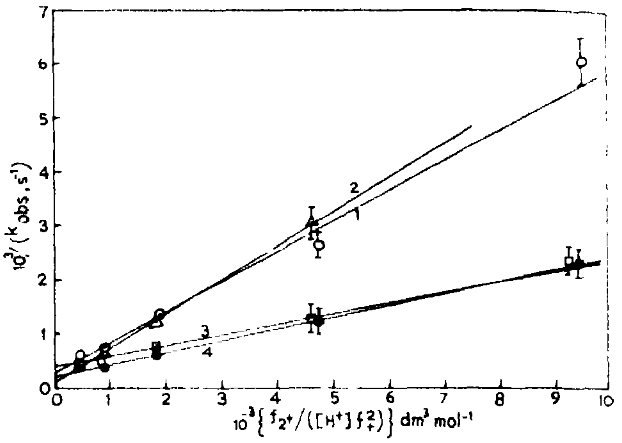

Fig 1—Plot of $10^3/(k_{obs}, s^{-1})$ versus $10^{-3}\{f_{2+}/([H^+]f_+^2)\}$ (dm^3 mol^{-1}) for acid-catalysed SO_2 elimination reaction of ($\alpha\beta S$)[(tetren)CoOSO$_2$]$^+$.[(1), 100% water; (2) 30% (v/v) MeOH, (3) 70% (v/v) DMSO; and (4) 30% (v/v) AN

Both DMSO and AN can not solvate the anionic oxygen site of ($\alpha\beta$S)(tetren)CoO^{2+} $-$ SO$_2^-$ while the dipolar protic MeOH can solvate it effectively by H-bonding. On the otherhand the protonated form of the complex ($\alpha\beta$S)[(tetren)CoOSO$_2$H]$^{2+}$, can be solvated by MeOH, DMSO and AN via H-bonding, e.g. CoOSOOH..S, (CoOSOOH..O=S(CH$_3$)$_2$, CoOSOOH..OHCH$_3$, CoOSOOH...N≡CCH$_3$). This differential solvation effect of the solvents is also responsible for the increased proton affinity of ($\alpha\beta$S)[(tetren)CoOSO$_2$]$^+$ in DMSO-water and AN-water media relative to that in MeOH-water media. The minima in the log K_H^T versus X_{AN} or X_{DMSO} plots presumably are consequences of the break down of normal water struc-

Table 2—Calculated Values of k_H and K_H^T at 25.0°C

Vol % of O.S.[a]	MeOH/W		AN/W		DMSO/W	
	$10^{-3} k_H$ (s^{-1})	K_H^T (dm^3 mol^{-1})	$10^{-3} k_H$ (s^{-1})	K_H^T (dm^3 mol^{-1})	$10^{-3} k_H^T$ (s^{-1})	K_H^T (dm^3 mol^{-1})
0	3.11 ± 0.73	573 ± 136	3.11 ± 0.73	573 ± 136	3.11 ± 0.73	573 ± 136
10.0	6.42 ± 2.50	290 ± 116	4.12 ± 0.20	452 ± 25	6.61 ± 0.90	400 ± 56
30.0	7.45 ± 0.86	215 ± 25	4.98 ± 0.40	876 ± 90	5.81 ± 1.50	475 ± 130
50.0	5.05 ± 3.20	206 ± 136	9.25 ± 2.83	1078 ± 369	3.23 ± 0.25	937 ± 81
70.0	11.3 ± 1 7	148 ± 24		—	2.52 ± 0.18	2016 ± 621

(a) Vol % refers to that of organic solvent component of the mixed solvent

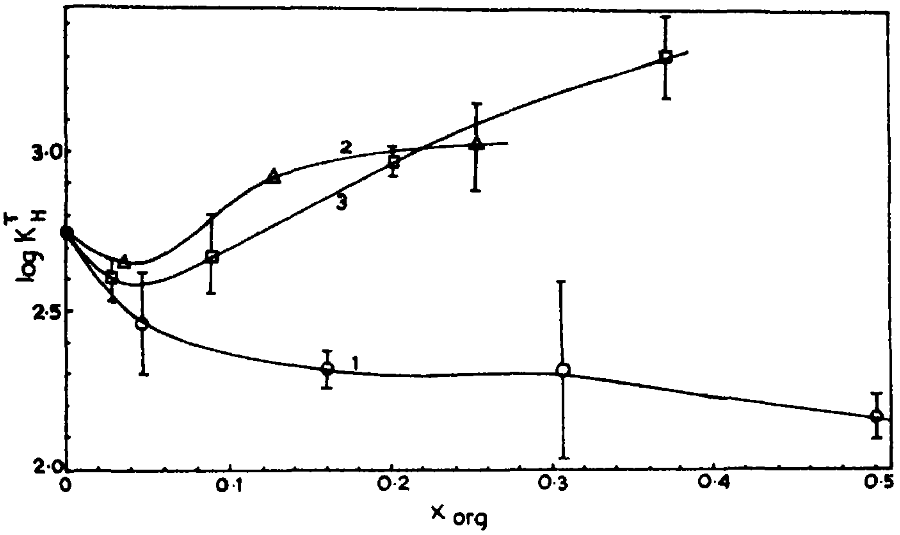

Fig. 2—Plots of log K^T_H versus mol fraction of cosolvent (X_{Org}) [(1) MeOH; (2) AN; and (3) DMSO]

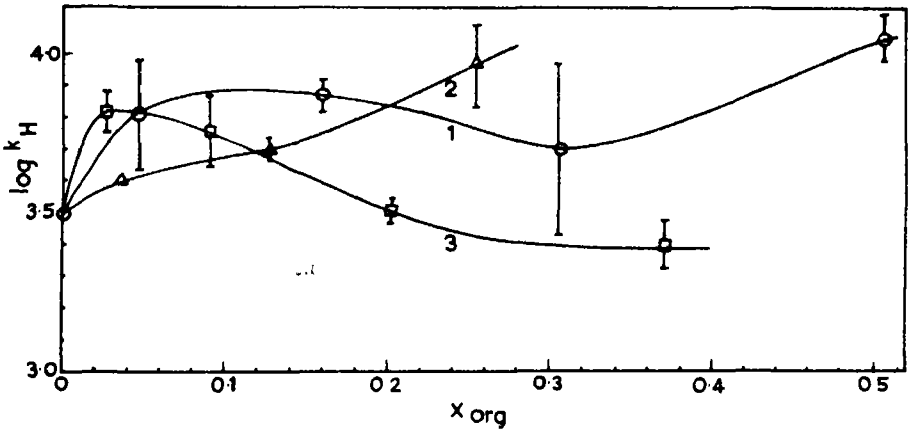

Fig. 3—Plot of log k_H versus mol fraction of cosolvent (X_{Org}) [(1) MeOH; (2) AN; and (3) DMSO]

ture by DMSO and AN at low mol fractions which consequently leads to production of more of monomeric water so that the H-bonding equilibrium (5)

$$(\text{tetren})\overset{III}{\text{Co}}\text{—O}-\text{SOO}^- + H_2O \rightleftharpoons$$

$$(\text{tetren})\overset{III}{\text{Co}}\text{—OSOO}^-\text{...HOH} \qquad \ldots(5)$$

becomes the most favourable. The formation of the proton solvation bridge acts against protonation of the oxygen site of O-bonded sulphito complex so that log K^T_H attains minimum around $X_{AN} = 0.038$ and $X_{DMSO} = 0.032$. Similar trends in the *pK* of phenols in DMSO water media have also been reported[5]. At higher mol fractions of AN and DMSO, however, both these cosolvents are involved in H-bonding with water molecules and DMSO can compete successfully with water for sovlation of H^+ ion. Electrostatic forces also dominate. Hence it is not unusual to expect that the proton affinity of the O-bonded sulphito species increases with increase in mol fraction of DMSO or AN.

Strikingly enough, log k_H versus X_{Org} plots (see Fig. 3) display well developed maximum around $X_{DMSO} = 0.03$; a broad maximum around $X_{MeOH} = 0.12$ and a minimum at $X_{MeOH} = 0.3$. Only a weakly developed inflexion is observed around $X_{AN} = 0.12$. The trend in the reactivities of the protonated species, ($\alpha\beta$S)[(tetren)CoOSO$_2$H]$^+$ (i.e. the rate of elimination of SO$_2$) in the mixed solvent media reflected in the log k_H versus X_{Org} plot leaves no doubt regarding the involvement of medium in the rate-determining process. It is likely that the process of proton transfer from the S−O site to the Co−O site (see the transition state I) is strongly mediated by the medium although the process is totally intramolecular.

The medium effect on the rate of SO_2 elimination reaction can be better understood considering the transfer free energy data for the initial and the transition state (I). On the basis of the transition state equation, $k_H = (kT/h)\exp(-\Delta G^{\pm}/RT)$ and the thermodynamic cycle shown in Scheme 1,

$$\begin{tikzcd}
(\text{i.s.})_s \arrow[r, "\Delta G_s^{\pm}"] & (\text{t.s.})_s \\
(\text{i.s.})_w \arrow[u, "{[\Delta G_t(\text{i.s.})]_{(s\leftarrow w)}}"'] \arrow[r, "\Delta G_w^{\pm}"] & (\text{t.s.})_w \arrow[u, "{[\Delta G_t(\text{t.s.})]_{(s\leftarrow w)}}"']
\end{tikzcd}$$

SCHEME − 1

where i.s. and t.s. denote the initial state and transition state of the reactant $(\alpha\beta S)[(\text{tetren})CoOSO_2H]^{2+}$ respectively; $\Delta G_j^{\pm}$ is the activation free energy in the medium j (j = w for water and s for the mixed solvent) and $[\Delta G_t(i)]_{(s\leftarrow w)}$ is the standard free energy of transfer of the species *i* (i.e. i.s. or t.s.) from water to the mixed solvent, the transfer free energy change of the transition state relative to that for the initial state for the transfer of the species from water to the mixed solvents, can be stated as in Eq. (6).

$$[\Delta G_t(\text{t.s.}) - \Delta G_t(\text{i.s.})]_{(s\leftarrow w)} = 2.303\, RT \log k_H^w/k_{H}s \tag{6}$$

Figure (4) depicts the variation of the relative transfer free energy changes at 25°C as a function of X_{Org} from which the differential solvating behaviour of different media for the initial state and the transition state is clearly evident. Minima in such plots for MeOH-water (at $X_{\text{MeOH}} = 0.15$) and DMSO-water (at $X_{\text{DMSO}} = 0.03$) media with nonlinear variation of the relative transfer free energy term with X_{Org} indicate that structural perturbations in the mixed solvent media also control the solvation of the initial and transition states. The linear decrease of the relative transfer free energy term with X_{AN}, however, would mean that the free energy changes associated with the structural perturbation in the medium is proportional to the variation of the relative transfer free energy function with increasing X_{AN}. It is, however, evident that $[\Delta G_t(\text{t.s.})]_{(s\leftarrow w)}$ is less than $[\Delta G_t(\text{i.s.})]_{(s\leftarrow w)}$ at all solvent compositions except for $X_{\text{DMSO}} > 0.2$. Hence relative to the initial state, the transition state is more stabilized in the mixed solvents. At

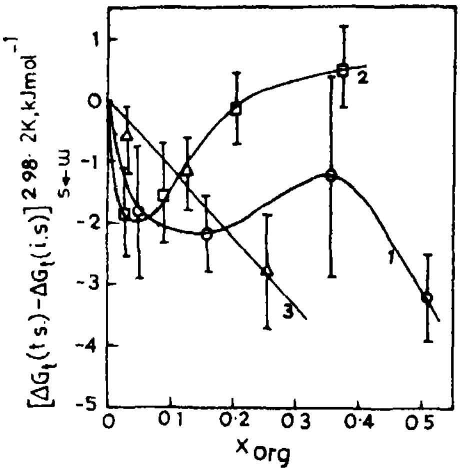

Fig. 4—Plots of $[\Delta G_t(\text{t.s.})-\Delta G_t(\text{i.s.})]_{(s\leftarrow w)}$ 298.2 K (kJ mol^{-1}) versus X_{Org} [(1) MeOH; (2) DMSO; and (3) AN]

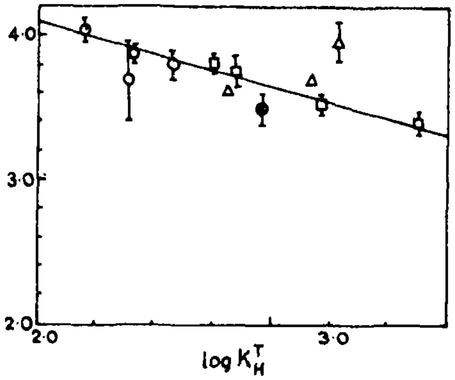

Fig 5—Plot of log k_H versus log K_H^T [○, MeOH; Δ, AN; □, DMSO; and ⊗, 100% water]

$X_{\text{DMSO}} = 0.2$ it appears that there is little difference between the solvational propensity of the initial and the transition states as the value of $[\Delta G_t(\text{t.s.}) - \Delta G_t(\text{i.s.})]_{(s\leftarrow w)}$ approaches zero. At $X_{\text{DMSO}} > 0.2$ the transition state appears to be more destabilized relative to the initial state in DMSO-water medium. Hence it is clear that medium does participate during proton transfer and SO_2 elimination processes and most likely both the processes are solvent-mediated to different degrees.

The solvent effect on the protonation equilibrium is virtually proportional to the solvent effect on the rate process following it. This is evident in the observed Bronsted correlation between log k_H and log K_H^T (see Fig. 5). The numerical value of the slope (= −0.58) of the plot is in keeping with the Marcus' theory for the rate-equilibrium relationship in proton transfer reactions[6]. Data point at high X_{AN} shows positive deviation from the Bronsted plot indicating that such proportionality between the rate and equilibrium parameters is adversely affected as the proportion of AN is increased.

Acknowledgement

This work is supported by a grant to ACD by the CSIR, New Delhi. ND is thankful to the CSIR for the award of a junior research fellowship.

References

1 Dash A C, El Awady A A & Harris G M, *Inorg Chem*, **20** (1981) 3160.

2 Dash A C, Roy A & Aditya S, *Indian J Chem*, **25A** (1986) 207.

3 Lindberg J J & Kenttamaa, *Soum Kemistil B*, **33** (1960) 104 as quoted in. Elgy N C & Wells C F, *J chem Soc Faraday Trans* 1, (1985) 2145; Moreau C & Douheret G, *J chem Thermody*, **8** (1976) 403.

4 Bates R G & Robinson R A in '*Chemical physics of ionic solutions*' edited by B E Conway and R G Barradas (Wiley, New York) pp. 211.

5 Buncel E & Wilson H in *Advances in physical organic chemistry*, Vol. 14, edited by V Gold and D Bethel (Academic Press, New York) 1977, pp. 143.

6 (a) Marcus R A, *J phys Chem*, **72** (1968) 891;
(b) Marcus R A, *J Am chem Soc*, **91** (1969) 7224.

Indian Journal of Chemistry
Vol. 27A, May 1988, pp. 404-406

'Antispectrochemical' Behaviour of Cobalt(II) & Nickel(II) Chelates of Substituted Trialkylphosphates

SURAJ P NARULA*, SUNITI KUMAR, S K BHARADWAJ & RAJEEV SHARMA
Department of Chemistry, Panjab University, Chandigarh 160 014

Received 14 *May* 1987; *revised* 8 *September* 1987; *accepted* 21 *September* 1987

The chelates of the type $M[O_2P(OR)_2]_2$ [where M = Co(II), Ni(II) and R = 2-chloroethyl and 2,2,2-trifluoroethyl] have been prepared by the solvolysis of the corresponding divalent metal chlorides or acetates by respective trialkylphosphates. While the cobalt(II) derivatives are tetrahedral with two $(RO)_2P(O)_2$ chelating groups, the nickel(II) derivatives have a distorted octahedral geometry resulting from the possible participation of the ethereal oxygen of the alkoxy group. The organophosphate chelating groups reveal 'antispectrochemical behviour' in these systems.

A large number of metal compounds of alkylphosphonates and alkylphosphates have been reported[1-4]. It is shown that an alkylphosphate generates a bidentate ligating group, $(RO)_2P(O)_2$ *in situ* upon solvolysis with metal halides. Mikulski *et al.*[1] have reported that the trivalent metals essentially form eight-membered rings due to the presence of bidentate ligating groups forming a bridge between two metal ions. These compounds are, however, polymeric. The divalent metal ions, it is claimed[2-4] retain a four-membered bidentate chelating structure comprising monomeric strucutral units. Nevertheless, no attempt has been made to elucidate the structure of cobalt(II) and nickel(II) chelates of the halo substituted trialkylphosphates, and hence the title investigation. Electronic spectra of chelates of triethylphosphate of these metals have also been studied.

Materials and Methods

Triethylphosphate (BDH, LR) was used as such. Tris(2-chloroethyl)- and tris(2,2,2-trifluoroethyl)-phosphates were prepared by the interaction of freshly distilled haloalcohols with freshly distilled $POCl_3$ (b.p. 105.3°) in the molar ratio 3.1:1. The reaction was vigorous in the beginning but could be taken to completion only by driving out HCl by a stream of dry N_2 at 100-120°C. The absence of Cl^- ions showed the complete conversion of $POCl_3$ into the corresponding ester. Excess haloalcohol was removed by distillation *in vacuo*. The purity of phosphoric ester was checked by its IR and ^1H NMR spectra.

Preparation of metal chelates

Bis(2-chloroethoxy)phosphato chelates of Ni(II) and Co(II) were obtained by refluxing metal chlorides or acetates (1 mmol) and tris(2-chloroethyl)phosphate (2.3 mmol) at 170-80°C *in vacuo*. The resultant oily product could be solidified by adding ether, the precipitates were filtered and dried *in vacuo*. The reactions of tris(2,2,2-trifluoroethyl)phosphate with the metal salts were carried out by refluxing the reaction mixture at 170-80° in a continuous stream of dry N_2. In both the cases the completion of the reaction was judged either by the absence of chloride ion or acetate group (IR). Bis(diethoxy)phosphato chelates of nickel(II) and cobalt(II) were prepared as described earlier[2].

Physical measurements

The infrared spectra were recorded as nujol mulls on a Perkin-Elmer 377 double beam grating spectrophotometer using NaCl optics and the electronic spectra on a Hitachi 330 spectrophotometer using MgO as standard. Magnetic moments were determined by Gouy's method.

Results and Discussion

Tris(2-chloroethyl)/(2,2,2-trifluoroethyl)phosphates are weakly co-ordinating ligands and give rise to syrupy complexes even with $SbCl_5$, $TiCl_4$ etc.[5] However, on reaction with cobalt(II) and nickel(II) chlorides or acetates, coloured solids are obtained (Table 1). The infrared spectra of the pure esters, $[(ClC_2H_4O)_3PO]$ and $[(CF_3CH_2O)_3PO]$ exhibit $\nu P{=}O$ modes at 1270 and 1290 cm^{-1} respectively. Upon chelation these bands are shifted to lower wavenumbers and appear in the range 1180-1190 cm^{-1}. On the other hand $\delta P{-}O{-}C$ (ester) modes remain more or less unperturbed and are observed at 970-980, 1020-1040 and 1060-1100 cm^{-1} in the case of 2-chloroethyl and 2,2,2-trifluoroethyl derivatives. Similar observations have also been reported by earlier workers[2-4]. The IR spectra of chelates,$M\{O_2P(OCH_2CF_3)_2\}_2$ exhibit $\nu_{as}CF_3$ and $\delta_{as}CF_3$ modes around 1280 and 660 cm^{-1}, respectively.

The electronic spectra of Co(II) chelates $Co\{O_2P(OC_2H_5)_2\}_2$, $Co\{O_2P(OC_2H_4Cl)_2\}_2$ and $Co\{O_2P(OC_2H_2F_3)_2\}_2$ have been examined. Among these, the ethyl derivative has already been reported[2] but no spectral data were mentioned. All of them display multiple bands, characteristic of tetrahedral cobalt(II) compounds[7]. Unlike the trivalent and the tetravalent metal organophosphates[1], these are soluble in several organic solvents and can, therefore, be visualized as monomers. The spectral data were processed by several methods suggested by König[6]. The ligand field parameters satisfying the best spectral fittings are given in Table 2. The average values of ν_2 and ν_3 were obtained considering spin-orbital coupling and taking a weighted average of components as suggested by Drago[8]. It is found, that the Δ_{tet} values for ethyl, 2-chloroethyl and tris(2,2,2-trifluoroethyl) derivatives are very close indicating a considerable π-character in the metal-ligand interaction. Contrary to expectations the fluoro substituted chelate, asserts the highest ligand field perturbation. The diffuse reflectance spectra of nickel(II) compounds are, noticeably, atypical of tetrahedral derivatives and exhibit three well-defined band envelops. All possible fittings of the spectral data assuming a tetrahedral geometry were computed but D_q and B' values so obtained are absurd. The conclusion of earlier workers[2-4] are based on analogies between cobalt(II) and nickel(II) chelates and are therefore subject to revision. It is also worth noticing that the band envelope, ν_1, of nickel(II) compounds is attended with some splitting, indicating slight distortion from octahedral geometry. The chelating moiety in the case of nickel(II) derivatives may have the structure (I).

Table 1—Analytical Data on Organophosphate Chelates of Cobalt(II) and Nickel(II)

Compound	Colour	Found (Calc.) %			
		C	H	P	Metal
$[Co\{O_2P(OC_2H_4Cl)_2\}_2]$	Deep blue	19.4 (19.0)	3.32 (3.28)	12.2 (12.3)	11.5 (11.7)
$[Co\{O_2P(OC_2H_2F_3)_2\}_2]$	Light blue	16.4 (16.5)	1.32 (1.37)	10.4 (10.6)	10.4 (10.5)
$[Ni\{O_2P(OC_2H_4Cl)_2\}_2]$	Yellow	19.1 (19.0)	3.37 (3.18)	12.4 (12.3)	11.6 (11.7)
$[Ni\{O_2P(OC_2H_2F_3)_2\}_2]$	Light yellow	16.4 (16.5)	1.35 (1.37)	10.6 (10.7)	10.6 (10.5)

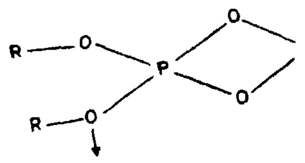

(I)

The 'satellite' ethereal site, it is argued, is engaged with Ni(II) of another molecule. Mikulski *et al.*[1] have proposed the existence of bridging bis(dialkylphosphato) groups in octahedral derivatives of transition metal ions. Thus there are two types of oxygen atoms in the $Ni[O_6]$ chromophore which should be represented as: $Ni[O^*_2O_4]$ (O^*, oxygen atom from the ethereal P–O–R group), and this not only explains the splitting of some of the electronic spectral bands but also the poor solubility of Ni(II) chelates in comparison to that of Co(II) chelates. The ligands follow the spectrochemical series: 2-chloroethyl > ethyl > 2,2,2-trifluoroethyl;

Table 2—Electronic Spectral Data and Ligand-Field Parameters of Organophosphate Chelates of Cobalt(II) and Nickel(II)

Compound	ν_1 (kK)	ν_2 (kK)	ν_3 (kK)	D_q (kK)	B' (kK)	Charge reduction
$[Co\{O_2P(OC_2H_5)_2\}_2]^*$	—	5 74	16.12	3.78	8.838	1.0
		6.45	18.50			
$[Co\{O_2P(OC_2H_4Cl)_2\}_2]^*$	—	5.81				
		6.51	16.67	3.86	0.837	1.0
		7.35	18.18			
$[Co\{O_2P(OC_2H_2F_3)_2\}_2]^*$	—	8.51 10.31	16.66 19.23	3.88	0.780	1.2
$[Ni\{O_2P(OC_2H_5)_2\}_2]^+$	7.23	11.83	21.98	7.29	0.800	1.5
$[Ni\{O_2P(OC_2H_4Cl)_2\}_2]^+$	7.02	12.50	23.80	7.52	0.926	0.7
$[Ni\{O_2P(OC_2H_2F_3)_2\}_2]^+$	7.40	12.90	23.80	7.14	0.959	0.5

*Values and assignments for tetrahedral disposition of ligands
+Values and assignments for octahedral disposition of ligands

and the nephelauxetic series: ethyl < 2-chloroethyl < 2,2,2-trifluoroethyl. The room temperature magnetic moment values of Ni(II) and Co(II) derivatives are in the ranges of 3.00 to 3.30 B.M. and 4.40 to 5.20 B.M., respectively. Based on these values alone it is not possible to distinguish between a bridging/chelating and only chelating organophosphate moiety.

In conclusion, it may be remarked that depending on the metal ion $(OR)_2PO_2$, species may act as a bidentate or as a terdentate ligand, [as in the case of Ni(II) chelates].

References

1 Mikulski C M, Karyannis N M & Pytlewski L L, *J inorg nucl Chem*, **36** (1974) 971.

2 Paul R C, Kapila V P, Battu R S & Bhatia J C, *Indian J Chem*, **10** (1972) 447.

3 Gutman V & Beer G, *Inorg chim Acta*, **3** (1969) 87.

4 Gutman V & Frankart F, *Mh Chem*, **99** (1961) 1452.

5 Bhardwaj S K, *Metal chelates of tris(2-chloroethyl)phosphate*, M.Phil Thesis, Panjab University, Chandigarh, 1983.

6 König E, *The nephelauxetic effect* in *structure and bonding*, Vol. 9 (Springer Verlag, Berlin) 1971.

7 Lever A B P, *Inorganic electronic spectroscopy* 2nd edition (Elsevier, New York), 1984.

8 Drago R S, *Physical methods in inorganic chemistry* (Reinhold, New York), 1965.

Indian Journal of Chemistry
Vol. 27A, May 1988, pp. 407-410

Metal Complexes of Some Nitrogen-Sulfur Donor Ligands

M T H TARAFDER* & S ROY
Department of Chemistry, University of Rajshahi, Rajshahi, Bangladesh

Received 31 *March* 1987; *revised and accepted* 26 *August* 1987

Several new complexes of Zr(IV), Th(IV) and U(VI) with S-benzyldithiocarbazate (NH$_2$NHCSSCH$_2$C$_6$H$_5$) and S-benzoyl-β-(N-benzoyl) dithiocarbazate (C$_6$H$_5$CONHNHCSSCOC$_6$H$_5$) have been synthesized only in alkaline medium where the ligands are deprotonated and act as bidentate uni-negative sulfur-nitrogen (NS$^-$) chelating agents forming the bis-chelated complexes of general formulae [M(NS$^-$)$_2$X$_2$] [M = Zr(IV) and Th(IV); X = NO$_3^-$ and NCS$^-$] and [U(O)(NS$^-$)$_2$X$_2$]. Analytical, conductivity and spectral data and magnetic measurements are consistent with six-coordination of Zr(IV) and Th(IV) atoms while the uranium analogues are seven-coordinate. S-Benzoyl-β-(N-benzoyl)dithiocarbazate also forms bis-chelated inner-complexes with Ni(II) and Zn(II) having a general composition of M(NS$^-$)$_2$. Magnetic and spectral data support a square-planar structure for Ni(II) and a tetrahedral geometry for Zn(II).

Preparation and characterization of lighter transition metal complexes of S-benzyldithiocarbazate and the schiff bases derived from it have been reported from our laboratory$^{1-8}$. Besides intrinsic academic interest, the work assumes importance as some of these compounds have been found to display carcinostatic activity[9]. Work on complexing of nitrogen-sulfur donor ligands with heavier transition metals is relatively unknown. As an extension, we report herein the complexes of Zr(IV), Th(IV) and U(VI) with S-benzyldithiocarbazate(SBDTC) and S-benzoyl-β-(N-benzoyl)dithiocarbazate (SBODTC). Complexation of the latter with Ni(II) and Zn(II) has also been investigated.

Materials and Methods

Infrared spectra were recorded in KBr on a Pye-Unicam SP3-300 infrared spectrophotometer. Conductivities of 10^{-3} M solutions of the complexes in dimethylformamide (DMF) were measured at 25°C using a WPA CM35 conductivity meter and a dip-type cell with platinized electrodes. Magnetic susceptibilities were measured at room temperature by the Faraday method. Diamagnetic corrections for the constituent elements were obtained using Pascal's law and employing tabulated constants[10]. Electronic spectra were recorded on a Shimadzu UV-180 double-Beam Spectrophotometer.

All chemicals used were of reagent grade (Merck). S-Benzyldithiocarbazate (SBDTC) was prepared as described previously[1]. S-Benzoyl-β-(N-benzoyl)dithiocarbazate (SBODTC) was prepared as follows: Potassium hydroxide (11.4 g) was dissolved in 90% ethanol (70 ml) and to this hydrazine hydrate (10 g) was added and the mixture was cooled to 0°C in an ice-salt bath. Carbon disulfide (15.2 g) was added dropwise to the above mixture with constant stirring during 1 hr, whereupon two layers were formed. The light brown layer was separated, dissolved in cold 40% ethanol (60 ml), kept in an ice-bath and to this benzoyl chloride (25 g) was added dropwise with vigorous stirring. A white product which separated out was filtered, washed with water, dried, recrystallized from ethanol and dried over anhydrous calcium chloride; yield 13 g (Found: C, 5.8; H, 3.8; S, 20.1. $C_{15}H_{12}N_2S_2O_2$ requires C, 56.9; H, 3.8; S, 20.2%).

General method for preparation of **1, 3, 5, 9, 11** *and* **13** *[M(NS)$_2$ (NO$_3$)$_2$] [M = Zr(IV) and Th(IV); NS = deprotonated form of SBDTC or SBODTC] and [U(O)(NS)$_2$(NO$_3$)$_2$]*

SBDTC or SBODTC (0.008 mol) was added to a solution of potassium hydroxide (0.008 mol) in water (25 ml). The solution was stirred for 5 min, filtered and to the filtrate was added, with stirring, a solution of appropriate hydrated metal nitrate (0.004 mol) in water (20 ml). The mixture was heated on a water-bath for 10-15 min, the resulting precipitate filtered, washed successively with water and ethanol and dried *in vacuo* over P_4O_{10}.

General method for preparation of **2, 4, 10** *and* **12** *[M(NS)$_2$ (NCS)$_2$] [M = Zr(IV) and Th(IV)]*

Metal nitrate tetrahydrate (0.004 mol) was dissolved in anhydrous methanol (20 ml) to which a solution of potassium thiocyanate (0.016 mol) in the same solvent (25 ml) was added. The precipitated potassium nitrate was discarded and the filtrate added to an aqueous solution (25 ml) of SBDTC or SBODTC (0.008 mol) containing potassium hydroxide (0.008 mol). The precipitate thus obtained was filtered, washed with water and ethanol and dried *in vacuo* over P_4O_{10}.

Preparation of **6** *and* **14** *[U(O)(NS)$_2$(NCS)$_2$]*

A solution of uranyl nitrate hexahydrate (0.008 mol) in anhydrous methanol (40 ml) was added to a solution of potassium thiocyanate (0.016 mol) in the same solvent (25 ml). The solution was filtered, the filtrate added to an aq. alkaline solution (45 ml) of SBDTC or SBODTC (0.016 mol) and the yellow precipitate obtained was filtered and stored as above.

Preparation of 7 and **8** *[M(NS)$_2$] [M = Ni(II) and Zn(II)]*

SBODTC (0.007 mol) was dissolved in aq. potassium hydroxide (0.007 mol in 30 ml water), filtered and to the clear solution, was added a solution of metal nitrate hexahydrate (0.0035 mol) in water (20 ml). The mixture was heated on a water-bath for 5 min, and the solid obtained filtered off and stored as above.

Results and Discussion

The analytical and molar conductance data of the complexes (Table 1) are consistent with six-coordinated Zr(IV) and Th(IV) complexes while the uranium complexes are seven-coordinated . The nickel and zinc complexes are four-coordinate. The complexes were soluble in almost all the polar solvents tried, and the electrical conductivities of 10^{-3} *M* solutions in DMF indicated that all the complexes were undissociated indicating that the anions are covalently bonded in all the cases.

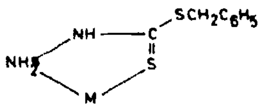
(1a)

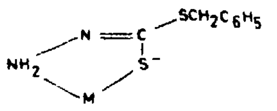
(1b)

Complexes **1-6**

We have previously demonstrated that SBDTC forms N, S chelated structure (**1a**) in a neutral medium. In alkaline medium, however, the ligand deprotonates and acts as a bidentate uni-negative ligand (**1b**)[1,7].

SBDTC reacts with the heavier metals only in an alkaline medium. Attempts to prepare complexes in neutral medium were unsuccessful. In the infrared spectra, the $\nu(NH_2)$ modes of the free SBDTC appearing at 3238 s, 3180 s cm^{-1} are shifted to lower wavenumbers in the complexes and appear around 3040-3080 and 3020-3060 cm^{-1}. This shift of $\nu(NH_2)$ modes is indicative of coordination of the ligand via the amino nitrogen. The shift of $\nu(NH_2)$ mode is much larger in Zr(IV) complexes (**1**: 3040, 3030; **2**: 3060, 3035 cm^{-1}) than those in Th(IV) analogues (**3**: 3080, 3060; **4**: 3070, 3050 cm^{-1}). This suggests that Zr(IV) is a stronger acceptor than Th(IV). The ν(NH) mode of SBDTC appearing at 3300 cm^{-1} disappears in the complexes (**1-6**), suggesting deprotonation and possible coordination ac-

Table 1—Characterization Data of Complexes[a] (**1-14**)

No.	Compd.	Colour	Calc (found) %			
			M[b]	C	H	S
1	$[Zr(NH_2NCSSCH_2C_6H_5)_2(NO_3)_2]$	Colourless	15.0 (14.9)	31.5 (31.2)	2.9 (2.9)	21.0 (20.9)
2	$[Zr(NH_2NCSSCH_2C_6H_5)_2(NCS)_2]$	-Do-	15.2 (15.1)	35.9 (35.7)	3.0 (3.0)	31.9 (31.5)
3	$[Th(NH_2NCSSCH_2C_6H_5)_2(NO_3)_2]$	-Do-	30.9 (30.6)	25.6 (25.5)	2.4 (2.4)	17.1 (17.0)
4	$[Th(NH_2NCSSCH_2C_6H_5)_2(NCS)_2]$	-Do-	31.3 (31.3)	29.1 (28.8)	2.4 (2.4)	25.9 (25.5)
5	$[U(O)(NH_2NCSSCH_2C_6H_5)_2(NO_3)_2]$	Yellow	30.8 (30.6)	24.9 (24.8)	2.3 (2.3)	16.6 (16.4)
6	$[U(O)(NH_2NCSSCH_2C_6H_5)_2(NCS)_2]$	—Do-	31.1 (31.0)	28.3 (28.0)	2.4 (2.3)	25.1 (25.0)
7	$[Ni(C_6H_5CONHNCSSCOC_6H_5)_2]$	Buff	8.5 (8.5)	52.3 (52.0)	3.2 (3.2)	18.6 (18.3)
8	$[Zn(C_6H_5CONHNCSSCOC_6H_5)_2]$	Colourless	9.4 (9.4)	51.8 (51.5)	3.2 (3.2)	18.4 (18.1)
9	$[Zr(C_6H_5CONHNCSSCOC_6H_5)_2(NO_3)_2]$	-Do-	10.8 (10.7)	42.6 (42.3)	2.6 (2.6)	15.1 (15.0)
10	$[Zr(C_6H_5CONHNCSSCOC_6H_5)_2(NCS)_2]$	-Do-	10.9 (10.7)	45.9 (45.5)	2.6 (2.6)	22.9 (22.8)
11	$[Th(C_6H_5CONHNCSSCOC_6H_5)_2(NO_3)_2]$	-Do-	23.5 (23.4)	36.5 (36.3)	2.2 (2.2)	12.9 (12.6)
12	$[Th(C_6H_5CONHNCSSCOC_6H_5)_2(NCS)_2]$	-Do-	23.7 (23.5)	39.3 (39.0)	2.2 (2.2)	19.6 (19.5)
13	$[U(O)(C_6H_5CONHNCSSCOC_6H_5)_2(NO_3)_2]$	Yellow	23.6 (23.5)	35.7 (35.6)	2.2 (2.2)	12.7 (12.5)
14	$[U(O)(C_6H_5CONHNCSSCOC_6H_5)_2(NCS)_2$	-Do-	23.8 (23.6)	38.4 (38.1)	2.2 (2.2)	19.2 (19.1)

[a] Organic moiety in 1-6 refer to the ligand SBDTC and that in 7-14 to the ligand SBODTC.

[b] Zr(IV)[11], Th(IV)[12] and U(VI)[13] were determined gravimetrically as oxides after complete ignition of the complexes. Ni(II) and Zn(II) were determined gravimetrically (as dimethyl glyoximato complex) and complexometrically (with EDTA) respectively[33].

cording to the structure (**1b**). This mode of N, S chelation in **1-6** is also evident from the appearance of bands at 267-350 and 230-280 cm^{-1} assigned tentatively to the $\nu(M-N)$ and $\nu(M-S)$ modes respectively[11-16]. The IR spectra of the complexes display $\nu(C=N)$ in the region 1520-1580 cm^{-1}. Complexes **1**, **3** and **5** show bands at about 1495, 1290, 1015 and 815 cm^{-1} characteristic of unidentate nitrate group[17-21]. The complexes **2**, **4** and **6** exhibit intense band in the region 2030-2060 cm^{-1} assignable to $\nu(C\equiv N)$ mode. This suggests that the thiocyanate is coordinated through the nitrogen[22-24], thus revealing "hard" acid properties of the Zr(IV), Th(IV) and U(VI) ions[25,26]. The uranium complexes, **5** and **6**, display band at 910 cm^{-1} due to $\nu(U=O)$ mode[13,27]. All the complexes display phenyl ring vibrations around 1600 cm^{-1}.

The complexes **1-6** are diamagnetic and their electronic spectra exhibit bands in the range 300-345 nm which are caused by charge transfer.

Complexes **7-14**

This is the first report on the complexation of SBODTC with lighter and heavier transition metals. The ligand was characterized on the basis of elemental analyses, IR, PMR and mass spectral data. The IR spectrum of this ligand exhibits bands at 3200 (νNH), 1625 ($\nu C=O$) and 1065 cm^{-1} ($\nu C=S$). Its PMR spectrum in DMSO-d_6 displays signals at δ 10.5 and 7.7 ppm corresponding to the $-NH-$ and phenyl protons, respectively. The mass spectrum shows the molecular ion peak at m/z 316 and other diagnostic peaks at m/z 240, 135, 105, 77, 51 and 28.

SBODTC reacts with the metal ions only in alkaline medium. We failed to prepare complexes of this ligand with lighter and heavier transition metals from a neutral medium. This suggests that the basicity of this ligand is markedly enhanced in an alkaline medium, probably due to creation of an anionic site *in situ*[1-9]. SBODTC (**2a**) has a proton adjacent to the thione group. The thione group is relatively unstable in the monomeric form and undergoes thione (**2a**) ⇌ thiol (**2b**) equilibrium[28]. Presumably, the ligand exists in thione and thiolo tautomeric forms (**2a** and **2b**), in solution although apparently not in the solid state (IR spectrum in the solid does not exhibit any νSH mode).

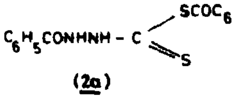

$C_6H_5CONHNH-C(=S)-SCOC_6H_5$

(2a)

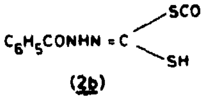

$C_6H_5CONHN=C(SH)-SCOC_6H_5$

(2b)

The deprotonation and consequent formation of an anionic site *in situ* is favoured by the basicity of the medium. Comparison of the IR spectra of the ligand and the complexes (**7-14**) indicate that the ligand is potentially bidentate, the coordination sites being the β-nitrogen and the thiolate sulphur. Molecular model shows that α-nitrogen is not bonded because of considerable steric strain. Besides, deprotonation of α-NH and concomitant formation of $C=N$ bonds are also indicative from the appearance of $\nu(C=N)$ modes in the region 1575-1585 cm^{-1} in the complexes (**7-14**). The $\nu(C=O)$ observed at 1625 cm^{-1} in the free ligand remains virtually unchanged in the complexes which precludes coordination to the metal ions through carbonyl oxygen. The β-nitrogen coordination is evident from the shift of ν(NH) mode of the free ligand appearing at 3200 cm^{-1} to lower wavenumbers (3100-3160 cm^{-1}) in **7-14**. The far IR spectra of the complexes exhibit bands in the region 270-470 and 225-360 cm^{-1} which are tentatively attributed to the $\nu(M-N)$ and $\nu(M-S)$ modes [M = Zr(IV), Th(IV) and U(VI)], respectively. It is noteworthy that the mode of coordinations of SBDTC and SBODTC closely resembles the coordination properties of thiosemicarbazide[9].

The four-coordinate nickel complex (**7**) is non-electrolyte and diamagnetic. This suggests that coordination actually occurs through the thiolate site of the ligand since the thiolates generated from thiols, but not the thio ethers, cause spin-pairing in complexes of nickel(II)[1,8,29]. The electronic spectrum of **7** is consistent with a square-planar nickel(II)[30,31]. The observed absorptions at 500, 385 and 350 nm correspond to $^1A_{1g} \rightarrow {}^1A_{2g}$, $^1A_{1g} \rightarrow {}^1B_{1g}$ and $^1A_{1g} \rightarrow {}^1E_g$ transitions in D_{4h} symmetry, respectively[30,31]. The four-coordinate zinc(II) complex (**8**) is diamagnetic and shows a charge transfer band only; the complex is probably tetrahedral.

That the complexes **9**, **11** and **13** have coordinated unidentate nitrate group[17-21] is evident from the appearance of bands around 1490, 1285, 1027 and 815 cm^{-1} in the IR spectra of the complexes. The IR spectra of **10**, **12** and **14** display $\nu(C\equiv N)$ mode characteristic of N-bonded isothiocyanate group at 2000-2025 cm^{-1} as a sharp band. It is noteworthy that $\nu(C\equiv N)$ modes in **2**, **4**, **6**, **10**, **12** and **14** are observed at much lower wavenumbers (2000-2060 cm^{-1}) than those observed for thiocyanate complexes of low valent transition metals. In particular, the $\nu(C\equiv N)$ mode in Ni(SBDTC)$_2$(NCS)$_2^+$ appears at 2095 cm^{-1} (see ref. 1). The present data thus suggest that Zr(IV), Th(IV) and U(VI) are stronger acceptors[32].

The complexes (**9-14**) are diamagnetic and exhibit only a charge transfer band. Excepting uranium, Zr(IV) and Th(IV) complexes are six-coordinate.

The uranium analogues are seven-coordinate of which the seventh coordination position is occupied by an oxo ligand. This is evident from the appearance of ν(U = O) mode at 910 cm^{-1} in the IR spectra of **13** and **14**.

Acknowledgement

We express our grateful thanks to Prof A D Westland, Department of Chemistry, University of Ottawa, Canada for the PMR and mass spectra.

References

1 Ali M A & Tarafder M T H, *J inorg nucl Chem*, **39** (1977) 1785.

2 Ali M A & Bose R, *J inorg nucl Chem*, **39** (1977) 265.

3 Tarafder M T H & Ali M A, *Can J Chem*, **56** (1978) 2000.

4 Ali M A, *Can J Chem*, **58** (1980) 727.

5 Tarafder M T H, Miah M A J, Bose R N & Ali M A, *J inorg nucl Chem*, **43** (1981) 3151.

6 Ali M A, Uddin M, Uddin M N, Chowdhury D A & Tarafder M T H, *Indian J Chem*, **25A** (1986) 238.

7 Tarafder M T H, Begum M & Rahman M L, *Indian J Chem*, **25A** (1986) 377.

8 Ali M A & Bose R N, *Polyhedron*, **3** (1984) 517.

9 Ali M A & Livingstone S E, *Coord chem Rev*, **13** (1974) 101.

10 Figgis B N & Lewis J, *Modern coordination chemistry*, edited by J Lewis & R G Wilkins (Interscience, New York) 1959; Selwood P W, *Magnetochemistry* (Interscience, New York) 1956.

11 Tarafder M T H & Miah M A L, *Inorg Chem*, **25** (1986) 2265.

12 Westland A D & Tarafder M T H, *Inorg Chem*, **21** (1982) 3228.

13 Westland A D & Tarafder M T H, *Inorg Chem*, **20** (1981) 3992.

14 Karayannis N M, Mikulski C M, Stroke M J, Pytlewski L L & Labes M M, *Inorg chim Acta*, **4** (1970) 455.

15 Agarwal R K, Srivastava A K, Srivastava M, Bakru N & Srivastava T N, *J inorg nucl Chem*, **42** (1980) 1778.

16 Agarwal R K, Srivastava M & Srivastava A K, *J inorg nucl Chem*, **43** (1981) 204.

17 Addison C C & Simpson W B, *J chem Soc*, (1965) 598.

18 Lever A B P, *Inorg Chem*, **4** (1965) 1042.

19 Mahanta H & Dash K C, *J inorg nucl Chem*, **39** (1977) 1345.

20 Barrister E & Cotton F A, *J chem Soc*, (1960) 2276.

21 Bakamoto K, *Infrared spectra of inorganic & coordination compounds* (John Wiley, New York) 1963, pp 161.

22 Bailey R a, Kezak S L, Michelsen T W & Mills W N, *Coord chem Rev*, **6** (1971) 407.

23 Basolo F, Baddley W H & Burmeister J L, *Inorg Chem*, **3** (1964) 1202.

24 Destefano N J & Burmeister J L, *Inorg Chem*, **10** (1971) 998.

25 Pearson R G, *J Am chem Soc*, **85** (1963) 3533.

26 Pearson R G, *J chem Educ*, **45** (1968) 581.

27 McGlynn S P, Smith J K & Neely W C, *J chem Phys*, **35** (1961) 105.

28 Mayer R, *Organosulphur chemistry*, edited by M J Jansen (Interscience, New York) 1967, pp 219.

29 Livingstone S E, *Quart Rev*, **19** (1965) 386.

30 Lever A B P, *Inorganic electronic spectroscopy* (Elsevier, Amsterdam) 1968, Chap. 9.

31 Gray H B & Ballhausen C J, *J Am chem Soc*, **85** (1963) 260

32 Ahrland S, Chatt J & Davies N R, *Quart Rev*, **12** (1958) 265.

33 Vogel A I, *A text book of inorganic quantitative analysis* (Longmans, London) 1962.

Indian Journal of Chemistry
Vol. 27A, May 1988, pp. 411-416

Preparation & Structural Investigations of Copper(II), Cobalt(II), Nickel(II) & Zinc(II) Derivatives of 2,9,16,23-Phthalocyanine Tetracarboxylic Acid

B N ACHAR*, G M FOHLEN†, J A PARKER‡ & J KESHAVAYYA
Department of Post-Graduate Studies & Research in Chemistry, Manasa Gangotri
University of Mysore, Mysore 570 006

Received 28 *April* 1987; *revised* 13 *July* 1987; *rerevised and accepted* 21 *September* 1987

An efficient method for the synthesis of pure 2,9,16,23-phthalocyanine tetracarboxylic acid derivatives of copper(II), cobalt(II), nickel(II) and zinc(II) has been developed. The complexes have been characterized on the basis of elemental analyses, titrimetric, FT-IR spectral, dynamic thermogravimetric, mass spectral, UV-visible and magnetic susceptibility studies. Copper(II) and nickel(II) compounds of phthalocyanine tetracarboxylic acid show more intense and sharper peaks in X-ray powder diffraction pattern than cobalt(II) and zinc(II) derivatives of phthalocyanine tetracarboxylic acids. This may be due to the greater crystalline nature of the former than that of their zinc(II) analogue.

Metal-phthalocyanine carboxylic acid derivatives have been synthesized, mostly for the preparation of inks, dyes and pigments[1-3]. Apart from colouring agents, the carboxylic acid derivatives have also been used as catalysts[4-7], curing agents for epoxy resins[8,9], sensitizers[10], in electrophotography[11,12], for preparing optical filters[13] and as deodorants[14]. A literature survey revealed that information on the synthesis and characterization of pure metal-phthalocyanine tetracarboxylic acid derivatives is meagre. Buc[15] has prepared copper(II)-phthalocyanine tetracarboxylic acid by first synthesizing tetracyanocopper(II) phthalocyanine and then hydrolyzing the cyano groups with 10% aqueous alkali solution. The material was found to contain significant impurities. Parry[8,9] reported the synthesis of copper(II)-phthalocyanine tetracarboxylic acid by heating cuprous chloride, trimellitic anhydride and urea in the presence of ammonium molybdate catalyst. This method was reported to give the compound with considerable amidized acid groups.

Keeping in view the valuable physicochemical properties of metal(II) phthalocyanine tetracarboxylate derivatives, we have evolved an efficient method for the synthesis of pure metal(II) phthalocyanine tetracarboxylic acid derivatives. The procedure outlined here is the improved version of the methods described in literature to synthesize various other types of metal phthalocyanine derivatives[16-19]. This series of pure metal(II) phthalocyanine tetracarboxylates led to synthesis of metal phthalocyanine sheet polymers which have very high thermal stability unknown in any of the phthalocyanine polymers heretofore synthesized[20,21].

Materials and Methods

Trimellitic anhydride was obtained from AMOCO Chemicals, USA and used as received. Ammonium chloride and ammonium molybdate were A.C.S. reagents from Aldrich Chemical Co. All the other chemicals were of analytical reagent grade. 2,9,16,23-Phthalocyanine tetracarboxylic acid-2-hydrates of copper(II), cobalt(II), nickel(II) and zinc(II) were synthesized as follows[20].

The metal(II) sulphate (0.048 mol), trimellitic anhydride (0.176 mol) and excess urea (1.0 mol) were finely ground along with a catalytic quantity of ammonium chloride/ammonium molybdate (0.085 mol/0.0004 mol). The mixture was placed in a 500 ml three-necked flask containing 25 ml nitrobenzene as solvent. The temperature of the reactants was increased to 185°C and maintained at 185 ± 2°C for 4h. The colour of the reaction mixture gradually deepened and finally a deep coloured solid was obtained. The product was ground well and washed with methanol until it was free from nitrobenzene. The solid product was added to 500 ml of 1.0 *N* hydrochloric acid saturated with sodium chloride, boiled briefly, cooled to room temperature and filtered. The resulting solid product was treated with 500 ml of 2.0 *M* sodium hydroxide containing 200 g sodium chloride and heated at 90°C until the evolution of ammonia ceased. The solution after filtration was treated with 500 ml 2.0 *N* hydrochloric acid and the product was separated by centrifugation. The residue was redissolved in 0.1 *N* sodium hydroxide and filtered to separate the insoluble materials. The compound was reprecipitated with 1.0 *N* hydrochloric acid and centrifuged to obtain the solid material. Dissolution and precipitation steps were repeated twice. Then the compound was washed until chloride-free and finally washed with methanol. The blue product was dried *in vacuo* over phosphorus pentoxide. The analytical data of the complexes are given in Table 1.

---

† Present address: Consultant in Chemistry, 1307, Vista Grande, Milbrae, CA 94030, USA.

‡ Present address: 1330 McClure Lane, Los Altos, CA 94022, USA.

Thermogravimetric studies were carried out with a Du Pont Model 990 thermal analyzer and a 951 thermogravimetric module. A heating rate of 10°C per min was used in air and nitrogen atmospheres with a flow rate of 100 ml/min. IR spectra were recorded using a Nicolet MX-1 FT—IR spectrophotometer. A Hewlett-Packard model 5980 mass spectrometer equipped with a data acquisition system was used for the mass spectral studies. Hewlett-Packard model 5830A gas chromatograph was used to study the volatile gaseous products formed during the thermal treatment. Carbon, hydrogen and nitrogen elemental analyses were done at the Huffman Laboratories, Inc., Co., USA. The metal contents of the metal(II) phthalocyanine tetracarboxylates were determined by decomposing a known amount of the complex with sulphuric acid-nitric acid mixture followed by careful evaporation and calcination to constant weight. A Gouy magnetic balance was used for measuring magnetic susceptibilities of the complexes. $Hg[Co(NCS)_4]$ was used as the calibration standard. Titrimetric analyses were performed with a Metrohm E 436 potentiograph. A Beckman Model DB spectrophotometer with 1 cm silica cells was used for UV and visible spectral studies. A JDK-8P Jeol X-ray diffractometer was used to study the X-ray diffraction patterns of the samples. The spectra were obtained with the following conditions: Target-Fe (Mn-filter); voltage 30 kV; current 30 mA; time constant 4; chart speed 10 mm/min; channel with 0.7 and channel centre 1.0.

Results and Discussion

The structure of the complexes of 2,9,16,23-phthalocyanine tetracarboxylic acid (PTC) with copper(II), cobalt(II), nickel(II), and zinc(II) is shown in Fig. 1.

All the phthalocyanines, which resist attack by concentrated sulphuric acid, contain metals whose atomic radii are close to 1.35 Å; they are also thermally very stable in air as well as in nitrogen atmosphere[22]. The complexes have deep blue to purple colour with crystalline appearance and metallic lustre. They are highly soluble in concentrated sulphuric acid and dilute sodium hydroxide but partially soluble in aprotic solvents like dimethyl sulphoxide, dimethylaceta-

Table 1—Elemental Analysis, Magnetic and Electronic Spectral Data of Metal(II) Phthalocyanine Tetracarboxylic Acids (MPTC)

Compounds	Field strength (Gauss)	$\mu_{eff.}$ (B.M.)	λ_{max}, nm (log ε)	Elemental analysis (%) Found (Calc.)
$CuPTC.2H_2O$	1024	2.479	232(4.79),	C: 54.95(54.86)
	1920	2.222	302(4.69),	H: 2.61(2.56)
	2816	2.092	416(4.28),	N: 14.50(14.22)
	3584	2.049	680(4.44),	Cu: 8.08 (8.06)
	4352	2.007	736(4.62)	
	4792	1.942		
	5632	1.940		
$CoPTC.2H_2O$	1024	2.987	232(4.87),	C: 55.66(55.18)
	1920	2.913	300(4.96),	H: 2.72 (2.57)
	2816	2.706	402(4.26),	N: 14.51(14.30)
	3584	2.466	748(4.55)	Co: 7.61(7.52)
	4352	2.377		
	4792	2.348		
	5632	2.221		
$NiPTC.2H_2O$	5632	—	232(4.71),	C: 56.01(55.20)
			306(4.63),	H: 2.66 (2.67)
			398(4.11),	N: 14.18(14.30)
			698(4.30),	Ni: 7.66 (7.50)
			755(4.28)	
$ZnPTC.2H_2O$	5632	—	232(4.76),	C: 55.01(54.74)
			304(4.61),	H: 2.63 (2.55)
			412(4.54),	N: 14.25(14.18)
			755(4.73)	Zn: 8.25 (8.28)

mide and dimethylformamide. The elemental analyses for carbon, hydrogen, and nitrogen agreed fairly well with the calculated values.

The FT—IR spectra of the complexes of copper(II), cobalt(II), nickel(II) and zinc(II) with phthalocyanine tetracarboxylic acid (Fig. 2) showed absorption bands at 1149-1153, 1086-1090, 1050-1055, 926-944.88-855 and 737-742 cm^{-1} assignable to phthalocyanine skeleton[23]. The strong broad absorption bands around 1696-1699 cm^{-1} are due to the carboxylic acid groups of the derivatives. The shift in their positions by 71-81 cm^{-1} towards the lower wavenumbers may be due to the inter- or intra-molecular hydrogen bonding involving either the two carboxylic acid groups or carboxylic group and a water molecule. The absorptions around 1410-1415 and 1189-1332 cm^{-1} may be due to the coupling between in-plane O—H bending and C—O stretching modes. The IR spectrum of zinc phthalocyanine tetracarboxylic acid seems to be slightly different which may be due to the presence of a small amount of demetallized product.

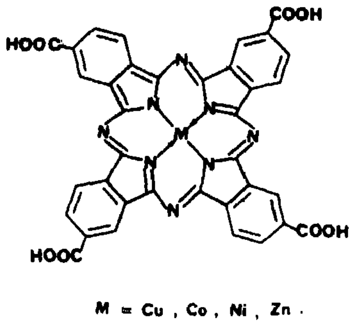

Fig. 1—Structure of metal(II) 2,9,16,23-phthalocyanine tetracarboxylic acid complexes

The thermogravimetric analytical curves obtained in air and nitrogen for CuPTC.2H$_2$O, CoPTC.2H$_2$O, NiPTC.2H$_2$O and ZnPTC.2H$_2$O are shown in Fig. 3. The nature of the curves indicates that these tetracarboxylic acids get degraded mainly in three steps in both the air and nitrogen atmospheres. The first mass loss ($\approx$ 5%) takes place between 50 and 150°C which corresponds to the loss of two water molecules. The second mass loss by about 25%, in nitrogen atmosphere, in the temperature range 300-500°C is due to

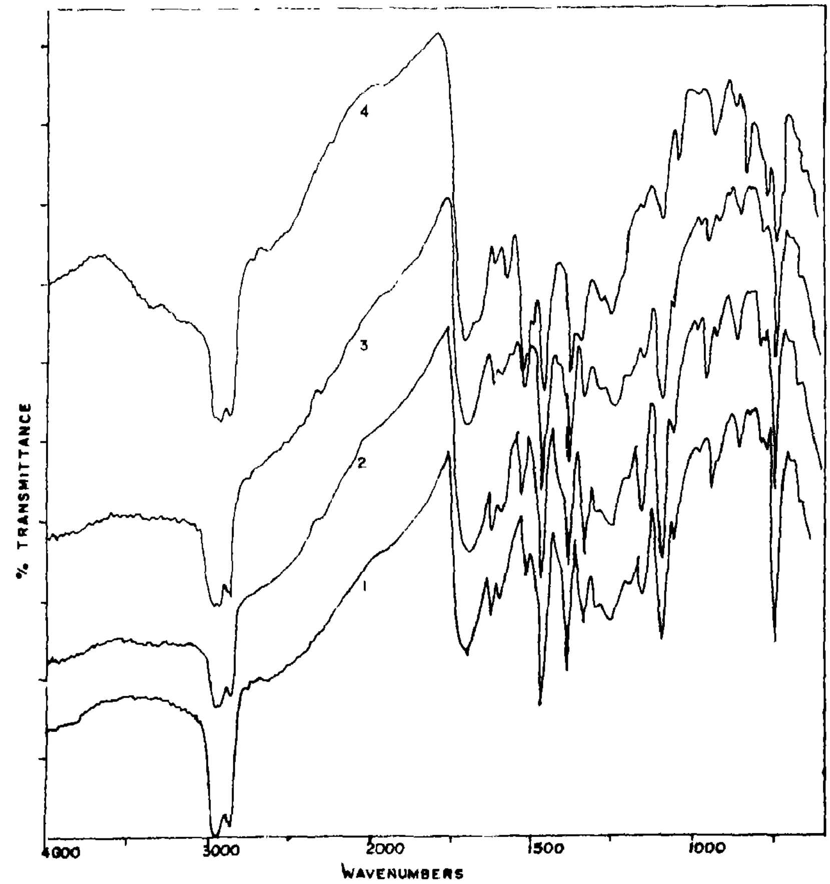

Fig. 2—FT-IR spectra of metal(II) complexes of 2, 9, 16, 23-phthalocyanine tetracarboxylic acid: (1) CuPTC.2H$_2$O; (2) CoPTC.2H$_2$O; (3) NiPTC.2H$_2$O and (4) ZnPTC.2H$_2$O

the decarboxylation reaction. The third step of degradation in nitrogen atmosphere takes place in a much higher temperature range, 700-800°C for CuPTC, 780-850°C for CoPTC, 825-900°C for NiPTC and 900-1000°C for ZnPTC. The mass loss is only about 10%. But this step occurs readily in oxidizing atmosphere and leads to accelerated loss of about 65% corresponding to the degradation of the unmetallated phthalocyanine structure in the temperature range 400-520°C which is very close to the second step; the two steps can hardly be differentiated from one another in the case of CuPTC, CoPTC and NiPTC complexes. The final products in the oxidizing atmosphere are copper oxide (CuO); cobalt oxide (CoO); nickel oxide (NiO); and zinc oxide (ZnO).

A known weight of metal(II)-phthalocyanine tetracarboxylic acid was taken in a reaction tube and heated to 400°C after evacuating the apparatus to ~ 2×10^{-5} torr. The gaseous mixture was analyzed by IR, GC, GC—MS and mass spectral studies. FT—IR spectra of the gaseous products showed the characteristic hyperfine structures around 3756, 3652 and 1596 cm^{-1} corresponding to the water molecules. The presence of bands with fine structures at 2143 cm^{-1} indicated the presence of carbon monoxide. Strong fine structures at 2349 and 667-720 cm^{-1} confirmed the formation of carbon dioxide.

Peaks corresponding to z/e, 18, 28 and 44 in the mass spectra of the gaseous product also confirmed the IR spectral results. Another series of mass spectra studies was carried out at 350-400°C by the direct injection method which also gave identical results. Qualitative gas chromatographic studies were performed and the results showed the presence of carbon dioxide, carbon monoxide, hydrogen and water. A trace quantity of blue material was found to be depo-

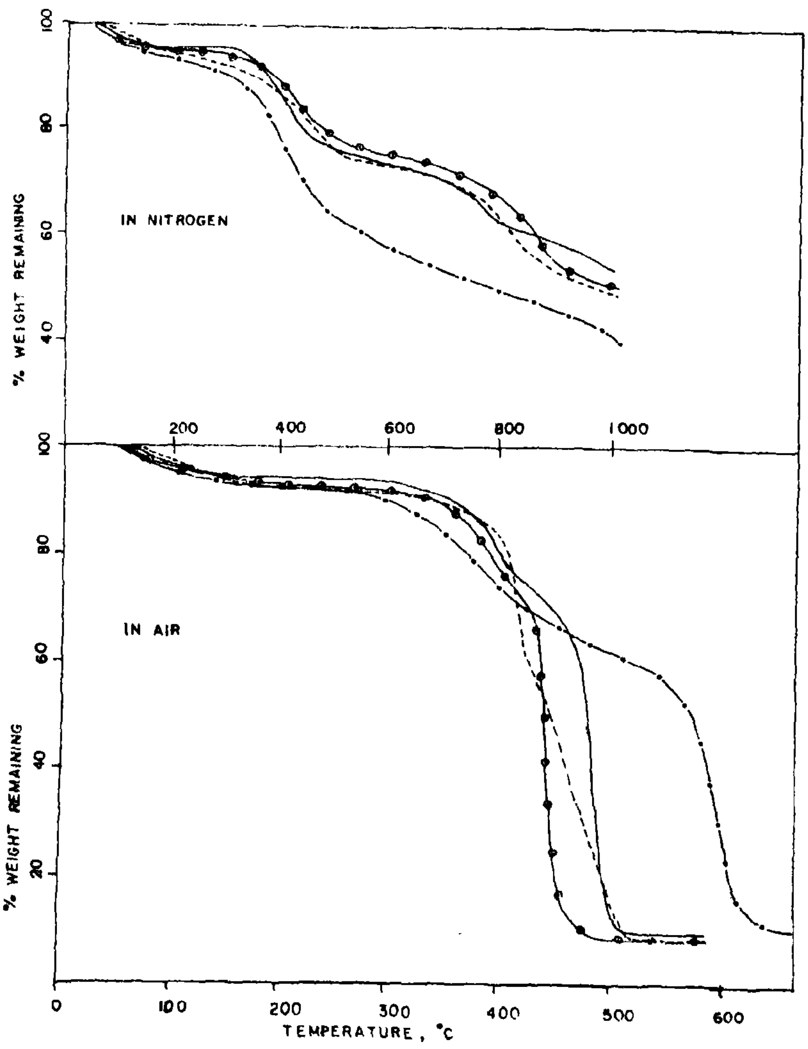

Fig. 3—The dynamic thermogravimetric analytical curves of (1) $CuPTC.2H_2O$ (——); (2) $CoPTC.2H_2O$ (- - -); (3) $NiPTC.2H_2O$ (-o-o-) and (4) $ZnPTC.2H_2O$ (—·—·—)

sited in the cooler portion of the vacuum apparatus and the IR spectra showed it to be identical with the parent phthalocyanine compound. From the observations of the amount of gaseous products, metal phthalocyanine and poly metal phthalocyanine formed, reaction leading to the formation of polymer seems to take place to an extent of > 90% (Eq. 1).

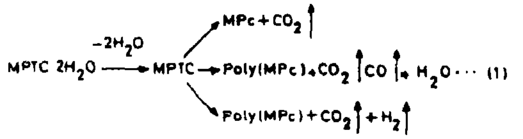

$$\mathrm{MPTC\ 2H_2O} \xrightarrow{-2H_2O} \mathrm{MPTC} \begin{array}{l} \nearrow \mathrm{MPc + CO_2}\uparrow \\ \rightarrow \mathrm{Poly(MPc) + CO_2}\uparrow \mathrm{CO}\uparrow + \mathrm{H_2O} \cdots \\ \searrow \mathrm{Poly(MPc) + CO_2}\uparrow + \mathrm{H_2}\uparrow \end{array} \quad (1)$$

The electronic absorption data for the MPTC complexes in 30 *N* sulphuric acid are listed in Table 1. All the derivatives show absorptions at 232, 300-306 and 736-750 nm. The deep blue or bluish green colour of the derivatives is due to the $\pi \rightarrow \pi^*$ transitions. Absorption bands at 402-416 nm are observed for CuPTC and CoPTC, which appear as a shoulder in the case of NiPTC and ZnPTC. In addition, an absorption band at 698 nm is observed for NiPTC and a shoulder around 680 nm is observed for CuPTC. The deep blue colour of the derivatives is due to the absorption around 736-750 nm which may be assigned to the $e_g \rightarrow a_{2u}$ transition. A nearly linear relationship between the electronegativity of the central metal ion and the absorption maxima of the red bands at 736-750 nm for the MPTC is observed. This small dependence of the spectrum upon the central metal ion may be either due to the involvement of the $p\pi(a_{2u})$ orbitals in the π-bonding of the phthalocyanine ring system or more probably due to the inducive effect[24].

The magnetic behaviour of the square planar phthalocyanine tetracarboxylic acid complexes of copper(II), cobalt(II), nickel(II) and zinc(II) has been investigated over the range of magnetic field strengths 1025-5632 gauss (Table 1). The experimental values are in agreement with the paramagnetic nature of the copper(II) and cobalt(II) complexes and, the diamagnetic nature of the nickel(II) and zinc(II) complexes. All the complexes have the dsp^2 covalent square planar structure (D_{4h}). The observed higher magnetic moment values than the expected spin-only value (1.73 B.M.) and variations of the same with varying magnetic field strengths may be due to the intermolecular co-operative effect[19].

X-ray diffraction spectrographs (Fig. 4) of copper(II), cobalt(II), nickel(II) and zinc(II) phthalocyanine tetracarboxylic acids taken through a range of 2θ angles 5-90° showed identical features. All these complexes showed two peaks, one sharper peak with maximum intensity at higher angle and another not well-resolved peak with lower intensity at lower angle. The interplanar spacings calculated based on these angles gave values (in Å): 3.329, 15.852 for CuPTC; 3.329, 14.785 for CoPTC; 3.329, 14.785 for NiPTC; and 3.329, 7.939 for ZnPTC respectively. CuPTC and NiPTC showed more intense and sharper peaks than CoPTC and ZnPTC, which may be due to the greater crystalline nature of the complexes.

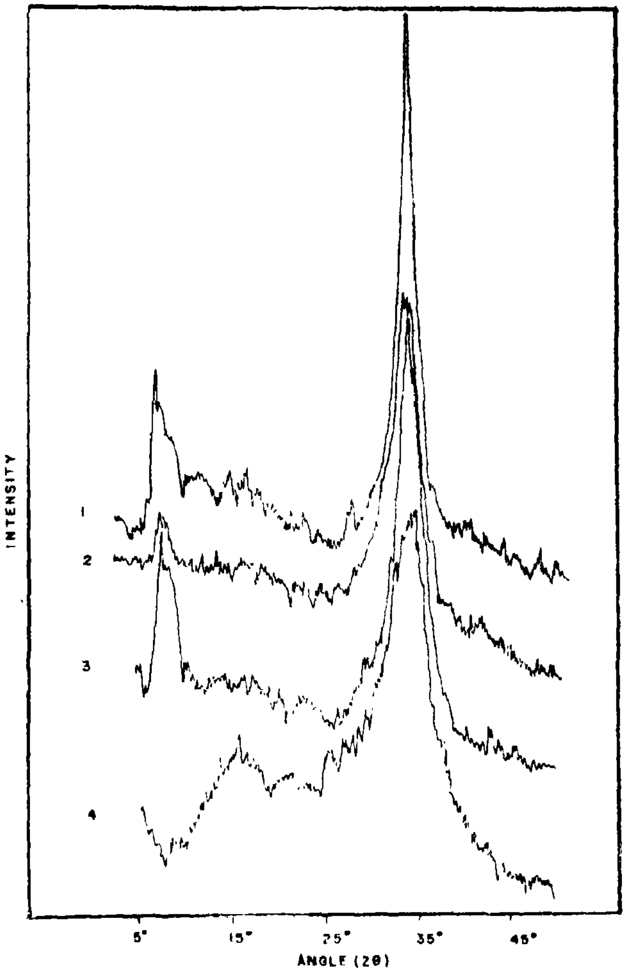

Fig. 4—X-ray diffraction photographs of (1) CuPTC.2H$_2$O; (2) CoPTC.2H$_2$O; (3) NiPTC.2H$_2$O; and (4) ZnPTC.2H$_2$O

References

1 Moser F H & Thomas A L, *Phthalocyanine compounds* (Reinhold, New York) 1963.
2 Potnis S P & Daruwala A P, *Paintindia*, (1969) 21.
3 Venkataraman K, *The chemistry of synthetic dyes*, Vol 2 (Academic Press, New York) 1952.
4 Shirai K, Maruyama A, Kobayashi K, Hojo N & Urushido K, *Macromol Chem*, **181**(3) (1980) 575.
5 Schutten J H, Van Hesternberg C H, Piet P & German Auton L, *Angew Macromol Chem*, **89** (1980) 201.
6 Universal Oil Product Co, *Neth Appl*, 6, 508, 611 (Cl B Olk) Jan. 6 (1967), Appl July 5 (1965), 9 pp.
7 Shirai H, Maruyama A, Takano J, Kobayashi K, Hojo N & Urushido K, *Macromol Chem*, **181** (1980) 565.
8 Parry H L, *T D Report*, ASD-TDR-63-396 April (1963).

9 Parry H L, *US Pat* 3,301,814 (Jan. 31, 1967).

10 Braun A & Lohses F, *Ger Offen*, 2,210,108 (Cl.B.01j). 05 Oct. (1972), *Swiss Appl* 3862/71, 16 March (1971), 30 pp.

11 Weigl J W, *US Pat*, 3,926,629 (Cl 9b, 1.5,G03G), 16 Dec (1975), Appl 468, 983, 01 Jul. (1965).

12 Nagashima S, Tsuchiya Y & Tsuenta T, Japan 73,25,665 (Cl G03y) 31 July (1973), Appl 6942, 577, 02 July (1969), 6 pp.

13 Soloveva L I, Lukyaneta E A & Kopylova E M, USSR 740,802 (Cl C09B47/04), June (1980), App. 2,506,813, 13 July (1977).

14 Gaspard S, Hochapfel A & Vivovy R, *Springer Ser Chem Phys*, **11** (1980) 298.

15 Buc S R (to General Aniline and Film Corp), *US Pat*, 2,647,908 Aug 4 (1953).

16 Baumann F, *US Pat*, 2,613,128 (1952).

17 Fukada N, *Nippon Kagaku Zaashi*, **75** (1954) 1141.

18 Fukada N, *Nippon Kagaku Zaashi*, **79** (1958) 396.

19 Weber J H & Busch D H, *Inorg Chem*, **4** (1965) 469.

20 Achar B N, Fohlen G M & Parker J A, *US Pat*, 4,450,268, May 22 (1984).

21 Achar B N, Fohlen G M & Parker J A, *J polym Sci Chem Ed*, **21** (1983) 589.

22 Berlin A A & Sherle A L, *Inorg Macromol Rev*, **1** (1971) 235.

23 Sidorov A N & Kotliar M P, *opt Spektrosk*, **11** (1961) 175.

24 Lever A B P, *Advan Inorg Chem Radiochem*, **7** (1965) 27.

Indian Journal of Chemistry
Vol. 27A, May 1988, pp. 417-420

Pd(II), Pt(II), Rh(III), Ir(III) & Ru(III) Complexes of Some Nitrogen-Oxygen Donor Ligands

SULEKH CHANDRA*
Department of Chemistry, Zakir Husain College, Ajmeri Gate, Delhi 110 006
and
RAJENDRA SINGH
Department of Chemistry, University of Delhi, Delhi 110 007

Received 8 *May* 1987; *revised* 22 *August* 1987; *rerevised and accepted* 9 *October* 1987

Pd(II), Pt(II), Rh(III), Ir(III) and Ru(III) complexes of propiophenone and butyrophenone semicarbazones (abbreviated as PSC and BSC, respectively) have been synthesised and characterised by elemental analyses, magnetic moments, IR and electronic spectral studies. The complexes have the compositions $M(ligand)_2Cl_2$ (M = Pd or Pt) and $M(ligand)_3Cl_3$ (M = Rh, Ir and Ru). All the complexes are diamagnetic except $Ru(ligand)_3Cl_3$, which is paramagnetic. Pd(II) and Pt(II) complexes are assigned square-planar geometry. Rh(III), Ru(III) and Ir(III) complexes are six-coordinate octahedral. Various ligand field parameters have been calculated and discussed.

The effect of platinum metal compounds on biological systems has evoked considerable interest[1-4]. There are very few reports[5-7] on platinum metal complexes of semicarbazones. Keeping in view the importance of compounds of platinum group metals in biological systems, we have synthesised and characterised the complexes of Pd(II), Pt(II),Rh(III), Ir(III) and Ru(III) with propiophenone and butyrophenone semicarbazones. The results of this study are reported here.

Materials and Methods

Preparation of ligands

Propiophenone and butyrophenone semicarbazones were prepared by the usual method reacting semicarbazide hydrochloride with the respective ketone in the presence of sodium acetate. The purity of the ligands was checked by elemental analyses and melting points.

Preparation of the complexes

The platinum metal salts were Johnson-Mathey (London) products. Commercial ruthenium chloride, which contained some ruthenium(IV), was evaporated several times with conc. HCl to ensure conversion of Ru(IV) into ruthenium(III) chloride.

The following general method was used for the preparation of the complexes. A hot aqueous solution (20 ml) of the metal chloride (0.1 mol) was mixed with a hot ethanolic solution (20 ml) of the semicarbazone (0.2 mol). The mixture was refluxed on a waterbath for 2-3 hr. On cooling, the coloured complex precipitated out in each case. The complex was filtered, washed with 50% aqueous ethanol and dried *in vacuo* over P_4O_{10}.

Magnetic measurements were carried out using a Princeton Applied Research Model 155 vibrating sample magnetometer, incorporating a digital readout. The instrument was calibrated using a standard (analytical) nickel pellet and cross-checked against $Hg[Co(SCN)_4]$. IR spectra were recorded on a Perkin Elmer 621 automatic recording (4000-400 cm^{-1}) spectrophotometer in KBr. Electronic spectra were recorded on a DMR-21 automatic recording spectrophotometer in nujol mull.

Analyses for carbon and hydrogen were carried out at the Microanalytical Laboratory of the Department of Chemistry, University of Delhi. Nitrogen was estimated at CDRI, Lucknow.

Results and Discussion

The formation of the complexes may be represented by the following reactions:

$K_2MCl_4 + 2L \rightarrow [ML_2]Cl_2 + 2\,KCl$
$M'Cl_3 + 3L \rightarrow [M'L_3]Cl_3$
M = Pd(II) or Pt(II); L = ligand (PSC and BSC);
M′ = Rh(III), Ir(III) or Ru(III)

Elemental analyses reveal that the complexes have the compositions $M(ligand)_2Cl_2$ (M = Pd or Pt) and $M(ligand)_3Cl_3$ (M = Rh, Ru and Ir) (Table 1). Conductivities of these complexes could not be measured due to their poor solubilities in the common organic solvents.

Table 1 — Colour, Composition and Magnetic Moment Data of the Complexes

Complex	Colour (yield, %)	m.p. (°C)	Found (Calc.) % M	C	H	N	μ_{eff} (B.M.)
Pd(PSC)$_2$Cl$_2$	Black (82)	158*	19.00 (19.02)	42.98 (42.98)	4.00 (4.65)	14.68 (15.02)	DM
Pt(PSC)$_2$Cl$_2$	Dull white (90)	190	30.00 (30.03)	37.00 (37.03)	4.00 (4.01)	12.82 (12.96)	DM
Ru(PSC)$_3$Cl$_3$	Light yellow (70)	210	13.66 (13.16)	30.70 (30.75)	3.12 (3.33)	11.00 (10.76)	1.80
Rh(PSC)$_3$Cl$_3$	Black (60)	270	13.76 (13.16)	30.22 (30.67)	3.42 (3.32)	10.44 (10.74)	DM
Ir(PSC)$_3$Cl$_3$	Light brown (55)	310	22.00 (22.05)	28.00 (27.53)	3.00 (2.98)	10.22 (09.64)	DM
Pd(BSC)$_2$Cl$_2$	Yellow (75)	300	17.67 (18.11)	44.90 (44.94)	4.88 (5 14)	13.66 (14.30)	DM
Pt(BSC)$_2$Cl$_2$	Greenish-yellow (92)	70*	28.00 (28.96)	39.00 (39.05)	4.22 (4.44)	12.00 (12.42)	DM
Ru(BSC)$_3$Cl$_3$	Dark brown (60)	195*	11.64 (12.29)	32.00 (32.07)	4.00 (3.63)	10.50 (10.21)	1.80
Rh(BSC)$_3$Cl$_3$	Light brown (56)	245	20.63 (21.04)	32.00 (32.02)	4.21 (3.64)	10.80 (10.18)	DM
Ir(BSC)$_3$Cl$_3$	Yellow (55)	300	12.08 (12.70)	29.22 (28.89)	4.11 (3.28)	09.20 (09.10)	DM

DM — Diamagnetic, *Decomposed without melting

Palladium(II) and platinum(II) complexes

The complexes are diamagnetic as expected for square-planar d^8 metal ion complexes. The electronic spectra of square-planar Pd(II) and Pt(II) complexes are expected to show three *d-d* bands due to the transitions[8,9], $^1A_{1g} \rightarrow {}^1A_{2g}$, $\rightarrow {}^1B_{1g}$ and $\rightarrow {}^1E_g$. The electronic spectra of the complexes under study display bands at 22200-24200 and 29200-31000 cm^{-1} (Table 2). The first band may be assigned[8,9] to the $^1A_{1g} \rightarrow {}^1B_{1g}$ transition and the second band in the UV region is undoubtly a charge-transfer band.

By assuming a value of $F_2 = 10F_4 = 600$ for Slatar-Condon interelectronic repulsion parameters for both Pd(II) and Pt(II), it is possible to calculate from the first spin allowed *d-d* transition[10] the value of Δ_1 (Table 2). The splitting parameters increase in the expected order, Pt > Pd.

Rhodium(III) and iridium(III) complexes

Elemental analyses of these complexes reveal the general composition M(ligand)$_3$Cl$_3$ (M = Rh or Ir). Conductance of these complexes could not be measured due to their poor solubilities in the common organic solvents. All the complexes are diamagnetic as expected. This is consistent with an octahedral arrangement of the donor atoms around the ion producing a strong field[11].

The electronic spectra of Rh(III) complexes display bands at 17500-17800, 20100-20200 and 24800 cm^{-1}. These resemble those reported for other six-coordinate rhodium(III) complexes[8,12-14] and may be assigned to $^1A_{1g} \rightarrow {}^3T_{1g}$, $^1A_{1g} \rightarrow {}^1T_{1g}$ and $^1A_{1g} \rightarrow {}^1T_{2g}$ transitions respectively. The electronic spectra of d^6 complexes can be used to evaluate[15] ligand field parameters. The values are given in Table 2. The values are comparable with those observed for other complexes of this metal ion with nitrogen-oxygen donor ligands[12-16]. The *B* values are 39-40% of the free ion values, suggesting considerable orbital overlap with strong covalency in the metal-ligand σ-bond.

Jorgensen[15] has demonstrated that a decrease in values of β is associated with a reduction in the positive charge of the cation and tendency towards reduction to the next lower oxidation state.

The electronic spectra of the iridium(III) complexes under study display bands around 30800 and 34000-34200 cm^{-1}, which may be assigned[16] to $^1A_{1g} \rightarrow {}^1T_{1g}$ (ν_1) and $^1A_{1g} \rightarrow {}^1T_{2g}$ (ν_2) transitions respectively. The ratio of ν_2/ν_1 in these complexes lies in the range 1.08-1.10. The two transitions ν_1 and ν_2 have been used to evaluate the ligand field parameters (Table 2). The values of these ligand field parameters are comparable with those reported for other iridium(III) complexes involving similar donors.[18-20]

Ruthenium(III) complexes

The room temperature magnetic moments of

Table 2 — Electronic Spectral Bands (cm^{-1}) and Ligand Field Parameters

Complex	λ_{max} (cm^{-1})	10 Dq (cm^{-1})	B (cm^{-1})	β	C (cm^{-1})	ν_2/ν_1	Δ_1 (cm^{-1})
$Rh(PSC)_3Cl_3$	17500 20200 24800	21550	288	0.39	1350	1.15	—
$Rh(BSC)_3Cl_3$	17800 20100 24800	21250	294	0.40	1150	1.13	—
$Ir(PSC)_3Cl_3$	30800 34000	31600	200	0.33	800	1.10	—
$Ir(BSC)_3Cl_3$	30800 34200	30850	212	0.32	850	1.08	—
$Ru(PSC)_3Cl_3$	13650 17600 22700	26259	494	0.78	2523	1.29	—
$Ru(BSC)_3Cl_3$	13700 17600 22600	26054	488	0.78	2479	1.28	—
$Pd(PSC)_2Cl_2$	22200 29200	—	—	—	—	—	24300
$Pd(BSC)_2Cl_2$	22200 29200	—	—	—	—	—	24300
$Pt(PSC)_2Cl_2$	24200 31000	—	—	—	—	—	25800
$Pt(BSC)_2Cl_2$	24200 31000	—	—	—	—	—	25800

the ruthenium(III) complexes of both the ligands lie in the range 1.08-1.82 B.M. (Table 2), which are lower than the predicted value of 2.10 B.M. The lowering in μ_{eff} values may arise due to presence of lower symmetry ligand fields, metal-metal interactions or extensive electron delocalisation[17].

The electronic spectra of ruthenium complexes display bands at 13650-13700, 17600 and 22600-22700 cm^{-1} which may be assigned[8,18-20] to ${}^2T_{2g}\rightarrow{}^4T_{1g}$, ${}^2T_{2g}\rightarrow{}^4T_{2g}$ and ${}^2T_{2g}\rightarrow{}^2A_{2g}$, ${}^2T_{1g}$ transitions, respectively. The electronic spectra of these complexes are further rationalised[19] in the terms of different ligand field parameters (Table 2). The ligand field parameters are comparable with those reported for other ruthenium(III) derivatives involving nitrogen-oxygen donor molecules[8,18-20].

Infrared spectra of complexes

A comparative study of the spectra of the ligands and complexes shows that both the semicarbazones behave as bidentate chelating agents coordinating to the metal ions through carbonyl oxygen and nitrogen of the C=N group. The ligands show bands at 1670 and 1570 cm^{-1} due to νC=O and νC=N modes[21]. These shift towards lower side (30-60 cm^{-1}) in the spectra of complexes, indicating that coordination takes place through oxygen of C=O group and nitrogen of C=N group. The other important bands in the li-

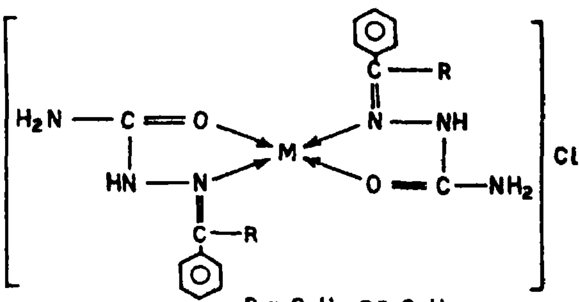

R = C_2H_5 or C_3H_7
M = Pd(II) or Pt(II)
(I)

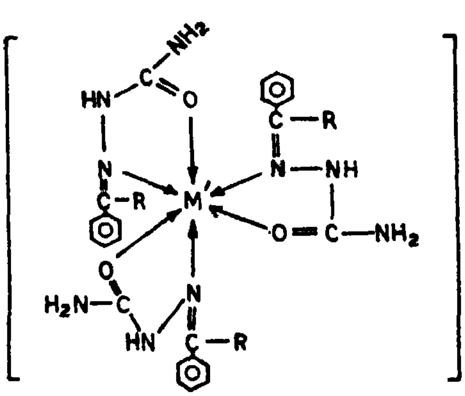

R = C_2H_5 or C_3H_7
M' = Rh(III), Ru(III) or Ir(III)
(II)

gand spectra occur in the region 3100-3500 cm^{-1} due to vNH modes of the NH and NH_2 groups[22-24]. It is difficult to assign these bands with certainty. These showed no definite pattern of shifts on complex formation and are probably not involved in coordination. On the basis of abvoe studies, structures I and II are assigned to the complexes.

References

1 Rosenberg B, *Plat Met Rev*, **16** (1971) 42.
2 Clears M J & Hoeschale J D, *Bio-inorg Chem*, **2** (1973) 187.
3 Rosenberg B & Blanz E J, *Brit J Dect*, **93** (1976) 71.
4 Rosenberg B, *Nature*, **222** (1969) 386.
5 Patil M M, Patel M R & Mankad B M, *J Indian chem Soc*, **53** (1976) 454.
6 Mahto C B, *J Indian chem Soc*, **57** (1980) 553.
7 (a) Thakur Y & Jha B N, *J inorg nucl Chem*, **42** (1980) 149.
(b) Kumar Y, Chandra S & Singh R P, *Synth React inorg met org Chem*, **15** (1985) 471.
8 Lever A B P, *Inorganic electronic spectroscopy*, edited by M F Lapport (Elsevier, Amsterdam) 1966.
9 Coggin P L, Goodfellow R J & Read F J S, *J chem Soc Dalton Trans*, (1972) 12198.
10 Bush D H & Gray H B, *Inorg Chem*, **6** (1967) 365.
11 Figgis B N & Lewis J, *Prog inorg Chem*, **6** (1964) 37.
12 Dwivedi J S & Agrawala U C, *Indian J Chem*, **10** (1972) 657.
13 Bartelli E, Preti C & Tosi G, *J inorg nucl Chem*, **37** (1975) 142.
14 Figgis B N, *Introduction to ligand fields* (Wiley Eastern Ltd, New Delhi) 1976.
15 Jorgensen C K, *Prog inorg Chem*, **4** (1962) 73.
16 Preti C & Tosi G, *Trans Met Chem*, **3** (1978) 17.
17 Livingston S E, Mayfield J H & Moors D S, *Aust J Chem*, **28** (1975) 2531.
18 Olliff R W & Odell A L, *J chem Soc*, (1964) 2467.
19 Tanabe Y & Sugano S, *J phys soc Japan*, **2** (1954) 766.
20 Gajendra M R & Agarwala U C, *J inorg nucl Chem*, 37 (1975) 2429.
21 Sterk H & Ziegler E, *Mh Chem*, **97** (1968) 1427.
22 Chatt J P, Duncanson L A & Vananzi L, *Nature*, **171** (1956) 1042.
23 Kovacic J K, *Spectrochim Acta*, **23A** (1967) 183.
24 Ali M A & Bose R, *J inorg nucl Chem*, **39** (1977) 265.

Indian Journal of Chemistry
Vol. 27A, May 1988, pp. 421-426

Characterisation of Some Copper(II), Nickel(II) & Cobalt(II) Complexes with Schiff Bases Derived from 3-Hydroxyiminobutane-2-one & Aromatic Amines

H C RAI*, (Mrs) JAYA TIWARY, (Mrs) RANJANA PRAKASH & (Mrs) SUSAN
Department of Chemistry, L S College, Bihar University, Muzaffarpur 842 001

Received 20 *April* 1987; *revised and accepted* 10 *November* 1987

A number of complexes of the types, CuL_2, $M(HL)_2X_2$ [$M = Co(II), Ni(II)$; $X = Cl^-, Br^-, I^-, NO_3^-, ClO_4^-$] and $Cu_2L_2X_2$ [$X = Cl^-, Br^-, NO_3^-, ClO_4^-$], where HL = schiff bases derived from 3-hydroxyiminobutane-2-one and aniline or toluidines, have been synthesised and characterised on the basis of elemental analyses, magnetic susceptibility, infrared and electronic spectral data.

Transition metal complexes with schiff bases as ligands have been amongst the most widely studied coordination compounds in the past few years, since they are becoming increasingly important as biochemical, analytical and antimicrobial reagents. Schiff bases derived from a large number of carbonyl compounds and amines have been used[1-8]; however, those derived from 3-hydroxyiminobutane-2-one have been comparatively less studied[9-11]. In the present investigation, a systematic study of the metal complexes of four schiff bases, all derived from 3-hydroxyiminobutane-2-one and aromatic amines is reported.

Materials and Methods

Bromide salts of Cu(II), Ni(II) and Co(II) as well as iodide salts of Ni(II) and Co(II) were prepared as reported in the literature[5,10]. An '*in situ*' method was adopted for the preparation of the complexes. 3-Hydroxyiminobutane-2-one (Loba), aromatic amines (BDH) and metal salts (S. Merck) were mixed together in the molar ratio 2:2:1 in an ethanolic medium and the mixture was warmed. The complexes of copper(II) separated as coloured crystalline products immediately; however, in the case of cobalt(II) and nickel(II) complexes, the colour of the solution changed immediately and solid products were obtained on allowing the mixture solution to stand overnight. All the complexes have been prepared under similar experimental conditions.

The compounds were analysed by standard procedures[12]. Infrared spectra of complexes were recorded on a Perkin Elmer spectrophotometer at IIT, Kharagpur. Electronic spectra were recordexed on a Beckman spectrophotometer. Magnetic susceptibilities were measured by a Gouy balance using $Hg[Co(CNS)_4]$ as the calibrant.

Results and Discussion

The molecular formulae of the complexes have been assigned on the basis of their analytical data (Table 1). The cobalt(II) and nickel(II) complexes are thus assigned the formulae, $M(HL)_2X_2$, whereas copper(II) complexes are of the types, CuL_2 and $Cu_2L_2X_2$ ($X = Cl^-, Br^-, NO_3^-, ClO_4^-$).

Although the infrared spectra of all the complexes are quite complex, structurally important bands have been identified which provide unequivocal evidence concerning the nature of bonding in the metal complexes. It is striking to note that important features of the spectra within one type of complexes resemble each other and can be clearly discriminated from those of other types. IR spectrum of 3-hydroxyiminobutane-2-one shows two fairly broad and strong bands at 3410 and 3350 cm^{-1} which are assigned to stretching mode of the hydrogen bonded N − O − H group[9]. These bands disappear in the spectra of the present complexes of the types CuL_2 and $Cu_2L_2X_2$ indicating breaking of N − O − H bonds and subsequent coordination of the ligands.

The spectra of the complexes of the type, $M(HL)_2X_2$ and ligand show an absorption band of medium intensity at about 1680 cm^{-1} while the spectra of other types of complexes, i.e., CuL_2 and $Cu_2L_2X_2$ do not contain this band. These characteristic features lead us to believe that this band is due to N − O − H deformation vibrations. Earlier studies on acetylacetonedioximato and diacetylazinedioximato metal chelates[13] containing the ligands in the neutral form assign the N-O − H deformation vibration around 1700 cm^{-1}. This band disappears from the spectra of the inner complexes. In the spectra of all the metal complexes, there appear two sharp bands of medium to strong intensity around 1600 and 1500 cm^{-1}. Considering their sharpness and in-

Table 1—Analytical Data of the Complexes

Compound	μ_{eff} (B.M.)	Colour	Found (Calc) %		
			Co	Halogen	N
Co(Hanilio)$_2$Cl$_2$	5.14	Brown	12.10	14.70	11.74
			(12.25)	(14.74)	(11.62)
Co(Hanilio)$_2$Br$_2$	5.10	Reddish Brown	10.82	28.52	9.65
			(10.33)	(28.02)	(9.80)
Co(Hanilio)$_2$I$_2$	5.00	Dark Brown	9.02	38.62	8.20
			(8.87)	(38.20)	(8.42)
Co(Hanilio)$_2$(NO$_3$)$_2$	4.98	Orange red	10.82	—	10.62
			(11.02)	—	(10.46)
Co(Hanilio)$_2$(ClO$_4$)$_2$	5.00	Brown	10.02	—	8.88
			(9.67)	—	(9.18)
Co(Hotoluio)$_2$Cl$_2$	5.16	Brown	11.42	13.10	10.43
			(11.52)	(13.93)	(10.99)
Co(Hotoluio)$_2$Br$_2$	5.12	Reddish	9.92	27.02	9.15
			(9.81)	(26.62)	(9.32)
Co(Hotoluio)$_2$I$_2$	5.06	Dark Brown	8.22	36.78	8.42
			(8.48)	(36.54)	(8.05)
Co(Hotoluio)$_2$(NO$_3$)$_2$	5.11	Orange red	10.26	—	10.02
			(10.44)	—	(9.91)
Co(Hotoluio)$_2$(ClO$_4$)$_2$	5.02	Brown	9.00	—	8.70
			(9.22)	—	(8.75)
Co(Hmetoluio)$_2$Cl$_2$	5.02	Brown	11.46	13.52	10.46
			(11.52)	(13.93)	(10.99)
Co(Hmetoluio)$_2$Br$_2$	5.12	Reddish Brown	9.91	27.01	9.16
			(9.81)	(26.62)	(9.32)
Co(Hmetoluio)$_2$I$_2$	5.09	Dark Brown	8.23	36.68	8.32
			(8.48)	(36.54)	(8.05)
Co(Hmetoluio)$_2$(ClO$_4$)$_2$	5.06	Brown	8.92	—	8.68
			(9.22)	—	(8.75)
Co(Hmetoluio)$_2$(NO$_3$)$_2$	5.07	Orange red	10.16	—	9.96
			(10.44)	—	(9.91)
Co(Hpatoluio)$_2$Cl$_2$	5.16	Brown	11.38	13.47	10.39
			(11.52)	(13.93)	(10.99)
Co(Hpatoluio)$_2$Br$_2$	5.12	Reddish Brown	9.84	27.00	9.08
			(9.81)	(26.62)	(9.32)
Co(Hpatoluio)$_2$I$_2$	5.14	Dark Brown	8.15	36.62	8.27
			(8.48)	(36.54)	(8.05)
Co(Hpatoluio)$_2$(ClO$_4$)$_2$	5.08	Brown	8.86	—	8.62
			(9.22)	—	(8.75)
Co(Hpatoluio)$_2$(NO$_3$)$_2$	5.10	Orange red	10.09	—	9.89
			(10.44)	—	(9.91)
Ni(Hanilio)$_2$Cl$_2$	2.90	Greenish Brown	12.00	14.81	11.72
			(12.25)	(14.74)	(11.62)
Ni(Hanilio)$_2$Br$_2$	2.88	Pale Yellow	10.78	28.42	9.60
			(10.33)	(28.02)	(9.80)
Ni(Hanilio)$_2$I$_2$	2.89	Yellow	8.68	38.52	8.20
			(8.87)	(38.20)	(8.42)
Ni(Hanilio)$_2$(NO$_3$)$_2$	2.86	Orange red	10.92	—	10.66
			(11.02)	—	(10.46)
Ni(Hanilio)$_2$(ClO$_4$)$_2$	2.82	Brown	10.15	—	9.20
			(9.67)	—	(9.18)
Ni(Hotoluio)$_2$Cl$_2$	2.85	Green	11.46	13.72	10.82
			(11.52)	(13.93)	(10.93)
Ni(Hotoluio)$_2$Br$_2$	2.83	Green	9.78	26.25	9.38
			(9.81)	(26.62)	(9.32)
Ni(Hotoluio)$_2$I$_2$	2.87	Yellowish	8.26	36.41	7.92
			(8.48)	(36.54)	(8.05)

Contd.

Table 1—Analytical Data of the Complexes—*Contd.*

Compound	μ_{eff} (B.M.)	Colour	Found (Calc) %		
			Co	Halogen	N
Ni(Hotoluio)$_2$(NO$_3$)$_2$	2.85	Pink	10.00	–	9.85
			(10.44)	–	(9.91)
Ni(Hotoluio)$_2$(ClO$_4$)$_2$	2.82	Brown	8.98	–	8.68
			(9.22)	–	(8.75)
Ni(Hmetoluio)$_2$Cl$_2$	2.82	Green	11.32	13.80	10.58
			(11.52)	(13.93)	(10.99)
Ni(Hmetoluio)$_2$Br$_2$	2.86	Yellowish Green	9.75	26.00	9.15
			(9.81)	(26.62)	(9.32)
Ni(Hmetoluio)$_2$I$_2$	2.78	Bright Green	8.32	36.18	8.00
			(8.48)	(36.54)	(8.05)
Ni(Hmetoluio)$_2$(NO$_3$)$_2$	2.84	Red	10.13	–	9.82
			(10.44)	–	(9.91)
Ni(Hmetoluio)$_2$(ClO$_4$)$_2$	2.83	Brown	9.00	–	8.68
			(9.22)	–	(8.75)
Ni(Hpatoluio)$_2$Cl$_2$	2.80	Green	11.46	13.70	11.12
			(11.52)	(13.93)	(10.99)
Ni(Hpatoluio)$_2$Br$_2$	2.85	Reddish Brown	9.72	26.30	9.00
			(9.81)	(26.62)	(9.32)
Ni(Hpatoluio)$_2$I$_2$	2.89	Red	8.35	36.13	8.00
			(8.48)	(36.54)	(8.05)
Ni(Hpatoluio)$_2$(NO$_3$)$_2$	2.80	Dark Brown	10.28	–	9.85
			(10.44)	–	(9.91)
Ni(Hpatoluio)$_2$(ClO$_4$)$_2$	2.84	Brown	9.20	–	8.65
			(9.22)	–	(8.75)
Cu(anilio)$_2$	1.75	Green	15.20	–	13.40
			(15.23)	–	(13.56)
Cu(otoluio)$_2$	1.70	Green	14.35	–	12.82
			(14.35)	–	(12.70)
Cu(metoluio)$_2$	1.70	Yellowish Green	14.25	–	12.78
			(14.35)	–	(12.70)
Cu(patoluio)$_2$	1.75	Green	14.50	–	12.80
			(14.35)	–	(12.70)
Cu$_2$(anilio)$_2$Cl$_2$	1.70	Green	23.28	13.02	10.32
			(23.17)	(12.95)	(10.22)
Cu$_2$(anilio)$_2$Br$_2$	1.90	Greyish Green	19.58	24.85	9.02
			(19.93)	(25.17)	(8.80)
Cu$_2$(anilio)$_2$(NO$_3$)$_2$	1.75	Green	21.42	–	9.42
			(21.13)	–	(9.32)
Cu$_2$(anilio)$_2$(ClO$_4$)$_2$	1.85	Green	18.85	–	8.42
			(18.78)	–	(8.28)
Cu$_2$(otoluio)$_2$Cl$_2$	1.75	Deep Green	22.05	12.32	9.56
			(21.97)	(12.28)	(9.68)
Cu$_2$(otoluio)$_2$Br$_2$	1.70	Brownish Green	19.22	24.12	8.28
			(19.04)	(23.98)	(8.40)
Cu$_2$(otoluio)$_2$(NO$_3$)$_2$	1.65	Green	19.85	–	9.20
			(20.12)	–	(8.87)
Cu$_2$(otoluio)$_2$(ClO$_4$)$_2$	1.70	Yellowish Green	18.10	–	8.02
			(17.98)	–	(7.93)
Cu$_2$(metoluio)$_2$Cl$_2$	1.80	Green	21.88	12.42	9.38
			(21.97)	(12.28)	(9.68)
Cu$_2$(metoluio)$_2$Br$_2$	1.85	Green	18.88	23.61	8.35
			(19.04)	(23.98)	(8.40)
Cu$_2$(metoluio)$_2$(NO$_3$)$_2$	1.75	Greyish Green	17.85	–	7.78
			(17.98)	–	(7.93)
Cu$_2$(metoluio)$_2$(ClO$_4$)$_2$	1.70	Green	18.20	–	8.15
			(17.98)	–	(7.93)

Contd.

Table 1—Analytical Data of the Complexes—*Contd.*

Compound	μ_{eff} (B.M.)	Colour	Found (Calc) %		
			Co	Halogen	N
$Cu_2(patoluio)_2Cl_2$	1.80	Green	22.02 (21.97)	22.18 (12.28)	9.66 (9.68)
$Cu_2(patoluio)_2Br_2$	1.70	Brownish Green	18.92 (19.04)	23.85 (23.98)	8.32 (8.40)
$Cu_2(patoluio)_2(NO_3)_2$	1.75	Green	20.00 (20.12)	– –	8.68 (8.87)
$Cu_2(patoluio)_2(ClO_4)_2$	1.70	Green	17.82 (17.98)	– –	7.86 (7.93)

Hanilio, Hotoluio, Hmetoluio and Hpatoluio are the schiff bases derived from 3-hydroxyiminobutane-2-one and aniline, *ortho-*, *meta-* and *para-*toluidines respectively.

tensity, they have been assigned to the $\nu C=N$ vibrations. The ligands contain two kinds of $C=N$ groups which are significantly different from each other. On comparison with IR data of structurally related molecules such as H_2dmg and schiff bases, the high frequency and low frequency bands have been assigned to azomethine and oxime $C=N$ groups respectively. The $\nu C=N$ mode due to $C=N-O-H$ group in H_2dmg appears at 1450 cm^{-1} which shifts to a higher frequency region (1590-1550 cm^{-1}) in the trinuclear dimethylglyoximato complexes.

It is conspicuous to observe that in the series of the metal complexes of the type, CuL_2, while the high frequency $\nu C=N$ band is shifted to lower frequency region, the low frequency oxime $\nu C=N$ band undergoes shift to high frequency region. It is believed that oxime ligands are bonded to the metal ions with both the imine and oxime nitrogen atoms by donating their non-bonding electron pairs with the simultaneous metal-ligand π-electron interactions. These spectral features lead us to conclude that complexes CuL_2 have the structure(I). The *cis* structure(I) is also supported by the experimental fact that copper(II) complexes are capable of forming binuclear metal chelates of the type, $Cu_2L_2X_2$. The shift in the $\nu C=N$ band and absence of hydrogen bonded $O-H$ group as evidenced by the infrared spectra of the complexes of the type $M(HL)_2X_2$ clearly indicate the *trans* structure(II) for these metal complexes. In the spectra of the complexes as well as the ligand, there appear three distinct bands in the region 1100-900 cm^{-1}, the strongest one being the middle one and most susceptible to change on coordination. This band, in our opinion, arises from the $N-O$ stretching vibration. In the ligand, this band appears at 1010 cm^{-1}.

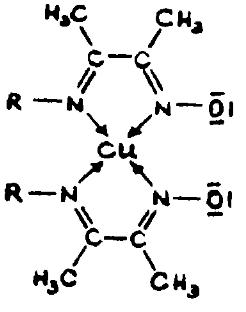
(I)

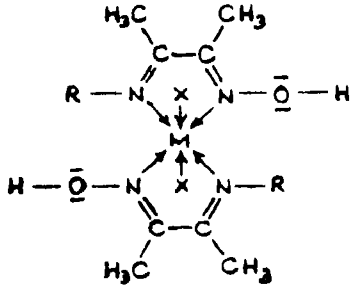
(II)

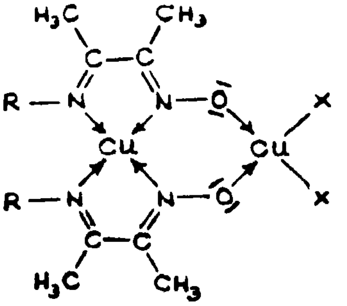
(III)

In 3-hydroxyiminobutane-2-one this band appears at 1020 cm^{-1}. In the complexes, $M(HL)_2X_2$, where M = Ni(II), Co(II), this band appears in the re-

Table 2—Electronic Spectra of Cu(II) Complexes with Imine Oxime Ligands (cm^{-1})

Complexes	Chromophore CuO_2X_2	Chromophore CuN_4
Cu_2(anilio)$_2Cl_2$	12000	17000
Cu_2(anilio)$_2Br_2$	12000	17500
Cu_2(otoluio)$_2Cl_2$	12500	17500
Cu_2(otoluio)$_2Br_2$	12200	17500
Cu_2(patoluio)$_2Cl_2$	12500	17000
Cu_2(patoluio)$_2Br_2$	12000	17000
Cu_2(metoluio)$_2Cl_2$	12300	17000
Cu_2(metoluio)$_2Br_2$	12000	17600

Table 3—Electronic Spectra of Ni(II) Complexes

Complexes	$^3B_{1g} \leftarrow {}^3A_{2g}$	$^3B_{1g} \leftarrow {}^3E_g$	$^3T_{1g}(P) \leftarrow {}^3A_{2g}$
Ni(Hanilio)$_2Cl_2$	13000	18700	24700
Ni(Hotoluio)$_2Cl_2$	13800	18500	24800
Ni(Hpatoluio)$_2Cl_2$	13700	17800	24000
Ni(Hmetoluio)$_2Cl_2$	13700	19200	24300

Table 4—Electronic Spectra of Co(II) Complexes

Complexes	$^4T_{1g}(F) \rightarrow {}^4T_{1g}(P)$
Co(Hanilio)$_2Cl_2$	15200
Co(Hotoluio)$_2Cl_2$	16100
Co(Hpatoluio)$_2Cl_2$	16100
Co(Hmetoluio)$_2Cl_2$	15800

gion 1115-1095 cm^{-1}. It is most striking to observe that in all the complexes of the type $Cu_2L_2X_2$, there is a decrease in the frequency of this band and the band appears in the region 1040-1000 cm^{-1} which undoubtedly occurs due to the formation of new links between the copper(II) inner complexes and copper(II) salts. This criterion when taken into account is reminiscent of the fact that the inner complexes act as exobidentate ligands giving rise to binuclear clusters which are postulated to possess the structure(III).

These structural assignments(I-III) are also supported by magnetic and electronic spectral studies (Tables 2-4).

It has been found that the binuclear complexes of copper(II) have magnetic moments in the range 1.70-1.90 B.M. per copper atom. The electronic spectra of the complexes have been studied in the region 10,000-25,000 cm^{-1}. In all the cases, the spectra appear to consist of two broad ligand field bands, the first one in the region 10,500-13,000 cm^{-1} and the second in the region 17,000-19,500 cm^{-1}. These spectral features resemble the features of the spectra reported for the bi- and tri-nuclear schiff base metal clusters and lead us to believe that the copper(II) ions are in similar ligand field environments respectively. Both the bands are due to $d-d$ transitions differing in their energies due to two different ligands fields. It would be reasonable to say that while the high frequency band arises from the chromophore, CuN_4 in a D_{4h} symmetry, the low frequency band originates from the chromophore, CuO_2X_2 in a lower symmetry, C_2.

Nickel(II) complexes of the type $Ni(HL)_2X_2$ show magnetic moments in the range 2.7-3.1 B.M. at room temperature which suggest octahedral arrangement of the ligand atoms around the central nickel(II) ion. Their electronic spectra show three bands (Table 3). The electronic spectral data indicate that the central nickel(II) ion is present in an octahedral field with certain amount of tetragonal distortion. The band at 24,000 cm^{-1} can be assigned to the transition, $^3T_{1g}(P) \leftarrow {}^3A_{2g}$, which, in some cases, overlaps with strong charge-transfer band.

The electronic spectra of several cobalt(II) complexes have been reported[14], their assignment have not been always unambiguous. The ligands field transitions $^4T_{2g} \leftarrow {}^4T_{1g}(F)$, $^4A_{2g} \leftarrow {}^4T_{1g}(F)$ and $^4T_{1g}(P) \leftarrow {}^4T_{1g}(F)$ are expected for octahedral Co(II) complexes to give rise to three bands. The first of these three bands generally appears in the near infrared range and the second one, being always weak, is scarcely observed. On the other hand, the third band appears as relatively intense band with some amount of structure.

The present series of compounds exhibit a multiplet band structure in the region 16,000-19,000 cm^{-1}, the band width spreading over ~ 3000 cm^{-1}. The band can be assigned to the transition, $^4T_{1g}(P) \leftarrow {}^4T_{1g}(F)$.

In general, the spectral and magnetic data provide consistent information with regard to the structure of the complexes i.e. all the complexes possess an approximately octahedral geometry with some amount of tetragonal distortion.

Acknowledgement

The authors are thankful to the Government of Bihar for a research fellowship to one of them (JT) and to Heads of the Departments of Chemistry, Patna University, patna and Bihar University, Muzaffarpur for laboratory facilities.

References

1 Holm R H, Everett (Jr) G W & Chakravorty A, *Progr inorg Chem*, 7 (1966) 83.

2 West B O, *New pathways in inorganic chemistry*, edited by E A V Ebsworth, A G Maddock & A G Sharpe (Cambridge University Press, Cambridge) 1968, 303.

3 Biradar N S, Pujari H A & Marathe U R, *Indian J Chem*, 8 (1971) 718.

4 Narang K K & Lal R A, *Curr Sci*, 47 (1978) 793.

5 Fider R C & Hill M C, *Inorg Chem*, **18** (979) 729.
6 Patil B R, Prabhakar B K & Kulkarni V H, *Curr Sci*, **48** (1979) 947.
7 Shukla P R, Jaiswal A M & Narain Gopal, *J Indian chem Soc*, **60** (1983) 1014.
8 El-Sharief A M Sh, Abu Gharib E A & Ammar Y A, *J Indian chem Soc*, **60** (1983) 1017.
9 Rai H C, Chakrabarti J & Sahoo B, *Indian J Chem*, **18A** (1979) 242.
10 Chakrabarti J & Sahoo B, *Indian J Chem*, **20A** (1981) 431.
11 Mahapatra B K & Sahoo B, *Indian J Chem*, **21A** (1982) 376.
12 Vogel A I, *A text book of quantitative inorganic analysis* (Longmans, London) 1981.
13 Singh C B, Rai H C & Sahoo B, *Indian J Chem*, **14A** (1976) 504.
14 Lever A B P, *Inorganic electronic spectroscopy* (Elsevier, Amsterdam) 1968, pp 318-333.

Indian Journal of Chemistry
Vol. 27A, May 1988, pp. 427-429

Synthesis & IR & NMR Spectral Studies on Some Triorganotin(IV) Compounds Containing 2-Pyridylcarbinols

R VISALAKSHI, V K JAIN* & G S RAO
Chemistry Division, Bhabha Atomic Research Centre, Bombay 400 085

Received 5 *June* 1987; *revised and accepted* 21 *September* 1987

Triorganotin isopropoxides, $[R_3Sn(OPr^i)]$ (R = Me, Et, Pr^n, Bu^n or Ph) react with 2-(hydroxymethyl)pyridine and 2-(2-hydroxyethyl)pyridine in refluxing benzene to afford moisture-sensitive complexes of the type $[R_3Sn\{O(CH_2)_nC_5H_4N\}]$ (n = 1 or 2). The trialkyltin compounds are colourless volatile liquids while the triphenyltin compound is obtained as a white crystalline solid. The complexes have been characterised by IR and NMR (^{1}H, ^{13}C and ^{119}Sn) spectral data. On the basis of NMR data, tetra-coordination is proposed for tin in these complexes.

8-Hydroxyquinolinol (oxine, OxH) (**I**) finds extensive uses in analytical and coordination chemistry[1]. To date compounds containing this ligand of virtually all metals and metalloids are known in which it behaves either in a monodentate or a bidentate fashion. The mode of coordination of 8-hydroxyquinolinate ligand in triorganotin(IV) compounds has been the subject of considerable discussion and various physical methods have been used to probe its nature in these compounds[2-9].

2-(Hydroxymethyl)pyridine (**II**) is isostructural to **I** as the two donor centers (O and N), like Ox, are separated by two carbon atoms. Consequently **I** and **II** may have similar coordination behaviour. Chelation and the changes in coordination number at tin can be detected by ^{119}Sn NMR spectroscopy[10,11]. The ^{119}Sn NMR shifts have also been shown to depend markedly upon the ring size when Sn atom is a part of a ring system. Incorporation of tin into a six-membered ring has the effect of shifting the ^{119}Sn resonance to lower frequency from its position in the five membered ring analogue[10]. If the pyridyl nitrogen participates in bonding, the ring effect should reflect in the ^{119}Sn NMR spectra of $R_3Sn(IV)$ complexes derived from 2-(2-hydroxyethyl)pyridine (**III**), a homologue of **II**. In this paper we have investigated the reactions of triorganotin isopropoxides with **II** and **III**.

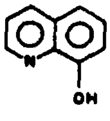

I

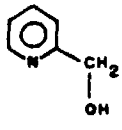

II

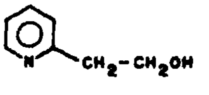

III

Materials and Methods

The ligands **II** and **III** (both Fluka reagents) were dried and distilled before use. Triorganotin isopropoxides were distilled prior to use. Solvents (AR) were dried and distilled under nitrogen atmosphere before use. Special precautions were taken to exclude moisture.

Infrared spectra were recorded either as neat liquids or as nujol mulls between CsI optics on a Perkin-Elmer-180 spectrophotometer. The ^{1}H, ^{13}C and ^{119}Sn NMR spectra were recorded on Varian FT-80 A spectrometer in $CDCl_3$ operating at 79.5, 20.0 and 29.6 MHz, respectively. Chemical shifts (^{1}H and ^{13}C) are reported in ppm from internal solvent peak ($CDCl_3$ δ 7.26 for ^{1}H; and δ 77.0 ppm for ^{13}C) and external 33% Me_4Sn in C_6D_6 for ^{119}Sn.

Reaction of triporpyltin isopropoxide with 2-(hydroxymethyl)pyridine (II)

A mixture of tripropyltin isopropoxide (2.71 g,

Table 1 — Boiling Points and Analytical Data for Triorganotin(IV) Compounds Containing 2-Pyridylcarbinols

Compound	b.p. °C/mm	Sn found (Calc.), %	
$[Me_3Sn(OCH_2C_5H_4N)]$	74/0.5	43.86	(43.65)
$[Et_3Sn(OCH_2C_5H_4N)]$	124/0.5	36.95	(37.8)
$[Pr_3Sn(OCH_2C_5H_4N)]$	116/0.2	32.81	(33.33)
$[Bu_3Sn(OCH_2C_5H_4N)]$	136/0.1	29.42	(29.81)
$[Ph_3Sn(OCH_2C_5H_4N)]^*$	—	24.60	(25.91)
$[Me_3Sn(OCH_2CH_2C_5H_4N)]$	85/0.2	41.73	(41.51)
$[Et_3Sn(OCH_2CH_2C_5H_4N)]$	135/0.5	35.79	(36.18)
$[Pr_3Sn(OCH_2CH_2C_5H_4N)]$	125/0.2	31.73	(32.07)
$[Bu_3Sn(OCH_2CH_2C_5H_4N)]$	140/0.1	28.17	(28.8)

*C, 61.53 (62.9); H, 4.51 (4.84); N, 2.48 (3.06)

Table 2 — ^{1}H, $^{13}C\{^{1}H\}$ and $^{119}Sn\{^{1}H\}$ NMR Data of Triorganotin(IV) Compounds Derived from 2-Pyridylcarbinols in $CDCl_3$

Compound	^{1}H NMR data δ Sn – R in ppm[a]	δ ^{119}Sn in ppm	$^{13}C\{^{1}H\}$ NMR data		
			δ Sn – R[b] in ppm		δ Ligand carbons (in ppm)
			Sn – C(1)	C(2), C(3), C)4)	
$[Me_3Sn(OCH_2-C_5H_4N)]$	0.31 (56) s	110	– 3.0 (407)	—	67.4, 120.3, 121.5, 136.2, 147.3, 162.7
$[Et_3Sn(OCH_2-C_5H_4N)]$	0.61-1.28 m	82	—	—	—
$[Pr_3Sn(OCH_2-C_5H_4N)]$	0.80-1.80 m	92	18.2 (375)[c]	18.9	68.4, 120.1, 121.0, 135.8, 147.6, 163.7
$[Bu_3Sn(OCH_2-C_5H_4N)]$	0.72-1.55 m	93	15.4	27.6, 26.7, 13.1	68.5, 120.2, 121.1, 135.8, 147.7, 163.8
$[Ph_3Sn(OCH_2-C_5H_4N)]$	7.05-7.80 m[d]	—	—	—	—
$[Me_3Sn(OCH_2CH_2-C_5H_4N)]$	0.23 (56) s	138	– 5.0 (395)	—	43.7, 65.3, 120.6, 123.4, 135.5, 148.9, 160.0
$[Et_3Sn(OCH_2CH_2-C_5H_4N)]$	0.52-1.70 m	103	5.3 (380)	9.3	43.8, 65.7, 120.4, 123.2, 135.2, 148.7, 160.0
$[Pr_3Sn(OCH_2CH_2-C_5H_4N)]$	0.82-1.62 m	104	—	—	—
$[Bu_3Sn(OCH_2CH_2-C_5H_4N)]$	0.77-1.52 m	105[c]	—	—	—

a s = singlet, m = multiplet; values in parantheses are $^{2}J(^{119}Sn-{}^{1}H)$ in Hz.
b Values given in paranetheses are $^{1}J(^{119}Sn-{}^{13}C)$ in Hz
c Merged with C(3)
d Pyridyl protons merged in Ph – Sn resonances
e Contains small impurities of $(Bu_3Sn)_2O$; δ ^{119}Sn 92 ppm, probably formed due to hydrolysis.

8.83 mmol) and **II** (0.98 g, 8.95 mmol) was refluxed in anhydrous benzene. The isopropanol liberated was removed azeotropically and determined. Excess benzene was distilled off and the product was distilled under reduced pressure.

Other reactions were also carried out similarly. The triphenyltin compound was a solid and hence it was recrystallised from benzene-hexane. Pertinent data for these compounds are summarised in Table 1.

Results and Discussion

Reactions of triorganotin(IV) isopropoxides, $[R_3Sn(OPr^i)]$, with **II** and **III** in refluxing benzene give products arising by replacement of the isopropoxy group by a 2-pyridylalkoxy group. Liberated isopropanol is fractionally distilled azeotropically with benzene and estimated. These reactions require 3-6 hr refluxing for completion and the progress of the reaction is monitored by the estimation of isopropanol in the azeotrope by an oxidometric method. While all the trialkytin compounds are obtained 55-70% yield as volatile liquids distillable under reduced pressure the triphenyltin compound is obtained as a white solid which can be recrystallised from benzene-hexane. These compounds are sensitive to moisture and hydrolyse readily when exposed to atmospheric air.

The broad bands appearing in the region 3500-3100 cm^{-1} in the IR spectra of the free ligands, assignable to νOH, are absent in the spectra of organotin compounds. The free ligands and the triorganotin(IV) compounds exhibit νC – O[12] in the region 1040-1080 cm^{-1}. The νSn – O and νSn – C modes in the region 470-700 cm^{-1} in organotin alkoxides are generally coupled and no clear distinction between them could be made[12-16]. In conformity the coupled νSn – O and νSn – C modes in the presently synthesised compounds appear in the region 500-700 cm^{-1}. The tripropyl and tributyltin compounds exhibit two bands in the region 585-610 and 500-515 cm^{-1} which may be assigned to νSn – C modes of *trans* and *gauche* conformations respectively. A strong band at ~ 270 cm^{-1} in triphenyltin compound can be assigned to νSn – C(Ph) modes[17,18].

In the PMR spectra of the ligands, **II** and **III**, the OH proton appears as a singlet at δ 4.90 and 4.56 ppm, respectively. These resonances are absent in the organotin(IV) compounds. The singlet due to CH_2 proton in **II** appearing at δ 4.68 is deshielded in the spectra of organotin(IV) compounds and appears at δ ~ 4.8 (for trialkyltin compounds) and at δ 5.38 in triphenyltin compound. In the case of **III** the methylene protons appear as two triplets at δ 2.94 ($-CH_2-$) and 3.93 ppm ($-CH_2O$); on complexation the triplet due to $-CH_2O$ protons is slightly deshielded. The signal due to methyl, ethyl, propy, butyl and phenyl groups attached to tin appear as a singlet (for methyltin) and as multiplets in other cases. The ^2J ($^{119}Sn-{}^1H$) for methyltin compounds is 56 Hz (Table 2) and is comparable to other four-coordinate trimethyltin compounds reported previously[19,20].

The $^{13}C\{^1H\}$NMR spectra of some of the organotin compounds were recorded and the data are summarised in Table 2. It has been shown recently that ^1J ($^{119}Sn-{}^{13}C$) values provide useful information regarding the coordination number and stereochemistry of organotin compounds[20,21]. The ^1J-values are directly proportional to the *s*-character of their hybrid orbitals when none of the participating bonding atoms have a lone electron pair. For tetracoordinate trialkyltin compounds the ^1J values were reported in the range 390 ± 20 Hz in non-coordinating solvents[20,22,23]. The observed ^1J values (Table 2) for our complexes are in the range expected for four-coordinate tin compounds. This suggests that the pyridyl nitrogen does not participate in bonding with tin. The methylene carbon(s) of the ligand moieties appeared as singlet(s).

The ^{119}Sn NMR shifts for trialkyltin compounds are reported in Table 2 which appear in the range δ 82 to 138 ppm. This is typical of ^{119}Sn shifts for four coordinate trialkyltin alkoxides (δ 60 to 134 ppm)[10]. As is evident from Table 2 that the ^{119}Sn NMR signal is deshielded by 12-28 ppm in $R_3Sn(IV)$ compounds containing **III** compared to the corresponding compounds derived from **II**. Shielding would have been observed in chelated compounds[10].

In conclusion, the NMR data suggest that the compounds reported in this paper contain four coordinate tin with unidentate 2-pyridyl-carbinol ligand and that any $Sn-N$ interaction, if present, must be very weak.

Acknowledgement

We are grateful to Dr J P Mittal, Head, Chemistry Division and Dr R M Iyer, Director, Chemical Group for their interest in this work.

References

1 Phillips J P, *Chem Rev*, **56** (1956) 271; Hollingshead R G W, *Oxine and its derivatives*, Part I (Butterworths, London) 1954.

2 Wada M, Kawakami K & Okawara R, *J organometal Chem*, **4** (1965) 159.

3 Kawakami Y, *Bull chem Soc Japan*, **49** (1976) 2319.

4 Kawakami K & Okawara R, *J organometal Chem*, **6** (1966) 249.

5 Barbieri R, Faraglia G, Giustiniani M & Roncucci L, *J inorg nucl Chem*, **26** (1964) 203.

6 Roncucci L, Faraglia G & Barbieri R, *J organometal Chem*, **6** (1966) 278; **1** (1964) 427.

7 Harrison P G & Phillips R C, *J organometal Chem*, **99** (1975) 79; Kawasaki Y, *Org Mag Res*, **2** (1970) 165.

8 Clark H C, Jain V K, McMahon I J & Mehrotra R C, *J oranometal Chem*, **243** (1983) 299.

9 Jain V K, Mason J, Saraswat B S & Mehrotra R C, *Polyhedron*, **4** (1985) 2089.

10 Smith P J & Tupeiauskas A P, *Annual reports on NMR spectroscopy*, **8** (1978) 291.

11 Harris R K, Kennedy J D & McFarlane W, *NMR and the periodic table*, edited by Harris R K & Mann B E (Academic Press, New York) 1978, p. 309.

12 Bradley D C, Mehrotra R C & Gaur D P, *Metal alkoxides and allied derivatives* (Academic Press, London) 1978 and references therein.

13 Cummins R A & Evans J V, *Spectrochim Acta*, **21** (1965) 1016.

14 Tanaka T, *Organometal Chem Rev*, **A5** (1970) 1.

15 Gaur D P, Srivastava G & Mehrotra R C, *J organometal Chem*, **63** (1973) 221.

16 Saraswat B S, Srivastava G & Mehrotra R C, *J organometal Chem*, **129** (1977) 155.

17 Tanaka T, *Inorg chim Acta*, **1** (1967) 217.

18 Poller R C, Ruddick J N R, Thevarasa M & McWhinnie W R, *J chem Soc A*, (1969) 2327.

19 Singh B P, Srivasvata G & Mehrotra R C, *J organometal Chem*, **171** (1979) 35; Rao R J, Srivastava G & Mehrotra R C, *J organometal Chem*, **258** (1983) 155.

20 Al-Allaf T A K, *J organometal Chem*, **306** (1986) 337.

21 Holecek J, Nadvornik M, Handlir K & Lycka A, *J organometal Chem*, **241** (1983) 177.

22 Domazetis G, Magee R J & James B D, *J organometal Chem*, **148** (1978) 339.

23 Poorter, B de, *J organometal Chem*, **221** (1981) 57.

Indian Journal of Chemistry
Vol. 27A, May 1988, pp. 430-433

Open Shell Hexamethyleneiminecarbodithioates of VO(IV), Cr(III), Mn(II & III), Fe(III), Co(II) & Cu(II)—Magnetic, Spectral & Antimicrobial Investigations

A K SINGH*, B K PURI & R K RAWLLEY
Department of Chemistry, Indian Institute of Technology, New Delhi 110 016,

Received 29 *April* 1987; *revised and accepted* 1 *July* 1987

The high spin complexes of sodium hexamethyleneiminecarbodithioate (NaHMICdt) with VO(IV), Cr(III), Mn(II and III), Fe(III), Co(II) and Cu(II) complexes have been prepared and characterized by elemental analyses, molar conductance and magnetic measurements (at 77 to 298 K) and electronic, IR, ESR and Mössbauer spectra. The Co(II) and Cu(II) complexes have square planar geometry and others octahedral except VO(IV), for which square pyramidal arrangement is indicated. The $Mn(HMICdt)_2OH$ has antiferromagnetic interaction and probably hydroxy-bridged dimeric structure. The $Fe(HMICdt)_3$ exhibits fast spin cross-over at room temperature. The ligand coordinates symmetrically through bisulphur fork. The Mn(II) complexes have been stabilised by the auxillary ligands, viz. 1,10-phenanthroline and 2,2'-bipyridyl. The ligand and its complexes have been tested for their activity against bacteria and fungi. The ligand and the Mn(II) and Fe(III) complexes are shown to possess both antibacterial and antifungal activity.

The chemistry of metal dithiocarbamates has attracted the attention of many research workers due to their applications[1-3] in diverse areas. The complexation of heterocyclic dithiocarbamates is less explored than that of N,N'-dialkyldithiocarbamates; however, it is found to be different in several respects[4] because donor properties of CSS^- group depend on the basicity of the parent amine. The behaviour of such a ligand having a seven-membered nonplanar saturated heterocyclic ring system linked to $-CSS^-$ group is expected to be different from that of planar heterocyclic dithiocarbamates. The seven-membered saturated ring system is expected to offer greater steric hindrance and thus can give metal complexes of unusual geometries. It is, therefore, thought worthwhile to examine the metal-hexamethyleneiminecarbodithioates and hence the title investigation.

Materials and Methods

Synthesis of ligand

Sodium hexamethyleneiminecarbodithioate ($NaHMICdt.2H_2O$) was prepared as follows: Sodium hydroxide pellets (2 g) were dissolved in a minimum amount of ethanol-water (4:1) mixture. Hexamethyleneimine (5 mg) in diethyl ether was stirred with the NaOH slurry for 5 min and CS_2 (4g) in diethyl ether (100 ml) was slowly added to the mixture under vigorous stirring during 1.5 hr. The contents were further stirred for another 1.5 hr and the precipitate was filtered, washed with diethyl ether and dried *in vacuo* over anhydrous calcium chloride. The recrystallized product from acetone-petroleum ether (m.p. 188-89°) yielded satisfactory elemental analyses, IR, PMR and mass spectra authenticating the purity of the compound. Thermogravimetric analysis confirmed the presence of 2 mol of water.

Synthesis of complexes

The complexes of VO(IV), Fe(II), Co(II) and Cu(II) were prepared respectively by reacting vanadyl sulphate, ferric ammonium sulphate, cobaltous nitrate and copper sulphate (0.25 g each), with 4-5 fold excess of NaHMICdt in aqueous solution. The compounds which precipitated out immediately were washed with cold water, filtered and dried *in vacuo* over anhydrous $CaCl_2$. On reacting commercially available (BDH) manganous chloride in a similar way a compound having the composition $Mn(HMICdt)_2OH$ was obtained instead of the expected $Mn(HMICdt)_2$. The complexes of Mn(II) were prepared only as mixed ligand complexes with nitrogen donors, viz. 1, 10-phenanthroline and 2,2'-bipyridine by the following procedure.

Phenanthroline or bipyridine (three-times over metal) dissolved in ethanol-water (2:1) was slowly added to an aqueous solution of commercially available (BDH) $MnCl_2.4H_2O$ (0.5 g). The resulting greenish-yellow solution was stirred with $NaHMICdt.2H_2O$ (1.18 g) dissolved in water. The precipitate was filtered, washed thoroughly with distilled water and dried *in vacuo* over anhydrous $CaCl_2$.

To synthesize the Cr(III) chelate the ligand in absolute ethanol was slowly added to a solution of $CrCl_3.6H_2O$ in absolute ethanol in a 3:1 mol ratio. The resulting mixture was filtered, washed with absolute ethanol, and dried *in vacuo* over anhydrous $CaCl_2$.

Analyses and spectral studies

The metals in the complexes after decomposing these with concentrated HNO_3 were estimated using a Pye-Unicam SP 191 atomic absorption spectrophotometer. The IR spectra of the samples were recorded in CsI discs in the range 4000-200 cm^{-1} on Perkin-Elmer 580 B and Nicolet 5 DX FT-IR spectrophotometers. Electronic spectra in nujol and chloroform were recorded on 554 Perkin-Elmer and Hitachi 330 UV-Vis spectrophotometers. ESR spectra were recorded on Varian E-12 and E-112 EPR spectrometers. Mössbauer spectrum of iron complex was recorded on a wiesel drive coupled to Canberra multichannel analyzer operating in the multiscaling mode, using a 25 mCi ^{57}Co radioactive source embedded in Pd-matrix. $Na_2[Fe(CN)_5NO].2H_2O$ was employed as the calibrant. The programme of E. Von Meerwall was executed on an ICL 2960 computer to obtain the computer generated plot of the Mössbauer spectrum. The magnetic susceptibilities of the polycrystalline samples were measured on a PARC model 155 vibrating sample magnetometer at room temperature and low temperatures down to 77 K. The conductance measurements were made on a W.G. Pye conductance bridge.

Results and Discussion

The results of elemental analyses recorded in Table 1 authenticate the assigned stoichiometries. All the complexes were found to behave as non-electrolytes in nitrobenzene as expected.

The observed μ_{eff} = 1.65 B.M. of $VO(HMICdt)_2$ is close to the spin only value for one unpaired electron, ruling out the possibility of direct intermolecular V-V interaction. The bands at 16.447, 18.382 and 21.008 kK observed in its electronic spectrum in nujol, have been assigned to $b_2 \rightarrow b_1^*$, $b_2 \rightarrow e_\pi^*$ and $b_2 \rightarrow a_1^*$ transitions respectively, indicating square pyramidal arrangement of ligands with C_{4v} symmetry around vanadium. A band around 24 kK is believed to be ligand to metal charge transfer in origin. The electronic spectra in pyridine and DMSO exhibit a new band in the region 12.903-13.158 kK and a shoulder in 16.26-16.40 kK region, due to coordination of the solvent molecule with vanadium. Moreover, the $b_2 \rightarrow e_\pi^*$ transition is found to decrease by 5 kK. These observations provide further support to square pyramidal structure. The ESR spectrum of the complex in DMF at room temperature was found to be isotropic containing eight lines. The $g_\parallel$ and $g_\perp$ values (1.9004 and 2.0268 respectively) indicate substantial covalent character of V-S bond. The IR spectrum of the complex exhibits a band at 952 cm^{-1} due to terminal ν(V=O), ruling out the presence of V—O—V—O chain. The nature and the extent of shift observed in ν(C—N), ν_s(C—S) and ν_{as}(C—S) modes on complexation are found to be of the same order as reported in literature[4], indicating symmetric bonding of the dithiocarbamate group. The IR spectrum of the complex also exhibits bands at 408 and 375 cm^{-1} due ν(V—S).

The magnetic moment of $Cr(HMICdt)_3$ (3.8 B.M.) is slightly less than the spin only value as is generally the case with octahedral chromium(III) complexes due to very small spin-orbit coupling constant of Cr^{3+}. Its electronic spectrum in chloroform displays two bands at 15.25 and 20.00 kK, assignable to $^4A_{2g} \rightarrow {}^4T_{2g}$(F) and $^4A_{2g} \rightarrow {}^4T_{1g}$(F) transitions respectively. The band at 33.50 kK is the charge transfer band masking the $\nu_3[^4A_{2g} \rightarrow {}^4T_{1g}(P)]$. These observations agree well with an octahedral arrangement around chromium in the complex. The values of parameters B, β, z and CFSE are calculated to be 446 cm^{-1}, 0.49, 0.68 and 218.92 kJ mol^{-1} respectively. The DT/DQ found to be lower than the limiting value (0.4226), supports the expected small trigonal distortion from the perfect cubic symmetry. The ESR spectrum of the powdered complex is isotropic at room temperature. The value of g (1.9742) and covalency parameter (γ, 0.60) suggest significant covalency of Cr-S bond. The ν(Cr—S) mode in the complex is observed at 378 cm^{-1}. A comparison of IR spectrum of the complex with that of ligand suggests symmetrical bonding of the bisulphur fork with chromium, as in the case of VO^{2+} complex.

The manganese complex $Mn(HMICdt)_2$ could not be isolated. This may be due to the tendency of Mn(II) to form an octahedral complex. The octahedral $Mn(HMICdt)_2(H_2O)_2$ is not stable and, therefore stabilization through relatively stronger auxiliary ligands is needed. The steric factor due to non-planarity of the ring, perhaps prevents the formation of a polymeric structure with composition $Mn(HMICdt)_2$ as is observed for diethyldithiocarbamate[5]. The isolation of Mn(II) as well as Mn(III) complex of HMICdt-(later in low yield) was possible from the commercially available manganese dichloride, without involving any additional oxidising agent. The presence of $(MnOH)Cl_2$ in commercial $MnCl_2$ seems to be responsible for the formation of Mn(III) complex, which contains an OH group.

The magnetic moments of $[Mn(HMICdt)_2phen]$ and $[Mn(HMICdt)_2bipy]$ in the range of 5.76-5.97 B.M., indicate these to be high spin octahedral complexes. The low temperature magnetic susceptibility measurements (upto 77 K) indicate that the complexes follow Curie-Weiss law. The bands observed in their electronic spectra at 16.67, 21.05-21.74, 27.78-28.57 and 36.10-37.04 kK are assigned to $^6A_{1g} \rightarrow {}^4T_{1g}$(G), $^6A_{1g} \rightarrow {}^4T_{2g}$(G), $^6A_{2g} \rightarrow {}^4T_{2g}$(D) and charge transfer transitions respectively. The first

Table 1—Physical Properties and Analytical Data of Metal-Hexamethyleniminecarbodithioates

Complex	Colour	m.p. (°C)	ΔM (Ω^{-1} cm^2.mol^{-1})	Calc (Found)%			
				M	C	H	N
VO(HMICdt)$_2$	yellow	81-83	0.90	12.26 (12.02)	40.47 (40.14)	5.82 (6.13)	6.74 (6.59)
Cr(HMICdt)$_3$	bluish-grey	> 250	0.44	9.04 (8.90)	43.87 (43.29)	6.31 (6.07)	7.31 (7.38)
[Mn(HMICdt)$_2$phen]	saffron	210	0.80	9.41 (9.20)	53.49 (53.76)	5.53 (5.46)	9.60 (9.80)
[Mn(HMICdt)$_2$bipy]	brick red	120	0.90	9.81 (9.56)	51.50 (52.61)	5.76 (5.62)	10.01 (10.40)
[Mn(HMICdt)$_2$OH]	violet-brown	98	1.43	13.06 (13.20)	39.95 (40.30)	5.99 (6.06)	6.66 (6.47)
Fe(HMICdt)$_3$	dark brown	247	0.25	9.64 (9.30)	43.58 (44.26)	6.27 (6.54)	7.26 (7.53)
Co(HMICdt)$_2$	dark green	> 250	0.46	14.46 (14.69)	41.26 (40.00)	5.94 (6.30)	6.87 (6.58)
Cu(HMICdt)$_2$	chocolate	145	0.40	15.42 (15.35)	40.80 (40.58)	5.87 (5.96)	6.80 (6.88)

three bands provide further support to octahedral geometry of the complexes. The value of β (0.723) indicates appreciable covalent character of Mn-S bond.

The magnetic moment of Mn(HMICdt)$_2$OH in the range of 4.35-4.9 B.M., is lower than the spin-only value. The low temperature magnetic measurements reveal that Curie-Weiss law is not followed and complex has a bi- or poly-nuclear structure having antiferromagnetic interactions. The electronic spectrum of this complex displays a shoulder at 16.5 kK assignable to ${}^5E_g \rightarrow {}^5T_{2g}$ transition as expected for octahedral geometry, and charge-transfer bands at 19.50, 27.50 and 36.78 kK. The ESR spectrum of the polycrystalline Mn(III)-complex exhibits a broad signal whereas that in chloroform solution, the spectrum exhibits a four-line signal. The $g_\parallel$ and $g_\perp$ are found to be 2.3314 and 1.9534 respectively (from spectrum of polycrystalline sample), indicating that metal-ligand bond does not have much covalency. The IR spectrum of this complex displays a band at 962 cm^{-1} which seems to arise from the bending mode of bridging[6] OH group and therefore, structure (A) seems logical for this Mn(III) complex. However, $\nu_{\text{Mn-O}}$ could not be unequivocally assigned in the far IR region. The IR spectra of Mn(II) complexes exhibit bands around 1300 cm^{-1} which seem to arise from the coordinated phen or bipy as reported in the literature[10]. In view of the above facts structure (B) seems more appropriate for the Mn(II) complexes.

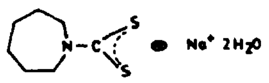

NaHMICdt.2H$_2$O

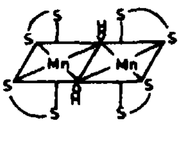

(A)

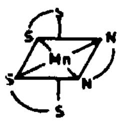

(B)

The room temperature magnetic moment of 4.65 B.M. of the Fe(HMICdt)$_3$ complex indicates the mixed ground state in octahedral geometry around Fe(III). The variation of μ_{eff} with temperature (77 to 293 K) suggests the existence of a spin state equilibrium (${}^6A_1 \rightleftharpoons {}^2T_2$). The Mössbauer spectrum of the Fe(III) complex at room temperature consists of quadrupole-split, well-resolved doublet with δ = 0.4 mm s^{-1} and ΔE_q = 0.53 mm s^{-1}. This implies that time of spin cross over is shorter than life-time of ^{57}Fe excited state (1.45×10^{-7}s). The δ-value is closer to the weak ligand field and supports electron donation from the ligand σ-orbitals to metal *d*-orbitals. The electronic spectrum of Fe(HMICdt)$_3$ has the charge transfer and intraligand transition bands in the range 25.64-37.74 kK. The band at 16.95 kK may be attributed to ${}^2T_2 \rightarrow {}^2T_1$ transition. These observations support an octahedral geometry for the complex. The $\nu_{(\text{Fe-S})}$ mode appears at 368 cm^{-1}. The difference between IR spectrum of HMICdt Na and its Fe(III)-complex is of the type observed in other complexes described above. Therefore, the ligand seems to be symmetrically bonded in the iron complex too.

The Co(HMICdt)$_2$ has the room temperature magnetic moment value of 2.51 B.M., as expected for a square planar complex. Its electronic spectrum in chloroform exhibits peaks at 15.75 (${}^2A_{1g} \rightarrow {}^2B_{2g}$), 20.83 (${}^2A_{1g} \rightarrow {}^2E_g$) and 25 kK (${}^2A_{1g} \rightarrow {}^2B_{1g}$) compatible with a square planar geometry. The ESR spectrum of the polycrystalline sample is anisotropic at room temperature as well as liquid N_2 temperature. The small difference in the *g* values may be due to the formation of a weak axial Co-S bond at liquid N_2 temperature. The low value of $g_\parallel$ (1.5262) arises from admixture of 4*s* and $3d_z^2$ orbitals, and intermolecular cobalt-sulphur interaction. The absence of s.h.f.s. in the spectrum indicates that the unpaired electron most probably residues in d_z^2 orbital[7]. The ν(Co-S) mode in the IR spectrum is observed at 360 cm^{-1}. The symmetric bonding of HMICdt is indicated by its IR spectrum.

The magnetic moment of $Cu(HMICdt)_2$ (1.73 B.M.) is close to the spin-only value and μ_{eff} is independent of temperature. Its electronic spectrum in chloroform displays a broad shoulder at 16.39 kK and an intense band at 22.99 kK due to $^2B_{1g} \rightarrow {}^2A_{1g}$ and $^2B_{1g} \rightarrow {}^2E_g$ transitions, respectively, indicating the square planar geometry. The ESR spectrum of polycrystalline copper complex is anisotropic. The ESR spectrum of frozen chloroform solution of the complex is very similar, probably due to weak Cu-S axial interactions. The $g_\parallel$ and $g_\perp$ values (~ 2.1292 and ~ 1.9764 respectively) are lower than those expected for an octahedral complex, and suggest that unpaired electron lies in $d_{x^2-y^2}$ orbital[8] and Cu-S bond has considerable covalent character[9]. The νCu-S mode in its IR spectrum appears at 368 cm^{-1}. The other IR frequencies are in favour of symmetrical bonding of bisulphur fork.

Antimicrobial screening

The HMICdtNa as well as its complexes have been tested for antbacterial activities against *Streptococcus faecalis* (I), *Klebsiella pneeumoniae* (II), *Escherichia coli* (III), *Pseudomonas aeruginosa* (IV) and *Staphylococcus aureus* penicillin-resistant (V) and for the antifungal activities against *Candida albicans* (VI), *Cryptococcus neoformans* (VII), *Sporotrichum schenckii* (VIII), *Trichophyton mentagrophytes* (IX) and *Aspergillus fumigatus* (X). The antibacterial tests were carried out in peptone broth and antifungal tests in Sabourand's broth. The 12.5 to 25 μg cm^{-3} of HMICdtNa was found to inhibit the growth of all fungi and bacteria except IV and VIII. For $[Mn(HMICdt)_2phen]$ and $[Mn(HMICdt)_2bipy]$ minimum inhibitor concentrations were in the range of 6.25 to 25 μg cm^{-3}. The 2,2′-bipyridyl derivative of Mn(II) was not active against III, IV, VI and IX whereas the 1,10-phenanthroline derivative was active against I, II, III, V and X only. The 12.5 to 25 μg cm^{-3} of $Fe(HMICdt)_3$ inhibited the growth of I, V, VII and IX. The other complexes have not been found active against these bacteria and fungi.

References

1 Eisenberg R, *Progr Inorg Chem*, **12** (1970) 295.
2 Coucouvanis D, *Progr Inorg Chem*, **11** (1970) 234.
3 Jones M M & Jones S G, *Inorg chim Acta*, **79** (1983) 288.
4 Fabretti A C, Forghieri F, Giusti A, Pretti C & Tosi G, *Inorg chim Acta*, **86** (1984) 127 and references therein.
5 Cotton F A & Wilkinson G, *Advanced inorganic chemistry* (Wiley, New York) 1980, pp 739.
6 Nakamoto K, *Infrared and Raman spectra of inorganic and coordination compounds* (Wiley, New York) 1978, pp 230.
7 Assour J M & Kahn W K, *J Am chem Soc*, **87** (1965) 207.
8 Ballhausen C J, *Introduction to ligand field theoy* (McGraw Hill, New York) 1962, pp 134.
9 Kivelson D & Neiman R, *J chem Phys*, **35** (1961) 149.
10 McWhinnie W R & Miller J D, *Adv Inorg Chem Radiochem*, **12** (1969) 135.

Indian Journal of Chemistry
Vol. 27A, May 1988, pp. 434-435

Notes

Solvent Effects on Rates of Reduction of *trans*-Diazidobis(dimethylglyoximato)-cobaltate(III) by Iron(II)

N MANI & V R VIJAYARAGHAVAN*

Department of Physical Chemistry, University of Madras,
A.C. College Campus, Madras 600 025

Received 27 *April; revised and accepted* 29 *September* 1987

The kinetics of Fe(II) reduction of $[Co(dmgH)_2(N_3)_2]^-$ in aqueous methanol, ethanol, isopropanol and 2-methyl-2-propanol have been studied at $I = 1.0$ mol dm^{-3} ($LiClO_4$), temp = 30°C and $[H^+] = 0.10$ mol dm^{-3}. It has been observed that the rate increases with increase in substitution of alkyl group in alcohols. This kinetic behaviour is attributable mainly to structural changes in the inner sphere of Fe(II).

Electron transfer reactions involving cobaloximes have been extensively studied in this laboratory[1-4] and it has been observed[1] that (i) iron (II) reduction of these complexes shows an inverse dependence on $[H^+]$ with a limiting rate at high $[H^+]$ and (ii) the probable site of bridging in the complex by iron(II) is the oxime oxygen[2]. The effect of solvent on the rates of reduction of cobaloximes has not been investigated in detail and hence the title investigation using aqueous CH_3OH, C_2H_5OH, $(CH_3)_2CHOH$ and 2-methyl-2-propanol. It may be mentioned that such studies on carboxylato[5] and halogenopentammine[6-8] complexes of cobalt(III) are available.

The complex *trans*-$Na[Co(dmgH)_2(N_3)_2]^-$ was prepared and purified by literature method[9] and its purity confirmed by UV-vis and IR spectra, conductivity measurements and elemental analyses. Ferrous perchlorate was prepared[10] and stored under nitrogen.

Kinetic studies were carried out using a 10-fold excess of Fe(II) over [complex]. Preequilibrated solutions of the reactants in the desired alcohol-water mixtures were mixed under oxygen-free conditions and the cells used were sealed carefully using serum caps and flushed with nitrogen. Reactions were followed spectrophotometrically at 540 nm employing a Carl-Zeiss SPECORD UV-Vis recording spectrophotometer. Reactions were carried out in perchlorate medium and the ionic strength was adjusted to 1.00 mol dm^{-3} with lithium perchlorate. The plot of $\log (A_0 - A_\infty)(A_t - A_\infty)^{-1}$ versus time were linear upto 3 half-lives. The pseudo-first order rate constants were calculated from the slopes of such plots.

The 1:1 stoichiometry of the reaction was determined as follows: The reaction mixture containing a 10-fold excess of Fe(II) over [complex] was acidified with excess $HClO_4$ (1 mol dm^{-3}) after completion of reaction and passed through a Dowex 50WX8 resin (H^+-form). Cobalt(II) and Fe(III) which eluted out were determined in the presence of Cl^- and NCS^- respectively[11].

The rate constants for the Fe(II) reduction of *trans*-$[Co(dmgH)_2(N_3)_2]^-$ at $[H^+] = 0.10$ mol dm^{-3} in various water-alcohol mixtures containing alcohol in the mol fraction range of 0.05 to 0.50 are presented in Table 1. At $[H^+]$ used in this work, the complex should be in the form *trans*-$Co(dmgH)(dmgH_2)(N_3)_2$ (ref. 2).

The overall solvent effect (Table 1) may be analysed in terms of the following factors: (i) formation of species such as $Fe(H_2O)_{6-n}(ROH)_n^{2+}$ and the effect of coordinated ROH on the ease of formation of Fe(III), i.e. the redox potential of Fe^{2+} and (ii) effect of solvent on the equilibrium for precursor complex formation.

Considering the formation of $Fe(H_2O)_{6-n}(ROH)_n^{2+}$ and its oxidation, it is known that in the presence of methanol, Fe(II) is easily oxidised to Fe(III) forming the species $Fe(H_2O)_n(ROH)_n^{3+}$ in water-methanol mixtures. The ease of formation of Fe(III) in the various alcohol-water mixtures should increase from methanol to 2-methyl-2-

Table 1—Rate Constants for Fe(II) Reduction of $Co(dmgH)_2(N_3)_2^-$ in Different Water-Alcohol Mixtures

$[Co(III)] = 4.06 \times 10^{-4}$ mol dm^{-3}; $[Fe(II)] = 4.03 \times 10^{-3}$ mol dm^{-3} $I = 1.0$ mol dm^{-3} ($LiClO_4$); $[H^+] = 0.10$ mol dm^{-3}; Temp. = 30 ± 0.1°C

Mol fr of alcohol	*k* (dm^3 mol^{-1} s^{-1})	Mol fr of alcohol	*k* (dm^3 mol^{-1} s^{-1})
Methanol		Ethanol	
0.05	0.10	0.06	0.15
0.10	0.15	0.11	0.21
0.20	0.24	0.21	0.32
0.31	0.38	0.30	0.43
0.40	0.48	0.40	0.61
0.51	0.76	0.50	1.12
Propan-2-ol		2-Methyl-propan-2-ol	
0.06	0.20	0.05	0.36
0.12	0.30	0.11	0.45
0.21	0.42	0.21	0.69
0.33	0.66	0.31	1.09
0.40	0.98	0.40	1.47
0.50	1.50		

propanol in the series of alcohols studied. This is a reasonable assumption, since [alcohol] in the primary coordination sphere of Fe(II) would increase from methanol to 2-methyl-2-propanol, due to a relatively greater repulsion of the latter from the bulk aqueous phase[13].

The solvent is expected to make a significant contribution to the ease of formation of the precursor complex between Fe(II) and the substrate complex. The solvent dielectric constant should decrease with increasing mol fraction of alcohol and with increasing number of carbon atoms in the alcohol molecule. Decreasing dielectric constant of the solvent mixture (i.e. increase in mol fraction of alcohol) should favour the precursor complex formation in a preequilibrium step if the reactants are oppositely charged but not when reactants are like-charged. Hence the effect of solvent is explained as due to the presence of species $Fe(ROH)_x\ (H_2O)^{2+}_{n-x}$. If the complex were considered as an anion, the Fuoss equation[14] could be used to calculate the ion-pair association constants (K_{ip}) as a function of solvent dielectric constant in different solvent mixtures. This was done using a value of 3.45Å (ref. 15) for the radius of the complex and 0.83Å for the radius of Fe^{2+}_{aq} (ref. 16). The dielectric constants were obtained literature[17]. It was found that the slope of the log k versus log K_{ip} plot decreased in the order: CH_3OH (0.8) > C_2H_5OH (0.5) > *i*-PrOH (0.38) ~ 2-Me-2-PrOH (0.37). In the light of Ohashi's observations that the same solvent order is observed for a cation-cation reaction, one should expect the slopes to increase from MeOH to 2-Me-2-PrOH, as ion-association effects should complement the effects due to the $[Fe(ROH)(H_2O)]^{2+}$ species. It appears, therefore, that the solvent effects should be attributable to the species $Fe(ROH)_{n-x}(H_2O)^{2+}_x$ and that the complex is a neutral species $[Co(dmgH)(dmgH_2)(N_3)_2]$ obviating the possibility of ion-association. However, Fe^{2+} reduction of the complex cation *cis*-$[Co(Cl)(NH_2CH_2CH_2OH)(en)_2]^{2+}$ in alcohol-water mixtures indicated a behaviour[5] similar to that observed in the present work.

It may be concluded that the solvent effects on the rate of reduction may be understood mainly in terms of the influence of solvent on the inner sphere structure of Fe(II) in such media and on the equilibrium constant for precursor complex formation between the substrate complex and Fe(II).

References

1 Balasubramanian P N & Vijayaraghavan V R, *Inorg Chim Acta*, **38** (1980) 49.

2 Balasubramanian P N & Vijayaraghavan V R, *Inorg Chim Acta*, **53** (1981) L209.

3 Arunachalam M K, Balasubramanian P N & Vijayaraghavan V R, *J inorg nucl Chem*, **43** (1981) 753.

4 Balasubramanian P N & Vijayaraghavan V R, *Indian J Chem*, **20A** (1981) 892.

5 Ohashi K, Amano T & Yamamoto K, *inorg Chem*, **16** (1977) 3364.

6 Matthews B A & Watts D W, *Inorg Chim Acta*, **11** (1974) 127.

7 Matthews B A & Watts D W, *Aust J Chem*, **29** (1976) 97.

8 Matthews B A, Turner J V & Watts D W, *Aust J Chem*, **29** (1976) 551.

9 Vijayaraghavan V R, Thillaichidambaram N, Raghavan A & Santappa M, *J Indian chem Soc*, **55** (1978) 532.

10 Wada G & Reynolds W, *Inorg Chem*, **5** (1966) 1354.

11 Kitson R E, *Analyt Chem*, **22** (1950) 664.

12 Ohashi K, Yamamoto K, Hirako J & Kurimura Y, *Bull Chem Soc Japan*, **45** (1972) 1712.

13 Watts D W, *Physical chemistry of organic solvent systems*, edited by A K Covington & T Dickinson, (Plenum Press, New York) 1973, Chap. 5.

14 Fuoss R M, *J Am chem Soc*, **80** (1958) 5059.

15 Chakravorty A, *Coord Chem Rev*, **13** (1974) 1.

16 *Advanced inorganic chemistry*, edited by F Albert Cotton & G Wilkinson (John Wiley, New York) 1980, Chapter 1 pp. 14.

17 Shedlovsky T & Spivey H O, *J phys Chem*, **71** (1967) 2165.

Indian Journal of Chemistry
Vol. 27A, May 1988, pp. 436-437

Kinetics & Mechanism of Oxidation of Diphenyl Sulphoxide by N-Chloro-3-methyl-2,6-diphenylpiperidin-4-one in Perchloric Acid Medium

K GANAPATHY* & K IYANAR
Department of Chemistry, Annamalai University,
Annamalainagar 608 002

Received 1 *May* 1987; *revised and accepted* 29 *September* 1987

The title reaction in the presence of perchloric acid in 75% (v/v) ethanol-water mixture at 30°C is of a total second order, being first order each in [oxidant] and [substrate]. Activation parameters have been evaluated. The results are discussed in terms of a mechanism involving a rate-determining formation of an intermediate between protonated oxidant and sulphur of the sulphoxide.

The kinetics and mechanisms of oxidation of sulphoxides to sulphones by different oxidants have been investigated by several groups[1-4]. The oxidant, N-chloro-3-methyl-2,6-diphenylpiperidin-4-one (NCP) has not been used so far for such kinetic investigations and hence the present investigation. The reaction has been carried out in perchloric acid medium, since in other media oxidation of sulphoxide to sulphone is very slow[5,6] in comparison to that of sulphide.

Kinetic runs were carried out in 75% (v/v) ethanol-water mixture under pseudo-first order conditions at the desired temperature which could be maintained with an accuracy of ±0.01°C. The rate of disappearance of oxidant was followed by the iodometric estimation of the unreacted oxidant as described by Kolthof and Carr (see ref. 6 for details).

The linearity of the rate profiles indicates that the rate of disappearance of oxidant follows first order rate law in each kinetic run. Pseudo-first order rate constants were evaluated from the gradients of the linear plots by the method of least squares using a computer IBM 1130 systems. The stoichiometry of the reaction comes out to be 1:1, i.e. 1 mol of oxidant consumed 1 mol of substrate to give diphenyl sulphone as the product which was identified by direct comparison (m.p. and m.m.p. 126°) with an authentic sample.

$$C_6H_5SOC_6H_5 + \rangle N-Cl + H_2O \rightarrow C_6H_5SO_2C_6H_5 + \rangle N-H + H^+ + Cl^-$$

The results of the kinetic runs reveal the following characteristic features.

(i) The reaction was first order in NCP as evidenced by the linearity of log titre versus time plots and the non-invariance of the rate constants at different [NCP].

(ii) The pseudo-first order constants increased with increase in [substrate]. The plots of log k_1 versus log [substrate] were linear with slope of unity indicating first order in [substrate].

(iii) Increase in ionic strength of the medium from 0.1040 to 0.3885 mol dm^{-3} ($NaClO_4$) increased the rate constants from 2.74×10^{-4} s^{-1} to 5.72×10^{-4} s^{-1} showing participation of charged particles in the rate-determining step.

(iv) At fixed [substrate] and [oxidant] and temperature the rate constant increased with increase in $[H^+]$, the order being one as revealed by the unit slope of linear plot of log k_1 versus log $[H^+]$.

(v) The rate constants increased with increase in water content of the reaction medium. For example in ethanol-water mixtures containing 60, 65, 70, 75 and 80% (v/v) ethanol, the rate constants were 3.86×10^{-4}, 2.88×10^{-4}, 2.26×10^{-4}, 1.75×10^{-4} and 1.63×10^{-4} s^{-1} respectively. The increase in the rate constant with increase in the dielectric constant of the medium may probably be due to the ion-dipole interaction of the reactants.

The kinetic runs were repeated at four different temperatures 25°, 30°, 35° and 40°C under the conditions: [substrate] $= 1.012 \times 10^{-2}$ mol dm^{-3}, [oxidant] $= 1.055 \times 10^{-3}$ mol dm^{-3}, $[H^+] = 6.0 \times 10^{-2}$ mol dm^{-3}. The rate constants (k_2) calculated were 1.01×10^{-2}, 1.73×10^{-2}, 2.71×10^{-2} and 4.09×10^{-2} dm^3 mol^{-1} s^{-1}, respectively. The enthalpy and entropy of activation were calculated and found to be 69.59 kJ mol^{-1} and -49.40 JK^{-1} mol^{-1} respectively by linear least squares method of a linear plot of log k_2/T versus $1/T$ of the logarithmic form of Eyring's equation.

Mechanism

In acid medium, the oxidant (NCP) is in equilibrium with its protonated form which is found to be an effective oxidising species[6-10]. The increase in the rate constant with increase in $[H^+]$ also confirms the existence of such an equilibrium.

Since the reaction is first order each in [oxidant], [substrate] and $[H^+]$ ion, it confirms the rate-determining electrophilic attack of the protonated NCP at the sulphur of the sulphoxide to form sulphone. The intermediate may decompose to give the sulphone by the attack of water.

The derived rate law is given below:

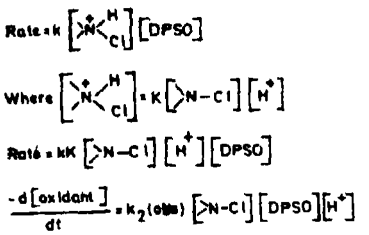

$$\text{Rate} = k\left[>\overset{+}{N}<^{H}_{Cl}\right][\text{DPSO}]$$

$$\text{Where } \left[>\overset{+}{N}<^{H}_{Cl}\right] = K[>N{-}Cl][H^+]$$

$$\text{Rate} = kK[>N{-}Cl][H^+][\text{DPSO}]$$

$$\frac{-d[\text{oxidant}]}{dt} = k_{2(\text{obs})}[>N{-}Cl][\text{DPSO}][H^+]$$

One of the authors (KI) is thankful to the UGC, New Delhi, for the award of a research fellowship.

References

1 Srinivasan C, Pandarakutty Jegatheesan P & Arumugam N, *Indian J Chem*, **25A** (1986) 678.

2 Mahadevappa D S, Katgeri S N & Naidu H M K, *Indian J Chem*, **20A** (1981) 665.

3 Srinivasan C, Venkataswamy R & Rajagopal S, *Indian J Chem*, **20A** (1981) 505.

4 Durgadevi R, *M. Phil Thesis*, Annamalai University (1985).

5 Howard H & Levitt L S, *J Am chem Soc*, **75** (1973) 6171.,

6 Ganapathy K & Iyanar K, *J Indian chem Soc*, **62** (1985) 483.

7 Ganapathy K & Vijayan B, *J Indian chem Soc*, **55** (1978) 957.

8 Ganapathy K, Kumarachakravarthy T & Vijayan B, *Indian J Chem*, **19B** (1980) 76.

9 Ganapathy K & Vijayan B, *Indian J Chem*, **21B** (1982) 1136.

10 Ganapathy K & Kabilan S, *Indian J Chem*, **25A** (1986) 681.

Indian Journal of Chemistry
Vol. 27A, May 1988, p. 438

Kinetics & Mechanism of Oxidation of *m*-Cresol by Osmium Tetroxide in Alkaline Medium

A K SINGH*, SANGEETA SAXENA, MADHU SAXENA, RANJANA GUPTA & R K MISHRA

Chemistry Department, University of Allahabad, Allahabad

Received 10 *June* 1987; *revised* 31 *August* 1987; *accepted* 15 *October* 1987

The title reaction is first order each in $[OsO_4]$ and [substrate]. First order dependence in OH at low $[OH^-]$ becomes zero at higher $[OH^-]$. Kinetic results indicate the formation of a complex between the substrate and reactive species of Os(VIII) i.e. $[OsO_4(OH)_2]^{2-}$ which disproportionates in a slow step into the products and Os(VI) species.

Although osmium tetroxide has been extensively used as a catalyst, it has been seldom used as an oxidant. Silverton[1] has reported the oxidation of 4,5-dihydrobenzophrine by osmium tetroxide. The title investigation is an extention of our earlier work[2,3] on the application of OsO_4 as an oxidising agent.

The standard solution of OsO_4 was prepared by dissolving the sample (Johnson Matthey) in KOH solution. Standard solution of *m*-cresol was prepared by weight. The progress of reaction was followed spectrophotometrically at 420 nm.

Kinetic results can be summarised as follows:

(i) Order in $[OsO_4]$ is unity as revealed by the constancy in k_1 values (both graphical as well as calculated) at varying $[OsO_4]$. For example, under the conditions, [*m*-cresol] = 1.2×10^{-2} mol dm^{-3}, [NaOH] = 1.6×10^{-2} mol dm^{-3} at 32.7°C the value of $k_1 \times 10^3$ s^{-1} remained constant at 3.61 ± 0.30 when $[OsO_4] \times 10^3$ was varied from 1.2 to 4.2 mol dm^{-3}.

(ii) Order in *m*-cresol is one as revealed by the constancy of k_1/[*m*-cresol] values at varying [*m*-cresol]. Under the conditions $[OsO_4] = 1.25 \times 10^{-3}$ mol dm^{-3}, [NaOH] = 2.5×10^{-2} mol dm^{-3} and temp. = 31.7°C, k_1/[*m*-cresol] remained constant (0.27 ± 0.01) when [*m*-cresol] $\times 10^3$ was varied from 4 to 20 mol dm^{-3}.

(iii) Order in $[OH^-]$ changed from unity at low $[OH^-]$ to zero at high $[OH^-]$.

(iv) There is no change in reaction rate by varying ionic strength of medium.

(v) Activation parameters have been calculated (temp. = 35.3°C) to be $E_a = 71.65$ $kJmol^{-1}$, $A = 9.49 \times 10^9$ mol^{-1} dm^{-3} s^{-1}, $\Delta G^{\ddagger} = 67.58$ $kJmol^{-1}$, $\Delta S^{\ddagger} = 4.96$ JK^{-1} mol^{-1}.

It is reported[4] that OsO_4 in alkaline medium exists mainly as $[OsO_4(OH)_2]^{2-}$ species.

Based on the kinetic results the mechanism in Scheme 1 has been proposed.

$$[OsO_4(OH)H_2O]^{1-} + OH^- \overset{K_1}{\rightleftharpoons} [OsO_4(OH)_2]^{2-} + H_2O \quad \ldots (1)$$

$$CH_3C_6H_4OH + [OsO_4(OH)_2]^{2-} \overset{K_2}{\rightleftharpoons} [CH_3C_6H_4O-OsO_3(OH)_3]^{2-} \quad \ldots (2)$$

$$[CH_3C_6H_4O-OsO_3(OH)_3]^{2-} \xrightarrow[\text{slow}]{k} CH_3C_6H_4O + [OsO_2(OH)_4]^{2-} \quad \ldots (3)$$

Scheme 1

Scheme 1 leads to rate law (4)

$$-\frac{d[Os(VIII)]}{dt} = \frac{2kK_1K_2[Os(VIII)]_T[S][OH^-]}{1+K_1[OH^-]\{1+K_2[S]\}} \quad \ldots (4)$$

since $1 \gg K_2[S]$, Eq. (4) reduces to Eq. (5)

$$\frac{1}{k_1} = \frac{1}{[S]}\left\{\frac{1}{2kK_1K_2[OH^-]} + \frac{1}{2kK_2}\right\} \quad \ldots (5)$$

$$\text{where } k_1 = -\frac{d[Os(VIII)]}{dt} / [Os(VIII)]_T$$

The rate equation (5) predicts that the plot of $1/k_1$ versus $1/[OH^-]$ should be linear with a positive intercept. It is found to be so and from the slope value of kK_1K_2 (13.54) and from intercept the value of kK_2 (0.416) are calculated.

Similarly a plot of $1/k_1$ and $1/[S]$ is linear passing through origin. From the slope the value of kK_2 has been calculated to be 0.422.

References

1 Silverton, *Tetrahedron Lett*, **19** (1976) 1557.
2 Singh B, Singh M B, Singh A K & Singh A P, *Tetrahedron*, **42** (1986) 715.
3 A K Singh, A K Sisodia, Sangeeta Saxena & Madhu Saxena, *Indian J Chem*, **26A** (1987) 600-602.
4 Griffith, W P, *Quart Rev*, **19** (1665) 254.

Indian Journal of Chemistry
Vol. 27A, May 1988, pp. 439-441

Effect of Ion-pairing on Solvolytic Aquation of Bromopentaamminecobalt (III) Ion in Presence of Oxalate Anion

A PANDA
Department of Chemistry, G.M. College, Sambalpur 768 004
and
N C NAIK*†
Principal, Bonaigarh College, Bonaigarh 770 038

Received 25 *March* 1987; *revised and accepted* 29 *June* 1987

The rate of solvolytic aquation of bromopentaamminecobalt (III) ion has been measured in aqueous medium in the presence of exalate anion at 40°, 45° and 50°C. The rate accelerating effect of oxalate has been attributed to the formation of more labile bromopentaamminecobalt (III)-oxalate ion-pair. The rate and association constants have been calculated. The activation parameters of each of the pathways and the thermodynamic parameters for the ion-association process have been evaluated and discussed.

We have already reported[1] that the rate of solvolytic aquation of bromopentaamminecobalt (III) ion is significantly accelerated in the presence of sulphate anion. The rate-accelerating influence has been ascribed to more labile bromopentaamminecobalt (III)-sulphate ion-pair. As a sequel to this, we report herein the result of study on rate-accelerating action of oxalate anion on acid hydrolysis reaction of bromopentaamminecobalt (III).

Bromo[2,3]-, aquo[4]-, and oxalato[5,6]-pentaamminecobalt (III) perchlorates were prepared and purified by literature methods and their purity was checked by elemental analyses and by measuring molar absorptivities which were in excellent agreement with the reported values[4,7-10].

Sodium salts of oxalic acid (NaHOx, Na_2Ox) were prepared in the laboratory. Sodium perchlorate (extra pure) was used for adjusting ionic strength. Doubly distilled water was used for preparing all solutions.

The rate of aquation and the formation of the oxalato complex were followed by methods reported earlier[1].

The pseudo-first order rate constants for the release of bromide ion from the complex were calculated from the plots of $\log(V_\infty - V_t)$ versus time (t) where V_t and V_∞ are the volumes of silver nitrate consumed after time 't' and after completion of the reaction respectively. The results at 40°, 45° and 50°C are recorded in Table 1.

The free complex ion reacts with the added oxalate anion and produces ion-pairs of the type, $\{Co(NH_3)_5Br^{2+}, HOx^-\}$ and $\{Co(NH_3)_5Br^{2+}, Ox^{2-}\}^+$. Hence the observed rate constant would be a composite term consisting of acid hydrolysis rate constant of the free complex ion and the product of aquation rate constant of the ion-pair and its equilibrium constant. The data were analysed in the same manner as described in our earlier communication[1] taking into account the observations reported by Wyatt and Davies[11] and Monk *et al.*[12] and assuming the reactivities of the H-oxalate ion-pair and the free complex to be the same. Taking pK $(HOx^-) = 4.27$ (ref. 13), pH value of reaction was calculated to be 5.67 (Table 1). Under this condition the base hydrolysis of the complex[14] does not contribute significantly towards the overall rate and as such this path of bromide release has been neglected. Equations (1-3) were utilised to calculated the rate constants and the association constants of the ion-pair by the method of successive approximations.

$$\text{Rate} = \frac{-dC}{dt} = k_{obs} \times C = k_1 [C_p^{2+}] + k_{ip}[C_p O_x] \qquad (1)$$

$$\frac{1}{k_{obs} - k_1} = \frac{1}{k_{ip} - k_1} + \frac{1}{(k_{ip} - k_1) K_{ip}[O_x^{2-}]_f} \qquad (2)$$

$$[O_x^{2-}]_f = \frac{[O_x^{2-}]_T}{1 + \frac{[HO_x^-]_t}{[O_x^{2-}]_t} + \frac{K_{ip}C}{1 + K_{ip}[O_x^{2-}]_f} + K_{As}[Na^+]_T} \qquad (3)$$

where $[C_p^{2+}] = [C_p^{2+}]_f + [C_pHOx^+]$, C = total initial [complex], k_1 = acid hydrolysis rate constant of the free complex ion, $[C_p^{2+}]_f$ = free [complex ion], $[C_pOx]$ = [ion-pair] of free complex ion with oxalate ion, $[C_pHOx^+]$ = [ion-pair] of free complex ion with the bioxalate ion, k_{ip} = acid hydrolysis rate constant of the ion-pair, C_pOx, K_{ip} = association constant of the oxalate ion-pair, $[Ox^{2-}]_f$ = free [oxalate ion], $[Ox^{2-}]_T = [Ox^{2-}]_t + [HOx^-]_t$, $[Ox^{2-}]_T$ = total initial [oxalate], $[Ox^{2-}]_t$, $[HOx^-]_t$ = total initial concentrations of the added oxalate and bioxalate ions respectively in the absence of the complex, and K_{As} = ion-pair association constant involving ions $(Na^+)_f$ and $(Ox^{2-})_f$. The values of K_{As} were calculated from the available

---

†Present address: Deputy Registrar, Utkal University, Bhubaneswar 751004

Table 1 — Acid Hydrolysis of $[Co(NH_3)_5Br](ClO_4)_2$ in Aqueous Solution in Presence of Oxalate (Ox^{2-}) Ion

[complex] = 5×10^{-3} mol dm^{-3}; ionic strength = 0.3 mol dm^{-3}

$[HClO_4] \times 10^3$ (mol dm^{-3})	$[HOx^-] \times 10^3$ (mol dm^{-3})	$[Ox^{2-}] \times 10^3$ (mol dm^{-3})	$k_{obs} \times 10^5 (s^{-1})$[(a)]			$k_{ip} \times 10^5 (s^{-1})$		
			40°	45°	50°C	40°	45°	50°C
10	—	—	4.40	8.10	14.70	—	—	—
—	0.2	5	4.78	8.56	15.55	7.61	12.59	23.28
—	0.4	10	5.05	8.96	16.18	7.53	12.71	23.27
—	0.8	20	5.56	9.60	17.40	7.65	12.71	23.27
—	1.2	30	5.87	—	—	7.61	—	—
						(30)	(26.1)	(23)

(a) The observed rate constants are accurate upto ± 1%. K_{ip} values are given in parentheses.

data[15,16]. The k_{ip} and K_{ip} values are collected in Table 1.

The possible pathways for formation of $Co(NH_3)_5H_2O^{3+}$, $[Co(NH_3)_5H_2O, Ox]^+$ and $[Co(NH_3)_5Ox]^+$ have been delineated in Scheme 1.

The release of bromide ion, according to Scheme 1 takes place through three pathways, viz k_1, k_{ip}' and $k^0_{3(ip)} \cdot k^0_{3(ip)}$ was calculated in the same manner as reported previously[1,17], using the Eqs (4) and (5)

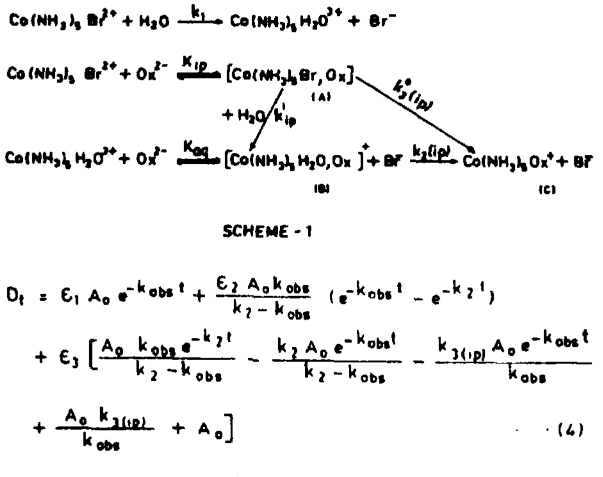

SCHEME - 1

$$D_t = \varepsilon_1 A_0 e^{-k_{obs} t} + \frac{\varepsilon_2 A_0 k_{obs}}{k_2 - k_{obs}} (e^{-k_{obs} t} - e^{-k_2 t}) + \varepsilon_3 \left[\frac{A_0 k_{obs} e^{-k_2 t}}{k_2 - k_{obs}} - \frac{k_2 A_0 e^{-k_{obs} t}}{k_2 - k_{obs}} - \frac{k_{3(ip)} A_0 e^{-k_{obs} t}}{k_{obs}} + \frac{A_0 k_{3(ip)}}{k_{obs}} + A_0 \right] \quad \ldots (4)$$

$$k_{3(ip)} = \frac{k^0_{3(ip)} K_{ip} [O_x^{2-}]_t}{1 + K_{ip} [O_x^{2-}]_t} \quad \ldots (5)$$

In Eq. (4) D_t is the absorbance of the reaction mixture at time t in a cell of 1 cm path length, and ε_1, ε_2 and ε_3 represent the molar absorptivities of the bromo-, aquo-, and oxalato-pentaamminecobalt (III) complexes respectively. A_0 refers to the concentration of $Co(NH_3)_5Br^{2+}$ at zero time and other terms have their usual meaning[1]. The k_2, k_{ip}, $k_{3(ip)}$ and $k^0_{3(ip)}$ values are given in Table 2. $\Delta G^{\neq}$ at 40°C (kJ mol^{-1}), $\Delta H^{\neq}$ (kJ mol^{-1}) and $\Delta S^{\neq}$ (JK^{-1}mol^{-1}) for the k_1, k_{ip} and $k^0_{3(ip)}$ paths have been estimated and are respectively as follows; 102.9; 98.3; −14.6; 101.3, 77.8, −75.3; 110.5, 92.5, −58.6. Values of ΔG (40°C) (kJ mol^{-1}), ΔH (kJ mol^{-1}) and ΔS (JK^{-1}mol^{-1}) for the ion-association process are found to be −8.8, −24.9 and −51.5 respectively.

Table 2 — Rate constants for k_{ip}, k_2, $k_{3(ip)}$ and $k^0_{3(ip)}$ Paths of Reaction

Pathway	Temp (°C)		
	40	45	50
$k_{ip} \times 10^5 (s^{-1})$	7.60 ± 0.05	12.67 ± 0.04	23.25 ± 0.03
$k_2 \times 10^4 (s^{-1})$	1.13	2.15	4.00
$k_{3(ip)} \times 10^6 (s^{-1})$ at $[Ox^{2-}] \times 10^3$ mol dm^{-3}			
2.5	—	1.22 ± 0.10	2.95 ± 0.22
5	1.12 ± 0.10	1.75 ± 0.12	3.98 ± 0.28
10	1.48 ± 0.08	2.10 ± 0.15	4.62 ± 0.28
15	1.63 ± 0.12	—	—
$k^0_{3(ip)} \times 10^6 (s^{-1})$	2.12 ± 0.05	2.94 ± 0.08	5.88 ± 0.30

The results clearly reveal that the rate of aquation of complex is markedly accelerated in the presence of oxalate ion. The rate-accelerating influence has been ascribed to the formation of more labile bromopentaamminecobalt (III)-oxalate ion-pair. The rate constant increases with increase in added [oxalate ion] and levels off at $[Ox^{2-}] = 0.03$ mol. The rate constants of the ion-pair bear no correlation with the basicity and size of the dicarboxylate ions[18] [$k_{ip} \times 10^6 s^{-1}$ ($K_{HL^-} \times 10^5$); 16.03 (26.7), 14.98 (0.845), 16.21 (1.03) at 25°C for L^{2-} = oxalate, malonate and succinate respectively].

A predominantly electrostatic process is thus visualised to account for the greater reactivity of the ion-pair with a dissociative mechanistic pathway. This would result in a transition state having considerable degree of charge separation, leading to loss of activation entropy. The entropy of activation for the aquation of the ion-pair is found to be negative and low which according to Tobe[19], is indicative of a dissociative pathway proceeding possibly through an incipient tetragonal pyramid intermediate.

The extent of bromide release through $k^0_{3(ip)}$ path is limited to 4% of the minimum of total bromide release via k_1, k_{ip} and $k^0_{3(ip)}$ pathways taken together. The rate constant for the formation of oxalatopentaamminecobalt (III) complex through $k^0_{3(ip)}$ path is calculated to be $3.3 \times 10^7 s^{-1}$ at 25°C which is only 2.1% of the k_{ip} value at the same temperature. Thus it is reasonable to assume that the bromide release takes place predominantly through the formation of the aquo complex. At 350 nm, the molar absorptivities of bromo-, aquo-, and oxalato-pentaamminecobalt (III) complexes are found 232, 43 and 160 $dm^3 mol^{-1} cm^{-1}$ respectively. The minima in the absorbance versus time plots[1,20] lead us to believe that the formation of the oxalatopentaamminecobalt (III) complex takes place predominantly through the anation of the intermediate aquo-oxalate ion-pair (at 25°C, $k_{2(ip)} = 1.42 \times 10^{-6} s^{-1}$ and $k^0_{3(ip)} = 0.33 \times 10^{-6} s^{-1}$). This gains further support from the excellent agreement between the experimental absorbance and that calculated on the basis of Scheme 1.

The outer sphere association of bromopentaamminecobalt (III) with oxalate is exothermic and is associated with the negative entropy change. This is expected considering the loss of translational entropy in the process.

The authors are thankful to Prof R K Nanda and Dr A C Dash of the Department of Chemistry, Utkal University for helpful discussions.

References

1 Panda A & Naik N C, *Indian J Chem*, **25A** (1986) 858.

2 *Inorganic synthesis*, **4** (1953) 171.

3 Chan S C, Hui K Y, Miller J & Tsong N S, *J chem Soc*, (1965) 3207.

4 Splinter R C, Herris S J & Tobias R S, *Inorg Chem*, **7** (1968) 898.

5 Saffir P & Taube H, *J Am Chem Soc* **82** (1960) 13.

6 Tuig I F, Kelm H & Harris G M, *Inorg Chem*, **5** (1966) 696.

7 Linck R G, *Inorg Chem*, **9** (1970) 2529.

8 Buckingham D A, Olsen I I, Sargeson A M & Satrapa H, *Inorg Chem*, **6** (1967) 1027.

9 Andrade C & Taube H, *Inorg Chem*, **5** (1966) 1087.

10 Naik N C & Nanda R K, *Indian J Chem*, **19A** (1980) 113.

11 Wyatt P H & Davies C W, *Trans Faraday Soc*, **45** (1949) 778

12 Campbell M B M, Wendt M R & Monk C B, *J chem Soc*, (Dalton) (1972) 1714

13 Eldik R V & Harris G M, *Inorg Chem*, **14** (1975) 10.

14 Basolo F & Pearson R G, *Mechanisms of inorganic reactions*, (Wiley, New York), 1967, pp 180

15 Archer D W, East D A & Monk C B, *J chem Soc*, (1965) 720.

16 Izatt R M, Eatough D, Christensen J J & Bartholomew C H, *J chem Soc*, (1969) 45

17 Naik N C & Nanda R K, *J inorg nucl Chem*, **36** (1974) 3793.

18 Panda A, Ph.D. Thesis, Sambalpur University (1983).

19 Tobe M L, *Inorg Chem*, **6** (1968) 1261.

20 Moore J W & Pearson R G, *Inorg Chem*, 3 (1964) 1334.

Indian Journal of Chemistry
Vol. 27A, May 1988, pp. 442-443

Kinetics of Chlorination of Some Substituted Piperidin-4-ones by 1-Chlorobenzotriazole

R GURUMURTHY* & E ARUNANTHI

Department of Chemistry, Annamalai University,
Annamalainagar 608 002

Received 18 *May* 1987; *revised* 5 *October* 1987; *accepted* 28 *October* 1987

The title halogenation reaction is first order each in the substrate and the chlorinating agent in 30% aq. acetic acid at 303 K. While increase in $[H^+]$ decreases the rate, the rates are not much affected by the change in dielectric constant and by added salts. It is likely that the reaction occurs between two neutral species.

Table 1—Effect of Varying [CBT], [Ketone] on the Reaction Rate

[Ketone] = 0.01 mol dm^{-3}; [CBT] = 0.001 mol dm^{-3}; [HOAC] = 30% (v/v); temp = 30°C

[Ketone] (mol dm^{-3})	[CBT] (mol dm^{-3})	$k \times 10^4$, (s^{-1})
0.01	0.0007	8.57
0.01	0.0008	8.55
0.01	0.0009	8.56
0.01	0.0011	8.57
0.005	0.001	4.22
0.0075	0.001	6.23
0.0125	0.001	9.91
0.02	0.001	15.90

Table 2—Effect of Varying [$HClO_4$], [$NaClO_4$] and Dielectric Constant on Reaction Rate

[Ketone] = 0.01 mol dm ^{3}[CBT] = 0.001 mol dm^{-3}; temp 30°

[$HClO_4$] (mol dm^{-3})	[$NaClO_4$] (mol dm^{-3})	Acetic acid %	$k \times 10^4$ (s^{-1})
0.025	0.075	30	4.17
0.05	0.05	30	2.18
0.075	0.025	30	1.54
0.1	0.0	30	1.08
—	0.08	30	9.52
—	0.16	30	9.90
—	0.24	30	10.50
—	0.32	30	10.40
—	—	20	8.41
—	—	40	8.46
—	—	50	8.52
—	—	60	8.38

The earlier work[1-3] from our laboratory reported the kinetics and mechanism of chlorination of organic substrates by 1-chlorobenzotriazole(CBT). The title investigation is in continuation of this earlier work.

1-Chlorobenzotriazole(CBT) and the ketones, viz. N-methyl-2,3,5,6-tetraphenyl-(I)-, N-methyl-2,6-diphenyl-(II)-, N,3-dimethyl-2,6-diphenyl-(III)-, N,3,3-trimethyl-2,6,-diphenyl-(IV)- and N,3,5-trimethyl-2,6-diphenyl(V)-piperidin-4-ones were prepared by literature methods[4-6]. The reactions were followed iodometrically under pseudo-first order conditions ([ketone] > > [CBT]). The stoichiometric runs indicated that one mol of ketone consumed one mol of CBT to give α-haloketone and benzotriazole.

The rate constants at varying [CBT] and [substrate], given in Table 1, show that the reaction is first order each in the reactants. The results on the effect of change of ionic strength, dielectric constant and $[H^+]$ on the reaction rate are given in Table 2. The various thermodynamic parameters calculated for the chlorination (followed at four temperatures) of the representative ketone(III) are: $E_a = 83.44$ kJ mol^{-1}; $\Delta H^{\ddagger} = 80.78$ kJ mol^{-1}; $\Delta S^{\ddagger} = -37.36$ JK^{-1} mol^{-1}.

All these observations indicate that the chlorination does not proceed by an ion-dipole reaction in the rate-limiting step, but occurs between two neutral species. The rate expression should be of the form: Rate = k_1 [substrate] [oxidant] and that the reaction is simple and straightforward involving CBT and piperidone[7].

The rate constants of chlorination of ketones (I-V) in 30% acetic acid are: 19.1×10^{-4}, 11.2×10^{-4}, 8.51×10^{-4}, 3.61×10^{-4} and 3.35×10^{-4} s^{-1} respectively. All the ketones investigated in this study have been shown to exist in simple chair conformation[8] with equatorial alkyl group(s) and further chlorination occurs by the displacement of hydrogenes alpha to the carbonyl group because of stereo-electronic reasons.

Eventhough the electron density of both the H atoms at 3,5-positions is much less due to the inductive effect of the carbonyl function at position-4, the H atom at each of the equatorial position is easily approached by the molecule of CBT. Thus when 3 and 5 positions are being successively occupied by methyl groups there is striking retardation in the rate. Increasing substitution of the active H atoms by alkyl groups not only increases the steric hindrance to the attacking species but also enhances the shift of electron density towards the ring. The presence of electron releasing methyl group thus opposes the buildup of a partial positive charge on the hydrogen and counteracts the electron-withdrawing effect of the carbonyl group. This effect may be more significant when there are two methyl groups at the same carbon of the ring.

Thus N-methyl-2,6-diphenylpiperidin-4-one(II), which has two equatorial H atoms that can be attacked, undergoes chlorination at a much faster rate as compared to other ketones. On the other hand, in N,3,5-trimethyl-2,6-diphenylpiperidin-4-one(V) both the bulky methyl groups at 3 and 5 positions are equatorially placed, the attacking CBT has to approach only the axial hydrogen atoms. Because of the steric hindrance the reaction is expected to be the slowest and this is found to be so.

The much faster rate of chlorination of N-methyl-2,3,5,6-tetraphenylpiperidin-4-one(I) indicates that in this compound the electronic effect outweighs the steric effect.

References

1 Ganapathy K, Gurumurthy R, Mohan N & Sivagnanam G, *Acta Ciencia Indica*, **12C** (1986) 175.

2 Ganapathy K, Gurumurthy R, Mohan N & Sivagnanam G, *Indian J Chem*, **25A** (1986) 478.

3 Ganapathy K, Gurumurthy R, Mohan N & Sivagnanam G, *Mh Chem*, **330** (1986) 1266.

4 Rees C W & Storr R C, *Chem Commun*, (1969) 1474.

5 Baliah V & Noller C, *J Am chem Soc*, **70** (1948) 3853.

6 Chandrasekaran J, Ph D Thesis, Annamalai University, 1964.

7 Arunandhi M, Phil Thesis, Annamalai University, 1987.

8 Balasubramanian M & Padma N, *Tetrahedron*, **19** (1966) 2135.

Indian Journal of Chemistry
Vol. 27A, May 1988, pp. 444-446

^{13}C NMR Studies of Thiocyanato Complexes

M T H TARAFDER* & KANIZ FATEMA
Department of Chemistry, University of Rajshahi, Rajshahi, Bangladesh

Received 2 *March* 1987; *revised and accepted* 23 *July* 1987

Several thiocyanato complexes of nickel(II), zinc(II), palladium(II) and cadmium(II) containing auxiliary ligands PPh_3, $OPPh_3$, C_5H_5N and C_5H_5NO have been synthesized. ^{13}C NMR spectra of the complexes reveal the relative acceptor properties of different metal ions. The study indicates that the heavier metals in a group are always weaker acceptors.

The mode of coordination of SCN^- moiety has been investigated by different workers[1-10] on the basis of IR data. However, report on the ^{13}C NMR spectra of the thiocyanato complexes is lacking. We present here the ^{13}C NMR spectral data of several thiocyanato complexes to describe their bondings.

^{13}C NMR spectra in DMSO-d_6 were obtained on AM-250 and FT-80 spectrophotometers. Tetramethylsilane was employed as internal standard.

All the chemicals used were Merck reagents and were used as such.

Microanalyses for carbon and hydrogen were done by Mickro-analytisches Labor Pascher, Germany. For metal analyses the complexes were decomposed by a mixture of sulphuric, nitric and perchloric acids; nickel was estimated gravimetrically while zinc was estimated complexometrically[11].

General method for the preparation of complexes

Hydrated metal nitrate (0.005 mol) was dissolved in absolute ethanol or acetonitrile (10-20 ml) to which a solution of potassium thiocyanate (0.01 mol) in the same solvent (15 ml) was added. The precipitated potassium nitrate was filtered off and the filtrate was treated with the solution of a stoichiometric amount of an ancillary ligand (PPh_3, $OPPh_3$, C_5H_5N or C_5H_5NO) in ethanol or acetonitrile (10-25 ml). The complexes obtained were separated, washed with hot ethanol and dried *in vacuo* over P_4O_{10}.

The analytical data of the complexes are given in Table 1. Compound **3** has been reported previously[2]. However, report on its ^{13}C NMR spectrum is lacking. ^{13}C NMR assignments are based partly on the proton couplings in off-resonance spectra and partly on a consideration of nuclear Overhauser enhancement. Signals of C-1 carbon of PPh_3 and that of NCS^- carbon are less intense than those of the other carbons in the ring. Upon coordination of the phosphino ligand in **1-4**, all the ring carbons shift upfield compared to the free ligand values[12] (Table 2). Paramagnetic anisotropy attributable to the metal is a major influence in causing upfield shifting[13,14]. The upfield shifting may also be attributed to the π-acidity of the phosphine ligand. In **1-4**, the ^{13}C resonance of NCS^- group appears at 131.6-133.4 ppm. The assignments are based upon the comparison of the ^{13}C resonance absorptions for SCN^- group in a number of inorganic and organic compounds[15]. The ^{13}C resonance for the carbon of the isothiocyanato moiety in **1** appears at 1.3 ppm downfield compared to that of **3**. This arises because of stronger coulombic interaction of Ni^{2+}-NCS^- than that of Pd^{2+}-NCS^-. The ^{13}C NMR chemical shifts of $OPPh_3$ in DMSO-d_6 (Table 2) are similar to the literature values[16]. Upon coordination, the ring carbon resonances are slightly shifted upfield com-

Table 1 — Analytical Data of the Complexes

Compd.	Found (Calc.) %		
	M	C	H
$[Ni(NCS)_2.2PPh_3]$ (**1**)	8.2 (8.4)	66.0 (65.3)	4.4 (4.3)
$[Zn(NCS)_2.2PPh_3]$ (**2**)	9.1 (9.3)	64.3 (64.6)	4.3 (4.3)
$[Pd(NCS)_2.2PPh_3]$ (**3**)	—	61.2 (61.2)	4.0 (4.0)
$[Cd(SCN)_2.PPh_3.H_2O]$ (**4**)	—	47.4 (47.2)	3.2 (3.3)
$[Zn(SCN)_2.2OPPh_3]$ (**5**)	8.9 (8.9)	61.5 (61.8)	4.1 (4.1)
$[Cd(SCN)_2.OPPh_3.H_2O]$ (**6**)	—	46.1 (45.8)	3.0 (3.2)
$[Zn(NCS)_2.2C_5H_5N]$ (**7**)	19.1 (19.3)	42.2 (42.4)	2.9 (2.9)
$[Cd(SCN)_2.2C_5H_5N]$ (**8**)	—	36.9 (37.3)	2.7 (2.6)
$[Zn(SCN)_2.2C_5H_5NO]$ (**9**)	17.3 (17.6)	39.3 (38.8)	2.8 (2.7)
$[Cd(SCN)_2.C_5H_5NO.H_2O]$ (**10**)	—	25.0 (24.6)	1.9 (2.0)

Table 2 — Chemical Shifts Relative to that of Me_4Si in ^{13}C NMR Spectra of the Ligands and Their Complexes[a]

Compd. No.	C-1	C-2	C-3	C-4	C of NCS group
Ph_3P[b]	138.3	134.4	129.2	129.3	
1	129.5	129.3	124.9	125.2	132.9
2	133.1	129.0	128.7	128.8	133.4
3	131.3	130.8	128.0	128.6	131.6
4	136.6	133.3	128.9	129.1	131.7
Ph_3PO	133.6	133.1	129.8	132.5	
5	133.3	132.0	128.6	131.4	131.7
6	133.3	132.1	128.8	131.5	131.7
C_5H_5N[b]	150.5(α)	124.7	136.9(γ)		
7	149.1	124.5	137.6		135.5
8	149.2	124.4	137.4		133.7
C_5H_5NO[b]	139.0	126.7	125.2		
9	139.1	127.0	126.9		135.3
10	139.2	127.1	126.7		133.3

[a]In ppm downfield relative to Me_4Si as internal standard.
[b]Chemical shifts for carbons of the free ligands refer to the literature values.

pared to the free ligand values. This slight shifting arises because of the ring carbons being far away from the first coordination site. Paramagnetic anisotropy attributable to the metal is a major influence in causing upfield shifting[14,15,17]. Both the compounds **5** and **6** show ^{13}C resonance of SCN^- carbon at 131.7 ppm characteristic of covalently bonded thiocyanato group[15]. Upon complexation, in **7** and **8**, the α- and β-carbon resonances of C_5H_5N are slightly shifted upfield whereas the γ-carbon resonance is shifted downfield (Table 2). Lavalle *et al.*[17] pointed out that the upfield shift of α-carbon arises because of change in bond order of the N − C bond upon complexation. Apparently, this effect is caused by a change in the electron distribution about the α-carbon atom rather than the net electron density. The shifting of electron density from the nitrogen toward metal causes a polarization of density from the α-carbon which, in turn, is compensated by a shift in density toward the α-carbon from the β-carbon which is again compensated by the drift of electron density from the γ-carbon. The net effect is anisotropic with respect to the α- and β-carbons. This electric field effect and/or paramagnetic shift caused by anisotropy in electron distribution should cause an upfield shift at the α- and β-carbons. The downfield shift of γ-carbon in **7** and **8** may be explained in terms of the inductive effect originating at the nitrogen hetero atom of pyridine which is strengthened upon coordination[13,14,17]. The downfield shift of the ^{13}C resonance of NCS^- in **7** compared to that of **8** again indicates that Zn^{2+} is "harder" than its heavier analogue. The ^{13}C NMR spectra of **9** and **10** afforded further comparisons of the relative acceptor properties of Zn^{2+} and Cd^{2+} ions. The chemical shifts for the free pyridine oxide refer to the literature values[15]. Upon complexation, the γ-carbon and the NCS carbon resonances in **9** display larger downfield shifts compared to those in **10**. This again demonstrates that Zn^{2+} is a stronger acceptor than Cd^{2+}.

We thank Dr. M. A. Jalil Miah of the Chemistry Department, University of Ottawa, Canada for helping us with the ^{13}C NMR spectroscopic measurements. Special allocation of funds by Prof. M. A. Raqib, Vice-Chancellor of Rajshahi University to support the cost of microanalyses from Germany is gratefully acknowledged.

References

1. Ahrland S, Chatt J & Davies N R, *Quart Rev*, **12** (1958) 265.
2. Basolo F, Baddley W H & Burmeister J L, *Inorg Chem*, **3** (1964) 1202.
3. Melpolder J B & Burmeister J L, *Inorg Chem*, **11** (1972) 911
4. Lauer J L, Peterkin M E, Burmeister J L, Johnson K A & Lim J C, *Inorg Chem*, **11** (1972) 907.
5. Destefano N J & Burmeister J L, *Inorg Chem*, **10** (1971) 998.
6. Westland A D & Tarafder M T H, *Can J Chem*, **61** (1983) 1573.
7. Pearson R G, *J Am chem Soc*, **85** (1963) 3533.
8. Pearson R G, *J chem Soc*, **45** (1968) 581.
9. Gelbman P & Westland A D, *J chem Soc (Dalton Trans)* (1975) 1598.
10. Makhija R & Westland A D, *J chem Soc (Dalton Trans)* (1977) 1707.
11. Vogel A I, *A text book of quantitative inorganic analysis*, (Longmans, Green & Co, London) 1961.

12 Gansow O D & Kimura B Y, *Chem Commun*, (1970) 1621.

13 Westland A D & Tarafder M T H, *Inorg Chem*, **21** (1982) 3228.

14 Tarafder M T H & Miah M A L, *Inorg Chem*, **25** (1986) 2265.

15 Levy G C, Lichter R L & Nelson G L, *Carbon-13 nuclear magnetic spectroscopy*, 2nd Edn (John Wiley, N.Y.) 1980.

16 Albright T A, Freeman W J, Schweizer E E, *J org Chem*, **40** (1975) 3437.

17 Lavalle D K, Baughman M D & Phillips M P, *J Am chem Soc*, **99** (1977) 718.

Indian Journal of Chemistry
Vol 27A, May 1988, pp. 447-448

Complexes of La(III), Pr(III), Nd(III), Sm(III) & Tb(III) with 2-Thioorotic Acid

MADHULIKA SHRIVASTAVA & G S PANDEY*
Department of Chemistry, Ravishankar University,
Raipur 492 010

Received 28 *April* 1986; *revised* 2 *September* 1986, *rerevised and accepted* 3 *August* 1987

Complexes of 2-thioorotic acid have been prepared with La(III), Pr(III), Nd(III), Sm(III) and Tb(III). Their probable structures have been postulated on the basis of their chemical analysis, magnetic moments and infrared spectra.

The complexes of 2-thioorotic acid (I) with a number of metal ions have been studied[1-3].

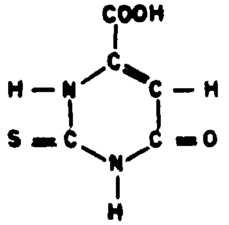

(I)

This compound and its salts have a number of therapeutic[4-6] and industrial[7-9] applications. In this note the preparation and spectral and magnetic properties of the complexes of La(III), Pr(III), Nd(III), Sm(III) and Tb(III) with (I) are reported.

All the chemicals used were of AR or CP grade. 2-Thioorotic acid (I) was prepared by the method described in the literature[10-12]. The ammonium and sodium salts of (I) and their deuterated forms were prepared by procedures described in earlier work[1].

Tris(2-thioorotato)(tetraaquo)lanthanum (III)

$La(NO_3)_3.6H_2O$ (1.3 g, 3 mmol) was dissolved in 25 ml of distilled water, and slightly acidified with dilute HNO_3 (1:10). Ammonium salt of 2-thioorotic acid (1.7 g, 9 mmol) was dissolved in 50 ml of distilled water. The two solutions were mixed together in hot condition. A light yellow complex slowly formed on heating the mixture on a water bath for about 2 hr. The product was centrifuged and washed repeatedly with hot water and finally with ethanol, and dried at 110°C.

The deuterated form of the complex was obtained by refluxing ~0.21 g of the complex with 15 ml of D_2O for two hours. The residue was then centrifuged, washed with D_2O and dried in an oven at 110°C.

Corresponding compounds with Pr(III), Nd(III), Sm(III) and Tb(III) were prepared similarly using 1:3 (metal:ligand) molar ratio of the reactants. The complexes are yellow to light pink in colour and are insoluble in common solvents.

Sulphur in the complexes was estimated by fusing a known amount of the compound in a mixture of KNO_3 and KOH (1:8, w/w) followed by extraction with distilled water, acidification with HNO_3 and estimation of sulphate ions as $BaSO_4$ (ref. 13). Analyses of La(III), Pr(III), Nd(III), Sm(III) and Tb(III) were carried out by decomposing the complexes by aqua regia followed by evaporation to dryness, extraction with water and estimation of metal ions by standard methods[14]. Carbon, hydrogen and nitrogen were analysed at the Microanalytical Section of the Central Drug Research Institute, Lucknow.

The analytical data (Table 1) indicate that the rare earth metals studied here from complexes of the type $M(ligand)_3(H_2O)_x$ at 110°C (x = 2,4).

All the complexes (except that of lanthanum, which is diamagnetic) are paramagnetic. Their magnetic moments, as determined by a vibration magnetometer, are given in Table 1. The experimental values correspond very well with those calculated by the method of Van Vleck and Frank[15]. This shows that the metal ions are in the trivalent state.

The IR spectra of the ligand, and of its sodium and ammonium salts have been reported earlier[1]. It has been indicated that the predominant tautomeric form of the ligand present in the solid state is the thione form.

The ligand molecule contains $-COOH$, $-NH-C=S$ and $-NH-C=O$ groups, and shifts in the positions of the bands due to these groups in the spectra of the complexes should be expected.

The main bands and their assignments in the infrared spectra of these complexes are as follows:

(i) The bands due to $\nu(O-H)$, $\nu(N-H)$ and $\tau(N-H)$ occurring around 3440, 3260 and 720 cm^{-1} in the ligand remained unchanged in the spectra of complexes. These bands shifted to 2550, 2300 and 520 cm^{-1} respectively in the deuterated species. The band due to $\nu(C-H)$ at 3160 cm^{-1} remained unchanged.

(ii) The bands of the (COO) group observed at 1740, 1450 and 1355 cm^{-1} in the spectrum of ligand shifted to 1720 and 1430 cm^{-1} in the spect-

Table 1—Analytical Data and Magnetic Moments of the Complexes

Complexes	Calc. (Found), %					Magnetic Moments	
	C	H	N	S	M	Van Vleck & Frank (B.M.)	Experimental (B.M.)
$La(C_5H_3N_2O_3S)_3.4H_2O$	24.86 (24.90)	2.35 (2.36)	11.60 (11.58)	13.26 (13.30)	19.19 (19.24)	0.00	0.00
$Pr(C_5H_3N_2O_3S)_3.4H_2O$	24.53 (25.39)	2.11 (2.10)	11.87 (11.84)	13.56 (13.58)	19.41 (19.45)	3.62	3.07
$Nd(C_5H_3N_2O_3S)_3.4H_2O$	24.68 (24.71)	2.33 (2.35)	11.52 (11.50)	13.16 (13.21)	19.78 (19.88)	3.68	2.91
$Sm(C_5H_3N_2O_3S)_3.2H_2O$	25.74 (25.72)	1.86 (1.87)	12.01 (12.06)	13.73 (13.70)	21.50 (21.55)	1.55-1.65	1.81
$Tb(C_5H_3N_2O_3S)_3.2H_2O$	24.43 (25.48)	1.84 (1.85)	11.86 (11.82)	13.56 (13.60)	22.45 (22.52)	9.72	9.17

ra of complexes. In the spectra of complexes with deuterated species these bands appeared at 1720 and 1420 cm^{-1}. The positions of these bands are similar to those found in the spectrum of the sodium salt of the ligand. It indicates bonding of the metal ions with the (COO) group.

(iii) The amide—I, −IV and −VI bands at 1680, 680 and 620 cm^{-1} in the ligand shifted to 1650, 660 and 590 cm^{-1} respectively in the complexes. There was no change in the positions of these bands on deuteration.

(iv) The thioamide bands at 1030 and 950 cm^{-1} remained unchanged.

(v) Two broad bands appearing at 1550 and 1410 cm^{-1} have contributions from $\delta(N-H)$, $\delta(O-H)$, $\nu(C=C)$ and $\nu(C-N)$ modes. On deuteration, the 1550 cm^{-1} band disappeared and three new bands appeared at 970, 1060 and 1130 cm^{-1}, while the band at 1450 shifted to 1430 cm^{-1}. The positions of the bands obtained on deuteration were the same as those observed in the deuterated ligand. Hence, it is inferred that N − H groups do not interact with the metal ions.

(vi) Two new bands appeared at 520 and 400 cm^{-1}.

All these shifts in the positions of the bands in the IR spectra of the complexes are in keeping with the bonding scheme proposed below (II):

The stoichiometry of complexes obtained after drying at 110°C shows the presence of water molecules. On heating the complexes at 160°C, the mass loss in each case corresponded to the loss of water molecules present. The anhydrous residual mass in each case, which was subjected to elemental analysis, corresponded to the stoichiometry $M(Ligand)_3$, which confirmed that the water molecules were not present in the coordinated form, but as water of crystallisation.

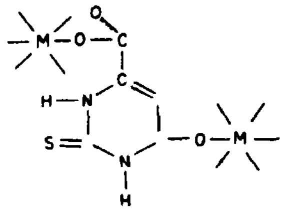

(II)

Hence, in the present complexes, bonding through oxygen of carboxylate group and O of the $-NH-C=O$ has been proposed.

References

1 Pandey G S, Nigam P C & Agarwala U, *J inorg nucl Chem*, **39** (1977) 1877.
2 Pandey G S, Nigam P C & Agarwala U, *Indian J Chem*, **14A** (1976) 884
3 Pandey G S, Nigam P C & Agarwala U, *Indian J Chem*, **15A** (1977) 537.
4 Moor H, *Brit Pat*, 1193 (1970); *Chem Abstr*, **73** (1970) 698525X.
5 Chelbova K V, Golovinski E & Hadjiolov A A, *Biochem Pharmac*, **19** (1970) 2785.
6 Rendina G, Sarcione E J, Lee O T & Barrett H W, *Proc Soc Exp Biol Med*, **95** (1957) 350.
7 Chemoforma A G, *Fr Pat*, 1,569,124 (1969); *Chem Abstr*, **72** (1970) 419732.
8 Thomas Murray J, *U S Pat*, 909, 023 (1973).
9 Scheibitz M , Kabbe J H, Von Koning A, Goetze J & Wegde E, *German Pat*, 2, 013, 423 (1971).
10 Johnson T B & Schroeder Elmer F, *J Am chem Soc*, **53** (1931) 1989.
11 Johnson T B & Cretcher, *J Am chem Soc*, **37** (1915) 2144.
12 Johnson T B & Schroeder Elmer F, *J Am chem Soc*, **54** (1932) 2941.
13 Treadwell E P & Hall W T, *Analytical chemistry*, Vol. 2 (John Wiley, New York), 1958, 199, 977.
14 Kotthoff I M & Elving Philip J, *Treatise on analytical chemistry*, Part 2, Vol. 5 (Interscience, New York) 1961, 189.
15 Van Vleck J H & Frank A, *Phys Rev*, (1929) 1494, 1625.

Indian Journal of Chemistry
Vol. 27A, May 1988, pp. 449-450

Studies on Lanthanide(III) Hexamethylenedithiocarbamate Complexes

K K DAHIYA & N K KAUSHIK*

Department of Chemistry, University of Delhi, Delhi 110 007

Received 10 *June* 1987; *revised and accepted* 9 *September* 1987

Hexamethylenedithiocarbamate complexes of the type $Ln(C_6H_{12}NCS_2)_3$ [where Ln = La, Pr, Nd, Sm, Tb and Dy] have been synthesized and characterized on the basis of elemental analysis, conductance measurements and magnetic, spectral (IR, UV, visible, ^1H NMR) and fluorescence studies. IR and UV spectral studies show that the dithiocarbamate group behaves as a S-S bonding bidentate ligand.

The present note deals with the preparation and characterization of some lanthanide(III) hexamethylenedithiocarbamate complexes. Sodium hexamethylenedithiocarbamate was prepared by the modified method given by Gilman and Blatt[1]. Anhydrous trichlorides (MCl_3) of the lanthanides (M = La, Pr, Nd, Sm, Tb, Dy) were prepared by the method reported by Taylor and Carter[2]. All the complexes were prepared by a similar method. The complexes(I) were prepared, in anhydrous and inert atmosphere, by refluxing ethanolic solutions of the metal trichloride and the ligand in 1:3 stoichiometric ratio in nitrogen atmosphere for 30-45 min. The solvent was removed under reduced pressure and the residue extracted into ~ 45 ml acetonitrile. The solution was filtered and the filtrate was concentrated under reduced pressure to about one third of its original volume. Anhydrous petroleum ether (60-80°C) (~ 30 ml) was added to it with vigorous shaking. Solid crystals separated out, which were filtered, washed with ether and dried *in vacuo*. These were recrystallized from acetonitrile.

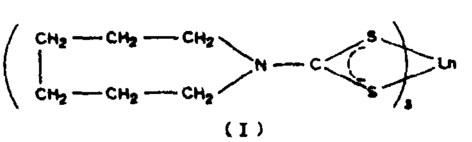

(I)

Ln = La, Pr, Nd, Sm, Tb, Dy

Conductance measurements were carried out on an Elico conductivity bridge (model CM-82). IR of the compounds in nujol were recorded on a Shimadzu infrared spectrophotometer IR-435 in the range 4000-400 cm^{-1}. The far IR spectra were recorded on a Perkin-Elmer 621 grating spectrophotometer. Perkin-Elmer UV-Vis spectrometer, model 554, was used for recording the UV and visible spectra of the compounds. The PMR spectra were recorded at room temperature on a Jeol FX-200 FT-NMR spectrometer at a spectral width of 1000 Hz. Fluorescence studies were carried out on a Jasco FP-500 spectrofluorometer. Gouy's method was chosen for the magnetic moment studies[3].

Molar conductance values of these complexes in 10^{-3} *M* nitrobenzene solution are of the order of 0.50 Ohm^{-1}cm^{2}mol^{-1}, indicating that the complexes are non-electrolytes. The complexes are soluble in acetonitrile, methylene chloride and DMSO. The paramagnetic behaviour of the lanthanide(III) ions is consistent with the presence of unpaired 4*f* electrons. The magnetic moment, μ_{eff}.(B.M. at 300 K) values for the complexes are as follows: La(dtc)$_3$, diamag.; Pr(dtc)$_3$,3.62; Nd(dtc)$_3$,3.50; Sm(dtc)$_3$, 1.46; Tb(dtc)$_3$, 9.48; Dy(dtc)$_3$, 10.40.

All the complexes possess only one medium intensity band in their IR spectra at ~ 1000 cm^{-1}. This indicates the presence of a four-membered ring system[4,5] and also supports the bidentate nature of dithiocarbamate ligand[6]. The frequency of the thioureide band at ~ 1500 cm^{-1} lies in between that of C-N (1350-1250 cm^{-1}) and C = N (1690-1640 cm^{-1}), which suggests that this band possesses partial double bond character. The non-ligand bands occurring at ~ 375 cm^{-1} have been tentatively assigned to ν(M-S) modes[7,8].

Since in lanthanide ions the 4*f* orbitals are effectively shielded by the $5s^2 5p^6$, octet, the lines appearing in their absorption spectra arise from electronic transitions within the 4*f* levels, which are normally forbidden, but are allowed after the removal of degeneracy in the 4*f* orbitals by external crystal fields[9,10]. The absorption bands in Pr(III), Nd(III), Sm(III), Tb(III) and Dy(III) appear due to the transitions from the ground levels $^3H_4$, $^4I_{9/2}$, $^6H_{5/2}$, $^7F_6$ and $^6H_{15/2}$ respectively to the excited *J* levels of the 4*f* configuration[11,12]. The states arising from various f^n configurations are only slightly affected by the surrounding ions and are practically invariant for a given ion in all of its compounds. Electronic spectral bands (cm^{-1}) with assignments for the complexes are presented in Table 1.

In the UV region an intense band appears at ~ 260 nm (log ε ~ 4.0) due to the interligand π-π^* transition of the $N \overset{\cdots}{-} C \overset{\cdots}{-} S$ group[13-15]. The intraligand π-π^* transition of the $S \overset{\cdots}{-} C \overset{\cdots}{-} S$ group generally appears as a shoulder and is associated with the inequivalance of the $C \overset{\cdots}{-} S$ bonds of the ligand[16]. Thus, in dithiocarbamate complexes this band is observed in cases where the dithiocarbamate moiety is bonded inequiv-

Table 1—Electronic Spectral Bands (cm^{-1}) with Assignments for the Complexes

Complex	Bands	Assignments
$Pr(C_6H_{12}NCS_2)_3$	20800	$^3H_4 \rightarrow {}^3P_0$
	22700	$\rightarrow {}^3P_1$
	25600	$\rightarrow {}^1P_2$
$Nd(C_6H_{12}NCS_2)_3$	17000	$^4I_{9/2} \rightarrow {}^4G_{5/2}$
	20000	
	21300	
	24300	$\rightarrow {}^2P_{1/2}$
$Sm(C_6H_{12}NCS_2)_3$	19100 20500	$^6H_{5/2} \rightarrow {}^4F_{3/2}, {}^4G_{7/2}$
$Tb(C_6H_{12}NCS_2)_3$	28100	$^7F_6 \rightarrow {}^5D_2, {}^5G_4, {}^5L_3$
$Dy(C_6H_{12}NCS_2)_3$	20200	$^6H_{15/2} \rightarrow {}^4F_{9/2}$
	22100	$\rightarrow {}^4I_{15/2}$
	26000	$\rightarrow {}^4G_{11/2}$

alently to the metal ions or when the dithiocarbamate moiety is monodentate[14]. In the present compounds, although this band is observed at 320 nm (log ε 3.75) in the spectrum of the ligand, sodium hexamethylenedithiocarbamate, it tends to disappear in the spectra of metal complexes, showing thereby that the dithiocarbamate ligand is S - S bonded to the metal ions. This fact is in agreement with IR studies.

The ^1H NMR spectra of the ligand and the complexes were recorded in DMSO-d_6. The resonance signal due to N-CH_2 protons appears at ~ δ 3.0 (t, 4H, J 7Hz) and that due to $-CH_2-$ protons appears at δ 1.4-1.9 (d, 8H, J 10Hz)[17]. A shift towards lower field of N-CH_2 signal in the complexes, in comparison to that of the free ligand, may be attributed to a change in the electronic environment as a result of coordination of the ligand to the metal atom. Of course, the resonance signals are shifted only to a small extent, since the N-CH_2 protons are distant from the coordinating centres. The signals are sharp, without being split. The spectra show no trace of the ligand indicating that the complexes do not dissociate on dissolution in DMSO-d_6.

From the fluorescence spectra, quantum yield of fluorescence (ϕ_f) has been calculated using a relative method and taking anthracene as the reference material[18]. The areas under the emission curves for the standard and experimental samples were calculated by the planimetric integration method.

The quantum yields of fluorescence show deviation from unity. Thus, fluorescence remains the dominant but certainly not the exclusive mode of emission. The non-radiative processes like intersystem crossing and internal conversion are probably contributing to the emission process. The ϕ_f values are as follows: La(dtc)$_3$, 0.47; Pr(dtc)$_3$, 0.15; Nd(dtc)$_3$, 0.17; Sm(dtc)$_3$, 0.43; Tb(dtc)$_3$, 0.12; Dy(dtc)$_3$, 0.13; (dtc = $C_6H_{12}NCS_2$).

References

1 Gilman H & Blatt A H, *Organic synthesis collective Vol I* (John Wiley, New York) 1958, 448.
2 Taylor M D & Carter C P, *J inorg nucl Chem*, **24** (1962) 387.
3 Figgis B N & Lewis J, *Modern coordination chemistry* (Interscience, New York) 1960.
4 Kumar S & Kaushik N K, *Synth react inorg met-org Chem*, **11** (1981) 649.
5 Kumar S & Kaushik N K, *Inorg nucl chem Lett*, **16** (1980) 389.
6 Bonati F & Ugo R, *J organometal Chem*, **10** (1967) 157.
7 Bhat A N, Fay R C, Lewis D F, Lindmark A R & Strauss S H, *Inorg Chem*, **13** (1974) 886.
8 Bradley D C & Gitlitz M H, *J chem Soc A*, (1969) 1152.
9 Yost D M, Russel H & Garner C S, *The rare earth elements and their compounds* (Wiley, New York) 1947.
10 Lapitakaya A V & Pirkes S B, *Zh neorg Khim*, **16** (1971) 369.
11 Dieke G H, *Spectra and energy levels of rare earth ions in crystals*, edited by H M Croswhite & H W Mose (Interscience, New York) 1968.
12 Sinha S P, *Complexes of rare earths* (Pergamon Press, London) 1966.
13 Jorgensen C K, *J inorg nucl Chem*, **24** (1962) 1571.
14 Tsipis C A & Manoussakis G E, *Inorg chim Acta*, **18** (1976) 35.
15 Takami F, Wakahara S & Maeda T, *Tetrahedron Lett* (1971) 2645.
16 Janssen M L, *Recl Trav chim Pays Bas Belg*, **79** (1960) 1066.
17 Bajaj R K, Ph D Thesis, Delhi University, 1984.
18 Calvert J G & Pitts J N, *Photochemistry* (John Wiley, New York) 1966.

Indian Journal of Chemistry
Vol. 27A, May 1988, pp. 451-453

Magnetic, Spectral & Thermal Studies on Some New Polymeric Complexes of Mn(II), Co(II), Ni(II), Cu(II) & Zn(II) with Bis-phenylhydrazides of Suberic & Sebacic Acids

H D JUNEJA & K N MUNSHI*
Department of Chemistry, Nagpur University Campus,
Nagpur 440 010

Received 9 *December* 1986; *revised* 4 *May* 1987; *revised and accepted* 27 *August* 1987

Coordination polymers of Mn(II), Co(II), Ni(II), Cu(II) and Zn(II) with bis-phenylhydrazides of suberic acid and sebacic acid have been prepared. These polymers have been characterized on the basis of the elemental analysis, magnetic susceptibility, reflectance and infrared spectral, and thermogravimetric data.

Transition metal complexes with hydrazides have played a vital role in the development of coordination chemistry. In continuation of our earlier work[1] we are reporting in this note, the preparation and characterisation polymeric chelates of Mn(II), Co(II), Ni(II), Cu(II) and Zn(II) with suberic acid bis-(phenylhydrazide) [SABPH] and sebacic acid bis-(phenylhydrazide) [SEABPH].

All the chemicals used in the preparation of the ligands and the complexes were of AR grade.

The infrared spectra of the ligands and coordination polymers were recorded in the region 400-4000 cm^{-1} on a Specord-75 infrared spectrophotometer using nujol mull technique. Magnetic susceptibilities of polymeric complexes were measured by the Gouy method. A single beam Carl-USU-2-P-spectrophotometer was used for recording reflectance spectra of the polymers. The thermogravimetric studies were carried out using an apparatus fabricated at the Department of Chemistry, Nagpur University; heating rate was maintained at 5°/min. Carbon and hydrogen contents of the complexes were analysed using a Colemen's analyser and nitrogen by a Colemen's nitrogen analyser.

The ligands were prepared by refluxing a mixture of suberic acid or sebacic acid (0.1 *M*) and distilled thionyl chloride (0.2 *M*) for 2 hr on a steam-bath till a clear solution was obtained. This solution was again heated for 30 min to ensure complete removal of hydrochloric acid. The acid dichlorides so obtained was added to phenylhydrazine in stoichiometric ratio of 1:2 and the mixture was refluxed in benzene medium for 2 hr. A white solid, suberic acid bis-(phenylhydrazide) or sebacic acid bis-(phenylhydrazide), was obtained. The product was filtered and crystallized from ethanol-benzene mixture. The melting point and elemental analysis data of ligands are given in Table 1.

The coordination polymers were prepared by refluxing for 4 hr an equimolar mixture of the ligand (0.1 *M*) and metal acetate (0.1 *M*) dissolved in minimum quantity of dimethylformamide-ethanol mixture (4:1). The product formed were filtered and washed a number of times with hot dimethylformamide and then with ethanol to remove unreacted ligands and metal acetate. The purified sample was then dried *in vacuo*. All the products were found to be insoluble in common organic solvents. On the basis of elemental analysis (Table 1), the compositions of these polymeric products have been suggested.

A medium band observed around 3380 cm^{-1} in the IR spectrum of SABPH and at 3360 cm^{-1} in the spectrum of SEABPH is assigned to stretching vibration of $-$NH group[2] while a band appearing in the region 1610-1670 cm^{-1} may be assigned to $C=O$ stretching vibration[3]. The bis-(hydrazide) undergoes keto-enol tautomerism during polymerization which is supported by the fact that the $\nu C=O$ band around 1610-1670 cm^{-1} in free ligands disappears in polymers and a new band appears at 1550-1590 cm^{-1} which is due to $C=N$ stretching[4]. Another band appearing around 1100 cm^{-1} in polymers is assigned to $\nu C-O$ mode observed subsequent to deprotonation of the OH group (enolic). Additional band at 560-650 cm^{-1} found in the spectra of polymers may be assigned to metal-oxygen bonding[5]. Another weak band in the region 490-550 cm^{-1} may be assigned to $M-N$ stretching vibration. Due to formation of $N-N\rightarrow M$ coordinate bond, the $\nu N-H$ mode is shifted towards lower frequencies in polymers. The free $H-O-H$ stretching frequencies of water have been found merged with $\nu N-H$ band which thus appears as a broad band in polymers.

The $\pi-HOH$ mode of coordinated water is found in the region 780-810 cm^{-1} in cobalt(II) and nickel(II) polymers only[5].

Electronic spectral and magnetic moment studies

Mn(II) polymers—The band which appears at 20.50 kK in Mn(II)-SEABPH and at 19.23 kK in Mn(II)-SABPH polymers is assigned to $^6A_1 \rightarrow {}^4E(G)$ transition while the band observed at 15.15 kK in Mn(II)-SEABPH and at 16.18 kK in Mn(II)-SABPH complexes is assigned to charge-transfer.

Table 1—Elemental Analysis of Ligands and Complexes

Proposed composition (Dec. Tem., °C)	Found (Calc.), %				$\mu_{eff.}$ (B.M.)
	C	H	N	M	
SABPH	68.02	7.55	16.00	—	—
(217)	(67.79)	(7.34)	(15.81)		
SEABPH	68.29	7.92	14.75	—	—
(226)	(69.10)	(7.85)	(14.65)		
$\{[\text{Mna}]\text{H}_2\text{O}\}_n$	57.00	5.50	13.72	13.60	5.66
(300)	(56.47)	(5.64)	(13.17)	(12.97)	
$[\text{Co(a)}2\text{H}_2\text{O}]_n$	55.05	5.80	13.10	13.25	4.75
(340)	(54.21)	(5.42)	(12.64)	(13.26)	
$[\text{Ni(a)}2\text{H}_2\text{O}]_n$	55.25	5.88	13.61	14.00	3.53
(340)	(54.21)	(5.42)	(12.64)	(13.25)	
$[\text{Cua}]_n$	58.00	5.46	13.45	15.26	2.16
(380)	(57.75)	(5.77)	(13.47)	(15.29)	
$[\text{Zna}]_n$	57.26	5.84	13.37	15.60	—
(320)	(57.50)	(5.75)	(13.41)	(15.66)	
$\{[\text{Mnb}]\text{H}_2\text{O}\}_n$	59.10	6.50	12.92	12.57	5.90
(320)	(58.28)	(6.18)	(12.36)	(12.12)	
$[\text{Co(b)}2\text{H}_2\text{O}]_n$	56.00	6.05	12.70	13.10	5.20
(360)	(55.61)	(5.89)	(11.79)	(12.36)	
$[\text{Ni(b)}2\text{H}_2\text{O}]_n$	55.50	6.00	12.10	13.00	3.52
(370)	(55.61)	(5.89)	(11.79)	(12.36)	
$[\text{Cub}]_n$	59.60	6.30	12.68	14.50	2.15
(400)	(59.51)	(6.31)	(12.62)	(14.33)	
$[\text{Znb}]_n$	56.30	6.34	12.60	14.65	—
(380)	(56.37)	(6.01)	(12.08)	(14.10)	

a = SABPH, b = SEABPH

The magnetic moment values of Mn(II) complexes of SABPH and SEABPH are 5.66 and 5.90 B.M. respectively which correspond to five unpaired electrons, indicating presence of high spin Mn(II) ion. The electronic spectra and magnetic moment data thus support tetrahedral geometry for this polymer.

Co(II) polymers—The octahedral complexes of Co(II) ion have been reported to show magnetic moment values ranging from 3.82 to 5.50 B.M.[7], corresponding to three unpaired electrons. In the present study, the Co(II)-SEABPH and -SABPH complexes show magnetic moment values of 5.20 and 4.75 B.M. respectively.

The reflectance spectra of Co(II) octahedral complexes are generally reported to show three bands. A band near 8,000-10,000 cm^{-1} can be assigned to $^4T_{1g}\rightarrow{}^4T_{2g}$ transition. A multiple band is observed in visible region near 20,000 cm^{-1} which may be due to $^4T_{1g}\rightarrow{}^4T_{1g}$ (P) transition and a band observed in the region 11,800-17,200 cm^{-1} may be assigned due to $^4T_{1g}\rightarrow{}^4A_{2g}$ transition.

In the case of Co(II)-SEABPH and -SABPH polymeric complexes, bands observed at 14.28 kK, 20.83 kK and 11.90 kK, 19.85 kK may be assigned to $^4T_{1g}\rightarrow{}^4A_{2g}$ and $^4T_{1g}\rightarrow{}^4T_{1g}(P)$ transitions respectively. Thus, the magnetic moment and reflectance spectra correspond to the octahedral geometry for Co(II) complexes.

Ni(II) complexes—The magnetic moment values of 3.5 and 3.53 B.M. for Ni(II) complexes of SABPH and SEABPH respectively show the presence of two unpaired electrons and are within the range expected for octahedral Ni(II) complexes.

The reflectance spectra of six coordinate nickel(II) complexes generally exhibit three spin-allowed transitions to the $^3T_{2g}$, $^3T_{1g}(F)$ and $^3T_{1g}(P)$ levels and these occur in the ranges 7000-13,000, 11,000-20,000 and 19,000-27,000 cm^{-1} respectively[6].

In case of Ni(II)-SEABPH and -SABPH polymeric complexes, bands appearing around 22.76, 16.12, 13.51 kK and 23.00, 16.12, 11.76 kK may be assigned to $^3A_{2g}\rightarrow{}^3T_{1g}$ (P), $^3A_{2g}\rightarrow{}^3T_{1g}$ (F) and $^3A_{2g}\rightarrow{}^3T_{1g}$ transitions respectively.

The magnetic moment value and reflectance spectra support octahedral geometry for Ni(II) polymeric complexes.

Cu(II) complexes—The μ_{eff} value in the range 2.15-2.16 B.M. for Cu(II) polymeric complexes corresponds to presence of one unpaired electron.

The reflectance spectra of Cu(II) polymers show two bands, around 22.00 and 15.62 kK in SABPH, and around 21.70 and 13.51 kK in SEABPH polymer. These may be due to charge-transfer and d_{yz}, $d_{xz} \rightarrow d_{x^2-y^2}$ transitions respectively.

Thermal properties of polymers

The Mn(II) complexes show mass loss around 80-120°C in thermogravimetric curve; this is due to the loss of water of hydration. From 120 to 240°C, no mass loss is observed in both the Mn(II) polymers indicating that water of coordination is not present. These polymers have been found to be stable up to 260°C.

TG curve of Co(II) and Ni(II) polymers show a mass loss in the range 150-240°C indicating the presence of two coordinated molecules of water, thus supporting the octahedral geometry of these polymers as suggested on the basis of spectral and magnetic studies.

TG curves of Cu(II) – SABPH and – SEABPH polymers show absence of the water of hydration as well as water of coordination. These polymers have been found to be stable up to 320°C. TG curves of Zn(II) polymers also show no mass loss up to 240°C indicating the absence of water of hydration and water of coordination. These polymers are, however, stable up to 300°C. The decomposition temperatures were found out by half decomposition curve technique and are given in Table 1.

On the basis of the results reported above, the coordination polymers may be suggested to have structure I when M = Mn(II), Cu(II), and Zn(II); and structure II when M = Co(II) and Ni(II).

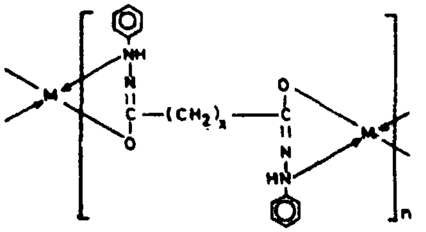

Where x = 6 in case of SABPH
x = 8 in case of SEABPH
(I)

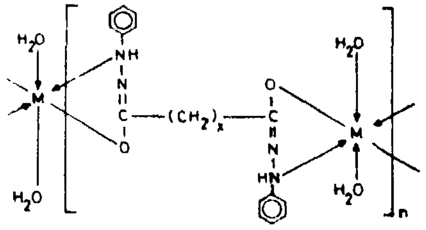

Where, x = 6 in case of SABPH
x = 8 in case of SEABPH
(II)

References

1 Juneja H D, Chakravarty B B & ,Munshi K N, *Nagpur University Journal*, Vol. 5, 1986, 510..

2 Dyer R J, *Applications of absorption spectroscopy of organic compounds* (Prentice Hall of India, New Delhi) 1978, 37.

3 Alpert N L, Keiser W E & Szymanski H A, *IR-Theory and practice of infrared spectroscopy* (Plenum, New York) 1970, 268.

4 Silverstein R M, Bassler G C & Morrill T C, *Spectrometric identification of organic compounds* (John Wiley, New York) 1974, 111.

5 Nakamoto K, *Infrared spectra of inorganic and coordination compounds* (John Wiley, New York) 1970, 167, 220.

6 Lever A B P, *Inorganic electronic spectroscopy* (Elsevier, new York) 1968, 320, 333, 334.

7 Selwood P W, *Magnetochemistry* (Interscience, New York) 1943, 174.

Indian Journal of Chemistry
Vol. 27A, May 1988, pp. 454-455

Stability Constants of N-(2-Hydroxy-3-methoxybenzylidene)phenylhydrazine, N-(2-Hydroxy-3-methoxybenzylidene)semicarbazide & N-(2-hydroxy-3-methoxybenzylidene)thiosemicarbazide Complexes with La^{3+}, Y^{3+}, Nd^{3+}, Dy^{3+}, Pr^{3+} & Sm^{3+}

M S MAYADEO* & SUJATA S KALE
Department of Chemistry, Ramnarain Ruia College, Matunga, Bombay 400019

Received 13 *February* 1987; *revised and accepted* 8 *October* 1987

Complexation of La^{3+}, Y^{3+}, Nd^{3+}, Dy^{3+}, Pr^{3+} and Sm^{3+} with N-(2-hydroxy-3-methoxybenzylidene)phenylhydrazine, N-(2-hydroxy-3-methoxybenzylidene)semicarbazide and N-(2-hydroxy-3-methoxybenzylidene)thiosemicarbazide, has been studied by potentiometric titration technique in 75:25 dioxan-water medium at 30 ± 0.1°C and at ionic strength of 0.1 *M*. The stability constants of the above three reagents follow the orders: $Y^{3+} > Sm^{3+} > Dy^{3+} > Pr^{3+} > Nd^{3+} > La^{3+} >$; $Dy^{3+} > Nd^{3+} > Y^{3+} > Sm^{3+} > Pr^{3+} > La^{3+}$ and $Pr^{3+} > Sm^{3+} > Nd^{3+} > Dy^{3+} > Y^{3+} > La^{3+}$, respectively.

Potentiometric studies on La^{3+}, Y^{3+}, Dy^{3+}, Sm^{3+}, Nd^{3+} and Pr^{3+} chelates with N-(2-hydroxy-3-methoxybenzylidene)phenylhydrazine, N-(2-hydroxy-3-methoxybenzylidene)semicarbazide and N-(2-hydroxy-3-methoxybenzylidene)thiosemicarbazide have been carried out following the Calvin-Bjerrum *p*H titration technique as adopted by Irving and Rossotti[1], at 30 ± 0.1°C and ionic strength of 0.1*M* in 75:25 (v/v) dioxan-water medium.

An Elico model-LI-15 *p*H-meter equipped with a glass electrode and a calomel reference electrode was used for *p*H measurements.

The reagents (A) N-(2-hydroxy-3-methoxybenzylidene)phenylhydrazine, (B) N-(2-hydroxy-3-methoxybenzylidene)semicarbazide and (C) N-(2-hydroxy-3-methoxybenzylidene)thiosemicarbazide were prepared by condensing equimolar ethanolic solutions of 2-hydroxy-3-methoxybenzaldehyde with the respective amines. The products obtained were repeatedly crystallised and their purities were checked by TLC and elemental analysis.

The experimental details and computational methods were the same as described in our earlier publication[2].

From the titration data, $\bar{n}_A$ values were determined and plotted against B (*p*H-meter readings) to obtain *p*K values. These were further corroborated by linear plots of $\text{Log}\,\bar{n}_A/1-\bar{n}_A$ versus B.

From the metal titration curves $\bar{n}$ and *p*L values were calculated. The $\bar{n}$ values were plotted against the corresponding *p*L values to get the formation curves of the metal complex ion equilibria. $\text{Log}K_1$ and $\text{Log}K_2$ were evaluated from these curves. They were further corroborated by linear plots of $\log \bar{n}/1-\bar{n}$ versus *p*L and $\log 2-\bar{n}/\bar{n}-1$ versus *p*L.

The stability constant data are presented in Table 1.

The pK^{H}_{OH} value of N-(2-hydroxy-3-methoxybenzylidene)thiosemicarbazide was found to be less than that of N-(2-hydroxy-3-methoxybenzylidene)semicarbazide, while that of N-(2-hydroxy-3-methoxybenzylidene)phenylhydrazine was higher than that of N-(2-hydroxy-3-methoxybenzylidene)semicarbazide.

The order of stability constants for metal chelates with N-(2-hydroxy-3-methoxybenzylidene)phenylhydrazine is: $Y^{3+} > Sm^{3+} > Dy^{3+} > Pr^{3+} > Nd^{3+} > La^{3+}$, with N-(2-hydroxy-3-methoxybenzylidene)semicarbazide it is: $Dy^{3+} > Nd^{3+} > Y^{3+} > Sm^{3+} > Pr^{3+} > La^{3+}$, and with N-(2-hydroxy-3-methoxybenzylidene)thiosemicarbazide, the order is: $Pr^{3+} > Sm^{3+} > Nd^{3+} > Dy^{3+} > Y^{3+} > La^{3+}$.

The complex forming abilities of metal ions are frequently characterised by stability orders as pointed out by Irving and Williams[3,4] and this is particularly important and valid for most nitrogen and oxygen donor ligands irrespective of the nature of the ligand. To explore the possible correlation, $\text{Log}K$ values of Pr^{3+} complexes of the present series of related ligands were plotted against the $\text{Log}K$ values of Sm^{3+} complexes of corresponding ligands. A linear relationship was ob-

Table 1—Stability Constants of the Ligands and Their Metal Complexes

{Temp. = 30 ± 0.1°C; ionic strenghth $\mu = 0.1\,M$}

	H^+	La^{3+}	Y^{3+}	Sm^{3+}	Dy^{3+}	Pr^{3+}	Nd^{3+}
N-(2-Hydroxy-3-methoxybenzylidene)phenylhydrazine							
$\text{Log}K_1$	12.62	8.08	9.03	8.96	8.93	8.83	8.70
$\text{Log}K_2$	—	—	8.62	—	—	—	—
N-(2-Hydroxy-3-methoxybenzylidene)semicarbazide							
$\text{Log}K_1$	10.94	8.13	10.50	10.26	10.95	9.85	10.91
$\text{Log}K_2$	—	—	—	—	—	—	—
N-(2-Hydroxy-3-methoxybenzylidene)thiosemicarbazide							
$\text{Log}K_1$	10.48	6.73	6.96	7.26	7.10	7.36	7.20
$\text{Log}K_2$	—	—	—	—	—	—	—

served in the present study, in consonance with that of Irving and Williams.

Similarly the Log K values of the present complexes were plotted against the reciprocal ionic radii of the metal ions. The first formation constants were found to increase rather uniformly with decreasing ionic radii, irrespective of the ligands, as would be expected if the interaction is predominantly electrostatic. With the heavier lanthanide ion, Dy^{3+} however, the variations are not regular and uniform and may be dependent upon the nature of the ligand itself.

References

1 Irving H & Rossotti H S, *J chem Soc*, (1954) 2904.
2 Mayadeo M S, Chaubal A M & Vartak S D, *J Indian Chem Soc*, **55** (1978) 456.
3 Irving H & Williams R J P, *Nature*, **162** (1948) 746.
4 Irving H & Williams R J P, *J chem Soc*, (1953) 3192.

Indian Journal of Chemistry
Vol. 27A, May 1988, pp. 456-457

Stability Constants of Some Bivalent Metal Ion Chelates of Schiff Bases Derived from 2-Hydroxy-5-bromobenzaldehyde

M S MAYADEO* & JYOTI V NALGIRKAR
Ramanarain Ruia College, Department of Chemistry, Matunga, Bombay 400 019

Received 6 *April* 1987; *revised* 10 *July* 1987; *rerevised and accepted* 24 *August* 1987

Potentiometric studies have been carried out on metal chelates of Mg^{2+}, Cd^{2+}, Zn^{2+}, Co^{2+}, Ni^{2+} and Cu^{2+} with N-(2-hydroxy-5-bromobenzylidene)-aniline, N-(2-hydroxy-5-bromobenzylidene)-4-methylaniline, and N-(2-hydroxy-5-bromobenzylidene)-4-chloroaniline. The dissociation constants of the reagents and formation constants of their metal chelates have been determined by Calvin-Bjerrum *p*H titration technique as adopted by Irving and Rossotti, at 28 ± 0.1°C and at an ionic strength of 0.1 *M* in 75:25 (v/v) dioxan-water medium.

The chelating properties of schiff bases of *o*-hydroxyaldehydes and ketones are well established. These ligands show useful analytical applications as well as biological activities. In view of this, in the present study, schiff bases of 2-hydroxy-5-bromobenzaldehyde have been synthesised and the stability constants of their metal chelates have been determined potentiometrically, by Calvin-Bjerrum technique, as adopted by Irving and Rossotti[1].

The reagents (A) N-(hydroxy-5-bromobenzylidene)aniline, (B) N-(2-hydroxy-5-bromobenzylidene)-4-methylaniline and (C) N-(2-hydroxy-5-bromobenzylidene)-4-chloroaniline were prepared by condensing equimolar ethanolic solutions of 2-hydroxy-5-bromobenzaldehyde and the respective amines. The products obtained were repeatedly crystallised to obtain analytically pure samples. Their purities were tested by TLC and elemental analyses.

The experimental details and computational methods were the same as described in our earlier publication[2].

Calculations

From the titration data, $\bar{n}_A$ values were determined and were plotted against B (pH meter readings) to obtain values of pK_1 and pK_2. These values were further corroborated by straight line plots of log $\bar{n}_A/1-\bar{n}_A$ versus B and log $2-\bar{n}_A/\bar{n}_A-1$ versus B respectively.

From the metal ion titration curves, $\bar{n}$ and pL values were calculated. The $\bar{n}$ values were plotted against the corresponding pL values to get the formation curves of the metal complex-ion equilibria. From these plots, values of log K_1 and log K_2 were evaluated. These were further corroborated by straight line plots of log $\bar{n}/1-\bar{n}$ versus pL and log $2-\bar{n}/\bar{n}-1$ versus pL respectively.

Table 1—Stability Constants of the Ligands and Their Metal Complexes
[Temp. = 28 ± 0.1°C; μ = 0.1 *M*]

N-(2-Hydroxy-5-bromobenzylidene)aniline

	H^+	Cu^{2+}	Co^{2+}	Ni^{2+}	Zn^{2+}	Cd^{2+}	Mg^{2+}
Log K_1	9.27	7.95	5.73	5.72	5.56	4.51	3.72
Log K_2	2.72	6.82	—	—	—	—	—

N-(2-Hydroxy-5-bromobenzylidene)-4-methylaniline

	H^+	Cu^{2+}	Zn^{2+}	Ni^{2+}	Co^{2+}	Cd^{2+}	Mg^{2+}
Log K_1	10.05	9.60	6.32	6.24	6.02	4.97	4.32
Log K_2	3.30	8.49	—	—	—	—	—

N-(2-Hydroxy-5-bromobenzylidene)-4-chloroaniline

	H^+	Cu^{2+}	Ni^{2+}	Co^{2+}	Zn^{2+}	Cd^{2+}	Mg^{2+}
Log K_1	8.78	7.56	5.32	5.15	5.07	4.00	3.64
Log K_2	1.86	6.25	—	—	—	—	—

The pK^{H}_{OH} value of (B), i.e., N-(2-hydroxy-5-bromobenzylidene)-4-methylaniline, (10.05) is found to be higher than that of (A), i.e., N-(2-hydroxy-5-bromobenzylidene)aniline (9.27). The methyl group at *para* position increases the electron density on the azomethine N through hyperconjugation as well as through $+I$ effect resulting in stronger chelation. This accounts for the higher pK^{H}_{OH} value of the compound (B) as compared to that of compound (A).

In the case of compound (C), i.e., N-(2-hydroxy-5-bromobenzylidene)-4-chloroaniline, the pK^{H}_{OH} value is found to be 8.78 which is lower than that of (A) (9.27). This is due to the $-I$ effect exerted by the chloro substituent at the *para* position in (C).

The orders of the stability constants (Table 1) for the ligands are:

(A) *N-(2-Hydroxy-5-bromobenzylidene)-aniline*:
$Cu^{2+} > Co^{2+} \approx Ni^{2+} > Zn^{2+} > Cd^{2+} > Mg^{2+}$

(B) *N-(2-Hydroxy-5-bromobenzylidene)-4-methylaniline*:
$Cu^{2+} > Zn^{2+} \approx Ni^{2+} > Co^{2+} > Cd^{2+} > Mg^{2+}$

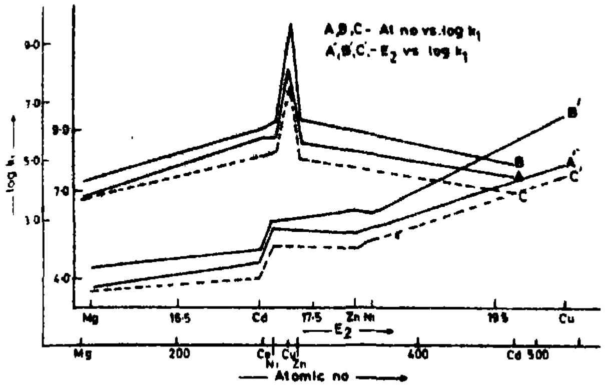

Fig. 1—Plots of log K_1 values against atomic numbers (A, B and C) and log K_1 values against ionization potential (A', B' and C')

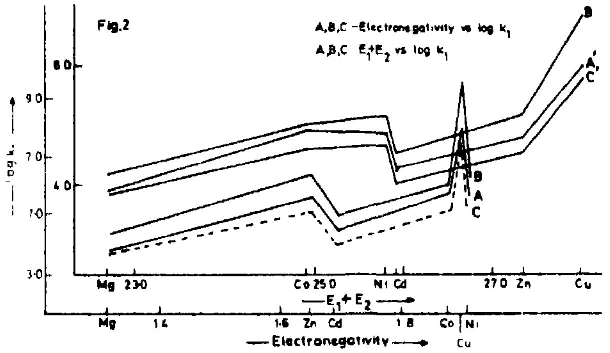

Fig. 2—Plots of log K_1 values against electronegativities (A, B and C) and log K_1 values against $E_1 + E_2$ (A', B' and C')

(C) *N-(2-Hydroxy-5-bromobenzylidene)-4-chloroaniline*:

$Cu^{2+} > Ni^{2+} > Co^{2+} \simeq Zn^{2+} > Cd^{2+} > Mg^{2+}$

The log K_1 values of the metal-ligand systems were plotted against the atomic numbers of the metal ions (Fig. 1). The plots showed a monotonic rise with a maximum at Cu, followed by a fall and lower value of Zn. A similar relationship was observed by Irving and Williams[3]. The above plot shows that stability decreases with increase in basicity of the metal, i.e., weakly basic metal Cu forms stronger chelates and strongly basic metal like Mg forms weaker chelates[4].

In the plots of log K_1 versus second ionisation potential of the metal (Fig. 1), it is observed that for ligands A and C, stability increases from Mg to Co, falls marginally at Zn and then again increases upto Cu, whereas in the case of ligand B, it increases steadily from Mg to Cu, Zn and Ni having practically same stability. This is in consonance with the fact that Zn is not a member of the first transition series[6].

The log K_1 values of the metal-ligand systems were plotted against the electronegativities of the metals (Fig. 2). The stabilities of complexes formed by any ligand with a series of metals may be expected to increase with the increase in electronegativity[5]. In the present case, it is observed that stability increases with the electronegativity of the metal except for Cd and Ni. In the case of Ni it falls rather abruptly.

The stability constants for the ligands A, B and C increase approximately linearly with the sum of the first two ionisation potentials of the gaseous metal atoms, with the exception of Cd where the value falls down (Fig. 2). This presumably indicates an underlying similarity between the electron energy levels in the complex ions and in the corresponding metal atoms[7].

The reagents used in the present investigation are good chelating agents and like EDTA they form strong chelates with Ca^{2+}. It was thought worthwhile to investigate their anticoagulant properties. The anticoagulant activity of these reagents was evaluated by employing 'Dale and Laidlaw' technique[8]. The *in vitro* test was carried out using rabbits whole blood. Normal clotting time was first determined using capillary technique with twenty blood samples drawn from the marginal ear vein of the animal. In order to test for the anticoagulant activity of the compounds, the freshly drawn sample was mixed with about 3-4 mg of the test compound in a glass vial. The capillary was then quickly filled with the blood sample and the clotting time was determined. The normal clotting time was found to be (2.5 ± 0.5 min). The clotting time observed for the compound (A) was 2.5 ± 0.5 min, for compound (B) was 8.25 ± 0.5 min and that for (C) was 15.5 ± 0.2 min.

References

1 Irving H M & Rossotti H S, *J chem Soc*, (1954) 2904.
2 Mayadeo M S, Chaubal A M & Vartak S D, *J Indian chem Soc*, **55** (1978) 450.
3 Irving H & Williams R J P, *J chem Soc*, (1953) 3192.
4 Martell A E & Calvin M, *Chemistry of metal chelate compounds* (Prentice Hall, N.Y.) 1956.
5 Irving H & Williams R J P, *Nature*, **162** (1948) 746.
6 Calvin M & Melchoir N C, *J Am chem Soc*, **70** (1948) 3270.
7 Schwarzenbach G, Ackermann H & Prue J, *Nature*, **163** (1949) 723.
8 Dale H H & Laidlaw P P, *J Pathology Bacteriology*, **16** (1911-12) 351; *Chem Abstr*, **6** (1912) 1016.

Indian Journal of Chemistry
Vol. 27A, May 1988, pp. 458-459

Extraction Chromatographic Separation of Cobalt (II) Thiocyanate Complex with Dibenzo-18-Crown-6

YI YU VIN & S M KHOPKAR*
Department of Chemistry, Indian Institute of Technology, Bombay 400 076

Received 17 *July* 1987; *revised and accepted* 17 *September* 1987

Cobalt is separated from 0.25-2 *M* thiocyanate as a complexing agent with Dibenzo-18-Crown-6 in 1,2-dichloroethane by extraction chromatography. It is stripped with various mineral acids in concentration ranges of 0.5-2 *M* of hydrochloric or sulphuric acid as well as with 0.01-0.5 *M* ammonium chloride. The metal from aqueous phase after stripping has been determined spectrophotometrically with Nitroso-R-salt at 530 nm. Separation of cobalt from its binary mixtures with metal ions such as chromium, molybdenum, nickel, copper, lead, bismuth, vanadium, iron, zinc, cadmium, manganese and aluminium is described.

Several macrocyclic polyethers have been recently used for solvent extraction of *S*-block elements[1]. However similar work on *d*-block elements is rather scanty. Yoshio and Noguchi[2] have described the exractive spectrophotometric determination of cobalt at *p*H 5.0-7.5 with 18-Crown-6 in the presence of protonated *n*-hexylamine and with 4-(2-pyridylazo) resorcinol (PAR) as a counter ion. Yoshio *et al.*[3] attempted to extract cobalt thiocyanate complex with 18-Crown-6 in 1,2-dichloroethane between *p*H 1.0 and 7.0 and its subsequent spectrophotometric determination. However, systematic investigations on the extraction chromatographic separation of cobalt with crown ether as the stationary phase are lacking. The results of such a study are reported in this note.

Standard cobalt solution was prepared by dissolving cobalt chloride (BDH, AR) in deionised water and standardized complexometrically[4]. Dibenzo-18-Crown-6 (Aldrich Chemicals) was used as such. Purified silica gel (100-200 mesh) was rendered hydrophobic by the procedure described earlier[5] and coated with Dibenzo-18-Crown-6 taken in 1,2-dichloroethane. This gel was used both for column extraction and separation work.

To an aliquot of solution containing 15 μg/ml of cobalt, ammonium thiocyanate was added so as to have its concentration as 1 *M*. The solution was passed through the column at a flow rate of 0.5 ml/min. The extracted cobalt was stripped with various mineral acids. Ten fractions of 5 ml each were collected and cobalt from each fraction was determined spectrophotometrically as its complex with Nitroso-R-salt at 530 nm[6].

The results of varying ammonium thiocyanate concentration (from 0.25 to 2.0 *M*) indicate that the extraction of cobalt was quantitative (100%) at 0.5 and 1.0 *M* ammonium thiocyanate. Above or below these concentrations, extraction was less than 99.0% only.

Stripping of cobalt was quantitative with 0.5-2.0 *M* hydrochloric or sulphuric acids or 0.2-1.0 *M* nitric acid. It was also quantitative with 0.01-5.0 *M* ammonium chloride. The stripping was incomplete in concentration less than 0.1 *M* acid.

Certain elements like alkali and alkaline earths as well as chromium, nickel, silver, tin, lead and bismuth do not form extractable complexes in the presence of 1 *M* ammonium thiocyanate. Hence, when the binary mixtures containing cobalt and any of these ions were passed through the column, only cobalt was retained by the column, which could be eluted with 1 *M* ammonium chloride.

Similarly elements like vanadium (V), iron (III), aluminium and antimony form extractable complexes which cannot be stripped with 0.5 *M* ammonium chloride. Hence when binary mixtures containing any of these ions were passed through the column both species were extracted. However, cobalt was first stripped with 0.1 *M* ammonium chloride while other ions were stripped with 4 *M* hydrochloric acid.

Beryllium, cadmium, zinc and manganese also formed thiocyanate complexes along with cobalt and

Table 1—Separation of Cobalt from Binary Mixtures with Other Metal Ion (Co = 15 μg)

Metal ion	Amount taken mg	% Recovery of Co(II)
Na	2.5	100.0
K	2.5	99.3
Cs	2 5	98.7
Be	0.2	100.0
Ca	2.5	101.0
Sr	2.5	99.3
Ba	2.5	100.0
V(V)	0.1	102.0
Cr(VI)	2.0	98.0
Fe(III)	0.1	99.3
Mn(II)	0.1	102.0
Ni	2.5	99.3
Ag	5.0	98.0
Zn	0.1	100.0
Cd	0.1	101.0
Bi	2.0	99.3
Sb	2.5	99.3
Pb	5.0	101.0
Sn	5.0	95.0
Al	2.5	99.0

were co-extracted. They were then separated by stripping cadmium with 0.2 *M* ammonium acetate followed by cobalt with 2 *M* ammonium chloride. Similarly in mixtures of cobalt and beryllium or cobalt and manganese, first cobalt was eluted with 0.01 *M* ammonium chloride while beryllium or manganese was eluted with 0.5 *M* hydrochloric acid. It was thus possible to separate the elements which are generally associated with each other in binary mixtures in ratios varying from 1:1 to 1:10. In all the cases cobalt after stripping was determined spectrophotometrically at 530 nm (Table 1).

The method is simple, rapid and reproducible and permits separation of cobalt at microgram concentration.

We are thankful to Dr(Mrs) Chhaya Dixit for carrying out a part of the work and to the CSIR, New Delhi, for the award of a junior research fellowship to Yi Yu Vin.

References

1 Mohite B S, *Solvent extraction separation of alkali and alkaline earths with macrocyclic polyethers* (i.e. Crown Ethers), Ph D Thesis, IIT Bombay (1987).

2 Yoshio M & Noguchi H, *Anal Lett*, **A15** (1982) 1197.

3 Yoshio M, Ugamara M & Nagamatsu M, *Anal Lett*, **A 11** (1978) 281.

4 Vogel A I, *A textbook of quantitative inorganic analysis* (Longman Green, London) 1962, 443.

5 Bhosale S N & Khopkar S M, *Talanta*, **26** (1979) 889.

6 Sandell E B, *Colorimetric determination of traces of metals* (Interscience, New York) 1959, 415.

Indian Journal of Chemistry
Vol. 27A, May 1988, pp. 460-462

Use of Nickel Phosphate Membrane as an Ion Sensor with Special Reference to Phosphate Ion

M N BEG* & M ARSHAD
Department of Chemistry, Aligarh Muslim University,
Aligarh 202 001

Received 21 *May* 1987; *revised and accepted* 9 *November* 1987

The parchment supported nickel phosphate membrane electrode has been tested for its ability to sense various inorganic ions in aqueous solution using potentiometric method. The electrode is found to have optimum sensitivity with 0.1 M KH_2PO_4 as the internal solution. The test solutions used are KCl, KBr, KI, NaCl, LiCl, $MgCl_2$, $CoCl_2$, KNO_3, K_2SO_4, K_3PO_4, $K_4Fe(CN)_6$ and $K_3Fe(CN)_6$. The electrode shows dynamic response and the shapes of EMF versus concentration curves are similar to those obtained with an ion selective electrode. The potentiometric selectivity for phosphate ion as compared to SO_4^{2-}, $Fe(CN)_6^{4-}$, $Fe(CN)_6^{3-}$ has been also determined in terms of apparent selectivity and effective ΔE value.

The development of phosphate ion selective electrodes has received special attention during the past decade because of their possible use in environmental monitoring, sewage treatment, detection of phosphate ions in boiler water, fertilizers and soils etc. Guilbault[1] prepared various inorganic phosphates embedded in silicon rubber and utilized them as phosphate sensors. Nanjor *et al.*[2] investigated the use of polyphenyl-onium bases in the preparation of phosphate ion selective electrodes. Midgley[3] prepared composite-pressed membrane electrode using Ag_2S, PbS and $PbHPO_4$ while Novozamski[4] used Ag_3PO_4 to develop a phosphate ion selective electrode. All these electrodes gave reproducible results, showed dynamic Nernstian response but lacked in selectivity, had high response time and even serious interferences. Attempts[5] have also been made to develop phosphate ion selective electrode using liquid membranes but due to the lack of selectivity, complications arising from unfixed sites and short life span, little progress has been achieved with such electrodes[6]. We have in a series of communications, demonstrated that parchment supported inorganic precipitate membranes carry small density of fixed charge and that the interionic jump distance is about 1.5 Å (refs 7-13). In this note we describe the use of parchment supported nickel phosphate membrane as an ion sensor with special reference to phosphate ion.

Nickel phosphate membrane was prepared by the method of Beg *et al.*[13]. The membrane electrode was assembled as shown in Fig. 1. Two saturated calomel electrodes and a Pye-precision vernier potentiometer were used to monitor the electrical potential. Different concentrations of KH_2PO_4 and K_3PO_4 were used as internal reference and external test solutions. It was observed that the best data could be obtained with 10^{-1} M solution. If the concentration of the internal reference solution was higher, the electrode response was poor, whereas at lower concentration, the results were not reproducible. The various electrolyte solutions of type 1:1, 1:2, 1:3, 1:4 and 2:1 at different concentrations were used as test solutions. These solutions were kept stirred by a glass coated magnetic stirrer. The whole cell assembly was kept in a water thermostat maintained at 25 ± 0.1°C. The results were reproducible to better than ± 0.5mV. The electrolyte solutions were prepared using AR grade chemicals (BDH, India) and deionized water.

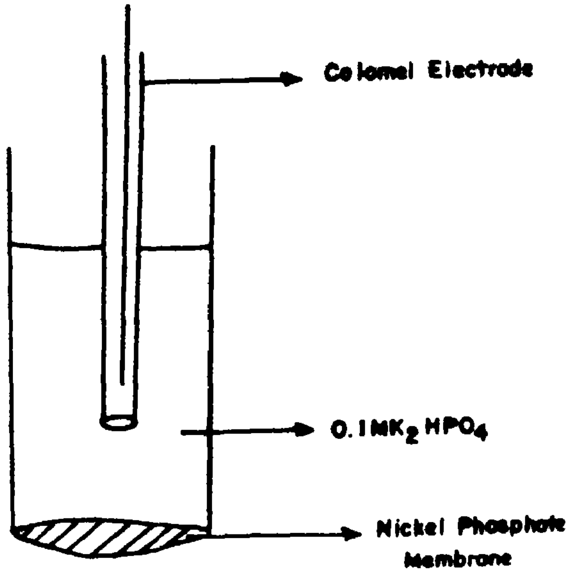

Fig. 1—Nickel phosphate membrane electrode

The electric potentials observed across nickel phosphate membrane using 10^{-1} M KH_2PO_4 as reference solution and a number of 1:1, 1:2, 1:3, 1:4 and 2:1 electrolytes at different concentrations as test solutions are depicted in Figs 2 and 3. The value of E with 1:1 and 2:1 electrolytes is positive when the membrane is in contact with concentrated solutions, whereas it gradually decreases with decrease in electrolyte concentration and finally becomes negative. In the case of 1:2, 1:3 and 1:4 electrolytes an opposite phenomenon is observed, i.e., E is negative at higher electrolyte concentration and increases with decrease in concentration. This type of change in mem-

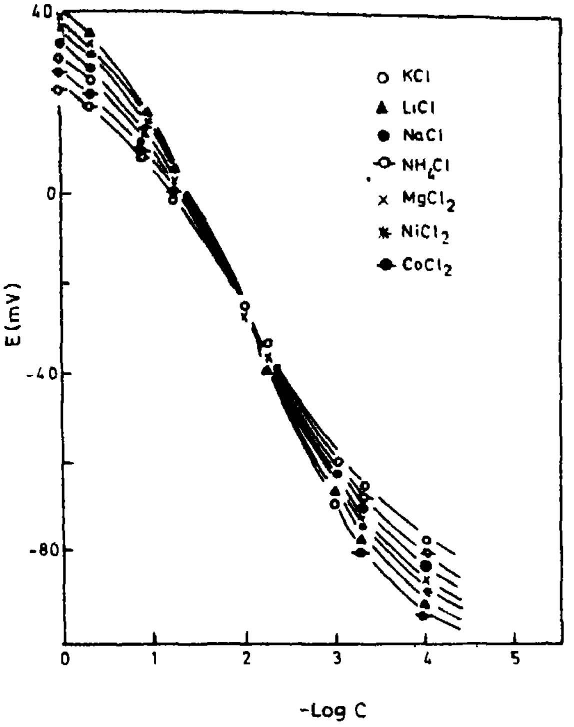

Fig. 2—Response of nickel phosphate membrane electrode with various 1:1 and 2:1 electrolyte solutions at different concentrations using $10^{-1}M$ KH$_2$PO$_4$ as reference solution at 25 ± 0.1°C

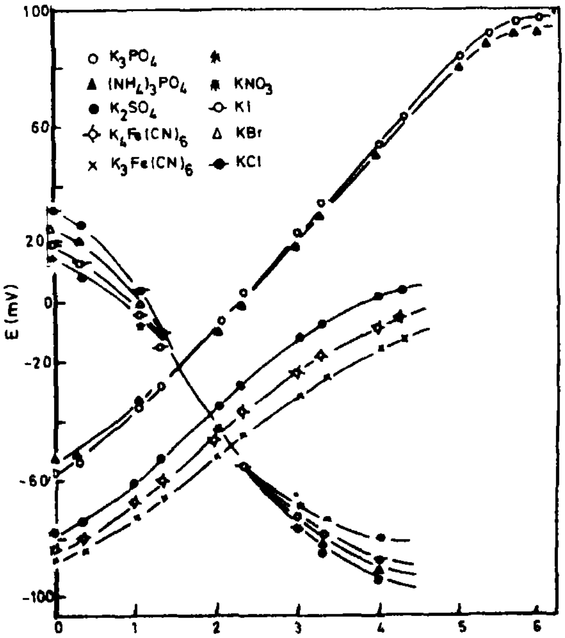

Fig. 3—Response of nickel phosphate membrane electrode with various 1:1, 1:2, 1:3 and 1:4 electrolyte solutions at different concentrations using $10^{-1}M$ KH$_2$PO$_4$ as reference solution at 25 ± 0.1°C

Table 1—Potentiometric Selectivity of Nickel Phosphate Membrane Electrode with $10^{-1}M$ Salt Solutions at 25 ± 0.1°C

Parameter	Anion pairs		
	SO_4^{2-}/PO_4^{3-}	$Fe(CN)_6^{4-}/PO_4^{3-}$	$Fe(CN)_6^{3-}/PO_4^{3-}$
Apparent selectivity	10.0	31.7	78.5
Effective ΔE(mV)	27.4	34.5	41.0

brane potential vis-a-vis reversal in the selectivity character of the membrane is not particular to this system[14,15].

It is noted in Figs 2 and 3 that potential changes with ionic concentrations and that Nernstian trend is followed with every electrolyte used as test solution. The slopes of the lines are negative with 1:1 and 2:1 electrolytes whereas these are positive with 1:2, 1:3 and 1:4 electrolytes. The potential versus concentration curves for NaCl, LiCl, MgCl$_2$, CoCl$_2$, KNO$_3$, KBr and KI lie closer to each other whereas for the electrolytes of the type 1:2, 1:3 and 1:4, the curves are separated, the curves for K$_3$PO$_4$ being at one extreme end. These investigations reveal that the electrode with $10^{-1}M$ KH$_2$PO$_4$ *as reference solution may be utilized for the* quantitative estimation of a number of electrolytes; the membrane cannot distinguish significantly between cations but has preferential selectivity for multivalent anions. The selectivity sequence of the membrane electrode for anion is (Fig. 3): $PO_4^{3-} > SO_4^{2-} > Fe(CN)_6^{4-} > Fe(CN)_6^{3-}$.

The selectivity of membrane electrode for an ion was examined by comparing potentiometric response of the membrane electrode to $10^{-1}M$ K$_3$PO$_4$ with the response of $10^{-1}M$ potassium salts of other common anions. The results of these investigations are given in Table 1, both in terms of apparent selectivity ratio and EMF difference, ΔE. The selectivity has been defined here as the ratio of anion to phosphate ion concentration required to yield same cell EMF under identical conditions; ΔE value is the difference in cell EMF obtained when a $10^{-1}M$ of potassium salt of the anion is compared with a $10^{-1}M$ solution of K$_3$PO$_4$. It is seen from Table 1 that the selectivity sequence $PO_4^{3-} > SO_4^{2-} > Fe(CN)_6^{4-} > Fe(CN)_6^{3-}$ obtained in this way is the same as found by plotting method described earlier. Since the values of the apparent selectivity and ΔE for the three anion pairs SO_4^{2-}/PO_4^{3-}, $Fe(CN)_6^{4-}/PO_4^{3-}$, and $Fe(CN)_6^{3-}/PO_4^{3-}$ are quite high, it may be concluded that the presence of a small amount of anion like SO_4^{2-}, $Fe(CN)_6^{4-}$ or $Fe(CN)_6^{3-}$ will not cause serious error in the estimation of phosphate ions using potentiometric method.

References

1 Guilbault G G, *Analyt Chem*, **41** (1969) 1156.
2 Nanjor M, *Analyt chim Acta*, **77** (1975) 19.
3 Midgley D, *Talanta*, **26** (1979) 267.
4 Novozomski J, *Analyt chim Acta*, **84** (1978) 41.
5 Guilbault G G & Brignac P J, *Analyt chim Acta*, **56** (1971) 139.
6 Al-Sibaac A A, *Proc Anal Div Chem Soc*, **12** (1975) 65.
7 Beg M N, Siddiqi F A & Shyam R, *Can J Chem*, **55** (1977) 1680.
8 Beg M N, Siddiqi F A, Shyam R & Altaf I, *J electro Chem*, **98** (1979) 231.
9 Beg M N, Siddiqi F A & Prakash P, *J polym Sci*, **17** (1979) 539.
10 Beg M N, Ahmad K, Altaf I & Arshad M, *J membrane Sci*, **9** (1981) 303.
11 Beg M N, Siddiqi F A, Ahmad K & Altaf I, *J electro Chem*, **122** (1981) 313.
12 Beg M N, Shyam R & Khandedval, *Acta chim Acad Sci Hung*, **110** (1982) 65.
13 Beg M N, Siddiqi F A, Shyam R & Arshad M, *J membrane Sci*, **2** (1977) 362.
14 Tien H T & Ting H P, *J Colloid Interface Sci*, **27** (1968) 702.
15 Beg M N, Siddiqi F A, Shyam R & Altaf I, *J electroanal Chem*, **89** (1978) 141.

Indian Journal of Chemistry
Vol. 27A, May 1988, pp. 463-464

Extractive Spectrophotometric Determination of Zirconium with Ferron

S P ARYA* & (Miss) VEENA SLATHIA
Department of Chemistry, Kurukshetra University, Kurukshetra 132 119

Received 23 *January* 1987; *revised* 1 *June* 1987; *rerevised and accepted* 21 *Sepetmber* 1987

Zirconium(IV) has been extracted as its ferron complex with tribenzylamine in chloroform and determined spectrophotometrically by measuring the absorbance of the complex at 400 nm. Beer's Law is obeyed over the range 0.2-7 μg Zr/ml with a sensitivity of 0.006 μg Zr/cm^2. The method is free from interference of large amounts of manganese(II), iron(III), cobalt(II), nickel(II), zinc(II), aluminium(III), uranium(VI), thorium(IV), silver(I), mercury(II), and lead(II). The tolerance limit for tungsten(VI), titanium(IV), copper(II), tin(II), chromium(VI), vanadium(V) and molybdenum(VI) is comparatively low.

Ferron has been used as a spectrophotometric reagent for many elements[2-5] either in aqueous solution or after extracting the corresponding ferronate complexes into water-immiscible solvents. Zirconium has been found to form a complex with ferron which is extractable into tribenzylamine in chloroform and we report here the results of our studies on this system.

A zirconium stock solution (5 mg/ml) in 0.1 *N* HCl was prepared from zirconium oxychloride. 5 ml of the stock solution on dilution to 250 ml with distilled water afforded a solution with 100 μg Zr/ml. A stock solution of ferron (0.15%) in distilled water was prepared. Tribenzylamine (TBA) solution (1%) was prepared in chloroform.

Absorbance measurements were carried out using a 550 S Perkin-Elmer spectrophotometer having a pair of matched 1 cm glass cells.

Determination of zirconium

An aliquot containing 5-175 μg of zirconium was taken and its *p*H was adjusted to about 5 followed immediately by the adition of 1 ml of 2*N* sulphuric acid and 10 ml of aqueous ferron solution; enough distilled water was added to get a 20-ml aqueous phase. The contents were heated on a water bath for 10 min. The contents were allowed to cool and transferred to a 100-ml separatory funnel containing 10 ml of TBA-chloroform solution. The contents were shaken gently for 2 min. After the separation of the two phases, the solvent phase was removed into a 25-ml volumetric flask. The extraction was repeated with another 10 ml portion of TBA-chloroform solution and the two extracts were combined; then the volume was made up to the mark with chloroform. The absorbance of the greenish yellow complex was measured at 400 nm against a similarly treated reagent blank. Zirconium content was computed from a calibration curve.

The complex shows λ_{max} at 400-405 nm while the reagent blank shows strong absorption at 340 nm which decreases sharply to a very low value as the wavelength reaches 400 nm.

The effect of various parameters on the extraction of zirconium(IV)-ferronate complex is shown in Table 1. These parameters were studied by keeping the optimum concentration of other parameters constant and varying the one under study. On the basis of these studies, the optimum conditions for maximum absorbance have been found to be: 0.08-0.1 *N* sulphuric acid in the aqueous phase, 10-15 ml of 0.1% ferron, 1-2% TBA in chloroform, and 2-4 min of equilibration time. The reaction of zirconium(IV) with ferron is found to be slow at room temperature as zirconium(IV) is extensively hydrolysed in neutral or slightly acidic solutions resulting in precipitation depending on its concentration. The hydrolysed and polymerized species of zirconium(IV) does not react readily with the reagents. Hence 10-20 min of heating is required to obtain maximum absorbance. The reaction is dependent on the temperature of water-bath and it is found that the absorbance increases with the temperature, becoming highest at 100°C.

Table 1 — Dependence of the Zr(IV)-Ferronate Extraction on Different Parameters

[Zr(IV) = 6 μg/ml in the solvent phase]

Acidity	Ferron conc.	TBA conc.	Absorbance
(*N*, H_2SO_4)	(0.1%)	(in $CHCl_3$)	
0	10 ml	1%	0.001
0.02	10 ml	1%	0.16
0.04	10 ml	1%	0.518
0.08-0.1	10 ml	1%	0.992
0.2	10 ml	1%	0.682
0.4	10 ml	1%	0.21
0.08	2 ml	1%	0.171
0.08	4 ml	1%	0.674
0.08	8 ml	1%	0.896
0.08	10 ml	1%	0.992
0.08	10 ml	0.1%	0.673
0.08	10 ml	0.5%	0.908
0.08	10 ml	1.0%	0.992
0.08	10 ml	2.0%	0.992

The complex is not extracted by benzene, chloroform, carbon tetrachloride, carbon disulphide, nitroethane, nitromethane, isoamyl acetate, methyl isobutyl ketone or ethyl acetate; it is slightly extracted by isoamyl alcohol and better by *n*-butanol. The complex is readily extracted by tertiary amines, and tribenzylamine dissolved in chloroform has been found to be the most suitable extractant. Beer's law is obeyed in the range 0.2-7 μg of Zr/ml of solvent phase with a Sandell sensitivity of 0.006 μg Zr/cm^2 which can be further enhanced to 0.0038 μg Zr/cm^2 if a single extraction is carried out. The complex is stable for at least 24 hr.

Effect of diverse ions

The effect of various anions and complexing agents on the extraction of zirconium has been studied. Chloride and sulphate do not interfere. The tolerance to other anions and complexing agents is limited. Only 0.1 g each of hydrazine sulphate, sulphosalicylic acid, sodium acetate; 0.05 g of sodium sulphite; and 0.01 g each of thiourea and ascorbic acid are tolerated. Phosphate, citrate and tartrate lower the extration considerably. Oxalate, fluoride and ethylenediaminetetraacetic acid, even in small amounts, mask the zirconium extraction completely.

Iron(III) gives a green coloured complex with ferron which is extractable into TBA-chloroform solution. Extraction of iron can be prevented by reducing it to iron(II) by hydrazine sulphate and then passing carbon dioxide through the aqueous phase which prevents the reoxidation of any iron(II) during shaking. Chromium(VI) gives orange coloured extract. Chromium(VI) is also reduced to chromium(III) by hydrazine sulphate, which is not extracted when alone but suppresses the extraction of zirconium. Thorium gives a white precipitate under the proposed conditions and causes emulsion formation thus lowering its tolerance limit; otherwise it is not extracted and so is the behaviour of bismuth(III). Silicon taken as silicate does not interfere. Uranium(VI) gives a faint yellowish green colour when present in large amounts but is tolerated in amounts as mentioned. Calcium, strontium and barium form insoluble sulphates which need not be filtered. The tolerance limits for these elements in 20 ml of solution are: 100 mg each of beryllium, magnesium, mercury, silicon; 50 mg each of aluminium, calcium, strontium, barium, cadmium, nickel, cobalt, manganese, iron, zinc, silver, thalium, lanthanum; 10 mg of thorium; and 5 mg each of bismuth and uranium. The tolerance limits (in μg amounts) for W(VI) 500; Ti(IV) 50; Cu(II) 20; Sn(II) 20; Cr(VI) 10; V(V) 10; Mo(VI) 5 is rather low.

The authors are thankful to the Chemistry Department, University of Jammu, for providing facilities to carry out a part of this work during the tenure of one of the authors (SPA) there.

References

1 Kolthoff I M & Elving P J, *Treatise on analytical chemistry*, Part 2, Vol 5 (Interscience Publishers, New York), 1961, 66.
2 Yatirajam V & Arya S P, *Anal chim Acta*, **86** (1976) 209.
3 Malik A U, *Indian J Chem*, **3** (1965) 446.
4 Brady J B & Frantz J D, *Year book—Carnegie inst Washington*, 1978, 676.
5 Rusheed A, Ahmed S & Fjaz M, *J radioanal Chem*, **49** (1979) 205.

Indian Journal of Chemistry
Vol. 27A, May 1988, pp. 465-466

Thioridazine Hydrochloride as a New Reagent for Rapid Spectrophotometric Determination of Iridium(IV)

H SANKE GOWDA* & G K REKHA
Department of Chemistry, Central College,
Bangalore University, Bangalore 560 001

Received 24 *July* 1987; *revised and accepted* 21 *August* 1987

Thioridazine hydrochloride is proposed as a new reagent for the rapid spectrophotometric determination of iridium(IV). The reagent instantaneously forms a blue coloured species with iridium(IV) at room temperature in 4*M* phosphoric acid medium having an absorption maximum at 635nm. Beer's law is obeyed over the concentration range 0.2-9.0 μg/ml of Ir(IV) with an optimum concentration range of 2.0-8.0 μg/ml of Ir(IV). The method has been used for the selective determination of Ir(IV) in the presence of Pt(IV), Rh(III) and Pd(II).

Methods for the spectrophotometric determination of iridium are limited in number and in most of these methods separation of rhodium, palladium and platinum is necessary or the time for maximum colour development is long. We have presently found that 2-methylmercapto 10-[2-(1-methyl-2-piperidyl)ethyl] phenothiazine hydrochloride or thioridazine hydrochloride (TH) instantaneously forms a blue coloured species with Ir(IV) at room temperature in acid solution. This colour reaction has been used for the spectrophotometric determination of Ir(IV).

Stock solution of Ir(IV) was prepared in doubly distilled water containing a little HCl from sodium chloroiridate(IV) (Johnson Matthey, London) and standardised potentiometrically[1]. Appropriate dilution of the stock solution gave the working solution containing 100 μg/ml of Ir(IV). The reagent solution (0.2% wt/vol) was prepared in doubly distilled water and stored in an amber coloured bottle. Solutions of diverse ions of suitable concentrations were prepared using AR grade reagents. Hitachi 150-20 spectrophotometer with matched 1cm quartz cells was used for absorbance measurements.

Procedure

To an aliquot of stock solution containing 50-200μg of Ir(IV) were added phosphoric acid (5*M*, 20ml) and the reagent solution (2ml) and the volume was made upto 25ml with doubly distilled water. The solution was mixed well and its absorbance measured at 635nm against the corresponding reagent blank. The amount of iridium in the sample was deduced from the standard calibration curve.

Phosphoric acid is chosen because in the presence of hydrochloric acid, sulphuric acid or walpole buffer media, the reaction is less sensitive, the blue coloured species is less stable and many foreign ions interfere even at low concentrations. The maximum colour development is observed in 3-6 *M* phosphoric acid. The absorbance decreases below 3*M* and slightly increases above 6*M* phosphoric acid. A 4 *M* phosphoric acid medium is chosen in which the absorbance is stable for 1hr. A 10-fold molar excess of the reagent is necessary for maximum colour development. The blue species exhibits maximum absorption at 635nm. The reagent blank and the metal ion under similar conditions do not absorb around this wavelength. There is no appreciable change in the absorbance if the order of addition of reactants is varied. The absorbance values are not affected over the temperature range 5-40°C, but beyond 40°, the absorbance gradually decreases. The blue species is cationic in nature as revealed by ion-exchange experiments.

Table 1—Determination of Iridium in Synthetic Mixtures

Synthetic mixture	Amount of Ir(IV)taken (ppm)	Metal ion added (ppm)			Amount of Ir(IV) found* (ppm)	Relative error %
		Rh	Pt	Pd		
In-Rh-Pt	3.0	16.0	4.0	4.0	3.02	+0.66
	5.0	20.0	7.0	8.0	5.03	+0.60
Ir-Rh-Pd	4.0	12.0	6.0	10.0	4.04	+1.00
	6.0	18.0	5.0	12.0	5.98	−0.33
Ir-Rh-Pd-Pt	4.0	24.0	6.0	9.0	3.97	−0.75
	7.0	20.0	7.0	12.0	6.94	−0.85

*Average of six determinations

Beer's law is obeyed over the concentration range 0.2-9.0 μg/ml of Ir(IV). The optimum concentration range as evaluated by Ringbom's method[2] for the effective spectrophotometric determination of Ir(IV) is 2.0-8.0 μg/ml. The Sandell's sensitivity and molar absorptivity are 25 ng cm^{-2} and $7.59 \times 10^3 dm^3 cm^{-1} mol^{-1}$ respectively. The standard deviation calculated from six determinations in a solution containing 4 μg/ml of Ir(IV) is 0.003 and the relative error is less than 2%.

Effect of diverse ions

The interference of 33 ions was studied in the determination of 4 μg/ml of Ir(IV). The following amounts (μg/ml) of foreign ions give an error of less than 2%: Pt(IV), 2; Pd(II), 0.5; Rh(III), 36; Ru(III), 0.8; Os(VIII), 0.5; Au(III), 0.4; Ag(I), 8; Fe(III), 50; Ni(II), 100; Cu(II), 100; Cr(III), 400; Mg(II), 8000; U(VI), 850; Th(IV), 1990; Zr(IV), 1000; Zn(II), 700; Pb(II), 2000; Hg(II), 200; Mo(VI), 400; Bi(III), 8; acetate, 2800; tartrate, 1200; citrate, 5000; oxalate, 3000; fluoride, 400; bromide, 1600; iodide, 35; sulphate, 7000; nitrate, 40; EDTA, 50; DMG, 200; thiourea, 2; and thiocyanate, 5. The tolerance limit of Ru(III) and Pt(IV) could be raised to 2.0 and 8.0 μg/ml respectively using 2 μg/ml of thiourea as masking agent, that of Pd(II) to 16 μg/ml using 50 μg/ml of DMG and that of Au(III) to 10 μg/ml using 1 μg/ml of thiocyanate.

Analysis of synthetic mixtures

Synthetic mixtures containing varying compositions of Ir(IV), Pt(IV), Rh(III) and Pd(II) were prepared and the Ir(IV) content was determined following the standard procedure. The results presented in Table 1 show that determination of Ir(IV) is possible in presence of Pt(IV), Rh(III) and Pd(II). DMG and thiourea were used as masking agents for Pd(II) and Pt(IV) respectively.

The authors thank the UGC, New Delhi, for financial assistance.

References

1 Beamish F E, *The analytical chemistry of noble metals* (Pergmon Press, Oxford), 1966, pp 332 and 334.
2 Ringbom A Z, *Analyt Chem*, **115** (1938) 332.

Indian Journal of Chemistry
Vol. 27A, May 1988, p. 467

Potassium Butyl Xanthate as a Spectrophotometric Reagent for Iron(III)

P K PARIA* & S K MAJUMDAR
Department of Chemistry,
North Bengal University, Darjeeling 734430

Received 29 *December* 1986; *revised* 30 *July* 1987; *accepted* 11 *September* 1987

Iron(III) forms a brown 1:3 (metal:ligand) complex with potassium butyl xanthate in aqueous solution. A single extraction in the *p*H range 3-6 is adequate for quantitative extraction of the complex into chloroform. Beer's law is obeyed over a concentration range 2-25 ppm of iron. The system tolerates 10 to 50-fold excess of diverse ions. Palladium, vanadium, molybdenum, fluoride and citrate interfere. The molar absorptivity of the complex is 1.14×10^3 dm^3 mol^{-1} cm^{-1} and Sandell's sensitivity is 0.008 μg/cm^2 at 460 nm.

Iron(III) is known to interfere in the spectrophotometric determination of nickel, palladium and cobalt when xanthates are used as a spectrophotometric reagents[1]. Analytical application of potassium butyl xanthate has now been extended for the spectrophotometric determination of iron(III).

A Shimadzu PR-1 spectrophotometer fitted with optically matched quartz cells of 10 mm path lengths was used for absorbance measurements. Potassium butyl xanthate was prepared and purified in the laboratory[2] and the solution (0.25%) was prepared in conductivity water. Stock solution of iron(III) was prepared from ferric chloride and standardised volumetrically[3]. A working solution (107.7 μg Fe/ml) was prepared by dilution. Standard solutions of diverse ions were prepared from their chlorides, sulphates or from sodium/potassium/ammonium salts. Acetate buffer was used to maintain the required *p*H.

General procedure

To an aliquot containing 20-250 μg of iron was added the reagent solution (1 ml), diluted to 10 ml with acetate buffer (*p*H 4) and left for 1 min to ensure completion of reaction. The reaction mixture was extracted with pre-distilled chloroform (10 ml) for 1 min. The organic extract was separated, dried over anhydrous Na_2SO_4, and its absorbance was measured at 460 nm against a reagent blank. Iron(III) was determined from a calibration curve. To study the interference the respective foreign ions were added to the system before the dilution step.

Though the brown coloured iron complex exhibits absorption maxima at 555 nm, the shoulder around 460 nm was chosen for absorbance measurements. The reagent blank did not absorb from 400 nm onwards. It was observed that the extraction of iron complex by chloroform was complete in the *p*H range of 3-6. Further 1 ml of 0.25% reagent solution was sufficient to extract 107.7 μg iron in a single extraction. Larger amounts of the reagent have been used to study the interference of diverse ions. The system conformed to Beer's law both at 555 and 460 nm over a concentration range of 2-25 ppm of iron. The molar absorptivity of the complex was calculated to be 1.14×10^3 dm^3 mol^{-1} cm^{-1} and Sandell's sensitivity worked out to be 0.008 μg/cm^2 at 460 nm.

Mol ratio method indicated 1:3 stoichiometry (metal:ligand) for the complex. Colour was stable at least for 24 hr.

In order to study the effect of diverse ions on the extraction behaviour, a definite amount of iron(III) was extracted and determined according to the general procedure in the presence of the respective foreign ions. An ion was considered to interfere if the recovery of iron(III) differed by more than ± 3% from the actual amount taken. It was found that 107.7 μg of Fe could easily be determined without any interference in the presence of the following cations, the amounts (mg) taken being mentioned in parentheses: Ca(II)(5), Ba(II)(5), Sr(II)(5), Pb(II)(3), Zr(IV)(2), U(VI)(5), Rh(III)(5), Zn(II)(5), Mn(II)(2), Al(III)(5), Pt(IV)(1), Ce(III)(5), Be(II)(5), Cd(II)(2), Hg(II)(2), Th(IV)(5), Cu(II)(5), Cr(III)(5), Mg(II)(5), La(III)(5), Ti(IV)(5), Sn(II)(3). The interference due to nickel(II) and cobalt(II)(5) was masked by adding EDTA. Vanadium(V), Pd(II) and Mo(IV) interfered. Among the anions tested citrate and fluoride were found to interfere.

The accuracy of the proposed method was 1.91% and the method took 10-15 min for analysis.

References

1 Paria P K & Majumdar S K, *Indian J Chem*, **24A** (1985) 629.
2 Vogel A I, *A textbook of practical organic chemistry* (Orient Longmans, London), 1969.
3 Vogel A I, *A textbook of quantitative inorganic analysis* (Orient Longmans, London), 1978.

Indian Journal of Chemistry
Vol. 27A, May 1988, p. 468

Announcements

National Conference on Coordination Chemistry

A national conference on "Coordination Chemistry: Modern Trends and Future Prospects" will be held during January 15-20, 1989 at the Department of Chemistry, University College of Science, 92, A.P.C. Road, Calcutta 700009.

The following subject areas will be covered: (A) synthesis, structure and bonding; (B) thermodynamics of metal-ligand interaction; (C) energetics, dynamics and reaction mechanisms; (D) environmental and biological coordination chemistry; (E) coordination chemistry in catalysis and other applications; and (F) coordination chemistry in curriculum. The last date for registration is 31 August 1988. Further information may be obtained from:

Prof. D Banerjea
Department of Chemistry
Calcutta University
92, A.P.C. Road, Calcutta 700009

International Symposium on Gas Separation Technology

An international symposium on Gas Separation Technology will be held in Antwerp, Belgium, from 10 to 15 September 1989. The symposium will deal with both fundamental aspects and practical applications of gas separation and purification. Major emphasis will be laid on the latest developments in these fields using sorbents, membranes, cryogenic techniques and chemical processes (including catalysis). A special session will be devoted to accurate gas measurements.

For further information contct Dr R. Dewolfs (Secretary), University of Antwerp (U.I.A.), Dept. of Chemistry, Universite-itsplein 1, B-2610 Antwerp-Wilrijk, Belgium.

Indian Journal of Chemistry
Vol. 27A, June 1988, pp. 469-473

Topological Investigations of the Viscous Behaviour of Binary Mixtures of Non-electrolytes

PREM PAUL SINGH
Department of Chemistry, Maharshi Dayanand University, Rohtak 124 001

Received 9 *June* 1987; *revised* 21 *September* 1987; *accepted* 9 *November* 1987

A graph theoretical approach has been developed to evaluate viscosity change ($\Delta\eta$) data on mixing components of binary mixtures of non-electrolytes. The approach describes well the ($\Delta\eta$) data of those binary mixtures whose components do not undergo complexation reaction. A simple relation has also been developed between ($\Delta\eta$) and molar excess volume (V^E) of an (A+B) mixture. The relationship is quite successful in describing ($\Delta\eta$) data of even those (A+B) mixtures which are characterised by specific interactions between their components or when A is associated in the pure state and the addition of B causes rupture of this association.

A binary (A+B) mixture is formed by the replacement of like contacts in the pure A and B by unlike contacts A−B in the mixture. Consequently, there must be some correlation between the molar excess volume (V^E) and the viscosity change ($\Delta\eta$) data of a binary liquid mixture. The rupture of like contacts in the pure A and B and the formation of new A−B contacts in the (A+B) mixtures may be described mathematically using graph theory[1-6] treating structural formulas of organic compounds as molecular graphs. In the present investigation an approach has been developed to (i) evaluate ($\Delta\eta$) data and (ii) correlate V^E and ($\Delta\eta$) data of an (A+B) mixture.

Method of Calculation & Results

The resistance to flow of a liquid has been attributed to velocity gradient between the liquid layers. Each layer exerts a drag on the next layer, and for Newtonian flow the magnitude[7] of the retarding force has been taken to be proportional to the velocity gradient and to the area of contact between the moving liquid layers. In the case of the organic molecules the effective area of contact between the moving liquid layers depends on the length of the carbon-carbon (C−C) backbone and the degree of branching of the molecules of the liquid. Larger the C−C chain length, larger would be the effective area of contact of the moving liquid layers, and hence larger would be the viscosity. But larger the degree of branching in a molecule, smaller would be the area in effective contact between the moving liquid layers, and so smaller would be the viscosity. This is corroborated by the available viscosity data[8-12] at 288.15K of a number of liquid non-electrolytes where η is found to vary as: isopentane < *n*-pentane; *n*-heptane < 2, 3-dimethyl-pentane; 3,3-dimethylpentane < *n*-nonane; chloroform < carbon tetrachloride, chlorobenzene < bromobenzene; benzene < *m*-xylene < *p*-xylene. It is interesting to point out that the molar volumes of these liquids also vary in the same manner. Kier[13] and Singh *et al.*[14] have shown that the molar volumes of most of the liquid non-electrolytes depend directly on ${}^1\zeta$ and inversely on ${}^3\zeta$ parameters of these molecules. It appears, therefore, that the viscosity, η, of these liquids must have a similar type of dependence on ${}^1\zeta$ and ${}^3\zeta$ parameters of these molecules. Consequently, following Kier[13] and Singh *et al.*[14], we express η of a liquid by,

$$\eta = \alpha_V{}^3\zeta + \beta_V{}^1\zeta + \gamma_V \qquad \dots (1)$$

where α_V, β_V and γ_V are constants and ${}^1\zeta$ and ${}^3\zeta$ are connectivity parameters of the first and the third degree respectively and are defined[14] by,

$${}^1\zeta = \sum_{i<j} (\delta_i\delta_j)^{-0.5} \qquad \dots (2)$$

$${}^3\zeta = \sum_{i<j}\sum_{j<k}\sum_{k<l} (\delta_i\delta_j\delta_k\delta_l)^{-0.5} \qquad \dots (3)$$

where δ_i denotes the valency[14] of the *i*th vertice in the graph of the molecule.

In order to check as to how well Eq. 1 reproduces the η values of liquid non-electrolytes, we utilized the η values[12] at 288.15K of *n*-pentane, *n*-hexane and *n*-heptane to evaluate α_V, β_V and γ_V parameters of Eq. (1), and these in turn were used to evaluate η of a number of alkanes. These η values are recorded in Table 1 and are also compared with the corresponding literature values[8-12]. It is quite apparent from Table 1 that the predicted η values are mostly within 10 percent (20 percent in a few cases)

Table 1—Comparison of η Values Calculated at 288.15K from Eq. 1 with The Corresponding Literature Values for Some Liquid Non-electrolytes

	η (millipoise)		$^3\zeta$	$^1\zeta$
	Calc.	Lit.		
Isopentane	2.18	2.34[12(b)]	0.817	2.27
2-Methylpentane	3.08	3.24[9]	0.866	2.770
3-Methylpentane	3.20	3.39[9]	1.393	2.807
2,2-Dimethylpentane	3.62	4.01[10]	1.000	3.061
2,3-Dimethylpentane	3.85	4.36[9]	1.213	3.180
2,5-Dimethylhexane	4.63	5.12[12(f)]	1.322	3.614
n-Octane	5.17	5.79[12(e)]	1.457	3.914
n-Nonane	6.88	7.50[12(g)]	1.707	4.414

of the literature values. We next employed η data[15] at 298.15K of benzene *m*-xylene and *p*-xylene to evaluate η of toluene. The calculated η (toluene) value of 6.80 millipoise agrees within 10 percent with the corresponding literature value[15] (6.23 millipoise) even though the molar valume of toluene is more than that of benzene and its viscosity is less than that of benzene. We hope that Eq. 1 would also describe well the η data of other liquid non-electrolytes.

The ideal viscosity, η_{id}, of the mixture ($x_A A + x_B B$) (where x_A is the mole fraction of A), would then be given by,

$$\eta_{id} = \Sigma x_A \cdot \eta_A = x_A \alpha_{V_A}/{}^3\zeta_A + x_A \beta_{V_A}{}^1\zeta_A + x_A \gamma_{V_A} + x_B \alpha_{V_B}/{}^3\zeta_B + x_B \beta_{V_B}{}^1\zeta_B + x_B \gamma_{V_B} \quad \ldots (4)$$

The viscosity, η_m, of this mixture would also be expressible[14] by an expression analogous to Eq. 1, i.e.,

$$\eta_m = \alpha_{V_m}/{}^3\zeta_m + \beta_{V_m}{}^1\zeta_m + \gamma_{V_m} \quad \ldots (5)$$

we now assume[14] that

$$^3\zeta_m = \Sigma x_A \cdot {}^3\zeta_A \quad \ldots (6)$$

$$\beta_{V_m}({}^1\zeta_m) = \Sigma x_A . \beta_{V_A}{}^1\zeta_A \quad \ldots (7)$$

$$\gamma_{V_m} = \Sigma x_A \gamma_{V_A} \quad \ldots (8)$$

and

$$\alpha_{V_m} \approx \alpha_{V_A} \approx \alpha_{V_B} \approx \alpha \quad \ldots (9)$$

so that the viscosity change ($\Delta\eta$) on mixing the components of this binary mixture would be given by,

$$(\Delta\eta) = \eta_m - \eta_{id} = \alpha \left[\frac{1}{\Sigma x_A \cdot {}^3\zeta_A} - \sum \frac{x_A}{{}^3\zeta_A} \right] \quad \ldots (10)$$

Evaluation of ($\Delta\eta$) of a binary mixture (A+B) would thus require a knowledge of its α parameter; the $^3\zeta$ parameters of A and B can be calculated from Eq. 3 in the manner described elsewhere[16] utilizing δ^v (δ^v = valence δ values[13,16]) of the vertices of their molecular graphs. For the present investigations we evaluated α for an (A+B) mixture by utilizing its ($\Delta\eta$) value at $x_A = 0.5$. This value of α was next employed to evaluate ($\Delta\eta$) for the mixture at $x_A = 0.1$, 0.3, 0.7 and 0.9. Such ($\Delta\eta$) values are recorded in Table 2 and are also compared with the corresponding literature values[17-20]. Examination of Table 2 shows that Eq. 10 is successful in reproducing ($\Delta\eta$) values of mixtures No. 1-11, and 14. It is interesting to note that even though there is evidence[21] for complex formation between benzene (A) and carbon tetrachloride (B), Eq. 10 reproduces its ($\Delta\eta$) data. Again although methylene chloride (A) + aromatic hydrocarbons (B) mixtures have been charactgerized[20,22] by weak specific interactions between A and B, yet their ($\Delta\eta$) data are also well described by Eq. 10. For methylene chloride (A) + *p*-xylene (B) mixture, however, ($\Delta\eta$) values calculated from Eq. 10 compare resonably well with the corresponding literature[19] values in the range $x_A < 0.3$; in the rest of the composition range, while the calculated ($\Delta\eta$) values are positive the experimental ($\Delta\eta$) values are negative. Further, for chloroform (A) + 1,4-dioxane or ether (B) system, while the calculated ($\Delta\eta$) values have the same sign as the experimental ($\Delta\eta$) values, the agreement between these values is not good in the range $x_A \geqslant 0.6$. This is understandable since in the latter mixtures[23] specific interactions exist between their components which form well characterized molecular species in solution. This approach, however, cannot be worked out for methanol (A) + aromatic hydrocarbons (B) since A in these mixtures is known to be associated in the pure state, and as the degree or the extent of association in A is not known with certainty[24-27], the $^3\zeta$ parameter of A cannot be evaluated in the pure state. The addition of B to A in these mixtures would further complicate the matters so far as the evaluation of $^3\zeta$ values in (A+B) mixtures is concerned. In fact in ROH(A) (R = CH_3 or C_2H_5) + CHX_3(B) (X = Cl or Br) or CH_2Br_2(B) mixtures, A has been shown[28] to be self-associated in the pure state, i.e.. while methanol has been shown[29] to exist mainly as a cyclic dimer (with open chain dimers and trimers), ethanol exists mainly as an open chain trimer. It has further been shown[28] that in these mixtures $^3\zeta$ values of A are indeed different the pure A and (A+B) mixtures. Again, these mixtures have been shown[28] to be characterized by the presence of AB and or A_2B molecular species in solution. Such (A+B) mixtures where complexation reaction takes place between A and B leading to the formation of molecular species in so-

Table 2—Comparison of ($\Delta\eta$) Values Calculated (for $x_A = 0.1, 0.3, 0.7$ and 0.9 at 298.15K) from Eqs 10 and 14 with the Corresponding Literature Values for Some (A+ B) Mixtures

Sl No.	Mixture	$\Delta\eta$ (Millipoise)	x_A			
			0.1	0.3	0.7	0.9
1	Benzene (A) + ethylene chloride (B)	Calc.	−0.240	−0.527	−0.545	−0.239
		Expt.[17]	−0.270	−0.650	−0.600	−0.223
		(Calc.)*	(−0.307)	(−0.657)	(−0.657)	(−0.284)
		$[{}^3\zeta_A = 0.667, {}^3\zeta_B = 0.714, \alpha = 378.767, K = 3.304]$				
2	Benzene (A) + cyclohexane (B)	Calc.	−0.386	−1.019	−1.390	−0.728
		Expt.[17]	−0.550	−1.300	−1.050	−0.400
		(Calc.)*	(−0.540)	(−1.209)	(−1.167)	(−0.480)
		$[{}^3\zeta_A = 0.667, {}^3\zeta_B = 1.500, \alpha = 8.7484, K = -2.1212]$				
3	Benzene (A) + chlorobenzene (B)	Calc.	−0.016	−0.040	−0.048	−0.022
		Expt.[18]	−0.030	−0.040	−0.042	−0.016
		(Calc.)*	(−0.020)	(−0.050)	(−0.040)	(−0.020)
		$[{}^3\zeta_A = 0.667, {}^3\zeta_B = 1.007, \alpha = 0.10115, K = -0.260]$				
4	Benzene (A) + bromobenzene (B)	Calc.	−0.069	−0.179	−0.230	−0.115
		Expt.[18]	−0.080	−0.180	−0.196	−0.070
		(Calc.)*	(−0.077)	(−0.200)	(−0.200)	(−0.078)
		$[{}^3\zeta_A = 0.667, {}^3\zeta_B = 1.273, \alpha = 0.2153, K = 7.74194]$				
5	Benzene (A) + *n*-pentane (B)	Calc.	−0.320	−0.848	−0.870	−0.30
		Expt.[19]	−0.300	−0.700	−1.000	−0.40
		(Calc.)*	(−0.430)	(−0.880)	(−0.870)	(−0.40)
		$[{}^3\zeta_A = 0.667, {}^3\zeta_B = 0.707, \alpha = 82.4, K = 1.021]$				
6	Benzene (A) + *n*-hexane (B)	Calc.	−0.330	−0.859	−0.948	−0.440
		Expt.[19]	−0.300	−0.800	−1.000	−0.450
		(Calc.)*	(−0.380)	(−0.881)	(−0.900)	(−0.390)
		$[{}^3\zeta_A = 0.667, {}^3\zeta_B = 0.957, \alpha = 2.5884, K = -0.2540]$				
7	Benzene (A) + carbon tetrachloride	Calc.	−0.014	−0.036	−0.042	−0.020
		Expt.[17]	−0.014	−0.038	−0.034	−0.012
		(Calc.)*	(−0.044)	(−0.061)	(−0.034)	(−0.021)
		$[{}^3\zeta_A = 0.667, {}^3\zeta_B = 1.000, \alpha = 0.9224, K = 9.7561]$				
8	Toluene (A) + Chlorobenzene (B)	Calc.	0.032	0.075	0.077	0.033
		Expt.[18]	0.031	0.061	0.100	0.045
		(Calc.)*	(0.032)	(0.075)	(0.076)	(0.033)
		$[{}^3\zeta_A = 0.94, {}^3\zeta_B = 1.007, \alpha = -7.39, K = -0.08867]$				
9	Toluene (A) + bromobenzene (B)	Calc.	−0.100	−0.250	−0.280	−0.129
		Expt.[18]	−0.120	−0.260	−0.280	−0.120
		(Calc.)*	(−0.110)	(−0.260)	(−0.260)	(−0.110)
		$[{}^3\zeta_A = 0.94, {}^3\zeta_B = 1.273, \alpha = 1.4806, K = 0.2352]$				
10	Methylenechloride (A) + Benzene (B)	Calc.	−0.170	−0.365	−0.311	−0.124
		Expt.[19]	−0.130	−0.350	−0.330	−0.150
		(Calc.)*	(−0.150)	(−0.340)	(−0.339)	(−0.150)
		$[{}^3\zeta_A = 1.0, {}^3\zeta_B = 0.667, \alpha = 0.8028, K = -0.1520]$				
11	Methylenechloride (A) + Toluene (B)	Calc.	−0.013	−0.031	−0.036	−0.017
		Expt.[19]	−0.010	−0.030	−0.040	−0.023
		(Calc.)*	(−0.010)	(−0.028)	(−0.038)	(−0.018)

(Cont.)

Table 2—Comparison of ($\Delta\eta$) Values Calculated (for $x_A = 0.1, 0.3, 0.7$ and 0.9 at 298.15K) from Eqs 10 and 14 with the Corresponding Literature Values for Some (A+B) Mixtures—*Contd.*

Sl No.	Mixture	$\Delta\eta$ (Millipoise)	x_A 0.1	0.3	0.7	0.9
		[$^3\zeta_A = 1.0, {}^3\zeta_B = 0.94, a = 0.1525, K = -0.0181$]				
12	Methylenechloride (A)+ *m*-xylene (B)	Calc.	0.031	0.065	0.070	0.035
		Expt.[19]	0.010	0.070	0.020	0.000
		(Calc.)*	(0.023)	(0.065)	(0.086)	(0.04)
		[$^3\zeta_A = 1.0, {}^3\zeta_B = 1.174, a = -1.5267, K = 0.027$]				
13	Methylenechloride (A)+ *p*-xylene (B)	Calc.	0.018	0.044	0.048	0.021
		Expt.[19]	0.040	0.060	−0.020	−0.020
		(Calc.)*	(0.013)	(0.038)	(0.054)	(0.027)
		[$^3\zeta_A = 1.0, {}^3\zeta_B = 1.217, a = 0.6288, K = 0.0239$]				
14	Acetone (A)+ Benzene (B)	Calc.	−0.154	−0.329	−0.280	−0.112
		Expt.[19]	−0.140	−0.290	−0.230	−0.050
		(Calc.)*	(−0.090)	(−0.251)	(−0.250)	(−0.075)
		[$^3\zeta_A = 1.0, {}^3\zeta_B = 0.667, a = 0.7219, K = 0.4656$]				
15	Chloroform (A)+ 1,4-Dioxane (B)	Calc.	−0.273	−0.598	−0.532	−0.216
		Expt.[19]	−0.040	−0.339	−0.717	−0.420
		(Calc.)*	(−0.040)	(−0.278)	(−0.860)	(−0.440)
		[$^3\zeta_A = 1.0, {}^3\zeta_B = 0.744, a = 2.6531, K = -0.3289$]				
16	Chloroform (A)+ ether (B)	Calc.	—	—	—	—
		Expt.[19]	−0.060	−0.181	−0.460	−0.242
		(Calc.)*	(−0.083)	(−0.236)	(−0.232)	(−0.090)
		[$K = -0.0278$]				
17	Methanol (A)+ benzene (B)	Expt.[20]	−0.162	−0.376	−0.329	−0.131
		(Calc.)*	(−0.124)	(−0.342)	(−0.330)	(−0.135)
		[$K = 0.1515$]				
18	Methanol (A)+ Toluene (B)	Expt.[20]	−0.000	−0.030	−0.070	−0.050
		(Calc.)*	(−0.020)	(−0.040)	(−0.055)	(−0.032)
		[$K = 0.0319$]				
19	Methanol (A)+ *m*-xylene (B)	Expt.[20]	0.025	0.068	0.067	0.000
		(Calc.)*	(0.025)	(0.068)	(0.080)	(0.040)
		[$K = 0.0270$]				

*Values in parenthesis are those calculated by using Eq. 14.

lution, ($\Delta\eta$) values should be expressed (in view of equations 4, 5, 7-9) by

$$(\Delta\eta) = a\left[\frac{1}{{}^3\zeta_m} - \sum \frac{x_A}{{}^3\zeta_A}\right] \quad \ldots (11)$$

where $^3\zeta_m$ is the $^3\zeta$ of the (A+B) mixture and is not given by Eq. 6. Since no method is available for the evaluation of a and $^3\zeta_m$ for these (x_AA+ x_BB) mixtures from the $^3\zeta$ values of pure A and B, we devised an alternative approach.

Expressing ($\Delta\eta$) of these (A+B) mixtures by Eq. (11) would require that the molar excess volume, V^E, of these mixtures be also expressed by,

$$V^E = a_{AB}\left[\frac{1}{{}^3\zeta_m} - \sum \frac{x_A}{{}^3\zeta_A}\right] \quad \ldots (12)$$

In fact, (V^E) data for ROH(A) (R = CH_3 or C_2H_5) + CHX_3 (X = Cl or Br) or CH_2Br_2 (B) mixtures have been best reproduced[28] by Eq. 12 and the information[28] that this equation has yielded about the nature of the molecular species in these mixtures has further been substantiated by independent ideal associated approach study[29] on the thermodynamic excess properties of ROH(A) (R = CH_3 or C_2H_5) + CHX_3(B) (X = Cl or Br) mixtures.

Consequently, Eqs 11 and 12 yield,

$$\frac{\Delta\eta}{V^E} = \frac{\alpha}{\alpha_{AB}} = K \qquad \ldots (13)$$

or

$$(\Delta\eta) = K\,V^E \qquad \ldots (14)$$

Equation 14 thus provides a very simple relationship between $(\Delta\eta)$ and (V^E) values of an (A+B) mixture.

Evaluation of $(\Delta\eta)$ values for a binary mixture from Eq. 14 requires a knowledge of its K parameter provided its V^E data are available. For the present analysis we employed $(\Delta\eta)$ and V^E values for $x_A = 0.5$ to compute its K parameter. This value of K was further coupled with the V^E data at any x_A to evaluate $(\Delta\eta)$ value for the mixture at that x_A. Such $(\Delta\eta)$ values at $x_A = 0.1$, 0.3, 0.7 and 0.9 are recorded (in paranthesis) in Table 2 and are also compared with the corresponding literature values[17-20]; the necessary V^E data were taken from literature[22,29-32].

Examination of Table 2 reveals that Eq. 14 describes reasonably well $(\Delta\eta)$ values of all the present (A+B) mixtures. However, Eq. 14 gives a poorer description of methylene chloride (A) + *o*-xylene (B) mixture than does Eq. 10.

Thus, in those (A+B) mixtures where it is possible to compute $^3\zeta$ of A and B, Eq. 10 provides a convenient means to evaluate $(\Delta\eta)$ for the mixture provided its $(\Delta\eta)$ value at $x_A = 0.5$ is available. On the other hand, when V^E data at various x_A and $(\Delta\eta)$ value at any one x_A are available. $(\Delta\eta)$ values for the mixture can be easily evaluated from Eq. 14 for any x_A.

Acknowledgement

The author expresses his thanks to the Head of the Chemistry Department of Maharshi Dayand University, Rohtak for providing necessary facilities.

References

1 Hosoya H, *Bull chem Soc Japan*, **44** (1971) 2332.
2 Rouvary D H, *RIC Rev*, 4 (1971) 173.
3 Graovac A, Gutaman I, Trinajstic N & Tivkovic T, *Theor chim Acta*, **26** (1970) 67.
4 Balaban A T, *Chemical applications of graph theory* (Academic press, London), 1976.
5 Hall L H & Kier L B, *J pharm Sci*, **67** (1978) 1743.
6 Coulson C A, *Proc Cambridge Philos Soc*, **46** (1950) 202.
7 Atkins P W, *Physical chemistry* (W H Freeman, San Fransisco), (1978) 805.
8 Chaoanne G & Risseghem H V, *Bull Soc chim Belg*, 31 (1922) 87.
9 Graef H D, *Bull Soc chim Belg*, 34 (1925) 427.
10 Edgar G, *Ind Eng Chem*, **19** (1927) 145.
11 Smyth C P & Stoops W N, *J Am chem Soc*, **50** (1928) 1883.
12 Timmerman J, *Physico-chemical constants of pure organic compounds* (Elsevier, Amsterdam), 1950, pp, (a) 34; (b) 38; (c) 44; (d) 63; (e) 86; (f) 91; (g) 98.
13 Kier L B, *Physico-chemical properties of drugs*, edited by S H Yolkowsky, A A Sinkula & S C Valvani (Marcel Dekker, New York) Chap. 9, p. 297.
14 Singh P P, Nigam R K, Singh K C & Sharma V K, *Thermochim Acta*, **46** (1981) 175.
15 *CRC handbook of chemistry and physics*, 58th Edn, 1977-78, pp. F-62, F-57.
16 Singh P P, *Thermochim Acta*, **66** (1983) 37.
17 Fort R J & Moore W R, *Trans Faraday Soc*, **62** (1966) 1112.
18 Nigam R K & Singh P P, *Indian J Chem*, **9** (1971) 691.
19 Mahl B S, Ph.D thesis, Kurukshetra University, 1973.
20 Maini N N, Ph.D thesis, Kurukshetra University, 1971.
21 Rowlinson J S, *Liquid and liquid mixtures*, (Butterworths, London), 1959, p. 182.
22 Nigam R K & Mahl B S, *J chem Soc, Faraday Trans-I*, **68** (1972) 1508.
23 McGlashan M L & Rastogi R P, *Trans Faraday Soc*, **54** (1958) 496.
24 Mecke R, Reuter A & Schupp R, *Z Naturforsch*, **49** (1949) 182.
25 Pimental G C & McClellan A L, *The hydrogen bond* (Freeman, San Fransisco) 1960.
26 Whetsel K B & Lady J H, *Spectroscopy of fuels* (Plenum, New York), 1970, pp. 259-279.
27 Woolley E M, Travers J G, Erno B P & Hepler L G, *J phys Chem*, **75** (1971) 3591.
28 Singh P P, Sharma V K & Sharma S P, *Thermochim Acta*, **106** (1986) 293.
29 Singh P P, Sharma B R & Sindhu K S, *Aust J Chem*, **30** (1977) 1241.
30 Nigam R K & Singh P P, *Trans Faraday Soc*, **65** (1969) 950.
31 Mishra R, Ph.D thesis, M.D. University, Rohtak, 1980.
32 Levien B J & Marsh K N, *J chem thermodyn*, **5** (1973) 651.

Indian Journal of Chemistry
Vol. 27A, June 1988, pp. 474-478

Charge-Transfer Complexes of Hydroxystyrylcyanine Dyes & Their Analogues with Nicotine: Structure—Activity Relationship Studies

MAHER M GIRGIS* & ZARIF H KHALIL
Chemistry Department, Faculty of Science, Assiut University Assiut, Egypt.

Received 20 *July* 1987; *revised and accepted* 3 *November* 1987

UV-visible spectrophotometric studies on the interaction of nicotine with hydroxystyrylcyanine dyes and their analogues [dyes (I-IX)] in 10% (v/v) aq ethanol at 29°C demonstrate the formation of charge-transfer complexes of dyes (I, III-VI) only. Addition of increasing amounts of nicotine to a solution containing fixed [dye] causes a decrease in the dye absorptivity with a gradual development of a new band at considerably longer wavelength characteristic of the complex formed. The spectra exhibit a clear unique isosbestic point. The stability constants and the molar absorptivities of the complexes formed have been calculated assuming the formation of 1:1 complexes. The experimental results have been interpreted in terms of molecular structure of the interacting molecules.

Nicotine finds growing interest for its biochemical[1] and pharmacological[2,3] effects. The biological activity of cyanine dyes is attributed to the adsorption of the dye molecules on active sites of the living cells[4]. Structure-activity relationship has been conducted on styryl and aza cyanine dye analogues to study their effect on breaking period of dormancy in garlic[5], essential oil production in sweet marjoram (*Origanum majorana* Linn)[6] and chromosomal behaviour in *Vicia faba* seeds[7]. To shed some light on the cause of bioeffect of aza cyanine dyes, formation of charge-transfer (CT) complexes between one of the nucleic acid bases (adenine) and azacyanine dyes has been investigated[8], and the results obtained were in accord with the biological activity of aza cyanine dyes when applied as bioregulator for *V. faba* seeds in the field.

The interactions between nicotine and drugs have been the subject of many investigations[3,9]. The interactions between nicotine and cyanine dyes have not been investigated. In this work we aim to study the CT interaction of nicotine with hydroxystyrylcyanine dyes and their analogues and the effect of geometry[10] on the complexation with a view to selecting an appropriate configuration for the development of radio immunoassay for tobacco alkaloids[11].

Materials and Methods

Nicotine (BDH) was used as such. Styrylcyanine dyes (I-IX) were prepared by the method described before[12] and recrystallized from ethanol. Their purity was checked by elemental analyses and spectral data.

All experiments were carried out in 10% (v/v) ethanol-water mixture. The calculated volumes of nicotine (0.05 mol dm^{-3}), dye (0.001 mol dm^{-3}) and ethanol were mixed together and the volume made up to 10 ml in a dark-coloured bottle by adding doubly dis-

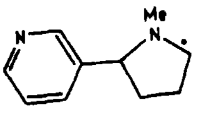

3 [1-Methyl-2-pyrrolidinyl]-pyridine
(Nicotine)

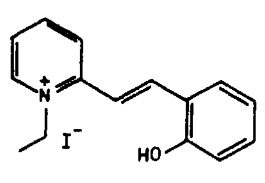

2 [2-Hydroxystyryl] pyridinium-1-ethyl iodide. (Dye I)

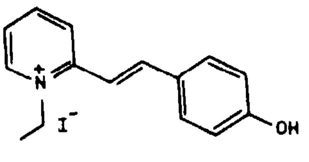

2 [4-Hydroxystyryl] pyridinium-1-ethyl iodide. (Dye II)

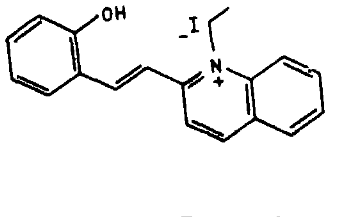

2 [2-Hydroxystyryl] quinolinium-1-ethyl iodide. (Dye III)

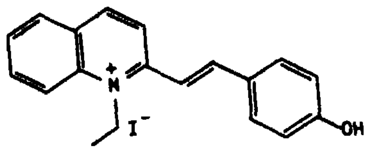

2 [4-Hydroxystyryl] quinolinium-1-ethyl iodide. (Dye IV)

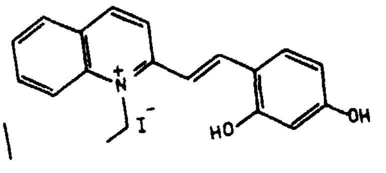

2 [2,4-Dihydroxystyryl] quinolinium-1-ethyl iodide. (Dye V)

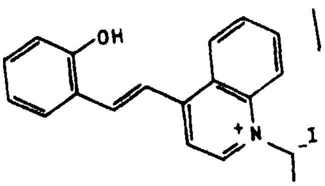

4 [2-Hydroxystyryl] quinolinium-1-ethyl iodide. (Dye VI)

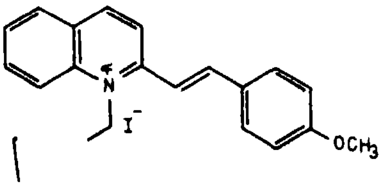

2 [4-Methoxystyryl] quinolinium-1-ethyl iodide. (Dye VII)

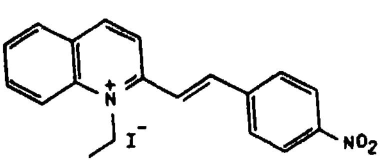

2 [4-Nitrostyryl] quinolinium-1-ethyl iodide. (Dye VIII)

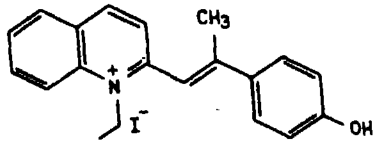

2 [2-Methyl-2(4-hydroxyphenyl)ethenyl] quinolinium-1-ethyliodide. (Dye IX)

tilled water. The solutions were freshly prepared each day, and their aborbances were measured within 5 hr. All the operations were performed at 22°C in subdued light.

Spectrophotometric measurements were made on a Shimadzu UV-200S double beam spectrophotometer, using a rectangular cell of 1 cm pathlength against solvent as the blank. The absorbances were measured at fixed wavelengths to minimize errors arising from the steepness of absorption spectra. The absorption band of the complex formed between nicotine and the dye was detected at wavelength longer than those of the individual components at concentrations identical to that in the mixture. The absorbances were measured within ~ 10 min after mixing the solutions and placing the cell in a thermostated cell holder for equilibrium. The accuracy of the measurement was ± 0.01 absorbance unit.

Results and Discussion

The absorption spectra of the dyes I, III, IV and VI are presented in Fig. 1. For some dye-nicotine mixtures, the visible absorption band of the dye diminishes gradually with increase in nicotine content in the mixture and a new band gradually appears at longer wavelength. The spectra of the mixture show a clear unique isosbestic point (Fig. 2). This behaviour is noticed only for nicotine-dye (I, III-VI) combinations, but not with other nicotine-dye (II, VII-IX) combinations. The appearance of this new longer wavelength band is attributed to the formation of a charge-transfer (CT) complex between nicotine and the dyes I and III-VI.

The stoichiometry of the CT complex ($N_n D_d$) of nicotine (N) and dye (D),

$$nN + dD \rightleftharpoons N_nD_d \qquad \ldots(1)$$

was determined applying Eq. (2)[13]

$$A_\lambda^{CT} = K_c^{CT} \cdot \varepsilon_\lambda^{CT} [N]^n [D]^d \qquad \ldots(2)$$

where A_λ^{CT} and ε_λ^{CT} are the absorbance and the molar absorptivity, respectively, of the complex at wavelength λ, and K_c^{CT} is the thermodynamic equilibrium constant. A plot of A_λ^{CT} versus concentration of one component, that of other being kept constant, on log paper, proved that the complex has 1:1 composition. Thus, for the equilibrium

$$N + D \rightleftharpoons ND \qquad \ldots(3)$$

the equilibrium constant (K_c^{ND}) is given by Eq. (4)

$$K_c^{ND} = \frac{[ND]}{[N][D]} = \frac{[ND]}{\{[N]_0 - [ND]\}\{[D]_0 - [ND]\}} \qquad \ldots(4)$$

where ND is the complex formed, and $[N]_0$ and $[D]_0$

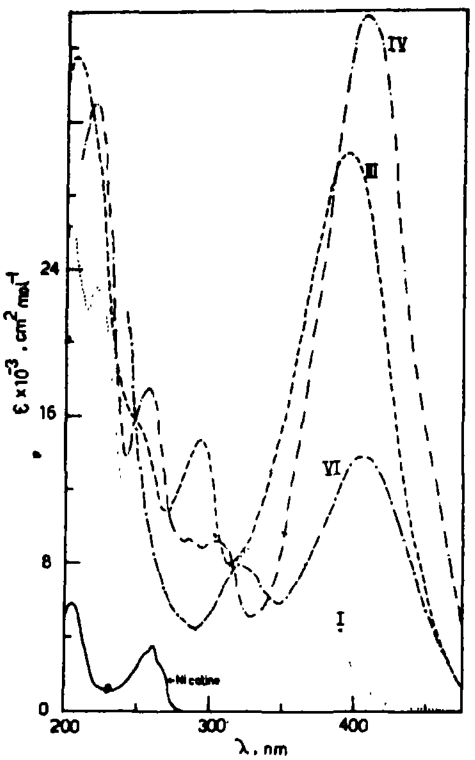

Fig. 1—Electronic absorption spectra of dyes (I, III, IV and VI) and nicotine in 10% (v/v) aq ethanol at 29°C.

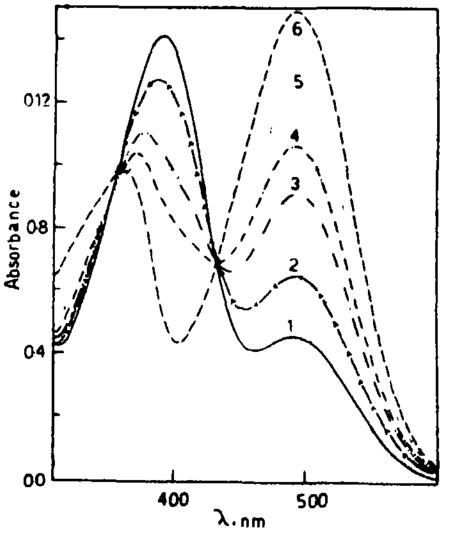

Fig. 2—Absorption spectra of 5.56 × 10^{-5} mol dm^{-3} dye(III) in 10% (v/v) aq ethanol at 29°C to which the following amounts of nicotine (mol dm^{-3} × 10^4) were added: (1) 0.50; (2) 0.86; (3) 1.72; (4) 2.50; (5) 5.00; (6) 50.00.

are the initial concentrations of nicotine and the dye respectively. Eq. (4) may be rearranged to obtain Eq. (5)

$$\frac{[D]_0}{[ND]} = \frac{1}{K_c^{ND}} \cdot \frac{1}{[N]_0} + \frac{[D]_0}{[N]_0} + 1 - \frac{[ND]}{[N]_0} \qquad \ldots(5)$$

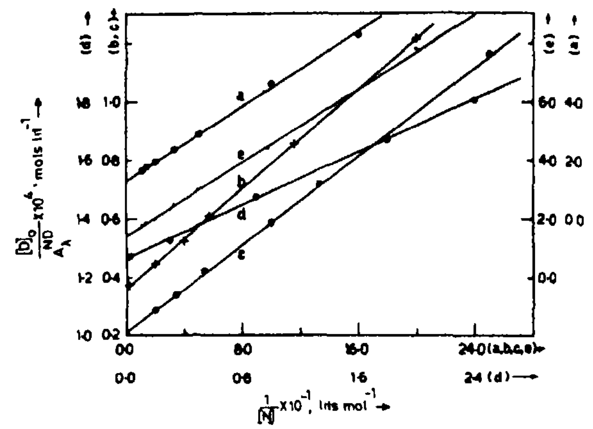

Fig. 3—Plots of $[D]_0/A_\lambda^{ND}$ versus $1/[N]_0$ for 10% (v/v) aq ethanol containing fixed [dye] and different [nicotine] at 29°C. [The combinations are: (a) nicotine-dye(I) ([dye I] = 7.40 × 10^{-5} mol dm^{-3}); (b) nicotine-dye(III) ([dye III] = 5.58 × 10^{-5} mol dm^{-3}); (c) nicotine-dye(IV) ([dye IV] = 3.87 × 10^{-5} mol dm^{-3}); (d) nicotine-dye (V) ([dye V] = 9.27 × 10^{-5} mol dm^{-3}); (e) nicotine-dye(VI) ([dye VI] = 9.30 × 10^{-5} mol dm^{-3})].

Since the absorbance in the region of the new band is due to the complex ND (Fig. 2), and the solution is of 1 cm pathlength, for two molecules forming complex in accordance with Eq. (3), the molar absorptivity of the complex at wavelength λ is given by Eq. (6)

$$\varepsilon_\lambda^{ND} = \frac{A_\lambda^{ND}}{[ND]} \qquad \ldots(6)$$

where A_λ^{ND} is the absorbance of the complex (ND) at the wavelength λ.
Combining Eqs (5) and (6), we get

$$\frac{[D]_0}{A_\lambda^{ND}} = \frac{1}{K_c^{ND} \cdot \varepsilon_\lambda^{ND}} \cdot \frac{1}{[N]_0} + \frac{[D]_0}{[N]_0 \varepsilon_\lambda^{ND}} + \frac{1}{\varepsilon_\lambda^{ND}} - \frac{[ND]}{[N]_0 \varepsilon_\lambda^{ND}} \qquad \ldots(7)$$

Since $[N]_0 \gg [ND]$ it is possible to neglect the last term in the right hand side of Eq. (7)[14a], so that

$$\frac{[D]_0}{A_\lambda^{ND}} = \frac{1}{[N]_0}\left(\frac{1}{K_c^{ND} \varepsilon_\lambda^{ND}} + \frac{[D]_0}{\varepsilon_\lambda^{ND}}\right) + \frac{1}{\varepsilon_\lambda^{ND}} \qquad \ldots(8)$$

For a series of solutions of constant $[D]_0$ and varying $[N]_0$ a plot of $[D]_0/A_\lambda^{ND}$ against $1/[N]_0$ should be linear. The intercept of the line with ordinate gives $(\varepsilon_\lambda^{ND})^{-1}$ and the gradient is equal to $[(K_c^{ND} \cdot \varepsilon_\lambda^{ND})^{-1} + [D]_0(\varepsilon_\lambda^{ND})^{-1}]$, so that K_c^{ND} and ε_λ^{ND} can be evaluated. Plots of Eq. (8) for nicotine-dye (I, III-VI) mixtures at 29°C are represented in Fig. 3 while K_c^{ND} and ε_λ^{ND} values are given in Table 1.

Various pyridinium salts are utilized as coenzyme models. Pyridine and its derivatives, e.g. nicotinic acid, act as electron donors on mixing with electron acceptors such as riboflavin[15] and iodine[16] forming CT

Table 1—$\lambda_{max}(\varepsilon_{max})$ Values of CT Bands of Styrylcyanine Dyes (I-IX) and Nicotine-Dye (ND) Combinations, Isosbestic Points and Equilibrium Constants (K_c^{ND})$^{a-c}$

	CT-band			Isosbestic point (nm)	$K_c^{ND} . 10^{-3}$ (dm^{3}mol^{-1})
Dye	$\lambda_{max}^{D}(\varepsilon_{max}^{D} . 10^{-3})$	Combination	$\lambda_{max}^{ND}(\varepsilon_{max}^{ND} . 10^{-3})$		
I	348(9.7)	Nicotine-dye(I)	424(7.7)	375	5.99
II	330*sh*(8.3)	Nicotine-dye(II)	—	—	—
III	394(30.2)	Nicotine-dye(III)	506(27.4)	434	16.40
IV	406(37.7)	Nicotine-dye(IV)	496(47.6)	436	7.08
V	511(4.0)	Nicotine-dye(V)	549(7.9)	473	11.66
VI	404(13.7)	Nicotine-dye(VI)	505(7.1)	444	7.61
VII	400(29.0)	Nicotine-dye(VII)	—	—	—
VIII	364(29.5)	Nicotine-dye(VIII)	—	—	—
IX	585(6.3)	Nicotine-dye(IX)	—	—	—

(a) λ_{max} in nm; ε_{max} in cm^{2}mol^{-1}.

(b) All measurements were carried out in 10% (v/v) aq ethanol at 29°C.

(c) Nicotine has a characteristic band: $\lambda_{max} = 261$ nm ($\varepsilon_{max} = 3.5 \times 10^3$ cm^2 mol^{-1}).

complexes. Kosower and coworkers[17] have shown that pyridinium ion acts as an electron acceptor during formation of a CT complex with iodide ion as the electron donor. Such complexes are essentially ion-pairs in the ground state[14b]. Absorption of energy within the CT-band causes excitation to a covalent excited state. The coloured nature of the quinolinium iodide[18] as compared to the lack of absorption in the visible region by most of other quinolinium salts has been explained in terms of CT interaction between the two ions. Bispyridinium cation derivatives form 1:1 CT complexes with neutral donor species[19].

Experimental results show that the absorption spectrum of nicotine is not changed by the addition of iodide ions, indicating that there is no CT interaction between nicotine and iodide ions.

The spectra of nicotine-dye (I, III-VI) mixtures exhibit (Fig. 2) isosbestic point which may be taken as an evidence for 1:1 complex formation[20]. Application of Eq. (8) gives linear slopes (Fig. 3) supporting 1:1 complex formation. The results show wavelength-independence of the equilibrium constant indicating the formation of only one type of complex[21].

Exact geometry of the complex cannot be determined from the present absorption measurements, but parallel stacking interactions between nicotine and dye can be invoked as have been for similar systems[22].

In the present investigation, it is found that the ability of nicotine to form CT complexes with styrylcyanine dyes depends mainly on their molecular structures. Thus, 2-(2-hydroxystyryl)-pyridinium-1-ethyl iodide (dye I) forms CT complex on mixing with nicotine. This CT complex is assumed to be formed by 1:1 parallel stacking interaction between nicotine as an electron donor and dye(I) as an electron acceptor. The acceptor character of the dye results from the two partially positive centres located at the quaternary nitrogen and the oxygen atom of the hydroxystyryl moiety (Scheme 1A). The hydrogen atom of the hydroxyl group may act as a bridge between the O-phenyl of dye (I) and the unshared electron pair located at

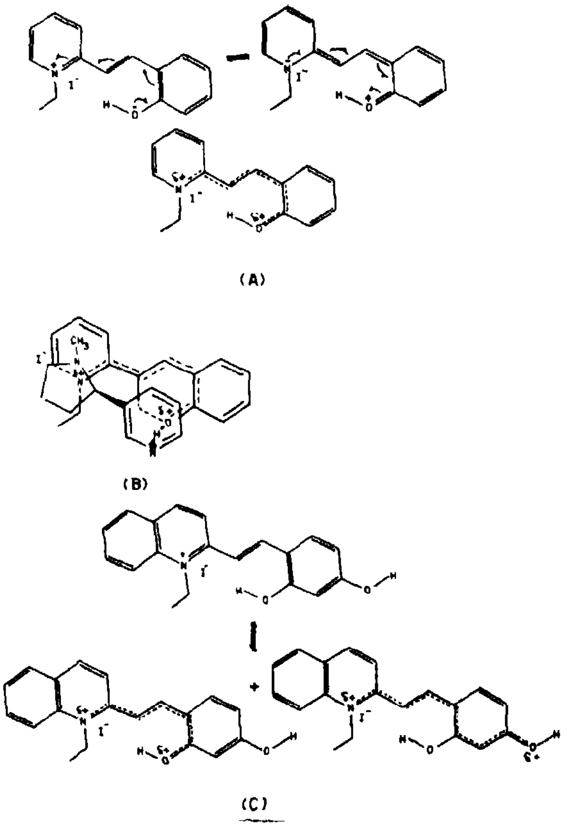

Scheme 1

the N-pyridine of nicotine molecule. The two partially positive centres of dye(I) are located at a distance equal to the distance between the two N-atoms of pyridine and pyrrolidinyl moieties of nicotine, since the distance geometry[10] is approximately the same. The suggested 1:1 parallel stacking interaction is presented in Scheme 1 B[23]. In support of this suggestion, 2-(4-hydroxystyryl)-pyridinium-1-ethyl iodide (dye II) does not form CT complex with nicotine as the two positive centres of dye(II) do not fit the distance geometry[10] and the ring-ring[24] size formation with nicotine.

On the other hand 2-(2-hydroxystyryl)-quinolinium-1-ethyl iodide (dye III) and 2-(4-hydroxystyryl) quinolinium-1-ethyl iodide (dye IV) form CT complexes. This behaviour of dye(IV) in contrast to that of dye(II) may be attributed to greater delocalisation of the positive charge at the N-quaternary atom of quinolinium moiety, due to the extra-fused benzene ring which enables the formation of a stable CT complex with nicotine. The stability constant (K_c^{ND}) of nicotine-dye(IV) complex (7.08×10^3 dm^3 mol^{-1}) is much less than that of nicotine-dye (III) complex (16.40×10^3 dm^3 mol^{-1}). The dye 2-(2,4-dihydroxystyryl)-quinolinium-1-ethyl iodide (dye V) forms a CT complex with $K_c^{ND} = 11.66 \times 10^3$ dm^3 mol^{-1}, a value which is half of the sum of stability constants of CT complexes of nicotine with dyes III and IV (Table 1). This may be attributed to the fact that dye(V) has two resonance hybrid structures giving two types of complexes (of Scheme 1C). 4-(2-Hydroxystyryl)-quinolinium-1-ethyl iodide (dye VI) forms a CT-complex with nicotine having $K_c^{ND} = 7.61 \times 10^3$ dm^3 mol^{-1}. This value is much less than that of nicotine-dye(III) complex, but is approximately the same as that of nicotine-dye (IV) complex. This is due to the fact that dyes(IV) and (VI) have approximately the same distance geometry[10] between two partially positive centres.

Substitution of the hydroxyl group in 4-hydroxystyryl moiety by a methoxyl group (electron releasing) as in dye (VII), or a nitro group (electron withdrawing) as in dye(VIII) does not help in the formation of CT complexes. This provides further new evidence for the formation of H-bridge between the hydroxystyryl and the N-pyridine moieties, since this H-bridge is absent in the dyes (VII) and (VIII), and consequently no CT complexes are formed.

Substitution at the ethenyl moiety ($-CH=CH-$) of the 4-hydroxystyryl group (dye IX) also does not lead to CT complex formation with nicotine. This may be due to steric congestion between the interacting molecules and the inability to adopt ring-ring conformations needed[24].

References

1 Aceto M D, Martin B R & May E L, *CRC Handbook stereoisomers: Drugs psychopharmacol*, edited by Donald F Smith (CRC, Boca Raton, Fla) 1984, p. 67-78.

2 Balfour D J K, *Int encycl pharmacol Ther*, edited by D J K Balfour (Pergamon, UK.) 1984, pp. 101-12.

3 Masafumi H & Gerhard L, *J pharm Sci*, **74** (1985) 412.

4 Terada H, Nagamune H, Morikawa N & Ikuno M, *Biochem Biophys Acta*, **807** (1985) 168

5 Abdou R F, Waly E A, Abdel [illegible] A & Khalil Z H, *Assiut J Agric Sci, Egypt*, **14** (198[illegible]) 415.

6 El-Keltawi N E & Khalil Z H, *Flavour Fragrance J*, **1** (1986) 63.

7 Abdou R F, Omara M K, Hussein M Y & Khalil Z H, *Assiut J Agric Sci, Egypt*, **13** (1982) 117.

8 Girgis M M & Khalil Z H, *Croat Chem Acta*, **2** (1987) 225.

9 Jusko W J, *J Pharmacokinet Biopharm*, **6** (1978) 7.

10 Sheridan R P, Nilakantan R, Dixon J S & Venkataraghavan R, *J mednl Chem*, **29** (1986) 899.

11 (a) Shibagaki M, Matsushita H, Shibata S, Saito A, Ysujino Y & Kaneko H, *Heterocycles*, **19** (1982) 1641.
(b) Castro A, Monji N, Ali H, Yi M, Bowman E R & Mckennis H, *Eur J Biochem*, **104** (1980) 331.

12 Phillips A P, *J org Chem*, **12** (1947) 233.

13 Slifkin M A, *Charge transfer interactions of biomolecules* (Academic Press, London) 1971, p. 17.

14 Foster R, *Organic charge-transfer complexes* (Academic Press, London) 1969, (a) p. 135, (b) p. 340.

15 (a) Draper R D & Ingraham Li L, *Archs Biochem Biophys Acta*, **139** (1970) 265, (b) Mc Cormick D B, Heng-Chun Li & Mackenzie R E, *Spectrochim Acta*, **23** (1967) 2353.

16 (a) Krishna V G & Bhowmik B B, *J Am chem Soc*, **90** (1968) 1700. (b) Popov A I & Rygg R H, *J Am chem Soc*, **79** (1957) 4622. (c) Srivastava R D & Prasad G, *Spectrochim Acta*, **22** (1966) 825. (d) Bhaskar K R & Singh S, *spectrochim Acta*, **23** (1967) 1155. (e) Mckinney W J, wong M K & Popov A I, *Inorg Chem*, **7** (1968) 1001.

17 (a) Kosower E M & Klinedinst P E, Jr., *J Am chem Soc*, **78** (1956) 3493. (b) Kosower E M, *J Am chem Soc*, **78** (1956) 3497. (c) Kosower E M & Burbach J C, *J Am chem Soc*, **78** (1956) 5838. (d) Kosower E M, *J Am chem Soc*, **80** (1958) 3253. (e) Kosower E M, Skorez J A, Schwarz W M, Jr. & Patton J W, *J Am chem Soc*, **82** (1960) 2188. (f) Kosower E M & Skorez J A, *J Am chem Soc*, **82** (1960) 2195. (g) Kosower E M, *Molecular biochemistry*, (McGraw-Hill, New York) (1962), p. 180.

18 (a) Mason S F, *J chem Soc* (1960) 2437. (b) Briegleb G, Jung W & Herre W, *Z phys Chem Frankf Ausg*, **38** (1963) 253.

19 (a) Nakahara A & Wang J H, *J phys Chem*, **67** (1963) 496. (b) Ledwith A & Iles D H, *Chem Brit*, **4** (1968) 266.

20 Gouterman M & Stevenson P E, *J chem Phys*, **37** (1965) 2266.

21 Johnson G D & Bower R E, *J Am chem Soc*, **87** (1965) 1655.

22 (a) Dimicoli J L & Helene C, *J Am chem Soc*, **95** (1973) 1036. (b) Dimicoli J L, *Biochem Biophys Acta*, **254** (1971) 349.

23 Tsibris J C M, Mc Cormick D B & Wright L D, *Biochemistry*, **4** (1965) 504.

24 Jaffrey I S, Henry V S, Homer H & Roseanne G, *J Am chem Soc*, **102** (1980) 7741.

Indian Journal of Chemistry
Vol. 27A, June 1988, pp. 479-481

Solution Densities of Aqueous Potassium Chloride-Barium Chloride Mixtures at 298.15 K & Different Ionic Strengths

ANIL KUMAR†
Institute of Physical Chemistry, University of Karlsruhe, 7500, Karlsruhe, F.R. Germany

Received 16 *July* 1987; *accepted* 14 *September* 1987

The solution densities of aqueous KCl-$BaCl_2$ mixtures are reported at 298.15K from ionic strength 0.5 to 4.5 mol kg^{-1} of water. The negative excess volumes (ΔV_m) obtained from the experimental mean apparent molal volumes are fitted to the Friedman equation. The reliable estimates of the mixture densities can be made by the Young's rule with the addition of the ΔV_m values. In general, the densities can be predicted to within 14 ppm with the use of ΔV_m term as compared to 211 ppm obtained without the use.

Recently, there has been growing interest in the thermodynamic properties of concentrated electrolyte mixtures. Although, a large number of papers have appeared on osmotic and activity coefficients of these mixtures, only a little[1-3] has been accomplished as regard their PVT properties in concentrated region. A knowledge of PVT properties is essential in obtaining the pressure dependence of activity coefficients in these solutions. Thus, the present investigation reports the densities and mean apparent molal volumes of aqueous KCl-$BaCl_2$ mixtures at 298.15K and at ionic strengths of 0.5, 1, 3 and 4.5 mol kg^{-1} of water. The experimental measurements cover the range from pure KCl to pure $BaCl_2$ solutions.

Materials and Methods

Both KCl and $BaCl_2$ (Baker analysed) were recrystallized twice from water before use. The stock and working solutions were prepared by dissolving a definite weight in degassed ion-exchanged water. The concentrations of these solutions were determined gravimetrically using $AgNO_3$ solution. The mixtures of KCl and $BaCl_2$ were prepared at constant ionic strength as $Y_{BaCl_2} = 3m_{BaCl_2}/(m_{KCl} + 3m_{BaCl_2})$, where m and Y respectively refer to molality and ionic strength fraction of an electrolyte in mixture and $Y_{KCl} + Y_{BaCl_2} = 1$.

The densities were measured using a Paar vibrating tube densimeter[4]. The relative densities (Δd) were evaluated as the difference between density of solution (d) and that of pure water (= 0.997047 gm^{-3} at 298.15K). The densimeter was calibrated with the known densities of water[5] and NaCl solutions[6]. The temperature of the densimeter was controlled within ± 0.005°C and the densities were precise to ± 3 ppm.

Results and Discussion

In Table 1 are reported the relative densities (Δd) as a function of Y_{BaCl_2} for aqueous KCl-$BaCl_2$ at $I = 0.5$, 1, 3 and 4.5 mol kg^{-1} of water.

Apparent molal volumes, ϕ_V of pure KCl and $BaCl_2$ solutions were calculated using Eq (1)[7]

$$\phi_V = [10^3(d_0 - d)/mdd_0] + (M/d) \quad \dots (1)$$

where M refers to the formula weight of an electrolyte.

The mean apparent molal volumes in mixtures, ϕ_V^* were obtained using Eq. (2)

Table 1—Experimental Density Differences (Δd/g cm^{-3}) as a Function of Y_{BaCl_2} for the System aq. KCl-$BaCl_2$ at 298.15K

Y_{BaCl_2}	$\Delta d \times 10^3$ g cm^{-3}	Y_{BaCl_2}	$\Delta d \times 10^3$ g cm^{-3}
$I = 0.5$ mol kg^{-1}		$I = 3$ mol kg^{-1}	
0	22.721	0	121.266
0.1253	23.618	0.1259	127.482
0.2317	24.379	0.2483	133.577
0.3518	25.238	0.3596	139.152
0.4006	25.603	0.4929	145.844
0.5001	26.300	0.6103	151.800
0.6198	27.165	0.7185	157.309
0.7251	27.902	0.8399	163.509
0.8098	28.524	0.9385	168.575
0.9321	29.225	1.0000	171.750
1.0000	29.877		
$I = 1$ mol kg^{-1}		$I = 4.5$ mol kg^{-1}	
0	44.291	0	171.038
0.1582	46.628	0.1195	180.054
0.3051	48.805	0.2428	189.556
0.4182	50.481	0.3775	199.945
0.4995	51.685	0.4952	209.155
0.6128	53.366	0.6111	218.349
0.7523	55.437	0.7275	227.684
0.8951	57.556	0.8505	237.643
1.0000	59.115	0.9301	244.152
		1.0000	249.950

---

† Present address: Department of Sugar Chemistry, Deccan Sugar Institute, Manjari (BK), Pune 412 307

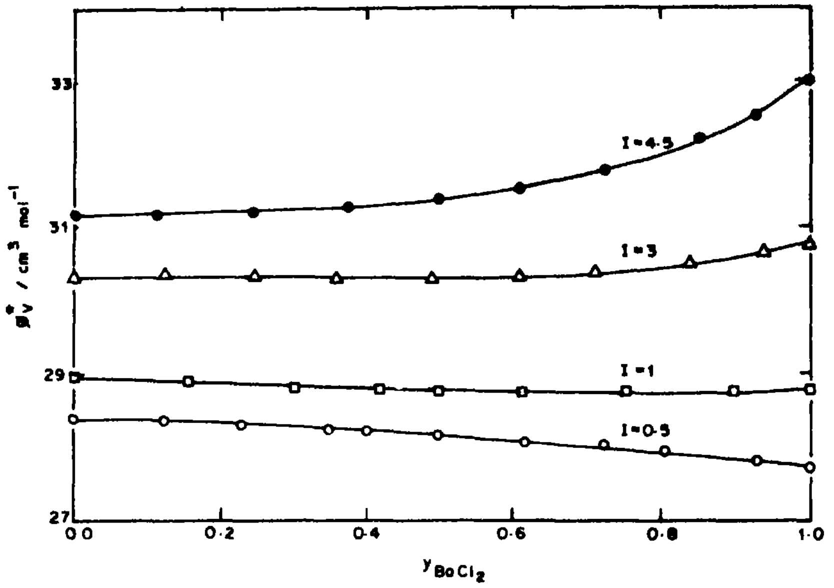

Fig. 1 – Experimental mean apparent molal volumes (ϕ_V^*) as a function of Y_{BaCl_2} at different ionic strengths for aq. KCl-BaCl$_2$

$$\phi_V^* = [10^3(d_0 - d)/m_T d d_0] + (M_T/m_T d) \quad \dots (2)$$

where $m_T = m_{KCl} + m_{BaCl_2}$;
$M_T = (m_{KCl}M_{KCl} + m_{BaCl_2}.M_{BaCl_2})$.

The values of ϕ_V^* at each ionic strength are plotted as a function of Y_{BaCl_2} in Fig. 1 showing nonlinear variation.

The excess volumes of mixing, ΔV_m were calculated by the expression (3)

$$\Delta V_m = \phi_V^* m_T - \phi'_{V,KCl} \cdot m_{KCl} - \phi'_{V,BaCl2} \cdot m_{BaCl_2} \quad \dots (3)$$

Where ϕ'_V refers to the apparent molal volume of an individual electrolyte solution at the ionic strength of mixture. The ΔV_m values, thus obtained can be fitted to Friedman's equation[8] (see Eq. 4),

$$\Delta V_m = Y_{BaCl_2}(1 - Y_{BaCl_2})I^2[v_0 + v_1(1 - 2Y_{BaCl_2})] \quad \dots (4)$$

where v_0 and v_1 indicate the binary (K^+, Ba^{2+}) and ternary ($K^+, Ba^{2+} Cl^-$) interactions respectively. In Fig. 2, the ΔV_m values are plotted against Y_{BaCl_2}, except at $I = 0.5$ mol kg^{-1} because of extremely small ΔV_m values. The ΔV_m values are negative throughout. The plots in Fig. 2 exhibit symmetrical parabola at $Y_{BaCl_2} = 0.5$. Thus, v_1 in Eq. (4) may be neglected. The values of v_0 obtained from Eq (4) are -0.122, -0.178, -0.272 and -0.528 at $I = 4.5, 3, 1$ and 0.5 mol kg^{-1} of water, respectively with an average standard deviation of fit for ΔV_m to be 0.01 cm^{3}kg^{-1} of water.

Wood and Gamkhar[9] have reported the heats of mixing (ΔH_m) data for this system, and fitted these data to an equation analogous to Eq. (4) and obtained h_0 and h_1 values similar to v_0 and v_1. The decrease v_0 with increase in ionic strength is supported by a similar trend in h_0 values reported by Wood and Gamkhar[9]. The magnitude of h_1 is extremely small, thus suggesting negligible triple interactions. A similar situation is found for ΔV_m. In addition, Pitzer and Kim[10] analysed the osmotic and activity coefficient data[11] on aq. KCl-BaCl$_2$ system using their virial coefficient approach. They obtained negative binary mixing and zero ternary terms supporting our ΔV_m results.

The need for considering ΔV_m values in estimating the densities of mixtures can be demonstrated by comparing the experimental densities with those calculated by Eq. (5)

$$d = d_0 (1000 + M_T)/(\phi^*_{V,est} m_T d_0 + 1000) \quad \dots (5)$$

where

$$\phi^*_{V,est} = x_{KCl}\phi'_{V,KCl} + x_{BaCl_2}\phi'_{BaCl_2} + \Delta V_m/m_T \quad \dots (6)$$

and $x = m/m_T$

The first two terms on the right hand side of Eq. (6) represent the well known Young's rule[12], which states that no volume change occurs on mixing the solutions of equal ionic strength. The last term on right hand side of Eq. (6) gives the correction term or excess property.

In Eq. (6), $\phi^*_{V,est}$ can be calculated with and without ΔV_m and so the values of d can be obtained. Table 2 reports the maximum and minimum differences (δ) between experimental and those obtained with and without the use of ΔV_m. One, for example, can see that

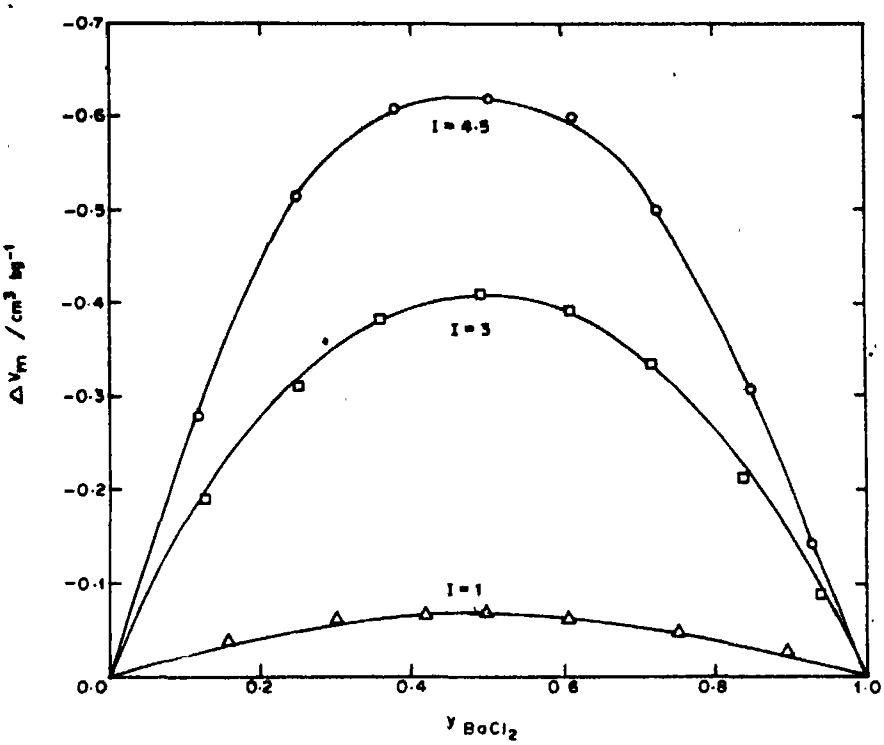

Fig. 2—Excess volumes of mixing ΔV_m as a function of y_{BaCl_2} at different ionic strengths for aq. KCl-BaCl$_2$

Table 2—Differences (δ, in ppm) between Experimental Densities and Densities Calculated with and without Addition of ΔV_m to Young's Rule for Aqueous KCl-BaCl$_2$ at 298.15K

Ionic strength (mol kg^{-1})	δ (ppm)			
	Without ΔV_m		With ΔV_m	
	Av.	Max.	Av.	Max.
0.5	12	17	6	9
1	44	61	10	14
3	299	411	18	25
4.5	490	672	21	29

densities at $I = 4.5$ mol kg^{-1} can be measured to 15 ppm with the use of ΔV_m values as compared to 490 ppm obtained without its use. As an average, the differences δ are 211 ppm at $I = 0.5$-4.5 mol kg^{-1} without the use of ΔV_m. These differences are reduced to 14 ppm with the use of ΔV_m.

To summarise, the densities of concentrated mixtures of 1-1 and 2-1 electrolytes can be estimated with the Young's rule[12], combined with the correction term or excess volumes. One notes that the average difference δ of 14 ppm remains slightly higher than the experimental accuracy.

Acknowledgement

The author is grateful to the authorities of University of Karlsruhe for permitting him to use the experimental facilities.

References

1 Wirth H E & Mills W L, *J chem engng Data*, **13** (1968) 102.
2 Kumar A, Atkinson G & Howell R D, *J solution Chem*, **11** (1982) 857.
3 Millero F J, Connaughton L M, Vinokurova F & Chetirkin P V, *J solution Chem*, **14** (1985) 837.
4 *DMA instruction manual*, Anton Paar K G, A-8054 Graz, Austria.
5 Kell G S, *J chem engng Data*, **20** (1975) 97.
6 Losurdo A, Alzola E M & Millero F J, *J Chem Thermodyn*, **14** (1982) 649.
7 Millero F J, *Activity coefficients in electrolyte solutions*, Vol II, edited by R M Pytkowicz (CRC Press, Boca Raton) 1979 pp 63.
8 Friedman H L, *Ionic solution theory* (Wiley-Interscience, New York) 1962 pp 265.
9 Wood R H & Gamkhar M, *J phys Chem*, **73** (1969) 3959.
10 Pitzer K S & Kim J J, *J Am chem Soc*, **96** (1974) 5701.
11 Robinson R A & Bower V E, *J Res NBS*, **69A** (1965) 439.
12 Young T F & Smith M B, *J phys Chem*, **58** (1954) 716.

Indian Journal of Chemistry
Vol. 27A, June 1988, pp. 482-486

Electrochemical Behaviour of Bisazo Dye, Acid Red-150

R N GOYAL* & ANOOP KUMAR
Department of Chemistry, University of Roorkee, Roorkee 247 667

Received 30 *July* 1987; *revised* 21 *September* 1987; *accepted* 16 *October* 1987

The electrochemical behaviour of Acid Red-150 has been studied in the *p*H range of 2.2-11.2. Unlike the reduction of bisazobenzene to bishydrazo-benzene, the reduction of azo group attached to napthol moiety in this dye takes place in a ($4e, 4H^+$) reduction step to give amino compound as product of electrode reaction. The products of electrolysis have been separated and identified.

An excellent review is available on the polarographic reduction of azo dyes in aqueous and non-aqueous media[1]. However, most of the studies are confined to the reduction of monoazo compounds and very little is known about the azo compounds containing two azo groups and hence the title investigation was undertaken.

Materials and Methods

Acid Red-150 (I) (Sigma Chemical Co) was used as received. Its stock solution (2 m*M*) was prepared in doubly distilled water. Universal Britton-Robinson[2] buffers (*p*H 2.2-11.2) were used. The *p*H was measured using an ECIL expanded scale *p*H meter (model *p*H 821) after due standardisation with potassium hydrogen phthalate and borax buffers.

Polarograms were recorded on a Cambridge pen recording polarograph. The capillary used had the following characteristics: $m = 1.25$ mgs^{-1}, and $t = 3.90$ at $h = 60$ cm.

For recording polarograms and voltammograms 1 ml of the stock solution of the dye was mixed with 9.0 ml of buffer of appropriate *p*H under total nitrogen blanket. Voltammetric studies were carried out using Micronic cyclic voltammeter and a digigraphic X, Y-t recorder. The details of instruments used for spectral studies have been described elsewhere[3]. Pyrolytic graphite electrode was prepared by the method reported earlier[4]. It had an area ~ 1.8 mm^2. All potentials refer to SCE at 25°C.

Controlled potential electrolysis and product identification

Controlled potential electrolysis of 1 m*M* solution of the dye was carried out in a three-compartment cell at potential more negative to peak Ic or IIc or at the plateau potential of the first or second polarographic wave. The working electrode was pyrolytic graphite plate (area 6 cm^2) or mercury pool, counter electrode was the cylindrical platinum gauze and the reference electrode was a saturated calomel electrode. Nitrogen was bubbled throughout electrolysis and progress of electrolysis was monitored by recording cyclic voltammograms at different intervals of time until the reduction wave completely disappeared.

For the separation and identification of products, the dye (8-10 mg) was electrolysed in a H-type cell. At Hg pool, plateau potential corresponding to first or second wave was applied and at pyrolytic graphite electrode potential more negative to peak Ic or IIc was applied. When electrolysis was complete (~ 99%) the electrolysed solution was made sufficiently acidic and lyopholised. The freeze-dried material was dissolved in water (1-2 ml) and passed through a glass column (70 × 1.6 cm) packed with sephadex G-10 (Sigma Chemical Co) using doubly distilled water as the eluent. Different fractions (10 ml each) were collected. The absorbance of each tube was monitored at 215 nm and was plotted against volume. The first peak (volume 50-200 ml) contained phosphate, borate and acetate, hence was discarded. Other three peaks in the volume ranges 200-270, 280-350, 360-450 ml, respectively were collected separately, freeze-dried and analysed. TLC of electrolysed solution was carried out on silica gel-G plates using methanol-acetic acid-benzene (80:10:10) as developer.

Results and Discussion

Polarographic behaviour

Polarographic reduction of Acid Red-150 occurred in one well-defined diffusion-controlled wave below *p*H 5.5. In the *p*H range of 5.6-8.0, the wave splitted into two waves and the limiting current of the first wave was almost 1/3 of the second wave. At *p*H > 8.0, two waves of equal height were observed. The nature of the waves was found to be diffusion-con-

Table 1—Polarographic Characteristics of Acid Red-150 in B.R. buffers of different *p*H

*p*H	$(-E_{1/2})$ (V)	i_d (μA)	αn	
			log plot method	Oldham's method
2.2	0.22	2.62	1.10	1.12
3.4	0.26	2.62	1.00	1.16
4.4	0.34	2.69	0.90	1.00
5.5	0.45	2.54	1.12	0.98
6.4	0.32	0.825	0.96	0.98
	0.48	1.500	0.98	1.06
7.2	0.37	0.750	1.13	0.98
	0.54	1.650	1.08	1.08
8.6	0.44	1.275	1.12	1.06
	0.65	1.350	0.96	0.96
10.0	0.52	1.350	1.00	1.10
	0.70	1.275	1.10	1.14
11.2	0.58	1.275	1.14	1.12
	0.73	1.275	1.12	1.12

trolled as evidenced by i_d versus $\sqrt{h}$ and low temperature coefficient value (1.2% deg^{-1}). The $E_{1/2}$ was dependent on *p*H and shifted towards more negative value with increase in *p*H. The plots of $E_{1/2}$ versus *p*H were linear for both the waves and can be represented by Eqs (1) and (2),

$$(-E_{1/2})_1 = [0.054\,p\text{H} + 0.02] \qquad \ldots(1)$$

$$(-E_{1/2})_2 = [0.066\,p\text{H} + 0.09] \qquad \ldots(2)$$

The limiting current of the wave < 5.5 was practically equal to the sum of the limiting current of the two waves at *p*H > 5.5. This indicates that overall electrode reaction is the same in the entire *p*H range. The effect of dye concentration on $E_{1/2}$ and limiting current was studied in the dye concentration range of 0.05-1.0 m*M*. The i_d versus concentration plot was linear passing through the origin indicating that this dye can be safely estimated in this concentration range by polarographic method. However, $E_{1/2}$ shifted towards more negative value with increase in dye concentration showing irreversible nature (also confirmed by log plot analysis[5]) of the electrode process and possible role of adsorption[5]. The values of αn were determined by log plot analysis as well as the method of Oldham and Perry[6]. The values of αn determined by the two methods at different *p*H values are practically same (Table 1).

Linear and cyclic sweep voltammetry

Linear sweep voltammetry at a sweep rate of 5 mVs^{-1} exhibited one well-defined reduction peak in the *p*H range of 2.2-11.2. The peak potential was dependent on *p*H and shifted towards more negative potential with increase in *p*H. Cyclic sweep voltammetry at a sweep rate of 100 mVs^{-1} exhibited two reduction peaks Ic and IIc, when sweep was initiated in the negative direction. In the reverse sweep, three oxidation peaks were observed. On the second sweep towards positive potential two new cathodic peaks (IIIc and IVc) were noted (Fig. 1). To confirm whether oxidation peaks are due to the oxidation of products formed in Ic/IIc reaction or are due to an independent oxidation of Acid Red-150, cyclic voltammograms were also recorded by initiating the sweep in the positive direction. The absence of oxidation peaks clearly indicated that peaks IIIa-Va are due to oxidation of the product formed in Ic/IIc reaction.

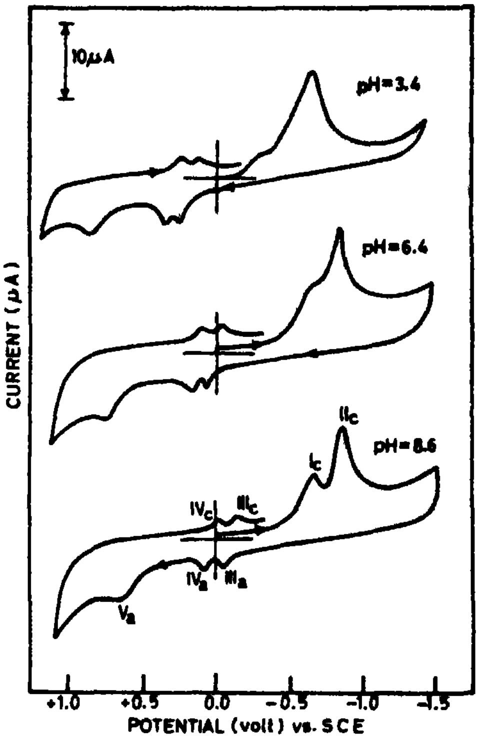

Fig. 1—Cyclic voltammograms observed for 0.2 m*M* Acid Red-150 at PGE. Sweep rate 150 mVs^{-1}

At *p*H 8.6 where two reduction peaks were well-defined, cyclic voltammograms were recorded by changing the direction of the sweep after peak Ic. The peaks IIIa-Va and reduction peaks IVc and Vc were not visible, indicating that these peaks are observed only after complete reduction of the dye. Peaks IIIa/IIIc and IVa/IVc formed an irreversible couple and were observed clearly only at a scan rate > 100 mVs^{-1}. The peak potential of the reduction peaks Ic to IVc was dependent on *p*H and shifted towards more negative potential with increase in *p*H. On the other hand peak potentials of oxidation peaks IIIa to Va also shifted towards less positive value with increase in *p*H.

Controlled potential coulometry of Acid Red-150 was carried out at mercury pool cathode and at plateau potential of first or second wave. Below *p*H 5.5, where only one wave was observed the value of *n* determined by graphical integration of current-time curve was found to be 8.0 ± 0.2. In the *p*H range 5.6-8.0 the first wave involved 2.0 ± 0.1 electrons whereas second wave involved 6.0 ± 0.2 electrons. This observation was in accordance with the observed limiting currents for the first and second wave. At *p*H > 8.0, the two waves involved 4.0 ± 0.15 electrons as confirmed by practically same equal limiting currents. The values of *n* were also determined using pyrolytic graphite plate. At *p*H < 8.0, the first peak was not very well-defined; hence the value of *n* determined at potentials more negative to peak IIc was found to be 8.0 ± 0.15. At *p*H > 8.0, the value of *n* for the peaks Ic and IIc, was 4.0 ± 0.3 electrons each. The large deviation in *n*-value from the average value at *p*H > 8.0 may be due to the fact that the potential applied for peak Ic also contributed partially to peak IIc, as the potentials of peaks Ic and IIc are very close.

The progress of electrolysis was monitored by recording cyclic voltammograms at different time intervals. On applying potential corresponding to peak IIc, a systematic decrease in peaks Ic and IIc was observed. Whereas the peaks IIIa to Va and IIIc, IVc were clearly visible in exhaustively electrolysed solution. A cyclic voltammogram of exhaustively electrolysed solution at *p*H 3.4 is presented in Fig. 2D. This voltammogram did not change even when the electrolysed solution was left at room temperature for several hours. Thus it is concluded that product or products of electroreduction are electroactive in nature. Similar behaviour was observed at *p*H 7.0 and 10.6.

The progress of electrolysis was also monitored by UV/vis spectra at different interval of times. The UV/VIS spectra of Acid Red-150 in the entire *p*H range, exhibit λ_{max} at 235, 356 and 513 nm, indicating that the dye exists as a neutral species in the entire *p*H range studied. At *p*H 6, upon application of potential more negative to peak IIc, absorbances at 356 and 513 nm systematically decrease whereas the absorbance at 235 nm increases. After about 3 hr of electrolysis the absorbance at 235 nm reaches a maximum while those at 356 and 513 nm reach minimum values. These observations show that no intermediate with sufficient half-life is generated during electrooxidation of the dye.

Product identification

The products of electroreduction at *p*H 3.0, 6.0 and 10.2 at mercury pool or at pyrolytic graphite electrode were characterised as follows: The volumes obtained corresponding to three peaks in liquid chromatography over sephadex G-10 were lyopholised and analysed by TLC, m.ps and IR spectra. The volumes 200-270 (peak 2), 280-350 (peak 3) and 360-450 (peak 4) ml were lyopholised and exhibited R_f values 0.65, 0.47, and 0.19 respectively. Thus it is clear that three products are formed during complete electroreduction of the dye.

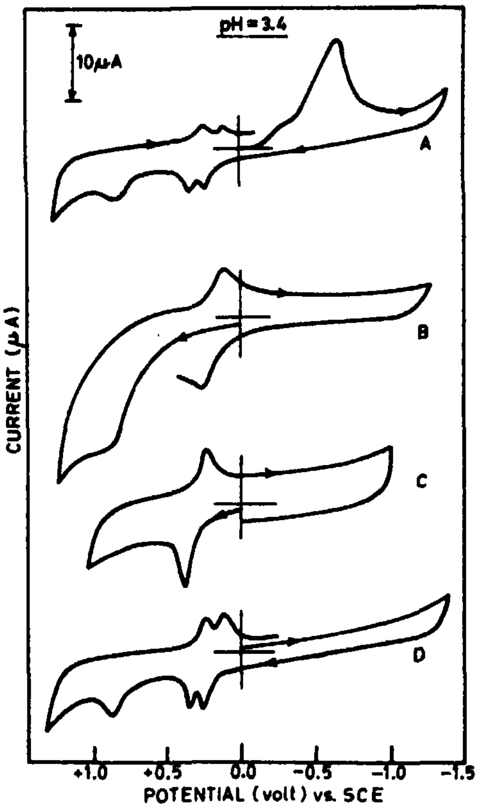

Fig. 2—Cyclic voltammograms observed at *p*H 3.4 for (A) Acid Red-150, (B) aniline, (C) *p*-phenylenediamine, (D) exhaustively electrolysed solution of Acid Red-150 at *p*H 3.4.

The product with R_f 0.65 (peak 2) was identified as aniline by comparison (R_f and IR) with an authentic sample. The product with R_f 0.47 (peak 3) had the m.p. 290°. The IR spectrum of this product exhibited peaks corresponding to SO_3H (1030, 1100 cm^{-1}) and phenolic OH (1250, 1360 cm^{-1}). Based on this the product should have structure similar to 1-amino-2-hydroxynaphthalene-3, 6-disulphonic acid. This product could not be completely identified at this stage due to non-availability of its authentic sample.

The product with R_f 0.19 (peak 4), melted at 140° and exhibited in its IR spectrum bands at 820, 1120, 1260, 1300, 1500 and 1600 cm^{-1}. This product was identified as *p*-phenylenediamine by direct comparison with an authentic sample.

Hence it is clear that the products of complete electroreduction of Acid Red-150 are aniline, *p*-phenylenediamine and 1-amino-2-hydroxynaphthalene-3, 6-disulphonic acid.

The formation of aniline and *p*-phenylenediamine was further confirmed by recording cyclic voltammograms of authentic samples of aniline and *p*-phenylenediamine, which have been reported electroactive in nature[7,8]. It was interesting to observe that aniline exhibits peaks IIIa, Va and IIIc as reported in literature[9,10] and *p*-pheylenediamine gives peaks IVa and IVc at the same potentials as observed for the dye. Cyclic voltammograms of Acid Red-150, *p*-phenylenediamine and aniline at *p*H 3.4 are presented in Fig. 2, for comparison.

The products corresponding to (4e, $4H^+$) reduction of the dye (I) were also characterised at neutral and alkaline *p*H, where two waves in polarography and two peaks in cyclic voltammetry with equal limiting currents were observed. For this purpose the dye was reduced at peak Ic potential or plateau potential of the first wave. The TLC of this solution gave two spots with $R_f = 0.47$ and 0.56 thus indicating that (4e, $4H^+$) reduction of the dye gives two products. The spot with R_f 0.47 indicates the formation of 1-amino-2-hydroxynaphthelene-3, 6-disulphonic acid as observed earlier. Cyclic voltammogram of this solution was recorded by initiating the sweep in the positive direction. The absence of oxidation peak IIIa-Va and reduction peaks IIIc-IVc clearly indicate that 4e, $4H^+$ reduction of the dye does not give aniline or *p*-phenylenediamine as the product. Thus (4e, $4H^+$) reduction causes cleavage of bulky naphthol moiety to give 1-amino-2-naphthol-3, 6-disulphonic acid (sodium salt) and 4-aminoazobenzene.

Redox mechanism

On the basis of the results obtained, it is clear that the dye undergoes reduction by 8e, $8H^+$ process at d.m.e and pyrolytic graphite electrode in the *p*H range of 2.2-11.2. The (4e, $4H^+$) reduction in neutral and alkaline *p*H ranges does not indicate the formation of aniline and *p*-phenylenediamine. It can be safely concluded that reduction of $-N=N-$ attached to bulkier naphthol moiety takes place easily in comparison to azo group attached to phenyl moiety.

As the final products of electroreduction are aniline, *p*-phenylenediamine and 1-amino-2-naphthol-3, 6-disulphonic acid it is clear that electroreduction of the two azo groups does not stop at hydrazo stage but further reduction of hydrazo group in II takes place to give amino compounds as the ultimate products (Scheme 1). The first (4e, $4H^+$) reduction of the dye causes cleavage of $-N=N-$ to give *p*-aminoazobenzene (III) and aminonaphthol moiety (IV). Further (4e, $4H^+$) reduction causes the cleavage of second $-N=N-$ to give aniline and *p*-phenylenediamine as the products.

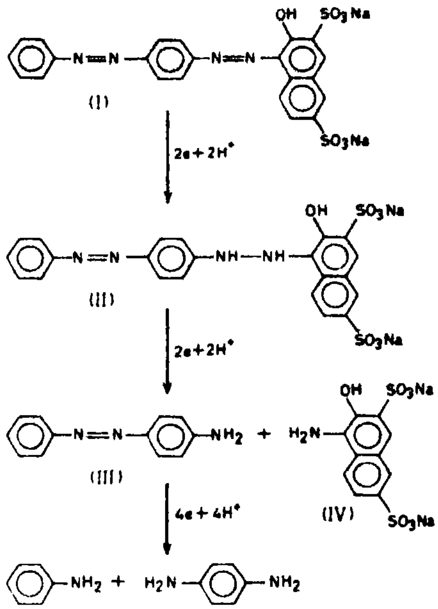

Scheme 1 – Tentative mechanism proposed for the electroreduction of Acid Red-150.

Previous results[12] reported in literature indicate that electroreduction of bisazodyes occurs by first taking (4e, $4H^+$) to give bishydrazo derivatives. Bisazobenzene and similar dyes have been reported[13,14] to form bishydrazobenzene at d.m.e. Further (4e, $4H^+$) reduction of bishydrazo derivatives is reported to give amino compounds as the products of reduction. However, in our case bishydrazo derivative is not formed, rather cleavage at $-N=N-$ attached to bulkier naphthol moiety takes place. This difference in behaviour can be due to steric hindrance to coplanarity[15,16] in the molecule, due to the bulkier naphthol group, thereby facilitating cleavage via $-N=N-$. It has also been observed that reduction potentials at pyrolytic graphite are 250 to 500 mV more negative in comparison to that at d.m.e. This behaviour can be explained on the basis of adsorption on the solid electrodes[17]. The solid electrodes also do not permit the free orientation of the species undergoing reduction and hence the potentials observed are always more negative in comparison to those at d.m.e.

Acknowledgement

Thanks are due to M/s Pfizer, USA for the gift of pyrolytic graphite. One of the authors (AK) is thankful to the UGC, New Delhi for the award of a junior research fellowship.

References

1 Eisner U & Eisner E K, in *Encyclopedia of electrochemistry of the elements*, edited by A J Bard (Marcel Dekker, New York) 1979.
2 Britton H T S, *Hydrogen ions* (D Van Nostrand, New York) 1956 P 360.
3 Goyal R N, Bhushan R & Agarwal A, *J electroanal Chem*, **171** (1984) 281.
4 Goyal R N, Srivastava S K & Agarwal R, *Bull Soc Chim Fr*, **4** (1985) 656.
5 Meites L, *Polarographic techniques* (Interscience, New York) 1967 pp 228.
6 Oldham K B & Perry E P, *Analyt Chem*, **40** (1968) 65.
7 Lee H Y & Adams R N, *Analyt Chem*, **34** (1962) 1587.
8 Bacon J & Adams R N, *J Am chem Soc*, **65** (1945) 1938.
9 Wawzonek S & McIntyre T W, *J electrochem Soc*, **114** (1967) 1025.
10 Melchior & Maki A H, *J chem Phys*, **34** (1961) 471.
11 Zeweig A, Lancaster J E, Negalia M T & Jura W H, *J Am chem Soc*, **86** (1964) 4130.
12 Saber T M H, Ali M I & Abed N M, *J electroanal Chem*, **28** (1970) 177.
13 Florence T M, Johnson D A & Batley G E, *J electroanal Chem*, **50** (1974) 411.
14 Florence T M, *J electroanal Chem*, **52** (1974) 115.
15 Zuman P, *Colln Czech chem Commun*, **27** (1962) 648.
16 Charton M, *J org Chem*, **34** (1969) 278.
17 Adams R N, *Electrochemistry at solid electrodes* (Marcel Dekker, New York) 1969, pp 120.

Indian Journal of Chemistry
Vol. 27A, June 1988, pp. 487-493

Redox Chemistry of Hyponitrous Acid: Part I—Stoichiometry, Kinetics & Mechanism of Its Oxidation by Ethylenediaminetetraacetatothallium (III) in Aqueous Perchloric Acid Medium

MUNI R GOYAL, RAMA K MITTAL & Y K GUPTA*
Department of Chemistry, Rajasthan University, Jaipur 302 004

Received 23 *June* 1987; *revised* 21 *September* 1987; *accepted* 16 *November* 1987

One mol of hyponitrous acid ($H_2N_2O_2$) reacts with one mole of thallium (III) in acidic perchlorate solution initially yielding one mol of HNO_2 and 1/2 mol of N_2O gas. The likely subsequent steps are the oxidation of HNO_2 by Tl(III), and the reaction between $H_2N_2O_2$ and HNO_2. In the absence of EDTA, oxidation by Tl(III) occurs and ultimately two mol of Tl(III) are consumed for each mol of $H_2N_2O_2$. In the presence of EDTA the stoichiometry is not definite for solutions in which $[HClO_4]$ is < 1.0 mol dm^{-3}, but in solutions where $[HClO_4]$ is > 1.5 mol dm^{-3}, one mol of Tl(III) consumes two mol of $H_2N_2O_2$. Kinetics studied in the presence of EDTA shows an induction period which is ascribed to the formation of HNO_2

No mechanistic studies on the oxidation of hyponitrite seem to have been made so far; only its decomposition kinetics[1-6] have been studied. During investigations on the oxidation of hydroxylamine in our laboratory, hyponitrite was found to be one of the intermediate products[7,8]. Also *trans* and *cis* forms of $H_2N_2O_2$ have been reported[2] and it is not known whether the unstable[9,10] *cis*-form has any role in the redox systems. The present paper describes the results of oxidation of $H_2N_2O_2$ with thallium (III). Only one redox reaction in which $H_2N_2O_2$ acts as an oxidizing agents is reported in literature[11].

Our preliminary results revealed that the oxidation of $H_2N_2O_2$ by Tl(III) in acid perchlorate solutions (0.1-0.6 mol dm^{-3}) occurs in two stages. The first reaction is very fast and is over within the time of mixing and corresponds to the stoichiometry of 1:1 ([Tl(III)]:[$H_2N_2O_2$]). This fast reaction is followed by a slow reaction characteristic of the oxidation of nitrite[12]. Literature survey reveals that hyponitrous acid is oxidized to oxyhyponitrous acid ($H_2N_2O_3$) which decomposes[13,14] readily yielding HNO_2 and N_2O in aqueous acidic solutions. Our aim is to characterize these two steps separately and to know the product of oxidation of the fast step.

Oxidation of HNO_2 by Tl(III) is slow in the presence of EDTA (0.015 mol dm^{-3}) and yielded HNO_3 as the final product. The reaction[11] of $H_2N_2O_2$ and HNO_2 is also slow in the presence of EDTA. However, the rate of the reaction increases with increase in acidity and is instantaneous in 1.5 mol dm^{-3} $HClO_4$ even in the presence of EDTA. This reaction could not be studied kinetically owing to interference in spectrophotometric measurements by EDTA. Only qualitative tests for HNO_2 could be done.

The main oxidation reaction in the presence of EDTA is attended by an induction period which decreases by the addition of trace amounts of $HNO_2$and disappears completely in the presence of 5×10^{-5} mol dm^{-3} NO_2^-. The magnitude of induction period also decreases with increase in $[H_2N_2O_2]$ and $[HClO_4]$, and no induction period is observed in 1.5 mol dm^{-3} or more $HClO_4$. Hence kinetic runs were made in the presence of 1×10^{-4} mol dm^{-3} NO_2^- so that the induction period is completely eliminated.

Since oxyhypointrous acid (trioxodinitrate or Angeli's salt)[14] is said to be the intermediate oxidation product prior to the formation of HNO_2, this was prepared[9] and a few experiments were also carried out with it to verify whether it could be the intermediate product of fast reaction.

Materials and Methods

Sodium hyponitrite was prepared by the electrolytic method[15] and its purity checked by standard method[16,17]. Solutions of $H_2N_2O_2$ were prepared whenever required in aqueous 0.5 mol dm^{-3} $HClO_4$ to which ethyl alcohol (0.1mol%) was added to prevent its decomposition[4]. For all kinetic experiments *p*H was kept < 3 so that the decomposition of $H_2N_2O_2$ did not occur during the time the kinetics were followed.

Thallic perchlorate solutions were prepared from thallic oxide (BDH, AR) and 70% $HClO_4$ (E. Merck) and were standardized iodometrically. Solutions of $LiClO_4$ were prepared by neutralizing

70% $HClO_4$ with Li_2CO_3 (BDH, AR) to *p*H 6.8. All other chemicals were either AR (BDH) or GR (E. Merck) quality. doubly distilled, conductivity water was used for preparing all solutions.

Oxyhyponitrous acid was prepared by the literataure method[18]. Ethyl nitrate was prepared by mixing calculated amounts of ethyl iodide and solid silver nitrate and distilling under reduced pressure. The solid compound after recrystallisation was stored in ethyl alcohol in the cold. Its analysis corresponded to $Na_2N_2O_3$. Alkaline solutions ($0.1\ mol\ dm^{-3}$) of the salt absorbed at 248 nm ($\varepsilon = 8.0 \times 10^3$). In aqueous solution it decomposed slowly, but in acidic solutions it decomposed readily[13] and gave no absorption in UV region except that characteristic of HNO_2. Aqueous solutions of the salt were prepared only when needed.

Kinetic procedure

Reaction was initiated by adding the required quantity of $H_2N_2O_2$ to a mixture of Tl(III) and other reactants. Aliquots were added to an equal volume of 6 *N* HCl to quench the reaction [since chloro-complexes of Tl(III) are are not reactive], and analysed iodometrically for unreacted Tl(III). Nitrite was decomposed by the addition of urea before carrying out iodometric determination. Initial rates were detrmined by the plane mirror method. These were reproducible within ± 5%.

Spectrophotometric measurement was carried out on a Perkin-Elmer spectrophotometer fitted with a cell of 1cm path length. *p*H determinations were made on an EC Digital *p*H meter.

Results

Stoichiometry

This was determined in the absence and presence of EDTA. Excess thallium (III) was determined iodometrically and excess hyponitrite determined by the precipitation method[12]. Excess hyponitrite could not be employed in the presence of EDTA since the latter interfered with the precipitation method. UV spectrophotometry also could not be adopted because of the presence of EDTA and possibly other unknown intermediates. Nitrous oxide was collected over water saturated with N_2O. The results are given in Table 1.

The stoichiometry was determined under two conditions: In the absence of EDTA one mol of Tl(III) reacted with one mol of $H_2N_2O_2$ according to Eq. (1).

$$\mathrm{Tl(III)} + H_2N_2O_2 + \tfrac{1}{2}H_2O \rightarrow \tfrac{1}{2}N_2O + HNO_2 + \mathrm{Tl(I)} + 2H^+ \qquad \ldots (1)$$

Table 1 — Initial Rates (v_0) at DIfferent [Tl(III)] in Reaction of Tl(III) with $H_2N_2O_2$

[EDTA] = $0.015\ mol\ dm^{-3}$; [NO_2^- = $1.0 \times 10^{-4}\ mol\ dm^{-3}$; [$HClO_4$ = $0.5\ mol\ dm^{-3}$; temp = 35°C

$10^3\ [H_2N_2O_2]$ (mol dm^{-3})	10^3 [Tl(III)] (mol dm^{-3})	$10^7\ (v_0)$ (mol $dm^{-3}s^{-1}$)	
		Obs	Calc[a]
1.0	0.5	2.2	2.2
1.0	0.6	2.5	2.5
1.0	0.8	3.3	3.2
1.0	1.0	4.0	3.7
1.0	2.0	6.0	5.7
1.0	3.0	6.5	6.9
1.0	4.0	7.0	7.7
1.0	6.0	7.0	—
2.0	0.5	4.8	4.4
2.0	1.0	7.8	7.4
2.0	2.0	11.5	11.3
2.0	3.0	13	13.8
2.0	4.0	14.5	15.4
2.0	6.0	14.5	—
3.0	0.5	7.0	6.6
3.0	0.6	7.5	7.6
3.0	0.8	10	9.5
3.0	1.0	12	11.2
3.0	2.0	17.5	17
3.0	3.0	21	20.7
3.0	5.0	21.5	—
3.0	7.0	21.5	—

[a] Calculated from Eq. (14) with $k_1 = 1.2 \times 10^{-3}s^{-1}$ and $k_5/k_4 = 4.5 \times 10^2$.

The reaction mixture containing 5ml of $0.1\ mol\ dm^{-3}$ $H_2N_2O_2$ and 25ml $0.02\ mol\ dm^{-3}$ thallium (III) in $0.5\ mol\ dm^{-3}$ $HClO_4$ yielded an average of 5.4 ml of N_2O at N.T.P. which compared well with the value of 5.6 ml expected from Eq. (1). The mixture responded to tests for HNO_2. One of the forms of oxyhyponitrous acid ($H_2N_2O_3$) reported earlier[13] may be an intermediate in reaction (1), decomposing quickly according to Eq. (2).

$$H_2N_2O_2 \rightarrow \tfrac{1}{2}H_2O + \tfrac{1}{2}N_2O + HNO_2 \qquad \ldots (2)$$

The same mixture consumed one more mol of Tl(III), if excess Tl(III) was determied after 2hr. The overall stoichiometry of 2:1 ([[Tl(III)]:[$H_2N_2O_2$]]) therefore corresponded to reaction (3)

$$2\mathrm{Tl(III)} + H_2N_2O_2 + 1.5H_2O \rightarrow 0.5N_2O + HNO_3 + 2\mathrm{Tl(I)} + 4H^+ \qquad \ldots (3)$$

This was further supported by the quantitative determination of N_2O and qualitative tests for

HNO_3. Equation (3) is in fact a combination of Eqs (1) and (3a).

$$Tl(III) + HNO_2 + H_2O \rightarrow Tl(I) + HNO_3 + 2H^+ \quad \ldots (3a)$$

The stoichiometry ([Tl(III)]:[$H_2N_2O_2$]) in the presence of EDTA and 0.5 mol dm^{-3} $HClO_4$ was not definite and it always varied between one and two depending on the concentrations of the reactants. The products responded to tests for NO_3^-, N_2 and N_2O. In the presence of EDTA, reaction (1) was slow and subsequent reaction (oxidations of HNO_2 and $H_2N_2O_2$) was still slower.

In (1.5-2.0) mol dm^{-3} $HClO_4$ and in the presence of EDTA, one mol of Tl(III) reacted with two mol of $H_2N_2O_2$. In such a situation reaction (1) seems to be followed by a fast reaction (4)

$$H_2N_2O_2 + HNO_2 \rightarrow N_2 + H_2O + HNO_3 \quad \ldots (4)$$

with an overall stoichiometry given by Eq. (5).

$$2H_2N_2O_2 + Tl(III) \rightarrow N_2 + HNO_3 + Tl(I) + 2H^+ + 0.5N_2O + 0.5H_2O \quad \ldots (5)$$

Nitrogen was estimated after dissolving N_2O in water. In four experiments 10 ml of 0.1 mol dm^{-3} of $H_2N_2O_2$ and 25 ml of 0.02 mol dm^{-3} solution of Tl(III) in 2.0 mol dm^{-3} $HClO_4$ and 0.015 mol dm^{-3} EDTA, yielded an average of 10.8 ml of N_2 at N.T.P. The expected value is 11.2 ml. It is therefore obvious that the intermediate product in all cases is HNO_2 which is oxidized to HNO_3 by Tl(III) in the absence of EDTA, and by $H_2N_2O_2$ in the presence of EDTA both according to definite stoichiometries.

An attempt was made to determine the stoichiometry of the oxidation of oxyhyponitrous acid by Tl(III) and it was found to be between 2:1 and 3:1 ([Tl(III)]:[$H_2N_2O_3$]). Oxyhyponitrous acid partly decomposed in acid solution and stoichiometry was not definite. It we assume that $H_2N_2O_3$ was completely decomposed, then one mol of Tl(III) would be required for one mol of $H_2N_2O_3$ indicating oxidation of decomposition product HNO_2. It was therefore obvious that greater part of $H_2N_2O_3$ was oxidized. The reaction was initiated by the addition of $Na_2N_2O_3$ and excess Tl(III) was determined after about 5 hr. Incidently this also proved that $H_2N_2O_3$ as such was not the intermediate product of the fast reaction between $H_2N_2O_2$ and Tl(III).

Reaction in presence of EDTA and 0.5 *mol dm*$^{-3}$ *$HClO_4$: Thallium (III) dependence*

The results presented in Table 1 show that the rate increases and tends to a limiting value with increase in [Tl(III)] from 6.0×10^{-4} to 7.0×10^{-3} mol dm^{-3} and follows the general rate law (6).

$$-d[Tl(III)]/dt = A[Tl(III)]/(1 + B[Tl(III)]) \quad \ldots (6)$$

where A and B are constants.

The rate was first order in [$H_2N_2O_2$] (from 7.0×10^{-4} to 1.25×10^{-2} mol dm^{-3}) at different [Tl(III)] and [H^+] as revealed by the results in Table 2. Above 1.0 mol dm^{-3} $HClO_4$ when the stoichiometry was definite, the rate was first order in [H^+] (Table 3).

Reaction in presence of EDTA and 2.0 *mol dm*$^{-3}$ *$HClO_4$: First stage reaction*:

A typical plot under the conditions for decrease in [Tl(III)] with time (Fig. 1) gave the stoichiometry 1:2 ([Tl(III)]:[$H_2N_2O_2$]). The order in [Tl(III)], [$H_2N_2O_2$] and [H^+] was unity in each case as re-

Table 2—Effect of Varying [$H_2N_2O_2$] on Initial Rate (v_0) in Oxidation of $H_2N_2O_2$ by Tl(III)

[EDTA] = 0.015 mol dm^{-3}; [NO_2^-] = 1.0×10^{-4} mol dm^{-3}; [$HClO_4$] = 0.5 mol dm^{-3}; temp. = 35°C

10^3 [$H_2N_2O_2$] (mol dm^{-3})	10^7 (v0) (mol dm^{-3}s^{-1})	10^3 [$H_2N_2O_2$] (mol dm^{-3})	10^7 (v_0) (mol dm^{-3}s^{-1})	10^3 [$H_2N_2O_2$] (mol dm^{-3})	10^7 (v_0) (mol dm^{-3}s^{-1})
[Tl(III)] = 3.0×10^{-3}mol dm^{-3}		[Tl(III)] = 2.0mol dm^{-3}		[Tl(III)] = 7.0×10^{-3}mol dm^{-3}	
0.7	3.2				
1.0	6.4	1.0	5.0	1.0	7.0
2.0	13	2.0	12	2.0	14
3.0	21	3.0	18	3.0	21
4.0	27				
5.0	31	5.0	27	5.0	38
6.0	36			7.0	52
8.0	50				
10.0	56	10.0	54	10.0	69
12.5	72				

Table 3—Effect of Varying [H^+] on Initial Rates (v_0) in Reaction of Tl(III) with $H_2N_2O_2$

[Tl(III)] = 2.0×10^{-3}mol dm^{-3}; [$H_2N_2Q_2$] = 1.0×10^{-3}mol dm^{-3}; [NO_2^-] = 1.0×10^{-4}mol dm^{-3}; [EDTA] = 0.015mol dm^{-3}; I = 2.0 mol dm^{-3}; temp. = 35°C

[$HClO_4$] (mol dm^{-3})	[H^+] (mol dm^{-3})	10^7 (v_0) (mol dm^{-3}s^{-1})	[$HClO_4$] (mol dm^{-3})	[H^+] (mol dm^{-3})	10^7 (v_0) (mol dm^{-3}s^{-1})
0.16	0.08	5.0	0.96	0.68	4.7
0.24	0.15	5.7	1.12	0.76	4.8
0.42	0.22	7.3	1.28	0.86	5.5
0.40	0.30	6.7	1.44	1.04	7.0
0.48	0.37	5.8	1.60	1.04	8.5
0.64	0.50	4.2	1.76	1.43	10
0.80	0.60	4.2	1.92	1.64	11

Table 4—Effect of Varying [Tl(III)], [$H_2N_2O_2$] and [$HClO_4$] on Initial Rates (v_0) at 35°

[EDTA] = 0.015mol dm^{-3}; [NO_2^-] = 1.0×10^{-4}mol dm^{-3}

10^3 [Tl(III)] (mol dm^{-3})	10^3 [$H_2N_2O_2$] (mol dm^{-3})	[$HClO_4$] (mol dm^{-3})	[H^+] (mol dm^{-3})	10^7 (v_0) (mol dm^{-3}s^{-1})	v_0/Tl(III)][$H_2N_2O_2$][H^+] (dm^{6}mol^{-2}s^{-1})
0.6	3.0	2.0	1.7	9.5	0.31
1.0	3.0	2.0	1.7	16	0.31
2.0	3.0	2.0	1.7	33	0.32
3.0	3.0	2.0	1.7	50	0.33
6.0	3.0	2.0	1.7	100	0.32
2.0	2.0	2.0	1.7	22	0.32
3.0	2.0	2.0	1.7	34	0.32
2.0	1.5	2.0	1.7	17	0.33
2.0	1.0	2.0	1.7	11	0.32
2.0	1.0	1.75	1.4	10	0.36
2.0	1.0	1.50	1.1	7.3	0.33
2.0	1.0	1.25	0.84	5.7	0.34
2.0	1.0	1.0	0.70	4.7	0.33

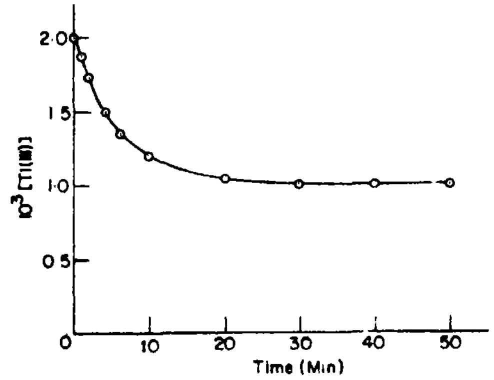

Fig. 1—Plots of Tl(III) versus time at 35°C: Tl(III) = 2.0×10^{-3} mol dm^{-3}; $H_2N_2O_2$ = 2.0×10^{-3} mol dm^{-3}; $HClO_4$ = 2.0×10^{-3} mol dm^{-3}; and EDTA = 0.015 mol dm^{-3}

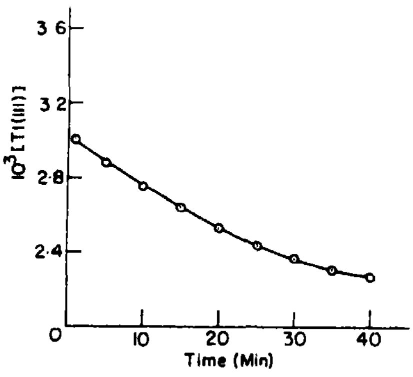

Fig. 2—Plot of Tl(III) versus time at 35°C; Tl(III) initial = 4.0×10^{-3} mol dm^{-3}; Tl(III) after 1 min = 3.0×10^{-3} mol dm^{-3}; $H_2N_2O_2$ = 1.0×10^{-3} mol dm^{-3}; $HClO_4$ = 0.5 mol dm^{-3}

vealed by the result given in Table 4. The otherwise complicated reaction seems to behave in a simple manner in high acid medium, but in order to know more about the products and the mechanism, several reaction mixtures were prepared by mixing Tl(III) and $H_2N_2O_2$ in equivalent amounts corresponding to the stoichiometry of 1:2. After 20 min when the reaction was almost over, more Tl(III) was added to see whether it reacted with the products. These results showed that there was no reducing product in the system and that added Tl(III) reacted only when excess

Table 5—Effect of Oxidation Product of Fast Reaction

[$HClO_4$] = 0.5mol dm^{-3}; temp. = 35°C

10^3 [Tl(III)]$_i$ (mol dm^{-3})	10^3 [$H_2N_2O_2$]$_i$ (mol dm^{-3})	10^3 [Tl(III)]^a (mol dm^{-3})	·10^3 [Product]^a (mol dm^{-3})	10^6 (v_0)^a (mol dm^{-3}s^{-1})
3.0	2.0	1.0	2.0	7.5
4.0	2.0	2.0	2.0	5.0
5.0	2.0	3.0	2.0	3.1
6.0	2.0	4.0	2.0	2.2
7.0	2.0	5.0	2.0	1.8
3.0	1.0	2.0	1.0	1.2
4.0	2.0	2.0	2.0	3.2
5.0	3.0	2.0	3.0	15
6.0	4.0	2.0	4.0	18
8.0	6.0	2.0	6.0	21
10.0	8.0	2.0	8.0	28
12.0	10.0	2.0	10.0	30
22.0	20.0	2.0	20.0	26
32.0	30.0	2.0	30.0	24

a After 1 min

Table 6—Oxidation of Oxyhyponitrous Acid by Tl(III)

[oxyhypointrite] = 0.001mol dm^{-3}; [$HClO_4$] = 0.5mol dm^{-3}; temp. = 35°C

Time (min)	Iodometric titre values at different times for 10^3 [Tl(III)](mol dm^{-3})				
	5.0	4.0	2.0^a	2.0^{a,b}	2.0^{a,c}
0	10	8.0	8.4	8.4	8.4
1	8.5	6.4	5.5	7.9	8.4
5	8.1	5.8	2.6	6.4	8.4
10	7.8	5.3	1.3	5.0	8.3
20	7.3	4.5	0.3(0)^d	4.1	8.3
30	6.8	4.1	—	4.1(4.2)^e	8.2
45	—	3.8	—	8.2	
60	6.3	—	—	—	—
300	5.2(5.1)^d	—	—	—	8.1
		3.0 (3.1)^d			

(a) Different solutions of thiosulphate used for titration(b) Reaction initiated by addition of Tl(III)

(c) Reaction in the presence of EDTA

(d) Figures in parentheses give the expected titre values on the arbitrary assumption that 75% $H_2N_2O_3$ undergoes oxidation and 25% of it decomposed.

(e) Figures in parentheses give the expected titre value on the assumption of overall 1:1 stoichiometry.

$H_2N_2O_2$ (> 2 molar proportion as required by 1:2 stoichiometry) was initially taken. Further the decrease in [Tl(III)] was characteristic of the plot in Fig. 1.

Reaction with the product of fast reaction: Second stage reaction:

The fast reaction between Tl(III) and $H_2N_2O_2$ which followed 1:1 stoichiometry and slowed down after 1 min was initially studied. A typical plot is shown in Fig. 2. The results at different [product] and unconsumed [Tl(III)] after 1 min, are presented in Table 5. At fixed [product] and different [Tl(III)], the rate decreased. At fixed [Tl(III)] and different [products], the rate increased, passing through a maximum and then decreased. These are characteristics of the oxidation[12] of HNO_2 where 1:2 complex of Tl(III) and HNO_2 was considered to be reactive and 1:1 and 1:3 complexes were considered to be unreactive. The maximum rate at 0.01 mol dm^{-3} HNO_2 is 30×10^{-6} mol dm^{-3}s^{-1} at 35°. In the oxidation[14] of HNO_2, the maximum rate at 0.009 mol dm^{-3} HNO_2 was 8×10^{-6} mol dm^{-3}s^{-1} at 25°. The product of fast reaction therefore appears to be HNO_2.

Reaction of oxyhyponitrous acid with thallium (III)

The reaction conditions for this reaction are shown in Table 6. The reaction was initiated by the addition of a solution of oxyhypointrite. Four facts are obvious from these results: (i) There was a fast reaction between $H_2N_2O_3$ and Tl(III), but Tl(III) consumed was always less than that corresponding to 1:1 stoichiometry, indicating thereby that part of $H_2N_2O_3$ decomposed. Hence oxidation and decomposition of $H_2N_2O_3$ are competitive processes, (ii) After the fast reaction, the magnitude of decrease in [Tl(III)] was less with increase in [Tl(III)]—a characteristic of the oxidation of HNO_2 by Tl(III). Hence the product of fast reaction was HNO_2. (iii) If the reaction was initiated by the addition of Tl(III), $H_2N_2O_3$ already present in the reaction mixture decomposed completely into HNO_2 and there was no initial fast reduction of Tl(III). Total Tl(III) consumed corresponded to 1:1 stoichiometry. (iv) In the presence of EDTA the fast reaction became slow—much slower then the oxidation of $H_2N_2O_2$ under similar conditions.

Immediate product of oxidation of hyponitrous acid

In the absence of EDTA the first step of the oxidation of hyponitrous acid is fast. If oxyhyponitrous acid was the product, its oxidation would be fast and hence the stoichiometry of the fast reaction would require more than one mol of Tl(III) for each mol of $H_2N_2O_2$. Since the stoichiometry of the fast reaction is 1:1 and the reaction mixture immediately after mixing of the reactants does not show absorption at 248 nm the possibility of oxyhyponitrous acid as the reaction product is ruled out. Further the works of Bonner and coworkers[19,20], and Hughes and Wimbledon[21] on the isotopic exchange studies on nitrogen and decomposition of $H_2N_2O_3$, catalyzed by HNO_2 showed that in acid solution NO was formed. We could not detect the presence of NO in the present redox system.

Discussion

The two acid dissociation constants of $H_2N_2O_2$ are reported to be $\sim 10^{-7}$ and $\sim 10^{-11}$ at ordinary temperature and hence hyponitrous acid would exist as $H_2N_2O_2$ under the acid conditions employed in the present investigation. Monoprotonated form $H_3N_2O_2^+$ has also been reported[5] in highly acidic medium. The hydrolysis constant[22] for Tl^{3+} is small and it forms strong complexes[23] with EDTA (H_4L). EDTA can exist in five different forms H_2L^{2-}, H_3L^-, H_5L^+ and H_6L^{2+} and all of them may form complexes with Tl^{3+}.

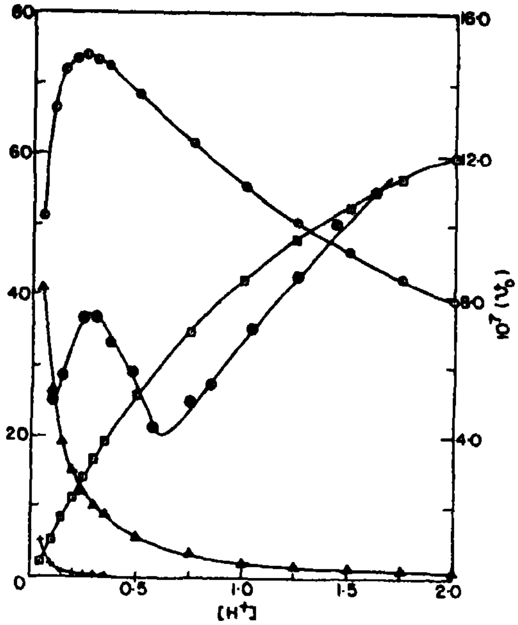

Fig. 3—Plots of percentage of different EDTA species and initial rates at various $[H^+]$ at 35°C (+), H_3L^-; (Δ), H_4L; (○), H_5L^+; (□), H_6L^{2+}; ⊗, initial rate; [EDTA] = 0.015 mol dm ^{3})

A calculation[24] of the population of vairous speciess of EDTA and the rate profile at different $[H^+]$ (Fig. 3) show that perhaps H_5L^+-complex of Tl(III) is the most important reactive species in the lower range of $[H^+]$. Any quantitative interpretation of $[H^+]$ dependence in the lower range of concentration is not reliable in view of the varying stoichiometry at different $[H^+]$.

Induction period

The role of nitrite in eliminating the induction period should be through its reaction with $H_2N_2O_2$ via formation of HNO_2 in the slow step to produce an adduct[11] (HO.N:N.O.NO), which then directly reacts with Tl(III). In highly acidic medium it decomposes to N_2 and HNO_3 without reacting with Tl(III) (see Eqs 7 and 8)

$$H_2N_2O_2 + HNO_2 \rightarrow HO.N{:}N.O.NO + H_2O \quad \ldots (7)$$

$$HO.N{:}N.O.NO \rightarrow N_2 + HNO_3 \quad \ldots (8)$$

Hughes and Stedman[11] consider a reaction between $HN_2O_2^-$ and $H_2NO_2^+$ instead of that shown in Eq. (7). It is difficult to distinguish between the two propositions.

Hyponitrous acid is said to exist in, *trans-* and *cis*-forms. The latter form has been indicated only as a transient intermediate in the reaction[9] of HNO_2 with NH_3OH^+ and in the reduction[25] of HNO_2 with europium (II). In the decomposition[2] of $H_2N_2O_2$ also, *cis*-form is proposed to be as transient intermediate. Since the rate of reaction is independent of large [Tl(III)], hyponitrous acid must be involved in a pre-equilibrium step, with two different forms, active and inactive, or *cis*- and *trans*-. Thus if we ignore [H⁺] despendence, mechanism outlined in Eqs (9-12) may be suggested in 0.5 mol dm⁻³ HClO₄.

$$\mathrm{H_2N_2O_2\,(trans)} \underset{k_2}{\overset{k_1}{\rightleftharpoons}} \mathrm{H_2N_2O_2\,(cis)} \qquad \ldots(9)$$

$$\begin{matrix}\mathrm{H_2N_2O_2}\\ \mathrm{(cis)+HNO_2}\end{matrix} \xrightarrow{k_3} \mathrm{HO.N{:}N.O.NO + H_2O} \qquad \ldots(10)$$

$$\mathrm{HO.N{:}N.O.NO} \xrightarrow{k_4} \mathrm{N_2 + HNO_3} \qquad \ldots(11)$$

$$\mathrm{HO.N{:}N.O.NO + Tl(III) + 2H_2O} \xrightarrow{k_5} \mathrm{H_2N_2O_3 + Tl(I) + HNO_2 + 2H^+} \qquad \ldots(12)$$

The above mechanism leads to the rate law (13).

$$-d[\mathrm{Tl(III)}]/dt = \frac{k_1k_3k_5[\mathrm{Tl(III)}][\mathrm{H_2N_2O_2}][\mathrm{HNO_2}]}{(k_4 + k_5[\mathrm{Tl(III)}])(k_2 + k_3[\mathrm{HNO_2}])} \qquad \ldots(13)$$

where the concentrations refer to total analytical concentrations. In the presence of 1×10^{-4} mol dm⁻³ NO_2^-, k_3 [HNO₂] appears to be much larger than k_2 and hence rate law (13) reduces to (14).

$$-d[\mathrm{Tl(III)}]/dt = k_1k_5[\mathrm{H_2N_2O_2}][\mathrm{Tl(III)}]/(k_4 + k_5[\mathrm{Tl(III)}]) \qquad \ldots(14)$$

Again for large [Tl(III)], the rate law (14) is reduced to (15).

$$-d[\mathrm{Tl(III)}]/dt = k_1[\mathrm{H_2N_2O_2}] \qquad \ldots(15)$$

A plot of (rate)⁻¹ versus [Tl(III)]⁻¹ is linear with a non-zero intercept and from this k_1 and k_3/k_4 have been calculated as $(1.2 \pm 0.08) \times 10^{-3}\,s^{-1}$ and $(4.5 \pm 0.6) \times 10^2$ dm³ mol⁻¹ respectively in 0.5 mol dm⁻³ HClO₄ and at 35°C.

The reaction at [H⁺] > 0.7 mol dm⁻³ appears to follow a different mechanism since it has altogether different stoichiometry and Tl(III) dependence, and has no induction period. The reaction is first order in [Tl(III)], [H₂N₂O₂] and [H⁺] and these results can be explained by the mechanism represented by Eqs. (16-19).

$$\mathrm{H_2N_2O_2 + H^+} \overset{K_{\mathrm{H^+}}}{\rightleftharpoons} \mathrm{H_3N_2O_2^+} \qquad \ldots(16)$$

$$\mathrm{H_3N_2O_2^+ + Tl(III) + H_2O} \xrightarrow{k} \mathrm{H_2N_2O_3 + 3H^+ + Tl(I)} \qquad \ldots(17)$$

$$\mathrm{H_2N_2O_3} \xrightarrow{\text{fast}} \tfrac{1}{2}\mathrm{N_2O} + \tfrac{1}{2}\mathrm{H_2O + HNO_2} \qquad \ldots(18)$$

$$\mathrm{H_2N_2O_2 + HNO_2} \xrightarrow{\text{fast}} \mathrm{N_2 + H_2O + HNO_3} \qquad \ldots(19)$$

Assuming K_{H^+} to be small, rate law (17) is obtained.

$$\begin{aligned}-d[\mathrm{Tl(III)}]/dt &= kK_{\mathrm{H^+}}[\mathrm{Tl(III)}][\mathrm{H_2N_2O_2}][\mathrm{H^+}]\\ &= k'[\mathrm{H_2N_2O_2}][\mathrm{Tl(III)}][\mathrm{H^+}]\end{aligned} \qquad \ldots(20)$$

k' is found to be (0.33 ± 0.01) dm⁶ mol⁻² s⁻¹ at 35°.

The rate constant (k_1) *for trans-cis* conversion (Eq. 9) is much larger than the corresponding rate constant for the decomposition[2] of H₂N₂O₂. Althogh the actual decomposition step may be preceded by a *trans-cis* conversion, the conditions are entirely different in the two cases. The presence of EDTA, NO_2^- and Tl(III) may greatly influence the rate.

References

1 Buchholz J R & Powell R E, *J Am chem Soc*, **87** (1965) 2350.
2 Hughes M N & Stedman G, *J chem Soc*, (1964) 163.
3 Polydoropoulos C N & Pipinis M, *Z physik chem*, **40** (1964) 322.
4 Buchholz J R & Powell R E, *J Am chem Soc*, **85** (1963) 509.
5 Hughes M N & Stedman G, *J chem Soc*, (1963) 1239.
6 Abel E & Proisl J, *Mh Chem*, **72** (1938).
7 Keshwani P, Goyal M R & Gupta Y K, *J chem Soc Dalton Trans*, (1983) 1831.
8 Thakuria B M & Gupta Y K, *J chem Soc Dalton Trans*, (1975) 77.
9 Hughes M N & Stedman G, *J chem Soc*, (1963) 2824.
10 Hussain M A, Stedman G & Hughes M N, *J chem Soc (A)*, (1968) 597.
11 Hughes M N & Stedman G, *J chem Soc*, (1963) 4230.
12 Thakuria B M & Gupta Y K, Inorg chem, **16** (1977) 1399.
13 Addison C C, Gamlen G A & Thompson R, *J chem Soc*, (1952) 338.
14 Addison C C, Gamlen G A & Thompson R, *J chem Soc*, (1952) 346.
15 Polydoropoulos C N, *Chem & Industry*, (1963) 1686.
16 Polydoropoulos C N & Pipinis M, *Chimica Chromica*, **28A** (1963) 107.
17 Polydoropoulos C N & Voliotis S D, *Anal chim Acta*, **40** (1968) 170.
18 Angeli A, *Gazz*, **30** (1900) 593.
19 Javaid A M, Lutz C A & Bonner F T, *Inorg chem*, **18** (1979) 2369.
20 Bonner F T & Ravid B, *Inorg chem*, **14** (1975) 558.
21 Hughes M N & Wimbledon P R, *J chem Soc Dalton Trans*, (1977) 1650.
22 Biederman G, *Arkiv Kemi*, **6**(5) (1964) 527.
23 Stability Constants, Special Publication No. 17, Chemical Society, London, p 640.
24 Anderegg G, *Helv chem Acta*, **50** (1967) 2333.
25 Fraser R T M, Lee R N & Hayden K, *J chem Soc (A)*, (1967) 741.

Indian Journal of Chemistry
Vol. 27A, June 1988, pp. 494-497

Chromium(VI) Oxidation of Thallium(I) in Aqueous Acetic Acid & Effect of Added Vanadium(V) on the Reaction

G S GOKAVI & J R RAJU*
Department of Chemistry, Karnatak University, Dharwad 580003

Received 10 *June* 1987; *revised* 30 *October* 1987; *accepted* 13 *November* 1987

Chromium(VI) oxidation of thallium(I) in 60% acetic acid containing 1.25 mol dm^{-3} hydrochloric acid is a second order reaction, understood to be between CrO_3Cl^- and TlCl. Increase in [H^+] and [Cl^-] accelerates the reaction. Added V(V) accelerates the reaction till [V(V)] slightly exceeds [Tl(I)] because of a 1:1 interaction between V(V) and Tl(I). At higher [V(V)], the rate constant is lowered due to a specific cation effect. No interaction between added V(V) and Tl(I) is encountered in the case of the reaction in 40% aqueous acetic acid; however, in 80 and 90% aqueous acetic acid, 2:3 and 1:2 interactions between V(V) and Tl(I) are observed.

The oxidation of Tl(I) by Cr(VI) does not occur to any extent in aqueous perchloric and sulphuric acids but the reaction is facile in conc hydrochloric acid medium ($\geqslant 3$ mol dm^{-3}; the reaction is slow at [HCl] lower than 3 mol dm^{-3})[1]. The species in 3.0 mol dm^{-3} HCl solution[1] are reported to be thallium(I) chloride (TlCl) and chlorochromate (CrO_3Cl^-). The formation of chlorochromate is known to be greatly facilitated in aqueous acetic acid solutions as indicated by an equilibrium constant of 14 in water[2] rising to 1×10^5 in 86.5% acetic acid[3]. It was, therefore, worthwhile studying the reaction in 60% (v/v) aqueous acetic acid containing 1.25 mol dm^{-3} HCl. In view of the particular retarding effect of V(V), a product in the Cr(VI)-V(IV) reaction[4], the effect of added V(V) on the title reaction has also been studied.

Materials and Methods

Reagent grade chemicals were used. Doubly distilled water was used throughout this work. Chromium(VI) solution was obtained by dissolving potassium dichromate (BDH, AR) in water and standardised spectrophotometrically. Applicability of Beer's law at 360 nm was tested in the case of the 1.25 mol dm^{-3} HCl in 60% acetic acid solution containing 2.0×10^{-4} to 6.0×10^{-4} mol dm^{-3} Cr(VI) using matched 1 cm cells ($\varepsilon = 1250$). Concentrations of Cr(VI) higher than 6.0×10^{-4} mol dm^{-3} were not required in any of the kinetic runs, because of the limited solubility of Tl(I) in the reaction solution.

The Tl(I) solution was obtained by dissolving thallium(I) chloride (BDH) in water and standardising with bromate. Vanadium(V) solution was obtained by dissolving ammonium vanadate (BDH, AR) in water. Applicability of Beer's law was also tested for the latter solution at 360 nm ($\varepsilon = 75$). Hydrochloric acid (Glaxo, AR) was used throughout this work. Acetic acid was purified by standard procedure.

Kinetic runs

These runs were carried out with solutions of 1.25 mol dm^{-3} HCl in 60% acetic acid at $\mu = 1.26$ mol dm^{-3}. In a typical run, [Cr(VI)] and [Tl(I)] were 2.0×10^{-4} and 3.0×10^{-4} mol dm^{-3} respectively and kinetics were followed spectrophotometrically at 360 nm by mixing the thermally equilibrated reactant solutions and transferring the reaction solution to a 1 cm cell kept in the thermostated cell compartment. The temperature was maintained at 25 ± 0.1°C. Kinetic results could be reproduced to ± 5% and runs were usually followed upto 80% of the reaction.

Results

Since oxidation of HCl by Cr(VI) in the absence of Tl(I) was marginal (0.8% in 50 min), no correction for the oxidation of hydrochloric acid was made.

Stoichiometry

Different reaction mixtures were prepared in 60% acetic acid containing 1.25 mol dm^{-3} HCl at $\mu = 1.26$ mol dm^{-3} and analysed after keeping them for over 3 hr at 25°C. Chromium(VI) was estimated spectrophotometrically at 360 nm while Tl(III) was found as difference of total oxidant titrated by iodometry with 2.0×10^{-3} mol dm^{-3} thiosulphate. The results indicate a 2:3 stoichiometry for Cr(VI) oxidation of Tl(I) in these solutions (see Eq. 1).

$$2Cr(VI) + 3Tl(I) = 2Cr(III) + 3Tl(III) \qquad \ldots(1)$$

Order of reaction

The reaction followed second order rate law at [Tl(I)] in the range of 1.0×10^{-4} to 3.0×10^{-4} mol dm^{-3} and [Cr(VI)] in the range of 2.5×10^{-4} to

4.5×10^{-4} mol dm^{-3}. Since [Cr(VI)] was followed by spectrophotometry, its concentration was close to that of Tl(I). The kinetic study was restricted to the narrow range of reactant concentrations because of the low solubility of Tl(I) in 60% acetic acid containing 1.25 mol dm^{-3} HCl.

Effect of added products

The effect of added products, Cr(III) and Tl(III), was studied at $\mu = 1.26$ mol dm^{-3}, [HCl] = 1.25 mol dm^{-3}, [oxidant] = 2.0×10^{-4} mol dm^{-3} and [substrate] = 3.0×10^{-4} mol dm^{-3}. Under these conditions, no variation in second order rate constant was observed. In case of runs involving non-equivalent concentrations of reactants, the rate constant (k) was evaluated using Eq. (2) with a and b representing the initial [Tl(I)] and [Cr(VI)] respectively and x representing the decrease in reactant concentration in time t. Rate constants were determined graphically, the second order plots being linear over 80% of the reaction (Fig. 1).

$$k = \left\{\frac{2.303}{t(a-3b/2)}\right\} \log \left\{\frac{b(a-3x/2)}{a(b-x)}\right\} \qquad \ldots(2)$$

Effect of chloride and hydrogen ions

At fixed [reactant], [H$^+$] and [Cl$^-$] and $\mu = 1.26$ mol dm^{-3}, the second order specific rate constant (k) increased with increase in [Cl$^-$] and/or [H$^+$] (Table 1). The orders of reaction in [Cl$^-$] and [H$^+$] were 1.2 and 2.0 respectively.

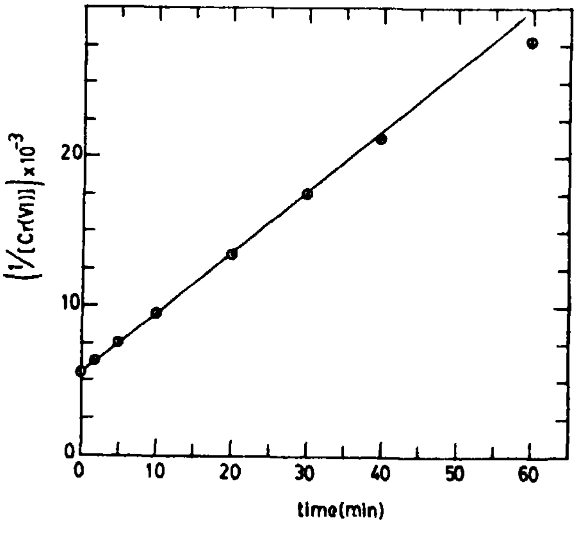

Fig. 1—Second order plot of chromium(VI)-thallium(I) reaction in 60% acetic acid containing 1.25 mol dm^{-3} hydrochloric acid at 25°C ([Cr(VI)] = 2.0×10^{-4} mol dm^{-3}, [Tl(I)] = 3.0×10^{-4} mol dm^{-3}, $\mu = 1.26$ mol dm^{-3})

Table 1—Effect of Varying [H$^+$] and [Cl$^-$] on Chromium(VI)-Thallium(I) reaction

[Cr(VI)] = 2.0×10^{-4} mol dm^{-3}; temp. 25°C;
[Tl(I)] = 3.0×10^{-4} mol dm^{-3}; solvent medium: 60% acetic acid.

[Cl$^-$] (mol dm^{-3})	k (dm^{3}mol^{-1}s^{-1})	[H$^+$] (mol dm^{-3})	k (dm^{3}mol^{-1}s^{-1})
[H$^+$] = 1.25 mol dm^{-3}		[Cl$^-$] = 1.25 mol dm^{-3}	
0.25	0.91	0.50	1.0
0.50	1.6	0.75	2.3
0.75	2.9	1.00	3.5
1.00	5.0	1.25	6.3
1.25	6.3		

Effect of added vanadium(V)

The effect of added V(V) on the reaction was studied by taking into account the absorption due to both V(V) and Cr(VI) at 360 nm in runs where [Tl(I)] was greater (1.5 times) than [Cr(VI)]. Under the condition [Cr(VI)] > [Tl(I)], the absorption at 360 nm was regarded as due to the Cr(VI) exclusively, that due to V(V) being neglected in view of the very much higher ε of the former over that of V(V). In the presence of added V(V), the stoichiometry and the effect of added products remained the same as in the absence of V(V). Second order rate constant (k) in 60% acetic acid containing 1.25 mol dm^{-3} HCl in the presence of V(V) first increased till added [V(V)] exceeded that of the [Tl(I)] used; while, with further increase in [V(V)], the k-value progressively decreased. Hence, the order of reaction was determined in the two ranges of increasing and decreasing k in the presence of V(V). In the increasing range of k([V(V)] < [Tl(I)]), the orders in [Cr(VI)], [Tl(I)] and [V(V)] were 0.85, 1.0 and 0.60 respectively while in the decreasing range of k ([V(V)] > [Tl(I)]), the orders were 0.91, 0.90 and − 1.0 respectively. In almost all runs, second order plots were linear practically throughout the 80% reaction range at all [V(V)] used. Such a behaviour of k was not observed in 40% acetic acid solution in the presence of 1.25 mol dm^{-3} HCl and k decreased continuously with increase in [V(V)].

In view of the distinctive effect of added V(V) on the reaction, the spectra of Tl(I) and V(V) were examined in 60% acetic acid containing 1.25 mol dm^{-3} HCl, individually and also together as mixed solution in the range of 250 to 350 nm. In the presence of both Tl(I) and V(V), there was a distinct change in the spectrum and the low intensity absorption bands of Tl(I) and V(V) were replaced by a high intensity band at 252 nm ($\varepsilon \sim 8200$), the latter being presumably due to the interaction between V(V) and Tl(I). Furthermore, a detailed study of the Job's curves[5] in respect of this system at 250, 260 and 270 nm each showed the composition of the V(V)-Tl(I) complex as 1:1, 1:1, 2:3 and 1:2 in 60, 70, 80 and 90% acetic acid solutions in the presence of 1.25 mol dm^{-3} HCl in each case.

Effect of Mn(II), Ce(III), Th(IV) and U(VI) on the reaction

Significantly, added Mn(II), Ce(III), Th(IV) and U(VI) in the concentration range of 0.5×10^{-3} to 1.5×10^{-3} mol dm^{-3} did not affect the reaction.

Discussion

The rate data in 60% acetic acid containing 1.25 mol dm^{-3} HCl parallel the results of an earlier study[1b] in 3 mol dm^{-3} HCl solution with respect to reaction order, effect of added products and the influence of Cl^- ions. However, with respect to H^+ ions, the order in the present case is two as against one found in the earlier study[1b]. In the presence of large [Cl^-] and [H^+], Cr(VI) and Tl(I) mainly exist in the form of chlorochromate[2], CrO_3Cl^-, and thallium(I) chloride, TlCl, respectively[1b]. These species may be expected to form in prior equilibria in the present case. The experimental results lead to the mechanism shown in Scheme 1

$$HCrO_4^- + Cl^- + H^+ \rightleftharpoons CrO_3Cl^- + H_2O \quad \ldots(K_1)$$

$$Tl^+ + Cl^- \rightleftharpoons TlCl \quad \ldots(K_2)$$

$$CrO_3Cl^- + H^+ + TlCl \rightleftharpoons HCrO_3 + TlCl_2 \quad (k_1, k_2)$$

$$CrO_3Cl^- + H^+ + TlCl_2 \rightarrow HCrO_3 + TlCl_3 \quad (k_3)$$

$$2(HCrO_3 + TlCl + 5H^+ \rightarrow Cr^{3+} + TlCl^{2+} + 3H_2O) \quad (k_4)$$

Scheme 1

Chromium(VI) in acid solutions exists mainly as acid chromate ion[6] ($HCrO_4^-$) and chlorochromate (CrO_3Cl^-) is formed from this species in a preequilibrium. The latter and TlCl, also formed in a preequilibrium, react in a one equivalent reversible step (k_1, k_2) yielding the reactive Cr(V) and Tl(II) species. The Tl(II) interacts (k_3) with a second Cr(VI) ion giving a second Cr(V). The Cr(V) formed oxidises Tl(I) subsequently in a two-equivalent step (k_4). Scheme 1 does not involve any Cr(IV) species but includes Cr(V). However, no direct evidence for Cr(V) could be obtained. While induction experiments[6] with iodide could not be performed to show the intermediacy of Cr(V) as one of the products, Tl(III), also oxidises iodide along with Cr(VI). The Cr(V)-Tl(I) reaction, being a complementary reaction, is also expected to be fast and, as a result, Cr(V) is expected to be present in very low concentrations. In this respect, it is noteworthy that the evidence for the involvement of Cr(IV) in the reaction is negative. Added Mn(II) ions do not influence the reaction to any significant extent. If Cr(IV) was implicated in the mechanism, the presence of Mn(II) ions in the reaction solution would have caused substantial changes[6] in stoichiometry and rate constant.

The application of the steady state approximation to the reactive intermediates, Tl(II) and Cr(V), of Scheme 1 leads to the rate equation (3) which is in agreement with the experimental results and the experimental second order rate constant (k) may be identified with the constant factors in Eq. (3) at fixed [H^+] and [Cl^-]. In Eq. (3), K_1 and K_2 are the equilibrium constants of formation of CrO_3Cl^- and TlCl respectively and k_0 is a constant given by Eq. (4), k_1, k_2, k_3 and k_4 in Eq. (4) being the rate constants of the

$$-\frac{d[Cr(VI)]}{dt} = \left\{ \frac{k_0 K_1 K_2 [H^+]^2 [Cl^-]^2}{(1 + K_1[H^+][Cl^-])(1 + K_2[Cl^-])} \right\} \times [Cr(VI)][Tl(I)] \quad \ldots(3)$$

$$k_0 = (k_3 k_4 / k_2)\left[\{1 - (4k_1 k_2 / k_3 k_4)\}^{1/2} - 1\right] \quad \ldots(4)$$

different steps shown in Scheme 1. An alternative pathway, almost identical to that of Scheme 1, except that the reactive intermediates, Cr(V) and Tl(II), are formed in an irreversible step in contrast to the reversible step of Scheme 1, can also be conceived. However, both Cr(V) and Tl(II) are usually formed in reversible steps[7] in noncomplementary electron transfer reactions of Cr(VI) and Tl(I) and Scheme 1 is therefore preferred.

In the presence of added V(V), it is observed that the Cr(VI)-Tl(I) reaction is accelerated till the added [V(V)] is slightly greater than [Tl(I)]. Thereafter, further addition of V(V) lowers the rate constant. In view of the rate law of Scheme 1, the nature of the distinctive effect of V(V) on the reaction needs to be understood. The experimental kinetic and spectroscopic results confirm the formation of a 1:1 V(V)-Tl(I) species and it is this species which is responsible for the initial rate acceleration in 60% acetic acid containing 1.25 mol dm^{-3} HCl. The active reductant under these conditions is a $(VO_2TlCl)^+$ species. Once the latter is completely formed, the rate constant is lowered on the further addition of V(V) because the latter manifests a specific cation effect on the CrO_3Cl^--TlCl reaction. Perhaps the V(V)-V(IV) cycle is now involved. That the influence of V(V) on the reaction is specific and limited to this ion is shown by the fact that the reaction is unaffected by ions of different valences and sizes such as Mn^{2+}, Ce^{3+}, Th^{4+} and UO_2^{2+} in a range of concentrations from one to four times that of the reductant. Because of the specific cation effect,

Table 2—Effect of Added Vanadium(V) on Chromium(VI)-Thallium(I) Reaction at 25°C

$[V(V)] \times 10^4$ (mol dm^{-3})	$k^{a,b}$ (dm^{3}mol^{-1}s^{-1})	$k^{a,c}$ (dm^{3}mol^{-1}s^{-1})	k^d (dm^{3}mol^{-1}s^{-1})
0.0	6.9	5.0	1.9
1.0	8.3	7.7	1.8
2.0	10	8.7	1.7
3.0	12	9.6	1.5
4.0	14	8.8	1.4
5.0	11	8.3	1.3
7.5	8.3		

(a) $[Cr(VI)] = 2.0 \times 10^{-4}$ mol dm^{-3}; $[HCl] = 1.25$ mol dm^{-3}; 60% acetic acid solution.

(b) $[Tl(I)] = 3.0 \times 10^{-4}$ mol dm^{-3}.

(c) $[Tl(I)] = 2.0 \times 10^{-4}$ mol dm^{-3}.

(d) $[Cr(VI)] = 2.0 \times 10^{-4}$ mol dm^{-3}; $[Tl(I)] = 3.0 \times 10^{-4}$ mol dm^{-3}; $[HCl] = 1.25$ mol dm^{-3}; 40% acetic acid solution.

there are two paths now for the reaction: one involving the reductant, $(VO_2TlCl)^+$, and the other, involving TlCl itself. It is noteworthy that the order of reaction in added V(V) is fractional (0.60) in the range of increasing rate constant and 1.0 for the range of decreasing rate constant. While excess V(V) is needed to drive the equilibrium towards complex formation, after the complex is fully formed, all added V(V) contributes to retardation of reaction. It is also possible that the V(V)-V(IV) cycle, marginally involved during catalysis, might be more active during retardation. However, there has been no evidence of any V(IV) during the reaction under a variety of conditions but it is also true that any V(IV) formed will be short-lived in the presence of several powerful oxidants in the reaction.

In 40% acetic acid containing 1.25 mol dm^{-3} HCl, there is no evidence of any V(V)-Tl(I) complex formation and hence the rate decreases with increase in [V(V)] (Table 2), again reinforcing the specificity of V(V) effect. As would be expected, there is no initial acceleration of reaction because no complex is formed in these solutions of higher dielectric constant. It is also apparent from the results of Table 2 that added V(V) decreases the rate much more efficiently in the absence of complex formation in 40% acetic acid solution than in solutions where the complex formation is facilitated.

References

1 (a) Sagi S R, Prakasa Raju G S & Ramana K V, *Talanta*, **22** (1975) 93; (b) Gokavi G S & Raju J R, *Polyhedron*, **6** (1987) 1721.

2 Haight G P Jr, Richardson D C & Coburn N W, *Inorg Chem*, **3** (1964) 1777.

3 Cohen M & Westheimer F H, *J Am chem Soc*, **74** (1952) 4387.

4 Davies K M & Espenson J H, *J Am chem Soc*, **92** (1970) 1889.

5 Job P, *Ann Chim (Paris)*, **9** (1928) 113.

6 Wiberg K B, *Oxidation by chromic acid and chromyl compounds in oxidation in organic chemistry, Part A* (Academic Press, New York) 1965.

7 Basolo F & Pearson R G, *Mechanisms of inorganic reactions*, (Wiley Eastern, New Delhi) 1973, 487-9.

Indian Journal of Chemistry
Vol. 27A, June 1988, pp. 498-503

Kinetics & Mechanism of Oxidation of Glutamine & Serine by Peroxomonosulphate in the Absence & Presence of Acetaldehyde & Propionaldehyde

M S RAMACHANDRAN*, T S VIVEKANANDAM & C NEWMAN PAUL DEVASINGH
School of Chemistry, Madurai Kamaraj University, Madurai 625 021

Received 2 *April* 1987; *revised* 14 *September* 1987; *accepted* 21 *October* 1987

The kinetics of oxidation of three structurally different amino acids, viz. serine, glutamine and alanine by peroxomonosulphate (PMS) in the absence and presence of aldehydes have been investigated in HOAc-NaOAc buffer medium. Analysis of kinetic results in the absence of aldehyde shows that SO_5^{2-} is the reactive species. The kinetic parameters such as rate constant, $\Delta H^{\ddagger}$ and $\Delta S^{\ddagger}$ show a correlation with pK_2 of the amino acid. The results have been analysed on the basis of a mechanism wherein the schiff base is proposed as the reactive intermediate.

In our earlier report[1] on the kinetics and mechanism of oxidation of amino acids (AA) by peroxomonosulphate (PMS)[1], it was observed that the first order plots showed curvature after 5-10% conversion of PMS which we believed was due to the effect of the product formed during the course of reaction. This was confirmed by studying the reactions in the presence of formaldehyde[2]. In order to have some insight in to the mechanism in the presence of aldehyde, presently we have investigated the kinetics of PMS oxidation of three structurally different amino acids namely alanine, serine and glutamine in the presence of acetaldehyde and propionaldehyde. Serine and glutamine have been chosen, in particular, to arrive at any correlation of the rate of oxidation with the structure of amino acids.

Materials and Methods

Potassium peroxomonosulphate (Du Pont) was found to be > 96% pure and its solution was always prepared afresh before use. The solution was standardised by cerimetry using ferroin as an indicator. Amino acids except glutamine were from Loba-Chemie Indo Austranal Co. Glutamine was from Koch-Light, England. Formaldehyde (S. Merck, 30%) was used as such and it was assayed by hypoiodite method[3]. Acetaldehyde and propionaldehyde were purified and assayed by standard procedures.

All the kinetic runs were followed by iodometry at constant $[H^+]$ using HOAc-NaOAc buffer. A high concentration of the buffer ($0.2M$) was maintained in the reaction mixture since the product HSO_4^- is a stronger acid than the oxidant HSO_5^-. No self-decomposition of PMS was observed under our experimental conditions.

Stoichiometry

Reaction mixtures containing large excess of [PMS] over [AA] or [AA + aldehyde] were allowed to stand for several hours (24 to 48 hr) at room temperature and constant $[H^+]$ (pH 4.8) and the unconsumed PMS was determined iodometrically. The stoichiometries of the reaction in the absence and presence of aldehyde were:

$$2\text{PMS} + 1\text{AA} \rightarrow \text{products;}$$

and

$$3\text{PMS} + 1\text{AA} + 1\,\text{aldehyde} \rightarrow \text{products.}$$

One of the oxidation products of serine with PMS both in the absence and presence of aldehyde was glycollic acid. An acid product was obtained in the case of glutamine also. However, in this case the product underwent further oxidation on long standing as in the case of glycollic acid (serine-PMS). In the presence of aldehyde the products of oxidation (CH_3COOH etc.) of aldehydes were also detected by spot tests.

Results

(*i*) *Oxidation of serine and glutamine in the absence of aldehyde*

All the experiments were carried out under pseudo-first order conditions: [AA] ≫ [PMS]. Plots of log V_t (V_t = volume of thiosulphate consumed) versus time were linear up to 60% conversion (Fig. 1A). At fixed [AA] and $[H^+]$ the values of pseudo-first order rate constant, (k_{obs}) were independent of the initial [PMS], indicating that rate was proportional to [PMS].

The values of k_{obs} increased linearly with [AA] and the plots of k_{obs} versus [AA] passed through the origin (Fig. 2A). The values of k_{obs} decreased with increase in $[H^+]$ and the plots of k_{obs} versus $1/[H^+]$ were linear and passed through the origin (Fig. 2B).

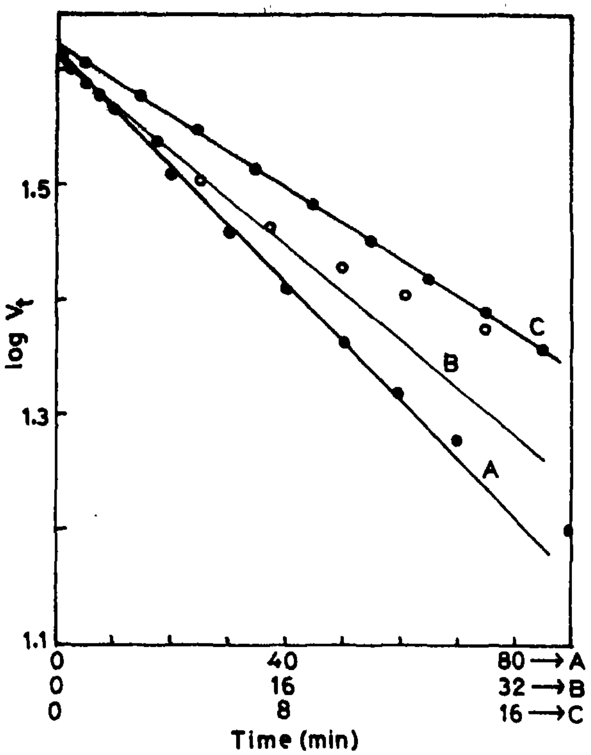

Fig. 1—(A) Plot of log V_t versus time at 31°C. ([glutamine] = 0.05 mol dm^{-3}, [PMS] = 4.19 × 10^{-3} mol dm^{-3}, *p*H = 5.2, μ = 0.25 mol dm^{-3}, (B) [alanine] = 0.05 mol dm^{-3}, [PMS] = 4.18 × 10^{-3} mol dm^{-3}, *p*H = 4.0; μ = 0.25 mol dm^{-3}, [acetaldehyde] = 2.8 × 10^{-3} mol dm^{-3}, (C) [serine] = 0.05 mol dm^{-3}, [PMS] = 4.2 × 10^{-3} mol dm^{-3}, *p*H = 4.0, μ = 0.25 mol dm^{-3}, [formaldehyde] = 3.03 × 10^{-3} mol dm^{-3})

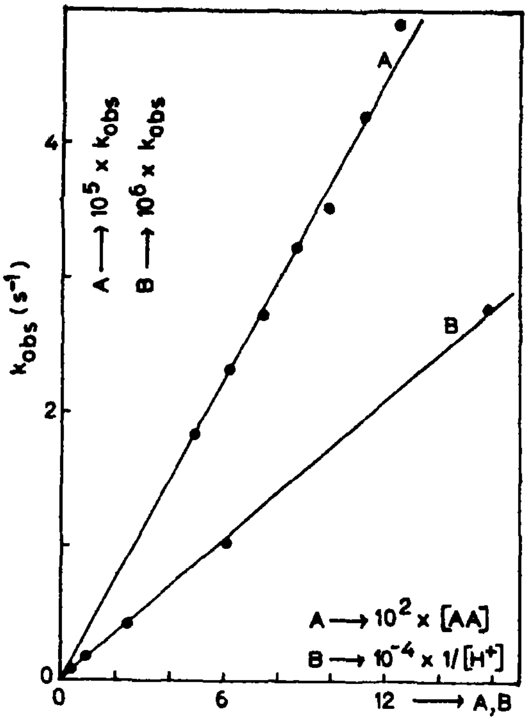

Fig. 2—(A) Plot of k_{obs} versus [amino acid] (AA) at 31°C ([AA] = [serine], [PMS] = 3.93 × 10^{-3} mol dm^{-3}, *p*H = 4.0, μ = 0.25 mol dm^{-3}, (B) Plot of k_{obs} versus 1/[H$^+$] at 31°C [Serine] = 0.05 mol dm^{-3}, [PMS] = 3.93 × 10^{-3} mol dm^{-3}, μ = 0.25 mol dm^{-3})

The change in ionic strength of the medium from 0.25 to 0.55 by adding potassium sulphate showed almost negligible increase in k_{obs}. The reactions were studied at four different temperatures (30-45°C) and from the temperature dependence of k_{obs} the activation parameters were calculated.

(*ii*) *Oxidation of alanine, serine and glutamine in the presence of aldehyde*

In these experiments pseudo-first order conditions were maintained only with respect to [AA]. The [aldehyde] was approximately equal to [PMS] in the oxidation reactions of amino acids in the presence of formaldehyde. But [acetaldehyde] and [propionaldehyde] were slightly less than [PMS]. In the presence of formaldehyde the plots of log V_t versus time were linear (Fig. 1C) even up to 70% conversion of PMS. In the presence of acetaldehyde and propionaldehyde the first order plots were curved (Fig. 1B) and the percentage of [PMS] conversion, corresponding to the point at which the curvature appeared, increased proportionally with increase in [acetaldehyde] and [propionaldehyde]. When the [aldehyde] in the case of acetaldehyde and propionaldehyde was greater than [PMS], the first order plots were linear upto 50% conversion. At fixed [AA], [H$^+$] and [aldehyde] the values of k_{obs} were independent of the initial [PMS], indicating first order dependence in [PMS].

The values of k_{obs} increased with increase in [AA]. Plots of k_{obs} versus [AA] were linear with a definite positive intercept (Fig. 3). At fixed [H$^+$] and [AA], the value of k_{obs} increased with increase in [aldehyde] and the plots of k_{obs} versus [aldehyde] were linear passing through the origin.

The values of k_{obs} decreased with increase in [H$^+$] and the plots of k_{obs} versus 1/[H$^+$] were linear with a positive intercept, indicating clearly that the reactions proceeded through two independent paths: one was [H$^+$]$^{-1}$ dependent and the other was [H$^+$] independent.

The change in ionic strength from 0.25 to 0.55 had negligible effect on k_{obs}. The reactions were studied at four different temperatures in the range 30-45°C and the activation parameters were calculated.

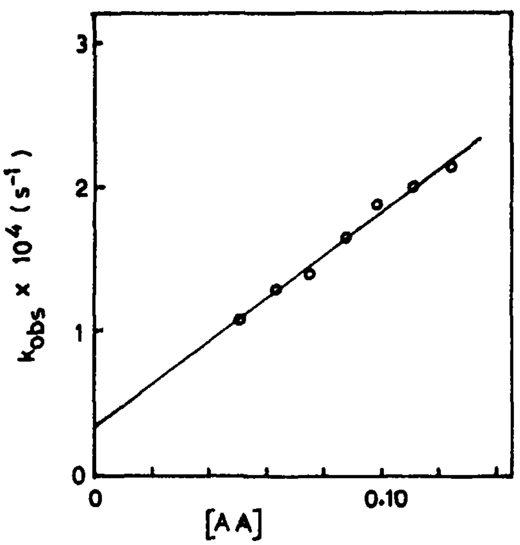

Fig. 3—Plot of k_{obs} versus [amino acid] (AA) at 31°C ([AA] = [glutamine], [PMS] = 4.2×10^{-3} mol dm^{-3}, pH = 4.0, μ = 0.25 mol dm^{-3}, [propionaldehyde] = 7.9×10^{-4} mol dm^{-3})

Discussion

Peroxomonosulphuric acid ($HO-OSO_3-H$) has two ionizable protons, viz. sulphuric acid proton and hydrogen peroxide proton. The pK_a value[4] of the sulphuric acid proton lies in a high acidity region and that of hydrogen peroxide proton is 9.4.

For amino acids, the following equilibria (1) exist in acidic/alkaline medium.

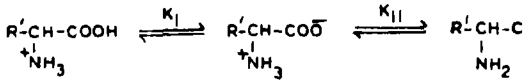

$$\underset{{}^{+}NH_3}{R'-CH-COOH} \underset{}{\overset{K_I}{\rightleftharpoons}} \underset{{}^{+}NH_3}{R'-CH-COO^-} \overset{K_{II}}{\rightleftharpoons} \underset{NH_2}{R'-CH-COO^-} \quad \ldots (1)$$

The values of pK_1 and pK_2 for the amino acids[5] studied are 2.2 and 9.1-9.7 respectively and the values are given in Table 1. Under our experimental conditions namely at pH = 4.0 all the amino acids would be in the form of zwitter ions. Therefore the amino acid in its zwitterionic form may be the reactive species.

It is well known that amino acids react with aldehyde to give schiff bases. The catalytic effect of pyridoxal phosphate in the amino acid metabolism by enzymes is attributed to the schiff base formed between the amino acid and pyridoxal phosphate[6-8]. We can therefore assume that the following equilibrium (2) exists under the present experimental conditions.

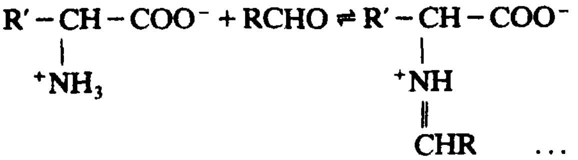

$$\underset{{}^{+}NH_3}{R'-CH-COO^-} + RCHO \rightleftharpoons \underset{\underset{CHR}{\|}}{\underset{{}^{+}NH}{R'-CH-COO^-}} \quad \ldots (2)$$

Mechanism of oxidation of serine and glutamine by PMS in the absence of aldehydes

From a knowledge of the possible reactive species that exist under the present experimental conditions oxidation of serine and glutamine in the absence of aldehydes may proceed as shown in Eqs (3) and (4).

$$HOOSO_3^- \overset{K}{\rightleftharpoons} {}^-OOSO_3^- + H^+ \quad \ldots (3)$$

$$\text{Amino acid} + {}^-OOSO_3^- \xrightarrow{k_1} \text{products} \quad \ldots (4)$$

Rate law corresponding to Eqs (3) and (4) is given by Eq. (5).

$$\frac{-d[PMS]}{dt} = k_1[\text{Amino acid}][SO_5^{2-}]$$

$$= Kk_1 \frac{[\text{Amino acid}][HSO_5^-]}{[H^+]}$$

$$k_{obs} = Kk_1 \frac{[\text{Amino acid}]}{[H^+]} \quad \ldots (5)$$

The rate equation (5) explains all the experimental facts. Using the literature[4] value of $K = 3.98 \times 10^{-10}$ the rate constants for the oxidation of SO_5^{2-} (k_1) have been obtained and the values are given in Table 1.

It is interesting to note that though serine is similar to threonine, it reacts only with SO_5^{2-} whereas threonine has been shown to react[9] with both SO_5^{2-} and HSO_5^-. Moreover the reaction of threonine with PMS was studied at pH 3.6, 4.0 and 4.4. In order to

Table 1—Kinetic Parameters for oxidation of Amino Acids at 31 °C in the Absence of Aldehydes[a]

Amino acid[b]	k_1		$\Delta H^{\ddagger}_{k_1}$ (K cal mol^{-1})	$\Delta S^{\ddagger}_{k_1}$ (cal deg^{-1} mol^{-1})	pK_2
Alanine	24.5	(21.0)	—	—	9.87
Butryne	32.0	(28.0)	—	—	9.83
Valine	10.6	(10.0)	22.6	62.6	9.74
Leucine	7.3	(7.0)	—	—	9.74
Isoleucine	18.4	(17.6)	16.4	46.9	9.76
nor-Leucine	28.0	(28.0)	—	—	9.83
Phenylalanine	47.2	(47.2)	18.0	50.5	9.18
Serine	87.0		17.6	51.4	9.21
Glutamine	60.0		13.4	35.5	9.13
Threonine	88.7	(76.2)	8.6	20.6	9.10

(a)Values given in parentheses are reported values taken from ref (2) and (9).

(b)Since in the oxidation of alanine, butryne and nor-leucine the first-order plots are linear only upto 10% conversion, a large error may be introduced in the calculation of k_{obs}. Therefore the $\Delta H^{\ddagger}$ and $\Delta S^{\ddagger}$ values are not calculated. We have calculated the $\Delta H^{\ddagger}$ and $\Delta S^{\ddagger}$ values only for the systems where the first order plot is linear atleast upto 50% conversion.

ascertain the above fact the kinetics were reinvestigated at *p*H 3.6 to 5.2 and from the plot of k_{obs} versus $1/[H^+]$ it was found that only SO_5^{2-} alone reacts with threonine since this plot also passed through origin. This led us to reexamine our earlier report[1] because in the earlier report we have studied the kinetics only upto 5-10% conversion of [PMS] and therefore there may arise some error in the calculation of k_{obs}. The recalculated results are given in Table 1. The values reported in Table 1 are the average of k_1 obtained as a result of $[H^+]$ and [AA] variations. Comparison of k_1 (Table 1) with the earlier reported values for the oxidation by SO_5^{2-} shows only a small difference.

Perusal of the results in Table 1 shows that there exists an approximate correlation between k_1 and pK_2 of the amino acid as expected since the reaction is a nucleophilic attack of SO_5^{2-} on $R'-CH(\overset{+}{N}H_3)COO^-$ at the $-\overset{+}{N}H_3$ group. From Table 1, we can infer that alanine, butryne etc. which are linear amino acids are more reactive than the branched chain amino acids such as leucine, isoleucine, etc. Similarly if we consider the reactivities of phenylalanine, glutamine and threonine, the reactivity order is threonine > glutamine > phenylalanine, as expected on the basis of pK_2 values. Based on this, the k_1 values of serine would be approximately equal to that of phenylalanine. But the observed value is equal to that of threonine. The above three amino acids, in comparison to serine have a different substituent at the β-position. The effect of the different bulkier groups at β-position may be complex and therefore it is difficult to arrive at any correlation in the case of serine.

From the effect of temperature on k_{obs} the activation parameters have been calculated (Table 1).

$$\Delta H^{\ddagger}_{obs} = \Delta H^{\ddagger}_{K} + \Delta H^{\ddagger}_{k_1}$$

$$\Delta S^{\ddagger}_{obs} = \Delta S^{\ddagger}_{K} + \Delta S^{\ddagger}_{k_1}$$

The values of $\Delta S^{\ddagger}_{k_1}$ for all the systems are surprisingly positive and this shows that more than one intermediate/transition state is involved in the reaction pathway.

From the results we can generalize the following facts: (i) The linear α-amino acids (i.e. with no β-substituent) show a curved first order plot after 5-10% conversion of PMS. This is due to the fact that the product aldehyde reacts with the amino acids to give a schiff base which reacts faster than the amino acid. (ii) α-Amino acids having a β-substituent, with the exception of threonine, do not show such a behaviour. This may be due to the fact that the product aldehyde, is not able to form a schiff base due to steric effet. Therefore the first order plots are linear even up to 50% conversion. In the case of threonine a curvature towards X-axis (k_{obs} increases) is noticed in the first order plot after 5-10% conversion and this may be due to further oxidation of product, aldehyde. (iii) All the amino acids are oxidised by SO_5^{2-} and the rate constants (k_1), $\Delta H^{\ddagger}$ and $\Delta S^{\ddagger}$ can approximately be correlated with pK_2. In the case of β-branched α-amino acids the observed rate constant is smaller than the unsubstituted one.

Mechanism of oxidation of alanine, glutamine and serine in the presence of aldehydes

The mechanism of oxidation of amino acids in the presence of HCHO has been discussed earlier in detail[2,9]. The kinetics of oxidation of amino acids in the presence of both acetaldehyde and propionaldehyde are similar to those of formaldehyde. Hence, the mechanism identical to that proposed in the presence of formaldehyde is valid in the case of acetaldehyde and propionaldehyde (see Scheme 1).

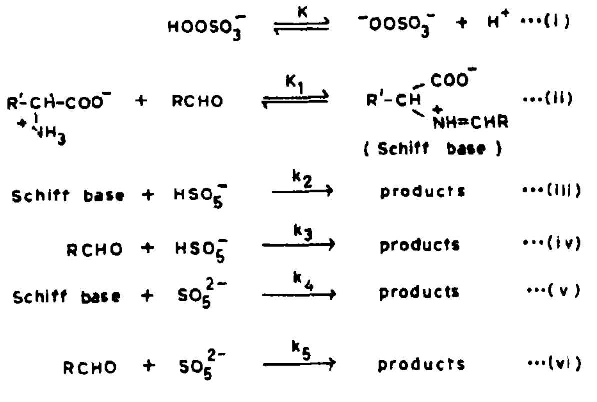
HOOSO3⁻ ⇌(K) ⁻OOSO3⁻ + H⁺ ...(i)
R'-CH-COO⁻ (+NH3) + RCHO ⇌(k1) R'-CH(COO⁻)(+NH=CHR) ...(ii)
(Schiff base)
Schiff base + HSO5⁻ →(k2) products ...(iii)
RCHO + HSO5⁻ →(k3) products ...(iv)
Schiff base + SO5²⁻ →(k4) products ...(v)
RCHO + SO5²⁻ →(k5) products ...(vi)

Scheme 1

Based on Scheme 1, the rate law at constant *p*H can be expressed by Eq. (6)

$$\frac{-d[PMS]}{dt} = \{k_a[AA][RCHO] + k_b[RCHO]\}[PMS]$$

$$k_{obs} = k_a[AA][RCHO] + k_b[RCHO] \quad \ldots (6)$$

where k_a and k_b represent the rate constants for oxidation of schiff base and aldehydes at constant *p*H. Equation (6) explains the effect of [AA] and [RCHO] variation on the rate. The values of k_b can be calculated from the plots of k_{obs} versus [AA] (Fig. 2) and these values can be compared with the values obtained from the direct oxidation of aldehydes[10]. These two values given in Table 2 agree well and this confirms the validity of the reaction mechanism shown in Scheme 1.

The rate law consistent with Scheme 1 can also be expressed by Eq. (7)

$$\frac{-d[\mathrm{PMS}]}{dt} = (k_4K_1[\mathrm{AA}] + k_5)[\mathrm{RCHO}]_T \frac{K[\mathrm{HSO_5^-}]}{[\mathrm{H^+}]} + (k_2K_1[\mathrm{AA}] + k_3)[\mathrm{RCHO}]_T[\mathrm{HSO_5^-}] \quad \ldots (7)$$

The values obtained for $(k_4K_1[\mathrm{AA}] + k_5)$ and $(k_2K_1[\mathrm{AA}] + k_3)$ from the plots of k_{obs} versus $1/[\mathrm{H^+}]$ are lower than the values of k_5 and k_3 respectively, which are the values from the direct oxidation of the concerned aldehydes[10]. This clearly shows that the rate constants k_5 and k_3 in the presence of amino acids are always smaller than the values obtained by the direct oxidation of aldehydes. This is due to our experimental conditions, viz. [AA] > [PMS] and [RCHO] ≤ [PMS]. Because of this the oxidation of RCHO by PMS may not follow the pseudo-first order kinetics. Therefore, as an approximation k_5 and k_3 can be neglected in Eq. (7) and approximate values of k_4K_1 and k_2K_1 are given in Table 3.

It is well known that the aldehydes in aqueous solution exist as a mixture of free carbonyl form and hydrated form[11]. From the foregoing results we could not say which form of aldehyde reacts with the amino group to form a schiff base. Moreover the values of the equilibrium constant (K_1) for the schiff base formation may be different for different aldehydes. Because of this we could not correlate the rate constants obtained for the oxidation of serine and glutamine in the presence of formaldehyde, acetaldehyde and propionaldehyde.

Table 2—Rate Constants (k_b)* for Oxidation of Aldehydes at 31°C

	k_b (from Eq. 6)		
	HCHO	CH_3CHO	CH_3CH_2CHO
Alanine	—	0.08	0.08
Serine	0.06	0.07	0.07
Glutamine	0.09	0.06	0.05
Experimental*•	0.11	0.26	0.19

*At pH = 4.0; μ = 0.25; temp. = 31°C.

•Obtained from direct oxidation of aldehydes by PMS (see ref. 10).

If the complex between SO_5^{2-} (HSO_5^-) and $-N=CHR$ is assumed as the activated complex, then the formation and decomposition of this activated complex depend on the electron density at the $-N=CHR$ group. According to the +I effect of alkyl group in $-N=CHR$, the electron density at the $-N=CHR$ may be in the order: propionaldehyde > acetaldehyde > formaldehyde. The observed $\Delta H^{\ddagger}$ values for oxidation of glutamine, serine and alanine in the presence of aldehyde show that the order is: propionaldehyde < acetaldehyde < formaldehyde. This clearly indicates that the electronic effect is more pronounced on the decomposition of the activated complex since the reverse order is expected if the complex formation is more pronounced due to increased electron density at $-N=CHR$. Moreoever, in our earlier work[1] the values of $\Delta H^{\ddagger}$ are almost same for various amino acids in the presence of formaldehyde, showing that $\Delta H^{\ddagger}$ values do not depend upon the alkyl part of the amino acid but depend only on the $-N=CHR$ group. This is also clearly borne out by the $\Delta H^{\ddagger}$ values obtained in the presence of acetaldehyde and propionaldehyde (Table 3).

Acknowledgement

The authors express their deep gratitude to Prof N R Subbaratnam for help and encouragement. One of them (CN) thanks the UGC, New Delhi for the award of a teacher fellowship under Faculty Improvement Programme and the Principal and Management of N.M.S.S.V.N. College for Study leave.

References

1 Ramachandran M S & Vivekanandam T S, *J chem Soc, Perkin Trans*, (1984) 1341.
2 Ramachandran M S, Vivekanandam T S & Malim Mani Raj R P, *J chem Soc, Perkin Trans*, (1984) 1345.
3 Mann F G & Saunders B C, *Practical organic chemistry*, (ELBS and Longman, London) 1974, pp 463.
4 Ball D L & Edwards J O, *J Am chem Soc*, **82** (1960) 1778.

Table 3—Kinetic Parameters for Oxidation of Amino Acids at 31°C in the Presence of Aldehydes

	Serine			Glutamine			Alanine	
	HCHO	CH_3CHO	CH_3CH_2CHO	HCHO	CH_3CHO	CH_3CH_2CHO	CH_3CHO	CH_3CH_2CHO
$10^1\ k_2K_1$ ($dm^6\ mol^{-2}\ s^{-1}$)	19.8	13.6	9.0	14.8	9.8	7.2	17.8	12.0
$10^{-5}\ k_4K^1$ ($dm^6\ mol^{-2}\ s^{-1}$)	8.3	5.8	5.0	8.2	7.4	8.4	3.2	2.8
$\Delta H''$ (k cal mol^{-1})	14.5	9.2	8.2	13.2	8.1	7.4	9.0	7.8

5 *Lange's hand book of chemistry*, edited by J A Dean, Ch 5-15, (McGraw-Hill, New York) 1973.
6 Bruice T C & Benkovic S J, *Bio-organic mechanisms*, Vol. II, (W A Benjamin, New York) 1966, Chapter 8.
7 Martell A E, *Chemical and biological aspects of pyridoxal catalysis*, edited by E E Snell, P M Fasella, A Braunstein & A Rossi Fanelli (Pergamon Press, New York) 1963, pp 13.
8 Braunstein A, *The enzymes*, Vol II, edited by F D Boyer, H Lardy & K Myrbach (Academic Press, New York) 1960, pp 113.
9 Ramachandran M S & Vivekanandam T S, *Tetrahedron*, **40** (1984) 4929.
10 Ramachandran M S, Vivekanandam T S & Arunachalam V, *Bull chem Soc, Japan*, **59** (1986) 1549.
11 Bell R P, *Advan phys org chem*, **4** (1968) 1.

Indian Journal of Chemistry
Vol. 27A, June 1988, pp. 504-506

Synthesis & Characterisation of Potassium, Cesium & Ammonium Oxotetrafluorotitanates(IV)

MIHIR K CHAUDHURI* & BIMAI ENDU DAS
Department of Chemistry, North-Eastern Hill University, Shillong 793 003

Received 7 *July* 1987; *revised and accepted* 24 *August* 1987

A high yield synthetic route to potassium and ammonium oxotetrafluorotitanates(IV) has been developed based on the reaction of freshly precipitated TiO_2 with 4 *M* sulphuric acid to produce TiO_2^{2+} cation which reacts with corresponding alkali fluorides (AF) in the molar ratio 1:7 (Ti:AF) to afford the desired compounds. The corresponding Cs^+ salt is prepared from the ammonium salt by metathesis. The compounds, all of which are white products, have been characterised on the basis of elemental analyses, room temperature magnetic susceptibility measurements, and IR and laser Raman (lR) spectral data. The IR and laser Raman (lR) spectra provide evidence for a distorted octahedral structure of $[TiOF_4]^{2-}$ ion with -Ti-O-Ti- interactions.

Solid oxo-complexes of Ti(IV) are rather fewer as compared to those of V(IV)[1-3]. In the case of Ti(IV), $[TiOF_5]^{3-}$ is the only well characterised[4] fluoro complex, although existence of $[TiOF_3]^-$ is also reported[5]. Of some interest is the complex oxotetrafluorotitanate(IV), $[TiOF_4]^{2-}$. Despite a number of attempts[6,7], synthesis of pure $[TiOF_4]^{2-}$ could not be achieved. In a recent study[8] involving high temperature thermal decomposition of a peroxo complex $K_2[Ti(O_2)F_4]$, $K_2[TiOF_4]$ has been obtained as one of the main products. As a sequel to our efforts on some aspects of titanium chemistry[1,9,10] and also in view of considerable interest on structural assessment of oxotitanates(IV)[11,12], we felt it imperative to synthesise the title compounds in pure forms and characterise them by elemental analyses, and IR and laser Raman (lR) spectral data.

Materials and Methods

Reagent grade chemicals were used throughout. IR spectra were recorded on a Perkin-Elmer model 983 spectrophotometer and laser Raman (lR) spectra on a SPEX Ramalog model 1403 spectrophotometer. The 4880 Å laser line from the Spectra-Physics model 165 argon laser was used as the excitation source. The scattered light at 90° was detected with the help of a cooled RCA 31034 photomultiplier tube followed by photon count processing system. The spectra were recorded at ambient temperature by holding the samples either in a quartz capillary or in the form of a pressed pellet. Magnetic susceptibility measurements were made at room temperature by Gouy's method using Hg $[Co(SCN)_4]$ as the calibrant.

Ammonium oxotetrafluorotitanate(IV), $(NH_4)_2[TiOF_4]$

Freshly prepared TiO_2 (lg, 12.5 mmol) was dissolved in 4 *M* sulphuric acid (36 ml) at room temperature to get a clear solution and to this was added a solution of ammonium fluoride (3.25g, 87.83 mmol) in water (10 ml) followed by addition of ethanol with constant stirring until thc white·product started appearing. The addition of ethanol was discontinued at this stage, the reaction mixture was cooled in an ice-water bath for 45 min until the preciiptation was complete, filtered, and the precipitate washed twice with ethanol and finally dried *in vacuo* over conc sulphuric acid, yield 1.8g (82%).

Potassium oxotetrafluorotitanate(IV), $K_2[TiOF_4]$

It was prepared as above, except ethanol was not added for precipitation since a white product appeared immediately. The reaction mixture was cooled in an ice-water bath for 15 min and the compound separated by filtration. It was dissolved in warm water (50 ml) which on cooling to room temperature afforded the desired compound which was filtered off, washed twice with ethanol and finally dried *in vacuo* over conc sulphuric acid, yield 1.9g (69.7%).

Cesium oxotetrafluorotitanate(IV), $Cs_2[TiOF_4]$

$Cs_2[TiOF_4]$ precipitated out spontaneously when solid $(NH_4)_2[TiOF_4]$ (2.84 mmol) was added to a clear solution of CsBr (8.52 mmol) dissolved in water (10 ml). The white product obtained was

Table 1 — Analytical Data of Potassium, Cesium and Ammonium Oxotetrafluorotitanates(IV)

Complex	Found (calc), %		
	K or N[a]	Ti[b]	F[c]
$K_2[TiOF_4]$	35.24 (35.77)	21.89 (22.01)	34.50 (34.86)
$Cs_2[TiOF_4]$		11.45 (11.82)	18.24 (18.71)
$(NH_4)_2[TiOF_4]$	15.45 (15.90)	26.80 (27.27)	42.98 (43.18)

(a) Determined as described earlier (see ref. 14)

(b) Determined after precipitation with cupferron (ref. 13a)

(c) Determined as lead chloride fluoride (ref. 13b)

washed with ethanol and finally dried *in vacuo* over conc sulphuric acid, yield 0.9g (78%).

Results and Discussion

The analytical data of the compounds are given in Table 1. Taking into account two important points, (i) that a number of direct methods[6,7] failed to provide pure $[TiOF_4]^{2-}$ and (ii) titanyl cation (TiO^{2+}) certainly exists[11,15,16] in solution, it was thought that an indirect route via the prior formation of an oxotitanates(IV) in solution might be appropriate for the synthesis of pure oxotetrafluorotitanates(IV) reported in this study. Thus freshly prepared TiO_2 (obtained by dissolving commercial titanium dioxide in 40% hydrofluoric acid and then treating with aqueous ammonia) was first dissolved in an excess of dil sulphuric acid to produce titanyl sulphates[17], $TiO(SO_4)$, in solution. The clear solution was then treated with alkali fluoride (AF) to produce the desired compound. The role of alkali fluoride was not only to fluorinate the titanyl (TiO^{2+}) but also to act as a source of counter alkali metal cation. For the preparation of the ammonium compound addition of ethanol was required to just initiate precipitation owing to high solubility of the ammonium salt. Recrystallisation of $K_2[TiOF_4]$ from water was necessary to remove any coprecipitated K_2SO_4. The method is fairly simple and does not involve hydrofluoric acid. The cesium salt $Cs_2[TiOF_4]$ was prepared by metathesis between $(NH_4)_2[TiOF_4]$ and CsBr. It is evident from the above discussion that fluoride is a better ligand for TiO^{2+} than sulphate. Indeed our endeavours to synthesise mixed ligand fluoro(sulphato)titanates(IV) have not been successful so far.

Potassium, cesium and ammonium oxotetrafluorotitanates(IV) are white solids and are stable when out of contact with water. All the compounds are diamagnetic, in conformity with the view that titanium occurs in its +4 oxidation state (d^0) in these compounds. They are also EPR silent. The IR and laser Raman (lR) spectra of all the compounds are identical except for $\nu(NH_4^+)$ mode of the ammonium salt. The occurrence of ν(Ti-F) mode due to coordinated fluoride around 605 cm^{-1} compares favourably with the literature reports[18-20]. The appearance of a medium intensity band at ~720 cm^{-1} may be assigned to ν(Ti-O-Ti)21. The absence of $\nu(Ti=O)$ mode at ~980 cm^{-1} indicates that the oxo group does not occur as a terminal one but is present as a bridging group. The band at ~300 cm^{-1} in the compounds may be assigned to a Ti-F deformation mode. The bands at 1400 (s), 3045(s) and 3155(m) cm^{-1} in the IR spectrum of ammonium salt have been attributed to ν_4, ν_1 and ν_3 modes of NH_4^+ (ref. 22), respectively.

The laser Raman (lR) spectra of all the three complexes are similar and exhibit a strong signal at ~610 cm^{-1} assignable to ν(Ti-F)[20]. The spectra also display medium intensity bands at ~650, ~530 and ~435 cm^{-1} originating from -Ti-O-Ti- interactions which, in accord with the literature[12], have been attributed to ν(-Ti-O-Ti-).

Thus, the results of IR and laser Raman (lR) spectral data suggest that the metal centre is hexacoordinated through a -Ti-O-Ti- interaction, and the complexes have polymeric distorted octahedral structures.

Acknowledgement

We thank the Department of Atomic Energy, Bombay for financial support.

References

1 Chaudhuri M K, Ghosh S K & Subramanian J, *Inorg Chem*, **23** (1984) 4439.

2 Ahrland S & Noren B, *Acta Chem Scand*, **12** (1958) 1595.

3 Ortolano T R, Selbin J & McGlynn S P, *J chem Phys*, **41** (1964) 262.

4 Dehnicke K, Pausewang G & Rudorff W, *Z anorg allgem Chem*, **366** (1969) 64.

5 Sengupta A K, Adhikari S K & Dasgupta H S, *J inorg nucl Chem*, **41** (1979) 161.

6 Dmitrevskii G E, Belitskaya A A, Savchenko M I & Kharchenko L P, *Zh Neorg Khim*, **13** (1968) 2663.

7 *Chem Abstr*, **73** (1970) 81105v; **79** (1973) 147791y; **79** (1973) 147794b.

8 Pausewang G & Schmidt R, *Z anorg allgem Chem*, **523** (1985) 213.

9 Chaudhuri M K & Das B, *Polyhedron*, **4** (1985) 1449; *Inorg Chem*, **25** (1986) 168.

10 Chaudhuri M K & Islam N S, *Inorg Chem*, **25** (1986) 3749; Bhattacharjee M & Chaudhuri M K, *J chem Soc, Dalton Trans*, (1987) 477.

11 Gratzel M & Rotzinger F P, *Inorg Chem*, **24** (1985) 2320.

12 Weighardt K, Quilitzch U, Weiss J & Nuber B, *Inorg Chem*, **19** (1980) 2514.

13 Vogel A I, *A text book of quantitative inorganic analysis*, (Longmans Green, London) 1962, (a) pp 544; (b) pp 269.

14 Chaudhuri M K & Ghosh S K, *Inorg Chem*, **21** (1982) 4020.

15 Caglilotì V, Ciavatta L & Liberti A, *J inorg nucl Chem*, **15** (1960) 115.

16 Ellis J D & Sykes A G, *J chem Soc, Dalton Trans*, (1973) 537; Ellis J D, Thompson G A K & Sykes A G, *Inorg Chem*, **15** (1976) 3172.

17 Clark R J H, Bradley D C & Thornton P, *The chemistry of titanium, zirconium and hafnium, Pergamon texts in inorganic chemistry*, vol 19 (Pergamon Press, Oxford) 1975, pp 377.

18 Dean P A W & Evans D F, *J chem Soc* (*A*), (1967) 698.

19 Lane A P & Sharp D W A, *J chem Soc* (*A*), (1969) 2942.

20 Milicev S & Macek J, *J chem Soc, Dalton Trans*, (1984) 297.

21 Coutts R S P & Wailes P C, *Inorg nucl chem Lett*, 3 (1967) 1.

22 Nakamoto K, *Infrared spectra of inorganic and coordination compounds*, (Wiley-Interscience, New York) 1970, pp 108.

Indian Journal of Chemistry
Vol. 27A, June 1988, pp. 507-509

Synthesis & Infrared, ^{1}H, ^{13}C, ^{119}Sn NMR & ^{119}Sn Mössbauer Studies of Some New Diorganotin Dichloride Adducts

A S KOTHIWAL, A SINGH, A K RAI & R C MEHROTRA*
Department of Chemistry, University of Rajasthan, Jaipur

Received 2 April 1987; revised and accepted 6 October 1987

Adducts of the type $R_2SnCl_2.O(R'')CC_6H_4NR'_2$ (R = Ph, Me; when R′ = H, R″ = CH_3 and R′ = CH_3, R″ = H) have been prepared and characterised by elemental analyses and spectral data (IR, PMR, ^{13}C, ^{119}Sn NMR, and ^{119}Sn Mössbauer).

Though the electrophilic nature of tin in organotin halides is weak, a large number of adducts of organotin halides have been synthesised and characterised. Addition complexes of diorganotin(IV) dihalides with monodentate Lewis bases, in general, depict 1:2 stoichiometry[1], $R_2SnX_2.2L$ (where R = alkyl, aryl; X = halogens; L = monodentate ligand) and octahedral geometry. In contrast, well characterised pentacoordinated complexes are comparatively limited in number[2,3].

In the present paper the mode of complexation of *p*-dimethylaminobenzaldehyde and *p*- or *m*-aminoacetophenone with dialkyl- and diaryl-tin dichlorides has been studied. The *p*- and *m*-aminoacetophenones have been chosen in order to rule out the possibilities of chelate formation. In view of the presence of both nitrogen as well as oxygen donor sites in the ligands, the following interesting possibilities can be envisaged for complexation in these systems: (i) $nNR'_2C_6H_4C(R'')O \rightarrow SnR_2Cl_2$; (ii) $nO(R'')CC_6H_4N(R'_2) \rightarrow SnR_2Cl_2$ and (iii) $R_2(Cl_2)Sn \leftarrow N(R'_2)C_6H_4C(R'')O \rightarrow SnR_2Cl_2$ (where n = 1 or 2).

Materials and Methods

The solvents used were dried before use. The ligands and reactants were purified by usual techniques. Molecular weights were determined in a semi-micro ebulliometer (Gallenkamp) equipped with thermistor sensing. IR spectra were recorded in the region 4000-200 cm^{-1} on a Perkin-Elmer 577 grating spectrophotometer and PMR spectra on Perkin-Elmer R-12B and Varian A-60 spectrometers. Carbon-13 and ^{119}Sn NMR spectra were recorded on a JEOL-PFT-100 FT spectrometer operating at 25.15 and 22.7 MHz respectively. Tin-119 Mössbauer spectra were recorded at 77 K using a conventional constant acceleration spectrometer.

Synthesis of complexes

When a solution of dialkyl/diaryltin dichloride in chloroform was mixed with a chloroform solution containing aminoacetophenone/dimethylaminobenzaldehyde in equimolar amount, heat was evolved and the colour of the reaction mixture changed from colourless to yellow. After stirring for 1 hr at room temperature, dry *n*-hexane was added gradually when a yellow precipitate was obtained leaving the supernatant liquid colourless, which was decanted off. The precipitate was filtered off, dried *in vacuo* at room temperature and recrystallised from benzene to afford a yellow solid. The characterisation data of diorganotin dichloride adducts thus prepared are listed in Table 1.

Results and Discussion

The reaction of dimethyl- and diphenyl-tin dichlorides with *p*-dimethylaminobenzaldehyde and *p*- or *m*-aminoacetophenone in chloroform can be represented by Eqs. (1) and (2), respectively:

$$R_2SnCl_2 + p\text{-}NMe_2C_6H_4CHO \rightarrow R_2SnCl_2.O(H)CC_6H_4NMe_2\text{-}p \quad \ldots (1)$$

$$R_2SnCl_2 + p \text{ or } m\text{-}NR'_2C_6H_4COCH_3 \rightarrow R_2SnCl_2.O(CH_3)CC_6H_4NR'_2\text{-}p \text{ or m} \quad \ldots (2)$$

$$(R = Ph, Me; R = H \text{ or } Me)$$

A noteworthy feature of the above reactions is the formation of addition complexes of 1:1 stoichiometry only even when two-fold excess of the ligand is used (Table 1). All the complexes obtained are coloured solids (organge, yellow, or brown), have sharp melting points and are soluble in common organic solvents. The adducts are monomeric in refluxing benzene.

The infrared spectra of the complexes did not exhibit any shift in νNMe_2 modes of the free ligands

Table 1—Physical and Analytical Data of Some Diorganotin Dichloride Adducts

Sl No.	Complex	m.p. (°C)	Physical state	found (calc.) %		
				N	Cl	Sn
1	p-$NH_2C_6H_4C(Me)O.Ph_2SnCl_2$	121	Orange powder	2.90 (2.94)	14.77 (14.83)	24.78 (24.83)
2	p-$NH_2C_6H_4C(Me)O.Me_2SnCl_2$	101	Yellow powder	3.89 (3.97)	19.87 (20.02)	33.39 (33.52)
3	m-$NH_2C_6H_4C(Me)O.Me_2SnCl_2$	95	Brown solid	3.85 (3.97)	19.85 (20.02)	33.26 (33.52)
4.	p-$NMe_2C_6H_4CHO.Me_2SnCl_2$	95	Yellow powder	3.80 (3.82)	19.17 (19.26)	32.06 (32.25)
5	p-$NMe_2C_6H_4CHO.Ph_2SnCl_2$	103	Lemon Yellow powder	2.80 (2.85)	14.36 (14.41)	24.06 (24.12)

Table 2—Spectral Data of Diorganotin Dichloride Adducts[a]

Sl No.	Complex	IR (cm^{-1})				^{1}H NMR (δ)		^{119}Sn Mössbauer[b]	
		νC=O	νSn−O	νSn−Cl		=C−H	−N(R′)$_2$	(ΔE) (mm s^{-1})	(δ) (mm s^{-1})
				asym	sym				
1	p-$NH_2C_6H_4C(CH_3)O.(CH_3)_2SnCl_2$	1675 (1645)	430	320	260	..	..	..	..
2	p-$NH_2C_6H_4C(CH_3)O\ (C_6H_5)_2SnCl_2$	1690 (1645)	440	320	265	..	..	2.81	1.38
3	p-$NMe_2C_6H_4C(H)O.(CH_3)_2SnCl_2$	1680 (1640)	435	330	275	9.55 (9.75)	3.02 (3.01)	3.88	1.48
4	p-$NMe_2C_6H_4C(H)O.(C_6H_5)_2SnCl_2$	1685 (1640)	435	332	278	9.48 (9.75)	3.01 (3.01)	2.89	1.24

(a) The values in parentheses are those of the ligands.
(b) The values are relative to SnO_2

suggesting non-involvement of amino and dimethylamino nitrogens in coordination. Lowering in the νC=O by ~40 cm^{-1} may be taken as an evidence for the coordination of the ligand with R_2Sn moiety through the oxygen of CO group. The aromatic νC=C modes were observed in the region 1590-1520 cm^{-1}. In the case of dimethyltin adducts, two medium intensity bands at 585 and 530 cm^{-1} could be assigned ν_{as}Sn-C and ν_sSn-C modes respectively. These modes in diphenyltin adducts appeared at 285 and 250 cm^{-1}, respectively. The appearance of both these modes suggests that C − Sn − C moiety is non-linear as suggested by Tanaka *et al*[2].

Generally,there are two structural possibilities (A and B) for pentacoordinated dialkyltin dihalide complexes in which the Lewis base(L) occupies the axial[4] or equatorial[5] site depending upon the electronegativity of the donor atom. Further, the positions of νSn-Cl modes are generally taken as diagnostic to distinguish among tetrahedral, trigonal bipyramidal and octahedral geometries. For trigonal bipyramidal geometry, a shift (compared to tetrahedral parent compound) of ~60 cm^{-1} in νSn-Cl is generally observed[6]. In the complexes studied presently, the observed shift (~50 *cm*$^{-1}$) *is consistent* with a trigonal bipyramidal geometry. Structure (A) should give rise to two νSn-Cl modes as a split band whereas structure (B) should give rise to only one νSn-Cl. The appearance of both ν_{as}Sn-Cl and ν_sSn-Cl modes, therefore, indicates that the ligand occupies the axial position, in a structure of the type (A). The appearance of a new band at ~435 cm^{-1} assignable[7] to νSn-O is also *confirms the coordination* through carbonyl oxygen.

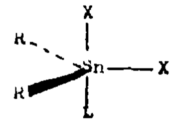

(A)

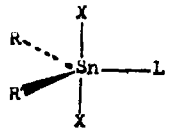

(B)

The significant characteristics revealed by the NMR(^{1}H, ^{13}C and ^{119}Sn) spectra of the complexes as compared with those of the free ligands are:

(i) The aldehydic proton in the adducts appears at higher field, shift being of the order of 0.25 ppm.

This is due to coordination through CO oxygen, which enhances the polarity of C − H bond resulting in greater concentration of electronic charges around the H atom.

(ii) The signals due to dimethylamino/amino protons, of the free ligands remain unaltered in the complexes, thereby providing indirect evidence for coordination through carbonyl oxygen.

(iii) Observed $^2J(^{119}Sn\text{-}^1H)$ values in the range 72-80 Hz provide evidence for pentaccordinated structures[8].

(iv) In the complex $Me_2SnCl_2.O(H)CC_6H_4NMe_2$-*p*, the $^1J(^{119}Sn\text{-}^{13}C)$ value of 597.72 Hz and $^1J(^{117}Sn-^{13}C)$ value of 610.75 Hz†, confirm that the tin atom has pentacoordinate environment[9].

(v) The ^{119}Sn chemical shift value (+26.8 ppm) observed for the complex $Me_2SnCl_2\cdot O(H)CC_6H_4$-$NMe_2$-*p* is in excellent agreement with that (δ, + 25.4 ppm) of $Me_3SnCl.NC_5H_5$ which has been shown to be pentacoordinated in a trigonal bipyramidal geometry[10].

The ^{119}Sn Mössbauer parameters (Table 2) obtained for these adducts reveal the following salient features:

(i) The lower isomer shift values for these complexes (1.24-1.48 mm/s) as compared to those reported for Me_2SnCl_2 (1.60 mm/s) and Ph_2SnCl_2(1.5 mm/s) are suggestive of the pentacoordinated geometry[11].

(ii) the higher quadrupole splitting values[12] (ranging between 2.74 and 3.86 mm/s)[13] indicate that the charge distribution around the tin nuclei is highly assymetric and the geometries are considerably distorted.

(iii) Further, the coordination number of the Mössbauer nuclei is also related to the ratio (ρ) of quadrupole splitting (ΔE) and isomer shift (δ). The observed ρ-values which range between 2.00 and 2.60, for the presently studies complexes, reflect a higher (may be pentacoordinated)[14-17] coordination number than the four coordination state at the tin atom, as concluded from other physicochemical studies.

On the basis of all the above findings these complexes may be assumed to possess five coordination around tin atom having a distorted trigonal bipyramidal geometry. These conclusions receive further, support from a recent X-ray diffraction authentication[18] of one of the derivatives, i.e. $Ph_2SnCl_2.OCHC_6H_4NMe_2$-*p*.

Acknowledgement

The authors thank the UGC, New Delhi for the award of a senior research fellowship to one of them (ASK). Sincere thanks are due to Prof. C L Khetrapal, Raman Research Institute, Bangalore for ^{13}C NMR and Prof. A G Davies, University College of London, London for the ^{119}Sn NMR and ^{119}Sn Mössbauer spectra.

References

1 Clark H C & Goel R G, *J organomet Chem*, **7** (1967) 263.
2 Tanaka T & Kamitani T, *Inorg Chim Acta*, **2** (1968) 175.
3 Matsubayashi G, Nishii N & Tanaka T, *Bull chem Soc Japan*, **42** (1968) 2369.
4 Cunningham D, Douek I, Frazer M J, Mc Partlin M & Matthews J D, *J Organomet Chem*, **90** (1975) C23.
5 Tzschack A, Weichmann H & Jurkschat K, *J organomet Chem Libry*, **12** (1981) 293.
6 Tzschack A & Jurkschat K, *Comments Inorg Chem*, **3** (1983) 35-50.
7 Saraswat B S, Srivastava G & Mehrotra R C, *J organomet Chem*, **164** (1979) 153; *Inorg Chim Acta*, **36** (1976) 289.
8 Simons P B & Graham W A G, *J organomet Chem*, **8** (1967) 479, and references therein.
9 Domazetis G, Magee R J & James B D, *J inorg nucl Chem*, **41** (1979) 1547.
10 Hunter B K & Reeves L W, *Can J Chem*, **46** (1968) 1399.
11 Parish R V & Platt R H, *J chem Soc* (*A*) (1969) 2145.
12 Bancroft G M & Platt R H, *Adv Inorg Radiochem*, **15** (1972) 59.
13 Naik D V & Curran C, *J organomet Chem*, **81** (1974) 177.
14 Zuckerman J J, *Adv organomet Chem*, **9** (1970) 21.
15 Lefferts J L, Molloy K C, Zuckerman J J, Haiduc I, Guta G & Ruse D, *Inorg Chem*, **19** (1980) 1662.
16 Lefferts J L, Molloy K C, Zuckerman J J, Haiduc I, Curtui M, Guta G & Ruse D, *Inorg Chem*, **19** (1980) 2861.
17 Mehrotra R C, Srivastava G & Chauhan B P S, *Coord Chem Revs*, **55** (1984) 207.
18 Mahadevan C, Seshasayee M & Kothiwal A S, *Cryst Struct Commun*, **11**(4B) (1982) 1725.

---

†Due to complexity of the spectra of other derivatives and weak ^{117}Sn and ^{119}Sn signals, the *J* values for all these could not be calculated.

Indian Journal of Chemistry
Vol. 27A, June 1988, pp. 510-513

Synthesis & Characterization of Complexes of Ru(II), Pt(II) & Pd(II) with Substituted Chalcones

T SEETHARAMA RAO, K LAXMA REDDY & P LINGAIAH*
Department of Chemistry, Kakatiya University, Warangal 506 009

Received 24 *February* 1987; *revised* 21 *July* 1987; *accepted* 8 *September* 1987

Complexes of Ru(II), Pd(II) and Pt(II) with 3-(2-furyl)-1-(2-hydroxyphenyl)-2-propen-1-one (FHPO), 3-(2-furyl)-1-(2-hydroxy-5-methylphenyl)-2-propen-1-one (FHMPO), 3-(2-thienyl)-1-(2-hydroxyphenyl)-2-propen-1-one (THPO), 3-(2-pyridyl)-1-(2-hydroxyphenyl)-2-propen-1-one (PHPO), 3-(1-naphthyl)-1-(2-hydroxyphenyl)-2-propen-1-one (NHPO) and 3-(3,4-dimethoxyphenyl)-1-(2-hydroxyphenyl)-2-propen-1-one (DMPHPO) have been synthesized and characterized by analytical, magnetic susceptibility, infrared, electronic and ESR data. Analytical data indicate a 1:2 (metal : ligand) stoichiometry. The IR spectral data of the metal complexes indicate that FHPO, FHMPO, THPO and PHPO act as mononegative tridentate towards Ru(II) and bidentate towards Pd(II) and Pt(II) metal ions, whereas NHPO and DMPHPO act as mononegative towards all the metal ions. The electronic spectral data susggest that all the Ru(II) complexes are octahedral whereas those of Pd(II) and Pt(II) are square planar.

Chalcones derived from *o*-hydroxyacetophenone and 2-furfural, thiophene-2-aldehyde, pyridine-2-aldehyde, naphthalene-1-aldehyde and veratraldehyde possess three coordinating sites for coordination to the metal ions, and therefore, these may act as monodentately, bidentately or tridentately with the different metal ions. In continuation of earlier publication[1], we report herein the synthesis and characterization of Ru(II), Pd(II) and Pt(II) complexes of these chalcones.

Materials and Methods

o-Hydroxyacetophenone, 2-furfural, thiophene-2-aldehyde, pyridine-2-aldehyde, naphthalene-1-aldehyde and veratraldehyde were Aldrich or BDH reagents. All the solvents used were of AR grade. The ligands, viz. 3-(2-furyl)-1-(2-hydroxyphenyl)-2-propen-1-one (FHPO), 3-(2-furyl)-1-(2-hydroxy-5-methylphenyl)-2-propen-1-one (FHMPO), 3-(2-thienyl)-1-(2-hydroxyphenyl)-2-propen-1-one (THPO), 3-(2-pyridyl)-1-(2-hydroxyphenyl)-2-propen-1-one (PHPO), 3-(1-naphthyl)-1-(2-hydroxyphenyl)-2-propen-1-one (NHPO) and 3-(3,4-dimethoxyphenyl)-1-(2-hydroxyphenyl)-2-propen-1-one (DMPHPO) were prepared as reported in literature[2,3] and their purities checked by TLC and melting point determinations. Ruthenium(III) chloride, platinum(II) chloride and palladium(II) chloride (all Johnson Mathew products) were used as such. The complex $RuCl_2 (DMSO)_4$ was prepared by the published method[4].

General procedure for the preparation of Ru(II) complexes

The complex $RuCl_2 (DMSO)_4$ (1 mol, 0.2 g) was suspended in toluene (30 ml) and refluxed for 1 hr with about four molar proportion of the appropriate ligand in methanol (10 ml). During the period of refluxing the suspension dissolved resulting in a clear solution, which was evaporated under reduced pressure to remove excess of solvent. The residue was treated with diethyl ether when the solid complex precipitated out. This was filtered off, washed several times with diethyl ether and dried *in vacuo* over fused calcium chloride.

General procedure for the preparation of Pt(II) and Pd(II) complexes

Platinum(II) and palladium(II) complexes were prepared by mixing 0.05 *N* HCl solution of metal chloride (0.056 mol) with methanolic solution of the ligands (0.112 mol) and heating the mixture on a hot water-bath for 30 min. The crystalline complexes formed were filtered under suction, washed with hot water followed by methanol and dried *in vacuo* over fused calcium chloride.

Results and Discussion

All the complexes are stable at room temperature, non-hygroscopic, insoluble in water and common organic solvents, but soluble slightly in acetone and freely in DMF and DMSO.

The analytical data presented in Table 1 indicate that the complexes have 1:2 (metal : ligand) stoichiometry. The molar conductances of 1×10^{-3} *M* solutions of the complexes in DMF are in the range of 10-20 $Ohm^{-1} cm^2 mol^{-1}$, indicating their non-ionic nature[5].

The complex, $RuCl_2 (DMSO)_4$ is an excellent precursor for the synthesis of many new ruthenium(II)

Table 1—Analytical and Electronic Spectral Data of Complexes of Ru(II), Pt(II) and Pd(II)

Compound	Found (Calc.) %			Electronic spectral bands (cm^{-1})
	C	H	S/N	
FHPO	72.56 (72.90)	4.82 (4.67)	—	—
[Ru(FHPO)$_2$]	59.22 (59.12)	3.68 (3.42)	—	19250, 23900
[Pd(FHPO)$_2$]	58.62 (58.57)	3.42 (3.38)	—	15600, 24600
[Pt(FHPO)$_2$]	50.42 (50.23)	2.92 (2.90)	—	20000, 23950
FHMPO	73.42 (73.68)	5.34 (5.26)	—	—
[Ru(FHMPO)$_2$]	60.42 (60.53)	3.86 (3.96)	—	19000, 24100
[Pd(FHMPO)$_2$]	59.91 (59.93)	3.89 (3.92)	—	15800, 25000
[Pt(FHMPO)$_2$]	51.86 (51.77)	3.42 (3.39)	—	19900, 24000
THPO	67.56 (67.83)	4.52 (4.35)	14.22 (13.91)	—
[Ru(THPO)$_2$]	55.86 (55.80)	3.26 (3.22)	5.86 (5.72)	18900, 24000
[Pd)THPO)$_2$]	56.12 (55.25)	3.76 (3.19)	5.92 (5.67)	15900, 24650
[Pt(THPO)$_2$]	47.92 (47.71)	2.76 (2.82)	4.82 (4.90)	20000, 24250
PHPO	.73.26 (73.56)	4.92 (4.72)	6.82 (6.60)	—
[Ru(PHPO)$_2$]	60.26 (59.65)	3.56 (3.44)	5.26 (5.35)	19500, 33000
[Pd(PHPO)$_2$]	59.82 (59.05)	3.56 (3.41)	5.42 (5.30)	15500, 20100
[Pt(PHPO)$_2$]	50.66 (50.56)	2.56 (2.92)	4.72 (4.54)	19500, 23200
NHPO	83.92 (83.21)	5.24 (5,11)	—	—
[Ru(NHPO)$_2$DMSO)$_2$]	62.82 (62.76)	4.92 (4.73)	8.12 (7.97)	19700, 33300
[Pd(NHPO)$_2$]	69.12 (69.90)	4.12 (3.99)	—	15500, 20250
[Pt(NHPO)$_2$]	61.66 (61.53)	3.62 (3.51)	—	19000, 24000
DMPHPO	72.26 (71.83)	5.12 (5.63)	—	—
[Ru(DMPHPO)$_2$DMSO)$_2$]	55.62 (55.40)	5.56 (5.10)	7.92 (7.78)	19000, 34000
[Pd(DMPHPO)$_2$]	60.72 (60.68)	4.52 (4.46)	—	15000, 35500
[Pt(DMPHPO)$_2$]	53.96 (53.61)	4.26 (4.94)	—	19100, 24000

complexes (Table 1) and the reactions involving this complex are mainly of the displacement type[6,7]. The reaction of this complex with substituted chalcones at reflux temperature in toluene was rapid and gave good yields of the complexes. Depending on the nature of the chelate this complex undergoes a variety of reactions.

Infrared spectra

The free ligands, FHPO, FHMPO, THPO, PHPO, NHPO and DMPHPO do not exhibit νOH in their IR spectra in KBr or CCl_4 solution, probably due to strong intramolecular H-bonding with oxygen of carbonyl group[8-10]; however, δOH modes appear at 1350, 1360, 1350, 1350, 1370 and 1370 cm^{-1} respectively. The disappearance of these bands in the spectra of the corresponding metal complexes indicates coordination of metal ions via deprotonation of phenolic OH of the ligands.

In the IR spectra of all the ligands, the $\nu C=O$ modes appear as an intense band around 1630 ± 10 cm^{-1} (ref. 12). This band is shifted to lower wavenumbers ($\Delta\nu = 50\ cm^{-1}$) in the spectra of the complexes indicating coordination through oxygen of $C=O$ group[13]. The medium intensity band appearing around 1560 ± 10 cm^{-1} in the ligands and the complexes can be assigned to the aromatic $\nu(C=C)$ vibrations, indicating non-participation of π-electron cloud in the $M-L$ bond formation[13].

The $O-O-O$ donor ligands FHPO and FHMPO contain furan ring, $O-O-S$ donor ligand THPO contains thiophene ring and $O-O-N$ donor ligands contain pyridine ring at 3-position. Strong bands at 1280 cm^{-1} in FHPO and FHMPO may be assigned to $\nu(C-O)$ of furan ring[14]; at 1100 cm^{-1} in THPO to $\nu(C-S)$ of thiophene ring[15]; and at 1600 cm^{-1} in PHPO to $\nu(C-N)$ of pyridine ring[16]. All these bands are shifted to lower wavenumbers in the spectra of Ru(II) complexes indicating coordination of oxygen of furan ring, sulphur of thiophene ring and nitrogen of pyridine ring to metal ions. However, all these bands do not undergo any shift in the spectra of Pd(II) and Pt(II) complexes indicating non-involvement of these atoms in coordination.

The ligand DMPHPO contains two methoxy groups in the phenyl ring causing a medium intensity band at 1245 cm^{-1} in its IR spectrum due to $\nu(C-O)$[17]. This band also appears at 1245 cm^{-1} in the IR spectra of complexes of the ligand. This band does not undergo any change.

The absence of DMSO in Ru(II) complexes of FHPO, FHMPO, THPO and PHPO was characterised by the absence of $\nu S=O$ mode of $RuCl_2(DMSO)_4$ in the region 1050-1100 cm^{-1} in the complexes[18]. The $\nu S-O$ modes in the complexes of $RuCl_2(DMSO)_4$ with NHPO and DMPHPO, appear at 1100 cm^{-1} indicating the presence of DMSO groups.

Thus it is clear from the IR data that the ligands FHPO, FHMPO, THPO and PHPO act as uninegative tridentate towards Ru(II), forming minimum possible six and seven-membered rings. However, these ligands also act as uninegative bidentate towards Pt(II) and Pd(II) forming minimum possible six-membered rings. The ligands NHPO and DMPHPO act as mononegative bidentate towards all the metal ions forming six-membered ring.

The participation of oxygen, sulphur and nitrogen is further supported by the appearance of bands at 450, 350 and 500 cm^{-1} due to $\nu(M-O)$, $\nu(M-S)$ and $\nu(M-N)$ respectively[19,20].

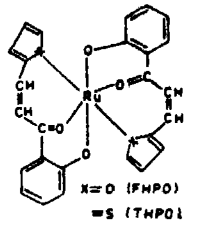

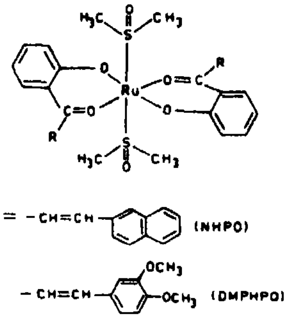

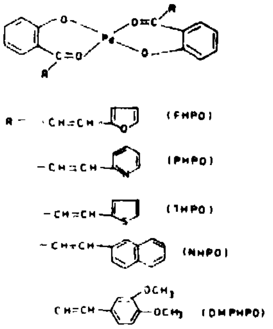

Electronic, ESR and magnetic data

All the ligands exhibit strong bands around 36000 and 30000 cm^{-1} assignable to $\pi^* \leftarrow \pi$ and $\pi^* \leftarrow n$ transitions, respectively. The two-spin allowed $d-d$ transitions in octahedral complexes are observed around 19000 and 24000 cm^{-1} corresponding to the ${}^1T_{1g} \leftarrow {}^1A_{1g}$ and ${}^1T_{2g} \leftarrow {}^1A_{1g}$ transitions, respectively[21]. Absence of splitting of lower energy band (19000 cm^{-1}) in the electronic spectra of Ru(II) complexes, indicates that there is no tetragonal distortion. Electronic spectra of Pd(II) complexes exhibit two bands at 15500 and 25000 cm^{-1} which may be assigned to ${}^1B_{1g} \leftarrow {}^1A_{1g}$ and ${}^1E_g \leftarrow {}^1A_{1g}$ transitions, respectively. These are characteristic of square planar geometry[22]. Platinum(II) complexes also exhibit two bands at 21000 and 24000 cm^{-1} characteristic of square planar geometry[23].

The complexes of Ru(II) are found to be diamagnetic, indicating that Ru(II) in the complexes is a low spin d^6-system. In general, all the octahedral complexes of Ru(II) known till now, are diamagnetic[21] and therefore, an octahedral geometry has been assigned to the complexes. The diamagnetic behaviour of Pd(II) and Pt(II) both belonging to d^8-system indicates the expected preferred square-planar geometry with $^1A_{1g}$ ground state around the metal ions. The diamagnetic behaviour of these complexes is also confirmed by the absence of a peak in their ESR spectra. The structures of Ru(II) and Pd(II) complexes are given in Structures 1 and 2.

References

1 Seetha Rama Rao T, Laxma Reddy K, Swamy S J & Lingaiah P, *Indian J Chem*, **24A** (1985) 942.
2 Ashanina T, *Bull chem Soc Japan*, **9** (1944) 133.
3 Geissman T A & Clinton R O, *J Am chem Soc*, **68** (1946) 697.
4 Evans I P, Spencer A & Wilkinson G, *J chem Soc, Dalton Trans*, (1973) 204.
5 Geary M J, *Coord chem Rev*, 7 (1971) 81.
6 Laxma Reddy K, Veera Reddy K & Lingaiah P, *Polyhedron*, **5(10)** (1986) 1519.
7 Ravinder V, Veera Reddy K & Lingaiah P, *Inorg chim Acta*, **87** (1984) 35.
8 Ingraham, Corsel Bailey & Stilt, *J Am chem Soc*, **71** (1952) 2297.
9 Rasmussen, Tunncliff & Brattain, *J Am chem Soc*, **21** (1949) 1068.
10 Koji Nakanshi, *Infrared absorption spectroscopy* (Practical Nankolo Company, London) (1964) 167.
11 Ramaswamy K K, Jose C I & Sen D N, *Indian J Chem*, **5** (1967) 156.
12 Dhar D N & Gupta V P, *Indian J Chem*, **9** (1971) 818.
13 Laxma Reddy K, Sri Hari S & Lingaiah P, *Indian J Chem*, **24A** (1985) 318.
14 Mahmoud M R, Hamide R & Haty M T, *Indian J Chem*, **19A** (1980) 345.
15 Centreras G & Cortes H, *J inorg nucl Chem*, **33** (1971) 1337.
16 Laxma Reddy K, Sri Hari S & Lingaiah P, *Indian J Chem*, **23A** (1984) 172.
17 Daniel J Pasto & Carl R Johnson, *Organic structure determination* (Prentice Hall Inc.) (1969) 172.
18 Reynolds M L, *Progr Inorg Chem*, **12** (1970) 1.
19 Laxma Reddy K, Sri Hari S & Lingaiah P, *Indian J Chem*, **24A** (1984) 318.
20 Shaw R N & Shaw J R, *Indian J Chem*, **22A** (1982) 372.
21 Pretic Tosi G & Zannini P, *J inorg nucl Chem*, (1979) 485.
22 Living Stones E, *The chemistry of ruthenium, rhodium, palladium, osmanium, iridium and platinum*, Vol. 25 (Pergmann Press Monograph) 1973, 1286.
23 Singh P P, Srivastava A K & Khan Sushil A, *Aust J Chem*, **28** (1975) 267.

Indian Journal of Chemistry
Vol. 27A, June 1988, pp. 514-518

Metal Complexes of Some Peptide Derivatives: Part V—Complex Formation of Copper(II) with N-Salicyloyl Derivatives of Some Amino Acids

G N MUKHERJEE* & (Miss) S SARKAR
Department of Chemistry, Calcutta University, University College of Science, 92 Acharya Prafulla Chandra Road,
Calcutta 700 009

Received 30 *March* 1987; *revised* 27 *July* 1987; *accepted* 24 *August* 1987

Complex formation of Cu(II) with N-salicyloyl derivatives of some amino acids has been studied by equilibrium method at 25, 30, 35 and 45°C in 50% v/v aq. ethanol and at $\mu = 0.2$ *M* ($NaNO_3$). Thermodynamic parameters associated with complexation equilibria have been correlated with the structure and bonding of the complexes.

Interactions of transition metal ions with amino acids and small peptide derivatives offer simple models for metal-protein interactions and enzymes[1-5]. In neutral solution protonation and metallation with the amide (–CONH–) bond occur at the amide carbonyl oxygen atom. Metallation at the amide nitrogen occurs only through substitution of the amide proton provided there is a possibility of chelation of the metal ions[2,5,6]. With a view to understanding the effect of an adjacent phenolic OH group on the coordinating properties of the amide bond we had earlier studied the complexation equilibria of Cu(II) with N-salicyloylglycine (SG)[7], and N-salicyloyl *dl*-α-alanine (SA)[8] at 30°C in 50% v/v aq. ethanol medium at a constant ionic strength ($\mu = 0.2$ *M* $NaNO_3$). Complexation equilibria of Cu(II) with N-salicyloyl-β-alanine (SB) and N-salicyloyl-*dl*-methionine (SM), in the same solvent medium have been studied. Complexation equilibria of the Cu(II)-SG and Cu(II)-SA system have also been studied at 25°, 35° and 45°C; the data for these systems at 30°C were obtained from literature[7,8]. Some solid complexes of Cu(II) have also been isolated and characterised on the basis of IR and UV-VIS spectral data.

Materials and Methods

All the ligands were prepared as described earlier[7,8] and their purities were checked by elemental analyses, m.ps, UV and IR spectra. All the other reagents used were of AR quality.

Bright green crystalline Cu(II) complexes, $Cu(HL\text{-}H).2H_2O$, (where $H_2L = SB$ and SM) were obtained by treating the monosodium salts (NaHL) of the respective ligands with Cu(II) sulphate in aqueous solution as described earlier[7,8]. These complexes on acetylation furnished the monoacetyl derivatives, $Cu(CH_3COL\text{-}H).2H_2O$.

The procedure for the *p*H-metric study was the same as described earlier[7,8]. Preliminary values of the equilibrium constants were evaluated by the procedure of Irving and Rossotti[9] and the values were finally refined employing the computer programme[10] SCOGS.

Results and Discussion

Characterisation of solid complexes $Cu(HL\text{-}H).2H_2O$ *and* $Cu(CH_3COL\text{-}H).2H_2O$ ($H_2L = SB, SM$)

The IR spectra of ligands in KBr exhibited νCOOH modes in the region 1740-1720 cm^{-1}. These modes were absent in the spectra of $Cu(HL\text{-}H).2H_2O$ or $Cu(CH_3COL\text{-}H).2H_2O$. However, the spectra of the complexes displayed two new bands at 1540-1530 and 1370-1330 cm^{-1} assigned to $\nu_{as}COO^-$ and ν_sCOO^- respectively, suggesting $Cu^{2+}-{}^-OOC$ bonding in the complexes[11]. The amide I and II bands in these complexes were observed at 1600-1590 and 1450-1440 cm^{-1} in comparison to those at 1660-1600 (br), 1550-1540 and 1300-1280 cm^{-1} respectively due to amide I, II and III bands for the free ligands. Such shifts of the amide bands indicated bonding of deprotonated amide nitrogen[3,4,12] to Cu(II) in these complexes. Both the series of complexes exhibited ν(O-H) mode in the region 3400-3300 cm^{-1} which, however, could not be considered as a diagnostic for the free phenolic OH group, as similar bands were expected to appear due to H_2O molecules. Formation of $Cu(CH_3COL\text{-}H).2H_2O$ through acetylation of $Cu(HL\text{-}H).2H_2O$ by the procedure usually applied for acetylation of phenols indicated the presence of free phenolic OH group in the parent $Cu(HL\text{-}H).2H_2O$ complexes. Analytical data of $Cu(CH_3COL\text{-}H).2H_2O$ also supported substitution

Table 1—Proton-Ligand Constants at Different Temperatures and Associated Thermodynamic Parameters at 25°C
[Solvent = 50% (v/v) aq. ethanol; $\mu = 0.2\ M(\mathrm{NaNO_3})$]

Ligand	Constant[c]	25°	30°	35°	45 ± 0.1°C	ΔG[a]	ΔH[a]	ΔS[b]
SG	$pK^{H}_{H_2L}$	4.00	3.98[7]	3.96	3.91	−23.0	−8.4	49
	pK^{H}_{HL}	8.86	8.83[7]	8.79	8.74	−50.8	−12.8	128
SA	$pK^{H}_{H_2L}$	4.22	4.18[8]	4.15	4.10	−24.2	−9.6	49
	pK^{H}_{HL}	9.36	9.30[8]	9.25	9.16	−53.7	−12.8	137
SB	$pK^{H}_{H_2L}$	4.82	4.80	4.77	4.73	−27.6	−8.5	64
	pK^{H}_{HL}	9.02	8.98	8.96	8.90	−51.7	−13.0	130
SM	$pK^{H}_{H_2L}$	4.05	4.04	4.02	3.98	−23.2	−8.7	49
	pK^{H}_{HL}	8.78	8.75	8.72	8.66	−50.4	−19.2	105

(*a*): kJmol^{-1} (*b*): JK^{-1}mol^{-1}; (*c*): error limits for constants, ± 0.05 in log scale; for ΔG, ΔH, ± 0.5 kJmol^{-1} and for ΔS, ± 3 JK^{-1}mol^{-1}.

of one hydrogen atom in Cu(HL-H).2H$_2$O, preferably phenolic proton by an acetyl group. This was supported by the fact that while Cu(HL-H).2H$_2$O gave intense violet colour with neutralised FeCl$_3$ solution, the corresponding acetyl derivatives did not give any colour with this reagent.

Electronic spectra of both Cu(HL-H).2H$_2$O and Cu(CH$_3$COL-H).2H$_2$O were almost superimposable and maximum absorption in the region 610-600 nm were indicative of coordination of Cu(II) by deprotonated amide nitrogen and carboxylate oxygen atoms in a square planar Cu(N,O)(H$_2$O)$_2$ geometry without having any apical coordination[5,13] as might be provided by the phenolic oxygen atom. As the ligand ion, (CH$_3$COL-H)$^{2-}$ could provide only bidentate (N,O) chelation via the deprotonated amide nitrogen and the carboxylate oxygen atoms, it may, therefore, be inferred that in Cu(HL-H).2H$_2$O the ligand (HL-H)$^{2-}$ is (N,O) bidentate leaving the phenolic OH intact. The possibilty of coordination of SCH$_3$ moiety of SM ligand was also ruled out because the electronic spectra of Cu(II) complexes of SM were superimposable with those of SG, SA and SB. Room temperature magnetic moment values of all the Cu(II) complexes were in the range 1.76-1.84 B.M. as expected for one unpaired electron and indicated the absence of any Cu...Cu interaction in these complexes.

Proton-ligand and Cu(II)-ligand equilibria

The ligands SB and SM like SG and SA could also be titrated as biprotic acids (H$_2$L), deprotonation occurring from −COOH and phenolic −OH groups in successive steps giving two well separated buffer regions in the *p*H ranges 2.5-6.5 and 8-12. That the phenolic OH and not the amide (−CONH−) group was deprotonated in the second step, was confirmed by the monoprotic nature of benzoylglycine (C$_6$H$_5$CONHCH$_2$COOH), which gave a single buffer region (*p*H 2.5-6.5) in the entire *p*H range (2-12) studied. Increase of K^{H}_{COOH} and K^{H}_{OH} values (Table 1) with increase in temperature indicated that COOH and OH are involved in H-bonding in the ligands. The H-bonding breaks down at higher temperature thus accounting for enhanced acidity. Positive entropy changes (ΔS) associated with proton-ligand equilibria indicate increased flexibility of the deprotonated forms of the ligands due to the absence of H-bonding. Enthalpy changes (ΔH) accompanying deprotonation of phenolic OH are found to be roughly 1.5 times higher than the corresponding values for the deprotonation of −COOH, probably due to the labilizing influence of C=O moiety of −COOH function on O−H bond. Higher acidities (K^{H}_{OH}) of phenolic OH of the ligands over that of salicylic acid may be due to stabilization of the L^{2-} anion by H-bonding involving amide proton.

Buffer regions (*p*H 2.5-6.5) are observed[7] at lower *p*H values in the presence of Cu(II) while the regions *p*H 8-12 do not show any change. Complexation with Cu(II), in solution, therefore, occurs only via deprotonation of −COOH. Four protons per Cu(II) are released in the *p*H range 2.5-6.5, where hydrolysis of the Cu^{2+} (*aq.*) ion does not occur. Mole ratio study of Cu(II)-H$_2$L mixtures at *p*H values corresponding to $\bar{n}$[†] > 4, by spectrophotometric method

---

[†] $\bar{n}$: Average number of protons released due to the reaction of Cu(II) with the ligands, H$_2$L.

Table 2—Formation Constants[a] of Cu(II) Complexes at Different Temperatures

[Solvent = 50% (v/v) aq. ethanol; $\mu = 0.2\ M(NaNO_3)$]

System	Temp. (±0.1°C)	$pK^{2H}_{Cu+H_2L}$	$pK^{2H}_{Cu(HL-H)+H_2L}$	$pK^{H}_{Cu(HL-H)_2}$	$pK^{H}_{Cu(L-H)(HL-H)}$
Cu(II) + SG	25	6.15	6.40	8.54	10.02
	30 (ref. 7)	6.06	6.32	8.43	9.98
	35	5.97	6.24	8.32	9.94
	45	5.81	6.10	8.14	9.82
Cu(II) + SA	25	6.52	6.90	8.77	10.53
	30 (ref. 8)	6.42	6.79	8.66	10.49
	35	6.33	6.68	8.55	10.45
	45	6.18	6.51	8.39	10.34
Cu(II) + SB	25	7.96	9.14	*b*	*b*
	30	7.87	9.03	*b*	*b*
	35	7.80	8.92	*b*	*b*
	45	7.66	8.73	*b*	*b*
Cu(II) + SM	25	6.39	6.59	8.40	10.35
	30	6.34	6.54	8.35	10.32
	35	6.29	6.49	8.31	10.29
	45	6.18	6.38	8.23	10.23

(*a*) Error limits for constants. ±0.05 in log scale; (*b*) constants could not be determined due to precipitation.

Table 3—Thermodynamic Parameters[a] Associated with Formation of Cu(II) Complexes at 25 ± 0.1°C

[Solvent = 50% (v/v) aq. ethanol, $\mu = 0.2\ M(NaNO_3)$]

Parameter	Cu(II)-SG	Cu(II)-SA	Cu(II)-SB	Cu(II)-SM
$Cu^{2+} + L^{2-} \rightleftharpoons Cu(HL-H)$				
$\log K^{Cu}_{Cu(HL-H)}$	6.71	7.05	5.88	6.44
ΔG (kJmol^{-1})	−38.5	−37.0	−33.7	−36.9
ΔH (kJmol^{-1})	12.8	3.0	9.6	2.0
ΔS (JK^{-1}mol^{-1})	172	146	145	131
$Cu(HL-H) + L^{2-} \rightleftharpoons Cu(HL-H)_2^{2-}$				
$\log K^{Cu(HL-H)}_{Cu(HL-H)_2}$	6.46	6.67	4.70	6.24
ΔG (kJmol^{-1})	−37.0	−40.4	−27.0	−35.8
ΔH (kJmol^{-1})	8.0	8.8	9.5	2.0
ΔS (JK^{-1}mol^{-1})	151	158	123	127
$Cu(HL-H)_2^{2-} \rightleftharpoons Cu(L-H)(HL-H)^{3-} + H^+$				
$pK^{H}_{Cu(HL-H)_2}$	8.54	8.77	*b*	8.40
ΔG (kJmol^{-1})	−49.0	−50.3	*b*	−48.2
ΔH (kJmol^{-1})	−38.5	−36.6	*b*	−16.5
ΔS (JK^{-1}mol^{-1})	35(40)	46(49)	*b*	106(49)
$Cu(L-H)(HL-H)^{3-} \rightleftharpoons Cu(L-H)_2^{4-} + H^+$				
$pK^{H}_{Cu(L-H)(HL-H)}$	10.02	10.53	*b*	10.35
ΔG (kJmol^{-1})	−57.4	−60.4	*b*	−59.3
ΔH (kJmol^{-1})	−19.2	−18.3	*b*	−11.5
ΔS (JK^{-1}mol^{-1})	128(128)	141(137)	*b*	160(105)

(*a*) Error limits: for the constants ±0.05 in the log scale; for ΔG and ΔH, ±0.5 kJmol^{-1}; and for ΔS, ±3 JK^{-1}mol^{-1}. (*b*) Could not be determined due to precipitation. Values in the parentheses are for the deprotonation equilibria of the free ligand.

at 610-600 nm established the 1:2 (Cu:ligand)stoichiometry. Therefore, hydroxo complexes and complexes higher than 1:2 were omitted in calculating the Cu(II)-ligand constants. Formation of Cu(II)-2H$_2$L complexes can, therefore, be accounted for by asuming the substitution of −COOH and amide (−CONH−) protons of the ligands by Cu(II) (Eqs 1 and 2):

$$\mathrm{Cu^{2+} + H_2L \rightleftharpoons Cu(HL-H) + 2H^+}$$

$$K^{2\mathrm{H}}_{\mathrm{Cu+H_2L}} = ([\mathrm{H}]^2[\mathrm{Cu(HL-H)}])/([\mathrm{Cu}][\mathrm{H_2L}]) \cdots\cdots\cdots\cdots (1)$$

$$\mathrm{Cu(HL-H) + H_2L \rightleftharpoons Cu(HL-H)_2^{2-} + 2H^+}$$

$$K^{2\mathrm{H}}_{\mathrm{Cu(HL-H)+H_2L}} = ([\mathrm{H}]^2[\mathrm{Cu(HL-H)_2}])/([\mathrm{Cu(HL-H)}][\mathrm{H_2L}]) \text{---} (2)$$

The higher *p*H buffer region (*p*H 8-12) arose because of the deprotonation of phenolic OH of the free ligand, HL^- ions, together with the deprotonation of uncoordinated phenolic OH in $Cu(HL\text{-}H)_2^{2-}$ complexes (Eqs 3 and 4):

$$\mathrm{Cu(HL-H)_2^{2-} \rightleftharpoons Cu(L-H)(HL-H)^{3-} + H^+}$$

$$K^{\mathrm{H}}_{\mathrm{Cu(HL-H)_2}} = ([\mathrm{H}][\mathrm{Cu(L-H)(HL-H)}])/[\mathrm{Cu(HL-H)_2}] \cdots\cdots (3)$$

$$\mathrm{Cu(L-H)(HL-H)^{3-} \rightleftharpoons Cu(L-H)_2^{4-} + H^+}$$

$$K^{\mathrm{H}}_{\mathrm{Cu(L-H)(HL-H)}} = ([\mathrm{H}][\mathrm{Cu(L-H)_2}])/[\mathrm{Cu(L-H)(HL-H)}] \cdots\cdots\cdots (4)$$

Charges were dropped from these expressions for clarity. The $(HL\text{-}H)^{2-}$ ions in the complexes stand for the ligand species which have lost their carboxylic (–COOH) and amide (–CONH–) protons while still retaining the phenolic OH protons and the $(L\text{-}H)^{3-}$ ions stand for the fully deprotonated ligand species[5,13]. Equilibria (3) and (4) could not be followed for Cu(II)-SB system due to precipitation at *p*H ≥ 9.5. Equilibrium constants for equilibria (1-4) are presented in Table 2.

Stability constants $K^{\mathrm{Cu}}_{\mathrm{Cu(HL-H)}}$ and $K^{\mathrm{Cu(HL-H)}}_{\mathrm{Cu(HL-H)_2}}$ (Table 3) were calculated with the help of the relations (5) and (6) respectively.

$$\log K^{\mathrm{Cu}}_{\mathrm{Cu(HL-H)}} = \log K^{2\mathrm{H}}_{\mathrm{Cu+H_2L}} + pK^{\mathrm{H}}_{\mathrm{COOH}} + pK^{\mathrm{H}}_{\mathrm{OH}} \cdots\cdots\cdots\cdots (5)$$

$$\log K^{\mathrm{Cu(HL-H)}}_{\mathrm{Cu(HL-H)_2}} = \log K^{2\mathrm{H}}_{\mathrm{Cu(HL-H)+H_2L}} + pK^{\mathrm{H}}_{\mathrm{COOH}} + pK^{\mathrm{H}}_{\mathrm{OH}} \cdots\cdots (6)$$

Formation of Cu(HL-H) and $Cu(HL\text{-}H)_2^{2-}$ complexes through metal-promoted deprotonation of the amide bond was accompanied by positive enthalpy change (Table 3). Positive entropy changes accompanying the formation of Cu(HL-H) and $Cu(HL\text{-}H)_2^{2-}$ complexes suggested their chelated structures. The $\bar{n}$(*p*H) plot corresponding to the two series of equilibria, (1), (2) and(3), (4) showed a sharp increase from $\bar{n} = 0$ to $\bar{n} = 4$ (*p*H 2.5-6.5) and a flat rise in the region from $\bar{n} = 4$ to $\bar{n} = 6$ (*p*H 8-12). Absorption maxima λ_{max} of 1:5 Cu(II):H_2L mixtures at *p*H values corresponding to $\bar{n} = 0$, 2, 4 and 6 were 730, 650, 620-610 and 620-610 nm respectively for all the systems. This blue shift of 90 nm in the absorption maxima indicated a change from an octahedral $Cu(O)_6$ system in Cu^{2+} (*aq.*) ion to a square planar $Cu(N,O)_2$ system in $Cu(HL\text{-}H)_2^{2-}$ complexes. The constancy of λ_{max} in going from $\bar{n} = 4$ to $\bar{n} = 6$ indicates the retention of square planar $Cu(N,O)_2$ geometry even in the fully deprotonated $Cu(L\text{-}H)_2^{4-}$ complexes. The observed λ_{max} values 620-610 nm for the $Cu(HL\text{-}H)_2^{2-}$ and $Cu(L\text{-}H)_2^{4-}$ complexes are quite close within experimental errors, to the calculated values[5] (605 nm) for square planar $Cu(N,O)_2$ systems, where Cu(II) is coordinated to two deprotonated amide nitrogen and two carboxylate oxygen atoms. This observation further rules out the possibility of apical coordination of Cu(II) by phenolic oxygen in the $Cu(L\text{-}H)(HL\text{-}H)^{3-}$ and $Cu(L\text{-}H)_2^{4-}$ complexes. However, the possibility of chelation *via* hydrogen bonding of the phenolic proton with the amide carbonyl oxygen in the $Cu(HL\text{-}H)_2^{2-}$ complexes cannot be ruled out. Comparable magnitudes of $pK^{\mathrm{H}}_{\mathrm{Cu(HL-H)}}$ and $pK^{\mathrm{H}}_{\mathrm{HL}}$ values for all these systems indicate deprotonation equilibria (3) and (4) of $Cu(HL\text{-}H)_2^{2-}$ complexes to be analogous to deprotonation of the phenolic moieties of the free ligands (HL^-) species. With the exception of Cu(II)-SM system, even the entropy changes (Δ*S*) corresponding to deprotonation of $Cu(HL\text{-}H)_2^{2-}$ complexes (Eqs 3 and 4) are comparable (Tables 1 and 3) with those of the free phenolic OH of the free ligand ion (HL^-). Positive Δ*S* values for these equilibria are the result of breakdown of H-bonding in uncoordinated phenolic OH with C = O of the amide group.

Comparable magnitudes of formation constants (Tables 2 and 3) and identical λ_{max} values of Cu(II) complexes derived from SG, SA and SB with those derived from SM which has an extra binding site, viz. the SCH_3 moiety, suggest similar type of coordination, viz. (N,O) bidentate chelation by all the four ligands. The SCH_3 moiety of SM was not probably associated to Cu(II) in the complexes. Compratively higher entropy change associated with deprotonation equilibria (3) and (4) of Cu(II)-SM system may be due to release of some sort of a hydrophopic strain involving $-CH_2CH_2SCH_3$ moiety. Stabilities of Cu(II) complexes follow the ligand order: SA > SG > SM > SB. The lowest stabilities of Cu(II)-SB complexes are probably the result of angle strain in the six-membered chelate rings without having a double bond[14] as against five-membered chelate rings in the complexes derived from the other three ligands. Electron releasing effect of CH_3 group at α-position to amide and COOH moieties in SA ligand provides additional basicity to the donor atoms and consequently Cu(II) complexes with SA ligands are more stable than those with SG. Similar trends in stability have also been observed for Cu(II) complexes with glycylglycinate[15] ad glycyl-*dl*-α-alaninate[16]. The bidentate (N,O) chelated square planar $Cu(HL\text{-}H)_2^{2-}$ complexes are predominant (≈ 95%) in Cu(II) containing species in the region of biological *p*H.

References

1 Dobbie H & Karmack W O, *Biochem J*, **59** (1955) 246.

2 Dutta S P & Rabin B R, *Trans Faraday Soc*, **52** (1956) 1123; *Biochem Soc Symp*, **15** (1958) 21.

3 Kim M K & Martell A E, *J Am chem Soc*, **84** (1963) 3080; *Biochemistry*, **3** (1964) 1169.

4 Nakon R & Angelici R J, *Inorg Chem*, **12** (1973) 1269.

5 Siegel H & Martin R B, *Chem Rev*, **82** (1982) 385.

6 Scheller-Krattiger V, Schellar K H, Sinn E & Martin R B, *Inorg chim Acta*, **60** (1982) 45.

7 Mukherjee G N, Sarkar (Miss) S & Chatterjee S K, *J Indian chem Soc*, **59** (1982) 1117.

8 Mukherjee G N & Sarkar (Miss) S, *Indian J Chem*, **22A** (1983) 539.

9 Irving H M & Rossotti H S, *J chem Soc*, (1954) 2904; (1953) 3397.

10 Sayce I G, *Talanta*, **15** (1968) 1397.

11 Bellamy L J, *The infrared spectra of complex molecules*, Vol 1, 3rd Ed (Chapman & Hall, London), 1975, Pp. 183-202.

12 Kabanos T A & Tangarish J M, *J coord Chem*, **13** (1984) 89.

13 Gamp H, Siegel H & Zuberbuhler A D, *Inorg Chem*, **21** (1982) 1190.

14 Siegel H, *Angew Chem* (Int Edn), **14** (1975) 394.

15 Martin R P, Mosoni L & Sarkar B, *J biol Chem*, **246** (1971) 5944.

16 Brunetti A, Burke E J, Lim M C & Nancollas G H, *J soln Chem*, **1** (1972) 153.

Indian Journal of Chemistry
Vol. 27A, June 1988, pp. 519-522

Coordination Compounds of Organometallic Bases of Group(IV) Elements: Part XI—Reactions of N,N'-(Phenyl/*o*-chlorophenyl/*p*-methylphenyl/benzyl/diethyl)-1,1-di-*n*-propoxy/*n*-butoxy-silanediamines[†] with Tin(IV) & Titanium(IV) Chlorides at -10°C

SURAJ P NARULA*, NEETA KAPUR, RAVI SHANKAR, ARUN CHODHA & RAJESH MALHOTRA
Department of Chemistry, Panjab University, Chandigarh 160 014

Received 5 *June* 1987; *revised and accepted* 1 *October* 1987

The title reactions in 1:1 molar ratio in petroleum ether (40-60°) afford adducts having rearranged bases with composition $[(RO)_nSi(NHR')_{4-n}.xMCl_4]$ where $R = C_3H_7$ or n-C_4H_9; $R' = C_6H_5CH_2$, o-ClC_6H_4 or p-$CH_3C_6H_4$; $n = 0$ or 1; and $x = 2$ or 3 as evidenced by elemental analyses, IR and PMR spectral data as well as base exchange reactions. Filtrates of these reactions after keeping at room temperature for 48-72 hr, give solid complexes of the type $[(RO)_2Si(NHR')_2.2MCl_4]$ in each case. The reaction with the tertiary amines such as N,N'-diethyl-1,1-di-*n*-propoxy/di-*n*-butoxysilanediamine form normal 1:1 adducts $[(n\text{-}C_3H_7O/n\text{-}C_4H_9O)_2\ Si[N(CH_2CH_3)_2]_2.MCl_4$ and no base rearrangement is observed. A tentative mechanism of the disproportionation reactions is proposed.

The conversion of triorganoxy/organo-organoxysilanamines into organoxy/organo-silanetriamines and even into silanetetramines in the presence of titanium(IV) and tin(IV) chlorides and antimony (III) halides, has been demonstrated by us[1-6]. It has further been shown that the electronic and steric effects of substituents on silicon and nitrogen atoms significantly influence the conversion into silane polyamines[4-7]. For example N-(2-fluorophenyl)-1,1,1-trialkoxy silanamine is converted into N,N'-(2-fluorophenyl)-1,1-dialkoxy silanediamine while N-*n*-butyl/*p*-methylphenyl-1-chloro-1,1-dialkoxy silanamines are converted into N,N',N",N‴-(*p*-methylphenyl/*n*-butyl)silanetetramines[6]. However, these studies have so far been confined to secondary silanamines $[(RO)_3SiNHR']$ containing single Si − N bond. With a view to checking the general validity of such reactions, it was thought appropriate to extend these investigations to other Si − N compounds. One such strategy is to attempt these reactions with secondary silanediamines $[(RO)_2Si\text{-}(NHR')_2]$ and tertiary silanediamines $[(RO)_2Si\text{-}(NR'_2)_2]$. The results of these studies are being reported here.

Materials and Methods

All experiments were carried out at -10°C under dry nitrogen atmosphere. The solvents used were dried by conventional methods. Tin(IV) and titanium(IV) chlorides (Reidel, pure) were distilled before use.

Infrared spectra were recorded in nujol on a Perkin-Elmer model 621, double beam grating spectrophotometer having NaCl/KBr optics and PMR spectra in $CDCl_3 + DMSO\text{-}d_6$ on a Varian 390, 90 MHz instrument; chemical shifts are in δ-scale downfield from TMS internal reference.

The constant reaction temperature (-10°) of the bath was maintained using "cryo cool" model CC-100 II Neslab, Italy.

The ligands, N,N'-(phenyl/*o*-chlorophenyl/*p*-methylphenyl/benzyl/diethyl)-1,1-di-*n*-propoxy/di-*n*-butoxysilanediamines were prepared by the reaction of corresponding dichlorosilanes with amines in 1:4 molar ratio in dry diethyl ether at 0°C. The filtrates obained after removal of the amine hydrochlorides were fractionally distilled under reduced pressure. All these silanediamines were characterised and their purity checked by IR and PMR spectral data.

Reactions of ligands with tin(IV) and titanium(IV) chlorides

Addition of a solution of tin(IV) or titanium(IV) chloride in petroleum ether to a solution of a silanediamine in the same solvent at -10°C in equimolar ratios resulted in the precipitation of a solid compound in each case. The compounds were filtered in the cold, washed and dried under reduced pressure. The filtrates on standing at room temperature for 48-72 hr afforded another solid in each case which was isolated as above and characterised.

Base exchange reactions

The above complexes (10 mmol) were added to

[†] Nomenclature in accordance with IUPAC rules

Table 1—Analytical Data of Complexes of N,N′-Organo-1,1-(diorganoxy)silanediamines

Sl No.	Compound	Found (Reqd) (%)			
		Cl	Ti/Sn	Si	N
1.	$(PrO)Si(NHC_6H_5)_3.2TiCl_4$	38.0 (38.22)	12.8 (12.92)	3.4 (3.77)	5.54 (5.65)
2.	$(PrO)Si(NHC_6H_5)_3.2SnCl_4$	32.21 (32.09)	26.70 (26.89)	2.91 (3.16)	4.65 (4.74)
3.	$(BuO)Si(NHC_6H_5)_3.2TiCl_4$	37.41 (37.52)	12.43 (12 68)	3.6 (3.7)	5.35 (5.55)
4.	$(BuO)Si(NHC_6H_5)_3.2SnCl_4$	31.41 (31.59)	26.35 (26.47)	2.99 (3.11)	4.53 (4.67)
5.	$Si(NHC_6H_4CH_3-p)_4.3TiCl_4$	41.75 (41.68)	14.29 (14.09)	2.4 (2.74)	5.38 (5.48)
6.	$Si(NHC_6H_4CH_3-p)_4.3SnCl_4$	34.2 (34.49)	28.4 (28.9)	2.15 (2.27)	4.40 (4.53)
7.	$(PrO)Si(NHC_6H_4Cl-o)_3.2TiCl_4$	33.43 (33.55)	11.2 (11.34)	3.2 (3.31)	4.8 (4.96)
8.	$(PrO)Si(NHC_6H_4Cl-o)_3.2SnCl_4$	28.4 (28.73)	23.79 (24.07)	2.57 (2.83)	4.12 (4.25)
9.	$(BuO)Si(NHC_6H_4Cl-o)_3.2TiCl_4$	32.72 (33.0)	10.9 (11.16)	3.0 (3.25)	4.75 (4.88)
10.	$(BuO)Si(NHC_6H_4Cl-o)_3.2SnCl_4$	28.19 (28.32)	23.59 (23.74)	2.60 (2.79)	4.10 (4.19)
11.	$(PrO)Si(NHCH_2C_6H_5)_3.2TiCl_4$	36.0 (36.18)	12.10 (12.23)	3.45 (3.51)	5.25 (5.35)
12.	$(PrO)Si(NHCH_2C_6H_5)_3.2SnCl_4$	30.57 (30.64)	26.35 (25.67)	2.94 (3.02)	4.44 (4.53)
13.	$(PrO)_2Si[N(C_2H_5)_2]_2.TiCl_4$	29.72 (29.58)	10.14 (10.00)	5.62 (5.83)	5.79 (5.83)
14.	$(BuO)_2Si[N(C_2H_5)_2]_2.TiCl_4$	27.72 (27.95)	9.52 (9.45)	5.39 (5.51)	5.47 (5.51)
15.	$(PrO)_2Si[N(C_2H_4)_2]_2.SnCl_4$	25.57 (25.77)	21.51 (21.60)	4.98 (5.08)	5.01 (5.08)
16.	$(BuO)_2Si[N(C_2H_5)_2]_2.SnCl_4$	24.69 (24.52)	20.42 (20.55)	4.67 (4.84)	4.87 (4.84)

ethylenediamine (25 mmol), molten 2,2′-bipyridyl (25 mmol) or pyridine-d_5 (25 mmol) under dry nitrogen atmosphere and kept at 35-40°C for 5-6 hr. Thereafter dry carbon tetrachloride was added, filtered, and the solids obtained identified by the chemical shifts and proton counts.

Results and Discussion

Analytical data (Table 1) of the adducts conform to the composition $[(RO)Si(NHR')_3.2MCl_4]$ except in the case of the ligands N,N′-*p*-methylphenyl-1,1-di-*n*-propoxy/*n*-butoxysilanediamines and N,N′-diethyl-1,1-di-*n*-propoxy/*n*-butoxysilanediamines. Whereas the former affords adducts of the type $Si(NHC_6H_4CH_3-p)_4$. $3MCl_4$, the latter forms normal 1:1 adducts and no rearrangement is observed in the ligands. All the adducts are extremely hygroscopic and insoluble in common organic solvents except DMSO.

Infrared spectra

Infrared spectra of adducts $[(RO)_2Si(NR')_2.2MCl_4]$, $[(RO)Si(NHR')_3.2MCl_4]$ and $[Si(NHR')_4.3MCl_4]$ are similar to those already reported[6]. However, the IR spectra of 1:1 adducts $[n-C_3H_7O/n-C_4H_9O]_2Si(NCH_2CH_3)_2].MCl_4$ display νCO and νSiO(C) modes at 1080 and 1020-30 cm^{-1} respectively. The νCN (aliphatic) modes at 1290 cm^{-1} in these ligands undergo shift to lower wavenumbers ($\Delta\nu = 15$-20 cm^{-1}) indicating coordination through nitrogen atom. The bands at 300 and 375 cm^{-1} have been assigned to coordinated νSnCl and νTiCl modes of the Lewis acids used.

PMR spectra

The chemical shift (δ) values along with the number of protons for each group are recorded in Table 2. From a comparison of proton counts of the parent ligand with those of the ligands in the

Table 2—PMR Spectral Data of Complexes of N,N′-(Phenyl/*o*-chlorophenyl/*p*-methylphenyl/benzyl/diethyl)-1,1-diorganoxy-silanediamines with Tin(IV) and Titanium(IV) Chlorides

Complexes*	CH_3	CH_2	CH_2O	CH_2N	NH	C_6H_5/C_6H_4	ring CH_3
1,2	0.85 (t, 3H)	1.2 (m, 2H)	3.6 (t, 2H)	—	4.2 (s, 3H)	7.4 (m, 15H)	—
3,4	0.90 (t, 3H)	1.2 (m,4H)	3.5 (t, 2H)	—	4.1 (s, 3H)	7.45 (m, 15H)	—
7,8	0.85 (t, 3H)	1.15 (m, 2H)	3.5 (t, 2H)	—	4.3 (s, 3H)	7.4 (m, 12H)	—
9,10	0.8 (t, 3H)	1.2 (m, 4H)	3.55 (t, 2H)	—	4.2 (s, 3H)	7.35 (m, 12H)	—
5,6	—	—	—	—	4.35 (s, 4H)	7.5 (m, 16H)	2.25 (s, 12H)
11,12	0.8 (t, 3H)	1.4 (q, 2H)	3.55 (t, 2H)	4.05 (s, 6H)	1.5 (s, 3H)	7.35 (s, 15H)	—
13,15	0.8 (t,6H)	1.4 (m, 12H)	3.6 (t, 4H)	2.85 (q, 8H)	—	—	—
14,16	0.85 (t, 6H)	1.4 (m, 14H)	3.6 (t, 4H)	2.90 (q, 8H)	—	—	—

*Sl nos refer to complexes listed in Table 1

adducts, it is apparent that the proton count due to alkylamino/anilino moieties in the ligands of the adducts have undergone three to four fold increase. On the other hand the proton count due to alkoxy groups in the adducts have suffered corresponding decrease. This shows that on reaction the ligands are disproportionated to alkoxysilanetriamines or silanetetramines, which are precipitated as the adducts. However, no such change is observed in the adducts of the tertiary amines such as $(n\text{-}C_3H_7O/n\text{-}C_4H_9O)_2Si\ [N(CH_2CH_3)_2]_2$. This observation indicates that no base rearrangement occurs for the ligand in tertiary silanamine which is contrary to the observations in secondary silanamine reactions.

Base exchange reaction

Further evidence in support of the compositions of the adducts is provided by the results of the base exchange reactions. Using the stronger electron donors such as 2,2′-bipyridyl, pyridine-d_5 and ethylenediamine in carbon tetrachloride separately, the silanamines could be regenerated and their identity confirmed through IR and PMR spectra.

From the foregoing data, it is apparent that under the same experimental conditions, the silanediamines like, silanamines[1-6] are converted into silanetriamines. N,N′-(*p*-Methylphenyl)-1,1-dialkoxysilanediamines are rearranged to silanetetramines[7]. The liberated silanamine from $(n\text{-}C_3H_7O/n\text{-}C_4H_9O)_2Si[N(CH_2CH_3)_2]_2.MCl_4$ is the original base molecule, which supports the view that tertiary silanamines do not undergo disproportionation in these donor-acceptor reactions.

Complexes isolated from filtrates

The filtrates of the above reactions at room temperature after 48-72 hr, afford another solid (15-20%), in each case. The composition of these compounds as evidenced by elemental analyses (Table 3), IR spectra [νNH 3200; νCO 1100-1080; νSiO(C) 1060 cm^{-1}], PMR spectra [CH_3, CH_2, CH_2O, C_6H_5, C_6H_5Cl and $CH_3(Ph)$ proton signals at 0.8 to 0.9, 1.3 to 1.4, 3.6 to 3.8, 6.8 to 7.5 and 2.4 ppm respectively along with proton integration] corresponds to $(OR)_2Si(NHR')_2.2MCl_4$. These adducts have also been isolated from the filtrates of the similar reactions of N-organo-1-chloro-1,1 dialkoxysilanamines[6]. In the case of N,N′-diethyl-1,1-dialkoxysilanediamines, only the residual normal 1:1 adducts were obtained.

The donor-acceptor reactions of organoxysilanamines studied so far[1-7], give adducts I-IV as the major reaction products.

$(RO)_2Si(NHR')_2.MCl_4$	$(RO)_2Si(NHR')_2.2MCl_4$
I	II
$(RO)Si(NHR')_3.2MCl_4$	$Si(NHR')_4.3MCl_4$
III	IV

Adducts (I) are obtained[4] from the ligands $[(RO)_3SiNHR']$ ($R = ClC_2H_4$; $R' = C_6H_5/C_6H_5CH_2$ and $R = CF_3CH_2$; $R' = C_6H_4F/C_6H_3F_2$). Adducts (II) are formed[4] from the ligand having mixed 2-chloroethoxy and *n*-propoxy/*n*-butoxy groups on silicon atom and $R' = C_6H_5/C_6H_5CH_2$. Adducts (III) are most common of the complexes isolated and are obtained from ligands having different R and

Table 3—Analytical Data of Complexes Isolated from Filtrates

Compound	Found (Reqd) %			
	Cl	Ti/Sn	Si	N
$(PrO)_2Si(NHC_6H_5)_2.2TiCl_4$	39.72	13.4	3.7	3.8
	(40.0)	(13.52)	(3.94)	(3.94)
$(PrO)_2Si(NHC_6H_5)_2.2SnCl_4$	33.16	27.7	3.0	3.2
	(33.33)	(27.93)	(3.29)	(3.29)
$(BuO)_2Si(NHC_6H_5)_2.2TiCl_4$	38.3	12.85	3.7	3.65
	(38.48)	(13.01)	(3.79)	(3.79)
$(BuO)_2Si(NHC_6H_5)_2.2SnCl_4$	32.02	27.16	2.9	3.22
	(32.27)	(27.04)	(3.18)	(3.18)
$(PrO)_2Si(NHC_6H_4Cl-o)_2.2TiCl_4$	36.29	12.24	3.7	3.65
	(36.45)	(12.34)	(3.59)	(3.59)
$(PrO)_2Si(NHC_6H_4Cl-o)_2.2SnCl_4$	30.95	25.7	2.8	3.16
	(30.84)	(25.84)	(3.04)	(3.04)
$(BuO)_2Si(NHC_6H_4Cl-o)_2.2TiCl_4$	35.05	11.7	3.27	3.42
	(35.19)	(11.89)	(3.47)	(3.47)
$(BuO)_2Si(NHC_6H_4Cl-o)_2.2SnCl_4$	29.85	25.12	2.9	3.01
	(29.93)	(25.08)	(2.95)	(2.95)
$(PrO)_2Si(NHC_6H_4CH_3-p)_2.2TiCl_4$	38.35	12.90	3.68	3.12
	(38.48)	(13.01)	(3.79)	(3.79)
$(PrO)_2Si(NHC_6H_4CH_3-p)_2.2SnCl_4$	32.14	27.15	3.02	3.12
	(32.27)	(27.04)	(3.18)	(3.18)
$(BuO)_2Si(NHC_6H_4CH_3-p)_2.2TiCl_4$	36.91	12.40	3.39	3.59
	(37.07)	(12.53)	(3.65)	(3.65)
$(BuO)_2Si(NHC_6H_4CH_3-p)_2.2SnCl_4$	31.15	26.07	3.21	3.01
	(31.27)	(26.21)	(3.08)	(3.08)
$(PrO)_2Si(NHCH_2C_6H_5)_2.2TiCl_4$	38.39	12.89	3.58	3.65
	(38.48)	(13.01)	(3.79)	(3.79)
$(PrO)_2Si(NHCH_2C_6H_5)_2.2SnCl_4$	32.35	26.92	3.0	3.11
	(32.27)	(27.04)	(3.18)	(3.18)

R′ groups[1-6]. Adducts (IV) are rare and are obtained as in the present case as well as when $R = CF_3CH_2$; $R' = C_6H_4F$. However, the present report and the literature observations also record the precipitation of adducts (II) as the minor products from the filtrates during the formation of III and IV. Even adduct III has been found in small amounts in the reaction giving IV as the main product[8].

Thus adducts (II) and (III) may be presumed to be the unconsumed intermediate products leading to the formation of the appropriate silane polyamines. The tentative mechanism may therefore, be written as shown in the Scheme 1.

(i) $(RO)_3SiNHR' + MCl_4 \rightarrow (RO)_3SiNHR'.MCl_4$

(ii) $(RO)_3SiNHR'.MCl_4 + (RO)_3SiNHR' \rightarrow (RO)_2Si(NHR')_2.MCl_4 + (RO)_4Si$

(iii) $(RO)_2Si(NHR')_2.MCl_4 + MCl_4 \rightarrow (RO)_2Si(NHR')_2.2MCl_4$

(iv) $(RO)_2Si(NHR')_2.2MCl_4 + (RO)_3SiNHR' \rightarrow (RO)Si(NHR')_3.2MCl_4 + (RO)_4Si$

(v) $(RO)Si(NHR')_3.2MCl_4 + MCl_4 \rightarrow (RO)Si(NHR')_3.3MCl_4$

(vi) $(RO)Si(NHR')_3.3MCl_4 + (RO)_3SiNHR' \rightarrow Si(NHR')_4.3MCl_4 + (RO)_4Si$

Scheme (1)

As mentioned above, adducts I-IV are stable and isolable under appropriate experimental conditions. However, the adducts $(RO)_3SiNHR'.MCl_4$ and $(RO)Si(NHR')_3.3MCl_4$ have not yet been isolated and/or identified. In the case of tertiary silanamines the reaction stops after the first reaction and affords only 1:1 adducts.

References

1 Narula S P & Kapur N, *Indian J Chem*, **22A**(1983) 557.

2 Narula S P & Kapur N, *Inorg chim Acta*, **73** (1983) 183.

3 Narula S P & Kapur N, *Inorg chim Acta*, **86** (1984) 37.

4 Narula S P, Shankar R & Kumar S, *Indian J Chem*, **23A** (1984) 661.

5 Narula S P, Shankar R & Kapur N, *J Indian chem Soc*, **62** (1985) 925.

6 Narula S P, Kapur N, Chodha A, Shankar R & Malhotra R, *Indian J Chem*, **26A**(1987) 135.

7 Narula S P, Kapur N, Shankar R & Kumar S, *Proc Indian natn Sci Acad*, **52A**(1986) 1049.

8 Shankar R, *Reactions of organoxy/organo-organoxy silicon compounds containing Si – N bond with Lewis acids*, Ph.D. Thesis, Panjab University, Chandigarh, 1985.

Indian Journal of Chemistry
Vol. 27A, June 1988, pp. 523-526

Solvent Extraction Studies of Mixed Chelates of Europium

P R SANGURDEKAR† & M SUDERSANAN*
Analytical Chemistry Division, Bhabha Atomic Research Centre, Trombay, Bombay 400 085

Received 27 *July* 1987; *revised and accepted* 5 *October* 1987

Mixed chelates of europium with β-diketones and oxine have been studied by solvent extraction using carbon tetrachloride as the medium. Extraction of europium by mixtures of HBFA–HFTA, HBFA–HTFA as well as oxine-HBFA/HFTA/HTFA have been studied (where HBFA = benzoyltrifluoroacetone, HTFA = trifluoroacetylacetone and HFTA = furoyltrifluoroacetone). Mixed complexes are formed in all the cases and the nature of the extracted species and their equilibrium constants have been evaluated by graphical methods.

Mixed chelate formation in solution has been studied by various methods[1,2]. Mixed chelates of metals like copper, zinc, indium and europium with ligands like HTTA and isopropyltropolone have been reported[3]. Mixed chelates of lutetium[4] and uranium[5] have been reported. In our laboratories, a systematic study of indium[6], hafnium[7] and uranium[8] systems have been carried out. In continuation of this work, solvent extraction studies on the formation of mixed chelates of europium with two β-diketones or a mixture of a β-diketone and oxine are presented here. The studies using oxine have been made with a view to assessing the possibility of formation of adducts besides mixed chelates.

Materials and Methods

Europium, in the form of $^{152+154}$Eu, was obtained from Isotope Group, BARC. Benzoyltrifluoroacetone (HBFA), furoyltrifluoroacetone (HFTA) and trifluoroacetylacetone (HTFA) (all from K&K Labs, USA) and oxine (BDH, AR) were used as a solution in carbon tetrachloride (E. Merck, GR).

Extraction experiments were carried out by equilibrating for 6 hr at 30 ± 2°C the aqueous phase (10 ml) containing europium ($\sim 10^{-5}$ *M*), sodium chloride to maintain the ionic strength at 0.5 and acetic acid + sodium hydroxide (~ 0.02 *M*) to adjust the *p*H with an equal volume of the organic phase containing the extractants. The two phases were separated and the *p*H of the aqueous phase was measured using a Beckman Expandomatic SS-2 *p*H meter (M/s Beckman Instruments Inc, USA). Europium in the two phases was assayed by gamma counting using a thallium-activated sodium iodide crystal with a single channel analyser (M/s ECIL, Hyderabad). Background corrections were applied in all the cases. The mass balance for europium was good.

Results and Discussion

The mixed chelate formation of europium with two ligands, HA and HB, can be described by Eq. (1)

$$\mathrm{Eu^{3+}} + \mathrm{n[HA]_0} + (3-\mathrm{n})\mathrm{[HB]_0} \rightleftharpoons \mathrm{[EuA_nB_{3-n}]_0} + \mathrm{3H^+} \quad \ldots (1)$$

and the equilibrium constant is given by Eq. (2)

$$K_{\mathrm{BA}} = K_{(3-\mathrm{n}),\mathrm{n}} = \{\mathrm{[EuA_nB_{3-n}]_0[H]^3[Eu]^{-1}[HA]_0^{-n}[HB]_0^{-(3-n)}}\} \quad \ldots (2)$$

where the charges have been omitted for convenience. The distribution ratio(D) is given by Eq. (3).

$$\mathrm{D} = \frac{\mathrm{[EuA_3]_0 + [EuA_2B]_0 + [EuAB_2]_0 + [EuB_3]_0}}{\mathrm{[Eu]}} \quad \ldots (3)$$

Substituting in terms of equilibrium constants and on rearranging, we get

$$\mathrm{F_0} = \mathrm{D[H]^3/[HA]_0^3} = K_{03} + K_{12}\mathrm{[L]} + K_{21}\mathrm{[L]^2} + K_{30}\mathrm{[L]^3} \quad \ldots (4)$$

where [L] represents $\mathrm{[HB]_0/[HA]_0}$ and can be solved for various equilibrium constants by graphical methods.

Extraction of europium was studied using a mixture of β-diketones or a β-diketone and oxine. Various β-diketones were selected in order to study the influence of the terminal groups of the β-diketones on the stability of mixed chelates.

Europium-HBFA-HFTA system

Extraction of europium was studied in the presence of a mixture of HBFA (HA) and HFTA (HB). The distribution ratio (D) was measured as a function of *p*H at fixed [HBFA] and [HFTA]. Studies were also made at varying [HBFA] or [HFTA]

[†] Health Physics Division, BARC, Bombay 400 085

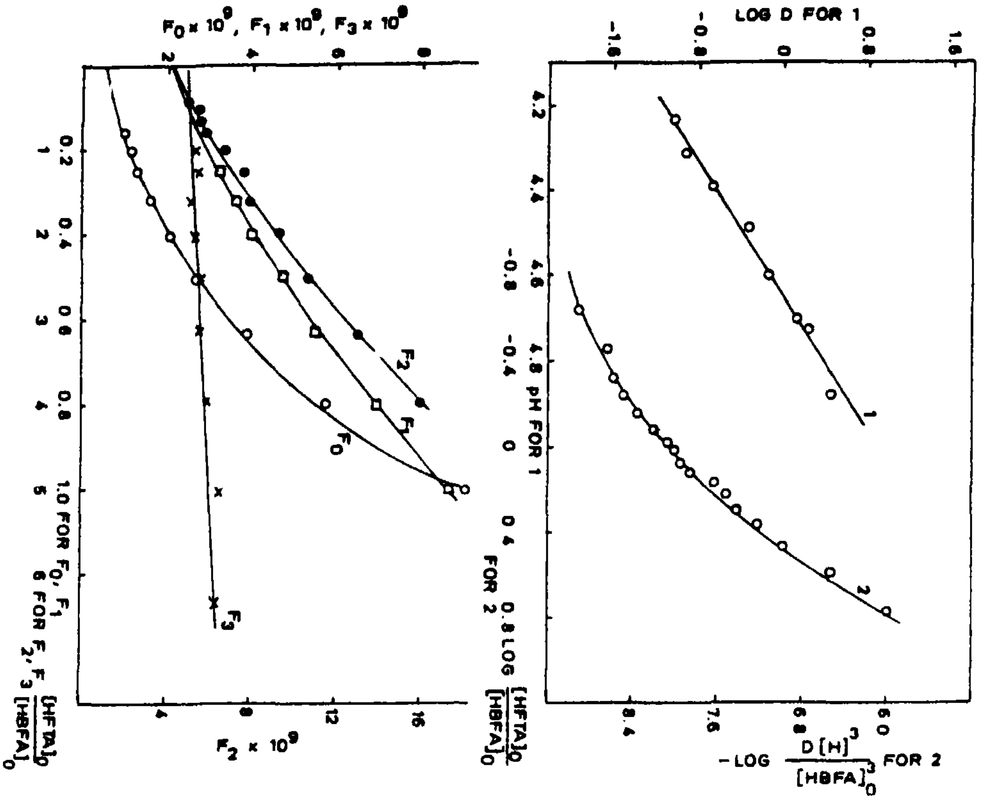

Fig. 1 — Europium-HBFA-HFTA system (Plots 1 and 2 represent the plot of log D versus pH and log $D\,[H]^3/[HBFA]_0^3$ versus $[HFTA]_0/[HBFA]_0$ respectively. Other plots represent the various F_j functions)

while maintaining the pH and concentration of the either β-diketone constant. The concentrations of the β-diketones were calculated taking into account the partition coefficients of the two β-diketones[9,10]. Values of partition coefficients were obtained from literature as log $P_{HA} = 2.47$ for HBFA and 0.82 for HFTA. The dissociation constants (pK) for HBFA and HFTA are 6.01 and 6.18 respectively[9].

The plot of function F_0, calculated using Eq. (4) resulted in a curve (Fig. 1) indicating the formation of mixed chelates. The plot of F_0 versus [L], when extrapolated to $[L] \rightarrow 0$, gives the value of K_{03} as the intercept. Another function F_1 can be written as

$$F_1 = \frac{F_0 - K_{03}}{[L]} = K_{12} + K_{21}[L] + K_{30}[L]^2 \qquad \ldots (5)$$

A plot of F_1 versus [L] gives the value of K_{12} as the intercept when $[L] \rightarrow 0$. Other functions can be written in a similar manner and solved to obtain the various equilibrium constants. Typical plots are given in Fig. 1 and the equilibrium constants are presented in Table 1.

Table 1 — Values of Equilibrium Constants

System (HA–HB)	K_{BA}	$-\log K_{BA}$
HBFA–HFTA	K_{03}	9.30
	K_{12}	8.70
	K_{21}	8.40
	K_{30}	8.60
HBFA–HTFA	K_{12}/K_1	7.66
	K_{21}/K_1	6.90
HFTA-oxine	K_{03}	7.92
	K_{12}	7.00
HBFA-oxine	K_{03}	8.36
	K_{12}	9.30
	K_{21}	8.32
HTFA-oxine	K_{12}/K_1	6.12

Europium-HBFA-HTFA system

Extraction of europium using a mixture of HBFA (HA) and HTFA (HB) was also studied in a similar manner. The concentration of HTFA in the organic phase was calculated taking into account the dissociation constant[9] (K_a) and partition coefficient (P) using the relation (6)

$$[HTFA]_0 = \frac{P_{HTFA}[HTFA]_{tot}}{1 + P_{HTFA} + K_a[H]^{-1}} \qquad \ldots (6)$$

where $P_{HTFA} = 0.646$ and $pK_a = 6.09$. Extraction of europium was studied around pH 5.6 by varying the concentration of HBFA (0.001 to 0.01 *M*) at a fixed concentration of HTFA (0.0165 *M*) and also at varying concentrations of HTFA and a fixed concentration of HBFA (0.01 *M*). Extraction of europium occurred at a higher pH of 5 to 6 and hence the aqueous phase complexes of Eu-TFA were to be considered for the analysis of data. The formation of $(\mathrm{Eu\ TFA})^{2+}$ can be described by the reaction (7)

$$\mathrm{Eu}^{3+} + [\mathrm{HTFA}]_0 \rightleftharpoons (\mathrm{Eu\ TFA})^{2+} + \mathrm{H}^+ \qquad \ldots (7)$$

with the equilibrium constant K_1 given by Eq. (8)

$$K_1 = [\mathrm{Eu\ TFA}][\mathrm{H}]/[\mathrm{Eu}][\mathrm{HTFA}]_0 \qquad \ldots (8)$$

Assuming Eu-TFA to be the predominant species in the aqueous phase, Eq. (5) can be rearranged to get

$$\mathrm{F}_0 = \frac{\mathrm{D}[\mathrm{H}]^3[\mathrm{HTFA}]_0}{[\mathrm{HBFA}]_0^3[\mathrm{H}]} = \frac{1}{K_1}\{K_{03} + K_{12}[\mathrm{L}] + K_{21}[\mathrm{L}]^2 + K_{30}[\mathrm{L}]^3\} \qquad \ldots (9)$$

where [L] represents $[\mathrm{HTFA}]_0/[\mathrm{HBFA}]_0$. Various functions were calculated from the data and were analysed to obtain the various constants by the graphical method. The values of K_{12}/K_1 and K_{21}/K_1 were calculated as 2.2×10^{-8} and 1.27×10^{-7} respectively, indicating the formation of mixed chelates. However, the higher pH of extraction and the presence of $(\mathrm{Eu-TFA})^{2+}$ complex in the aqueous phase complicates further analysis of the data.

Europium-HBFA-oxine system

Mixed complex formation of europium using mixtures of HBFA (HA) and oxine (HB) was also studied in a similar manner. Studies were made at fixed concentrations of HBFA and oxine of 0.01 *M* each and varying pH in the range of 4.2 to 4.6. Studies were also made at a nearly constant pH of about 4.5 and varying concentrations of one ligand at a fixed concentration (0.01 *M*) of the other ligand. The concentration of oxine in the organic phase was calculated taking into account the influence of protonation and partition coefficient of oxine[10], ($P_{Hox} = 10^{2.06}$) using Eq. (10),

$$[\mathrm{Hox}]_0 = \mathrm{P}_{\mathrm{Hox}}[\mathrm{Hox}]_{\mathrm{tot}}/\left\{1 + \mathrm{P}_{\mathrm{Hox}} + \frac{[\mathrm{H}]^2 + K_1K_2}{K_1[\mathrm{H}]}\right\} \qquad \ldots (10)$$

where K_1 and K_2 represent the dissociation constants of oxine[11], being equal to 5.09 for pK_1 and 9.02 for pK_2.

Extraction of europium in the presence of varying concentrations of HBFA and oxine was found to be higher than that due to the reagents alone. The data were analysed on the basis of formation of mixed chelates in order to obtain the values of equilibrium constants. The function F_0 or $\mathrm{D}[\mathrm{H}]^3[\mathrm{HBFA}]_0^{-3}$, plotted as a function of $\log\{[\mathrm{Hox}]_0/[\mathrm{HBFA}]_0\}$ resulted in a smooth curve indicating the presence of mixed chelates. The various constants were calculated as described earlier (Table 1). The value of K_{30} could not be evaluated because of relatively small changes in the values of F_j functions at higher concentrations of oxine indicating the contribution of $\mathrm{Eu(ox)_3}$ to the extraction to be small compared to those of mixed chelates. Details of analysis and the plots are not presented for the sake of brevity.

Europium-HFTA-oxine system

Extraction of europium in the presence of HFTA was studied in a similar manner around pH 4.3 and the data were analysed in a similar manner. The values of K_{03} and K_{12} were calculated as 1.2×10^{-8} and 1.0×10^{-7}, respectively while those for the higher complexes could not be evaluated from the data.

Europium-HTFA-oxine system

Studies were also extended to the extraction of europium by a mixture of HTFA and oxine around pH 4.9. The concentrations of oxine and HTFA in the organic phase were calculated using Eqs. (6) and (10), respectively. The data were analysed considering the presence of $(\mathrm{Eu-TFA})^{2+}$ in the aqueous phase as discussed in an earlier section. The plot of log F_0 versus log [L] where [L] represents $[\mathrm{Hox}]_0/[\mathrm{HTFA}]_0$ indicated the absence of extraction by HTFA alone under the present experimental conditions and the predominance of the first mixed chelate, $\mathrm{Eu(TFA)_2ox}$. The values of constants are summarised in Table 1.

The results obtained in the case of β-diketones can be attributed to the formation of mixed chelates. The values of stabilisation constants (K_s) were calculated for Eu-HBFA-HFTA system. The values of K_s given by Eq. (11)[1]

$$K_s = K_{\mathrm{obs}}/K_{\mathrm{stat}} \qquad \ldots (11)$$

were found to be 0.78 for $\mathrm{Eu(BFA)_2FTA}$ and 0.91 for $\mathrm{Eu(BFA)(FTA)_2}$, indicating that the complexes were stabilised as expected on the basis of statistical factors. However, in the case of Eu-β-diketone-oxine systems, the values of K_{03} obtained from the data on mixed chelates were somewhat higher than those obtained on binary systems.

This indicated the probable formation of adducts with oxine in addition to mixed chelates. Sekine and Dyrssen[3] also found evidence for the formation of self-adducts or adducts with one of the ligand (isopropyltropolone, IPT) in their studies on the formation of mixed chelates of europium with HTTA and IPT. An increase in the values of K_{03} by a factor of 5 to 10 can probably be attributed to this effect.

Acknowledgement

The authors wish to thank Dr A K Sundaram for his valuable guidance throughout the course of this work and Shri S Somasundaram, Head, R H C Section for keen interest in the studies.

References

1 Marcus Y & Eliezer I, *Coord chem Rev*, **4** (1969) 273.

2 Fridman Ya D, *Proceeding third symposium on coordination chemistry*, Vol 2, edited by M T Beck (Akademiai Kiado, Budapest) 1970, pp. 77.

3 Sekine T & Dyrssen D, *J inorg nucl Chem*, **26** (1964) 1727, 2013; **29** (1967) 1489.

4 Shigematsu T & Honjyo T, *Bull chem Soc Japan*, **43** (1970) 796.

5 Newman L & Klotz P, *Solvent extraction chemistry*, edited by D Dyrssen, J O Liljenzin & J Rydberg (North Holland, Amsterdam) 1967, pp. 128.

6 Sudersanan M & Sundaram A K, *Proc Indian Acad Sci*, **82A** (1975) 77.

7 Pushparaja & Sudersanan M, *J inorg nucl Chem*, **43** (1981) 1371.

8 Malhotra R K & Sudersanan M, *Indian J Chem*, **25A** (1986) 744.

9 Sekine T, Hasegawa Y & Ihara N, *J inorg nucl Chem*, **35** (1973) 3968.

10 Leo A, Hansch C & Elkins D, *Chem Rev*, **71** (1971) 525.

11 Smith R M & Martell A E, *Critical stability constants*, Vol 2 (Plenum, New York) 1975.

Indian Journal of Chemistry
Vol. 27A, June 1988, pp. 527-528

Notes

Application of Mean Spherical Approximation in Estimating Activity Coefficients of Aqueous Mixed Electrolyte Solutions

ANIL KUMAR
Department of Sugar Chemistry, Deccan Sugar Institute,
Manjari (Bk), Pune 412 307

Received 30 *July* 1987; *revised and accepted* 12 *October* 1987

The mean spherical approximation theory is applied to estimate the activity coefficients in aqueous mixed electrolyte solutions. The contribution due to hard-sphere term in the excess free energy is considered. The only adjustable parameter is the ionic diameter. The equations tested for aq. $HCl-CoCl_2$ at 25°C and aq. $HBr-CaBr_2$ from 5 to 45°C show excellent agreement with experimental data.

Recently there has been growing interest in developing methods for predicting thermodynamic properties of aqueous mixed electrolyte solutions. Of various methods, the mean spherical approximation (MSA) has frequently been employed[1-4] to predict thermodynamic properties of single electrolyte solutions. Humffray[5] included hard-sphere (non-electrostatic) terms into the MSA treatment of mixtures reported by Vericat and Grigera[6] and predicted the activity coefficients in aq. $NaCl-CaCl_2$ differing from the experimental values by 13%. Corti[7] applied the MSA theory to simple electrolyte mixtures like NaCl − HCl upto the ionic strength of 1 mol kg^{-1} of water.

In this note, an attempt is made to explore the possibility of using MSA theory to relatively complicated systems like $HCl-CoCl_2-H_2O$[8] at 25°C and $HBr-CaBr_2-H_2O$[9,10] from 5 to 45°C in the region of moderately concentrated electrolyte solutions. Temperature dependence of the adjustable parameter is also discussed.

Theoretical equation for estimating the free energy in a mixture of hard-spheres as applied to the systems undertaken here may be written as[11,12]

$$\begin{aligned}\ln \gamma_i^{hs} = {} & \ln\Delta\left(\gamma_i - 1 - \frac{2\eta_i}{\eta}y_3\right) \\ & + \frac{\eta}{\Delta^2}\left\{3(1-\alpha_i) + \gamma_i + \frac{3\eta}{2}(\alpha_i - \beta_i - \gamma_i - 1)\right\} \\ & + \frac{\eta}{\Delta^3}\left\{\eta\left[5y_3 - \frac{9}{2}y_1 - 2 + \eta\left(\frac{3}{2}y_1 - 3y_2\right.\right.\right. \\ & \left.\left.\left. - 4y_3 + 1\right)\right] - 2y_3 + 4\right\} \qquad \ldots(1)\end{aligned}$$

Equation (1) is consistent with Baxter equation[13], which is applicable for the calculation of activity coefficient in low concentration range.

According to unrestricted MSA model[14,15], the electrostatic contribution towards excess free energy of an electrolyte mixture, as applicable to present systems containing ionic species with charge Z_i and diameter σ_i, is given by Eq. (2)

$$\ln \gamma_i^e = \frac{\beta e^2 Z_i M_i}{\varepsilon_0} - \frac{P_n}{4\Delta}\left(\Gamma a_i + \frac{\pi}{12\Delta}\alpha^2 P_n \sigma_i^2\right) \qquad \ldots:(2)$$

The physical significance of various terms involved in Eqs (1) and (2) is discussed elsewhere[11,12,14,15].

The total exces free energy for an electrolyte mixture is given by Eq. (3), which is a combination of Eqs (1) and (2)

$$\ln \gamma_i = \ln \gamma_i^e + \ln \gamma_i^{hs} \qquad \ldots(3)$$

The values of σ for H^+, Co^{2+}, Ca^{2+}, Cl^- and Br^- were obtained by fitting the experimental activity coefficient data taken from literature[16]. Table 1 lists the σ-values at different temperatures. In this study, it is assumed that σ-values remain constant over the full range of concentration and composition. The ionic activity coefficients in a mixture obtained using σ-values given in Table 1 were converted into practical molal activity coefficients using densities of the mixtures. These densities were obtained from the viral coefficient approach of Pitzer[17]. The compressibility effects at atmospheric pressure were neglected.

In Fig. 1 are plotted the calculated results along with the experimental points as a function of Y_{CoCl_2}, the ionic strength fraction of $CoCl_2$ for aq. $HCl-CoCl_2$ at different ionic strengths. The results for aq. $HBr-CaBr_2$ at $Y_{CaBr_2} = 0.5$ at various temperatures are also shown in Fig. 1. The experimental mixture data fit the MSA theory with ex-

Table 1—Estimated Ionic Diameters (σ, Å) in MSA Theory at Different Temperatures

Ions	σ (Å) at temp				
	5°	15°	25°	35°	45°
H^+	5.20	4.70	4.45	4.21	4.10
Ca^{2+}	5.80	5.62	5.52	5.30	5.19
Co^{2+}	—	—	5.10	—	—
Cl	—	—	3.60	—	—
Br	4.00	4.00	3.90	3.82	3.78

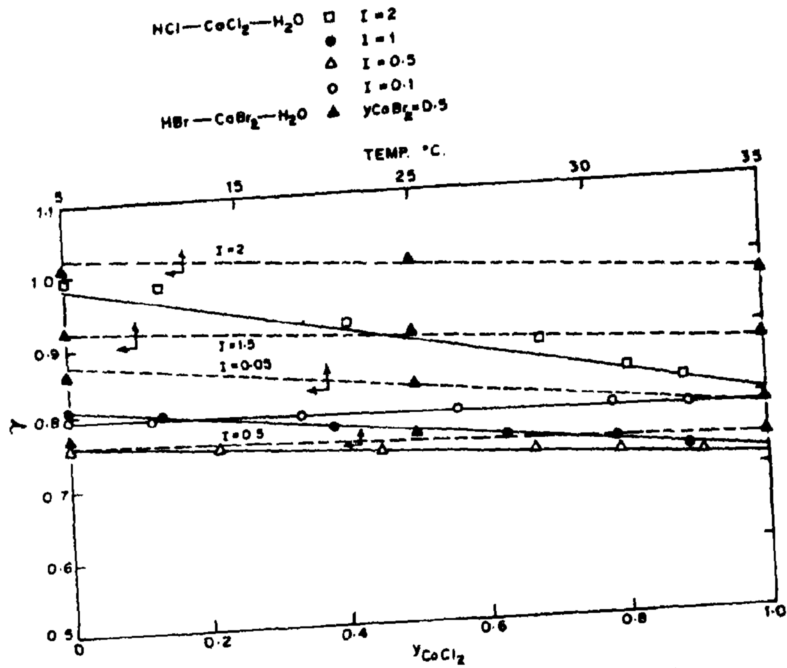

Fig. 1—Comparison of experimental and calculated activity coefficients for aq. $HCl-CoCl_2$ (———) and aq. $HBr-CaBr_2$ (– – ▲ – –) systems (Temperature dependence is at $y = 0.5$)

cellent accuracy upto ionic strength of 1 mol kg^{-1}, but a systematic deviation starts to occur beyond ionic strength of 2 mol kg^{-1}. The estimation for aq. $HBr-CaBr_2$ are fairly good even at ionic strength of 1.5. The poor fit in the range of high concentrations is due to the fact that the hydration around ions changes and thus the ionic diameters might be varying in the high concentration region. A consideration of concentration-dependent σ, however, will further complicate the system of equations. It was noted that σ_H· values for both aq. $HCl-CoCl_2$ and aq. $HBr-CaBr_2$ at 25°C were approximately the same and thus an average value at this temperature is given in Table 1. The values of σ decrease with increase in temperature; however, the temperature dependence of for H^+ is very strong.

In summary, the MSA theory with an adjustable parameter, acts as a powerful tool for predicting the activity coefficients.

The author is thankful to the referee for suggestions.

References

1 Triolo R, Grigera J R & Blum L, *J phys Chem*, **80** (1976) 1858.

2 Triolo R, Blum L & Floriano M A, *J phys Chem*, **82** (1977) 1368.

3 Corti H R & Fernandez Prini R, *J chem Soc Faraday Trans-I*, (1986) 921.

4 Ebling W & Grigo M, *Ann Phys* (Leipzig), **37** (1980) 21.

5 Humffray A A, *J phys Chem*, **87** (1983) 5521.

6 Vericat F & Grigera J R, *J phys Chem*, **86** (1982) 1030.

7 Corti H R, *J phys Chem*, **91** (1987) 686.

8 Khoo K H, Lim T K & Chan C Y, *J chem Soc Faraday Trans-I*, (1978) 2037.

9 Khoo K H, Lim T K & Chan C Y, *J chem Soc Faraday Trans-I*, (1979) 1067.

10 Roy R N, Wood M D, Johnson D & Roy L N, *J chem Thermodyn*, **19** (1987) 307.

11 Mansoori G A, Carnahan N F, Starling K E & Leland T W, *J chem Phys*, **54** (1971) 1523.

12 Ebling W & Scherwinski K, *Z phys Chem* (*Leipzig*), **264** (1983) 1.

13 Baxter R J, *J chem Phys*, **52** (1970) 4559.

14 Hoye J S & Blum L, *Mol Phys*, **35** (1978) 299.

15 Blum L & Hoye J S, *J phys Chem*, **81** (1977) 1311.

16 Robinson R A & Stokes R H, *Electrolyte solutions* (Butterworths, New York) 1959.

17 Kumar A, *J chem engng Data*, **32** (1987) 106.

Indian Journal of Chemistry
Vol. 27A, June 1988, pp. 529-531

Excess Properties of Binary Liquid Mixtures at 293.15 K†

T M AMINABHAVI*, L S MANJESHWAR,
S B HALLIGUDI† & R H BALUNDGI

Department of Chemistry,
Karnataka University Dharwad 580 003

Received 28 *July* 1987;
revised and accepted 16 *November* 1987

Reported values of density, viscosity and refractive index at 293.15 K for six binary mixtures, viz. benzene + cyclohexane, benzene + ethyl acetate, benzene + carbon tetrachloride, cyclohexane + ethyl acetate, cyclohexane + carbon tetrachloride, and ethyl acetate + carbon tetrachloride have been used to predict a number of thermodynamic, hydrodynamic and optical excess quantities. Results are discussed in terms of deviations from ideal behaviour.

In continuation of our earlier work on excess properties of binary solvent mixtures[1-3], we now report additional data on excess molar volume (V^E), excess Gibb's free energy of flow (G^E), excess viscosity (η^E), excess refractive index (n^E) and excess molar refraction (R^E) at 293.15 K for six binary mixtures, viz. (i) benzene + cyclohexane, (ii) benzene + ethyl acetate, (iii) benzene + carbon tetrachloride, (iv) cyclohexane + ethyl acetate, (v) cyclohexane + carbon tetrachloride and (vi) ethyl acetate + carbon tetrachloride. The properties are studied over the entire range of composition of the mixtures and the results are interpreted in terms of interaction forces and the nature of mixing components.

In view of the availability of the data[4-6] further experimentation appeared unnecessary. Solvents used were of the highest purity and their purities were checked by gas chromatography. Details of the measurements of density, viscosity and refractive index (at 589, 546 and 436 nm) have been outlined in previous papers[4,5]. All mixtutres were made on volume fraction (ϕ) basis and measurements at 293.15 ± 0.01 K were made on the same day on which mixtures were prepared.

Various excess quantities were calculated employing Eqs. (1-5)

$$V^E(\mathrm{cm^3/mol}) = V_m - V_1\phi_1 - V_2\phi_2 \qquad \ldots (1)$$

$$R^E(\mathrm{cm^3/mol}) = R_m - R_1\phi_1 - R_2\phi_2 \qquad \ldots (2)$$

$$n^E = n_m - n_1\phi_1 - n_2\phi_2 \qquad \ldots (3)$$

$$\eta^E(\mathrm{cP}) = \eta_m - \eta_1\phi_1 - \eta_2\phi_2 \qquad \ldots (4)$$

$$G^E(\mathrm{cal/mol}) = RT\,[\ln \eta_m V_m - \phi_1 \ln \eta_1 V_1 - \phi_2 \ln \eta_2 V_2] \qquad \ldots (5)$$

In the above equations $V_m[=(M_1\phi_1 + M_2\phi_2)/\rho_m]$ is the molar volume of the mixture (M_1, M_2 and ρ_m represent the molecular weights of components 1, 2 and density of the mixture respectively); V_1 ($= M_1/\rho_1$) and V_2($= M_2/\rho_2$) represent the molar volumes of components 1 and 2, respectively (ρ_1 and ρ_2 are their densities); R_1, R_2 and R_m are respectively the molar refractivities of components 1, 2 and their mixtures, respectively. The refractivity of the mixture (R_m) was calculated using Lorentz-Lorenz[7] mixing rule, i.e. $R_m = [(n_m^2 - 1)/(n_m^2 + 2)]\ (V_m)$, where n_m represents the refractive index of the mixture and n_1, n_2 are the refractive indices of components 1 and 2. η_1, η_2 and η_m are the viscosities of components 1, 2 and of the mixture respectively. The term *RT* has its usual meaning.

The excess quantities were fitted to a polynomial relation (Eq 6) to evaluate the coefficients (a_i)

$$X^E = \sum_{i=1}^{2} a_i(\phi_2 - \phi_1)^{i-1} \qquad \ldots (6)$$

where X^E represents the appropriate excess quantity. The fitted values were used to draw smooth curves in all the plots wherein the experimental data are given as points. The percentage error in the calculation of all the excess quantities seldom exceeded 5×10^{-4} units. All computations were done at CSMCRI, Bhavnagar, using HP 1000 computer.

Excess molar volumes are plotted against ϕ_1 in Fig. 1. A large negative V^E observed for cyclohexane + carbon tetrachloride mixture is due to the more flexible cyclohexane molecule, which seems to be oscillating rapidly between *cis*- and *trans*-configurations in the presence of a spherical molecule such as carbon tetrachloride leading to high levels of specific interactions between unlike species. Small negative V^E is observed for ethyl acetate + carbon tetrachloride mixture, again suggesting specific interactions between the components. Positive V^E values over the whole composition scale for the mixtures of benzene with cyclohexane, ethyl acetate and CCl_4 suggest that dis-

---

Based on the Ph D thesis of LSM submitted to Karnatak University (1987)

[†] Central Salt & Marine Chemicals Research Institute, Bhavnagar 364 002

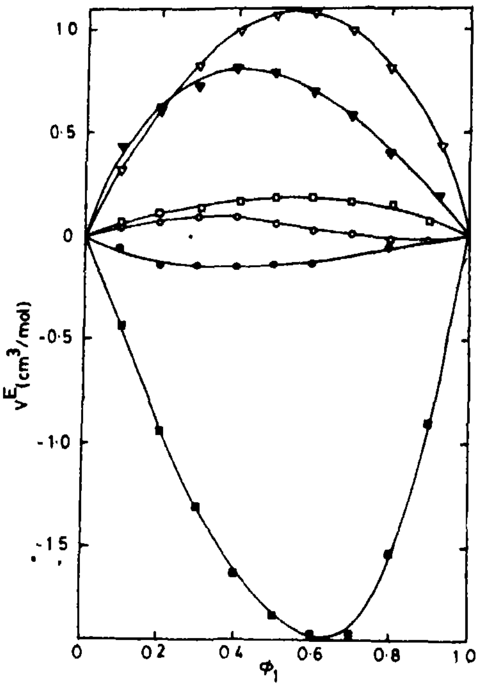

Fig. 1 – Excess molar volume (V^E) versus volume fraction (ϕ_1) of first component [○, benzene + cyclohexane; ▽, benzene + carbon tetrachloride; □, benzene + ethyl acetate; ■, cyclohexane + carbon tetrachloride; ●, ethyl acetate + carbon tetrachloride and ▼, ethyl acetate + cyclohexane]

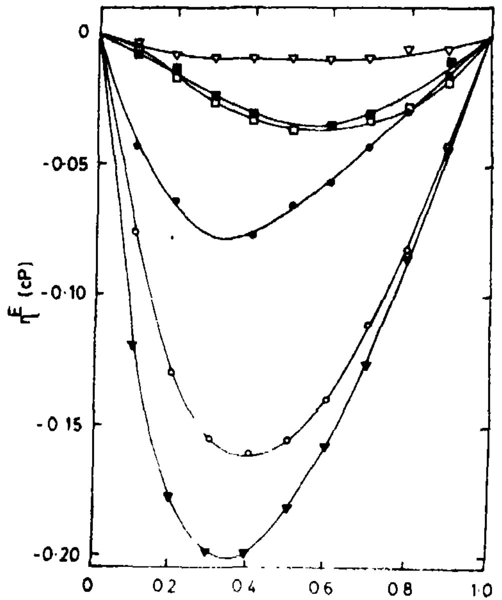

Fig. 2 – Excess viscosity (η') versus volume fraction (ϕ_1) of first component [symbols represent the mixtures given in Fig. 1]

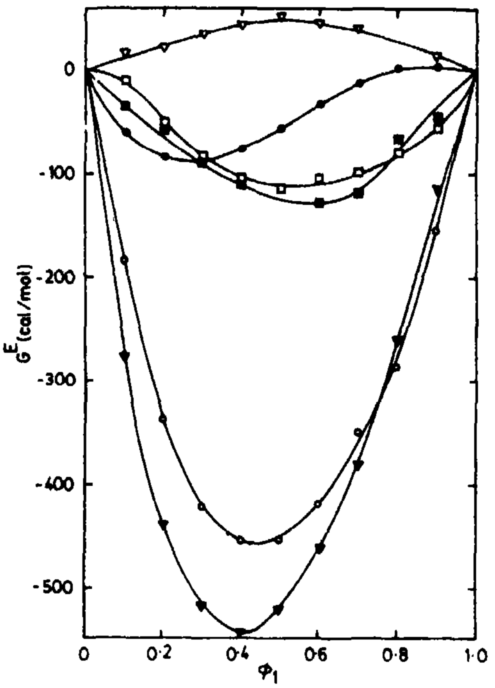

Fig. 3 – Excess Gibbs free energy (G^E) of flow versus volume fraction (ϕ_1) of first component [symbols have the same significance as in Fig. 1]

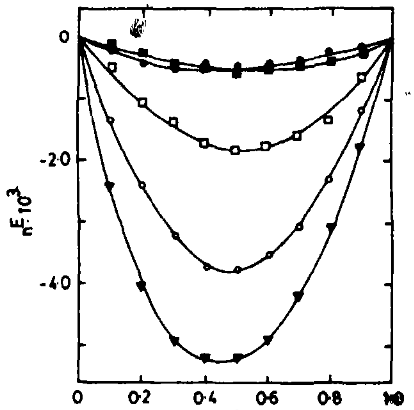

Fig. 4 – Excess refractive index (n^E) versus volume fraction (ϕ_1) of first component [symbols are the same as in Fig. 1]

persion forces are operative in these mixtures. When ethyl acetate (polar molecule) is mixed with cyclohexane (nonpolar molecule) again V^E is positive suggesting the existence of weak physical forces in the mixture.

The trend in the behaviour of η^E and G^E is similar for ethyl acetate + cyclohexane and benzene + cyclohexane mixtures as both of these exhibit large negative values with the minima occurring around $\phi_1 = 0.35$-0.5 on the composition scale (Figs 2 and 3). However, mixtures such as ethyl acetate + carbon tetrachloride and cyclohexane + carbon tetrachloride exhibit negative quantities but with different trend in their variations over the composition scale. A flattened U-shaped

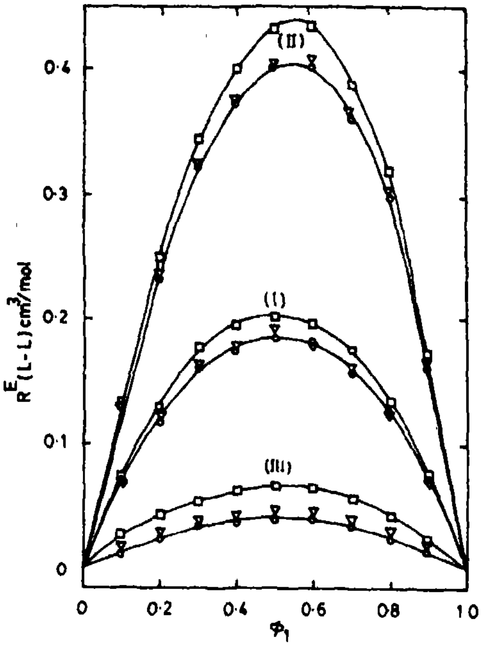

Fig. 5 – Excess molar refraction (R^E) versus volume fraction (ϕ_1) of benzene in mixtures with (I)-ethyl acetate, (II)-carbon tetrachloride and (III)-cyclohexane at wavelengths (O) 589 nm; (▽) 546 nm and (□) 436 nm.

behaviour is seen for G^E and η^E of benzene + carbon tetrachloride mixture whereas ethyl acetate + carbon tetrachloride shows a sigmoid behaviour for G^E. For benzene + ethyl acetate mixture, both G^E and η^E are negative.

Large negative n^E is observed for benzene + cyclohexane and ethyl acetate + cyclohexane mixtures at 589 nm (Fig. 4). However, benzene + ethyl acetate, cyclohexane + carbon tetrachloride and ethyl acetate + carbon tetrachloride mixtures at 589 nm show small negative n^E. The only system which exhibits positive n^E is benzene + carbon tetrachloride. It may be pointed out that for this system even values of V^E, G^E and R^E are also positive. The data at other wavelengths namely, 546 and 436 nm are not presented but the trend in their behaviour at these wavelengths is more or less the same. It should be noted that Eq. (3) used to compute n^E is identical to Heric and Posey relation[8]. The binary interaction term A_{12} as suggested by Heric and Posey[8] is the same as n^E of Eq. (3).

Dependence of ϕ_1 on excess molar refraction (R^E) as calculated from Lorentz-Lorenz mixing rule[7] is shown in Fig. 5 for only a few representative mixtures at three selected wavelengths. The curves are symmetric showing maxima around the middle of the composition scale. Larger positive values are seen for benzene + carbon tetrachloride mixture as compared to the mixture of benzene with either ethyl acetate or cyclohexane. However, for other mixtures namely, ethyl acetate + cyclohexane, ethyl acetate + carbon tetrachloride and cyclohexane + carbon tetrachloride negative values of R^E are observed (graphs not displayed). Very small negative values for ethyl acetate + carbon tetrachloride and large negative values for cyclohexane + carbon tetrachloride have been observed.

T M Aminabhavi wishes to thank Prof. P E Cassidy of Southwest Texas State University for facilities provided during the preparation of this manuscript.

References

1 Aminabhavi T M, Manjeshwar L S & Balundgi R H, *Indian J Chem*, **25A** (1986) 465.
2 Aminabhavi T M, Manjeshwar L S & Balundgi R H, *Indian J Chem*, **25A** (1986) 820.
3 Aminabhavi T M, Manjeshwar L S, Balundgi R H & Muddapur M V, *Indian J Chem*, **26A** (1987) 106.
4 Aminabhavi T M, *J chem Engng Data*, **32** (1987) 406.
5 Aminabhavi T M & Munk P, *Macromolecules*, **12** (1979) 607.
6 Aminabhavi T M & Munk P, *Macromolecules*, **12** (1979) 1186.
7 Lorentz H A, *Theory of electrons* (Teubner & Leipzig) 1909.
8 Heric E L & Posey C D, *J chem Engng Data*, **10** (1965) 340.

Indian Journal of Chemistry
Vol. 27A, June 1988, pp. 532-535

Studies of New Zeolite Derivatives of Stilbite

NEELU SINGHAI & SATI PRASAD BANERJEE*
Department of Chemistry, Dr H.S. Gour Vishwavidyalaya
Sagar 470 003

Received 15 *May* 1987; *revised and accepted* 16 *November* 1987

Natural zeolite stilbite and its Ag(I)-exchanged derivative have been studied by IR spectral, XRD and TG analyses and the results obtained have been reported. Both physical and chemical adsorptions have been indicated in the interactions of CO_2, NH_3 and H_2S adsorbates with adsorbents stilbite and its Ag(I)-exchanged form.

Naturally occurring mineral stilbite has been used to prepare cation-exchanged derivative with Ag(I) and both the zeolites have been used for adsorbing CO_2, NH_3 and H_2S. The aim of the present study is to test their suitability as cation exchangers and adsorbents for CO_2, H_2S and NH_3. Ag(I)-exchanged zeolites have found applications in radio-iodine monitoring[1] and isomerization of 1-butene[2]. Similarly, adsorbates like H_2S and NH_3 pose hazards both in the atmosphere and water and need to be controlled[3].

The stilbite specimen, from the region around Deccan trap, was obtained from GSI, Pune. It was finely powdered in a mechanical grinder and sieved to obtain uniform particle size. Its Ag(I)-exchanged derivative was prepared by treating a portion repeatedly with aqueous silver sulphate solution followed by filtration, washing and air-drying. The adsorbed derivatives were prepared by the procedures described in an earlier communication[4]. Both stilbite and Ag(I)-exchanged form were analyzed for Na(I), Ca(II) and Al(III) using a Varian Techtron AA-6 Atomic Absorption Spectrometer. TG analysis of the samples was carried out upto 800°C at a heating rate of 10°C min^{-1} on a thermobalance supplied by FCIL, Sindri IR spectra of the samples and their residues, after TG analysis, were recorded between 4000 and 200 cm^{-1} in KBr on a Perkin-Elmer IR spectrophotometer. The X-ray diffractograms, obtained between 2θ angles of 5° and 70° using a Philips PW1140 XRD unit and copper target, are reproduced in Figs 1 and 2.

Table 1—Analytical Data

Sample	Na%	Ca%	Al%	Si% + O% (by difference)	H_2O%
1. Stilbite	0.62 (0.79)†	4.76 (5.50)	8.15 (9.28)	68.81 (64.63)	17.66 (19.80)
2. Ag(I)–stilbite	0.46	0.80	6.57	71.18	20.99

† Figures in parentheses are for the ideal composition of stilbite: $NaCa_4Al_{10}Si_{26}O_{72}.32H_2O$[14]

The analytical data of stilbite sample are given in Table 1. TG analysis gave a mass loss of 17.66% which can be attributed to its dehydration. The analytical data for Ag(I)-exchanged stilbite are also given in Table 1. It showed a mass loss of 20.99% on TG analysis. The change in the composition is the direct result of cation exchange and can be interpreted as follows. Whereas stilbite showed Ca(II)/Na(I) ratio as 4.4:1, Ag(I)-exchange altered it to 1:1 thereby showing more than four times exchange of Ca(II) compared to that of Na(I). The reduction in the percentage of Al(III) is an indication of the extent of dealumination and increase in the Si/Al ratio. IR spectral data between 4000 and 200 cm^{-1} and XRD data using CuK$_\alpha$ radiation of both stilbite and the Ag(I)-exchanged form have been used to characterize them[5-7]. The results of IR spectral studies (Table 2) of the adsorbed derivatives exhibit the presence of the adsorbate species. Additional bands for free CO_3^{2-}(II) ions (1440 cm^{-1}), physically adsorbed H_2S (1390 cm^{-1}) and NH_4(I) ions (1450 cm^{-1}) are seen in the IR spectra of the CO_2, H_2S and NH_3 interacted derivatives of stilbite. On the other hand, IR band for physically adsorbed CO_2 (2300 cm^{-1} appears in the case of CO_2-interacted Ag(I)-exchanged stilbite. There is also definite indication of complex formation with NH_3, giving rise to $[Ag(NH_3)_2]^+$ species in the IR spectrum of ammonia interacted Ag(I)-exchanged stilbite which shows IR bands at 1500 and 250 cm^{-1}. The H_2S interaction results in the formation of a black sample, and the presence of Ag_2S species is indicated by the IR band at 2380 cm^{-1}. The IR spectra of the residues obtained after TG analysis show no bands for physically adsorbed water molecules and the adsorbed species indicating thereby dehydration, desorption and dehydroxylation as the major thermal events on heating the samples at a constant rate. Most of the TG plots exhibit loss of physically adsorbed water and the adsorbates at temperature upto 573K and dehydroxylation and decomposition above it. All the eight samples studied show distinct features in their TG plots and different values for total mass loss upto 1073K. Thus, H_2S interacted stilbite shows a fast rate of mass loss starting around 673 K over a 80 K stretch in its TG plot. Ammonia-interacted stilbite, on the other hand, shows an abrupt and very fast mass loss step around

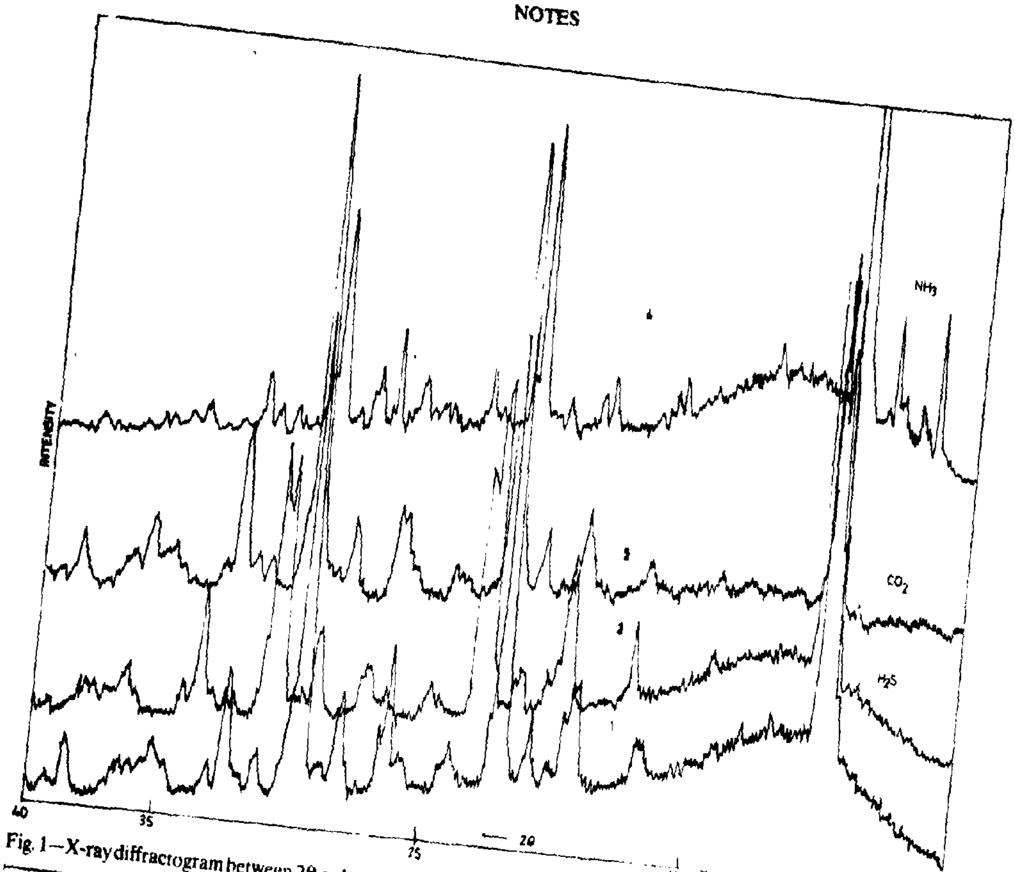

Fig. 1—X-ray diffractogram between 2θ-values of 5° & 40° of 1. stilbite, 2. stilbite + CO_2, 3. stilbite + H_2S, 4. stilbite + NH_3

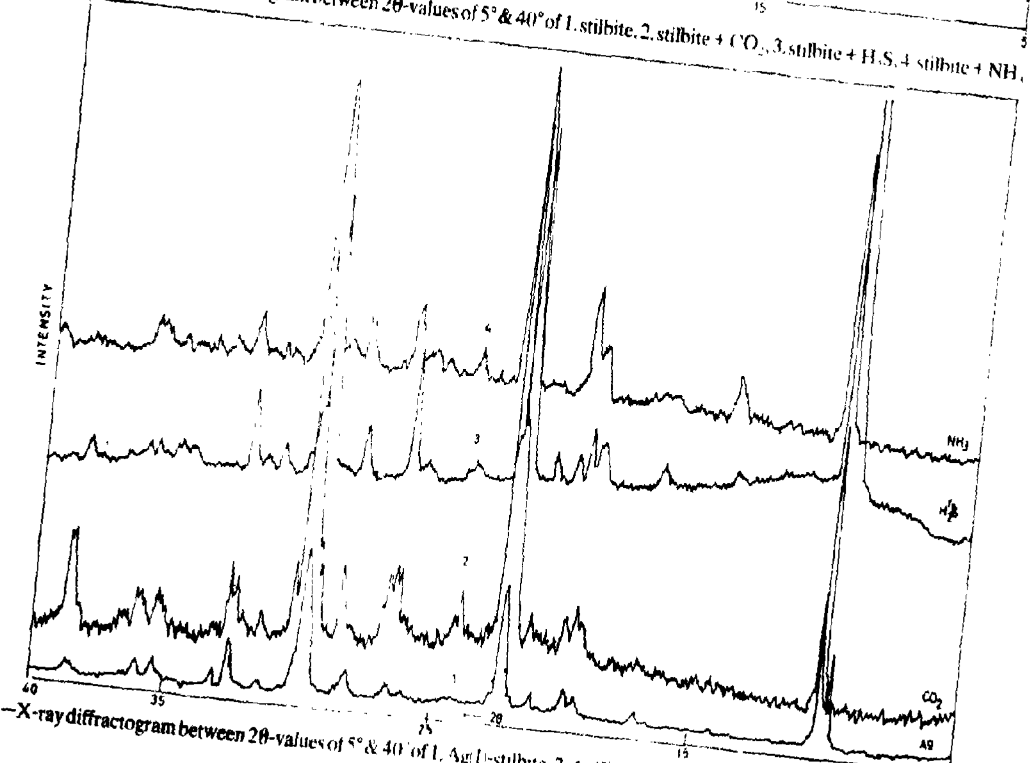

Fig. 2—X-ray diffractogram between 2θ-values of 5° & 40° of 1. Ag(I)-stilbite, 2. Ag(I)-stilbite + CO_2, 3. Ag(I)-stilbite + H_2S, 4. Ag(I)-stilbite + NH_3

Table 2—Summary of Thermal & IR Spectral Data

Sample	Total mass loss(%)	IR peaks (cm^{-1}) with assignments
1. Stilbite	17.66	3620 (O—H stretch), 1675 (O—H bend), 975-1095 (asymmetric T—O stretch), 710 (symmetric T – O stretch), 570 (double rings), 450 (T – O bend), 330 (pore opening).
2. Stilbite + CO_2	16.45	3600 (O – H stretch), 1670 (O – H bend), 1440, 1430 (CO_3^{2-}), 1050 (asymmetric T – O stretch), 715 (symmetric T – O stretch), 580 (double rings), 460 (T – O bend), 310 (pore opening).
3. Stilbite + H_2S	20.18	3630 (O – H stretch), 1680 (O – H bend), 1390 (H_2S phys.), 1030 (asymmetric T – O stretch), 710 (symmetric T – O stretch), 560 (double rings), 445 (T – O bend), 280 (pore opening).
4. Stilbite + NH_3	29.69	3590 (O – H stretch), 3470 (NH_4^+), 1695 (O – H bend), 1460 (NH_4^+), 960-1100 (asymmetric T – O stretch), 725 (symmetric T – O stretch), 580 (double rings), 450 (T – O bend), 360 (pore opening).
5. Ag(I)-Stilbite	20.99	3610 (O – H stretch), 1665 (O – H bend), 1030 (asymmetric T – O stretch), 710 (symmetric T – O stretch), 560 (double rings), 440 (T – O bend), 315 (pore opening).
6. Ag(I)-Stilbite + CO_2	16.55	3420, (O – H stretch), 2320 (CO_2 phys.), 1630 (O – H bend), 1020 (asymmetric T – O stretch), 690 (symmetric T – O stretch), 550 (double rings), 440 (T – O bend), 310 (pore opening).
7. Ag(I)-Stilbite + H_2S	25.10	3600 (O – H stretch), 2380 (H – S bend), 1665 (O – H bend), 1430 (H_2S phys.), 1080 (asymmetric T – O stretch), 565 (double rings), 430-460 (T – O bend, Ag – S bend), 345 (pore opening).
8. Ag(I)-Stilbite + NH_3	13.53	3600 (O – H stretch), 3480 (N – H stretch), 1690 (O – H bend), 1530 (N – H bend), 1040 (asymmetric T – O stretch), 720 (symmetric T – O stretch), 570 (double rings), 440 (T – O bend), 250 (Ag – N linkage).

T = (Al, Si)O_4 tetrahedron

733K due to the loss of adsorbed H_2S and NH_3 respectively. Loss of water and CO_2 from stilbite and the CO_2-interacted sample occurs in more gradual steps and above 673K mass loss in both these cases becomes negligible. Among the four zeolite samples prepared by Ag(I)-exchange and subsequent interaction with the three adsorbates the high temperature mass loss is most prominent only in the case of the H_2S interacted derivatives. From around 873K the TG plot of this derivative indicates a fast mass loss step, comprising almost one-third of the total mass loss, due primarily to the decomposition of Ag_2S. Influence of dehydration and repetitive oxidation and reduction steps on the structures of Ag(I)-Y type zeolites[8] and Ag(I)-stilbite[9] has been investigated earlier. During the reduction Ag metal was found to precipitate as cluster within the void of the zeolite network and as crystallites on the surface. XRD plots are reproduced in Figs 1 and 2. Crystal structure of stilbite is known from earlier studies[10]. Evidence of site selectivity of Ag(I) in synthetic zeolites A and Y is also available[11-13] and the knowledge of these structural orientations forms the basis in the interpretation of the XRD data of stilbite derivatives obtained with Ag(I) and the various adsorbates. The intensities of the peaks of stilbite are decreased as a result of exchange with Ag(I) ions showing loss of crystal structure. The (230) reflection at 3.98Å becomes very strong from the adsorption of carbon dioxide on Ag(I)-stilbite, while the intensity of (001) reflection is increased to a considerable extent as a result of adsorption of hydrogen sulphide. Ammonia adsorption on Ag(I)-stilbite produces a new (030) reflection at 6.23Å while the (600) reflection becomes diffused. It has been suggested by earlier workers that interference by the high scattering power of silver may be misleading. Some differences exist in the X-ray diffractograms of stilbite and its adsorbed derivatives. Intensity of (001) reflection is reduced as a result of adsorption of CO_2. The H_2S adsorbed derivative exhibits doublets at 8.95Å, 3.90Å and at 2.97Å. Ammonia adsorption produces some new reflections.

References

1 SooHoo G Y, Lin Chien-Chang, Norris R M & Wilkinson C D, *IEEE Trans Nucl Sci*, **22** (1975) 657.
2 Sugihara H, Chen L Y & Yasumori Iwao, *Bull chem Soc Japan*, **47** (1974) 2089.
3 Manahan S E, *Environmental chemistry* (Willard Grant Press, Massachusetts) 1975.
4 Bhattacharya S & Banerjee S P, *Indian J Chem*, **25A** (1986) 104.
5 Pechar F & Rykl D, *Chem Zvesti*, **35** (1981) 189.
6 Joshi M S & Bhaskar B T, *Indian J pure appl Phys*, **19** (1981) 560.
7 Breck D W, *Zeolite molecular sieves, structure, chemistry & use* (John Wiley, New York) 1974.

8 Gellens L R, Mortier W J & Uytterhoeven J B, *Zeolites*, **1** (1981) 85.

9 Herman K, Bica I & Jacob P A, *Magy Kim Foly*, **83** (1977) 34.

10 Slaughter M, *American Mineralogist*, **55** (1970) 387.

11 Nitta M, Matsumoto S & Aomura K, *JCS Chem Commun*, (1974) 552.

12 Nitta M, Ogawa K & Aomura K, *JCS Chem Commun*, (1974) 1015.

13 Matsumoto S, Nitta M, Ogawa K & Aomura K, *Bull chem Soc Japan*, **48** (1975) 1169.

14 Deer W A, Houri R A & Zussman J, *Rockforming minerals*, Vol. 4 (Longman, London) 1975.

Indian Journal of Chemistry
Vol. 27A, June 1988, pp. 536-537

Studies on New Mesogens: Part II-*p*-(*p*′-*n*-Alkoxycinnamoyloxy)benzylidene-*p*″-*n*-butoxyanilines

J M LOHAR & D N DHABHAI*
P G Chemistry Department, M L V Govt. College,
Bhilwara 311 001

Received 8 *April* 1987; *revised* 28 *July* 1987; *accepted* 6 *October* 1987

The title series (I) is a very high melting series and exhibits rich mesomorphism. The polymesomorphism prevails at about 85°C. The nematic-isotropic transitions show odd-even effect. The smectic-nematic transition curve rises smoothly enhancing the smectic mesophase range at the cost of nematic mesophase length. The nematic mesophase shows a threaded texture while the smectic mesophase exhibits a focal conic fan-shaped smectic A texture.

A new homologous series of mesogens, *p*-(*p*′-*n*-alkoxycinnamoyloxy) benzylidene-*p*″ -*n*-butyoxyanilines (I) has been synthesised and the behaviour of the compounds as liquid crystals has been studied.

Compounds (I) were synthesised as follows: A mixture of equimolar amounts (0.01 mol) of *p*-(*p*′-*n*-alkoxycinnamoyloxy)benzaldehyde[1] and *p*-*n*-butoxyaniline[2] in ethanol (20 ml) containing a few drops of acetic acid was refluxed for 1-3 hr depending upon the starting aldehyde. The solid products obtained were crystallized from benzene-ethylalcohol (20:80) mixture. The analytical data and transition temperatures of schiff base obtained are compiled in Table 1. Purity of the compounds was checked by TLC.

p-(*p*′-*n*-Alkoxycinnamoyloxy)benzylidene-*p*″-*n*-butoxyanilines (I) are high melting solids. The solid mesomorphic curve follows a zig-zag rising and falling pattern. The nematic-isotropic transition curves show a continuous falling tendency simultaneously displaying odd-even effect upto the eighth homologue, while the nematic property is exhibited upto the octadecyl homologue. Polymesomorphism is exhibited by the series from the sixth member and persists till the last octadecyloxy member. The sixth homologue shows monotropic smectic mesophase. The range of smectic mesophase gets enhanced as the series is ascended.

Extrapolation of the smectic-nematic transition curve to the left is rendered difficult on account of its extremely steep nature at the left tailing end.

The nematic mesophase, as observed under polarising microscope, shows a threaded texture while the smectic mesophase shows a focal conic fan-shaped smectic 'A' texture.

The thermal stabilities and other characteristics of the compounds(I) have been compared with other homologous series, viz. *p*-(*p*′-*n*-alkoxycinnamoyloxy)benzylidene-*p*″-anisidenes[3] (II), *p*-(*p*′-*n*-alkoxycinnamoyloxy)benzylidene-*p*″-phenetidenes[4] (III) and *p*-(*p*′-*n*-alkoxycinnamoyloxy)benzylidene-*p*″-*n*-propoxyanilines[5] (IV).

$$p\text{-R}-\text{O}-\text{C}_6\text{H}_4-\text{CH}=\text{CH}-\text{COO}-\text{C}_6\text{H}_4$$
$$-\text{CH}=\text{N}-\text{C}_6\text{H}_4-\text{R}'(p)$$

Series I: R′ = *n*-butoxy; II, R′ = methoxy; III, R′ = ethoxy and IV, R′ = *n*-propoxy.

Table 1 — Analytical Data & Transition Temperatures of *p*-(*p*′-*n*-Alkoxycinnamoyloxy)benzylidene-*p*″-*n*-butoxyanilines (I)

n-Alkyl group (R)	Mol. formula	Transition temperatures °C			Found (Calc) %			% Required		
		Smectic	Nematic	Isotropic	C	H	N	C	H	N
Methyl	$C_{27}H_{27}O_4N$	—	134	292	75.5	6.21	3.22	75.52	6.29	3.26
Ethyl	$C_{28}H_{29}O_4N$	—	150	295	75.8	6.52	3.13	75.7	6.6	3.2
Propyl	$C_{29}H_{31}O_4N$	—	145	278	76.1	6.7	3.02	76.15	6.78	3.06
Butyl	$C_{30}H_{33}O_4N$	—	145	283	76.41	6.9	2.95	76.43	7.00	2.97
Pentyl	$C_{31}H_{35}O_4N$	—	131	263	76.69	7.20	2.85	76.70	7.22	2.89
Hexyl	$C_{32}H_{37}O_4N$	(105)	120	270	76.90	7.40	2.80	76.95	7.41	2.81
Heptyl	$C_{33}H_{39}O_4N$	116	142	248	77.12	7.5	2.71	77.19	7.60	2.73
Octyl	$C_{34}H_{41}O_4N$	115	160	258	77.40	7.74	2.65	77.42	7 78	2.66
Decyl	$C_{36}H_{45}O_4N$	105	175	246	77.83	8.10	2.51	77.84	8.11	2.52
Dodecyl	$C_{38}H_{49}O_4N$	117	185	235	78.21	8.38	2.39	78.22	8.40	2.40
Tetradecyl	$C_{40}H_{53}O_4N$	105	188	223	78.55	8.65	2.28	78.56	8.67	2.29
Octaldecyl	$C_{44}H_{61}O_4N$	115	185	200	79.15	9.12	2.08	79.16	9.14	2.09

Value in parenthesis indicates monotropy

Table 2—Average Thermal Stabilities (°C) of Series I-IV

Phase	II	III	IV	I
Nematic-Isotropic	270 (C_6-C_8)	281.3 (C_6-C_8)	254.6 (C_6-C_8)	258.6 (C_6-C_8)
Smectic-nematic or Smectic-isotropic	167.2 (C_{12}-C_{18})	178.6 (C_{12}-C_{18})	182.6 (C_{12}-C_{18})	186 (C_{12}-C_{18})
Commencement of smectic phase	C_8	C_8	C_7 (C_6)*	C_6 (C_5)*

*Monotropy

It is observed that compounds belonging to series II-IV exhibit wider nematic mesomorphic range than those of series (I). These series (II-IV) have lesser smectic mesophase ranges. In terms of the substituent (R′) in the aniline moiety the series I-IV, show the nematic order: II⩾III>IV>I while the smectic order is: I⩾IV>III>II. This is also the sequence for the odd-even effect.

Thermal stabilities of the compounds of the present homologous series (I) have also been compared with those of the series II-IV. The calculated values of average thermal stabilities are given (Table 2).

The nematic-isotropic thermal stabilities of these series are quite high, the highest being for series (III). It is observed that as the $-CH_2$ units are added at the right terminal alkyl chain, the nematic-isotropic thermal stability decreases. The $-OC_2H_5$ group in series (III) is highly polar and hence gives rise to high end-to-end adhesion.

The more significant thing is the alternation of the nematic-isotropic stabilities of these series. The series (II and IV) having odd number of carbons at their right terminal alkyl chain show lower thermal stability as compared to that of series I and III having even number of carbons at their right terminal alkyl chain.

References

1 Lohar J M & Patel G H, Paper presented at International Liquid Crystal Conference, Bangalore, 1979.

2 Woodmansee W E, *Mater Evaluation*, **24** (1966) 504.

3 Lohar J M & Dave J, *Mol Cryst Liq Cryst*, **70** (1981) 279-287.

4 Lohar J M & Patel G H, Paper presented at the eleventh National Conference on Crystallography held in Calcutta, 1980.

5 Lohar J M & Dhabhai D N, *J Indian chem Soc*, **64** (1987) 600.

Indian Journal of Chemistry
Vol. 27A, June 1988, pp. 538-539

Charge Density—Activation Energy Correlations in Bromination of Thiophenes by N-Bromosuccinimide in Solution

LALITHA RAJARAMAN & M J NANJAN
Physical Chemistry Department, University of Madras, Madras 600 025
and
V KANNAPPAN*
Chemistry Department, Presidency College, Madras 600 005

Received 5 *August* 1986; *revised and accepted* 4 *August* 1987

The activation energies for N-bromosuccinimide bromination of several thiophene derivatives in 80% (v/v) aqueous acetic acid have been determined and discussed in the light of electron densities at the reaction site. The effect of substituents at different positions of thiophene ring has been investigated quantitatively by the actual calculation of total ($\pi + \sigma$) charge densities at various positions of the substituted thiophenes.

Earlier work from this laboratory reported on the charge-density distributions in several benzene and thiophene derivatives using Hückel LCAO MO and Del Re methods and their correlation with the experimental activation energy (E_a) values in the bromination of these compounds by molecular bromine in 100% acetic acid and acetic acid-water mixtures[1-3]. As an extension, charge densities of eleven thiophene derivatives have now been correlated with activation energies of their bromination by N-bromosuccinimide (NBS) in order to generalise the effect of substituents in thiophene ring towards electrophiles from quantum mechanical data.

Fluka (purum) samples of thiophene, 2-chlorothiophene and ethyl thiophene-2 carboxylate were used as such. 2-Bromothiophene (Fluka), 3-bromothiophene and 2-acetylthiophene were distilled before use. 2-Iodothiophene (b.p. 90°/30 mm) was prepared by iodination of thiophene[4]. 2-Fluorothiophene (b.p. 83°) was prepared by *ipso* fluorination of 2-iodothiophene[5]. Acetic acid (LR, BDH) was purified before use[6]. N-Bromosuccinimide (Riedel, m.p. 176°) was recrystallised and used. The procedure for the rate measurements has been described earlier[6].

The method of separation of bromination products under kinetic conditions has been described elsewhere[7]. The analysis of bromination product of thiophene was done at 220°C using a Varian GC dual column chromatograph model 3700 fitted with a 10%. OV-101 stainless steel column-chrom WHP 80/100 (2m × 1/8 inch) with nitrogen as the carrier gas. The GLC results showed the formation of only 2-bromothiophene. NBS bromination of 2-bromothiophene in 80% (v/v) aqueous acetic acid led to 2,5-dibromothiophene as confirmed by its PMR spectra. 3-Bromothiophene was bromination at position-2. Ethyl thiophene 2-carboxylate, 2-acetylthiophene and 3-acetylthiophene underwent bromination exclusively at 5-position[8-10]. Benzothiophene on bromination gave 3-bromobenzothiophene.

Charge-density calculations

The calculation of σ- and π-charges for 2-acetyl- and 3-acetyl-thiophenes was programmed in FORTRAN for the computer IBM 1130. The π-charges were calculated by the Hückel LCAO MO method. Del Re method was used for σ-charge calculations. Veillard and Pullman[11] have shown that with the correct choice of parameters, this method gives satisfactory charge density distributions comparable with those obtained by SCF calculations, even in large molecules of biological importance. Berthod-Pullman atom and bond parameters were used in these calculations. The π- and σ-systems have been treated separately and the total ($\pi + \sigma$) charge density (Table 1) on an atom was obtained as usual by adding the π- and σ-charge densities on that atom. The data used for other molecules have already been reported by us[2].

The kinetic data obtained for the bromination of thiophenes in aqueous acetic acid using NBS as the brominating agent are given in Table 2. On simple electrostatic considerations, the strong electrophile,

Table 1—π-Charges, σ-Charges and Total ($\pi + \sigma$) Charge Densities at Various Ring Positions in 2-Acetyl- and 3-Acetyl-thiophenes

Position	Charge Densities × 10^3		
	ΔQ_π	ΔQ_σ	ΔQ_t
		2-Acetylthiophene	
S_1	+799	+040	+839
C_2	−177	+003	−174
C_3	−134	−051	−185
C_4	−148	−042	−190
C_5	−151	−081	−232
		3-Acetylthiophene	
S_1	+785	+048	+833
C_2	−141	−089	−230
C_3	−169	+043	−126
C_4	−138	−045	−183
C_5	−156	−086	−242

Table 2—Rate Constants and E_a Values for NBS Bromination of Thiophenes and Charge Densities at Reaction Sites

([Substrate] = [NBS] = 2×10^{-3} mol dm^{-3}; solvent: 80% (v/v) aq. acetic acid)

Compound	$k_1 \times 10^3$ s^{-1} (20°C)	E_a (kJ mol^{-1})	$\Delta Q_t \times 10^3$
Thiophene	17.77	52.3	−256
2-Fluorothiophene	11.51	48.5	−258
2-Chlorothiophene	4.08	58.6	−249
2-Bromothiophene	4.08	51.5	−249
2-Iodothiophene	6.67	43.9	−254
3-Bromothiophene	27.29	55.2	−242
2,5-Dibromothiophene	5.33	63.2	−189
3-Acetylthiophene	1.92	55.2	−242
Benzothiophene	40.30	57.3	−254
Ethylthiophene-2 carboxylate	1.25†	55.2	−216
2-Acetylthiophene	1.38†	59.4	−232

†$k_2 \times 10^5$ (dm^3 mol^{-1} s^{-1}) values at 20°C.

Br^+ is expected to undergo electrophilic attack more easily than the dipolar bromine molecule. This should lead to smaller E_a values in NBS bromination. Contrary to expectations NBS bromination of thiophenes involves higher E_a value as compared to that by molecular bromine. This may be due to the fact that in NBS bromination the approaching electrophile Br^+ is not a bare cation but it is highly solvated in aqueous acetic acid and the extent of solvation should be more than that in the case of bromine molecule.

The experimental activation energy (E_a) value decreases as the total ($\pi + \sigma$) charge density at the reaction centre increases. There is a satisfactory linear correlation between the calculated charge densities and the experimental activation energies. This supports our earlier proposal that Arrhenius activation energy values can be explained on the basis of electron density at the reaction site for bromination of aromatic compounds[12,13]. The linear equations (1) and (2) can be obtained for the E_a values of bromination by molecular bromine and NBS respectively in terms of total charge density (ΔQ_t) at the reaction centre.

$$38.6 - 120 \times \Delta Q_t \qquad \ldots (1)$$

$$(n = 10; r = 0.99)$$

$$33.6 - 82 \times \Delta Q_t \qquad \ldots (2)$$

$$(n = 11; r = 0.98)$$

It is clear from the slopes that in the case of bromination by NBS the effect of total charge density in the E_a values is less than that in bromination by molecular bromine. Thus, the susceptibility of Br^+ to approach reaction centres of different total charge densities is less than that of molecular bromine, which is anticipated on the basis of their relative electrophilicities. Similar observation has also been made in the case of homocyclic aromatic compounds[6].

References

1 Nanjan M J, Kannappan V & Ganesan R, *Mh Chem*, **112** (1981) 581.

2 Nanjan M J, Kannappan V & Ganesan R, *Z Physik Chem, Frankfurt*, **127** (1981) 13.

3 Kannappan V, *Ph.D Thesis, University of Madras*, 1980.

4 Lew H Y & Noller C R, *Org Synth*, **30** (1950) 53.

5 Van Vleck R T, *J Am Chem Soc*, **71** (1949) 3256.

6 Sivakamasundari A S & Ganesan R, *Int J Chem Kinet*, **XII** (1980) 837.

7 Kannappan V, Nanjan M J & Ganesan R, *Indian J Chem*, **19A** (1980) 1183.

8 Marino G, *Prac Nauk Inst Chem Tech Naft Wegla Polit Wrocla*, **15** (1973) 89; *Chem Abstr*, **79**, 77565a.

9 Marino G, *Acad Naz Lineei Rend, Series VIII*, **38** (1965) 700.

10 Hartough H D, *The chemistry of heterocyclic compounds* (Interscience, New York) 1952.

11 Veillard A & Pullman B, *J theor Biol*, **4** (1963) 37.

12 Ganesan R, *Z physik Chem, Frankfurt*, **90** (1974) 82.

13 Nanjan M J & Ganesan R, *Mh Chem*, **110** (1979) 647.

Indian Journal of Chemistry
Vol. 27A, June 1988, pp. 540-541

Mechanism of Ligand Substitution Reaction of Monobipyridyl Complex of Manganese(II)

H M ABU EL-NADER* & M N H MOUSSA

Chemistry Department, Faculty of Science, Mansoura University, Egypt

Received 26 *February, revised* 27 *July* 1987; *accepted* 29 *October* 1987

The kinetics of ligand substitution reaction of $Mnbipy^{2+}$ complex with the trisoxalatocobalt(III) has been investigated spectrophotometrically at 600 nm. The reaction follows a first order kinetics. The rate of reaction increases with increase in [bipyridyl] in the reaction mixtures. Activation parameters have been evaluated. A mechanism consistent with the results has been suggested.

Complexes of Mn(II) are important due to their role in enzyme reactions[1]. The kinetics of complex formation of Mn(II) with bipyridyl was recently studied in different acidic solutions[2]. The relatively low value of the stability constant[3,4] of the complex, $Mnbipy^{2+}$ (4×10^{-4}), which is in accord with the low complexation reactivity of Mn^{2+} aqua ion led us to undertake the title investigation. The results of such studies using the trisoxalatocobalt(III) are reported in this note.

The substitution reaction was studied in the temperature range of 20-40°C, since in this temperature range the rate constant for the thermal decomposition of $K_3[Co(C_2O_4)_3]$ is extremely low[2].

$Mnbipy^{2+}$ complex was prepared in doubly distilled water using Merck grade $MnCl_2.4H_2O$ and 2,2'-bipyridyl. The complex $K_3[Co(C_2O_4)_3].3H_2O$ was prepared according to the method described before[5]. The reaction was followed at 600 nm, the λ_{max} of trisoxalatocobalt(III) using a Unicam SP 1800 UV spectrophotometer. All solutions were allowed to equilibrate at the desired temperature for 1 hr before mixing.

In a series of runs the [trisoxalate complex] was kept constant at 5×10^{-4} mol dm^{-3} while varying [$Mnbipy^{2+}$]. Under these conditions, the reaction followed first order kinetics as revealed by the linear plot of $2 + \log (A_t - A_\infty)$ versus time. It is seen that the rate constant decreased with increase in the concentration of $MnCl_2$ and bipyridyl mixtures (Table 1). To attain maximum degree of complexation ($\alpha = 0.997$) large excess of $MnCl_2$ solution was used (0.86 mol dm^{-3}).

Table 1—Rate Constants at Different Concentrations of $MnCl_2$ and Bipy
[$(K_3[Co(C_2O_4)_3] = 5 \times 10^{-4}$ mol dm^3 at 28°C)]

$[MnCl_2]_0$ (mol dm^{-3})	[bipy] (mol dm^{-3})	Degree of complexation	$10^4[Mnbipy^{2+}]$ (mol dm^{-3})	$10^3 k_1$ (s^{-1})
5×10^{-4}	5×10^{-4}	0.15	0.73	9.3
1×10^{-3}	1×10^{-3}	0.25	2.34	3.6
2×10^{-3}	2×10^{-3}	0.35	6.88	2.4

The kinetic measurements were performed at three different temperatures. The rate constants at 20°, 28°, and 35.5°C and [$Mnbipy^{2+}$] = [$K_3Co(C_2O_4)_3$] = 10^{-3} mol dm^{-3} came out to be 5.35×10^{-4}, 7.4×10^{-4} and 1.07×10^{-3} s^{-1} respectively. The system obeyed the Arrhenius equation. The values of E_a, A, $\Delta H^\ddagger$, $\Delta G^\ddagger$ and $\Delta S^\ddagger$ were evaluated as 34.02 kJ mol^{-1}, 1.2×10^{-3} s^{-1}, 31.51 kJ mol^{-1}, 92.42 kJ mol^{-1} and -202.86 JK^{-1} mol^{-1} respectively. Within the experimental errors, similar values of the activation parameters were obtained at [$K_3Co(C_2O_4)_3$] = 10^{-3} mol dm^{-3} and [$Mnbipy^{2+}$] = 3×10^{-3} mol dm^{-3}.

The composition of the complex formed between $Mnbipy^{2+}$ and $[Co(C_2O_4)_3]^{3-}$ applying Mauser's method[6,7] (Fig. 1) and Yoe-Jones[8] method was found to be 1:1 irrespective of [$Mnbipy^{2+}$].

Finally using different concentration ratios of the reactants it was observed that the rate constant increased with increase in [$Mnbipy^{2+}$] in the pres-

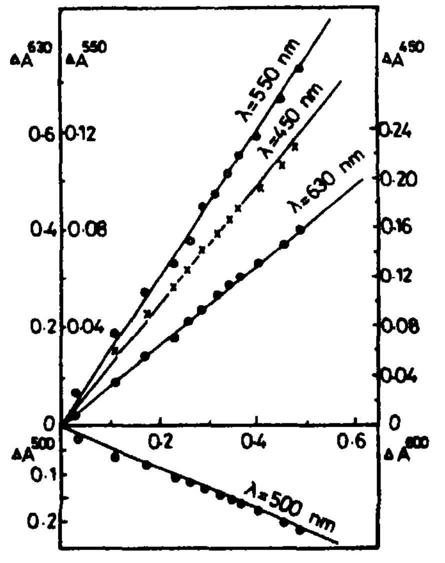

Fig. 1—ΔA diagram for $K_3[Co(C_2O_4)_3]$ and $[Mn\ bipy]^{2+}$ reaction

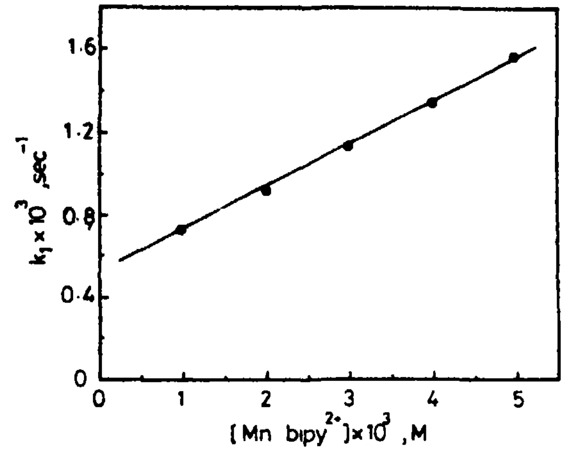

Fig. 2—Variation of k_1 with increasing [Mn bipy^{2+}] at 28°C

ence of large excess of $MnCl_2$ used to diminish the presence of free bipyridyl (Fig. 2). This behaviour is opposite to that observed on adding bipyridyl only to the $K_3[Co(C_2O_4)_3]$ complex[4].

On the basis of observation recorded above, a mechanism shown in Scheme 1 can be suggested for the ligand substitution reaction[9].

$$\mathrm{Mnbipy2+} \underset{k_{-1}}{\overset{k_1}{\rightleftharpoons}} \mathrm{Mn^{2+} + bipy} \qquad \ldots (1)$$

$$\mathrm{bipy + [Co(C_2O_4)_3]^{3-}} \underset{k_{-2}}{\overset{k_2}{\rightleftharpoons}} \mathrm{Co(C_2O_4)_2bipy^{-1} + C_2O_4^{2-}} \qquad \ldots (2)$$

$$\mathrm{C_2O_4^{2-} + Mnbipy^{2+}} \xrightarrow{k_3} \mathrm{MnC_2O_4 + bipy} \qquad \ldots (3)$$

$$\mathrm{C_2O_4^{2+} + Mn^{2+}} \xrightarrow{k_4} \mathrm{MnC_2O_4} \qquad \ldots (4)$$

Scheme 1

Based on Scheme 1 the rate-law (5) can be derived:

$$v = k_2[\mathrm{bipy}][\mathrm{Co(C_2O_4)_3}]^{3-} - k_3[\mathrm{C_2O_4^{2-}}][\mathrm{Mnbipy^{2+}}] \qquad \ldots (5)$$

The above mechanism is supported by the following observations:

(i) First order kinetics in [trisoxalate] at 600 nm. The formation of mixed ligand complex $[Co(C_2O_4)_2$ bipy] is an accepted fact since it has been synthesized and characterized spectrophotometrically[10]. (ii) Reaction rate increases with increase in [Mnbipy^{2+}]. (iii) Similar values of activation parameters obtained irrespective of reactant concentration ratios suggest the formation of only one activated complex. Also, Mouser's method sustains only one linear independent reaction (Fig. 1). (iv) High negative $\Delta S^{\dagger} (= -202.86\ JK^{-1}\ mol^{-1})$ confirms that the activated complex $[Co(C_2O_4)_3bipy]^{1-}$ results from $Co(C_2O_4)_3^{3-}$ in accordance with the extended Hückel theory[11].

References

1 Cohn M & Reuben J, *Account chem Res*, **4** (1971) 214.
2 Murgulescu I G & Oncescu T, *Z phys Chem*, (Leipzig) **214** (1960) 238.
3 Hague D N & Martin S R, *J chem Soc Dalton Trans*, (1974) 254.
4 Abu El Nader H M & Oncescu T, under publication.
5 Werner A, *Ann des Phys*, **59** (1919) 635.
6 Mauser H, *Z Naturforsch*, **23b** (1968) 1021.
7 Mauser H, *Z Naturforsch*, **23b** (1968) 1025.
8 Yoe J H & Jones A L, *Ind Eng Chem Anal Edition*, **16** (1944) 111.
9 Olson D C & Margerum D W, *J Am chem Soc*, **85** (1963) 297.
10 Broombhead J A, Dwyer M & Kane Maguire N, *Inorg Chem*, 7 (1968) 1388.
11 Benedix R, Reinhold J & Henning H, *Inorg chim Acta*, **40** (1980) 47.

Indian Journal of Chemistry
Vol. 27A, June 1988, pp. 542-544

Complexes of Oxovanadium(IV), Chromium(III), Manganese(II), Iron(II), Cobalt(II), Nickel(II) & Copper(II) with 6-Chloro-4-hydroxy-3-acetylcoumarin (Cl − HAC)

(Miss) L NALANDA SHARADA & M C GANORKAR*
Department of Chemistry, Osmania University,
Hyderabad 500 007

Received 18 *May* 1987; *revised* 16 *July* 1987; *rerevised and accepted* 7 *September* 1987

Complexes of 6-chloro-4-hydroxycoumarin (Cl − HAC) with oxovanadium(IV), chromium(III), manganese(II), iron(II), cobalt(II), nickel(II) and copper(II) have been prepared and characterised on the basis of analytical, conductance, magnetic moment and spectral data. Magnetic measurements, IR and electronic spectral studies suggest octahedral geometry for Cr(III), Mn(II), Fe(II), Co(II), Ni(II) and Cu(II) complexes and square-pyrimidal geometry for oxovanadium(IV) complex. Infrared spectral studies show monobasic bidentate behaviour of Cl − HAC with oxygen donor system.

Although solution chemistry of transition metal complexes of 4-hydroxy-3-acetylcoumarin is reported[1], no work is done on the synthesis and structural aspects of solid complexes. This note deals with the preparation and characterisation of oxovanadium(IV), Cr(III), Mn(II), Fe(II), Co(II), Ni(II) and Cu(II) complexes of 6-chloro-4-hydroxy-3-acetylcoumarin (Cl − HAC).

All the metal chlorides used were of AR grade. Malonic acid (Riedel), *p*-chlorophenol (Riedel), anhydrous aluminium chloride (Ranbaxy) and acetic anhydride (E. Merck) were used for the preparation of the ligand. The ligand (Cl − HAC) was prepared by reported procedure[2] and its purity was checked by TLC and melting point determination (m.p. 180°C).

The metal complexes were prepared by mixing the hot ethanolic solution of the metal chloride (0.01 mol) and the ethanolic solution of the ligand Cl − HAC (0.02 mol) in 1:2 molar ratio. Vanadyl sulphate and ferrous ammonium sulphate were used for the preparation of oxovanadium(IV) and Fe(II) complexes, respectively. The reaction mixture was refluxed for 2 hr and then cooled. The respective metal chelates separated from the solution at *p*H 6-7. The products thus obtained were filtered, washed successively with ethanol and petroleum ether (60-80°) and dried *in vacuo*. All the complexes are coloured and stable towards air and moisture. They decompose at 300°C. They are insoluble in common organic solvents and sparingly soluble in DMF, dioxane and DMSO. The molar conductance values of 1×10^{-3} *M* solutions of the complexes in DMF show their non-electrolytic behaviour (2-10 mhos cm^2 mol^{-1}). Electrical conductances were measured on a digital conductivity meter model D_1-909 (Digism Electronics) and digital direct reading conductivity meter 304 (Systronics).

The complexes were analysed for their metal contents employing standard procedures after destroying the organic matter with nitric acid. Chloride was estimated as AgCl. Nitrogen was determined by microanalysis.

The magnetic susceptibilities of the complexes were determined by the Gouy method using $Hg[Co(NCS)_4]$ as the calibrant, and experimental magnetic susceptibilities were corrected for diamagnetism[3]. Analytical data of the complexes are given in Table 1.

The electronic spectra of the complexes were recorded on a Carey-14 spectrophotometer in nujol. The infrared spectra of the ligand and the complexes were recorded on a Perkin-Elmer instrument in KBr. ESR spectra were recorded as powder at room temperature on a JEOL-JES-F3X spectrometer.

4-Hydroxycoumarins are known to exhibit tautomerism and the present ligand Cl − HAC can exist in the tautomeric lactone (a) and chromone (b)

Table 1—Analytical Data of the Complexes of Cl − HAC

Complex (molecular formula)	Found (Calc.) %			
	Metal	Carbon	Hydrogen	Chlorine
Cl − HAC	—	55.35	2.93	14.88
($C_{11}H_8O_4Cl$)		(55.34)	(2.99)	(14.90)
Oxovanadium (IV)				
(Cl − HAC)$_2$	9.50	48.82	2.22	12.90
($VC_{22}H_{12}O_9Cl_2$)	(9.40)	(48.83)	(2.210)	(12.93)
Cr(III)(Cl − HAC)$_2$Cl.H_2O	8.961	45.50	2.50	18.40
($CrC_{22}H_{14}O_9Cl_3$)	(8.959)	(45.48)	(2.41)	(18.26)
Mn(II)(Cl − HAC)$_2$.2H_2O	9.80	46.80	2.85	12.60
($MnC_{22}H_{16}O_{10}Cl_2$)	(9.707)	(46.65)	(2.82)	(12.52)
Fe(II)(Cl − HAC)$_2$.2H_2O	(9.90)	46.65	2.75	12.12
($FeC_{22}H_{16}O_{10}Cl_2$)	(9.85)	(46.57)	(2.82)	(12.09)
Co(II)(Cl − HAC)$_n$	10.37	46.45	2.81	12.45
Co($C_{11}H_6O_4Cl$)$_n$	(10.34)	(46.327)	(2.80)	(12.44)
Ni(II)(Cl − HAC)$_n$	10.33	46.40	2.90	12.45
Ni($C_{11}H_6O_4Cl$)$_n$	(10.30)	(46.34)	(2.808)	(12.44)
Cu(II)(Cl − HAC)$_n$	11.90	49.10	2.99	13.20
($CuC_{11}H_6O_4Cl$)$_n$	(11.80)	(49.02)	(2.97)	(13.16)

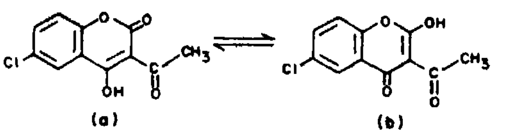

(a) Lactone form (b) Chromone form

forms. The lactone and chromone forms are expected to show νC=O at 1710 and 1665 cm^{-1}, respectively.

The IR spectrum of Cl−HAC shows a strong band at 1720 cm^{-1}, which confirms that the ligand is in the lactone form. The bands at 1610 and 1440 cm^{-1} are assignable to νC=O (acetyl) and νC−O (phenolic) respectively. The band due to νOH is observed at 3010 cm^{-1} in the ligand spectrum; its low position is attributed to the strong intramolecular hydrogen bonding between the hydroxyl group and acetyl group.

In the IR spectra of all the complexes of Cl−HAC, the band assigned to νOH in the free ligand is absent, suggesting the cleavage of intramolecular hydrogen bonded νOH[5] with subsequent deprotonation of the phenolic OH group and coordintion of oxygen to the metal ion. The positive shift of νC−O (phenolic) by 10 cm^{-1} in all the complexes further confirms coordination through the oxygen of the phenolic group[6]. A new broad absorption in the region 3150-3500 cm^{-1} is observed in case of Cr(III), Mn(II), and Fe(II) complexes which is attributed to the presence of coordinated water[7]. Its presence is further confirmed by the appearance of a non-ligand band at 820 cm^{-1} in Cr(III) and Fe(II) complexes, and at 840 cm^{-1} in Mn(II) complex. The presence of coordinated water was also confirmed by TG and DT analyses[8]. A negative shift of νC=O (acetyl) in all the complexes by 10 cm^{-1} shows the participation of oxygen of the acetyl carbonyl group in complexation. An interesting phenomenon that has been observed is the downward shift by 20-45 cm^{-1} of νC=O (lactone) in Ni(II), Co(II) and Cu(II) complexes indicating the participation of oxygen of the lactone carbonyl in coordination.

Coordination through the oxygen of lactone carbonyl was suggested by some earlier workers for the transition metal complexes of 4-hydroxycoumarins and coumarin-3-carboxylic acid[9]. In other complexes, i.e., complexes of oxovanadium (IV), Cr(III), Mn(II) and Fe(II), no change is observed in νC=O (lactone). New peaks of medium intensity are observed in the range 600-400 which are ascribed to νM−O vibrations[8,10]. For oxovanadium(IV) complex, a strong non-ligand band is observed at 900 cm^{-1} which is assigned to νV=O vibrations[11]. On the basis of IR spectral data, it is concluded that the ligand Cl−HAC utilizes the deprotonated phenolic oxygen and acetyl oxygen as coordinating centres in all the complexes. In addition to these centres, the oxygen of lactone carbonyl is coordinating in Co(II), Ni(II) and Cu(II) complexes.

The oxovanadium(IV) complex is paramagnetic and shows $\mu_{\text{eff.}}$ value of 1.75 B.M. which is in good agreement with the expected spin-only value for one unpaired electron at room temperature[12]. Its electronic spectrum displays two absorption bands at 15625 and 20408 cm^{-1} which are assigned to $b_2 \rightarrow e$ and $b_2 \rightarrow a$ transitions respectively[12-14] suggesting square-pyramidal geometry. The room temperature magnetic moment value of Cr(III) complex is 3.9 B.M. which is in agreement with the presence of three unpaired electrons. Irrespective of the strength of the ligand field, there will be three unpaired electrons in mononuclear Cr(III) complexes. The electronic spectrum of Cr(III) complex exhibits three bands at 17400, 24600 and 37060 cm^{-1}. They are assigned to $^4A_{2g} \rightarrow {}^4T_{2g}$, $^4A_{2g} \rightarrow {}^4T_{1g}(F)$ and charge-transfer respectively. From the electronic spectrum it is concluded that Cr(III) complex may have an octahedral geometry[14,15]. The observed magnetic moment value of Mn(II) complex of Cl−HAC is found to be 5.36 B.M. which is low compared to the spin-only value for high-spin Mn(II) complexes. The low value can be attributed to the presence of Mn(III) species[16]. The weak spectral bands in Mn(II) complex observed at 17241, 21276 and 24290 cm^{-1} are attributed to $^6A_{1g} \rightarrow {}^4T_{1g}$ (G), $^6A_{1g} \rightarrow {}^4T_{2g}$ (G) and $^6A_{2g} \rightarrow {}^4E_g$ transitions, respectively. They are in accordance with octahedral stereochemistry[17-19]. The room temperature magnetic measurements of Fe(II) complex show magnetic moment of 5.12 B.M. indicating the presence of four unpaired electrons[20]. The electronic spectrum of Fe(II) complex displays only one band at 12120 cm^{-1} which is assignable to $^5T_{2g} \rightarrow {}^5E_g$ transition. This is consistent with its high-spin octahedral geometry[21]. The magnetic moment of Co(II) complex is 4.46 B.M. suggesting a high-spin octahedral configuration[22]. The high value may be due to the orbital contribution. The Co(II) complex exhibits three bands at 11765, 18180 and 26660 cm^{-1} in the electronic spectrum. The bands can be assigned to $^4T_{1g} \rightarrow {}^4T_{2g}(F)$, $^4T_{1g} \rightarrow {}^4A_{2g}$ and $^4T_{1g}(F) \rightarrow {}^4T_{1g}(P)$ transitions respectively, which are in accordance with its high-spin octahedral geometry[19]. The Ni(II) complex is paramagnetic and shows an effective magnetic moment of 2.8 B.M. which is within the range expected for two

Table 2—Magnetic and Electronic Spectral Data of the Complexes of Cl – HAC

Complex	$\mu_{eff.}$ (B.M.)	λ_{max} (cm^{-1})
Oxovanadium(IV)(Cl – HAC)$_2$	1.75	15625
		20408
Cr(III)(Cl – HAC)$_2$Cl.H$_2$O	3.9	17400
		24600
		37060
Mn(II)(Cl – HAC)$_2$.2H$_2$O	5.36	17241
		21276
		24290
Fe(II)(Cl – HAC)$_2$.2H$_2$O	5.12	12120
Co(II)(Cl – HAC)$_n$	4.46	11765
		18180
		26660
Ni(II)(Cl – HAC)$_n$	2.8	10525
		20000
		25000
Cu(II)(Cl – HAC)$_n$	1.85	15385

unpaired electrons[23]. Its electronic spectrum shows three bands at 10525, 20000 and 25000 cm^{-1} which are attributed respectively to ${}^3A_{2g}\rightarrow{}^3T_{2g}(F)$, ${}^3A_{2g}(F)\rightarrow{}^3T_{1g}(F)$ and ${}^3A_{2g}(F)\rightarrow{}^3T_{1g}(P)$ transitions[19,24]. The observed magnetic moment of Cu(II) complex of Cl – HAC is 1.85 B.M. This value is in good agreement with the presence of one unpaired electron[22]. The Cu(II) complex exhibits an intense broad band in the range 15385 cm^{-1}, which is attributed to ${}^2T_{2g}\rightarrow{}^2E_g$ transition, suggesting distorted octahedral geometry[19]. The electronic spectral data and magnetic moment data are given in Table 2.

The ESR spectrum of Cu(II) complex is in agreement with the presence of one unpaired electron. The '*g*' value is calculated and found to be 2.545 which is characteristic of the octahedral Cu(II) complexes[25,26] and indicates strong interaction between the ligand and the metal ion.

On the basis of the analytical and conductivity data, magnetic susceptibility measurements, IR, electronic and ESR spectral data, it is concluded that the ligand Cl – HAC behaves as a monobasic bidentate oxygen donor system forming octahedral complexes in the case of Cr(III), Mn(II), Fe(II), Co(II), Ni(II) and Cu(II) and square-pyramidal complex with oxovanadium(IV) ion.

One of the authors (L N S) is thankful to the CSIR, New Delhi, for the award of a Junior as well as a Senior Research Fellowship.

References

1 Manku G S, *Aust J Chem*, **24** (1971) 925.

2 Venkateswara Rao K & Sundera Murthy, *Proc Indian Acad Sci*, **81A** (1975) 118.

3 Figgis B N & Lewis J, *Modern coordination chemistry*, edited by J Lewis & R G Wilkins (Interscience, New York) (1960) 403.

4 Hay R W & Williams P P, *J chem Soc*, (1964) 2270.

5 Rana A K & Shah J R, *J Indian chem Soc*, **58** (1981) 1100.

6 John R Dyer, *Applications of absorption spectroscopy of organic compounds* (Prentice-Hall, New Delhi) 1984.

7 Dutta R L & Ray R K, *J Indian chem Soc*, **60** (1983) 185.

8 Nakamoto K, *Infrared spectra of inorganic and coordination compounds* (Wiley Interscience, New York) 214.

9 Manku G S & Gurucharan S, *Fresenius Z Anal Chem*, **258** (1972) 365.

10 Narang K K & Agarwal A, *Inorg chim Acta*, **9** (1974) 137.

11 Selbin J, *Coord Chem Rev*, **1** (1966) 293.

12 Selbin J & Ortolano T R, *J inorg nucl Chem*, **26** (1964) 37.

13 Donini J C, Hollebone B R & Lever A B P, *Progr inorg nucl Chem*, **22** (1977) 225.

14 Thotia M P, Gurtu J N & Rana V B, *Indian J Chem*, **19A** (1980) 133.

15 Fatta A M & Lintredi R L, *Inorg Chem*, **10** (1971) 478.

16 Holm R H, Everett (Jr) G W & Chakravorty A, *Progr inorg Chem*, **7** (1966) 120.

17 Sengupta S K, Sahni S K & Kapoor R N, *Indian J Chem*, **20A** (1981) 692.

18 Preti C & Tosi G, *Aust J Chem*, **20A** (1976) 543.

19 Lever A B P, *Inorganic electronic spectroscopy* (Elsevier, Amsterdam) 1968, 294.

20 Cotton F A & Wilkinson G, *Advanced inorganic Chemistry*, 3rd Edn. (Wiley Eastern, New Delhi) 1976, 862.

21 Srivastava R S, Yadav L D S, Khare R K & Srivastava A K, *Indian J Chem*, **20A** (1981) 516.

22 Figgis B N & Lewis J, *Progr inorg Chem*, **6** (1964) 37, 67, 157, 185, 210.

23 Drago R S, *Physical methods in inorganic chemistry*, (East-West Press, New Delhi) 1971, 395, 328.

24 Singh N K, Agarwal Seema & Agarwal R C, *Indian J Chem*, **21A** (1982) 973.

25 Toy A D, Cheston S H A, Pilbrow I R & Smith T D, *Inorg Chem*, **10** (1971) 2219.

26 Hathway B J & Billing D E, *Coord Chem Rev*, **5** (1970) 143.

Indian Journal of Chemistry
Vol. 27A, June 1988, pp. 545-546

Lanthanide Nitrate Complexes of Schiff Base Derived from 1-Isonicotinyl-Hydrazide & 2-Hydroxy-1-Naphthaldehyde

H JAYASANKAR & P INDRASENAN*
Department of Chemistry,
University of Kerala, Trivandrum 695034

Received 31 *August* 1987;
revised and accepted 12 *October* 1987

New complexes of lanthanide nitrate with 1-isonicotinyl-2-(2-hydroxy-1-naphthylidene)hydrazine (INHNH) having the general formula [Ln(INHNH)$_2$NO$_3$] (where Ln = La, Pr, Nd, Sm, Gd, Dy and Y), have been synthesised and characterised by elemental analyses, and magnetic, conductance, IR and electronic spectral data. The ligand is shown to act as a monovalent terdentate ligand and the nitrate ion is coordinated monodentately offering a coordination number of seven to the lanthanide ion.

Recently, some interesting lanthanide complexes with schiff bases derived from salicylaldehyde, *o*-hydroxyacetophenone and 2-hydroxynaphthaldehyde and benzoyl- and 2-picolyl-hydrazides have been reported[1]. As a part of our programme on the synthesis and characteristion of solid lanthanide complexes[2-5], we report herein the synthesis and characterisation of lanthanide nitrate complexes with a schiff base derived from isonicotinylhydrazide and 2-hydroxy-1-naphthaldehyde. The ligand, 1-isonicotinyl-2-(2-hydroxy-1-naphthylidene) hydrazine (INHNH) is of special interest as it contains four potential donor sites.

The nitrates of lanthanum, praseodymium, neodymium, samarium, gadolinium, dysprosium and yttrium were prepared in the laboratory[5]. The ligand (INHNH) was prepared by a method similar to that given in literature[6,7]. The purity of the ligand was checked by its melting point, elemental analyses and IR spectrum.

Lanthanide nitrate (2 mmol) was dissolved in acetone (15 ml). The ligand, INHNH (4.1 mmol) was suspended in acetone (150 ml) and refluxed on a water-bath until it was completely dissolved. The lanthanide nitrate solution was slowly added to it. The resulting solution was further refluxed for 2 hr. The precipitated complex was filtered, washed several times with hot acetone and dried *in vacuo* over P_4O_{10}. The metal contents of the complexes were determined by conventional method[8].

The room temperature (28 ± 2°C) magnetic susceptibilities of the complexes were measured by Gouy's method and appropriate diamagnetic corrections were applied[9]. The molar conductances of 10^{-3} *M* solutions of the complexes in methanol were determined at 28 ± 2°C using an ELICO CM 82T conductivity bridge with a dip-type cell with platinum electrodes (cell constant = 1.32

Table 1 – Elemental Analysis, Magnetic Moment and Molar Conductivity Data of Lanthanide Nitrate Complexes of 1-Isonicotinyl-2-(2-hydroxy-1-naphthylidene)hydrazine (INHNH)

Complex	Elemental analysis*				Magnetic moment μ_{eff} BM	Molar conductivity in methanol Ohm^{-1}cm^{2}mole^{-1}
	Metal %	Carbon %	Hydrogen %	Nitrogen %		
[La(INHNH)$_2$NO$_3$]	17.54	52.10	3.12	12.32	0.0	58.08
	(17.78)	(52.25)	(3.32)	(12.54)	(0.0)	
[Pr(INHNH)$_2$NO$_3$]	17.47	52.04	3.20	12.28	3.4	31.68
	(17.99)	(52.11)	(3.32)	(12.52)	(3.6)	
[Nd(INHNH)$_2$NO$_3$]	18.00	51.75	3.18	12.16	3.5	32.47
	(18.34)	(51.89)	(3.30)	(12.46)	(3.6)	
[Sm(INHNH)$_2$NO$_3$]	19.32	51.32	3.14	12.15	1.5	36.83
	(18.97)	(51.49)	(3.28)	(12.37)	(1.5-1.6)	
[Gd(INHNH)$_2$NO$_3$]	20.07	50.92	3.08	12.02	7.6	32.52
	(19.77)	(51.04)	(3.25)	(12.26)	(7.9)	
[Dy(INHNH)$_2$NO$_3$]	20.04	50.52	3.02	11.96	10.6	48.31
	(20.10)	(50.71)	(3.23)	(12.18)	(10.6)	
[Y(INHNH)$_2$NO$_3$]	12.21	55.46	3.20	12.98	0.0	36.23
	(12.16)	(55.82)	(3.56)	(13.40)	(0.0)	

*Calculated values are in parentheses.

cm^{-1}). The IR spectra were recorded in KBr on a Perkin-Elmer 397 IR spectrophotometer. The electronic spectra were recorded in methanol (~ 10^{-4} *M*) on a Hitachi 220 A UV-visible spectrophotometer in the range 185-900 nm.

The analytical, magnetic moment and molar conductivity data are presented in Table 1. These complexes are reddish-violet, non-hygroscopic solids soluble in methanol and ethanol and insoluble in acetone, acetonitrile, nitrobenzene, benzene, petroleum ether and diethyl ether. These complexes have the general formula $Ln(INHNH)_2NO_3$ (where Ln = La, Pr, Nd, Sm, Gd, Dy and Y). Molar conductances of the complexes in methanol (Table 1) indicate their nonelectrolytic nature. This shows that the nitrate ion present in each complex is coordinated to the metal ion. The magnetic moments measured at room temperature show that La and Y complexes are diamagnetic and the other five complexes are paramagnetic as expected. The observed moments are generally found to agree well with the theoretical values calculated by the Van Vleck formula[10].

The ligand exhibits bands in its IR spectrum at 3200, 1670, 1600 and 1275 cm^{-1} assignable to νOH (H-bonded), νC = O, νC = N and νC − O (phenolic), respectively. However, in the spectra of the complexes, the νOH (phenolic) mode disappears indicating deprotonation followed by coordination to the metal ion. This agrees with the elimination of two of the three nitrate ions originally present in the metal salt used. The νC = O, νC = N and νC − O bands were found to shift and appeared at 1610, 1550 and 1300 cm^{-1}, respectively. These shifts indicate that the ligand acts as a monovalent terdentate ligand coordinating through the oxygen atoms of the phenolic − OH and > C − O groups and nitrogen atom of the > C = N group. The higher shift of phenolic νC − O (from 1275 to 1300 cm^{-1}) suggests the chelate formation on complexation.

The two medium bands at ~ 1455 and 1330 cm^{-1}, which are present only in the IR spectra of the complexes are assigned to ν_4 and ν_1 vibrations, respectively of the coordinated nitrate ion. The magnitude of $\nu_4 - \nu_1$ is ~ 125 cm^{-1} in these complexes, which indicates that the nitrate group is coordinated to the lanthanide ion in a monodentate fashion[11].

The electronic spectrum of the free ligand exhibits two $n \rightarrow \pi^*$ transitions at 27.02 and 30.30 kK, and a $\pi \rightarrow \pi^*$ transition at 42.55 kK. For the complexes, the higher freqency $n \rightarrow \pi^*$ transition is unchanged in energy, the lower energy $n \rightarrow \pi^*$ transition is not observed and the $\pi \rightarrow \pi^*$ band is split and appears at ~ 45.45 and ~ 39.21 kK. These complexes show a very broad band at 23.81 kK in the visible region, which is assigned to L → M charge-transfer transition. This band is so strong that the *f-f* bands of the lanthanide ions are obscured. No band due to hypersensitive transition is observed for the Nd^{3+} complex.

On the basis of the above discussion, in these complexes the ligand, INHNH forms two six-membered rings with the metal ion, which is a very stable arrangement. The ideal geometries for the complexes with a coordination number of seven are monocapped trigonal prism, monocapped octahedron and pentagonal bipyramid. The exact geometries of the present complexes can be ascertained only by X-ray diffraction studies on single crystals.

We are thankful to Prof C G R Nair for his keen interest and helpful suggestions and the University of Kerala for the award of a research fellowship to one of us (H J).

References

1 Dutta R L & Das B R, *Indian J Chem*, **22A** (1983) 207.
2 Giri V & Indrasenan P, *Polyhedron*, **2** (1983) 573.
3 Radhakrishnan P K, Indrasenan P & Nair C G R, *Polyhedron*, **3** (1984) 67.
4 Jayasankar H & Indrasenan P, *Indian J Chem*, **26A** (1987) 964.
5 Jayasankar H & Indrasenan P, *J Less-Comm Metals*, **132** (1987) 43.
6 Woodman A G & Seymour D E, *Brit*, **727** (1955) 486; *Chem Abstr*, **50** (1956) 5038f.
7 Vogel A I, *A text-book of practical organic chemistry* (Longmans, London), 1956; p. 653.
8 Kolthoff I M & Elving P J, *Treatise on analytical chemistry*, Vol 8, Part 2 (Wiley-Interscience, New York), 1960, p. 29.
9 Lewis J & Wilkins R G (Eds), *Modern coordination chemistry*, (Interscience, New York), 1960, p. 409.
10 Van Vleck J H & Frank N, *Phys Rev*, **34** (1929) 1494.
11 Curtis N F & Curtis Y M, *Inorg Chem*, **4** (1965) 804.

Indian Journal of Chemistry
Vol. 27A, June 1988, pp. 547-549

Mixed Valence Paramagnetic Trinuclear Complexes of Rhodium with N-alkylphenothiazines

B KESHAVAN* & R JANARDHAN

Department of Post-graduate Studies and Research in Chemistry, University of Mysore, Mysore 570 006

Received 24 *July* 1987; *revised and accepted* 7 *December* 1987

Eight mixed valence paramagnetic trinuclear complexes of rhodium, $Rh_3L_2Cl_8$ (L = N-alkylphenothiazine), have been synthesised. The complexes have been characterized on the basis of analytical, conductometric, magnetic, thermal, electronic, IR and EPR spectral data.

Rhodium complexes are receiving increasing attention in recent years owing to their potential as anticancer agents[1]. Paramagnetic complexes of rhodium(II)[2-7] and mixed valence complexes of Rh are rare. N-Alkylphenothiazines are extensively used as tranquilizers[8]. These are excellent electron donors[9]. Complex formation between Rh(III) and phenothiazines in aqueous medium has provided a basis for the spectrophotometric determination[10-12] of Rh(III). Lack of information on mixed valence complexes of Rh has prompted us to undertake the present study on the complexes of Rh with N-alkylphenothiazines.

Rhodium(III) chloride trihydrate and N-alkylphenothiazines (NAP) were used as received. Absolute ethanol and reagent grade ether (dried over sodium) were used.

The complexes were prepared as follows: An ethanolic solution of NAP was added slowly to a constantly stirred ethanolic solution of rhodium(III) chloride trihydrate at room temperature. The rhodium-NAP complexes precipitated immediately; these were filtered, washed several times with ethanol, ether and dried *in vacuo* over fused $CaCl_2$.

Analysis for carbon, hydrogen and nitrogen were performed at the Micro-analytical section of the Central Drug Research Institute, Lucknow. The electrical conductances of the complexes were measured in acetonitrile. The IR spectra were recorded on a Perkin-Elmer IR spectrophotometer Model 257 in KBr discs, far IR spectra on Fourier Transform far IR spectrophotometer Model PE 983 in polythene discs, electronic spectra on a Beckman Model DB spectrophotometer in methanol and EPR spectra on X-Band Varian E4 spectrometer at liquid nitrogen temperature (LNT). Magnetic susceptibilities were determined at room temperature using a Guoy balance. Thermograms were recorded using an Ulvac Sniku-Riko Thermal Analyser TA 1500.

Complexes reported in the present investigation are coloured, non-hygroscopic and are stable at room temperature for long periods. These do not possess sharp melting points. These are slightly soluble in acetonitrile and methanol, freely soluble in DMF and DMSO but insoluble in other common organic solvents and water. Analytical data (Table 1) suggest the formula $Rh_3L_2Cl_8$ {L = propionyl proma-

Table 1—Analytical and Magnetic Data of Rhodium Complexes

Compound	Colour	Found (Calc.), %				$\mu_{eff.}$ (B.M.)
		Rh	C	H	N	
$Rh_3(PP)_2Cl_8$	Violet	24.40	36.78	3.58	4.21	1.52
		(24.32)	(37.70)	(3.76)	(4.38)	
$Rh_3(MTM)_2Cl_8$	Red	24.62	36.21	3.72	4.71	1.22
		(24.71)	(36.50)	(3.84)	(4.48)	
$Rh_3(PPC)_2Cl_8$	Red	23.02	36.82	3.26	6.35	1.78
		(23.45)	(38.11)	(3.18)	(6.35)	
$Rh_3(P)_2Cl_8$	Dark brown	24.20	35.62	3.21	6.49	1.44
		(24.36)	(35.79)	(3.15)	(6.61)	
$Rh_3(CP)_2Cl_8$	Brown	22.55	34.92	3.46	4.02	1.20
		(22.72)	(33.58)	(3.39)	(4.12)	
$Rh_3(IP)_2Cl_8$	Brown	26.48	37.21	3.72	4.69	1.63
		(26.64)	(37.14)	(3.44)	(4.82)	
$Rh_3(AP)_2Cl_8$	Brown	24.82	36.42	3.88	6.48	1.80
		(24.88)	(36.56)	(4.00)	(6.73)	
$Rh_3(EI)_2Cl_8$	Brown	24.64	37.22	3.62	4.61	1.45
		(24.84)	(38.54)	(3.21)	(4.50)	

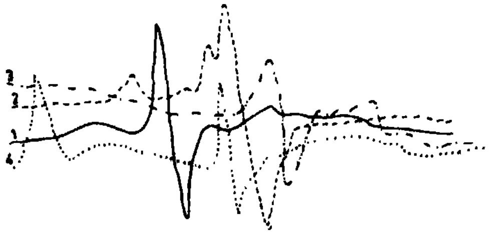

Fig. 1—Powder EPR spectra (LNT) of rhodium complexes of 1. PPC; 2. P; 3. IP; 4. PP

zine (PP), methotrimeprazine (MTM), propericiazine (PPC), perazine (P), chlorproethazine (CP), isopromethazine (IP), aminopromazine (AP) or ethylisobutrazine (EI)} for the complexes. The molar conductances of the complexes in acetonitrile are in the range 15-20 Ohm^{-1}cm^{2}mol^{-1} indicating the non-electrolytic nature of the complexes.

The $\mu_{eff.}$ values, assuming a trimeric structure for the complexes, are in the range 1.2 to 1.8 B.M per trimer. The paramagnetism of the complexes indicates the presence of Rh(II) in the complexes[2]. N-Alkylphenothiazines, being good reducing agents[9], bring about the reduction of Rh(III) to Rh(II). The EPR spectra of the complexes at LNT (field set: 3200, scan range: 4000, modulation frequency: 100 Hz, microwave frequency: 9.132 GHz, gain: 1.25 × 10^{2}g, M.A: 4 × 10° g) exhibit three anisotropic signals[2] (Fig. 1) confirming the presence of Rh(II). A trimeric structure is tentatively proposed for the complexes (Structure I). In this structure, two

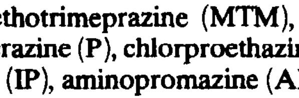

(I)

six-coordinated Rh(III) ions occupy the extreme positions while a four-coordinated Rh(II) ion occupies the middle position. The three metal ions are connected by dichlorobridges. Absence of hyperfine splitting indicates the absence of interacting atoms in the vicinity of Rh(II). Further, the anisotropic signals indicate a planar geometry around Rh(II). The four chlorine atoms surrounding the Rh(II) are probably responsible for the lower magnetic moments shown by the complexes. The insolubility of the complexes in water and common organic solvents and lack of sharp melting points support the polymeric nature of the complexes. The g values obtained for the complexes are in good agreement with those reported for the rhodium maleonitriledithiolate complex[2] (Table 2).

Sharp bands in the 240-270 nm region found in the UV spectra of both the ligands and their rhodium complexes are assigned to $\pi \rightarrow \pi^*$ transitions. Weak bands in the 300-320 nm region present in the spectra of ligands are shifted towards higher energy region in the spectra of their complexes. This band may be assigned to $n \rightarrow \pi$ transitions[8] and the shift may be due to coordination. Bands observed in the 405-420 nm region in the spectra of the complexes may be due to $^1A_{1g}$ - $^1T_{2g}$ transitions[13] of Rh(III).

Table 2—EPR Spectra of Rhodium Complexes at LNT

Complex	g_x	g_y	g_z
Rh$_3$(PP)$_2$Cl$_8$	2.092	2.014	1.982
Rh$_3$(MTM)$_2$Cl$_8$	2.106	2.016	1.952
Rh$_3$(PPC)$_2$Cl$_8$	2.102	2.012	1.948
Rh$_3$(P)$_2$Cl$_8$	2.108	2.010	1.966
Rh$_3$(CP)$_2$Cl$_8$	2.102	2.018	1.958
Rh$_3$(IP)$_2$Cl$_8$	2.102	2.016	1.984
Rh$_3$(AP)$_2$Cl$_8$	2.096	2.016	1.972
Rh$_3$(EI)$_2$Cl$_8$	2.098	2.012	1.964

In the N-alkylphenothiazine drugs $-R_3NH^+$ interaction with Cl$^-$ ion gives rise to a broad band in the 2500-2300 cm^{-1} region[14]. A broad band observed in the 2600-2350 cm^{-1} region in the infrared spectra of the free ligands corresponds to the $-CH_2NR_2H^+$ (R = Me, Et or Bu) moiety together with X$^-$ (X = Cl, PO$_4$, malonate or fumarate). In the infrared spectra of the corresponding rhodium complexes, this band either disappears or is reduced to a small hump showing that the tertiary nitrogen atom of the side chain of N-alkylphenothiazines is a site of coordination for the metal. Bands observed in the 2860-2825 cm^{-1} region in the infrared spectra of N-alkylphenothiazines may be assigned to the heterocyclic nitrogen atom attached to alkyl groups[15]. In the infrared spectra of the corresponding rhodium complexes, this band suffers a significant positive shift suggesting the participation of the heterocyclic nitrogen atom in coordination[15]. Thus, infrared spectra has shown that N-alkylphenothiazines act as bidentate chelating agents.

Bands in the 480-460 cm^{-1} region may be assigned to ν(Rh-N) modes and bands around 350 and 280 cm^{-1} are assigned to the terminal and bridging ν(Rh-Cl) modes[16]. Thus, far infrared spectra confirmed the presence of chlorine bridging in the complexes.

The thermal data of the rhodium complexes indicate that the complexes decompose at 190-240°C and attain constant weight at 500-580°C. The final product of decomposition has been characterised as metallic rhodium by X-ray diffraction. The final mass loss suffered by the complexes was in good agreement with the calculated mass loss in each case.

References

1 Cleare M J, *Coord Chem Rev*, **12** (1974) 349.

2 Billing E, Shupack S I, Waters J H, Williams R & Gray H B, *J Am chem Soc*, **86** (1964) 926.

3 Fischer E O & Wawersik H, *J organomet Chem*, **5** (1966) 557.

4 Masters C, Modonald W S, Raper G & Shaw B L, *J chem Soc Chem Commun*, (1971) 210.

5 James B R & Snynes D V, *J Am chem Soc*, **94** (1972) 6225.

6 Moers F G, Dejong J A M & Beanmont P M H, *J inorg nucl Chem*, **35** (1973) 1915.

7 Van Gaal H L M & Verlaak J M J, *Inorg chim Acta*, **23** (1977) 43.

8 Satoskar R S & Bhandarkar S D, *Pharmacology and pharmacotherapentics* (Popular Press, Bombay) 1976.

9 Dwivedi P C, Rao K G, Bhat S N & Rao C N R, *Spectrochim Acta*, **31A** (1975) 129.

10 Keshavan B & Nagaraja P, *Analyst*, **109** (1984) 835.

11 Keshavan B & Nagaraja P, *Mikrochim Acta*, **III** (1984) 283.

12 Keshavan B & Nagaraja P, *Ann Quim* (*Rome*), **75** (1985) 179.

13 Ball Hausen C J, *Introduction to ligand field theory* (McGraw Hill, New York) 1962, 276.

14 Katritzky A R & Boulton A J, *Advances in heterocyclic chemistry*, Vol 9 (Academic Press, New York) 1968, 336-338.

15 Garg S P, Srivastava N M & Sharma V N, *J Indian chem Soc*, **52** (1975) 1160.

16 Finch A, Gates P N, Radcliffe K, Dickson F N & Bentley F F, *Chemical applications of far infrared spectroscopy* (Academic Press, London) 1970, 148.

Indian Journal of Chemistry
Vol. 27A, June 1988, pp. 550-551

Molecular Adducts of Tellurocyclopentane Diperchlorate with Neutral Donors

T N SRIVASTAVA*, M A SIDDIQUI & S K SRIVASTAVA
Chemistry Department, University of Lucknow,
Lucknow 226 007

Received 11 *May* 1987; *revised and accepted* 23 *November* 1987

A freshly prepared solution of tellurocyclopentane diperchlorate reacts with Lewis bases to yield cationic complexes of the type $[C_4H_8Te(L)_2][ClO_4]_2$. These adducts have been characterised and a trigonal bipyramidal structure with one lone pair of electrons occupying one of the positions is proposed for the complex cations.

Triorganotellurium salts containing $[R_3Te]^+$ are known[1], but those containing $[R_2Te]^{2+}$ have been little studied. The first attempt was made by Lowry and Gilbert[2] who prepared dimethyltellurium(IV) diperchlorate, and on the basis of conductivity data formulated it as $[Me_2Te(ClO_4)]^+[ClO_4]^-$. In continuation of our work[3] on the synthesis and reactivity of diorganotellurium(IV) diperchlorates $[R_2Te(ClO_4)_2$, where R = Ph, p-$CH_3OC_6H_4]$, we report herein the preparation and characterisation of some molecular adducts of tellurocyclopentane diperchlorate with a few Lewis bases.

All operations were carried out under dry N_2 blanket. 1-Tellurocyclopentane diiodide[4] $(C_4H_8TeI_2)$ and silver perchlorate[5] were prepared by reported methods. The Lewis bases, viz. pyridine N-oxide (PyO), lutidine N-oxide(Lnt-O), β-picoline N-oxide (β-Pico), quinoline (Q), ν-picoline (ν-pic), 2,2′-bipyridyl (Bipy), phenanthroline (Phen), tetramethylethylenediammine (TMEN) and propylenediamine (pn) (all from BDH) were purified by distillation/recrystallisation.

In a typical preparation, a solution of the $C_4H_8TeI_2$ (0.87 g, 2 mmol) in dichloromethane (~ 30 ml) was stirred with $AgClO_4$ (0.83 g, 4 mmol) for 1 hr at room temperature. The precipitated silver iodide (0.93 g, 98%) was filtered off and the filtrate was treated with a solution of PyO (0.38 g, 4 mmol) in dichloromethane (~ 10 ml). The mixture was refluxed for 5 hr, excess of solvent distilled off, the product precipitated by the addition of excess pet ether (60-80°), filtered, washed repeatedly with the same solvent and dried *in vacuo*.

The analytical data of the molecular adducts are summarised in Table 1. The compounds which are light brown crystalline solids are stable in air and soluble in common organic solvents. These explode on heating. Molecular weights of the adducts were determined in freezing nitrobenzene and are found to be approximately one third of the calculated values indicating these to be 1:2 elecrolytes[6]. This is supported by their molar conductances in acetonitrile and ace-

Table 1—Analytical Data, Melting Points and IR Data of the Adducts

L	m.p.*	Found (Calc) %				$\nu N=O$ or $\nu C=N$	
		Te	C	H	N	Free Ligand	Complex
Pyo	210	22.2	29.2	3.0	4.8	1265	1235
		(22.2)	(29.3)	(3.1)	(4.8)		
LutO	185	20.2	34.3	4.1	4.4	1246	1230
		(20.2)	(34.3)	(4.1)	(4.4)		
β-PicO	182	21.2	32.1	3.7	4.5	1275	1240
		(21.2)	(31.9)	(3.6)	(4.6)		
Quo	170	18.8	39.3	3.2	4.1	1230	1210
		(18.9)	(39.2)	(3.2)	(4.1)		
ν-Pic	120	23.3	30.7	4.0	5.0	1578	1605
		(23.4)	(30.8)	(4.0)	(5.1)		
Bipy	130	23.2	31.1	3.1	5.1	1560	1575
		(23.6)	(31.1)	(3.2)	(5.1)		
TMEN	135	25.6	24.0	4.7	5.5	1253	1270
		(25.5)	(24.0)	(4.8)	(5.6)	1150	1170
						1130	1150
						1020	1025
Phen	210	22.6	34.1	3.0	5.0	1578	1585
		(22.6)	(34.1)	(2.8)	(4.9)	1485	1530
Pn	142	28.0	18.3	3.8	6.0	1370	1150
		(27.9)	(18.3)	(3.9)	(6.1)		

*Explode

tone ($10^{-3} M$ solutions) which fall in the range 258.5-278.5 and 185-193 mho mol^{-1} cm^2, respectively.

Infrared spectra of the complexes exhibit strong bands due to $\nu OClO_3$ around 1100 (ν_3) and 625 cm^{-1} (ν_4) indicating that both the perchlorate groups are ionic[7] in confirmity with their molecular weights and molar conductances. Their coordination with oxygen donor ligands occuring via the oxygen atom is revealed by the shift of the free ligand $\nu N = O$ to lower wavenumbers[8]. The ν C = N modes in free bipy[9], phen[10], ν-pic[11] and TMEN[12] undergo shifts to higher wavemembers in the spectra of the complexes suggesting coordination of the bases through nitrogen atoms. The $\nu C = N$ in pn shifts on to lower wavenumbers again indicating coordination through the nitrogen atom[13]. The complexes may be represented as $[C_4H_8Te(L)_2][ClO_4]_2$.

The PMR spectra of $[C_4H_8Te(Bipy)]$ $[ClO_4]_2$ and $[C_4H_8Te(PyO)_2][ClO_4]_2$ were recorded in $CDCl_3$ at room temperature. In the PMR spectra of the complexes, two multiplets of equal intensity appearing at δ 3.30(4H) and 2.38(4H) are attributed to CH_2-Te-CH_2 and $-CH_2$-C protons of the respective ring. In the spectrum of bipy in deuterated chloform, peaks appearing at δ 8.675, 8.490, 7.798 and 7.282 undergo significant shift and appear at δ 8.550(2H), 8.333(2H), 7.830(2H), and 7.349(2H) respectively on complexation. In the spectrum of $[C_4H_8Te(PyO)_2][ClO_4]_2$ phenyl protons of the ligand appear at δ 7.89. The spectra and their integration correspond to the proposed stoichiometry of the complexes. A trigonal bipyramidal structure with one lone pair of electrons occupying one of the positions is tentatively assigned for the complex cations.

Financial assistance from the UGC, New Delhi is gratefully acknowledged.

References

1 McWhinnie W R & Mallaki J, *Polyhedron*, **1** (1982) 13.
2 Lowry T M & Gilbert F L, *J chem Soc*, (1929) 2076.
3 Srivastava T N, Srivastava V K & Srivastava R C, *Polyhedron*, **4** (1985) 1223.
4 Morgon G T & Burstall F H, *J chem Soc*, (1931) 180.
5 Macy R, *J Am chem Soc*, **47** (1925) 1031.
6 Geary W J, *Coord chem Rev*, **7** (1971) 110.
7 Mathaway B J & Underhill A E. *J chem Soc*, (1961) 3091.
8 Sharp D W A, Brown D H & Amasa S, *J chem Soc* **A** (1969) 2892.
9 Carty A J & Tuck D G, *J chem Soc*, (1966) 1081.
10 Schilt A A & Tavlor R C, *J inorg nucl Chem*, **9** (1959) 211.
11 Cook D, *Can J Chem*, **42** (1964) 2523.
12 Srivastava T N & Kemboj P C, *Indian J Chem*, **19A** (1980) 167.
13 Srivastava T N, Singh Mala & Singh H B, *Indian J Chem*, **21A** (1982) 307.

Indian Journal of Chemistry
Vol. 27A, June 1988, pp. 552-554

Mixed Ligand Complexes of Uranium

S G DESHPANDE & S C JAIN*
Chemistry Division, Bhabha Atomic Research Centre,
Bombay 400 085

Received 27 *July* 1987; *revised and accepted* 13 *November* 1987

Mixed ligand complexes of U(IV) and dioxouranium(VI) such as $UCl_4.2DPC.EA$, $2UCl_4.DPC.2EA$, $UO_2Cl_2.2DPC.EA$, $2UO_2Cl_2.DPC.2EA$, $UO_2Cl_2.2DPTC.EA$, $UO_2(NO_3)_2.2DPC.EA$, and $UO_2(NO_3)_2.2DPTC.EA$ have been prepared by the interaction of UCl_4, UO_2Cl_2 or $UO_2(NO_3)_2$ with 1,5-diphenylcarbazide (DPC) or 1,5-diphenylthiocarbazide (DPTC) as primary ligand and ethyl acetate (EA) as secondary ligand. The compounds have been characterised by elemental analysis, infrared spectral data, molar conductance and thermogravimetric analysis.

1,5-Diphenylcarbazide (DPC) and 1,5-diphenylthiocarbazide (DPTC) are multidentate ligands having five donor atoms each. While in *trans* form these molecules can coordinate to two metal atoms forming two independent 5-membered chelates, in the *cis* form the molecules can form only one 5-membered chelate. The present work was taken up to study whether the ligand molecules could be stabilised in a particular isomeric form by varying the experimental conditions. It was also thought of interest to use ethyl acetate as secondary ligand to utilise other available coordination sites on the metal atoms to obtain mixed ligand complexes.

Uranium salts were prepared and purified by suitable methods[1]. The ligands (Aldrich) were used as such without further purification. The complex compounds were prepared in dry box flushed continuously with dry nitrogen by mixing the reactants in different stoichiometries using tetrahyrofugan (THF) as the solvent. typical examples for the two types of compounds synthesized are given below.

[$UO_2Cl_2.2DPC.EA$]: This class of compounds were prepared in two steps. In the first step, the uranium salt {UCl_4, $UO_2Cl_2.2H_2O$ or $UO_2(NO_3)_2.5H_2O$} and the primary ligand (DPC or DPTC in THF) were mixed in 1:2 molar ratio. The resulting mixture gave an oily product when *n*-hexane or pentane was added to it. The oily product gave a solid product on reacting with EA (secondary ligand). The product was filtered, washed with 50% (v/v) THF-pentane and dried *in vacuo* at room temperature for several hours.

[$(UO_2Cl_2)_2DPC(EA)_2$]: In this case the uranium salt and the primary ligand were reacted in 2:1 molar ratio respectively followed by the addition of EA (secondary ligand) to obtain free flowing solid. The compound was filtered, washed and dried *in vacuo*. The analytical results are reported in Table 1.

The IR spectroscopic measurements in nujol mull (4000-200 cm^{-1}) were carried out on a Perkin-Elmer grating spectrophotometer, Model 577. Molar conductances of the complexes in acetonitrile (10^{-3} *M* solutions) were measured with an Industrial Instrument Inc. conductivity bridge model RC-216-Bl at room temperature. Thermogravimetric measurements of some of the compounds were carried out (300 mg) in air (2.5 lit. h^{-1}) at a heating rate of 4 K min^{-1} using a Stanton thermobalance.

The IR spectra of the 1:2:1 complexes show that in

Table 1—Analytical Results

Compound	Colour (m.p., °C)	Found (Calc.), %					Molar conductance ($Ohm^{-1}cm^2mol^{-1}$)	Mass loss started at °C (TG Data)
		U%	Cl%	C	H	N		
$UCl_4(DPC)_2EA$	Pink	24.96	14.54	38.13	4.09	9.43	250	
	(85(d))	(25.00)	(14.90)	(37.79)	(3.78)	(11.76)		
$2UCl_4DPC\ 2EA$	Brick red	41.26	12.13	20.57	3.63	5.25	—	—
	(100(d))	(40.4)	(12.05)	(21.40)	(3.6)	(4.8)		
$UO_2Cl_2(DPC)_2EA$	Pink	26.0	7.07	38.1	2.74	10.4	255	160
	(140(d))	(26.1)	(7.78)	(39.4)	(3.9)	(12.27)		
$UO_2Cl_2(DPTC)_2EA$	Brown	25.41	7.13	39.09	2.81	9.19	260	145
	(160(d))	(25.21)	(7.52)	(38.1)	(3.8)	(11.85)		
$2UO_2Cl_2DPC_2EA$	Black	40.79	13.06	21.14	2.11	3.84	—	170
	(170(d))	(39.47)	(11.76)	(20.89)	(2.48)	(4.64)		
$UO_2(NO_3)_2(DPC)_2EA$	Blue	24.14	—	38.09	4.1	9.86	255	165
	(145(d))	(24.62)	—	(37.24)	(3.72)	(11.58)		
$UO_2(NO_3)_2(DPTC)_2EA$	Black	23.16	—	36.52	3.9	9.92	265	—
	(126(d))	(23.8)	—	(36.05)	(3.6)	(11.2)		

this class of compounds the ligand (DPC or DPTC) behaves as a bidentate molecule. The ν(C = O) and ν(C = S) bands for the free ligands at 1685 and 825 cm^{-1} shift to ~1616 and ~760 cm^{-1} respectively for the complexes. The N – H stretching frequencies for free DTC consist of several bands in the region 3480-3280 cm^{-1}. These bands in the complexes shift to 3500-3240 cm^{-1} indicating that all the nitrogen atoms are not involved in the coordination. Only the ν(N – H) bands associated with the coordinating nitrogen and the neighbouring nitrogen are expected to show a negative shift and the others are expected to show a positive shift. The ν(C = O) band for free ethyl acetate at 1740 cm^{-1} is shifted to 1680 cm^{-1} in the complexes. A bathocromic shift of 60 cm^{-1} suggests bonding of EA through CO group. Since the ν(C – O) band at 1250 cm^{-1} and ν(C′ – O) band at 1050 cm^{-1} for the free EA [$CH_3C = O - C'$] are also lowered by about 50 cm^{-1}, it is reasonable to propose that EA forms a four-membered ring chelate in the complexes[2].

In the case of 2:1:2 adducts the IR spectra in the ν(N – H) region show a general lowering of the bands from 3480-3280 cm^{-1} (free ligand) to 3240-3110 cm^{-1} (complex). The ν(C = O) band of DPC is again lowered from 1685 to 1615 cm^{-1} due to coordination[3]. The ν(C = O) and ν(O – C) bands of the secondary ligand EA also appear in the lower wave number region for the adducts. From this, it would seem that DPC molecule coordinates to two uranium atoms forming 5-membered chelate with each uranium atom and EA coordinates forming 4-membered chelate.

Molar conductance measurements of the compounds provide interesting results. While the 2:1:2 adducts in acetonitrile solutions are non-conducting, the 1:2:1 adducts appear to be 1:2 electrolytes[4,5] (Λ_M = 250-60 ohm^{-1} cm^2 mol^{-1}). From the available experimental results it would seem that the 1:2:1 adducts can be formulated as:

$[UCl_4.(DPC)_2.EA] \rightarrow [UCl_2.(DPC)_2.EA]^{2+} + 2Cl^-$

$[UO_2Cl_2.(DPC)_2.EA] \rightarrow [UO_2.(DPC)_2.EA]^{2+} + 2Cl^-$

$[UO_2(NO_3)_2.(DPC)_2.EA] \rightarrow [UO_2.(DPC)_2.EA]^{2+} + 2NO_3^-$

In such a formulation uranium would exhibit a coordination number of eight, the axial oxygens in UO_2 *being also considered as ligands. Appearance of IR bands at 1310, 750 and 700* cm^{-1} *for ionic nitrate further confirm the ionisation of* NO_3^- *in the compound*[6]. *In view of the above observations the 1:2:1 adducts can tentatively be assigned structure(I).*

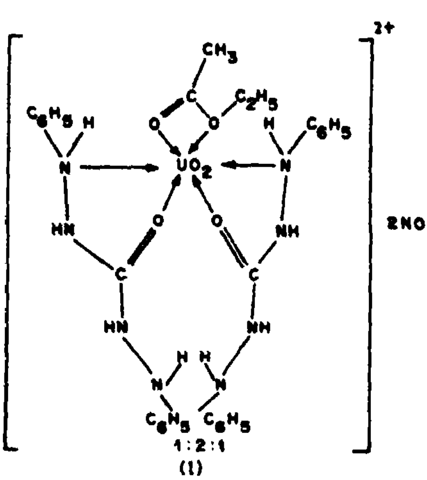

1:2:1
(I)

*In the case of the 2:1:2 adducts, the DPC molecule can be assumed as a tetradentate bridging ligand, co*ordinating to two uranium atoms. The EA molecules occupy two coordinating sites each as shown in structure II.

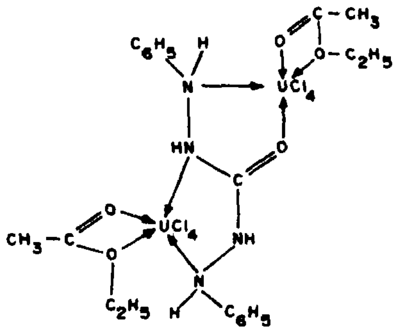

(II)

Thus, a coordination number of eight is attained by uranium atom in both the cases. In the case of $2UO_2Cl_2.DPC.2EA$ adduct, a similar structure would provide equatorial coordination number 6 and axial coordination number 2 to uranium. As expected, the ν(N – N) band at 985 cm^{-1} (ref. 7) for free DPC is lowered by about 60 cm^{-1} for the 2:1:2 adducts. For the 1:2:1 adducts, however, both shifted and unshifted bands of ν(N – N) are observed. This further indicates that in the former group of compounds the ligand is acting as tetradentate and in the latter group of compounds as bidentate.

In the case of DPTC adducts the involvement of the C = S group in bonding is supported by the lowering of the ν(C = S) band from 965 to 930 cm^{-1} *as a result of complex formation*[8]. *The* $\nu_{as}(UO_2)$ *band for free uranyl ion appears*[9] *at 965* cm^{-1}. *A ligand which forms strong bonding with the uranium atom of* UO_2 *moiety can effectively decrease the U = O bond or*der. As a result, $\nu_{as}UO_2$ lowered in the complexes[10]. *Using the magnitude of this shift as a criterion of the relative bonding ability of DPC and DPTC towards*

UO_2Cl_2 and $UO_2(NO_3)_2$, one can conclude that DPC forms stronger complexes than DPTC.

In the far infrared region, the new bands in the region 450-500 cm^{-1} can be assigned to ν(U-O)[11] where oxygen is of EA and/or DPC. The nitrogen is expected to form a weaker bond with uranium; therefore, the bands in the region 380-400 cm^{-1} are assigned to ν(U – N)[12] and the bands at 265 and 270 cm^{-1} to ν(U – S). For UCl_4.2DPC.EA and $2UCl_4$.DPC.2EA complexes the bands at 270 and 255 cm^{-1} are assigned to ν(U – Cl) modes[6].

Thermogravimetric analysis data of these complexes (Table 1) indicate that most of these compounds show major mass loss in the region 250°-400°C. There seems to be a simultaneous decomposition of organic moieties leading to the formation of U_3O_8 as the final residue in each case.

The authors sincerely thank Dr R M Iyer, Director, Chemical Group, Dr J.P. Mittal, Head, Chemistry Division and Dr A.J. Singh, Head, Inorganic Chemistry and Pure Materials Section for their interest in the work.

References

1 Brauer G, *Handbook of preparative inorganic chemistry*, 2nd edn, Vol. 2 (Academic Press, London) 1965.
2 Jain S C & Rivest R, *Can J Chem*, **40** (1962) 2243.
3 Jain S C & Rivest R, *Can J Chem*, **45** (1967) 139.
4 Geary W J, *Coord Chem Rev*, 7 (1971) 81.
5 Giesprecht E & Osorio V K L, *J inorg nucl Chem*, **37** (1975) 1409.
6 Jain S C, Gill M S & Rao G S, *J Indian chem Soc*, **58** (1981) 210.
7 Asmy A A H, Bekheit M, Ibrahim K M & Mostafa M M, *Acta chim hung*, **121** (1986) 391.
8 Beecroft B, Campbell J M & Grzeskowiak R, *J inorg nucl Chem*, **36** (1974) 55.
9 Balakrishnan P V, Patil S K, Sharma H D & Venkatasetty H V, *Can J Chem*, **43** (1965) 2052.
10 Rao G S, Jain S C & Gill M S, *Indian J Chem*, **21A** (1982) 526.
11 Sagoria V S, Gill M S, Jain S C, Ahuja H S & Rao G S, *Inorg chim Acta*, **121** (1986) 233.
12 Jain S C, Gill M S & Rao G S, *J Indian chem Soc*, **63** (1986) 195.

Indian Journal of Chemistry
Vol. 27A, June 1988, pp. 555-557

Studies on the Formation Equilibria of Binary & Ternary Complexes of Copper(II) with Acetylacetone & Some Amino Acids

Y ANJANEYULU*,
N KAMESWARA RAO & R PRABHAKARA RAO
Department of Chemistry,
Nagarjuna University, Nagarjuna Nagar 522 510

Received 5 *May* 1987; *revised* 7 *September* 1987;
accepted 3 *November* 1987

The formation equilibria of [CuAB] type of complexes in six ternary systems where HA = acetylacetone and H_2B = glycine, DL-α-alanine, DL-2-aminobutyric acid, DL-valine, DL-leucine and DL-β-phenylalanine have been studied *p*H metrically at 30°C and $\mu = 0.05$ *M* KNO_3 in 60% (v/v) water-ethanol medium. The acid dissociation constants of these ligands and the stability constants of their binary chelates with Cu(II) have also been determined under identical conditions by Irving-Rossotti method. The stability constants data are discussed in terms of the effect of basicity of the ligand, statistical factors and ring size upon chelation.

Though mixed ligand complexes of Cu(II) with various amino acids have been extensively investigated[1,2], no work has been reported so far on the formation constants of ternary complexes of Cu(II) with acetylacetone and amino acids. In this note a systematic *p*H-metric investigation has been carried out on the formation equilibria of ternary complexes of Cu(II) with acetylacetone and various amino acids viz. glycine (gly), DL-α-alanine (ala), DL-2-aminobutyric acid (2-aba), DL-valine (val), DL-leucine (leu), and DL-β-phenylalanine (pala).

All the chemicals used were of AR grade. Amino acids and cupric nitrate were BDH (India) reagents and acetylacetone Veb Chemie (Germany) reagent. All the amino acids were recrystallised from water-ethanol mixture and their purities were checked before use. Doubly distilled water was used in the preparation of the solutions.

A systronics digital *p*H-meter model No 335 with a combined glass electrode was used. The accuracy of the *p*H-meter was ±0.01 *p*H unit. It was calibrated by buffers of *p*H 4.00 and 9.20 at 30°C.

*p*H-metric titrations were carried out at 30±0.1°C and at an ionic strength of 0.05 *M* (KNO_3) under nitrogen gas free of O_2 and CO_2 atmosphere using a standard experimental set up described elsewhere[3]. The electrode system was calibrated by the method described by Uitert *et al*[4]. The metal to ligand ratio was maintained at 1:5 in the case of binary complexes and 1:1:1 in the case of ternary systems. Due to the low solubility of these complexes in water, the systems were studied in 60% (v/v) water-ethanol medium.

Stabilities of binary complexes

Although the *pK* values of the ligands and the stability constants of binary complexes of Cu(II) with these ligands have already been reported[1,2], we have redetermined these values for the sake of uniformity in experimental conditions, by Irving-Rossotti technique[5] in 60% (v/v) water-ethanol medium at 30°C and $\mu = 0.05$ *M* (KNO_3) and the results are presented in Table 1. The pK_1 and pK_2 values of amino acids agree well with reported values in 50-60% (v/v) isoproponol-water medium[6]. It can be seen from Table 1, that the log K^{Cu}_{CuB} and log $K^{CuB}_{CuB_2}$ metal-ligand formation constants of Cu(II) with amino acids follow the order, gly ≈ ala > 2-aba > val ≈ leu > pala. The values of proton-ligand stabilities of all these ligands are nearly same (except for β-phenylalanine which has low *pK* value) and it can be reasonably expected that their tendencies to form complexes would be similar. However, it can be seen that the complexes with glycine, α-alanine and 2-aminobutyric acid have almost the same log K^{Cu}_{CuB} and log $K^{CuB}_{CuB_2}$ values while valine and leucine, though having basicity closer to that of glycine, have lower values of metal-ligand formation constants. In case of valine and leucine the bulky methyl groups at α-carbon atom cause steric hindrance and make the chelate less stable (Structures A and B). It is also reported that an increase in

Table 1 – Stability Constants of Binary Complexes of Copper(II)

Ligand	pK_1	pK_2	log K^{Cu}_{CuB}	log $K^{CuB}_{CuB_2}$
Acetylacetone (A)	*9.80*		**9.50*	***8.12*
DL-Glycine	3.15	9.80	9.50	7.12
DL-α-Alanine	3.25	9.85	9.51	7.04
DL-2-Aminobutyric acid	3.23	9.90	9.47	6.99
DL-Valine	3.22	9.73	9.10	6.60
DL-Leucine	3.30	9.72	9.10	6.60
DL-β-Phenylalanine	3.30	9.25	8.90	5.90

*log K^{Cu}_{CuA}; **log K^{CuA}_{CuA}

chain length of amino acid results in the decrease in stability of the corresponding complex, which has been explained on the basis of restricted rotation of methyl group around C – C bond in solvent as the chain length is increased[7].

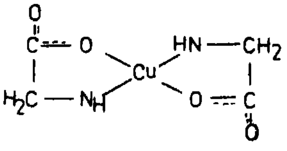

A

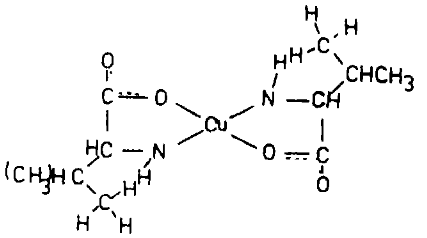

B

The metal-ligand formation constant in the case of β-phenylalanine which can form siz membered metal chelate rings, is found to be lower than those of complexes with all other α-amino acids which can form only five-membered metal chelate rings.

Stabilities of ternary complexes

The stability constants for the ternary systems were computed from the titrations in which the concentrations of Cu(II)(0.001 *M*):ligand A:ligand B were kept in the ratio 1:1:1. The acid dissociation constants of the ligands A and B, and the stability constant data for the parent binary complexes of Cu(II) with A and B, which were obtained by the Irving-Rossotti method were held constant in the computer calculations for the ternary systems.

The formation constants of ternary complexes (β_{MAB} = [MAB]/[M][A][B]) with HA and H_2B were calculated using appropriate mass balance equations and solving the corresponding cubic equations[8]. A computer programme written in Fortran IV was used to calculate the formation constants of ternary complexes and to calculate the concentrations of various species present in solution at each point on the titration. The calculations were restricted to *p*H value below 8, in order to avoid complications due to the hydrolysis of various complex species at higher *p*H. The results obtained are listed in Table 2. The charges for all the complex species reported in this paper are omitted for the sake of clarity.

Table 2 – Stability Constants of Ternary Complexes of Copper (II)

[$\mu = 0.05\ M\ KNO_3$; temp. = 30 ± 0.1°C]

Ligand	$\log K^{CuA}_{CuAB}$	$\log \beta_{CuAB}$	*Δ log *K*	log *X*	Δ log β
Glycine	8.54	18.04	−0.96	1.86	0.51
DL-α-Alanine	8.46	17.96	−1.05	1.75	0.56
DL-2-Aminobutyric acid	8.36	17.86	−1.11	1.64	0.53
DL-Valine	8.25	17.75	−0.85	2.18	0.56
DL-Leucine	7.91	17.41	−1.19	1.49	0.43
DL-β-Phenylalanine	6.94	16.44	−1.96	0.46	0.14

*$\Delta \log K = \log K^{CuA}_{CuAB} - \log K^{Cu}_{CuB} = \log K^{CuB}_{CuBA} - \log K^{Cu}_{CuA}$.

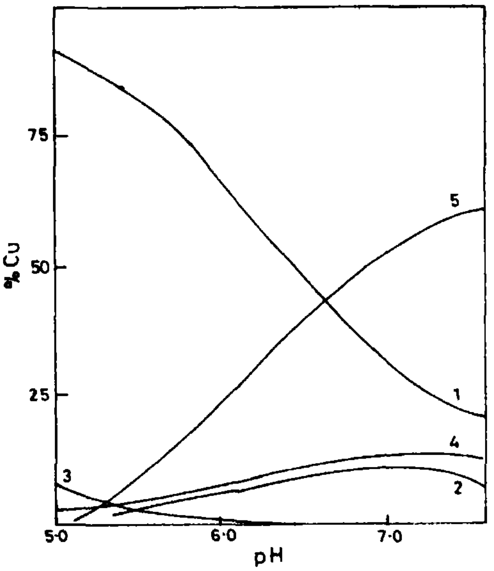

Fig. 1 – Distribution of complex species for Cu(II)-acetylacetone. (A) – glycine (B) system 1. CuA, 2. CuA_2, 3. CuB, 4. CuB_2, 5. CuAB.

The species distribution curve for copper(II)-acetylacetone-glycine system is shown in Fig. 1. It can be seen that under experimental conditions, nearly 90% of the total metal ion is present as CuA at *p*H 5 and the concentration of the complex decreases with increasing *p*H, at the same time the concentration of the ternary complex which is negligible at *p*H 5, gradually increases with increasing *p*H to a value of 60% at *p*H 7.5. The complexes CuA_2 and CuB_2 are formed to an extent of 10% and 12% respectively at *p*H 7. The CuB complex is formed in low concentration in the *p*H range 5 to 7. The species distribution diagrams for other systems exhibited similar qualitative features.

In order to compare the stabilities of the ternary complex species with those of the parent binary complexes, the values of Δlog *K*, the difference between the stabilities of the binary and the ternary complexes, log X, the disproportionation constant, were determined for all the ternary systems. From statistical considerations, it has been shown that considerably less negative values of $\Delta \log K$ and more positive values of $\log X$ indicate greater stabilities of the ternary complexes relative to those of the binary analogues.

The parameters $\Delta \log K$ and $\log X$ for the Cu-AB complexes are determined by Eqns 1 to 8,

$$\mathrm{Cu} + \mathrm{B} \rightleftharpoons \mathrm{CuB} \qquad \ldots (1)$$

$$\mathrm{CuA} + \mathrm{B} \rightleftharpoons \mathrm{CuAB} \qquad \ldots (2)$$

$$\Delta \log K = \log K^{\mathrm{CuA}}_{\mathrm{CuAB}} - \log K^{\mathrm{Cu}}_{\mathrm{CuB}} \qquad \ldots (3)$$

$$\mathrm{Cu} + \mathrm{A} \rightleftharpoons \mathrm{CuA} \qquad \ldots (4)$$

$$\mathrm{CuB} + \mathrm{A} \rightleftharpoons \mathrm{CuBA} \qquad \ldots (5)$$

$$\Delta \log K = \log K^{\mathrm{CuB}}_{\mathrm{CuBA}} - \log K^{\mathrm{Cu}}_{\mathrm{CuA}} \qquad \ldots (6)$$

$$\mathrm{CuA_2} + \mathrm{CuB_2} \rightleftharpoons 2\mathrm{CuAB}$$

$$X_{\mathrm{CuAB}} = [\mathrm{CuAB}]^2/[\mathrm{CuA_2}][\mathrm{CuB_2}] \qquad \ldots (7)$$

$$\log X_{\mathrm{CuAB}} = 2 \log \beta_{\mathrm{CuAB}} - (\log \beta_{\mathrm{CuA_2}} + \log \beta_{\mathrm{CuB_2}}) \qquad \ldots (8)$$

A critical examination of the values of $\Delta \log K$, $\log X$ and $\Delta \log \beta$ (Table 2) reveal that all the ternary complexes of Cu(II) with acetylacetone and amino acids, except that with β-phenylalanine, have $\Delta \log K$ values in the range -0.85 to 1.19. This range is close to -0.9, the value given by Sigel[1] as an indicator of strong ternary complex formation. These $\Delta \log K$ values are further supported by positive $\Delta \log X$ values occurring in the range 1.40-1.76, which are greater than 0.6, a value for the existence of 50% ternary complex species when the binary species are present to the extent of 25% each. Similarly, all the ternary complexes possess positive $\Delta \log \beta$ values.

The formation constant values of these ternary complexes (Table 2) show that in all these cases except with β-phenylalanine, the Cu(II)-acetylacetone-amino acid ternary complexes are more stable than the 1:2 Cu(II)-acetylacetone or Cu(II)-amino acid binary complexes. Further, the log $K^{\mathrm{CuA}}_{\mathrm{CuAB}}$ are in the order, gly > ala > 2-aba > val > leu > pala.

Thus the 1:1 copper(II)-acetylacetone complex has a greater tendency towards combination with any amino acid molecule (except with β-phenylalanine) rather than that with another acetylacetone molecule. It is well known that acetylacetone forms a six-membered metal chelate ring, while the α-amino acids can form only five-membered metal chelate rings. Thus the high stability of the ternary complexes may be due to the preference of Cu(II) ion to possess one five-membered ring and one six-membered ring over two five- or two six-membered rings. Similar observations were also made by several earlier workers[9-11]. This is further confirmed by the fact that the formation constant of ternary complex with β-phenylalanine, which can form only six-membered chelate ring with copper(II) has lower values of all the ternary complexes with other amino acids in the present investigations. It is also interesting to note that the 1:1 Cu(II)-acetylacetone complex has lesser tendency to combine with another molecule of β-phenylalanine than with acetylacetone.

Two of us (N K Rao & R P Rao) gratefully acknowledge the financial assistance from UGC, New Delhi for carrying out this work.

References

1 *Metal ions in biological systems*, Vol 2, edited by H Sigel (Marcel Dekker, New York) 1973.

2 Sivasankaram Nair M & Santappa M, *Indian J Chem*, **20A** (1981) 990.

3 Bond A M & Hefter G, *J electroanal Chem*, **68** (1976) 203.

4 Van Uitert L G & Haas C C, *J Am chem Soc*, **75** (1953) 451.

5 Irving H M & Rossotti H S, *J chem Soc*, (1954) 2904.

6 Dey B P, Dutta S & Lahiri S C, *Indian J Chem*, **21A** (1982) 886.

7 Irving H & Williams R J R, *J chem Soc*, (1953) 3192.

8 Beck M T, *Chemistry of complex equilibria* (Van Nostrand Reinhold Company, London) 1970, 70-73.

9 El Ezaby M S, Marafie H M & Fareed S, *J Inorg Bio Chem*, **11** (1979) 317.

10 Brookes G & Pettit L D, *J chem Soc* (*Dalton*), (1977) 1918.

11 Sigel H, Caraw R & Prijs B, *Inorg Chem*, **13** (1974) 462.

Indian Journal of Chemistry
Vol. 27A, June 1988, pp. 558-560

Atomic Absorption Spectrophotometric Determination of Copper after Adsorption of Its Rubeanate onto Microcrystalline Naphthalene

B K PURI
Department of Chemistry, Indian Institute of Technology, Hauz Khas, New Delhi 110 016
M KATYAL
St. Stephen's College, Delhi 110 007
and
M SATAKE* & L F CHANG
Faculty of Engineering, Fukui University, Fukui 910, Japan

Received 20 *July* 1987; *revised* 24 *September* 1987; *accepted* 23 *October* 1987

A highly sensitive and fairly selective atomic absorption spectrophotometric method has been developed for the determination of copper after adsorption of its rubeanate onto microcrystalline naphthalene in the *p*H range of 2.0-8.3. Beer's law is obeyed in the concentration range of 2.0-90.0 μg of copper at 324.7 nm in 10 ml of the final solution. Eight replicate analysis on a sample solution containing 45 μg of copper gave a mean absorbance of 0.250 with a relative standard deviation of ± 1.77%. The sensitivity for 1 % absorption is 0.079 μg/ml (0.133 μg/ml for the direct atomic absorption spectrophotometric method from the aqueous phase). The interference of various ions has been studied and the method has been employed for the determination of copper in various standard alloys and human hair etc.

Rubeanic acid(dithiooxamide) has been employed in the detection and determination of some metal ions[1-5]. The colorimetric method for the copper determination involves rigid conditions[6], e.g. absorbance has to be measured within 2-3 min. Preliminary observations reveal that copper reacts with rubeanic acid to form a coloured, water insoluble, thermally stable complex which cannot be extracted into any of the organic solvent but can be adsorbed onto microcrystalline naphthalene simply by shaking for a few seconds even from a large volume of the aqueous phase (~ 1.6 litres). In the present communication an atomic absorption spectrophotometric method has been developed for the trace determination of copper after adsorption of its rubeanate complex onto microcrystalline naphthalene. The interference of various ions has been studied and the method has been utilized for the determination of copper in various standard reference samples and complex materials like human hair etc.

Stock solution of copper sulphate was prepared in deionised, distilled water and standardized. A working solution(10 ppm) was prepared by appropriate dilution. A 0.1% solution of rubeanic acid was prepared in ethanol. Buffer solutions of *p*H 3-6 and 8-11 were prepared by mixing 1*M* acetic acid/1*M* ammonium acetate and 1*M* aqeous ammonia/1*M* ammonium acetate respectively. A 20% solution of naphthalene was prepared in acetone. For dissolving the metal complex and naphthalene, dimethylformamide (DMF, 100 ml), thiourea (300 mg) and 7.3*N* nitric acid(1ml) were mixed. These amounts were established by trial experiments. All other reagents used were of AR grade.

A Perkin-Elmer model 403 atomic absorption spectrophotometr and a Toa-Dempa model HM-5A *p*H meter were used. All absorbances were measured using an air-acetylene flame and a copper cathode lamp at 324.7 nm.

General procedure

To an aliquout of copper solution containing 2-90 μg of copper were added rubeanic acid(0.1%, 1 ml) and the buffer (*p*H 3.8, 2 ml). It was diluted to 50 ml with water, mixed well and allowed to stand for about 5 min at room temperature for complete formation of the complex. To this 20% naphthalene solution(1.2 ml) in acetone was added and shaken vigourously for 30 sec. The solid mass consisting of naphthalene and the metal complex was separated by filtration, dissolved in DMF-thiourea-nitric acid mixture and diluted to 10 ml in a standard flask. This solution was aspirated into air-acetylene flame at 324.7 nm using a copper hollow cathode lamp.

Reaction conditions were established by taking 45 μg of copper. The adsorption of copper rubeanate was maximum and constant in the *p*H range 2.0-8.3; below and above this *p*H range adsorption was incomplete. Addition of 0.5-5.0 ml of buffer (*p*H 3.8) virtually caused no variation in adsorbance and 2.0 ml were recommended in the all experiments.

A minimum of 0.05 ml of rubeanic acid(0.1%) was needed for the complete reaction. However, 1.0 ml of 0.1% rubeanic acid has been recommended to be on safe side. Absorbance increased with the increase in volume of naphthalene upto 0.25 ml of 20% naphthalene solution, then remained constant between 0.25 and 3.0 ml. Therefore, 1.2 ml of naphthalene were used. The formation of the copper rubeanate is fairly rapid at room temperature, however, a 5-min digestion time is maintained in all the cases. The adsorption is very rapid, being practically complete in less than 10 sec, and a shaking time of 30 sec gives an ample safety margin. Adsorption is quantitative when the volume of the aqueous phase does not exceed 1.6 litres and is best kept to 50 ml for convenience.

Table 1—Effect of Diverse Ions in Determination of Copper as Copper Rubeanate

Salt	Tolerance limit	Ion	Tolerance limit
$NaClO_4.H_2O$, NaCl,		Mg^{2+}, Ca^{2+}	500 mg
KNO_3, $CH_3COONa.3H_2O$,		Cr^{3+}, Cr^{6+}	100 mg
NH_4Cl, Na_2SO_4,		Mn^{2+}	50 mg
Sodium tartrate,		Cd^{2+}	20 mg
Sodium citrate	2 g	Pb^{2+}, Zn^{2+}	10 mg
KH_2PO_4	1 g	Al^{3+}, Fe^{3+}	10 mg
KI, KSCN, NH_4F	500 mg	Bi^{3+}	2 mg
Malonic acid,		Co^{2+}, Ni^{2+}	1 mg
Ethylenediamine	50 mg	V^{5+}	200 μg
DTCS, $Na_2S_2O_3$, $Na_2C_2O_4$,		Rh^{3+}	100 μg
thiourea	100 μg	Os^{8+}, Ir^{3+}	50 μg
Na_2-EDTA	10 μg	Hg^{2+}	30 μg
KCN	5 μg	Pd^{2+}, Mo^{6+}	20 μg
		W^{6+}	10 μg
		Ru^{3+}, Ag^{+}, Pt^{4+}, Au^{3+}	5 μg

Table 2—Analysis of Copper in Standard Reference Samples

Sample	Copper certified value (%)	Copper content⁺ (%)	
		Present method	DDTC-MIBK method
N.B.S., SRM-94c Die Casting alloy	1.01	1.017 ± 0.009	1.041 ± 0.007
N.B.S., SRM-629 Zinc-base alloy	1.50	1.671 ± 0.009	1.504 ± 0.008
JSS 611-7 High speed steel	0.036	0.0359 ± 0.0004*	0.0364 ± 0.0003
JSS 508-4 Ni-Cr steel	0.12	0.108 ± 0.003*	0.115 ± 0.002
JSS 513-4 Cr steel	0.074	0.0728 ± 0.0006*	0.0745 ± 0.0008
Nippon Aluminium Co., No. 3A-30 Al alloy	0.059	0.0601 ± 0.0017	0.0583 ± 0.0013

*Malonic acid (80 mg) was added as a masking reagent for Fe^{3+}.
⁺Mean of 5 individual determinations.

The composition of copper rubeanate was established by Job's method of continuous variation. A break at 0.50 mol fraction confirmed the formation of $Cu(C_2H_2N_2S_2)$ under these conditions which is the same as reported in the literature[1,2].

Copper rubeanate is insoluble in a large number of organic solvents, like benzene, toluene, xylene, *o*-chlorobenzene, *o*-dichlorobenzene, nitrobenzene, chloroform, carbon tetrachloride, 1,2-dichloroethane, isoamyl acetate, diethyl ether, *n*-amylalcohol, isoamylalcohol, ethanol, methyl isobutyl ketone, dioxane, DMF, dimethyl sulphoxide, propylene carbonate, acetonitrile, etc. It was also found to be insoluble in mixed solvents like DMF-HNO_3, DMF-$HClO_4$, DMF-HCl, *n*-butylamine-DMF, propylamine-DMF and isobutylamine-DMF. However, it is found to be soluble in DMF-thiourea-HNO_3 or DMF-*n*-butylamine-KCN. The results of preliminary observations reveal that a ternary mixture consisting of DMF(100 ml), thiourea(300 mg) and 7.3 *N* HNO_3 (1 ml) is the most suitable solvent for dissolving the metal complex. The calibration curve at 324.7 nm is found to be linear over copper concentration range of 2.0-90.0 μg in 10 ml in the ternary mixture solvent.

Table 3—Determination of Copper in Water Samples and Human Hair

Sample (vol taken)	Copper found (ppb)*	
	Present method	DDTC-MIBK method⁺
Hot spring water (Awara) (500 ml)	6.3 ± 0.2	5.5 ± 0.3
Lake water (Kitagata) (500 ml)	0.8 ± 0.1	0.8 ± 0.1
River water (Oyabe) (500 ml)	0.4 ± 0.1	0.4 ± 0.1
Human hair (male)	0.00153 ± 0.00007(%)	0.00159 ± 0.00004(%)

*Mean of 5 individual determinations.

⁺DDTC-MIBK method: Japanese Industrial Standard, JIS K0102, p.154 (1981)

Eight determinations of a sample solution containing 45 μg of copper gave a mean absorbance of 0.250 with a relative standard deviation of 1.77%. The sensitivity for 1% absorption is found to be 0.079 μg/ml (0.133 μg/ml for the direct atomic absorption spectrophotometric determination from the aqueous solution). The sensitivity of this method may be further improved by carrying out the adsorption from a larger volume of the aqueous phase(1.6 litres) instead of 50 ml as suggested in the general procedure.

Sample solutions containing 45 μg of copper and various amounts of different alkali metal salts or metal ions were prepared and the determination of copper was carried out by the general procedure. The tolerance limit(error ± 3%) of diverse ions is given in Table 1. Many ions can be tolerated upto mg level except oxalate, cyanate, EDTA, thiourea, thiosulphate, DTCS[N-(dithiocarboxy) sarcosine], o-phenanthroline, Mo^{6+}, W^{6+}, Hg^{2+}, V^{5+}, Ru^{3+}, Rh^{3+}, Os^{8+}, Ag^{+}, Au^{3+}, Ir^{3+}, Pt^{4+} and Pd^{2+}. The interference of the anions is probably due to the formation of more stable complexes with copper than copper rubeanate, while that of the metal ions it may be due to their reaction with the reagent under these conditions.

Determination of copper in standard reference materials

Sample (0.05-1 g) of the alloy was completely dissolved in 1:1 HCl (20-40 ml) by heating on a water-bath. To this 30% H_2O_2 (2-3 ml) was added. The excess of H_2O_2 was decomposed by heating the solution on a water-bath. The solution was cooled, filtered and diluted to 500 ml in a standard flask. An aliquot of this solution was taken and copper was determined by the general procedure (Table 2).

Determination of copper in water samples

The water samples from different sources were collected. Each of the water sample was adjusted to *p*H 1.0 with HNO_3, filtered through a filter paper No. 5C and copper was determined in the filtrate by the general procedure (Table 3).

Determination of copper in human hair

A sample(10 g) of human hair was taken and dissolved by heating it in a Kjeldahl flask containing conc HNO_3 (30 ml) and conc HCl (3 ml). The solution was cooled, filtered, diluted to 200 ml with distilled water and copper was determined in an aliquot of this solution by the general procedure (Table 3).

In all the cases the results were compared with the standard DDTC-MIBK method.

References

1 Welcher F J, *Organic analytical reagents*, Vol 4 (D Van Nostrand Company, London) 1948, p 148.
2 Kodama K, *Methods of quantitative inorganic analysis* (Interscience Publishers, London) 1963.
3 Chawla R S, Singh R P & Trikha K C, *Talanta*, **18** (1971) 1245.
4 Brajker K & Kozika U K, *Talanta*, **26** (1979) 417.
5 Saha M B & Chakraburtty A K, *J Indian chem Soc*, **60** (1983) 176.
6, West P W & Compare M, *Analyt Chem*, **21** (1949) 628.
7 Perrin D D, *Masking and demasking of chemical reactions* (Wiley-Interscience, London) 1970.